



# MARINE PHYSICAL LABORATORY

SCRIPPS INSTITUTION OF OCEANOGRAPHY

San Diego, California 92152

DTIC FILE COPY

## FREELY DRIFTING SWALLOW FLOAT ARRAY: JULY 1989 TRIP REPORT

G. C. Chen, G. L. D'Spain, W. S. Hodgkiss, and G. L. Edmonds

AD-A226 771

DTIC  
ELECTE  
SEP 28 1990  
S B D

MPL TECHNICAL MEMORANDUM 420

MPL-U-9/90  
February 1990

*Approved for public release; distribution unlimited.*

90 00 00 027

REPORT DOCUMENTATION PAGE				Form Approved OMB No. 0704-0188	
1a. REPORT SECURITY CLASSIFICATION UNCLASSIFIED			1b. RESTRICTIVE MARKINGS		
2a. SECURITY CLASSIFICATION AUTHORITY			3. DISTRIBUTION/AVAILABILITY OF REPORT Approved for public release; distribution unlimited.		
2b. DECLASSIFICATION/DOWNGRADING SCHEDULE					
4. PERFORMING ORGANIZATION REPORT NUMBER(S) MPL TECHNICAL MEMORANDUM 420 [MPL-U-9/90]			5. MONITORING ORGANIZATION REPORT NUMBER(S)		
6a. NAME OF PERFORMING ORGANIZATION University of California, San Diego		6b. OFFICE SYMBOL (If applicable) MPL	7a. NAME OF MONITORING ORGANIZATION Commanding Officer Naval Research Laboratory		
6c. ADDRESS (City, State, and ZIP Code) Marine Physical Laboratory Scripps Institution of Oceanography San Diego, California 92152			7b. ADDRESS (City, State, and ZIP Code) Washington, D.C. 20375		
8a. NAME OF FUNDING/SPONSORING Commanding Officer Naval Research Laboratory		8b. OFFICE SYMBOL (If applicable) ONR	9. PROCUREMENT INSTRUMENT IDENTIFICATION NUMBER N00014-88-K-2040		
8c. ADDRESS (City, State, and ZIP Code) Washington, D.C. 20375			10. SOURCE OF FUNDING NUMBERS		
			PROGRAM ELEMENT NO.	PROJECT NO.	TASK NO.
11. TITLE (Include Security Classification) FREELY DRIFTING SWALLOW FLOAT ARRAY: JULY 1989 TRIP REPORT					
12. PERSONAL AUTHOR(S) G. C. Chen, G. L. D'Spain, W. S. Hodgkiss, and G. L. Edmonds					
13a. TYPE OF REPORT technical memorandum		13b. TIME COVERED FROM _____ TO _____		14. DATE OF REPORT (Year, Month, Day) February 1990	
15. PAGE COUNT					
16. SUPPLEMENTARY NOTATION					
17. COSATI CODES			18. SUBJECT TERMS (Continue on reverse if necessary and identify by block number) Swallow floats, XBT and anemometer data, vlf hydrophones		
FIELD	GROUP	SUB-GROUP			
19. ABSTRACT (Continue on reverse if necessary and identify by block number)  Representative data collected by the Marine Physical Laboratory's (MPL) Swallow floats during the 8-9 July, 1989 deployment are presented herein. As part of the Downslope Conversion experiment, the Swallow float deployment was conducted near 34° 50' N, 122° 20' W, about 150 km west, northwest of Pt. Arguello, California. This report presents the Swallow float deployment locations, the positions and characteristics of known signal sources, expendable bathythermograph (XBT) and anemometer data, and representative Swallow float data from the experiment. The Swallow float data include battery voltage, compass heading, and automatic gain control (AGC) measurements, the 8 kHz acoustic localization ping arrivals, and the VLF pressure and particle velocity data. All 12 Swallow floats operated nearly flawlessly, resulting in a 95 % full data set. The data set is of extremely high quality and it appears to provide a rich source of information on signal propagation in the 1 to 20 Hz (VLF) band.					
20. DISTRIBUTION/AVAILABILITY OF ABSTRACT <input type="checkbox"/> UNCLASSIFIED/UNLIMITED <input type="checkbox"/> SAME AS RPT. <input type="checkbox"/> DTIC USERS			21. ABSTRACT SECURITY CLASSIFICATION UNCLASSIFIED		
22a. NAME OF RESPONSIBLE INDIVIDUAL W. S. Hodgkiss			22b. TELEPHONE (Include Area Code) (619) 534-1798		22c. OFFICE SYMBOL MPL

A number of interesting features can be seen in a preliminary look at these data. First, throughout the experiment, the Swallow floats were clearly able to hear the 14 Hz tone generated by the MARK VI source deployed by the Aloha, a source ship involved in a companion experiment, which was located about 2500 km to the west from the Swallow float array. At times, the array also appeared to hear the 11 Hz and 8 Hz tones generated by the MARK VI. Second, a 7 Hz line generated by the R/V New Horizon's blades, the research vessel used in this experiment, was at times audible to the floats, allowing for future efforts at beamforming the Swallow float data on a known source. Third, ship signatures of various commercial vessels in the VLF band were intermittently written into the Swallow floats' records, providing opportunity for future efforts in contact tracking and clutter suppression studies. Fourth, an arrival in the Swallow float time series has tentatively been identified as the arrival from a magnitude 3.5 earthquake in central California along the Calaveras fault.

A unique aspect of this experiment was the installation of VLF hydrophones on all of the floats. The calibrated pressure spectral levels estimated directly from data collected by the VLF hydrophones agree with those derived from the geophone data except near frequencies corresponding to float rocking resonances and at times when signal clipping or overloading was present. Also, in situ measurements of the floats' absolute clock drifts were obtained; the results from this deployment were consistent with those measured in the August 1988 deployment.

## Freely Drifting Swallow Float Array: July 1989 Trip Report

*G. C. Chen, G. L. D'Spain, W. S. Hodgkiss, and G. L. Edmonds*

Marine Physical Laboratory  
Scripps Institution of Oceanography  
San Diego, CA 92152

### ABSTRACT

Representative data collected by the Marine Physical Laboratory's (MPL) Swallow floats during the 8-9 July, 1989 deployment are presented herein. As part of the Downslope Conversion experiment, the Swallow float deployment was conducted near 34° 50' N, 122° 20' W, about 150 km west, northwest of Pt. Arguello, California. This report presents the Swallow float deployment locations, the positions and characteristics of known signal sources, expendable bathythermograph (XBT) and anemometer data, and representative Swallow float data from the experiment. The Swallow float data include battery voltage, compass heading, and automatic gain control (AGC) measurements, the 8 kHz acoustic localization ping arrivals, and the VLF pressure and particle velocity data. All 12 Swallow floats operated nearly flawlessly, resulting in a 95 % full data set. The data set is of extremely high quality and it appears to provide a rich source of information on signal propagation in the 1 to 20 Hz (VLF) band.

A number of interesting features can be seen in a preliminary look at these data. First, throughout the experiment, the Swallow floats were clearly able to hear the 14 Hz tone generated by the MARK VI source deployed by the Aloha, a source ship involved in a companion experiment, which was located about 2500 km to the west from the Swallow float array. At times, the array also appeared to hear the 11 Hz and 8 Hz tones generated by the MARK VI. Second, a 7 Hz line generated by the R/V New Horizon's blades, the research vessel used in this experiment, was at times audible to the floats, allowing for future efforts at beamforming the Swallow float data on a known source. Third, ship signatures of various commercial vessels in the VLF band were intermittently written into the Swallow floats' records, providing opportunity for future efforts in contact tracking and clutter suppression studies. Fourth, an arrival in the Swallow float time series has tentatively been identified as the arrival from a magnitude 3.5 earthquake in central California along the Calaveras fault.

A unique aspect of this experiment was the installation of VLF hydrophones on all of the floats. The calibrated pressure spectral levels estimated directly from data collected by the VLF hydrophones agree with those derived from the geophone data except near frequencies corresponding to float rocking resonances and at times when signal clipping or overloading was present. Also, in situ measurements of the floats' absolute clock drifts were obtained; the results from this deployment were consistent with those measured in the August 1988 deployment.

January 11, 1990



Session For	
IS GRA&I	<input checked="" type="checkbox"/>
IC TAB	<input type="checkbox"/>
announced	<input type="checkbox"/>
Justification	
By	
Distribution/	
Availability Codes	
Dist	Avail and/or Special
A-1	



## Table of Contents

	Introduction
I.	Deployment Geometry <ul style="list-style-type: none"><li>a) Swallow Float Deployment and Retrieval</li><li>b) Sonobuoy Deployment</li><li>c) Deployment Depths</li></ul>
II.	Known Sound Sources <ul style="list-style-type: none"><li>a) R/V New Horizon Ship Tracks</li><li>b) MARK VI Source Deployed from Aloha</li><li>c) Ship Sightings</li></ul>
III.	Swallow Float Log Summary
IV.	Environmental Data <ul style="list-style-type: none"><li>a) XBT Measurements</li><li>b) Anemometer Readings</li><li>c) Additional Environmental Information</li></ul>
V.	Swallow Float Data - General Indication of Data Integrity
VI.	Swallow Float Time Base Measurements
VII.	Battery Voltage, Float Heading, and AGC Level <ul style="list-style-type: none"><li>a) Battery Voltage</li><li>b) Float Heading</li><li>c) AGC Level</li></ul>
VIII.	The 8 kHz Surface and Bottom Bounce Data
IX.	The 8 kHz Interelement Range Data
X.	RMS Pressure and Velocity <ul style="list-style-type: none"><li>a) Midwater Swallow Float Data</li><li>b) Bottom-Mounted Swallow Float Data</li></ul>
XI.	Geophone and Hydrophone Time Series <ul style="list-style-type: none"><li>a) Comparison of Hydrophone and Geophone Time Series</li><li>b) Range Survey Pings in the GOES Clock Test</li><li>c) Tape Recorder Contamination</li><li>d) Gain Attenuation</li><li>e) New Horizon Radiated Noise</li><li>f) Mark VI Source</li><li>g) Other Unknown Signals in the Time Series</li><li>h) Geophone Time Series Recorded on the Sea Surface</li><li>i) Earthquake Arrival</li></ul>
XII.	Velocity and Pressure Power Spectra <ul style="list-style-type: none"><li>a) Hydrophone Pressure Spectra</li><li>b) New Horizon Radiated Noise</li><li>c) Tones from the MARK VI Source</li></ul>
	Acknowledgements
	References
	Appendix 1 - Swallow Float VLF Data Acquisition System
	Appendix 2 - Loran-C Position Fixes
	Figures

## Introduction

The Marine Physical Laboratory's (MPL) set of 12 Swallow floats were deployed for a 24-hour period on 8-9 July 1989 near  $34^{\circ} 50' \text{ N}$ ,  $122^{\circ} 20' \text{ W}$ , about 150 km west, northwest of Pt. Arguello, California. The Swallow float deployment was part of the Downslope Conversion experiment, whose primary objective was to study the physics of downslope signal propagation.

The Swallow floats, which have been under development for the past 8 years at the Marine Physical Laboratory, are neutrally buoyant, independently drifting, very low frequency (1-20 Hz), acoustic pressure and particle velocity sensors. They each contain within a 0.432 m diameter glass shell 3 orthogonally oriented geophones for measuring infrasonic particle velocity, a magnetic compass, and the data acquisition system [A-1]. They also contain an omni-directional hydrophone for measuring infrasonic pressure and an 8 kHz acoustic localization system [1,2,3,4,5]. Figure 1 is a schematic drawing of a typical midwater float.

In this experiment, 12 Swallow floats were deployed; 9 were freely drifting in the water column and 3 were tethered to the ocean bottom by 3.05-meter lines with 10-15 lb anchors. The 3 bottom-tethered floats were positioned at the corners of a triangle with sides of length about 6.3 km. The 9 midwater floats were deployed in a quasi vertical line array geometry with a vertical float separation of about 400 m, starting at about 600 m depth to about 3800 m. The midwater floats were put into the water at about the geometric center of the bottom-float triangle. All 12 floats operated nearly flawlessly during the experiment.

Also concurrently deployed were 3 DIFAR sonobuoys, model SSQ 53B, from the R/V New Horizon and 14 air-launched sonobuoys of various design from a P-3 aircraft. Jim MaEachern, from the Naval Air Development Center (NADC), was aboard the P-3 aircraft, monitoring the recording of the sonobuoy data. Data collected by the sonobuoys will be reported at a later time.

This report will be restricted to those data collected with the Swallow floats on 8-9 July and is organized in the following fashion: sections 1, 2, 3, and 4 present the instrument deployment locations, the positions and characteristics of known signal sources, Swallow float log summary, and expendable bathythermograph (XBT) and anemometer data; section 5 reports the data quality; section 6 discusses the clock drift measurement; sections 7, 8, 9, 10, 11, and 12 present the representative Swallow float data from the experiment which include battery voltage, compass heading, and automatic gain control (AGC) measurements, the 8 kHz acoustic localization ping arrivals, and the VLF pressure and particle velocity data.

Note that all times listed in this report are in local Pacific Daylight Time. To obtain Greenwich Mean Time, add 7 hours to the local time.

## I. Deployment Geometry

### a) Swallow Float Deployment and Retrieval

Figure I.1 shows the deployment and retrieval positions of all 12 Swallow floats. The symbols used for plotting the float positions are the float identification numbers (not the float serial numbers) in hexadecimal notation, i.e. float 10 is plotted as an "A" and float 11 is plotted as a "B".

The 3 bottom-mounted floats, floats 9, 10, and 11, formed a triangle about 6.3 km on a side. The 9 midwater floats, which were ballasted for a depth spacing about 400 meters, starting at 500 meters and extending to 3700 meters, were deployed in the approximate center of the triangle array (see Figure I.2). They drifted generally to the west during the deployment period. Note that float 0 was retrieved several kilometers northwest of its deployment position. It may have experienced some strong surface current during the deployment.

### b) Sonobuoy Deployment

Three DIFAR sonobuoys, model SSQ 53B, were deployed from the New Horizon in order to mark the spot of the Swallow float deployment for Jim McEachern from NADC. He arrived on station in a P-3 aircraft, around 9 p.m. local time on 8 July, and air-deployed 14 additional sonobuoys of various designs. The aircraft remained on station for 6 hours recording the sonobuoy data. The data from sonobuoys were multiplexed on several RF channels and transmitted back to the analog recorders aboard the P-3. Twelve of the 14 air-launched sonobuoys and all three ship-launched sonobuoys provided useable data. These data have been provided to us by NADC. The following table lists the number and type of sonobuoys which were deployed in the experiment.

Number Deployed	Type	Manufacturer (Air or Ship-launched)
2	53D	Hermes (Air)
2	53D	Spartan (Air)
3	53B	Magnavox (Ship)
2	77	Magnavox (Air)
2	57B	Spartan (Air)
2	VLF-IIa	Spartan (Air)
2	EARS	British (Air)
2	VLF-III	(Air)

### c) Deployment Depths

The planned deployment depths of the Swallow floats and the 3 ship launched sonobuoys are shown in Figure I.2. In Figure I.3, the set of horizontal dotted lines, starting at about 575 meters depth, indicate the depth at which the Swallow floats actually stabilized. Planned and actual deployment depths of the Swallow floats are shown in Table I-1.

**Table I-1: Planned and Actual Deployments Depths, July 1989 Experiment**

Float	Deployment Depth, m.	
	Planned	Achieved
0	500	575
1	900	1000
2	1300	1385
3	1700	1680
4	2100	2080
5	2500	2540
6	2900	2960
7	3300	3350
8	3700	3825
9	bottom	4080(bottom)
10	bottom	4080(bottom)
11	bottom	4080(bottom)

The equilibrium depths of freely drifting floats are controlled by the weight of the float release ballast, which must be carefully determined for each float prior to each experiment. Equilibrium depth is an extremely sensitive function of ballast weight, with a 1 gram change in ballast corresponding to approximately 10 meters change in equilibrium depth. All of the float components are compressible to some degree, which must be accounted for as the floats descend. Also, it is difficult to predict the exact density versus depth distribution for a particular experiment location.

In Figure I.3, the horizontal line of dots for each float is derived from the surface-bounce arrival in the 8 kHz localization data (converted to depth by using a speed of sound of 1500 m/sec). A discussion of the 8 kHz localization data is given in Section VIII.

The lower horizontal axis of Figure I.3 gives the record number in which the surface bounce detection was made. This axis is actually a measure of time elapsed since the time at which all floats were synchronously started; i.e. 11:28, 8 July. In this deployment, the floats did not start recording data until after an 8 hour (640 record) delay. To convert from record number to minutes, multiply the record number by 0.75 (since each record is 45 seconds long). Each float was programmed to ping every 12 records; the spacing between each of the dots in a given line is 12 records. The waviness of the midwater floats' dotted lines, due to their depths changing as a function of time, is indicative of the presence of internal waves. The gaps in the data, especially floats 7 and 8's data, are probably due to rough sea conditions; the wind gusted up to 35 knots at times during the deployment.

The final piece of information added to Figure I.3 is the sound velocity profile based upon historical salinity and temperature data [6] and an equation relating salinity, temperature, and depth to sound velocity [7]. The upper horizontal axis of the plot gives the sound velocity in meters/sec.

## II. Known Sound Sources

### a) R/V New Horizon Ship Tracks

Loran-C and GPS position fixes of the research vessel used in this experiment, the New Horizon, were recorded intermittently in the Swallow float log while the experiment was being conducted. All position fixes during the Swallow float data recording period, indicated by "+"s, are plotted in Figures II.1 and II.2.

The ship track in Figure II.1 began just to the southeast of the triangle of where the midwater floats were deployed. From there, the ship moved slowly north, northwest, as surveys of the ranges to the floats and float clock-drift measurements were made. At 20:40, 8 July, the New Horizon increased its speed to 5 knots (2.5 m/sec) and headed to the southeast away from the array toward the continental shelf for the night. In the morning of 9 July, as shown in Figure II.2 the New Horizon returned to the array, traversing a predetermined path so that it could be used as a source in future beamforming efforts. At 07:30, the ship was about 40 km away from the array traveling at about 3 knots (1.5 m/sec) and heading northwest across the slope and around 12:00 switched to 9 knots (4.5 m/sec) heading the southwest and finally at 6 knots (3 m/sec) heading the northwest toward the array.

In order to estimate the frequency of some of the possible narrow band signals generated by the R/V New Horizon, the following information was obtained from the ship's engineer. At a 10.25 knot speed, the ship's two engines rotate at 270 rpm. At this speed, then, the diesel shaft rate is 4.5 Hz. The reduction gear ratio is 3.9-to-1; the corresponding shaft rate is 1.15 Hz. Since the ship has 3 fixed blades on each of its 2 props, the blade rate is 3.5 Hz at this speed. An approximately linear relationship exists between engine rpm and ship speed when both screws are engaged. Sonobuoy measurements of the acoustic signature of the R/V New Horizon, made on May 23, 1989 for a ship speed of 5 knots, are given in Figures II.3 and II.4. A set of harmonically related lines at 7, 14, 21, 28, 35, 42, and 49 Hz are evident in the figures.

### b) MARK VI source Deployed from Aloha

A MARK VI source was deployed from the Aloha, a source ship involved in a companion experiment. This ship was located about 2500 km to the west of the Swallow float array during the Swallow float deployment. The broadcast plan of the Aloha was to transmit 14 Hz for a half hour, then 8 Hz for a half hour, then 14 Hz, then 11 Hz and then repeat the pattern. The Aloha also dropped SUS charges hourly, about 2 to 4 minutes before switching the MARK VI to a different frequency. Throughout the deployment, the Swallow floats can see quite clearly the 14 Hz line projected by the MARK VI source and, at times, the 11 Hz and the 8 Hz lines. The following table lists the arrival times and the duration of the 14-Hz tone heard by float 1. The arrival times at the Swallow float array are in local Pacific Daylight time.

Arrival Time Time (Date)	Duration (min)	Float 1 Record Interval
19:29(7-8)	31	642-682
20:28(7-8)	32	720-761
21:29(7-8)	30	802-841
22:29(7-8)	30	882-921
23:29(7-8)	31	962-1002
00:28(7-9)	31	1041-1081
01:28(7-9)	31	1121-1161
02:28(7-9)	30	1201-1240
03:38(7-9)	30	1281-1320
04:28(7-9)	30	1361-1400
05:28(7-9)	27	1441-1476
06:28(7-9)	30	1521-1560
07:28(7-9)	30	1601-1640
08:28(7-9)	28	1681-1717
09:28(7-9)	30	1761-1800
10:28(7-9)	31	1841-1881
11:28(7-9)	30	1921-1960
12:28(7-9)	31	2000-2040
13:28(7-9)	29	2080-2118

### c) Ship Sightings

The Swallow float deployment site is just to the west of the opening to the Santa Barbara Channel which is an area of heavy commercial shipping. The R/V New Horizon's radar was continuously monitored by the ship's crew during the course of the experiment for possible ship sightings. The following table lists the radar contacts obtained from the R/V New Horizon's Radar and Visual Contact Log during the Swallow float data recording period;

Radar and Visual Contact Log						
Time (Date)	Contact Bearing	Contact Range(n mi)	Contact Course	CPA (n mi)	Estimated Speed(kn)	Remarks
23:53(7-8)	020	3.4	297	3.4	11.3	Large vessel.
23:56(7-8)	056	4.2	139	3.1	2.7	Small vessel.
06:10(7-9)	345	5.5	119	3.6	16.0	Large SUBARU RO RO car carrier.
06:20(7-9)	250	8.2	110	5.6	21.0	Large con- tainer ship.
13:15(7-9)	074	1.8	287	1.7	14.0	Large TOY- OTA RO RO car carrier.

Also, while the P-3 was recording the sonobuoy data from 21:00, 8 July through 03:00, 9 July, the aircraft's radar made 6 contact maps. The following table lists the contact times and the number of ships sighted in each contact;

Contact Sequence Number	Contact Time Time (Date)	Number of Ships Sighted
1	21:35(7-8)	8
2	22:55(7-8)	4
3	23:35(7-8)	4
4	00:35(7-9)	3
5	01:42(7-9)	3
6	03:03(7-9)	3

The positions of ships sighted in each of the radar contact are labeled by the corresponding contact sequence number and are plotted on top of each other in Figure II.5 with reference to the Swallow float bottom-float triangle.

### III. Swallow Float Log Summary

Note: All times are in local Pacific Daylight Time. To obtain standard Greenwich Mean Time, add 7 hours.

8 July 1989

07:10 Finished downslope source tow and underway to Pt. SF.  
10:30 Arrive on station.  
10:56 XBT #28 T-5 is taken.  
11:28 Start all floats synchronously using GOES clock pulse.  
11:43 All Swallow floats are running properly.  
12:45 Deploy freely drifting Swallow floats (floats 0,1,2,3,4,5,6,7 and 8). Ship's position is 34° 50.080' N, 122° 20.045' W.  
12:53 Deploy last freely drifting float. Ship's position is 34° 50.037' N, 122° 20.160' W.  
12:57 Underway to deploy bottom float 10 and 10.5 kHz transponder.  
13:30 Deploy 10.5 KHz transponder. Ship's position is 34° 51.025' N, 122° 22.060' W.  
13:34 Deploy bottom float 10. Ship's position is 34° 51.067' N, 122° 22.115' W.  
13:38 Underway to deploy bottom float 11 and 11 kHz transponder.  
14:13 XBT #29 T-5 is taken.  
14:16 Arrive on station 11. Ship's position is 34° 48.018' N, 122° 20.071' W.  
14:21 Deploy 11 kHz transponder. Ship's position is 34° 48.023' N, 122° 20.096' W (GPS).  
14:23 Deploy bottom float 11. Ship's position is 34° 48.042' N, 122° 20.132' W.  
14:26 Underway to deploy bottom float 9 and 10.0 kHz transponder.  
15:10 Ship's position is 34° 51.088' N, 122° 17.697' W (GPS).  
15:17 Arrive on station 9. Ship's position is 34° 50.927' N, 122° 18.010' W.  
15:23 Deploy 10.0 kHz transponder. Ship's position is 34° 51.002' N, 122° 18.043' W.  
15:26 Deploy float 9. Ship's position is 34° 51.030' N, 122° 18.069' W.  
15:35 Begin float range survey. No floats on the surface.  
15:50 Begin transponder range survey. Ship's position is 34° 51.226' N, 122° 18.292' W.  
15:53 Ship's position is 34° 51.241' N, 122° 18.323' W.  
15:58 Start 3.5 kHz profiler.  
17:08 Begin another float range survey. Ship's position is 34° 50.665' N, 122° 19.765' W(GPS).  
17:12 Ship's position is 34° 50.787' N, 122° 19.855' W.  
17:14 Ship's position is 34° 50.852' N, 122° 19.904' W.  
17:15 Begin another transponder range survey. Ship's position is 34° 50.907' N, 122° 19.946' W(GPS).  
17:25 Ship's speed and heading are 2.7 knots and 333° magnetic. Ship's position is 34° 51.210' N, 122° 20.181' W(GPS).  
17:56 Deploy 3 SSQ 53B Sonobuoys (DIFAR). Ship's position is 34° 49.5' N, 122° 19.89' W(GPS).  
18:24 Ship's position is 34° 49.036' N, 122° 21.254' W(GPS).  
18:30 Begin another transponder and float range survey.  
19:28 Floats started recoding at record number 640 (synchronized at 11:28 with 8 hour delay).  
19:35 Ship's position is 34° 48.854' N, 122° 18.858' W(Loran).



19:44 Ship's position is 34° 49.193' N, 122° 19.005' W(Loran).  
19:53 Begin in situ measurement of the floats' clock drifts using the GOES clock for all floats.  
20:00 Ship's speed and heading are 2.4 knots and 350° magnetic. Ship's position is 34° 49.645' N, 122° 19.070' W.  
20:40 Start to steam away from Pt. SF at 5 knots and at heading 110° magnetic. Continue for two hours and then continue at comfortable ship speed and direction towards the continental shelf.  
22:15 Ship's heading and position are 110° magnetic and 34° 46.43' N, 122° 11.08' W(Loran). Ship is now picking up speed and steaming away at 7.0, 8.0 and 9.0 knots.

9 July 1989

06:39 Earthquake of magnitude 3.5 in central California along the Calaveras fault was reported on the radio.  
07:00 The HLF-3 will not be put into the water because of the rough sea conditions.  
07:30 Ship's position is 34° 54.841' N, 121° 53.664' W(Loran). Underway to pt. D to determine the water depth for NORDA VEKA array. The water depth is 2100 m. Ship's speed and heading are 6.0 knots and 175° magnetic.  
07:42 Turn to the Northwest. Ship's heading and position are 310° magnetic and 34° 53.318' N, 121° 54.672' W(Loran). The water depth is 2140 m at the 2nd VEKA array deployment site.  
07:56 Ship's position is 34° 53.412' N, 121° 55.201' W(Loran).  
08:21 Ship's position is 34° 54.277' N, 121° 56.178' W(Loran); heading 335° magnetic; speed 3.0 knots.  
08:37 Ship's position is 34° 55.041' N, 121° 56.793' W(Loran); heading 335° magnetic; speed 3.3 knots.  
09:04 Ship's position is 34° 56.395' N, 121° 57.740' W(Loran); heading 340° magnetic; speed 3.7 knots.  
09:27 Ship's position is 34° 57.608' N, 121° 58.235' W(Loran); heading 340° magnetic; speed 3.3 knots.  
09:35 Ship's position is 34° 58.053' N, 121° 58.463' W(Loran); heading 343° magnetic; speed 3.7 knots.  
09:40 XBT #35 T-5 is taken.  
09:48 Ship's position is 34° 58.808' N, 121° 58.749' W(Loran); heading 343° magnetic; speed 3.2 knots.  
10:22 Ship's position is 35° 00.813' N, 121° 59.506' W(Loran); heading 342° magnetic; speed 3.7 knots.  
10:49 Ship's position is 35° 02.478' N, 122° 00.591' W(Loran); heading 332° magnetic; speed 3.9 knots.  
11:11 Ship's position is 35° 03.873' N, 122° 01.453' W(Loran); heading 331° magnetic; speed 3.6 knots.  
11:22 Ship's position is 35° 04.582' N, 122° 01.931' W(Loran); heading 331° magnetic; speed 3.6 knots.  
11:41 Ship's position is 35° 03.917' N, 122° 03.068' W(Loran); heading 200° magnetic; speed 8.5 knots.  
11:59 Ship's position is 35° 01.429' N, 122° 04.234' W(Loran); heading 200° magnetic; speed 9.3 knots.  
12:22 Ship's position is 34° 58.035' N, 122° 05.677' W(GPS); heading 200° magnetic; speed 9.0 knots.

12:25 Ship's position is 34° 57.661' N, 122° 05.835' W(GPS). Ship's position is 34° 57.505' N, 122° 05.869' W(Loran).

12:45 XBT 036 is taken.

12:50 Ship's position is 34° 53.733' N, 122° 07.687' W; heading 210° magnetic; speed 9.8 knots.

13:10 Ship's position is 34° 50.986' N, 122° 09.733' W; heading 210° magnetic; speed 9.6 knots.

13:31 Ship's position is 34° 47.936' N, 122° 11.978' W; heading 210° magnetic; speed 9.9 knots.

13:55 Ship's position is 34° 46.297' N, 122° 14.457' W; heading 310° magnetic; speed 6.6 knots. A radio beacon at 160.725 MHz is detected on the surface. The signal is too weak to point to a correct heading.

14:11 Ship's position is 34° 47.530' N, 122° 16.276' W; heading 310° magnetic; speed 6.8 knots.

14:25 Ship's position is 34° 48.671' N, 122° 17.933' W; heading 310° magnetic; speed 7.4 knots.

14:34 Ship's position is 34° 49.383' N, 122° 19.067' W; heading 310° magnetic; speed 6.2 knots.

14:47 Ship's position is 34° 50.289' N, 122° 20.742' W; heading 305° magnetic; speed 6.1 knots.

14:53 Ship's position is 34° 50.722' N, 122° 21.589' W; heading to West and then South; speed 5.8 knots.

14:54 Ship's position is 34° 50.642' N, 122° 21.668' W; heading 205° magnetic; speed 6.5 knots.

14:55 Ship is speeding up to 9.3 knots.

15:02 Ship's position is 34° 49.546' N, 122° 22.210' W; heading 200° magnetic; speed 9.4 knots.

15:04 Ship turns to the Southwest. Float 5 was spotted on the surface; Ship then turns to port.

15:06 Ship's position is 34° 49.032' N, 122° 22.230' W.

15:07 Ship turns to the West.

15:13 Recover float 5. Ship's position is 34° 49.129' N, 122° 22.404' W. Its embedded microprocessor program is still running. It quick-released at 8 am on July 9 rather than 8 am, July 10. Float 5 was at 2500 m. It takes about 2 hours for it to come to the surface. It was probably on the surface for about 5 hours.

15:24 Ship's position is 34° 49.672' N, 122° 22.375' W; heading 20° magnetic; speed 5.2 knots. Underway for Pt. SF to conduct survey.

15:30 XBT 37 is taken.

15:33 Ship's position is 34° 50.491' N, 122° 22.002' W; heading 17° magnetic; speed 5.7 knots.

15:40 Ship turns to the East.

15:41 Ship's position is 34° 50.609' N, 122° 21.470' W; heading 117° magnetic; speed 3.6 knots.

15:52 Ship's position is 34° 50.295' N, 122° 20.795' W; heading 117° magnetic; speed 3.9 knots.

16:01 Conduct float range survey.

16:11 Begin in situ measurement of the floats' clock drifts using the GOES clock for all floats except float 5.

16:35 Recall float 3. Ship's position is 34° 51.521' N, 122° 20.903' W.

16:36 Recall float 2 and 1.

16:37 Try recalling float 0. Float 0 appears to be missing. Ship's position is 34° 51.626' N, 122° 20.931' W.

17:29 Range to float 0 is 3301 m. Ship's position is 34° 53.468' N, 122° 21.552' W. The ship is closing on float 0. Ship's heading and speed are 340° magnetic and 2.1 knots.

17:33 Recall float 0. Range to float 0 is 2692 m. Ship's position is 34° 53.837' N, 122° 21.708' W.

17:46 Conduct in situ clock drift measurement for float 0 using the GOES clock.

18:46 Recover float 0. Its embedded microprocessor program is still running and its time release was set properly. Ship's position is 34° 55.093' N, 122° 22.838' W.

18:57 XBT 38 is taken.  
19:29 Underway to the South to get floats 1,2, and 3. Ship's position is 34° 52.732' N, 122° 22.546' W(Loran).  
19:50 Recover float 1. Its embedded microprocessor program is still running. Ship's position is 34° 50.917' N, 122° 22.561' W.  
20:02 Recall float 4.  
20:03 Recall float 6.  
20:04 Recall float 7.  
20:40 Recover float 2. Its embedded microprocessor program is still running. Ship's position is 34° 49.444' N, 122° 21.981' W.  
20:56 Recover float 3. Its embedded microprocessor program is still running. Ship's position is 34° 49.226' N, 122° 22.783' W. Conduct float range survey.  
21:22 Ship's position is 34° 49.137' N, 122° 22.623' W; heading 110° magnetic; speed 4.0 knots.  
22:29 Recover float 4. Its embedded microprocessor program displays an HL message. Ship's position is 34° 49.630' N, 122° 22.242' W.  
23:31 Recover float 6. Its embedded microprocessor program is still running. Ship's position is 34° 49.364' N, 122° 20.784' W.  
23:56 Recover float 7. Its embedded microprocessor program is still running. Ship's position is 34° 49.335' N, 122° 19.685' W.

10 July 1989

00:05 Recall float 8.  
00:15 Conduct transponder range survey.  
01:00 Recall float 9.  
00:45 XBT #40 is taken.  
02:08 Recall float 11.  
02:58 Recall float 10.  
03:20 XBT #41 is taken.  
04:27 Recover float 8. Its embedded microprocessor program is still running. Ship's position is 34° 50.112' N, 122° 19.379' W.  
05:22 Recover float 9. Its embedded microprocessor program is still running. Ship's position is 34° 51.075' N, 122° 18.672' W.  
07:18 Recover float 11. Its embedded microprocessor program is still running. Ship's position is 34° 47.884' N, 122° 20.545' W.  
08:05 Recover float 10. Its embedded microprocessor program is still running. Ship's position is 34° 50.705' N, 122° 22.074' W. Continue on to the rest of downslope conversion experiment.

## IV. Environmental Data

### a) XBT Measurements

Expendable bathythermograph (XBT) measurements were made from the New Horizon at various times during the experiment. Sippican models T-5 and T-7 XBTs were used. These temperature measurements, along with historical salinity data archived by the National Oceanographic Data Center [6] and an equation relating temperature, salinity, and depth to sound speed [7], were used to derive sound velocity profiles. Shown in Figure IV.1 are the sound velocity profiles derived from XBTs 29, 30, and 31, which were taken near the Swallow float array on 8 July. For comparison, a sound speed profile based upon historical temperature data [6] is also plotted on the figure. Figure IV.2 shows the profiles derived from XBTs 37, 38, and 39, which were taken near the Swallow float array a day later, along with the historical-data-derived profile.

The sound speed profiles derived from the XBTs 29, 30, and 31 are quite similar to each other and they deviate only slightly from the historical profile. Other than showing more structure than the historical profile (the historical data are averaged and are reported only at standard oceanographic depths), the XBT-derived profiles in Figure IV.1 indicate a lower sound speed between 200 and 600 meters than the historical profile. The profiles derived from XBTs 37, 38, and 39 in Figure IV.2 also show a smaller sound velocity than in the historical profile between 200 and 600 meters.

Below is a listing of the times, in addition to the locations, at which all XBT measurements were taken during the Swallow float deployment period;

XBT Number	Position	Time (Date)
29	34° 48.4' N 122° 20.3' W	14:13(8 July)
30	34° 51.4' N 122° 20.4' W	17:35(8 July)
31	34° 49.5' N 122° 18.3' W	20:59(8 July)
32	34° 46.3' N 121° 56.2' W	00:45(9 July)
33	34° 51.4' N 121° 55.4' W	03:15(9 July)
34	34° 53.1' N 121° 50.2' W	06:30(9 July)
35	34° 58.1' N 121° 58.5' W	09:40(9 July)
36	34° 55.6' N 122° 06.7' W	12:40(9 July)
37	34° 49.2' N 122° 22.5' W	15:20(9 July)
38	34° 55.1' N 122° 22.9' W	18:55(9 July)
39	34° 49.0' N 122° 21.5' W	21:55(9 July)
40	34° 50.6' N 122° 20.4' W	00:40(10 July)

All times are in local Pacific Daylight time. To obtain standard Greenwich Mean Time, add 7 hours.

### b) Anemometer Readings

Anemometer readings taken from the bridge are recorded every two hours in the ship's log as standard practice. A plot of these wind velocity vectors for the 48-hour period of 8, 9 July is given in Figure IV.3. The vectors, starting at the dashed line, point in the direction the wind was blowing from; the lengths of the vectors, when measured against the plot's y axis, determine the wind speed. The wind direction in this plot is quite similar to the wind velocity plots for the August, 1988 experiment [Figure IV.3 of reference 5]. The weather in this part of the ocean typically comes from the northwest and the wind speed is usually around 10 to 15 knots. The notable difference is that the wind was blowing much harder in this experiment than in the August 1988 experiment.

c) Additional Environmental Information

Also recorded in the New Horizon's ship log every two hours are the sea state, the estimated wave swell height and direction, the temperature, barometric pressure, and cloud observations. During the experiment, the swell was observed to be 10 to 13 feet (3 to 4 meters) in height, coming from 330° magnetic. The temperature was in the low sixties (in degrees Fahrenheit).

A large volume of environmental information in addition to those mentioned above were collected as part of the Downslope Conversion experiment. Ten conductivity-temperature-depth measurements were collected from the New Horizon between 3 July and 13 July; 61 XBTs were taken between 2 July and 13 July including those listed under section a), and 58 air-launched bathythermographs (AXBT) were dropped by a P-3 aircraft on 8 July prior to the Swallow floats recording period. Reference [19] presents and discusses these data.

An additional source of information is the Fleet Numerical Oceanography Center, which has provided us with ocean wave spectra hindcasts and shipping density information during the experiment.

## V. Swallow Float Data - General Indication of Data Integrity

The first step in the data analysis of the Swallow floats is to scan all the floats' cassette tapes with a general screening program. This program checks each record for the proper location of resynchronization characters and the proper sum of byte values in a group prior to a checksum. The output from the screening program is given in Figure V.1. Note that the cassette-tape transcribing program attaches a zero-byte record with the same internal record number as the last record on the cassette tape onto the end of each float's data file; this allows the number of internal records to be determined. For example, float 0's last-written record was internal record number 2225. (The record number listed in the left-most column is assigned by the screening program itself). Since the internal record number begins with record 0 and the first 640 records (during float's descend) were not written onto tape, float 0 actually wrote 1586 (subtracting 640 from 2226 records) records onto tape.

The number of errors detected by the screening program is typical of that in other Swallow float deployments. The greatest source of lost data in past deployments [1,2,4] was due to floats which quit recording prematurely or which could not be synchronously started properly. In this deployment, all 12 floats which were taken on the trip were deployed and all recorded full data tapes except float 4 which quit recording about 4 hours earlier than expected due to a cassette tape defect. Also, float 5's time release occurred at 08:00, 9 July rather than at 08:00, 10 July due to a programming error which caused the float ascend back to the surface prematurely. In all, 95 % of the potential number of records which could have been recorded by 12 properly functioning floats were recorded and passed the screening test.

Although all of the Swallow floats are nearly identical in construction, the design of the experiment possibly resulted in a unique aspect being imparted to a given float. In addition, as in all deployments, unexpected events occur which may affect a float's data. The following table is a listing of some of the unique aspects of given floats in this deployment.

Unique Aspects of a Given Float in the July, 1989 Experiment

Float	Comments
0	It was retrieved several kilometers northwest of its deployment position; also, its geophone was accidentally rotated 180°.
3	Cross talk among geophone components due to cabling problem. This problem has also existed in float 3's data in past deployments.
4	It quit recording about 4 hours earlier than expected due to a cassette tape defect.
5	Its time release occurred one day earlier, at 08:00, 9 July, rather than at 08:00, 10 July, due to a programming error.
6	Its x and y geophone axes leads were accidentally reversed.
6-8	Floats lost sensitivity in their hydrophone channels while descending.
6,9	Floats equipped with CB radio beacons; all others had VHF beacons.
7,8	Floats had additional 1 lb ballasts on 6 hour galvanic time release (GTR).
9-11	Floats had 10-15 lb anchors on 3.05 meter tethers; floats had x and y geophone axes shorted and the fixed gain in z axis was reduced by 17.5 dB.

---

3,5,7-11	Floats equipped with "noisy" cassette tape recorders.
All floats	Antenna had tie-downs to side of float rather than across the float.

---

## VI. Swallow Float Time Base Measurements

As in the August, 1988 experiment, an attempt was made to measure the absolute drift of the individual float clocks in situ in this deployment. The time standard used was a Model 468-DC satellite-synchronized clock. This clock, when possible, phase-locks to one of two Geostationary Operational Environmental Satellites (GOES); when neither of the satellites is visible, the clock operates on its own internal crystal clock. It has an accuracy of  $\pm 1.0$  msec.

The individual float clock drifts were determined from the 8 kHz localization pulses. Once synchronized, the floats take turns pinging in sequence; one float pings approximately 10 seconds after the beginning of each record and since the floats ping in turn, a given float in this experiment pinged every 12 records, i.e. once every 9 minutes. The exact time that each float issues a localization ping is determined by its internal clock. Therefore, the times of localization pulse generation, as measured by an accurate time standard, can then be used to determine the drift of the floats' clocks.

The GOES clock was used to synchronously start the floats; synchronization occurred at 11:28:00, 8 July. The floats were then deployed and, after sufficient time had elapsed in order for them to stabilize at depth, their localization pings were used to trigger the oscilloscope on board ship in order to determine the time of ping arrival. Immediately upon hearing a given float's range ping, the float was acoustically requested to send a second range ping. This allowed the arrival time of the first range ping to be corrected for the travel time from the float to the ship. This procedure was repeated the next day after the floats had completed recording data and before they were recalled to the surface.

The following table lists the floats in the order in which they pinged and the travel-time-corrected times, according to the GOES clock, of their localization ping generation;

Time of Localization Ping Generation		
Float Number	After Stabilizing on 8 July	Before Recall on 9 July
0	*20:10:09.077*	-
1	19:52:55.610	16:25:55.254
2	19:53:40.285	16:17:39.508
	20:02:40.291	16:26:39.487
	20:11:40.372	
3	19:54:25.708	16:18:25.570
	20:03:25.644	16:27:25.574
	20:12:25.677	
4	19:55:10.653	
	20:04:10.670	-
	20:13:10.663	
5	20:13:55.549	-
6	19:56:40.371	16:20:39.787
	20:05:40.348	16:29:39.768
7	19:57:25.240	16:21:24.344
	20:06:25.387	16:30:24.332
8	19:58:10.496	16:31:10.068
	20:07:10.548	
9	19:58:55.365	16:22:54.587
10	19:59:40.332	16:23:10.559
11		16:15:25.839
	20:09:25.737	16:24:25.850



(\*) This time probably contains an error due to the uncertainty in reading the range data.

Since the floats each ping every 9 minutes, then, according to the floats, the difference between the times listed in the columns of the table above should be an integral multiple of 9 minutes. The following table lists the difference between the time measured by the floats and the time measured by the GOES clock, and the dimensionless float clock drift;

Difference between Float Time and GOES Clock Time and the Clock Drift				
Float Number	After Stabilizing on July 8 Difference (sec)	Clock Drift (X 10 <sup>-6</sup> )	Before Recall on July 9 Difference (sec)	Clock Drift (X 10 <sup>-6</sup> )
0	#+ 1.548#	#+49.41#	-	-
1	+ 0.015	+ 0.50	+ 0.371	+ 3.56
2	+ 0.340	+ 11.20	+ 1.117	+ 10.76
	+ 0.334	+ 10.82	+ 1.138	+ 10.91
	+ 0.253	+ 8.05		
3	- 0.083	- 2.73	+ 0.055	+ 0.53
	- 0.019	- 0.63	+ 0.051	+ 0.49
	- 0.052	- 1.65		
4	- 0.028	- 0.92		
	- 0.045	- 1.45	-	-
	- 0.038	- 1.21		
5	+ 0.076	+ 2.41	-	-
6	+ 0.254	+ 8.32	+ 0.838	+ 8.06
	+ 0.277	+ 8.92	+ 0.857	+ 8.20
7	+ 0.385	+ 12.60	+ 1.281	+ 12.32
	+ 0.238	+ 7.65	+ 1.293	+ 12.37
8	+ 0.129	+ 4.21	+ 0.557	+ 5.38
	+ 0.077	+ 2.55		
9	+ 0.260	+ 8.48	+ 1.038	+ 9.97
10	+ 0.293	+ 9.54	+ 0.066	+ 0.63
11	- 0.112	- 3.58	- 0.225	- 2.15

(#) This appears to be due to an erroneous reading.

(-) Measurements of floats 0, 4, and 5's localization ping arrivals could not be made; refer to the table in section V for explanations.

The float clock drift is defined as float elapsed time minus true elapsed time, normalized by the true elapsed time. The float clock rate is the ratio of float elapsed time to the true elapsed time so that float clock drift plus one equals the float clock rate (re [9]). Therefore, a positive clock drift in the table above indicates that a float's clock is fast, so that the float thinks it is later than it really is. The floats' clocks are expected to be fast; since the dimensions and elastic properties of a quartz crystal are used to determine time and since the crystal shrinks and becomes more "rigid" (its shear modulus increases) with decreasing temperature, then it will vibrate at a greater rate with decreasing temperature and keep faster time. It is surprising that floats 3, 4, and 11's clocks are slow. It is possible that these three floats were equipped with clocks which keep especially slow time at room temperature.

The clock drifts calculated from the absolute clock drift measurements in the table above agree quite well with the clock drifts from the August, 1988 data. The following table presents a comparison of the clock drifts measured in this experiment and in the August, 1988 experiment for those floats which operated properly in both deployments; and for which reliable GOES clock measurements were obtained;

Comparison of Float Clock Drift Measurements				
Float Number	1989 Experiment Using the GOES Clock		1988 Experiment Using the GOES Clock	
	After Stabilizing (X 10 <sup>-6</sup> )	Before Recall (X 10 <sup>-6</sup> )	After Stabilizing (X 10 <sup>-6</sup> )	Before Recall (X 10 <sup>-6</sup> )
1	+ 0.50	+ 3.56	+ 4.75 + 4.96	+ 3.52
2	+ 11.20 + 10.82 + 8.05	+ 10.76 + 10.91	+ 11.76 + 11.54	+ 11.45
5	+ 2.41	-	+ 3.22 + 3.65	+ 4.05
6	+ 8.32 + 8.92	+ 8.06 + 8.20	+ 6.28	+ 8.37
7	+ 12.60 + 7.65	+ 12.32 + 12.37	+ 5.81 + 12.30	+ 13.16
8	+ 4.21 + 2.47	+ 5.38	+ 3.09	+ 5.96 + 5.93
9	+ 8.48	+ 9.97	+ 6.62 + 8.02 + 7.99	+ 10.72
10	+ 9.54	+ 0.63	- 3.08	- 0.54
11	- 3.58	- 2.15	- 1.32	- 0.77

The consistency of these two independent sets of measurements supports the GOES clock method of estimating float clock drifts.

## VII. Battery Voltage, Float Heading, and AGC Level

The battery voltage, the compass reading, and the automatic gain control (AGC) level, measured once during each 45-second record, are plotted in Figures VII.1 through VII.12 for all Swallow floats. The plots are ordered according to the floats' deployment depths, from the shallowest (float 0) to the deepest (bottom floats 9, 10, and 11). This ordering scheme for the figures will be followed in all subsequent sections.

### a) Battery Voltage

The battery level for all floats remained constant at slightly more than 6 volts. The duration of the floats' deployment is therefore determined not by their power supply requirements, but by their recording capacity.

### b) Float Heading

Installed on the inside of each of the Swallow float glass spheres, at the sphere's south pole, is a compass for determining the orientation of the sphere, and thus, the orientation of the horizontal components of the float's geophone with respect to magnetic north. The compass heading during each 45-second record is shown in the middle plot of Figures VII.1 through VII.12. After being put into the water, the floats typically underwent rapid rotations as they descended. Once the midwater floats stabilized at depth, they twisted back and forth at a characteristic period of between 25 minutes to an hour. The twisting is believed to be caused by internal waves. As observed in previous deployments, the midwater floats' headings appeared to stabilize at about 300° near the end of the experiment (float 0's heading is a possible exception). The force responsible for this asymptotic approach to 300° magnetic is believed to be due to the interaction of a small, intrinsic magnetic field of the float (possibly due to the permanent magnets inside the geophone's components) with the earth's magnetic field.

The three bottom-mounted floats, floats 9, 10, and 11, were tethered to the bottom by 3.05-meter cotton lines; their compass headings usually remained approximately constant or varied slowly due to the constraining effects of the tether and the prevailing ocean current.

### c) AGC Level

The AGC is a variable gain amplifier, with a range of 0 to 36 dB gain, which allows the full dynamic range of the eight-bit A/D converter to be used. In this deployment, the AGC gain changes by a roughly 0.5 dB steps between records. After a five-second delay in the record, if more than 0.5 % of the points sampled on all 4 components (three components from geophone and one component from VLF hydrophone) are clipped, then the AGC decreases. Otherwise, it increases. Because of the slow adjustment time of the AGC gain, amplitude information for large impulsive arrivals cannot be obtained.

The bottom plot in each figure shows the automatic gain control (AGC) level during every 45-second record. Most of the dips in the AGC gain are probably due to the passage of ships; the deployment site is just to the west of the opening to the Santa Barbara Channel which is an area of heavy commercial shipping. An exception is the dip starting at record 1537; it is probably due to the arrival from a magnitude 3.5 earthquake along the Calaveras fault in central California.

## VIII. Swallow Float 8 kHz Surface and Bottom Bounce Data

Each Swallow float possesses an acoustic transducer, which generates and receives 8 kHz tone bursts, suspended 1.83 m below its glass sphere (see Figure 1). The source strength of the acoustic transducer is 192 dB re 1  $\mu$ Pa at 1 meter. Pulses 10 msec long are transmitted by the floats in a preprogrammed sequence. A different float transmits every 45 seconds. Twelve floats were deployed in this experiment, and each float transmits every 9 minutes, i.e. once every 12 records. Each float normally transmits 10 seconds after the beginning of each 45 second record.

The floats transmit and receive 10 msec pulses in order to measure interfloat and float-to-surface acoustic travel times. Figures VIII.1 through VIII.12 show each float's detection of its own 8 kHz pulses. The vertical axes in the figures have been scaled from travel time to depth (using half of 1500 m/s) so that float depth is indicated by the leading edge of pulses propagated from the float to the ocean surface and back. The horizontal axes are in units of record number, and may be converted to elapsed time after float synchronization using the conversion factor of 80 records per hour. The x axis begins at record 640. A line of 15 very faint dots descending from 0 range across the plot are discernible in some of the figures, e.g. Figure VIII.1. They are an artifact and should be ignored.

The general features of these plots have been discussed extensively elsewhere [3,4,5]. Following an arrival at 0 depth, which corresponds to the detection of the outgoing 8 kHz ping and its reflection off the float's glass sphere, the shallower floats first detect the arrival of the reflection off the underside of the air-sea interface and then the reflection off the ocean bottom. For those floats whose equilibrium depth exceeds half the total water depth (floats 4, 5, 6, 7, 8, 9, 10, and 11), the order of arrival of these two pulses is reversed.

The experiment test plan called for 9 floats to be deployed in a vertical string extending from 500 to 3700 meters in depth, spaced at 400 meter intervals. Figures VIII.1 through VIII.9 contain data for these 9 floats. The band of lines of varying length whose upper edge remains at approximately range 0 correspond to the outgoing acoustic pulse. The length of the lines after the floats reached equilibrium varies among the floats. The long outgoing pulse return seen in float 0 has been seen in other experiments when a float was deployed shallower than 500 meters. It may be caused by scatterers in the water volume [1,12] or by temperature-dependent resonance of the glass sphere excited by the 8 kHz acoustic pulse [11]. Factors which must be considered include a possible depth-dependent ambient ocean noise level (the range pulse detector circuit compares the signal level in a narrow band centered at 8 kHz to that in a broader band) and variations among the electronic components in each float's range pulse detection circuit (thus influencing the threshold).

Figures VIII.10 through VIII.12 pertain to floats 9, 10 and 11, which were deployed to the ocean bottom using a large weight (10 - 15 lb) and 3.05 meter tether to provide a fixed coordinate system for the experiment. The longer outgoing pulse return is due to scattering from the bottom.

The surface echoes for the bottomed floats, seen in Figures VIII.10 through VIII.12, are marked by a band of vertical lines stabilizing at approximately 4080 meters depth. The float depths are constant once their weights are resting on the bottom, although small-scale depth variations are apparent. These depth variations decrease the accuracy in estimating the positions of the floats as a prelude to beamforming the float acoustic data.

The seemingly random vertical lines appearing on the plots near record 640 and 700 are indicative of the floats being acoustically requested from the ship to transmit an 8 kHz pulse. This is done in order to survey floats' positions. Also, the gaps in the surface bounce returns are probably the result of the rough sea surface during the experiment.

## **IX. The 8 kHz Interelement Range Data**

Figures IX.1 through IX.12 contain the record of pulses transmitted by one float and received by another. As in Figure VIII.1 through VIII.12, the vertical axes have been scaled from travel time to range using 1500 m/s for the speed of sound, and the horizontal axes are record number. The starting record number is 640.

Figures IX.1a - i through IX.9a - i contain travel times between freely drifting floats. These plots include a strong direct path pulse arrival followed by a strong surface bounce pulse arrival, followed by much weaker multiple bounce pulse arrivals. The direct path arrivals are generally short, approximately the length of the pulse (10 msec). The surface bounce arrivals are much longer due to scattering by the ocean surface.

Both the direct path and surface bounce arrivals are longer early in the experiment. The period during which the arrivals are long appears to decrease with increasing float separation and float depth. Another interesting observation is that the duration of the longer returns is identical in reciprocal path plots.

Figures IX.1j - l through IX.9j - l contain travel times between freely drifting floats and the bottomed floats, 9, 10 and 11. These plots are also characterized by a strong, short direct path arrival followed by a strong surface bounce arrival and weaker multiple bounce arrivals.

Figures IX.10j - l through IX.12j - l contain the travel times between bottomed floats. Only the surface bounce arrivals are visible. The direct path pulse is bent upward by the sound speed gradient as sound travels between the floats, so that it is too weak to be detected by another bottomed float approximately 6.3 km away. Once the floats are bottomed, the leading edge of the band of surface bounce arrivals varies linearly with time. Since the floats are tethered to the bottom, their surface bounce travel time would be constant were it not for their clock rate differences. Random variations in surface bounce travel time are thought to be due to interference between multiple, scattered surface returns.

## X. RMS Pressure and Velocity

In order to quickly scan the VLF data from all channels of all floats, the root mean squared pressure (for the hydrophone) and root mean squared velocity (for the geophone) were calculated and are plotted in Figures X.1 through X.12. The plots are presented in order of increasing depth of deployment of the floats. These RMS power series have been corrected for the AGC gain, but are otherwise uncalibrated; the vertical axis is in units of volts at the A/D converter (re Appendix 1 for a block diagram of the VLF data recording system). Each RMS level value results from taking the square root of the average of the squared amplitude levels over a five second (or 250 point) period. Since each record is 2250 points long (which equals 45 seconds since the data sampling rate is 50 Hz), then nine RMS power values are calculated for each record.

Aspects of these plots common to all Swallow float deployments have been discussed elsewhere [1,2] and only the unique features of this data set will be discussed here.

### a) Midwater Swallow Float Data

Since the rms plots for the midwater floats show similar features, the following discussion will use float 1's plots (Figures X.2a through X.2i) as reference.

The large spikes appearing on the z component every 12 records (i.e. Figure X.2c) is caused by the 8 kHz localization ping issued by the float. Small inter-ping spikes, seen on the rms plots, are the impulses imparted to the float by the cassette tape recorder at the beginning of each record. The tape recorder impulses are especially strong in floats 3, 4, 5, 7, 8, 9, 10, and 11's data. In addition, data record drop-outs can be seen in float 1's data at about records 790 and 1440. These bad records were identified in the initial data screening discussed in Section V (re Figure V.1a).

The arrival identified as an earthquake in central California along the Calaveras fault occurs record 1530 (06:38 local time, 9 July). A plot of the earthquake time series recorded by float 0 is given in the next section.

Other jumps in RMS power levels consistent across the components of all midwater Swallow floats can be found in the data. One such prominent jump occurs around record 1730 (09:06, 9 July). Another jump in power levels occurs around record 2130 (14:05 9 July). These jumps are probably due to the passage of commercial vessels near the array (re Section IIc), although New Horizon-radiated sound which was topographically coupled into the sound channel may have contributed.

A spike around record 658 in float 7's data does not correspond to a spike in the other floats' data. The spike is possibly non-acoustic in nature.

### b) Bottom-Mounted Swallow Float Data

Since the bottom-mounted floats' geophone data are typically dominated by tether effects for much of the time after they reach the ocean bottom, in this experiment, floats 9, 10 and 11's horizontal geophones were shorted and their vertical geophones's fixed gain was decreased by 17.5 dB. Figures X.10 through X.12 show the RMS velocity plots for the bottom-mounted floats. As can be seen in these plots, periods of tether contamination on the vertical geophone component can be determined by the lack of corresponding increases in levels on the hydrophone channel. For example, the spikes in float 9's z axis data around records 930, 1025, 1125, 1785, 1840, 1865, and 2095 are probably the result of "jerking" on the float by the tether.

## XI. Geophone and Hydrophone Time Series

Selected time series recorded by the geophones and the hydrophones, corrected for the AGC level but otherwise uncalibrated, are presented in this section. Each figure shows the time series recorded by a given float's component over a 12-record (9 minute) period; the record numbers are given on the left hand side of the plot. The data are sampled at 50 Hz (re Appendix 1), so that 2200 points from each channel are collected in the 44 seconds of each record (the 45th second of the record is made up of 50 zeros). Only every other sampled point is plotted. The scale of the plots' vertical axis is given at the top of each figure.

The time periods selected for plotting are;

Swallow Float VLF Time Series				
Record Sequence	Local Time (Date)	Floats	Comments	Figure Numbers
673 - 684	19:52 - 20:01 (8 July)	All floats (z) & (h)	GOES clock test range pings.	XI.1 - XI.12
738 - 749	20:41 - 20:50 (8 July)	1 and 2	Unknown arrival is clearly visible on y axis in records 744 - 746.	XI.13 - XI.14
767 - 778	21:04 - 21:13 (8 July)	All floats	New Horizon was about 4 km to the southeast from the array; floats 4,5,6,7 and 8 were still descending.	XI.15 - XI.26
860 - 871	22:13 - 22:22 (8 July)	3	The float was struck by unknown object(s) twice in records 861 and 864.	XI.27
1030 - 1041	00:23 - 00:32 (9 July)	2	Cassette tape recorder contamination in record 1037 (float 2 has "quiet" recorder).	XI.28
1105 - 1116	01:16 - 01:25 (9 July)	0 and 1	Unknown arrival is clearly visible on x axis.	XI.29 - XI.30
1144 - 1155	01:46 - 01:55 (9 July)	All floats	14 Hz from Aloha.	XI.31 - XI.42
1280 - 1291	03:28 - 03:37 (9 July)	0 - 3	Unknown arrival is clearly visible on x axis in records 1285 - 1286.	XI.43 - XI.46
1530 - 1541	06:35 - 06:44 (9 July)	0	The Central Calif. earthquake arrival starting at record 1535.	XI.47
1680 - 1691	08:28 - 08:27 (9 July)	0 - 4	Unknown arrival in horizontal direction in records 1682 - 1687.	XI.48 - XI.52

1730 - 1741	09:05 - 09:14 (9 July)	All floats except 4	Unknown arrival; float 5 was on the surface.	XI.53 - XI.63
2120 - 2131	13:58 - 14:07 (9 July)	All floats except 4	TOYOTA car carrier and New Horizon radiated noises; float 5 was on the surface.	XI.64 - XI.74
2140 - 2151	14:13 - 14:22 (9 July)	0 - 2	Unknown transient arrival(10 seconds) in horizontal direc- tion in record 2145.	XI.75 - XI.77

The figures for this section are presented in chronological order, and in order of increasing depth of the floats.

#### a) Comparison of Hydrophone and Geophone Time Series

Plots of the hydrophone time series recorded by the floats appear following its geophone time series plots. The fact that the amplitudes recorded by the hydrophones were generally higher than those on the geophones is due to the greater sensitivity in the hydrophone channel versus the geophone channels. (Recall that the time series presented in this section are uncalibrated except for a correction of the AGC level).

The main difference between the hydrophone and geophone time series, besides the apparent difference in amplitude, is that the tape-recorder induced contamination at the beginning of most of the geophone records does not appear to be present in the hydrophone records. For example, the beginning of each record in the geophone time series for float 3 in Figures XI.18a through XI.18c shows a characteristic and repeatable pattern i.e. an initial upward swing from an initial large negative amplitude. The beginning of each hydrophone time series record shows no evidence of this contamination. Tape-recorder-induced contamination is therefore non-acoustic in nature since the float motions are not accompanied by water-borne pressure fluctuations and this results in differences between the geophone and the hydrophone data. Further discussion of tape recorder contamination is given in part c of this section.

The appearance of the 8 kHz localization ping arrival on the geophone time series is different than on the hydrophone time series. In Figure XI.2a and XI.2b, float 1's localization ping occurs 10 seconds after the beginning of record 673. On the vertical geophone component, the ping is a sharp, impulsive arrival of about 2 second duration (the localization ping itself is 10 msec in duration) with an approximately exponentially decaying amplitude; in the hydrophone time series, the ping arrival appears as a spike followed by 4 second of data of nearly zero amplitude. The difference in appearance is due to the difference in response of the geophone and the hydrophone circuits; the ping arrival is sufficiently loud to drive the hydrophone front-end amplifier circuit into saturation and the nearly zero amplitude period represents the recovery of the circuit, whereas the geophone circuit is only clipped for a short period.

#### b) Range Survey Pings in the GOES Clock Test

The GOES clock was used to synchronously start the floats; synchronization occurred at 11:28:00, 8 July. The floats were then deployed and, after sufficient time had elapsed in order for them to stabilize at depth, their localization pings were used to trigger the oscilloscope on board ship in order to determine the time of ping arrival. Immediately upon hearing a given float's range ping, the float was acoustically requested to send a second range ping, an 8 kHz pulse which is five times longer in duration than the floats' localization ping. This allowed the arrival time of the first range ping to be corrected for the travel time from the float to the ship.



Records 673 through 684 are plotted in Figures XI.1 through XI.12. The recording of the response pulses of float 1 occur in record 673. The beginning of float 2's response pulse occurs in the middle of record 674, the response pulse from float 3 appears in record 675. Float 4's response is recorded in the middle of record 676. Floats 5, 6, 7, 8, 9, 10 and 11's data show evidence of the corresponding response pulses.

#### c) Tape Recorder Contamination

The contamination at the beginning of each 45-second record caused by the "noisy" type of Swallow float cassette tape recorder can be seen in floats 3, 4, 5, 7, 8, 9, 10, and 11's data. ("Noisy" tape recorders are constructed so that their motor turns in the same direction as the cassette tape; "quiet" recorders are geared so that the motor and the tape turn in opposite directions). The tape recorder appears to impart an impulse to the float, causing the float to rock and thereby exciting other types of resonances, possibly including a radio beacon antenna oscillation at 4 to 5 Hz. However, the antenna oscillation amplitude has been strongly attenuated by the installation of nylon tie-downs on all the floats.

#### d) Gain Attenuation

Contamination by the tether has been seen in most of the bottom-mounted Swallow float time series in previous experiments but is not a dominant feature in this experiment. This is due to the fact that floats 9, 10, and 11 had their x and y axis geophones shorted and the fixed gain in z axis was reduced by 17.5 dB. The shorted channels provide an in situ measure of the amount of self noise in the data acquisition system.

#### e) New Horizon Radiated Noise

At 20:40, 8 July, the New Horizon finished the range survey and clock drift measurement; increased its speed to 5 knots (2.5 m/sec) and headed to the southeast away from the array toward the continental shelf. The New Horizon's sound is clearly recorded by all floats especially on the z geophone axis. In Figures XI.15 - XI.26) are plotted the data from records 767 through 778 when the ship was about 4 km from the array.

#### f) Mark VI Source

The 14 Hz tone generated by the Mark VI source is apparent in the time series. It is most strongly recorded on the horizontal geophone components. Records 1144 through 1155 are plotted in Fig XI.31 through Fig XI.42.

#### g) Other Unknown Signals in the Time Series

Spikes of unknown origin appear intermittently in some of the Swallow floats' time series. Float 1 and 2's y geophone axis (Figures XI.13b and XI.14b) recorded a noise of unknown origin for about 3 minutes beginning record 743. Also, float 0 and 1's x geophone axis heard a 10 minute arrival beginning record 1111 (Figures XI.29a and XI.30a). An unusual and predominant arrival, starting 28 seconds into record 1682 (08:29, 9 July) and 38 seconds into record 1684 occurs in all the midwater floats' time series (Figures XI.48 through XI.52). It is most strongly recorded on the horizontal geophone components suggesting a long range arrival. Another interesting set of unknown arrivals, in records 1730 through 1741, is composed of 4 second pulses every 8 seconds which dominates the time series (Figures XI.53 through XI.63).

#### **h) Geophone Time Series Recorded on the Sea Surface**

Figures XI.57a through XI.57c show the geophone time series recorded by float 5 while it was on the surface. The x and y axis time series show packets of clipped energy, each one to three seconds in duration, separated by a second or two of signal with relatively low amplitude. This pattern is probably a result of the rocking of the float under the influence of ocean surface waves.

#### **i) Earthquake Arrival**

As mentioned in Sections Xa, the Swallow floats detected a large amplitude signal starting about record 1535 (06:39, 9 July). It has tentatively been identified as arrival from a magnitude 3.5 earthquake in central California along the Calaveras fault. Figures XI.47a through XI.47d show a 12-record sequence (9 minutes) encompassing the arrival time of the earthquake.

## XII. Velocity and Acoustic Pressure Power Spectra

The calibrated power spectral estimates from data collected by each geophone and hydrophone component during selected periods of time are presented in Figures XII.1 through XII.19. The spectral estimates, except Figures XII.7, XII.9, and XII.10, were made by dividing a 40.96-second piece of data, gotten from the 44 seconds of data in each record after skipping the first three seconds in order to reduce tape recorder contamination, into seven 512-point segments (each segment is 10.24 seconds long) with a 50 % overlap between segments. The segments were Fourier transformed after being windowed with a Kaiser-Bessel window of  $\alpha = 2.5$ . The seven spectra were then incoherently averaged in order to reduce the variance of the power spectral estimates; the resulting 90 % confidence limits are + 3.3 dB to -2.3 dB. The power spectra were also properly normalized (re Appendix 1) to give the power in units of dB re 1 (m/sec)<sup>2</sup>/Hz for the geophone components and dB re 1 (μPa)<sup>2</sup>/Hz for the hydrophone component. Similarly, in calculating the spectra for Figures XII.7, XII.9, and XII.10, a FFT length of 2048 points (40.96 seconds) was used to increase the signal-to-noise ratio; and 40 such FFTs from 40 sequential records were then incoherently averaged to reduce the variance of the spectral estimates; the resulting 90 % confidence limits are plus and minus a half dB or so. Note that the derived pressure spectral estimates for bottom floats are calculated by tripling the z axis spectrum, rather than summing the 3 axes spectra because the bottom floats had their x and y geophone axes shorted.

The time periods selected for calculating the spectral estimates are;

Record Number	Times of Swallow Float Spectral Estimates			Figure Numbers
	Local Time (Date)	Floats	Comments	
745	20:46 (8 July)	1 and 2	Unknown broadband arrival is clearly visible on y axis.	XII.1
767	21:03 (8 July)	All floats	New Horizon (6.7 Hz) @ 5 kts was about 4 km to the southeast from the array.	XII.2
798	21:26 (8 July)	All floats	New Horizon (6.7 Hz) @ 5 kts was about 8 km to the southeast from the array.	XII.3
821	21:43 (8 July)	All floats	New Horizon (6.7 Hz) @ 5 kts was about 10 km to the southeast from the array.	XII.4
838	21:56 (8 July)	All floats	New Horizon (6.7 Hz) @ 5 kts was about 12 km to the southeast from the array.	XII.5
864	22:16 (8 July)	All floats	New Horizon (6.7 Hz) @ 5 kts was about 15 km to the southeast from the array.	XII.6
1081 - 1120	00:58 - 00:27 (9 July)	All floats	8 Hz line from Aloha.	XII.7

1114	01:23 (9 July)	1 and 2	Unknown arrival (7 Hz) is clearly visible on y axis.	XII.8
1121 - 1161	01:28 - 01:57 (9 July)	All floats	14 Hz line from Aloha.	XII.9
1161 - 1200	01:58 - 02:27 (9 July)	All floats	11 Hz line from Aloha.	XII.10
1286	03:32 (9 July)	1	Unknown arrival (9.2 Hz) is on x axis.	XII.11
1654	08:08 (9 July)	1	Unknown arrival (20 Hz) is on z axis.	XII.12
1732	09:07 (9 July)	1	CPA of a contact (8.4 Hz).	XII.13
1902	11:13 (9 July)	All floats except 4,5	New Horizon (7.0 Hz) @ 9 kts was about 40 km to the northeast from the array.	XII.14
1965	12:01 (9 July)	All floats except 4,5	New Horizon (7.0 Hz) @ 9 kts was about 30 km to the northeast from the array.	XII.15
2028	12:48 (9 July)	All floats except 4,5	New Horizon (7.0 Hz) @ 9 kts was about 20 km to the northeast from the array.	XII.16
2055	13:08 (9 July)	All floats except 4,5	New Horizon (7.0 Hz) @ 9 kts was about 17 km to the east from the array.	XII.17
2128	14:03 (9 July)	All floats except 4,5	New Horizon (6.8 Hz) @ 6 kts was about 10 km to the southeast from the array; TOY- OTA car carrier (7.1 Hz) was close to the array.	XII.18
2160	14:27 (9 July)	0,1,2,6,7, 9 and 10	New Horizon (6.8 Hz) @ 6 kts was about 5 km to the southeast from the array.	XII.19

The figures in this section are placed in chronological order, and in order of increasing depth of the floats.

#### a) Hydrophone Pressure Spectra

The installation of the VLF hydrophones on all of the Swallow floats allows for the comparison of the pressure spectra derived from the velocity data collected by the geophones with the pressure spectra estimated from the hydrophone data. The geophone and hydrophone spectral estimates are completely

independent of one another and are based upon data collected at the same time and the same place (that is, almost the same place; the VLF hydrophone and the geophone on a float are separated by about a half meter). The procedure used in deriving the pressure spectral estimates from the geophone velocity data is based upon an acoustic plane wave assumption [8].

The *derived* pressure spectral estimate (solid line) from the geophone data are plotted with the hydrophone pressure spectral estimate (dotted line) in the uppermost panel of each plot.

The pressure spectral levels derived from geophone particle velocity data in general agree with those calculated directly from hydrophone data. Differences between levels can usually be explained by clipping on either the hydrophone channel or one of the geophone channels, by the difference in the way the sensors' electronic circuits respond to large signals (e.g. the 8 kHz localization ping), or by the known, non-acoustic, float rotational resonances which contaminate the geophone data.

#### b) New Horizon Radiated Noise

The data written during record 767 were taken as the R/V New Horizon departed the Swallow float array area (Section IIa); ship-generated noise are clearly visible in float 0's (the shallowest float) time series, as discussed in Section XIe. Figures XII.2 present the calibrated component spectra for all of the floats at this time. The most remarkable feature of these spectra is the peak at 6.7 Hz. It stands out on the z axis spectra. Evidence that this peak is generated by the New Horizon can be gotten by looking at the spectra from data recorded while the ship was at various distances from the Swallow float array in records 798, 821, 838, 864, 1902, 1965, 2028, 2055, 2128, and 2160. The following is a list of the frequencies of the most prominent spectra peaks for the 11 records;

Record Number	New Horizon Speed in Knots	Spectral Peaks	Figure Numbers
767	5	6.7,8.0,9.2	XII.2
798	5	6.7,8.0,9.2,13.5	XII.3
821	5	6.7,8.0,9.2	XII.4
838	5	6.7,8.0,9.3,9.6,13.5,14	XII.5
864	5	6.7,8.0,9.1,9.6	XII.6
1902	9	7.0	XII.14
1965	9	7.0	XII.15
2028	9	7.0	XII.16
2055	9	7.0	XII.17
2128	6	6.8,7.1	XII.18
2160	6	6.8,7.9	XII.19

Since the R/V New Horizon's blade rate fundamental frequency is 3.5 Hz while the ship is traveling at a 10.25 knot speed (Section IIa), and an approximately linear relationship exists between engine rpm and ship speed when both screws are engaged, much of the variation in the spectra among the 11 recording times is probably associated with variations in speed of the ship. Therefore, the peaks 6.7 Hz, in Figures XII.2 through XII.6, 7.0 Hz in Figures XII.14 through XII.17, and 6.8 Hz in Figures XII.18 through XII.19 are believed to be due to the ship's blade rate series.

#### c) Tones from the MARK VI Source

Three tonals in the Swallow float frequency band, at 8 Hz, 11 Hz and 14 Hz, were generated by the MARK VI deployed from the Aloha.

Figures XII.9 show the spectra estimated from data collected by all of the floats during a 30 minute period when the 14 Hz tone was being broadcast by the MARK VI. A line at 14 Hz, about 20 dB above the

background noise, can be clearly seen in all floats' pressure spectra. For the shallower floats 0 through 5, the line is present on all three geophone components; for the deeper floats 6, 7, and 8, it occurs predominantly on the horizontal components.

The 11 Hz tone was being transmitted during the time when the data in records 1161 through 1200 were collected. A line at 11 Hz, about 10 dB above the background noise, can be clearly seen in all floats' pressure spectra. For floats 0 and 2, the line is present on all three geophone components; for floats 1, 3, 4, 5, 6, 7, and 8, it occurs predominantly on the horizontal components.

The detection of the 8 Hz line is shown in Figures XII.7. This line is the most difficult of the 3 tones to detect possibly because of the roll-off with decreasing frequency in the source level transmitted by the MARK VI. Nearly no detectable line at 8 Hz occurs in any of the vertical axis spectra. However, three floats, 1, 4, and 8, display a distinct line in one of their horizontal axes' spectra.

## **Acknowledgements**

We would like to thank Marvin Darling, Chris Nickles, and other members of MPL's Swallow float team, for their numerous and various contributions to the project. We would also like to thank Jim McEachern of the Naval Air Development Center for providing the sonobuoy instrumentation and expertise. The crew of the R/V New Horizon was very helpful and patient.

This work was supported by the Office of Naval Research under contract #N00014-88-K-2040.

## References

- [1] G. L. D'Spain, R. L. Culver, W. S. Hodgkiss, and G. L. Edmonds, "Freely drifting Swallow float array: April, 1987 trip report" MPL Tech. Mem. 397, Marine Physical Laboratory, Scripps Institution of Oceanography, San Diego, CA (1987).
- [2] G. L. D'Spain, R. L. Culver, W. S. Hodgkiss, and G. L. Edmonds, "Freely drifting Swallow float array: May, 1987 trip report" MPL Tech. Mem. 402, Marine Physical Laboratory, Scripps Institution of Oceanography, San Diego, CA (1988).
- [3] G. L. D'Spain, W. S. Hodgkiss, and G. L. Edmonds, "Freely drifting Swallow float array: September, 1987 trip report" MPL Tech. Mem. 413, Marine Physical Laboratory, Scripps Institution of Oceanography, San Diego, CA (1989).
- [4] R. L. Culver, W. S. Hodgkiss, G. L. Edmonds, and V. C. Anderson, "Freely drifting Swallow float array: September, 1986 trip report" MPL Tech. Mem. 391, Marine Physical Laboratory, Scripps Institution of Oceanography, San Diego, CA (1987).
- [5] G. L. D'Spain, R. L. Culver, W. S. Hodgkiss, and G. L. Edmonds, "Freely drifting Swallow float array: August, 1988 trip report" MPL Tech. Mem. 407, Marine Physical Laboratory, Scripps Institution of Oceanography, San Diego, CA (1989).
- [6] J. Churgin and S. J. Halminski, Temperature, Salinity, Oxygen, and Phosphate in Waters off the United States, Eastern North Pacific, National Oceanographic Data Center, 3, (1974).
- [7] K. V. Mackenzie, "Nine-term equation for sound speed in the oceans" J. Acoust. Soc. Am., 70 (3), (1981).
- [8] R. L. Culver, "Infrasonic ambient ocean noise spectra from freely drifting sensors" SIO Ref. 85-22, Marine Physical Laboratory, Scripps Institution of Oceanography, San Diego, CA (1985).
- [9] R. L. Culver, G. L. D'Spain, W. S. Hodgkiss, and G. L. Edmonds, "Estimating 8 kHz pulse travel times and travel time errors from Swallow float localization system measurements" Marine Physical Laboratory, Scripps Institution of Oceanography, San Diego, CA (in press).
- [10] G. L. D'Spain, "The calculation of acoustic pressure spectra from particle velocity spectra revisited" Marine Physical Laboratory, Scripps Institution of Oceanography, San Diego, CA (unpublished notes).
- [11] G. L. D'Spain, "Resonant response of the Swallow float glass sphere" Marine Physical Laboratory, Scripps Institution of Oceanography, San Diego, CA (unpublished notes).
- [12] R. L. Culver and G. L. Edmonds, "February, 1987 one-day Swallow float sea trip" Marine Physical Laboratory, Scripps Institution of Oceanography, San Diego, CA (unpublished memorandum).
- [13] R. Urick, Principles of Underwater Sound, 3rd ed., McGraw-Hill, (1983).
- [14] M. Pieuchot, Seismic Instrumentation, vol. 2, from Handbook of Geophysical Exploration, Section I - Seismic Exploration, ed. K. Helbig and S. Treitel, Geophysical Press (1982).



- [15] R. Urick, *Ambient Noise in the Sea*, Peninsula Publ. (1984).
- [16] A. B. Williams, *Electronic Filter Design Handbook*, McGraw-Hill (1981).
- [17] A. Antoniou, *Digital Filters: Analysis and Design*, McGraw-Hill (1979).
- [18] E. S. Maloney, *Dutton's Navigation and Piloting*, Naval Institute Press, 13th ed., (1978).
- [19] R. M. Olivera, "Downslope Conversion Experiment: Environmental Data Report", Marine Physical Laboratory, Scripps Institution of Oceanography, San Diego, CA (in preparation).

## Appendix 1 - Swallow Float VLF Data Acquisition System

### a) System Response

A block diagram of the Swallow float very low frequency (VLF) system appears in Figure A1.1. All of the floats were equipped with Ocean and Atmospheric Science (OAS) model E-4SD hydrophones in addition to the three-component Geo Space geophones. The geophone channels will be described first, followed by a description of the hydrophone channel.

The water particle motion (and float rocking) is first coupled into motion at the geophone. The particle velocity at the geophone is then converted into voltages representing the three orthogonal components of particle velocity. The geophones are electromagnetic transducers in which a voltage is produced across a moving, conducting coil by its motion through the magnetic field lines produced by a permanent magnet [14]. The resulting voltage is proportional to the velocity of the coil with respect to the magnet. Constraining the coil to move in only one direction are elastic springs connecting the coil to the instrument casing. (Laboratory tests have determined that the geophones can withstand a maximum tilt from vertical of about 15°). The geophone package in each Swallow float is composed of three such transducers oriented to measure in three orthogonal directions.

The geophone amplitude and phase response was calculated using the theoretical equation of motion for this system [14]. The amplitude response curve is nearly identical to the manufacturer's calibration curve provided with the geophones. Laboratory calibration measurements of the amplitude and phase response of all the geophone components has shown excellent agreement with the theoretically predicted response curves. Near-critical damping of the coil is achieved using a 60 k $\Omega$  shunt resistor. Note that the  $f^2$  roll-off of the geophone amplitude response below the natural frequency of 8 Hz effectively pre-whitens the ocean ambient noise so that no additional pre-whitening needs to be implemented.

The three signals next undergo a fixed gain of 95 dB before being input to the automatic gain control (AGC). (Note that in this experiment, the vertical geophone components in the bottom-tethered floats had a fixed gain of only 77.5 dB). Included in the geophone channel circuitry are nine RC circuits. Five of these RC circuits act as high pass filters, with poles located at 0.000034, 0.034, 0.07, 0.26, and 0.47 Hz, in order to eliminate DC bias and decrease ultra-low frequency self noise. The other four RC circuits act as low pass filters, with poles at 34, 34, 72, and 337 Hz, in order to eliminate AC coupling noise (i.e. "cross-talk"). These RC circuits are lumped together with the geophone channel "fixed gain" in Figure A1.1.

The water-borne pressure fluctuations (acoustic and non-acoustic) are converted into voltage fluctuations by the sensing material in the hydrophone. The sensing material is electrostrictive; that is, it develops a voltage in response to an implied stress [13]. (From laboratory tests, it has been determined that the sensing material is also pyroelectric, i.e. it generates a voltage in response to a change in temperature). The electrostrictive material in the OAS hydrophones is pre-polarized lead zirconate-titanate, a polycrystalline ceramic. The hydrophone has a sensitivity of -182 dB re 1 V/ $\mu$ Pa and a frequency response which is flat (within  $\pm 1$  dB) from 0 to 5 kHz. Because the ocean ambient noise spectrum increases as  $f^{-6}$  below about 5 Hz [15], the pressure-induced voltage output by the hydrophone is then passed through a pre-whitening filter. This high-pass filter is comprised of two RC circuits in cascade, both with corner frequencies of about 8 Hz, the same as the natural frequency of the geophone components.

The "fixed gain" triangle for the VLF hydrophone channel in Figure A1.1 represents somewhat different circuitry than in the geophone channels. The fixed gain is set to 80 dB, rather than 95 dB, since the hydrophones are more sensitive than the geophones; -182 dB re 1 V/ $\mu$ Pa for the hydrophones versus about -201 dB re 1 V/ $\mu$ Pa above 8 Hz for the geophones. Also, since the hydrophone pre-whitening filter already includes two high pass RC circuits, only two additional high-pass circuits, with poles located at 0.034 and 0.47 Hz, needed to be added. An additional equivalent high-pass RC circuit is formed by the capacitance of the hydrophone itself and the resistance of two diodes; for the August, 1988 sea trip the resonant pole for this circuit was located at about 2.6 Hz. As discussed in the following paragraph, the hydrophone circuit has since been changed so that this equivalent RC pole is now located at 0.2 Hz. These three high-pass RC circuits are included in the "fixed gain" triangle along with four low-pass circuits, with poles at 34, 34, 72, and 339 Hz.

Laboratory measurements made after the August, 1988 sea trip indicated that two silicon diodes, connected in parallel in the front end of the hydrophone system in order to protect the electronic components from large voltages, had finite equivalent resistances. The forward-biased diode had an equivalent resistance of about  $22\text{ M}\Omega$  and the reversed-biased diode had a resistance of  $53\text{ M}\Omega$ . These diodes, in series with the equivalent capacitance of  $0.004\text{ }\mu\text{f}$  of the hydrophone itself, form an additional RC circuit with a resonant pole at about 2.6 Hz. The laboratory tests also determined that the resistance of the silicon diodes was temperature sensitive; in the forward-biased state, it changed from  $12.5\text{ M}\Omega$  at  $22^\circ\text{C}$  to  $25\text{ M}\Omega$  at  $0^\circ\text{C}$ . The hydrophone's equivalent capacitance was also found to be slightly temperature dependent; however, the change in capacitance partially offsets the change in diode resistance. The total effect was a change in resonant pole frequency of 10 %, from 2.66 Hz to 2.41 Hz, for a temperature change of  $4.7^\circ\text{C}$  over the equilibrium depths of float 10 (425 meters) and float 11 (3360 meters) in the August, 1988 experiment. Even though this change in resonant pole location resulted in slight differences in the total hydrophone system response, the diodes have since been removed and replaced by a temperature-stable Zener diode. Also, a temperature-stable, metal film,  $200\text{ M}\Omega$  resistor was placed in series with the hydrophone in order to move the equivalent resonant pole location to 0.2 Hz.

The hydrophone component voltage and all three geophone component voltages are then sent to a automatic gain control (AGC) amplifier. The AGC is a variable gain amplifier with a range of 0 to 36 dB gain which allows the full dynamic range of the eight-bit A/D converter to be used. In this deployment, the AGC gain changes by a roughly 0.5 dB steps between records; if more than 0.5 % of all data samples from the last 40 seconds of each record are clipped, then the AGC decreases. Otherwise, it increases. Plots of the AGC level for each float during every record are given in Section VII.

Before digitizing, the signals are passed through a five-pole, four-zero, elliptic, anti-aliasing filter. Elliptic filters theoretically have the sharpest transition region for a given number of poles and circuit complexity. The filter frequency response and the pole, zero locations in the  $s$  plane are shown in Figure A1.2 [16,17]. Incoming signals are amplified by a maximum of 4.6 dB in the passband, which has a 0.28 dB equal ripple. The cut-off frequency (the highest frequency at which the amplitude gain is equal to the minimum passband gain) is 20 Hz, and the attenuation is 19.5 dB at the Nyquist frequency of 25 Hz. The maximum equal ripple level in the stop band is 50.1 dB below the level in the pass band and is first reached at 31 Hz. Before installation in the floats, all filters were adjusted so that broadband noise input to the filters yielded the same amplitude response and same null location at the filters' output.

The geophone channel response, including all components in the system except the AGC gain (which varies over the time of the experiment) is plotted in Figure A1.3. The hydrophone channel response, including all components in the channel except the AGC gain, is plotted in Figure A1.4. In deriving the phase response in Figure A1.4, it was assumed that no phase shift was introduced by the hydrophone's electrostrictive material in the conversion of pressure to voltage.

The four signals are then digitized at a 50 Hz sampling rate and put into a temporary buffer. After 44 seconds of data (equal to one data record) have accumulated in the buffer, a one second period of writing the data to cassette tape takes place. During this time, no data is sampled. The 45 second cycle then repeats until the cassette tape is full. The cassette tape can store up to 17 Mbytes of unformatted data, which is sufficient space for up to 1600 four-component data records.

Both the RMS power plots discussed in Section X and the time series plots of Section XI have been corrected for the variable AGC level. No other adjustments have been made in these plots. The power spectral plots of Section XII, however, have been corrected for all electronic system gains including the geophone/hydrophone sensitivities and the anti-aliasing filter response and therefore report estimates of the approximate power level at the input to the sensors.

Excellent agreement between the laboratory-measured and theoretically-predicted amplitude and phase responses of both the geophone and hydrophone channel circuitry, excluding the sensors themselves, has been obtained. In addition, the amplitude and phase response of all the geophone components and the amplitude sensitivity of two hydrophones have been measured and agree extremely well with the expected responses.

#### b) Correction to previous Swallow Float Calibrated Spectra

The nine RC circuits in the Swallow float geophone signal conditioning electronics had previously been assumed to have a negligible effect in the VLF band. However, the recent calibration measurements of the geophone system have shown that they actually have a significant effect at certain VLF frequencies. All previously reported Swallow float calibrated spectra, including those in references 1 through 4, 10, 12, and 14, have therefore under-estimated the power spectral levels. Figure A1.5 shows the amount to be added to the reported Swallow float geophone spectra in order to obtain the true calibrated spectral levels. The lower panel of Figure A1.7 shows these same data plotted on the same scale as the spectral plots in Section XII.

The hydrophone spectra were likewise previously uncorrected for the RC circuits' response, or for the diode-hydrophone equivalent RC response. Figure A1.6 shows the plot of the corrections to the hydrophone spectra to get the true calibrated spectra and the upper panel of Figure A1.7 shows these same data plotted on the same scale as the spectral plots in Section XII. The geophone and hydrophone spectra presented in this report were properly calibrated, i.e., the effect of all circuit components were taken into account.

#### c) Data Record Format

The installation of the VLF hydrophones required a change in the format of the data records. Shown in Figure A1.9 is the format of the old geophone-only records. Each record is composed of 7646 bytes, 7120 bytes of which are VLF acoustic data (including resynchronization and checksum bytes). Figure A1.10 presents the new 9766-byte record format for the VLF-hydrophone equipped floats. Interleaved with the geophone data are the hydrophone data, resulting in 9240 bytes of VLF data in each record.

## Appendix 2 - Loran-C Position Fixes

This short discussion is based upon the material on pp. 708-725 of [18].

Loran, or Long Range Navigation, is based upon the measurement of time differences between pulse radio emissions, with a carrier frequency of 100 kHz, issued from two or more transmitting stations. Loran-C is characterized by the use of multiple pulses, allowing a higher signal-to-noise ratio with the same power output at a transmitting station, and by the use of a phase matching procedure to refine the time-of-arrival estimates.

Position accuracy depends upon the variation in propagation conditions along the signal path and on the position of the ship with respect to the transmitting stations, as well as on the distance from the chain of stations. Therefore, an interval of accuracies, rather than a single value, is given.

Loran-C position fixes, however, can be expected to be much more precise than accurate. The relative distances between a number of fixes made in the same general area are much more reliable than the absolute position of any one fix. This is because all the fixes are affected by the same propagation effects and station-receiver geometry.

As an example, from the figure on the next page, based on data recorded a day after the end of the Swallow float experiment, the Loran-C position fixes are offset about 500 meters to the southwest from the GPS position fixes.

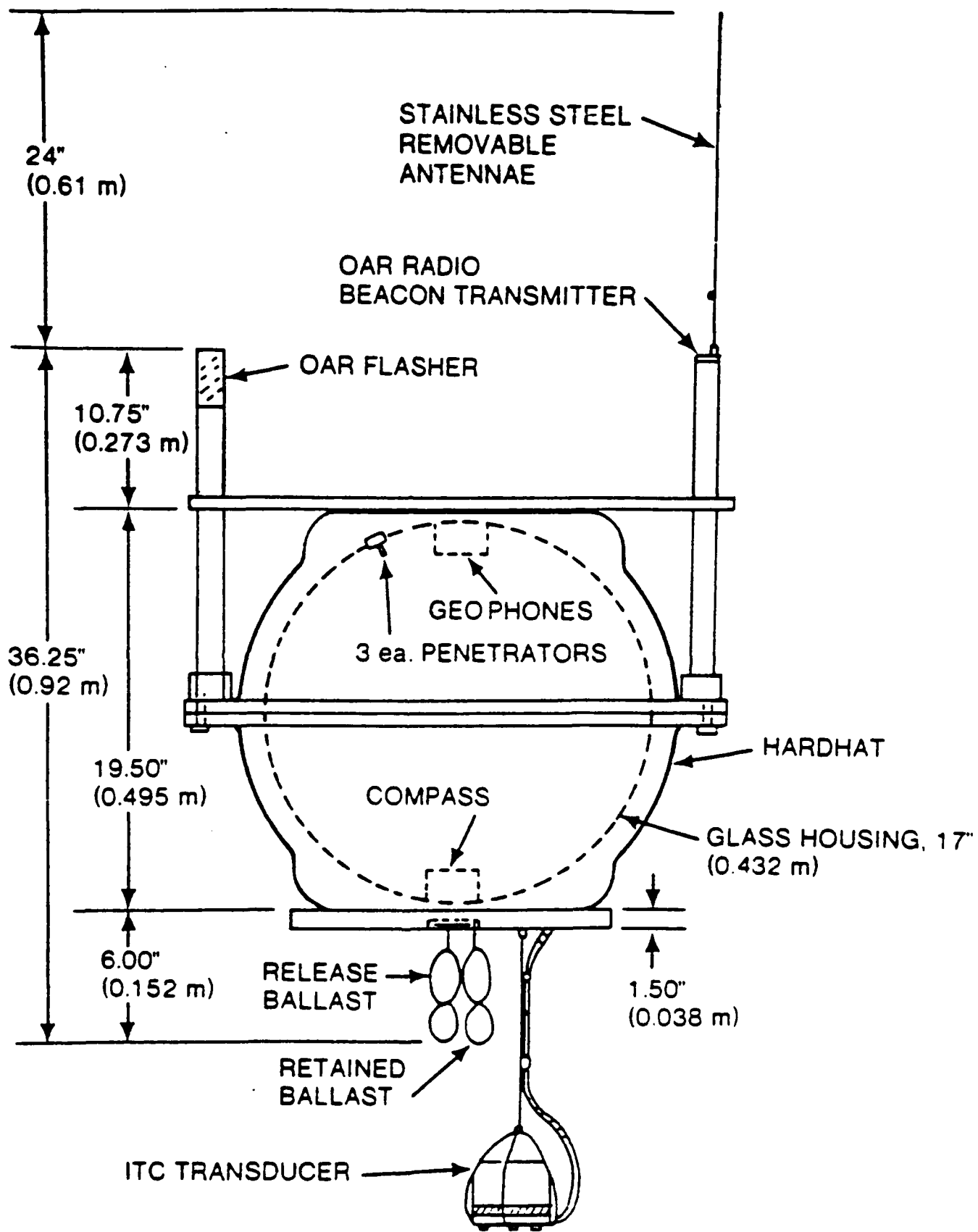


Figure 1

Figure 1

# Deployment Geometry, July, 1989 (34 deg N, 122 deg W)

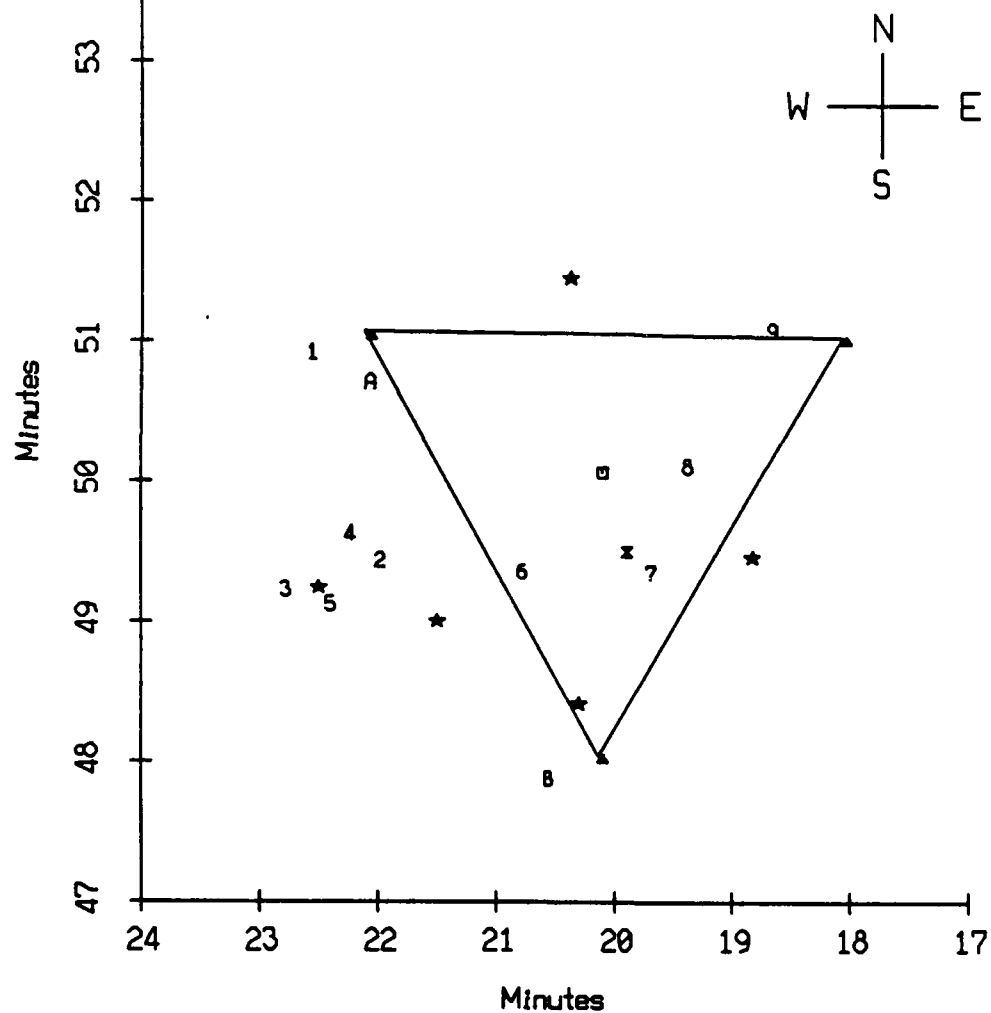


Figure I.1

Sound Speed Profile : Area 24, Months 7-9  
(34-36 deg N, 118-125 deg W)  
with Instruments' Deployment Depths

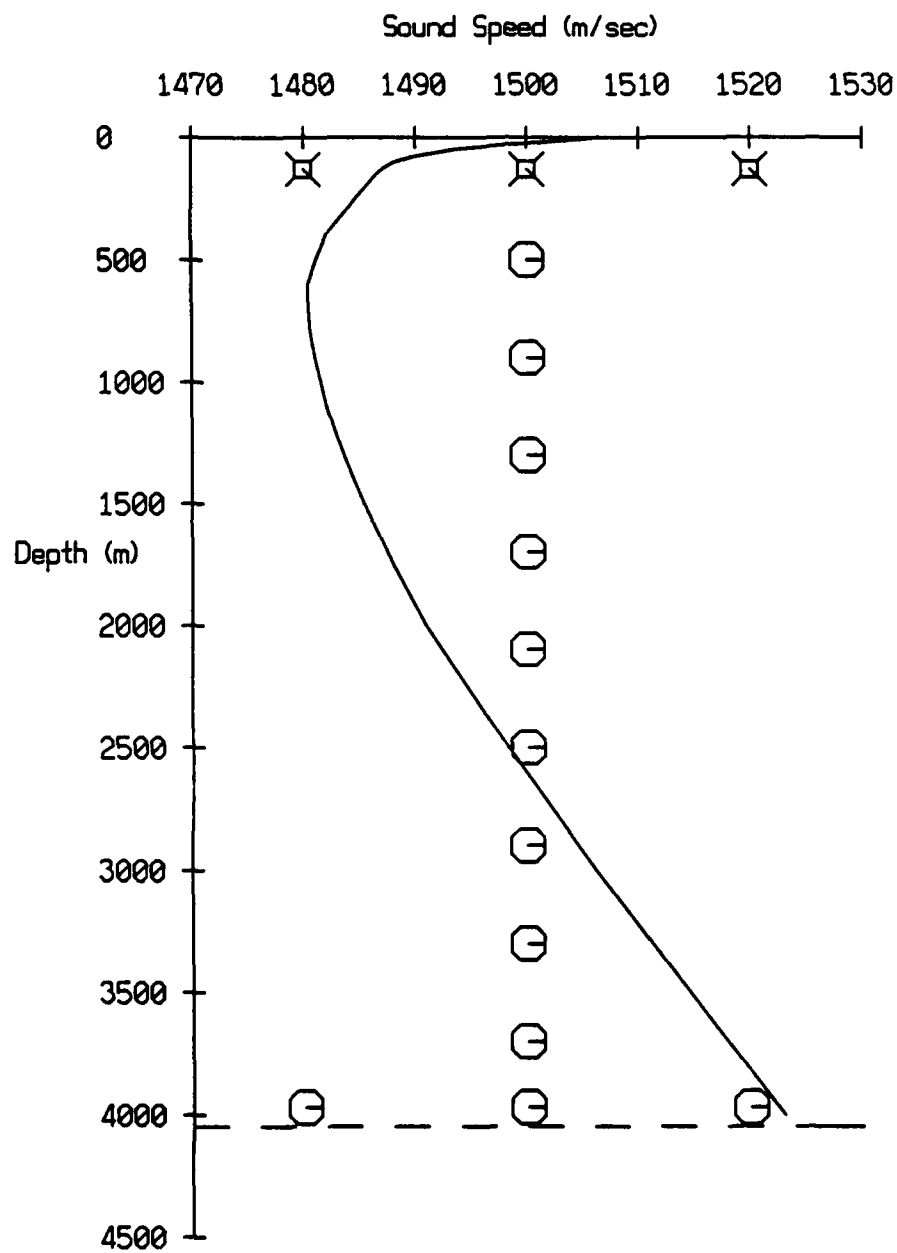


Figure I.2



# Deployment Depths and Times, July, 1989 Sea Trip

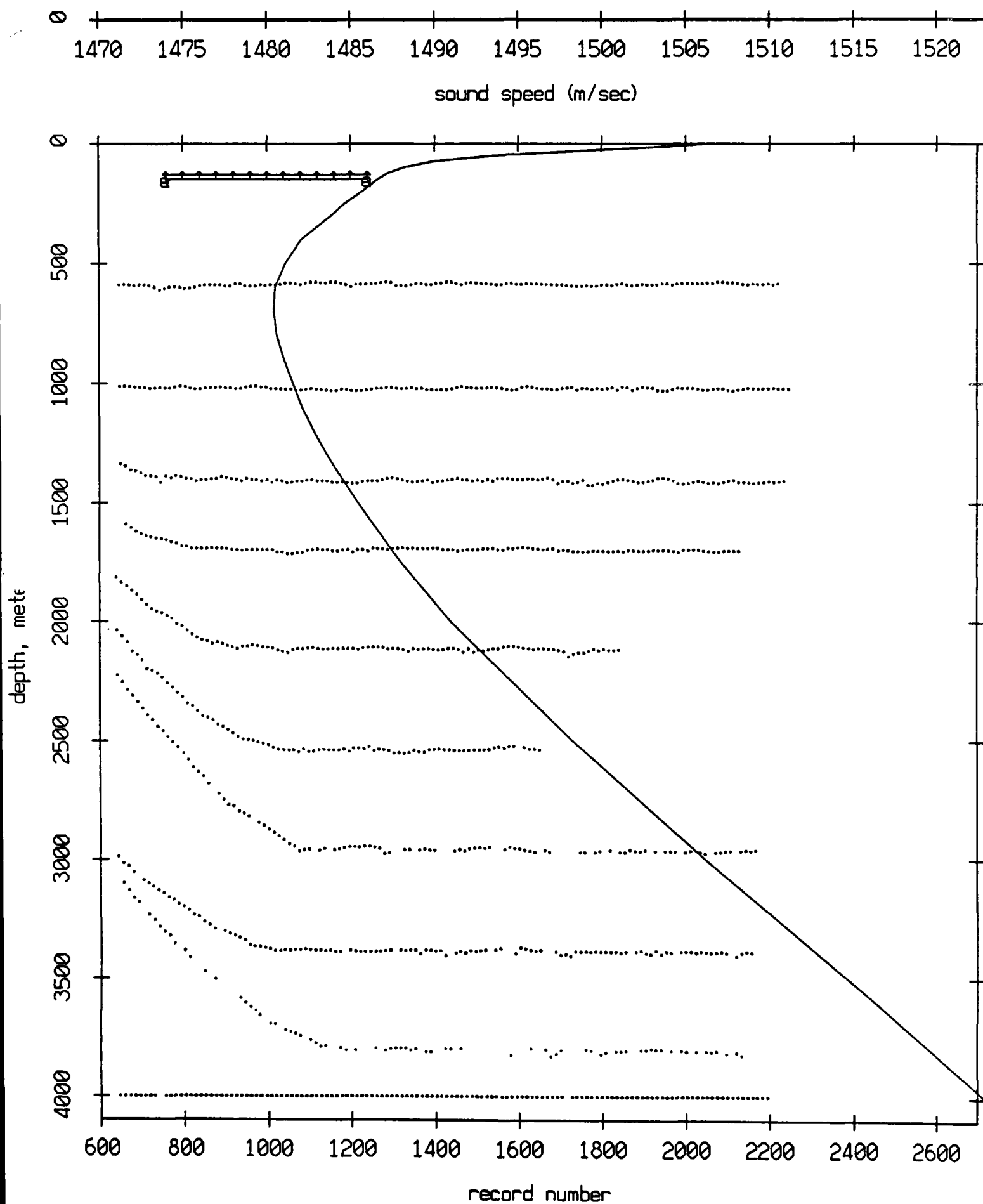


Figure I.3

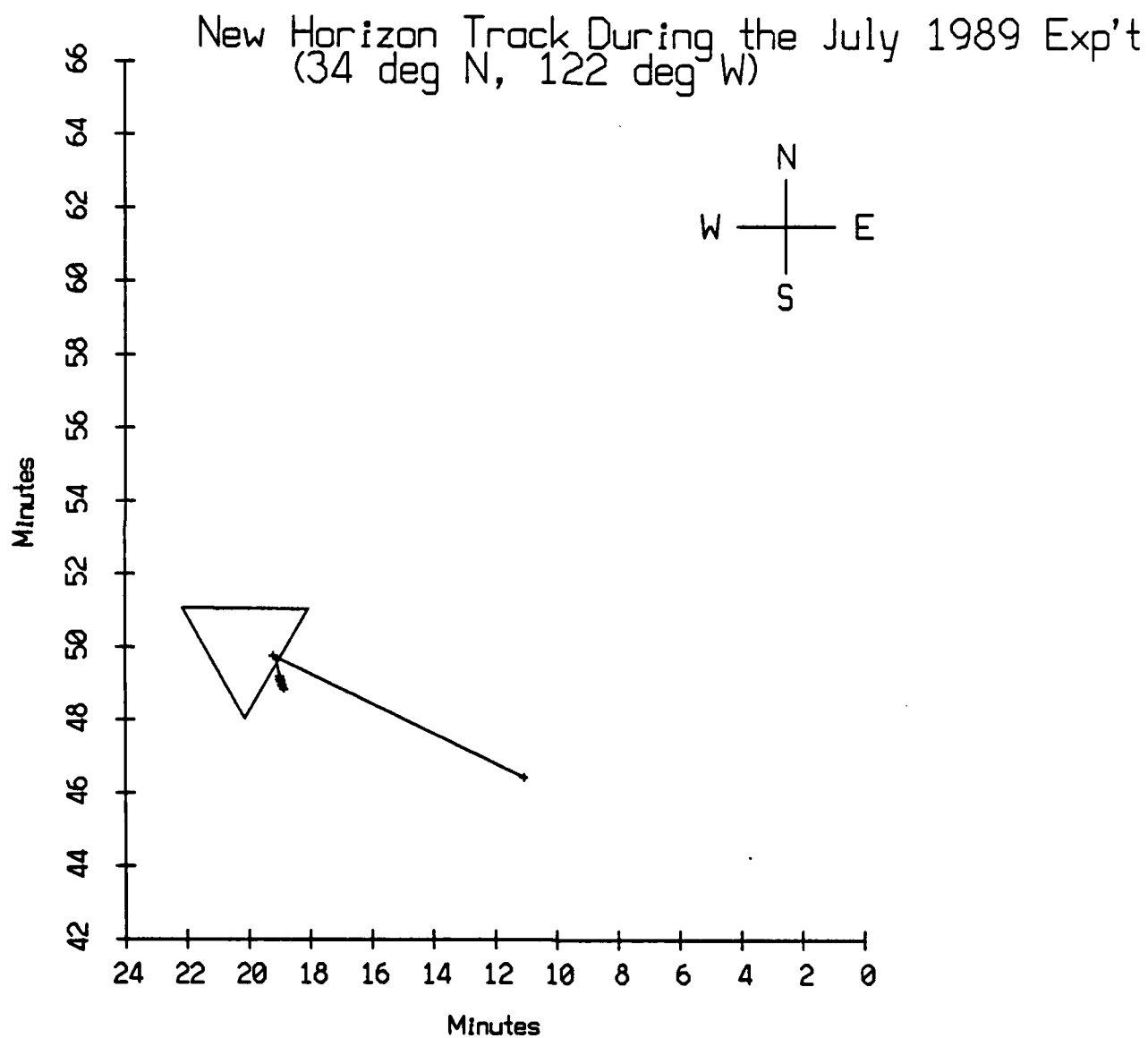


Figure II.1

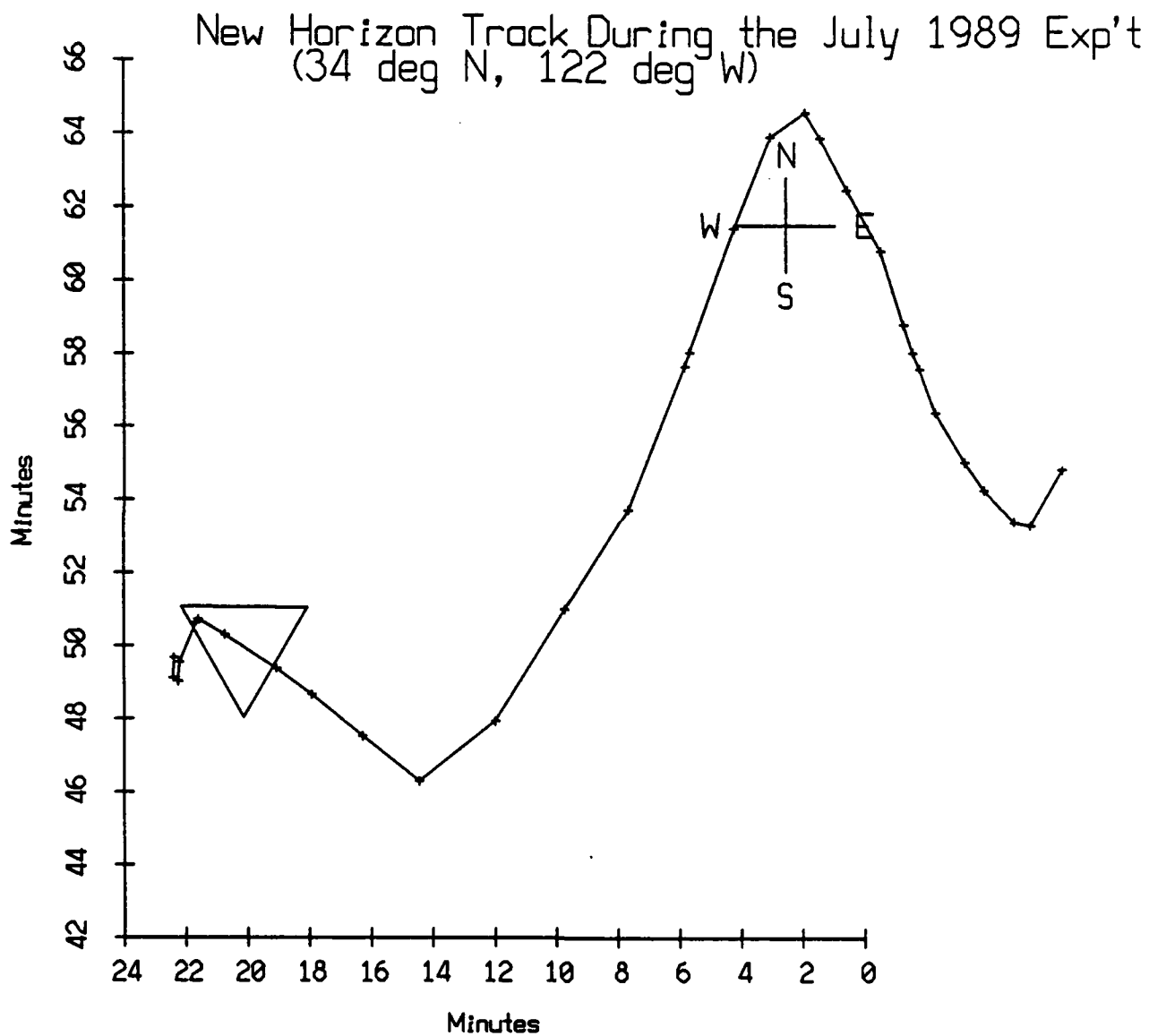


Figure II.2

#1

15:19:30 -  
15:20:35

RMS INPUT AC      #AVG(+)      FREE-RUN  
-20 DBV 100.MV      8/8

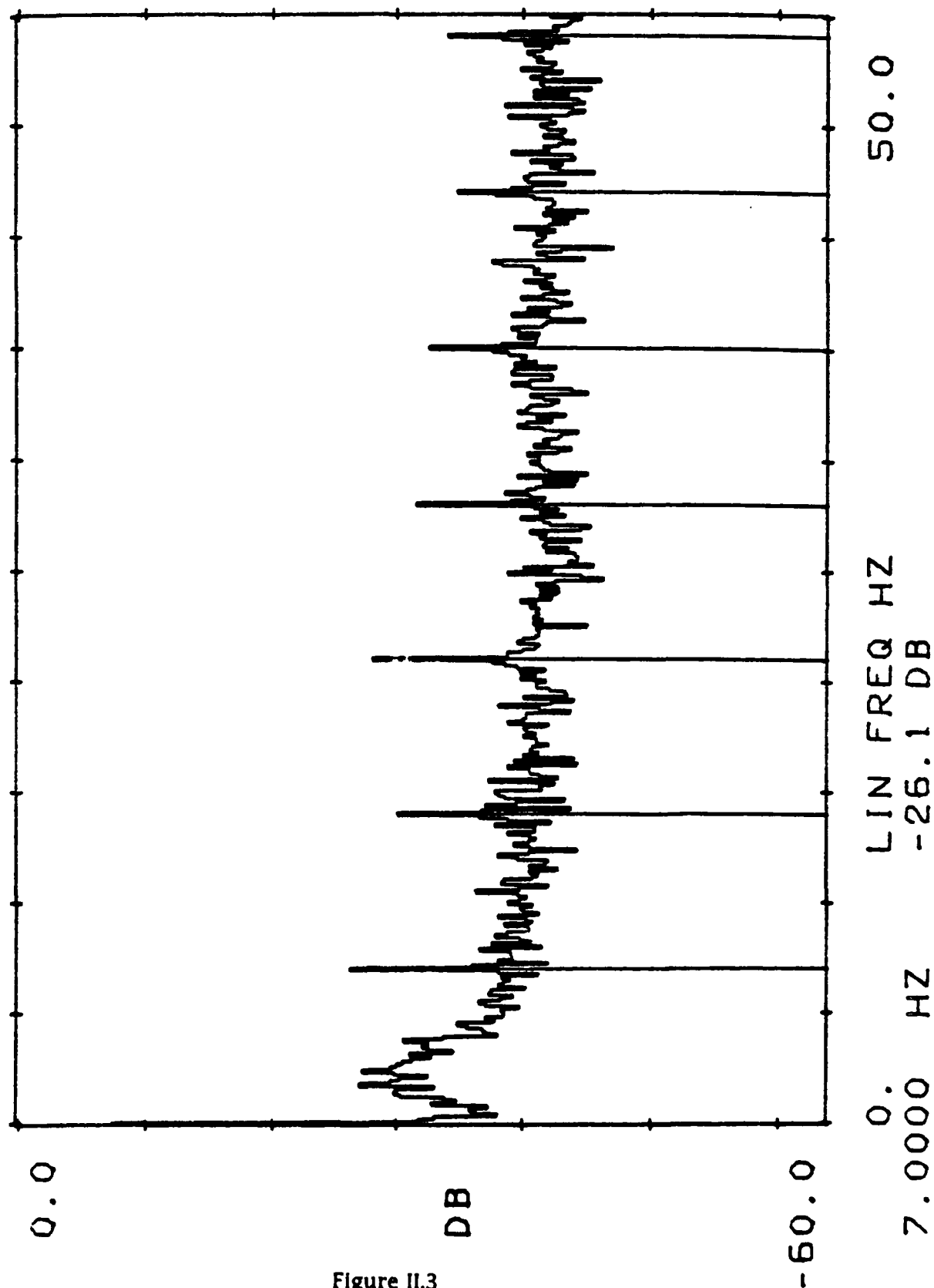


Figure II.3

#2

15:24:30 to  
15:25:45

FREE-RUN

#AVG(+) 8/8

RMS INPUT AC  
-20 DBV 100.MV

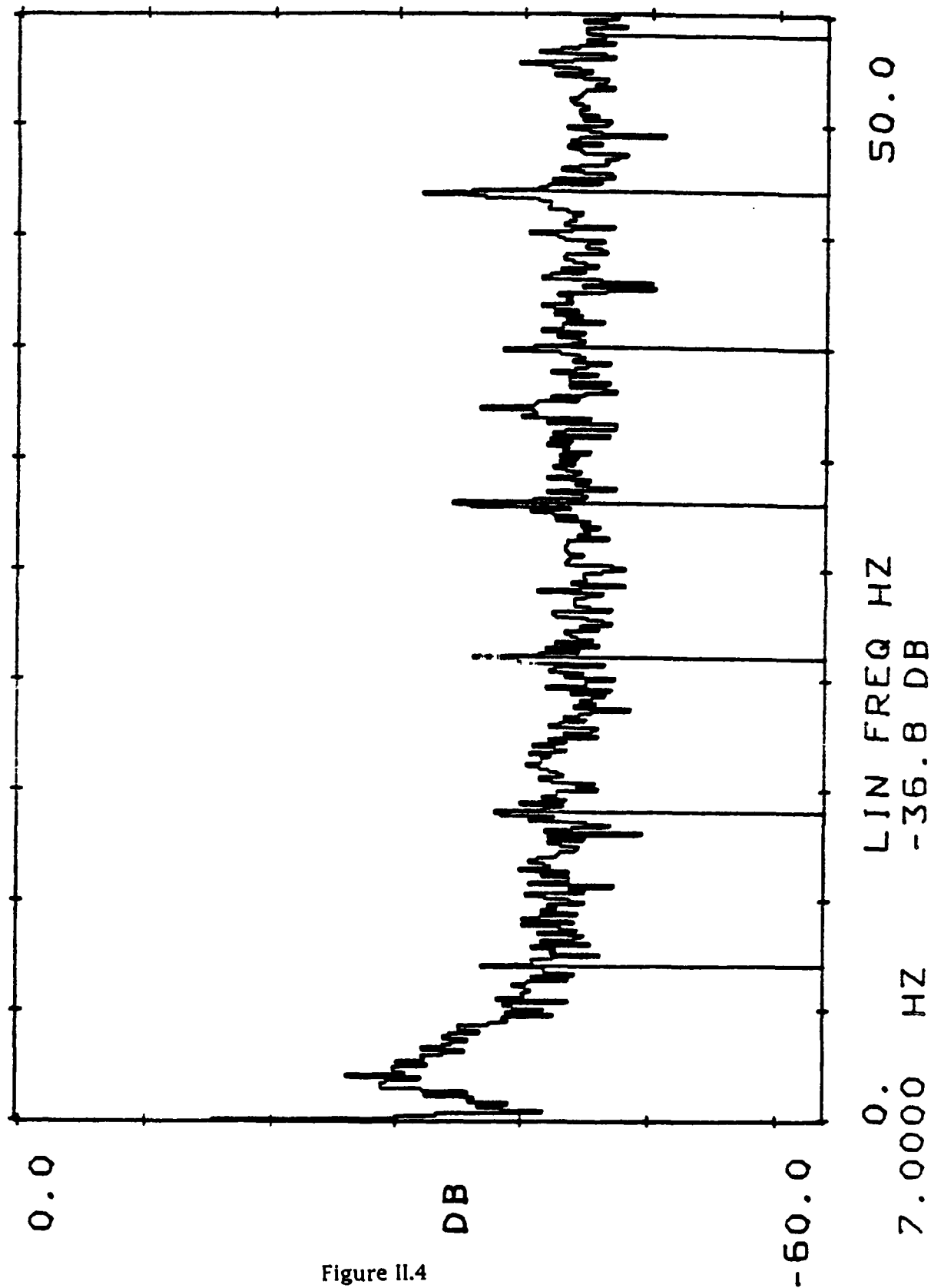


Figure II.4

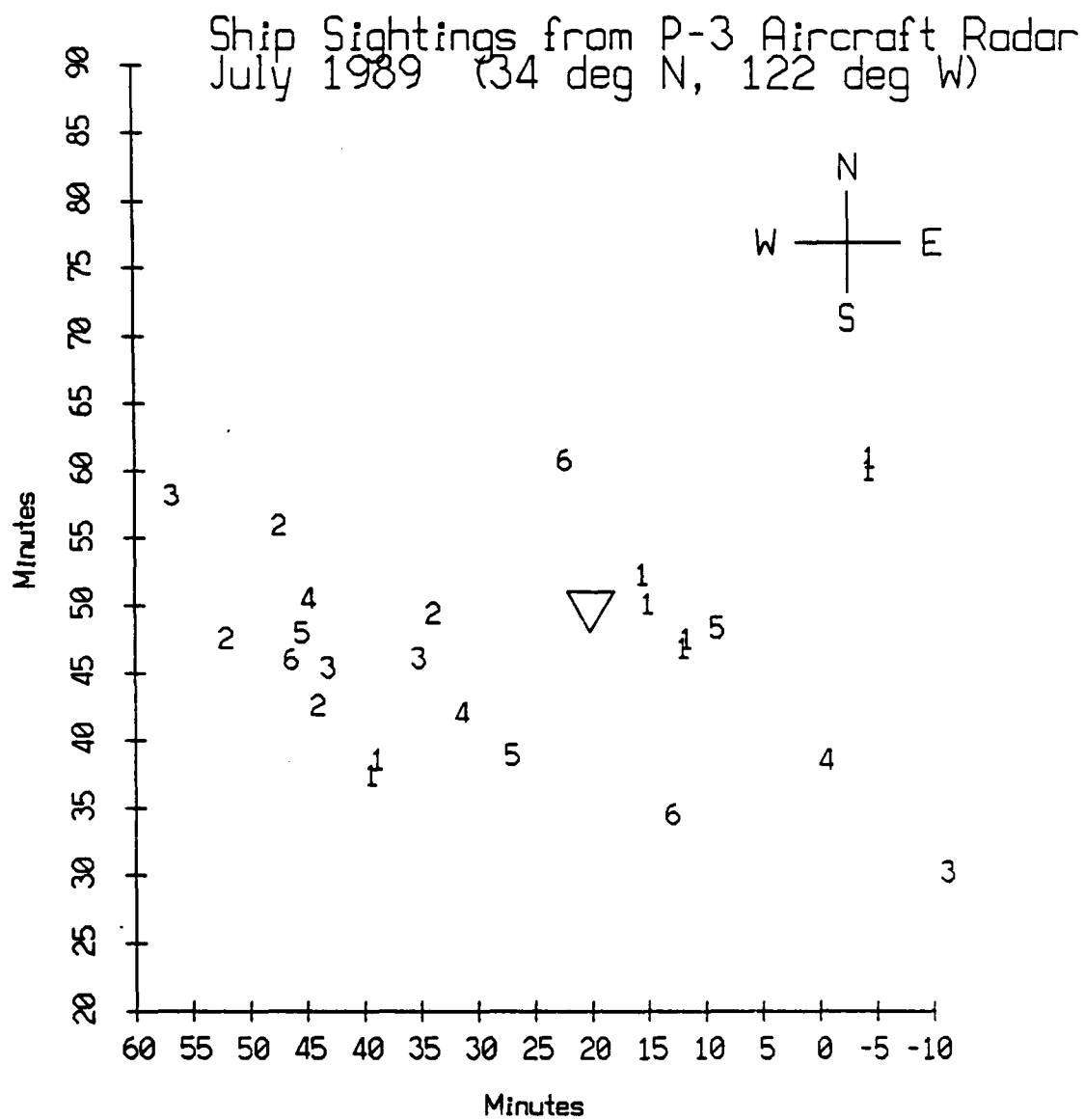


Figure II.5

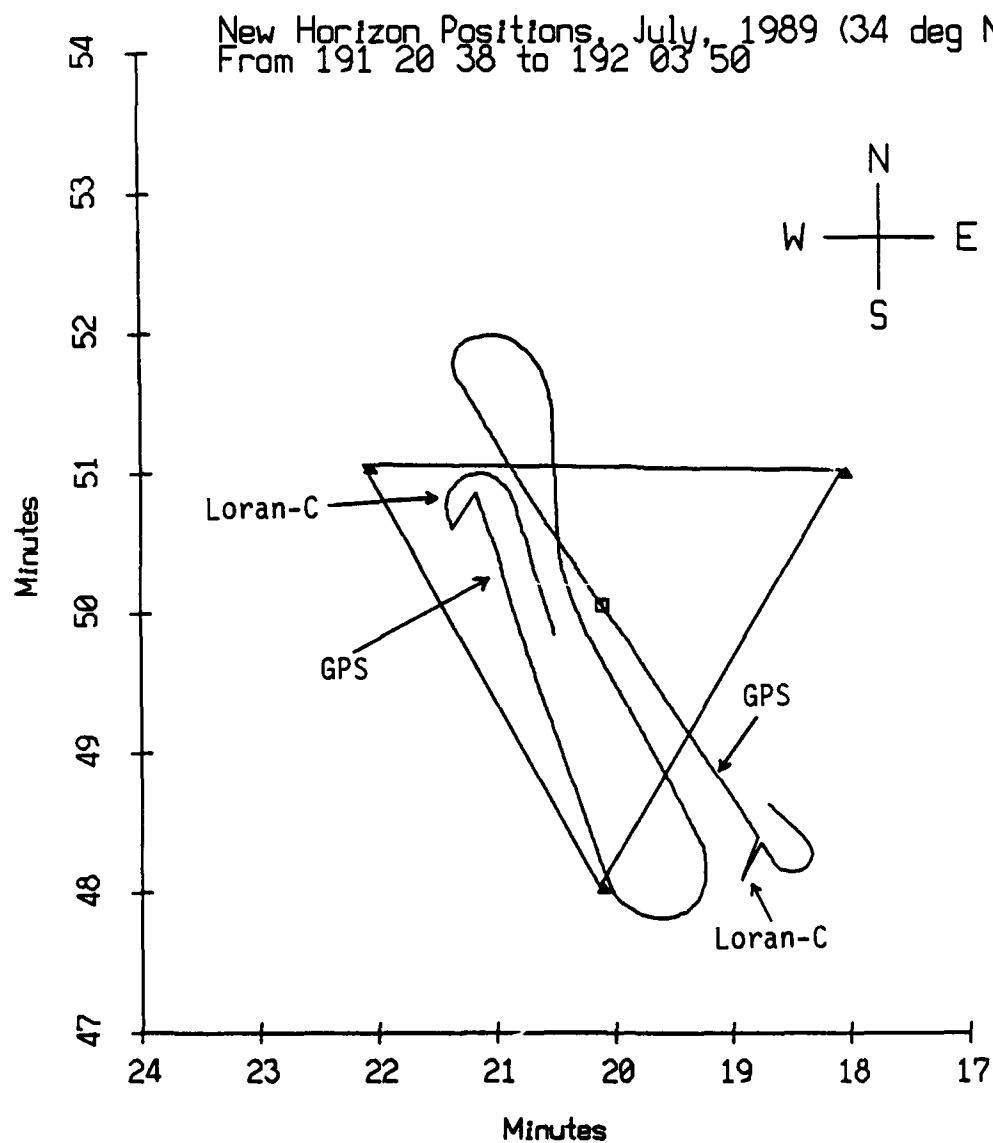


Figure III

Sound Speed Profile Area 24, Months 7-9  
(34-36 deg N, 118-125 deg W)  
with XBTs 29, 30, and 31

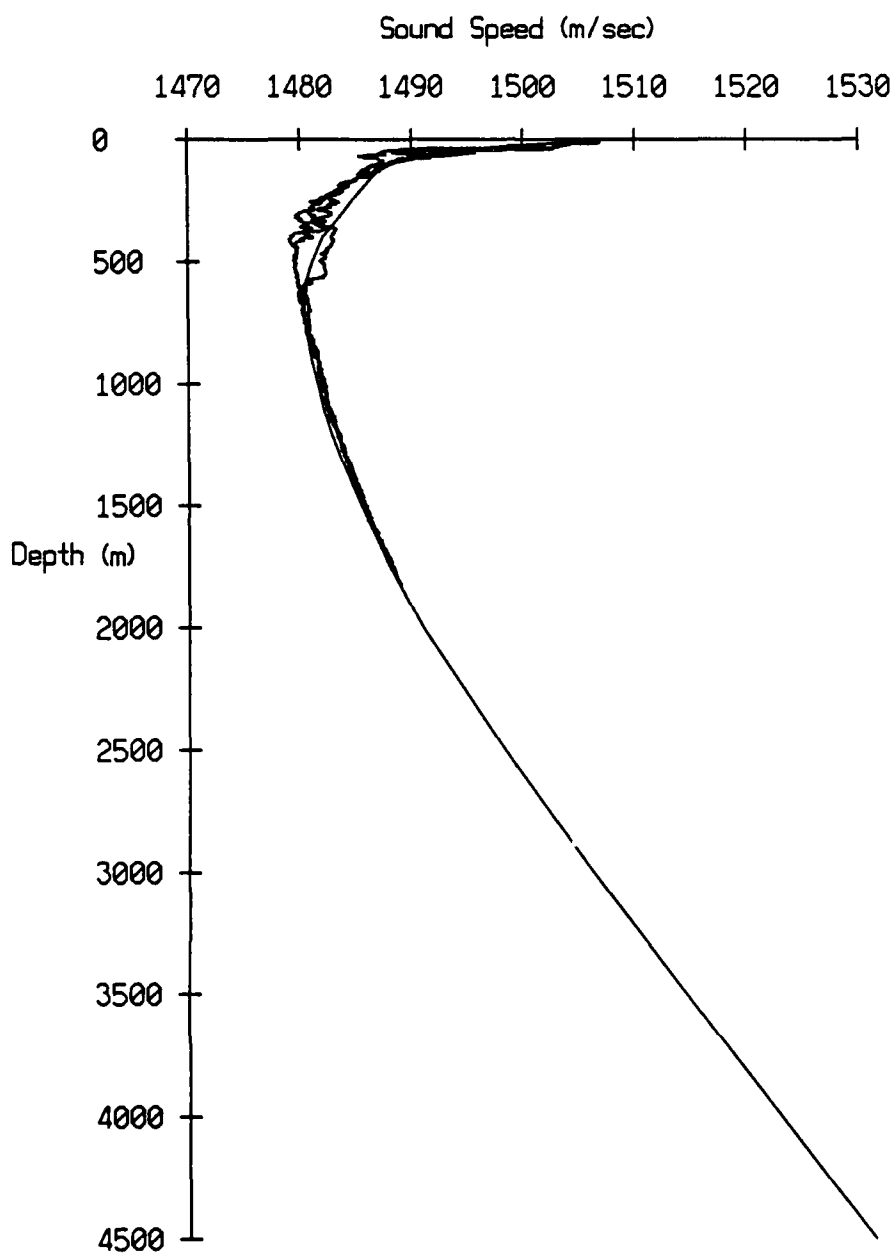


Figure IV.1



Sound Speed Profile Area 24, Months 7-9  
(34-36 deg N, 118-125 deg W)  
with XBTs 37, 38, and 39

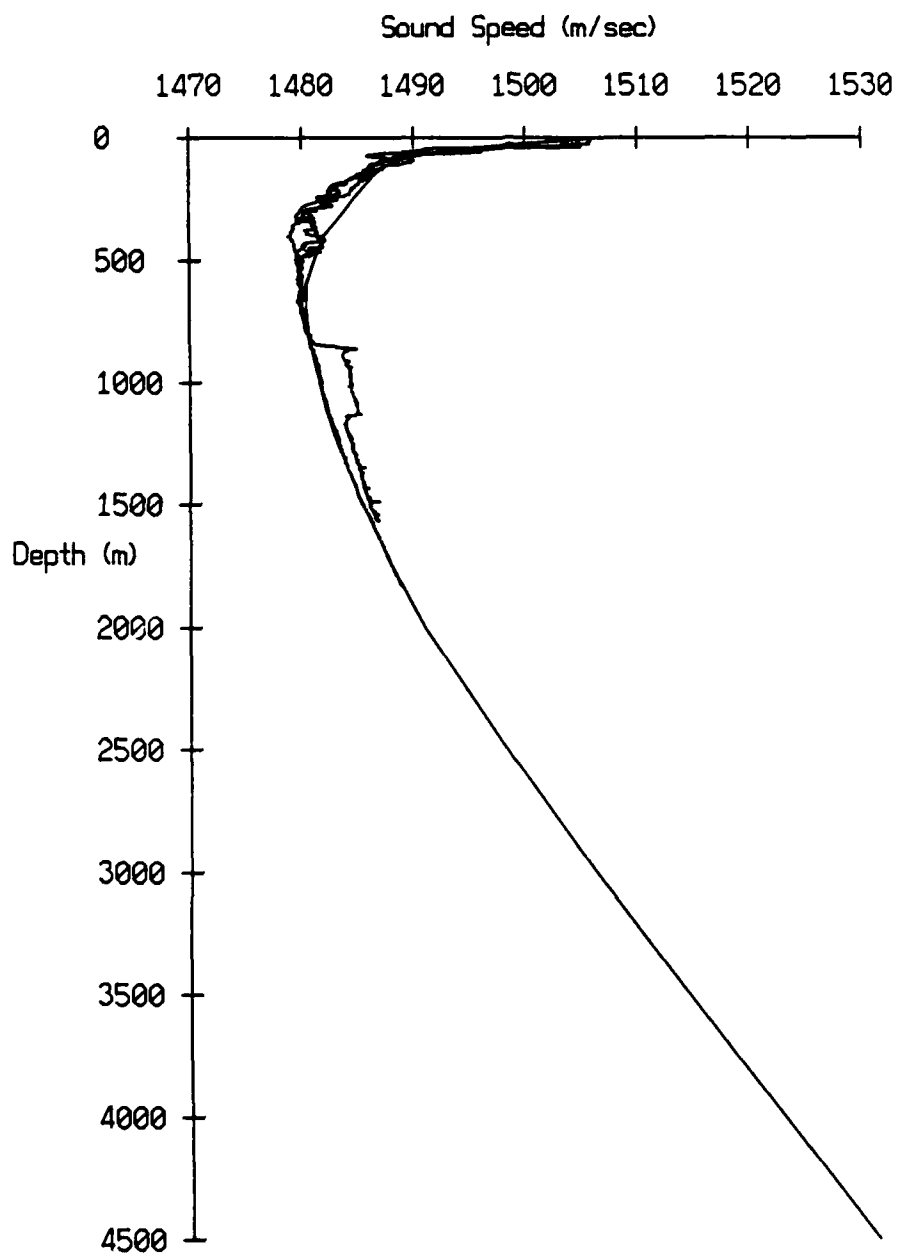


Figure IV.2

# Anemometer Readings after 00:00 a.m., 7-8-89 Measurements on the New Horizon

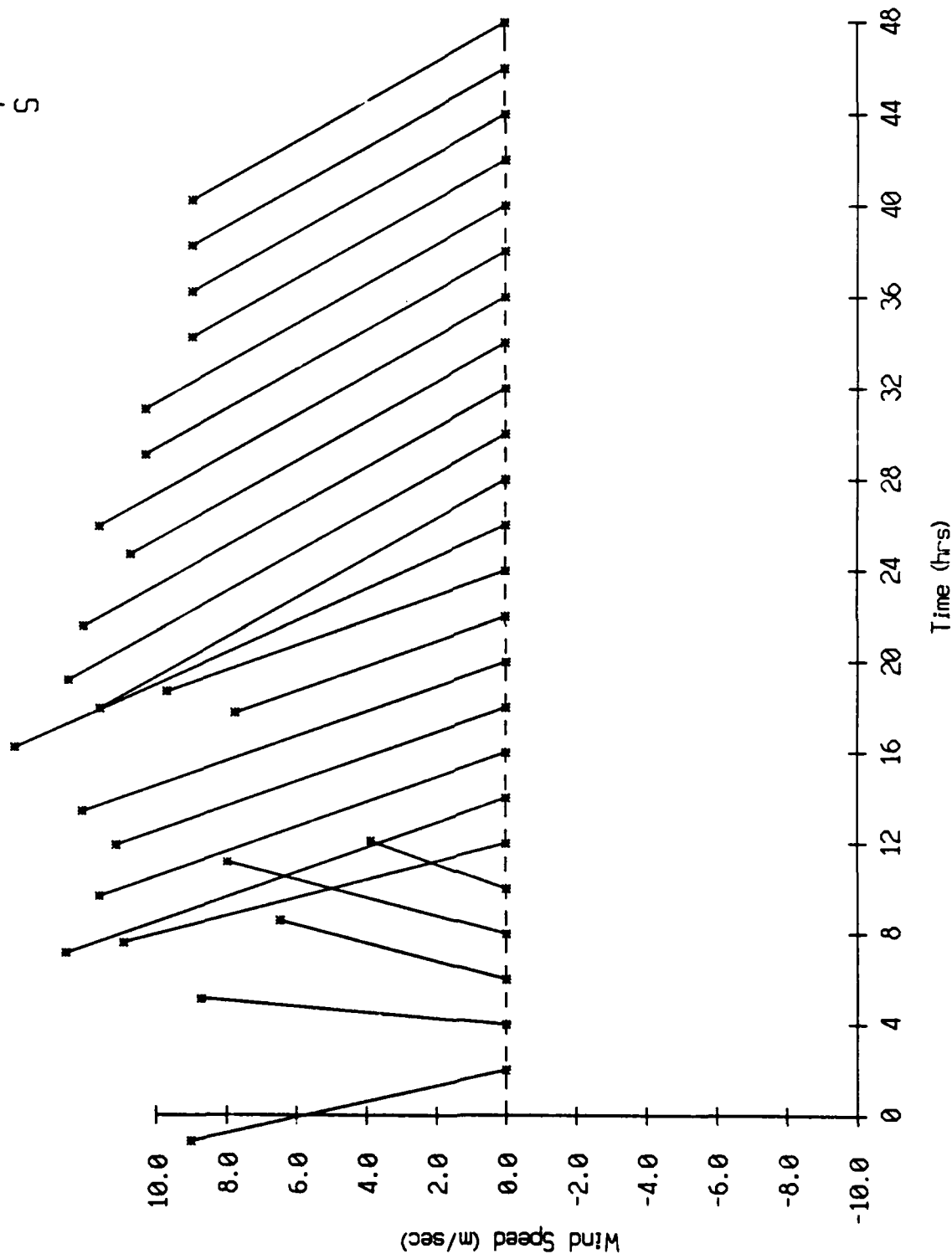
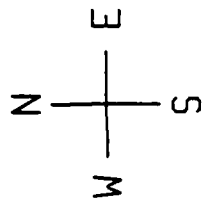


Figure IV.3

July 1989 Deployment Data Screening Results						
record number	internal record number	# of bytes written	first missing resync	pass header checksum?	pass range checksum?	# of failed acoustic checksums?
Float 0						
35	674	9028	0	yes	yes	0
36	****	14	1	no	no	0
795	1433	7594	0	yes	yes	1
796	****	2022	1	no	no	16
1589	2225	0	0	yes	yes	1
Float 1						
151	0	16	1	no	no	0
152	0	2	1	no	no	1
153	768	0	1	no	no	1
154	0	2	1	no	no	1
155	0	0	1	no	no	1
156	0	2	1	no	no	1
157	0	0	1	no	no	1
158	0	0	1	no	no	1
159	0	0	1	no	no	1
160	0	0	1	no	no	1
161	0	304	1	no	no	1
162	****	316	1	no	no	1
163	0	2	1	no	no	1
812	1439	7144	0	yes	yes	1
813	****	1932	1	no	no	15
814	1440	9764	21	yes	yes	70
1619	2245	5920	0	yes	yes	1
1620	****	4378	1	no	no	38
1621	****	0	1	no	no	39
1633	2245	5928	0	yes	yes	2
1634	****	3104	1	no	no	27
1635	****	0	1	no	no	27
Float 2						
4	643	258	0	yes	no	0
5	****	8818	1	no	no	79
35	673	9588	0	yes	yes	1
275	913	9766	0	yes	yes	1
319	957	5712	0	yes	yes	1
320	-1	3352	1	no	no	28
368	1005	9766	0	yes	yes	1

Figure V.1a

July 1989 Deployment Data Screening Results						
record number	internal record number	# of bytes written	first missing resync	pass header checksum?	pass range checksum?	# of failed acoustic checksums?
370	1007	9766	2	yes	no	88
386	1023	9768	20	yes	yes	71
392	1029	9766	80	yes	yes	11
1207	1844	9206	0	yes	yes	1
1604	2240	0	0	yes	yes	0
Float 3						
10	649	9766	0	yes	yes	1
159	798	4936	0	yes	yes	1
160	9345	4034	1	no	no	35
349	987	9796	15	yes	yes	76
1494	2131	0	0	yes	yes	1
Float 4						
1076	1715	9766	0	yes	yes	1
1211	1849	0	0	yes	yes	1
Float 5						
327	966	9766	75	yes	yes	16
343	982	64	0	yes	no	1
344	****	9796	1	no	no	88
390	1028	8254	0	yes	yes	2
391	****	786	1	no	no	5
1048	1685	5056	0	yes	yes	1
1049	****	5910	1	no	no	52
1543	2178	0	0	yes	yes	1
Float 6						
665	1303	1220	0	yes	yes	1
666	****	7832	1	no	no	70
684	1321	1860	0	yes	yes	1
685	****	9796	1	no	no	88
697	1333	9766	0	yes	yes	1
1496	2132	6760	0	yes	yes	1
1497	****	2304	1	no	no	18

Figure V.1b

July 1989 Deployment Data Screening Results						
record number	internal record number	# of bytes written	first missing resync	pass header checksum?	pass range checksum?	# of failed acoustic checksums?
1498	2133	2976	0	yes	yes	2
1499	****	6086	1	no	no	54
1513	2147	1640	0	yes	yes	1
1514	****	9796	1	no	no	88
1532	2165	3234	0	yes	yes	1
1533	****	5850	1	no	no	51
1535	2166	0	0	yes	yes	0
Float 7						
351	990	9766	46	yes	yes	45
783	1422	9796	31	yes	yes	60
1528	2166	0	0	yes	yes	0
Float 8						
6	644	9766	0	yes	yes	1
31	669	1990	0	yes	yes	1
32	1793	7068	1	no	no	63
91	728	4964	0	yes	yes	1
92	****	4104	1	no	no	36
1522	2157	0	0	yes	yes	0
Float 9						
370	1009	9766	40	yes	yes	51
1169	1808	9766	75	yes	yes	16
1560	2198	0	0	yes	yes	0
Float 10						
4	642	732	0	yes	yes	1
5	2433	8312	1	no	no	75
351	988	9766	43	yes	yes	48
962	1599	2978	0	yes	yes	1
963	****	6100	2	no	no	54
1556	2191	0	0	yes	yes	0

Figure V.1c

July 1989 Deployment Data Screening Results						
record number	internal record number	# of bytes written	first missing resync	pass header checksum?	pass range checksum?	# of failed acoustic checksums?
Float 11						
417	1056	9764	85	yes	yes	6
816	1455	9766	0	yes	yes	1
885	1524	9766	0	yes	yes	1
1000	1639	9766	0	yes	yes	1
1065	1704	9766	0	yes	yes	1
1518	2156	0	0	yes	yes	1

Figure V.1d

# AGC Level and Buoy Heading, Float 0, July 1989 Sea Trip

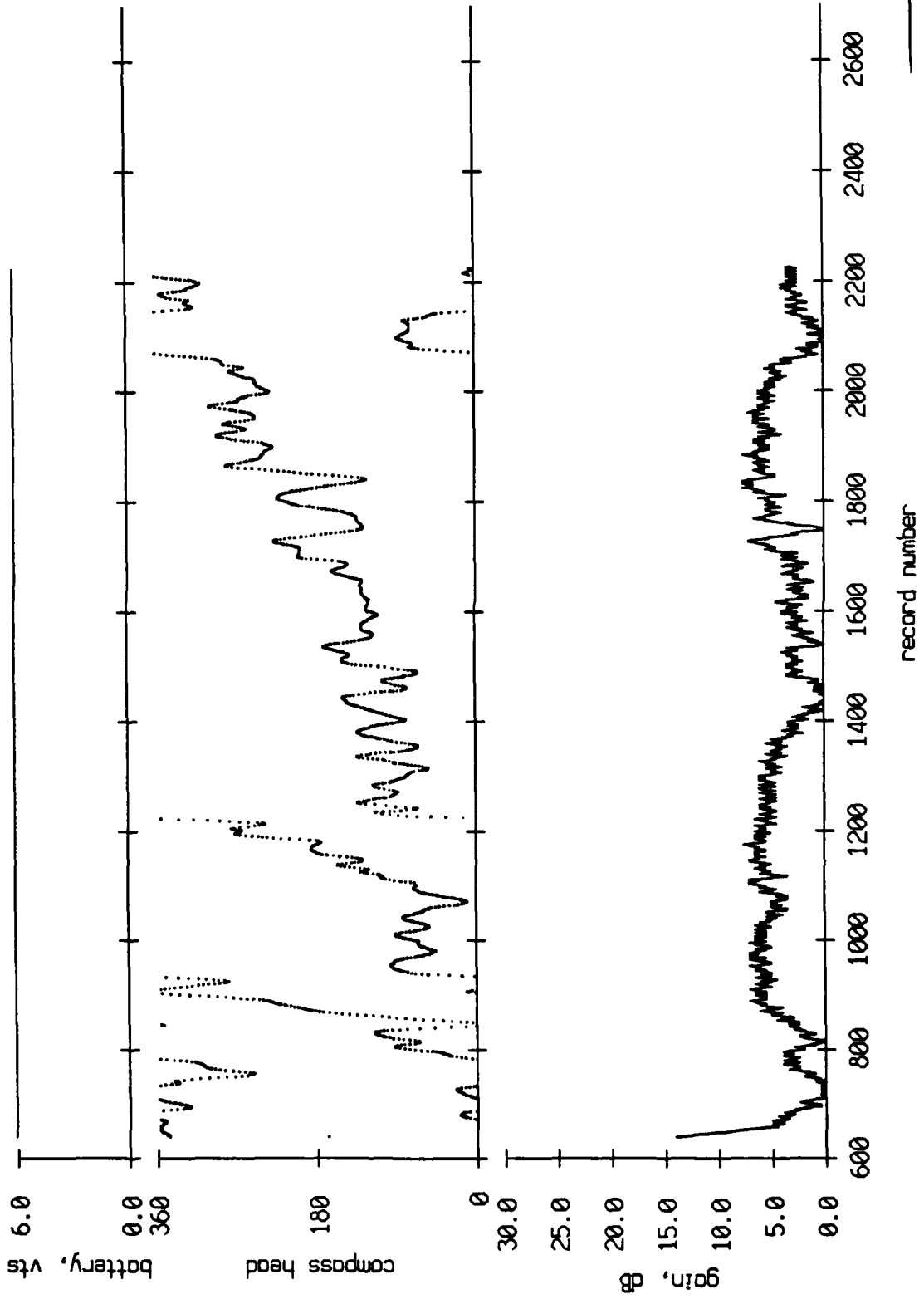


Figure VII.1

# AGC Level and Buoy Heading, Float 1, July 1989 Sea Trip

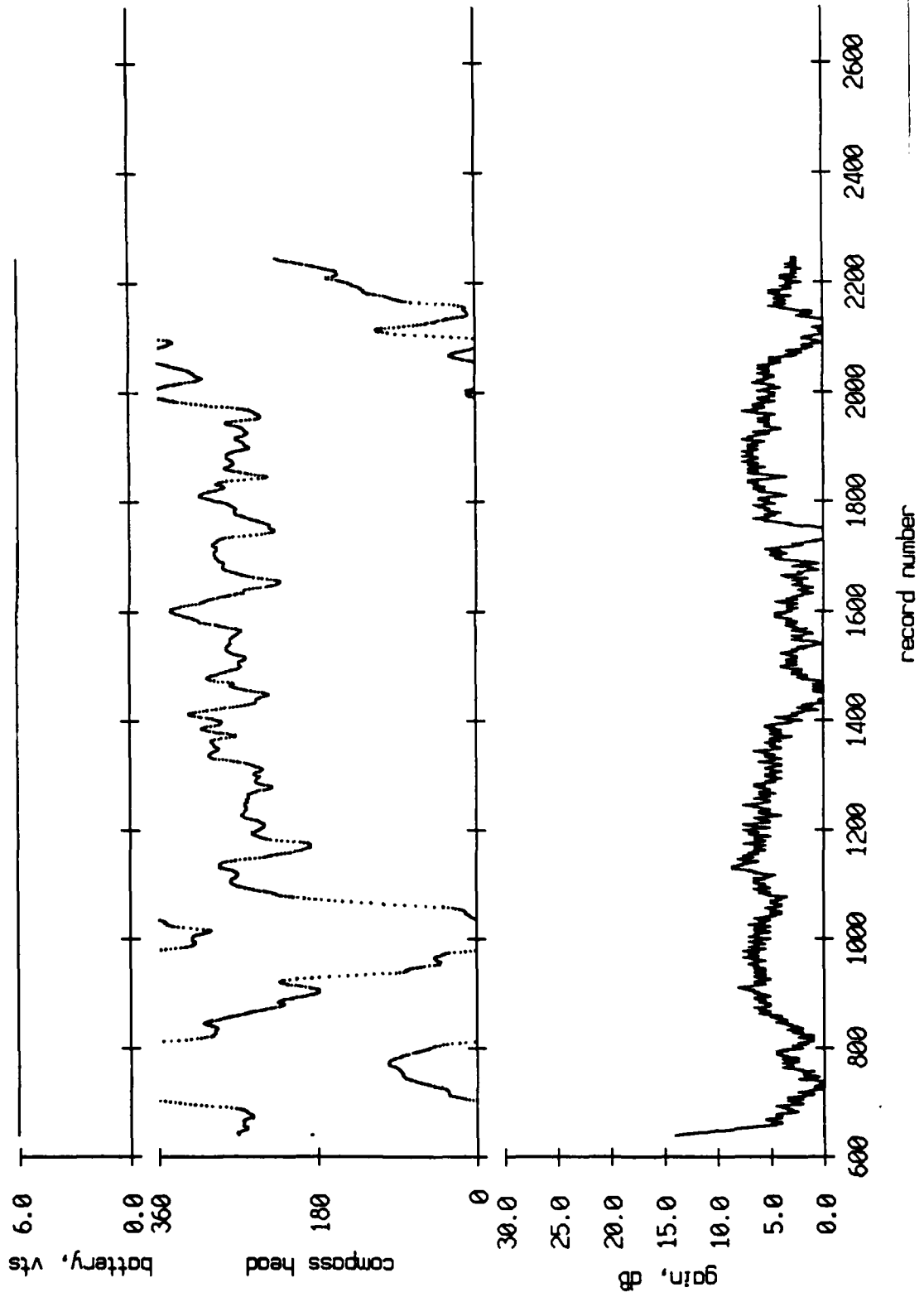


Figure VII.2



# AGC Level and Buoy Heading, Float 2, July 1989 Sea Trip

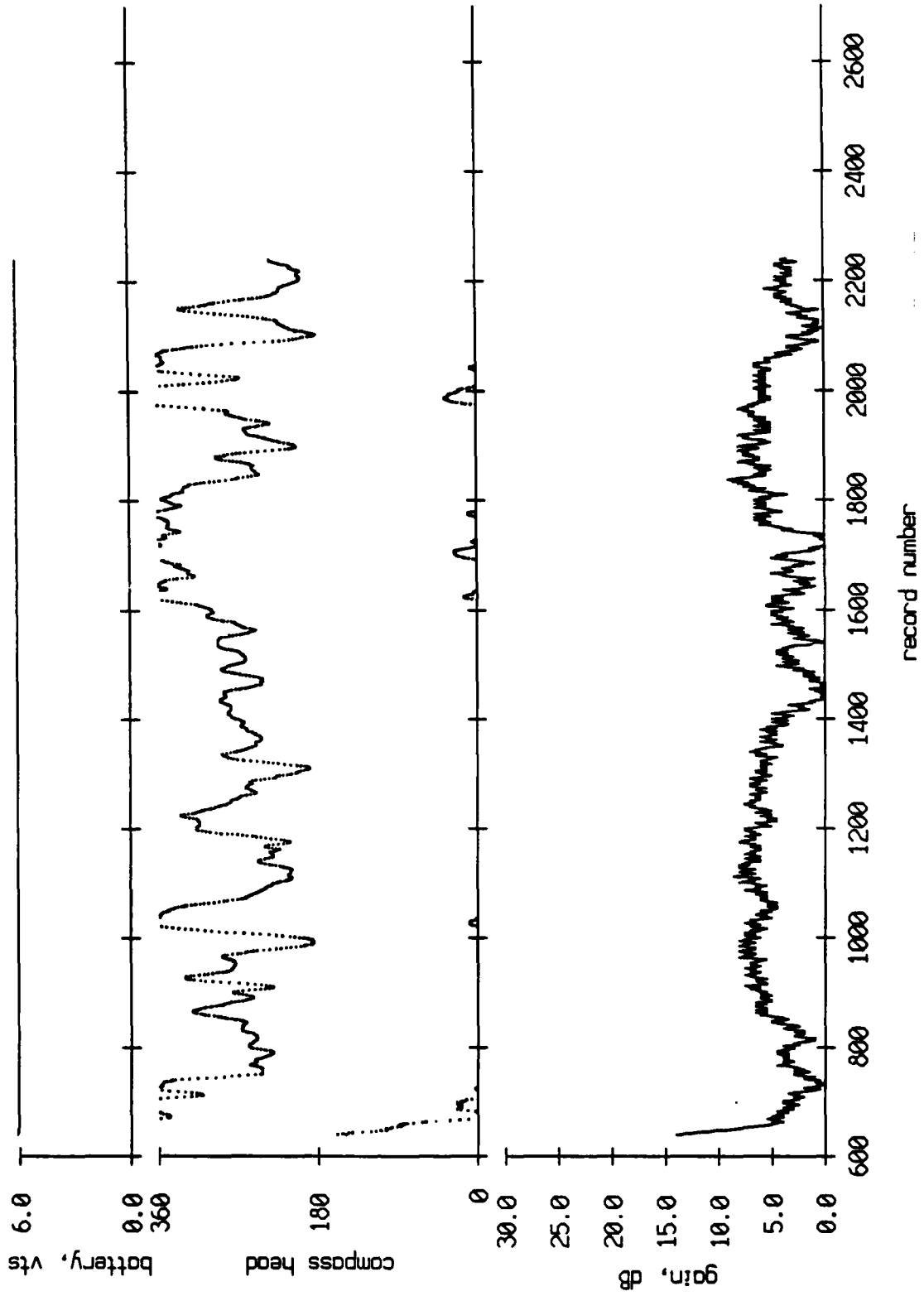


Figure VII.3

# AGC Level and Buoy Heading, Float 3, July 1989 Sea Trip

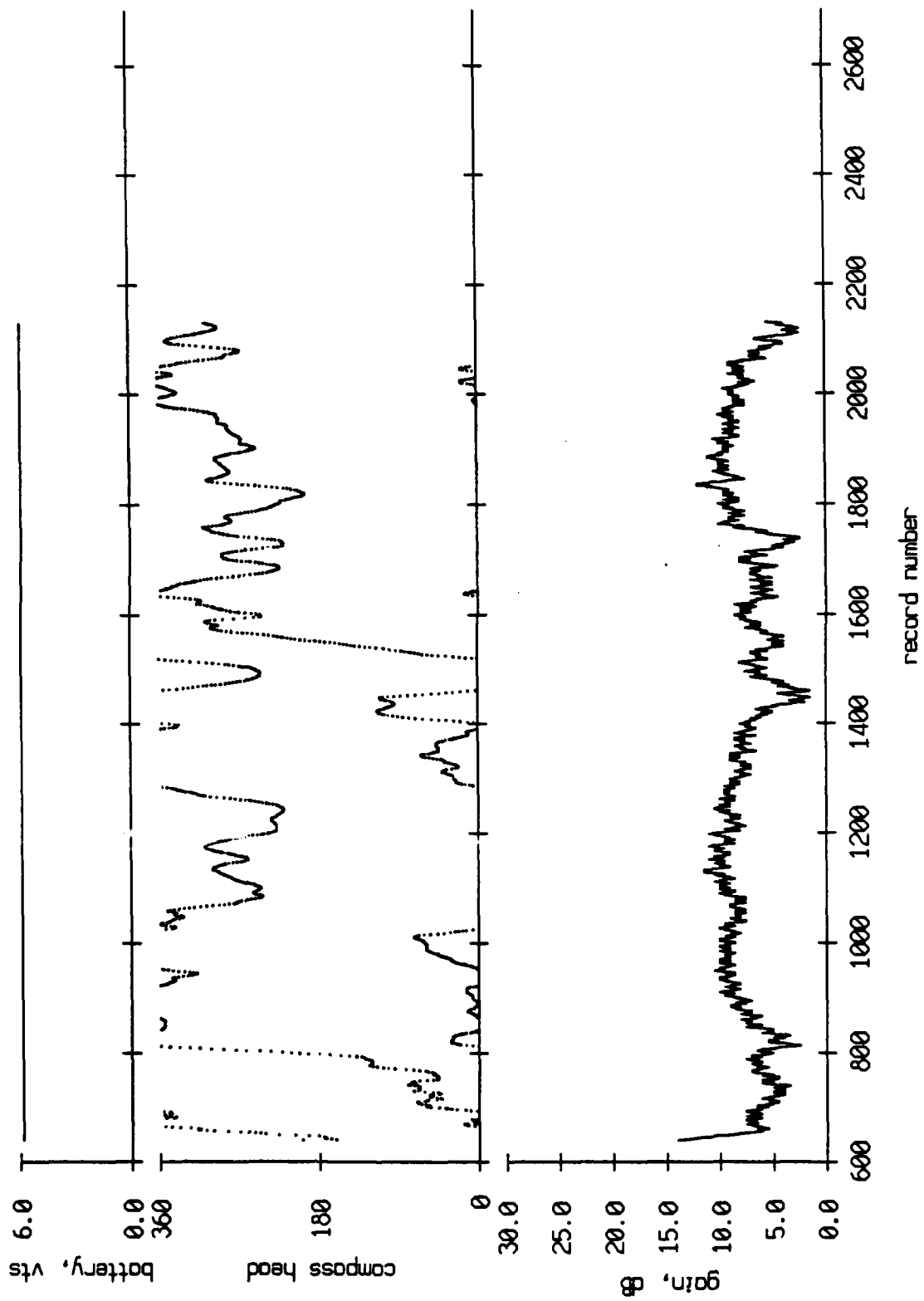


Figure VII.4

# AGC Level and Buoy Heading, Float 4, July 1989 Sea Trip

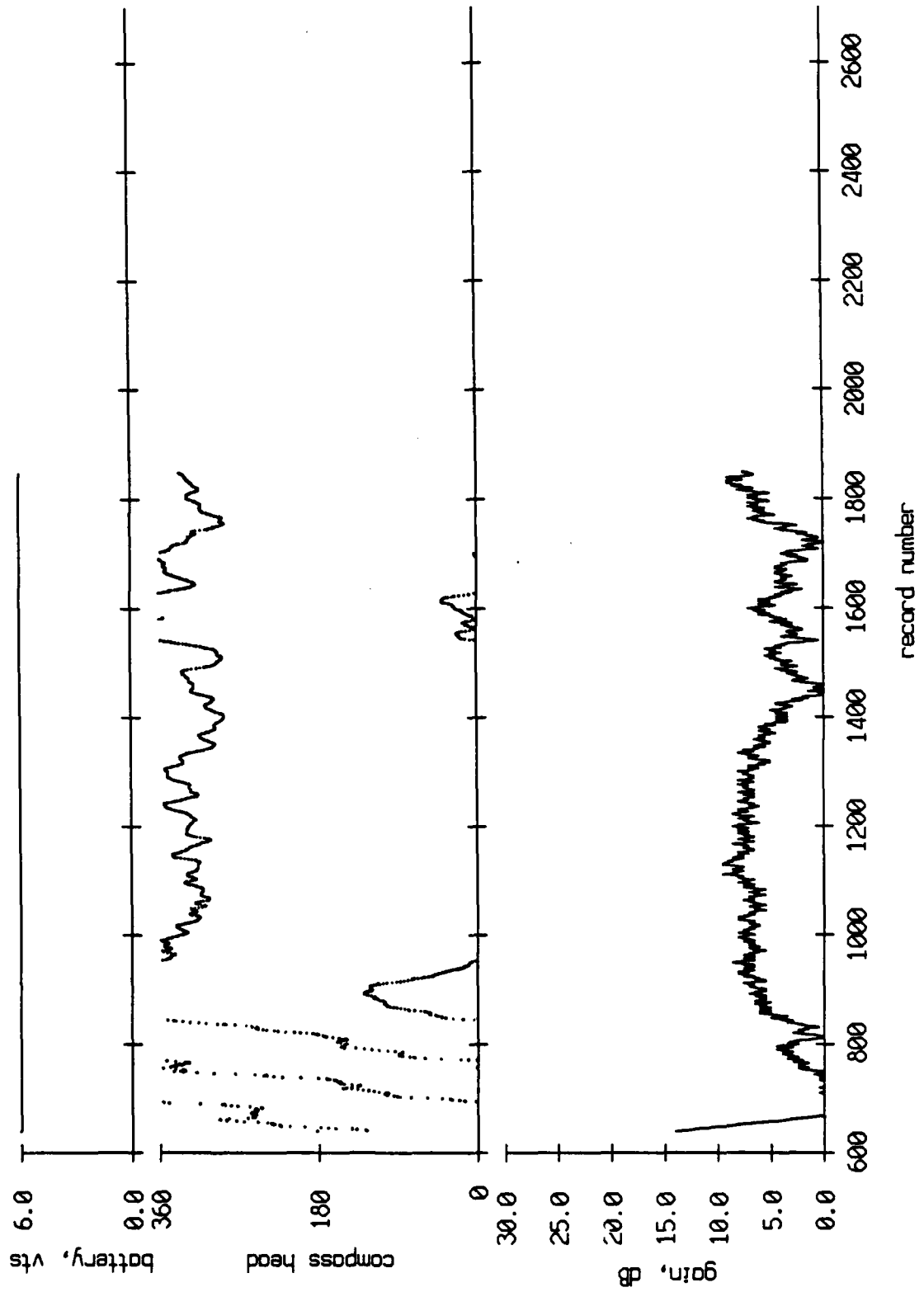


Figure VII.5

# AGC Level and Buoy Heading, Float 5, July 1989 Sea Trip

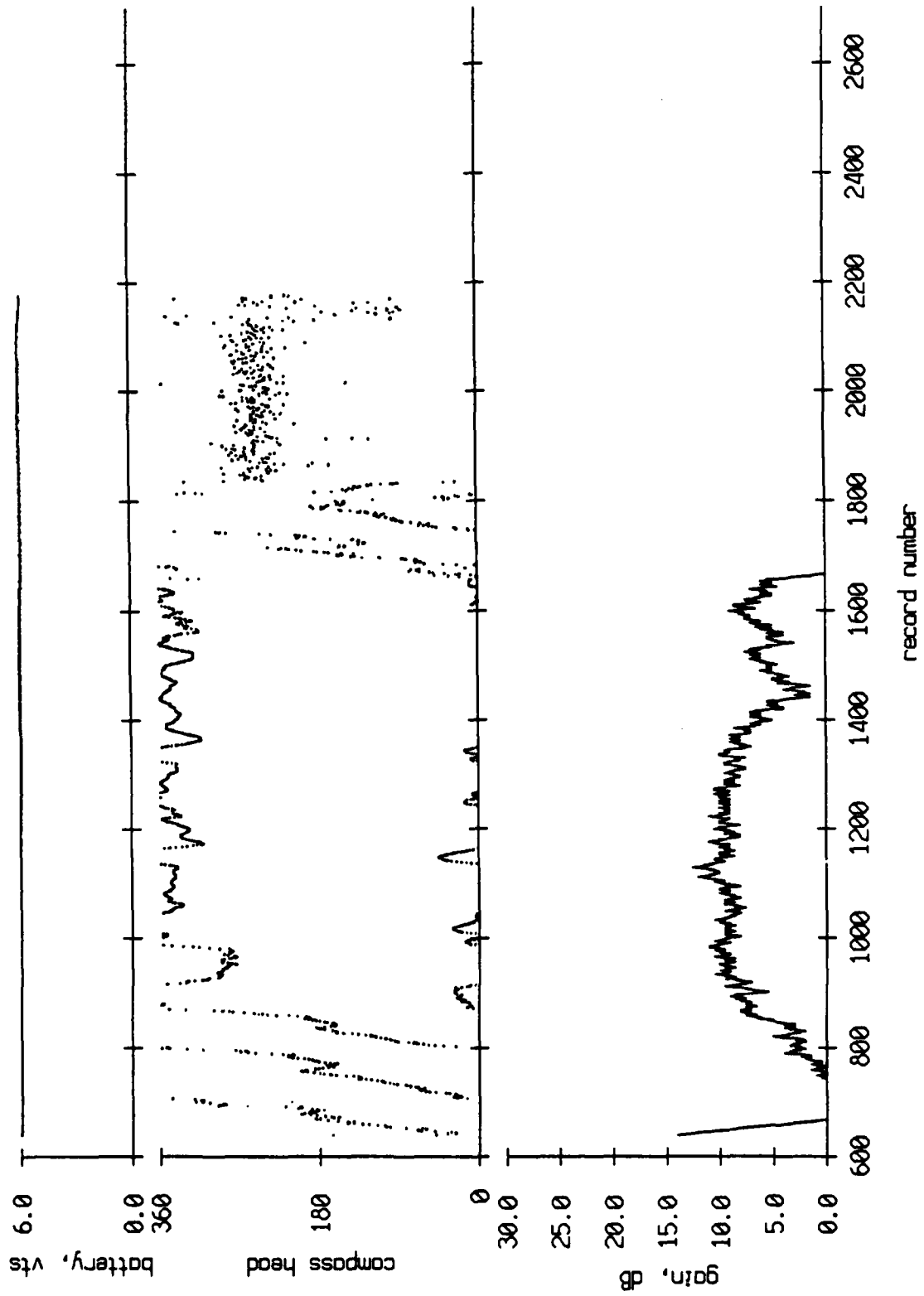


Figure VII.6

# AGC Level and Buoy Heading, Float 6, July 1989 Sea Trip

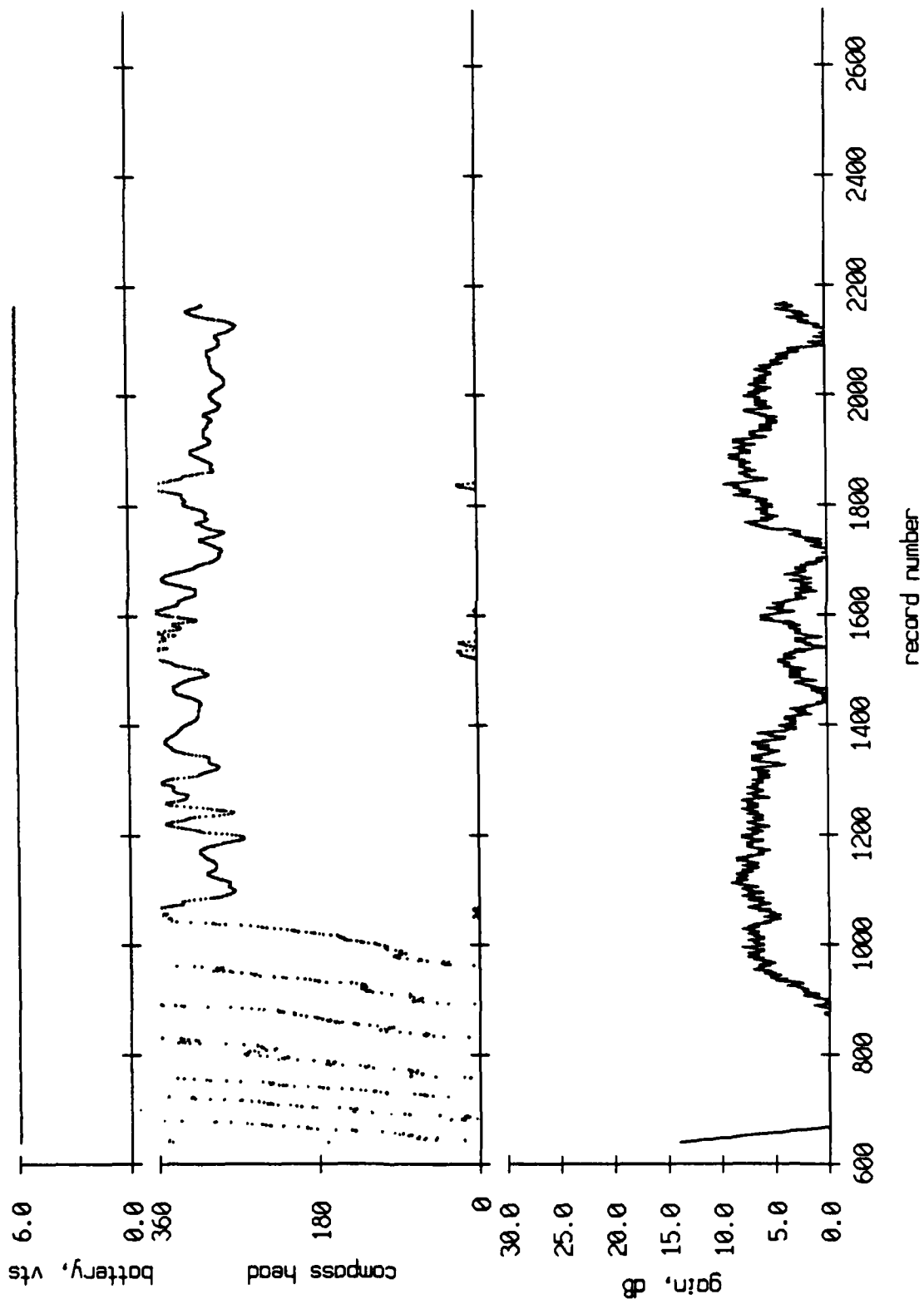


Figure VII.7

# AGC Level and Buoy Heading, Float 7, July 1989 Sea Trip

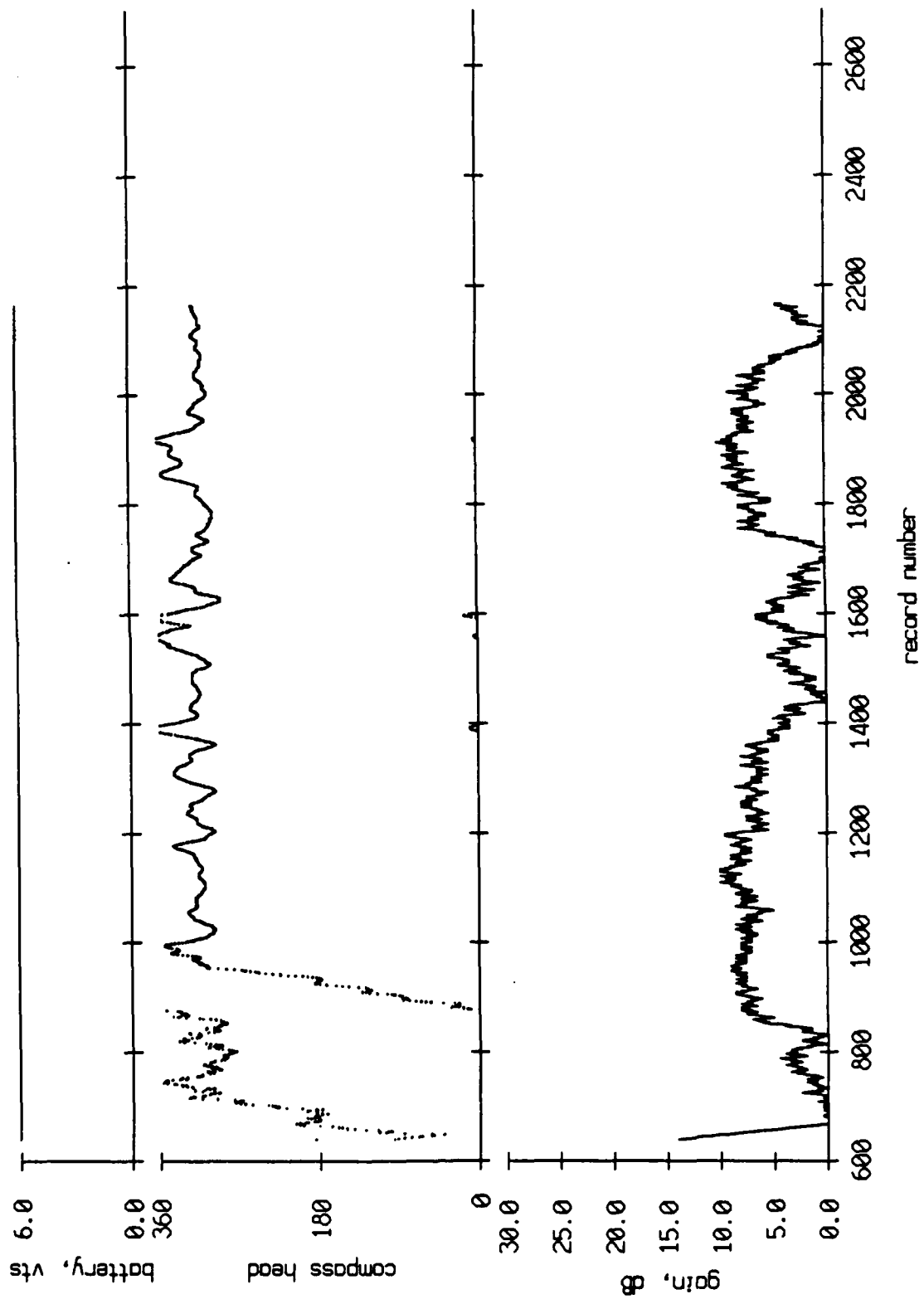


Figure VII.8

# AGC Level and Buoy Heading, Float 8, July 1989 Sea Trip

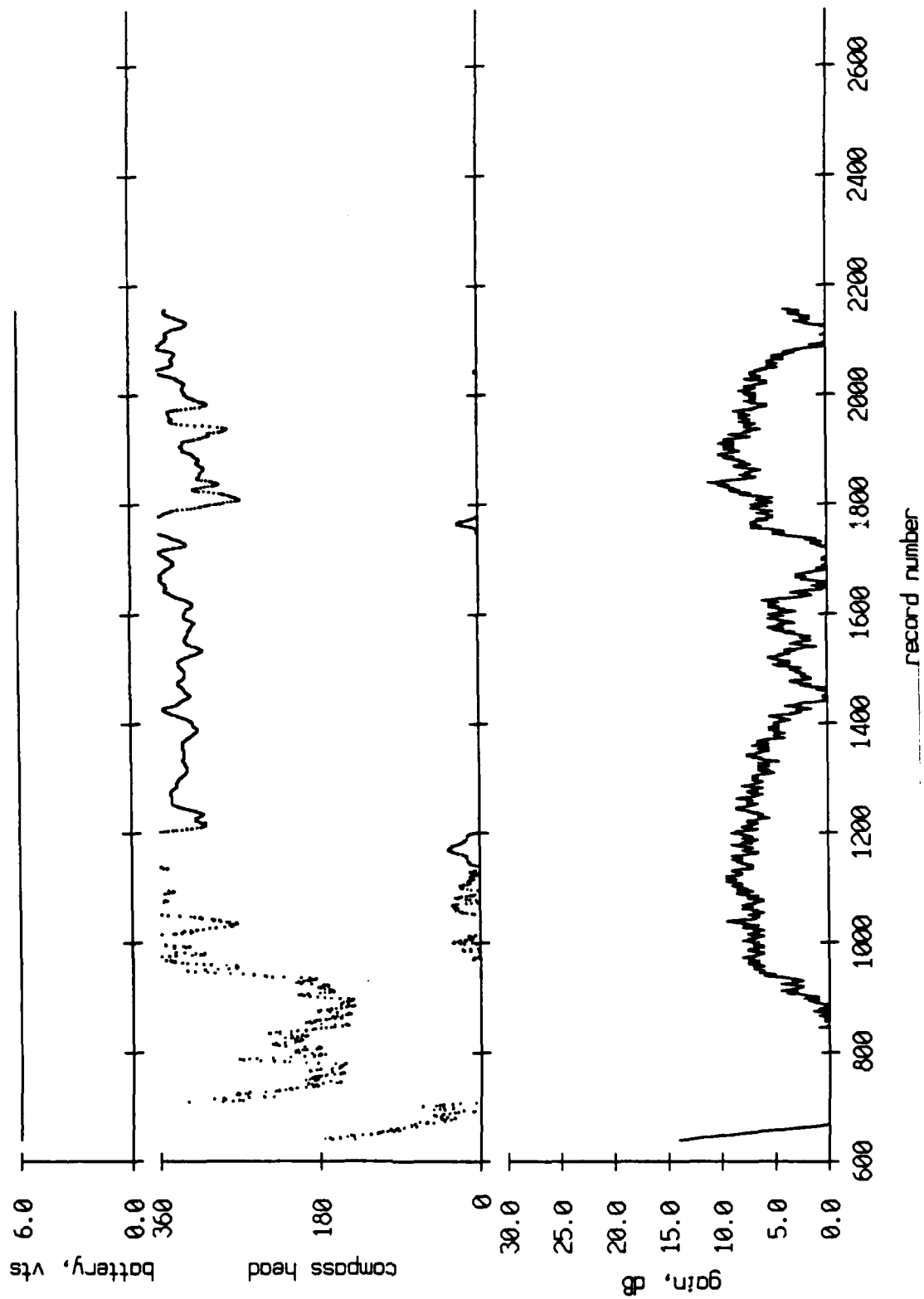


Figure VII.9

# AGC Level and Buoy Heading, Float 9, July 1989 Sea Trip

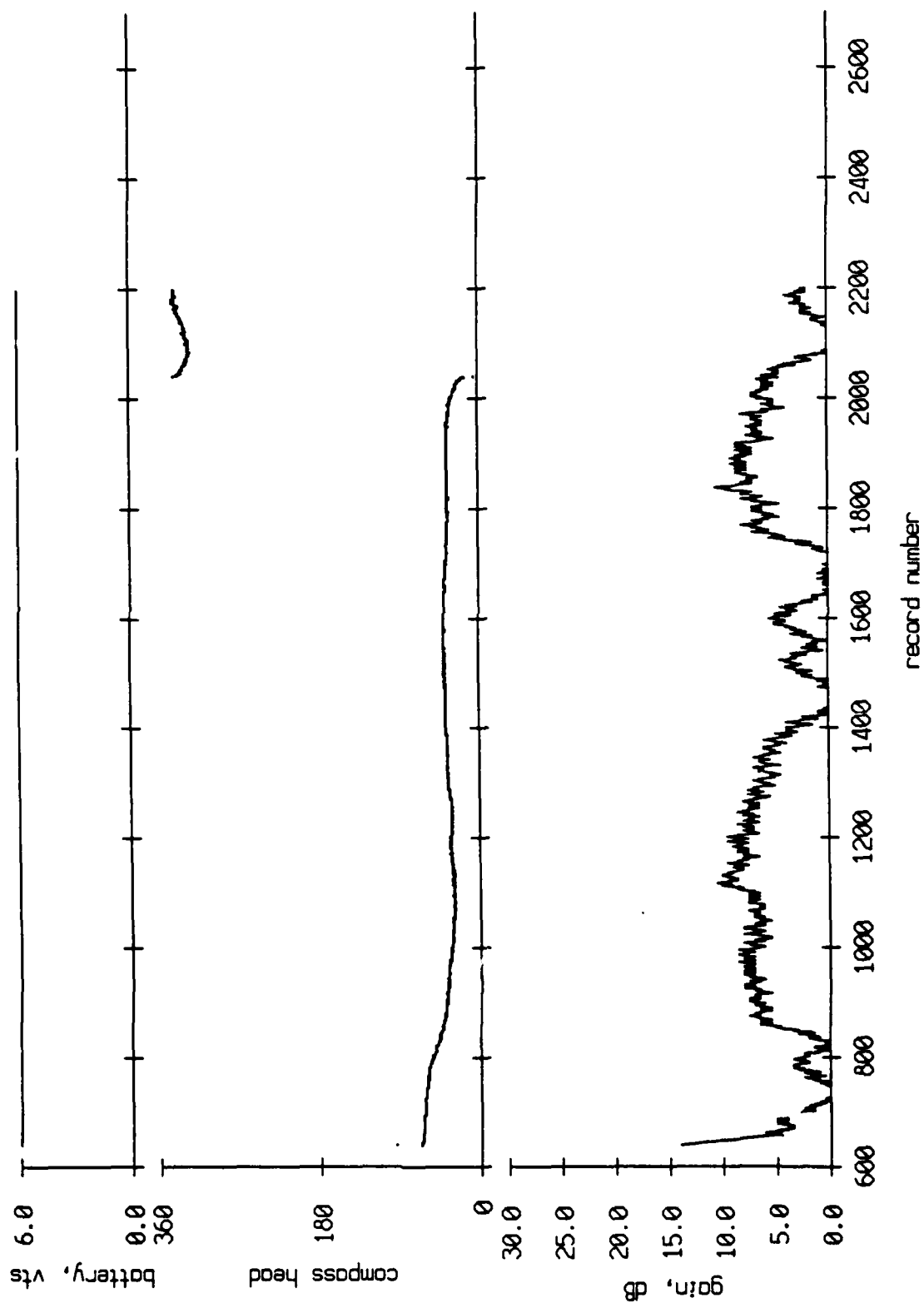


Figure VII.10



# AGC Level and Buoy Heading, Float 10, July 1989 Sea Trip

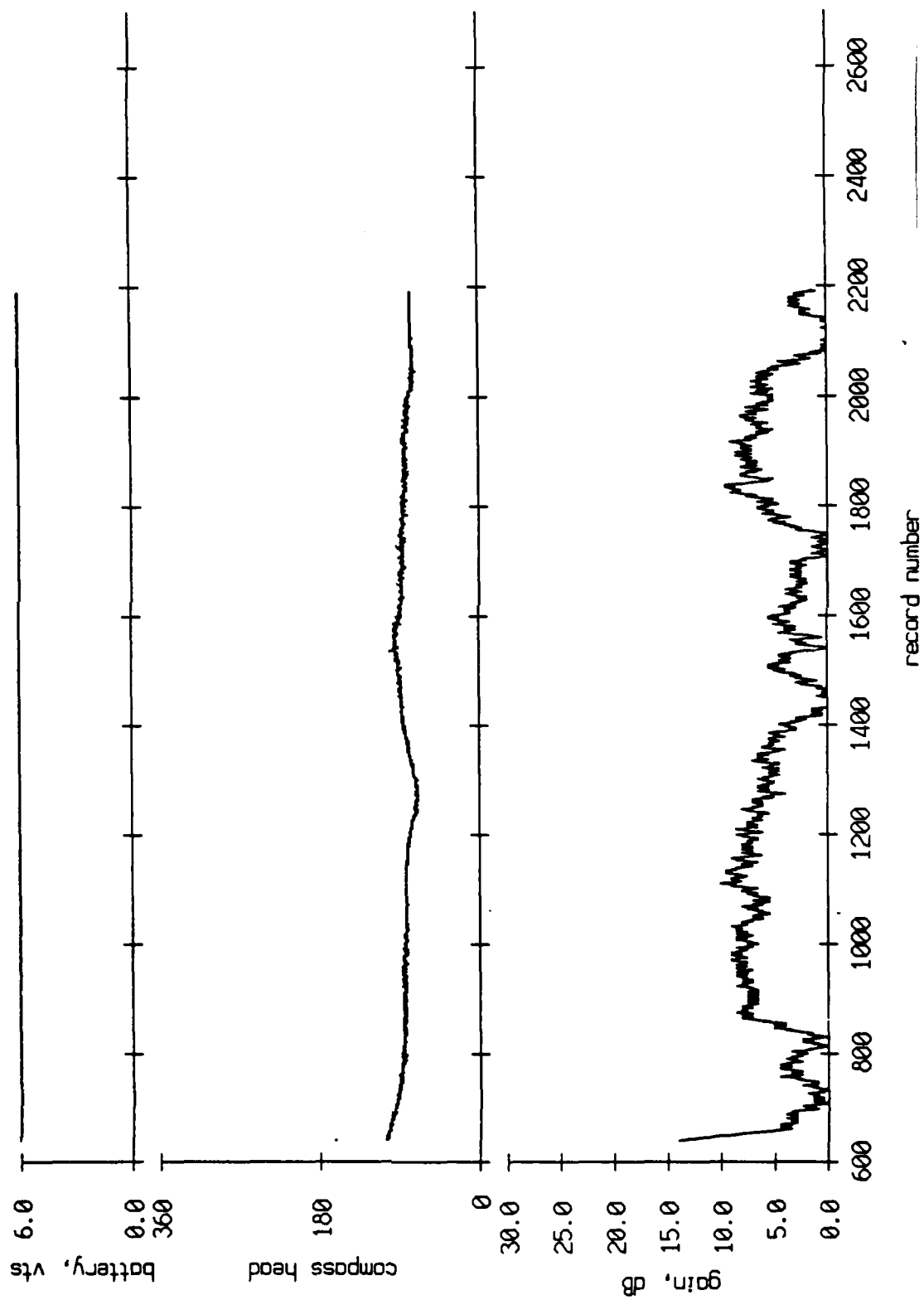


Figure VII.11

# AGC Level and Buoy Heading, Float 11, July 1989 Sea Trip

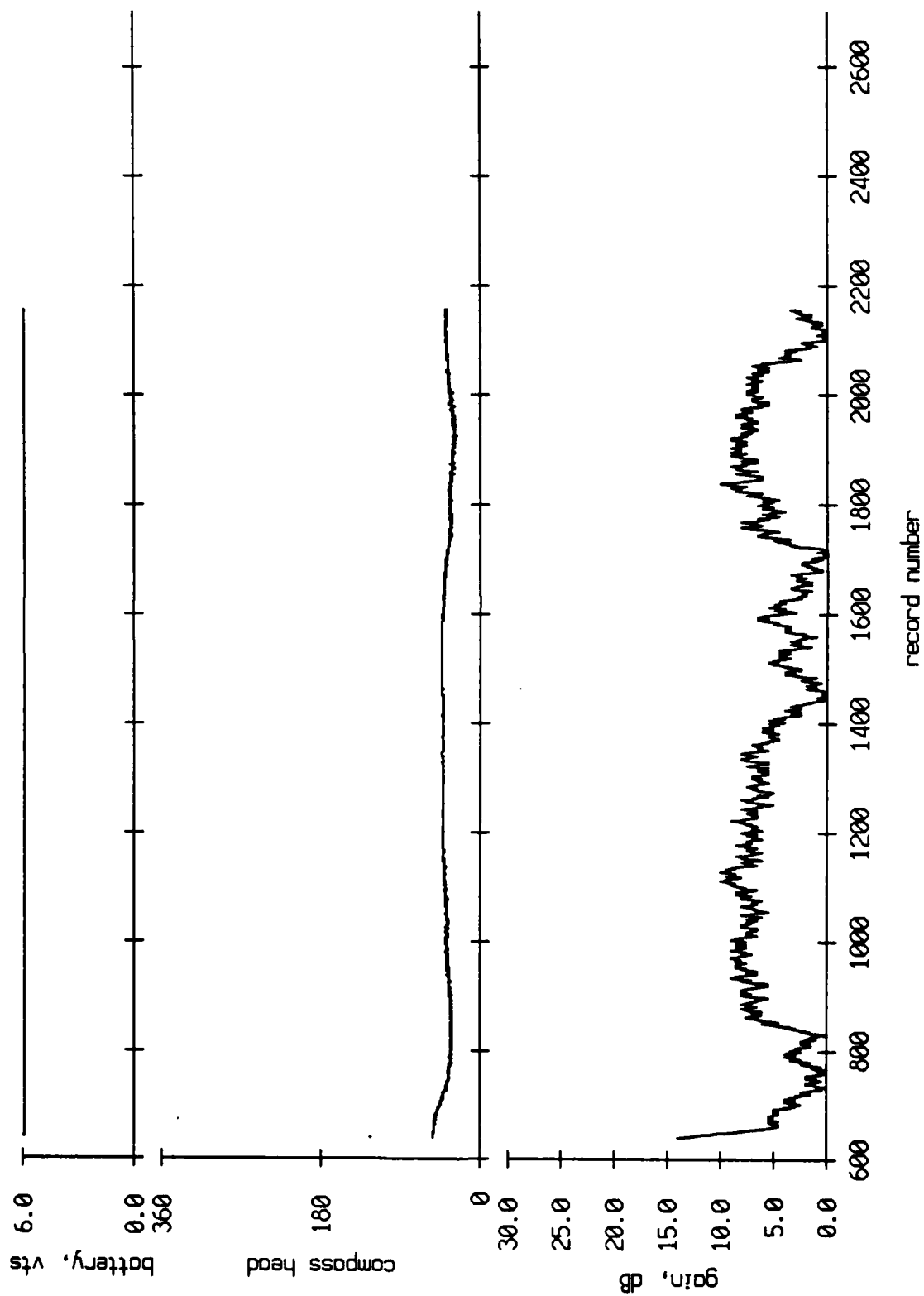
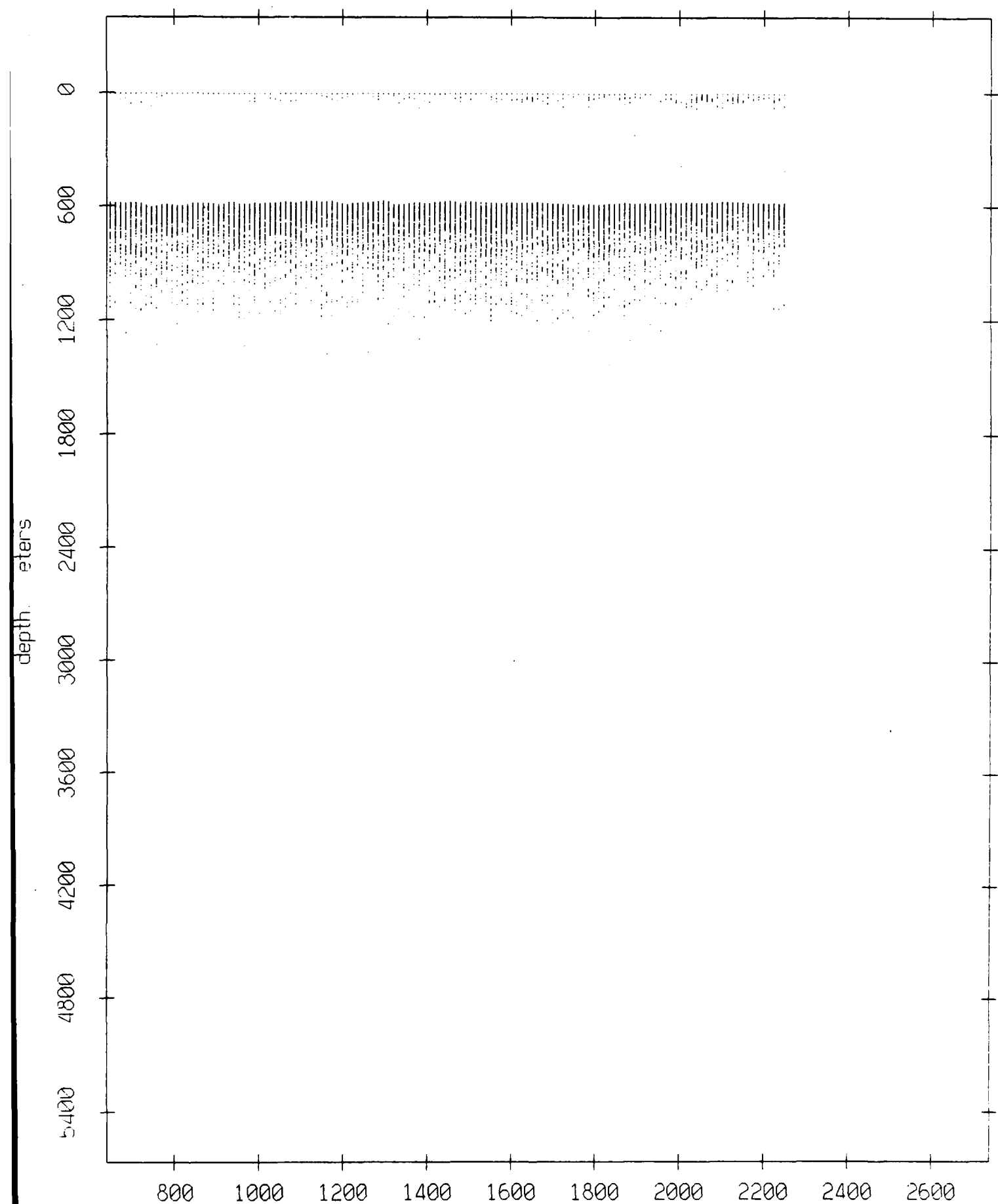


Figure VII.12

Float 0, July 1989 Trip: surface & bottom bounces



record number

Figure VIII.1

Float 1, July 1989 Trip: surface & bottom bounces

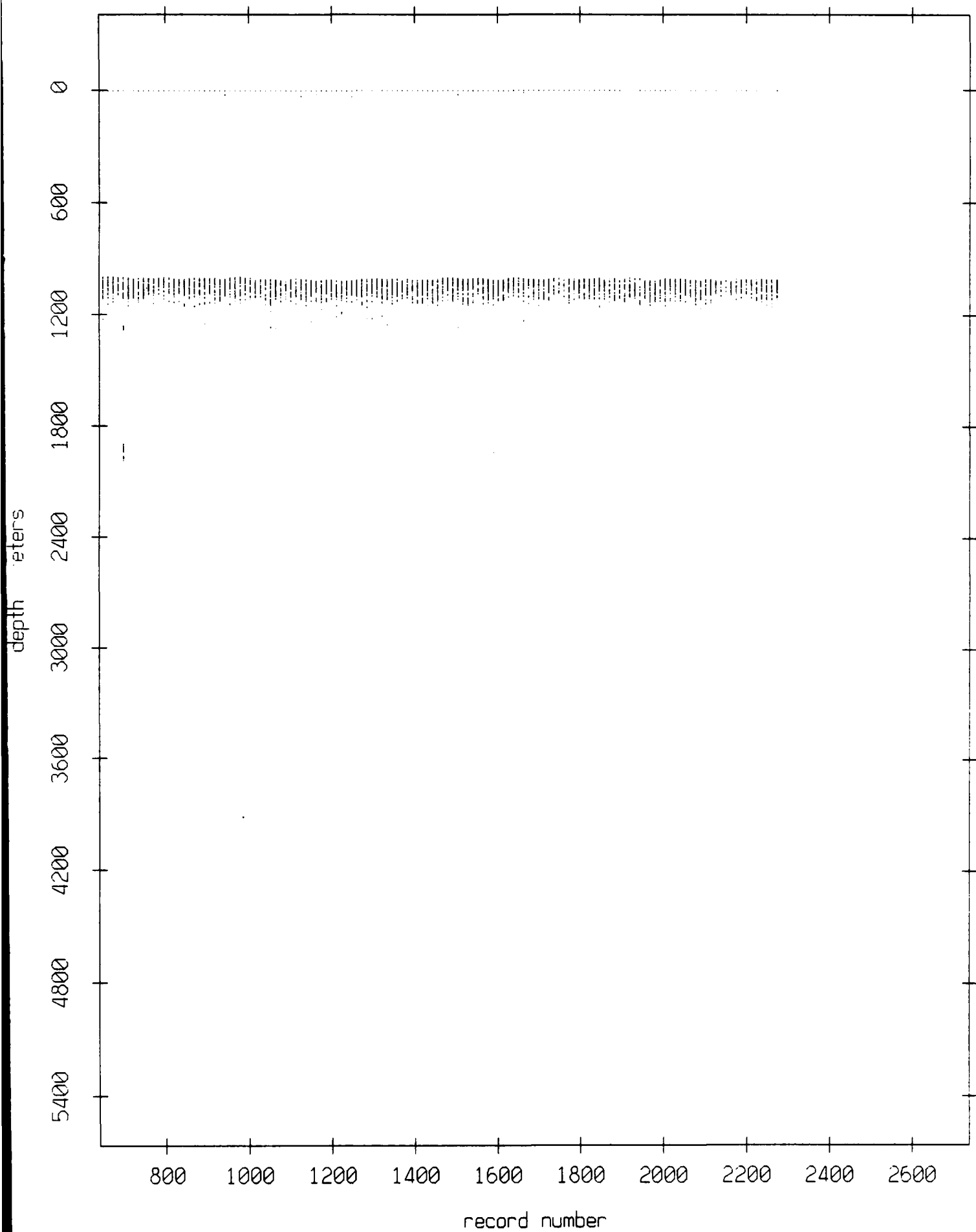


Figure VIII.2

Float 2, July 1989 Trip: surface & bottom bounces

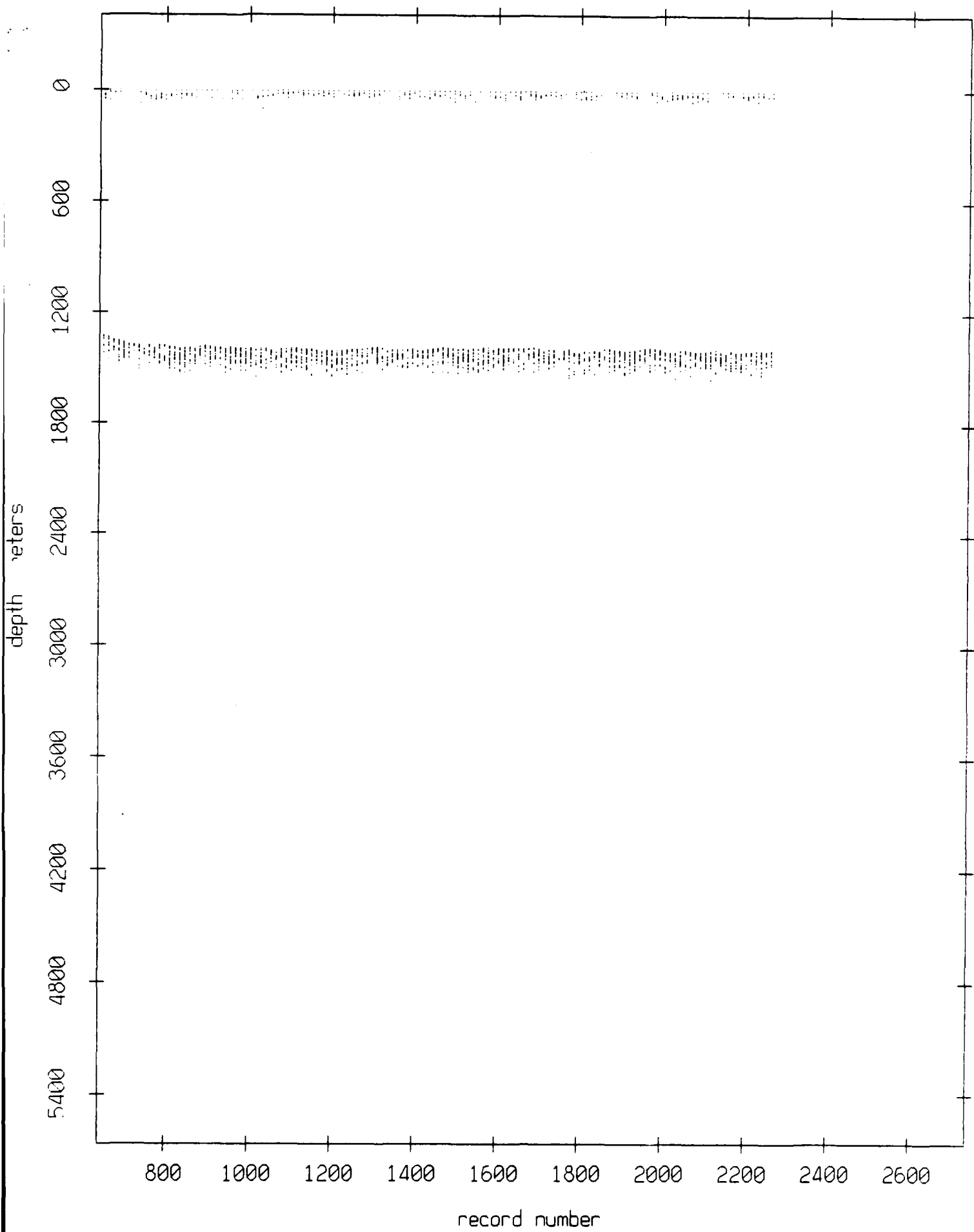
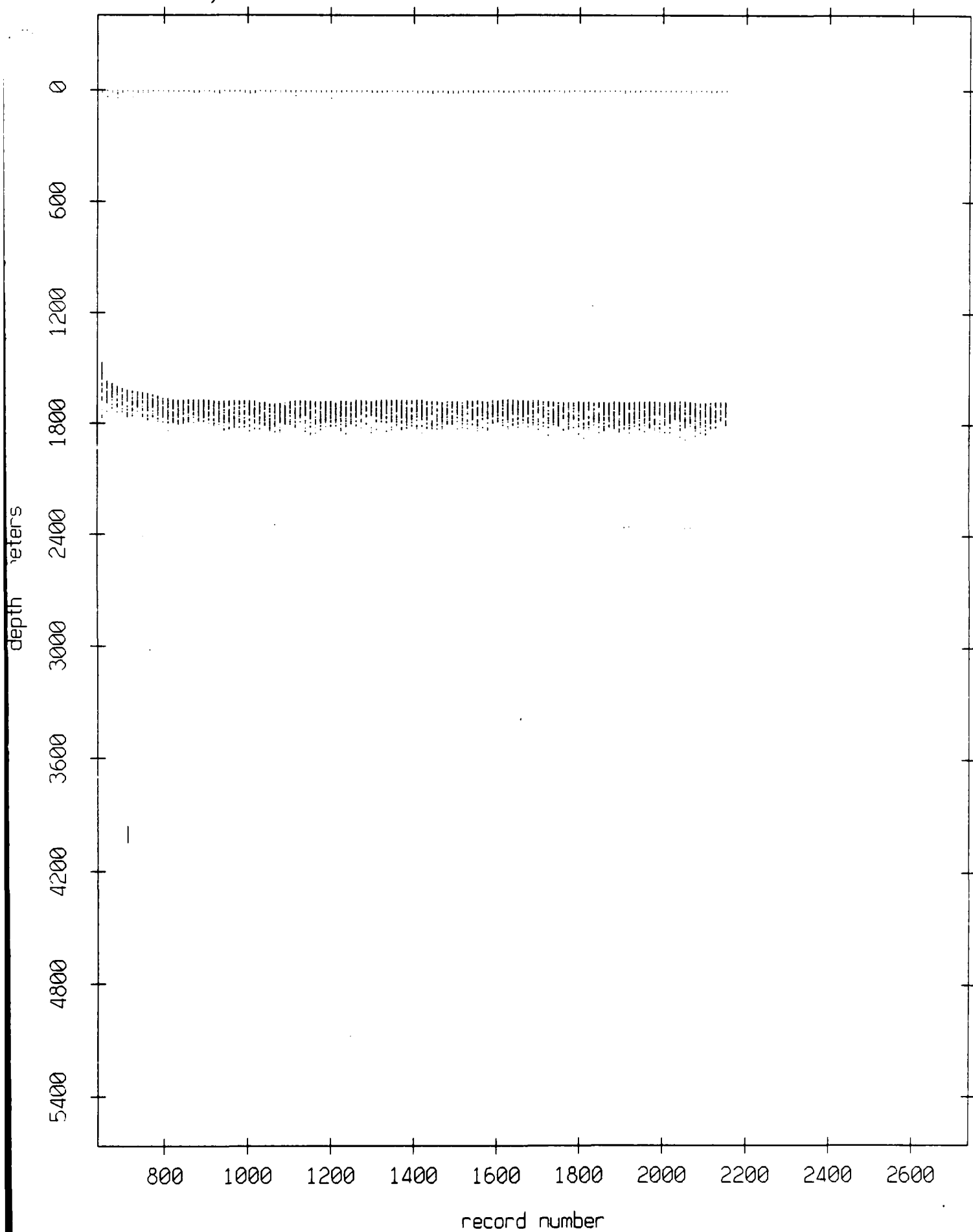
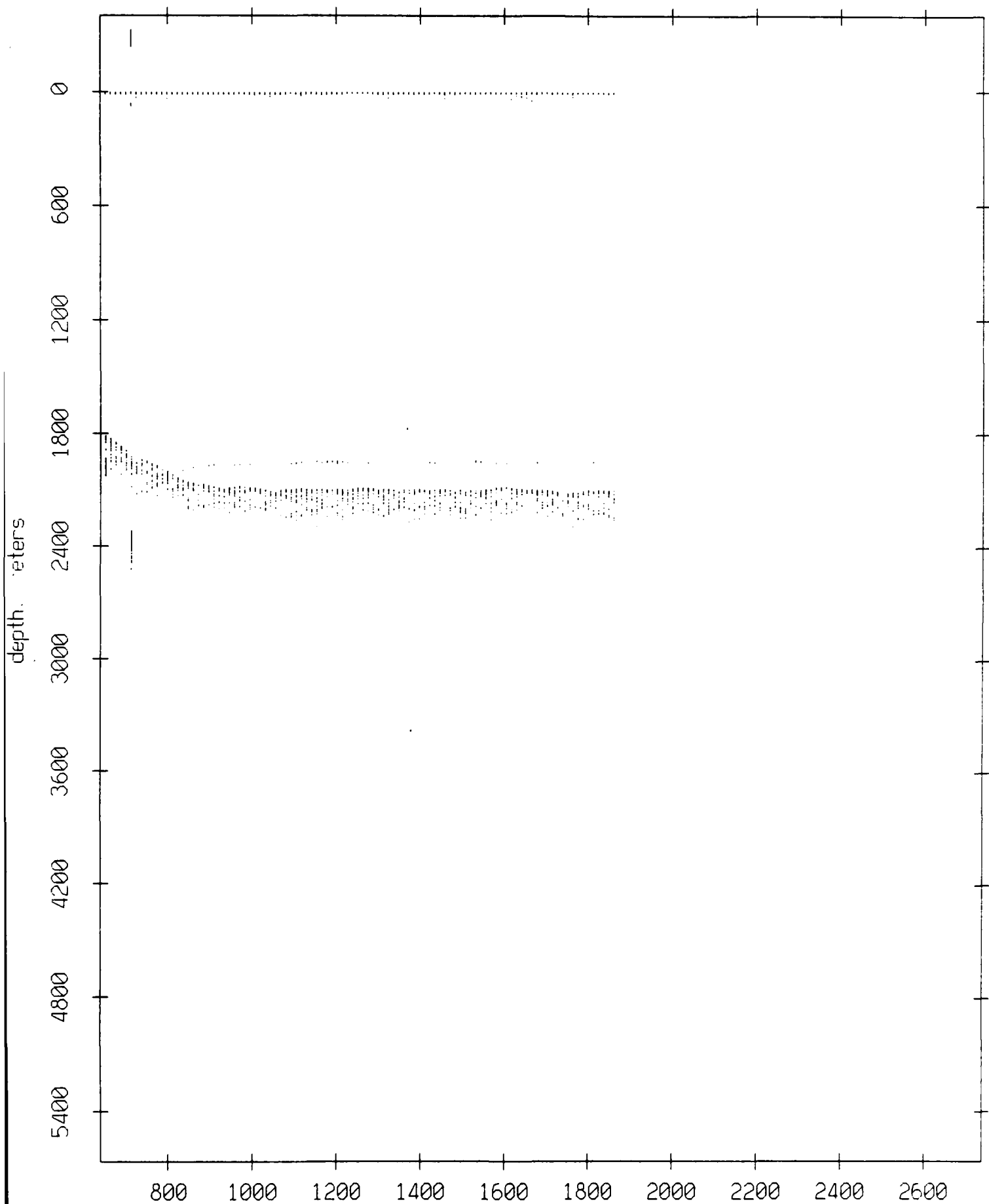


Figure VIII.3

Float 3, July 1989 Trip: surface & bottom bounces



Float 4, July 1989 Trip: surface & bottom bounces



record number

Figure VIII.5

Float 5, July 1989 Trip: surface & bottom bounces

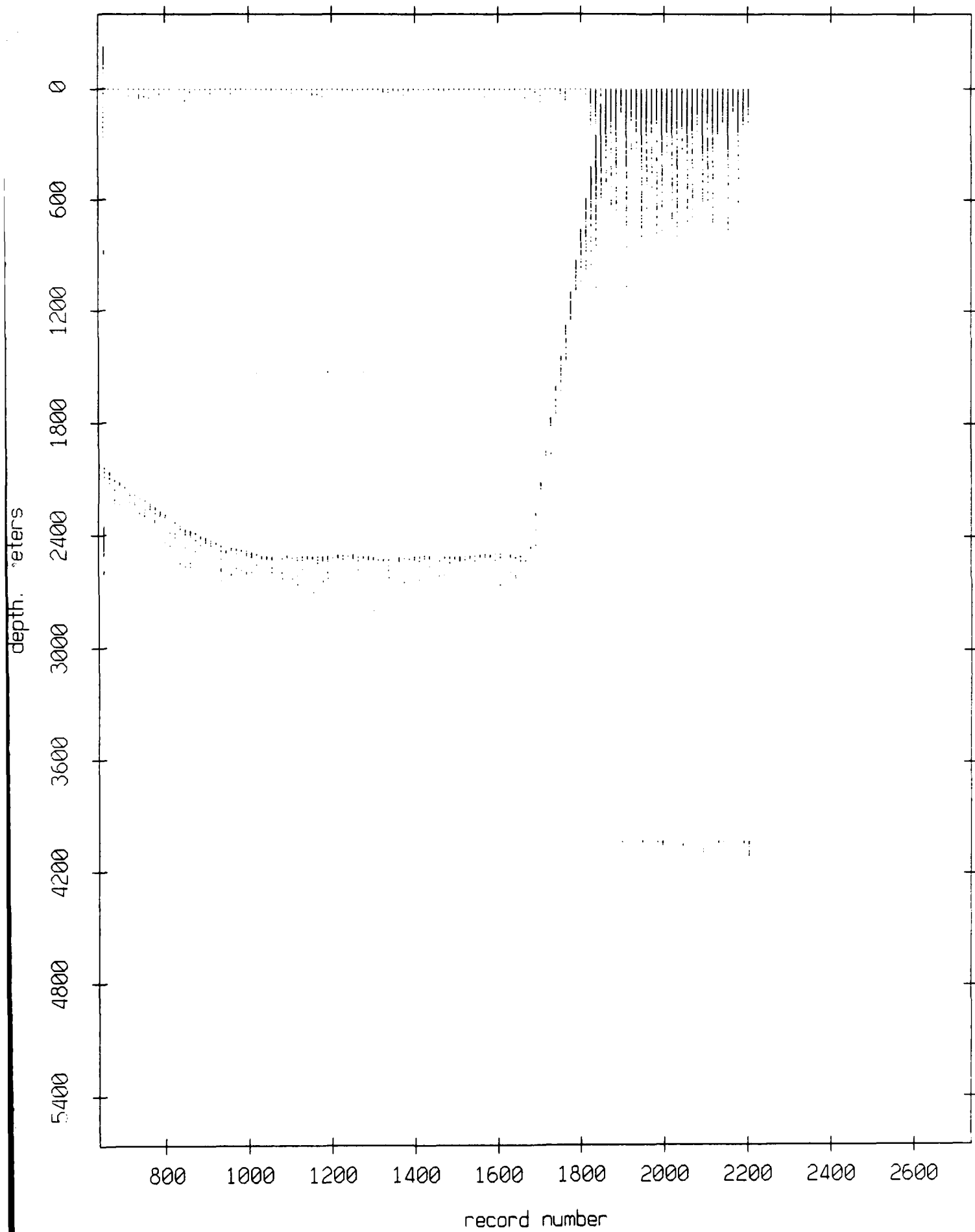
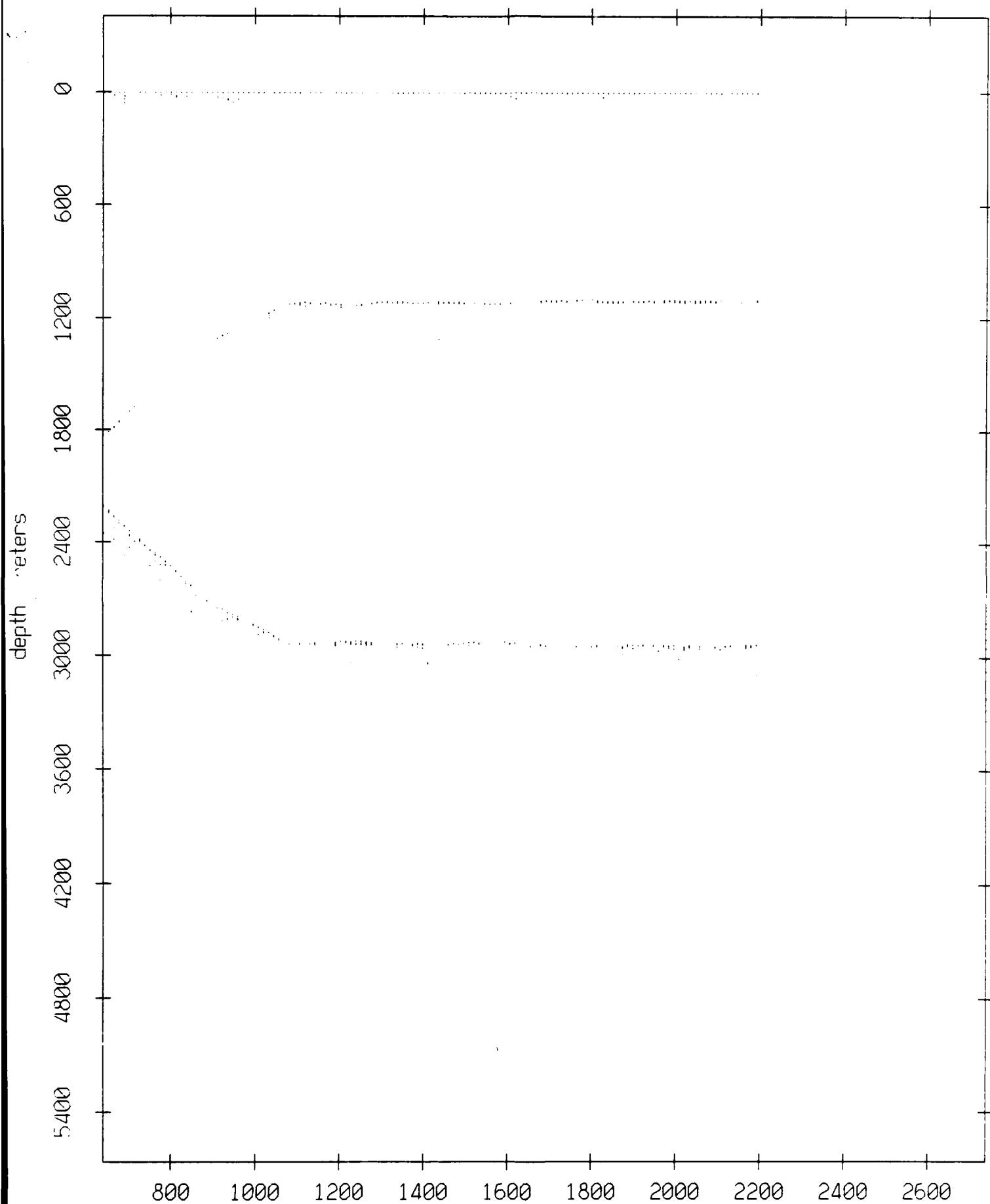


Figure VIII.6



Float 6, July 1989 Trip: surface & bottom bounces



record number

Figure VIII.7

Float 7, July 1989 Trip: surface & bottom bounces

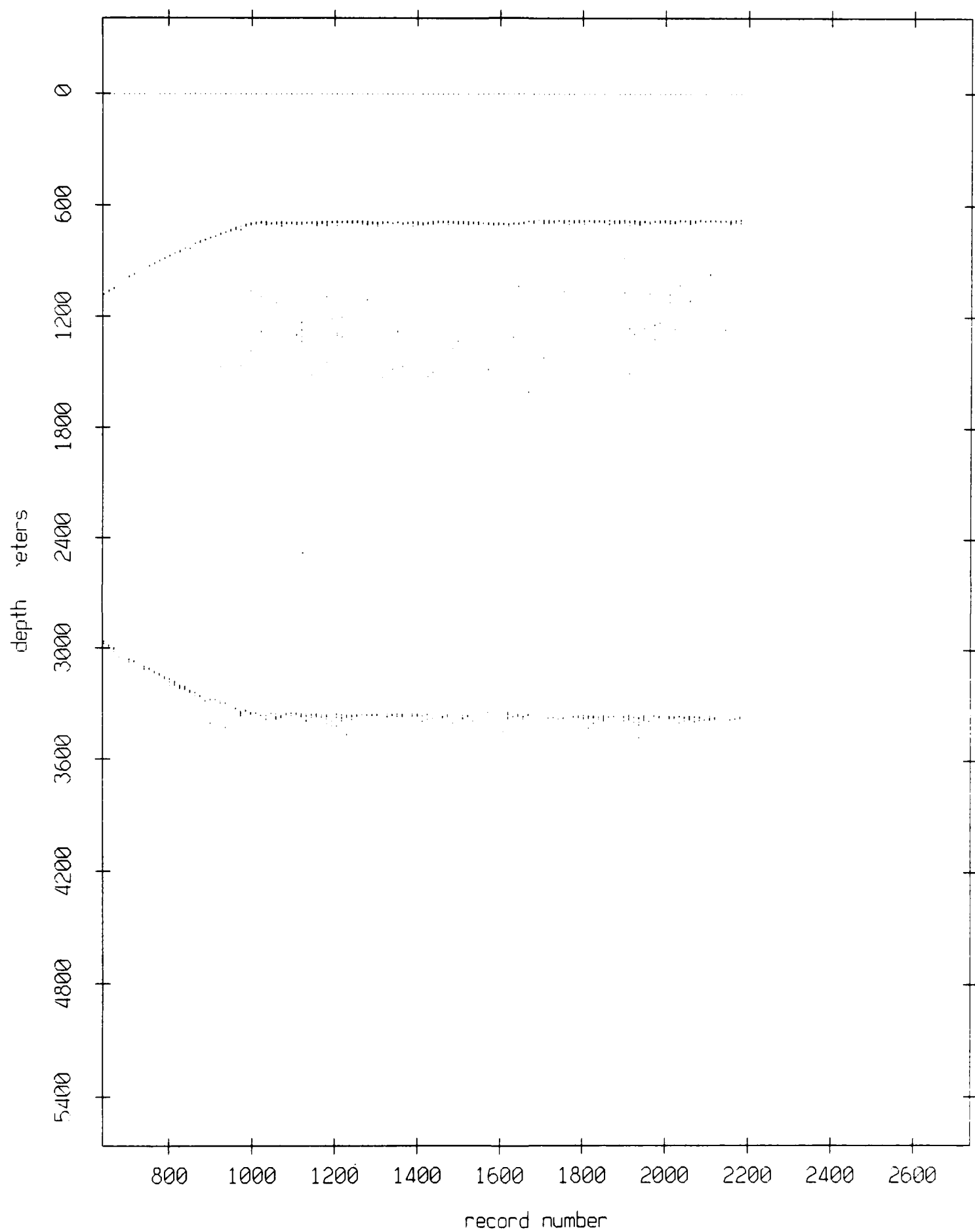
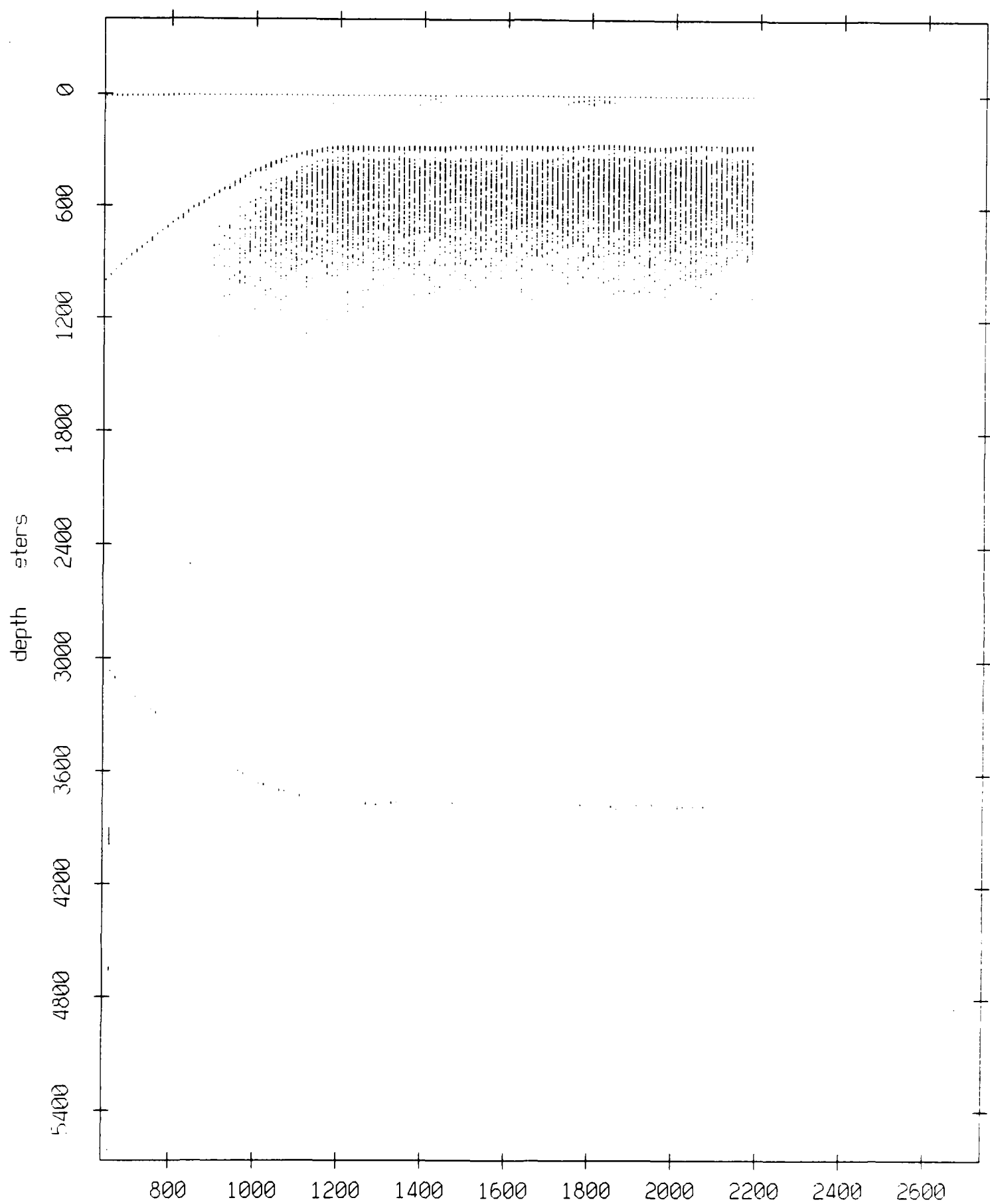


Figure VIII.8

Float 8, July 1989 Trip: surface & bottom bounces



record number  
**Figure VIII.9**

Float 9, July 1989 Trip: surface & bottom bounces

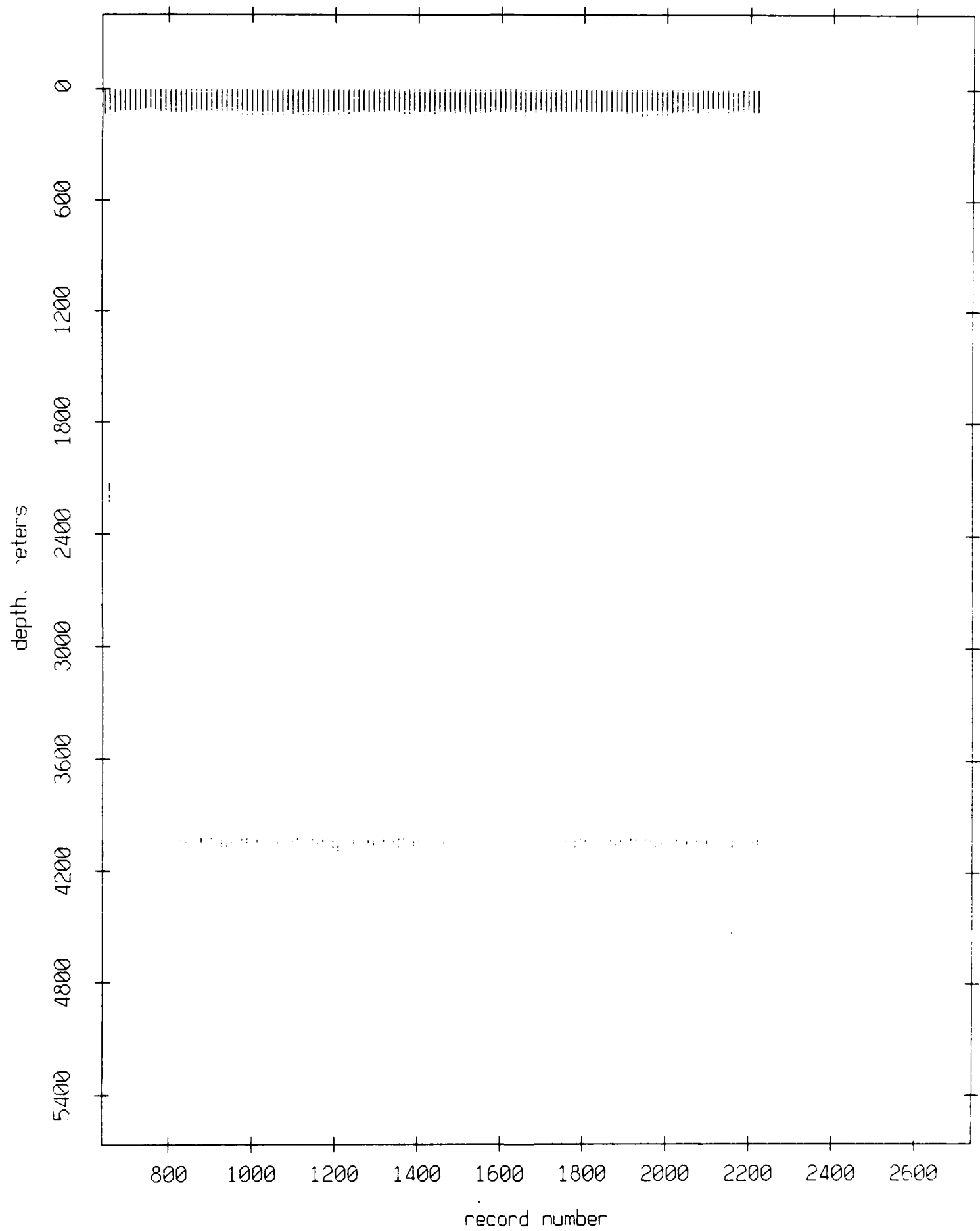


Figure VIII.10

Float 10, July 1989 Trip: surface & bottom bounces

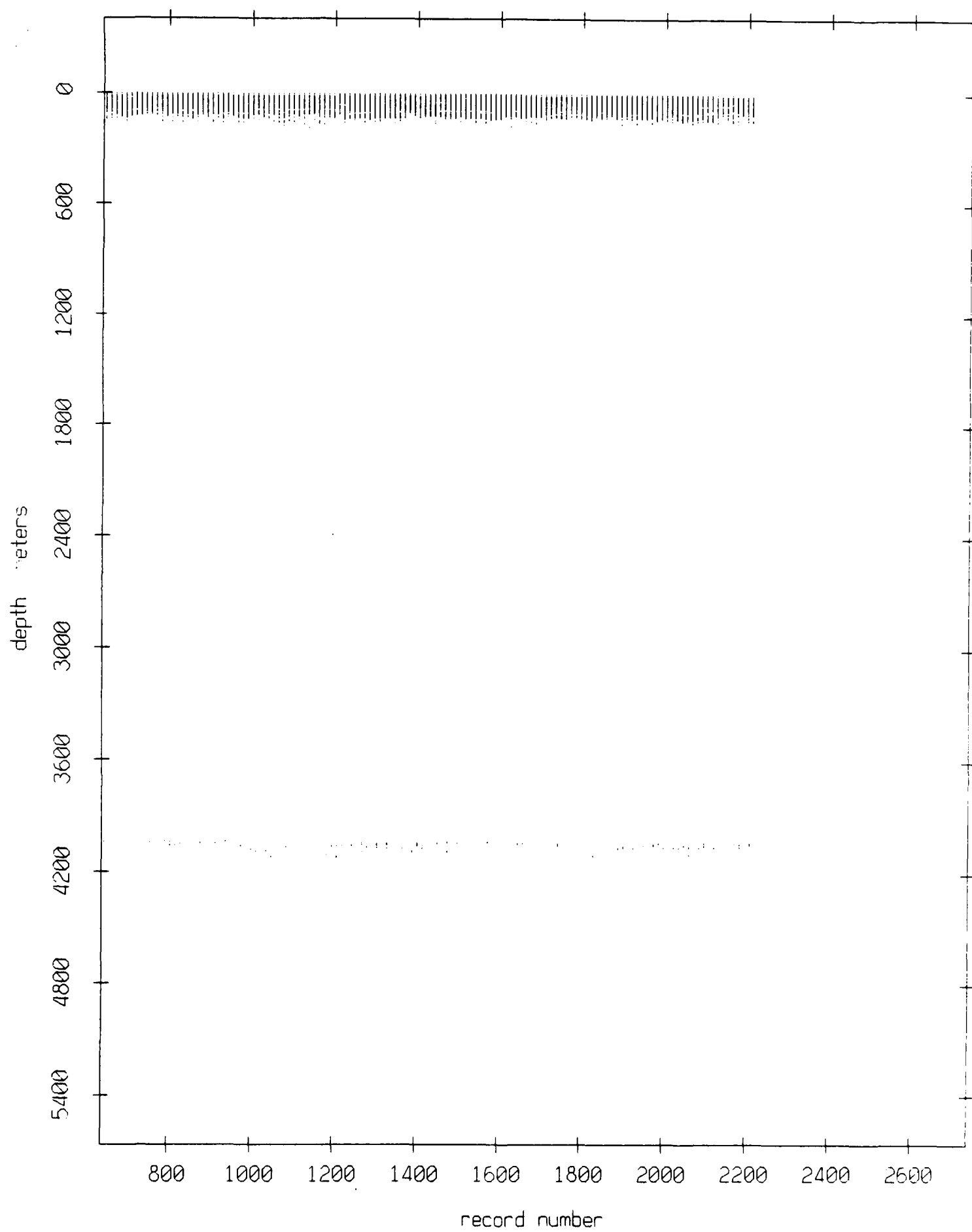
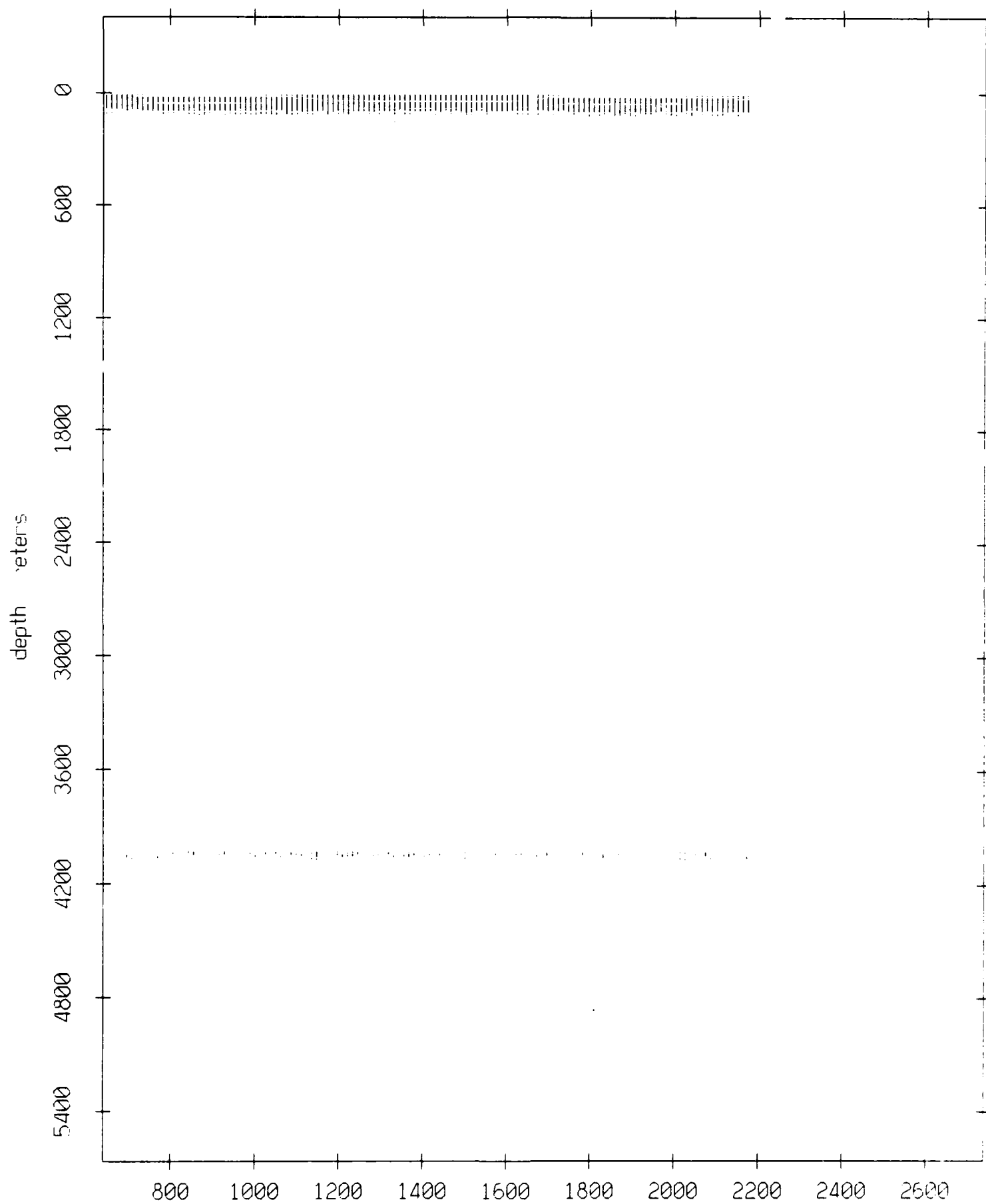


Figure VIII.11

Float 11, July 1989 Trip: surface & bottom bounces



record number  
**Figure VIII.12**

Float 0, July 1989 Trip: range from float 1

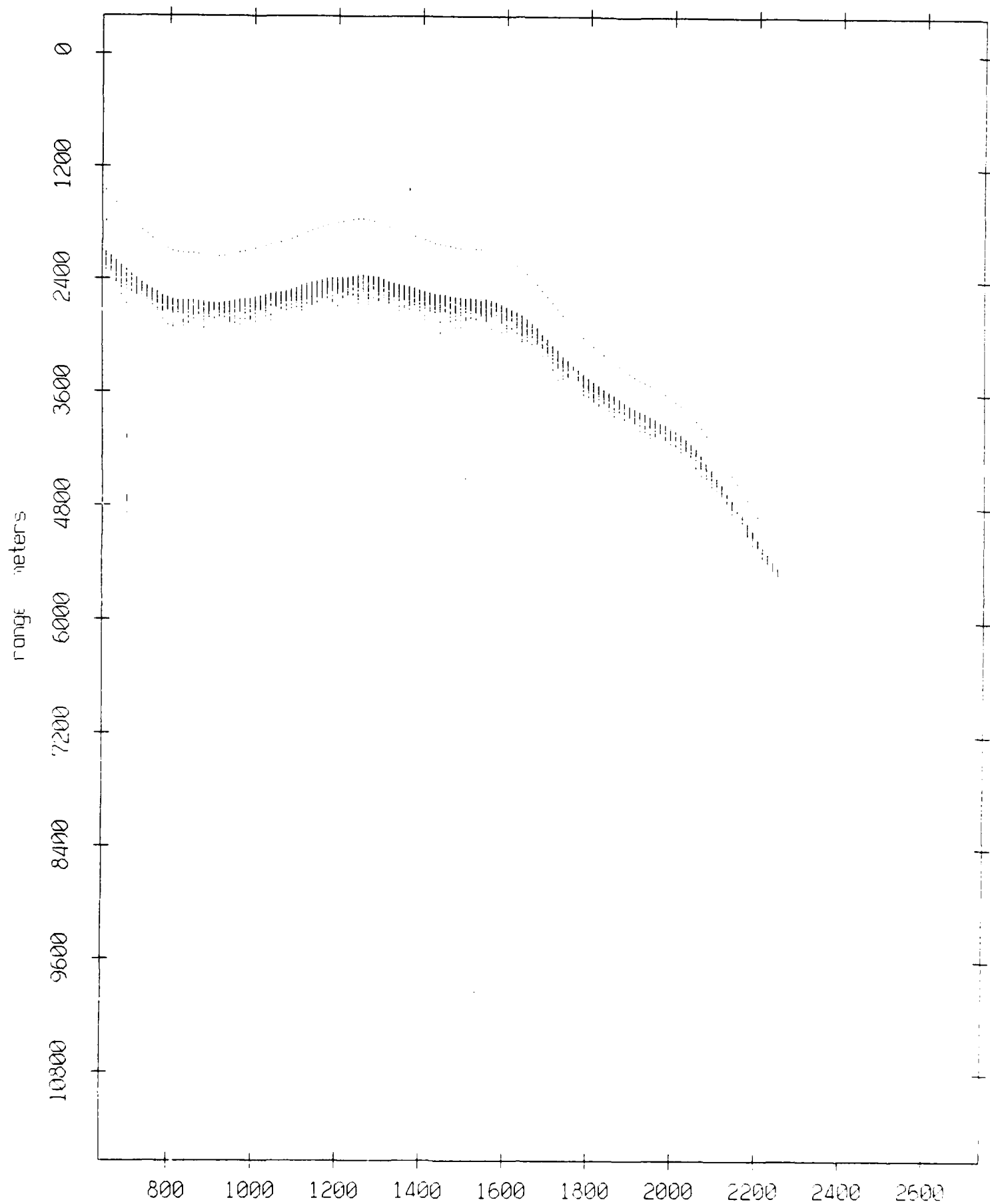
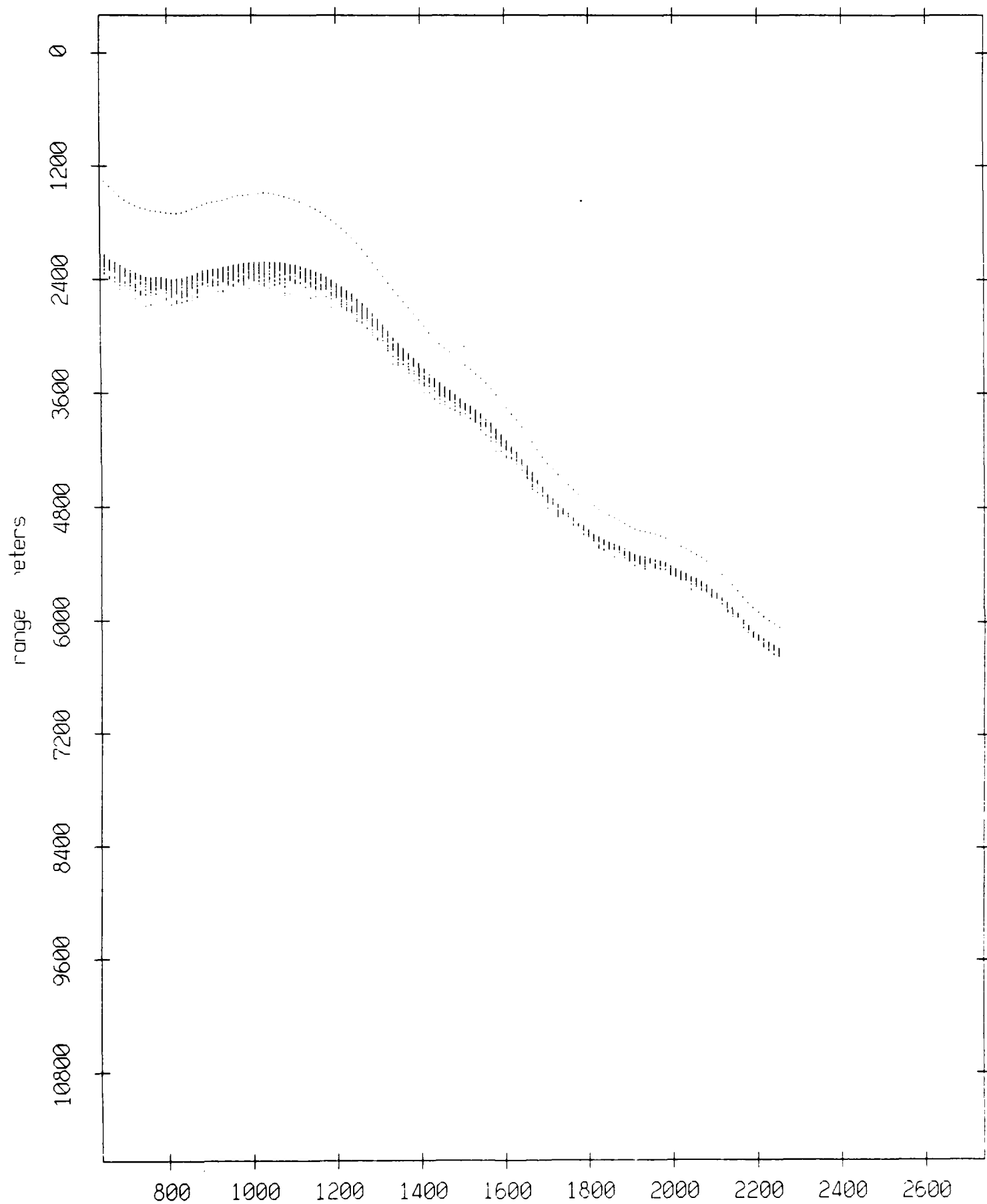


Figure IX.1a

Float 0, July 1989 Trip: range from float 2



record number

Figure IX.1b



Float 0, July 1989 Trip: range from float 3

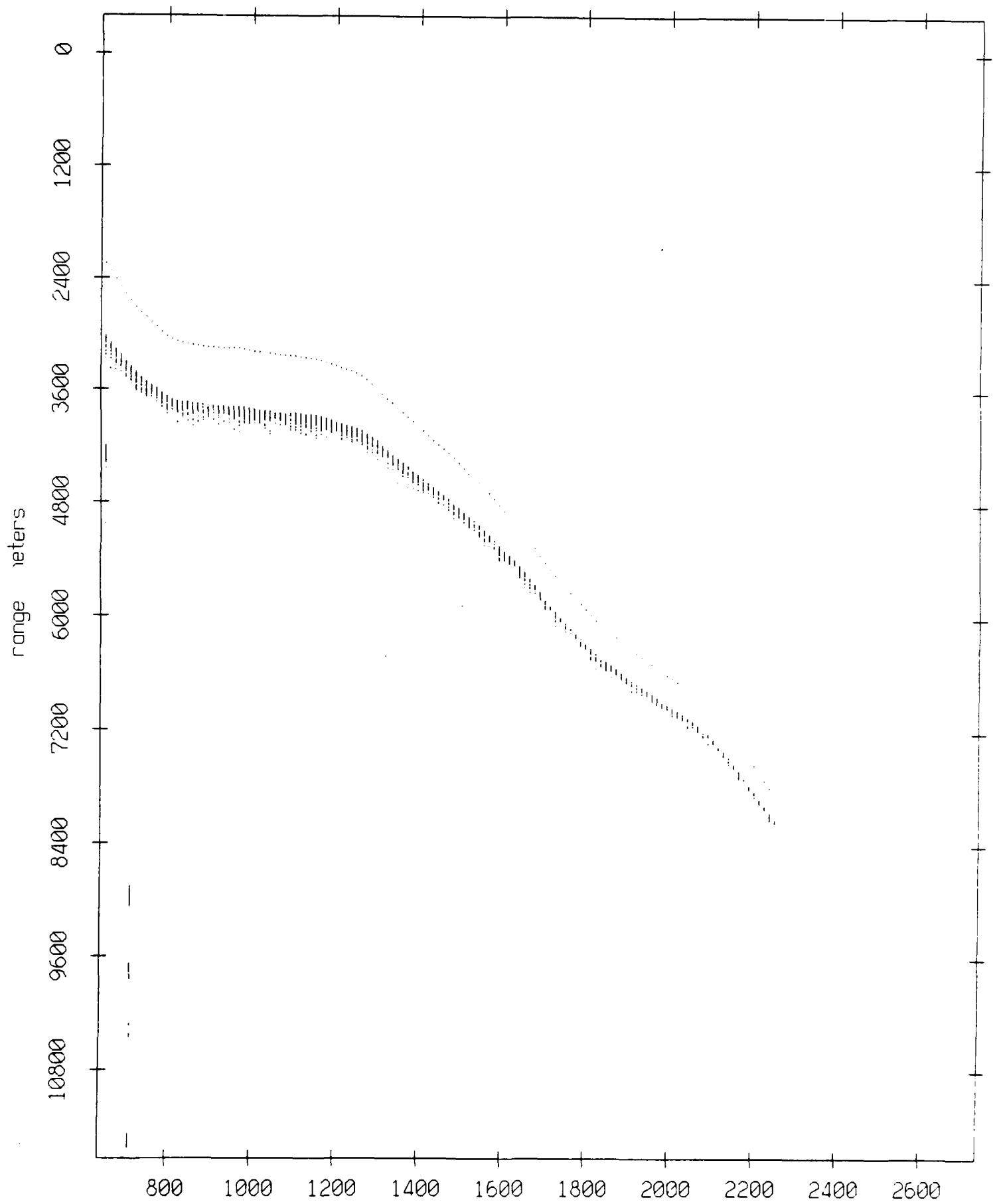
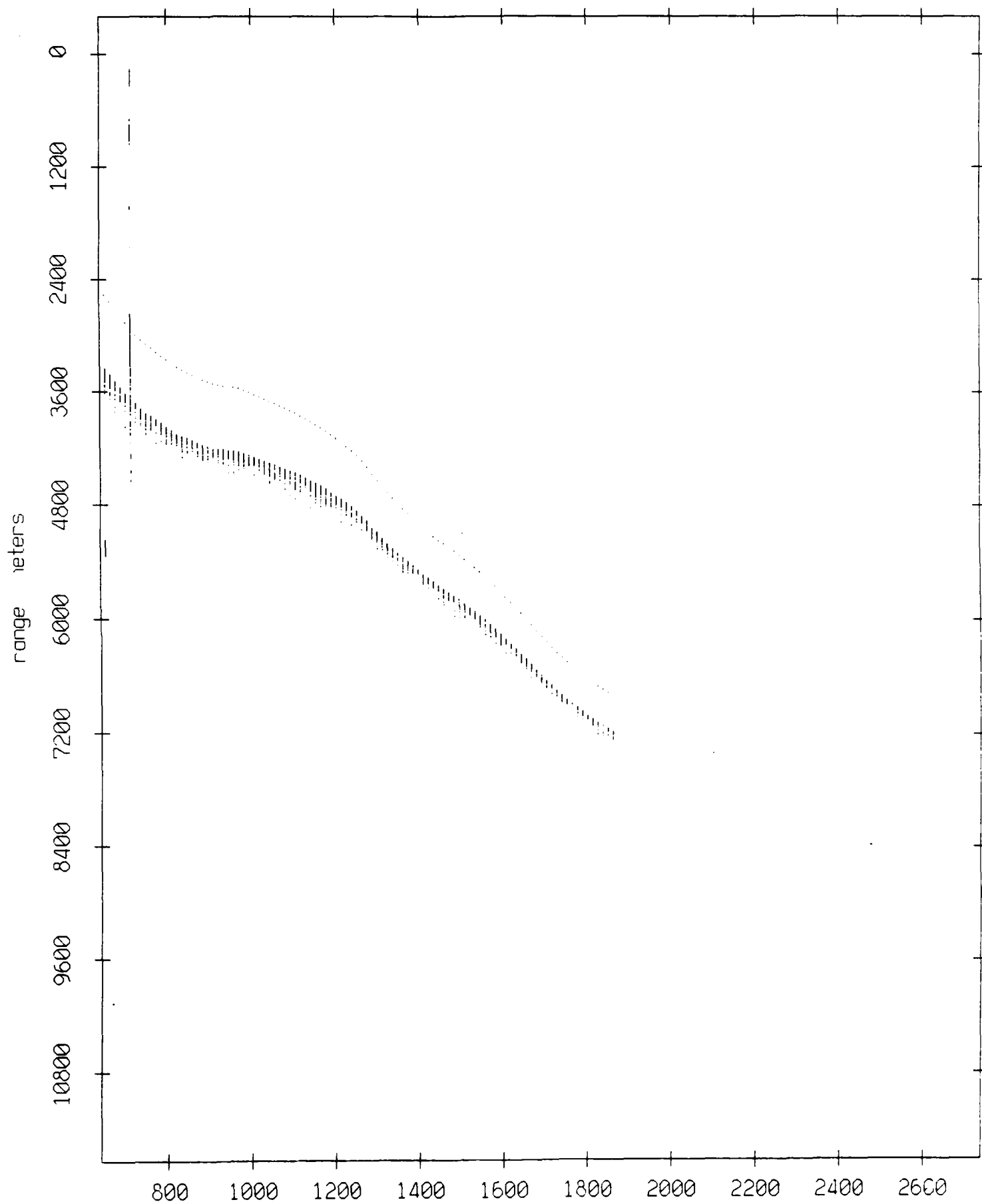


Figure IX.1c

Float 0, July 1989 Trip: range from float 4



record number

Figure IX.1d

Float 0, July 1989  $\tau$  :p: range from float 5

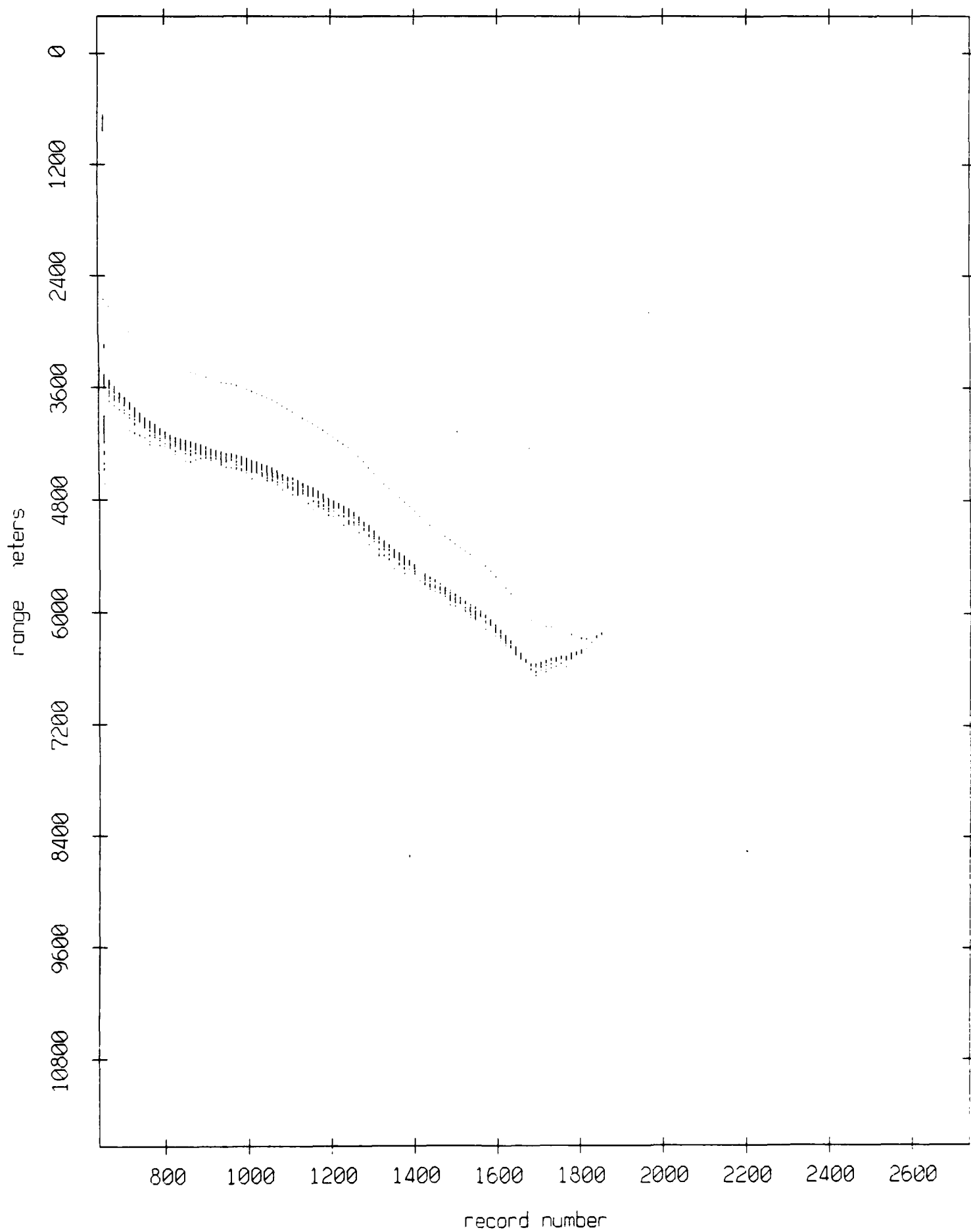


Figure IX.1e

Float 0, July 1989 Trip: range from float 6

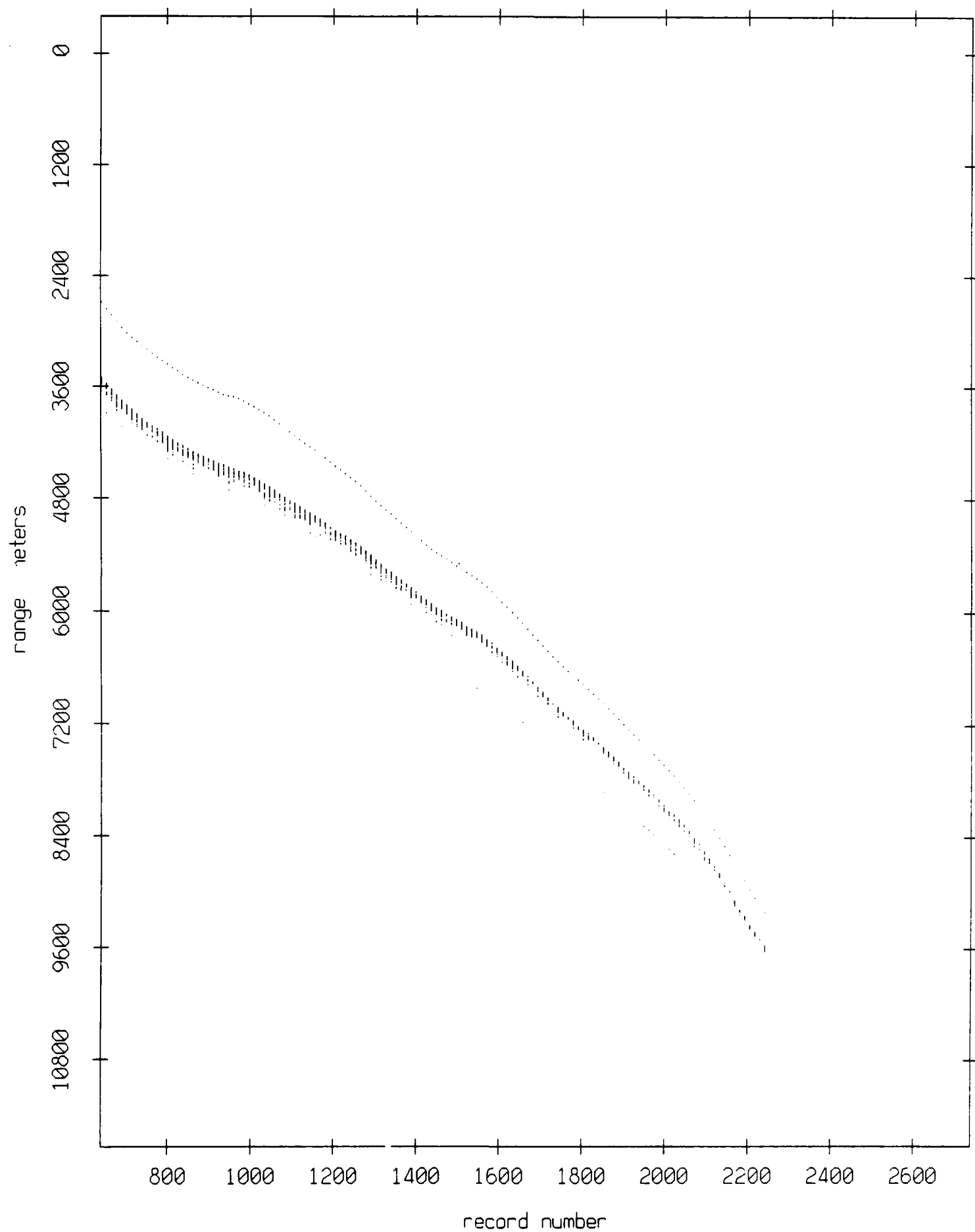
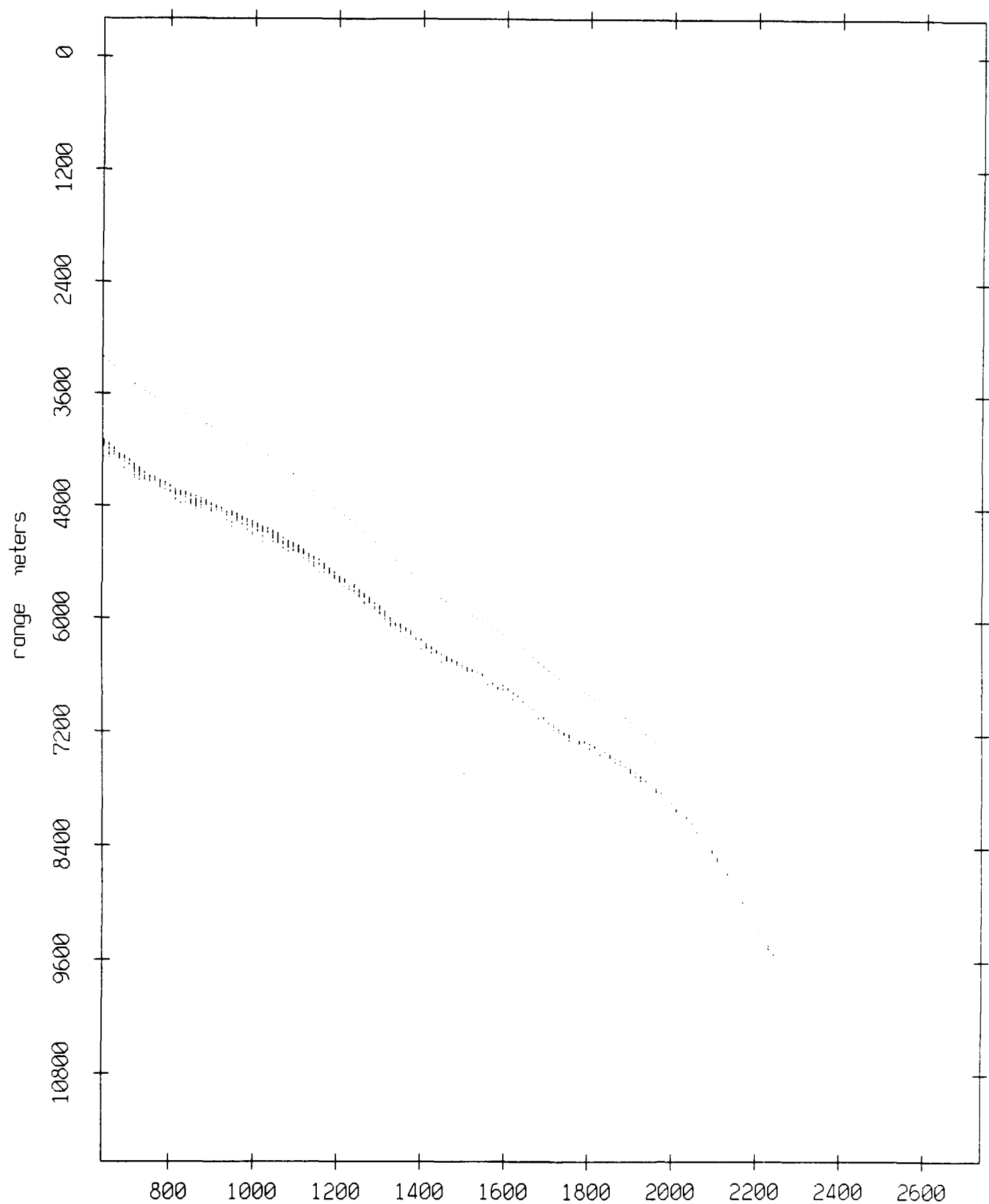


Figure IX.1f

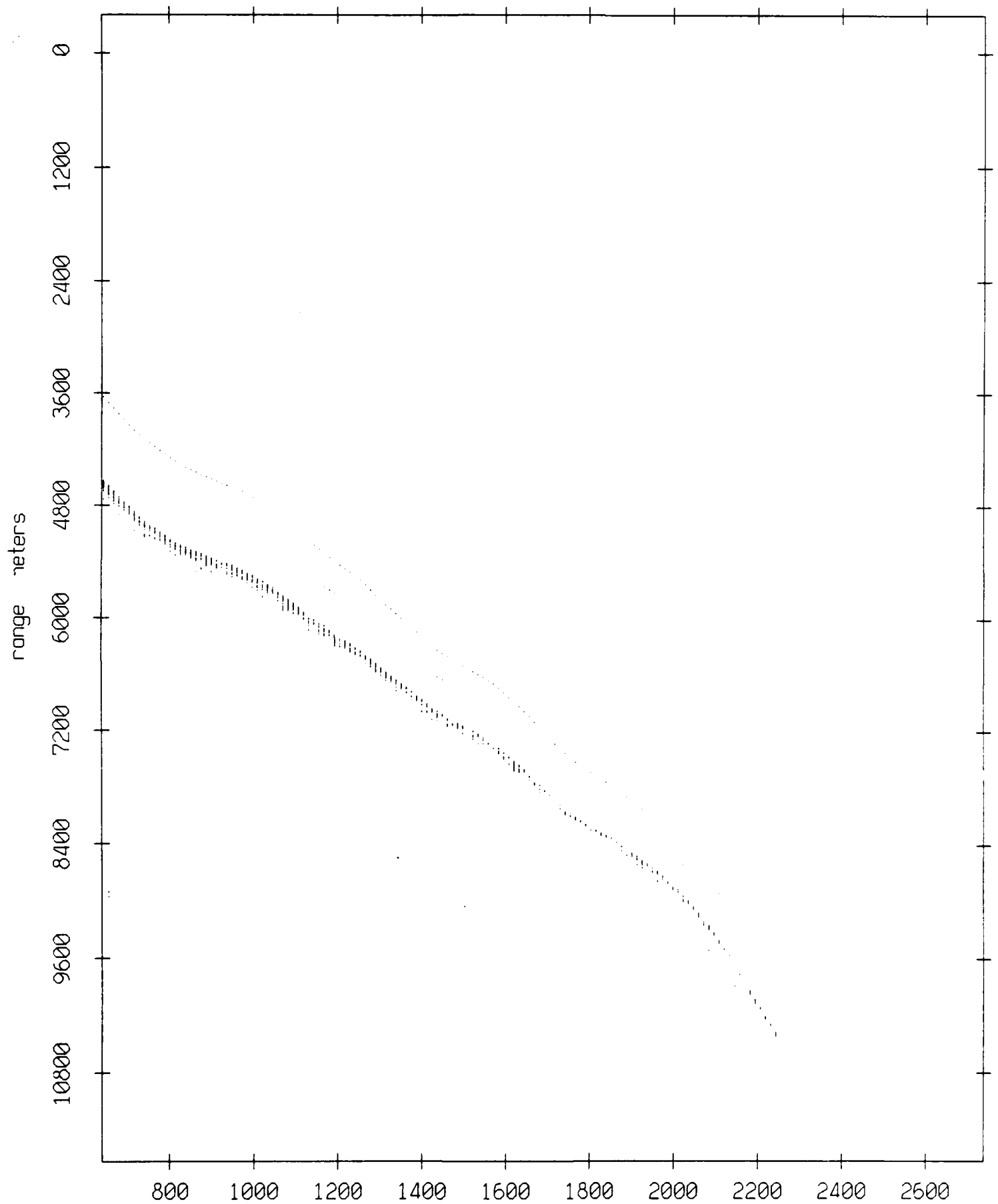
Float 0, July 1989 Trip: range from float 7



record number

Figure IX.1g

Float 0, July 1989 Trip: range from float 8



record number

**Figure IX.1h**

Float 0, July 1989 Trip: range from float 9

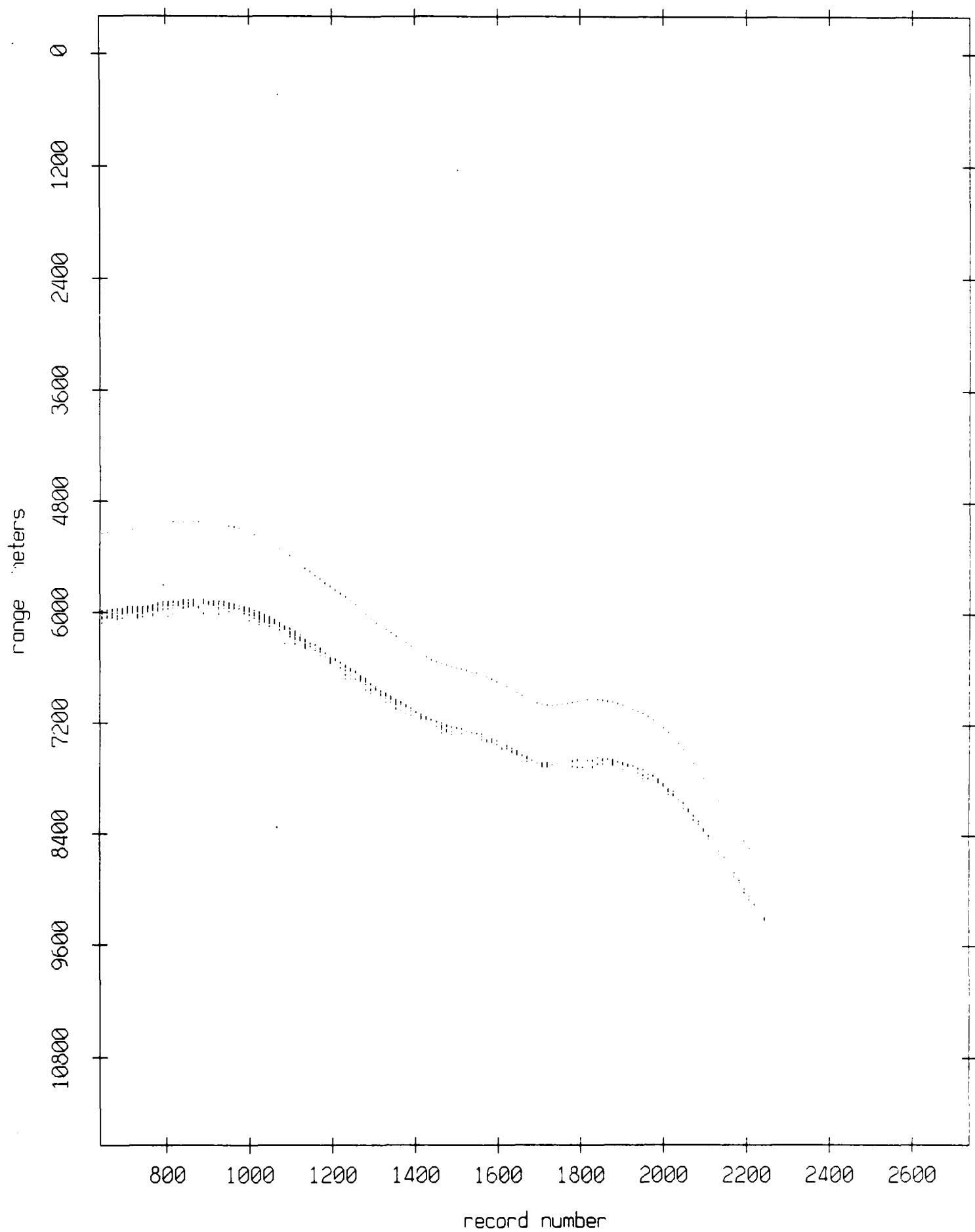


Figure IX.11

Float 0, July 1989 Trip: range from float 10

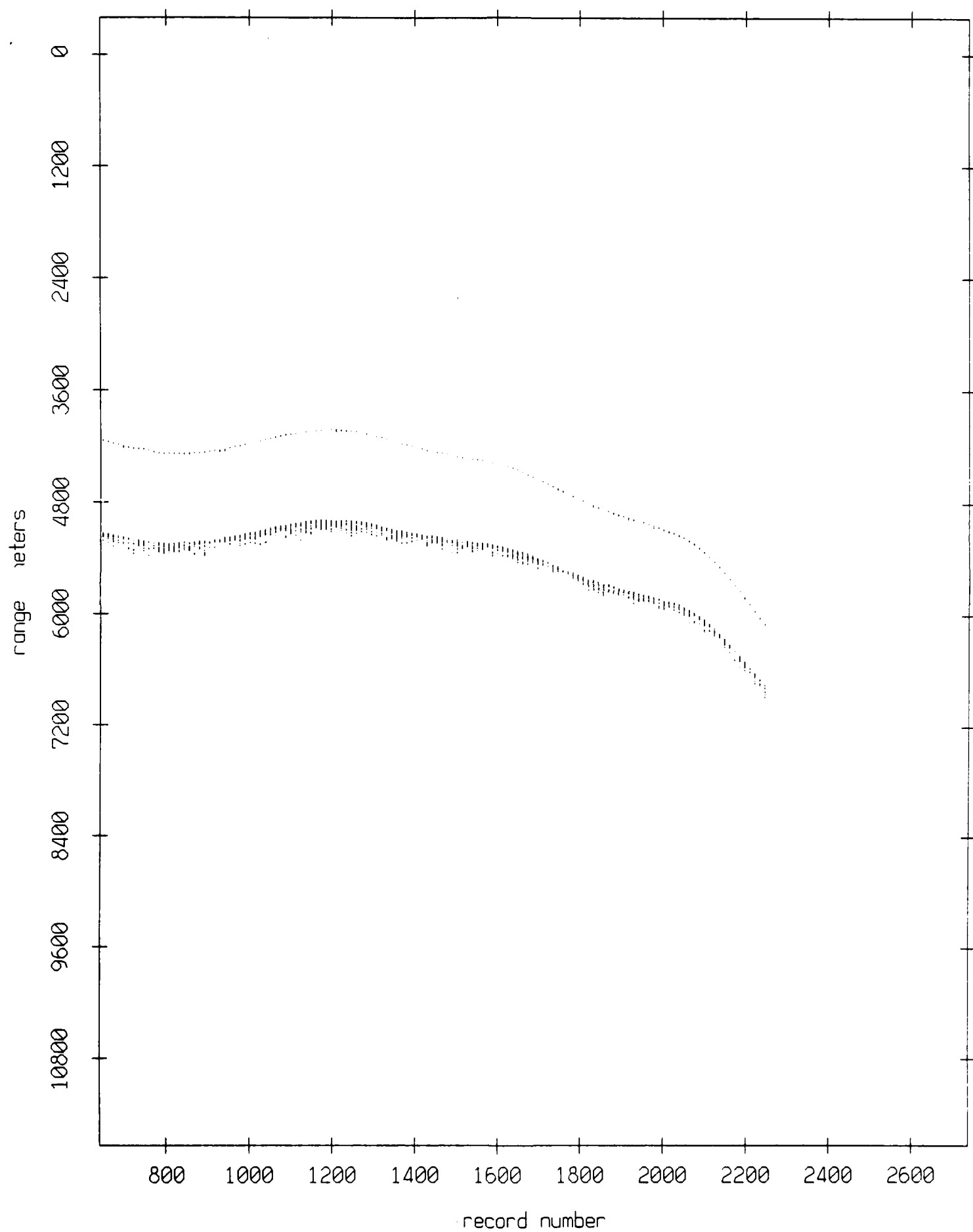


Figure IX.1j



Float 0, July 1989 Trip: range from float 11

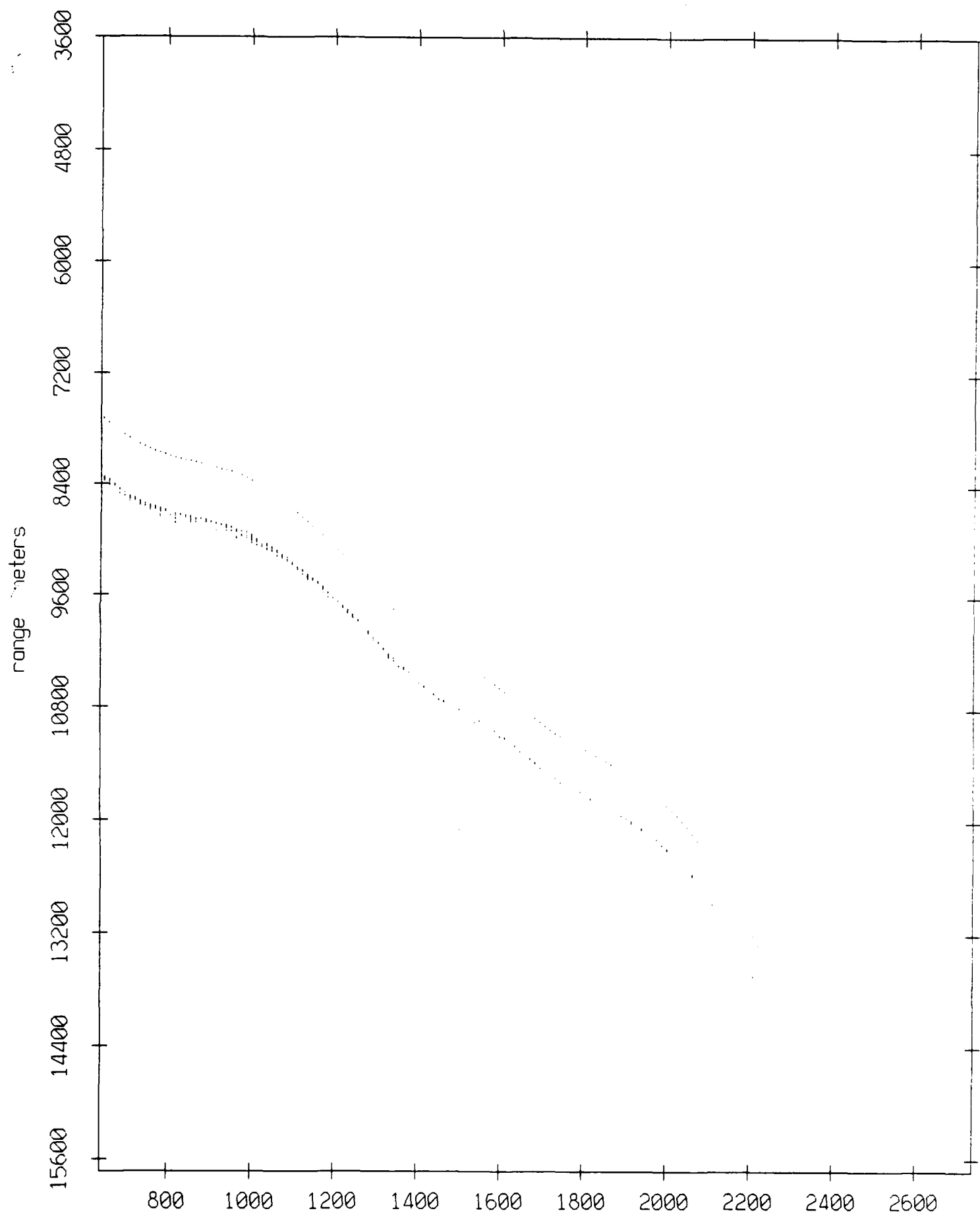
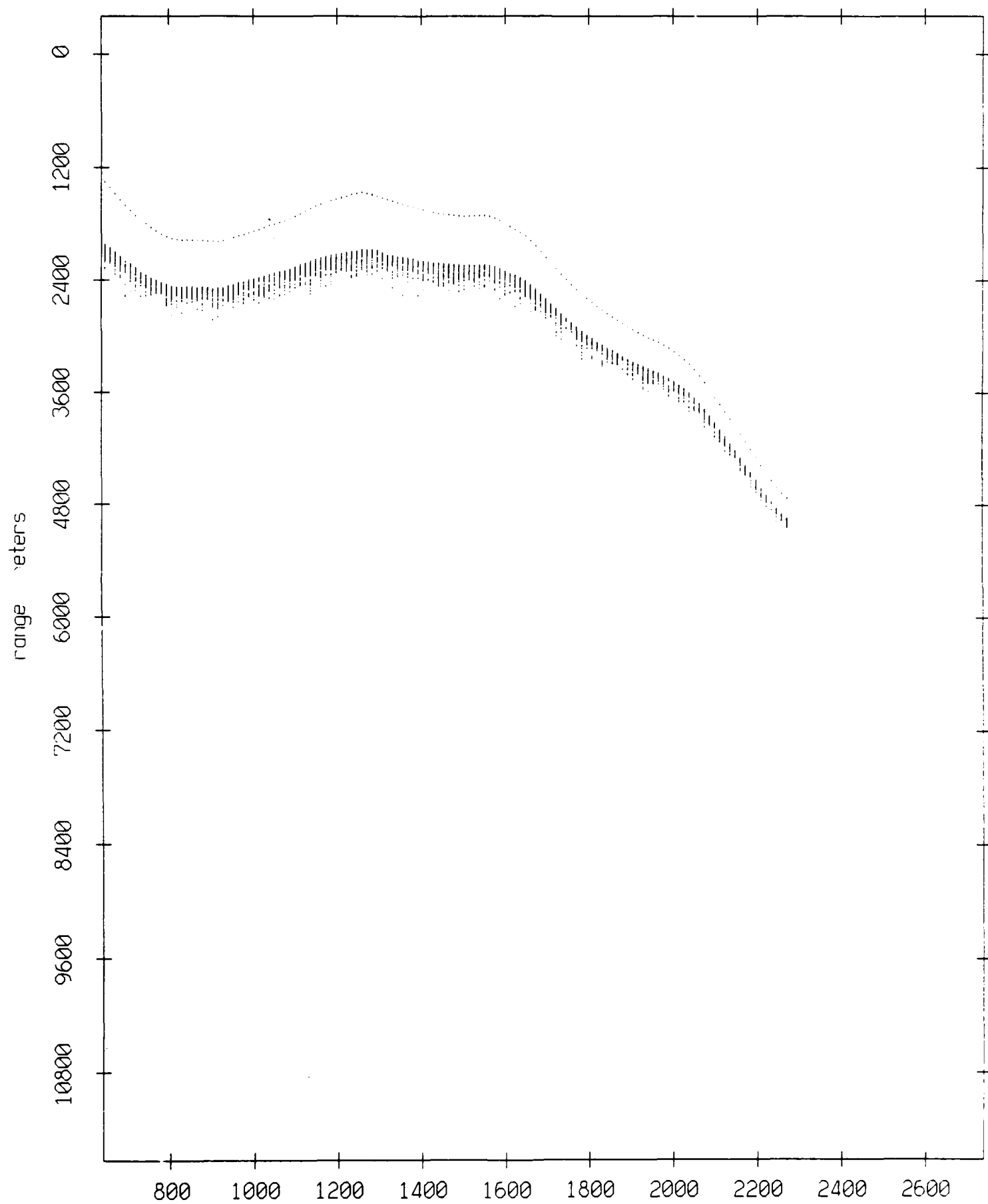


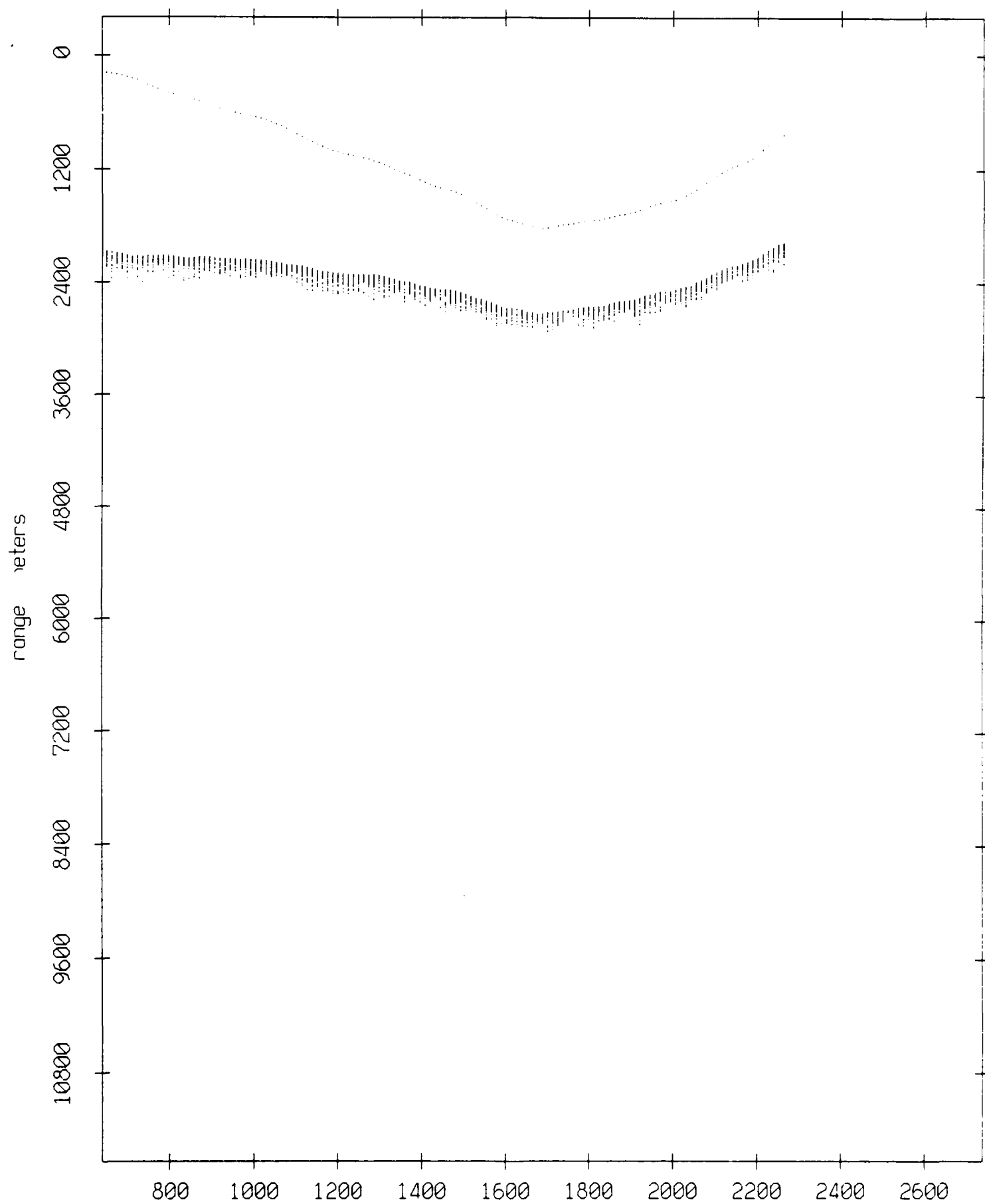
Figure IX.1k

Float 1, July 1989 Trip: range from float 0



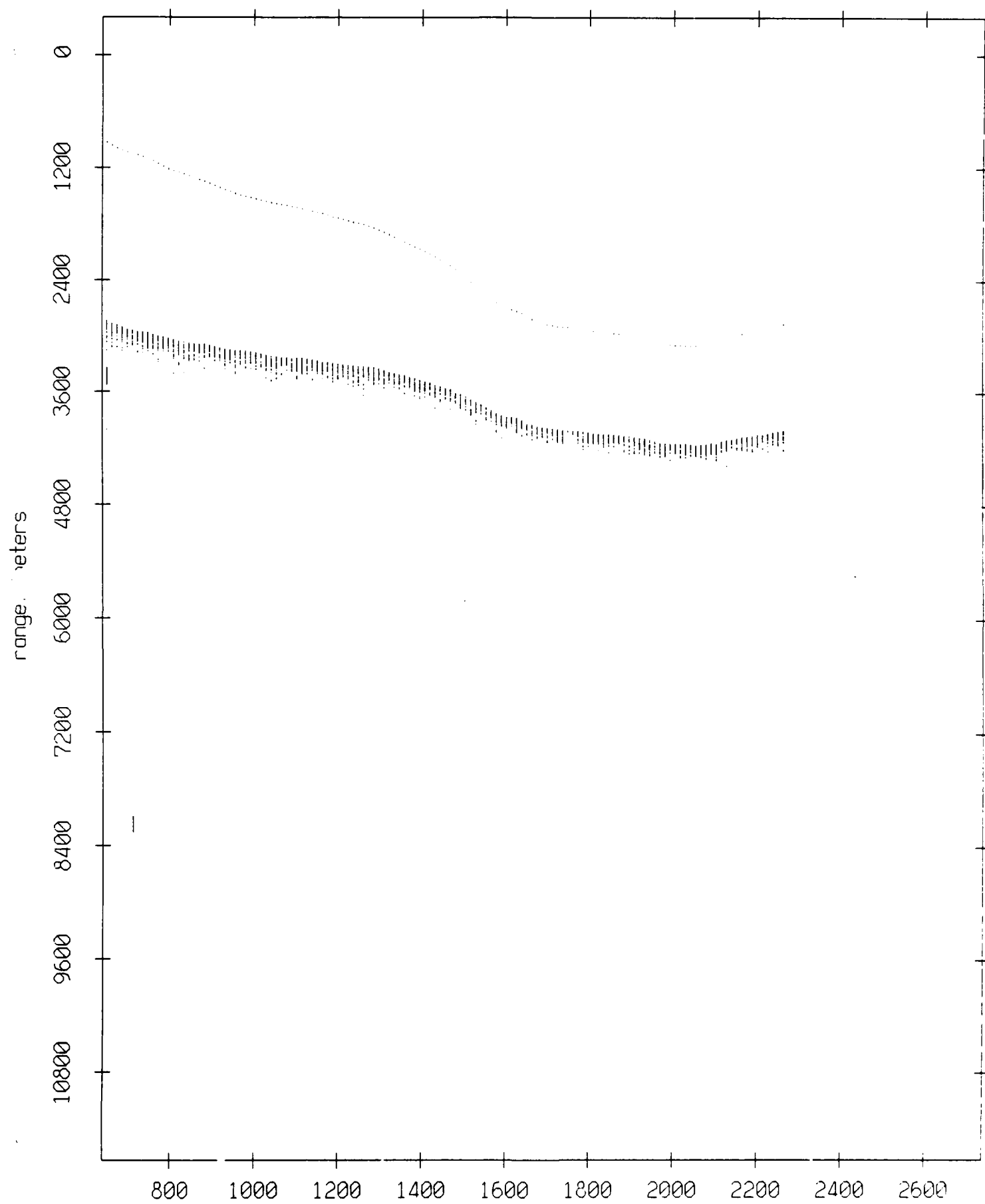
record number  
**Figure IX.2a**

Float 1, July 1989 Trip: range from float 2



record number  
**Figure IX.2b**

Float 1, July 1989 Trip: range from float 3



record number

Figure IX.2c

Float 1, July 1989 Trip: range from float 4

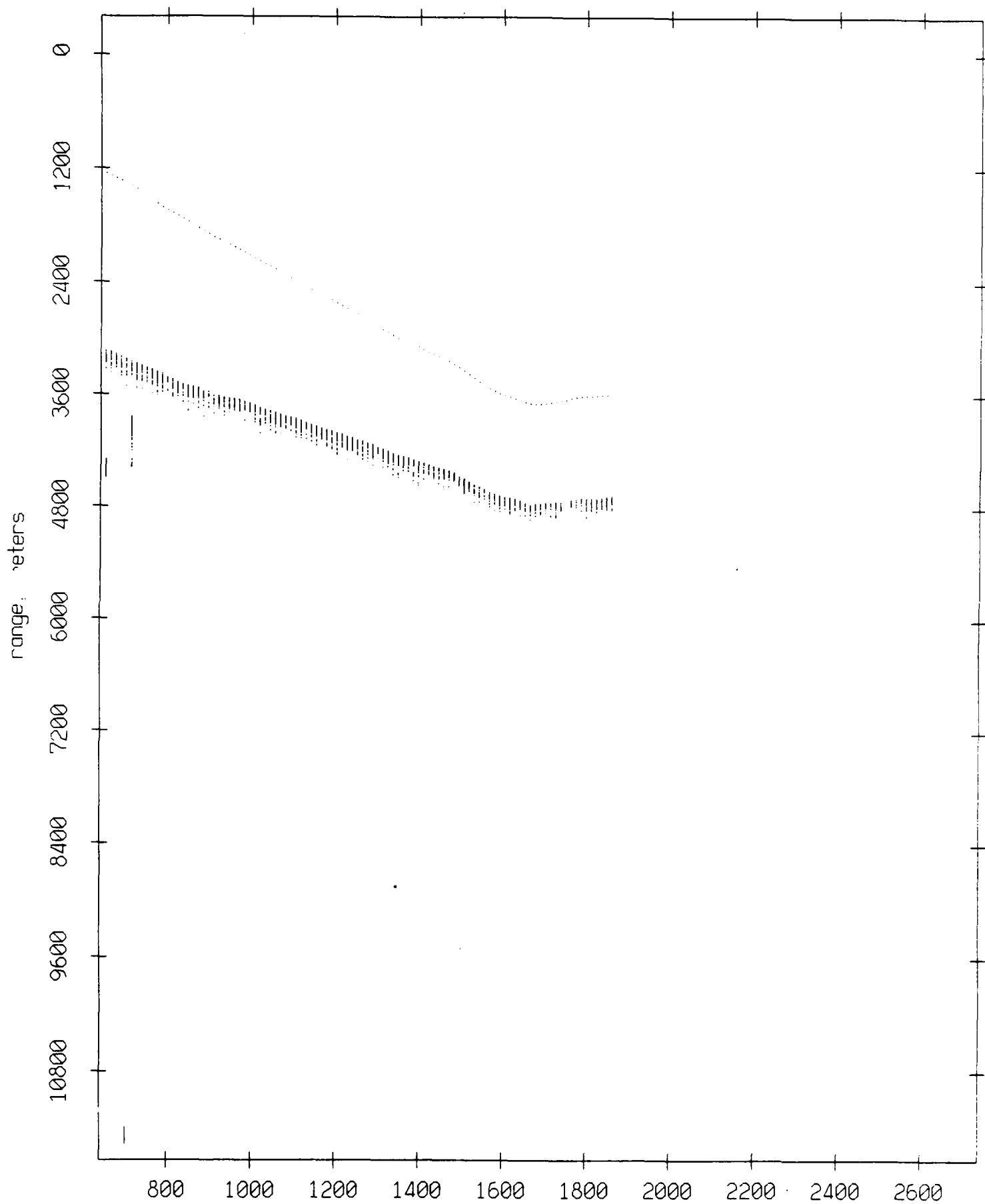
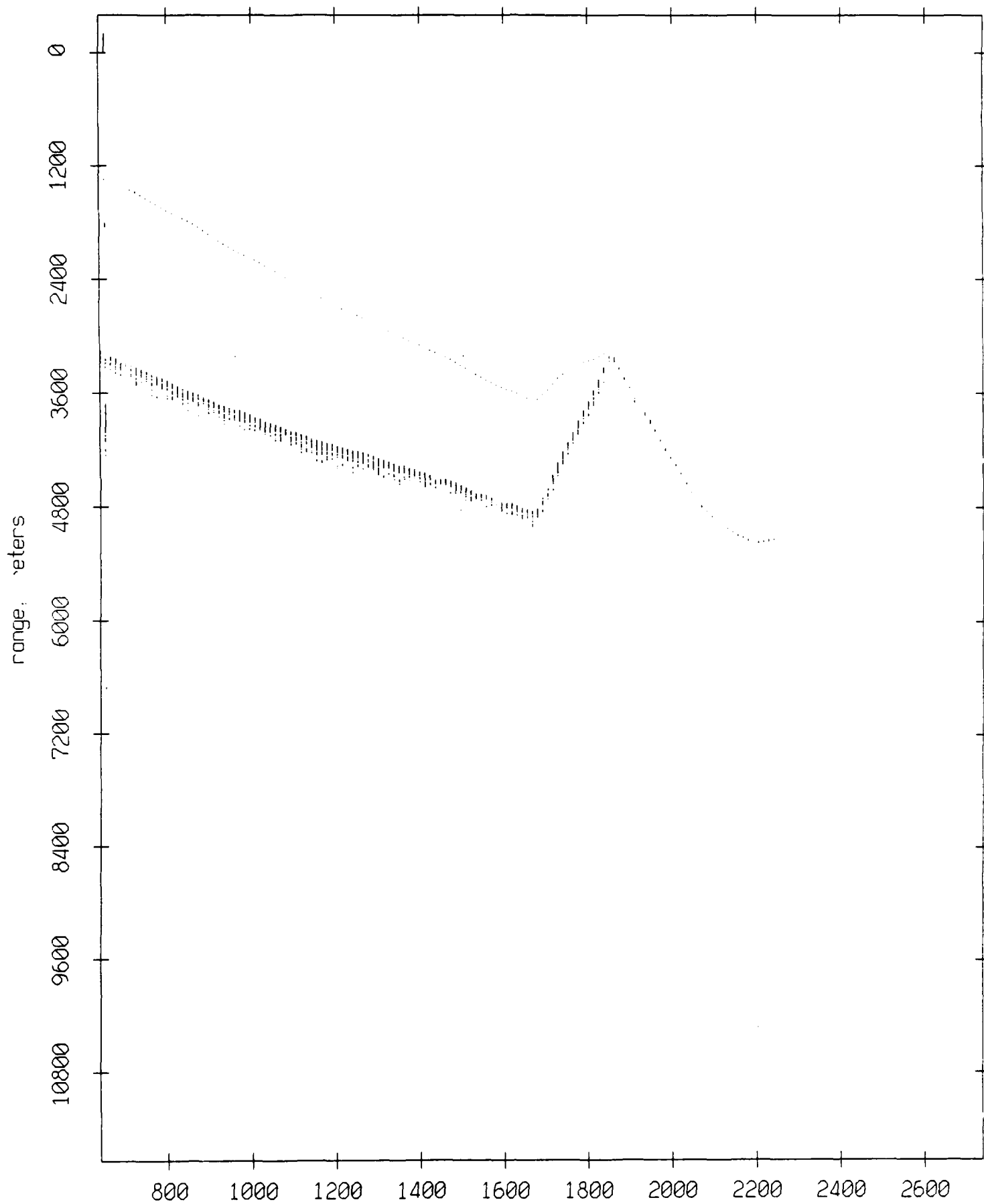


Figure IX.2d

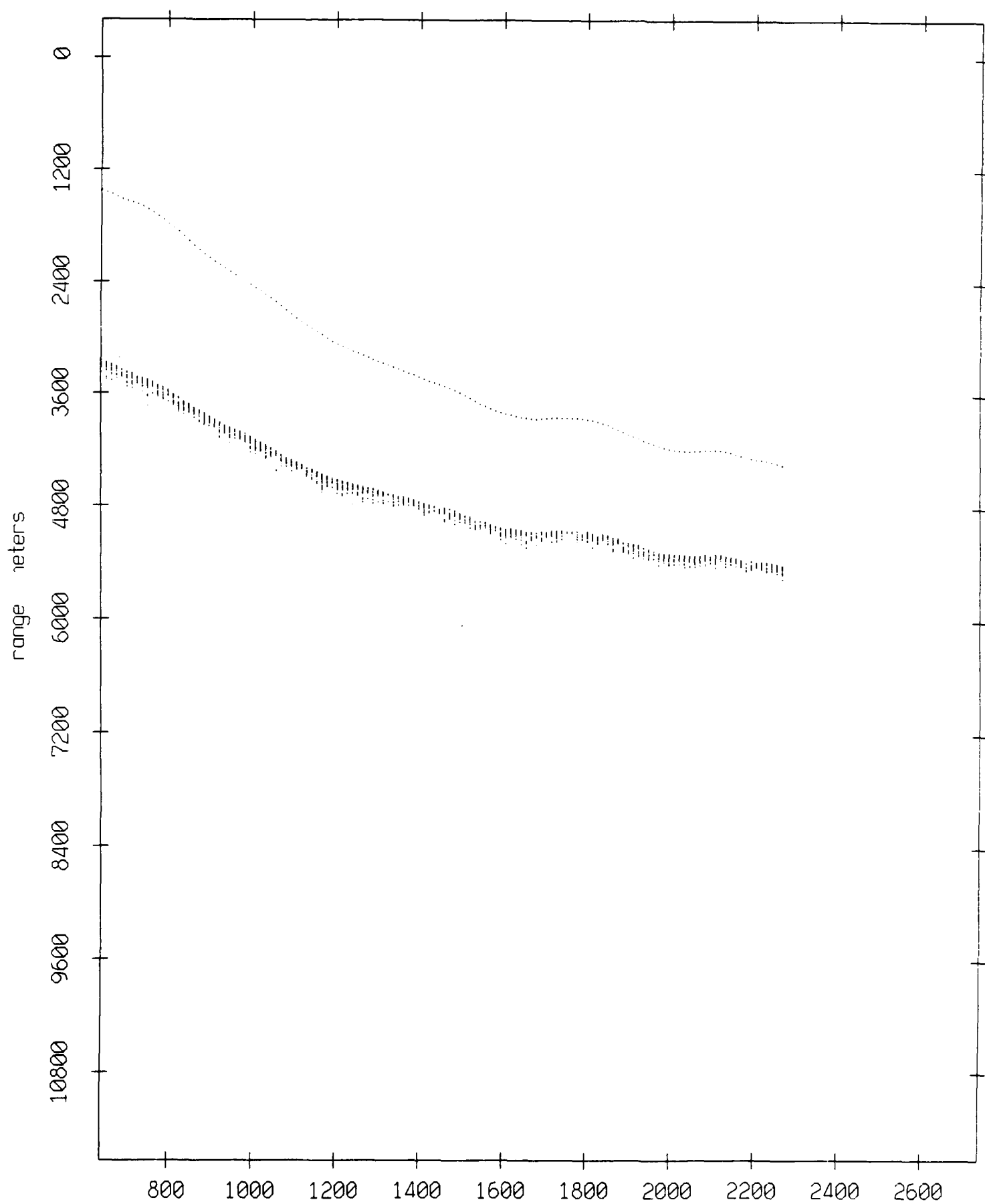
Float 1, July 1989 Trip: range from float 5



record number

Figure IX.2e

Float 1, July 1989 Trip: range from float 6



record number  
**Figure IX.2f**

Float 1, July 1989 Trip: range from float 7

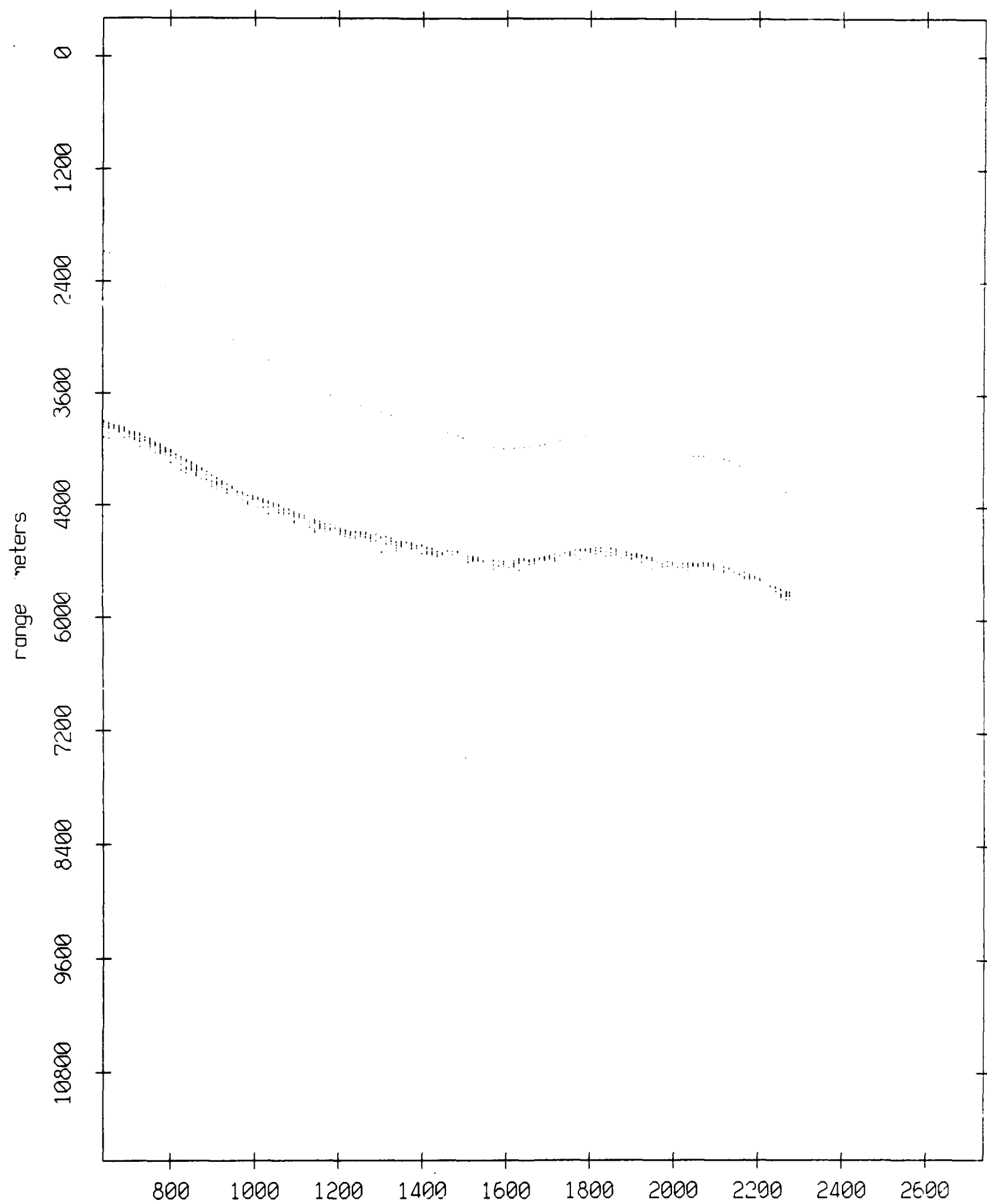


Figure IX.2g



Float 1, July 1989 Trip: range from float 8

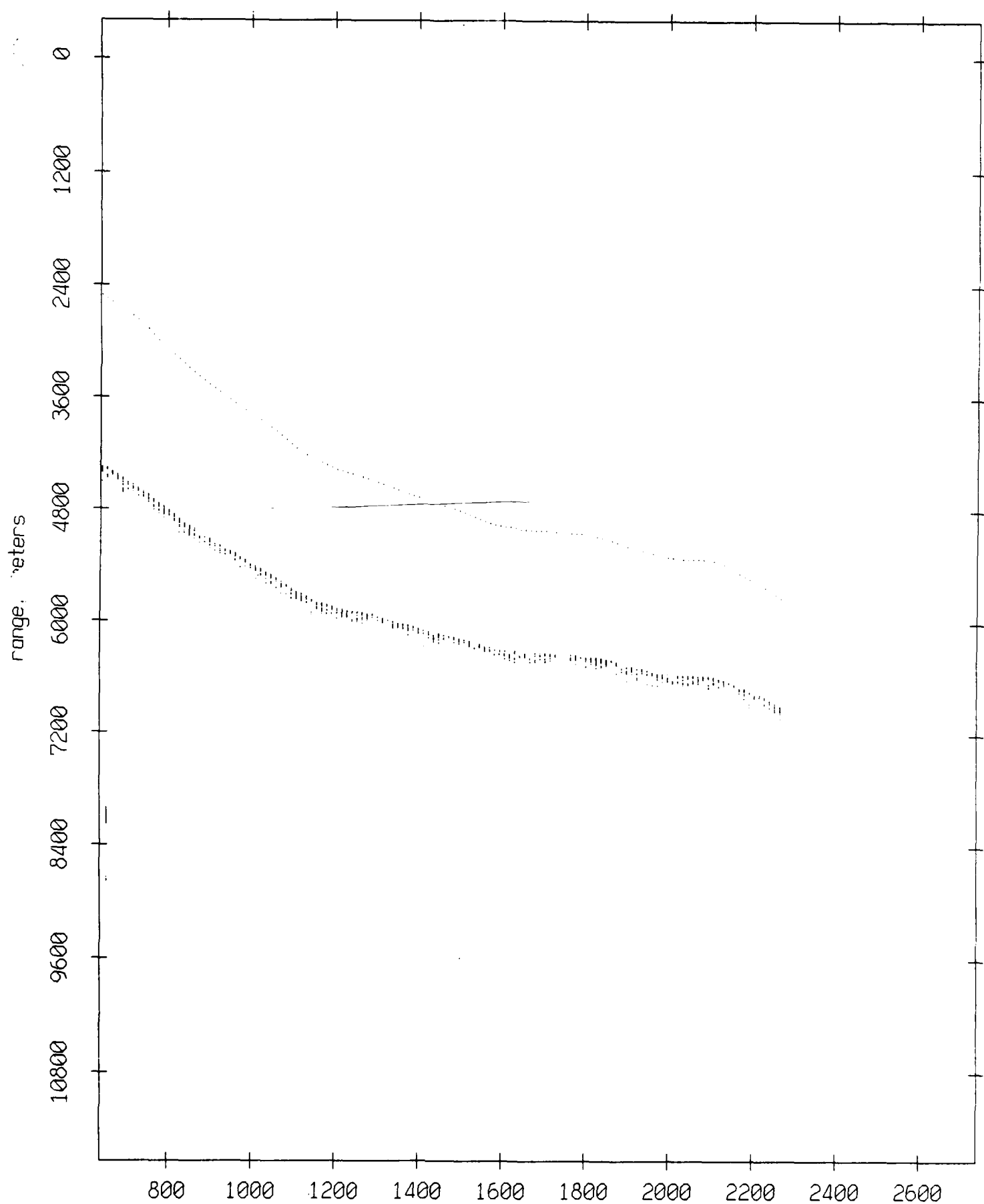
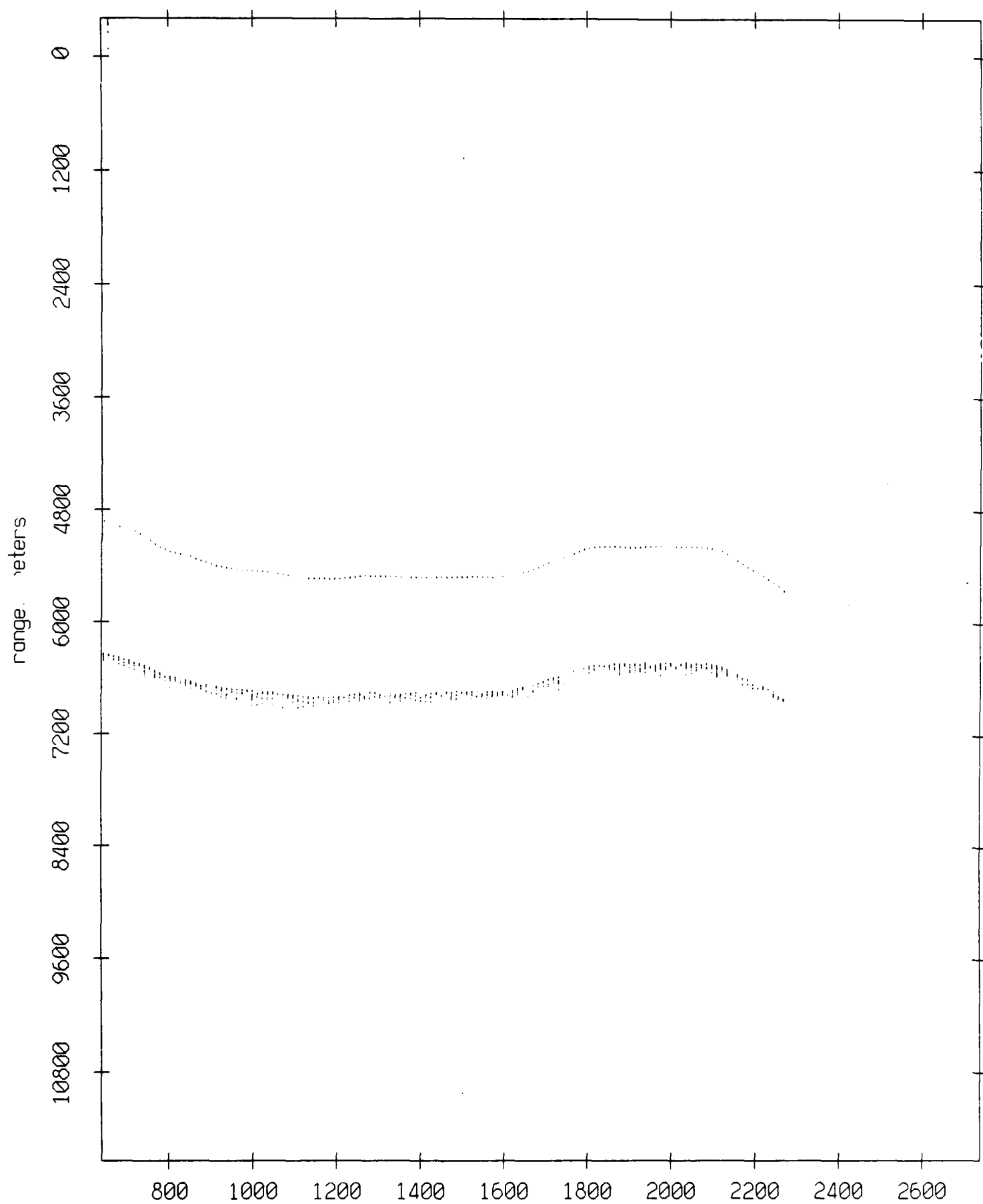


Figure IX.2h

Float 1, July 1989 Trip: range from float 9



record number

Figure IX.21

Float 1, July 1989 Trip: range from float 10

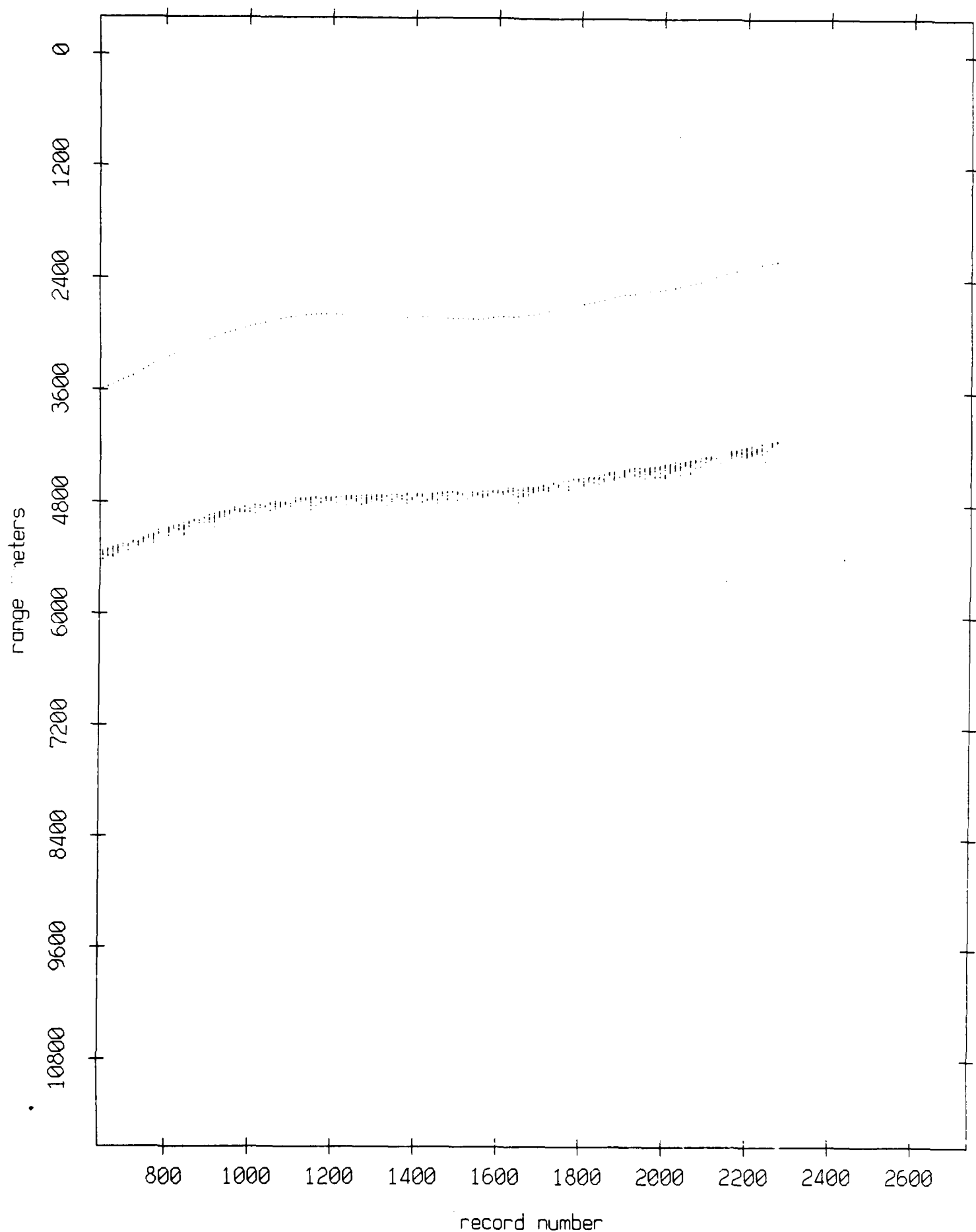


Figure IX.2j

Float 1, July 1989 Trip: range from float 11

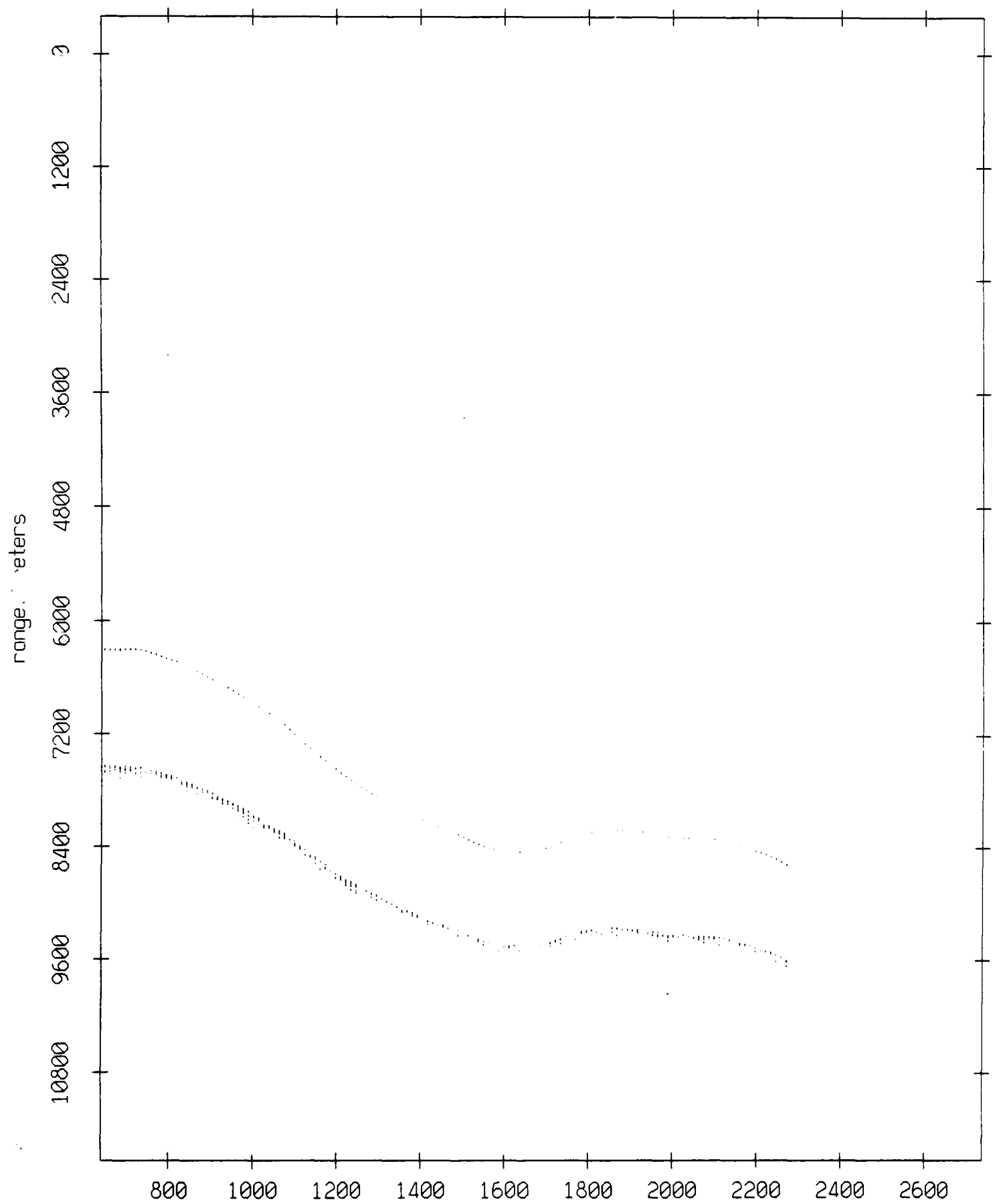
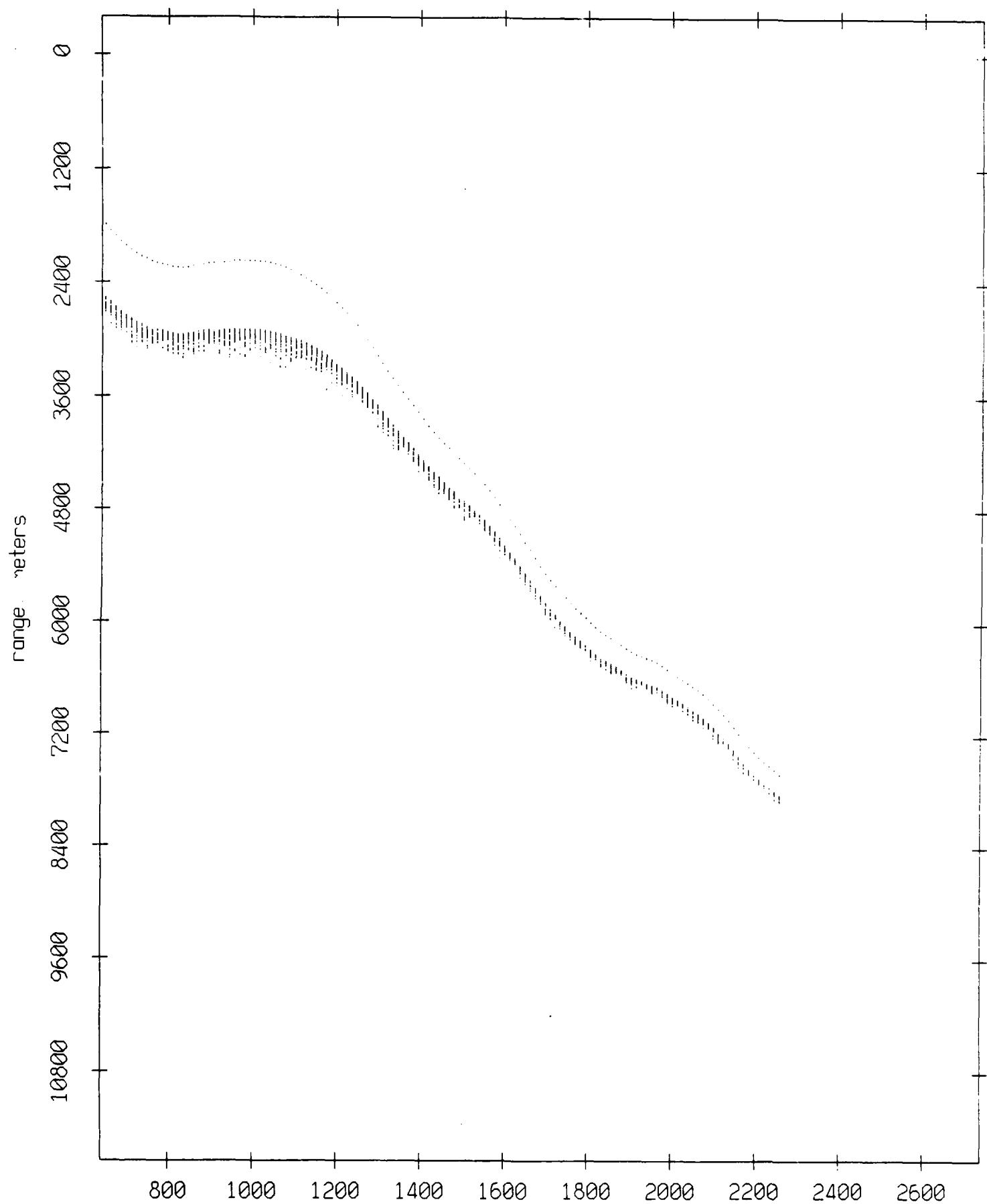


Figure IX.2k

Float 2, July 1989 Trip: range from float 0



record number

Figure IX.3a

Float 2, July 1989 Trip: range from float 1

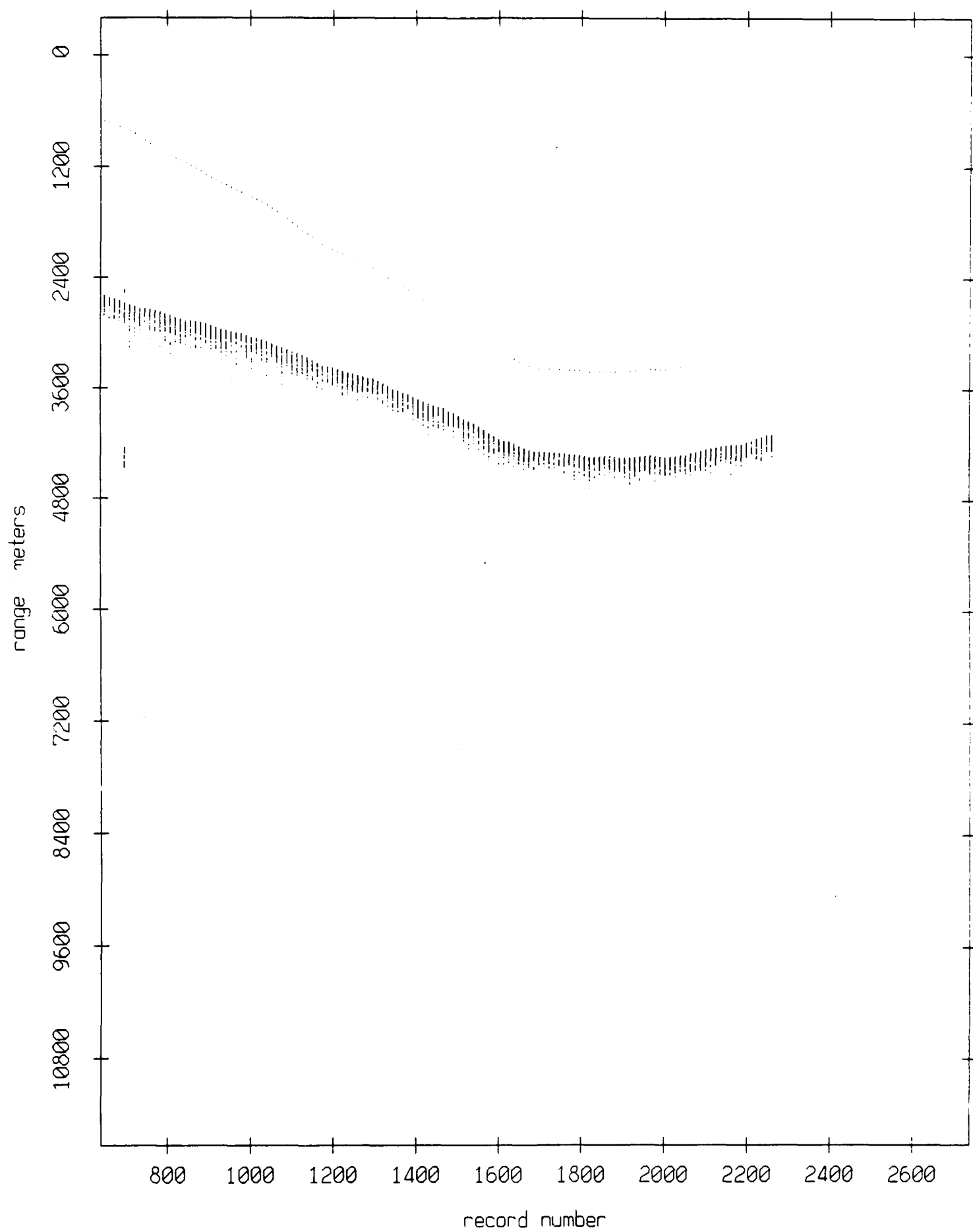
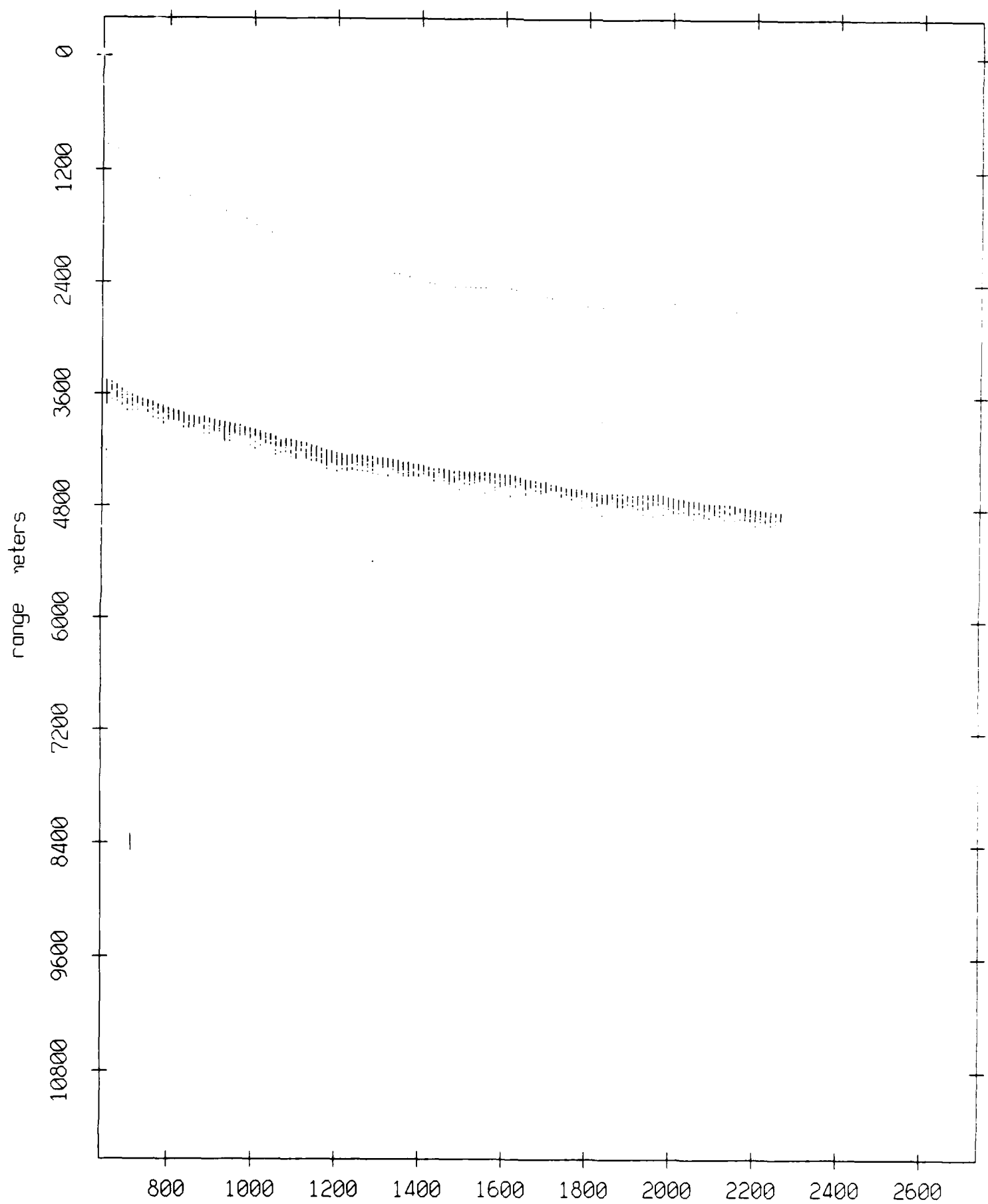


Figure IX.3b

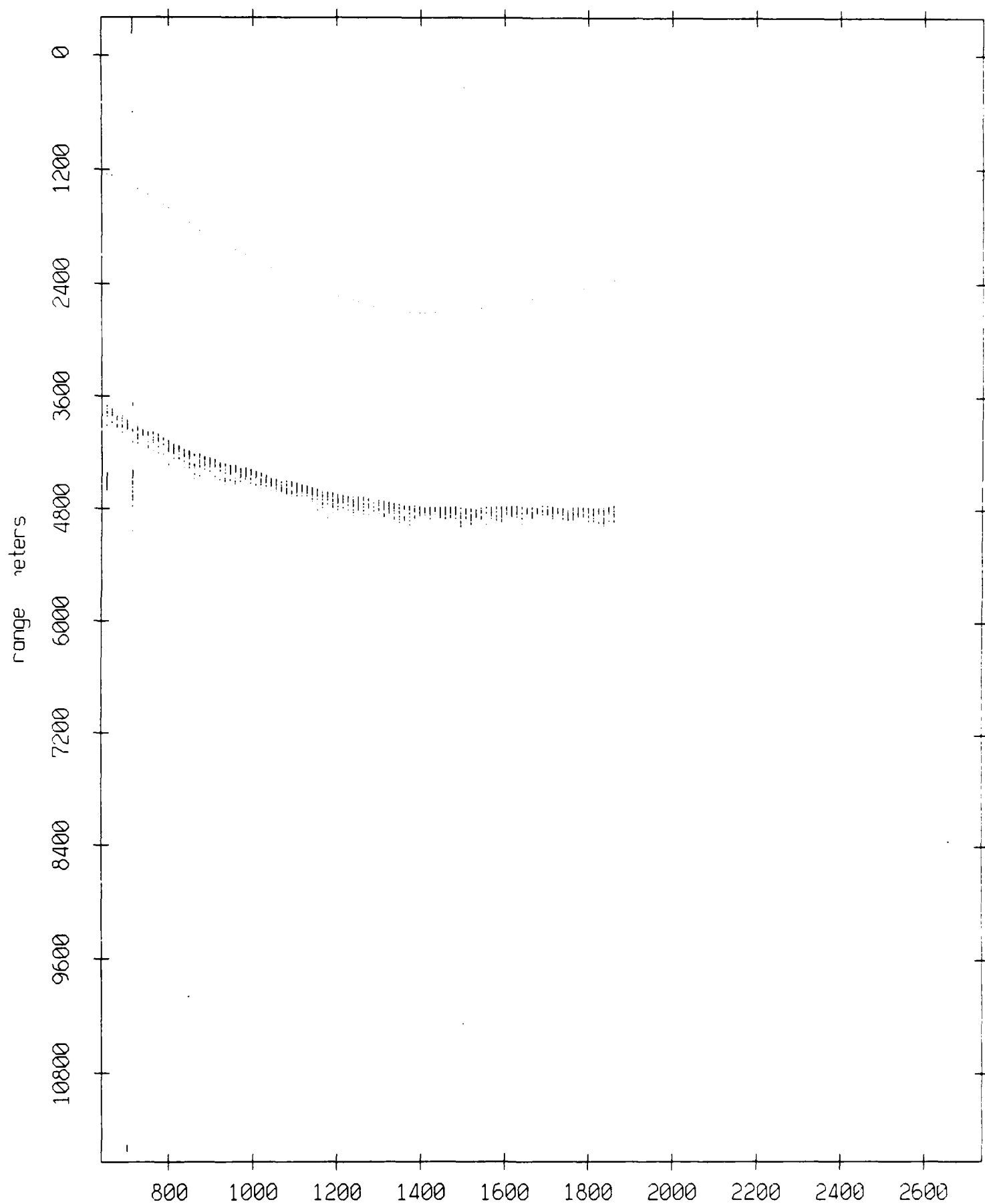
Float 2, July 1989 Trip: range from float 3



record number

Figure IX.3c

Float 2, July 1989 Trip: range from float 4

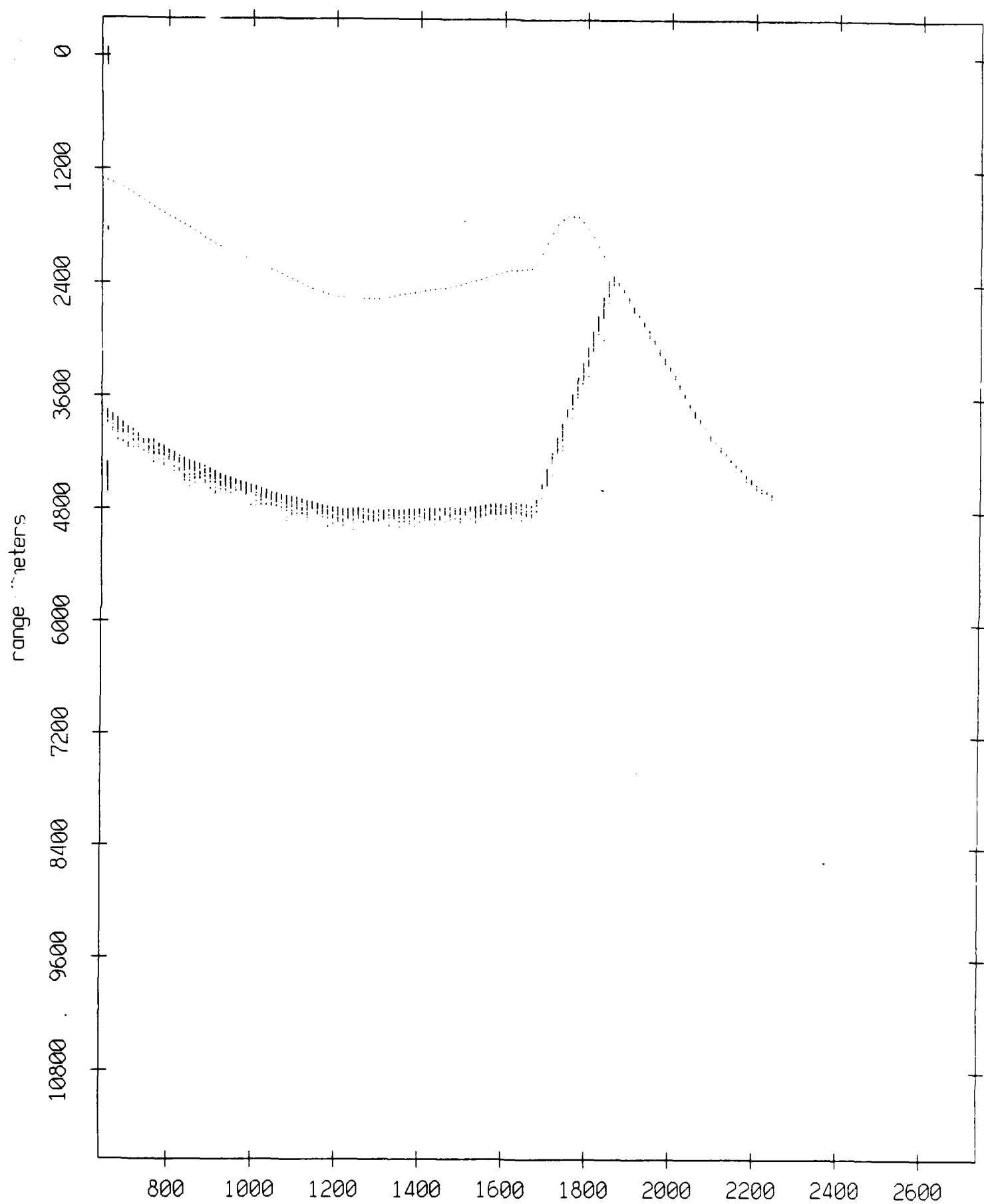


record number

Figure IX.3d



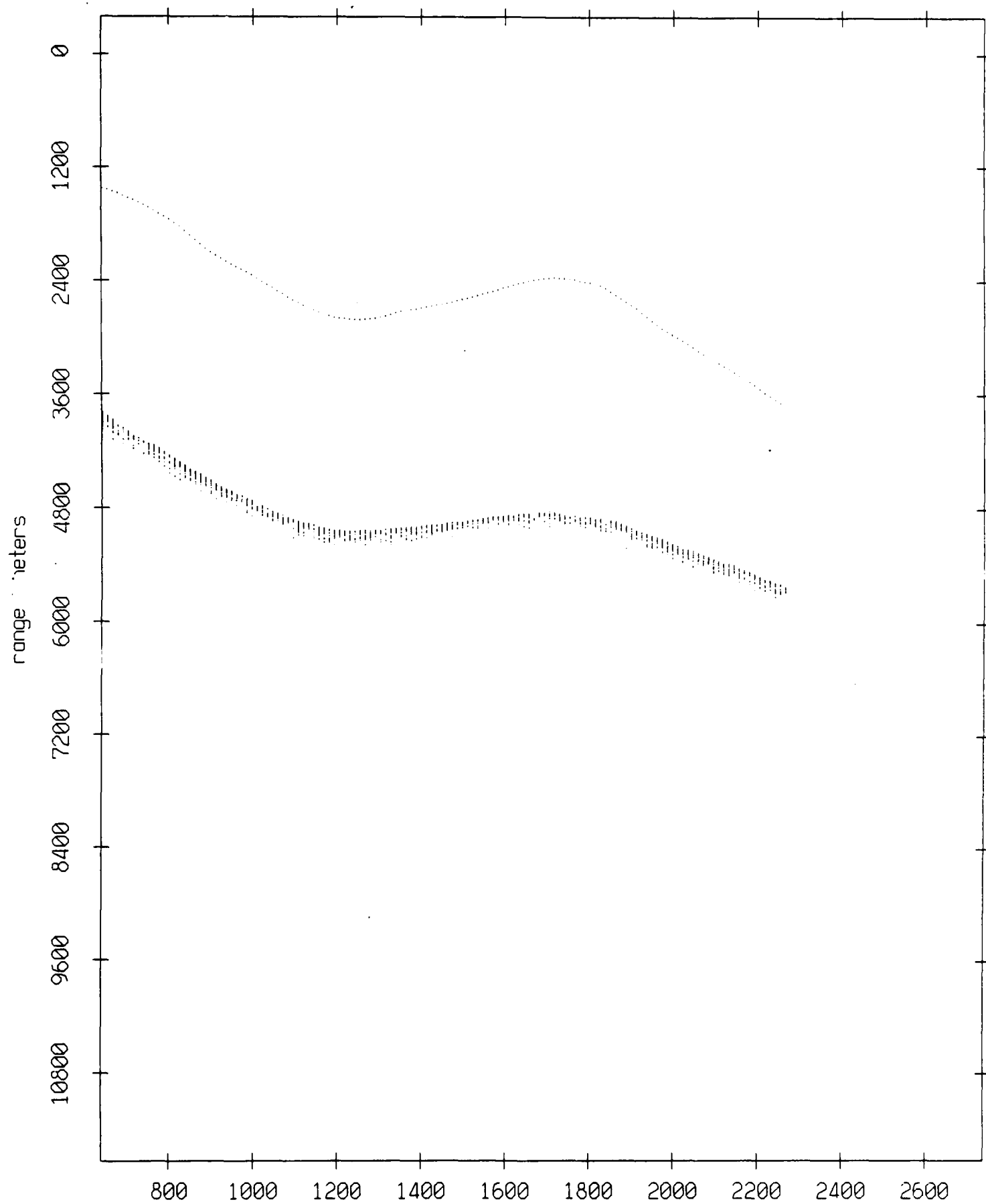
Float 2, July 1989 Trip: range from float 5



record number

Figure IX.3e

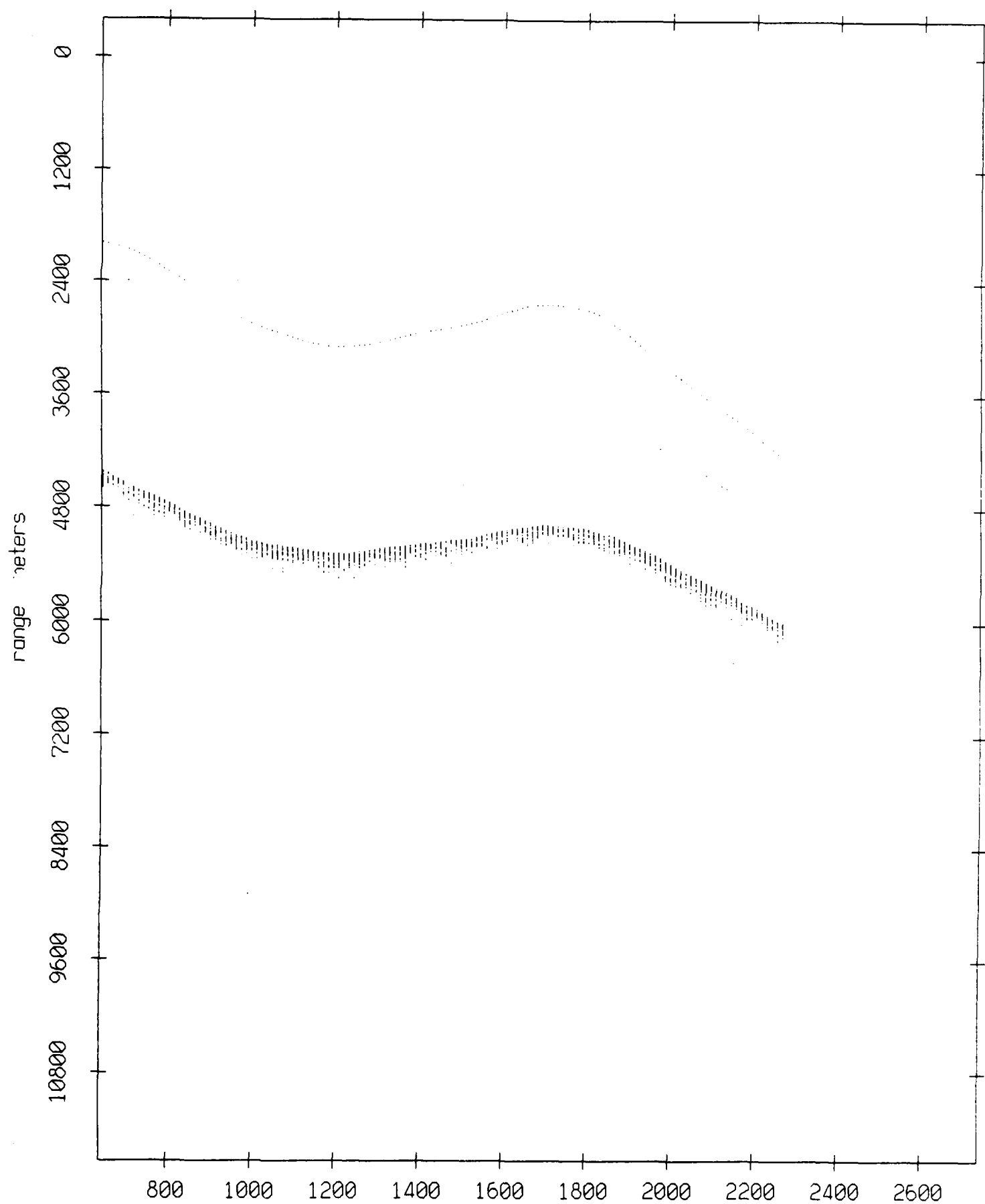
Float 2, July 1989 Trip: range from float 6



record number

**Figure IX.3f**

Float 2, July 1989 Trip: range from float 7



record number  
**Figure IX.3g**

Float 2, July 1989 Trip: range from float 8

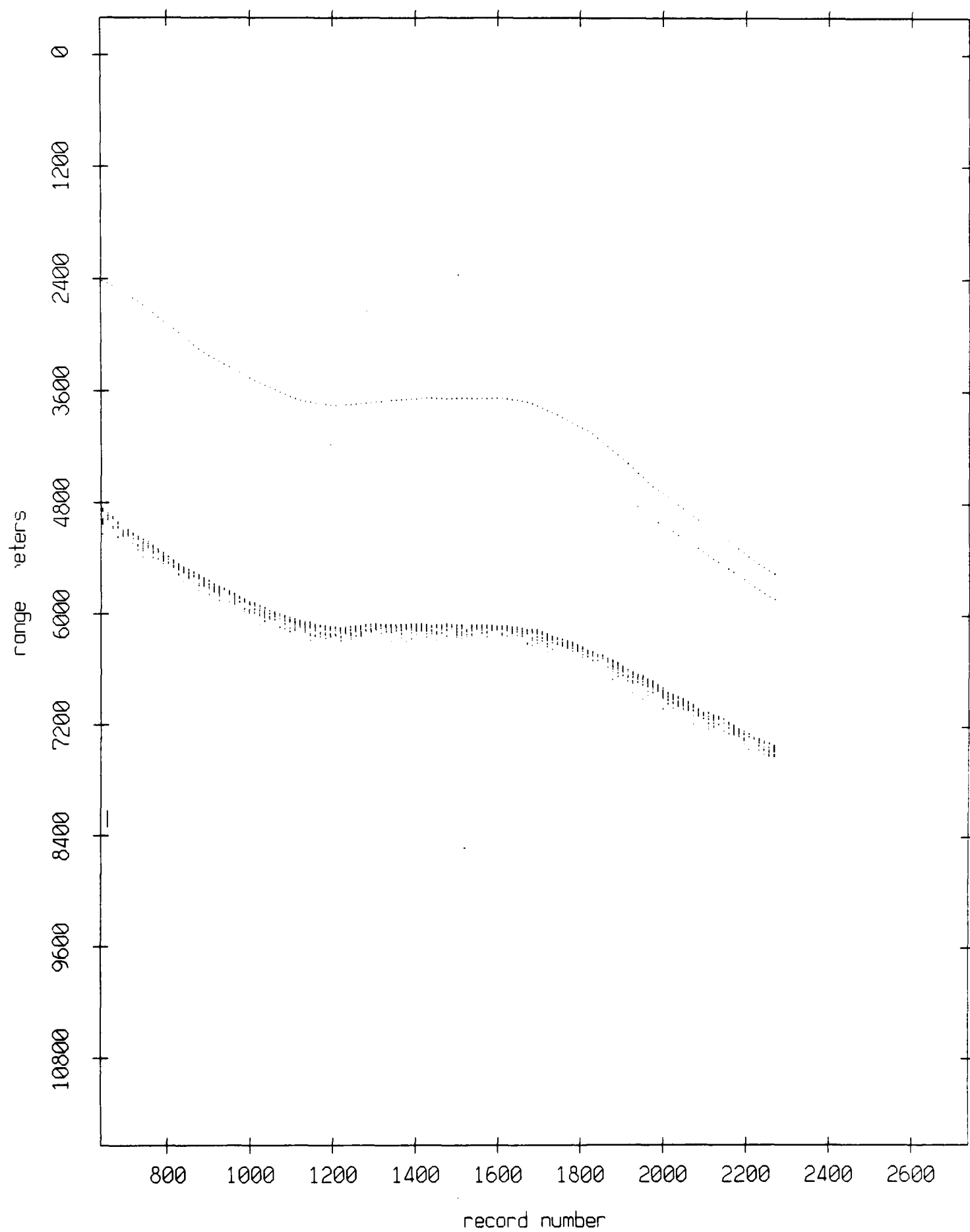
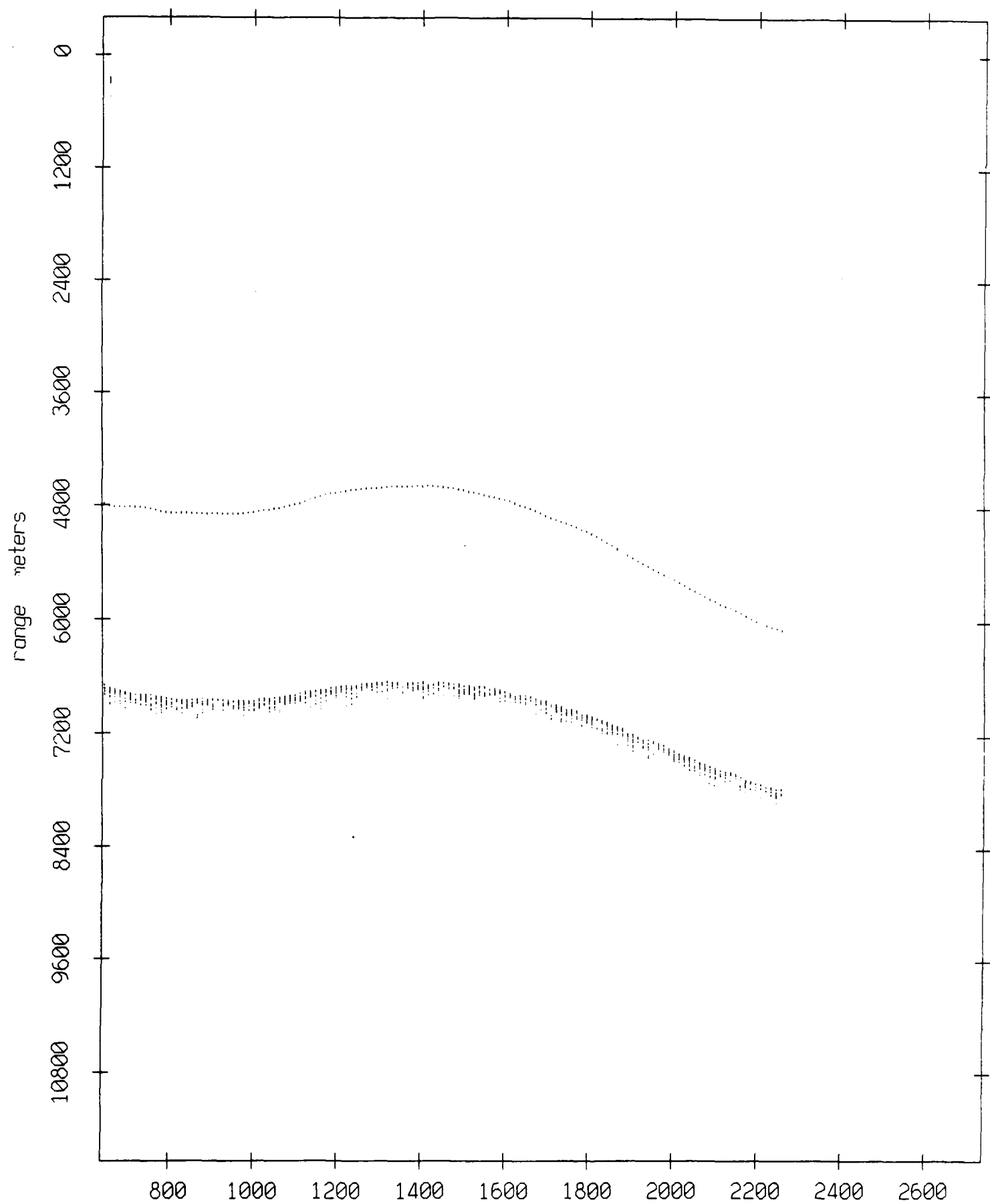


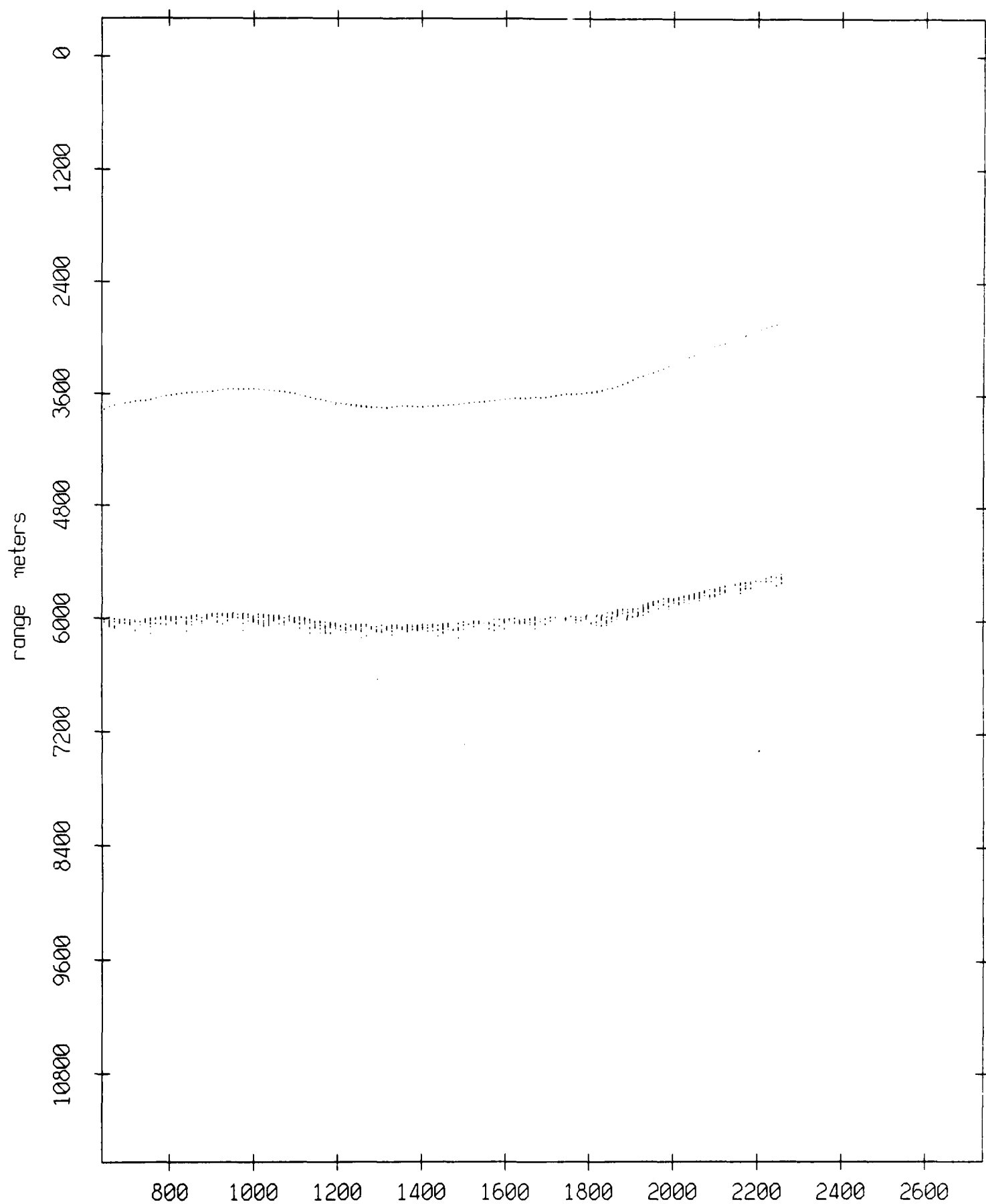
Figure IX.3h

Float 2, July 1989 Trip: range from float 9



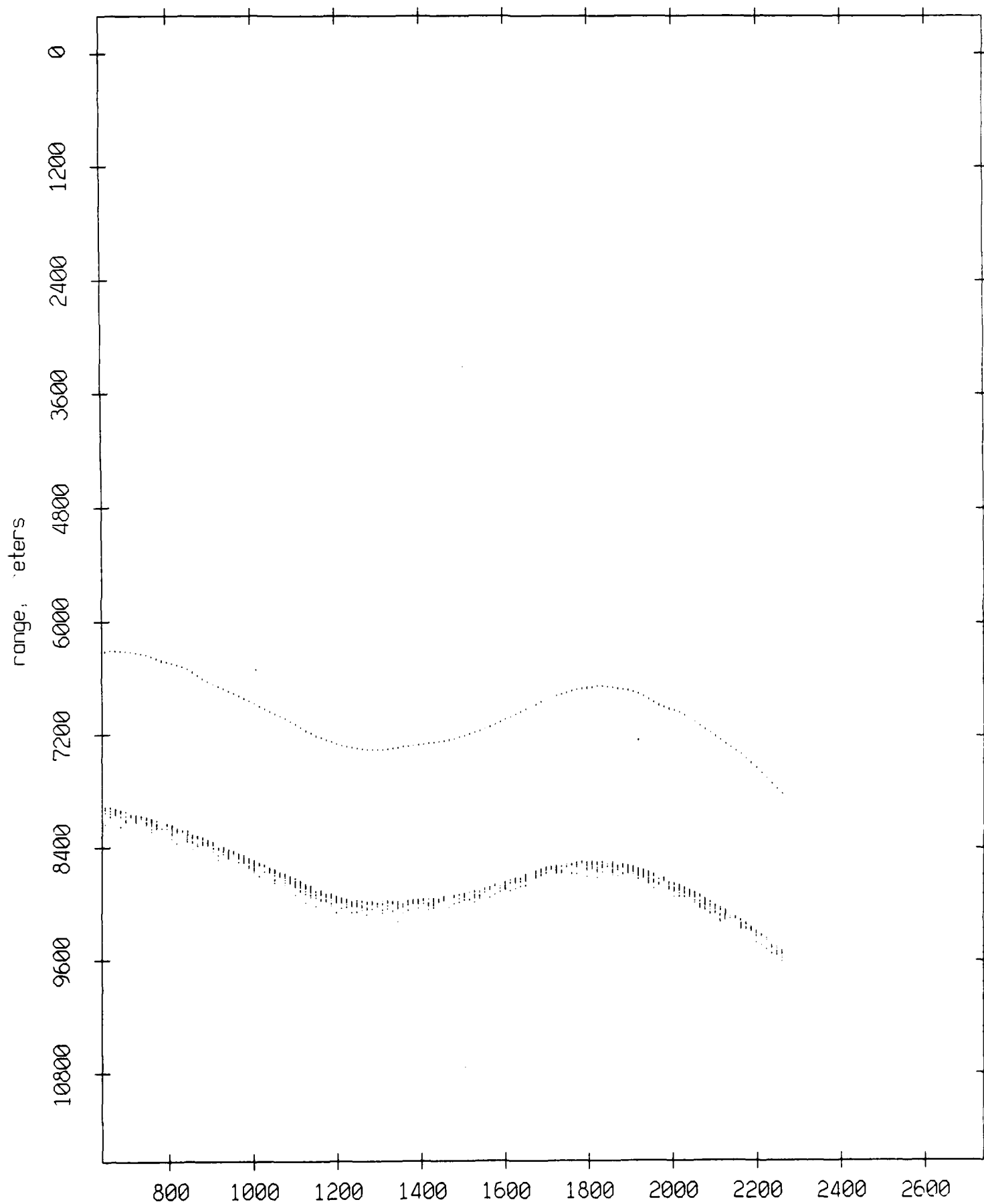
record number  
Figure IX.31

Float 2, July 1989 Trip: range from float 10



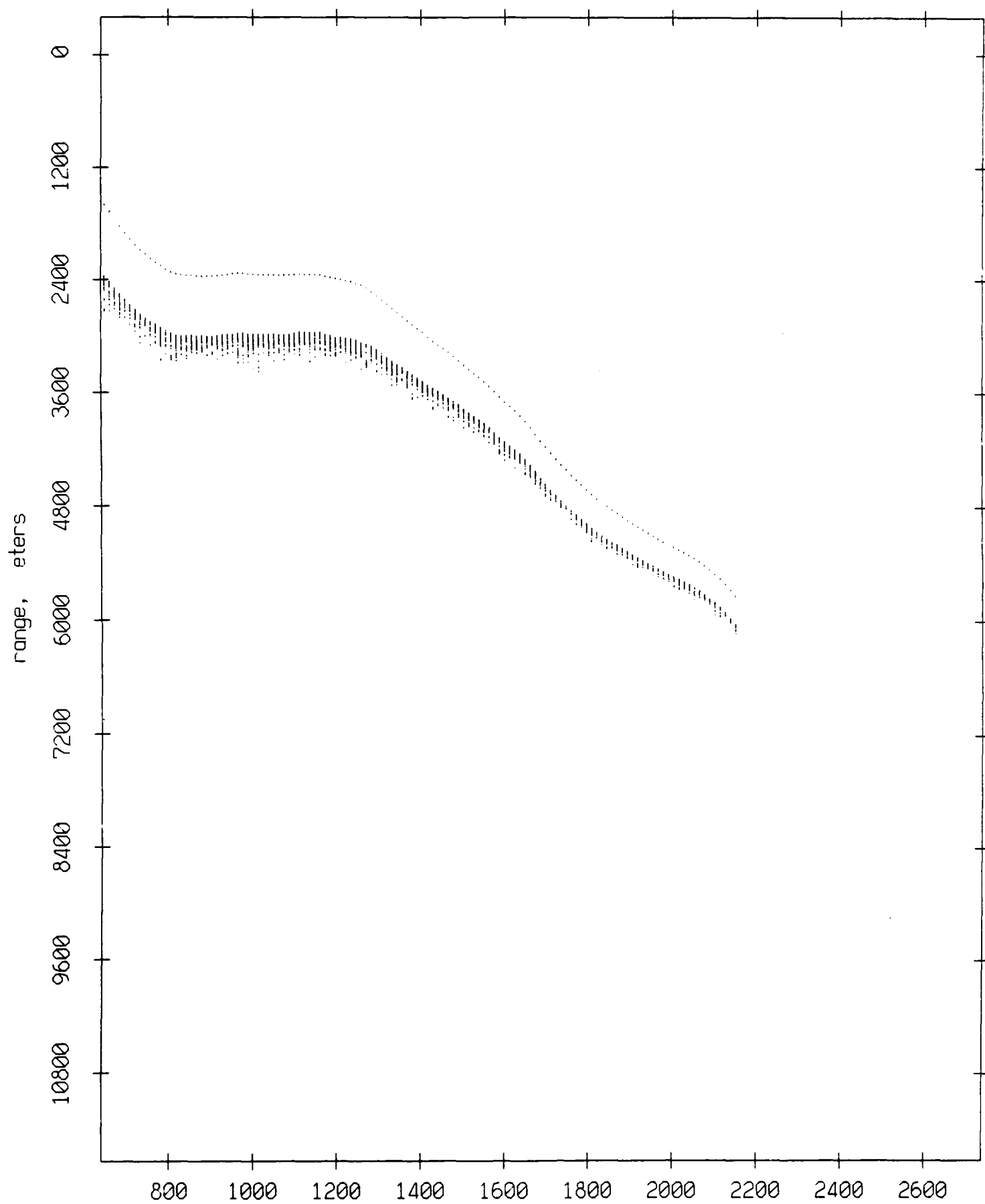
record number  
**Figure IX.3j**

Float 2, July 1989 Trip: range from float 11



record number  
**Figure IX.3k**

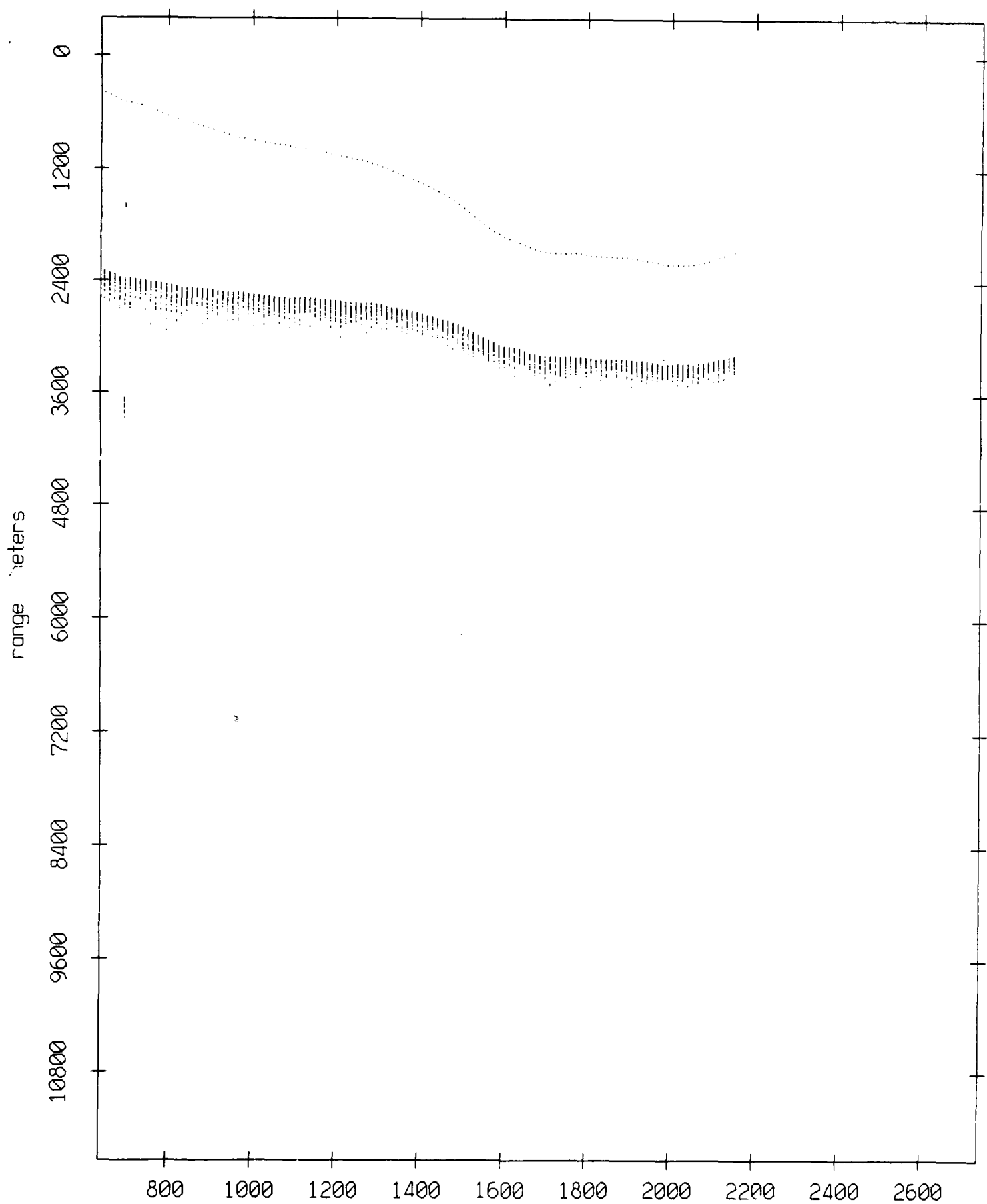
Float 3, July 1989 Trip: range from float 0



record number  
Figure IX.4a

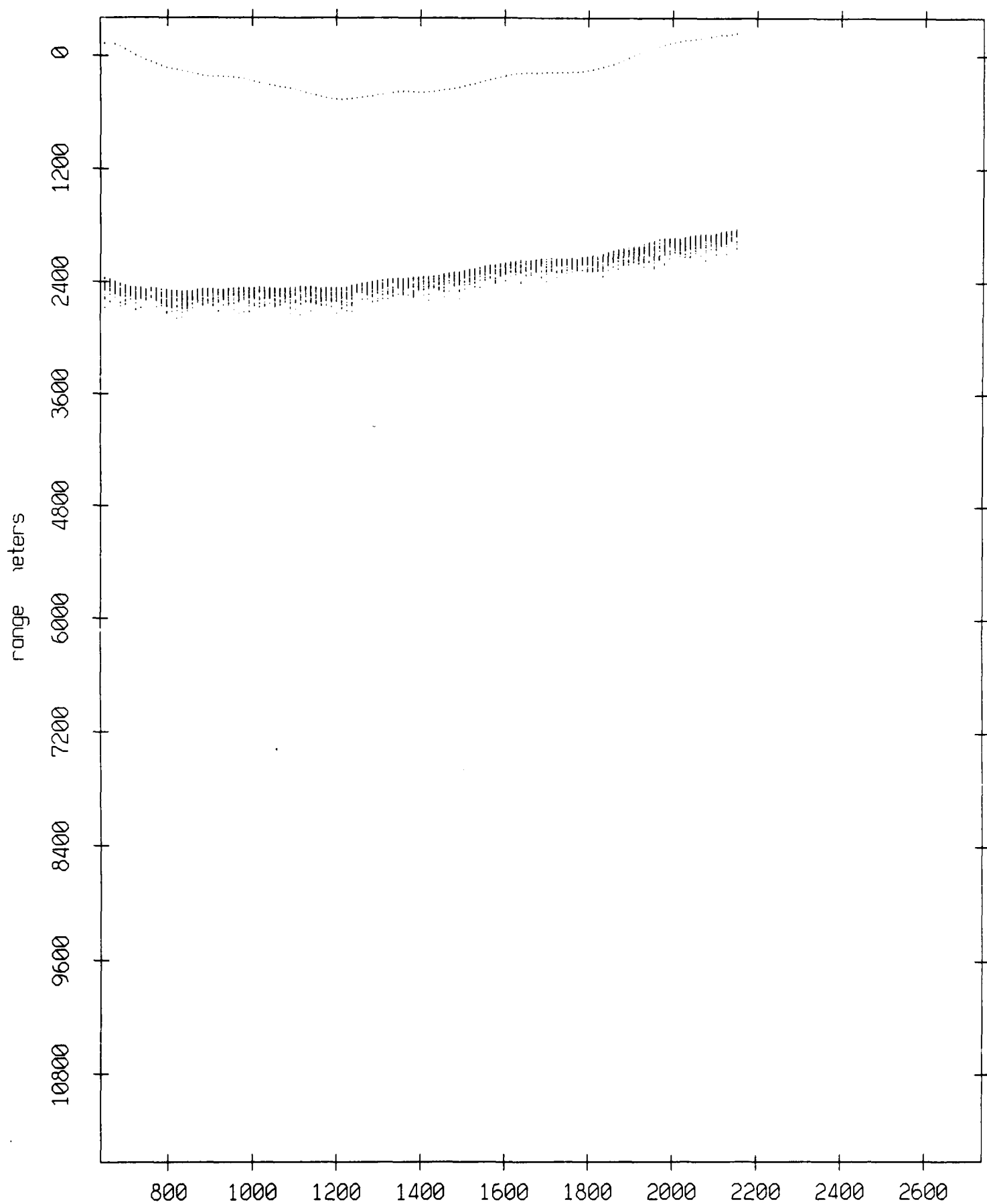


Float 3, July 1989 Trip: range from float 1



record number  
**Figure IX.4b**

Float 3, July 1989 Trip: range from float 2



record number

**Figure IX.4c**

Float 3, July 1989 Trip: range from float 4

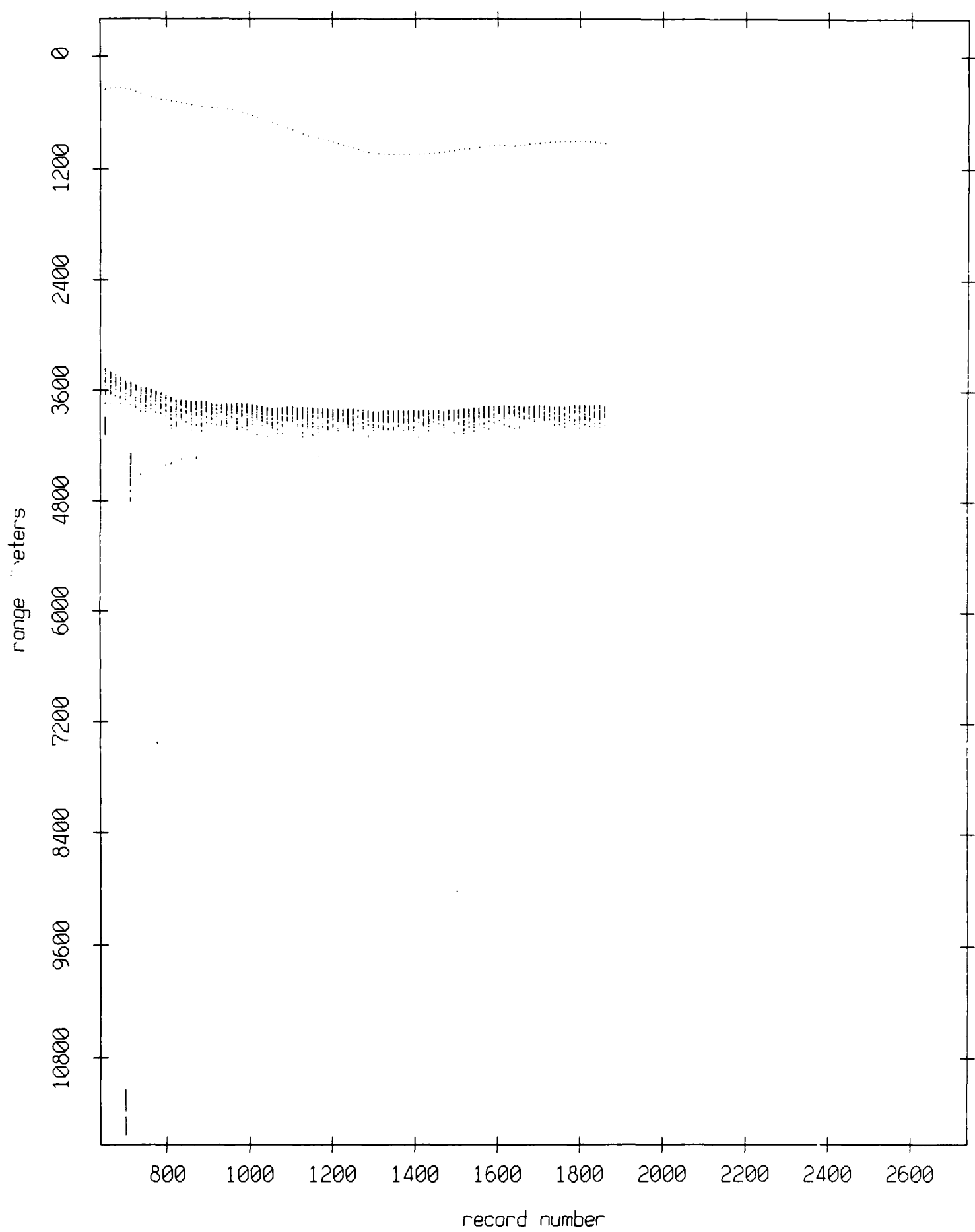
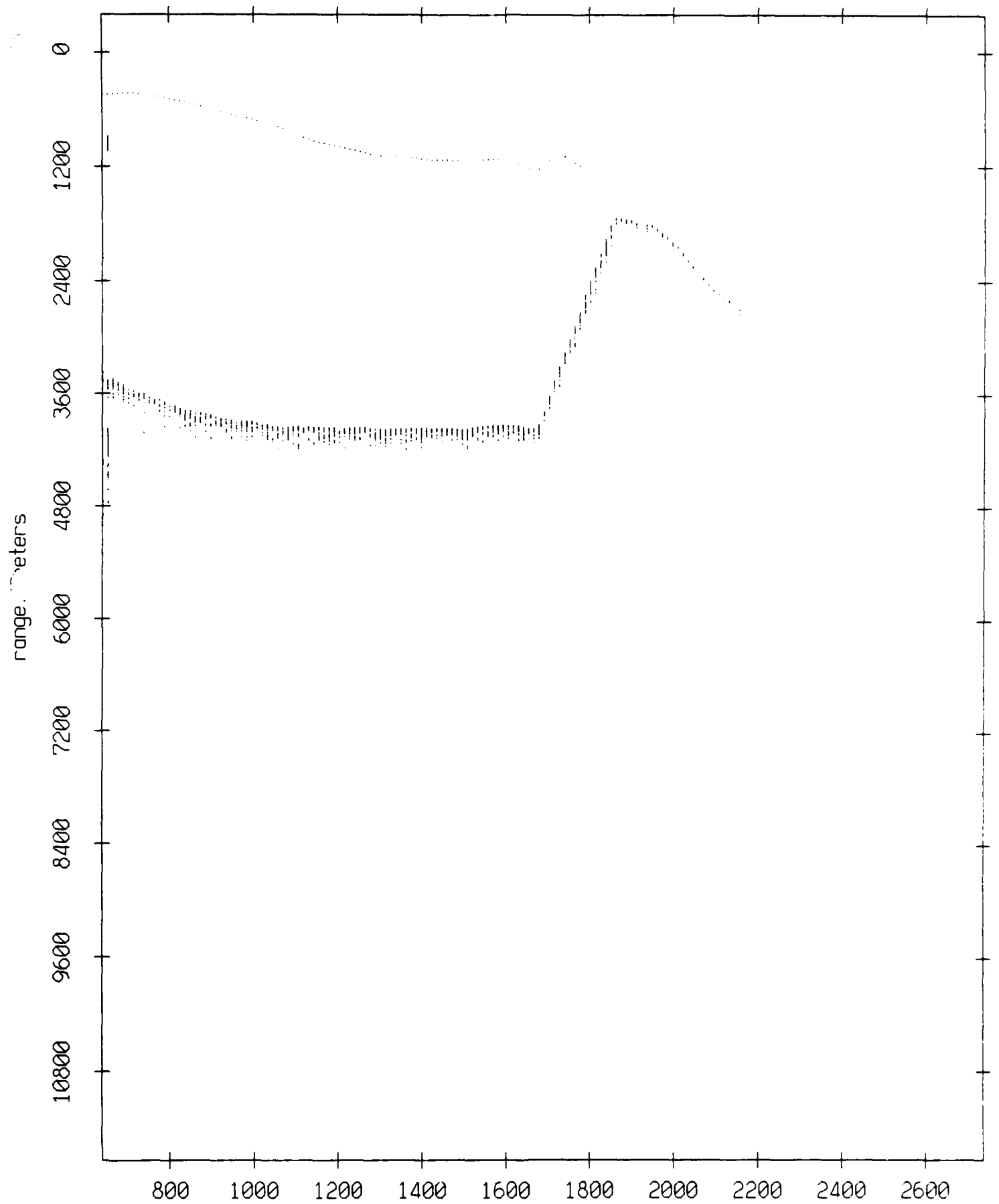


Figure IX.4d

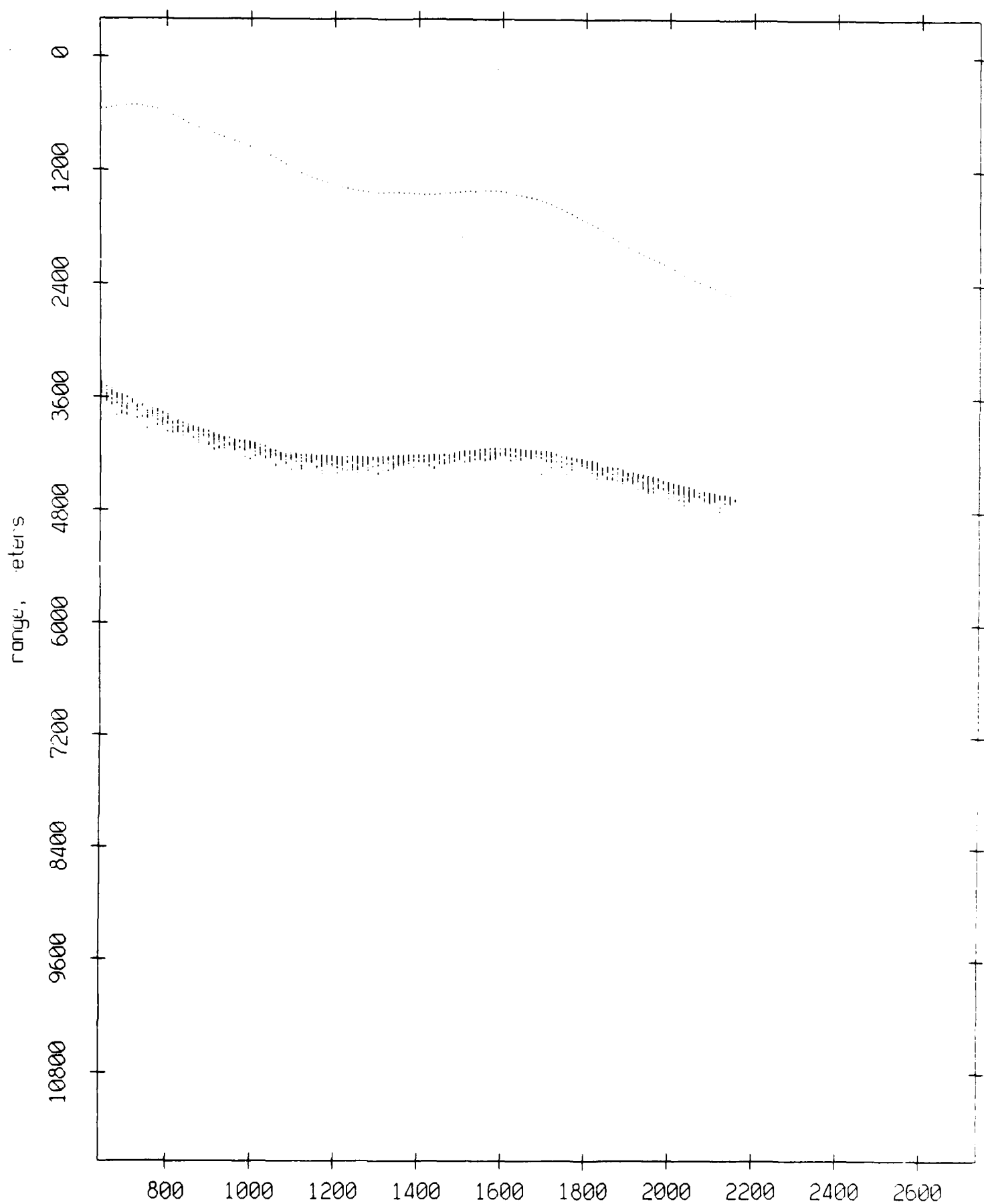
Float 3, July 1989 Trip: range from float 5



record number

Figure IX.4e

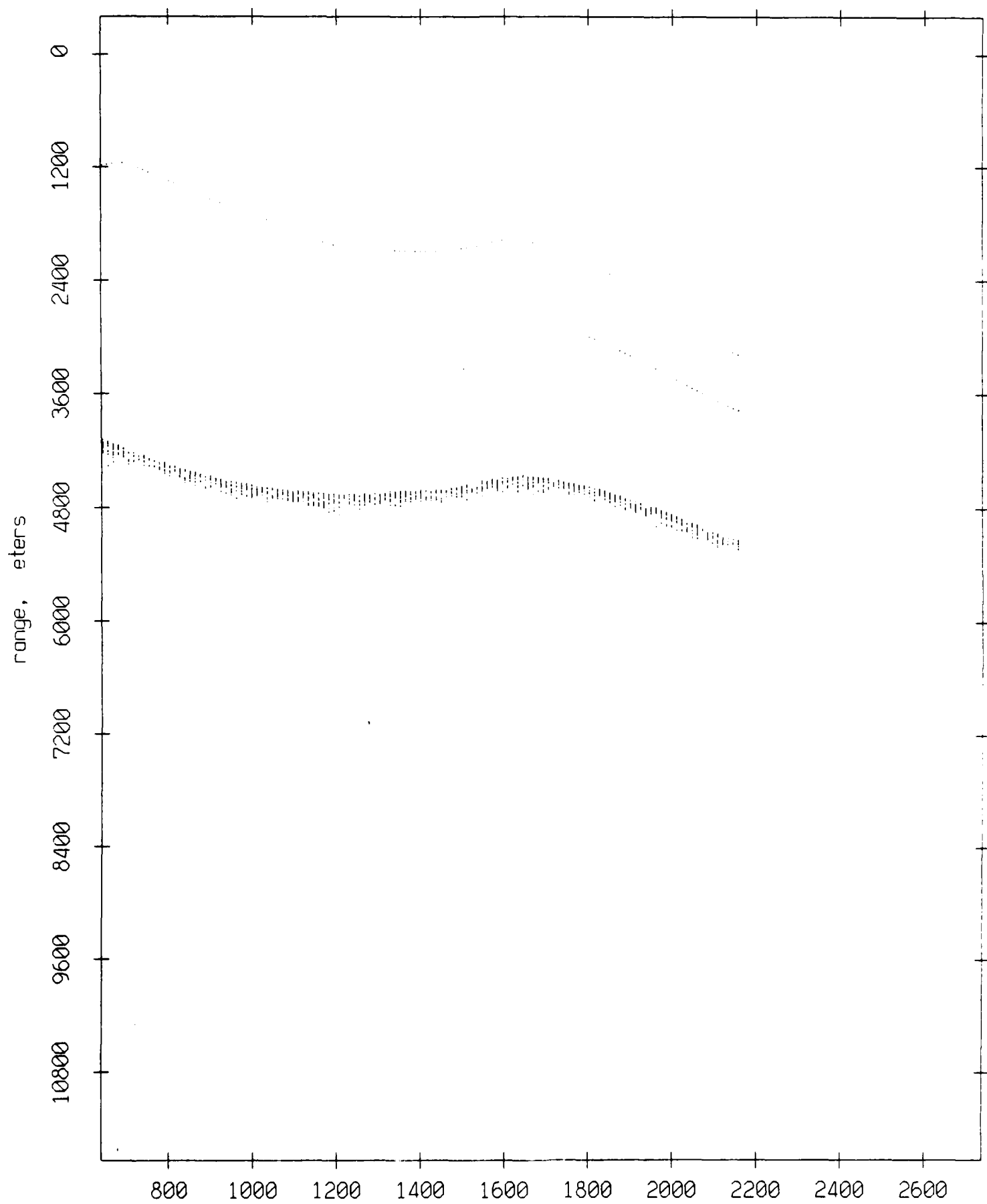
Float 3, July 1989 Trip: range from float 6



record number

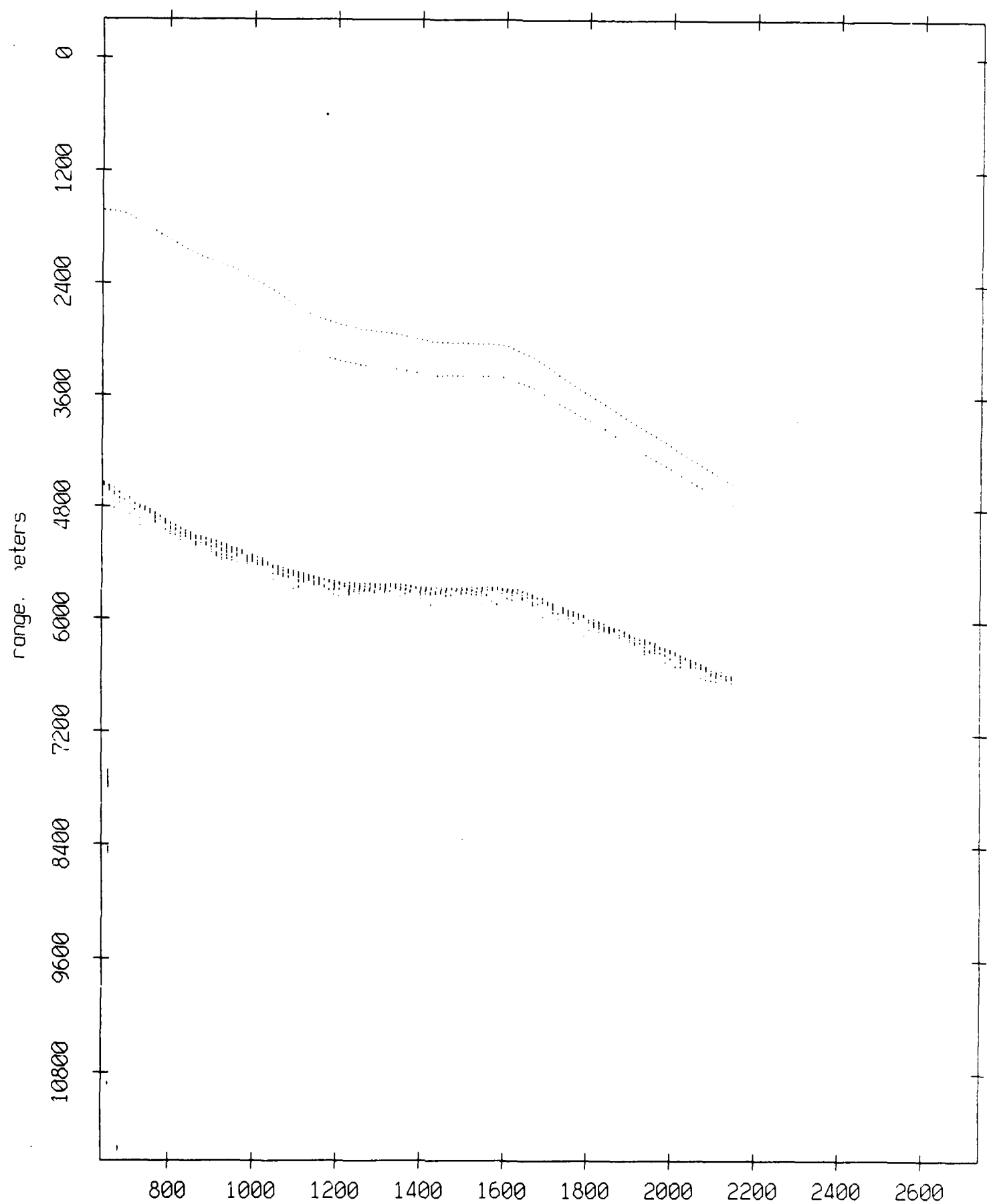
Figure IX.4f

Float 3, July 1989 Trip: range from float 7



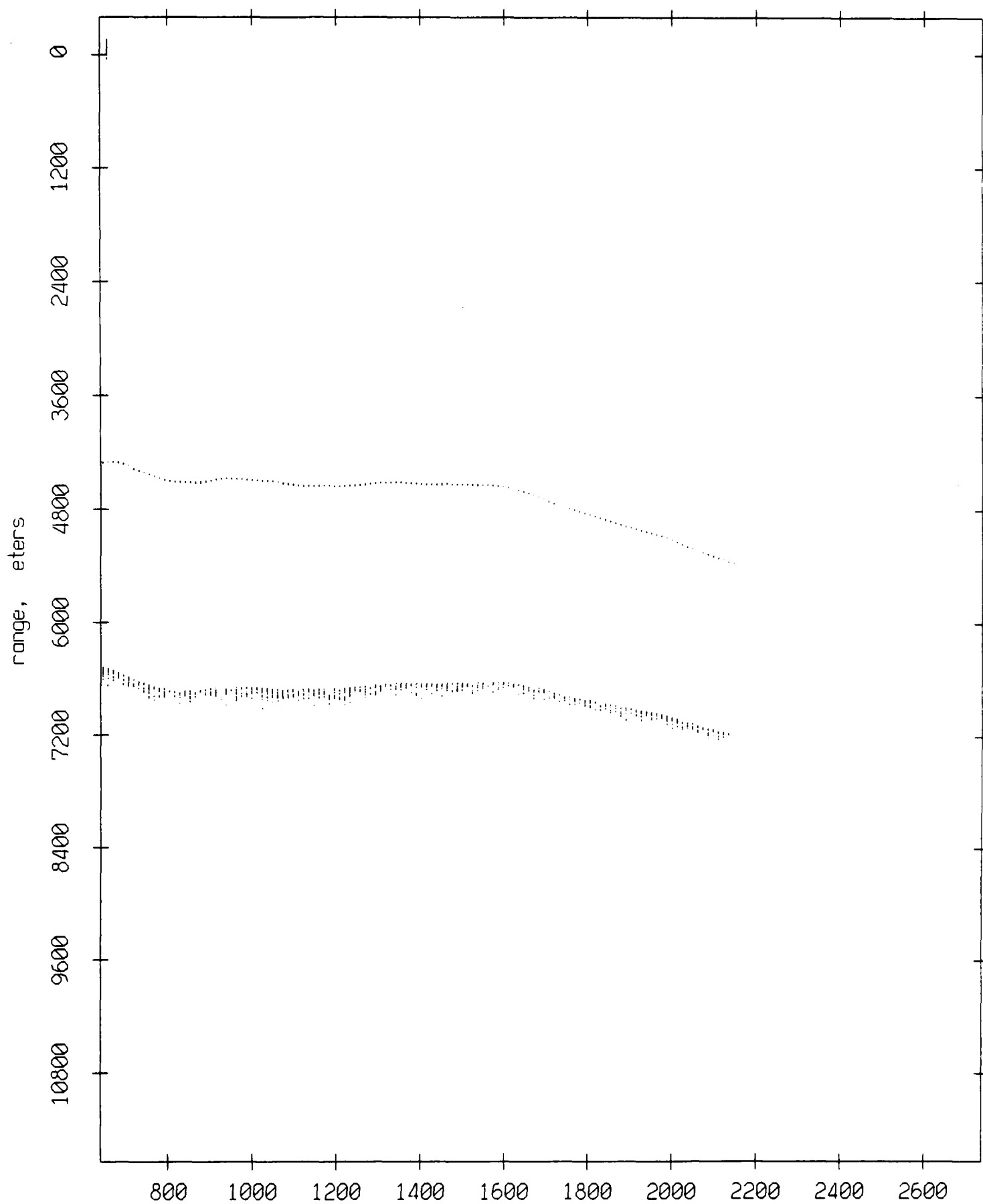
record number  
Figure IX.4g

Float 3, July 1989 Trip: range from float 8



record number  
Figure IX.4h

Float 3, July 1989 Trip: range from float 9

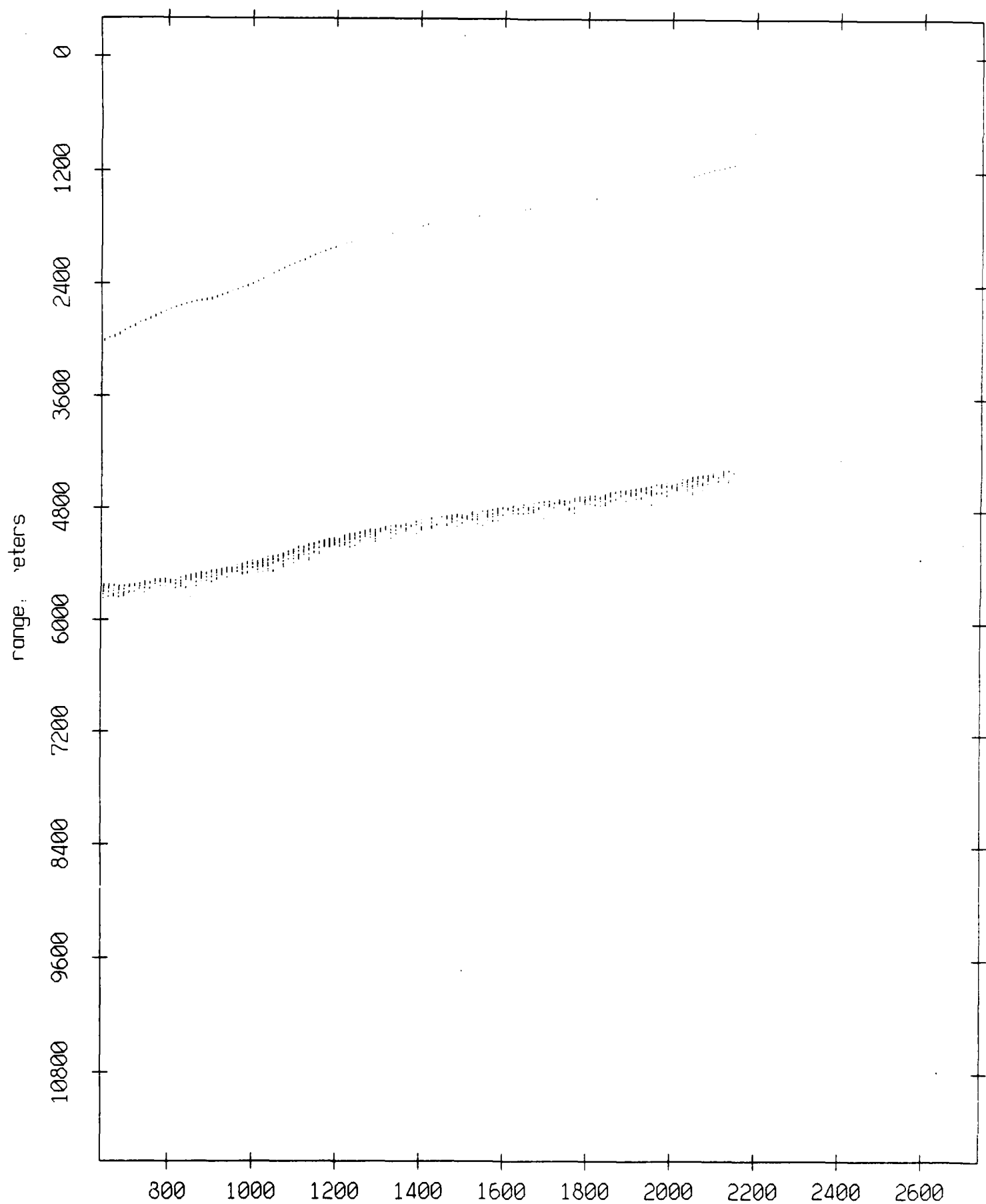


record number

Figure IX.41



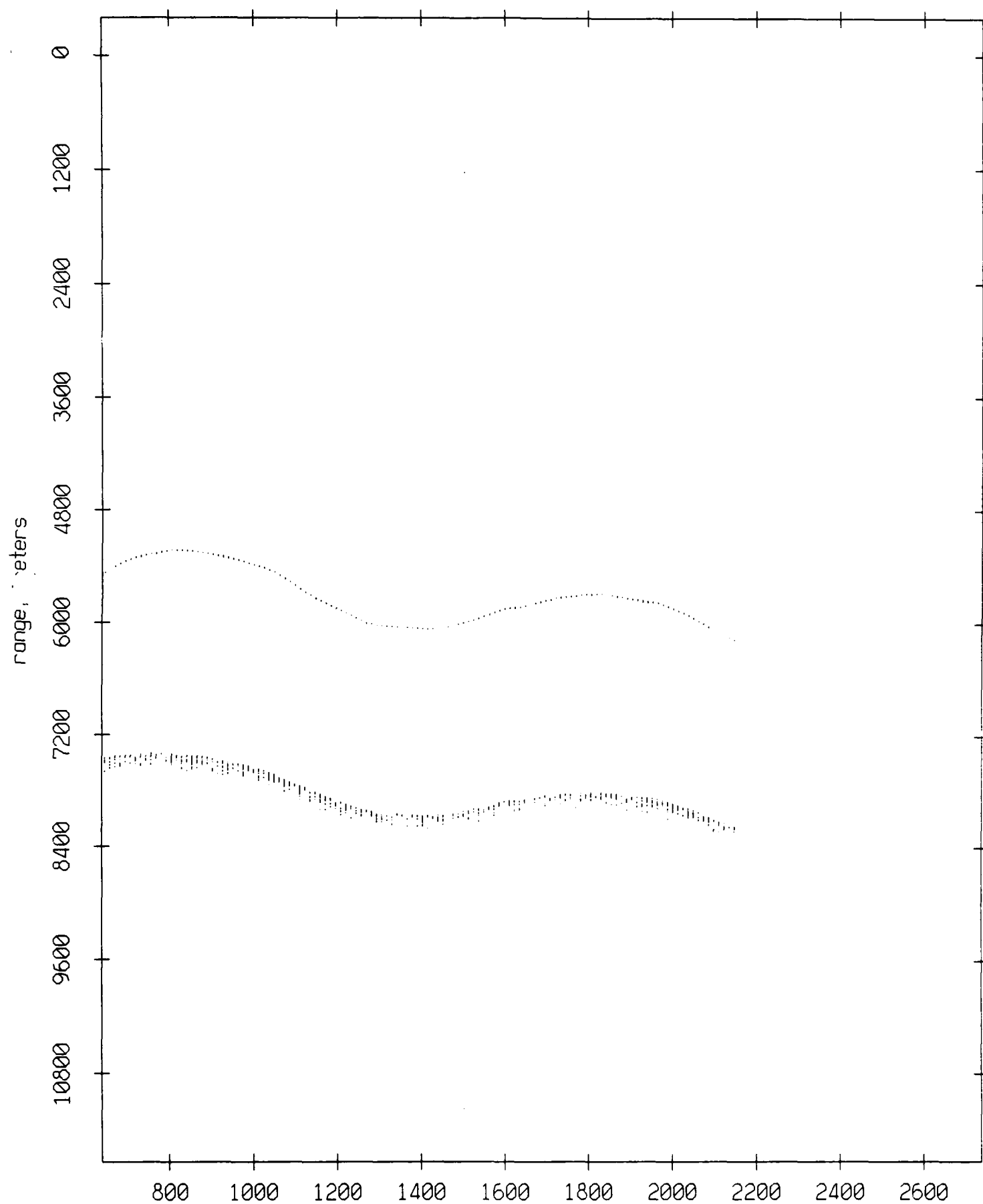
Float 3, July 1989 Trip: range from float 10



record number

Figure IX.4j

Float 3, July 1989 Trip: range from float 11



record number  
**Figure IX.4k**

Float 4, July 1989 Trip: range from float 0

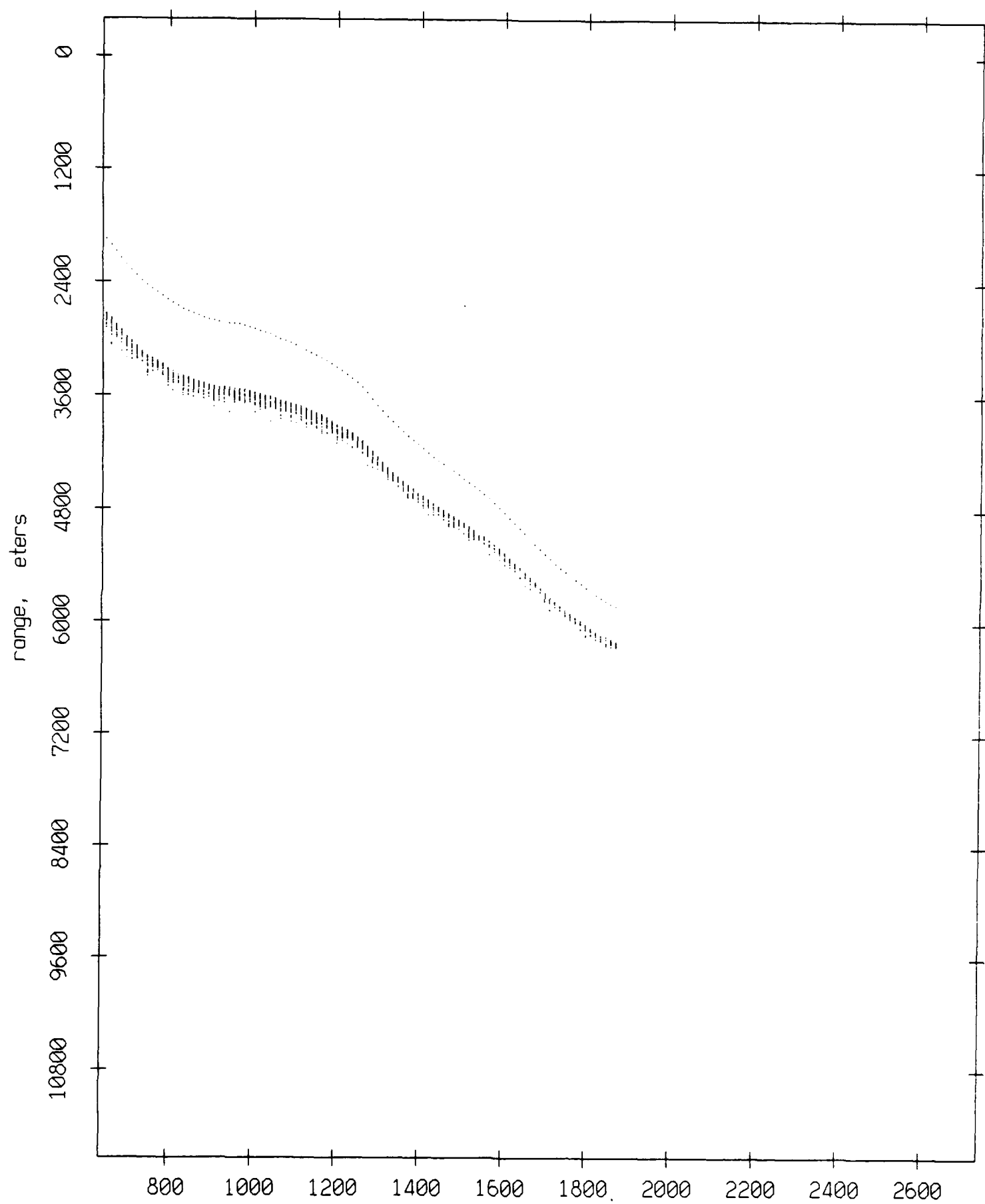


Figure IX.5a

Float 4, July 1989 Trip: range from float 1

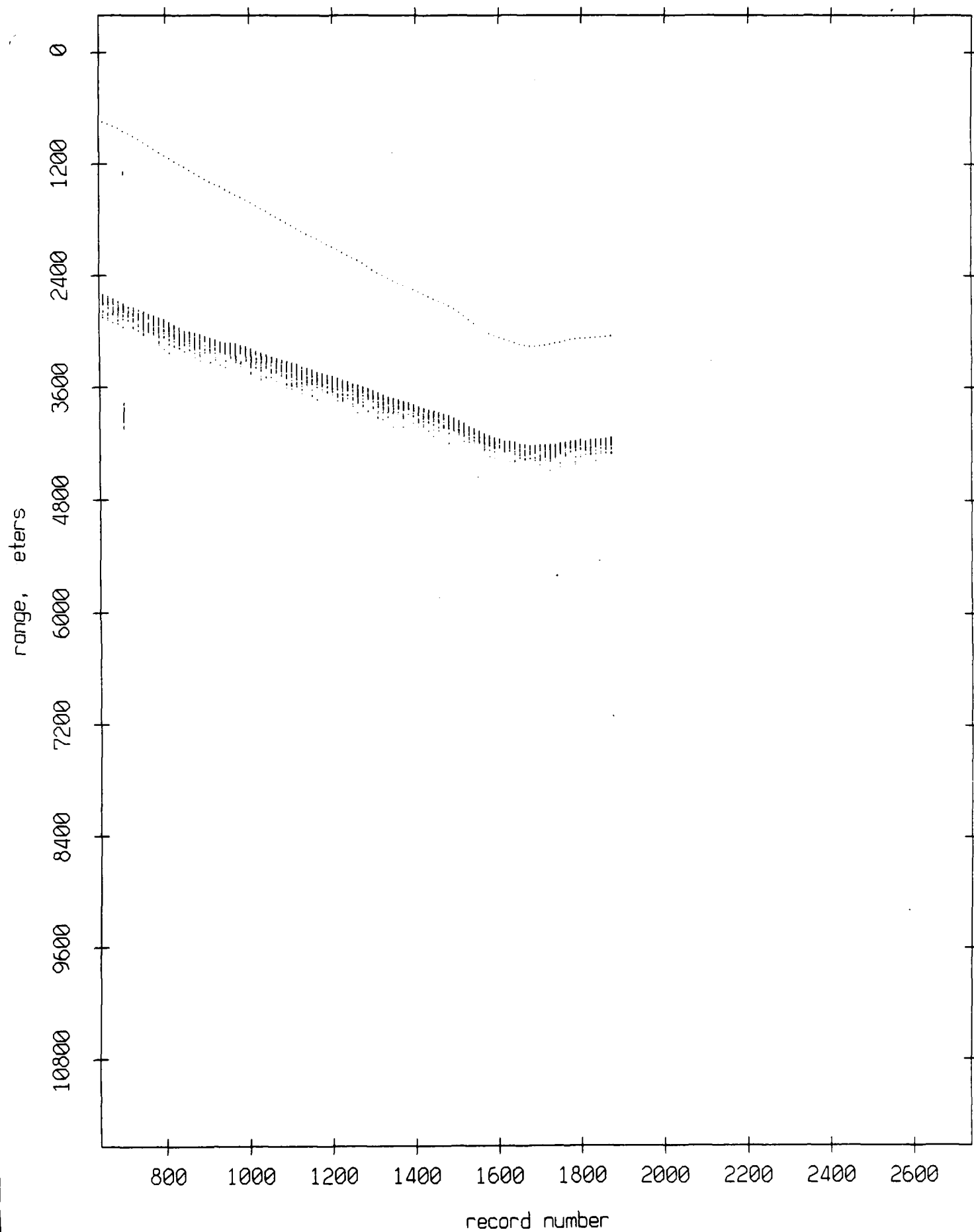


Figure IX.5b

Float 4, July 1989 Trip: range from float 2

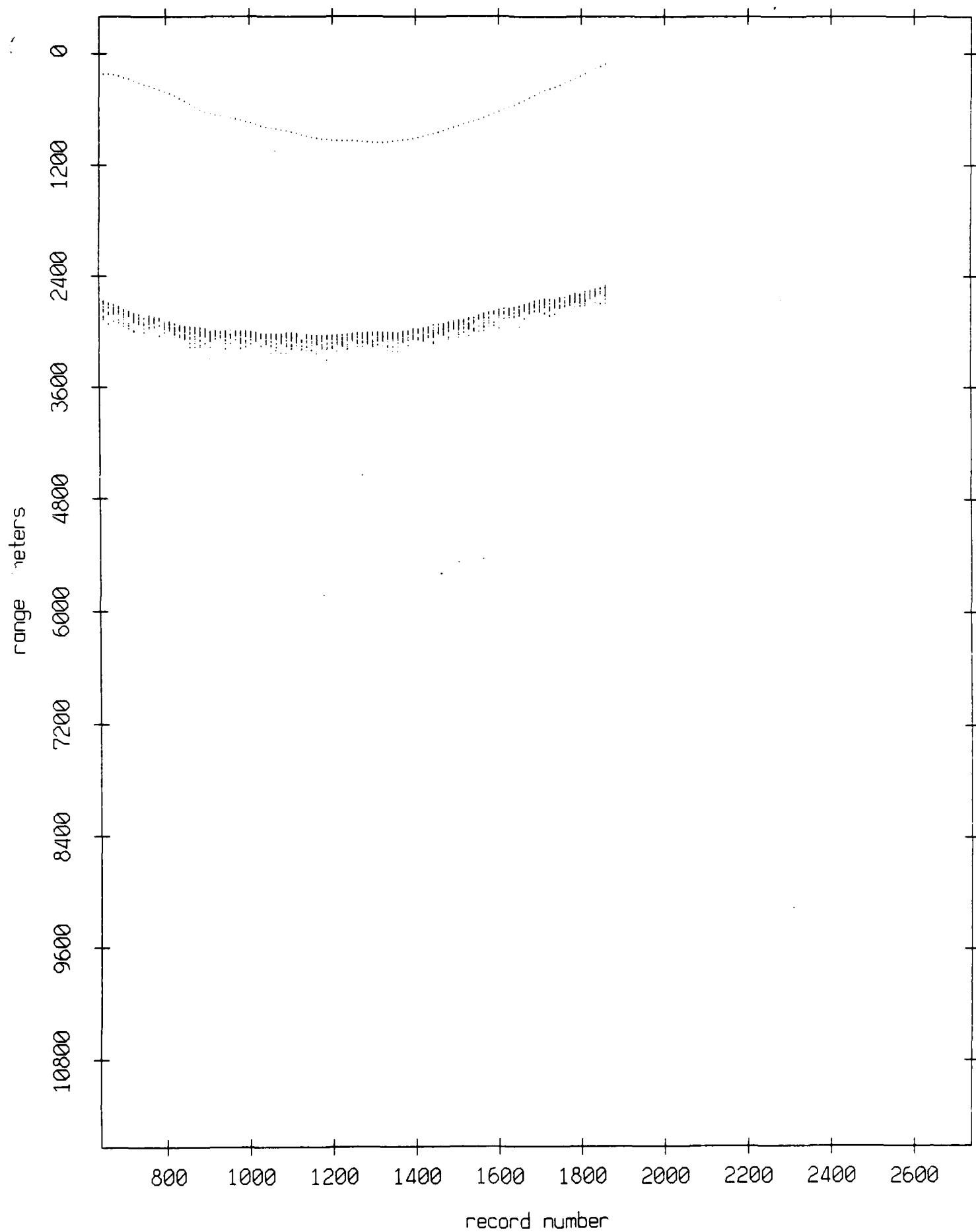
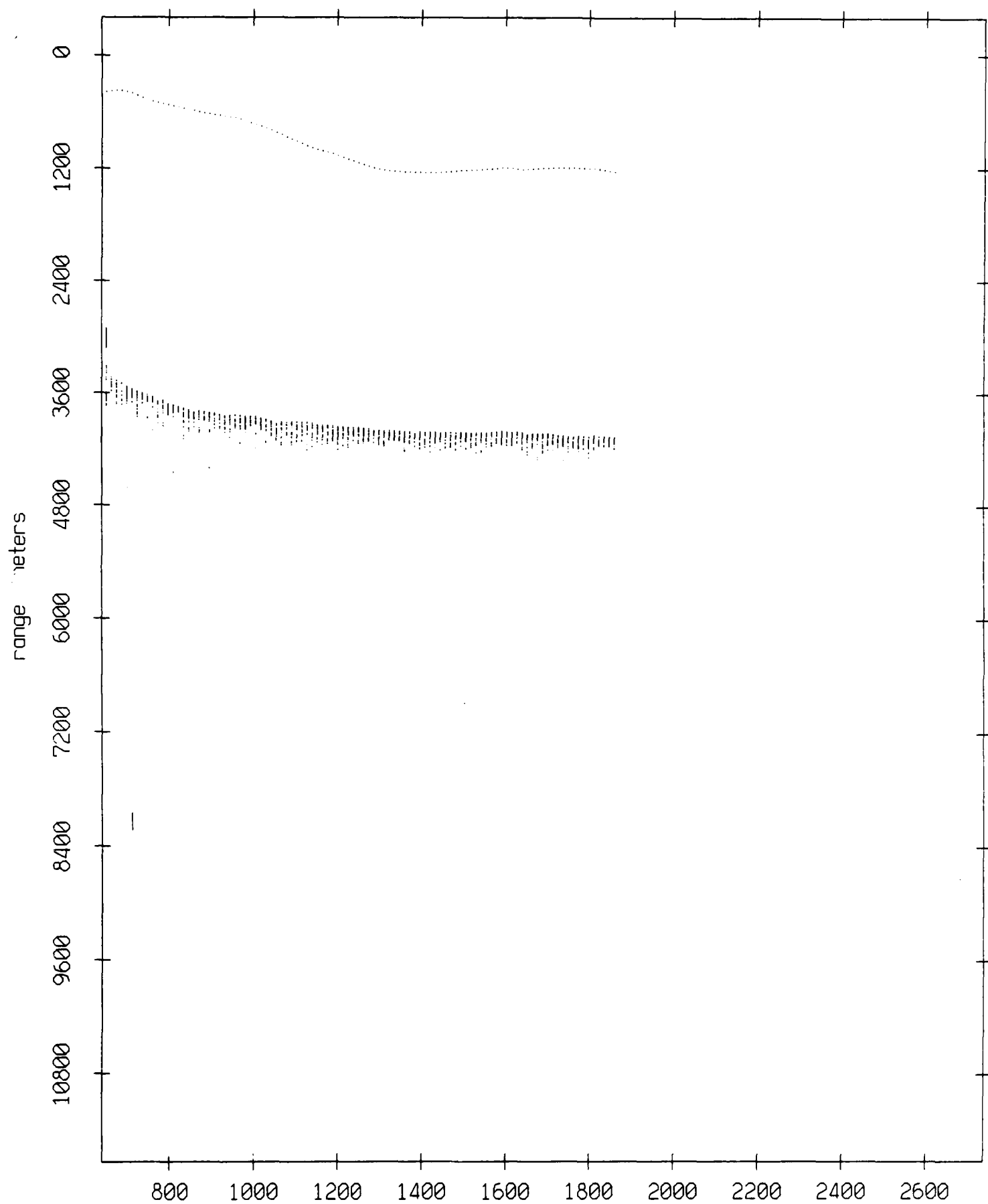


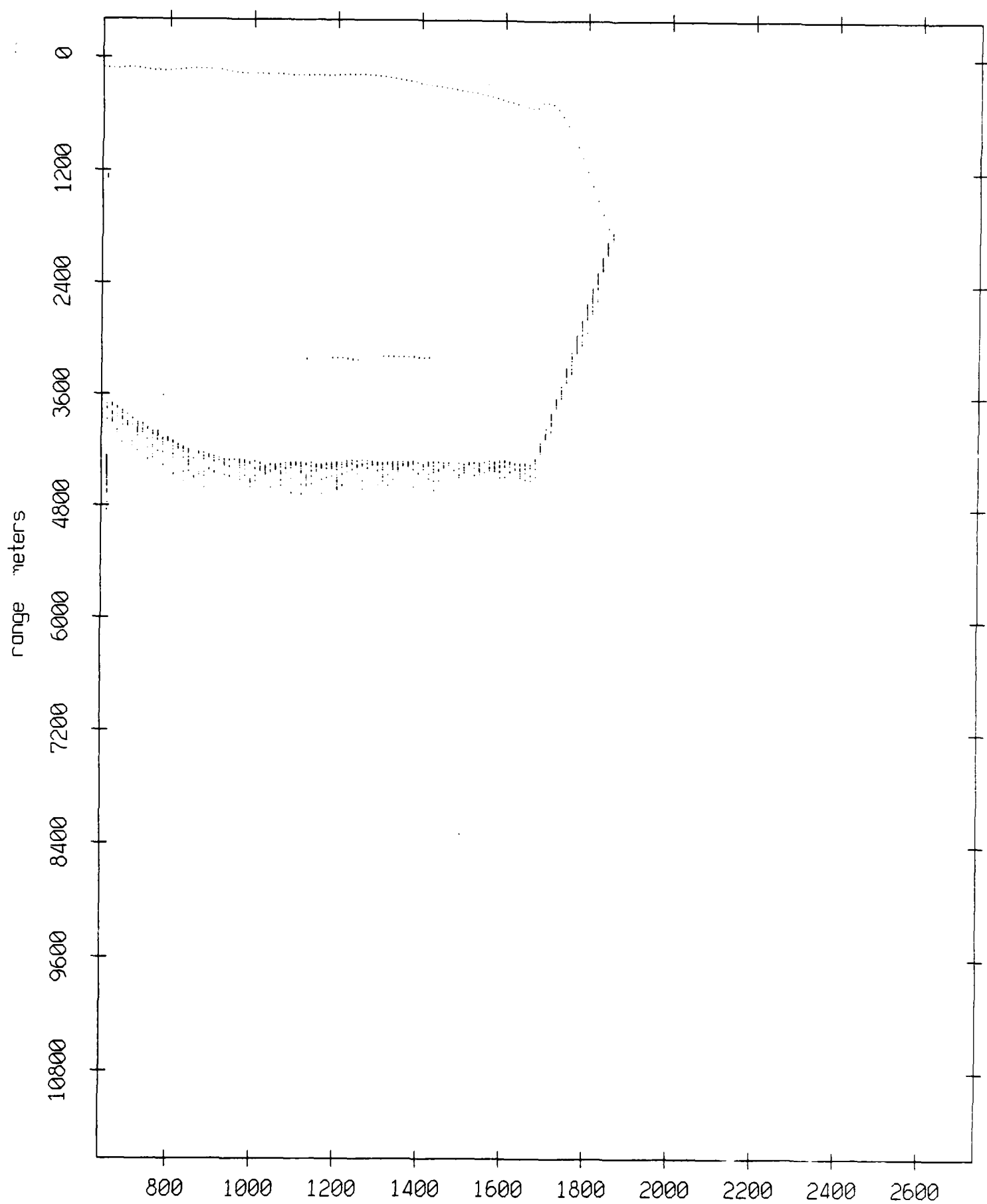
Figure IX.5c

Float 4, July 1989 Trip: range from float 3



record number  
**Figure IX.5d**

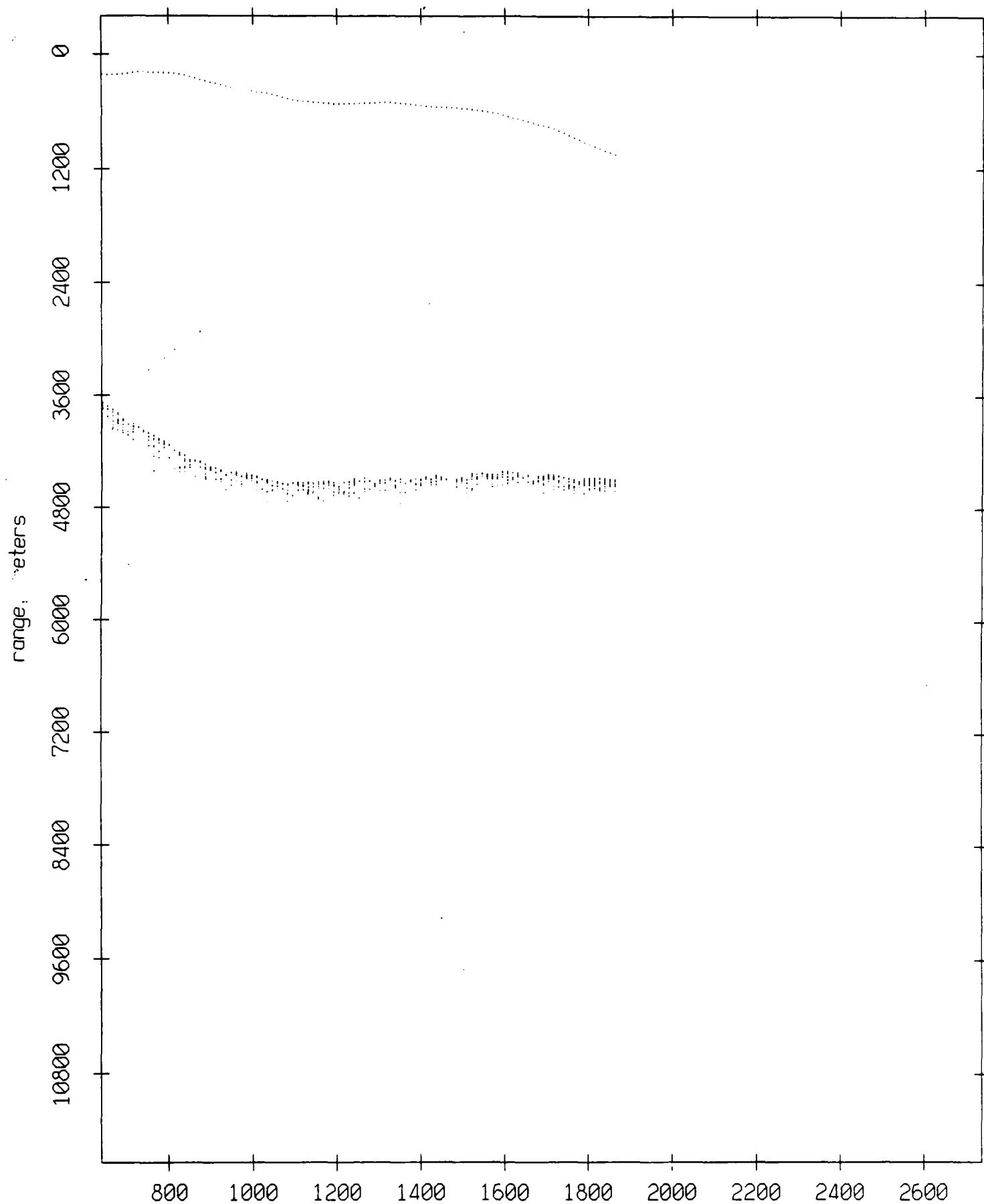
Float 4, July 1989 Trip: range from float 5



record number

Figure IX.5e

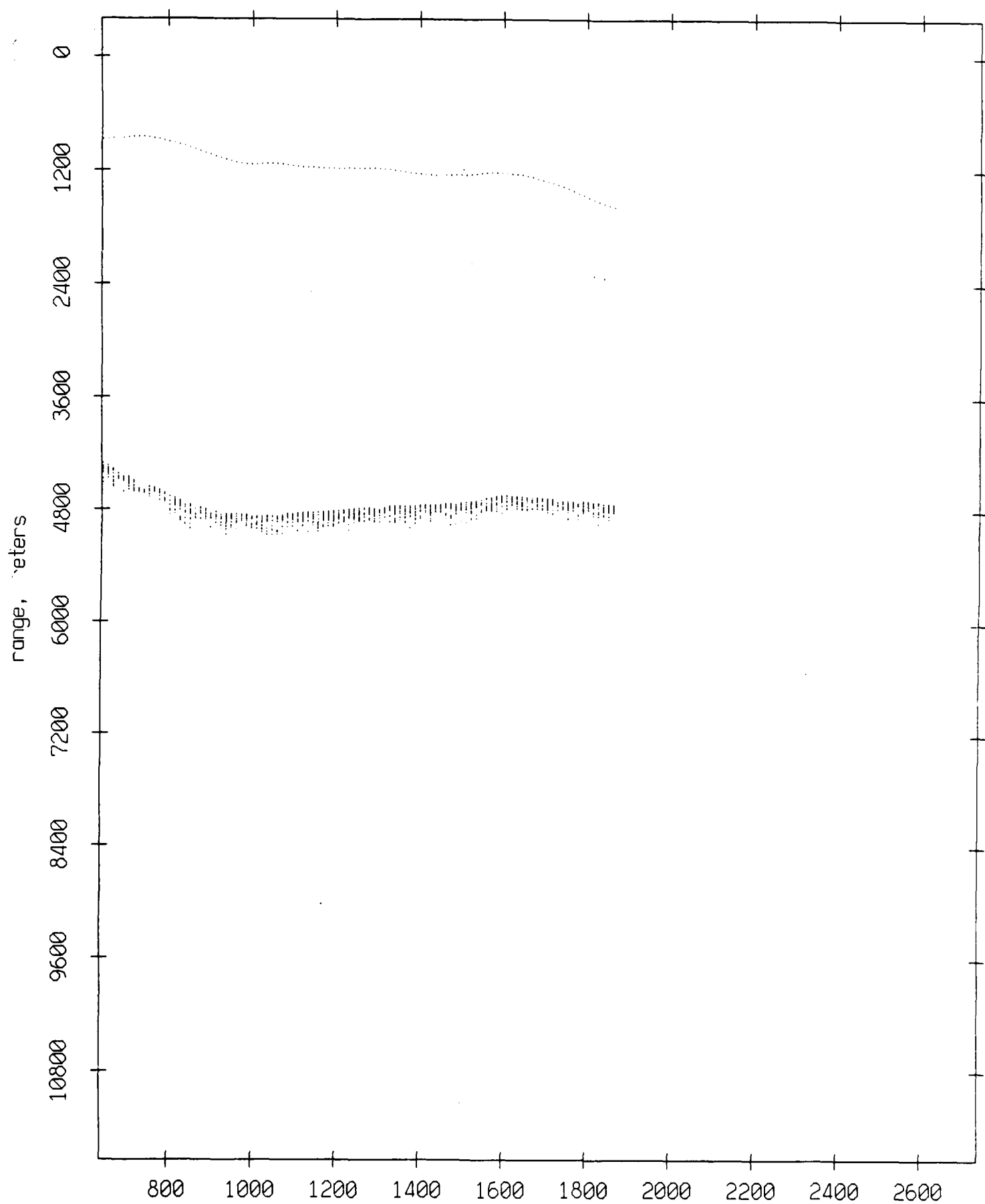
Float 4, July 1989 Trip: range from float 6



record number  
**Figure IX.5f**



Float 4, July 1989 Trip: range from float 7



record number  
**Figure IX.5g**

Float 4, July 1989 Trip: range from float 8

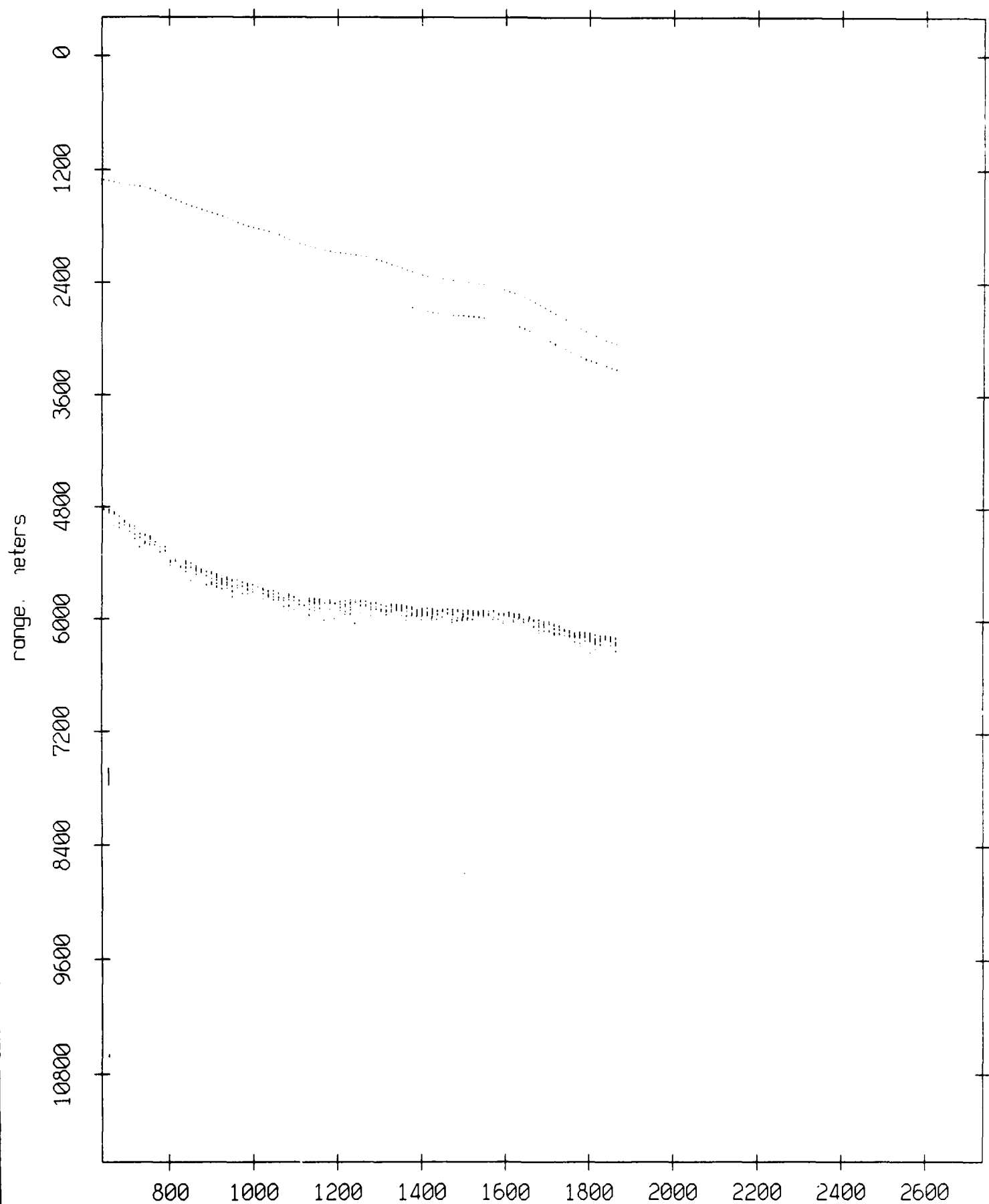
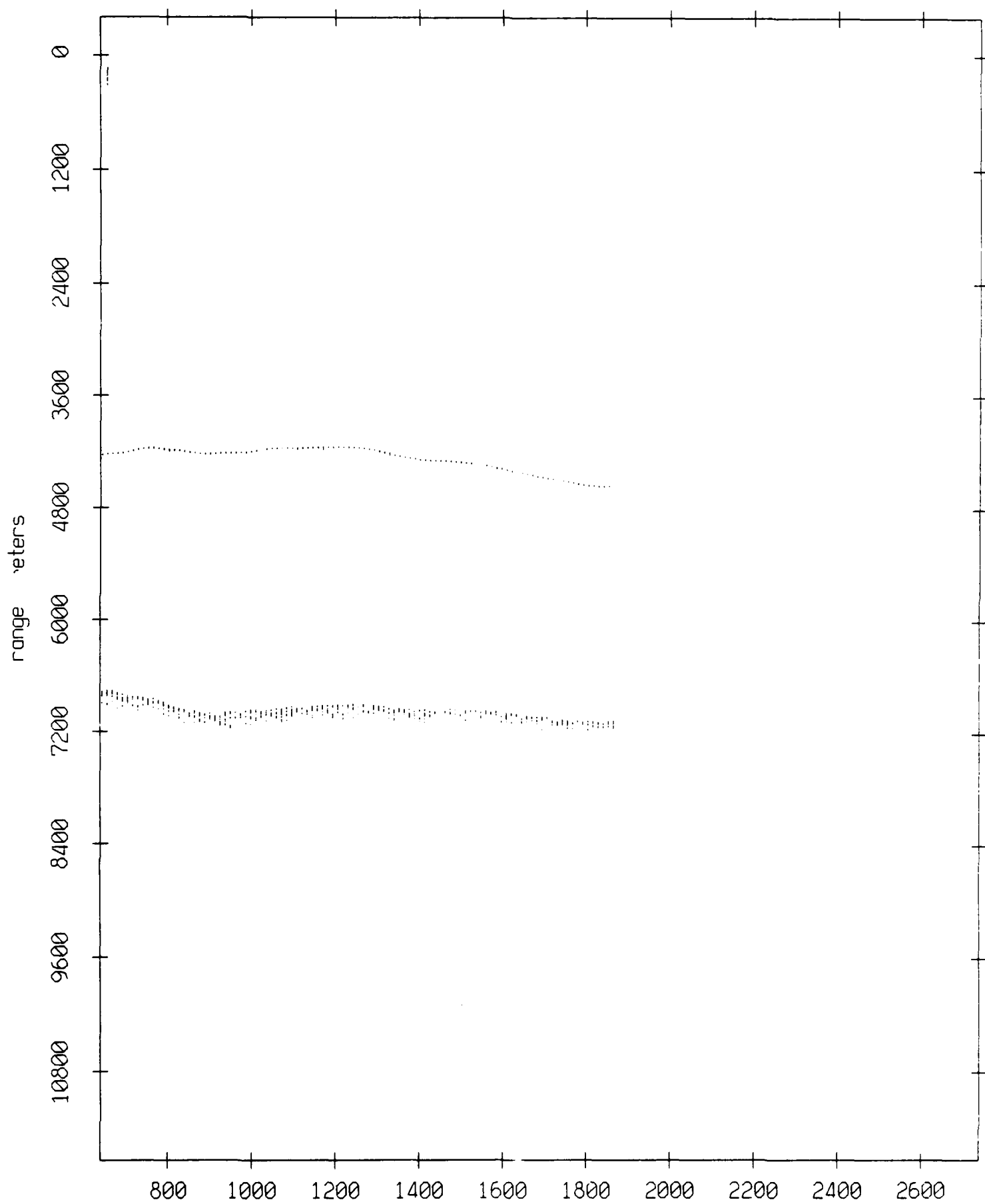


Figure IX.5h

Float 4, July 1989 Trip: range from float 9



record number  
Figure IX.51

Float 4, July 1989 Trip: range from float 10

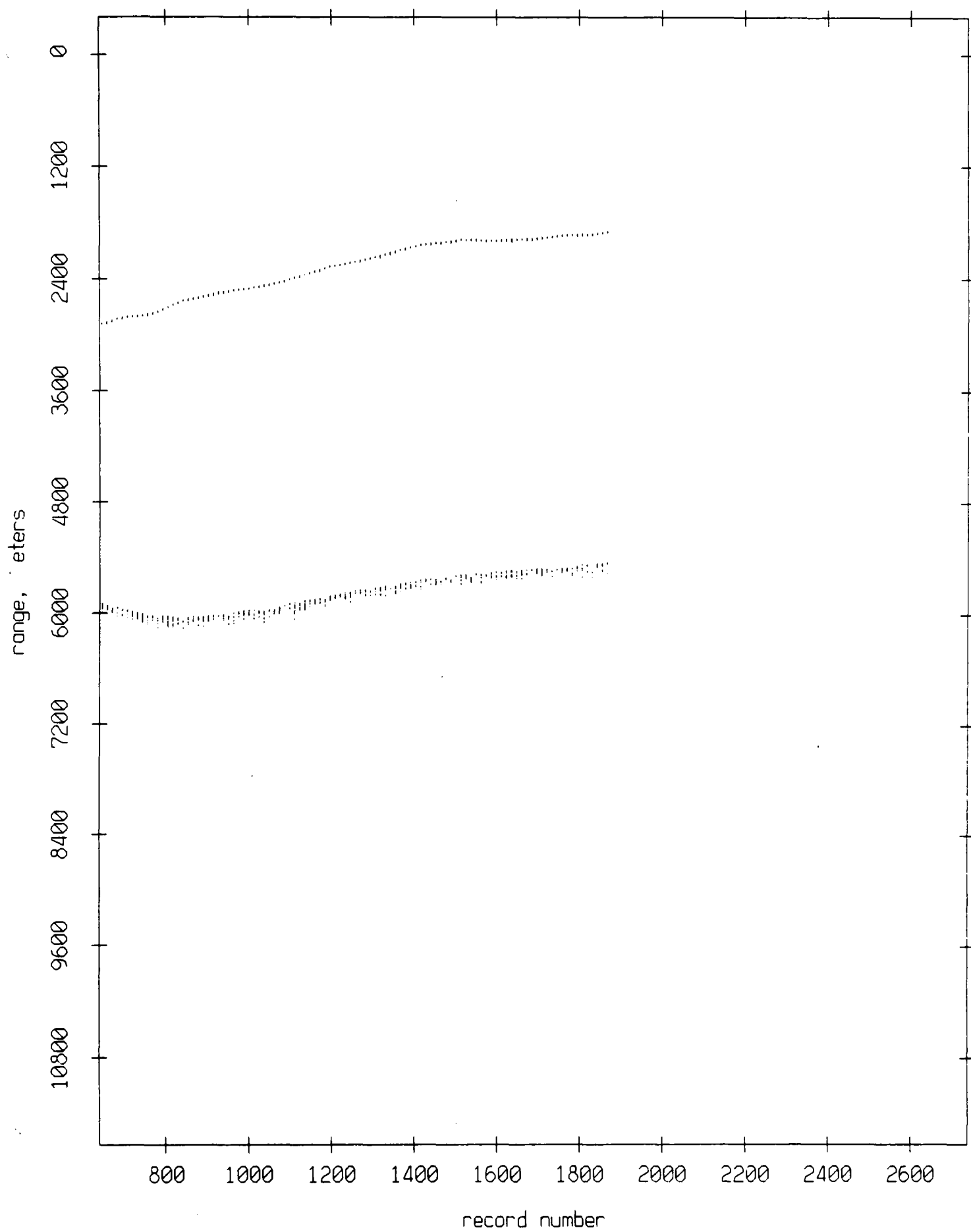
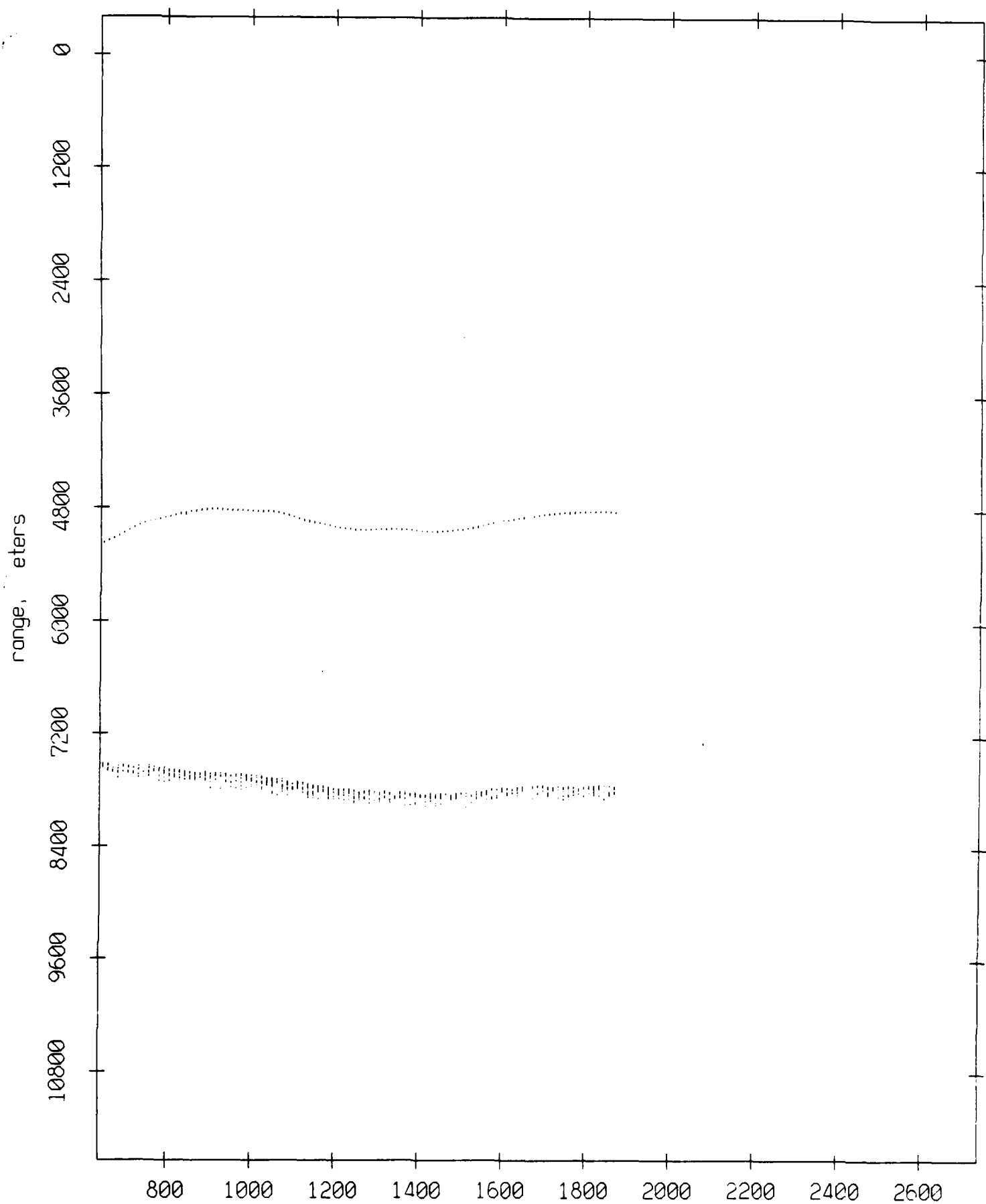


Figure IX.5j

Float 4, July 1989 Trip: range from float 11



record number

Figure IX.5k

Float 5, July 1989 Trip: range from float 0

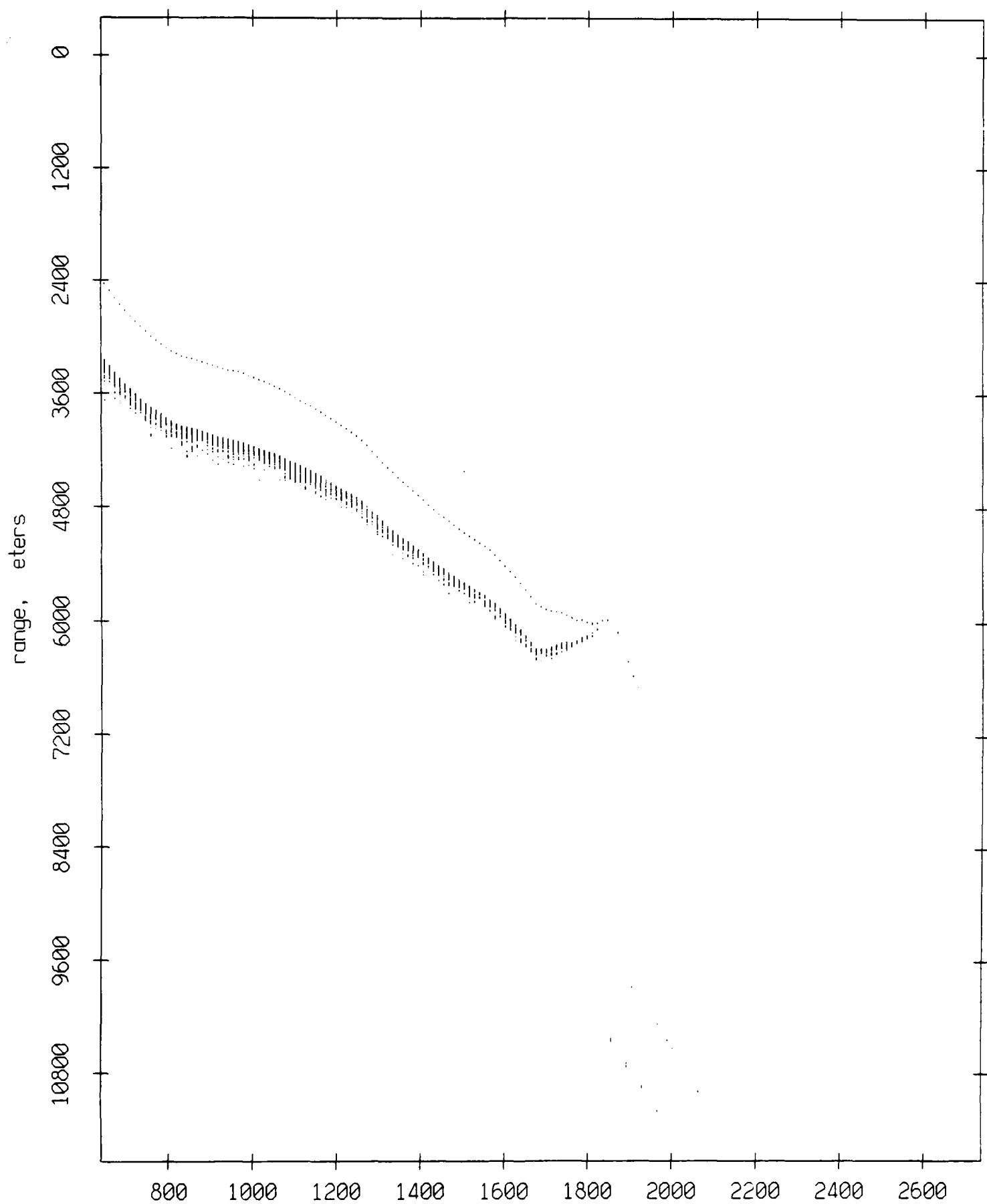
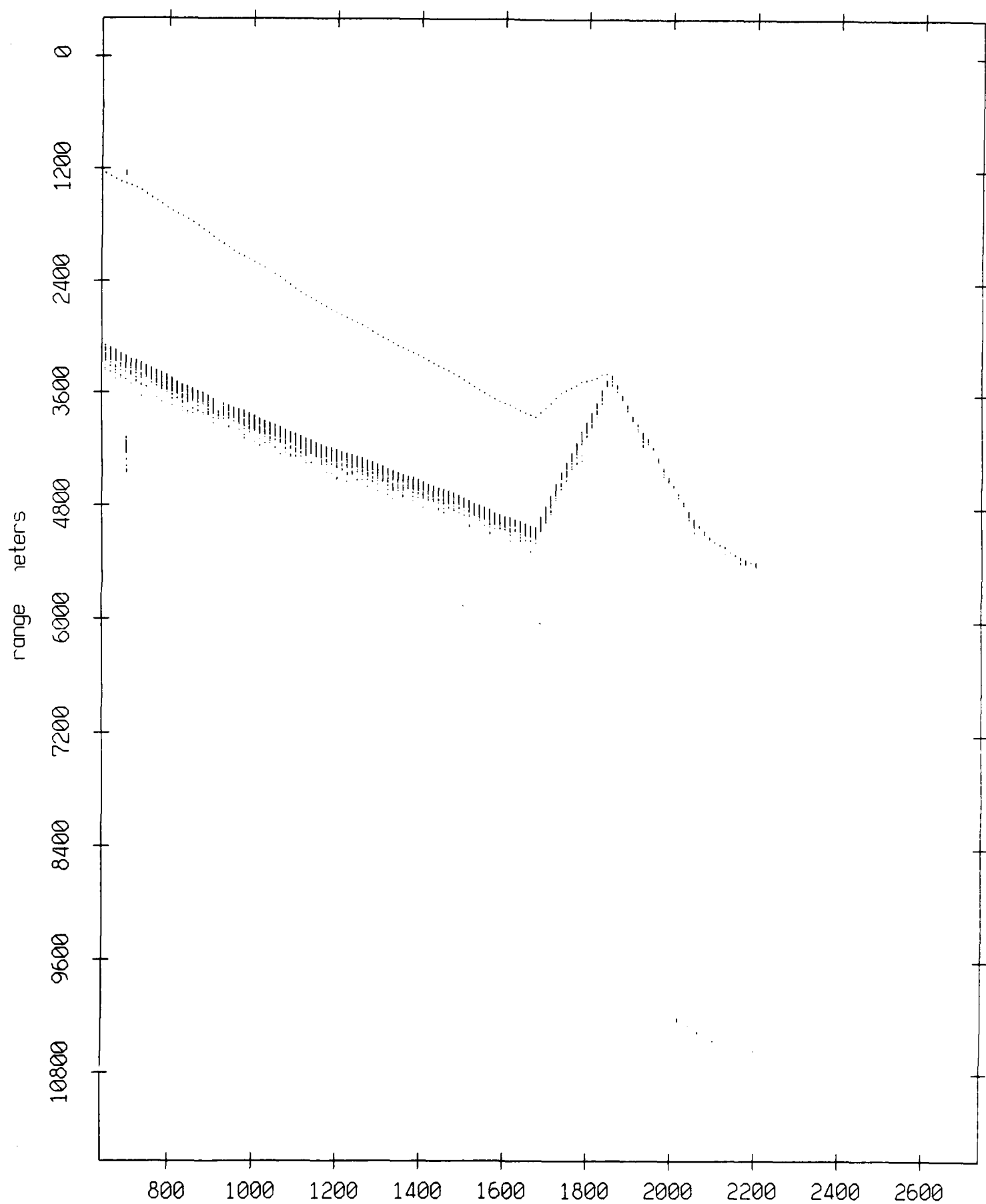


Figure IX.6a

Float 5, July 1989 Trip: range from float 1



record number

Figure IX.6b

Float 5, July 1989 Trip: range from float 2

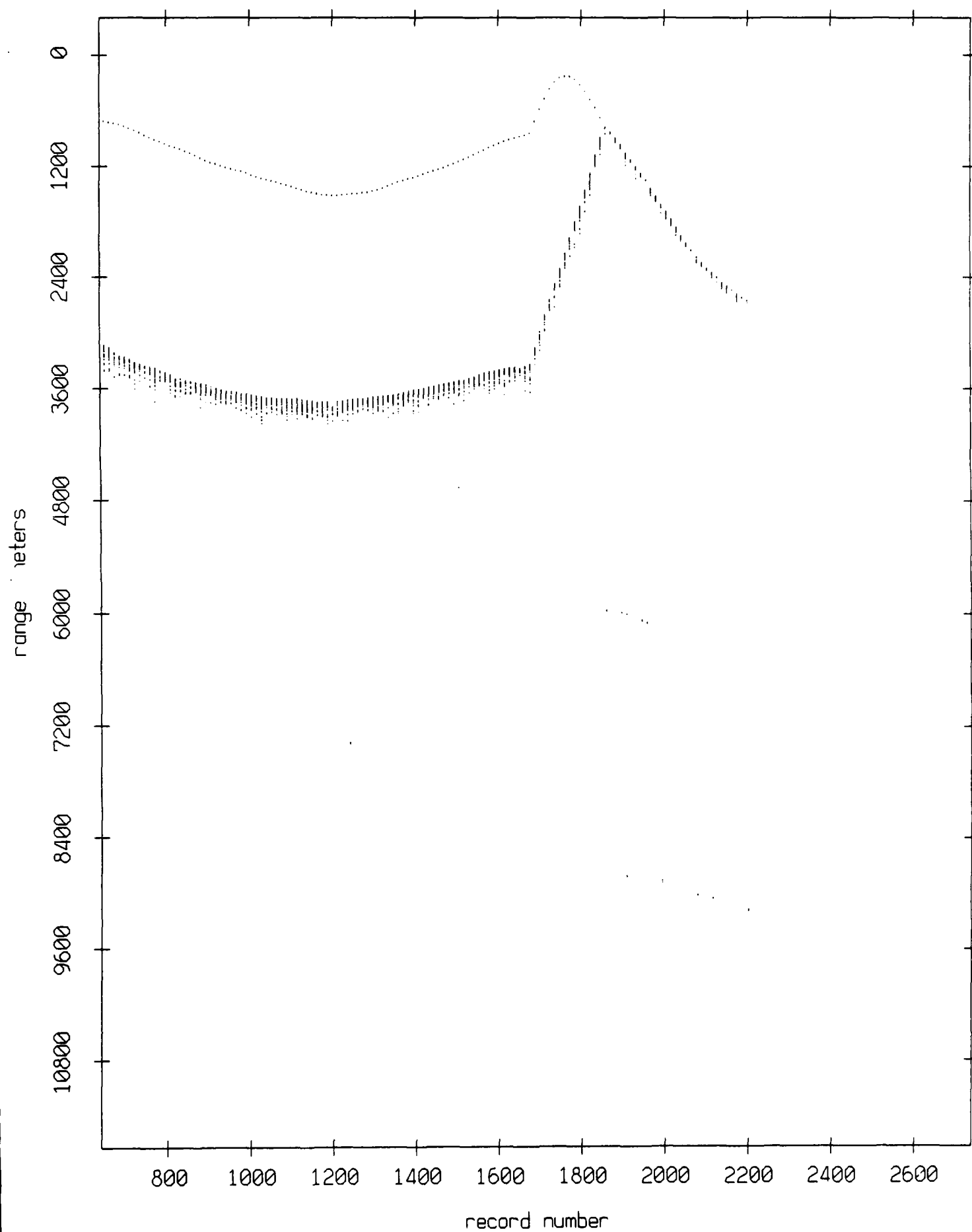
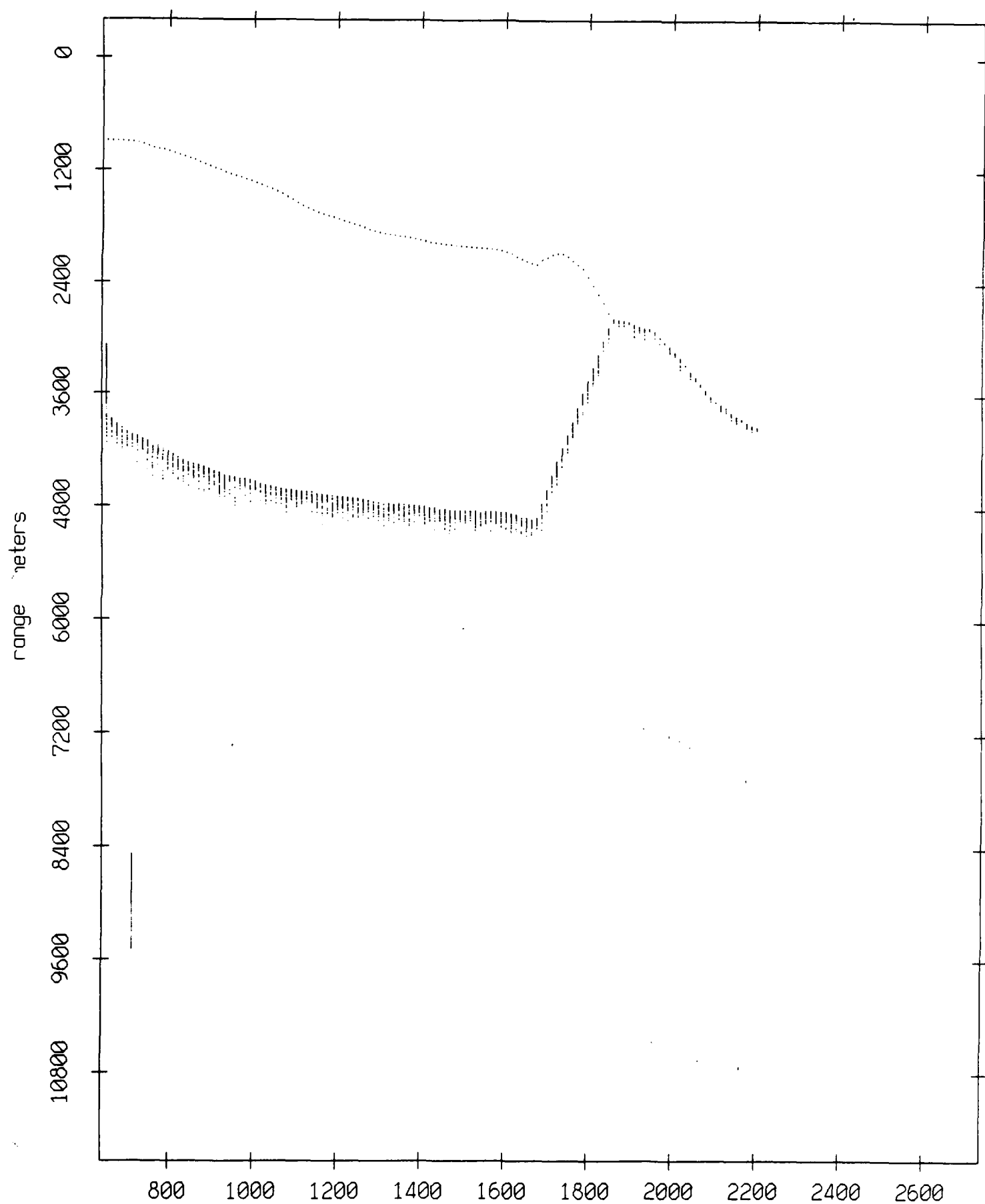


Figure IX.6c

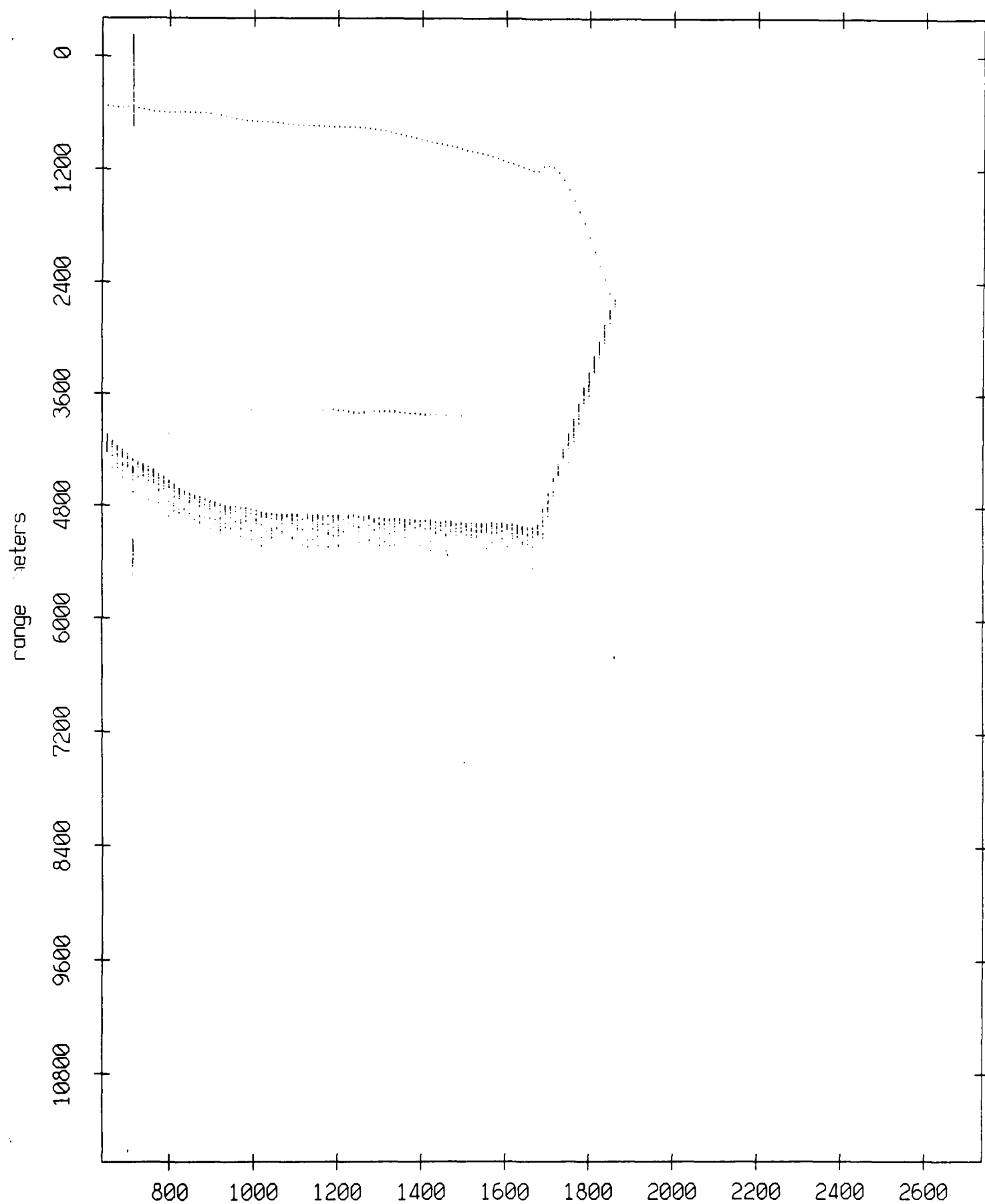


Float 5, July 1989 Trip: range from float 3



record number  
Figure IX.6d

Float 5, July 1989 Trip: range from float 4



record number

Figure IX.6e

Float 5, July 1989 Trip: range from float 6

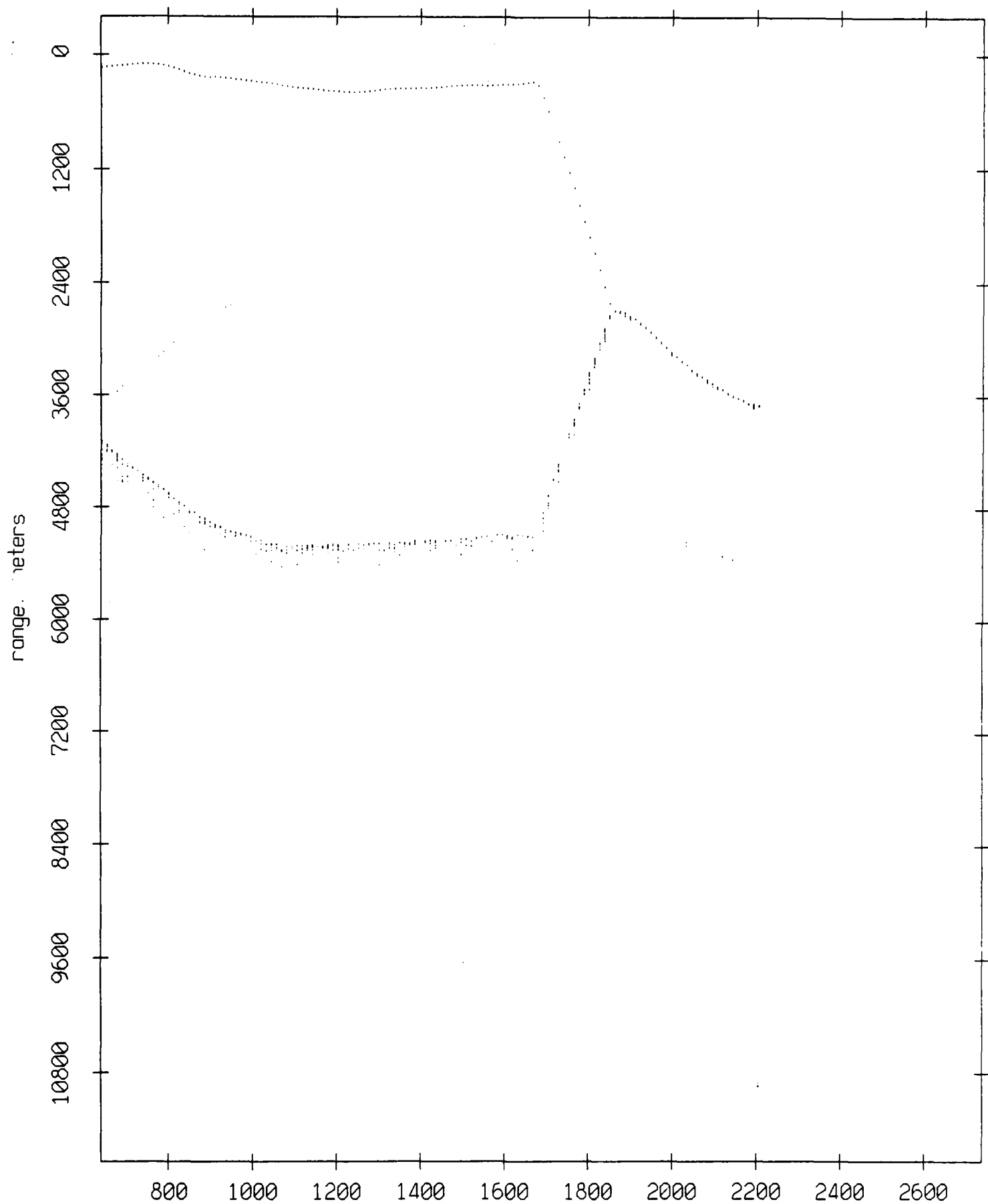


Figure IX.6f

Float 5, July 1989 Trip: range from float 7

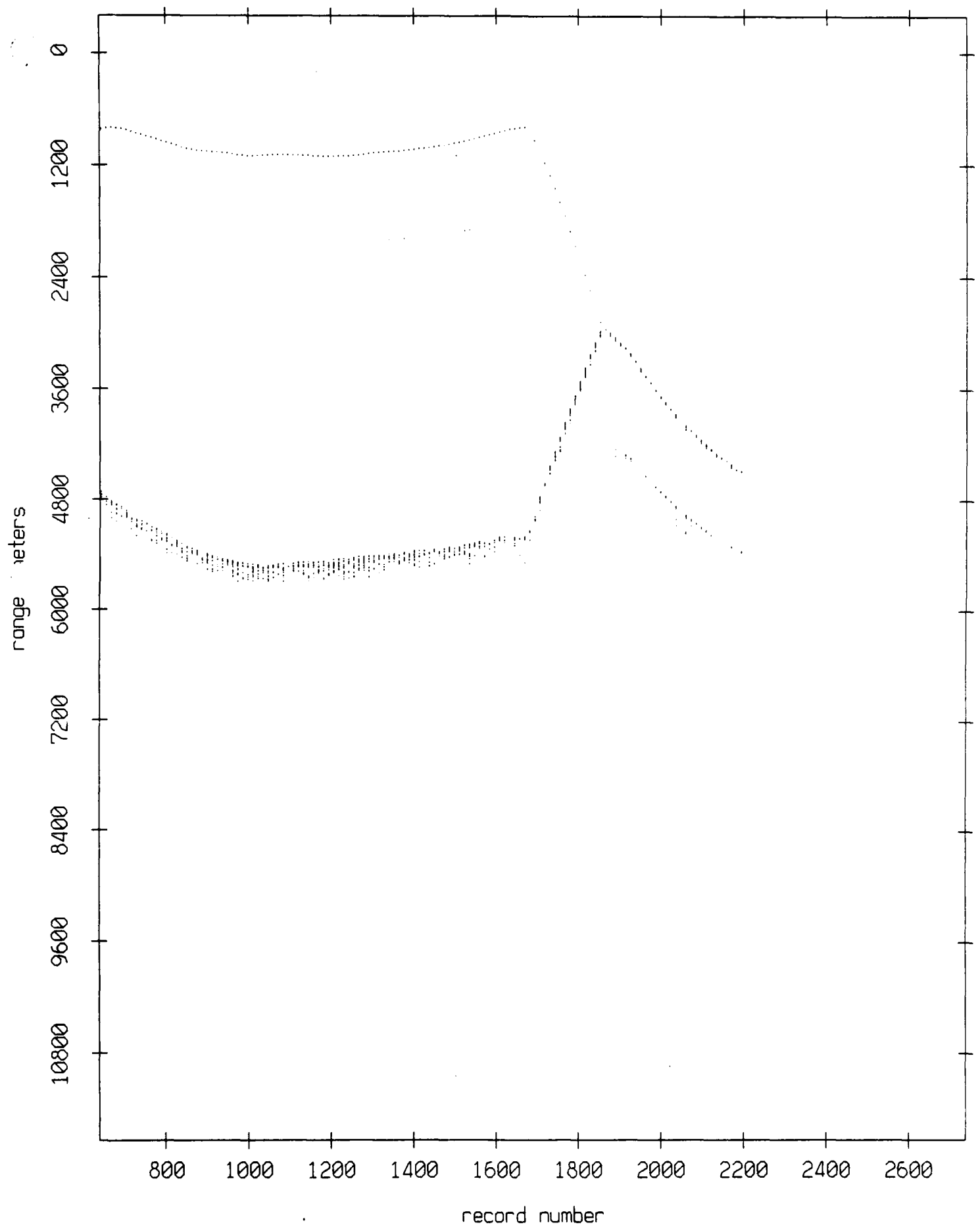
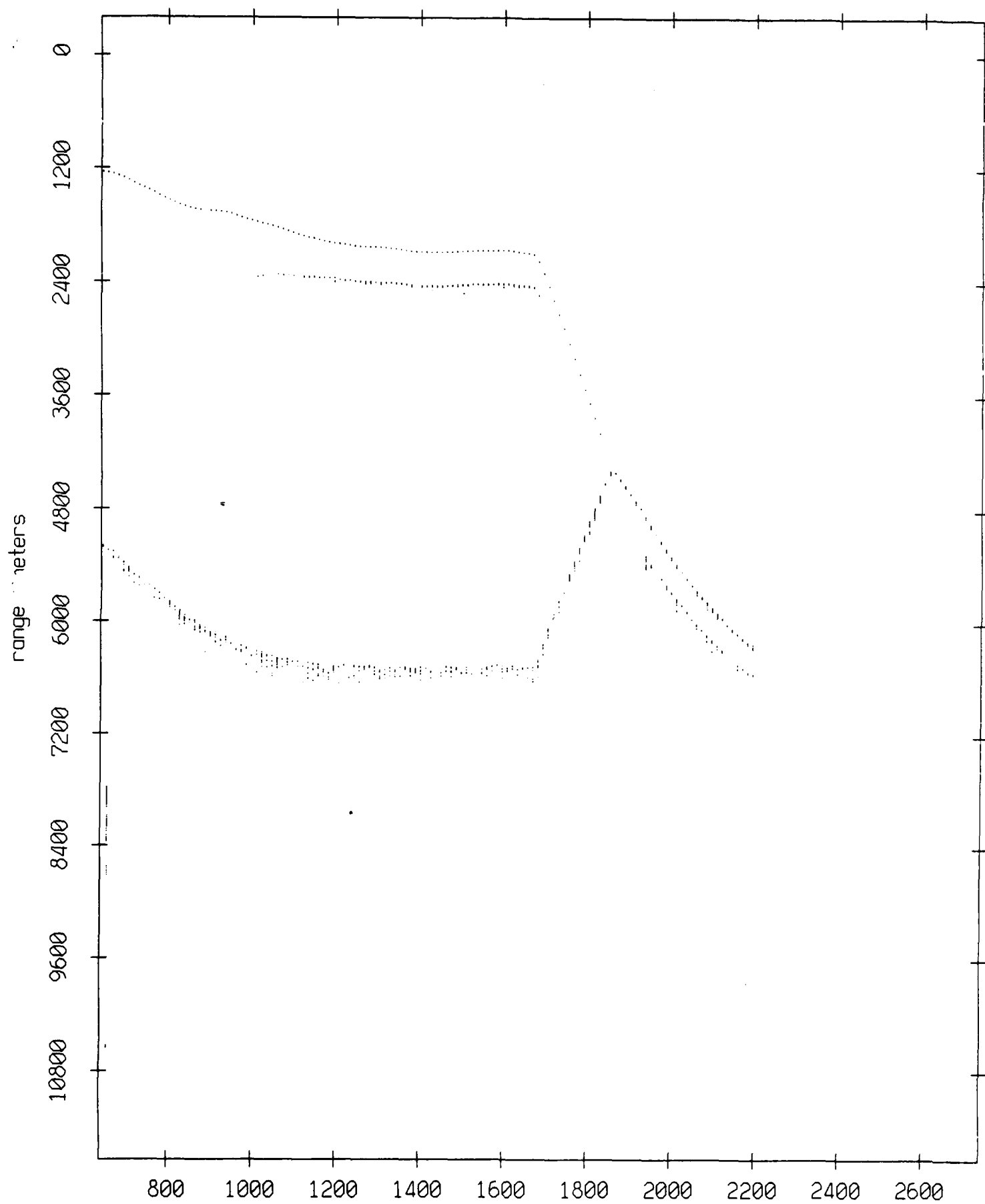


Figure IX.6g

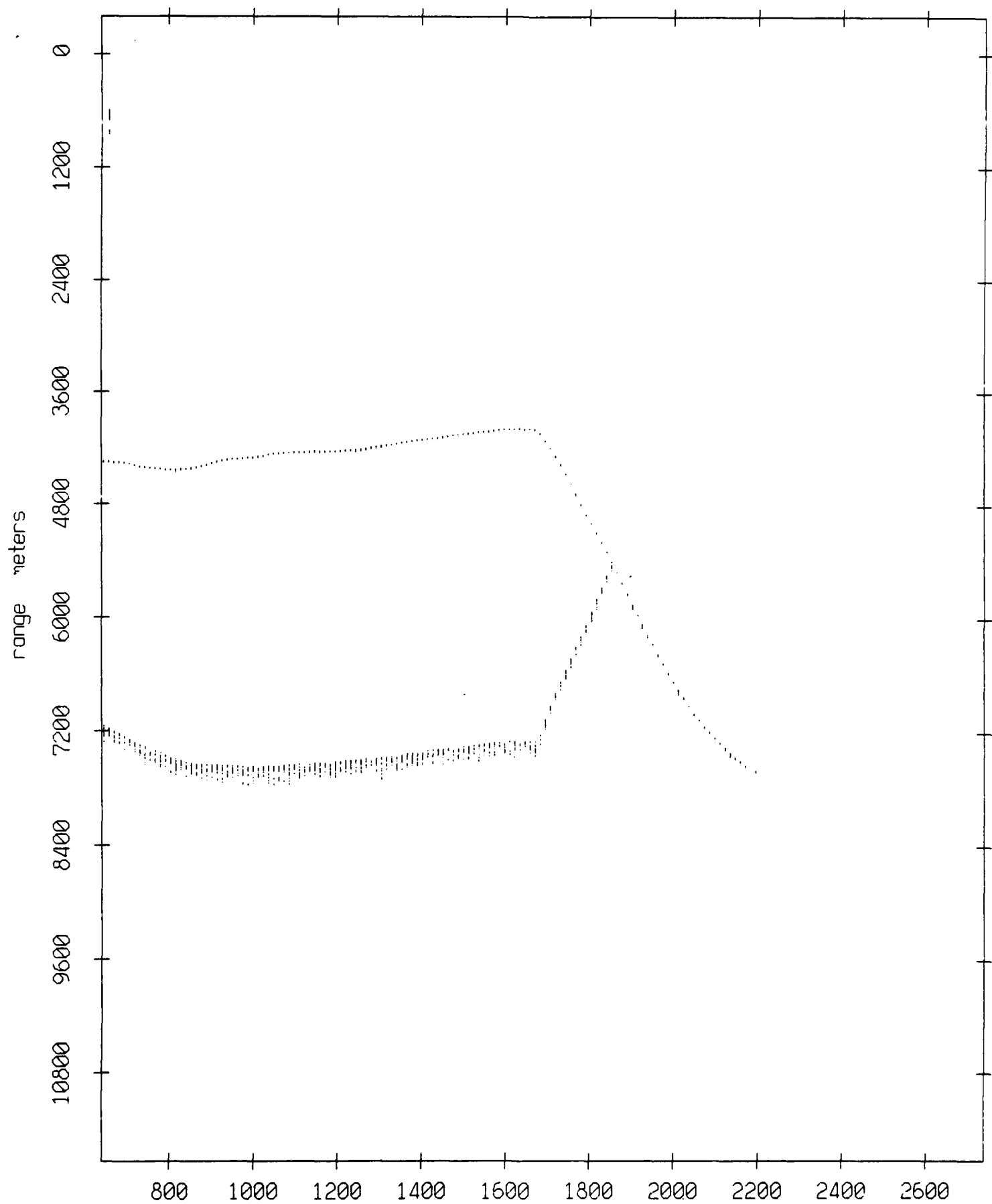
Float 5, July 1989 Trip: range from float 8



record number

Figure IX.6h

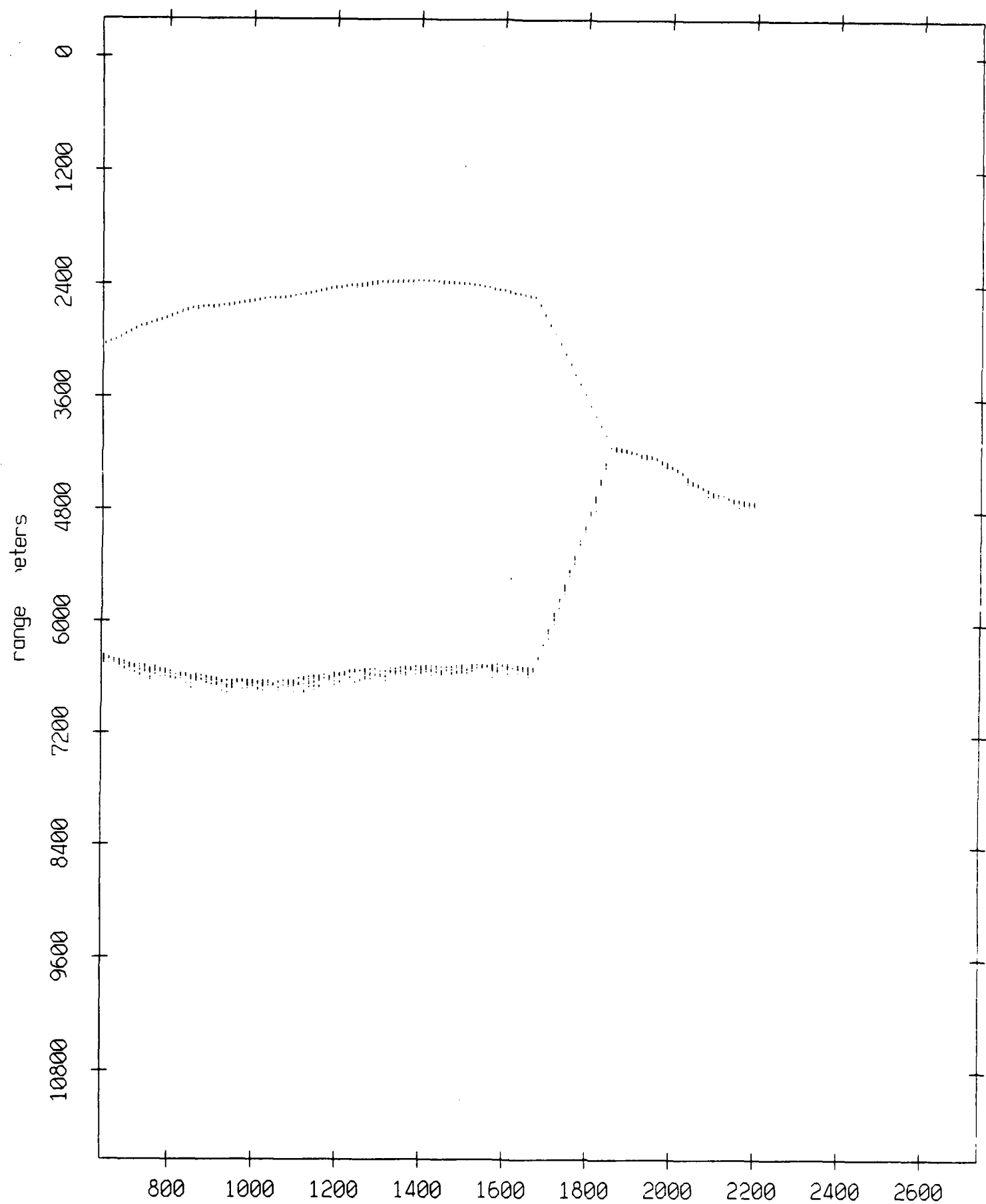
Float 5, July 1989 Trip: range from float 9



record number

Figure IX.61

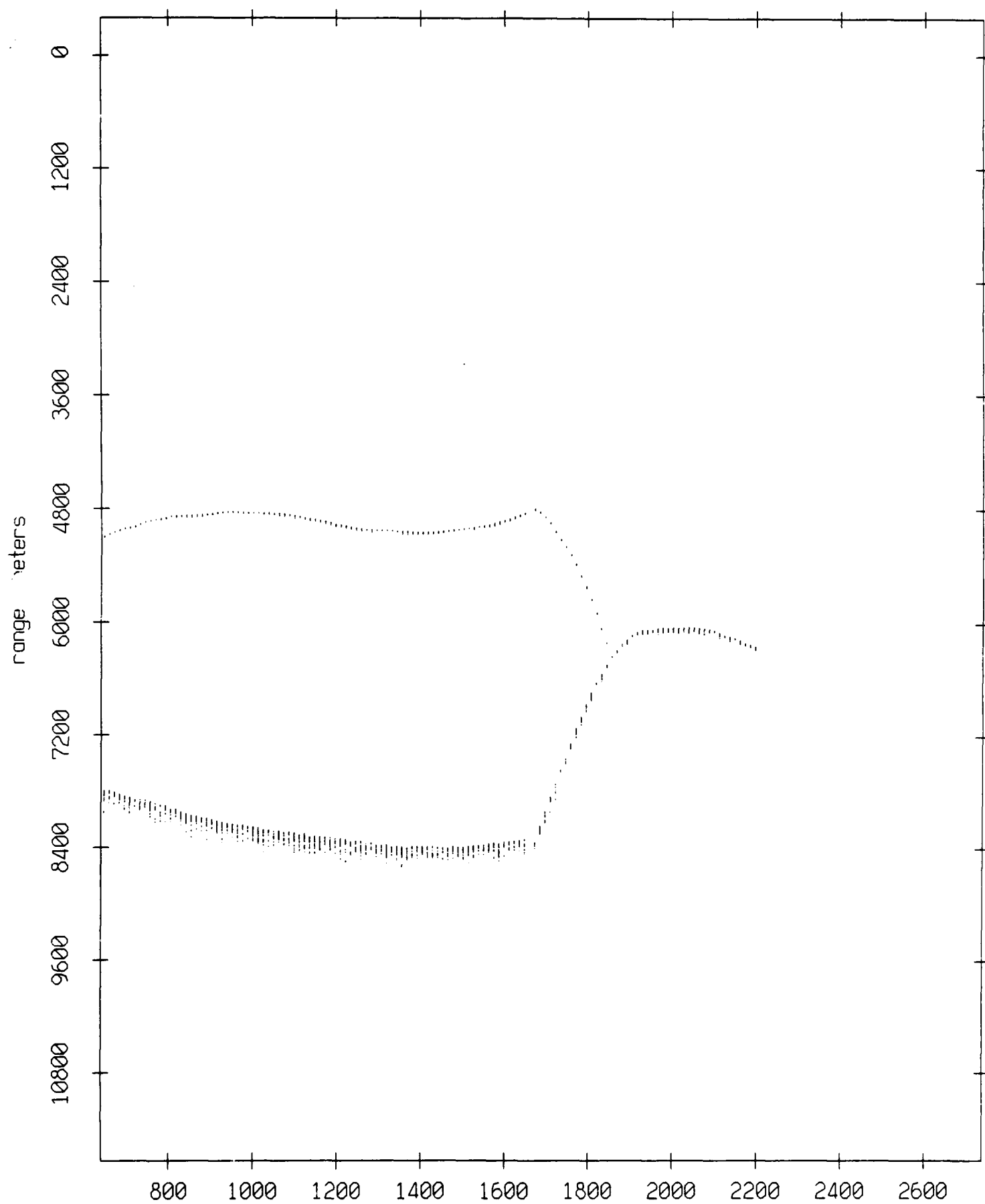
Float 5, July 1989 Trip: range from float 10



record number

Figure IX.6j

Float 5, July 1989 Trip: range from float 11

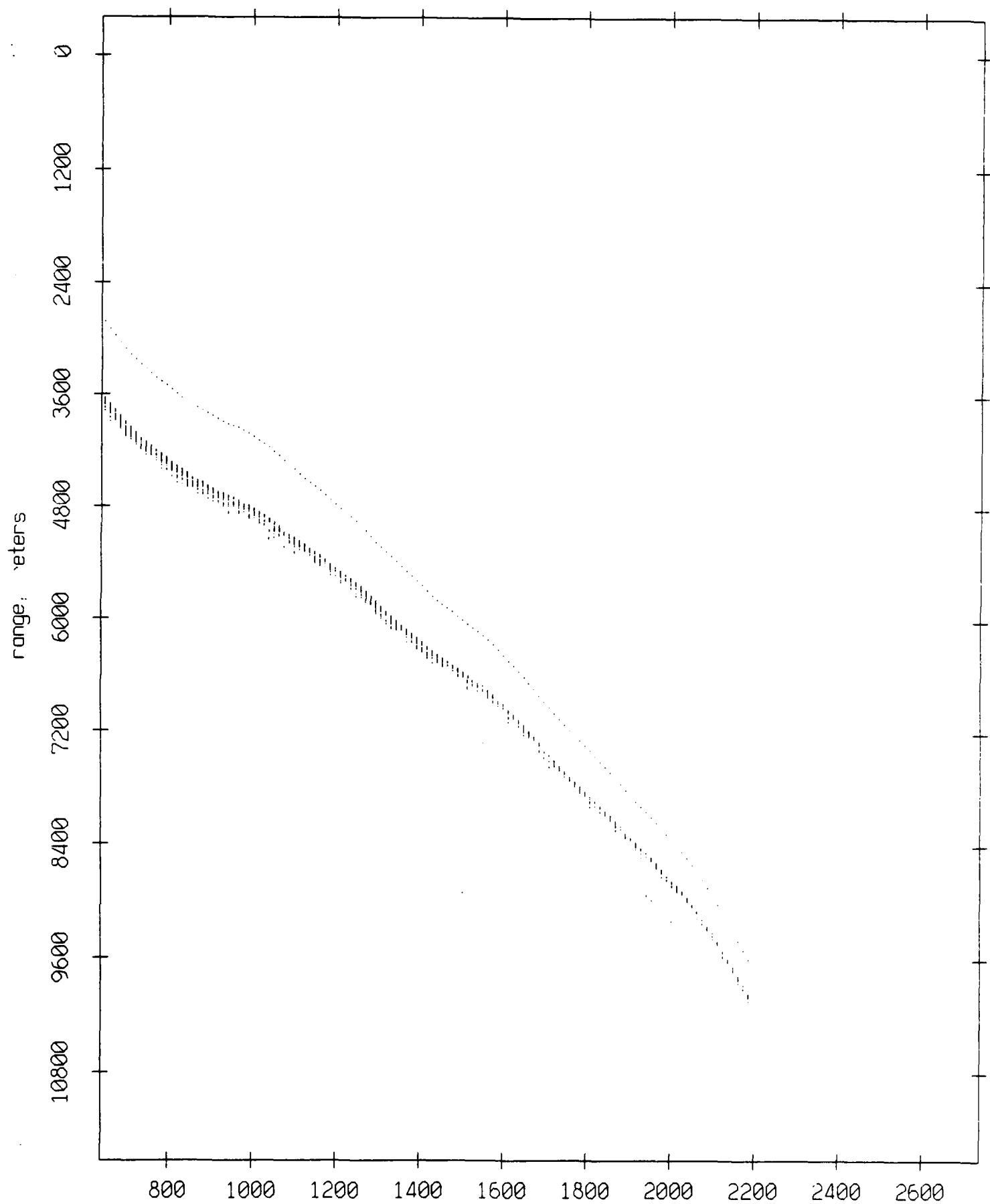


record number

Figure IX.6k



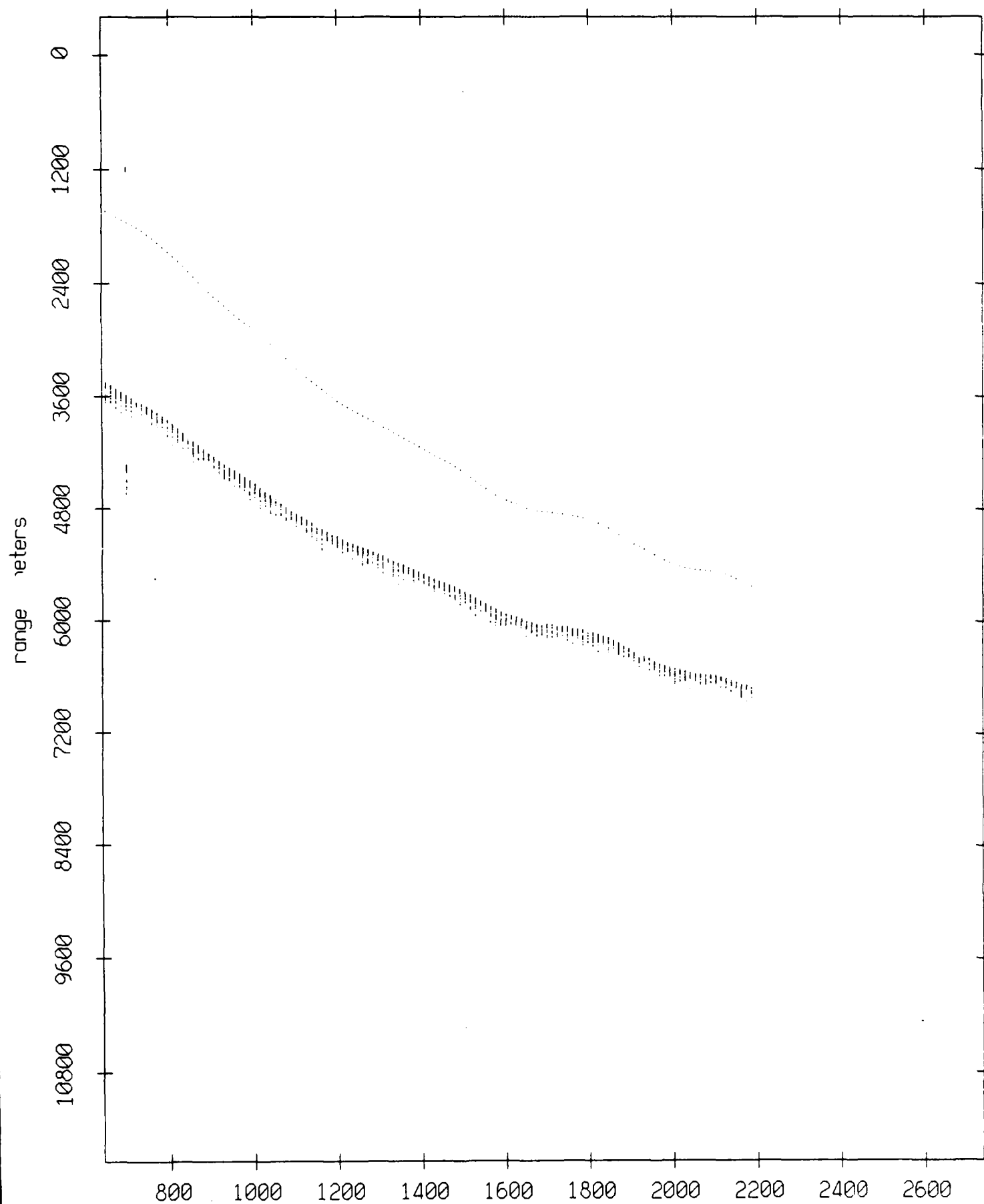
Float 6, July 1989 Trip: range from float 0



record number

Figure IX.7a

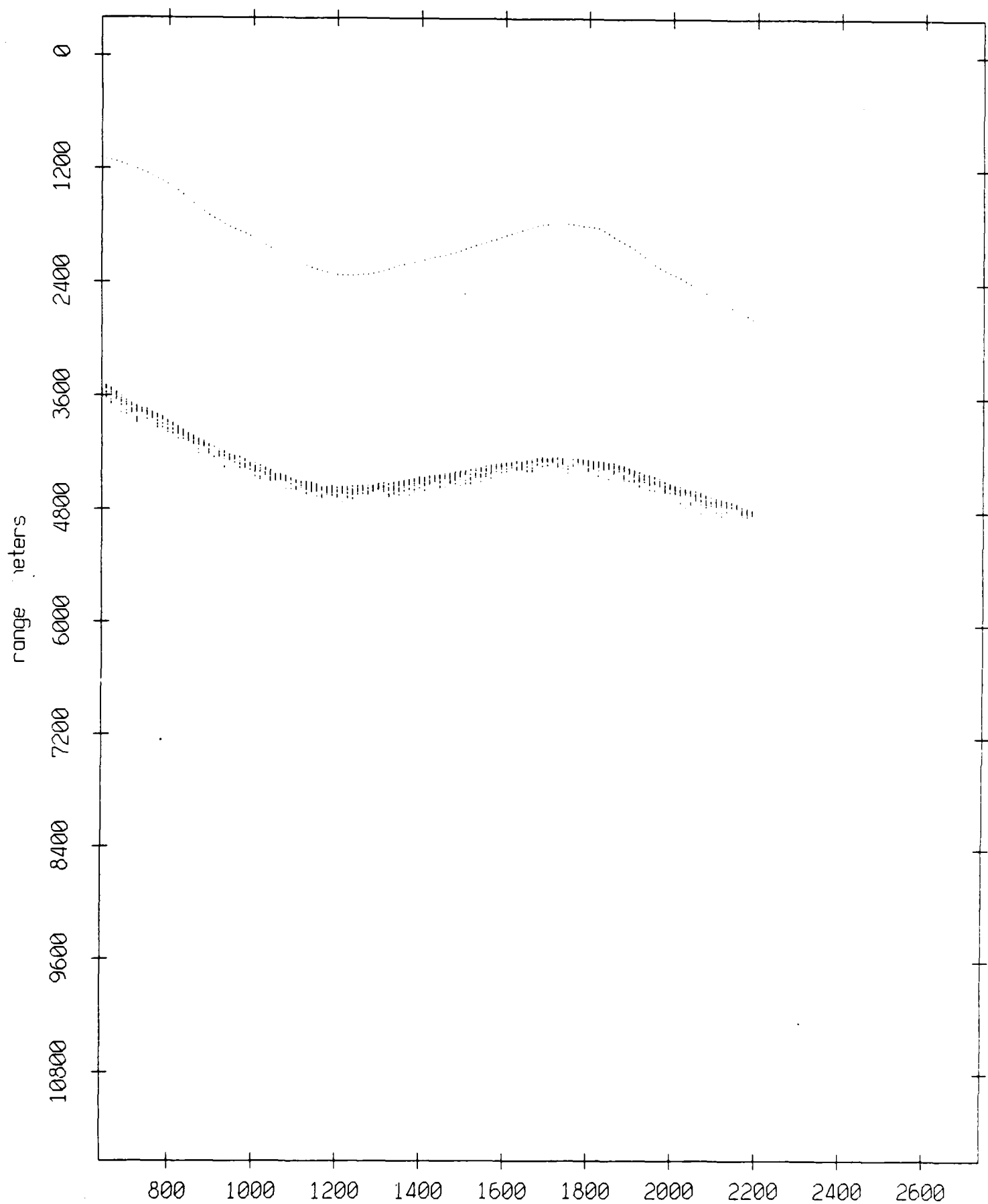
Float 6, July 1989 Trip: range from float 1



record number

Figure IX.7b

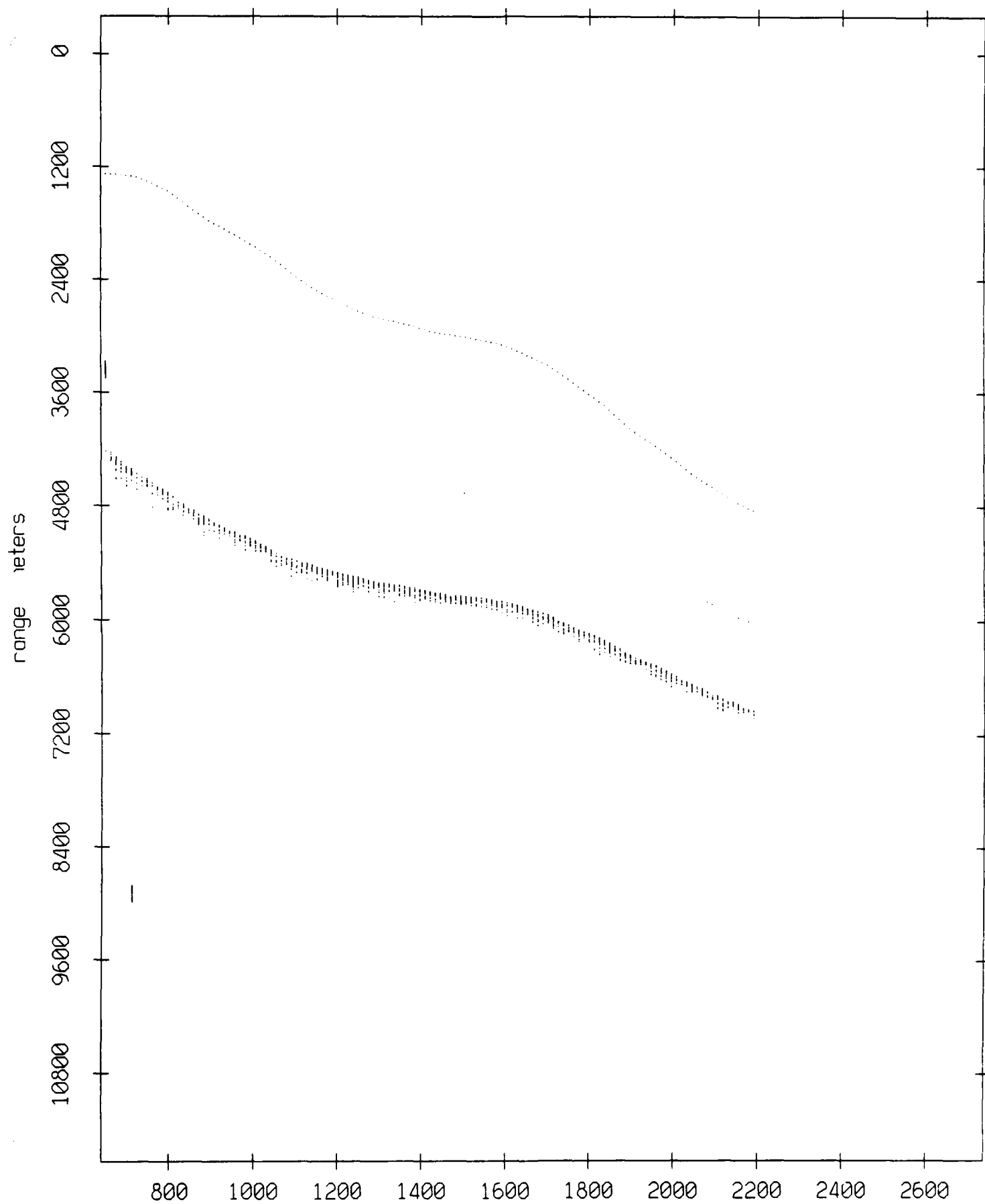
Float 6, July 1989 Trip: range from float 2



record number

Figure IX.7c

Float 6, July 1989 Trip: range from float 3



record number

Figure IX.7d

Float 6, July 1989 Trip: range from float 4

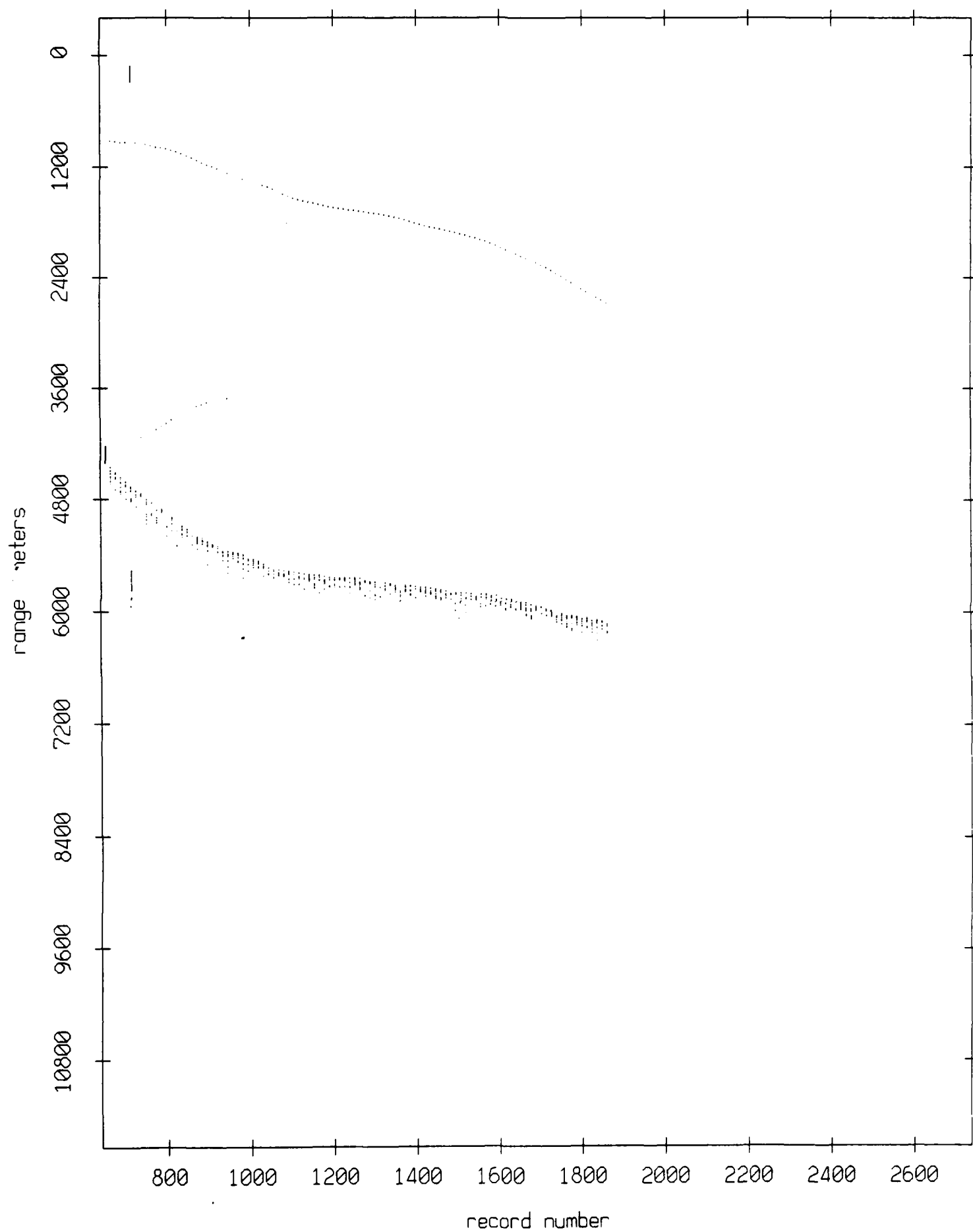
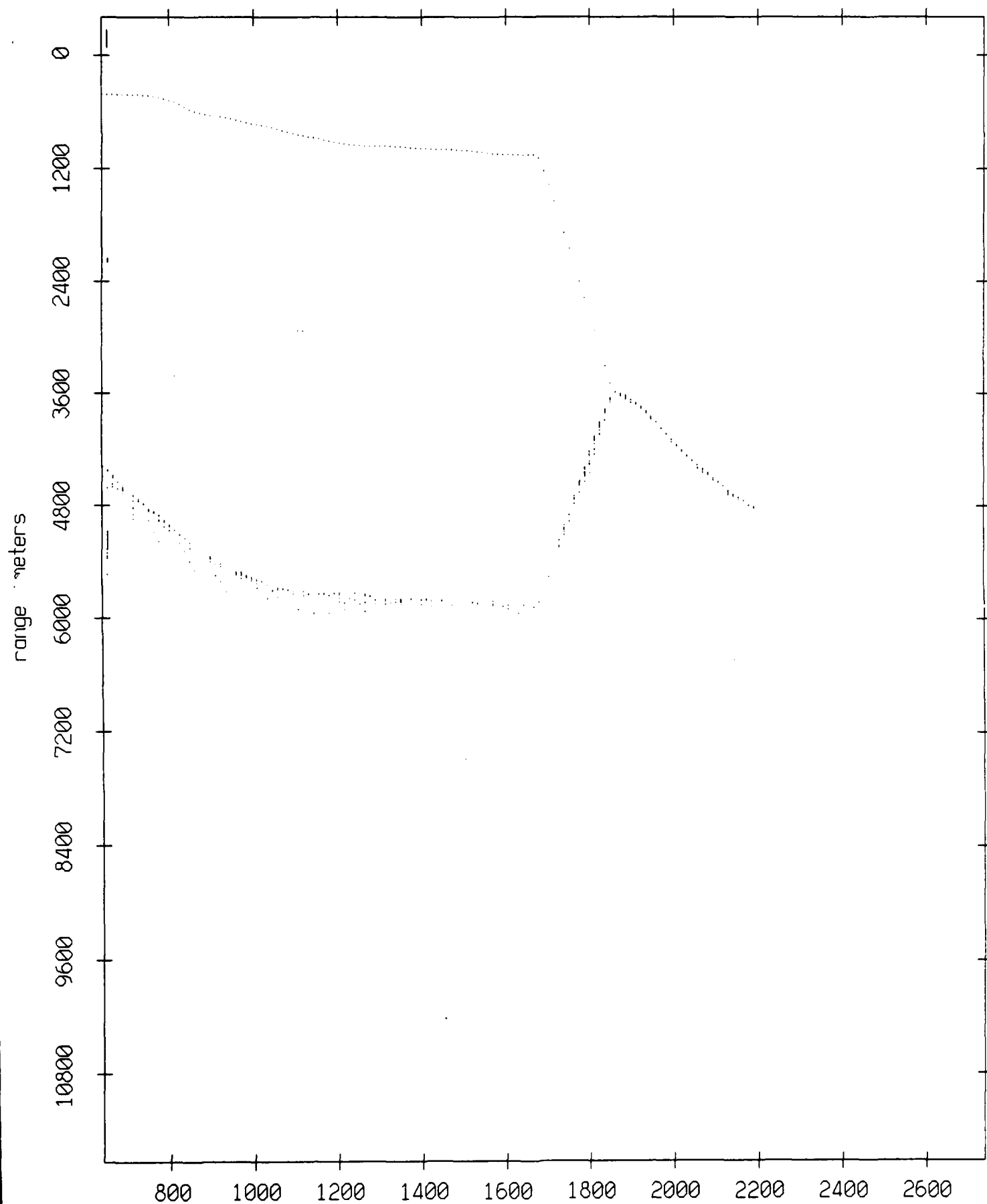


Figure IX.7e

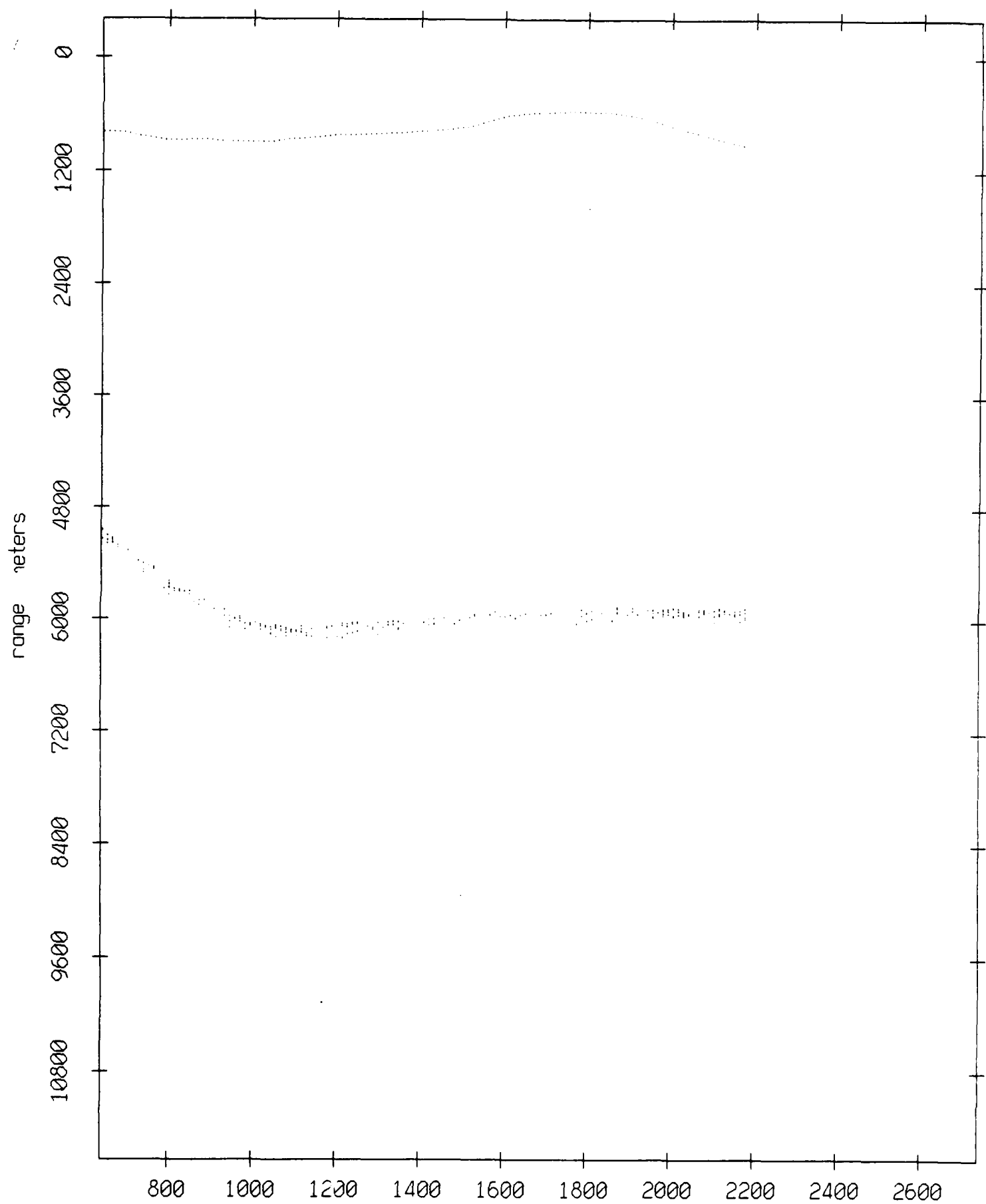
Float 6, July 1989 Trip: range from float 5



record number

Figure IX.7f

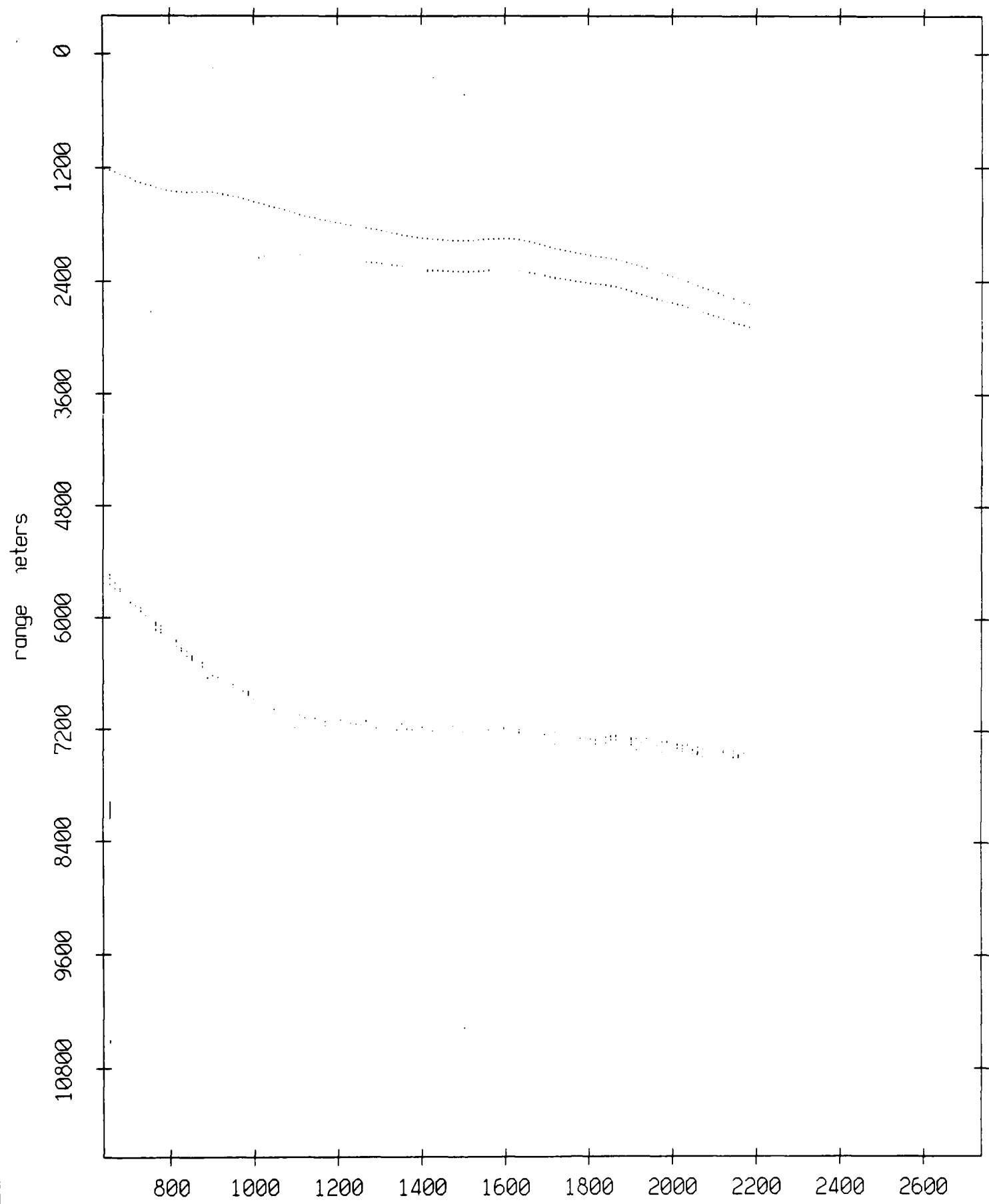
Float 6, July 1989 Trip: range from float 7



record number

Figure IX.7g

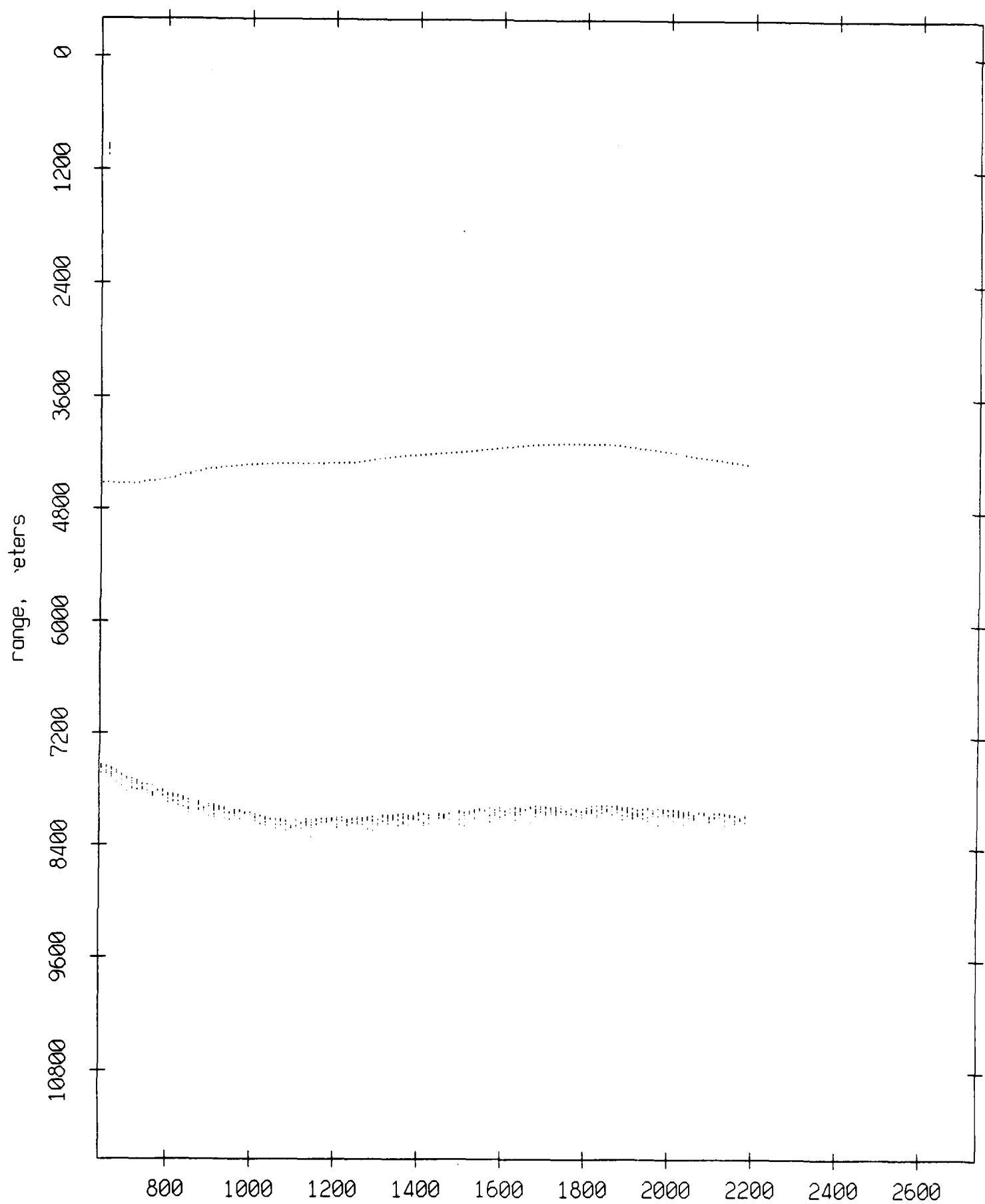
Float 6, July 1989 Trip: range from float 8



record number  
**Figure IX.7h**



Float 6, July 1989 Trip: range from float 9



record number

Figure IX.71

Float 6, July 1989 Trip: range from float 10

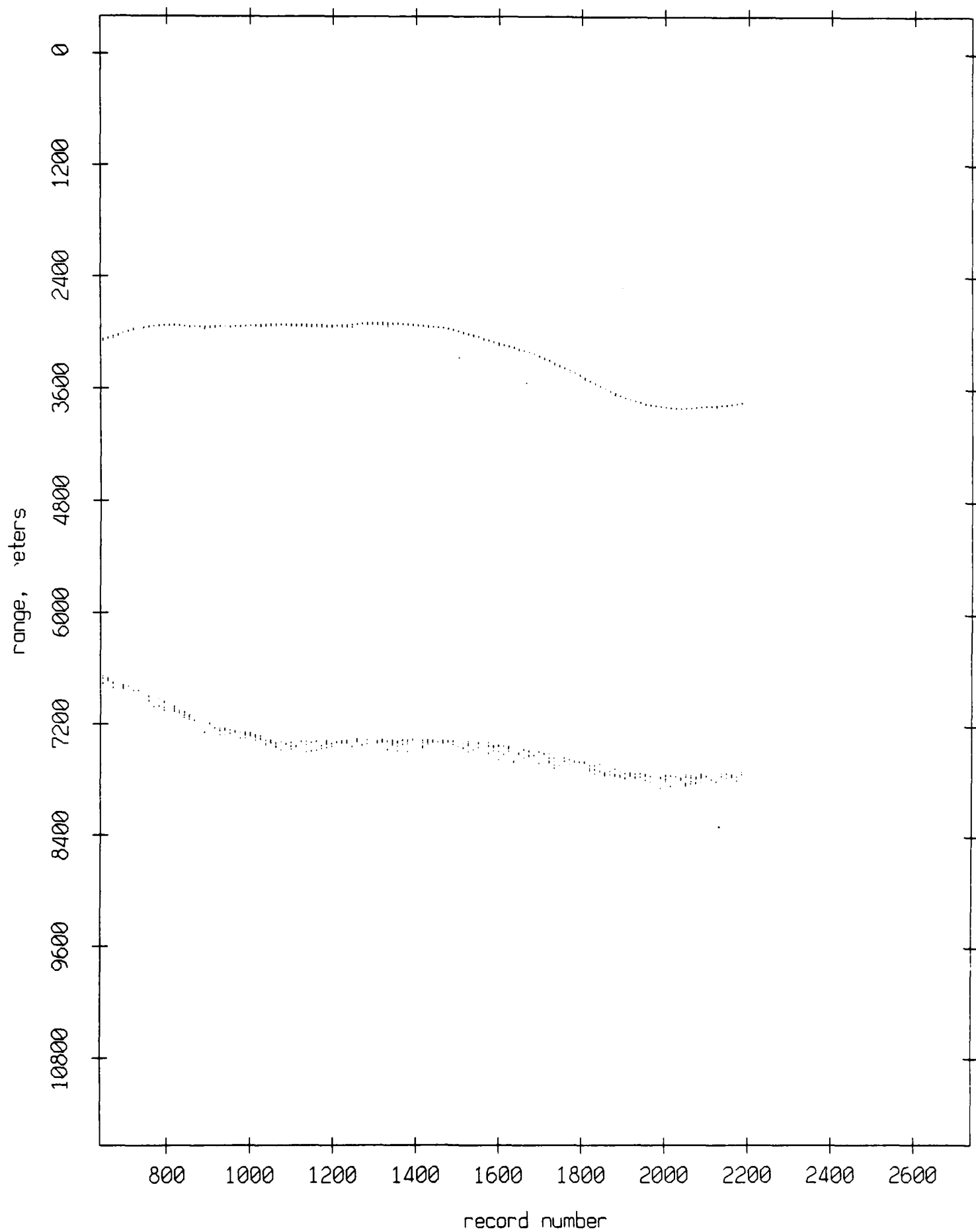


Figure IX.7]

Float 6, July 1989 Trip: range from float 11

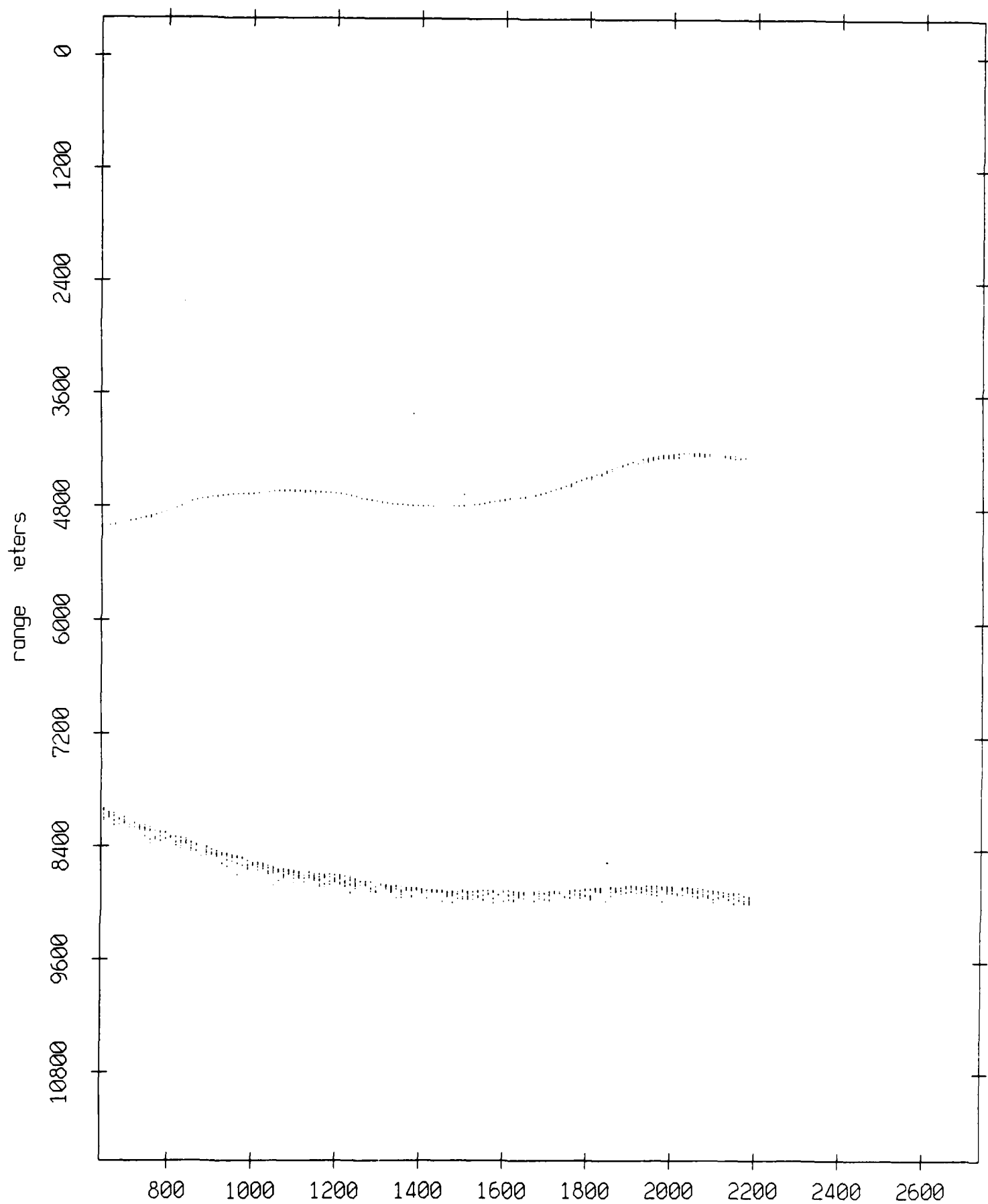
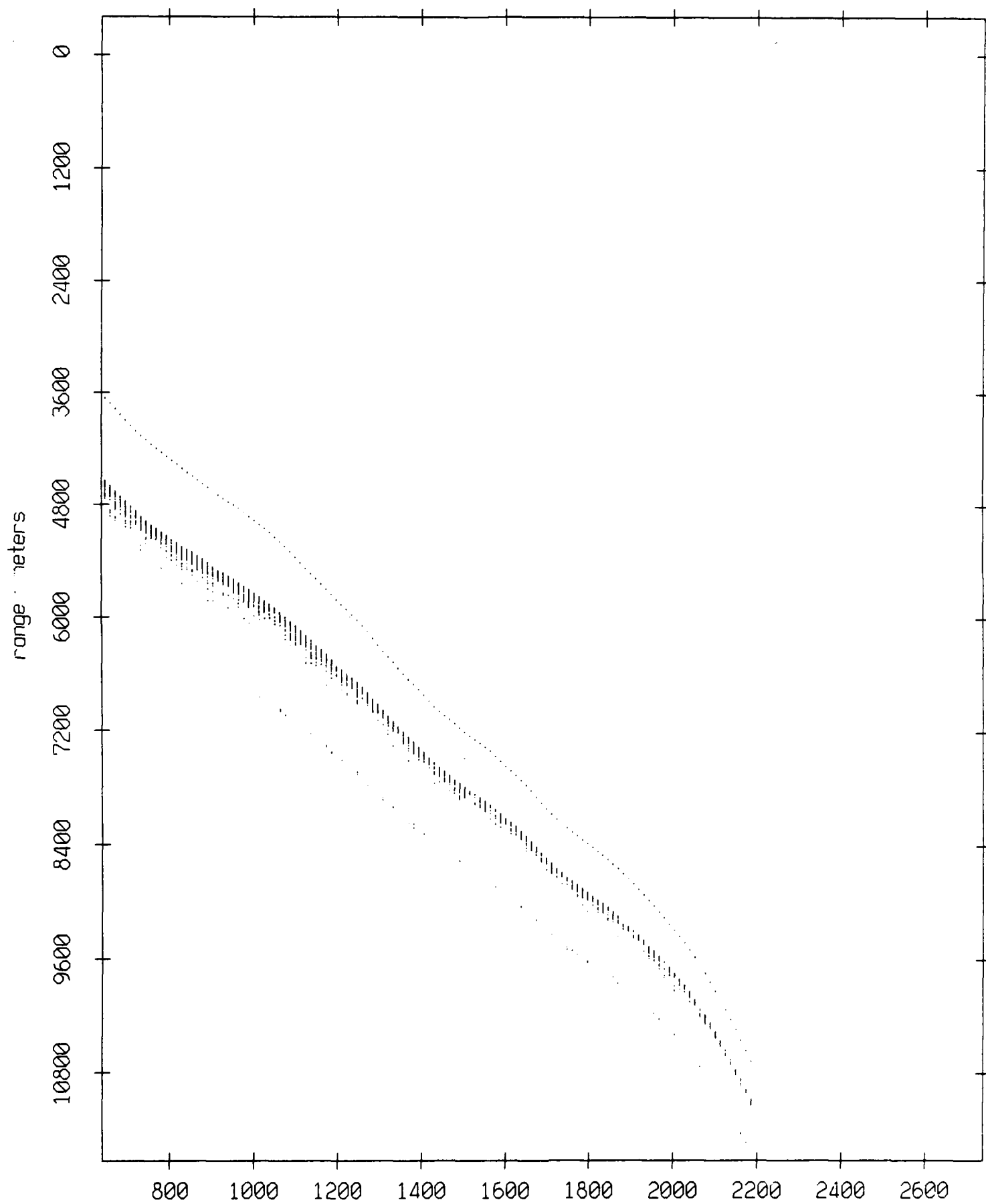


Figure IX.7k

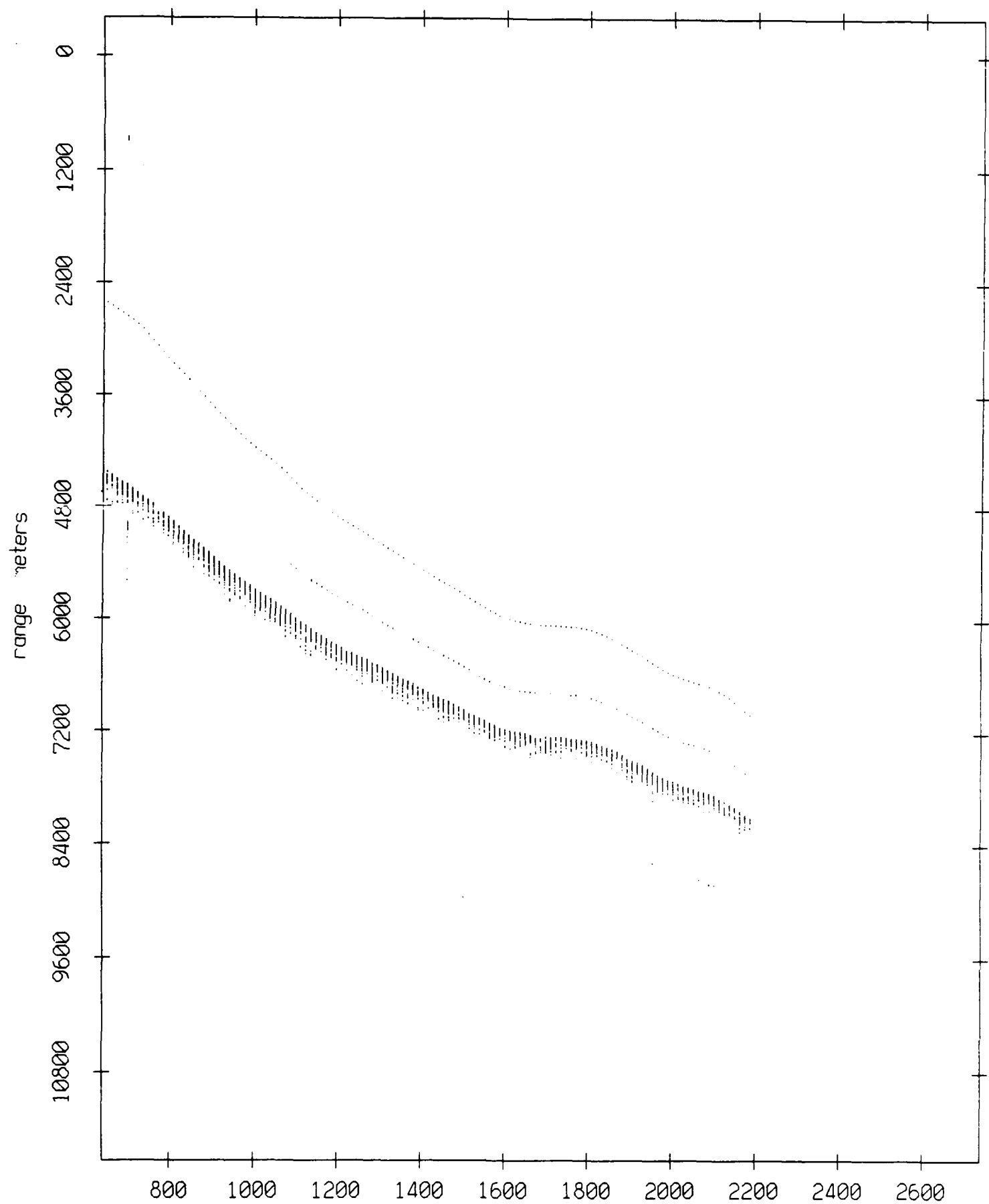
Float 7, July 1989 Trip: range from float 0



record number

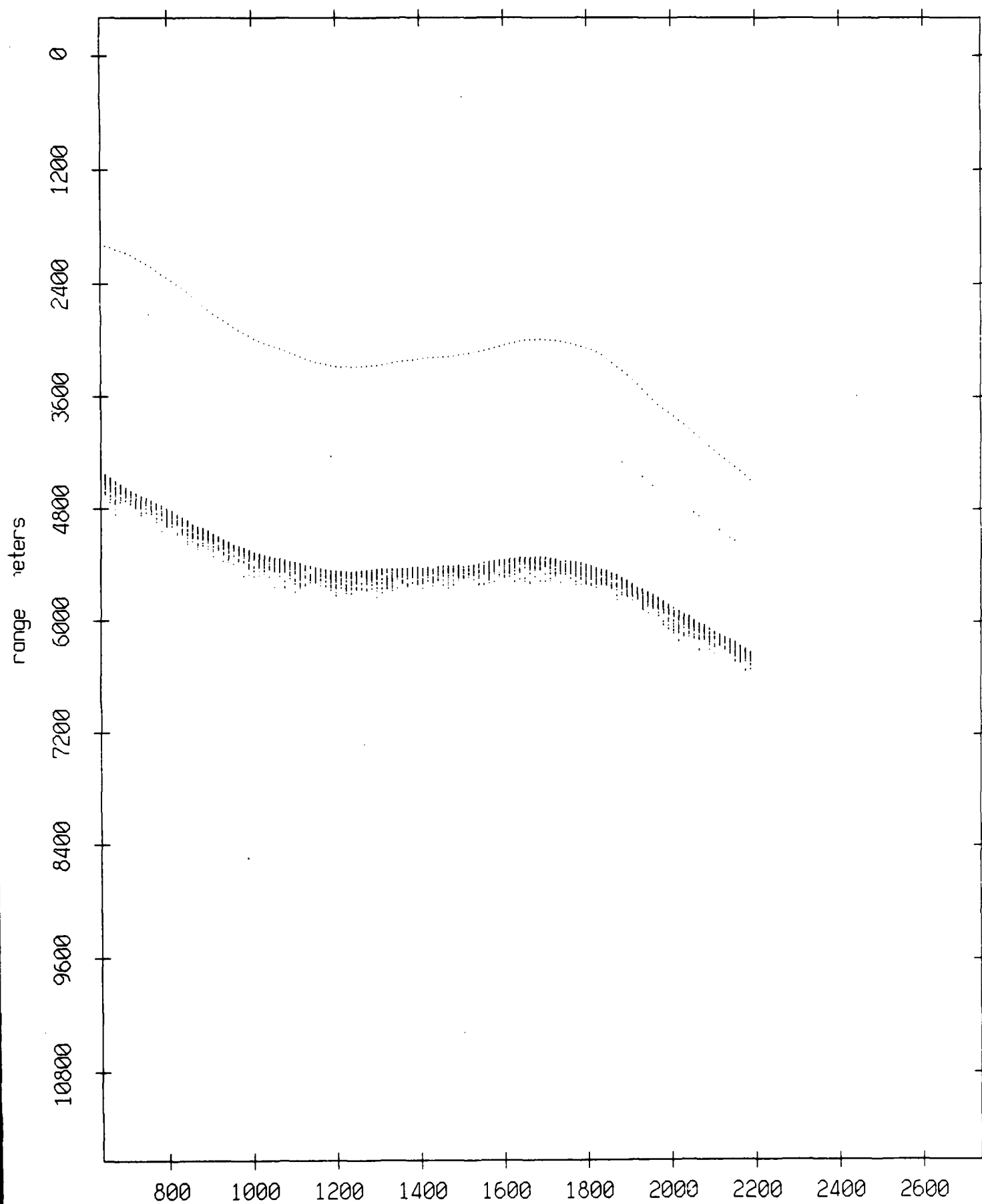
Figure IX.8a

Float 7, July 1989 Trip: range from float 1



record number  
**Figure IX.8b**

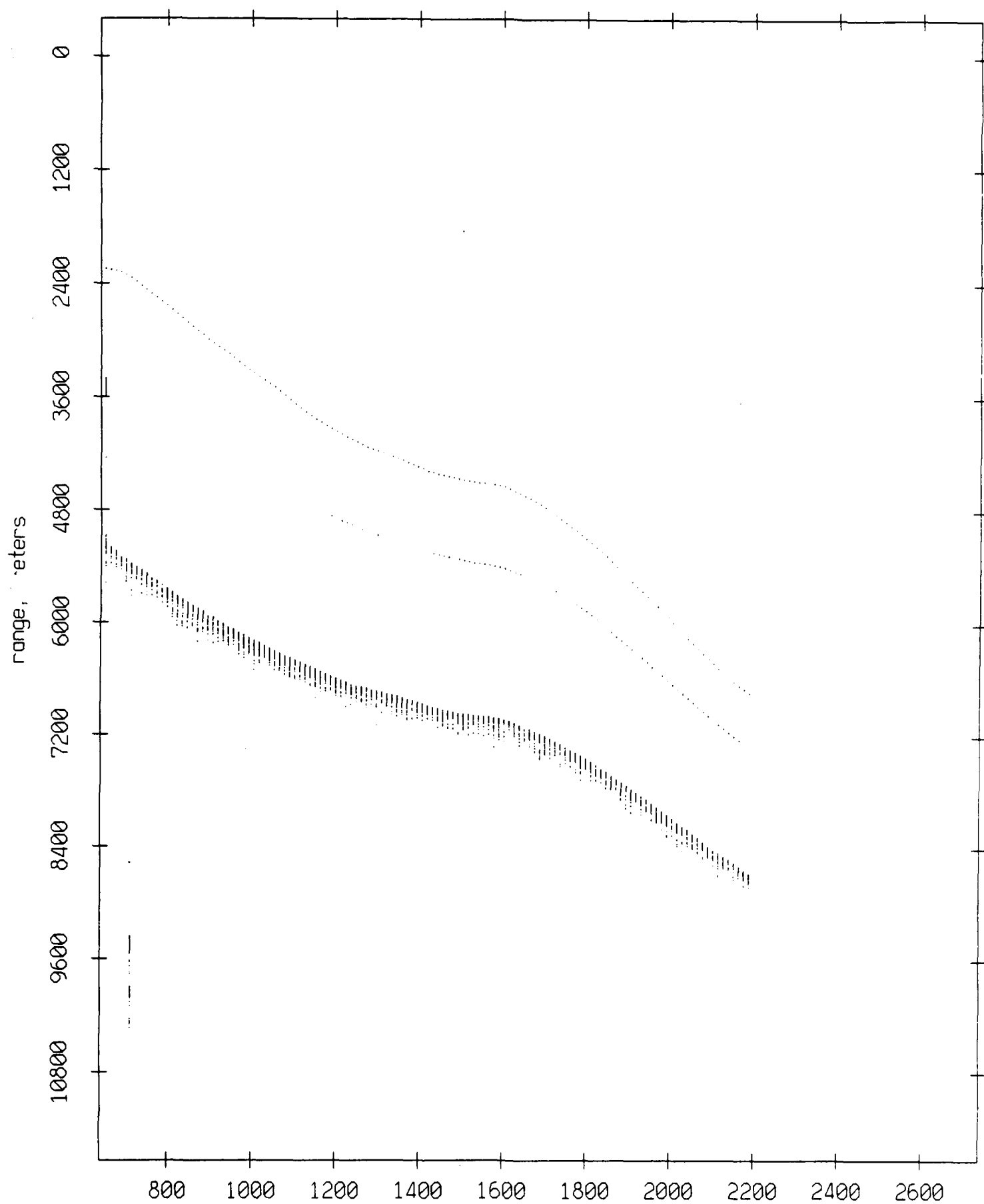
Float 7, July 1989 Trip: range from float 2



record number

Figure IX.8c

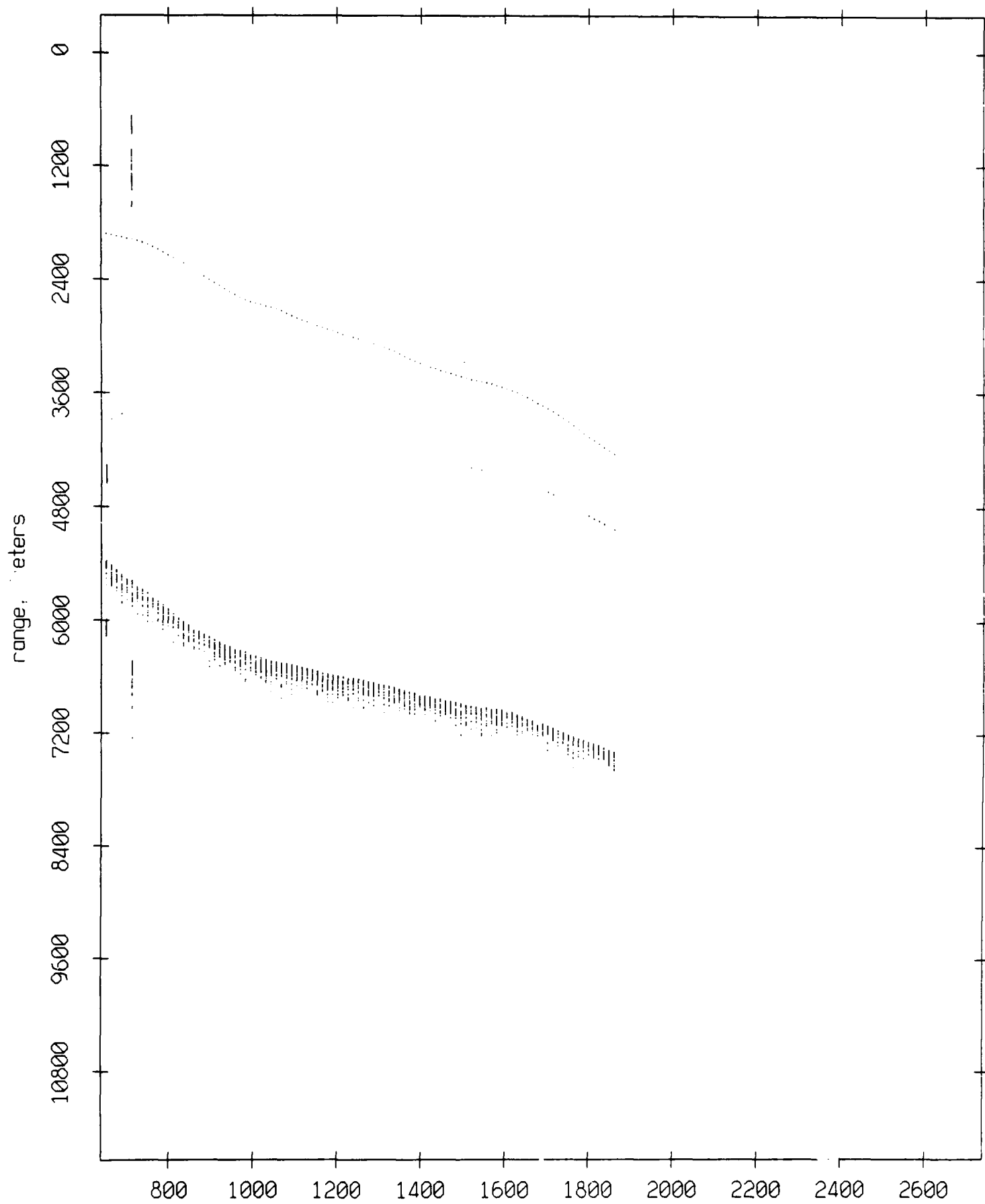
Float 7, July 1989 Trip: range from float 3



record number

Figure IX.8d

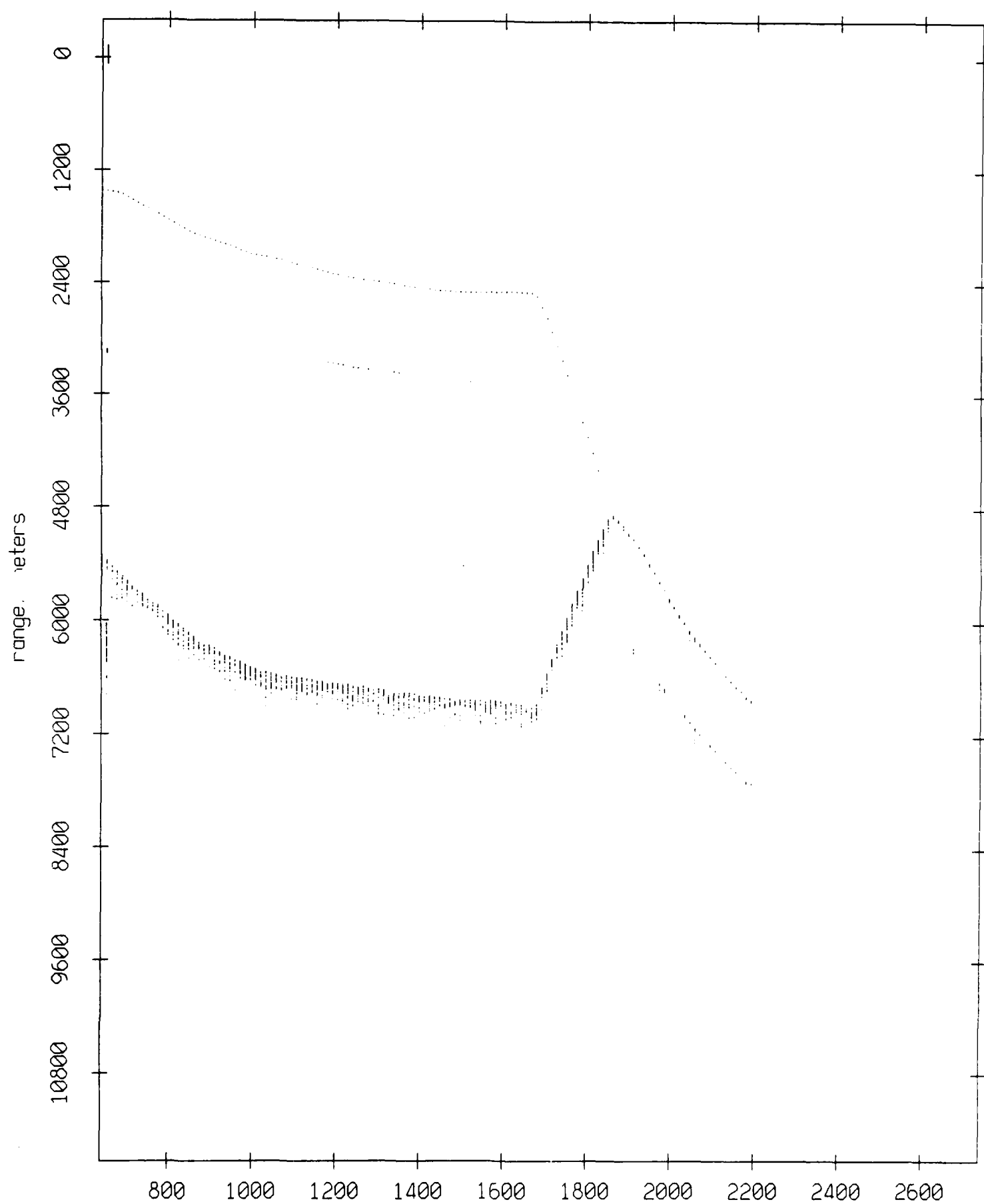
Float 7, July 1989 Trip: range from float 4



record number  
Figure IX.8e



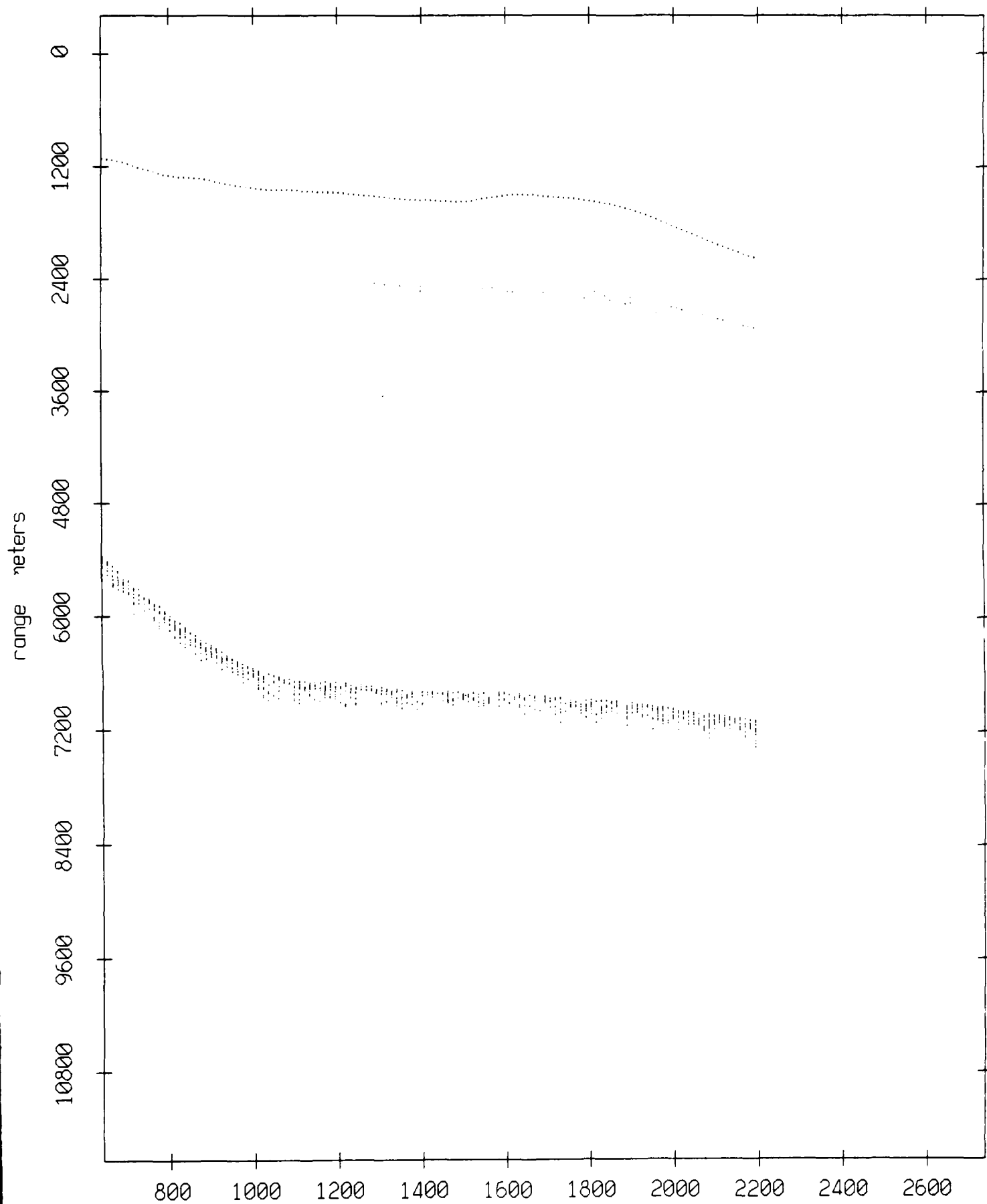
Float 7, July 1989 Trip: range from float 5



record number

Figure IX.8f

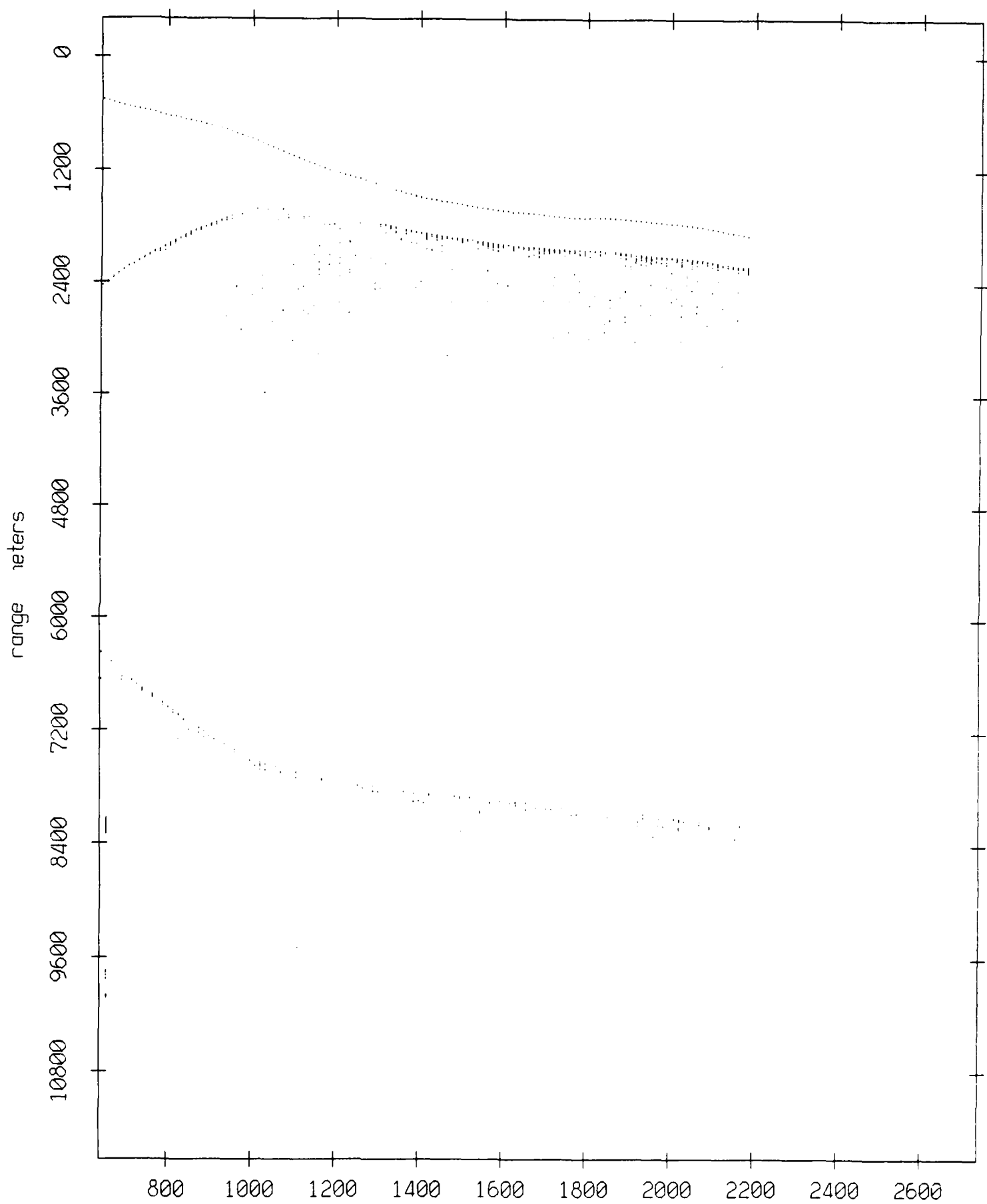
Float 7, July 1989 Trip: range from float 6



record number

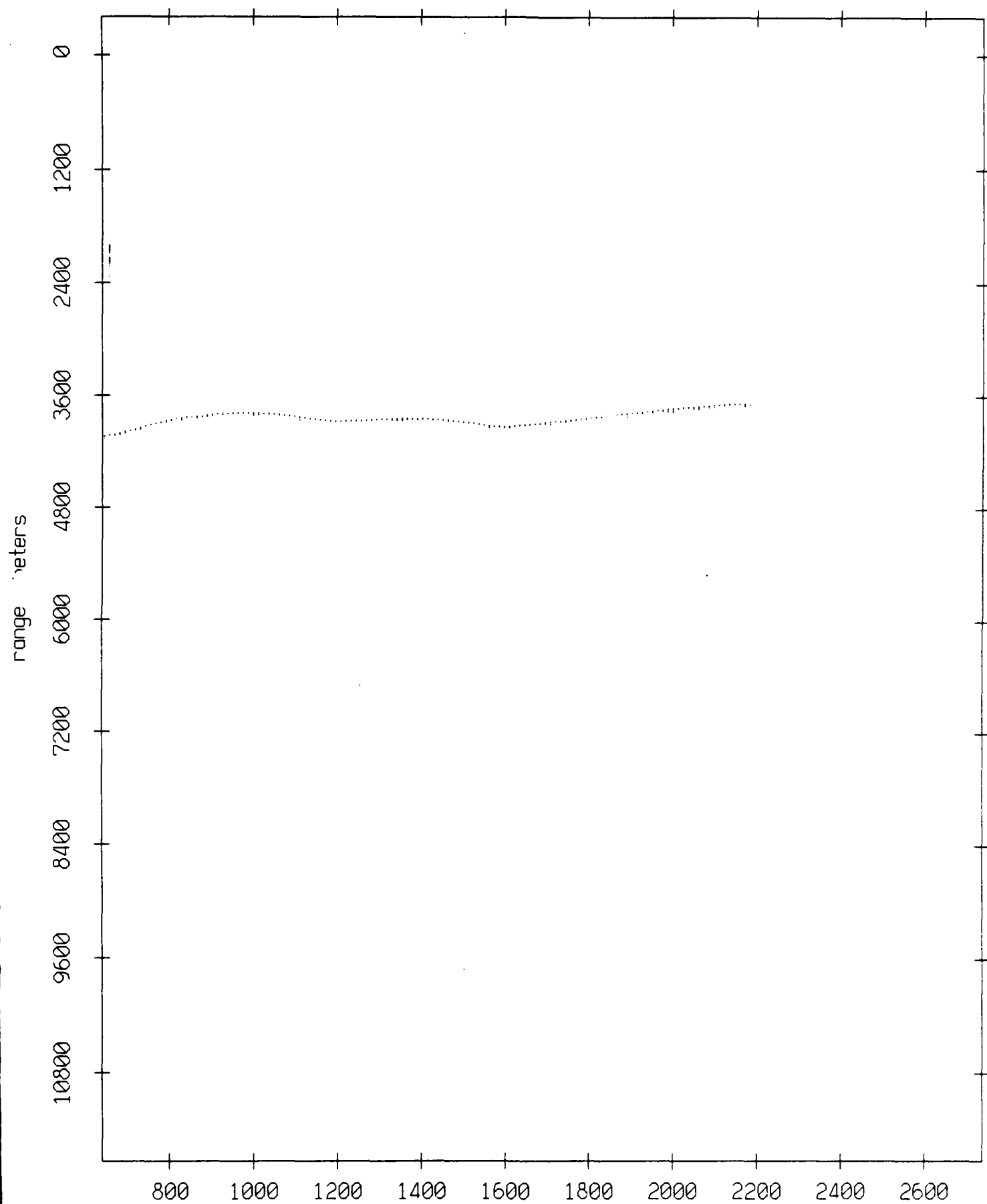
Figure IX.8g

Float 7, July 1989 Trip: range from float 8



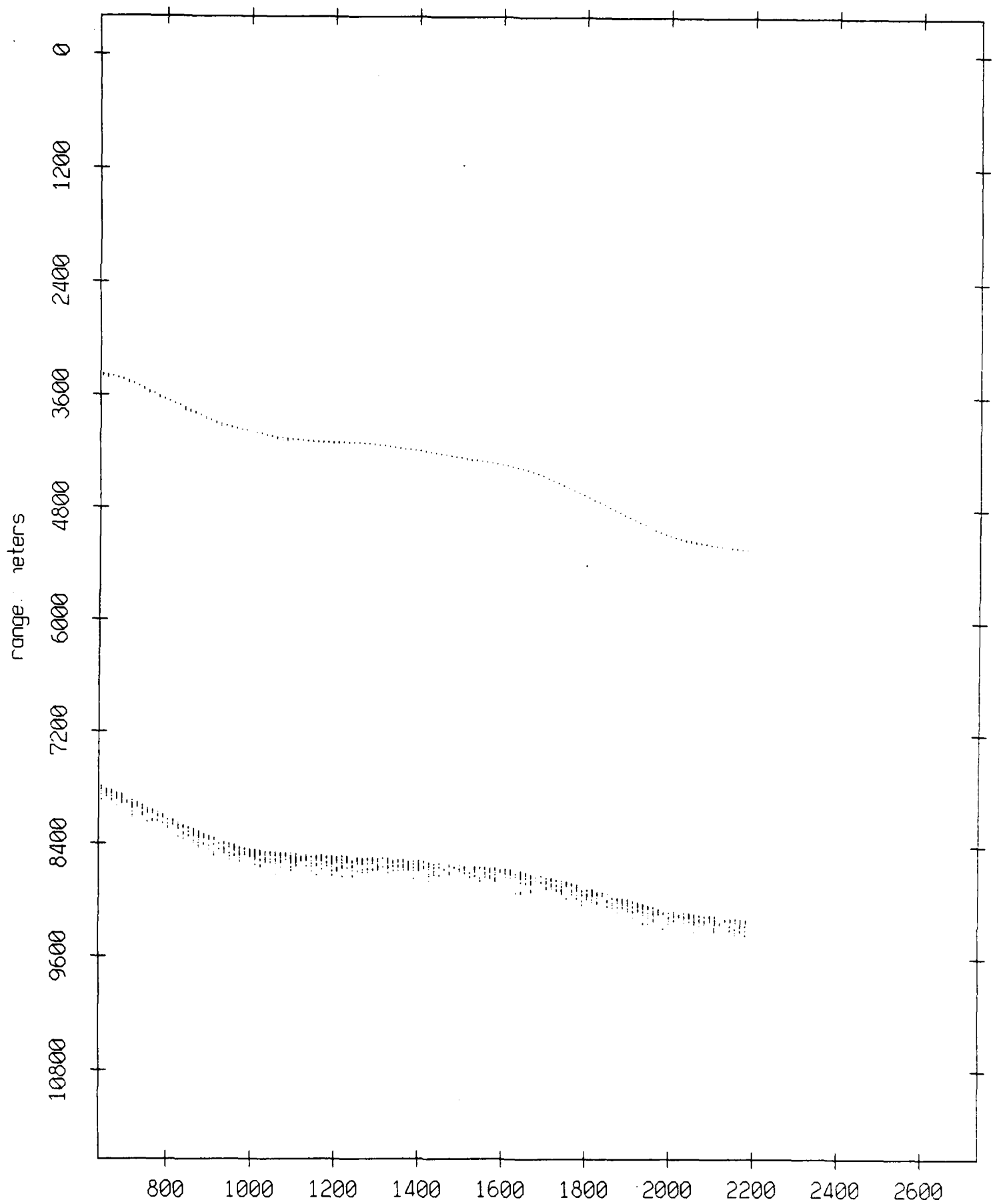
record number  
**Figure IX.8h**

Float 7, July 1989 Trip: range from float 9



record number  
**Figure IX.81**

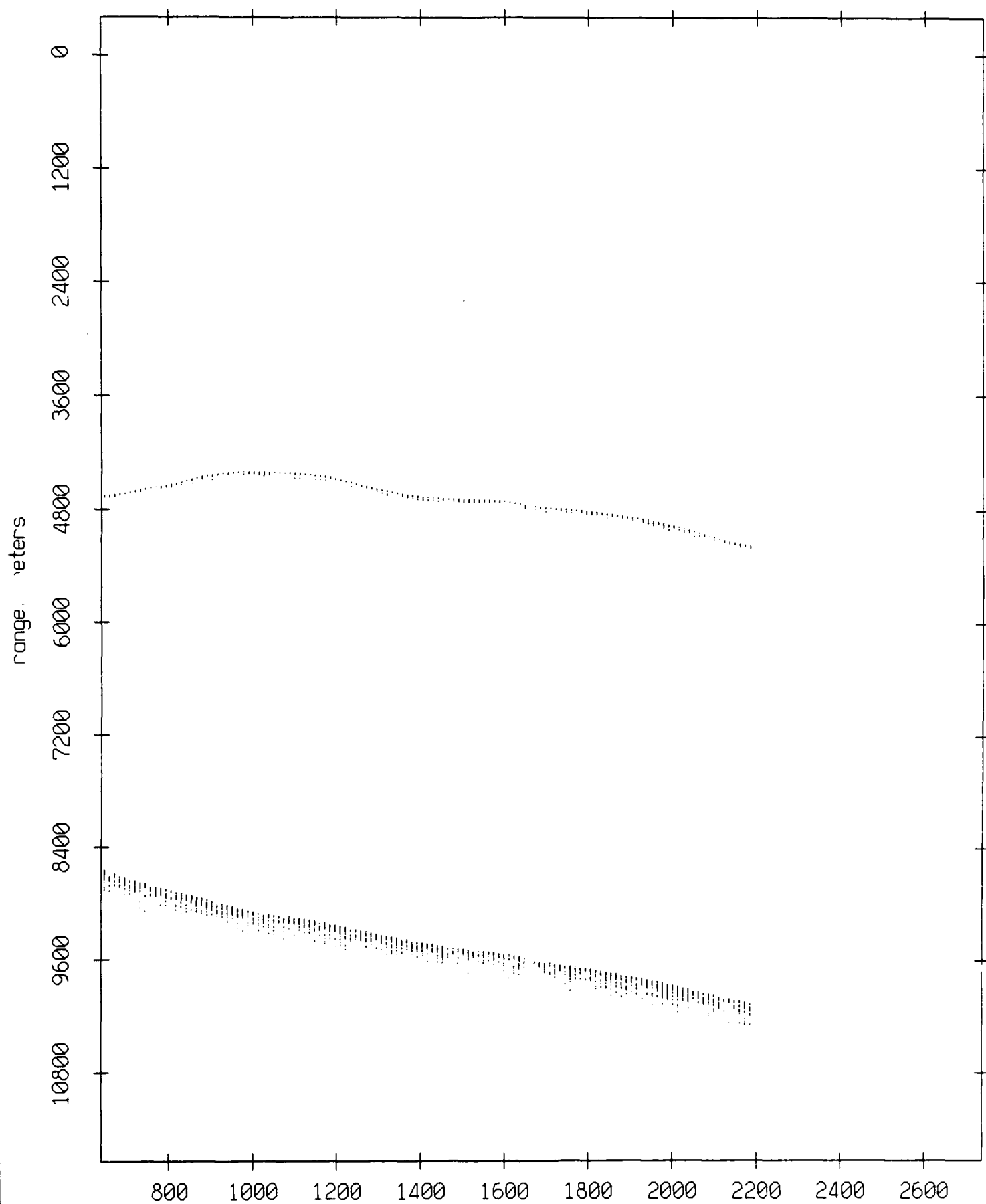
Float 7, July 1989 Trip: range from float 10



record number

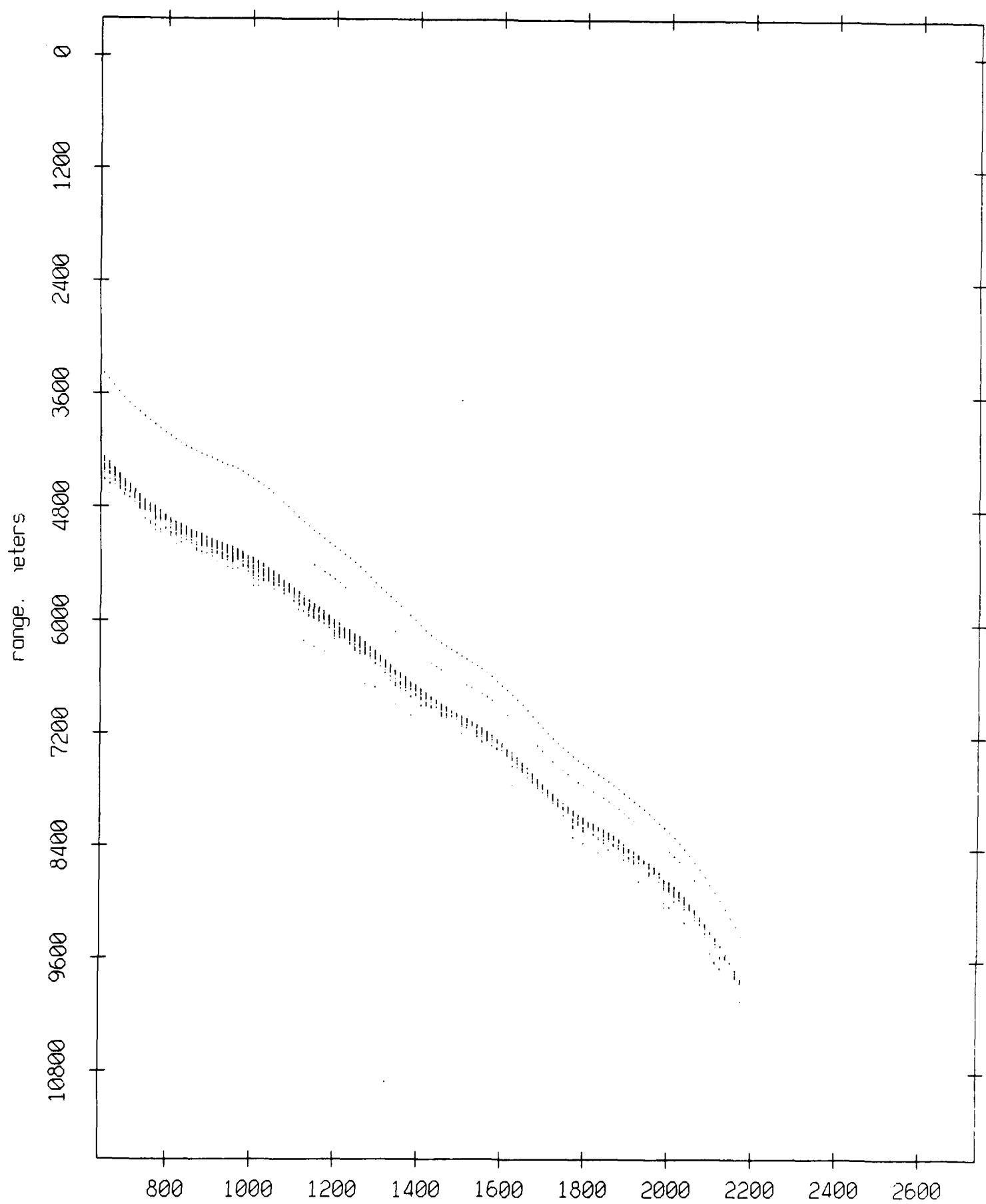
Figure IX.8j

Float 7, July 1989 Trip: range from float 11



record number  
**Figure IX.8k**

Float 8, July 1989 Trip: range from float 0



record number  
**Figure IX.9a**

Float 8, July 1989 Trip: range from float 1

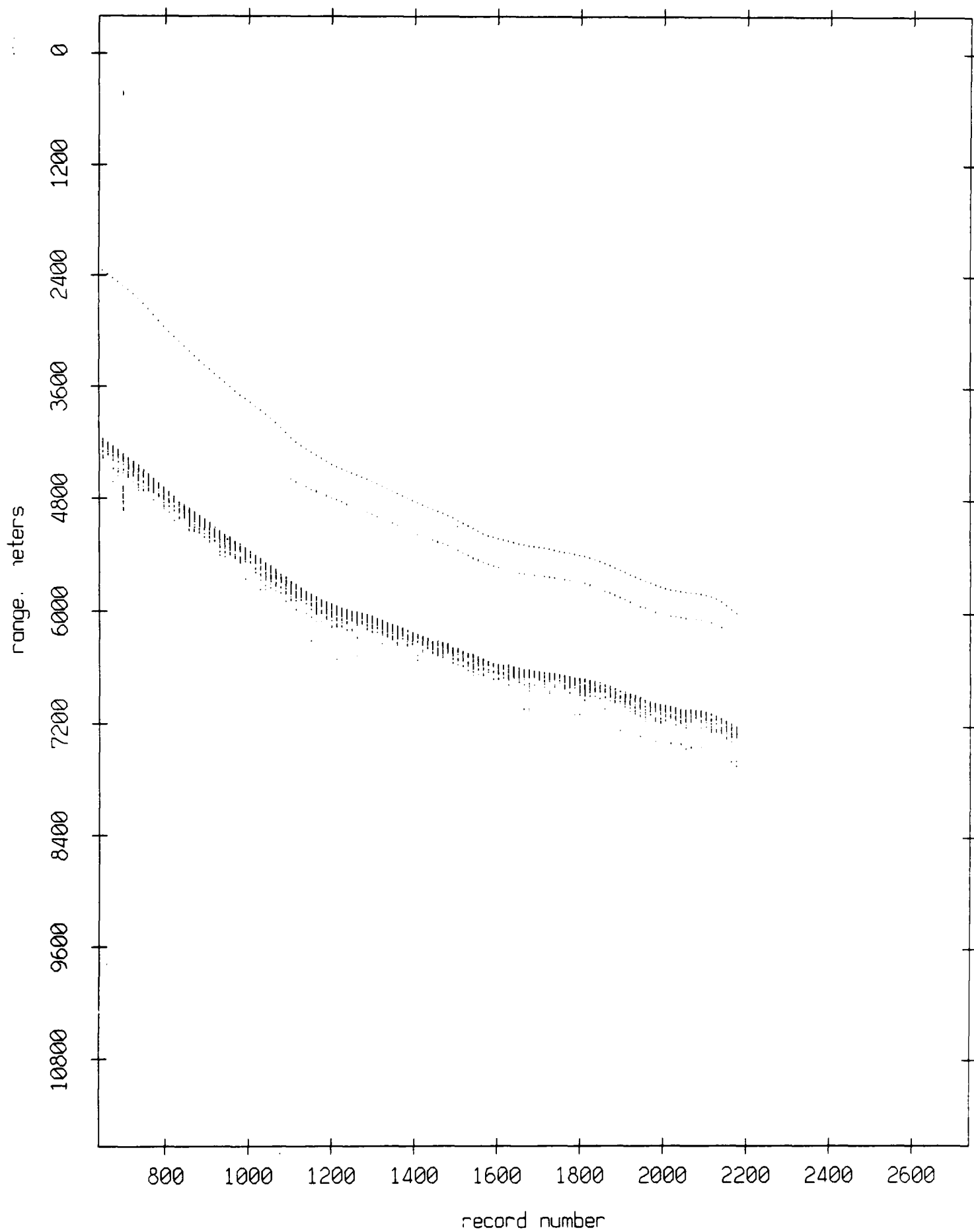
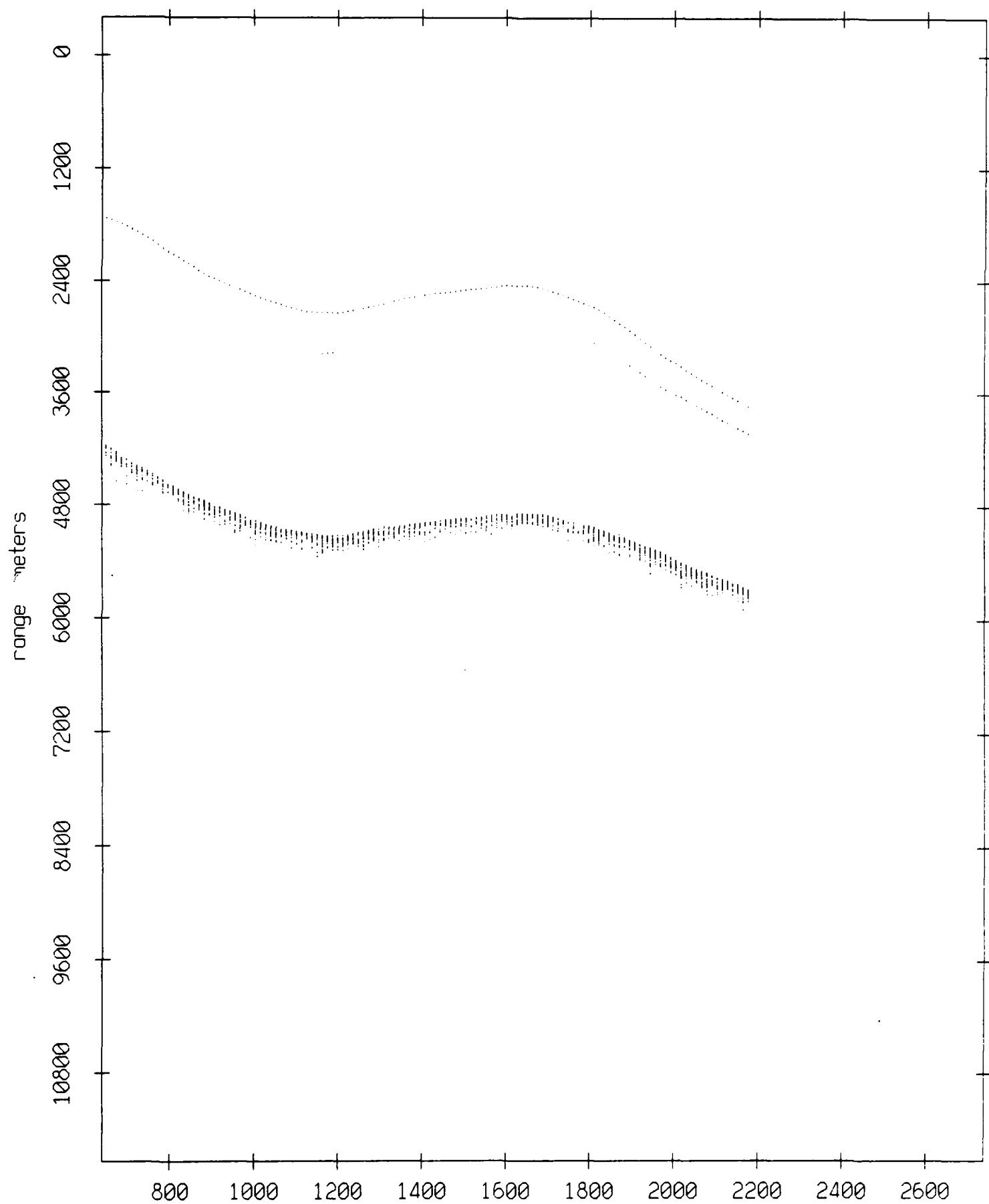


Figure IX.9b



Float 8, July 1989 Trip: range from float 2



record number

Figure IX.9c

Float 8, July 1989 Trip: range from float 3

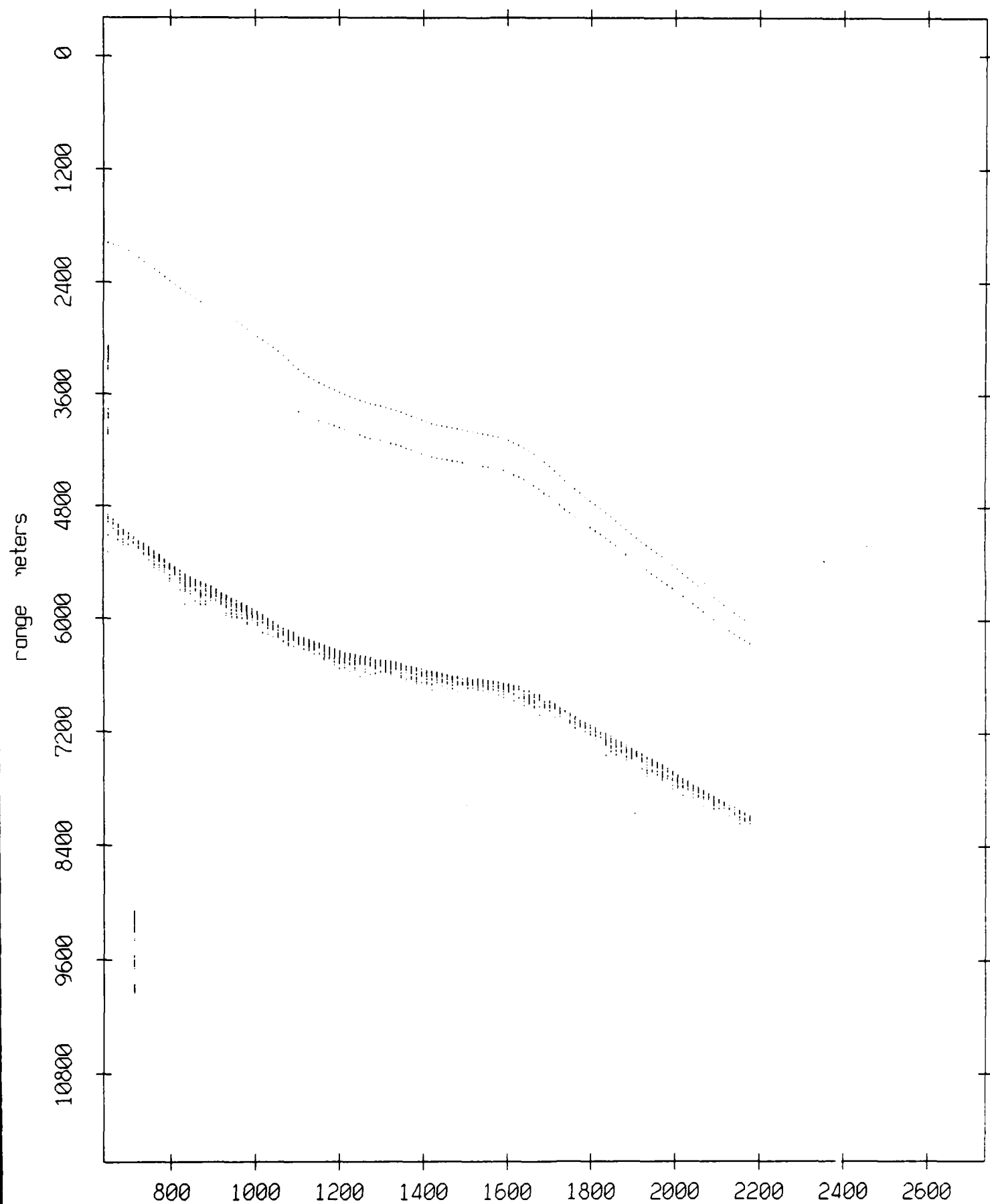
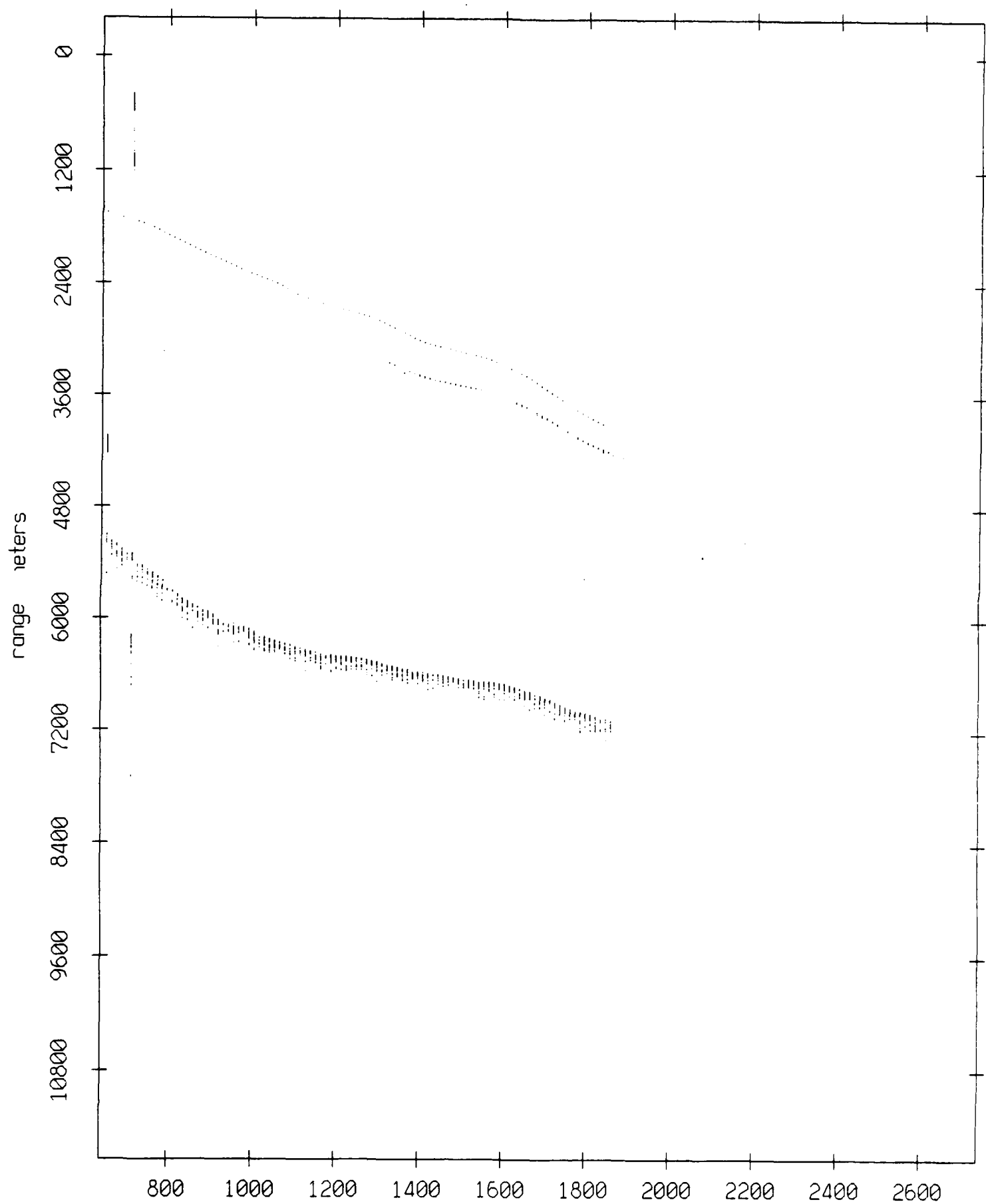


Figure IX.9d

Float 8, July 1989 Trip: range from float 4



record number

Figure IX.9e

Float 8, July 1989 Trip: range from float 5

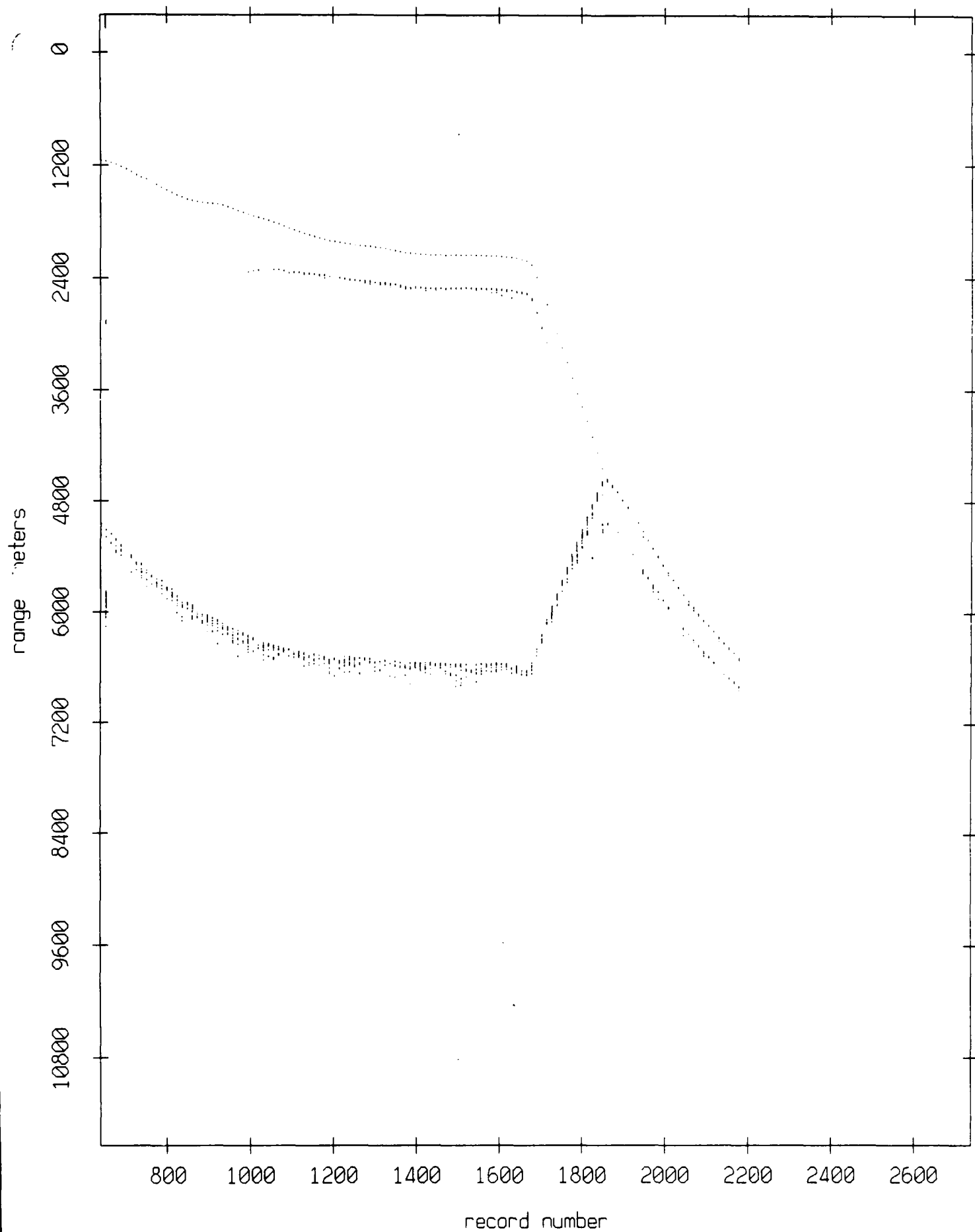
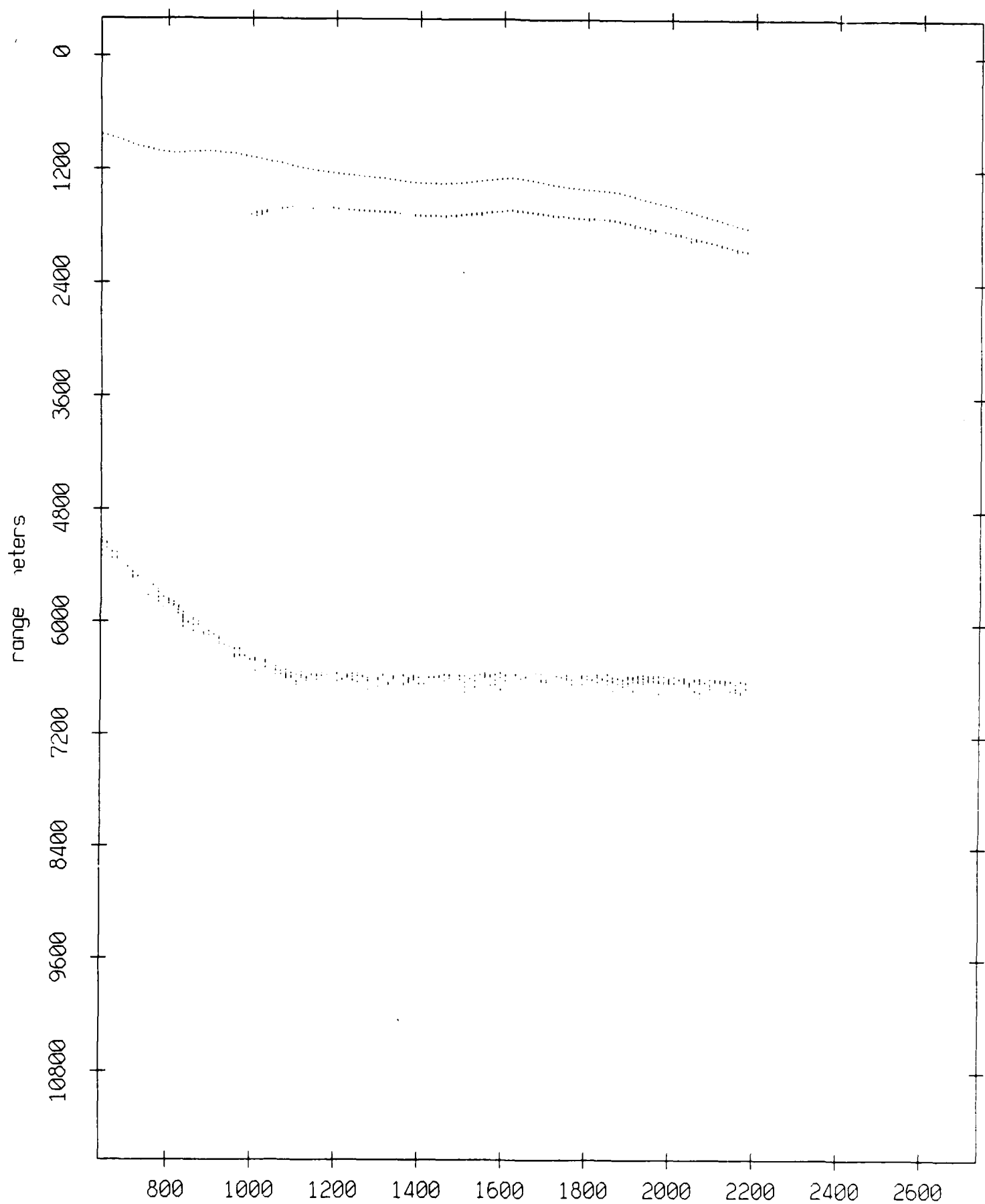


Figure IX.9f

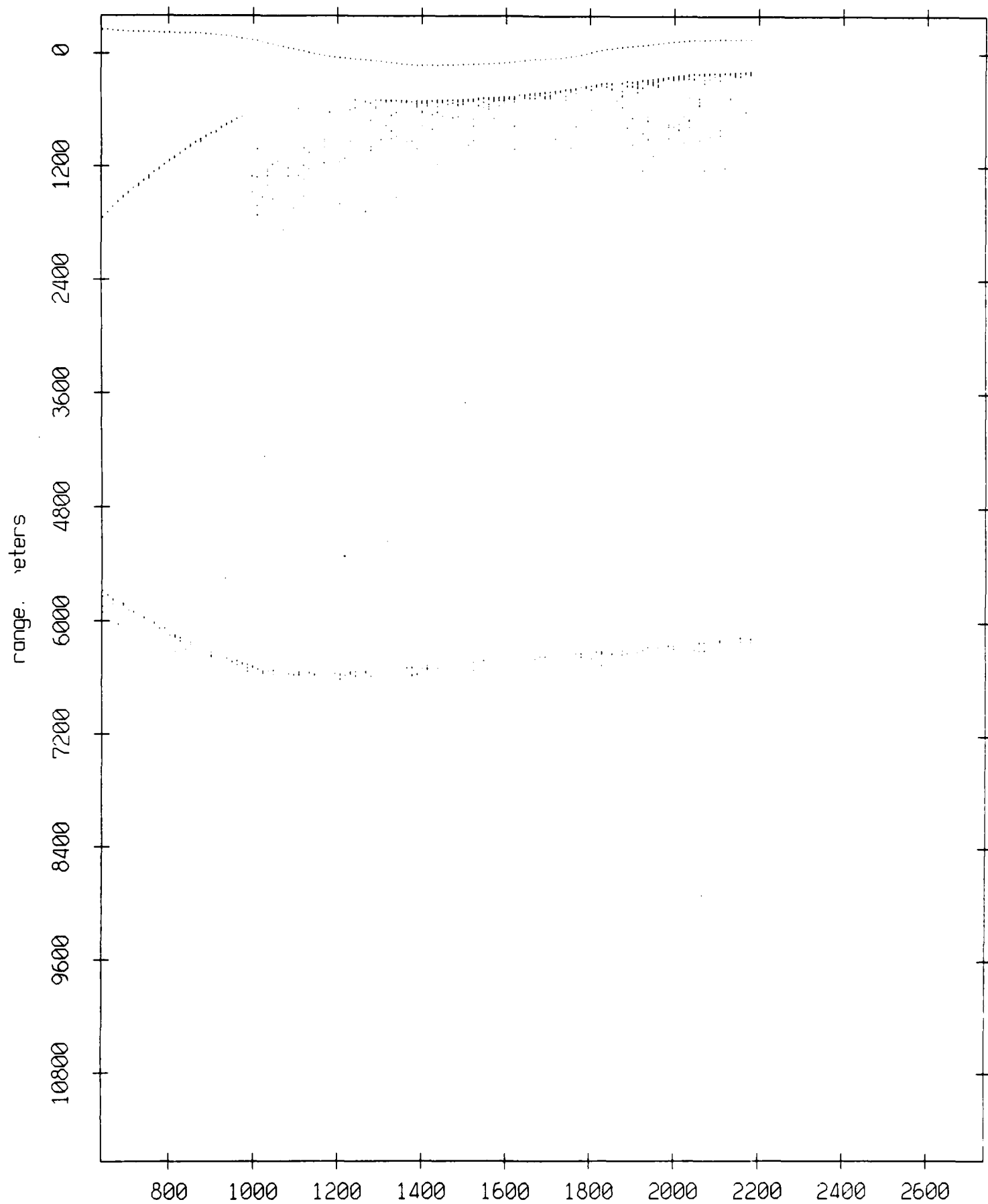
Float 8, July 1989 Trip: range from float 6



record number

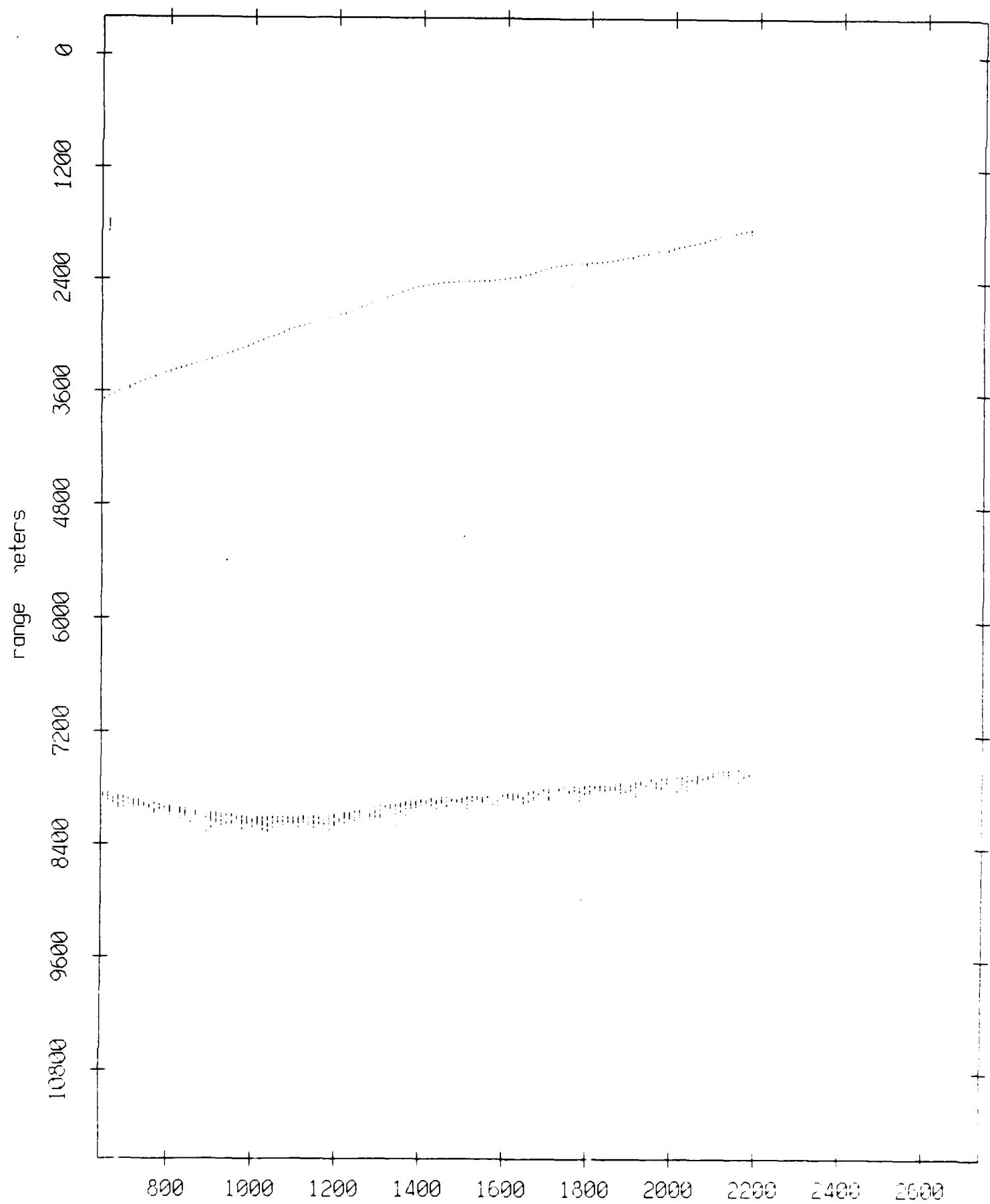
Figure IX.9g

Float 8, July 1989 Trip: range from float 7



record number  
Figure IX.9h

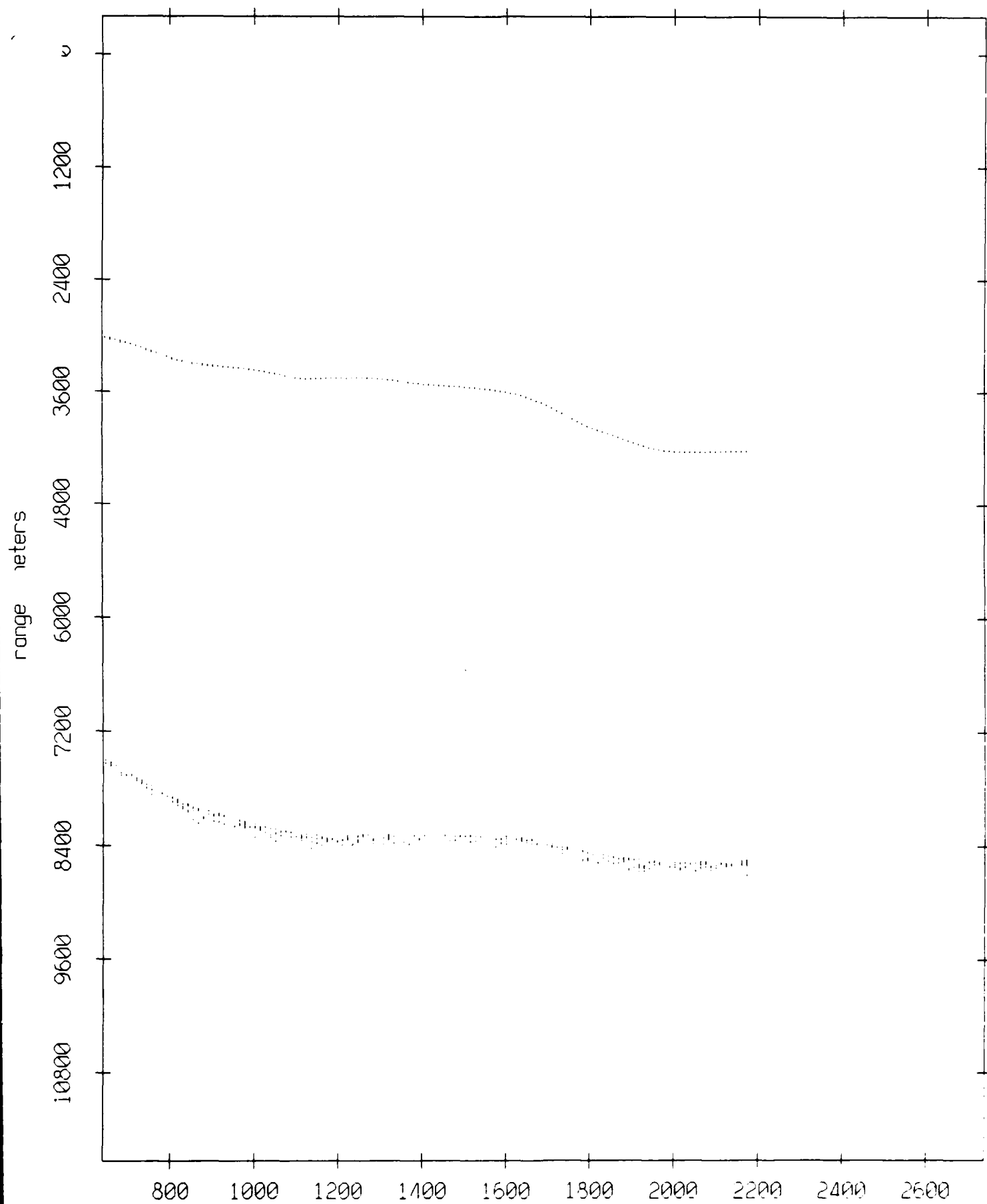
Float 8, July 1989 Trip: range from float 9



record number

Figure IX.91

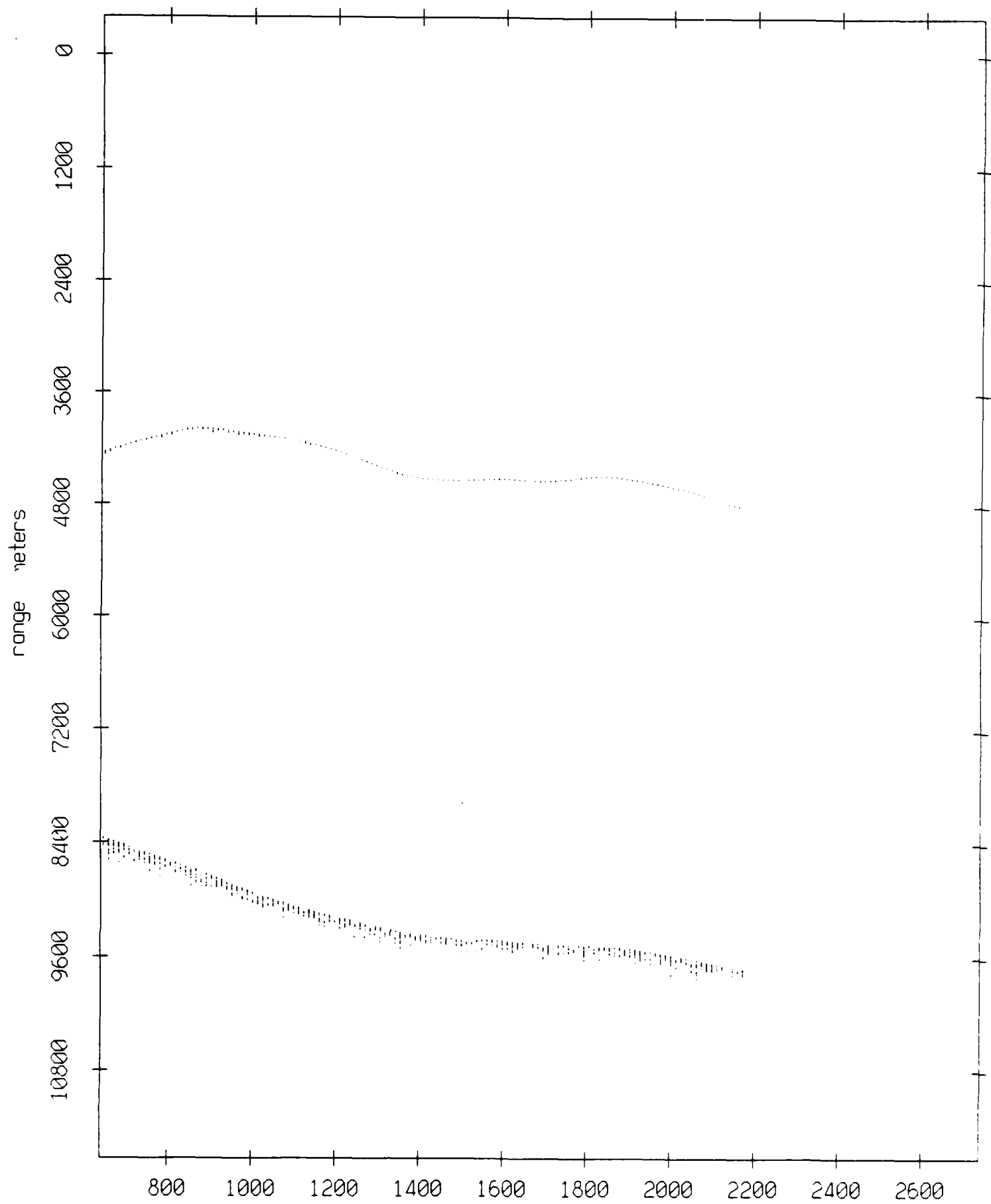
Float 8, July 1989 Trip: range from float 10



record number  
Figure IX.9j



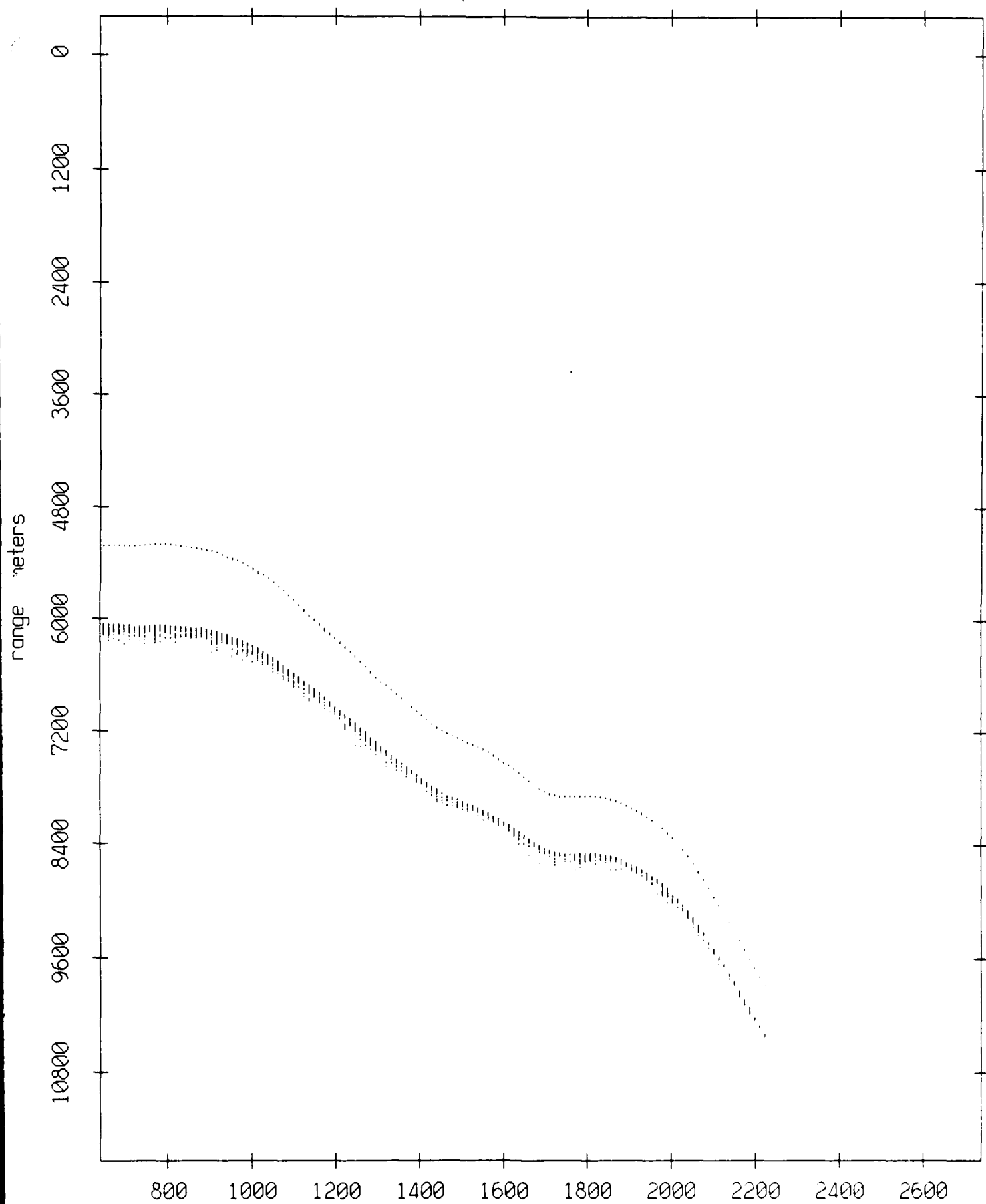
Float 8, July 1989 Trip: range from float 11



record number

Figure IX.9k

Float 9, July 1989 Trip: range from float 0



record number

Figure IX.10a

Float 9, July 1989 Trip: range from float 1

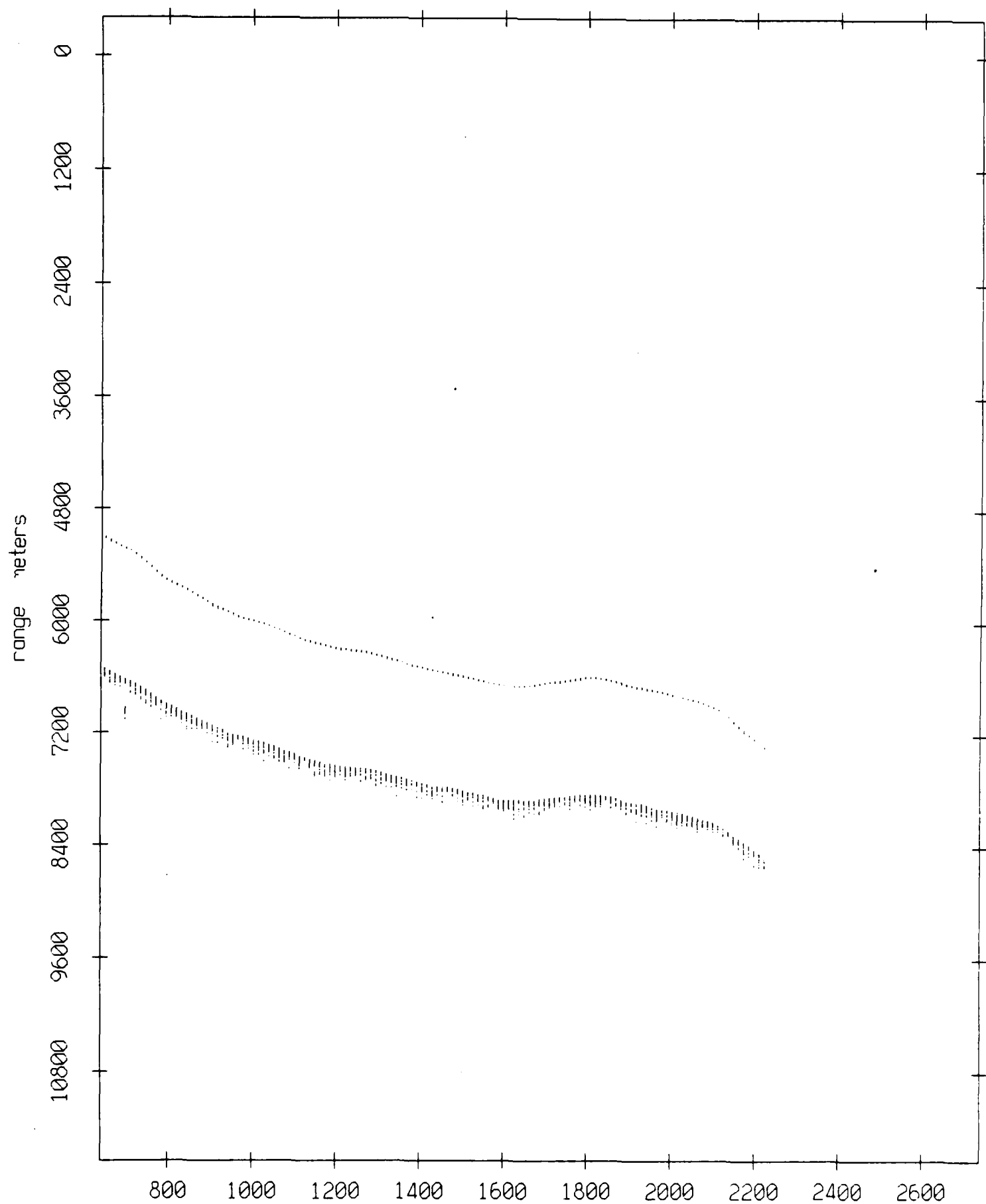
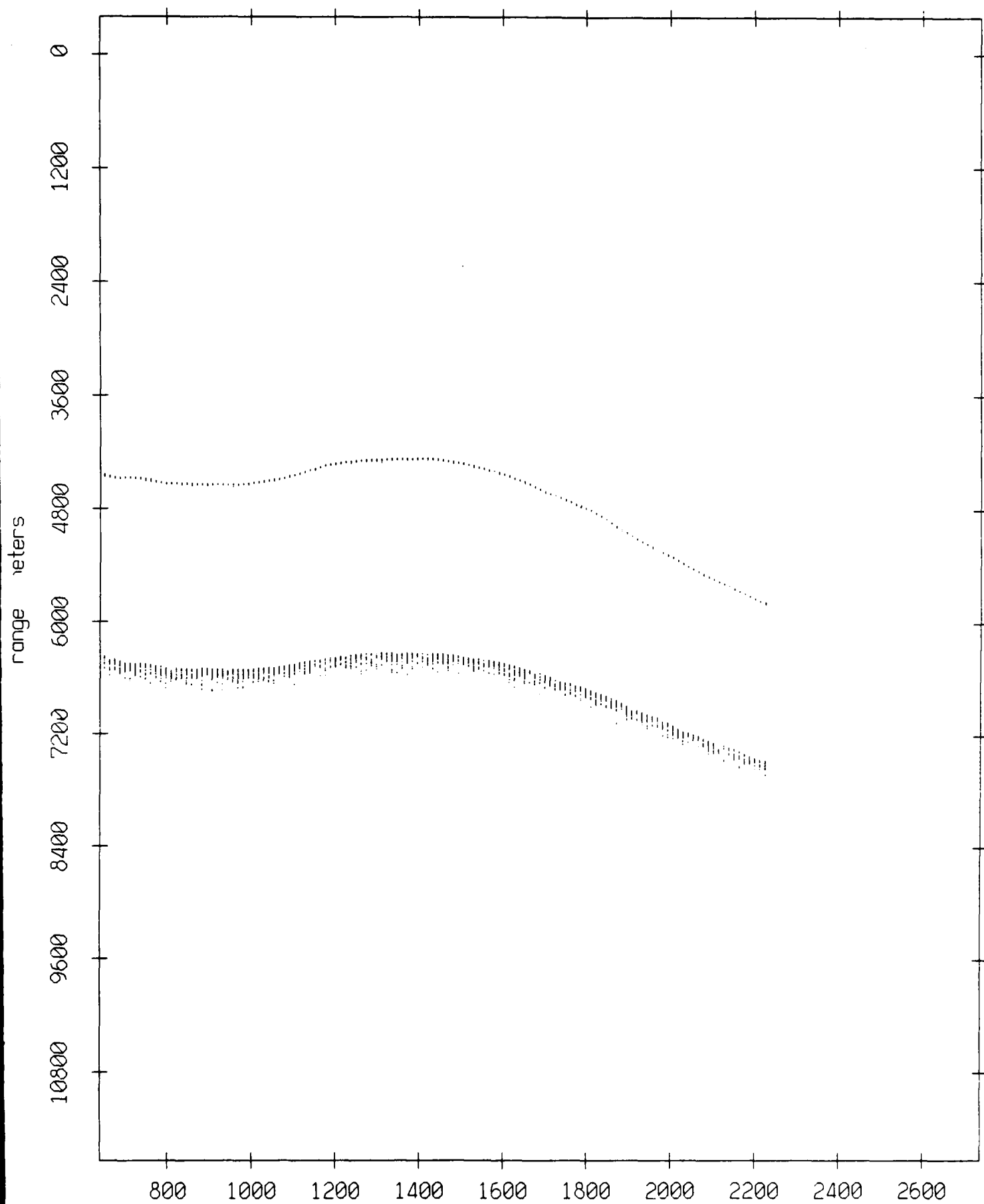


Figure IX.10b

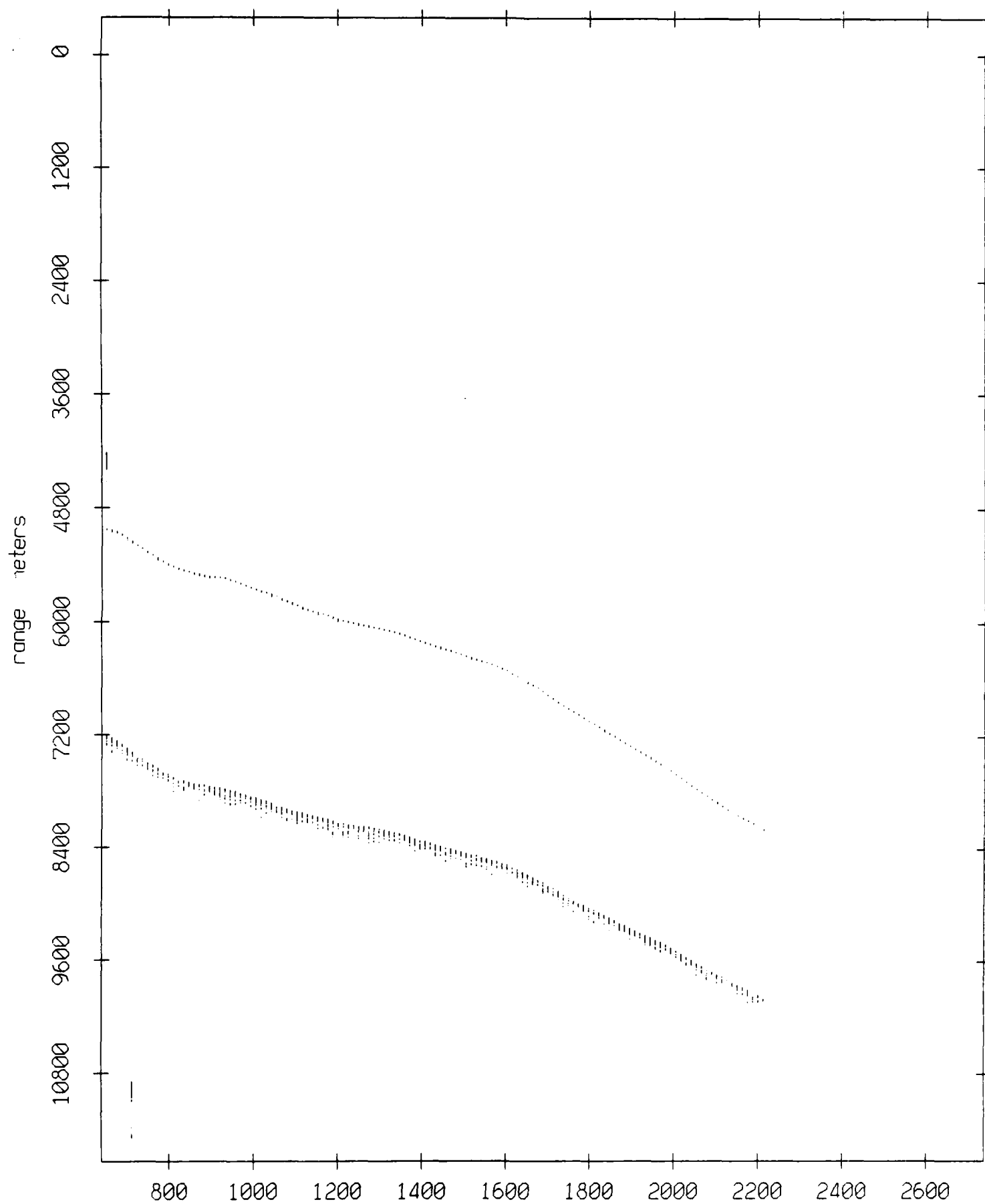
Float 9, July 1989 Trip: range from float 2



record number

Figure IX.10c

Float 9, July 1989 Trip: range from float 3



record number

Figure IX.10d

Float 9, July 1989 Trip: range from float 4

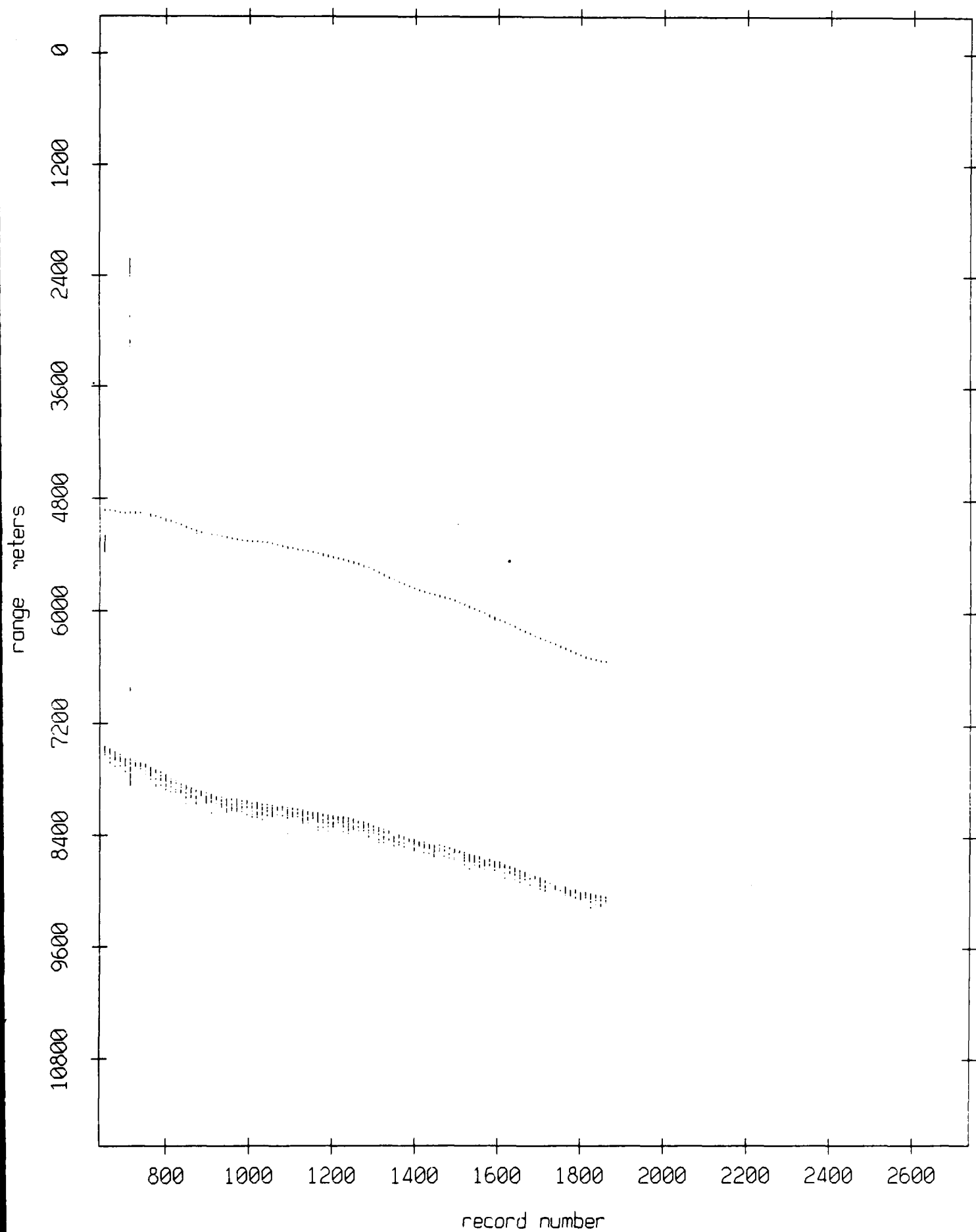


Figure IX.10e

Float 9, July 1989 Trip: range from float 5

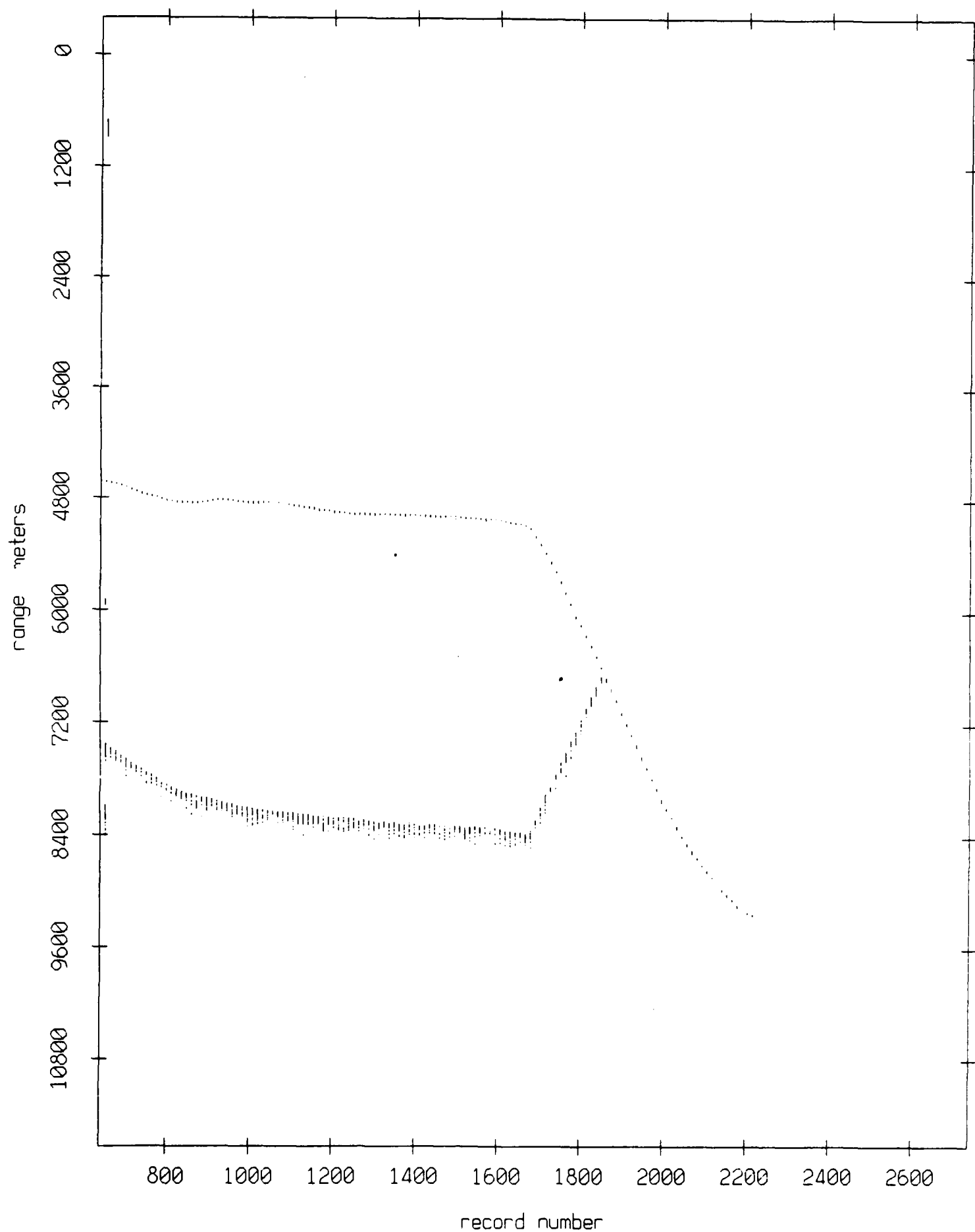
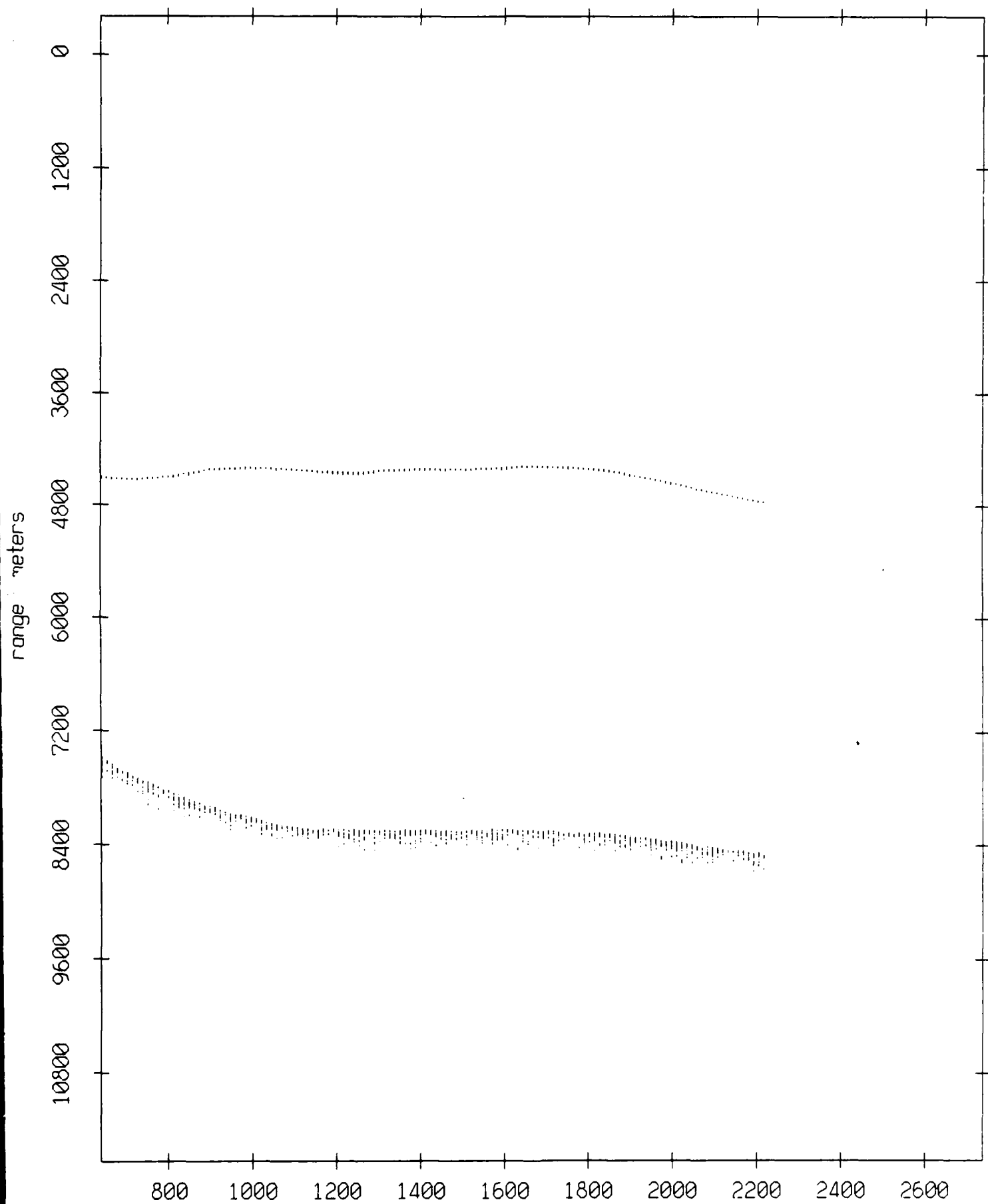


Figure IX.10f

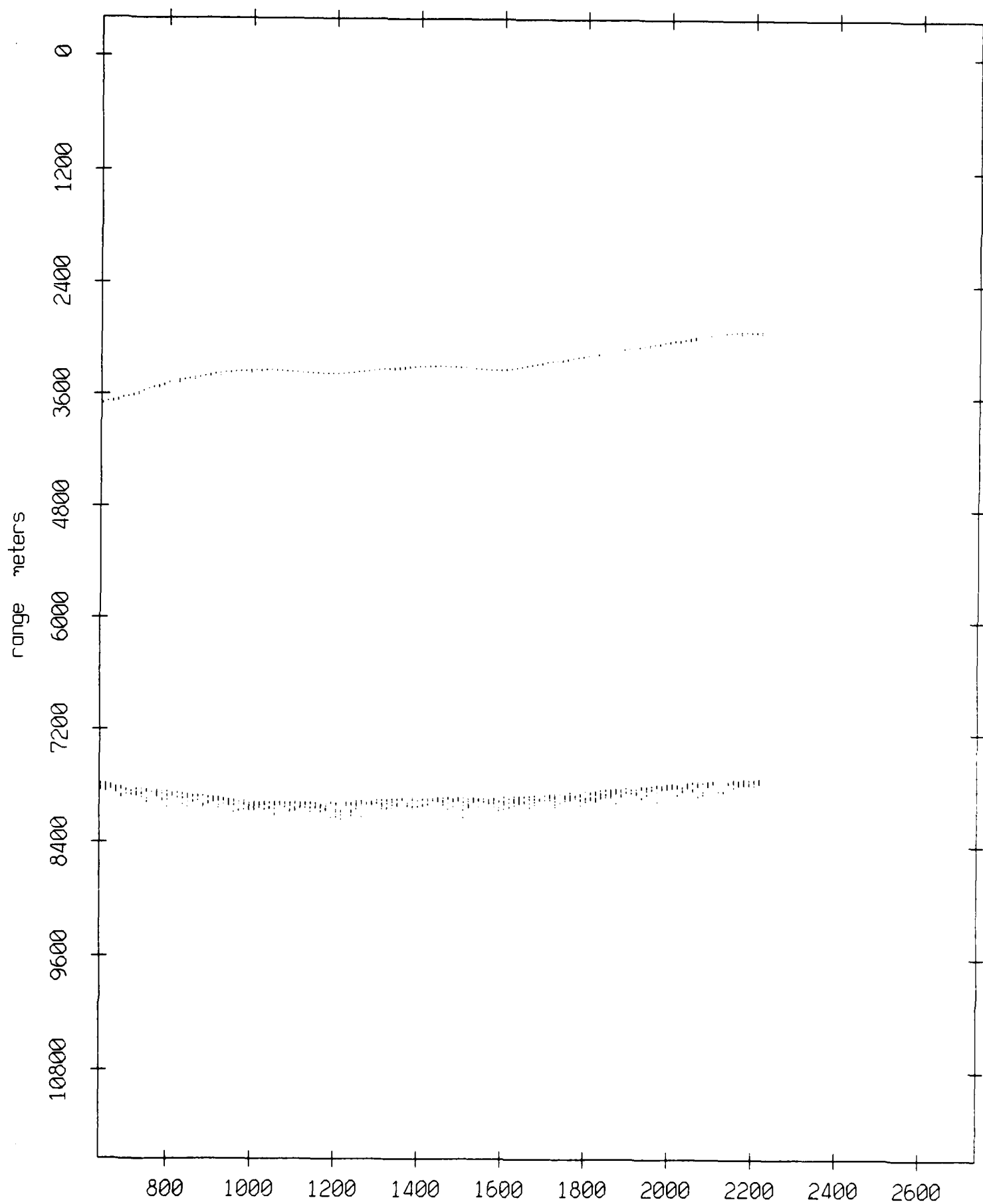
Float 9, July 1989 Trip: range from float 6



record number  
Figure IX.10g

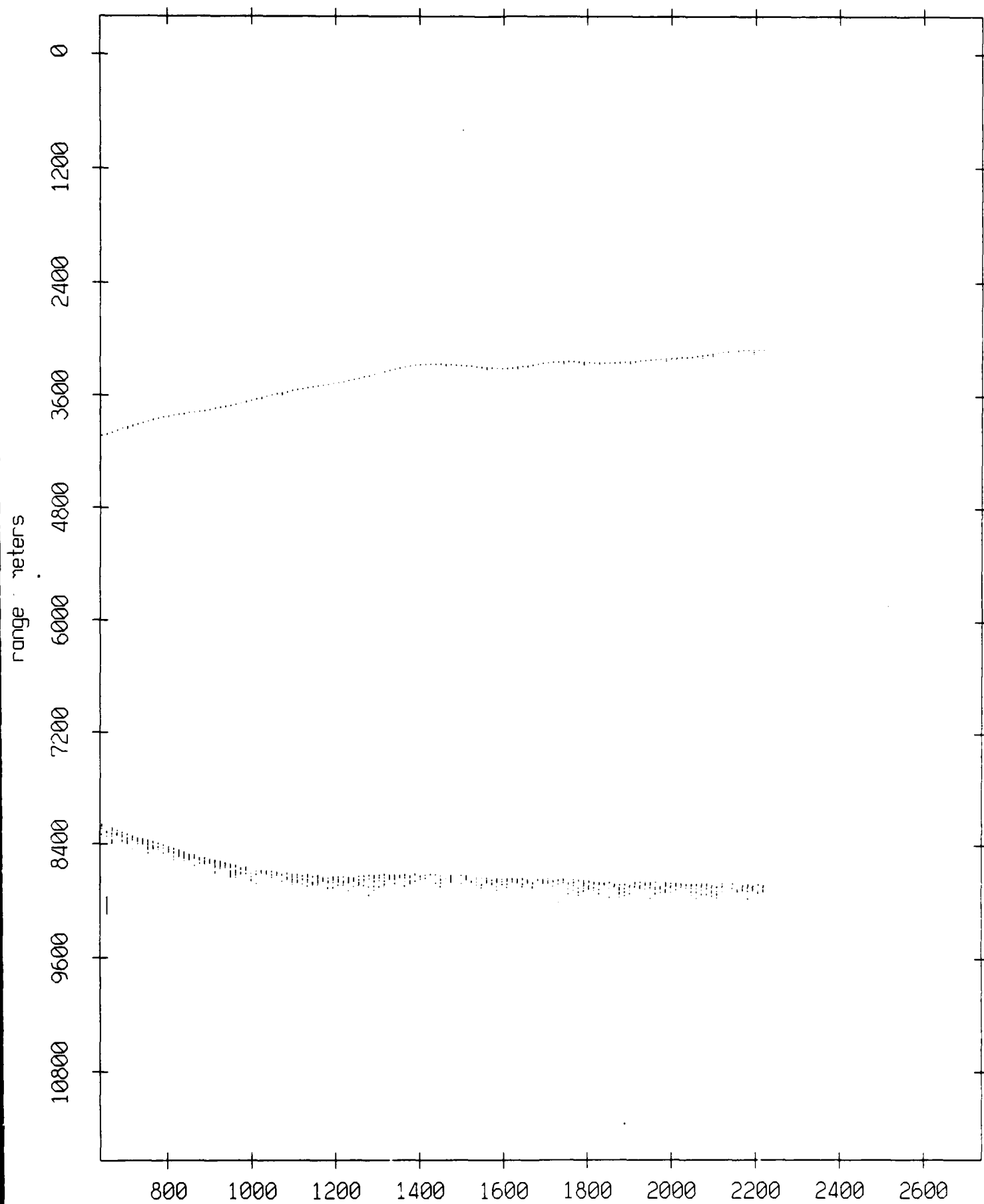


Float 9, July 1989 Trip: range from float 7



record number  
**Figure IX.10h**

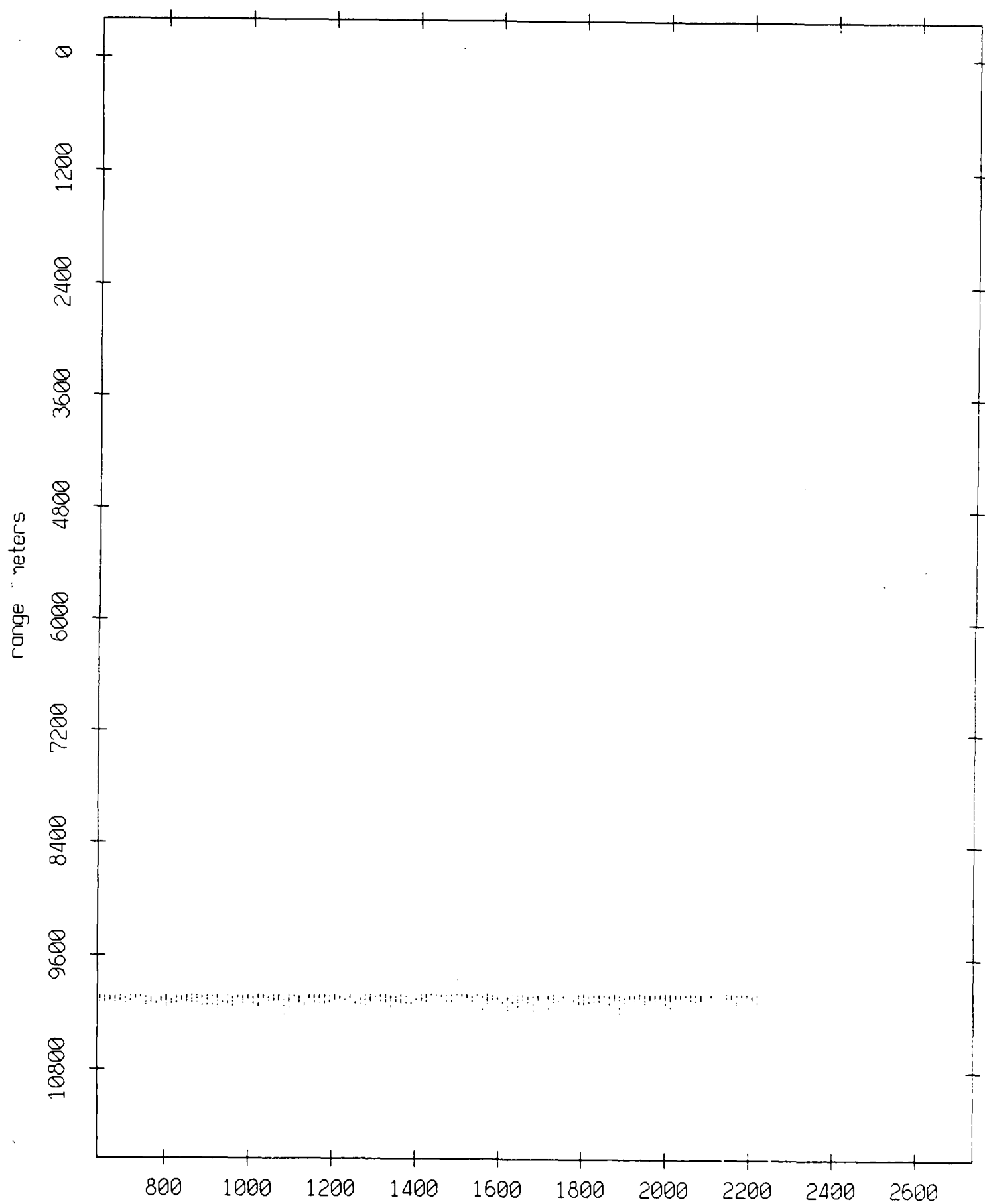
Float 9, July 1989 Trip: range from float 8



record number

Figure IX.101

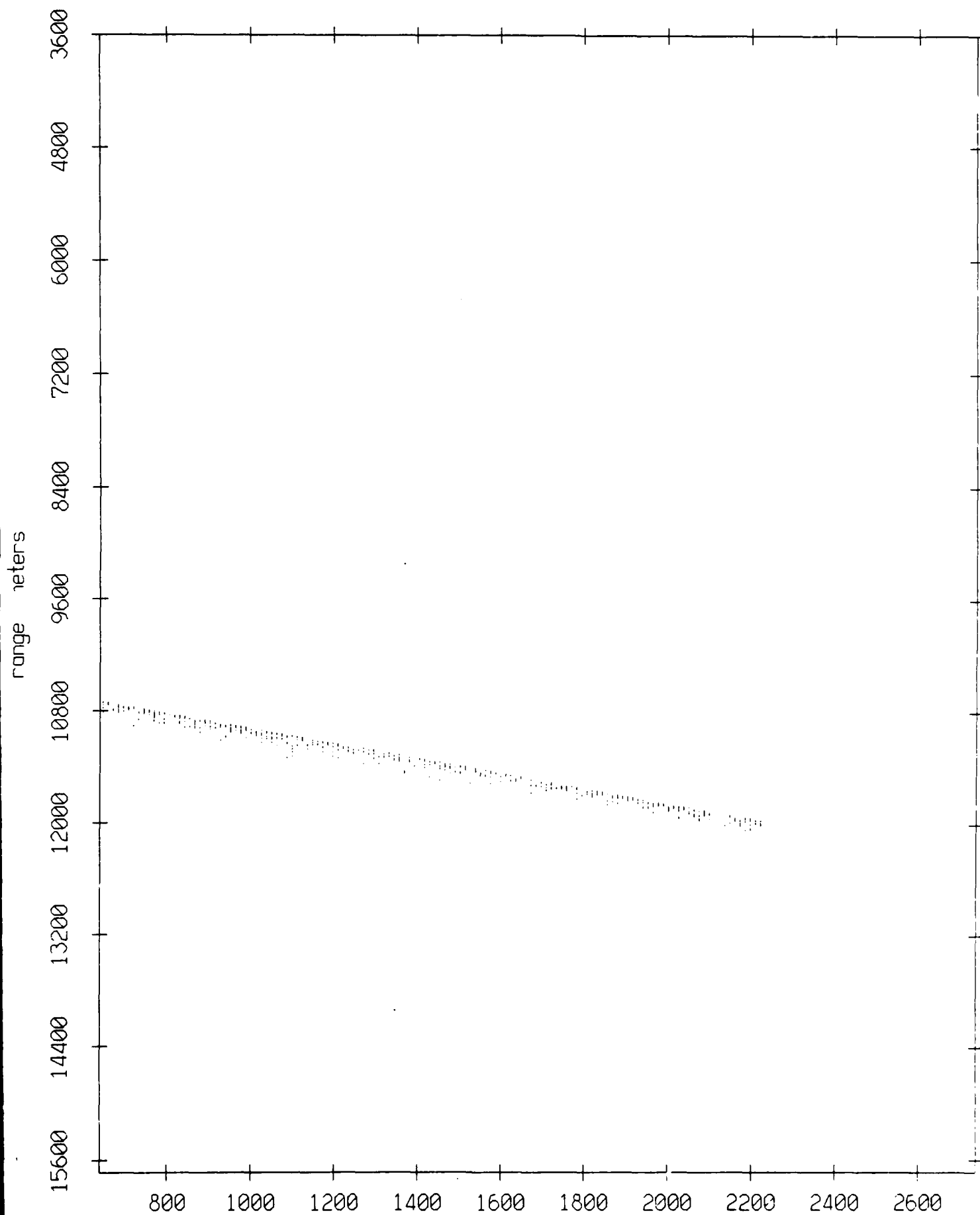
Float 9, July 1989 Trip: range from float 10



record number

Figure IX.10j

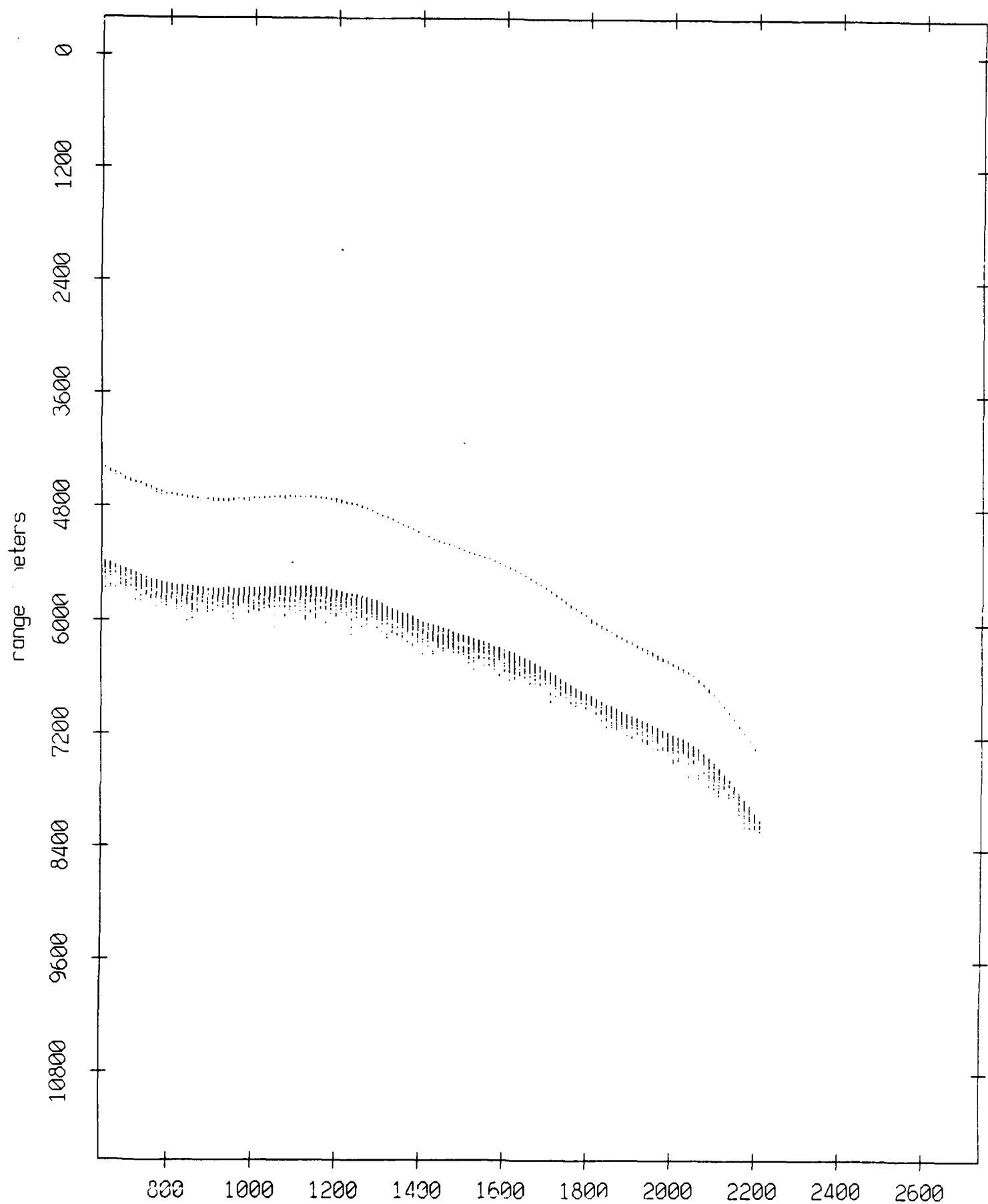
Float 9, July 1989. Trip: range from float 11



record number

**Figure IX.10k**

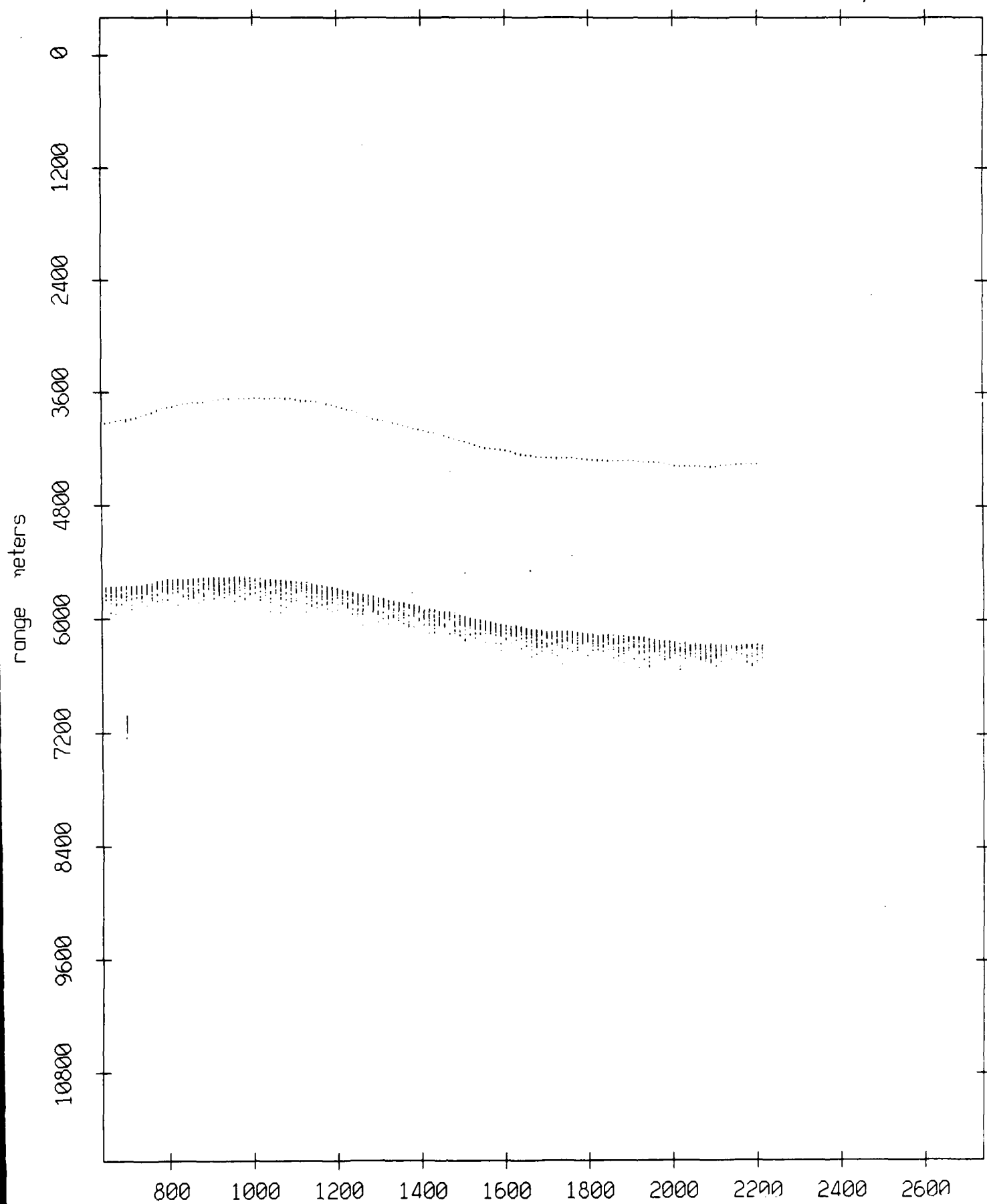
Float 10, July 1989 Trip: range from float 0



record number

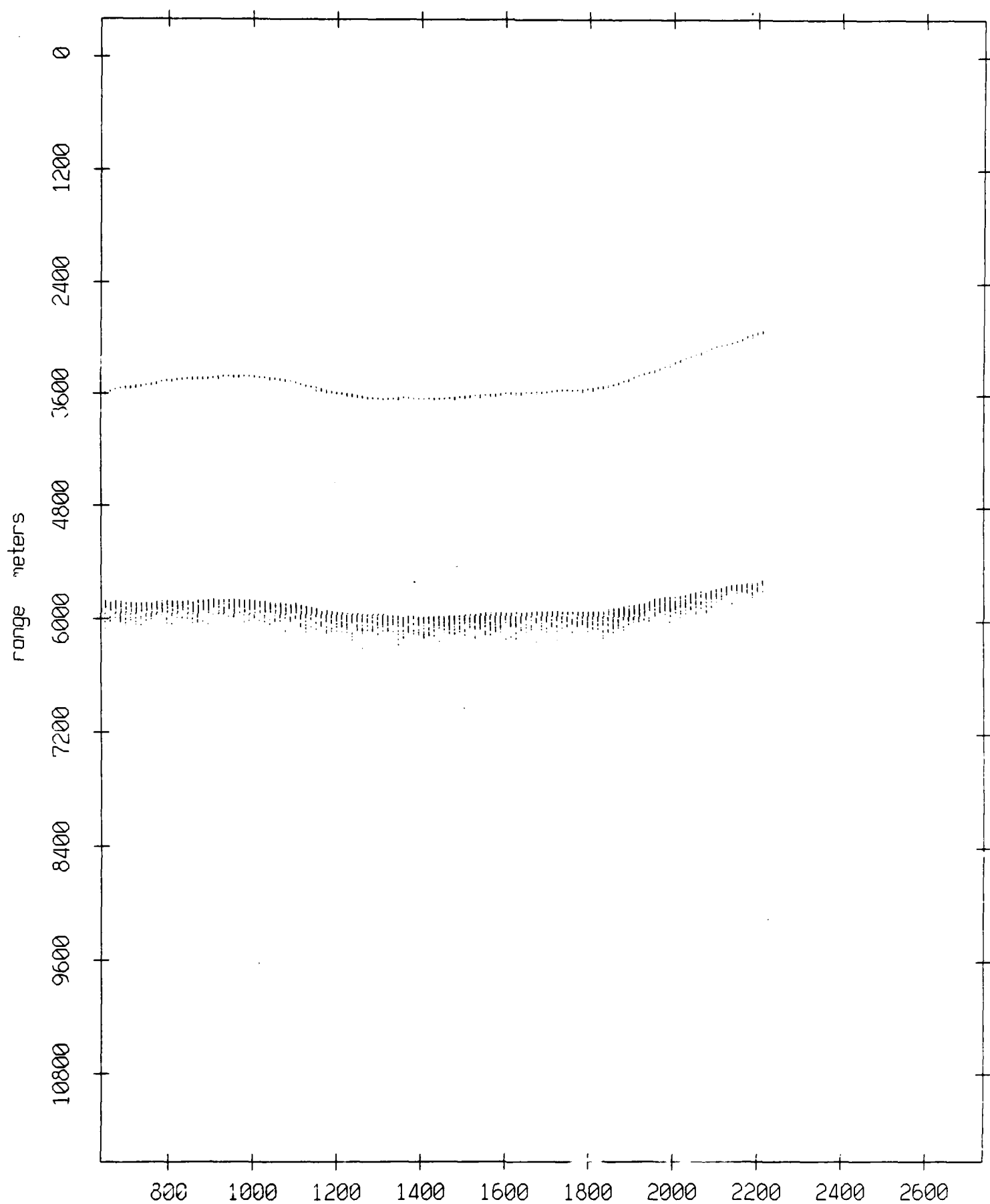
Figure IX.11a

Float 10, July 1989 Trip: range from float 1



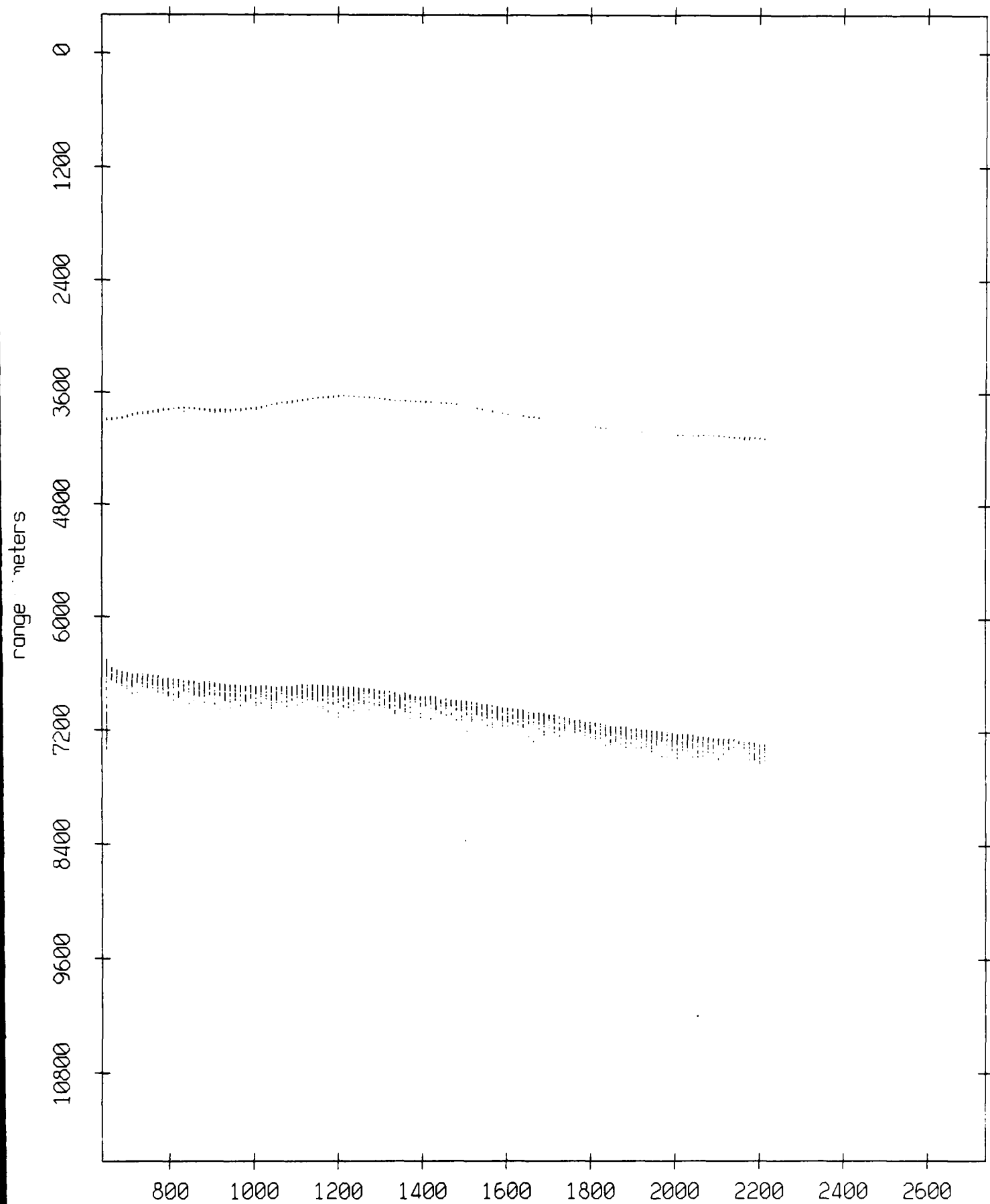
record number  
**Figure IX.11b**

Float 10, July 1989 Trip: range from float 2



record number  
Figure IX.11c

Float 10, July 1989 Trip: range from float 3

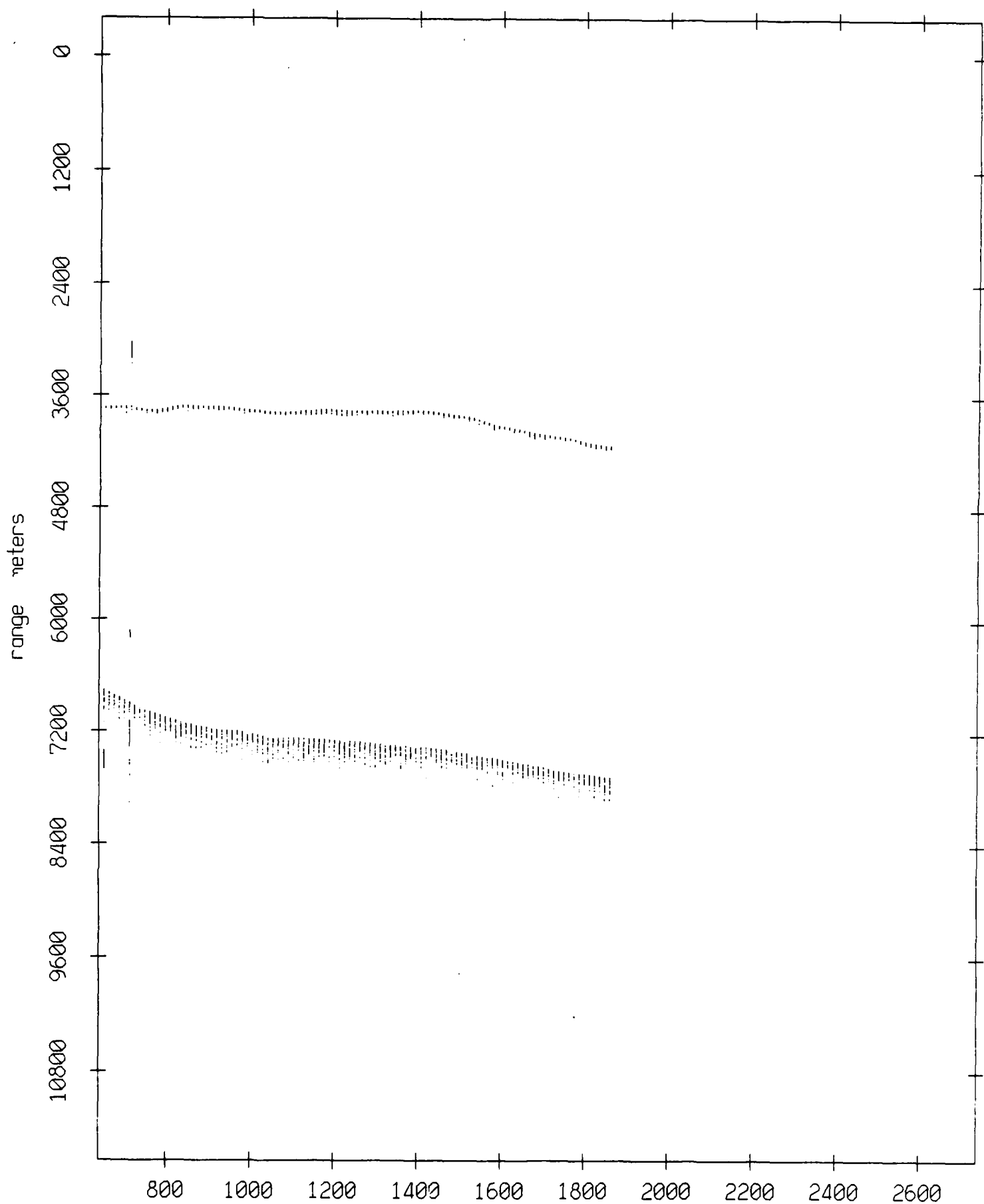


record number

Figure IX.11d



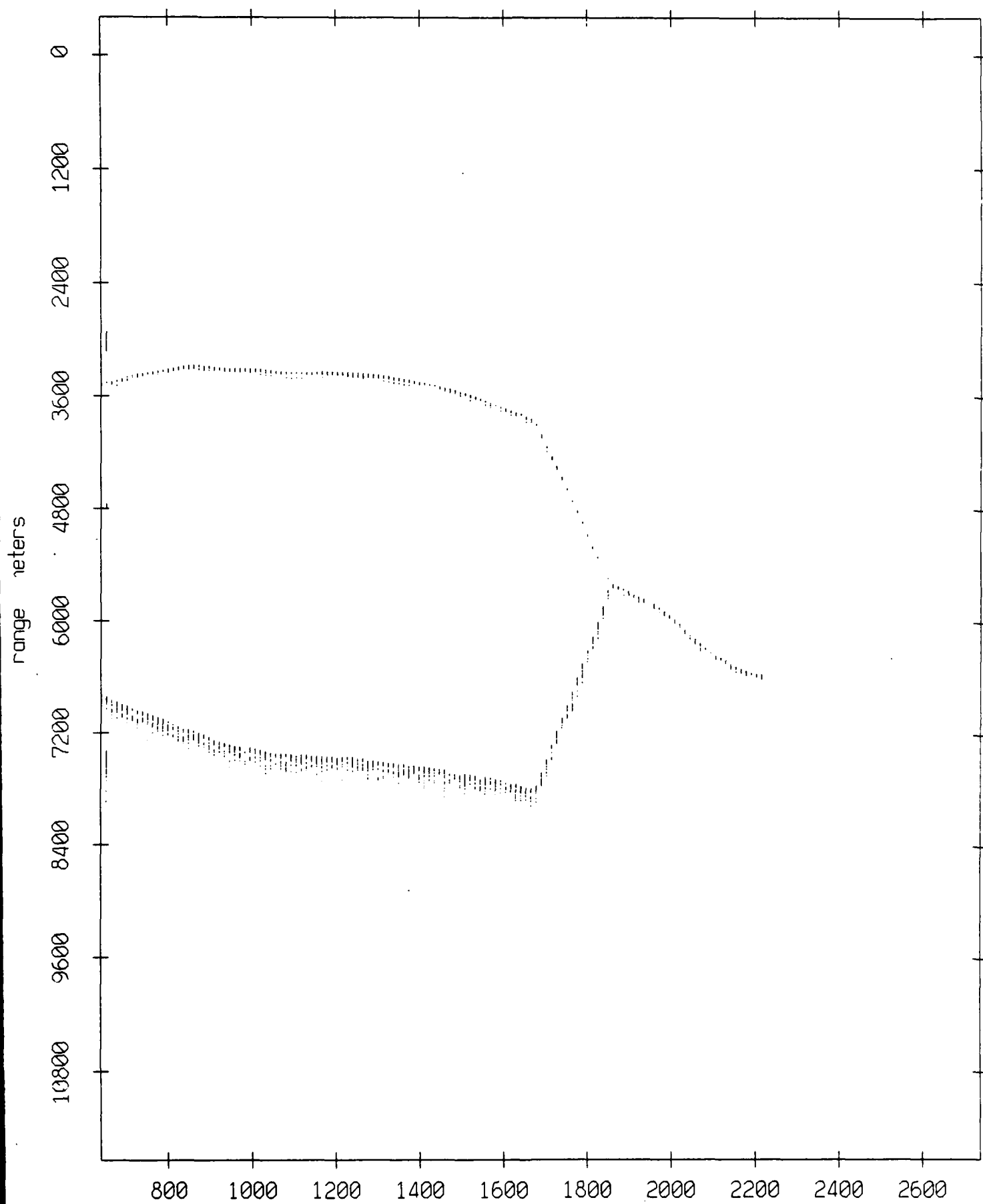
Float 10, July 1989 Trip: range from float 4



record number

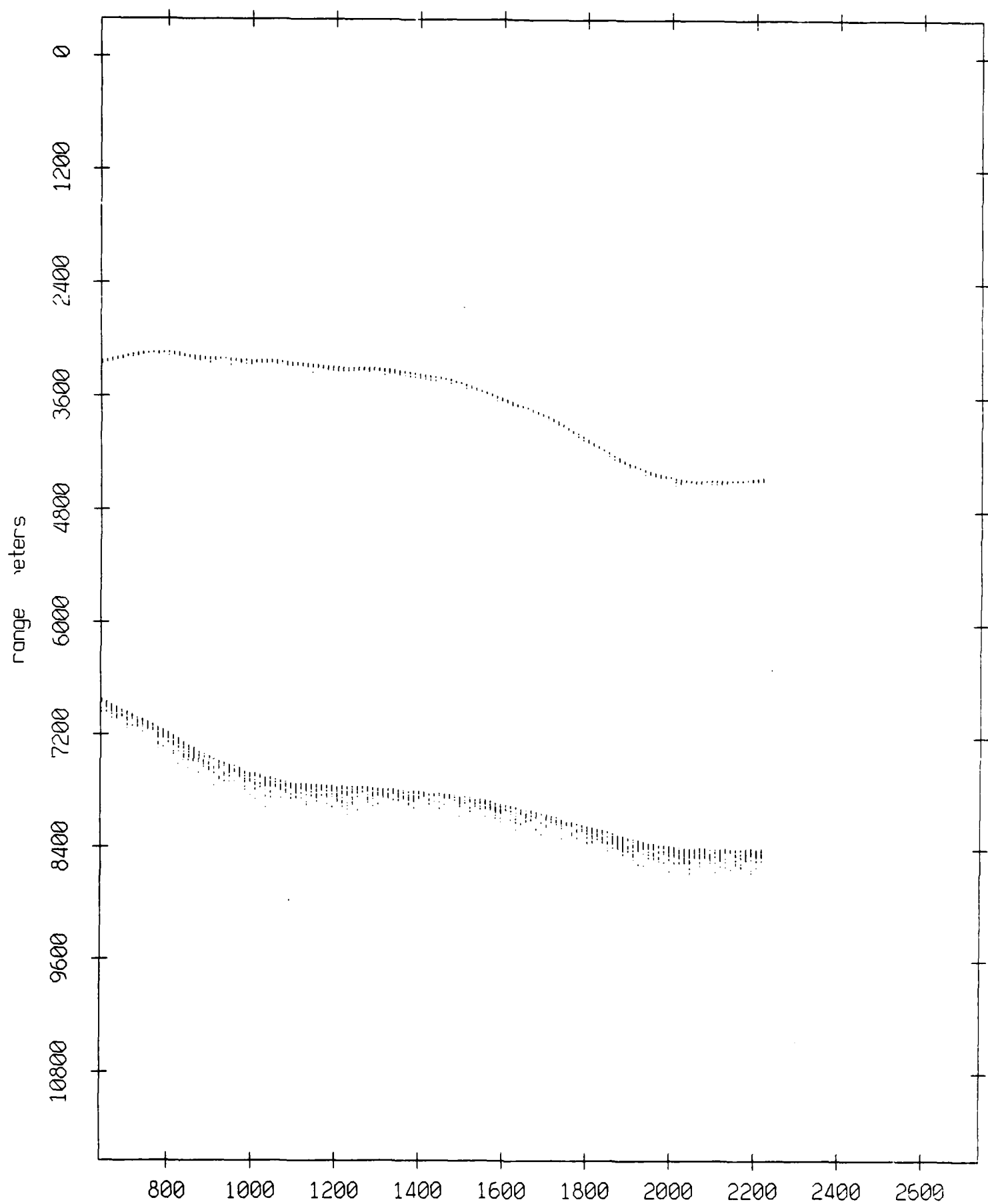
Figure IX.11e

Float 10, July 1989 Trip: range from float 5



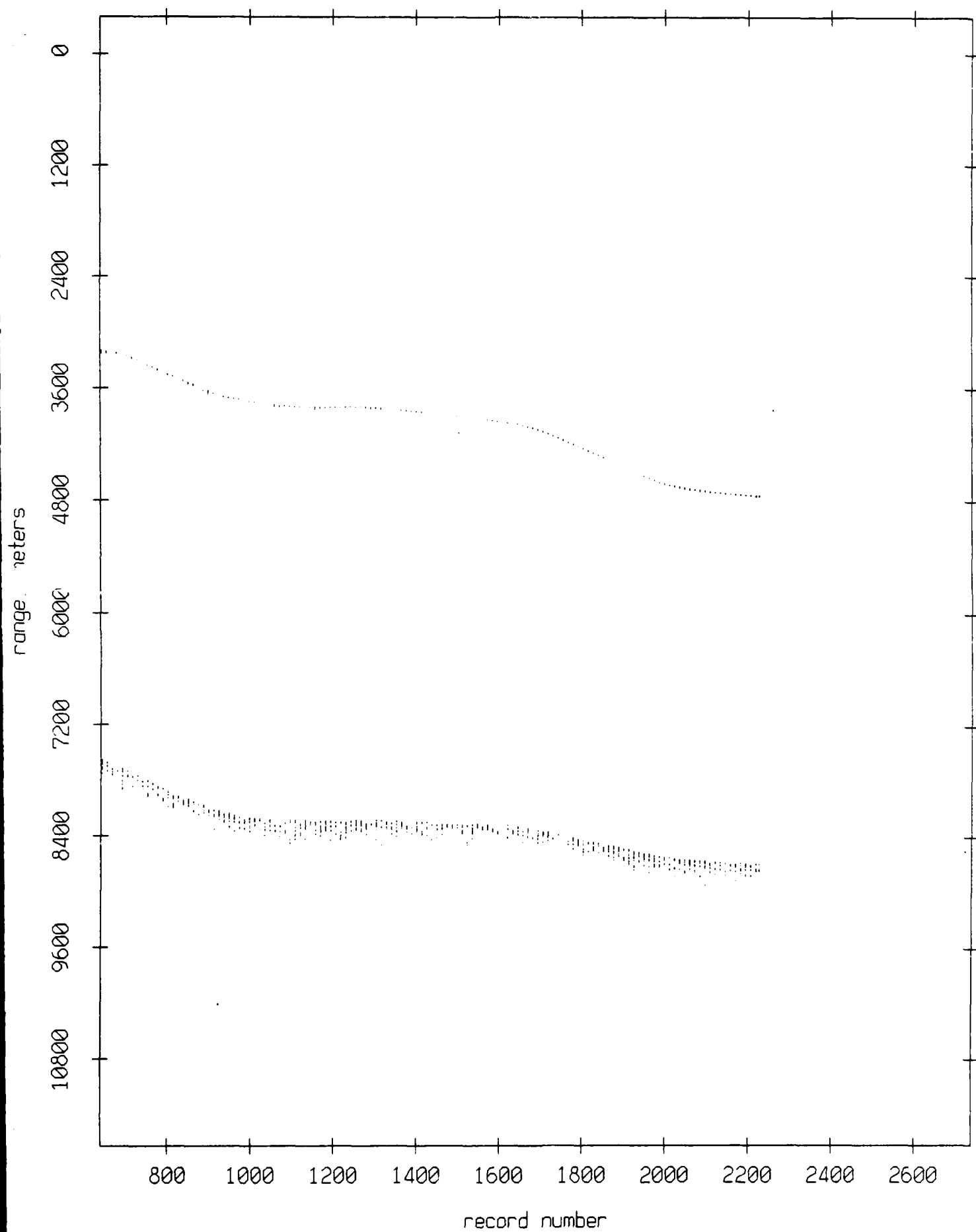
record number  
Figure IX.11f

Float 10, July 1989 Trip: range from float 6



record number  
**Figure IX.11g**

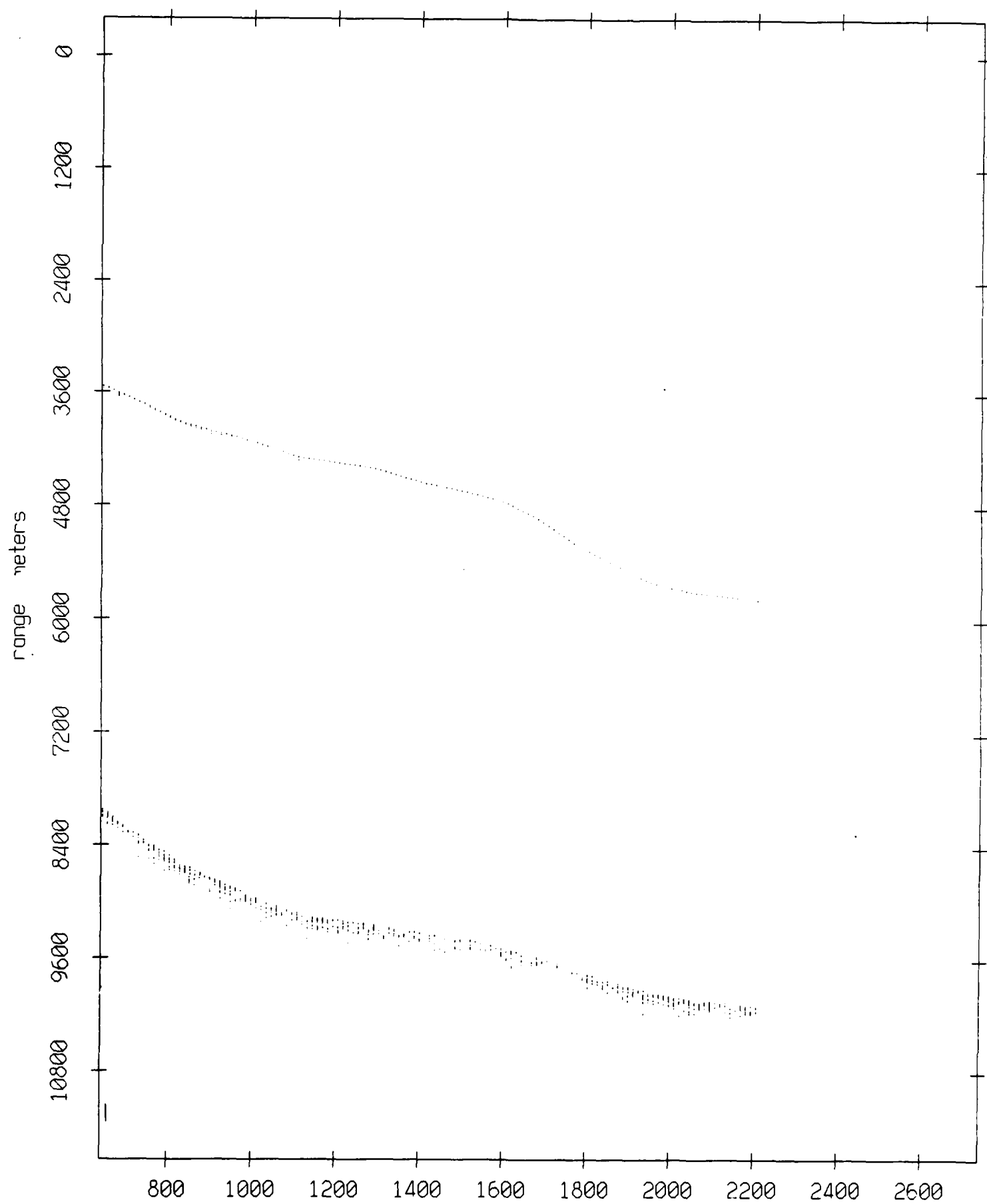
Float 10, July 1989 Trip: range from float 7



record number

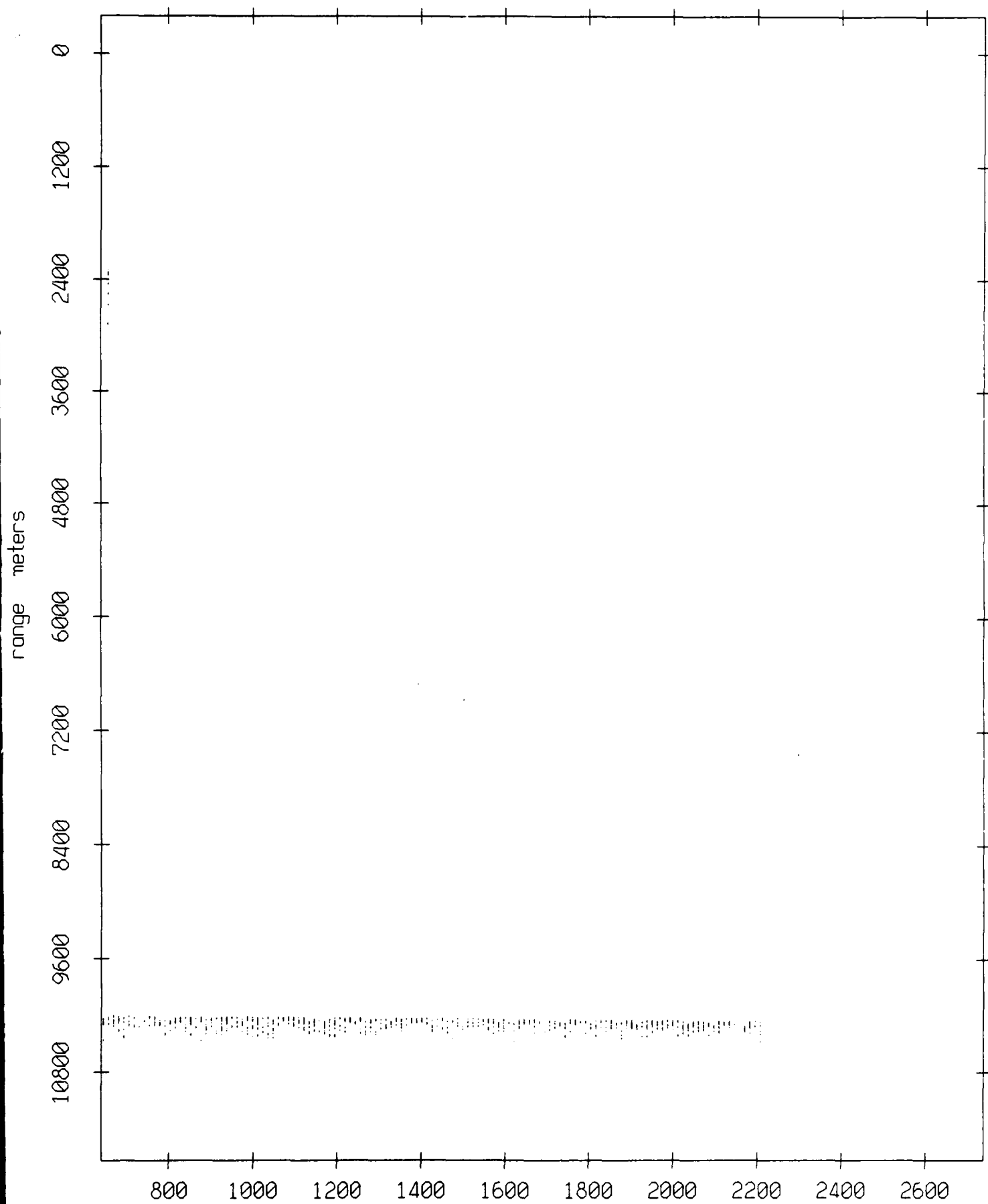
Figure IX.11h

Float 10, July 1989 Trip: range from float 8



record number  
Figure IX.111

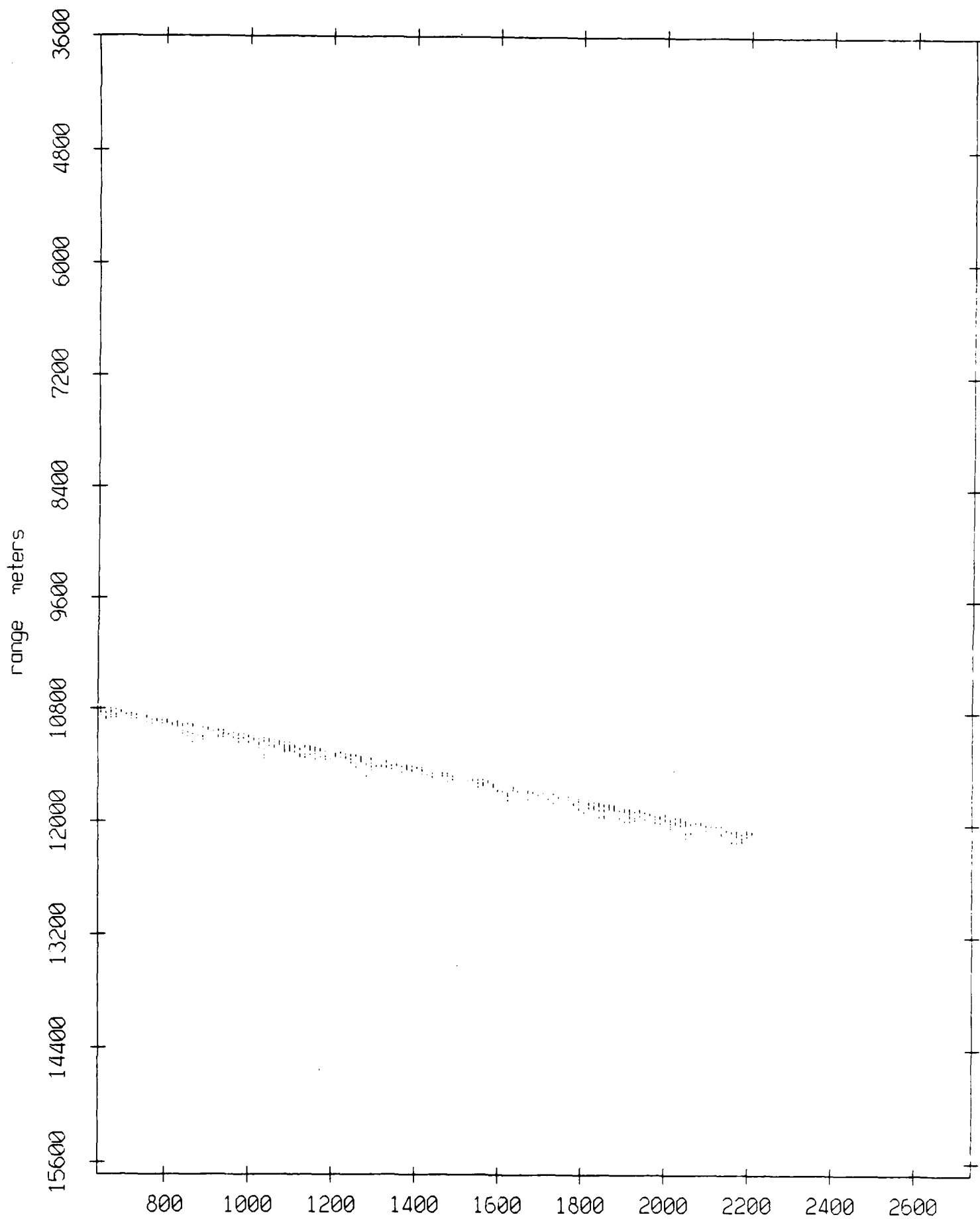
Float 10, July 1989 Trip: range from float 9



record number

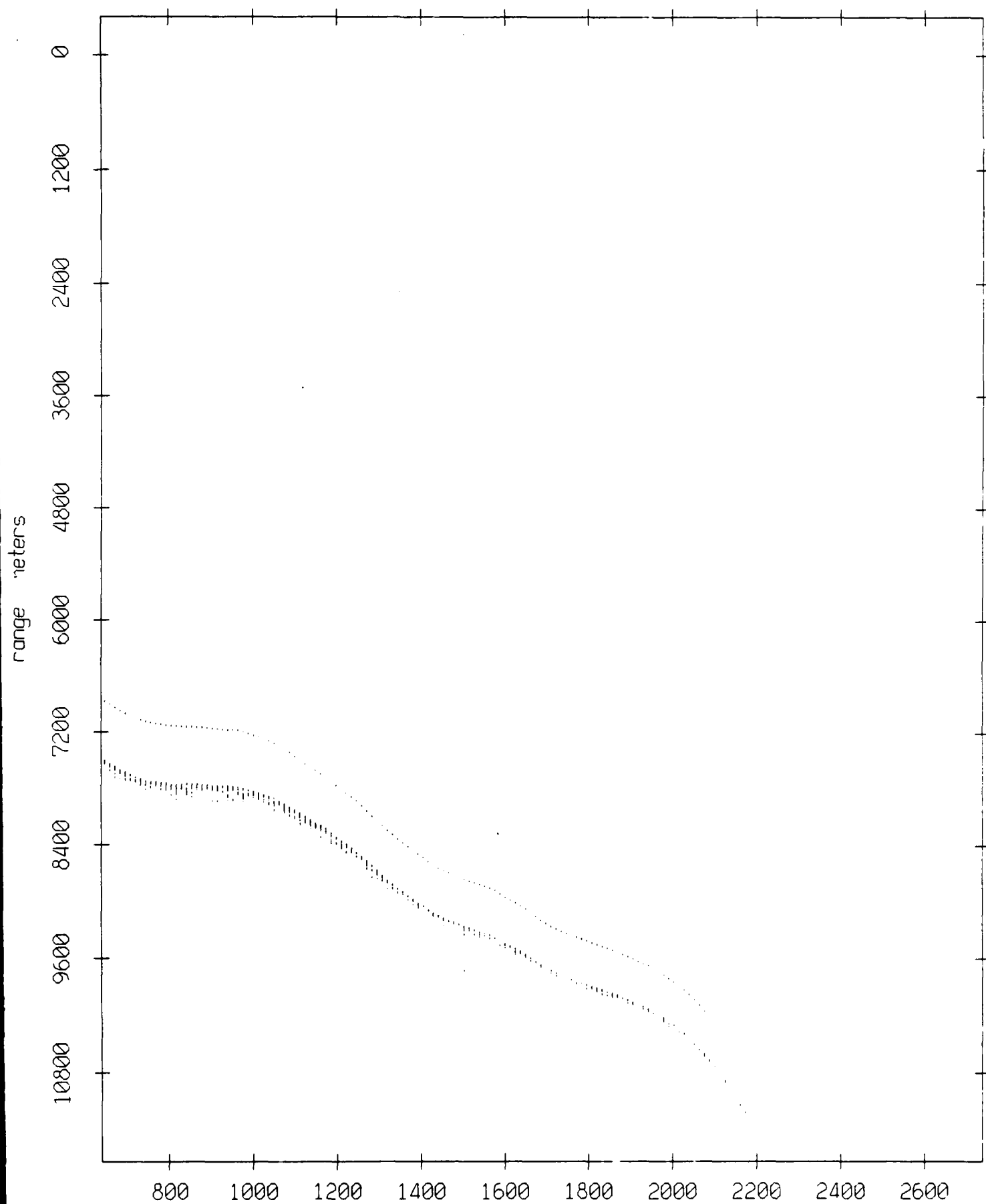
Figure IX.11j

Float 10, July 1989 Trip: range from float 11



record number  
**Figure IX.11k**

Float 11, July 1989 Trip: range from float 0

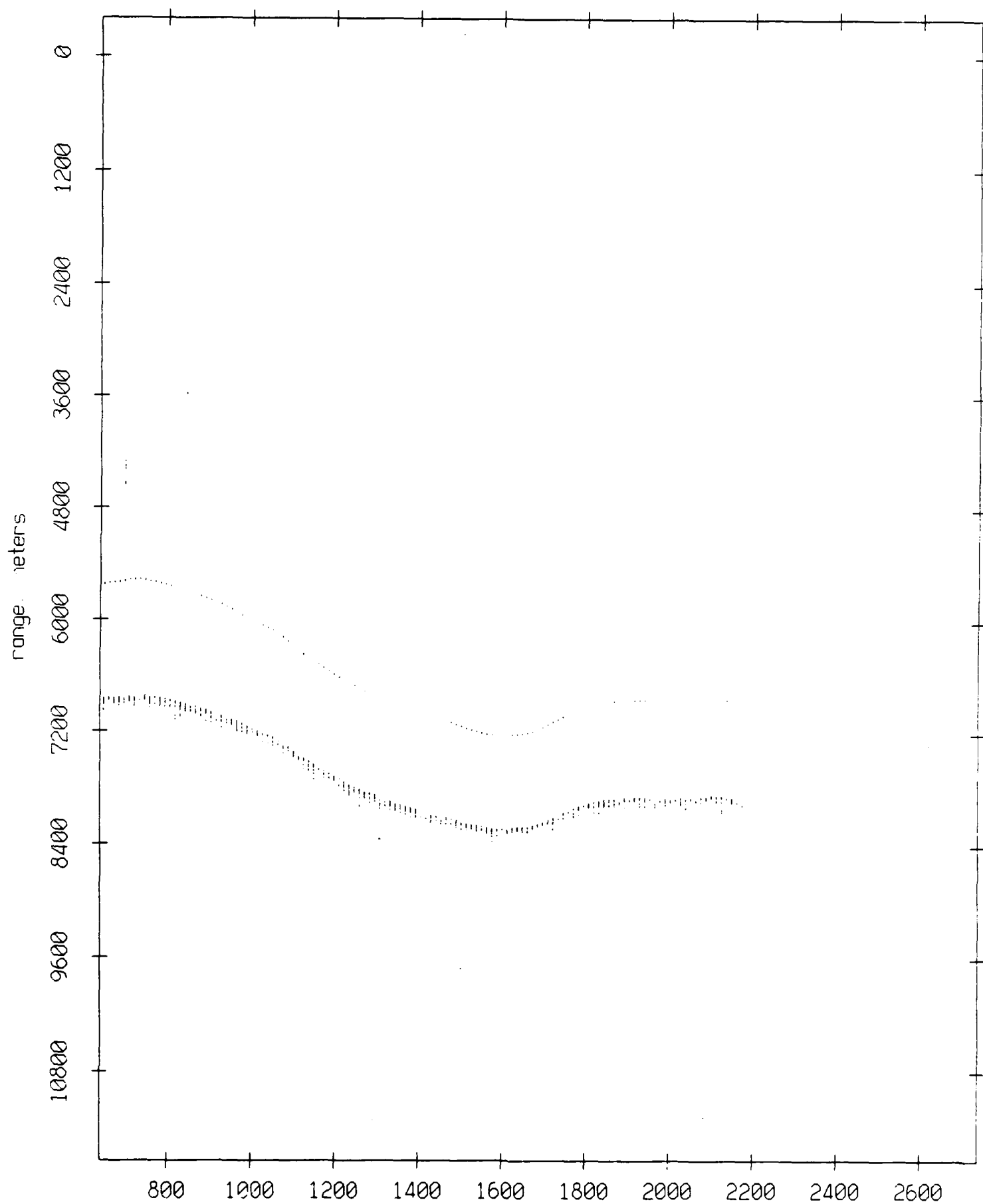


record number

Figure IX.12a



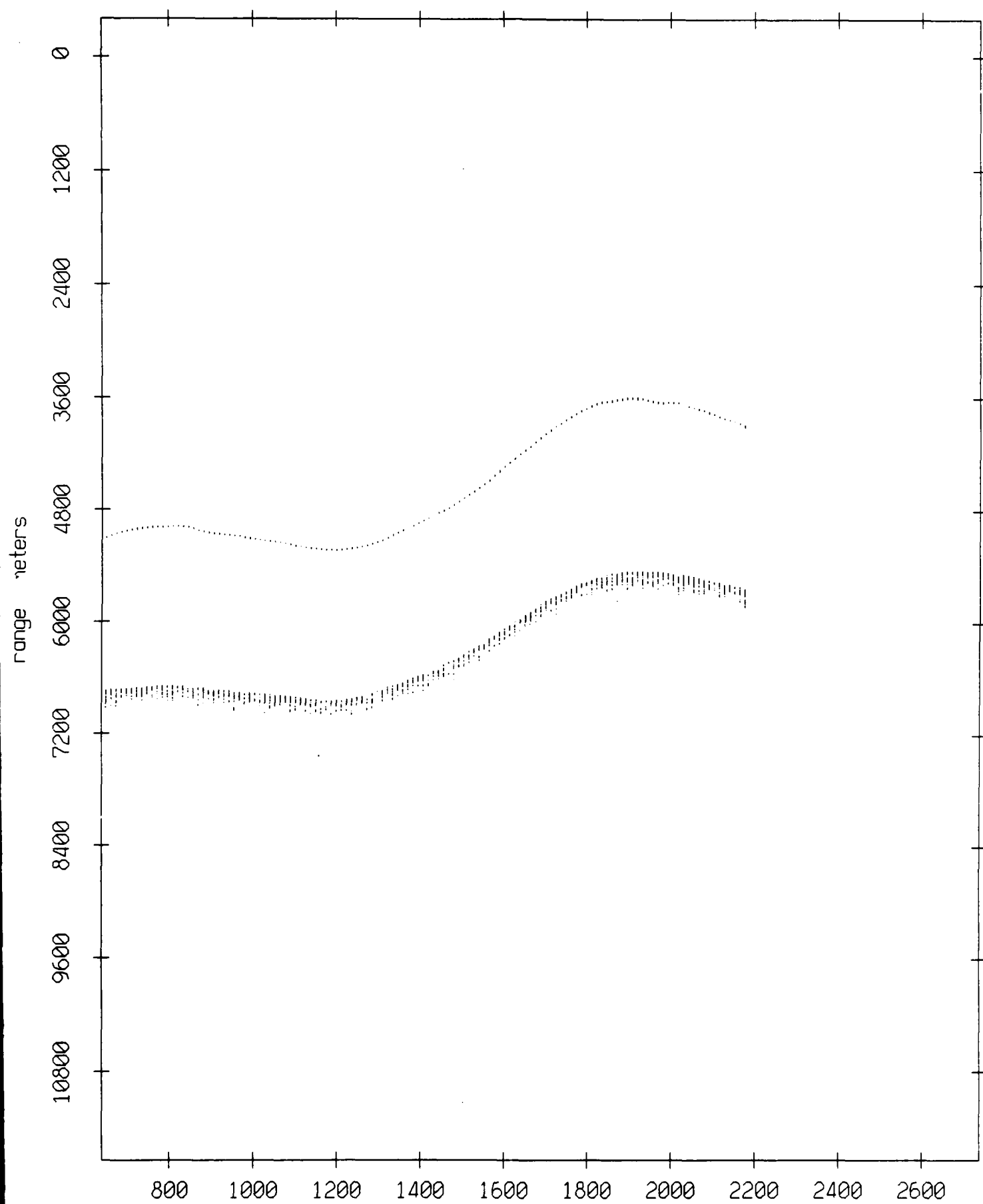
Float 11, July 1989 Trip: range from float 1



record number

Figure IX.12b

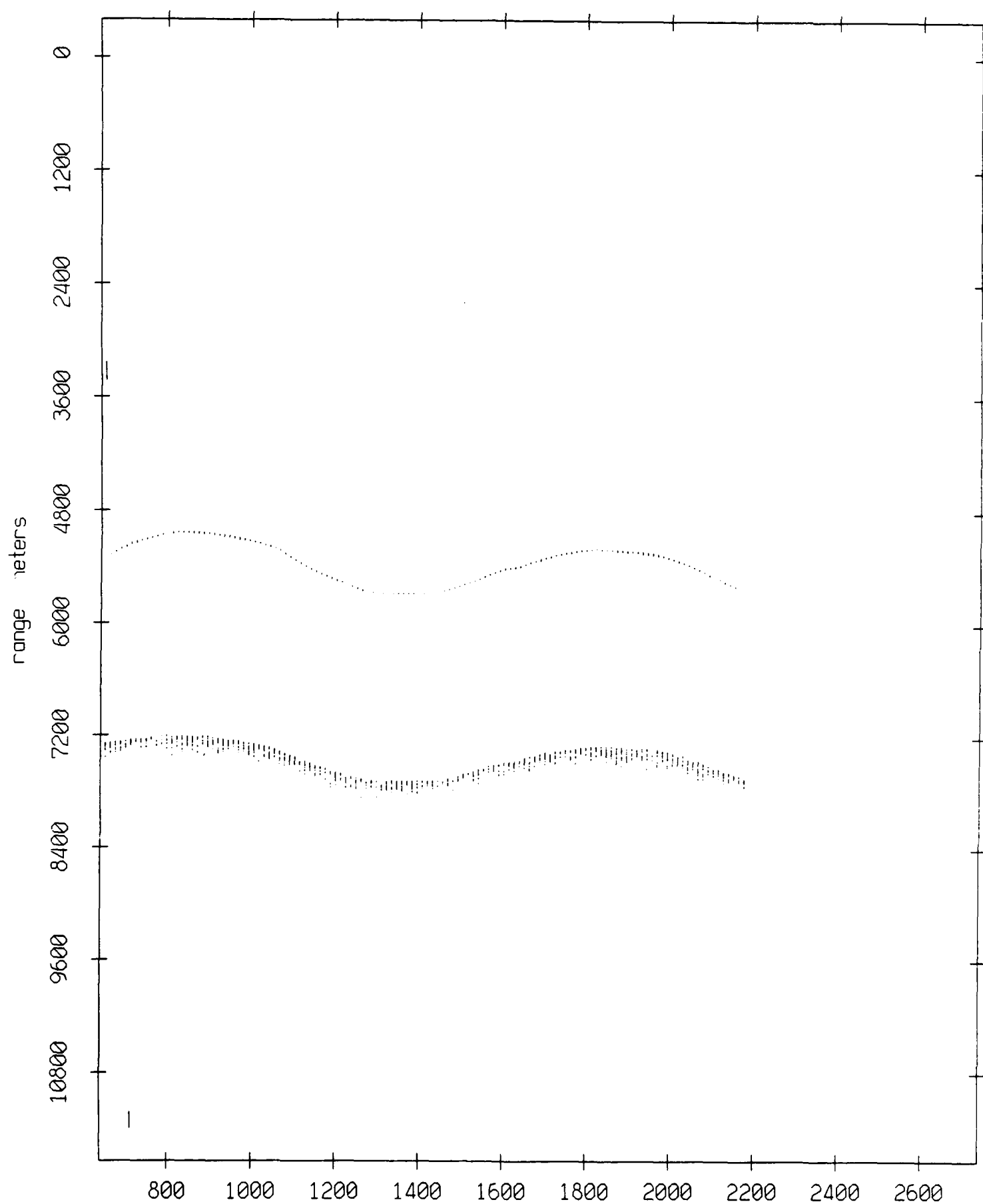
Float 11, July 1989 Trip: range from float 2



record number

Figure IX.12c

Float 11, July 1989 Trip: range from float 3



record number

Figure IX.12d

Float 11, July 1989 Trip: range from float 4

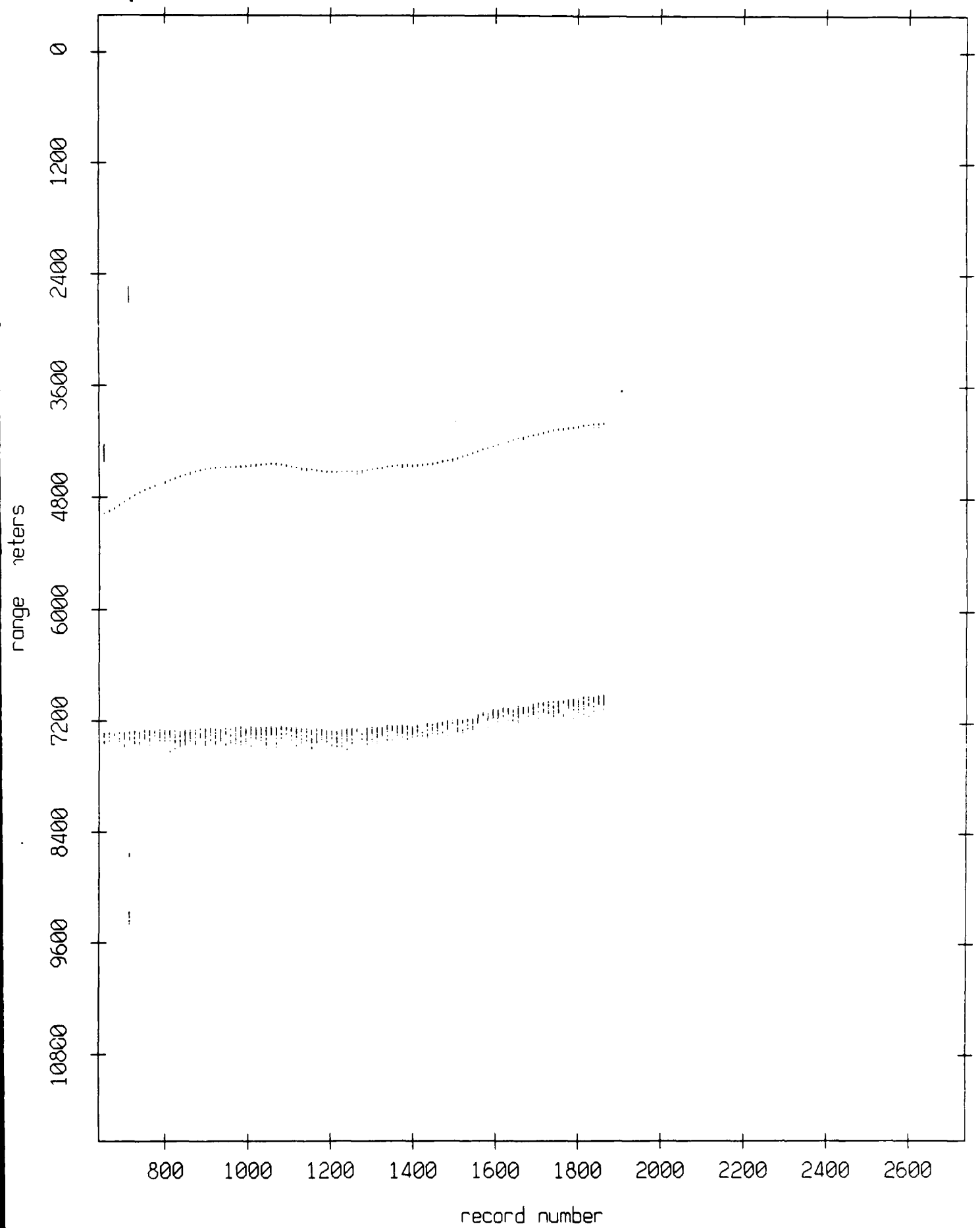
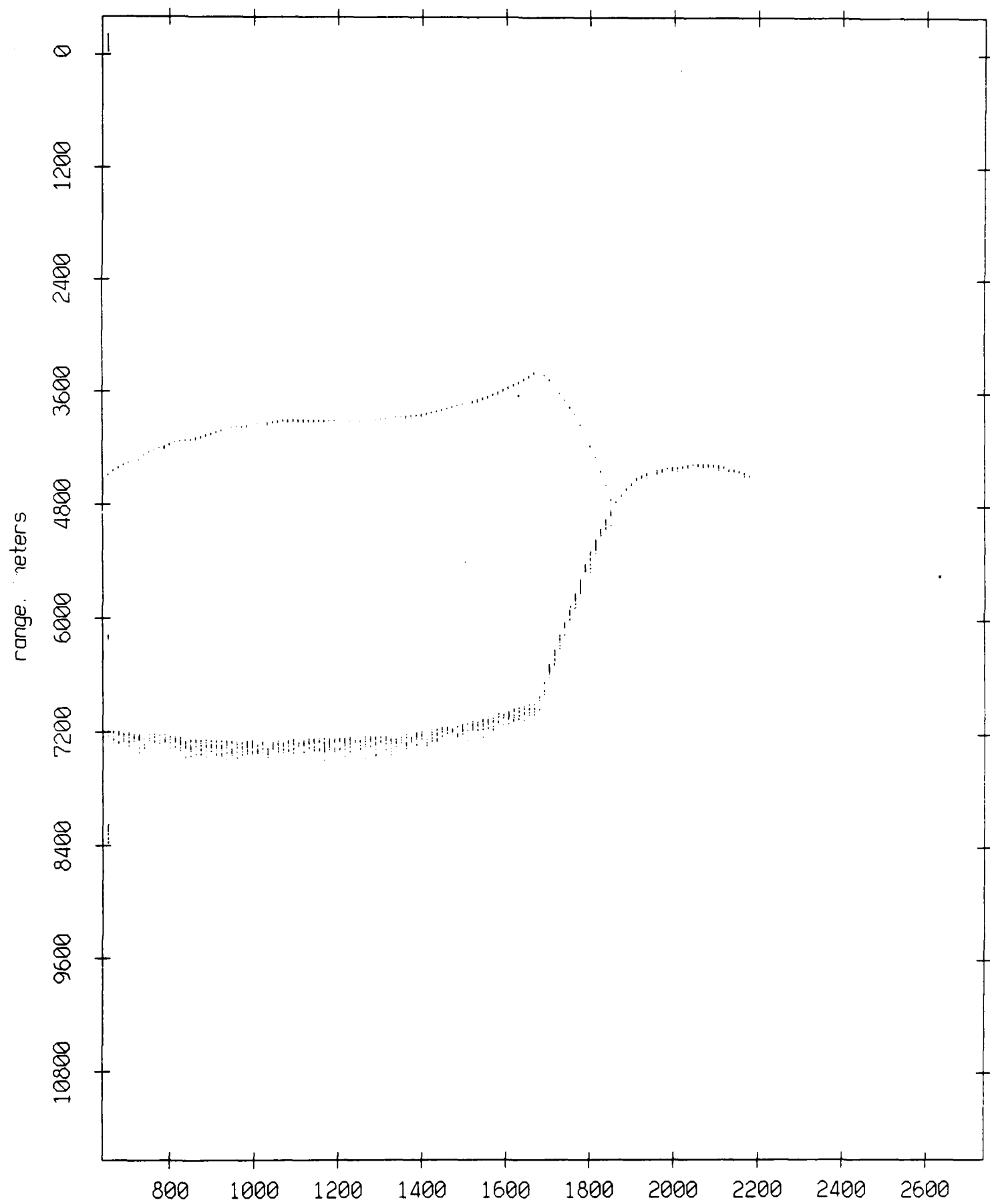


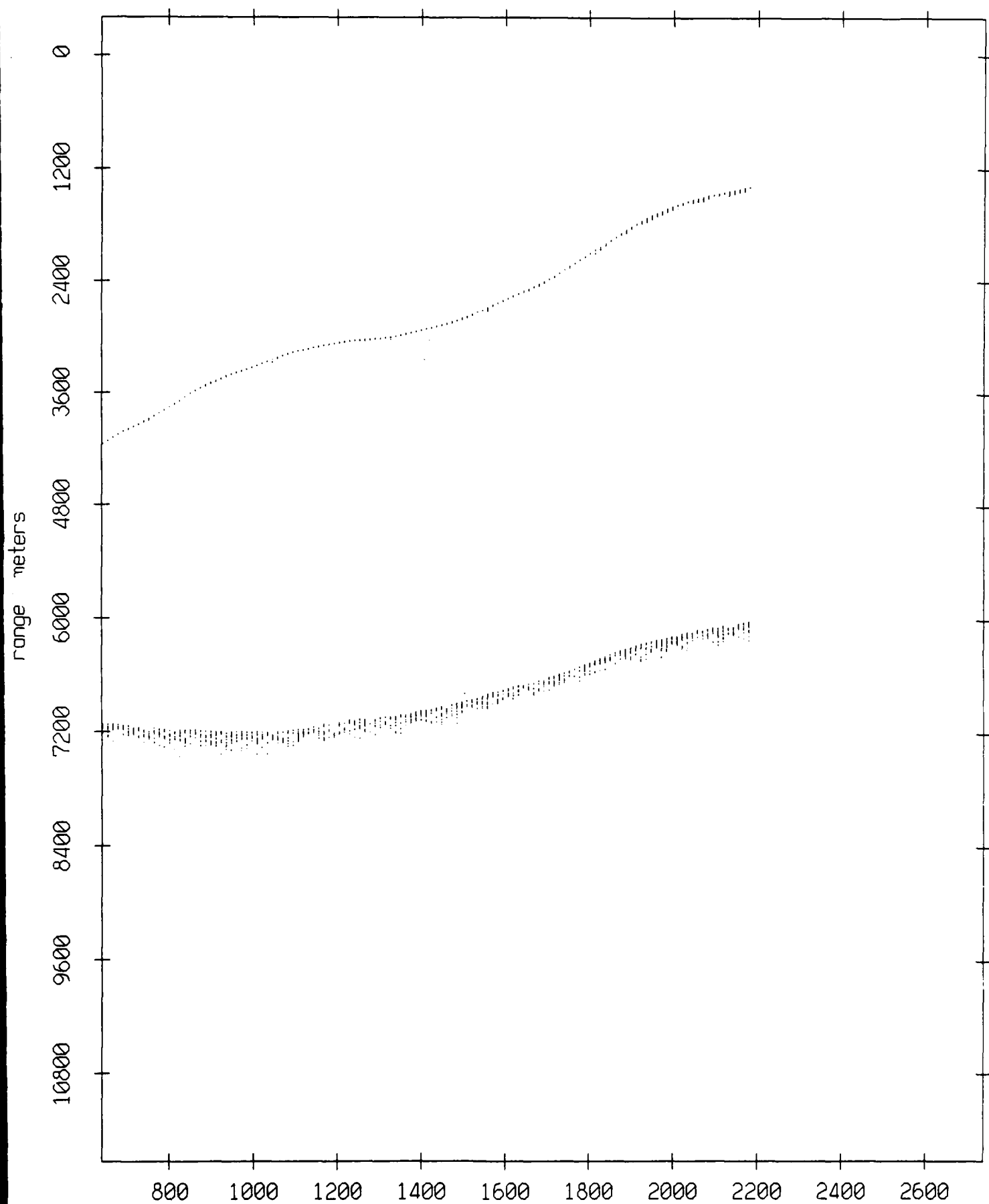
Figure IX.12e

Float 11, July 1989 Trip: range from float 5



record number  
**Figure IX.12f**

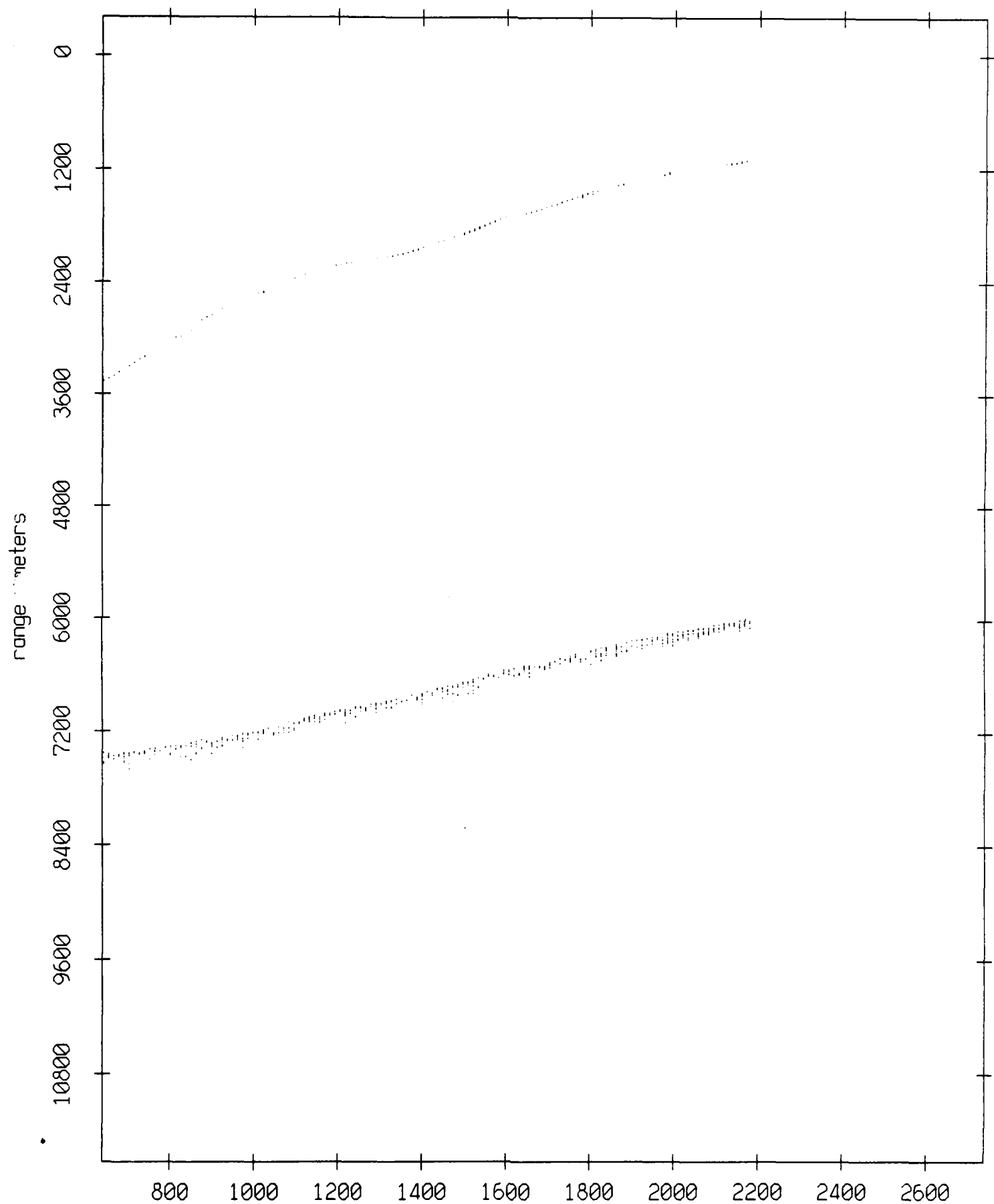
Float 11, July 1989 Trip: range from float 6



record number

Figure IX.12g

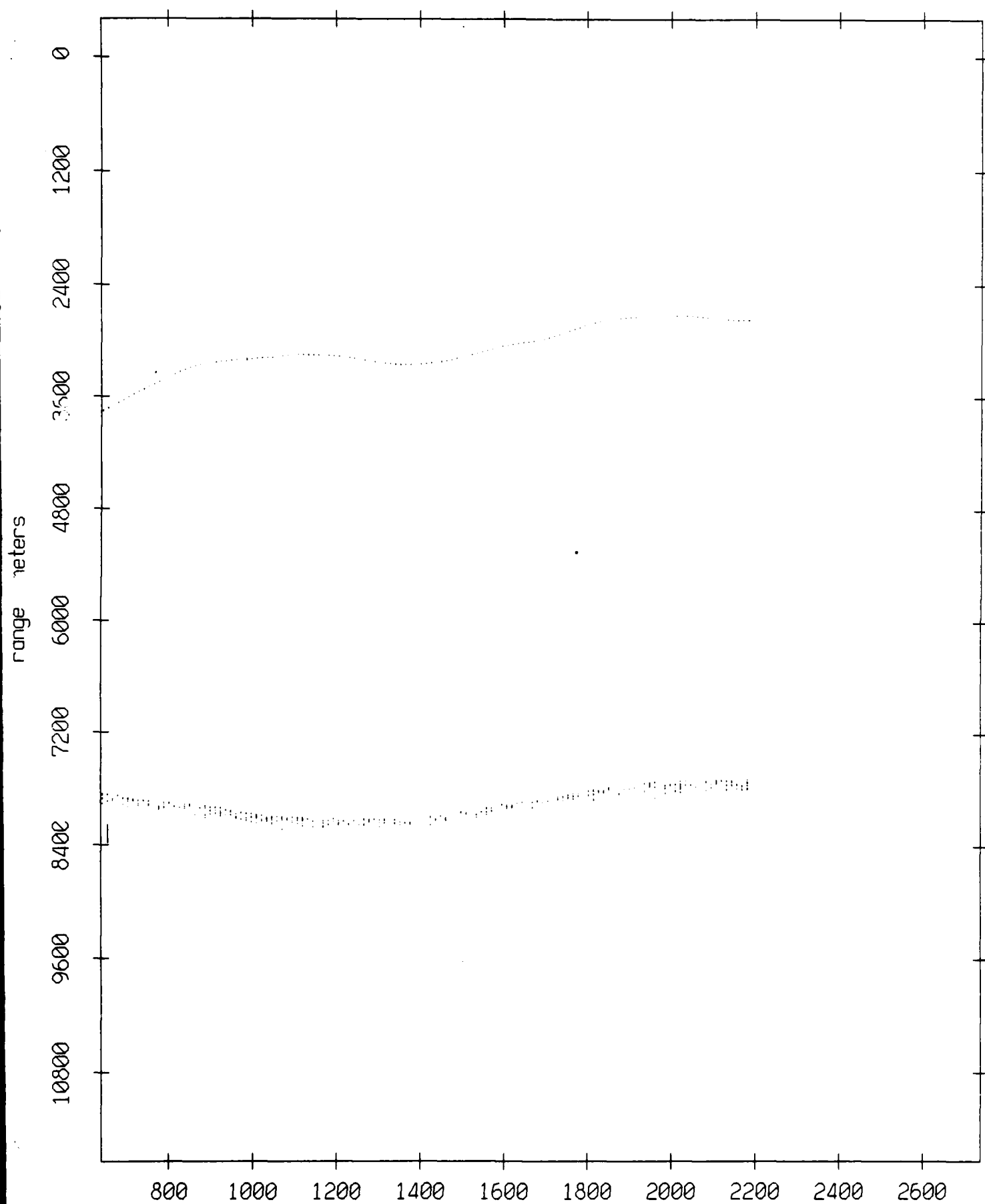
Float 11, July 1989 Trip: range from float 7



record number

Figure IX.12h

Float 11, July 1989 Trip: range from float 8

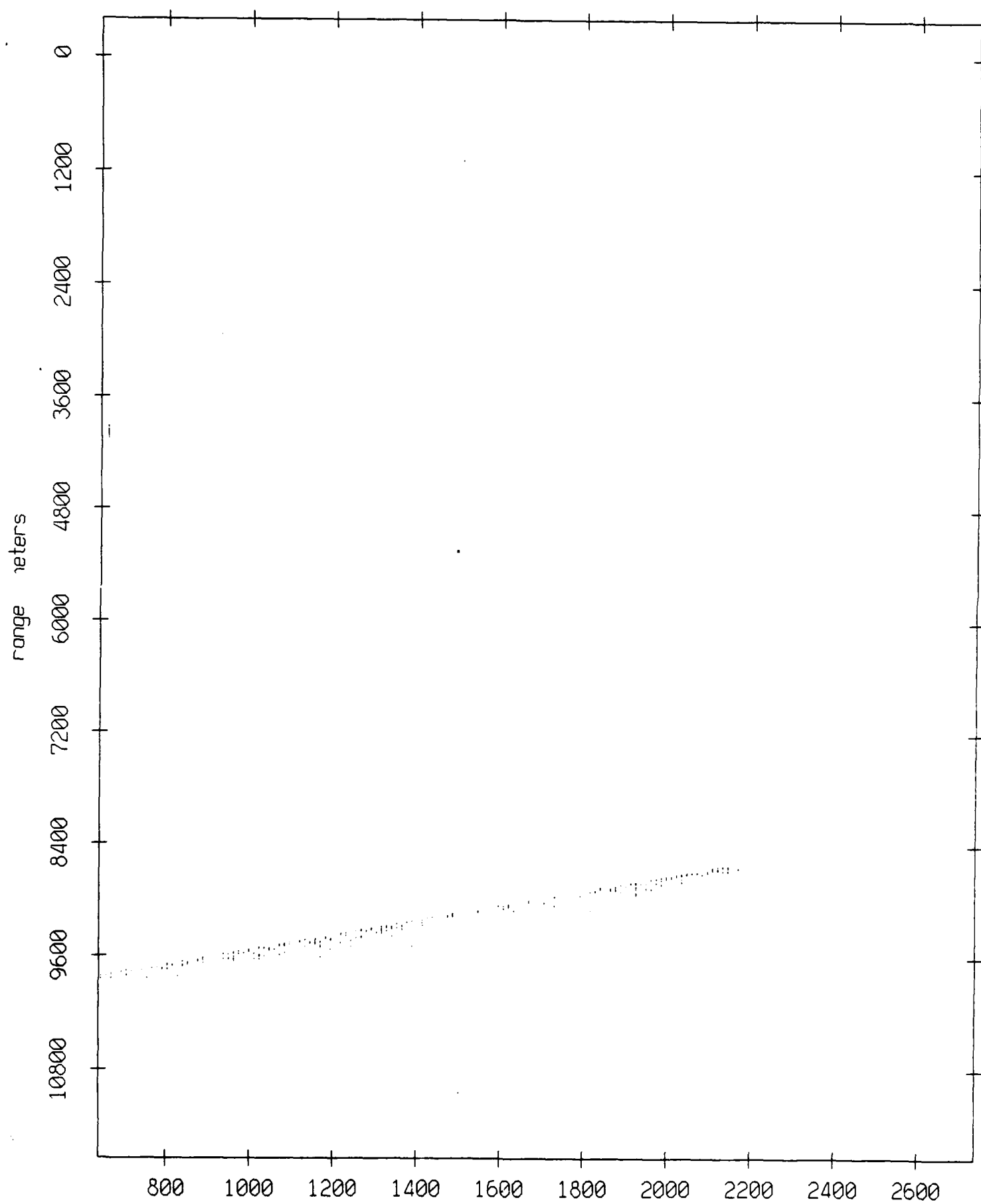


record number

Figure IX.121



Float 11, July 1989 Trip: range from float 9



record number

Figure IX.12j

Float 11, July 1989 Trip: range from float 10

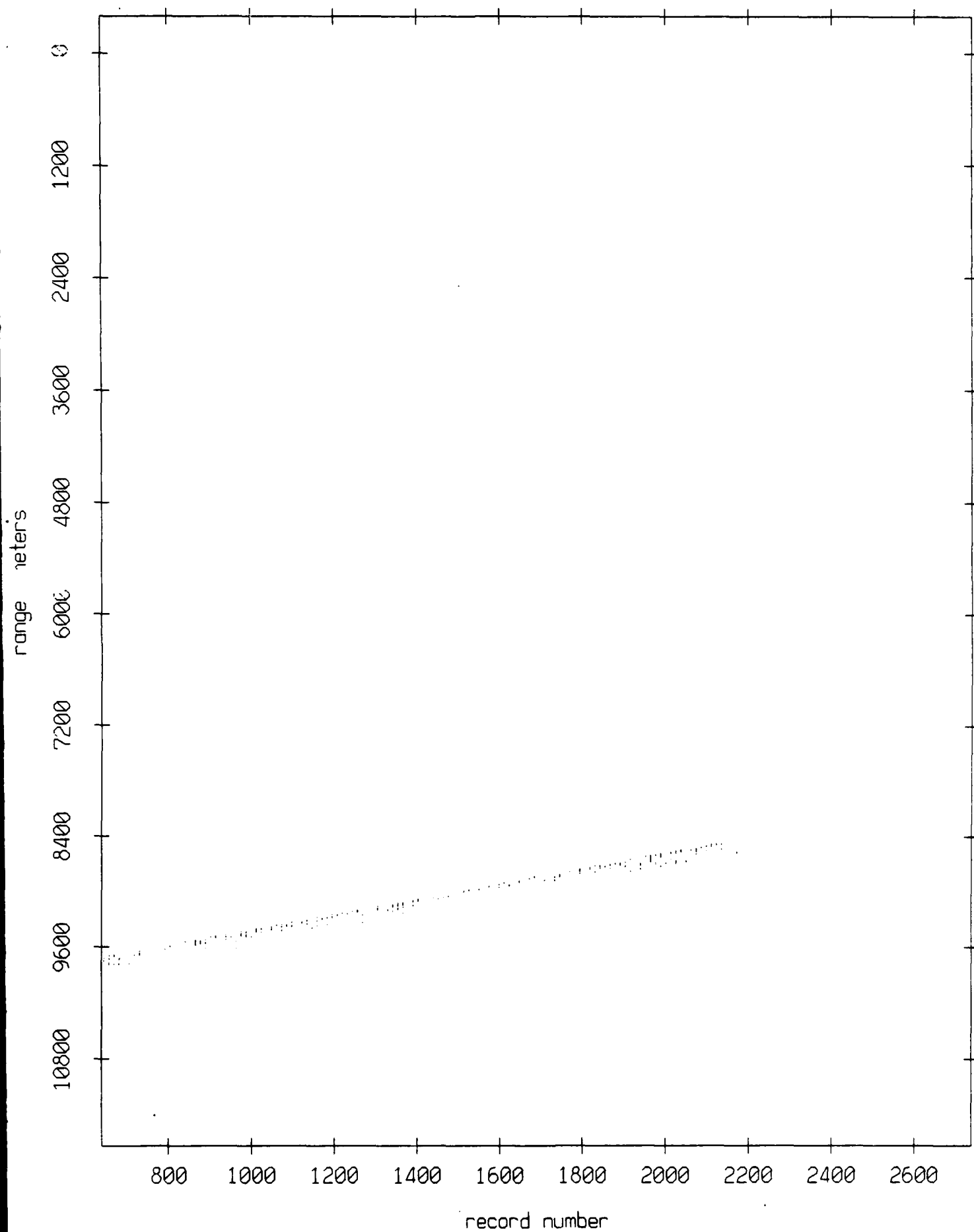


Figure IX.12k

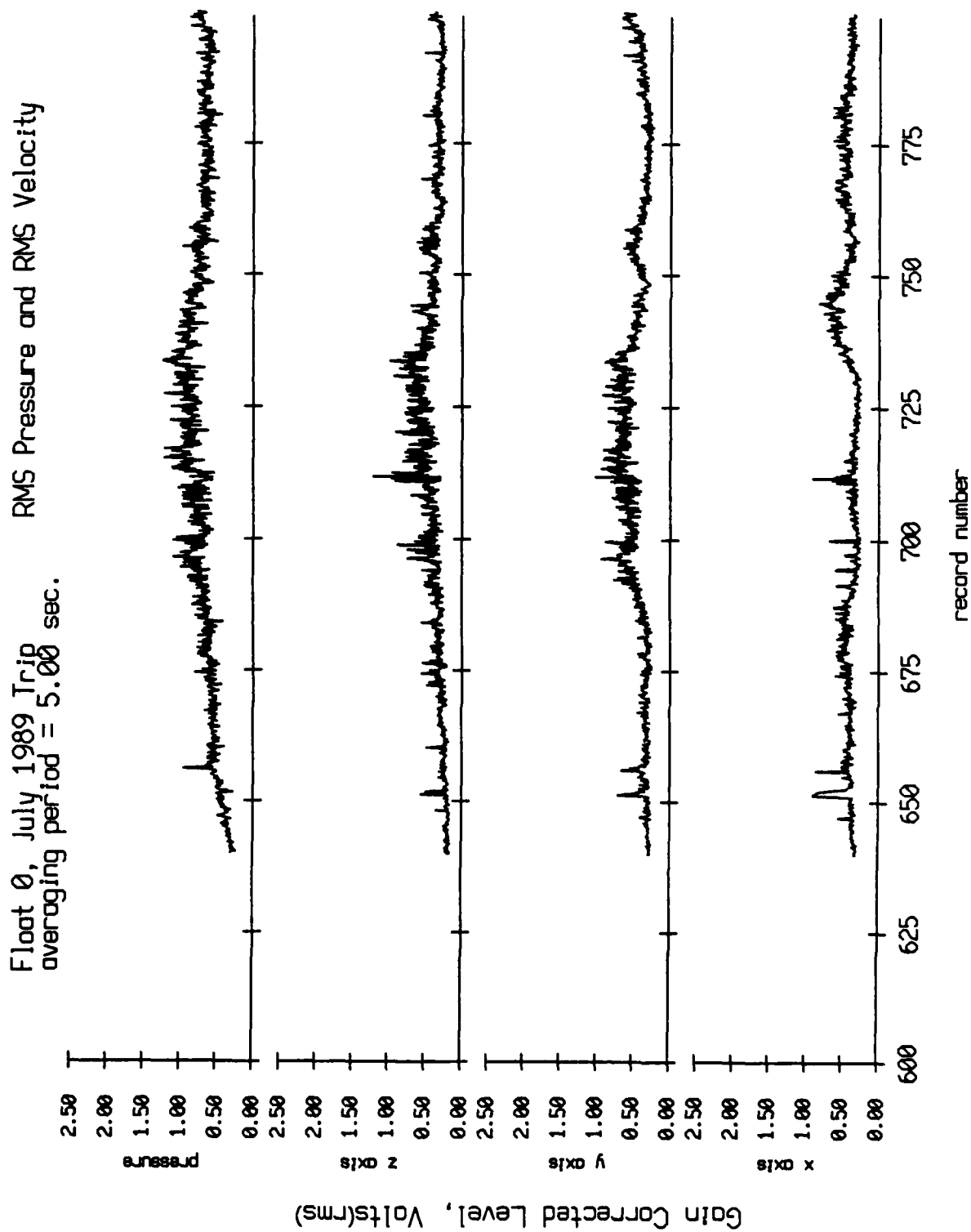


Figure X.1a

Float 0, July 1989 Trip  
 averaging period = 5.00 sec.

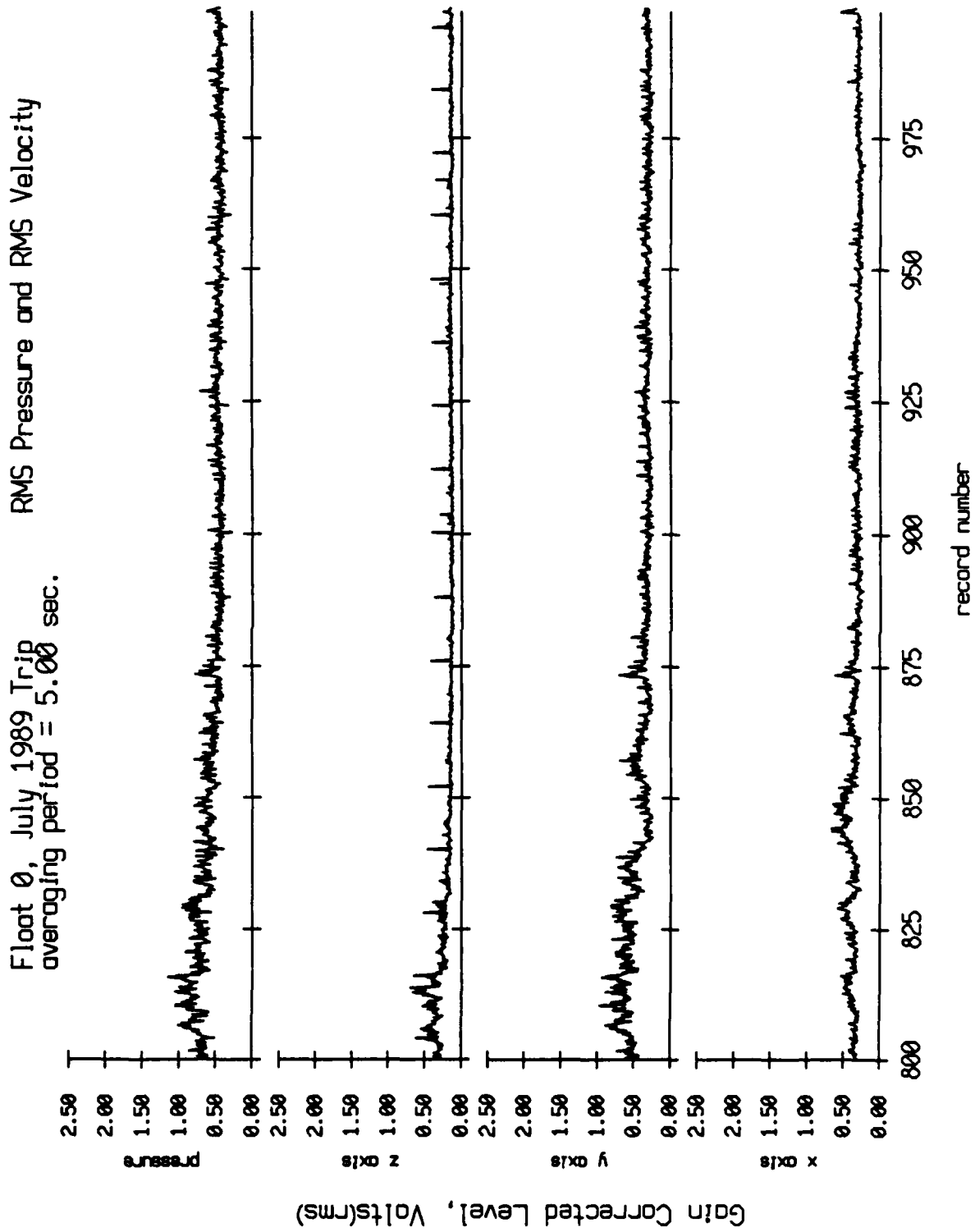


Figure X.1b

Float 0, July 1989 Trip  
 averaging period = 5.00 sec.

RMS Pressure and RMS Velocity

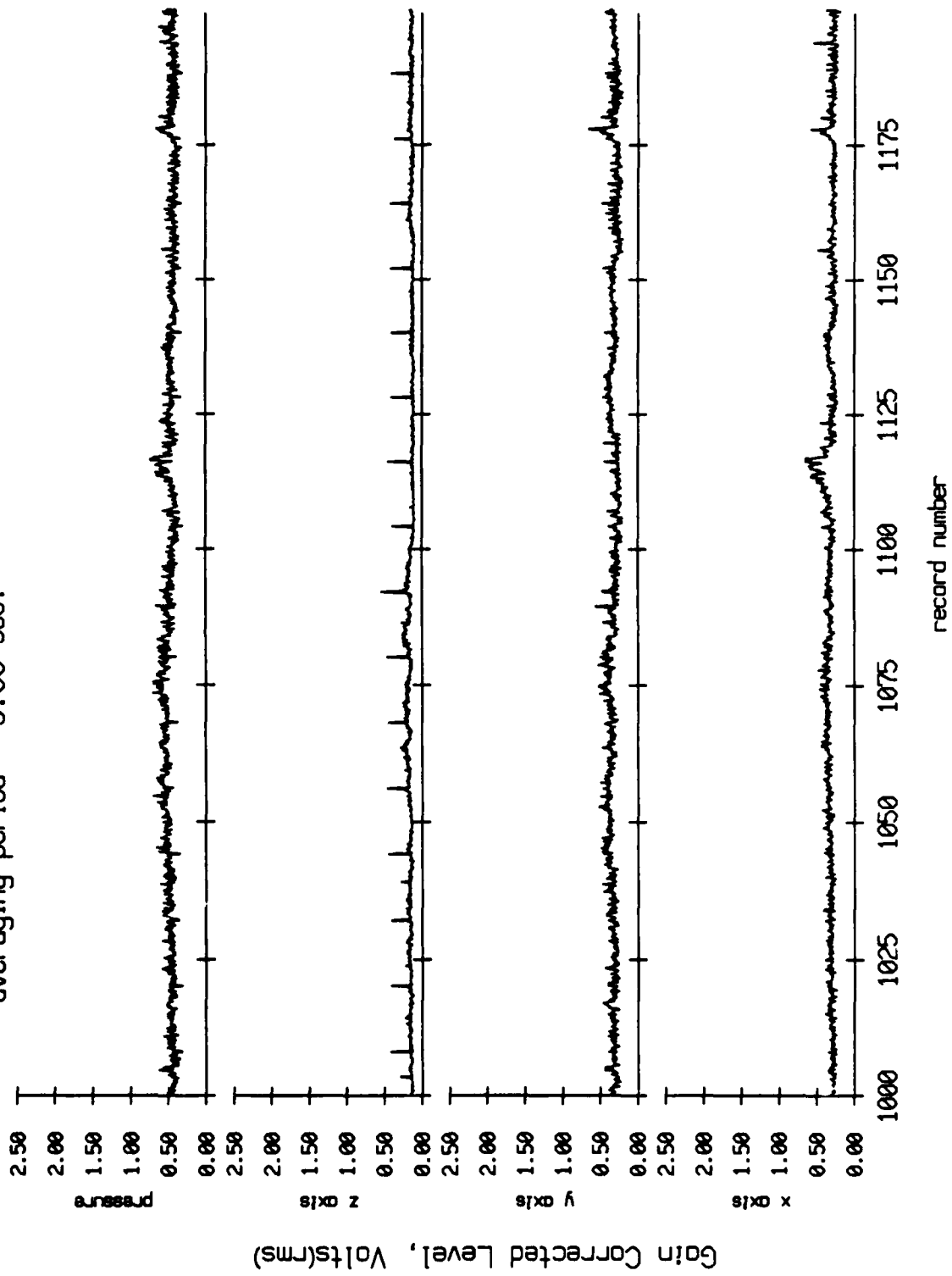


Figure X.1c

Float 0, July 1989 Trip  
 averaging period = 5.00 sec.

RMS Pressure and RMS Velocity

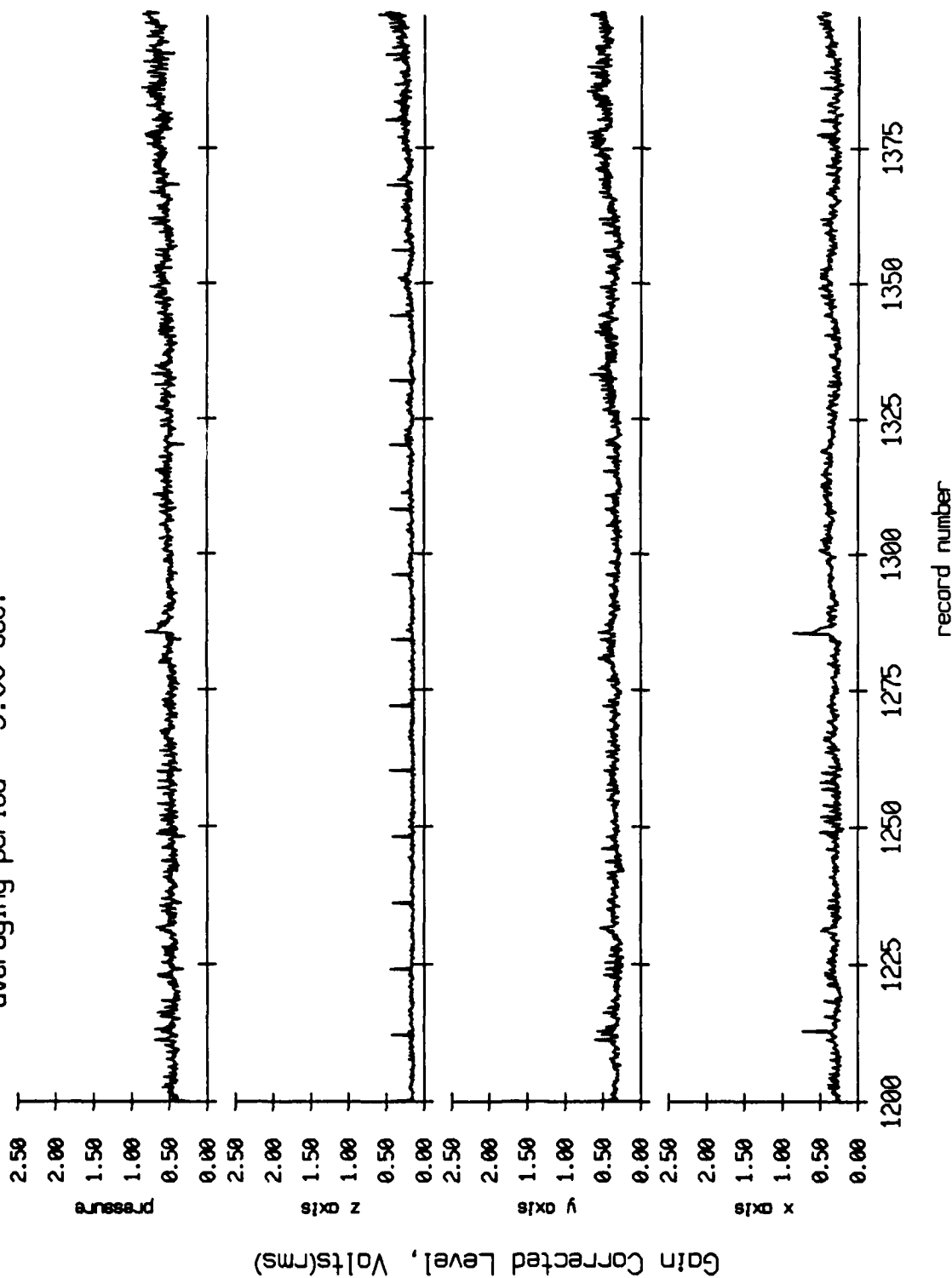


Figure X.1d

Float 0, July 1989 Trip  
 averaging period = 5.00 sec.

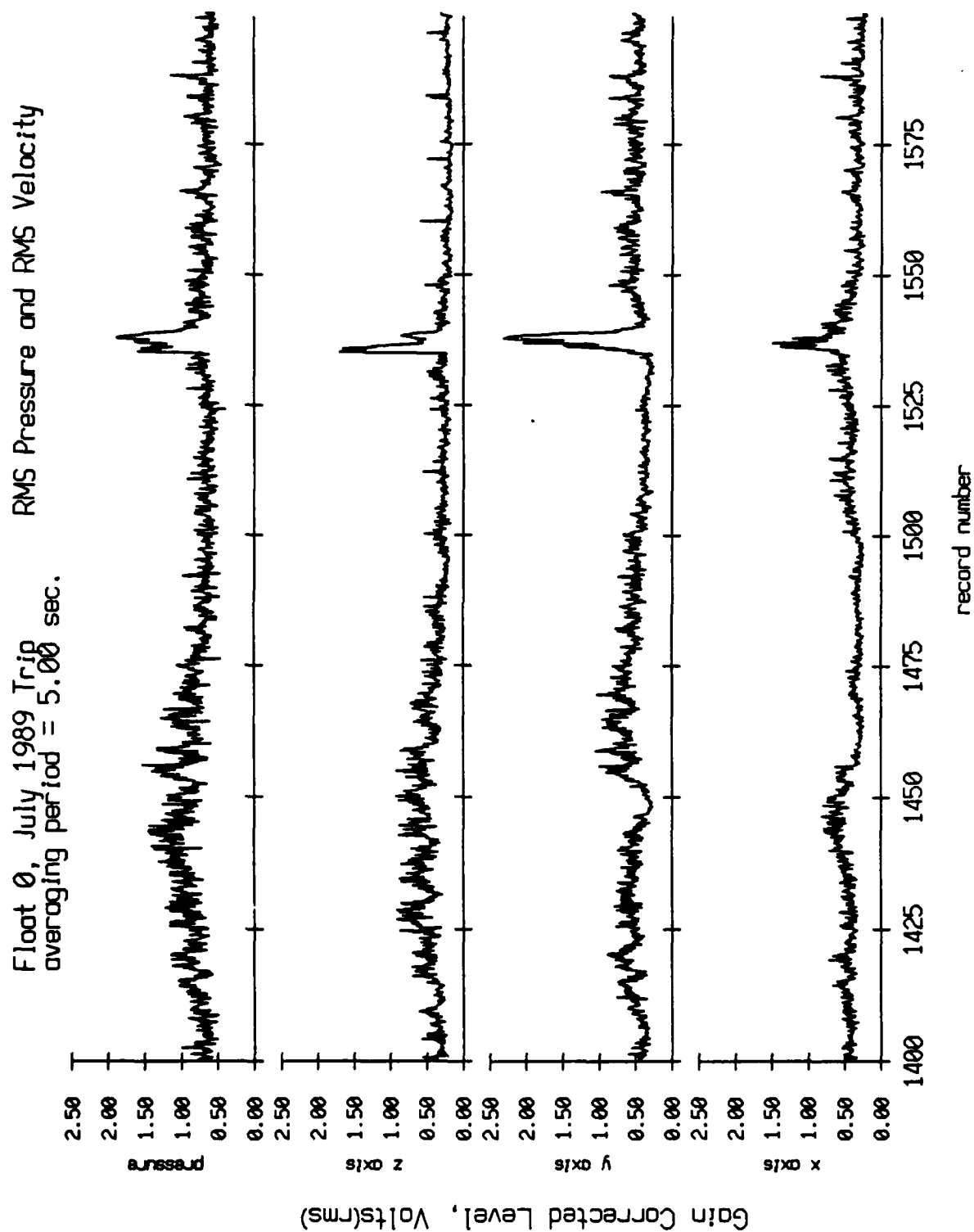


Figure X.1e

Float 0, July 1989 Trip  
 averaging period = 5.00 sec.

RMS Pressure and RMS Velocity

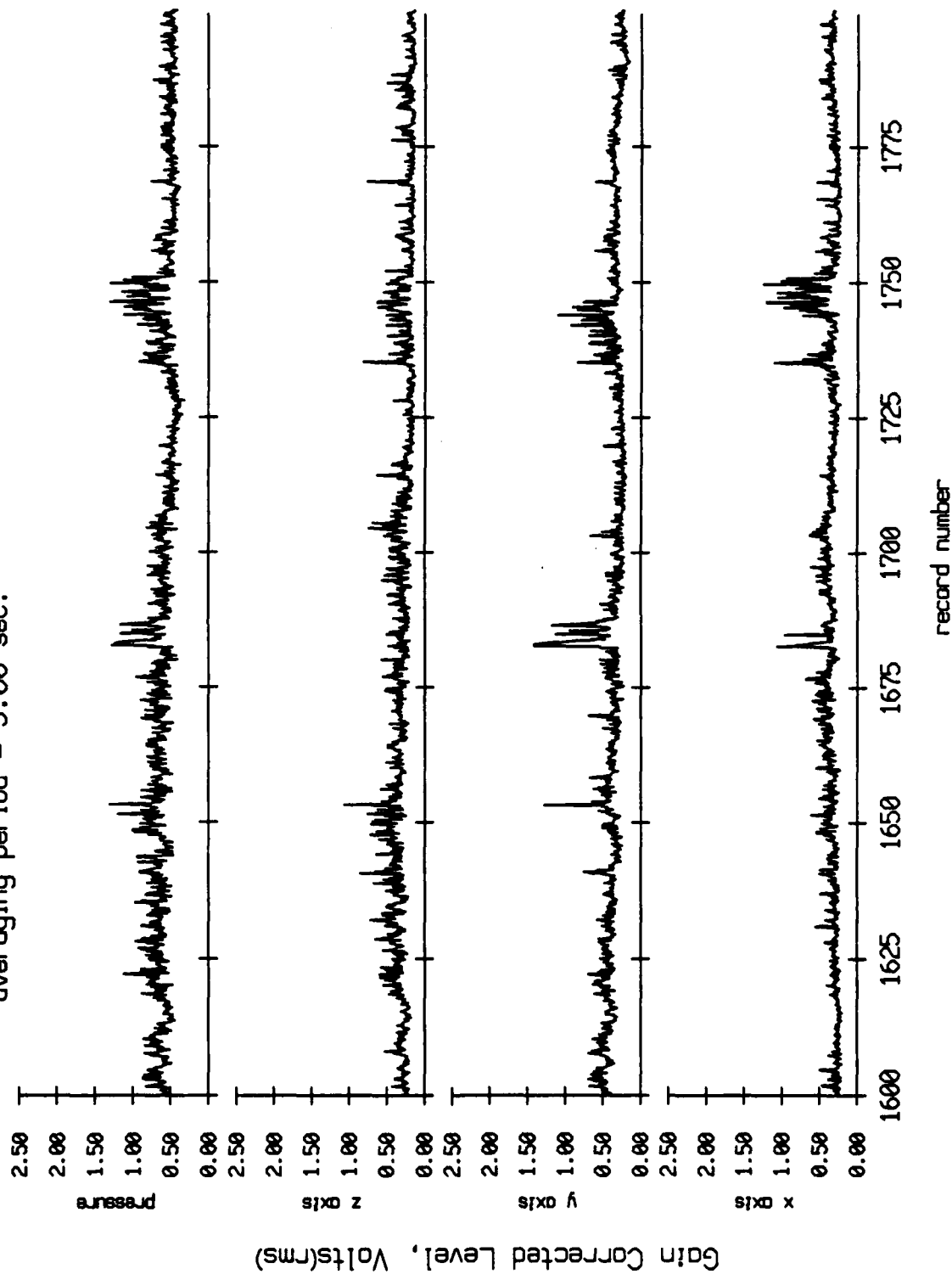


Figure X.1f



# Float 0, July 1989 Trip averaging period = 5.00 sec.

## RMS Pressure and RMS Velocity

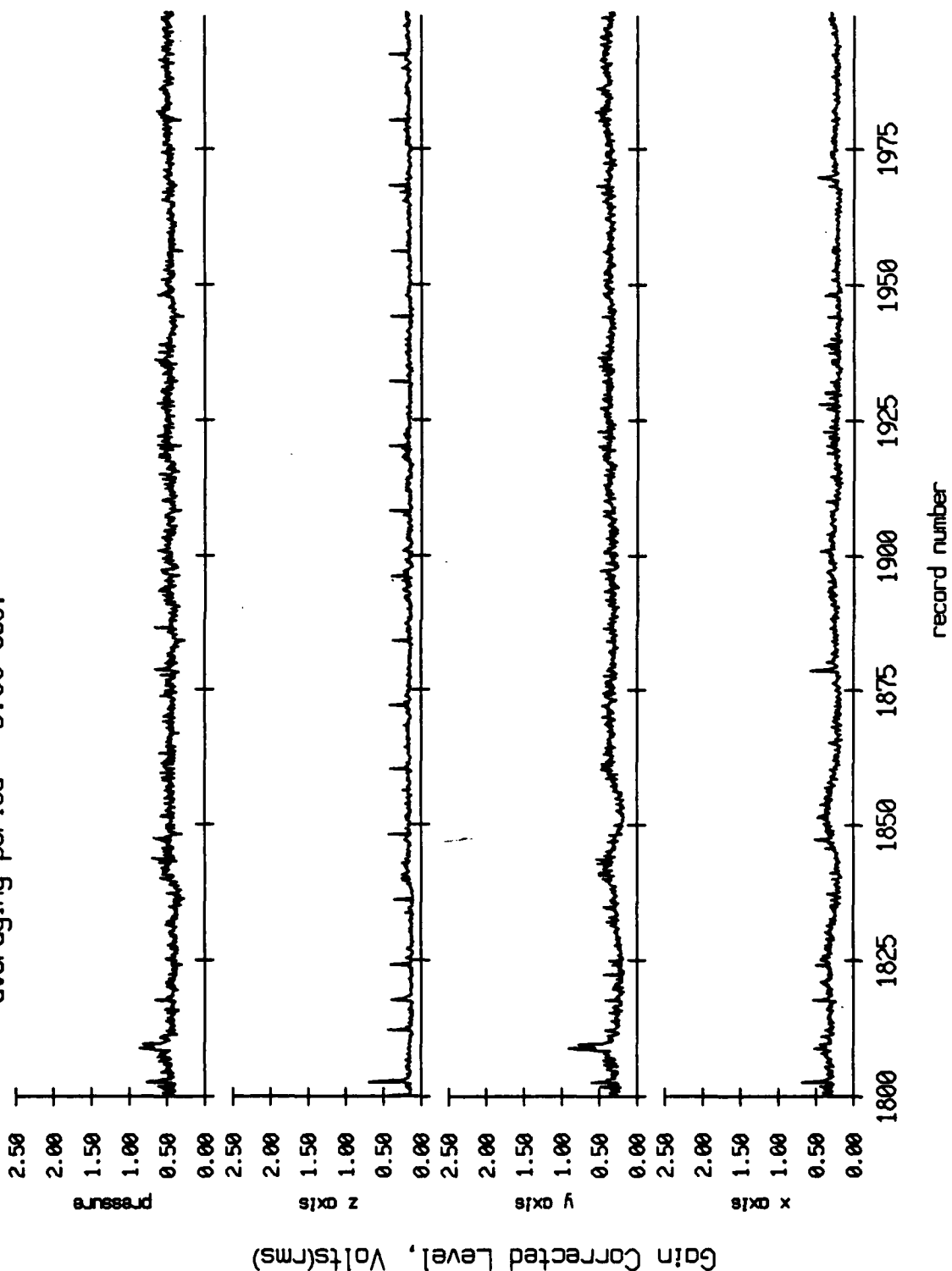


Figure X.1g

Float 0, July 1989 Trip  
 averaging period = 5.00 sec.

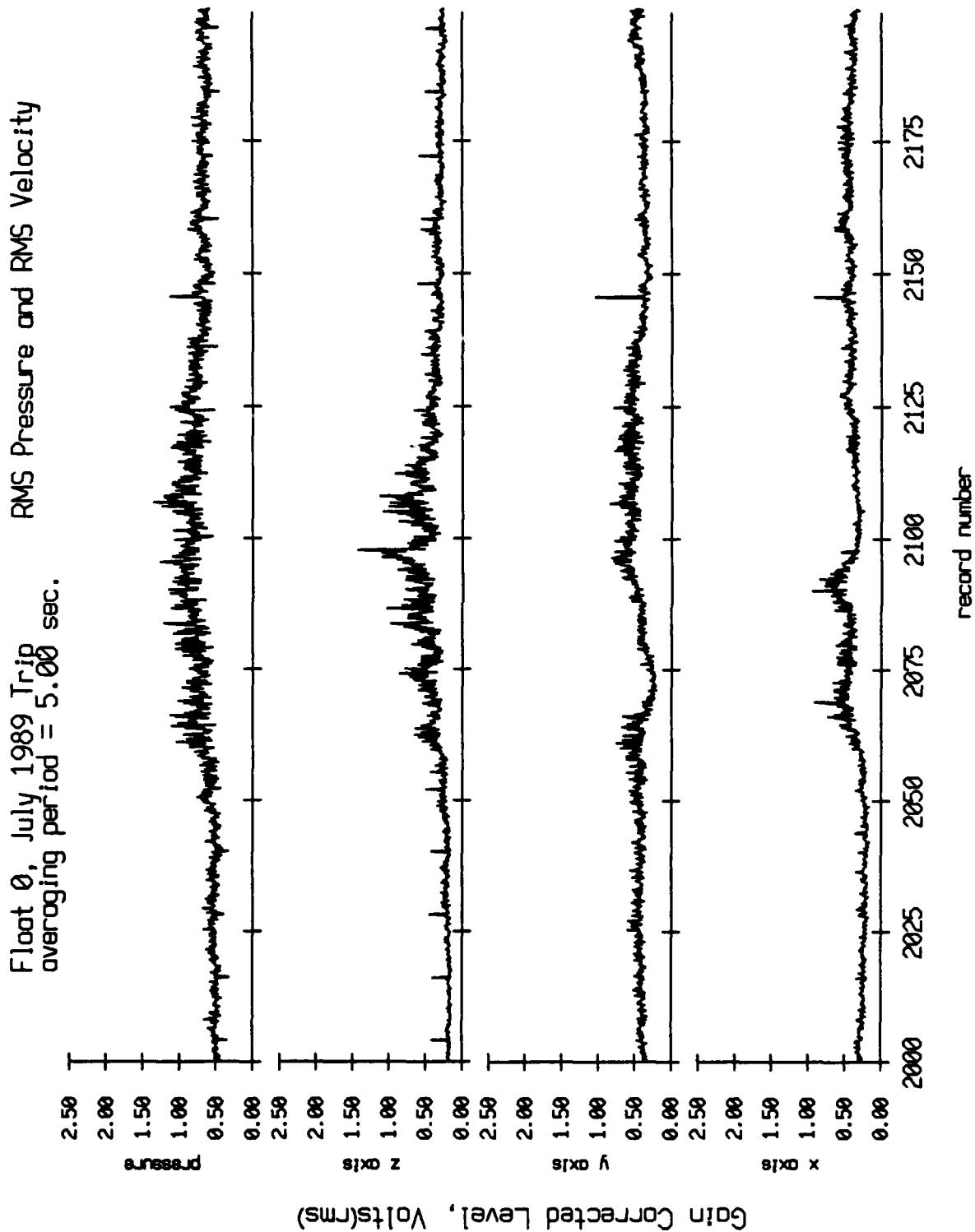


Figure X.1h

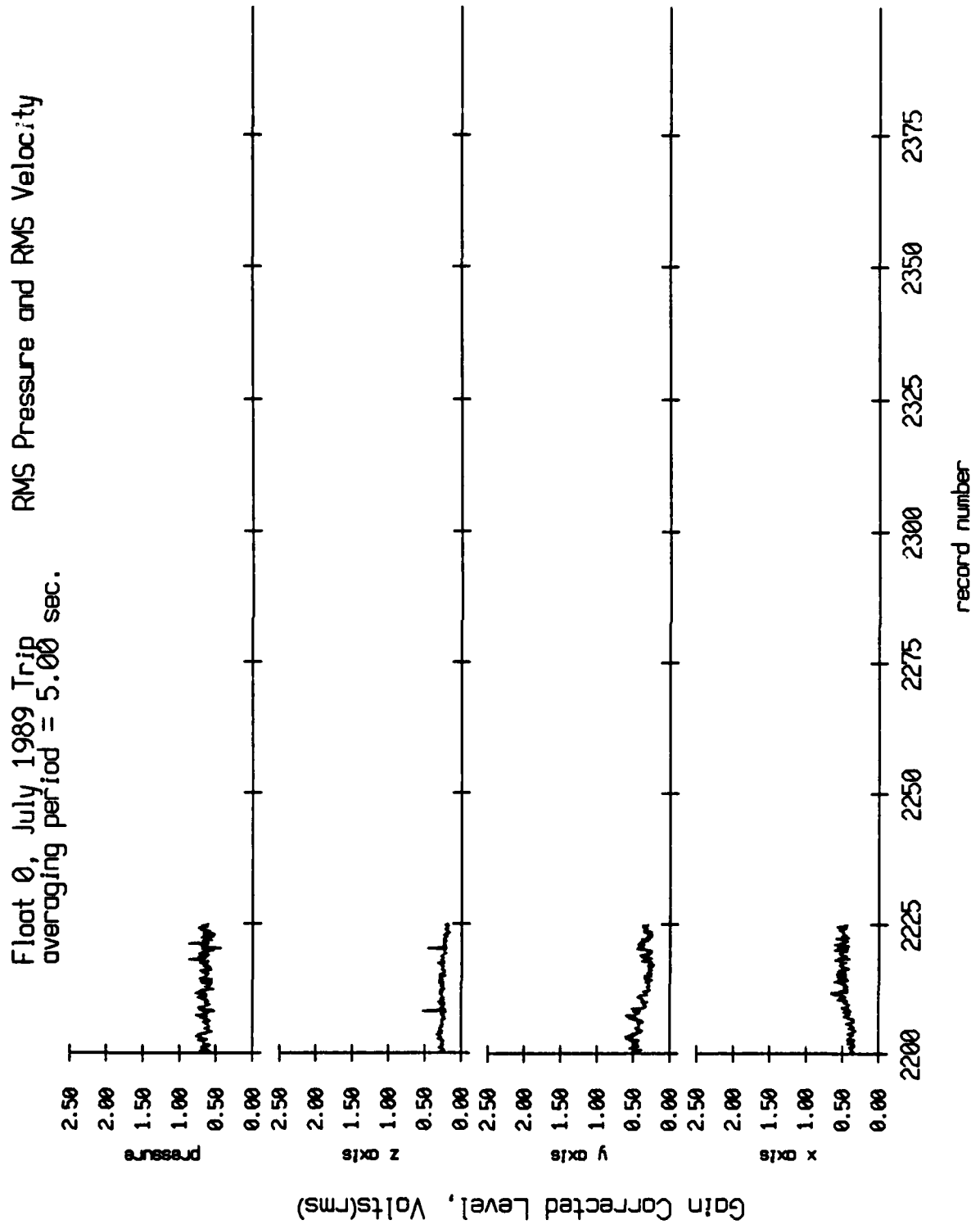


Figure X.11

Float 1, July 1989 Trip  
 averaging period = 5.00 sec.

RMS Pressure and RMS Velocity

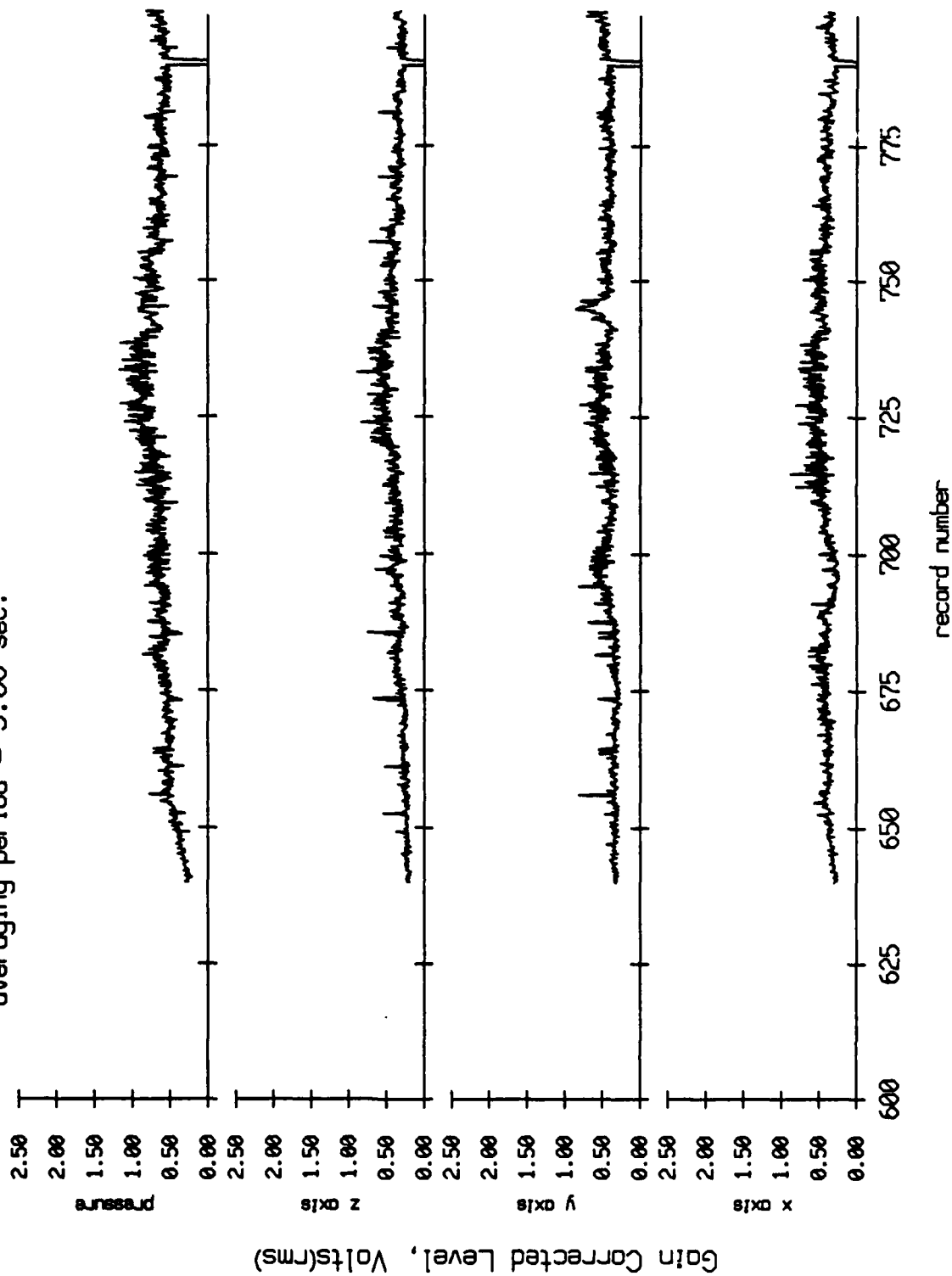


Figure X.2a

Float 1, July 1989 Trip  
 averaging period = 5.00 sec.

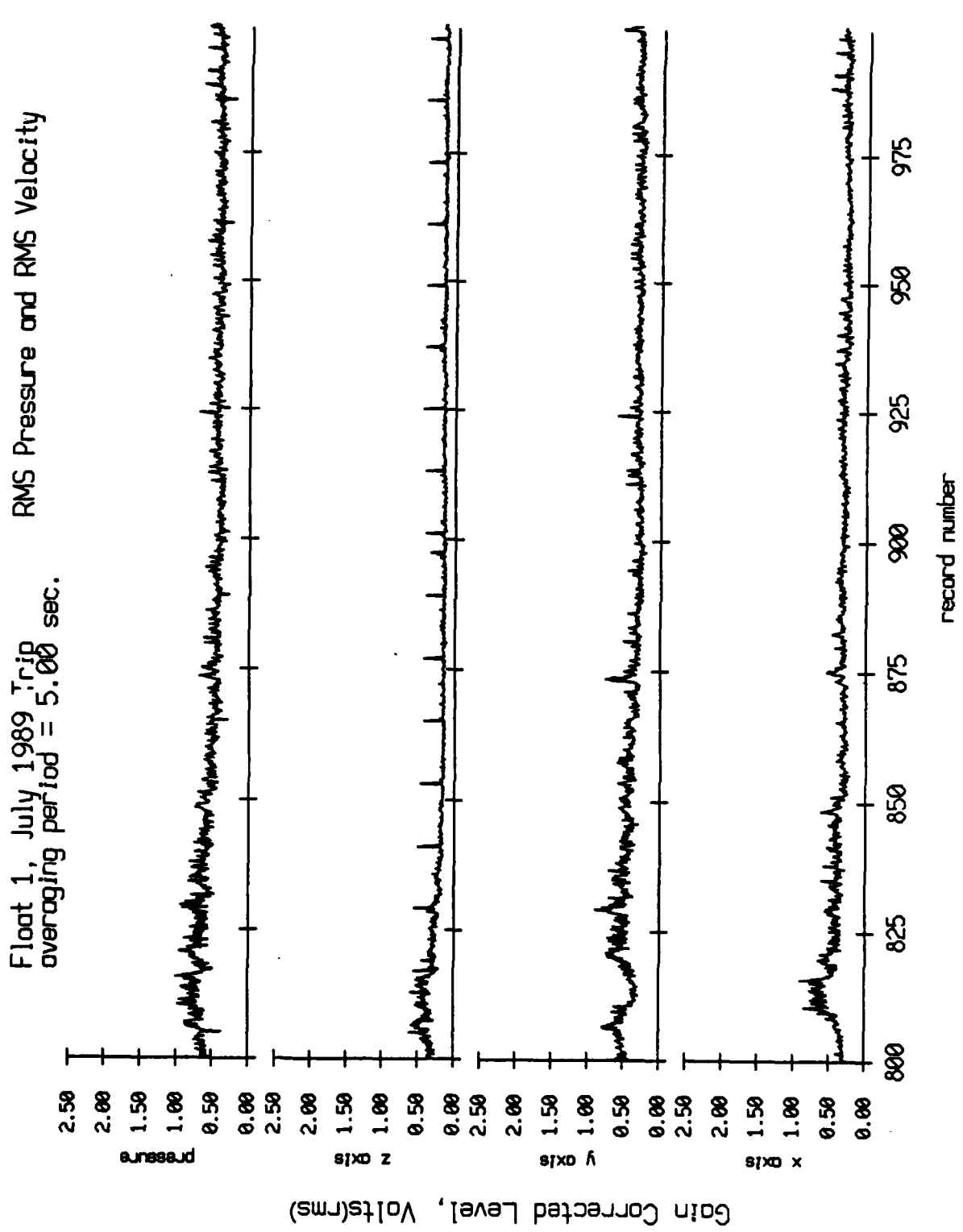


Figure X.2b

Float 1, July 1989 Trip  
 averaging period = 5.00 sec.

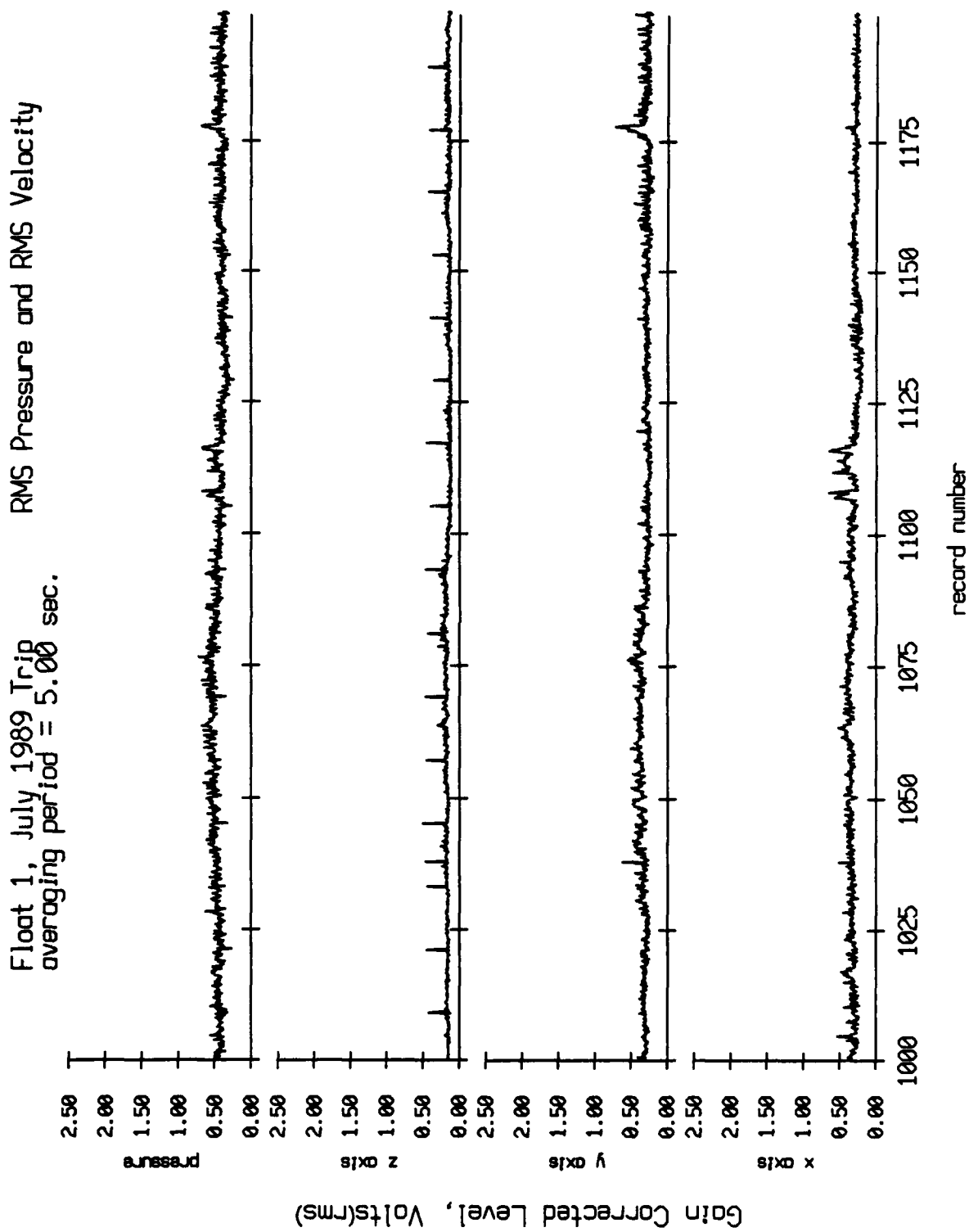


Figure X.2c

Float 1, July 1989 Trip  
 averaging period = 5.00 sec.

RMS Pressure and RMS Velocity

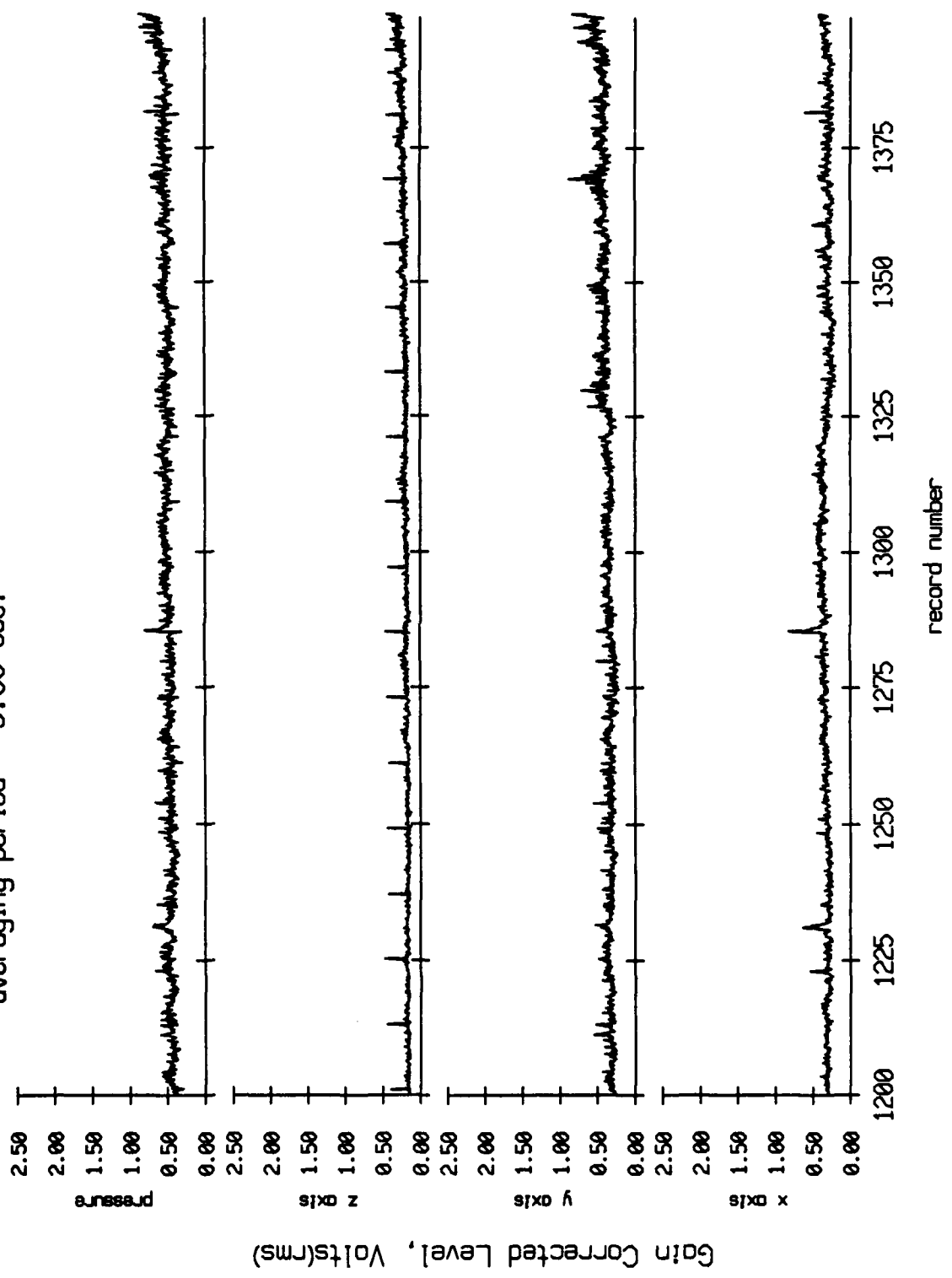


Figure X.2d

# Float 1, July 1989 Trip averaging period = 5.00 sec.

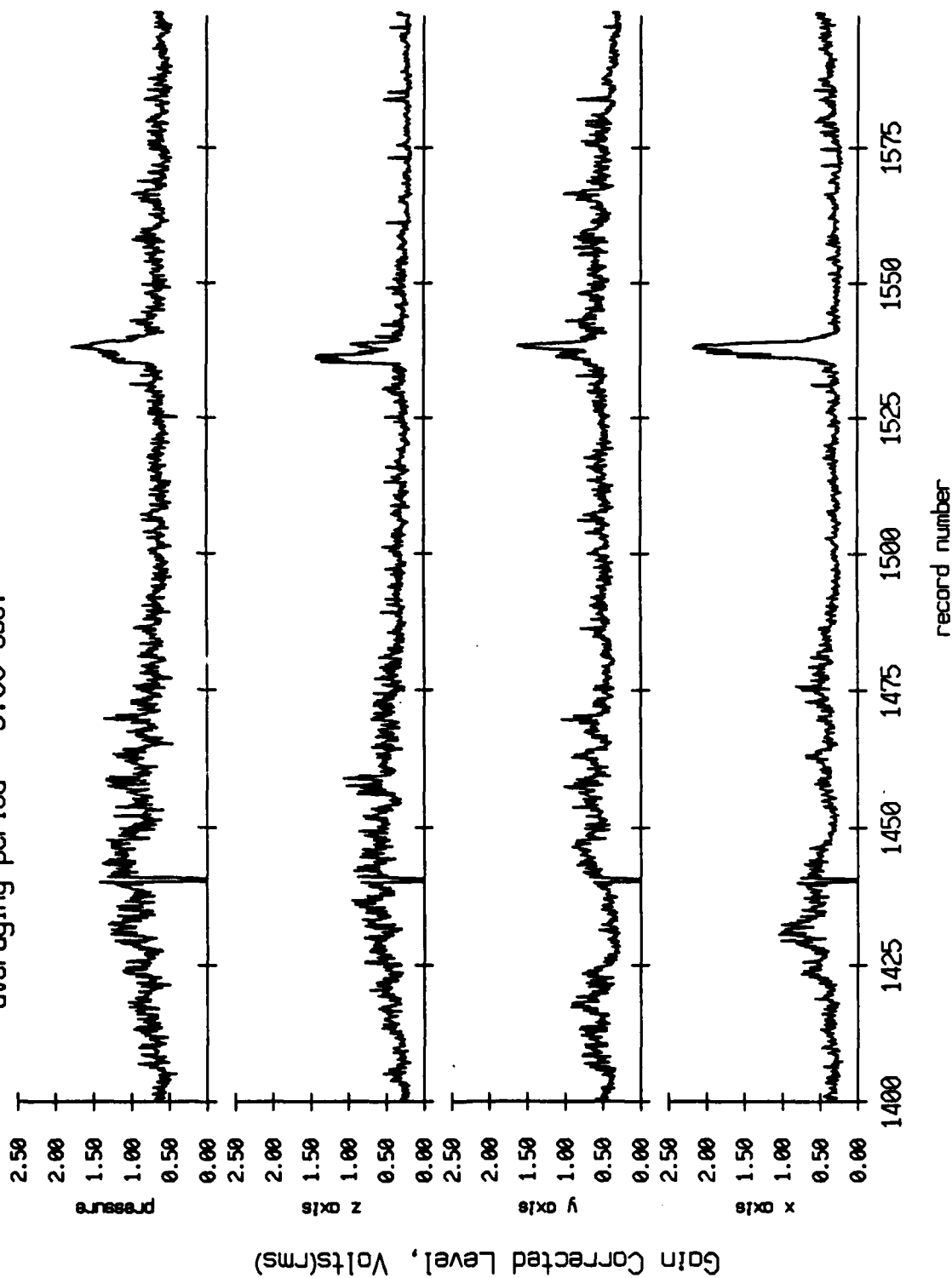


Figure X.2e



Float 1, July 1989 Trip  
 averaging period = 5.00 sec.  
 RMS Pressure and RMS Velocity

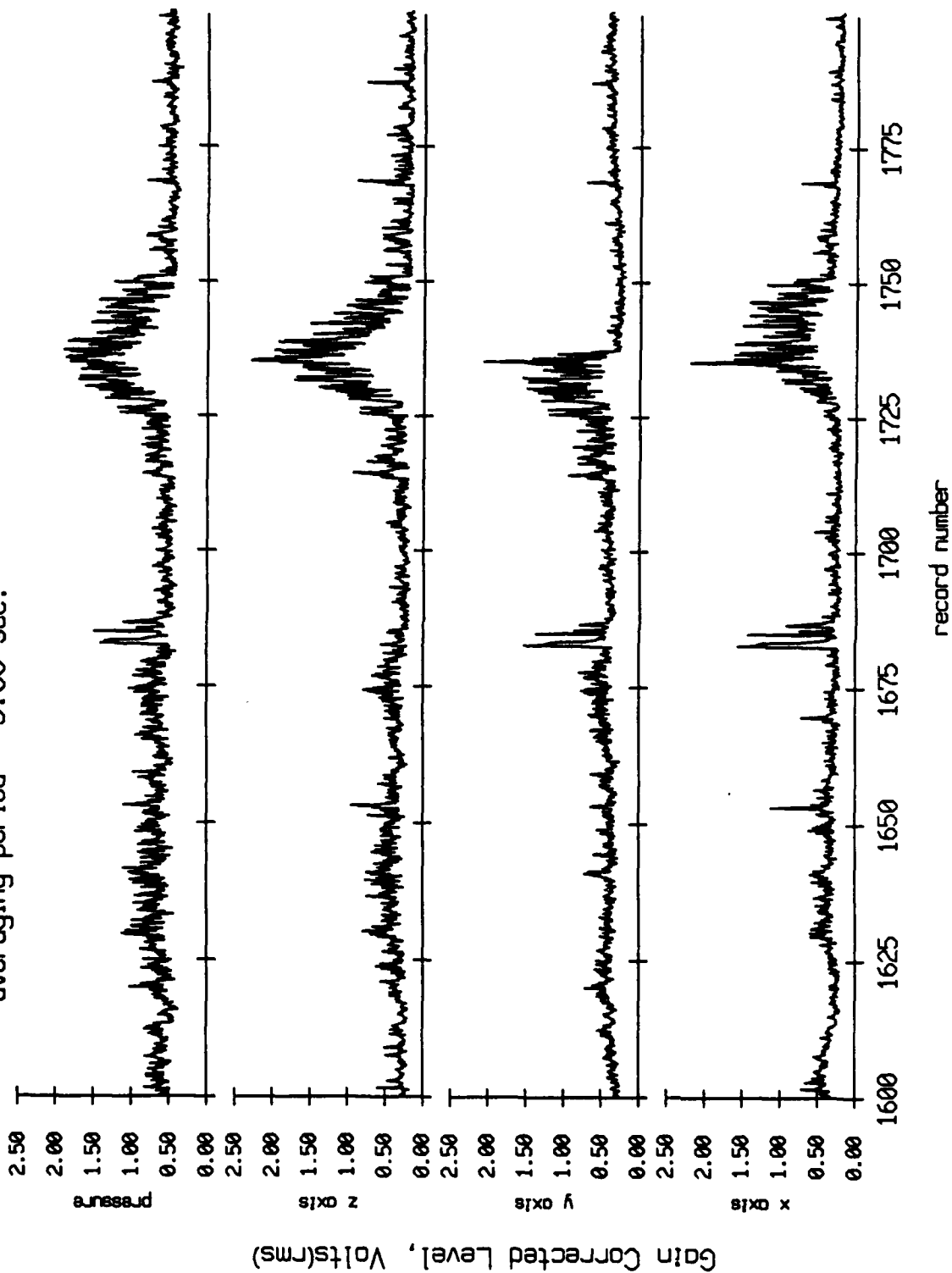


Figure X.2f

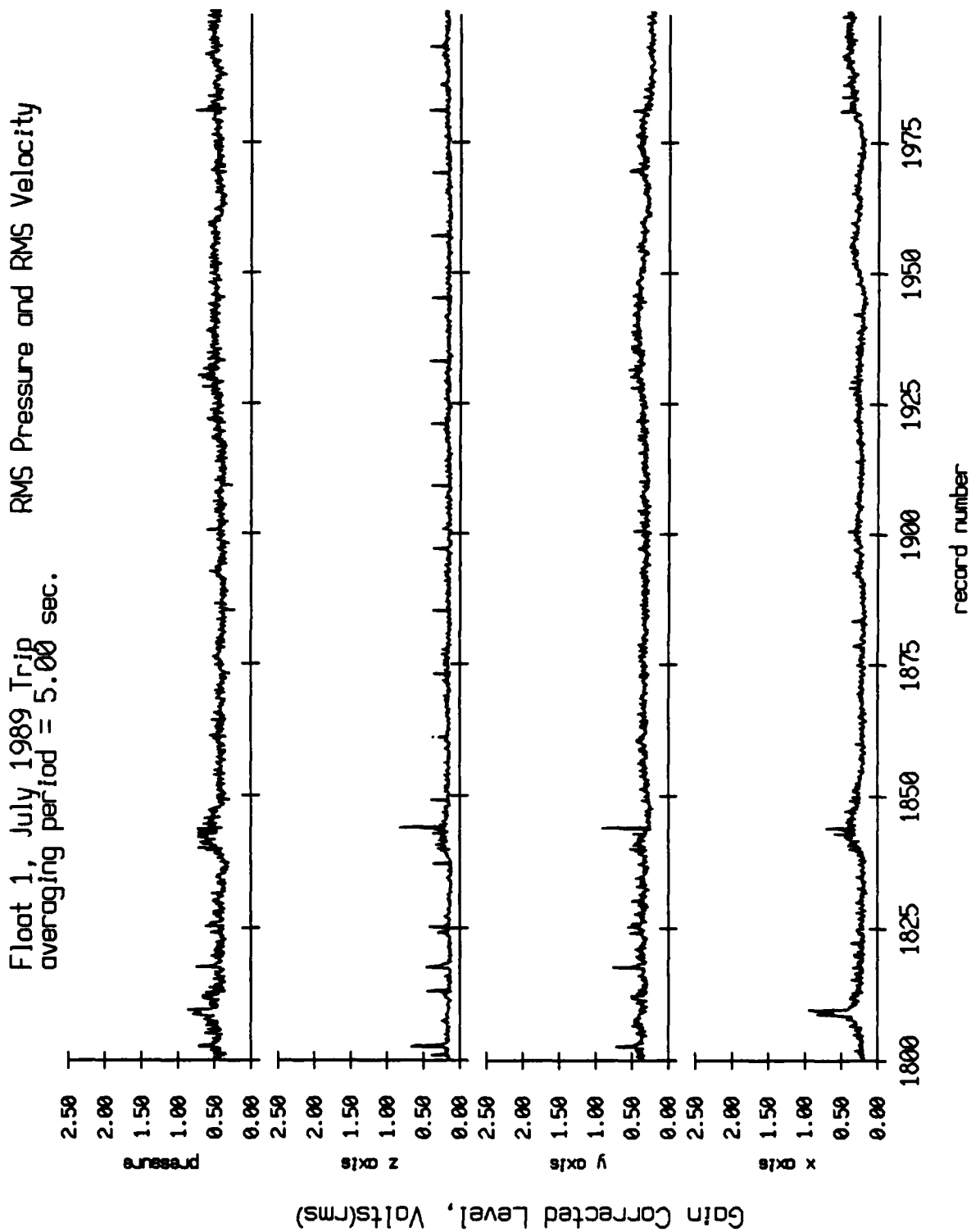


Figure X.2g

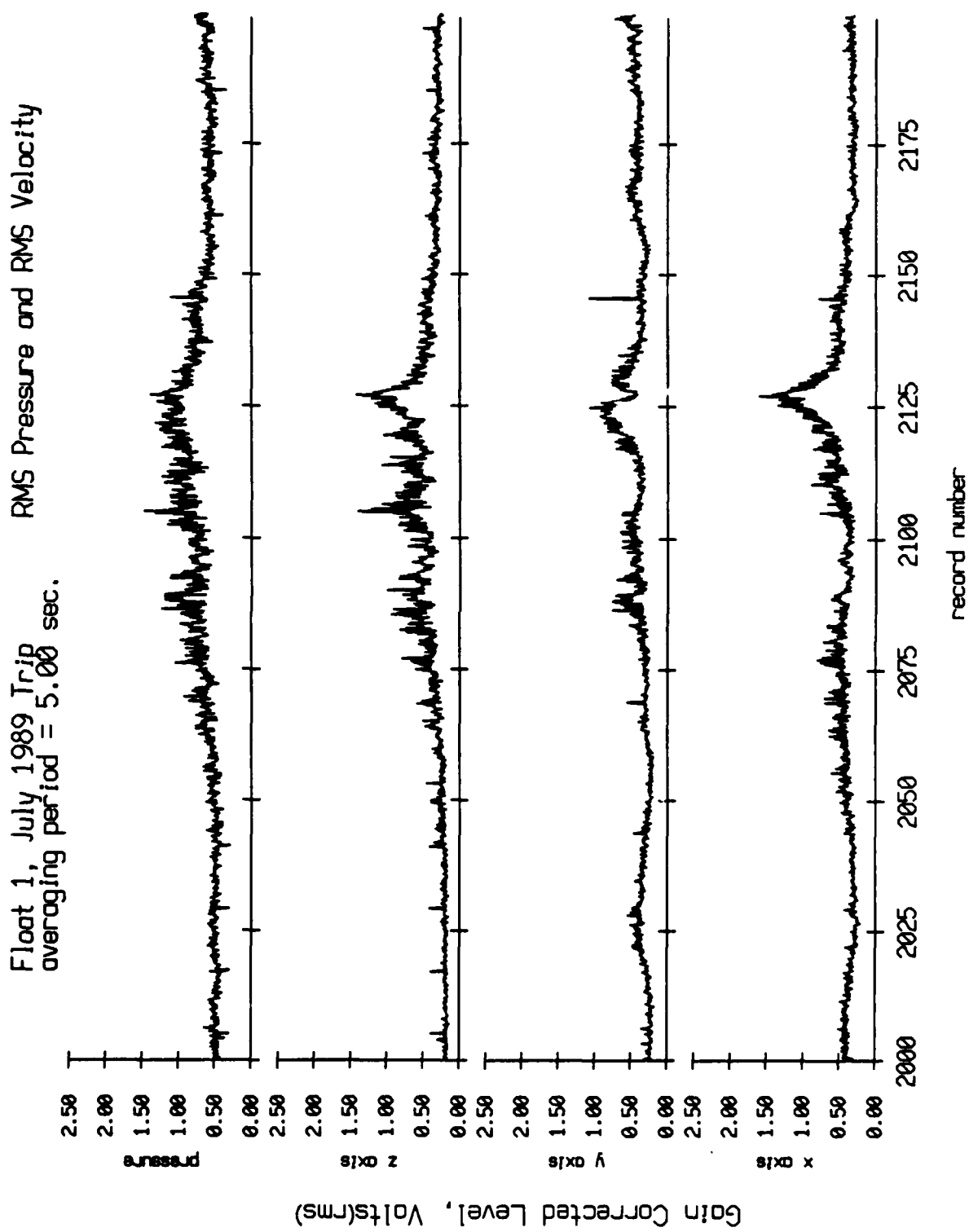


Figure X.2h

Float 1, July 1989 Trip  
 averaging period = 5.00 sec.

RMS Pressure and RMS Velocity

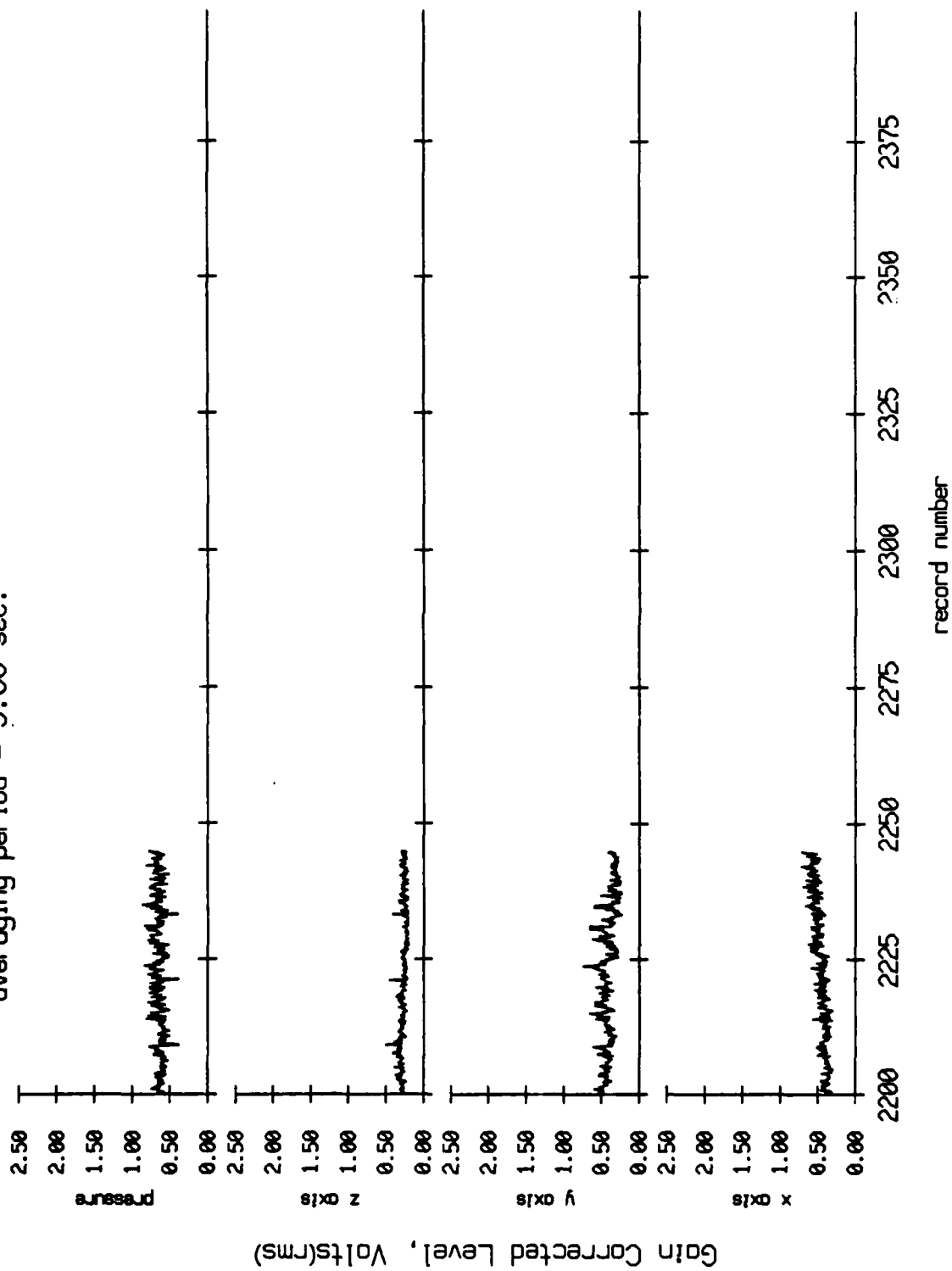


Figure X.21

# Float 2, July 1989 Trip averaging period = 5.00 sec. RMS Pressure and RMS Velocity

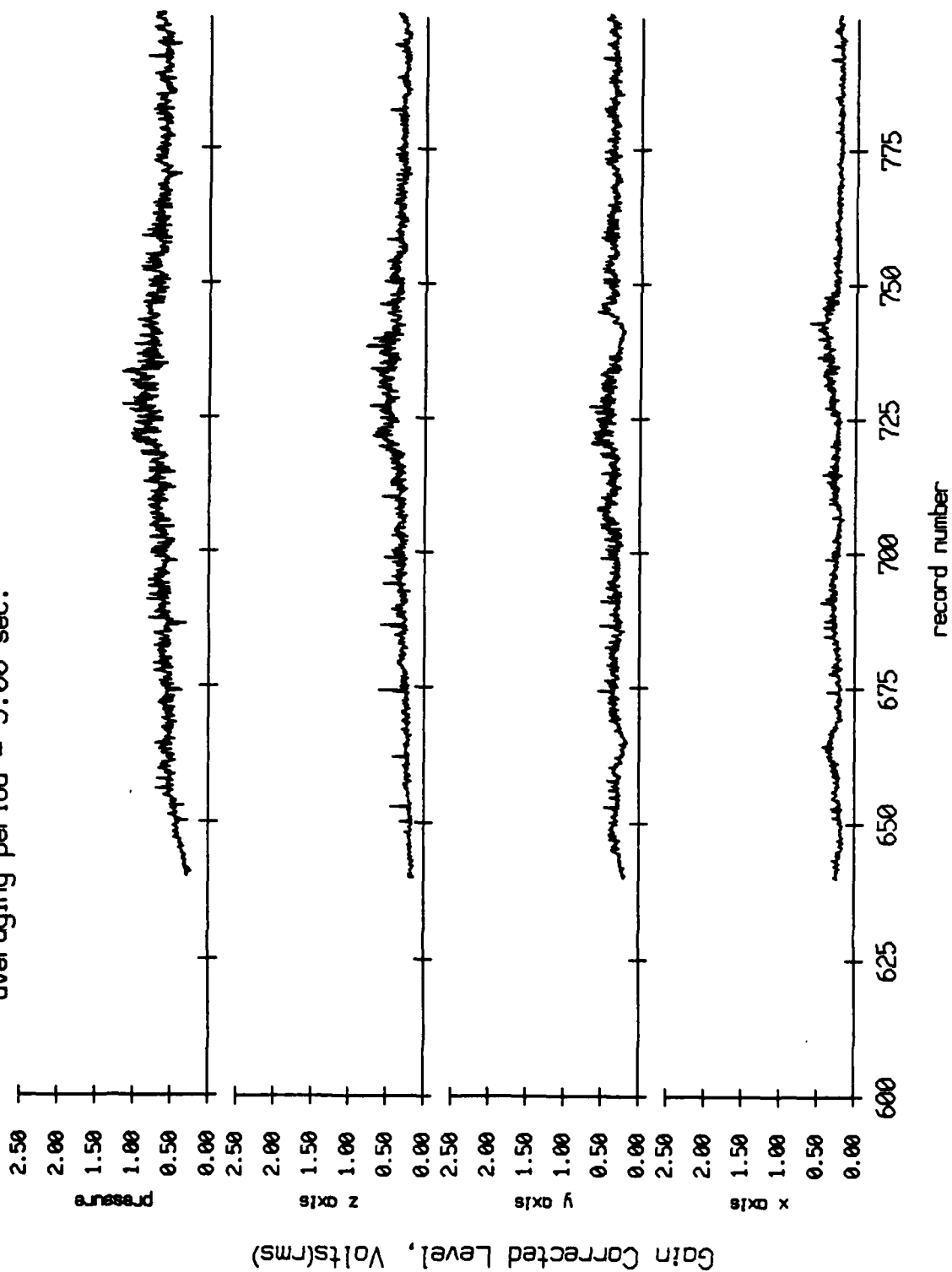


Figure X.3a

Float 2, July 1989 Trip  
 averaging period = 5.00 sec.

RMS Pressure and RMS Velocity

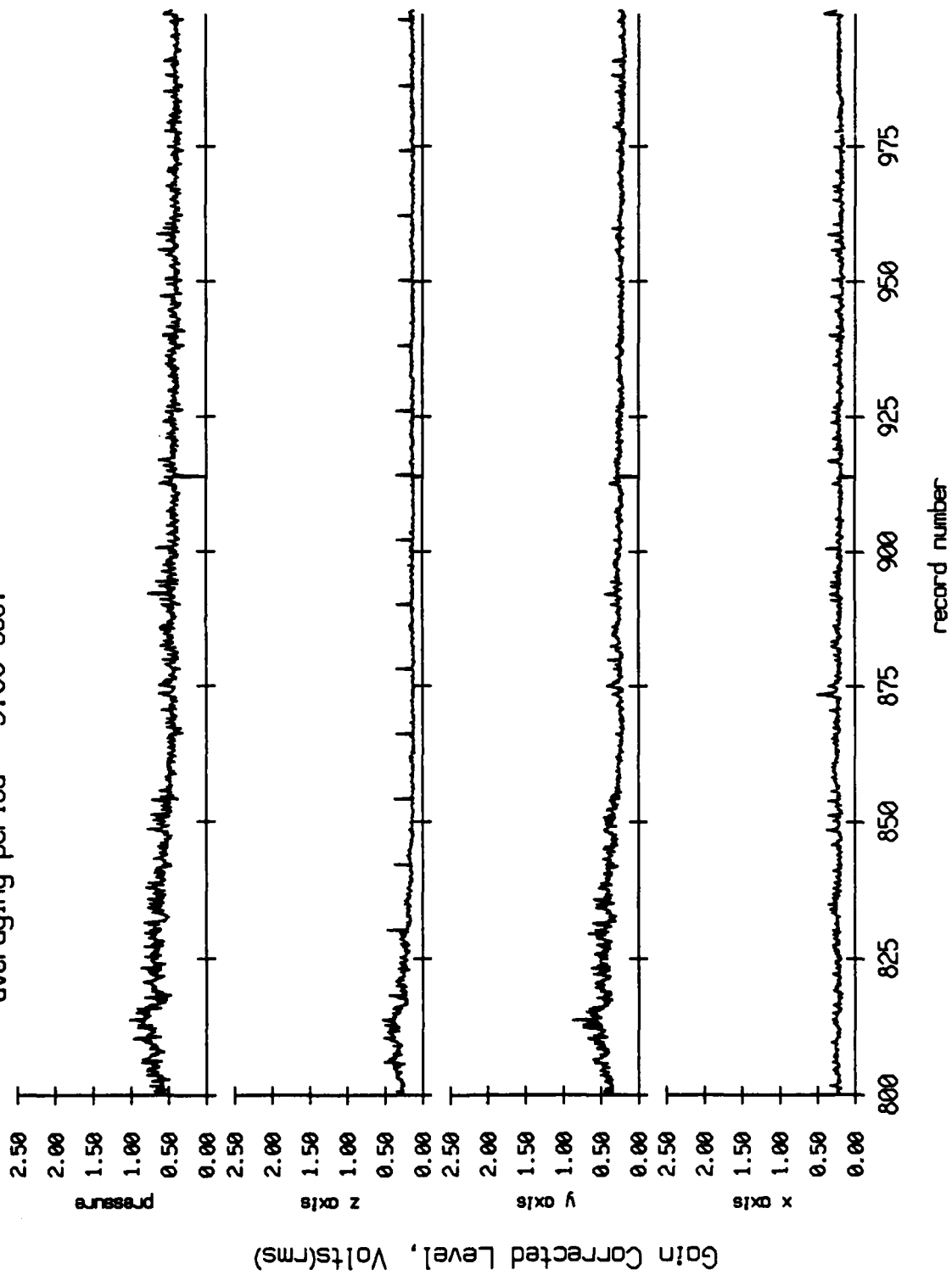


Figure X.3b

Float 2, July 1989 Trip  
 averaging period = 5.00 sec.

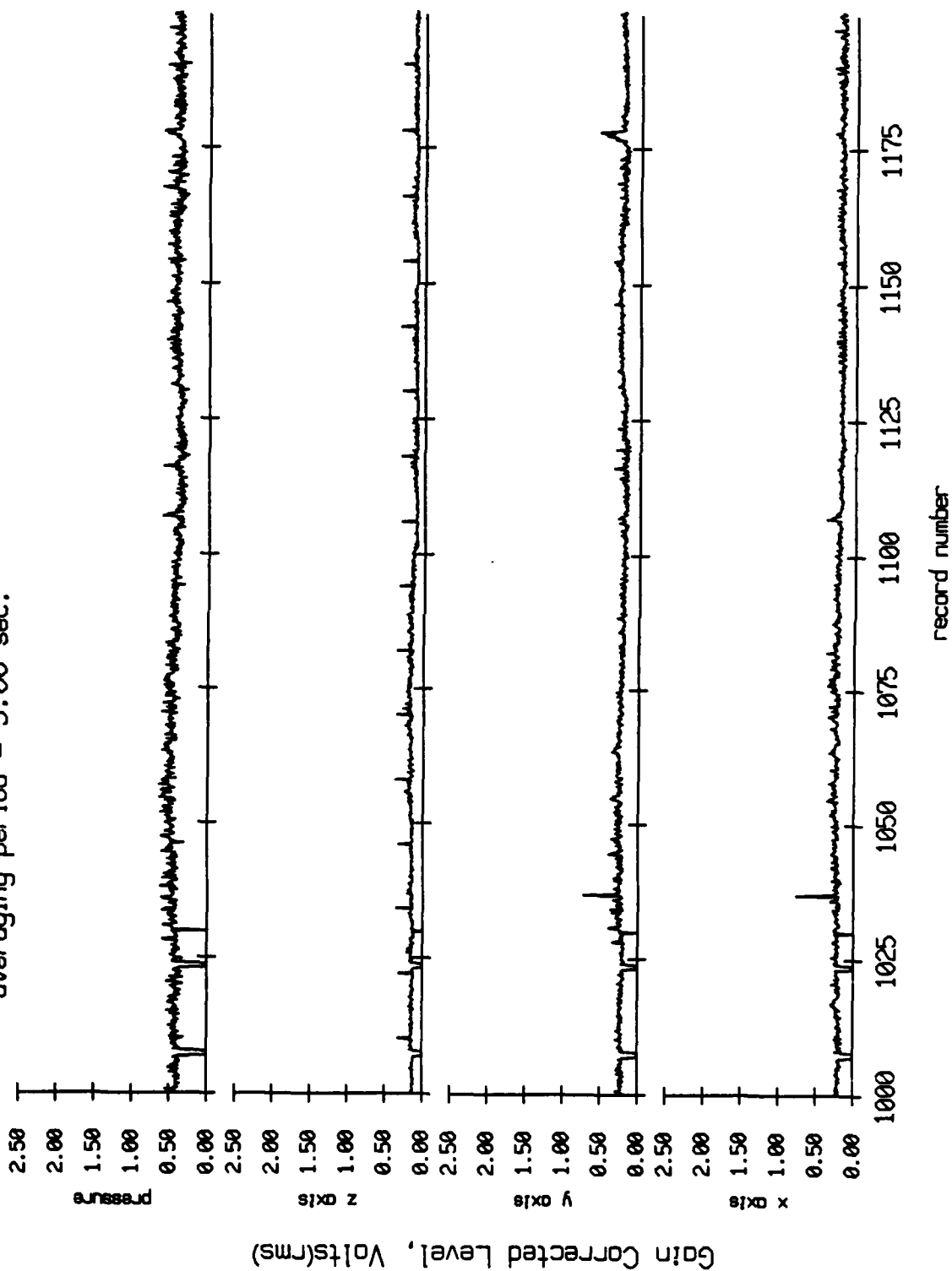


Figure X.3c

Float 2, July 1989 Trip  
 averaging period = 5.00 sec.

RMS Pressure and RMS Velocity

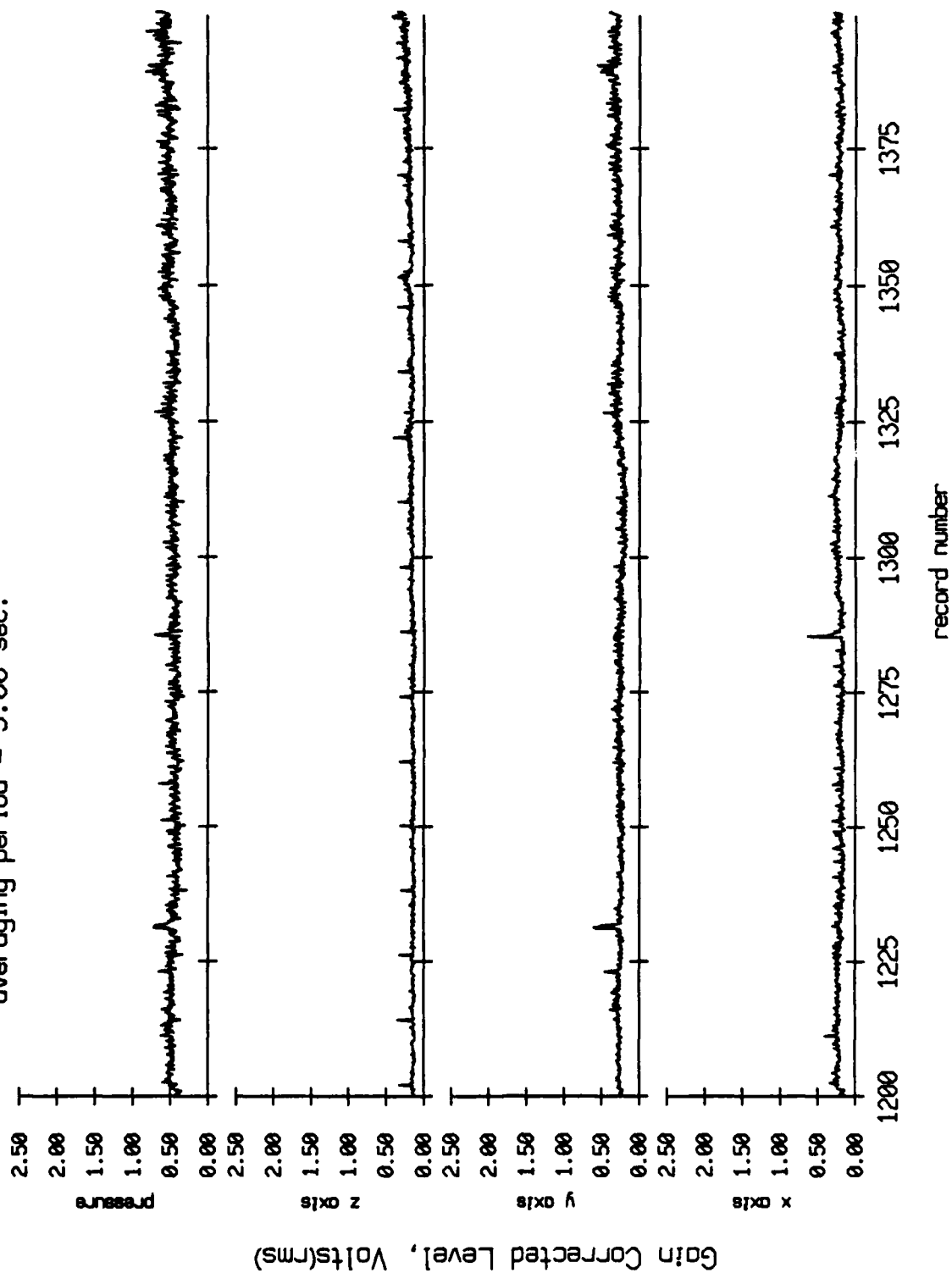


Figure X.3d



Float 2, July 1989 Trip  
 averaging period = 5.00 sec.

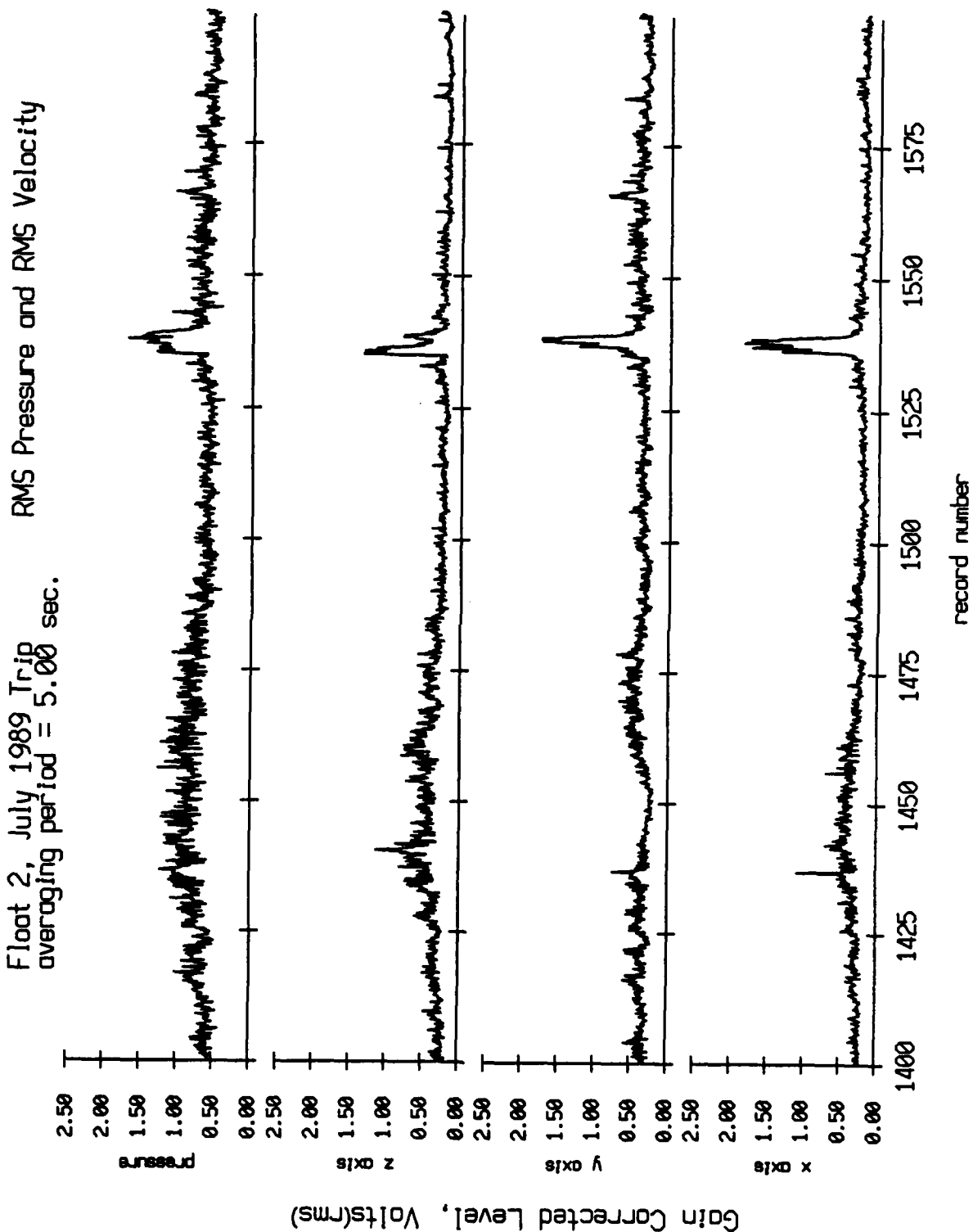


Figure X.3e

Float 2, July 1989 Trip  
 averaging period = 5.00 sec.

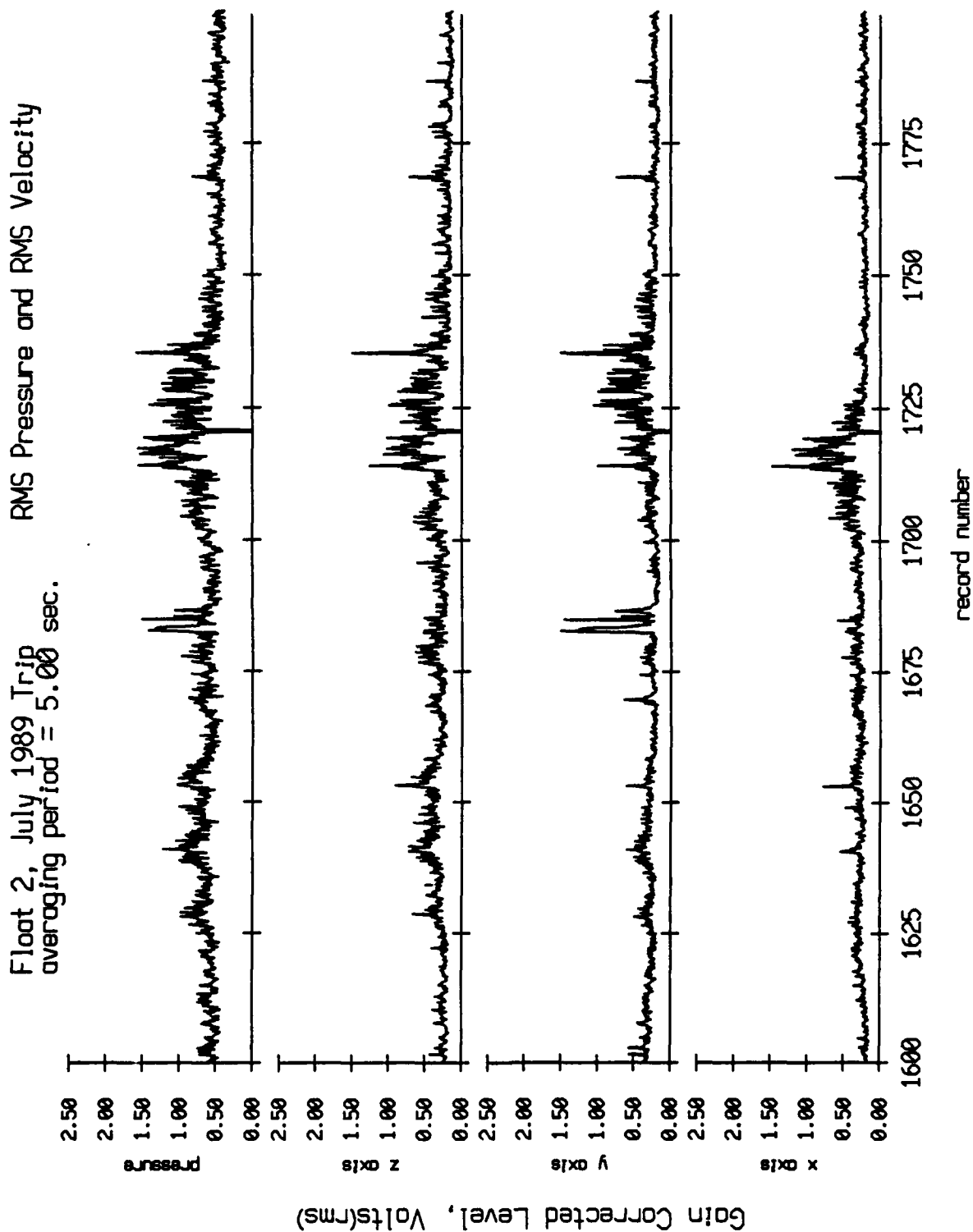


Figure X.3f

Float 2, July 1989 Trip  
 averaging period = 5.00 sec.

RMS Pressure and RMS Velocity

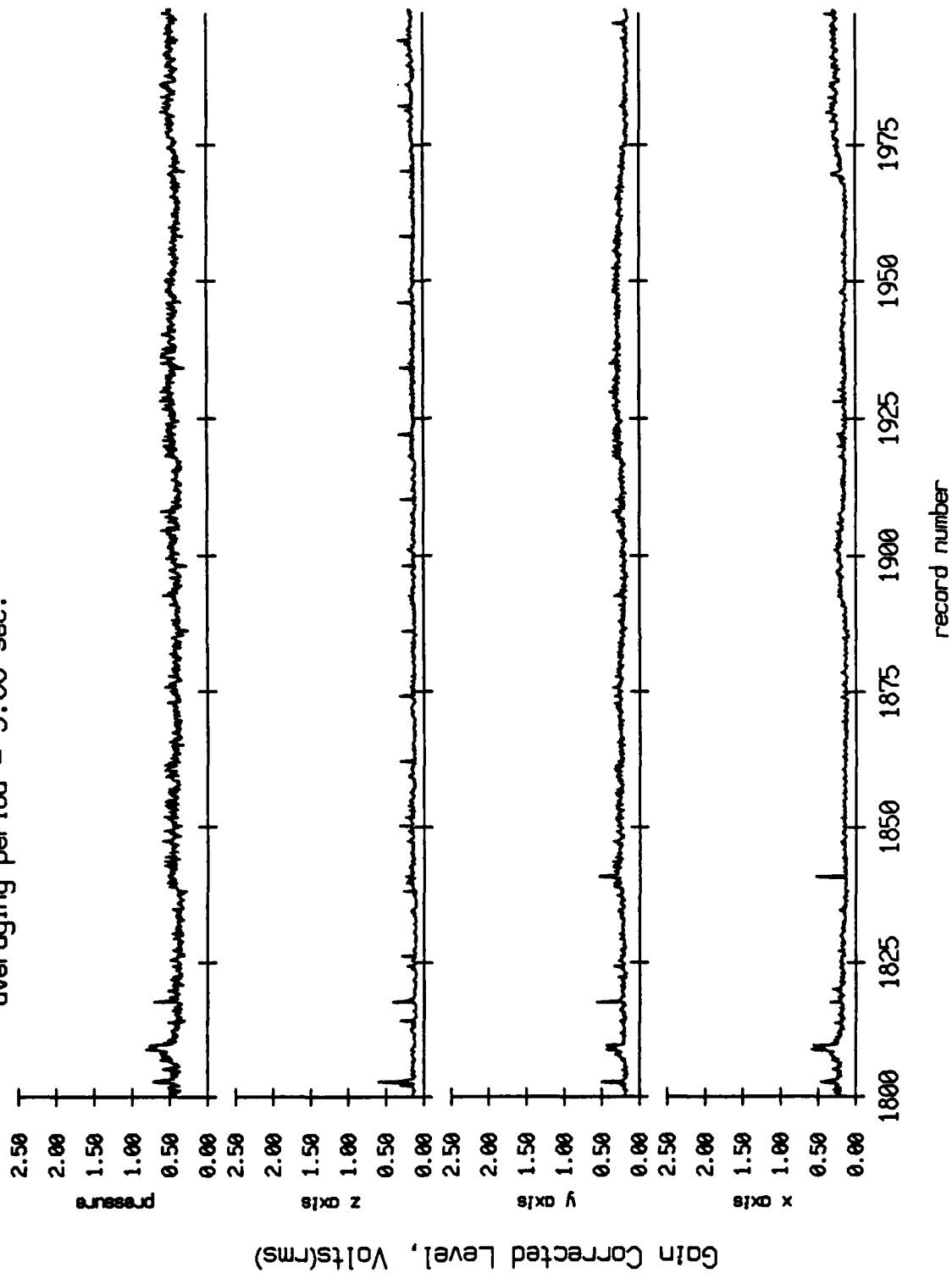


Figure X.3g

Floot 2, July 1989 Trip  
 averaging period = 5.00 sec.

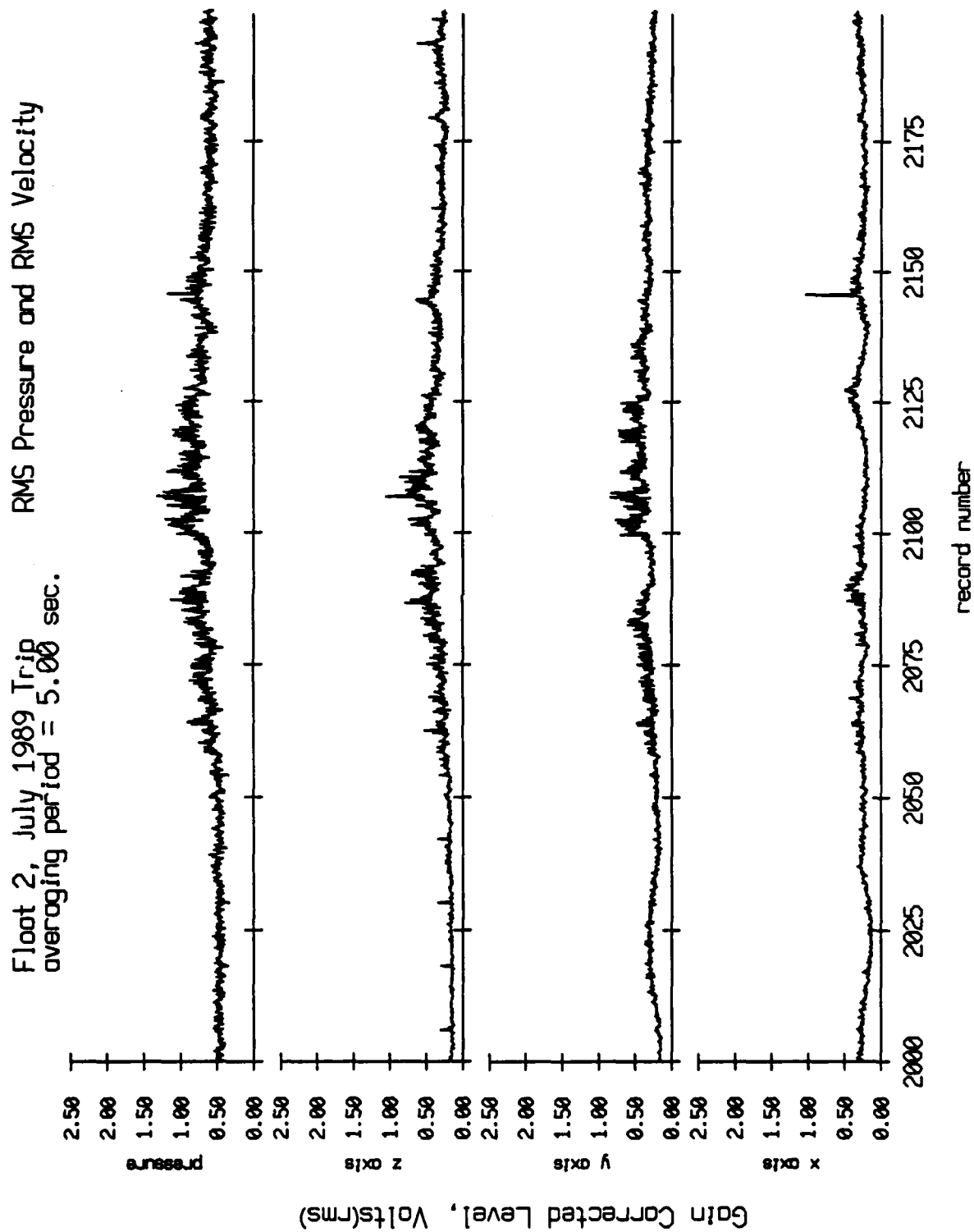


Figure X.3h

Floot 2, July 1989 Trip  
 averaging period = 5.00 sec.

RMS Pressure and RMS Velocity

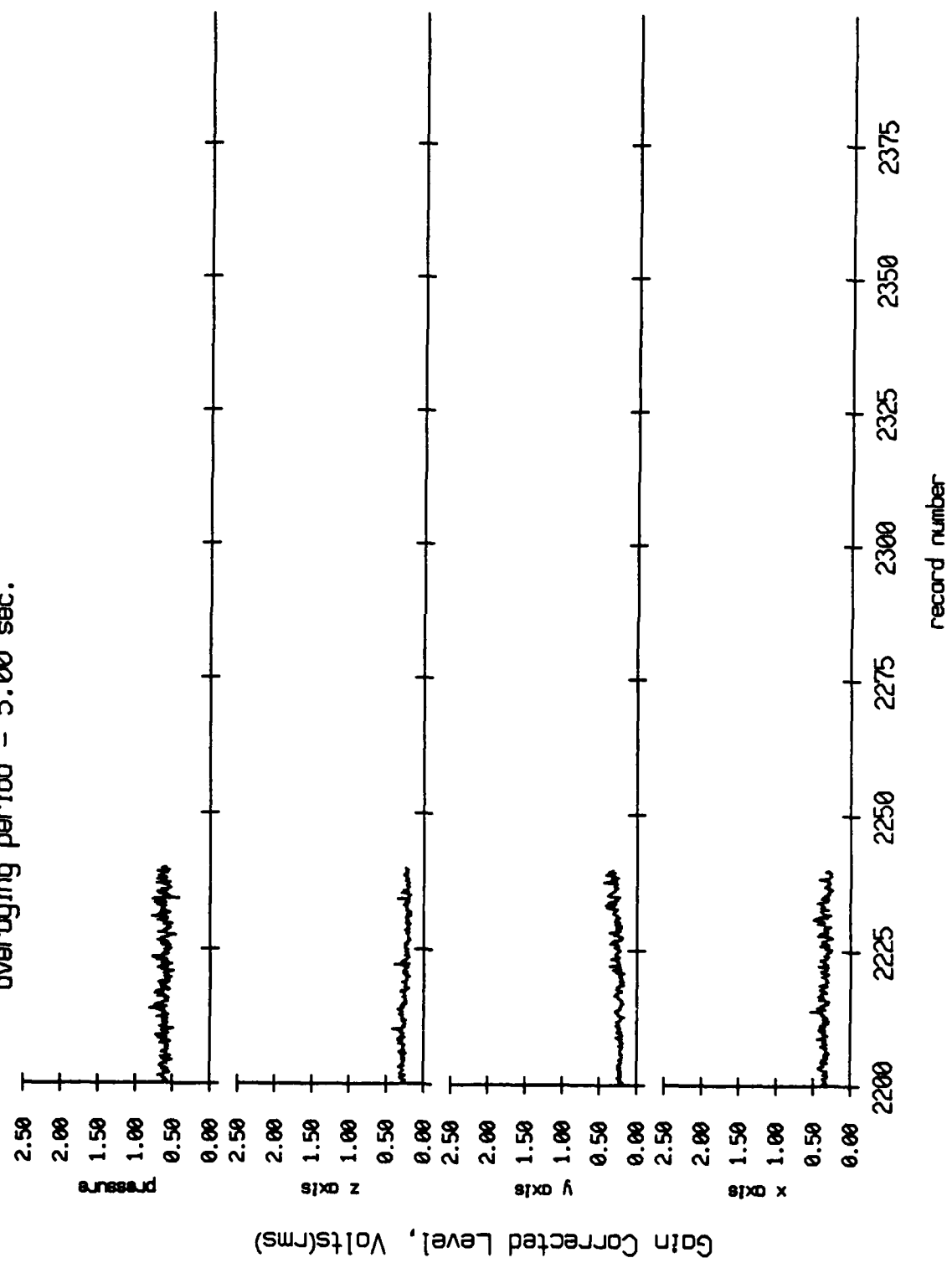


Figure X.31

Float 3, July 1989 Trip  
 averaging period = 5.00 sec.

RMS Pressure and RMS Velocity

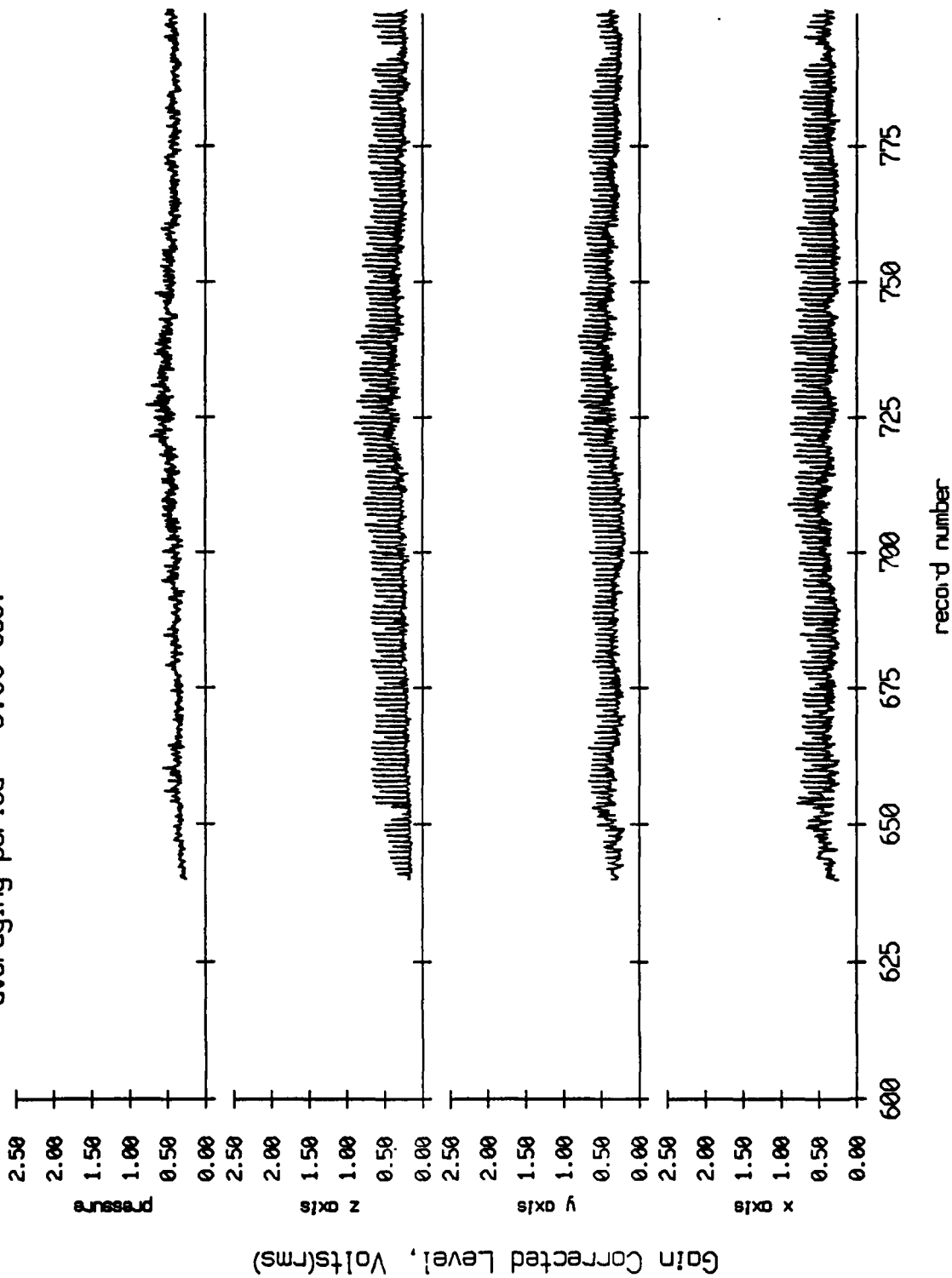


Figure X.4a

Float 3, July 1989 Trip  
 averaging period = 5.00 sec.

RMS Pressure and RMS Velocity

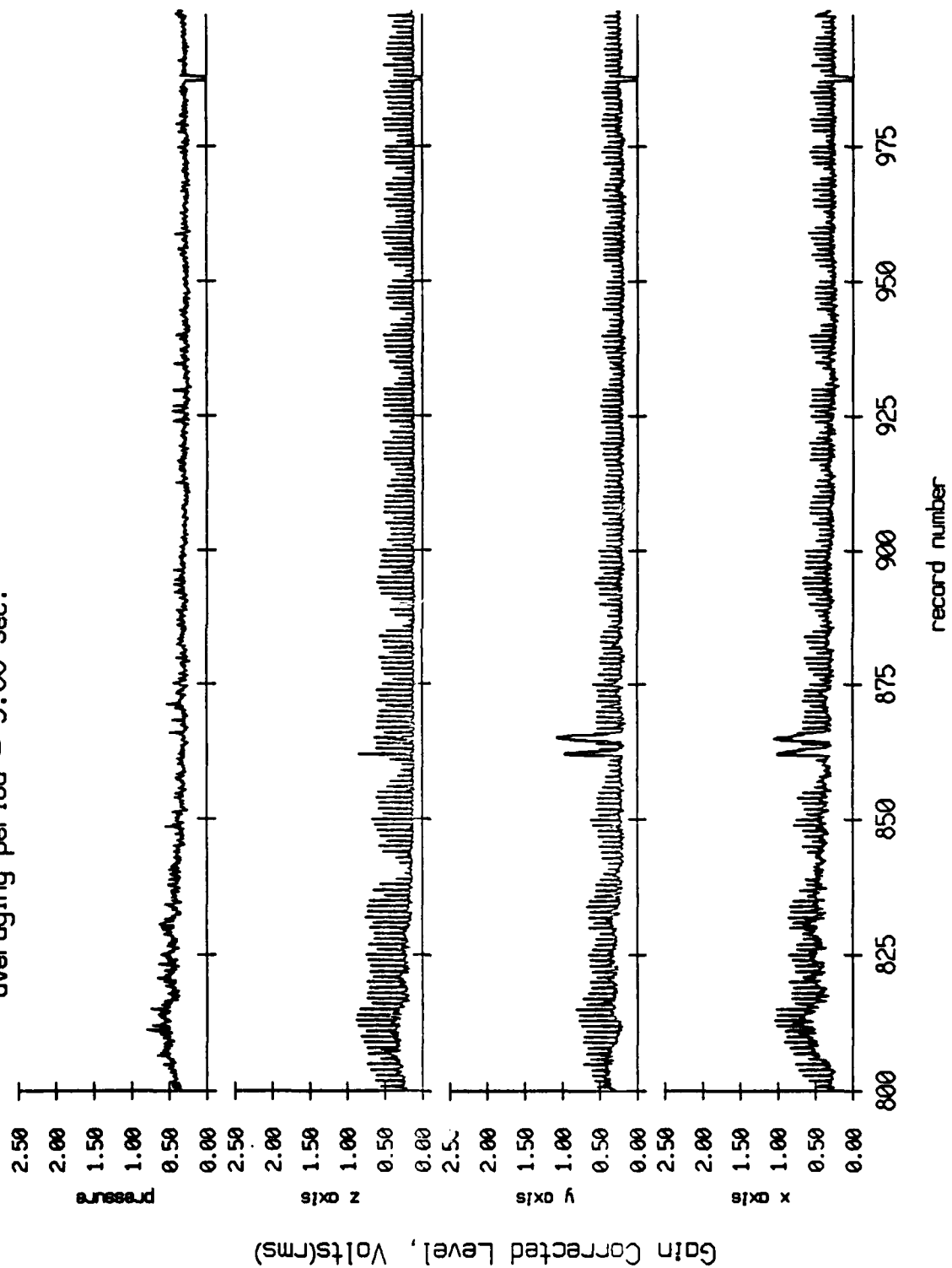


Figure X.4b

Float 3, July 1989 Trip  
 averaging period = 5.00 sec.  
 RMS Pressure and RMS Velocity

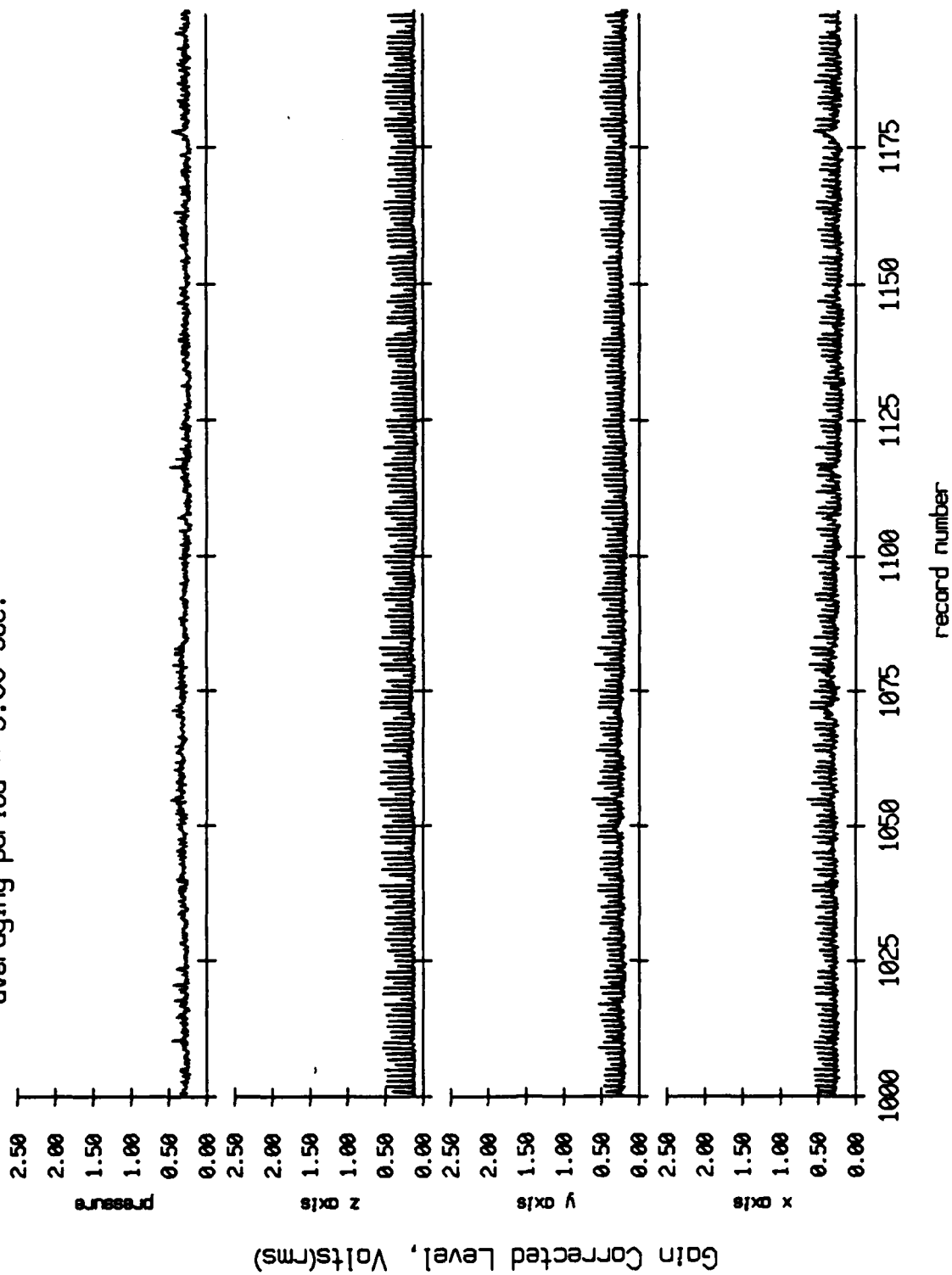


Figure X.4c



Float 3, July 1989 Trip  
 averaging period = 5.00 sec.

RMS Pressure and RMS Velocity

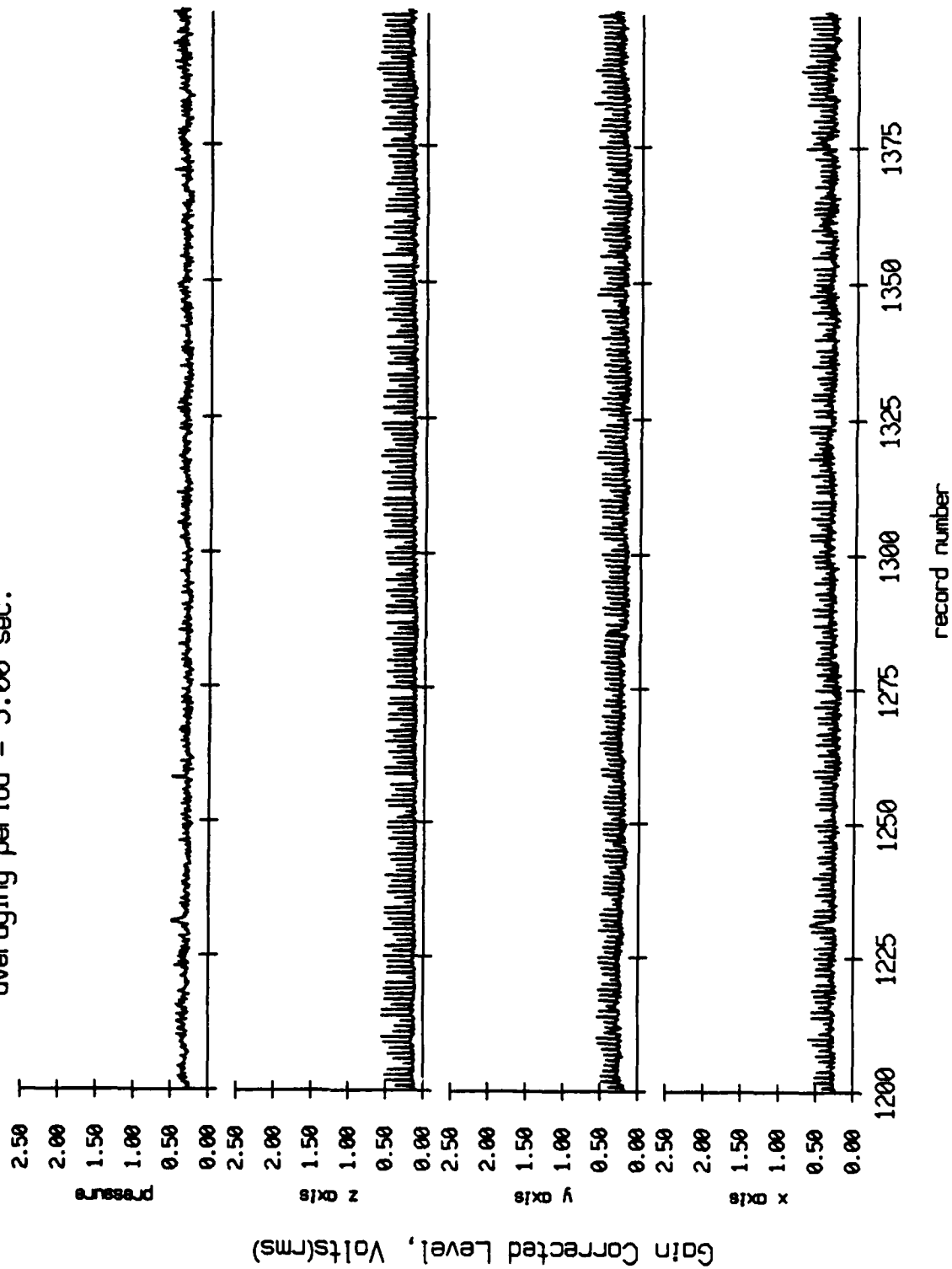


Figure X.4d

Float 3, July 1989 Trip  
 averaging period = 5.00 sec.

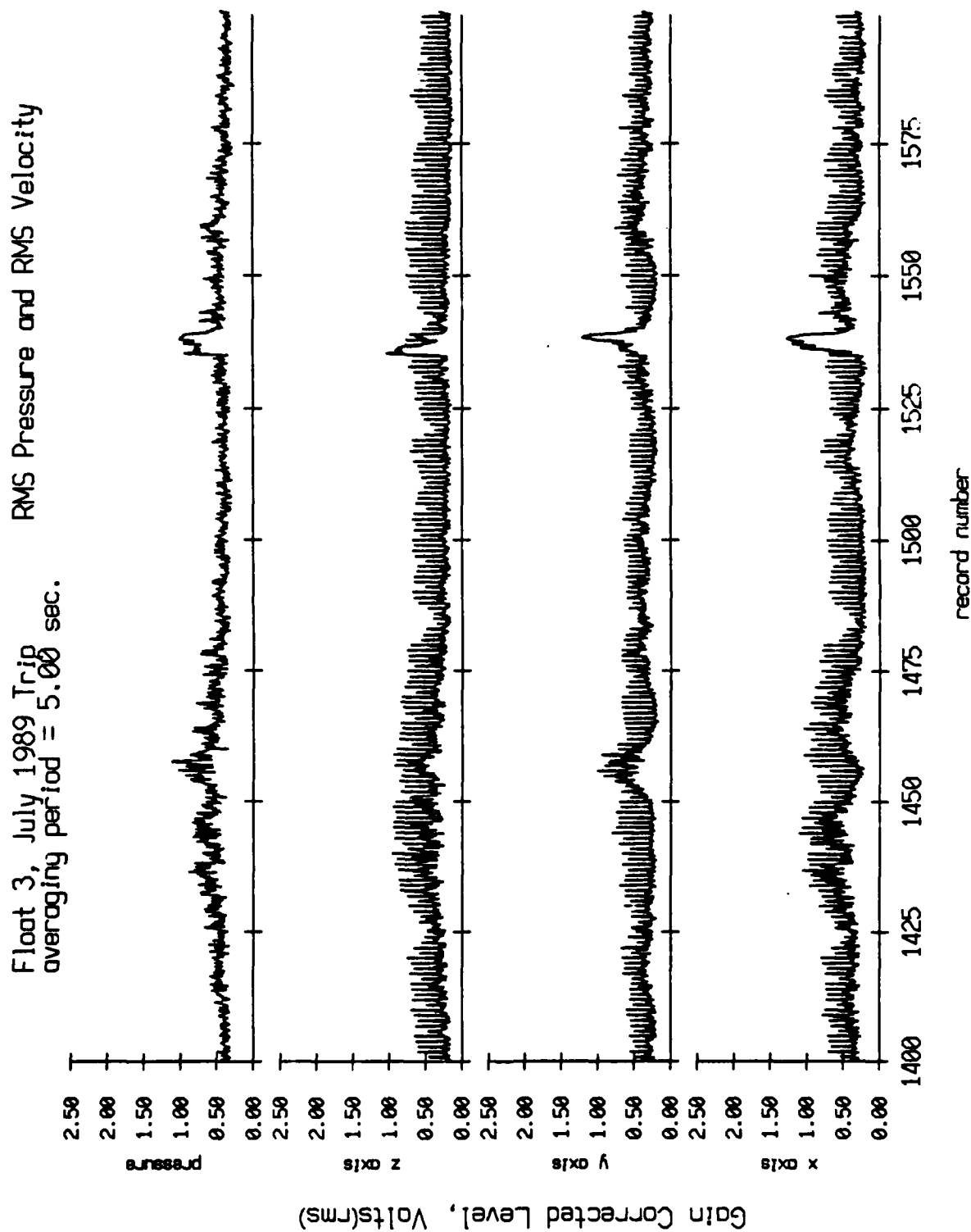
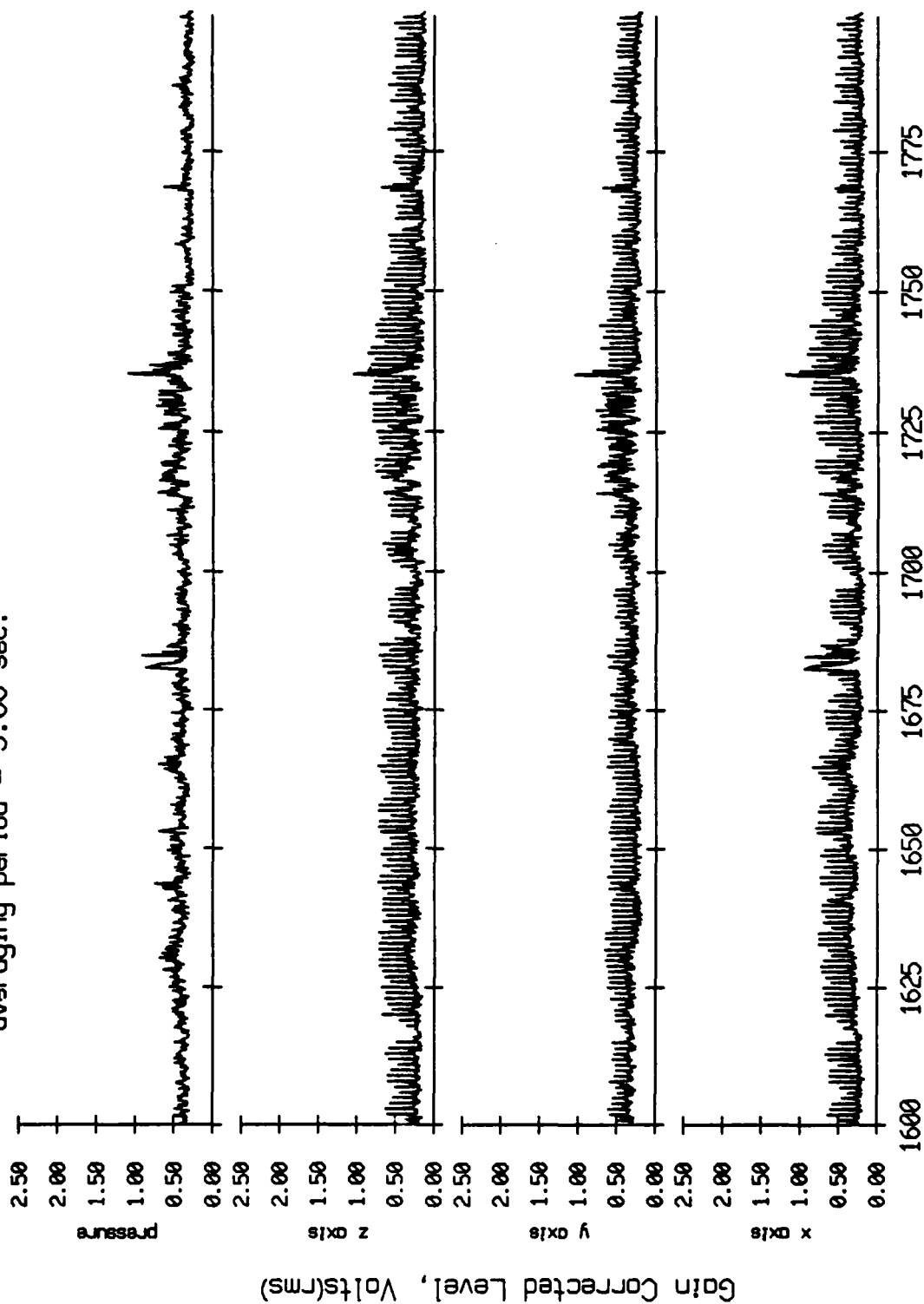


Figure X.4e

Float 3, July 1989 Trip  
 averaging period = 5.00 sec.

RMS Pressure and RMS Velocity



record number

Figure X.4f

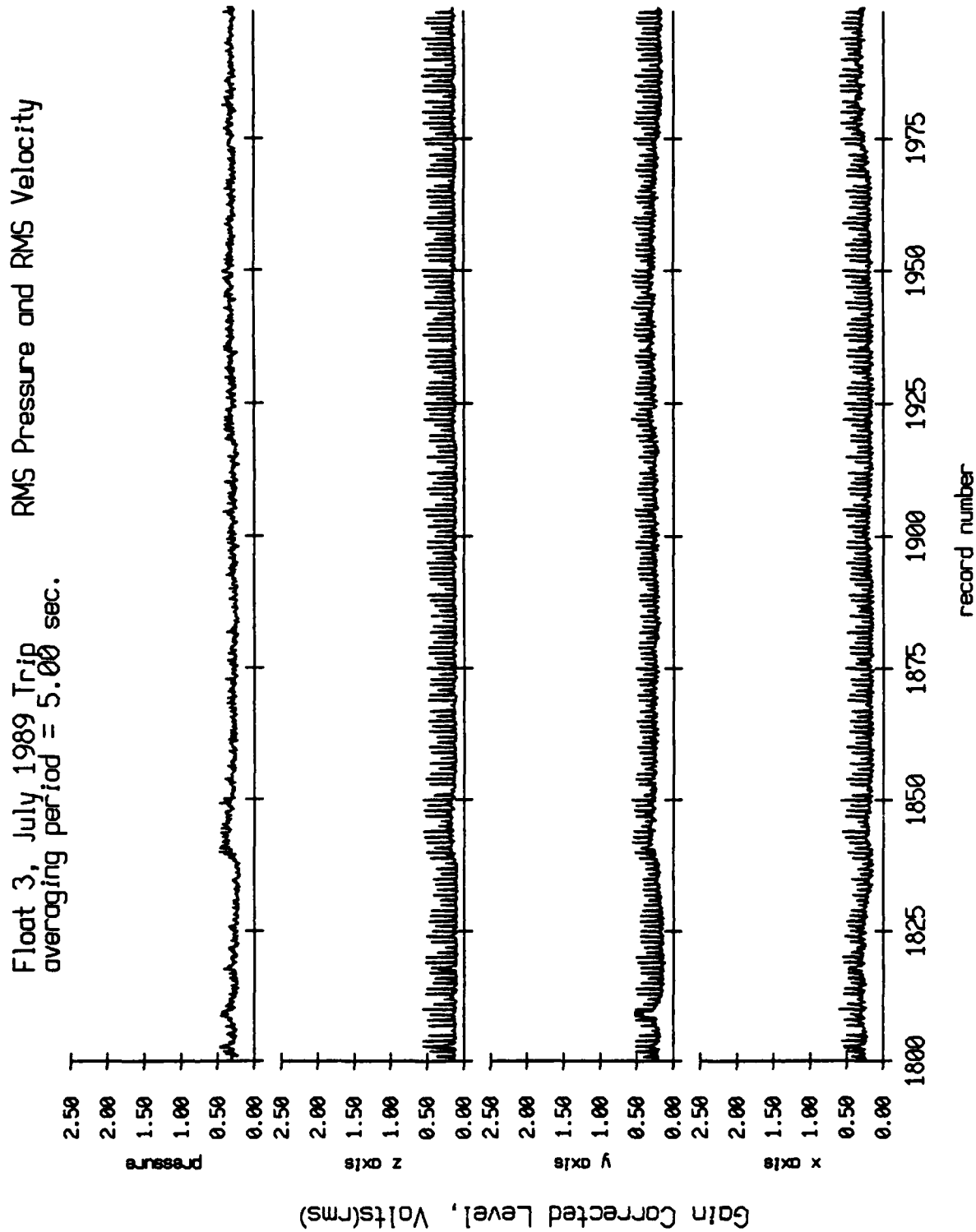


Figure X.4g

# Float 3, July 1989 Trip averaging period = 5.00 sec.

## RMS Pressure and RMS Velocity

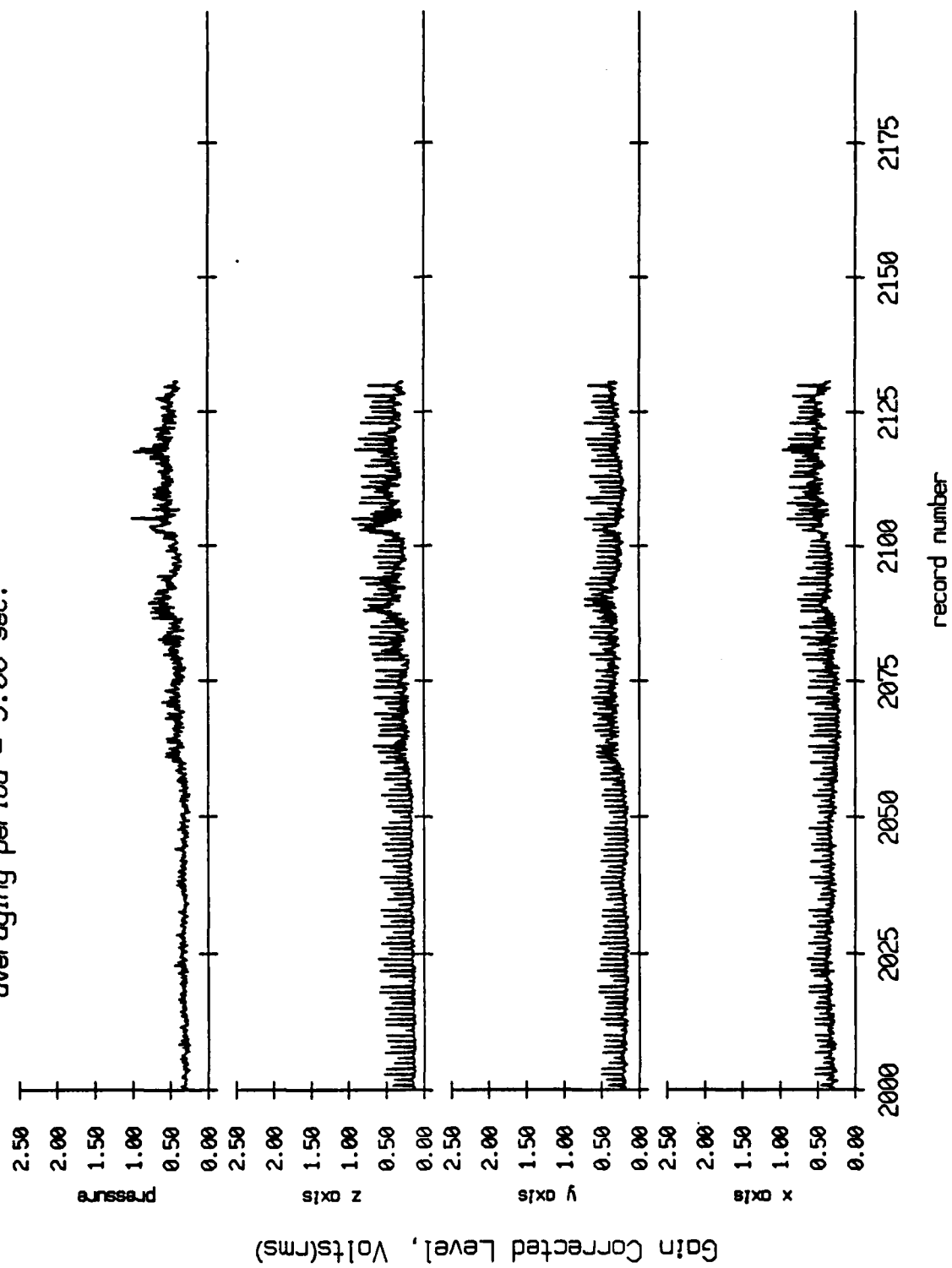


Figure X.4h

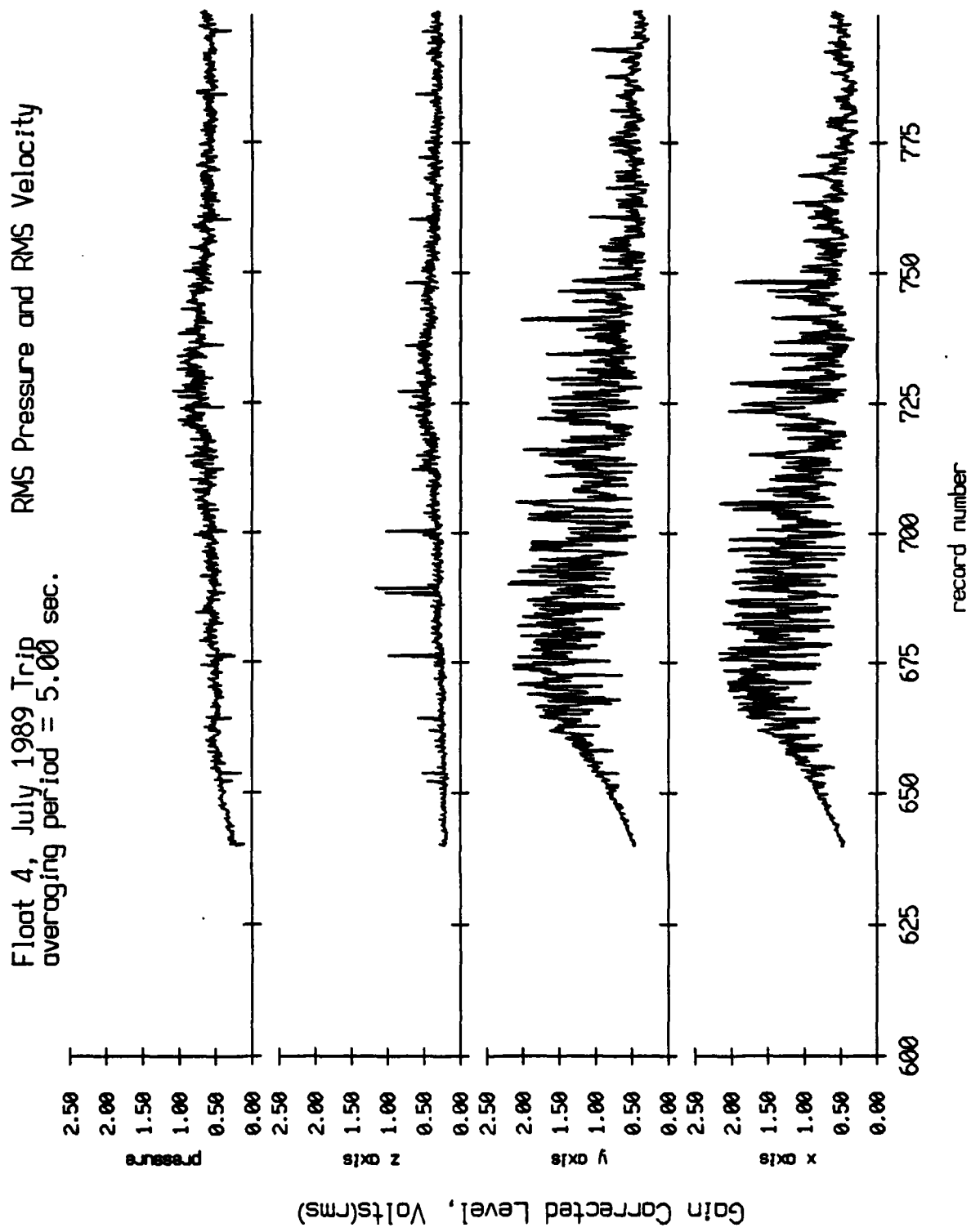


Figure X.5a

# Float 4, July 1989 Trip averaging period = 5.00 sec.

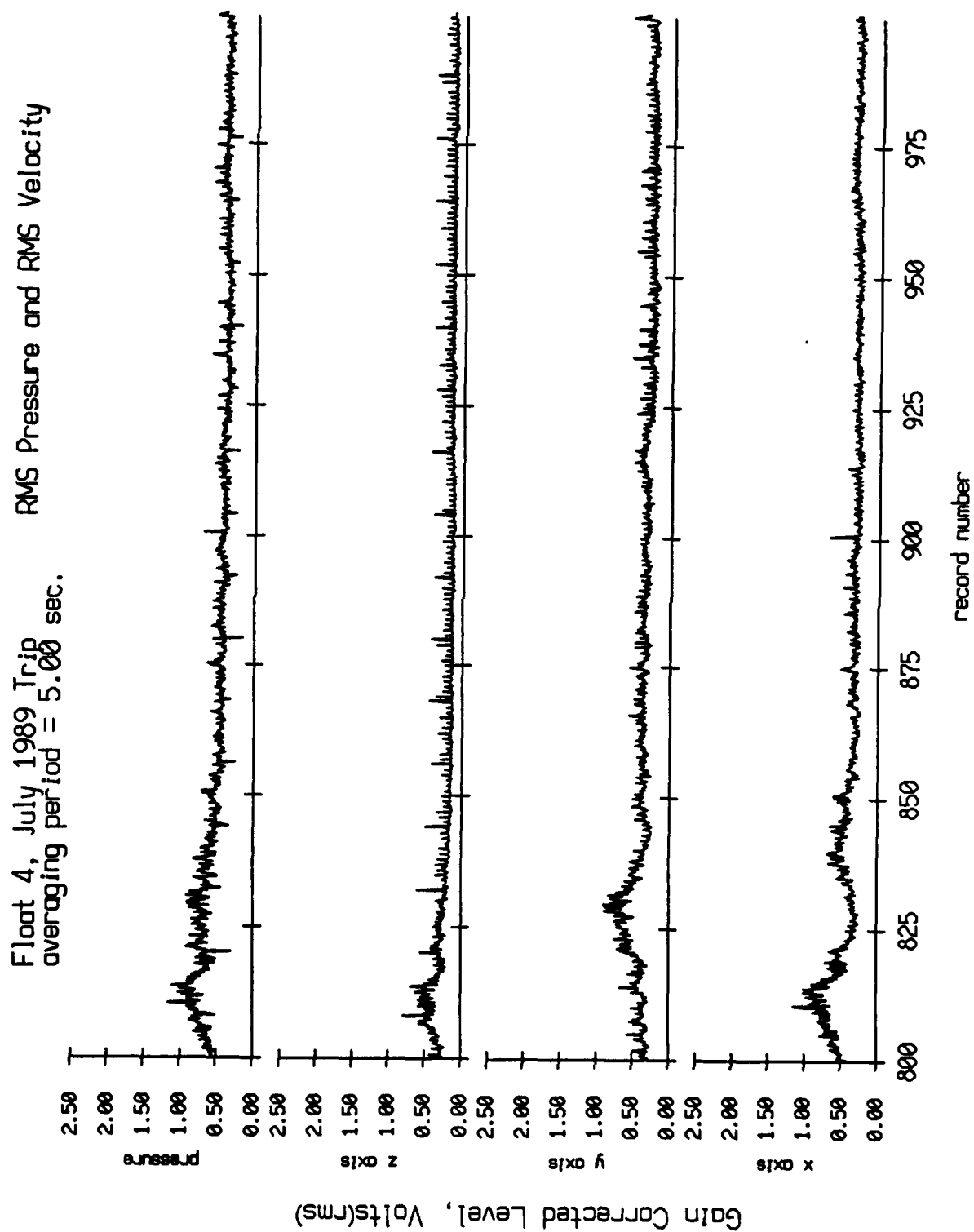


Figure X.5b

Float 4, July 1989 Trip  
 averaging period = 5.00 sec.

RMS Pressure and RMS Velocity

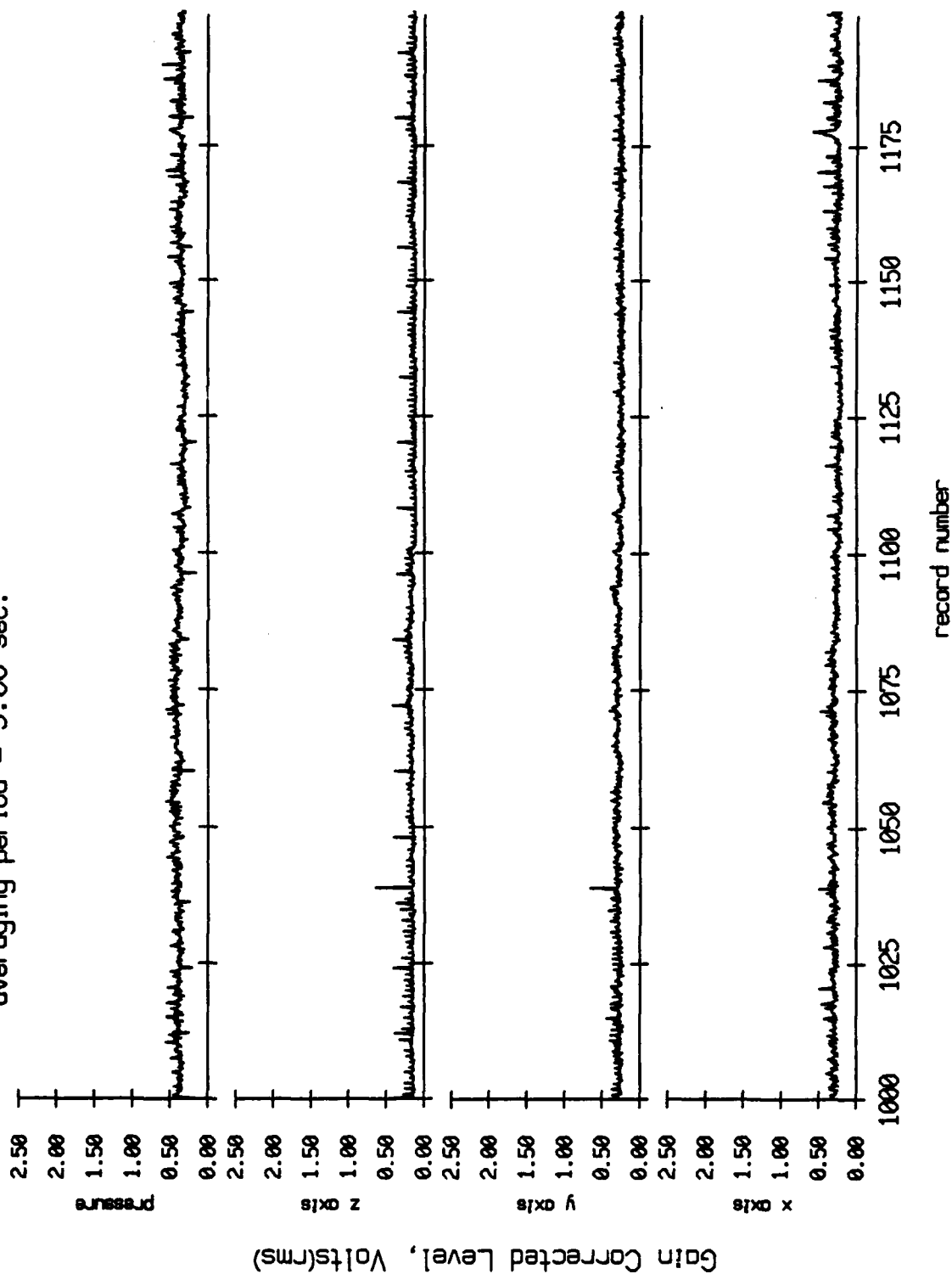


Figure X.5c



Floot 4, July 1989 Trip  
 averaging period = 5.00 sec.

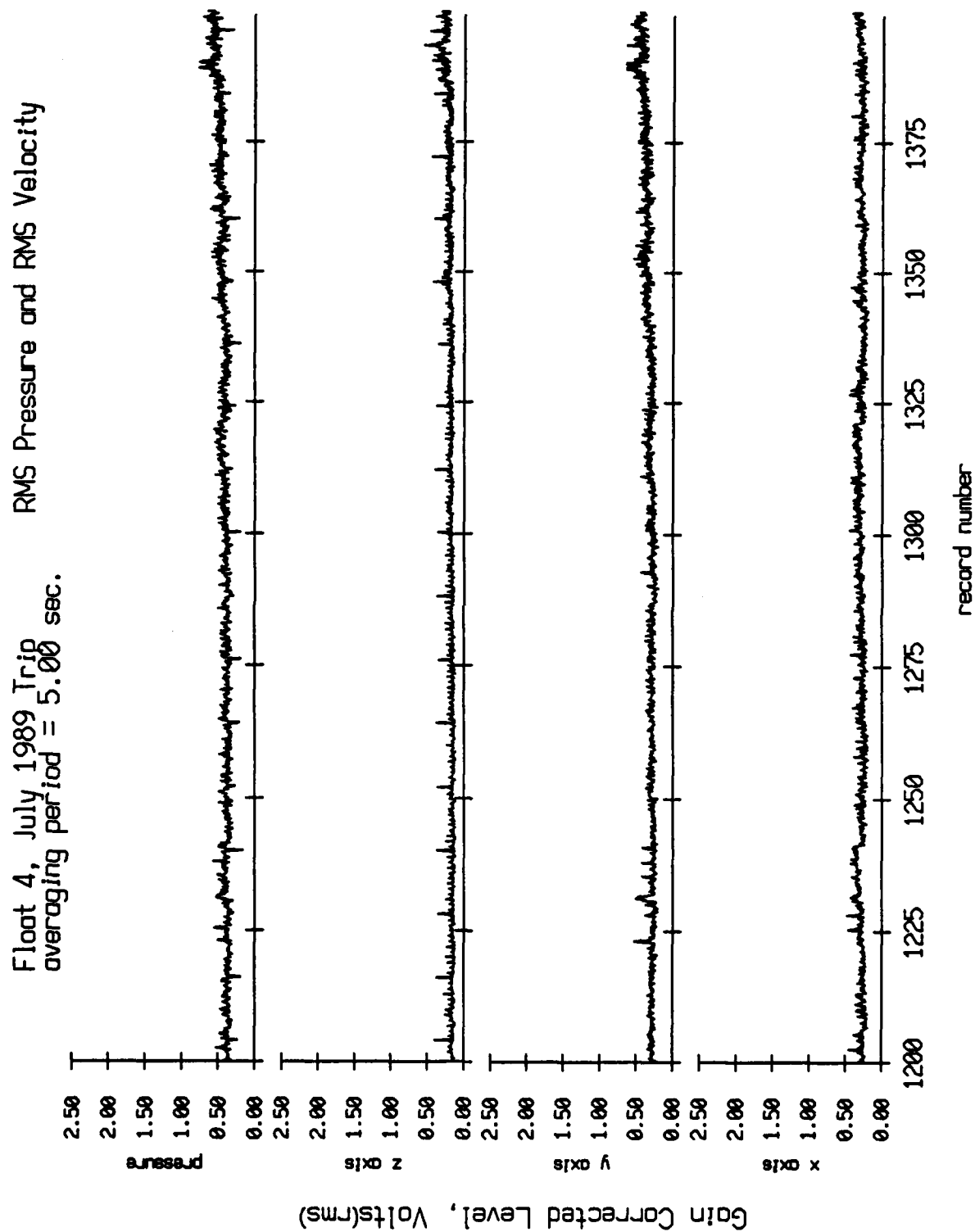


Figure X.5d

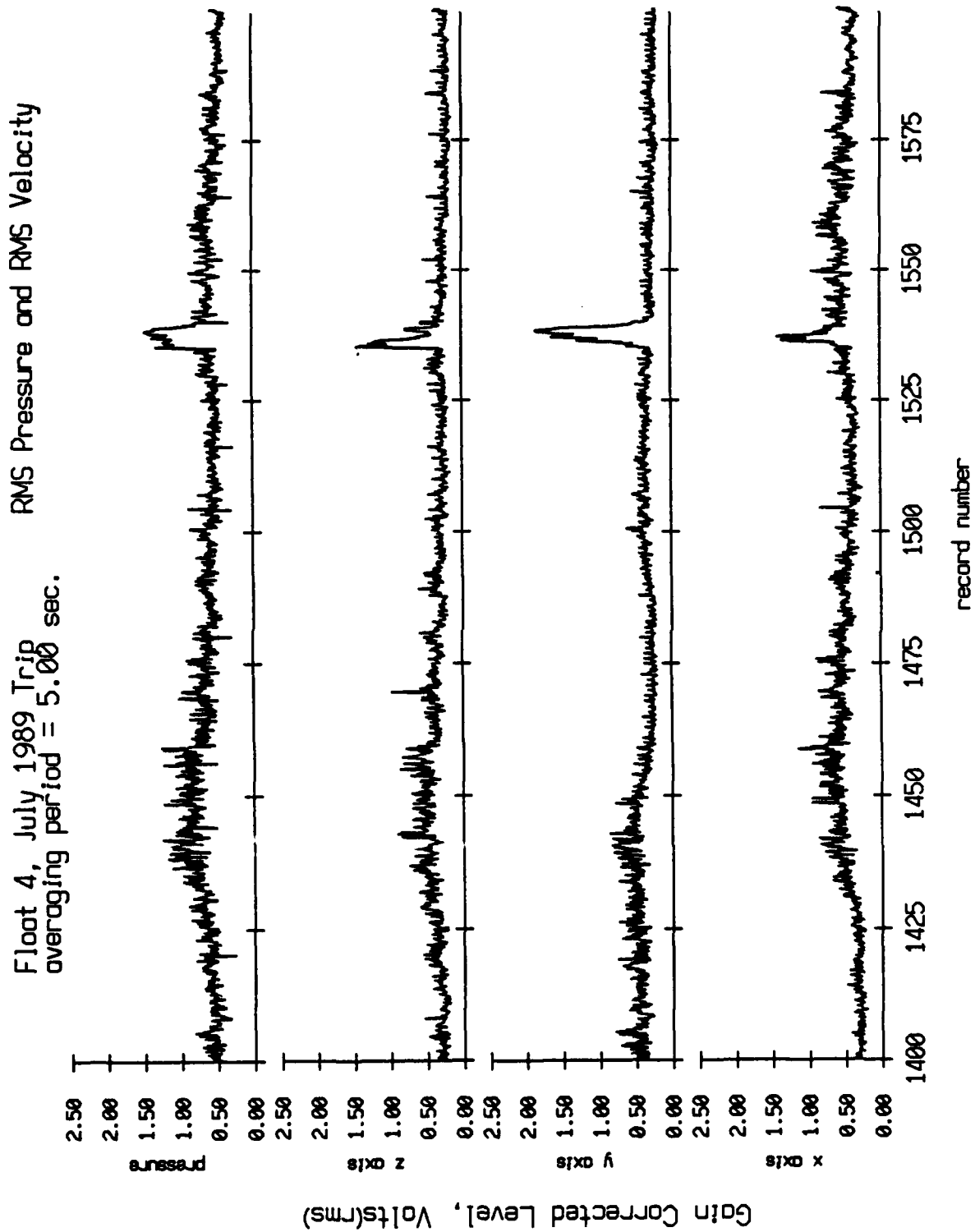


Figure X.5e

Float 4, July 1989 Trip  
 averaging period = 5.00 sec.

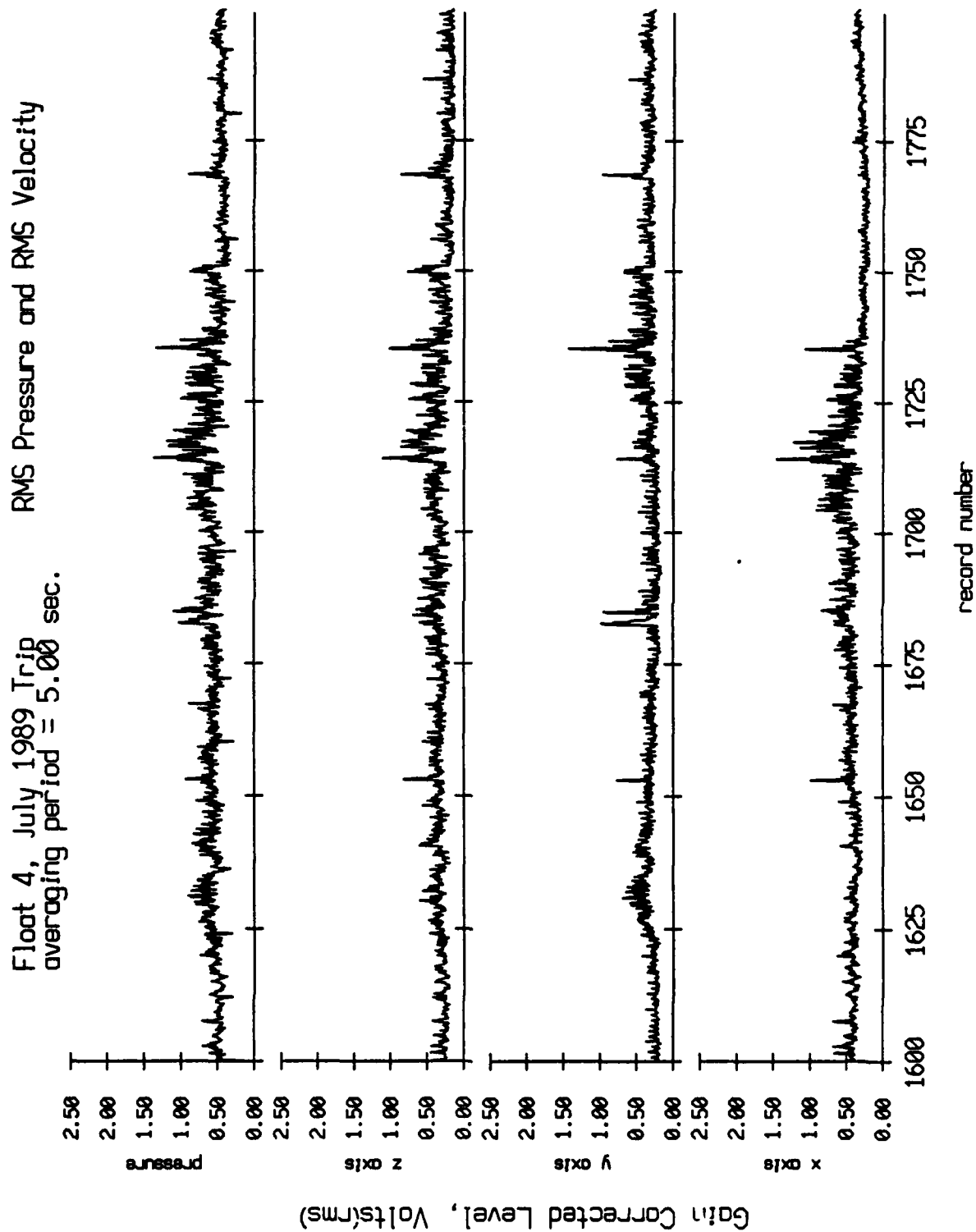


Figure X.5f

Float 4, July 1989 Trip  
 averaging period = 5.00 sec.

RMS Pressure and RMS Velocity

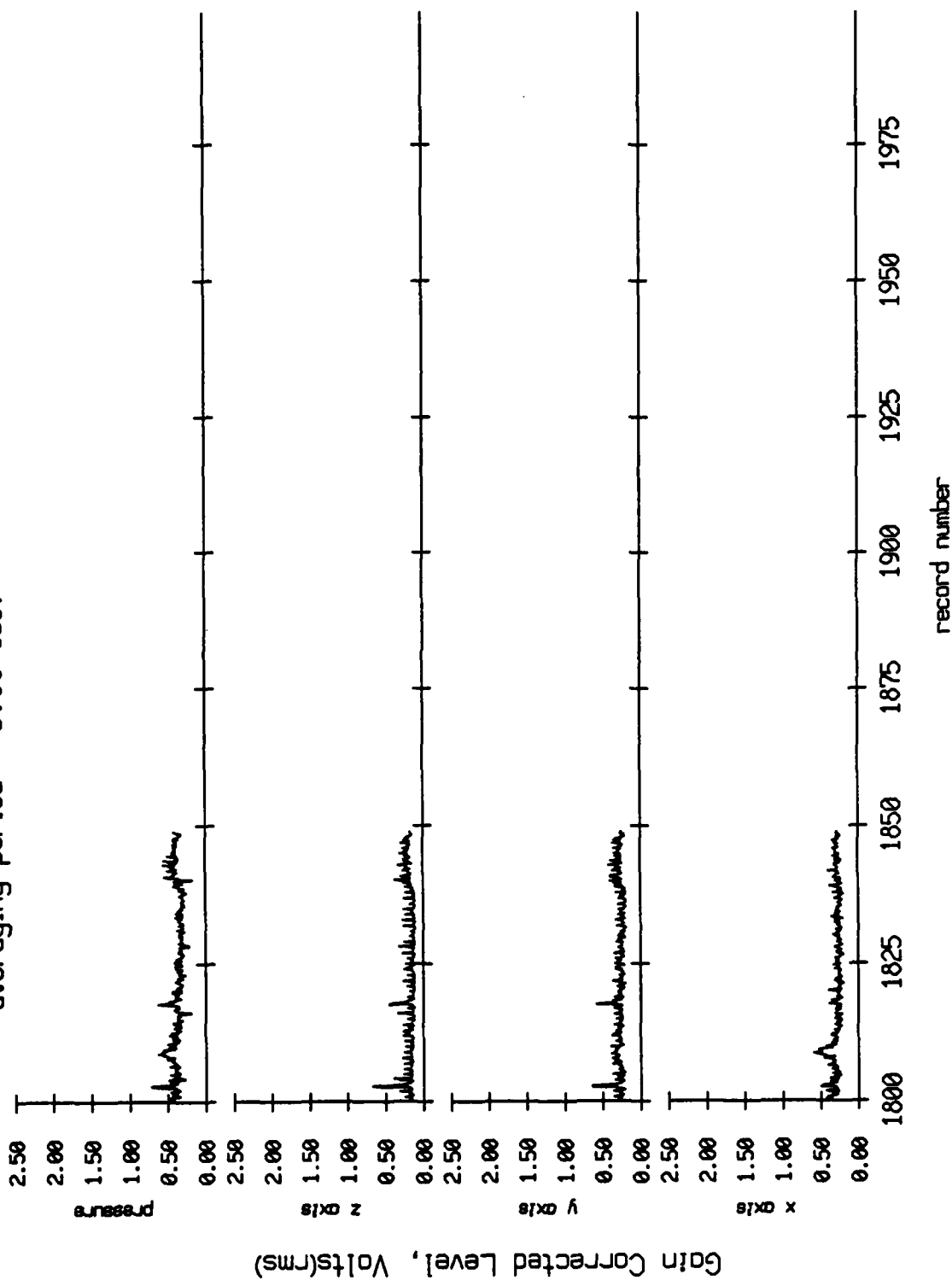


Figure X.5g

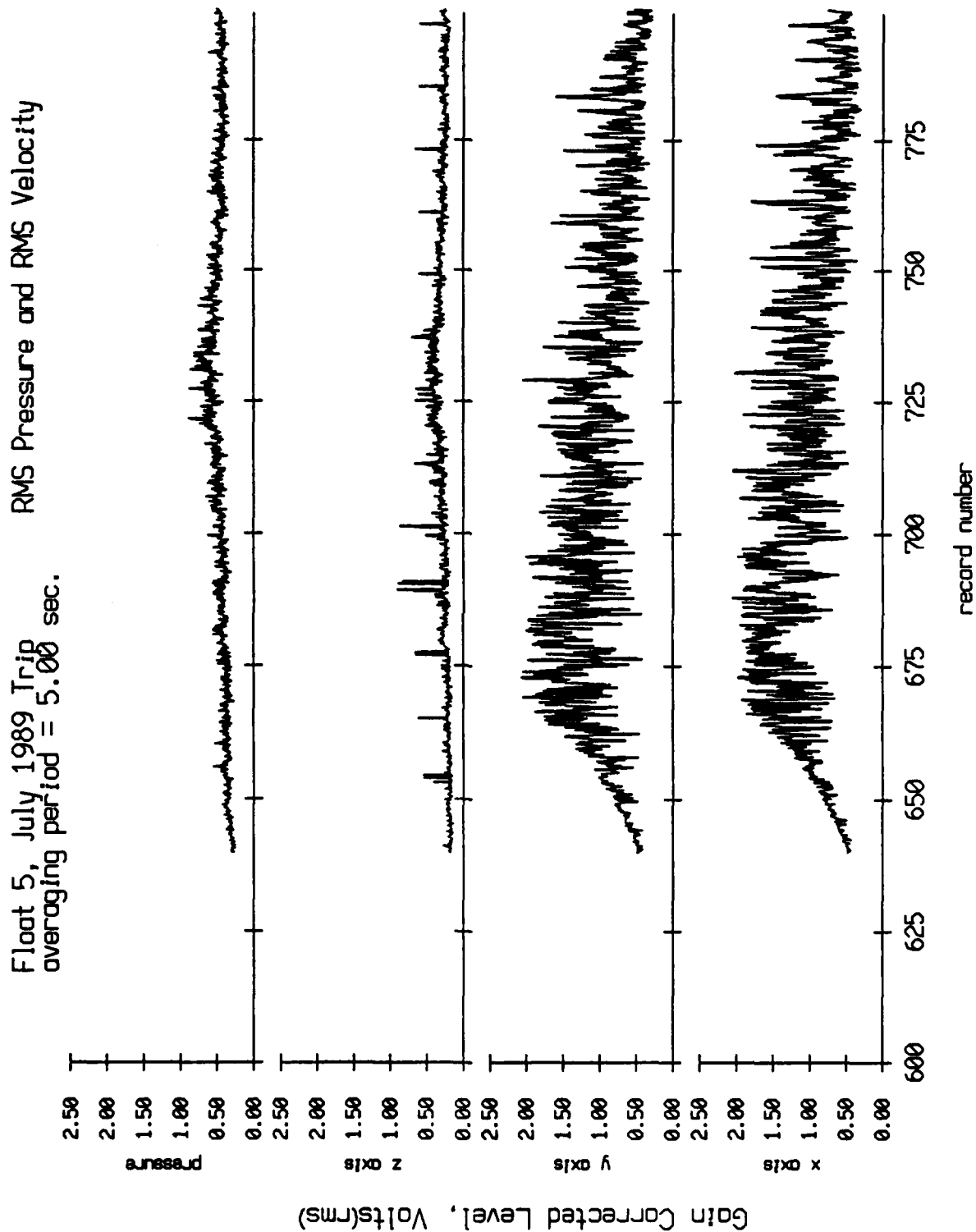


Figure X.6a

Float 5, July 1989 Trip  
 averaging period = 5.00 sec.

RMS Pressure and RMS Velocity

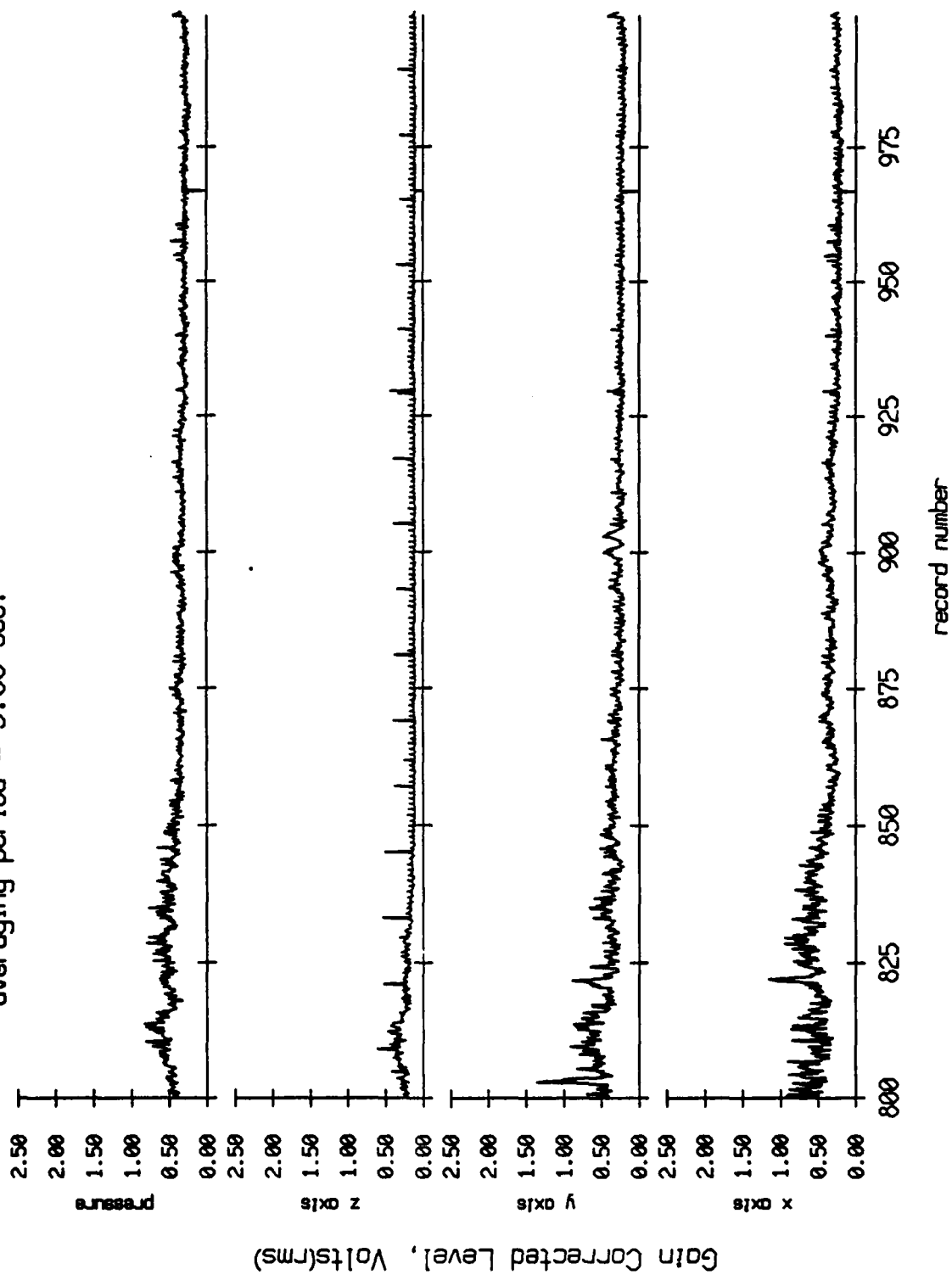


Figure X.6b

Float 5, July 1989 Trip  
 averaging period = 5.00 sec.

RMS Pressure and RMS Velocity

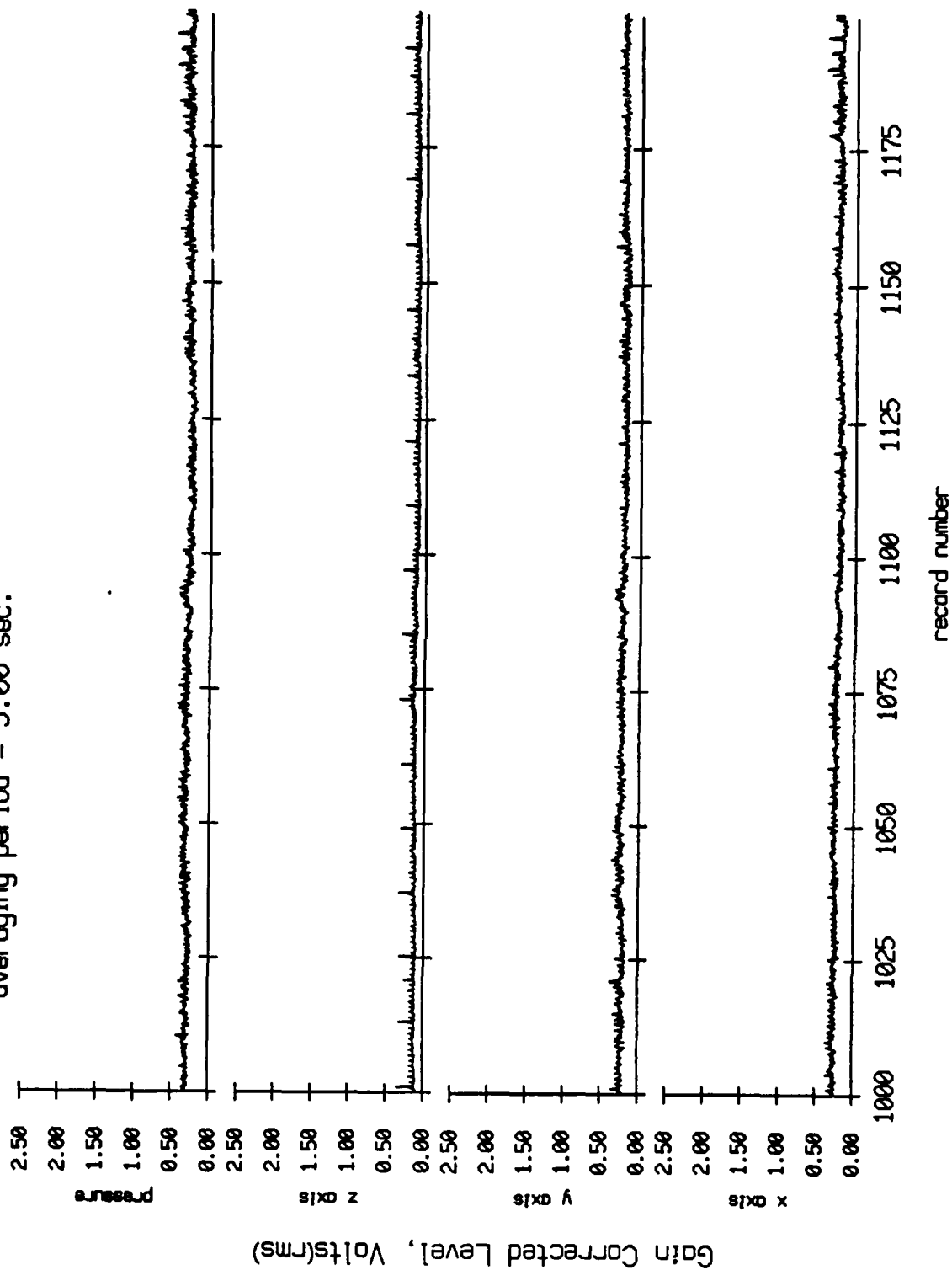


Figure X.6c

Float 5, July 1989 Trip  
 averaging period = 5.00 sec.

RMS Pressure and RMS Velocity

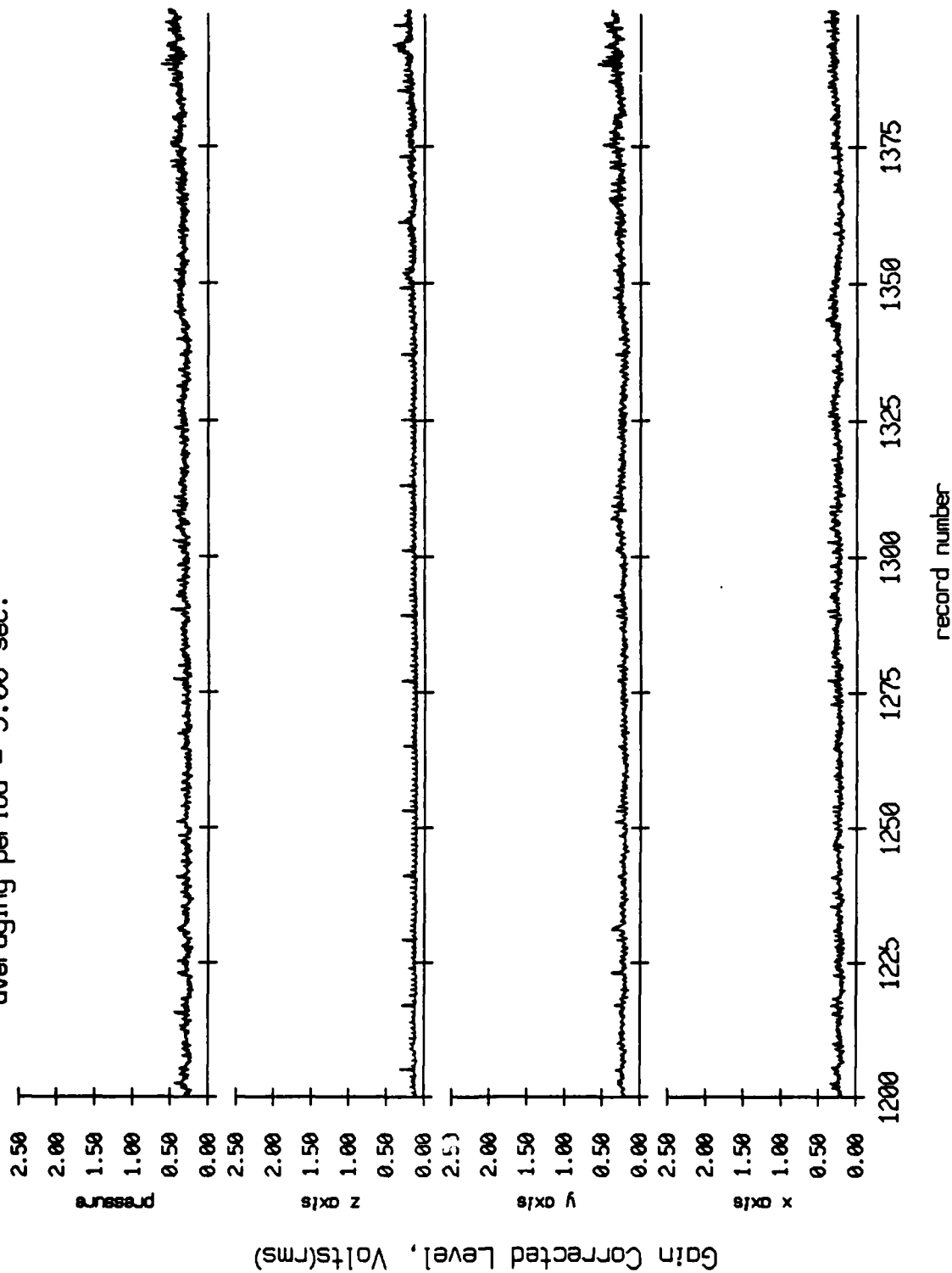


Figure X.6d



Float 5, July 1989 Trip  
 averaging period = 5.00 sec.

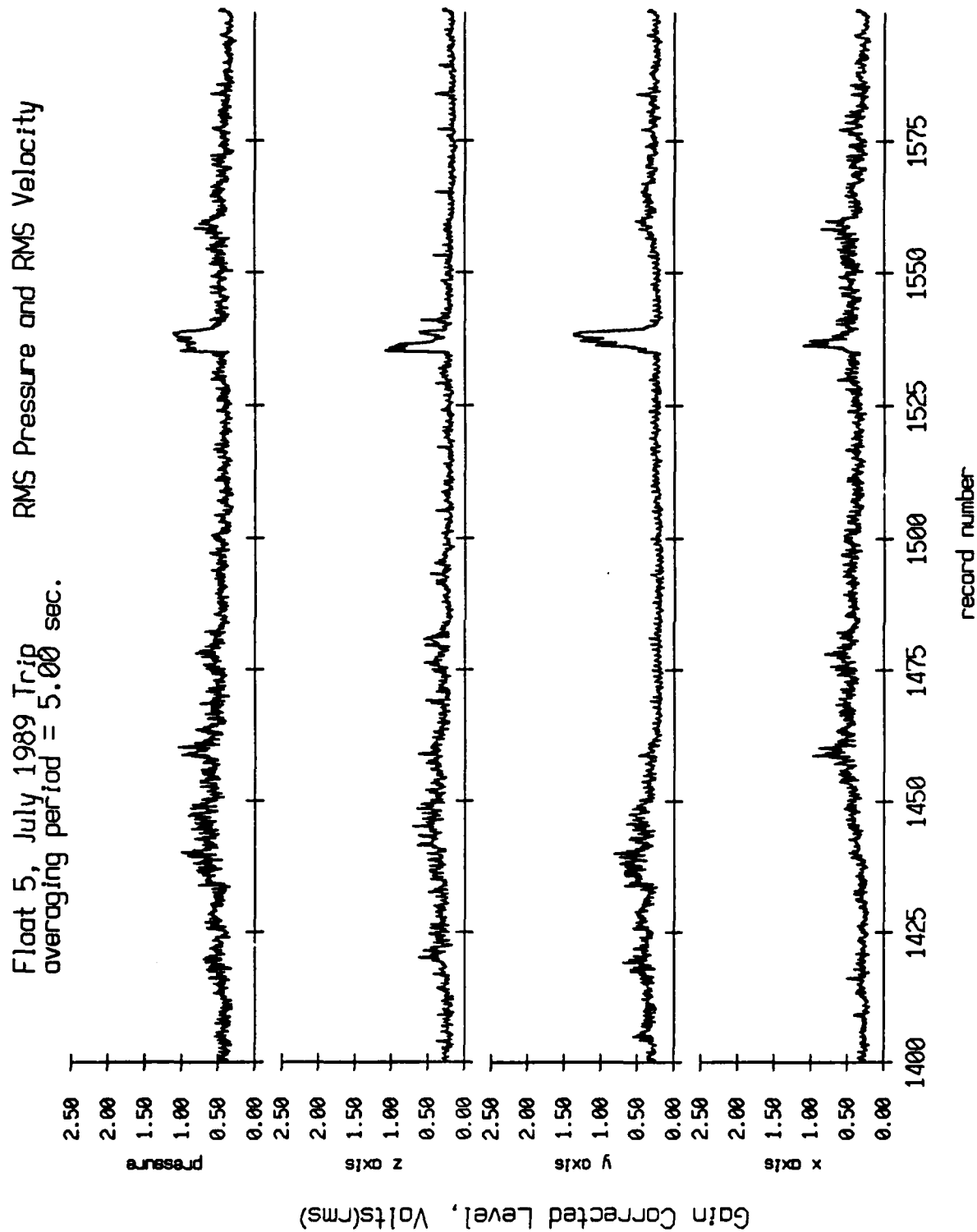


Figure X.6e

Float 5, July 1989 Trip  
 averaging period = 5.00 sec.

RMS Pressure and RMS Velocity

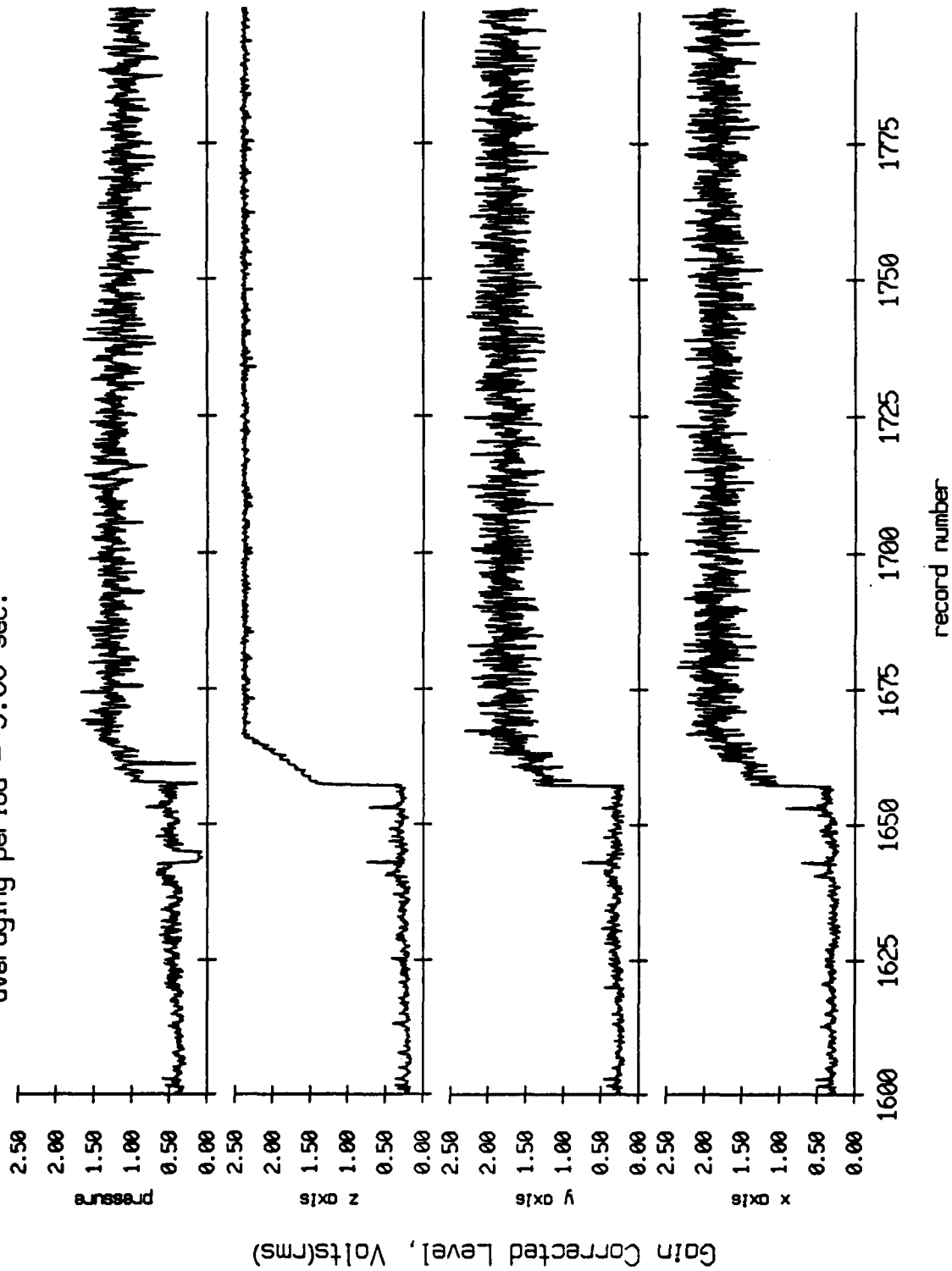


Figure X.6f

Float 5, July 1989 Trip  
 averaging period = 5.00 sec.

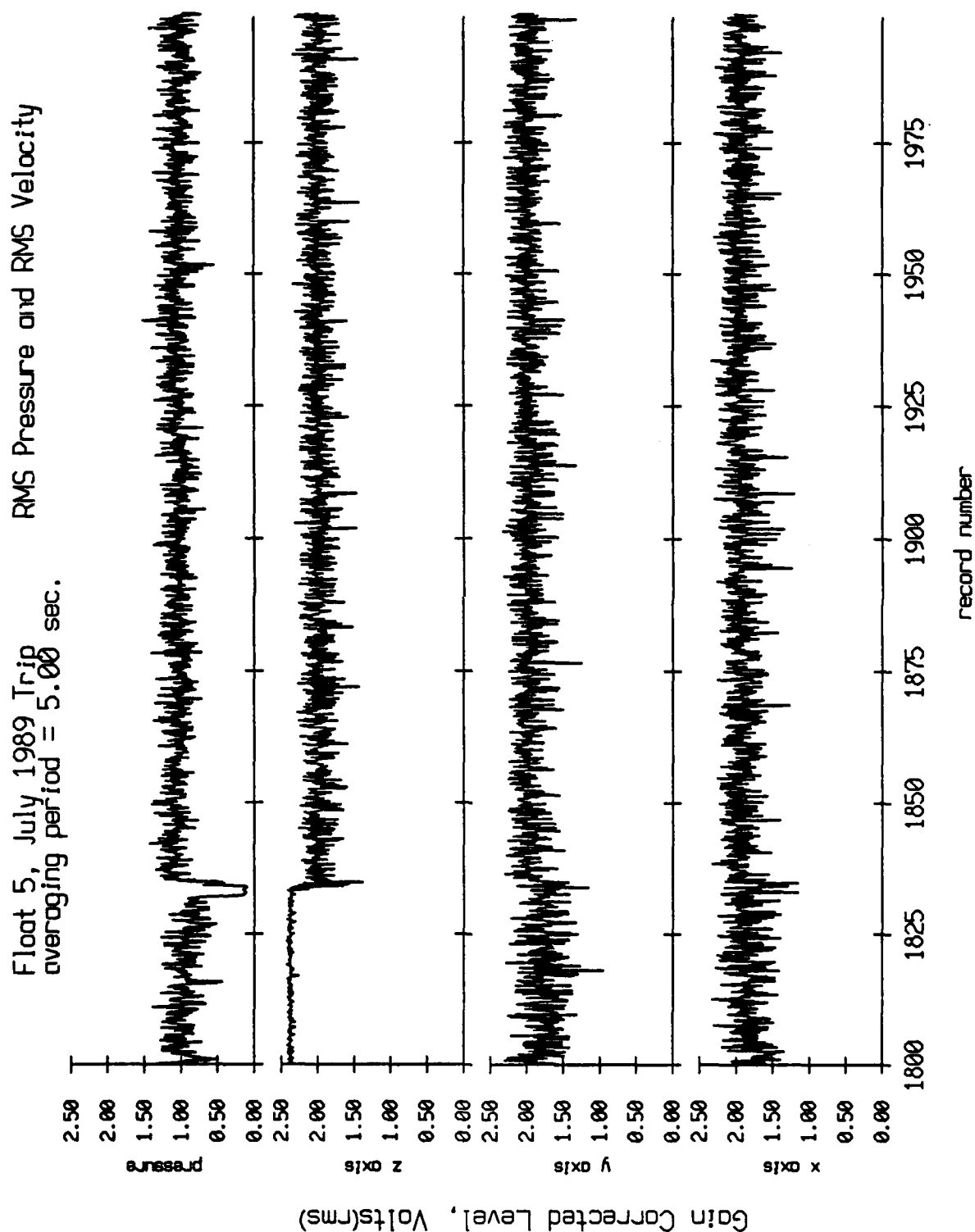


Figure X.6g

Float 5, July 1989 Trip  
 averaging period = 5.00 sec.

RMS Pressure and RMS Velocity

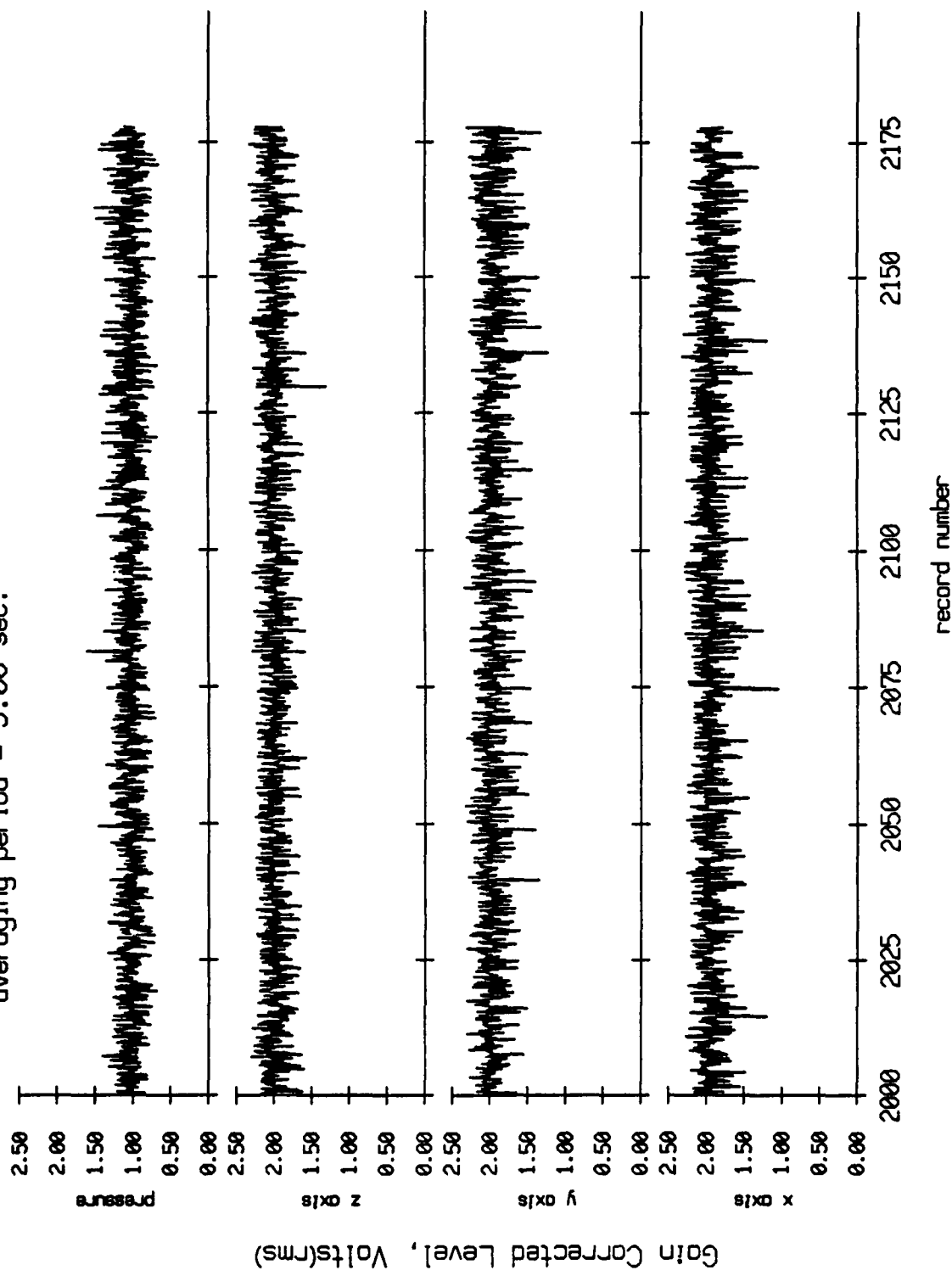


Figure X.6h

Float 6, July 1989 Trip  
 averaging period = 5.00 sec.      RMS Pressure and RMS Velocity

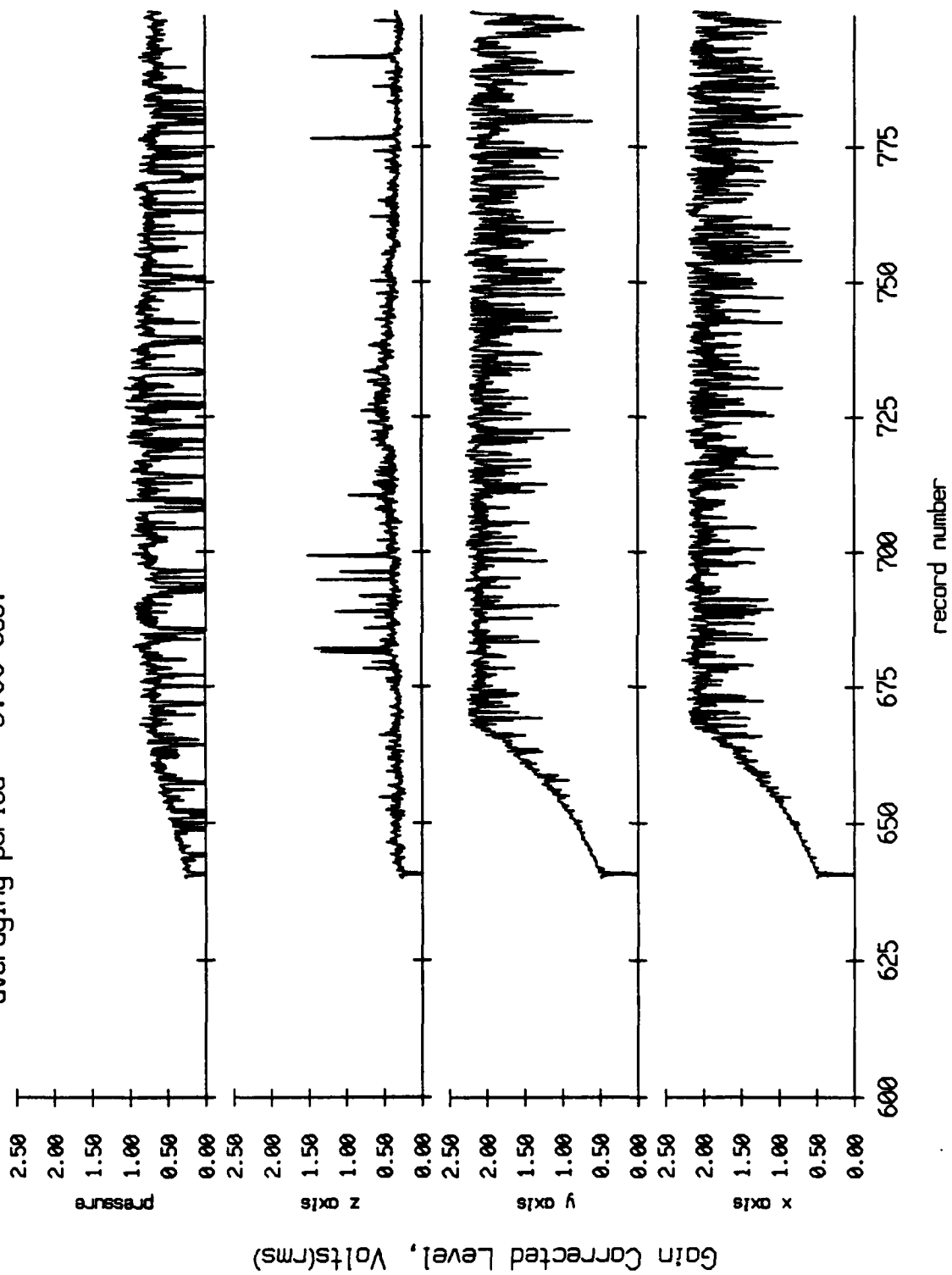


Figure X.7a

Float 6, July 1989 Trip  
 averaging period = 5.00 sec.

RMS Pressure and RMS Velocity

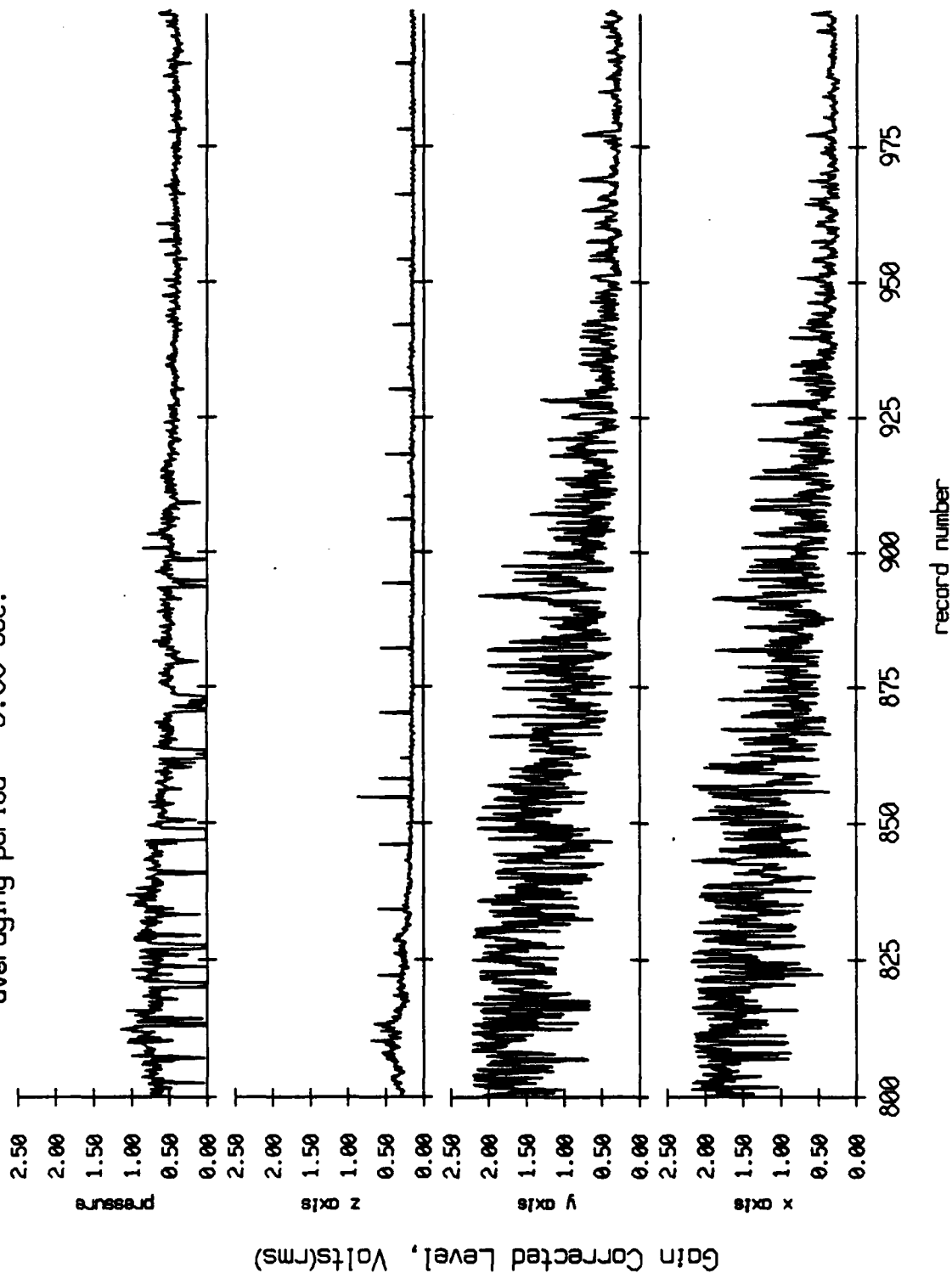


Figure X.7b

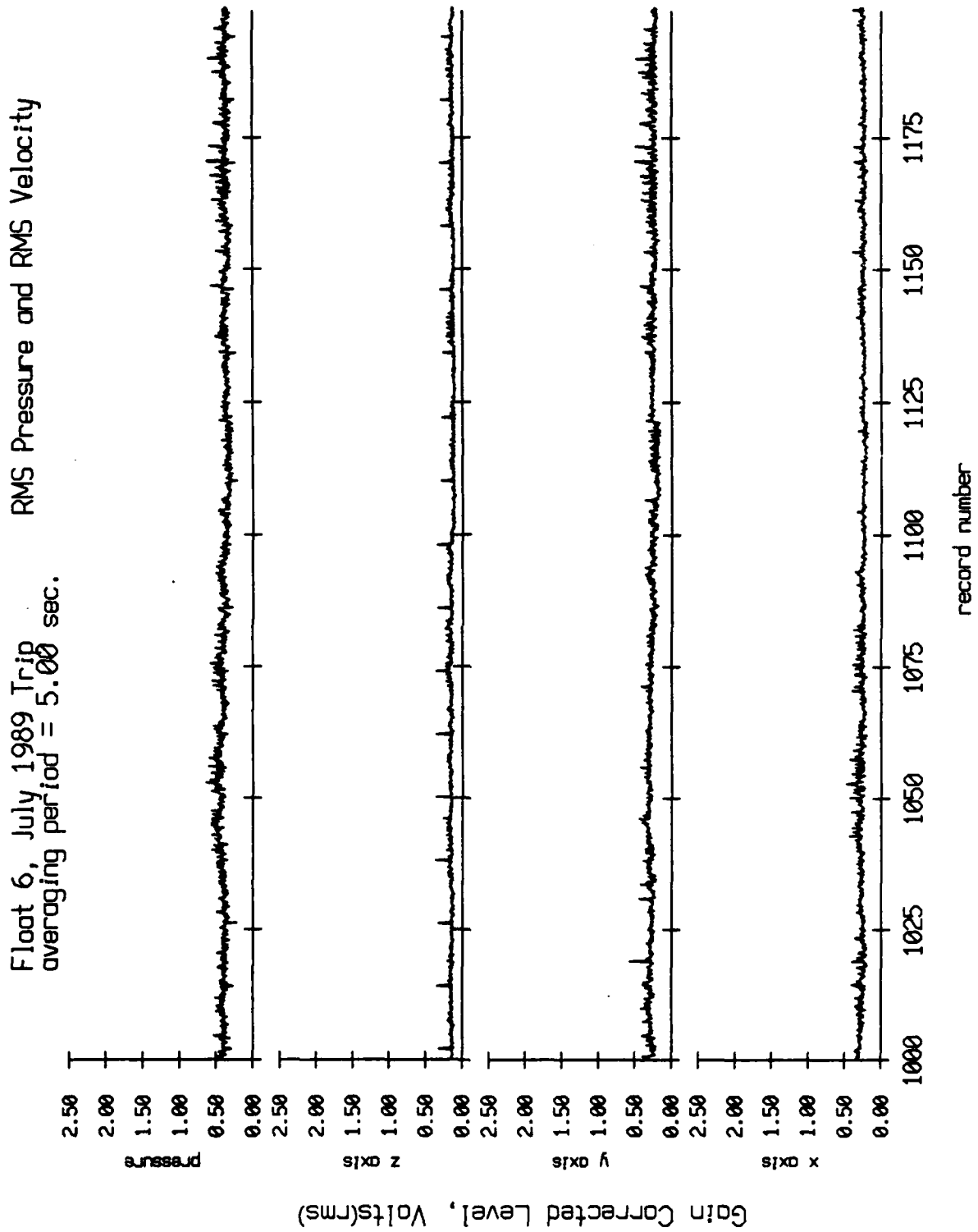


Figure X.7c

Float 6, July 1989 Trip  
 averaging period = 5.00 sec.  
 RMS Pressure and RMS Velocity

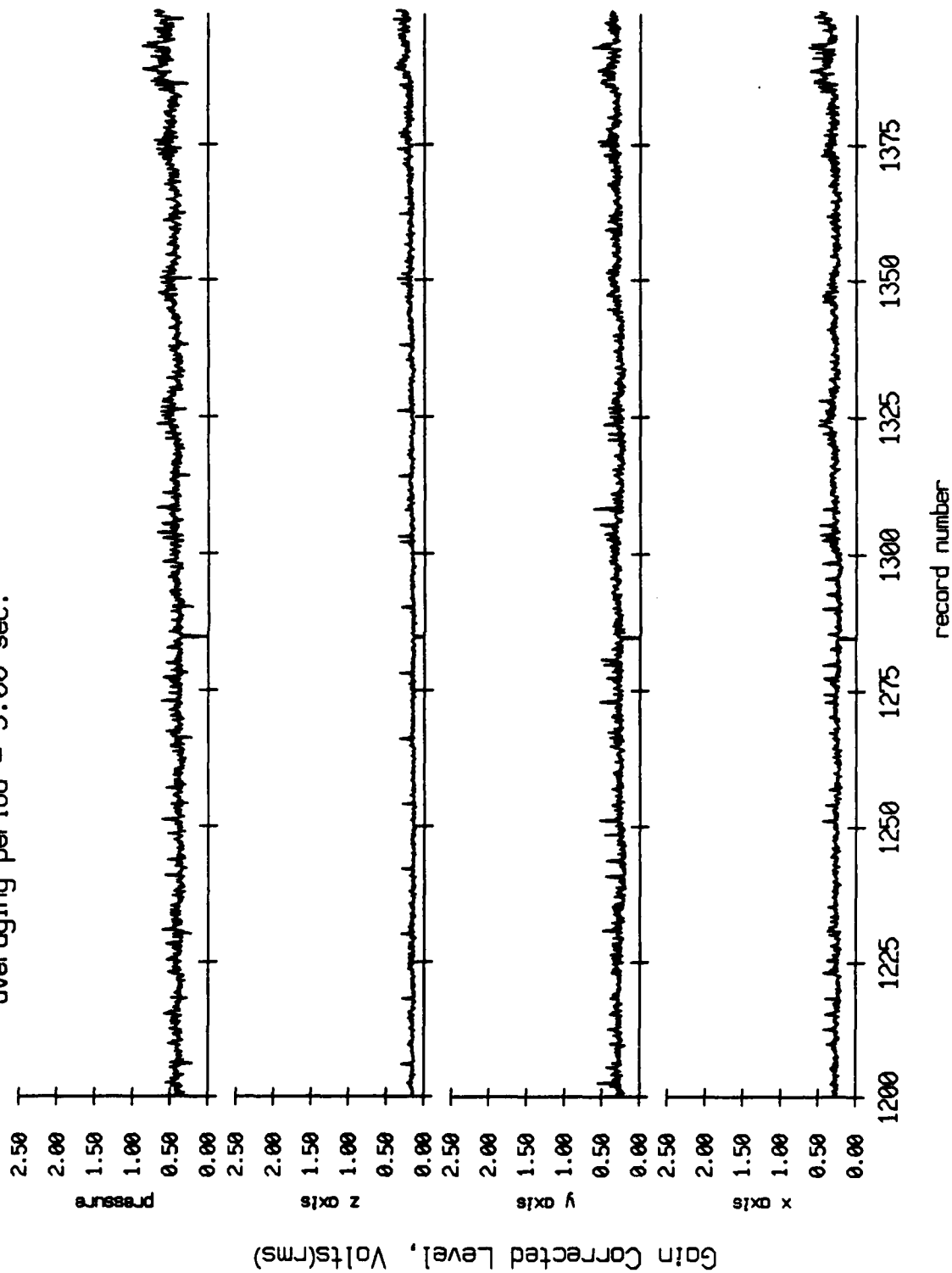


Figure X.7d



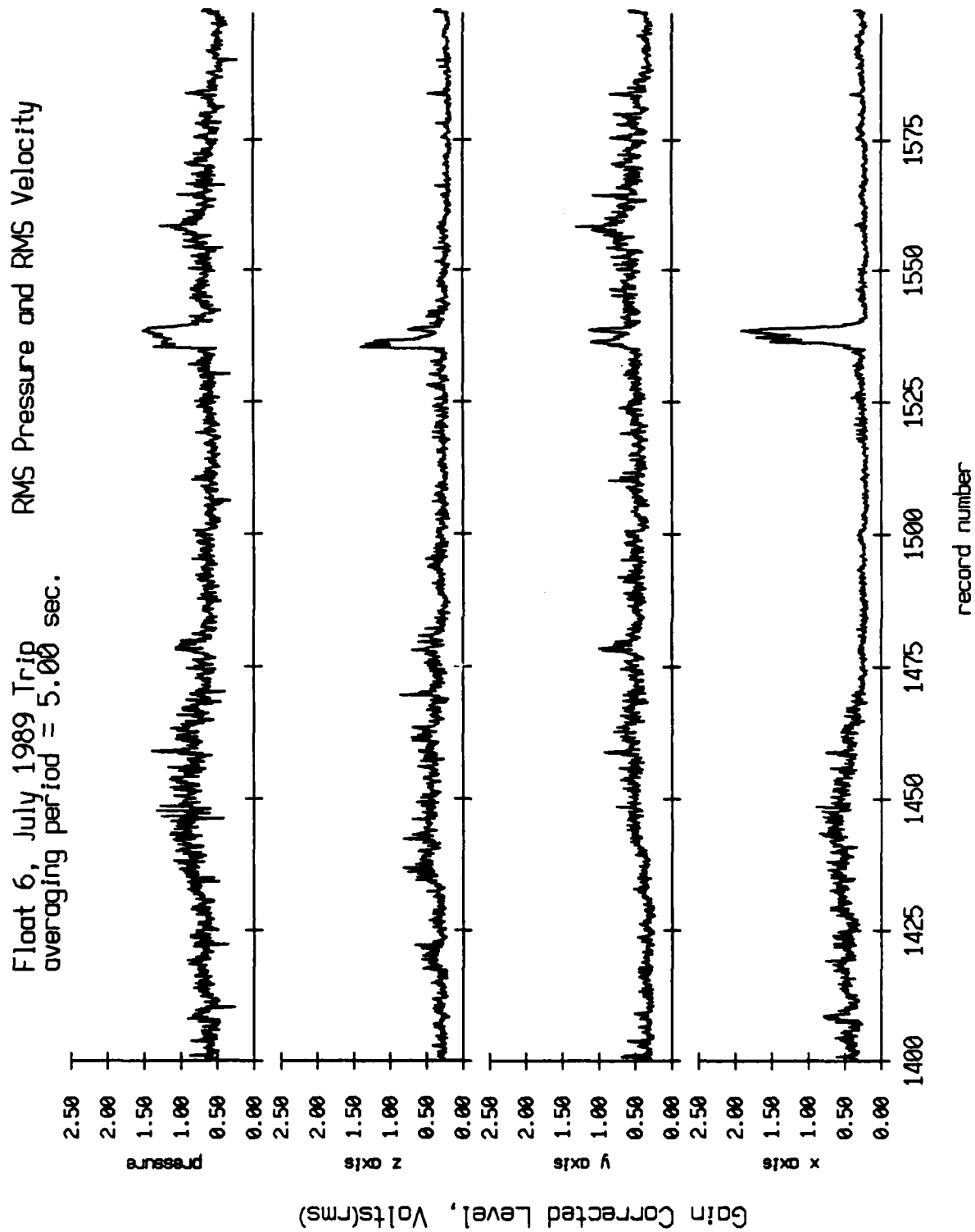


Figure X.7e

Float 6, July 1989 Trip  
 averaging period = 5.00 sec.  
 RMS Pressure and RMS Velocity

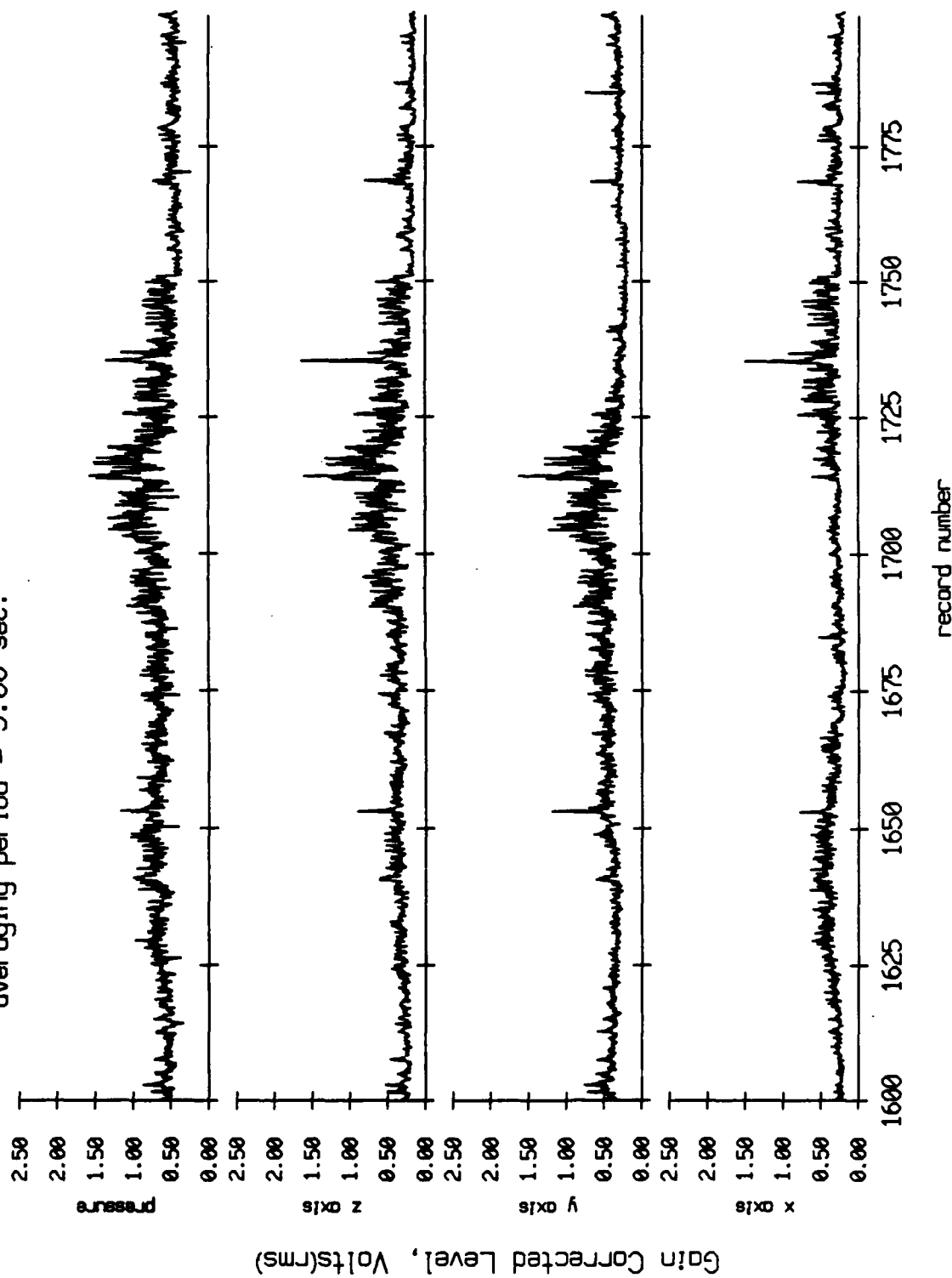


Figure X.7f

Float 6, July 1989 Trip  
 averaging period = 5.00 sec.

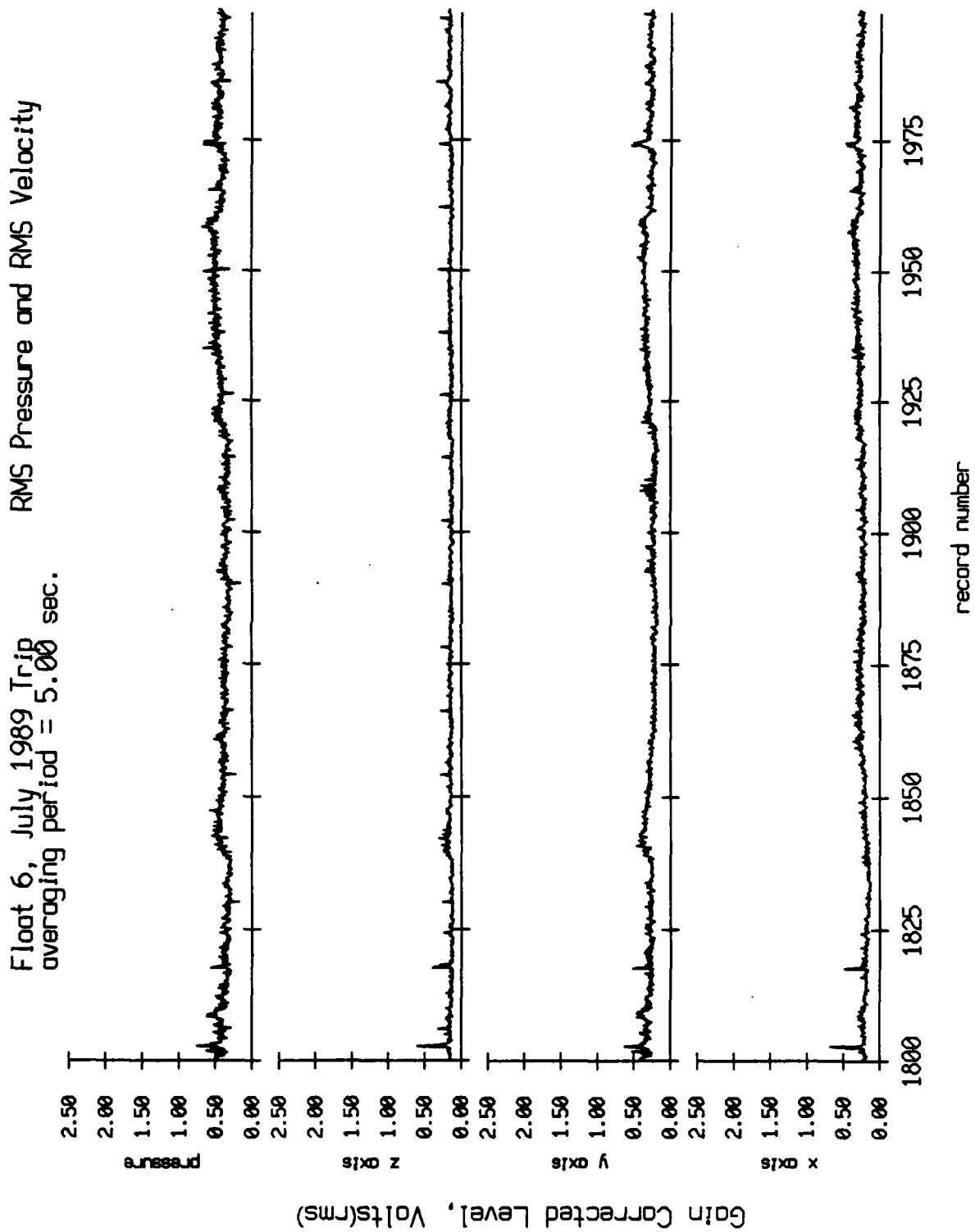


Figure X.7g

Float 6, July 1989 Trip  
 averaging period = 5.00 sec.

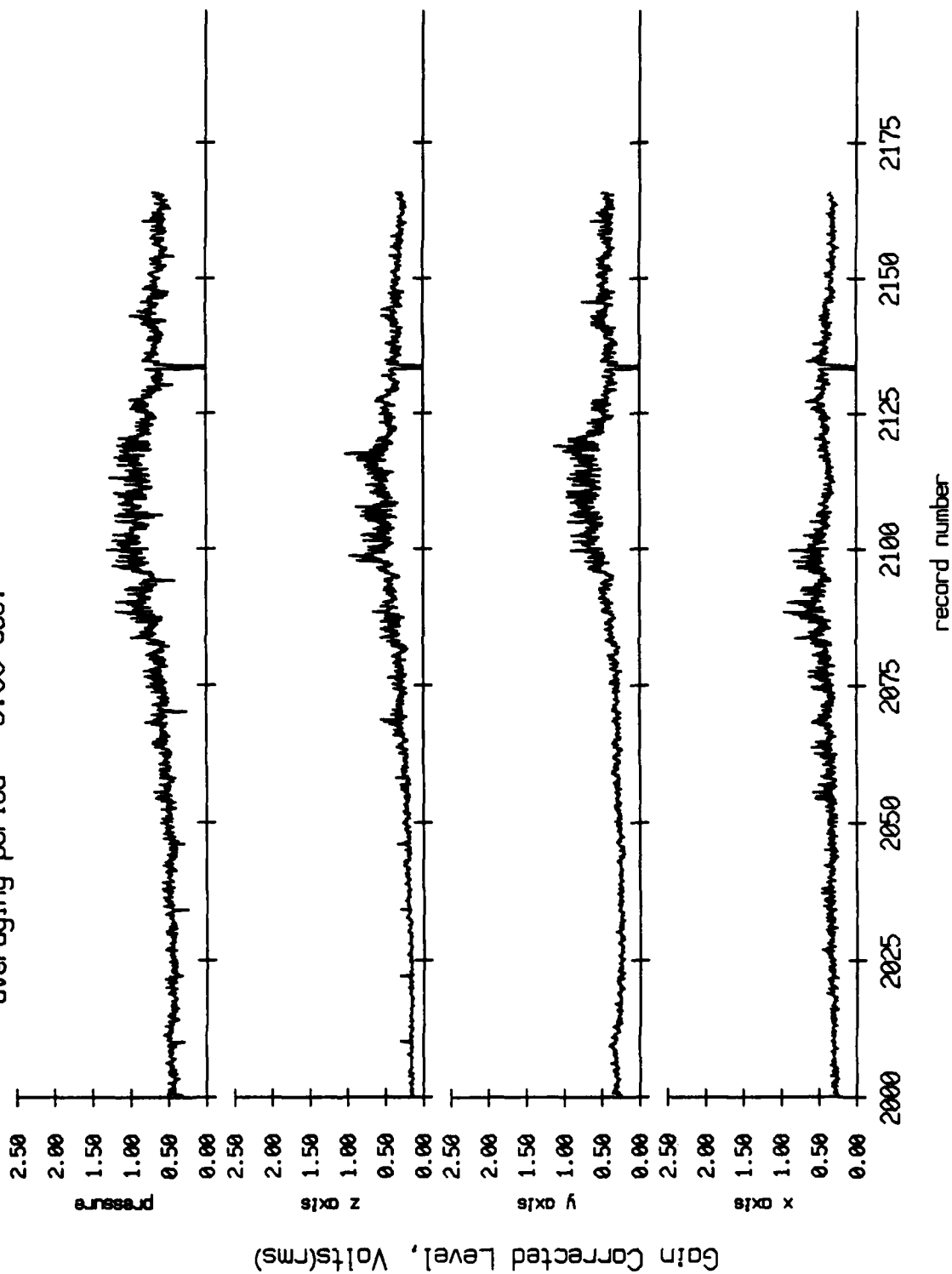


Figure X.7h

Float 7, July 1989 Trip  
 averaging period = 5.00 sec.

RMS Pressure and RMS Velocity

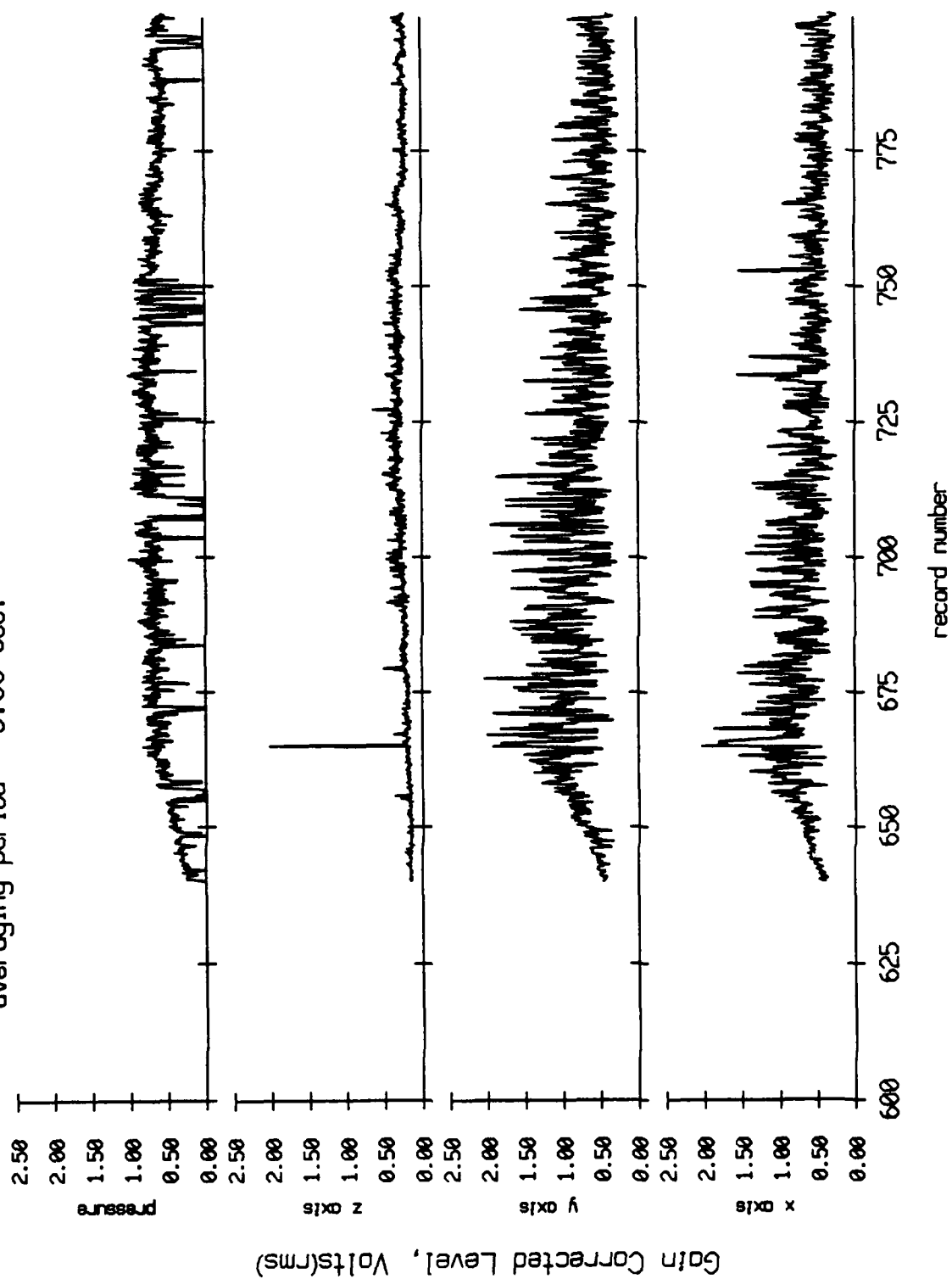


Figure X.8a

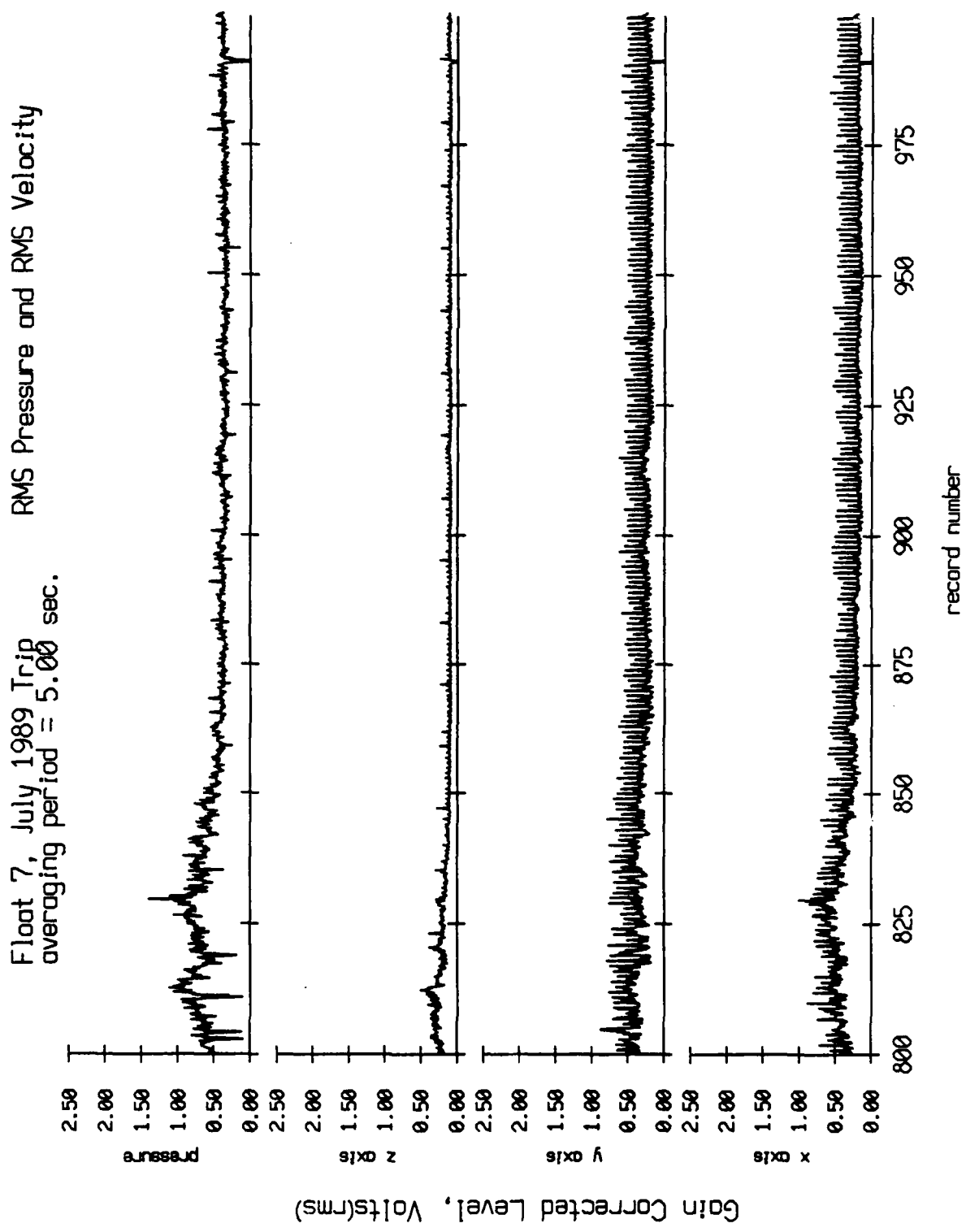


Figure X.8b

Float 7, July 1989 Trip  
 averaging period = 5.00 sec.

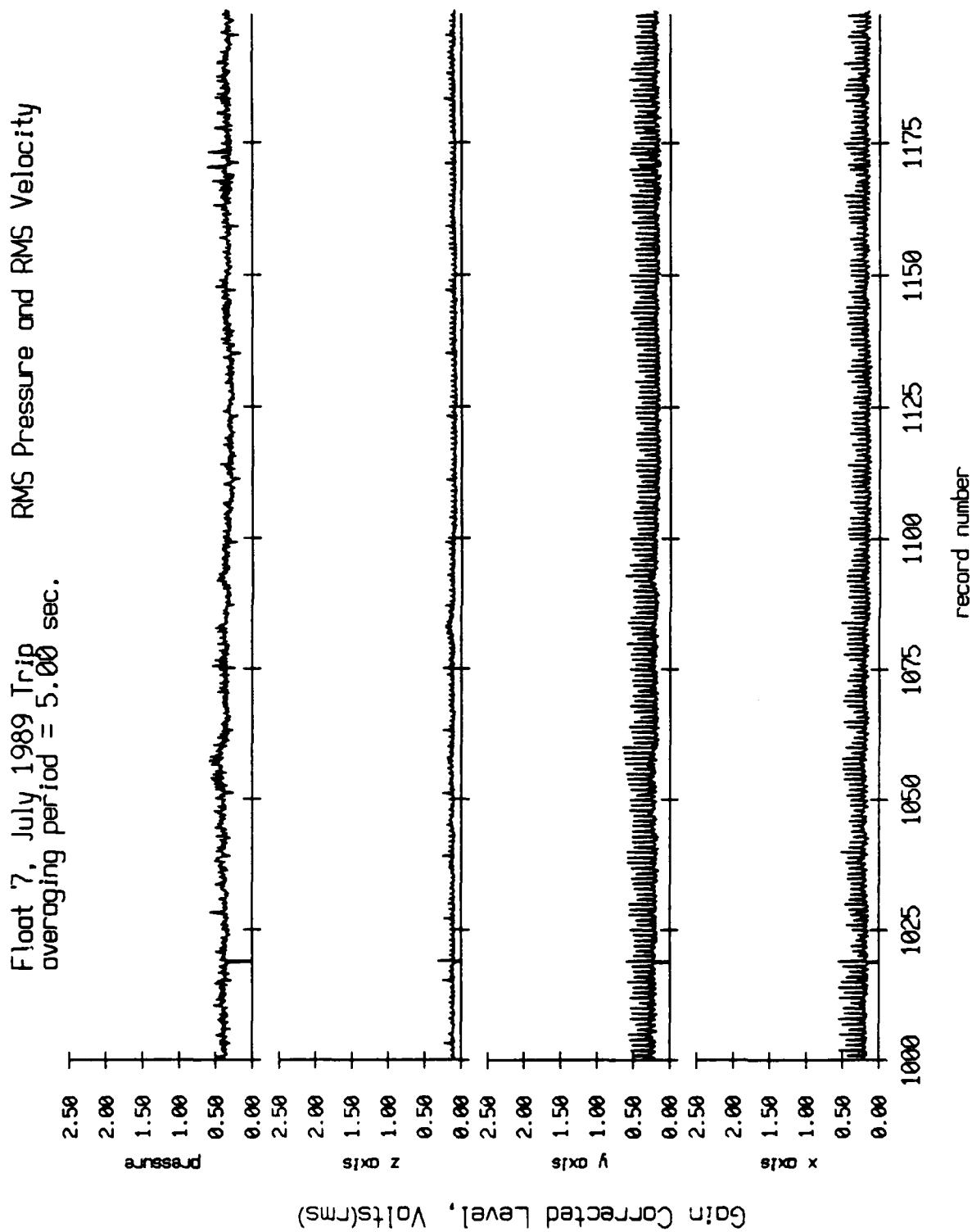


Figure X.8c

Float 7, July 1989 Trip  
 averaging period = 5.00 sec.

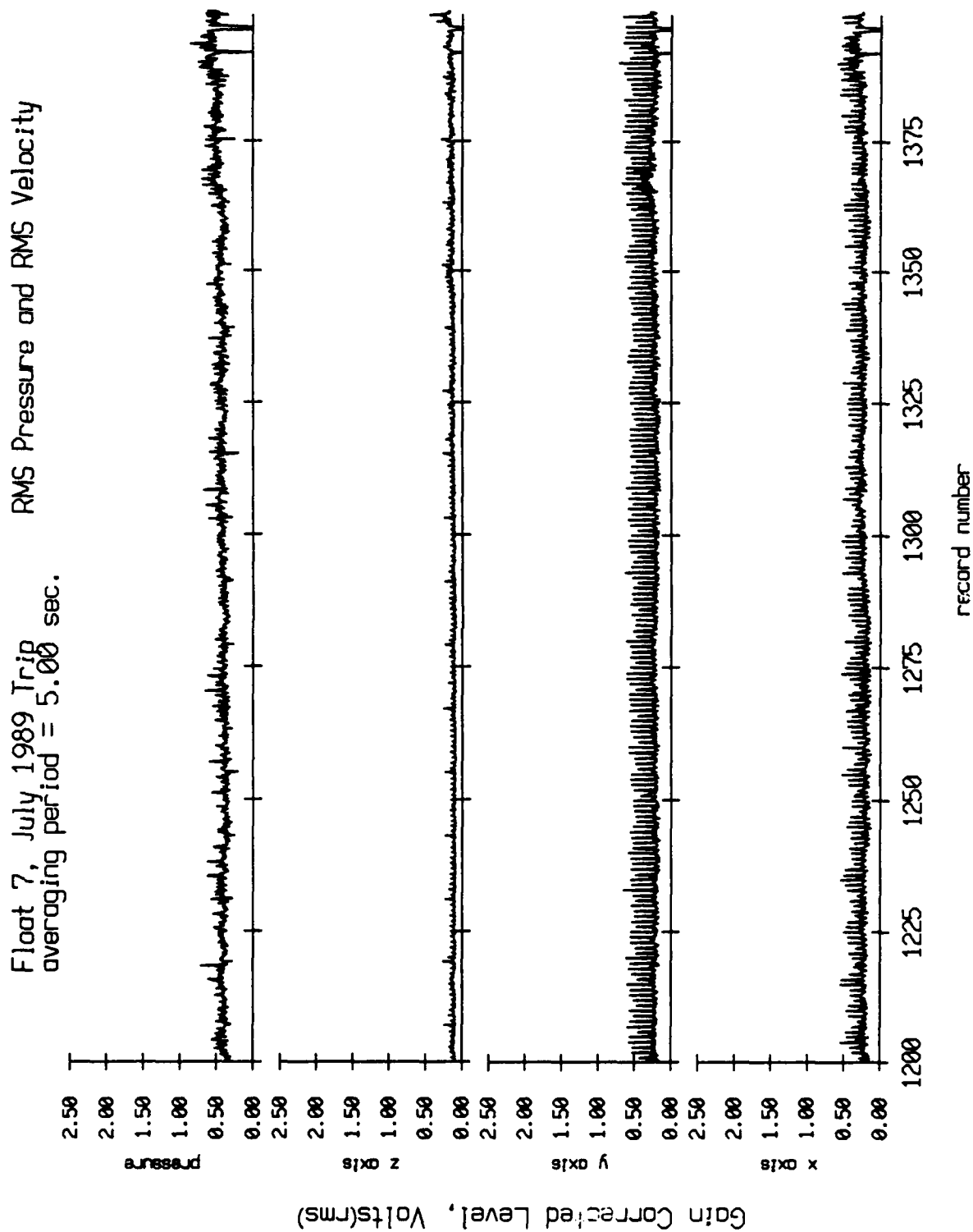


Figure X.8d



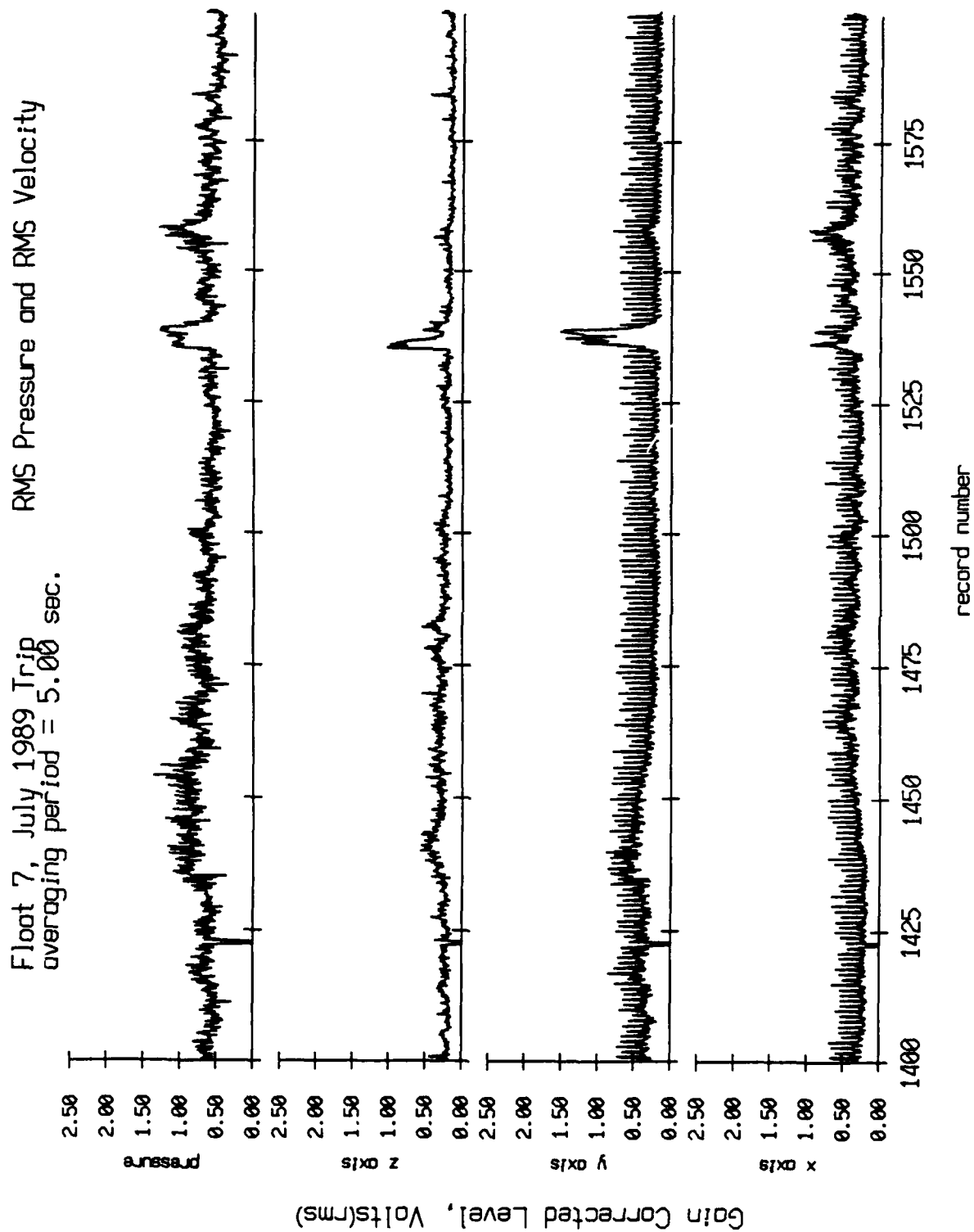


Figure X.8e

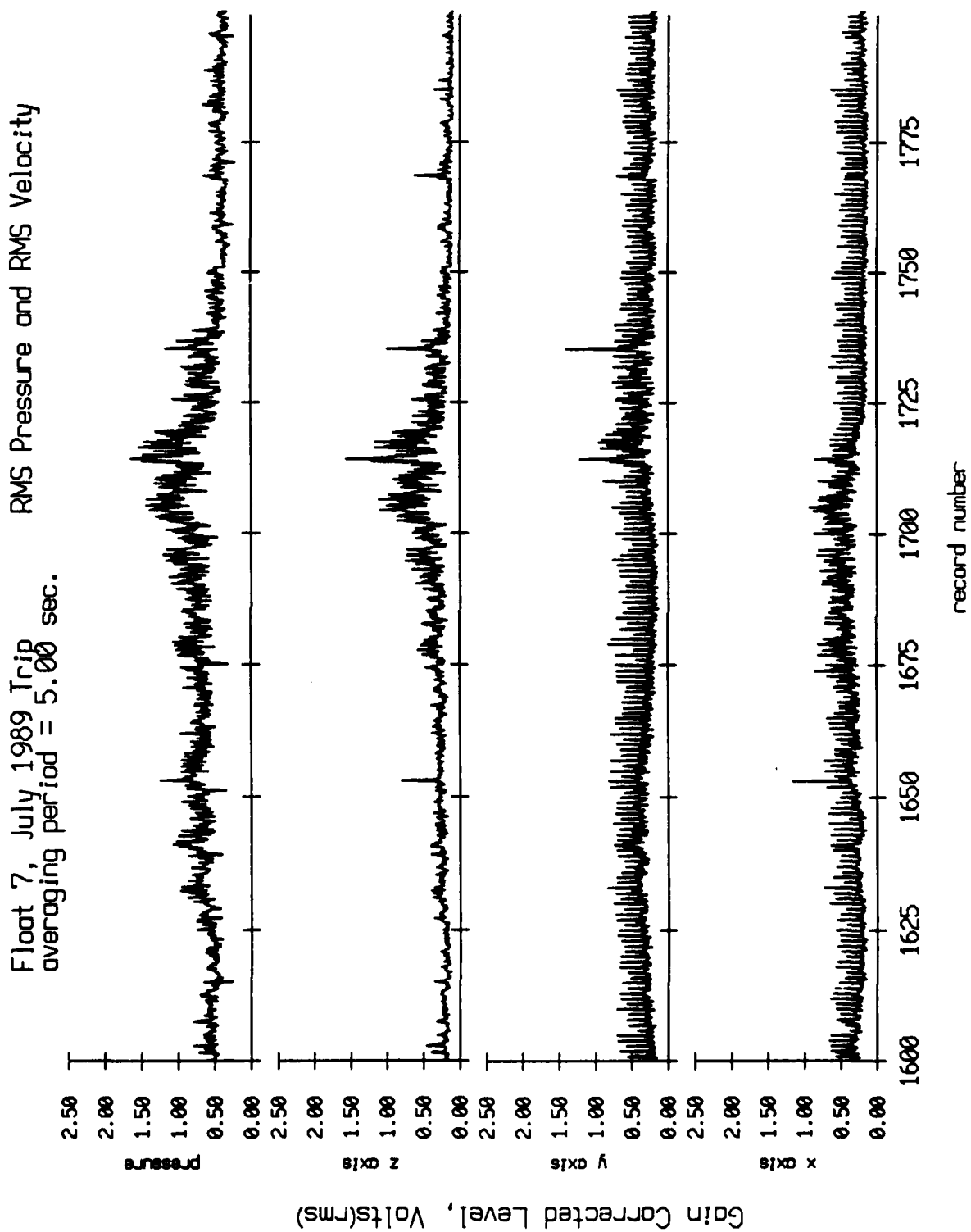


Figure X.8f

Float 7, July 1989 Trip  
 averaging period = 5.00 sec.

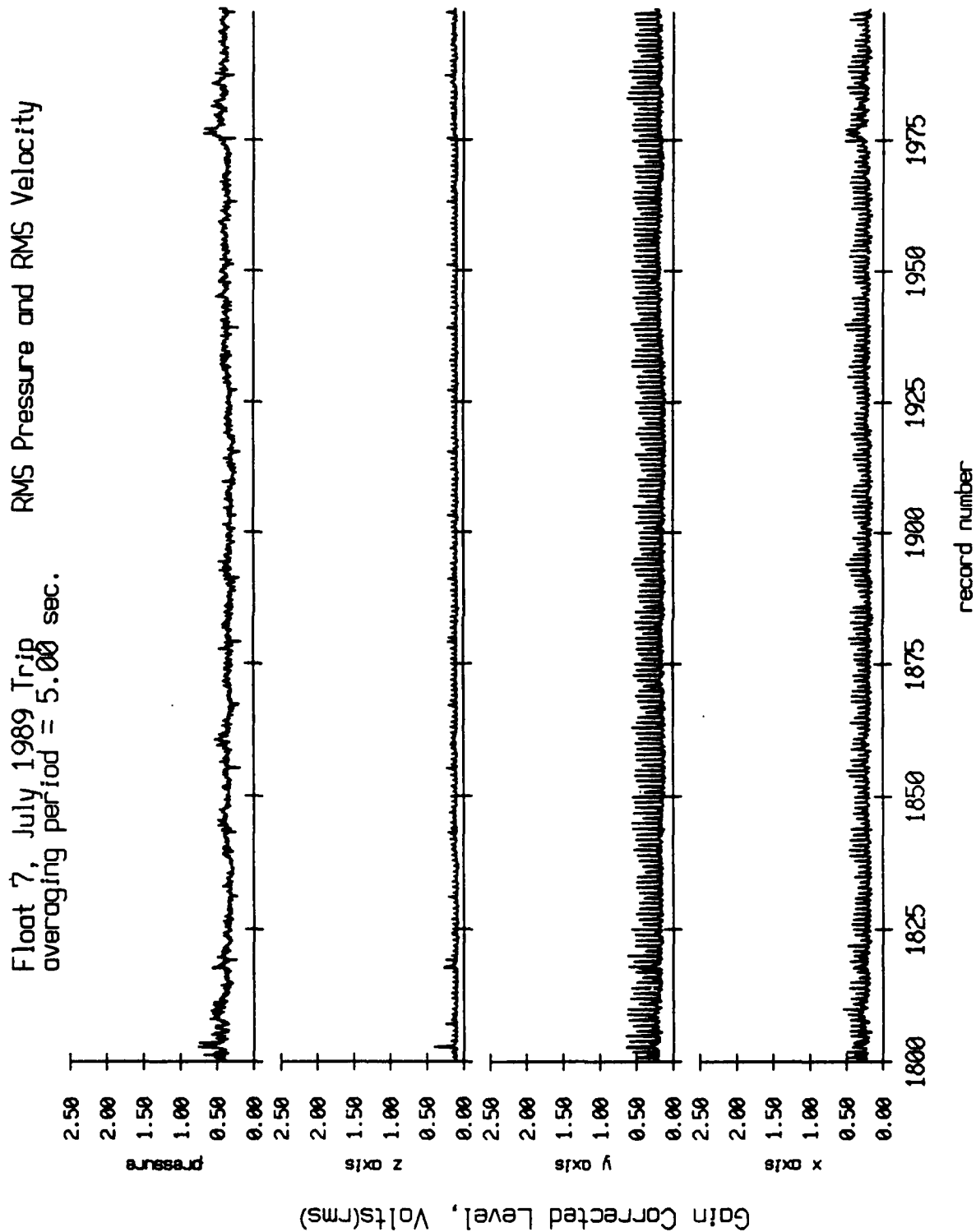
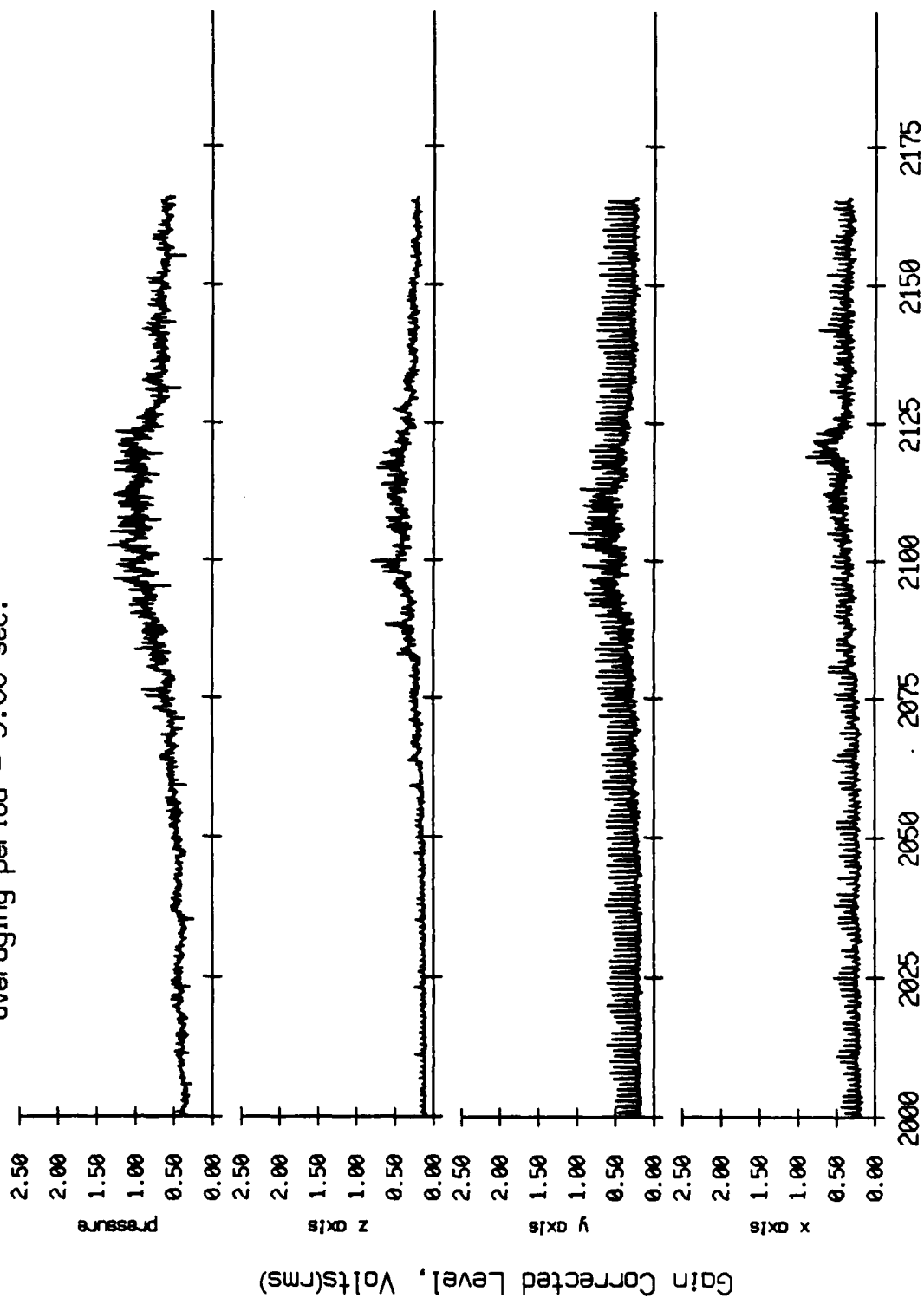


Figure X.8g

Float 7, July 1989 Trip  
 averaging period = 5.00 sec.

RMS Pressure and RMS Velocity



record number

Figure X.8h

Float 8, July 1989 Trip  
 averaging period = 5.00 sec.

RMS Pressure and RMS Velocity

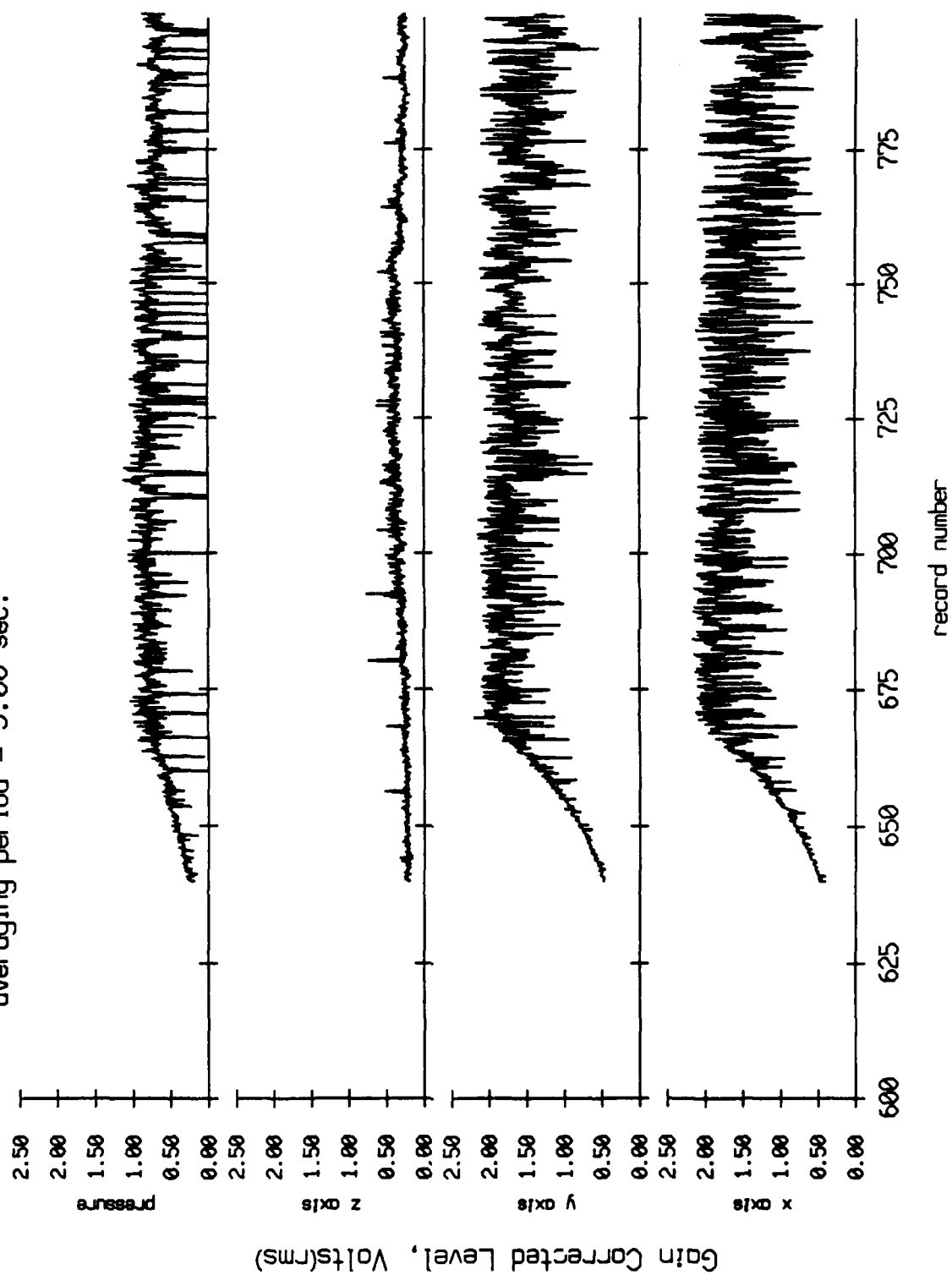


Figure X.9a

Float 8, July 1989 Trip  
 averaging period = 5.00 sec.

RMS Pressure and RMS Velocity

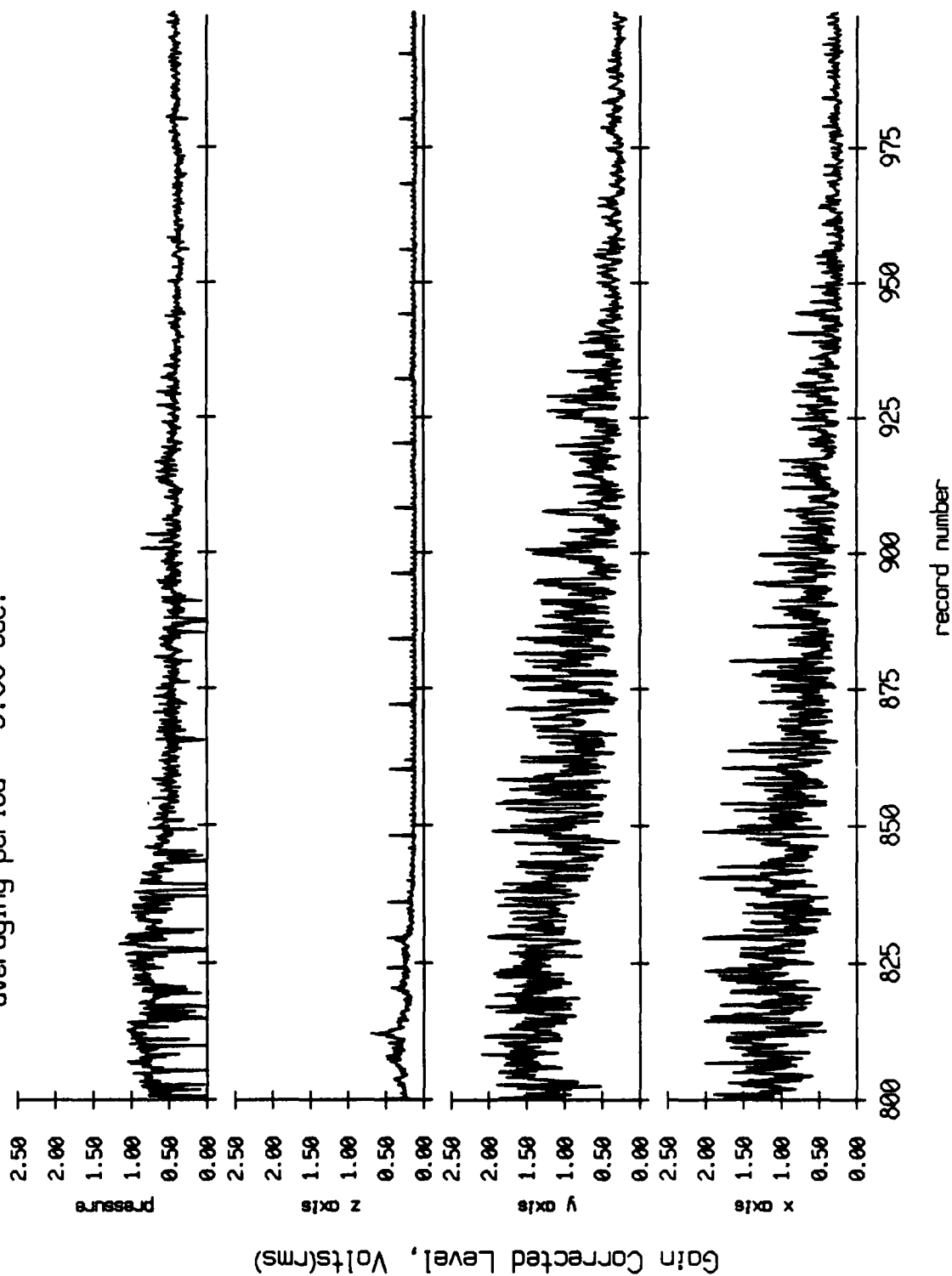


Figure X.9b

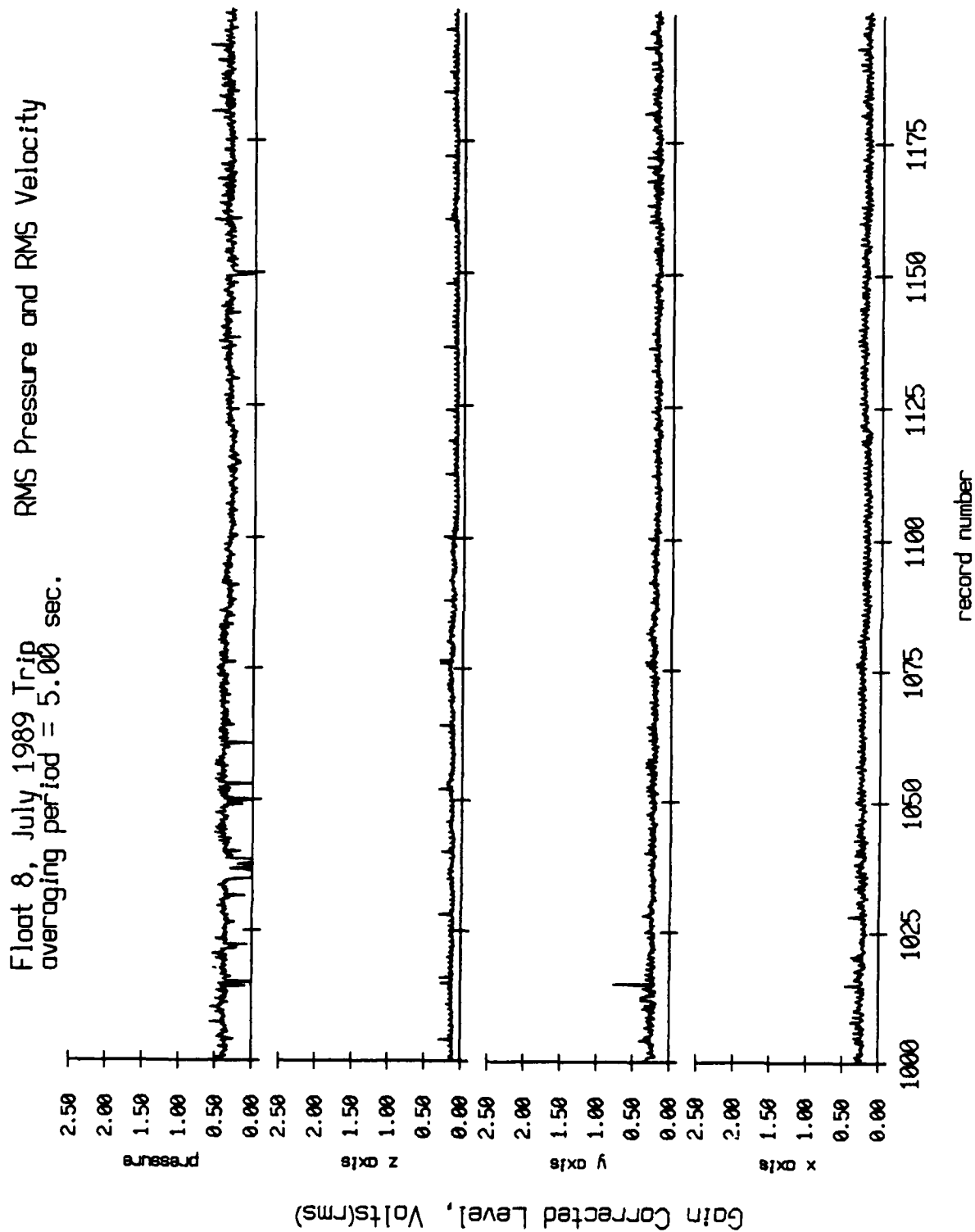


Figure X.9c

Float 8, July 1989 Trip  
 averaging period = 5.00 sec.

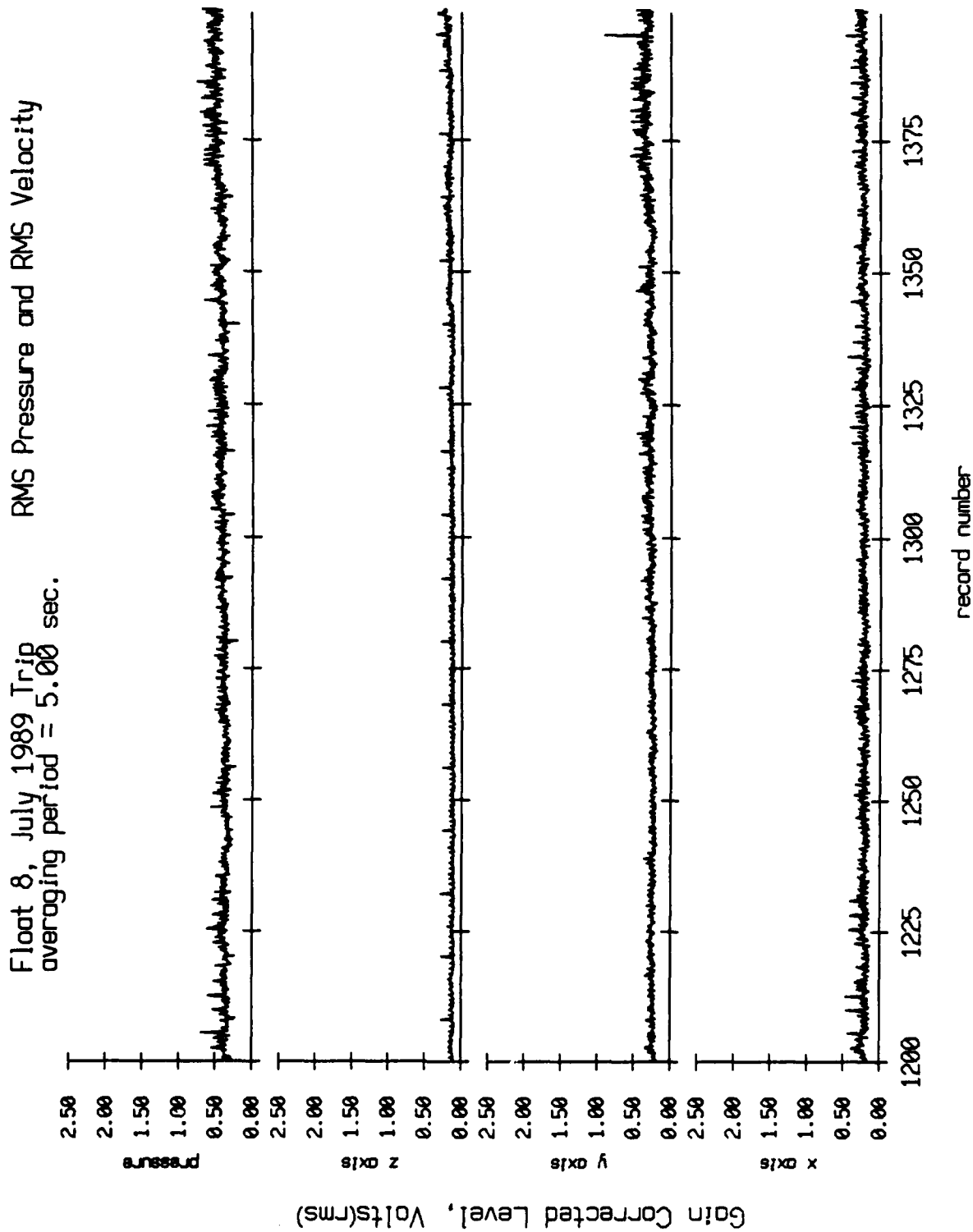


Figure X.9d



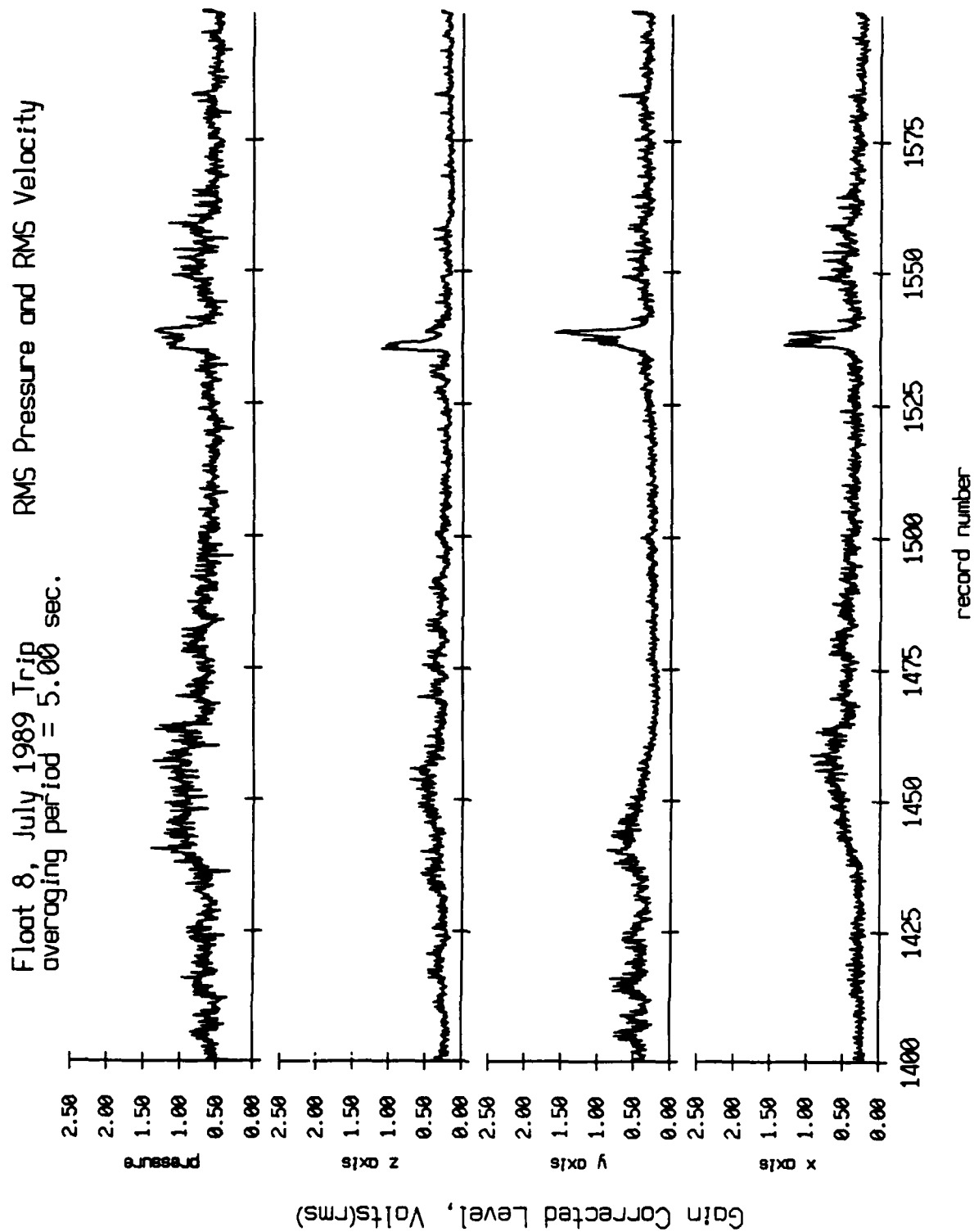


Figure X.9e

Float 8, July 1989 Trip  
 averaging period = 5.00 sec.

RMS Pressure and RMS Velocity

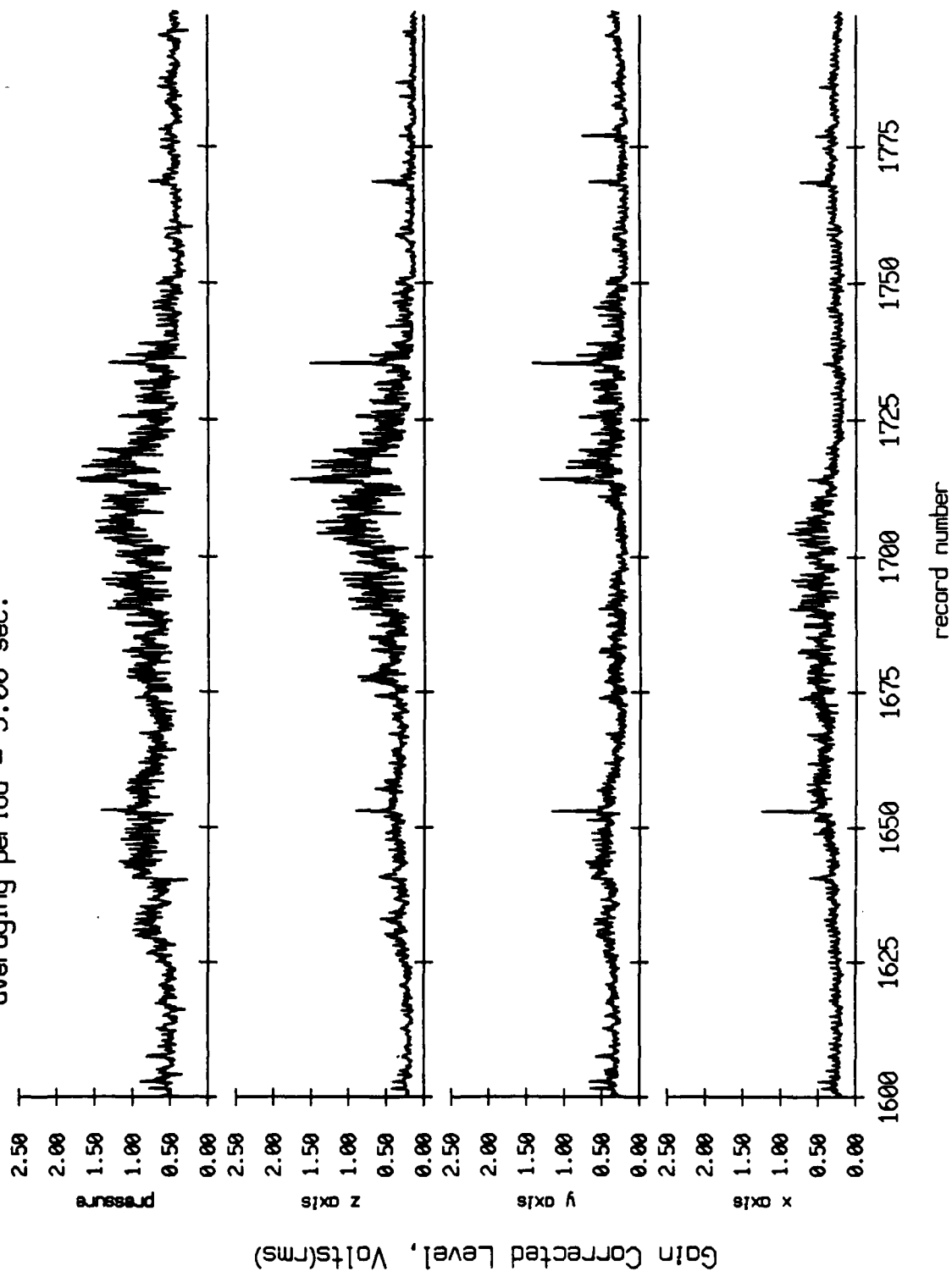


Figure X.9f

Float 8, July 1989 Trip  
 averaging period = 5.00 sec.

RMS Pressure and RMS Velocity

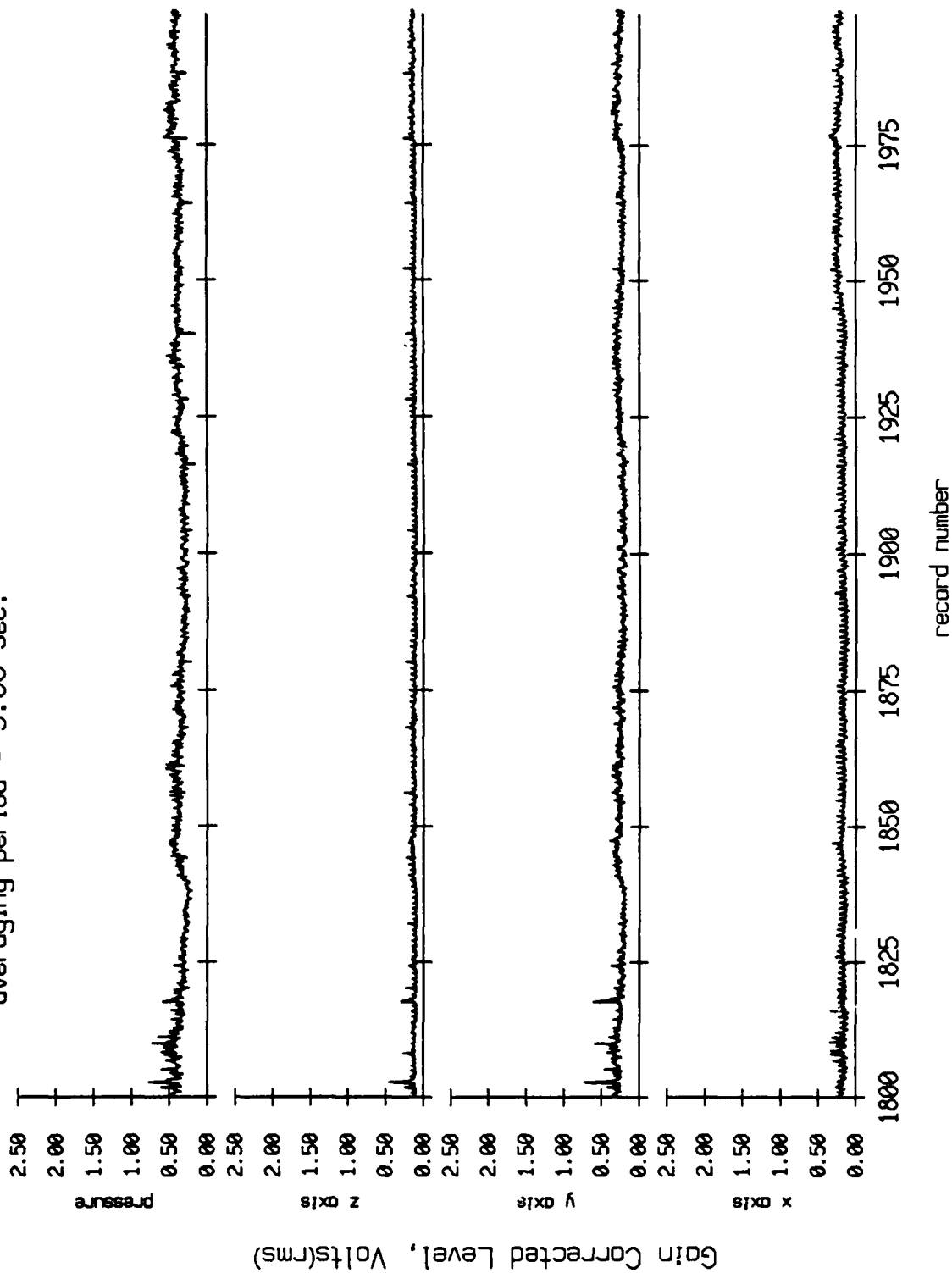


Figure X.9g

Floot 8, July 1989 Trip  
 averaging period = 5.00 sec.

RMS Pressure and RMS Velocity

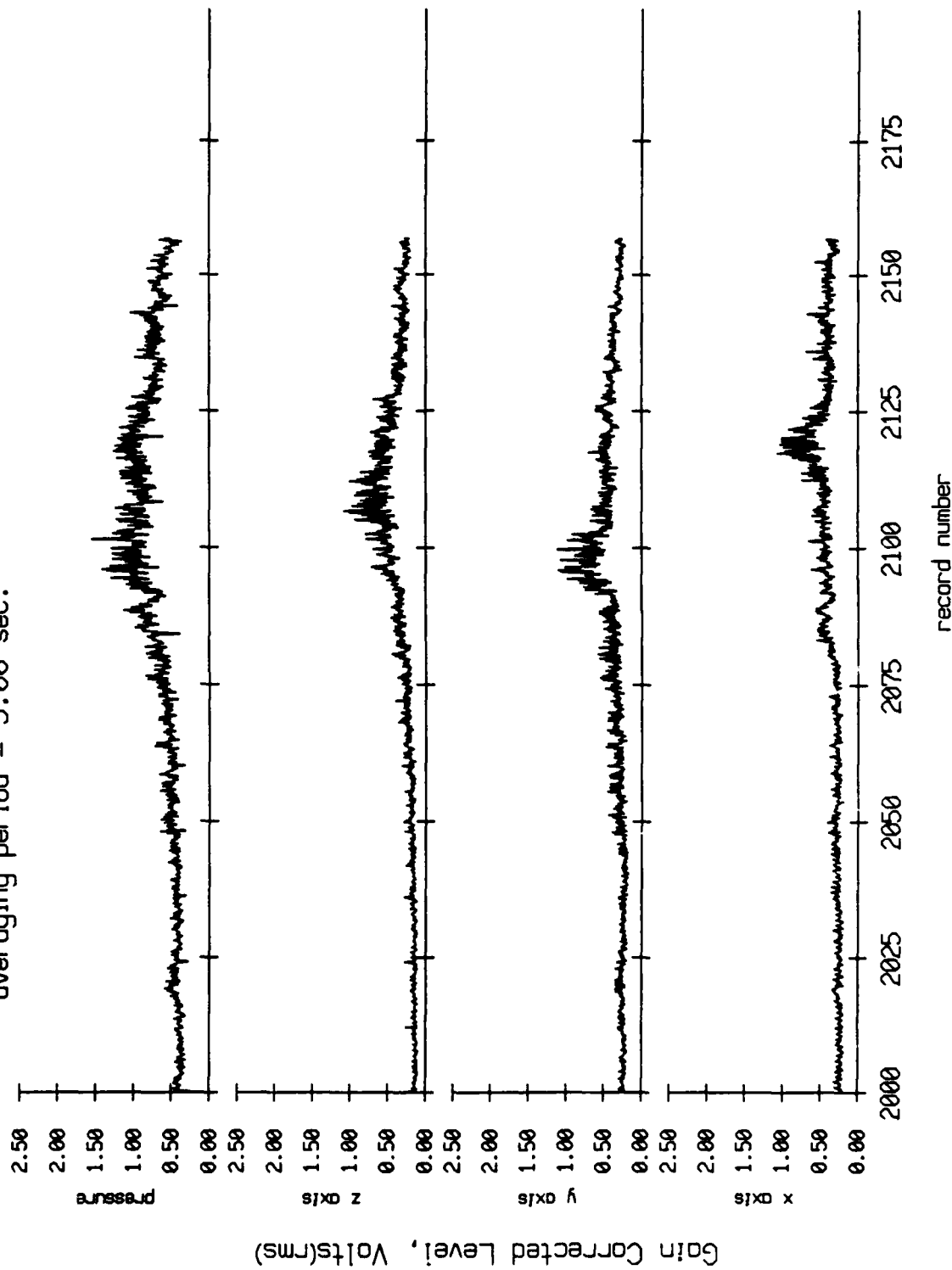


Figure X.9h

Float 9, July 1989 Trip  
 averaging period = 5.00 sec.

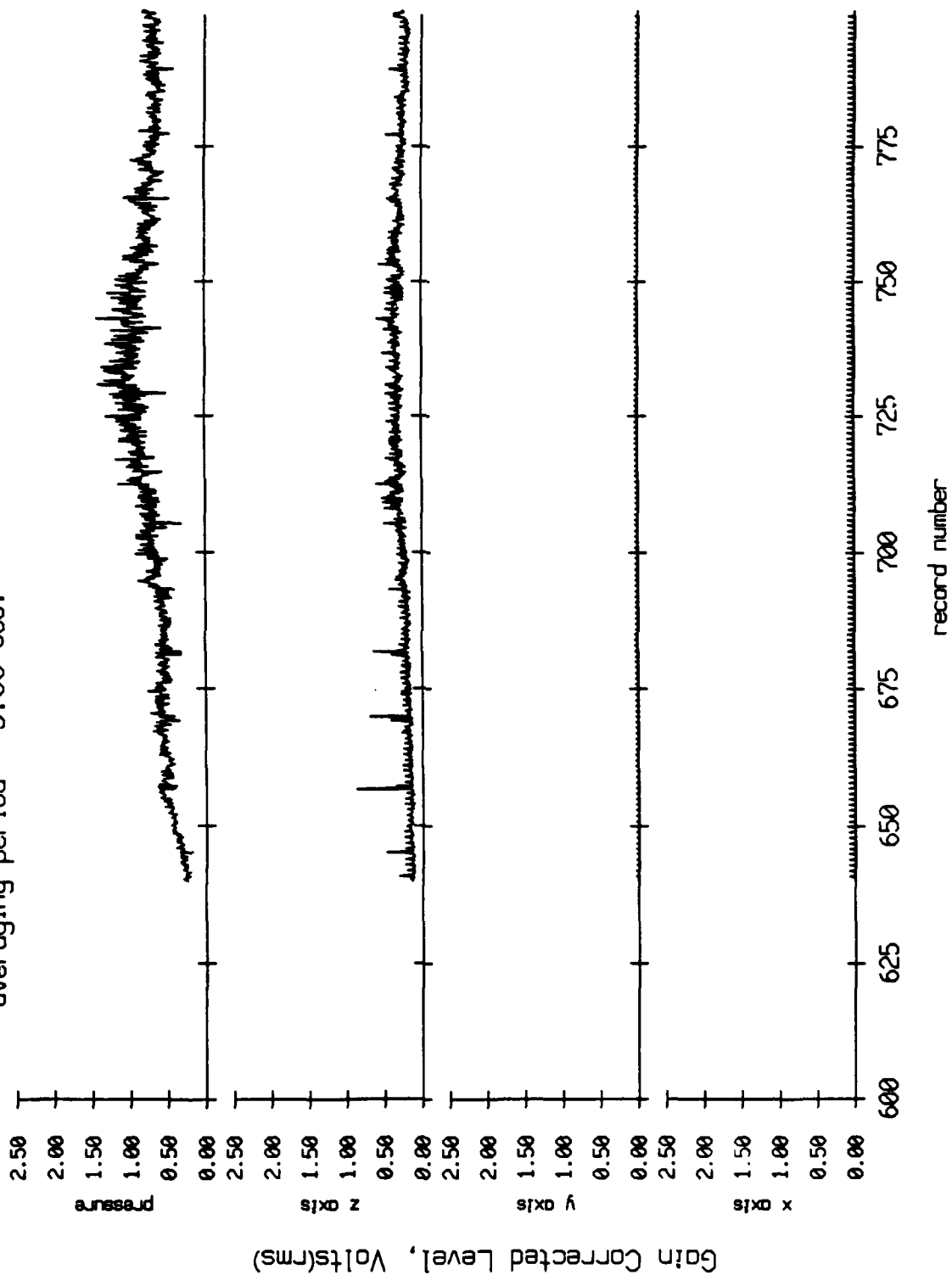


Figure X.10a

Float 9, July 1989 Trip  
 averaging period = 5.00 sec.  
 RMS Pressure and RMS Velocity

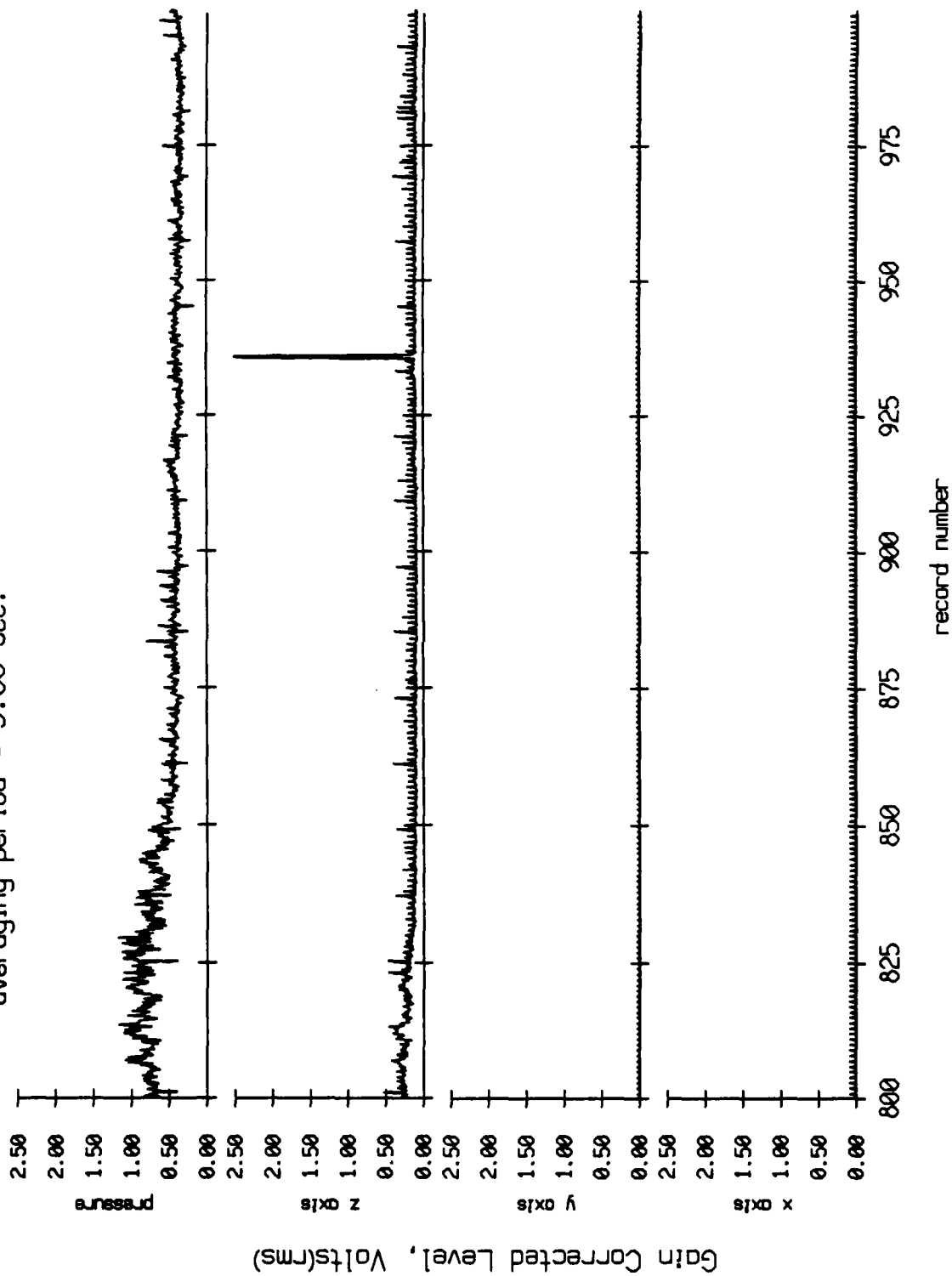


Figure X.10b

Float 9, July 1989 Trip  
 averaging period = 5.00 sec.

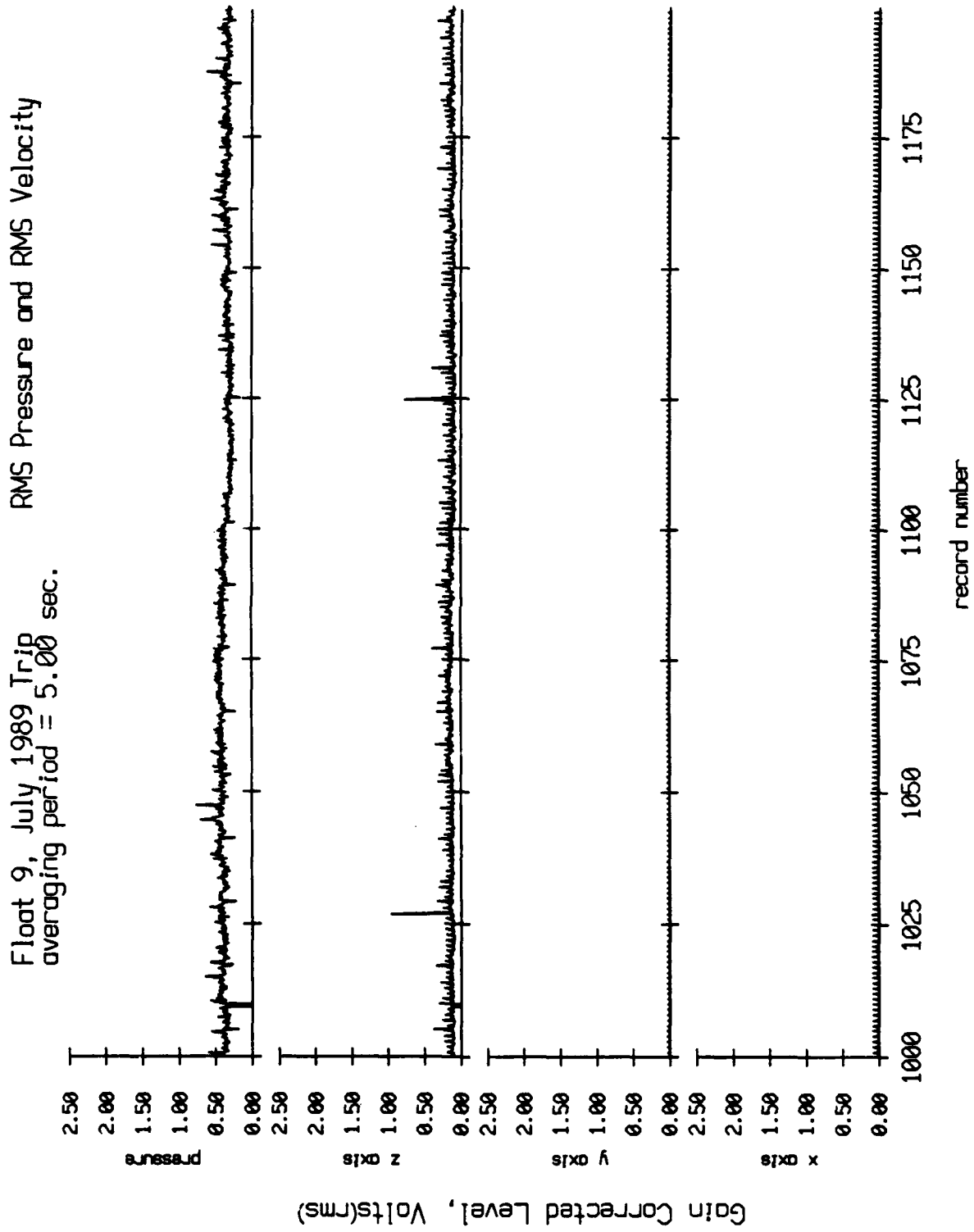


Figure X.10c

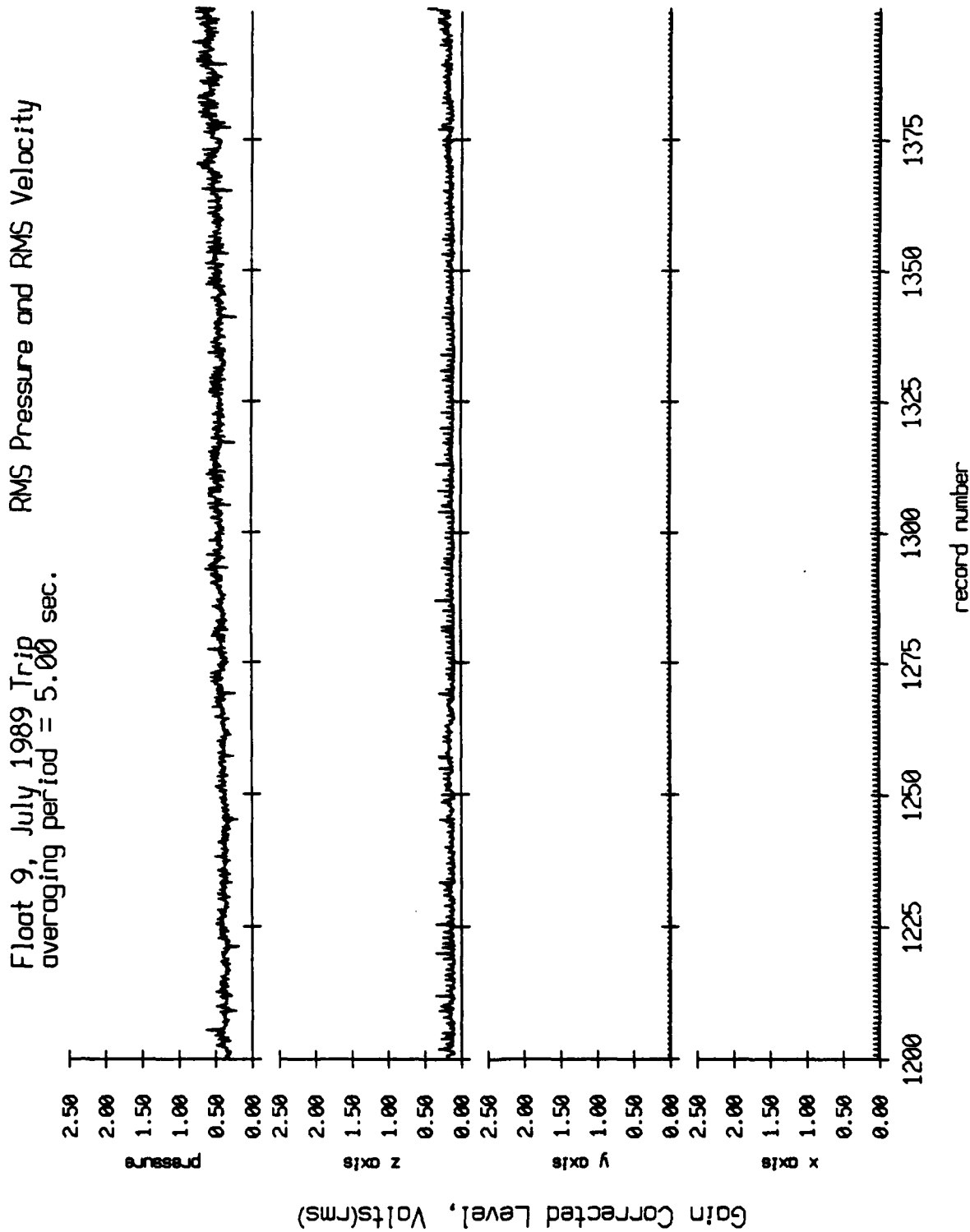


Figure X.10d



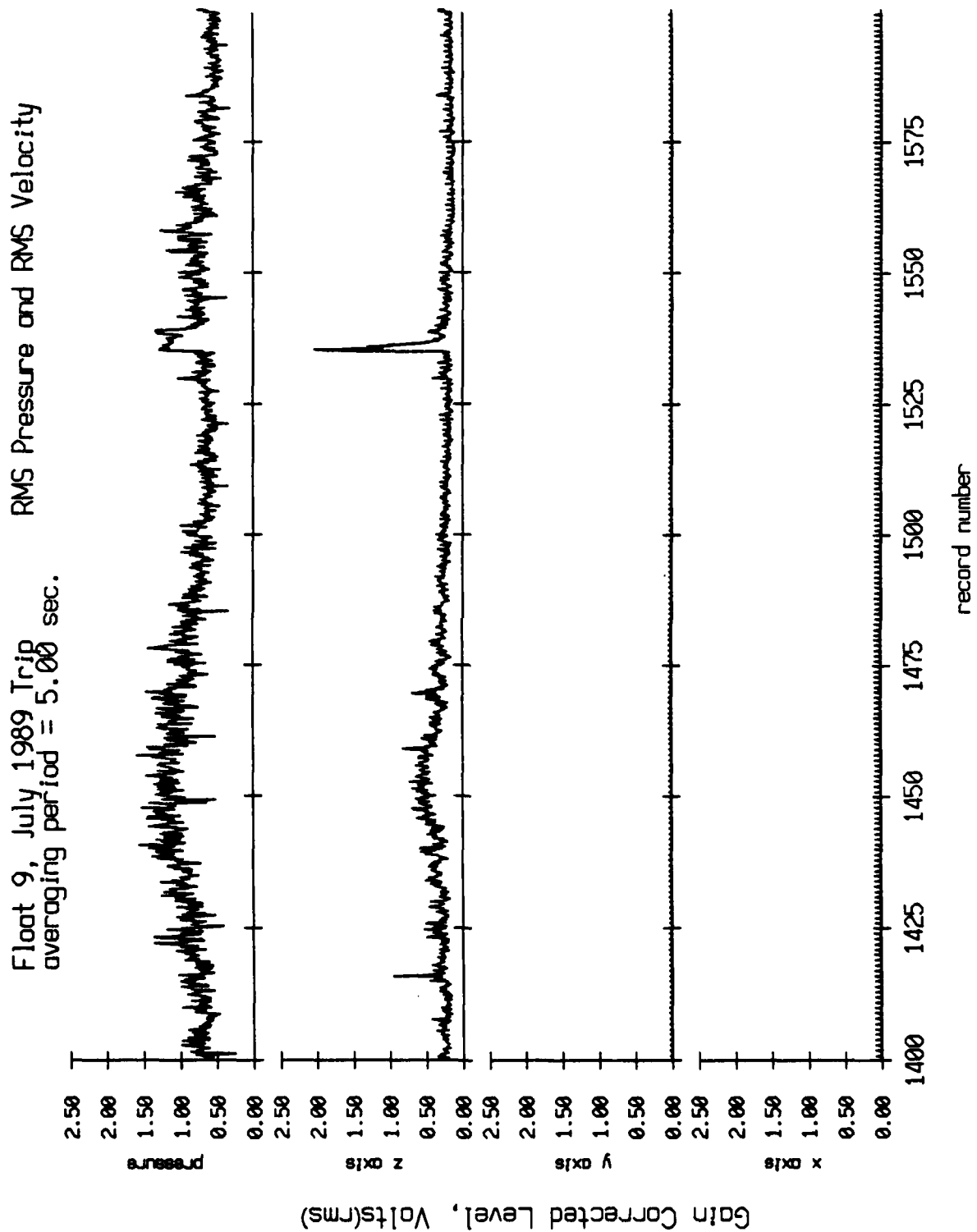


Figure X.10e

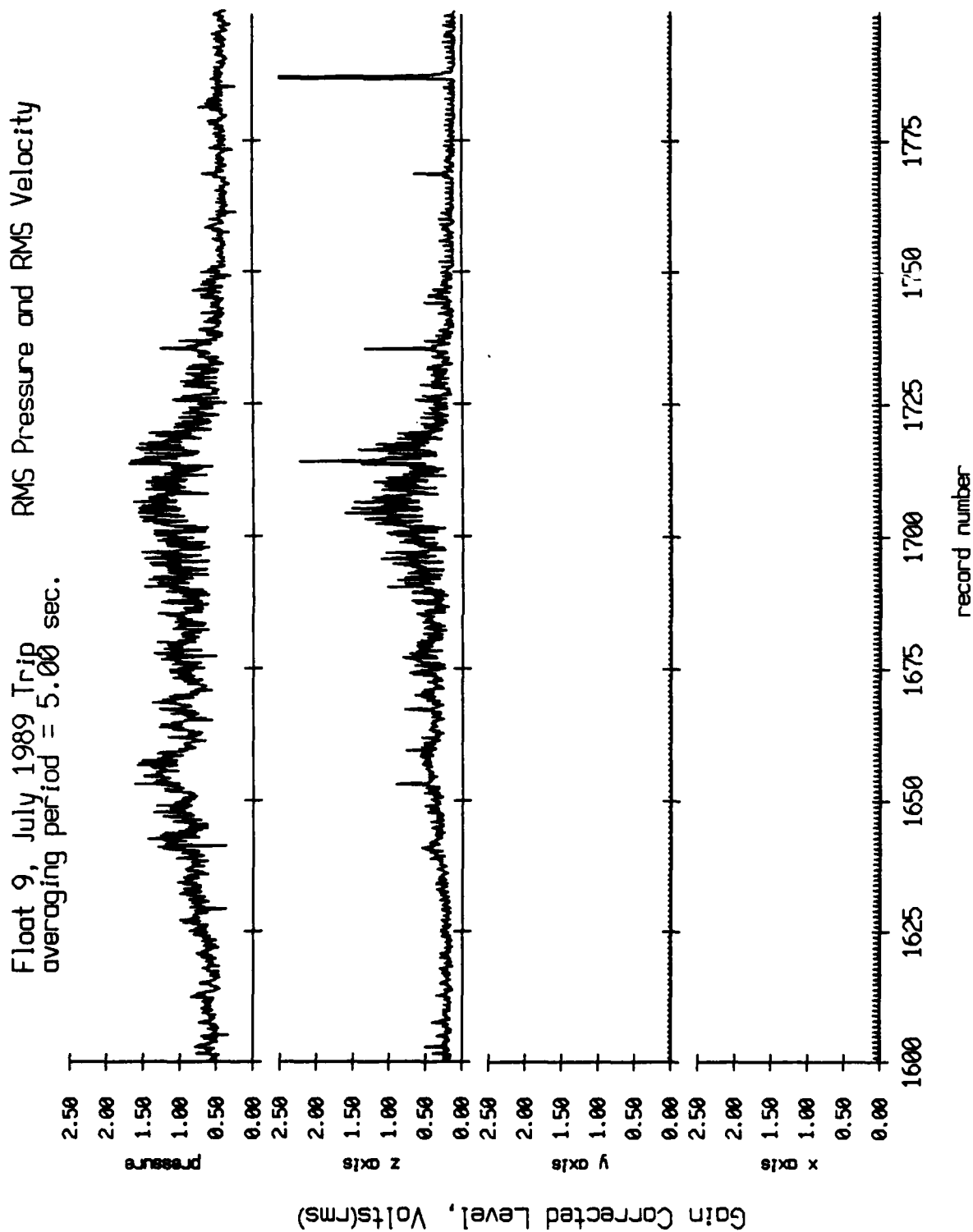


Figure X.10f

Float 9, July 1989 Trip  
 averaging period = 5.00 sec.

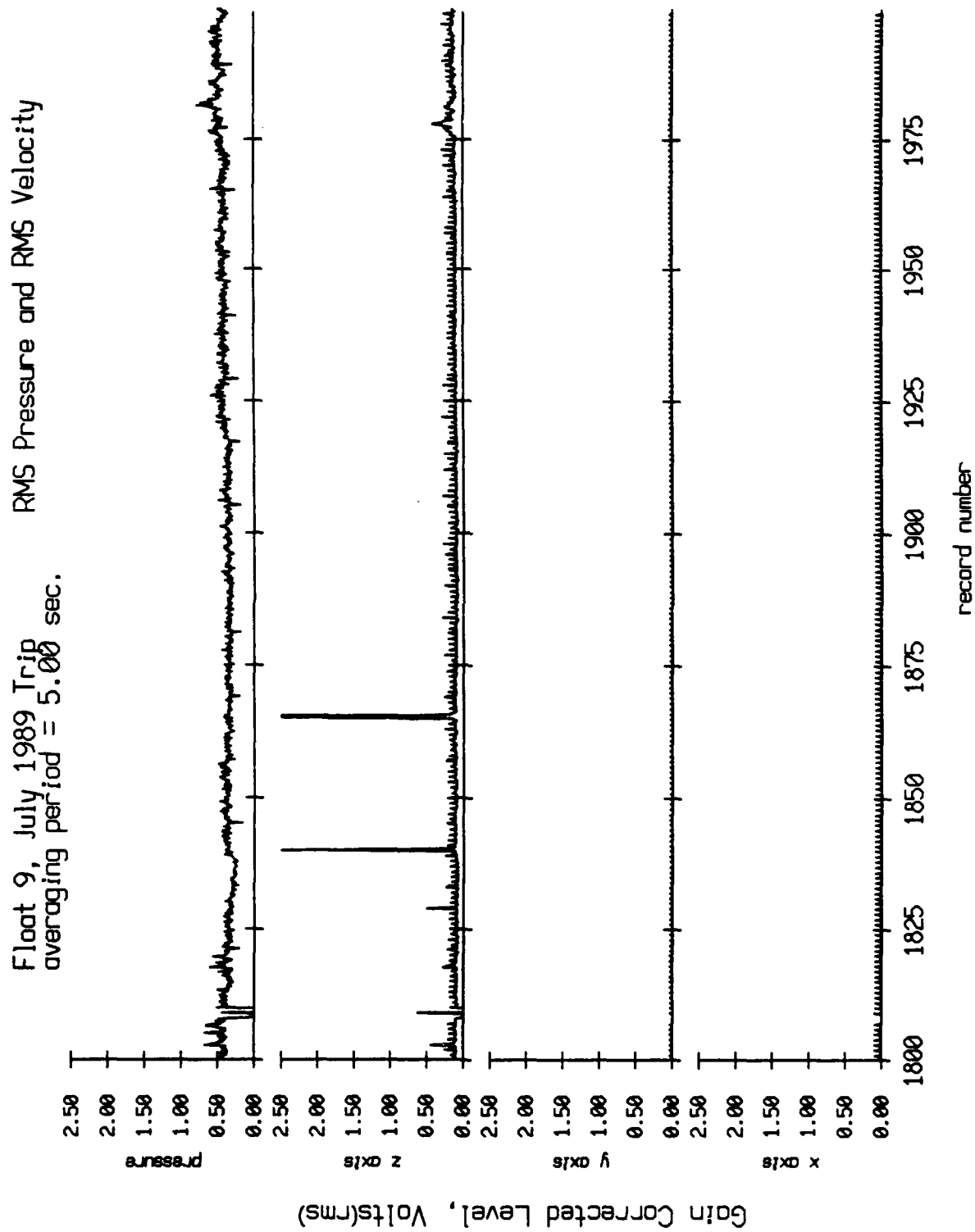


Figure X.10g

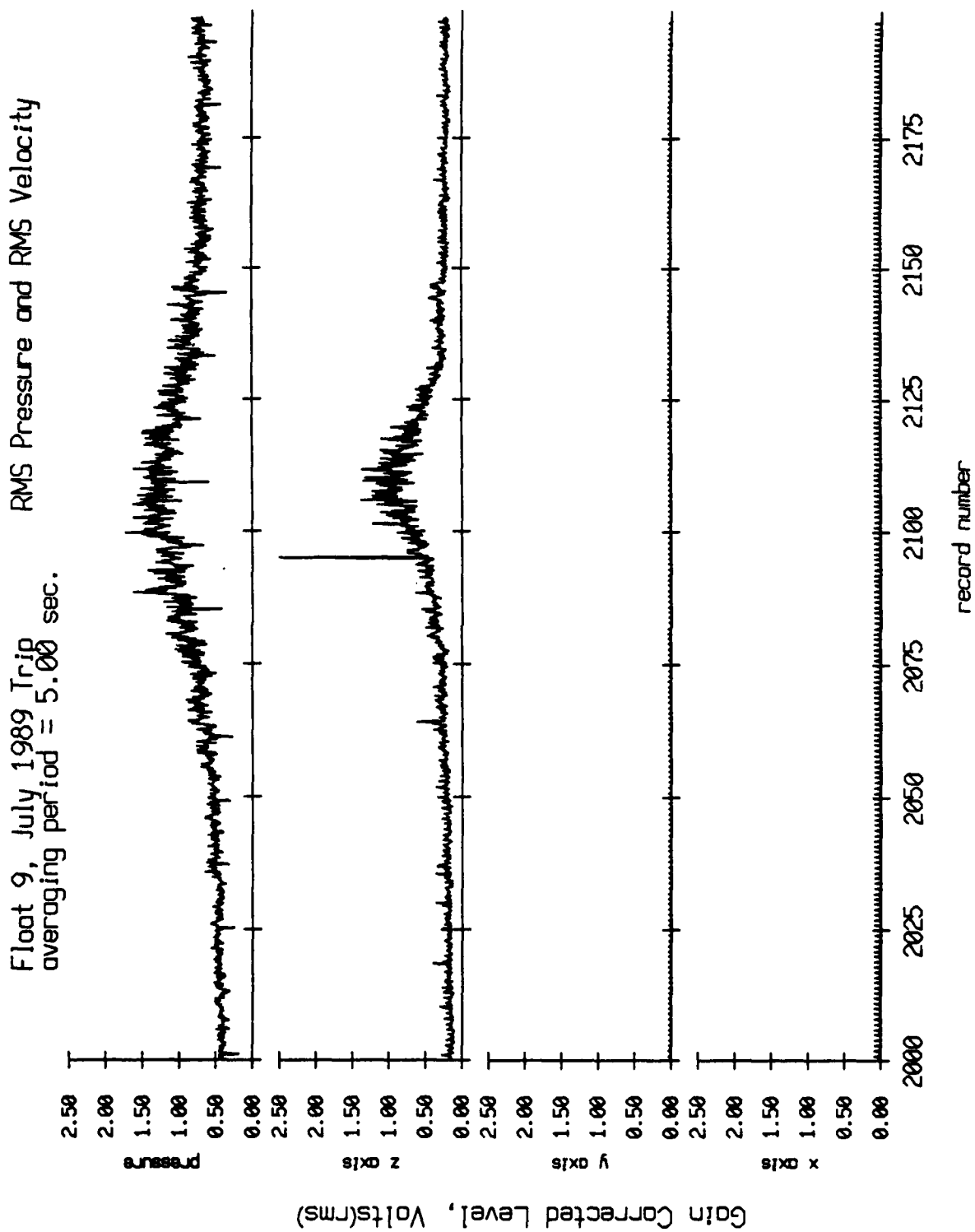


Figure X.10h

Float 10, July 1989 Trip  
 averaging period = 5.00 sec.

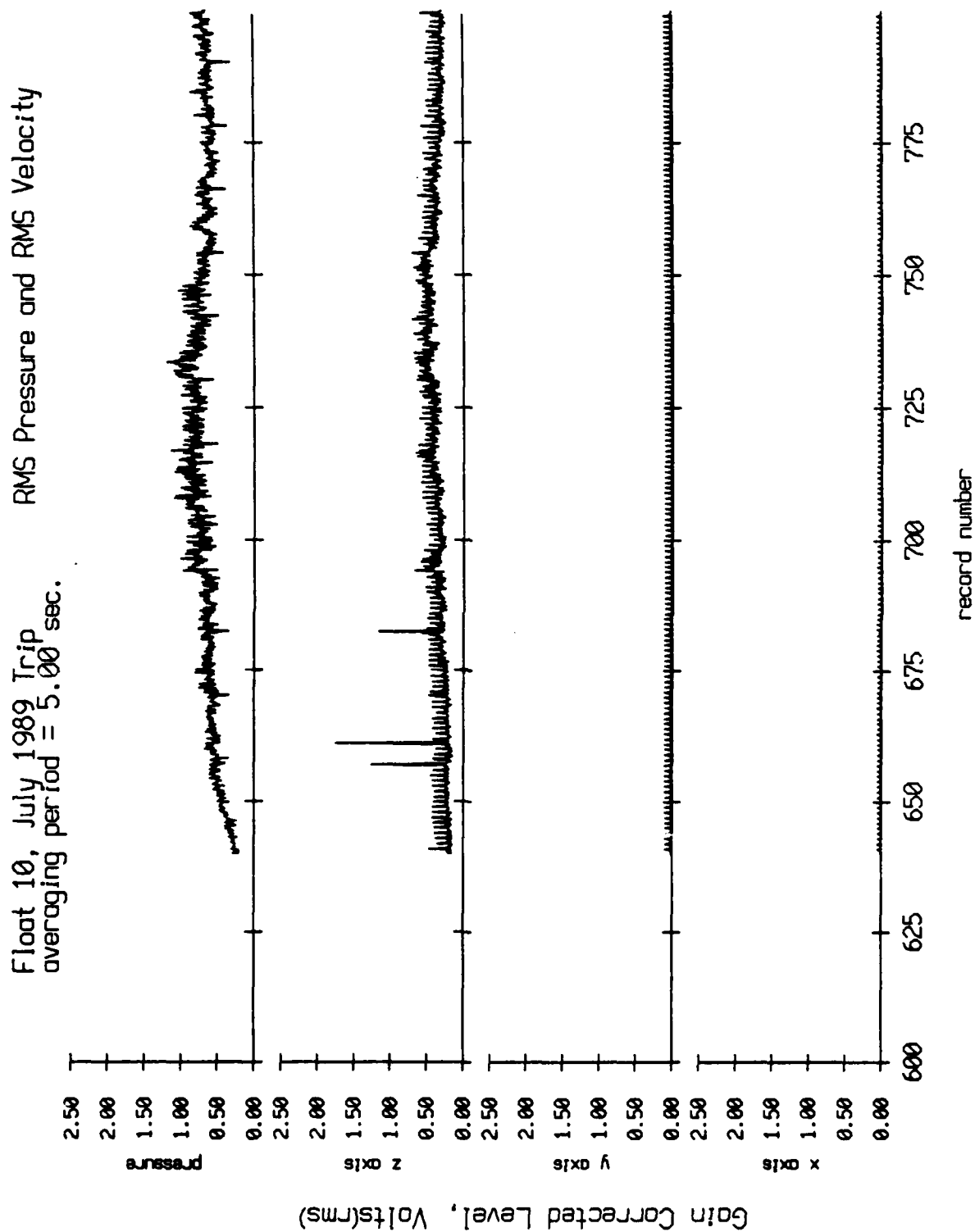


Figure X.11a

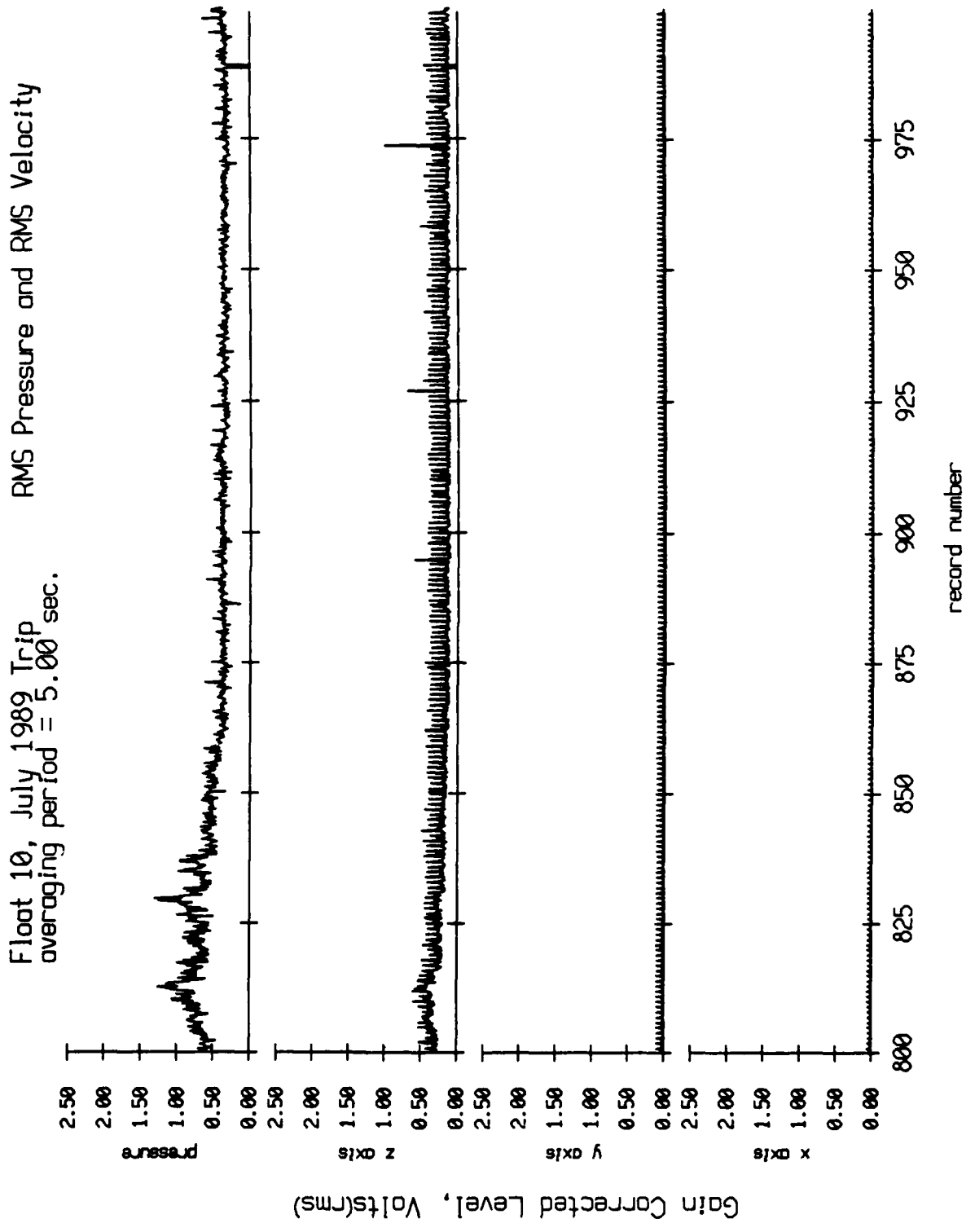
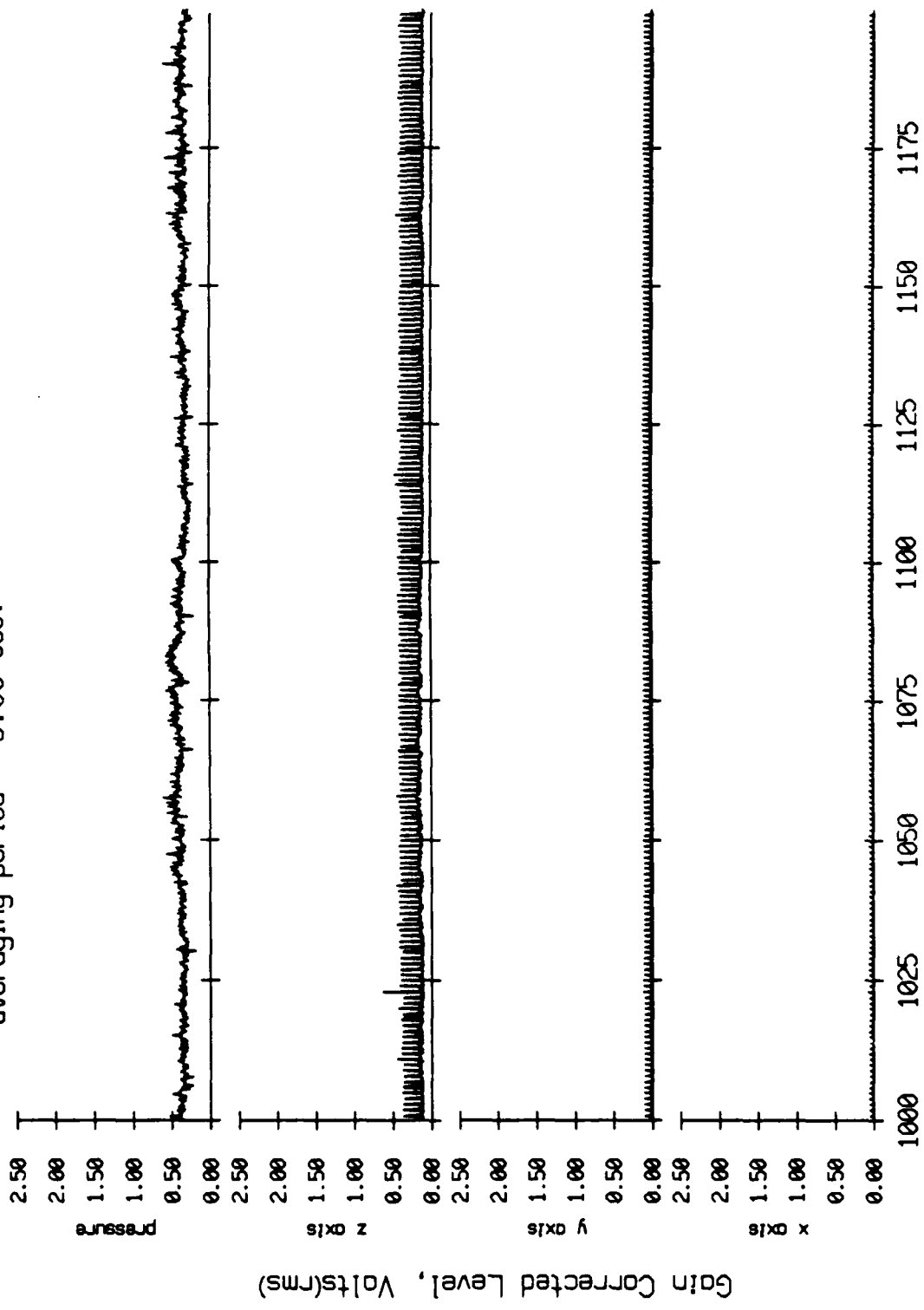


Figure X.11b

Float 10, July 1989 Trip  
 averaging period = 5.00 sec.



record number

Figure X.11c

Float 10, July 1989 Trip  
 averaging period = 5.00 sec.

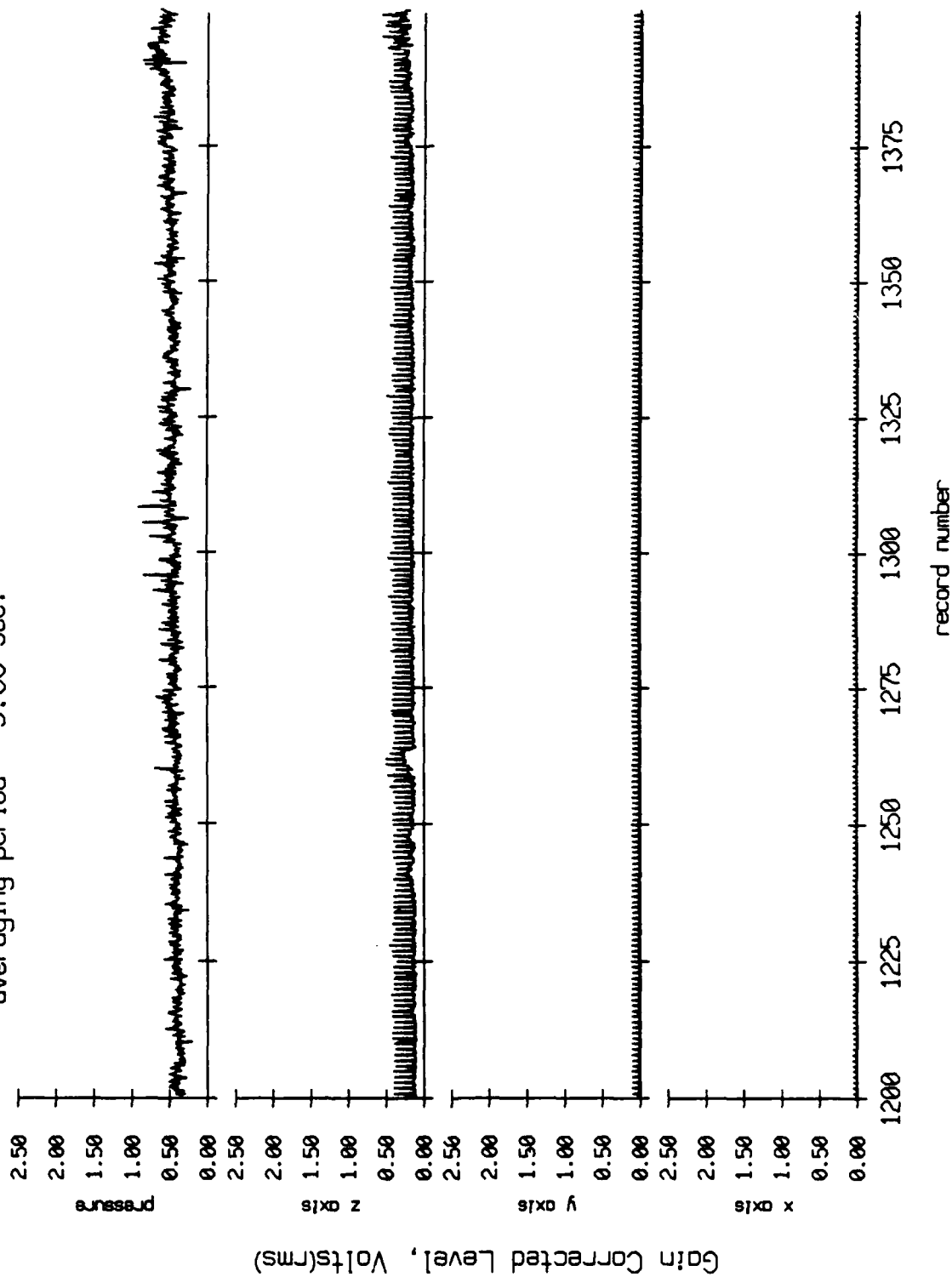


Figure X.11d



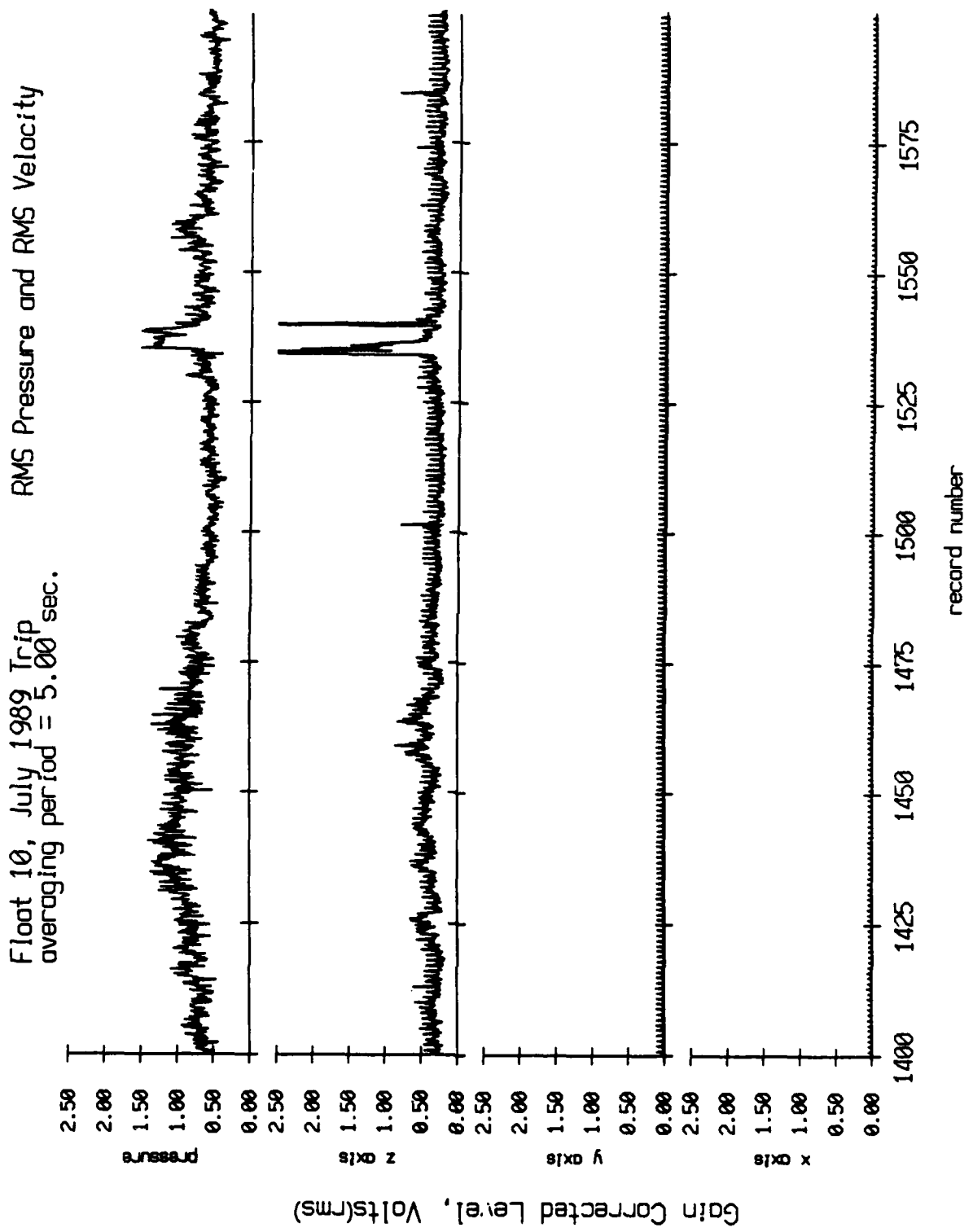


Figure X.11e

Float 10, July 1989 Trip  
 averaging period = 5.00 sec.

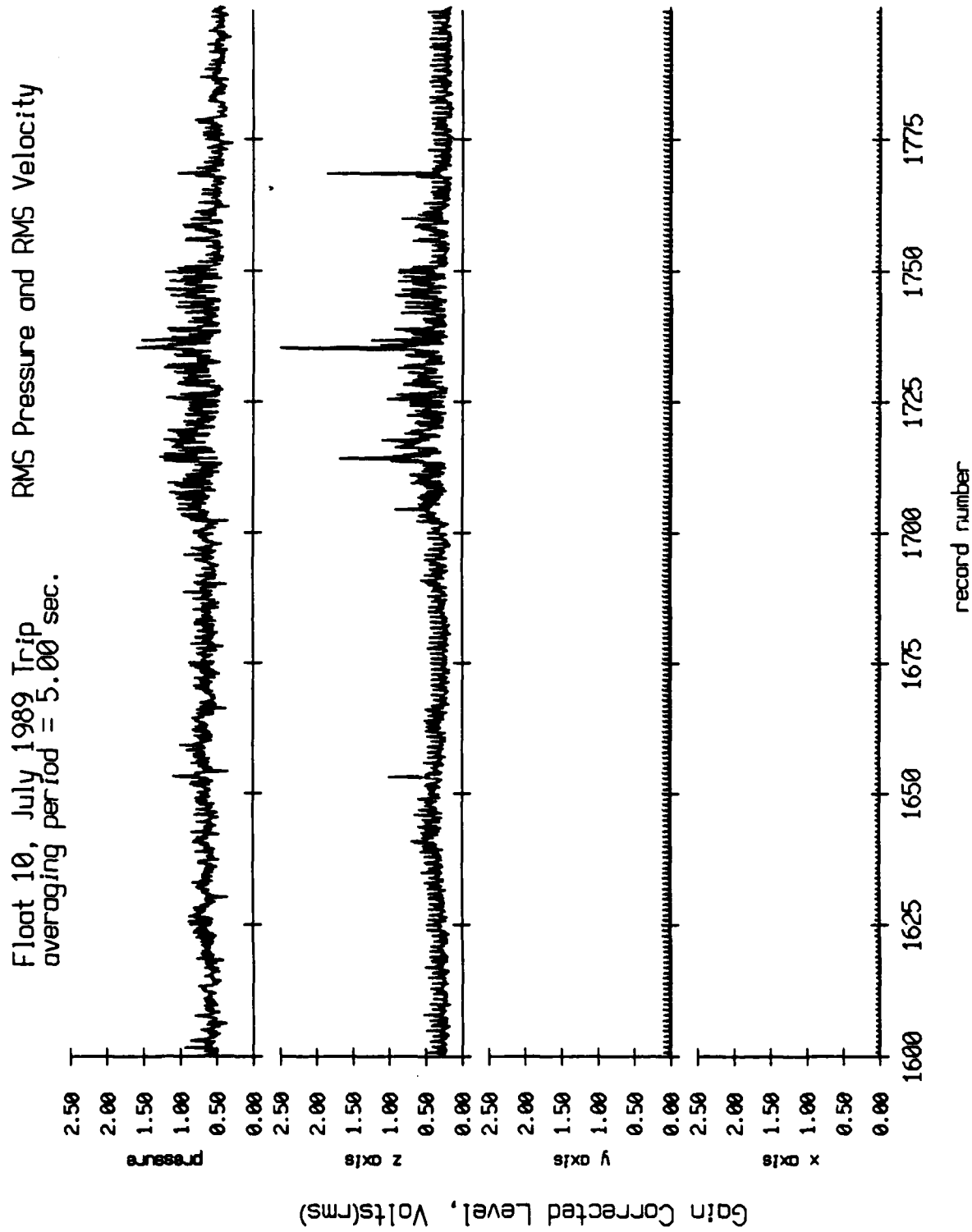


Figure X.11f

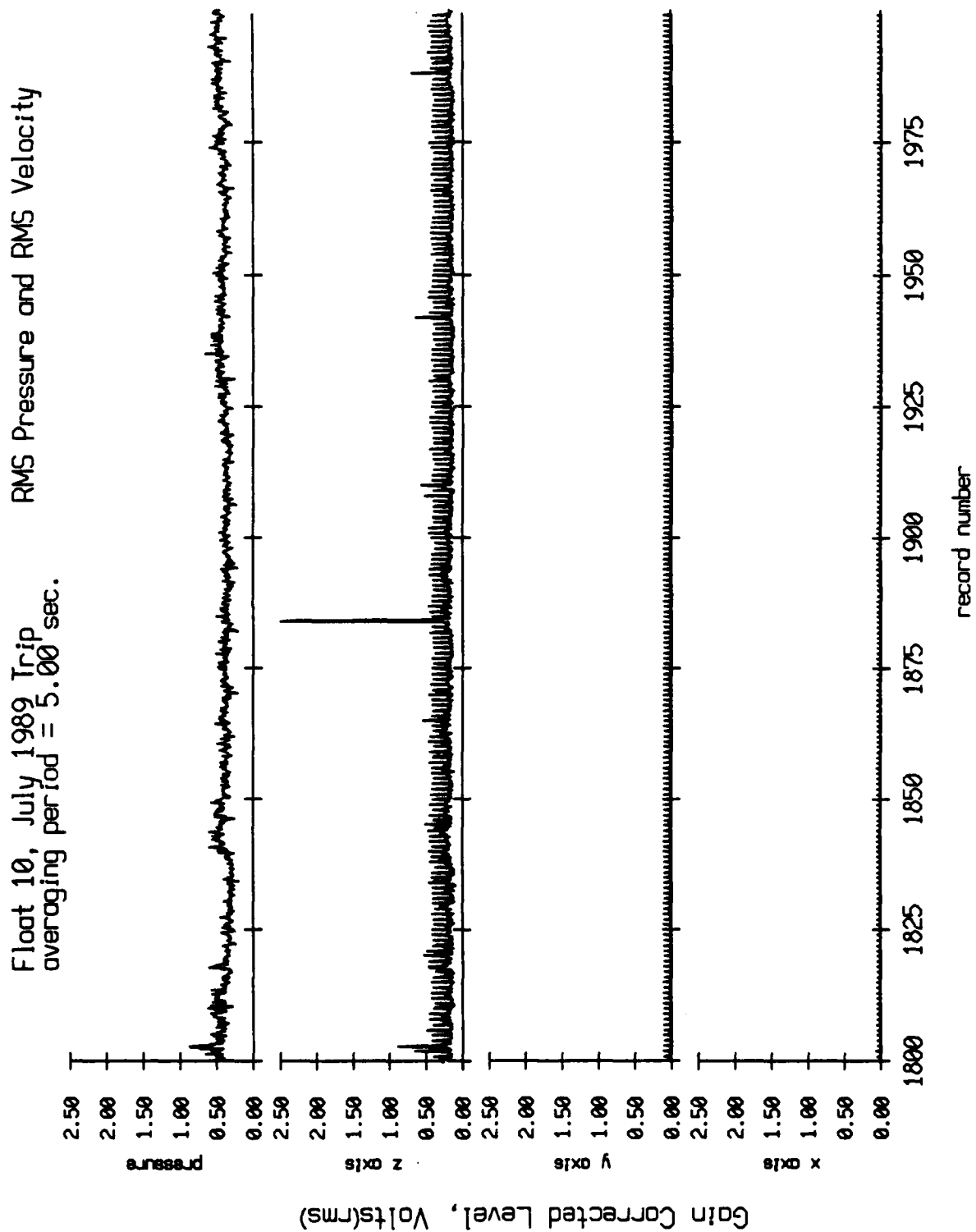
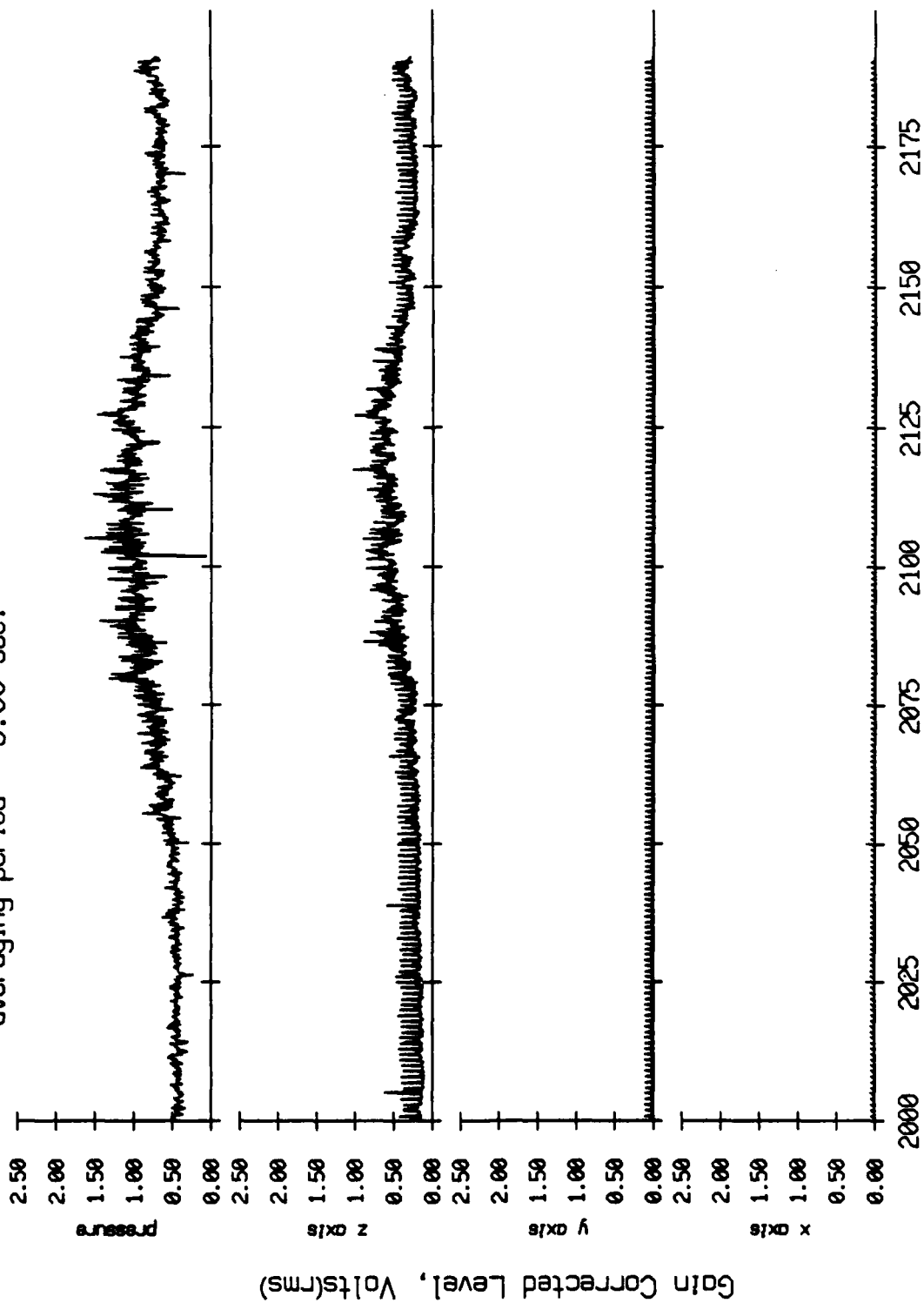


Figure X.11g

Float 10, July 1989 Trip  
 averaging period = 5.00 sec.

RMS Pressure and RMS Velocity



record number

Figure X.11h

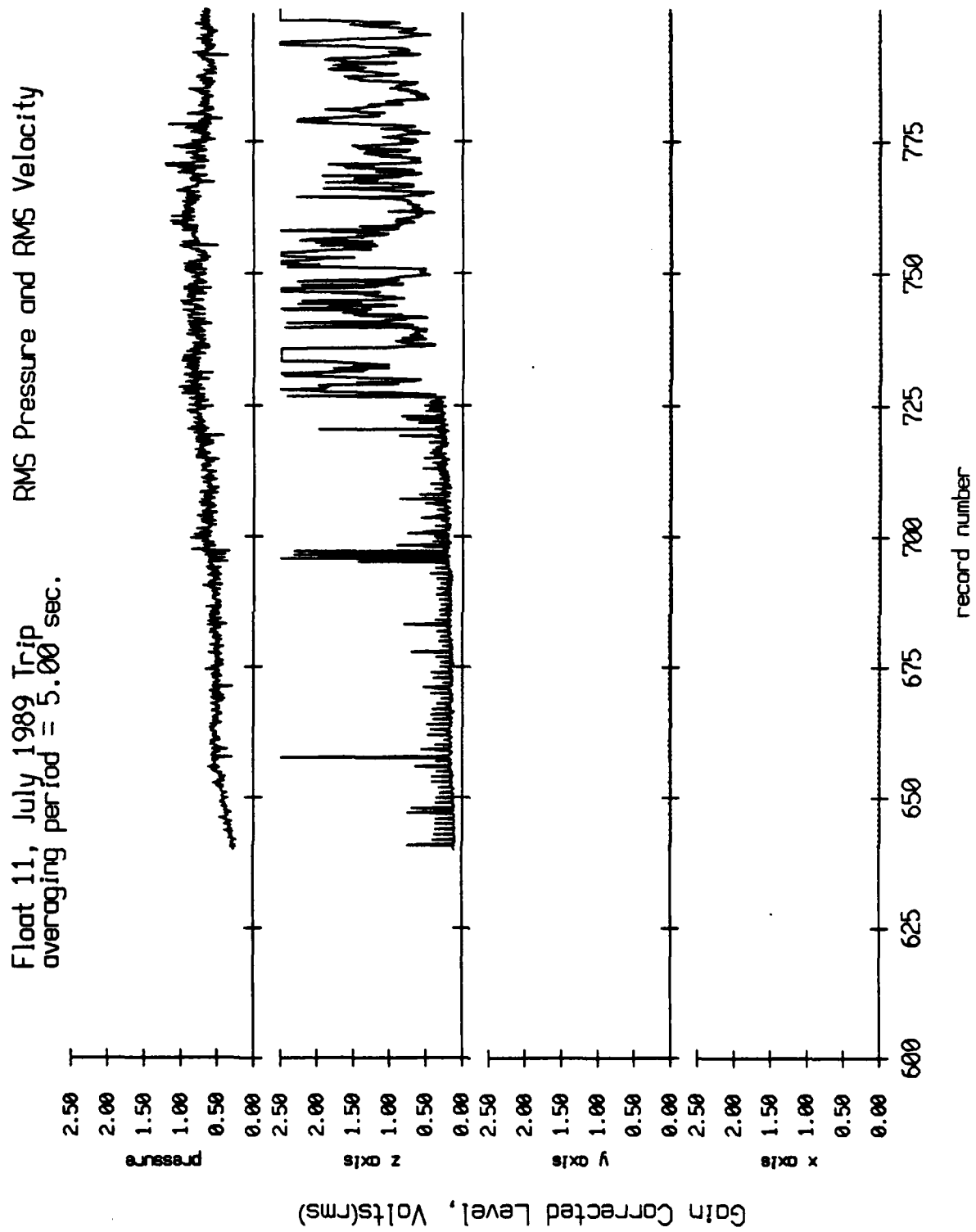


Figure X.12a

Float 11, July 1989 Trip  
 averaging period = 5.00 sec.

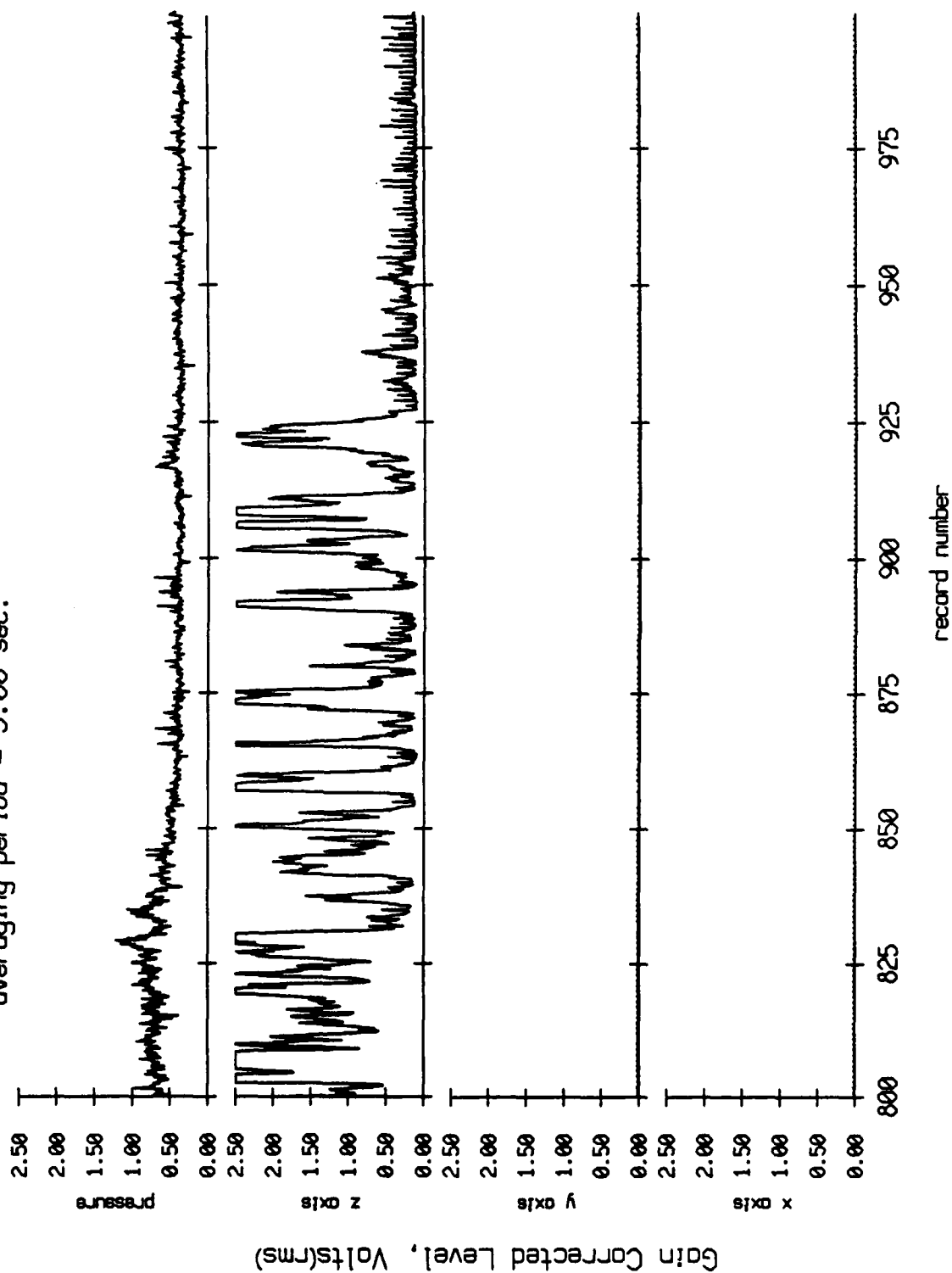


Figure X.12b

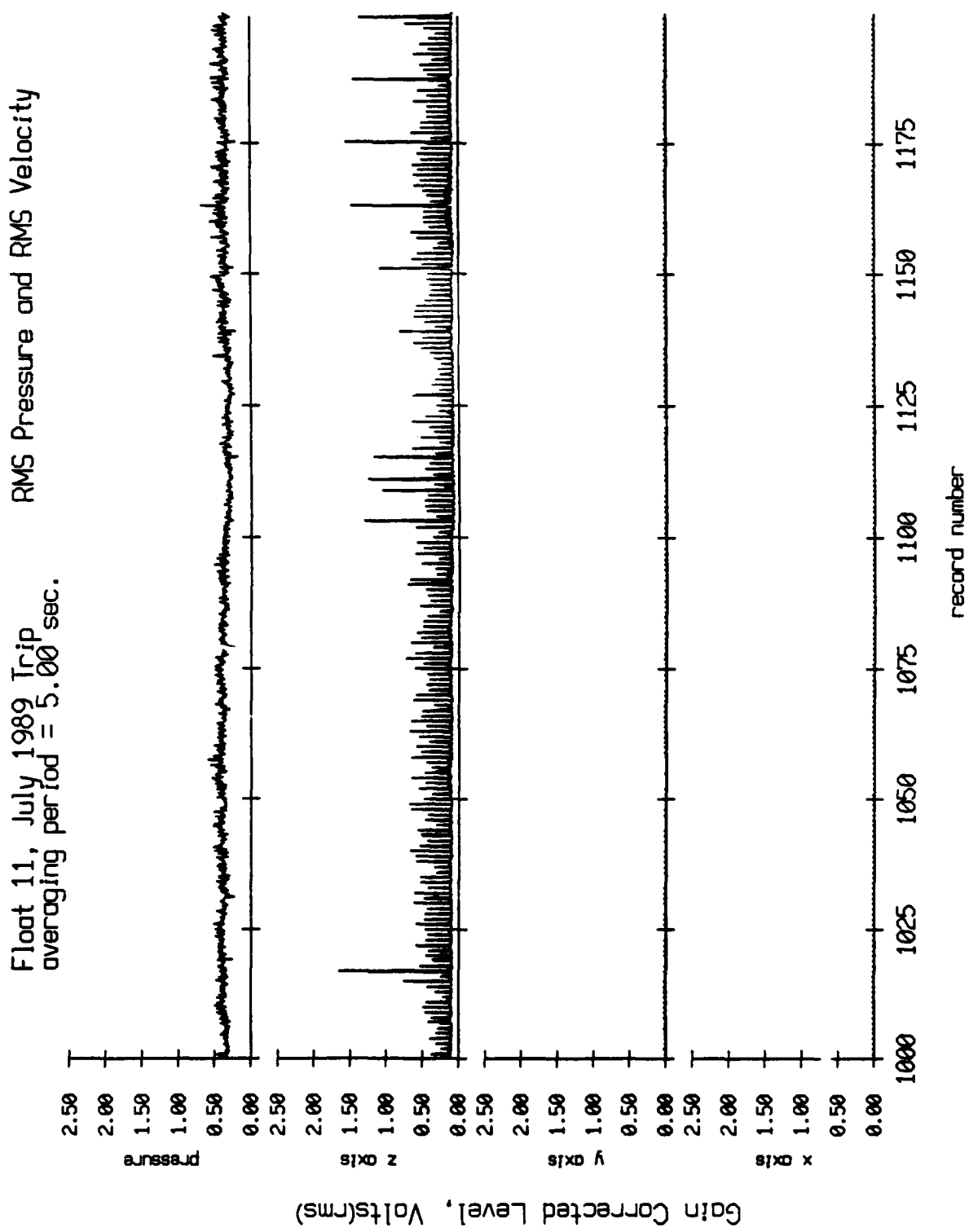


Figure X.12c

Float 11, July 1989 Trip  
 averaging period = 5.00 sec.  
 RMS Pressure and RMS Velocity

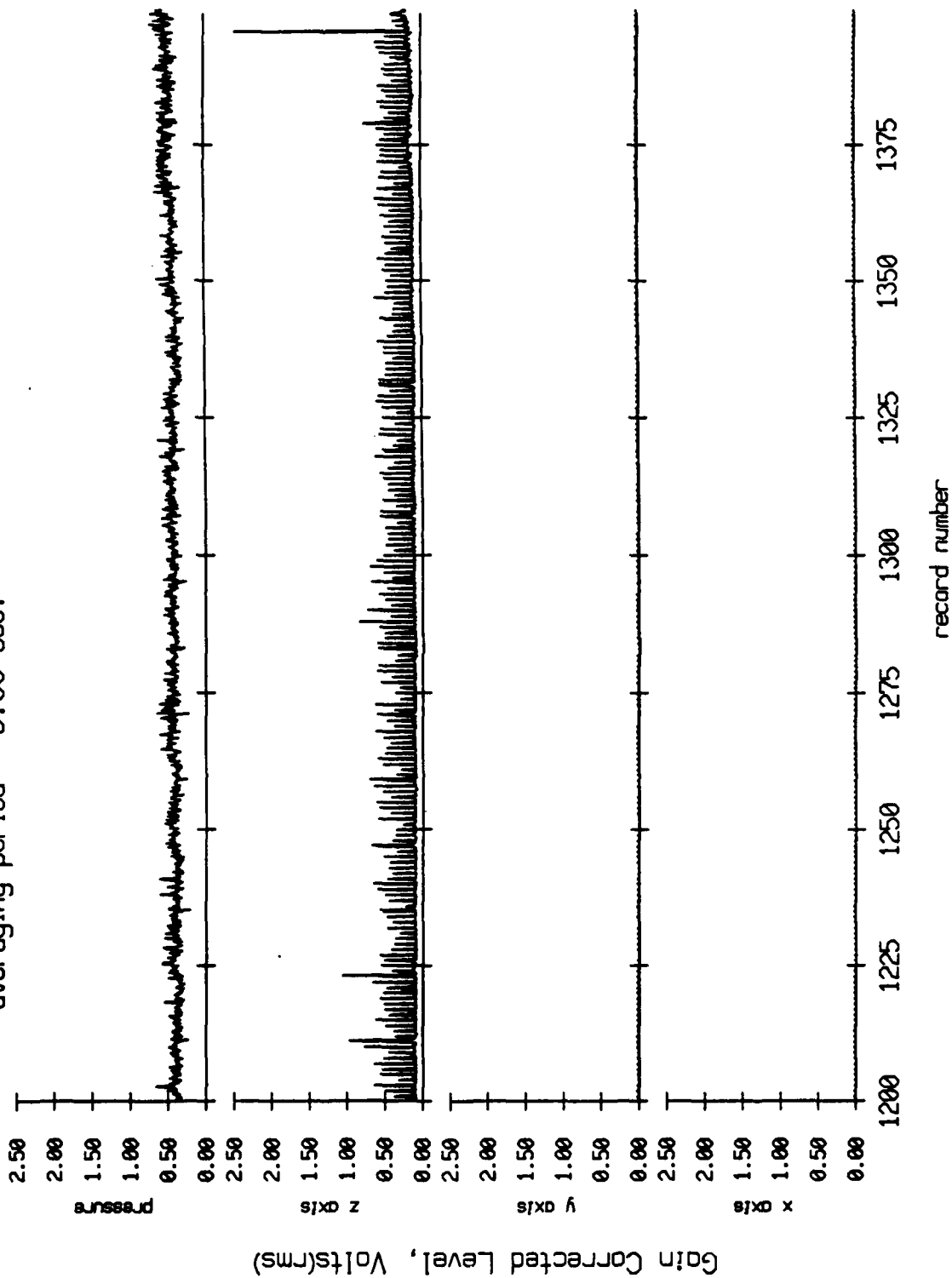


Figure X.12d



Float 11, July 1989 Trip  
 averaging period = 5.00 sec.

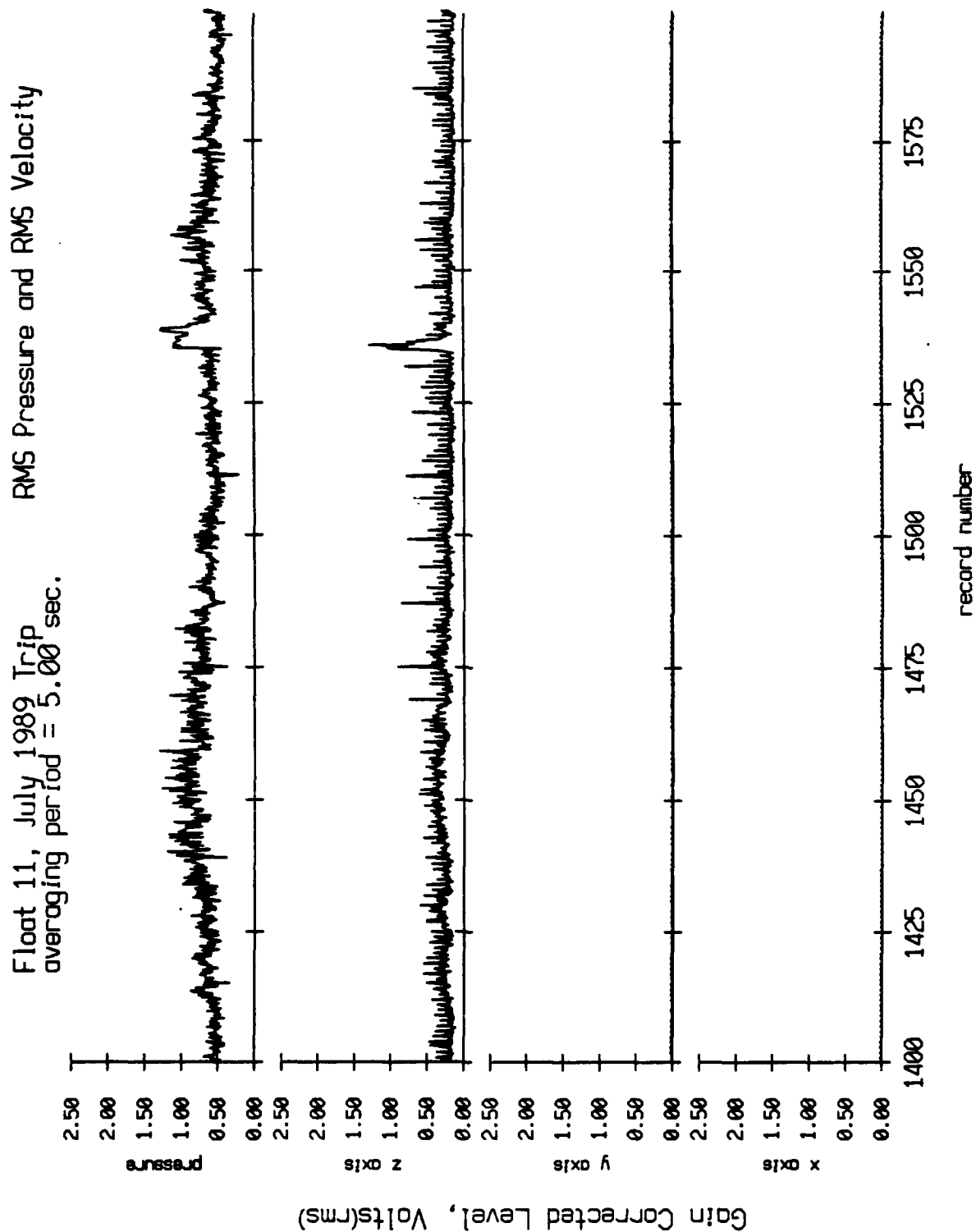


Figure X.12e

Float 11, July 1989 Trip  
 averaging period = 5.00 sec.

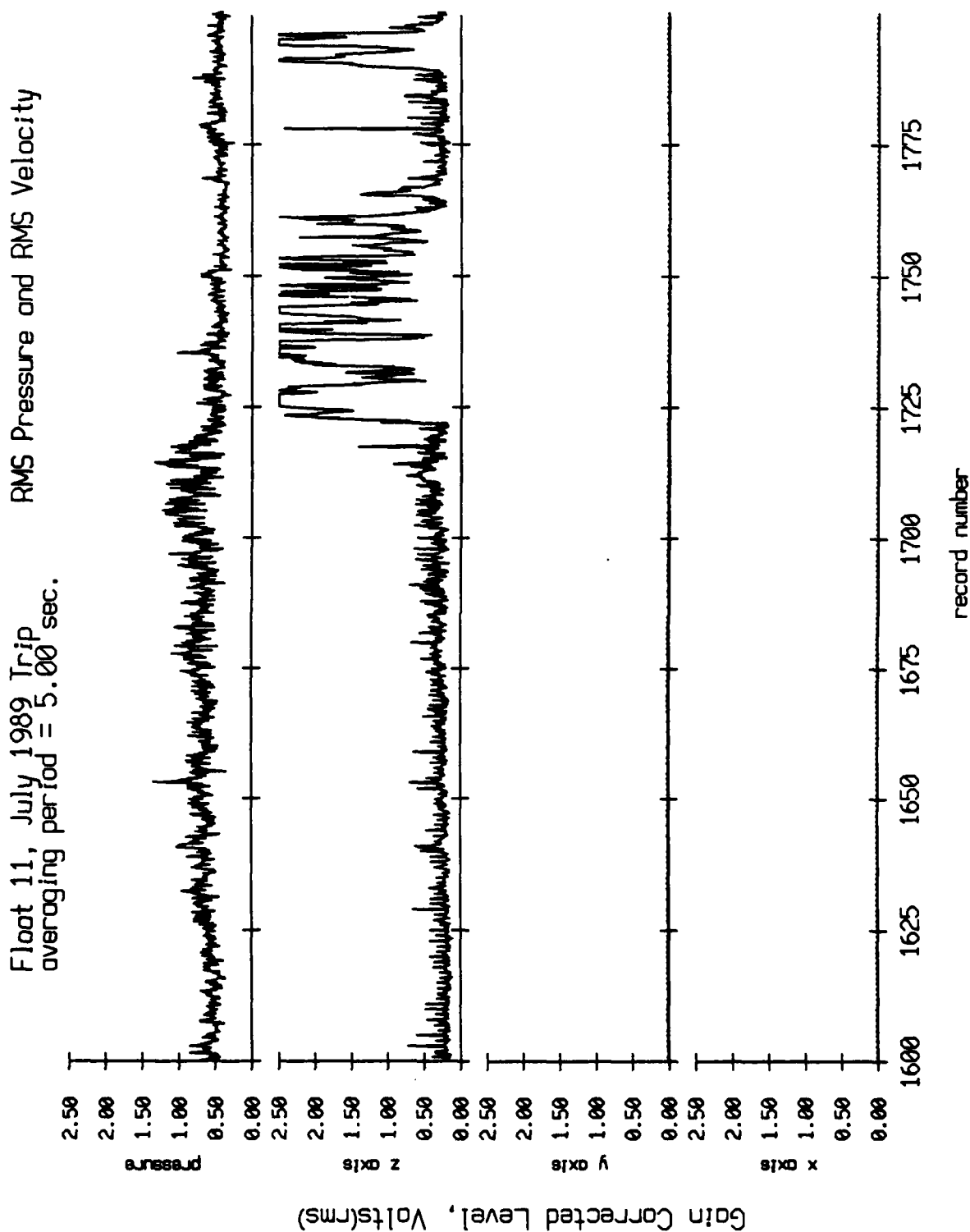


Figure X.12f

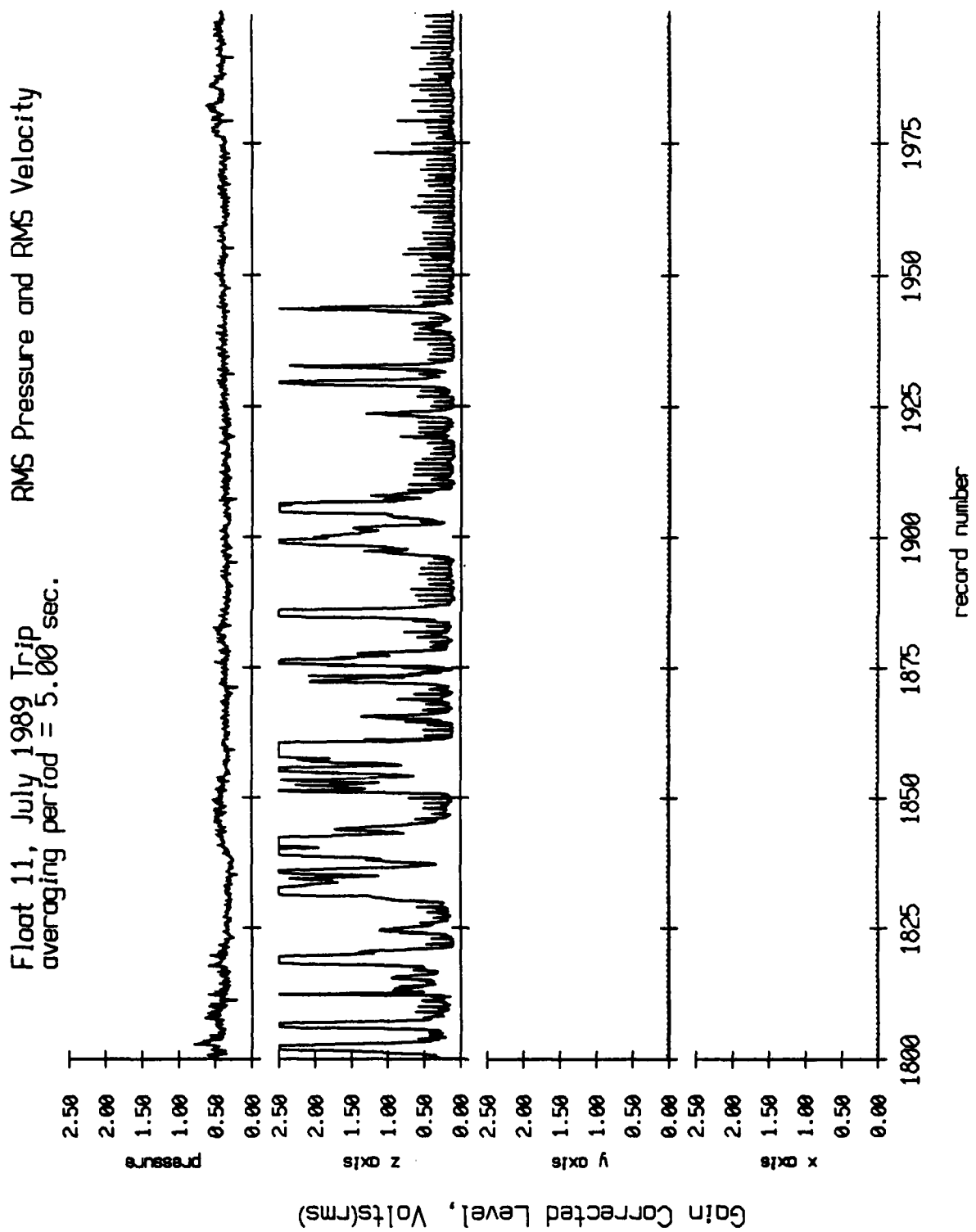


Figure X.12g

Float 11, July 1989 Trip  
 averaging period = 5.00 sec.

RMS Pressure and RMS Velocity

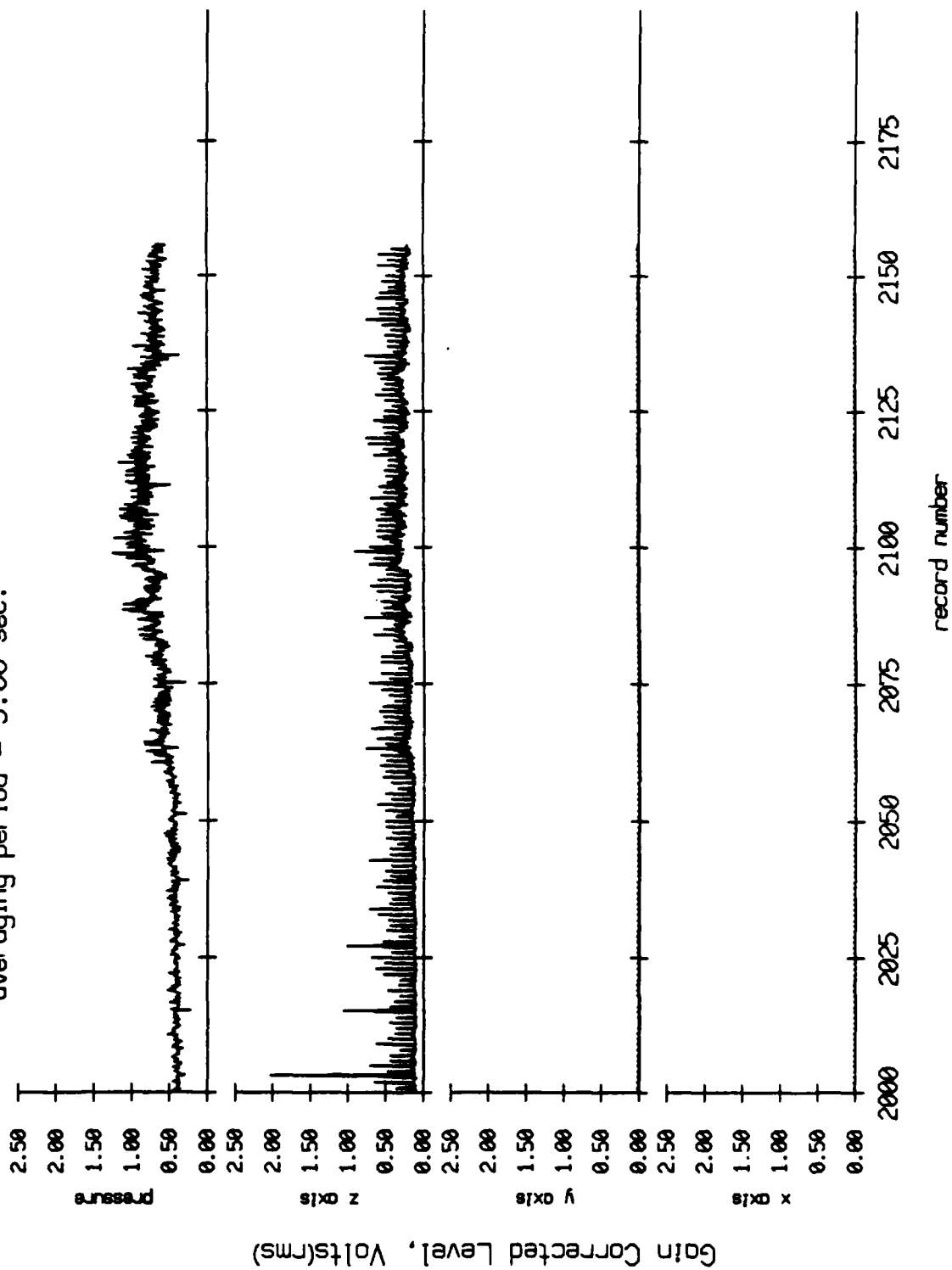
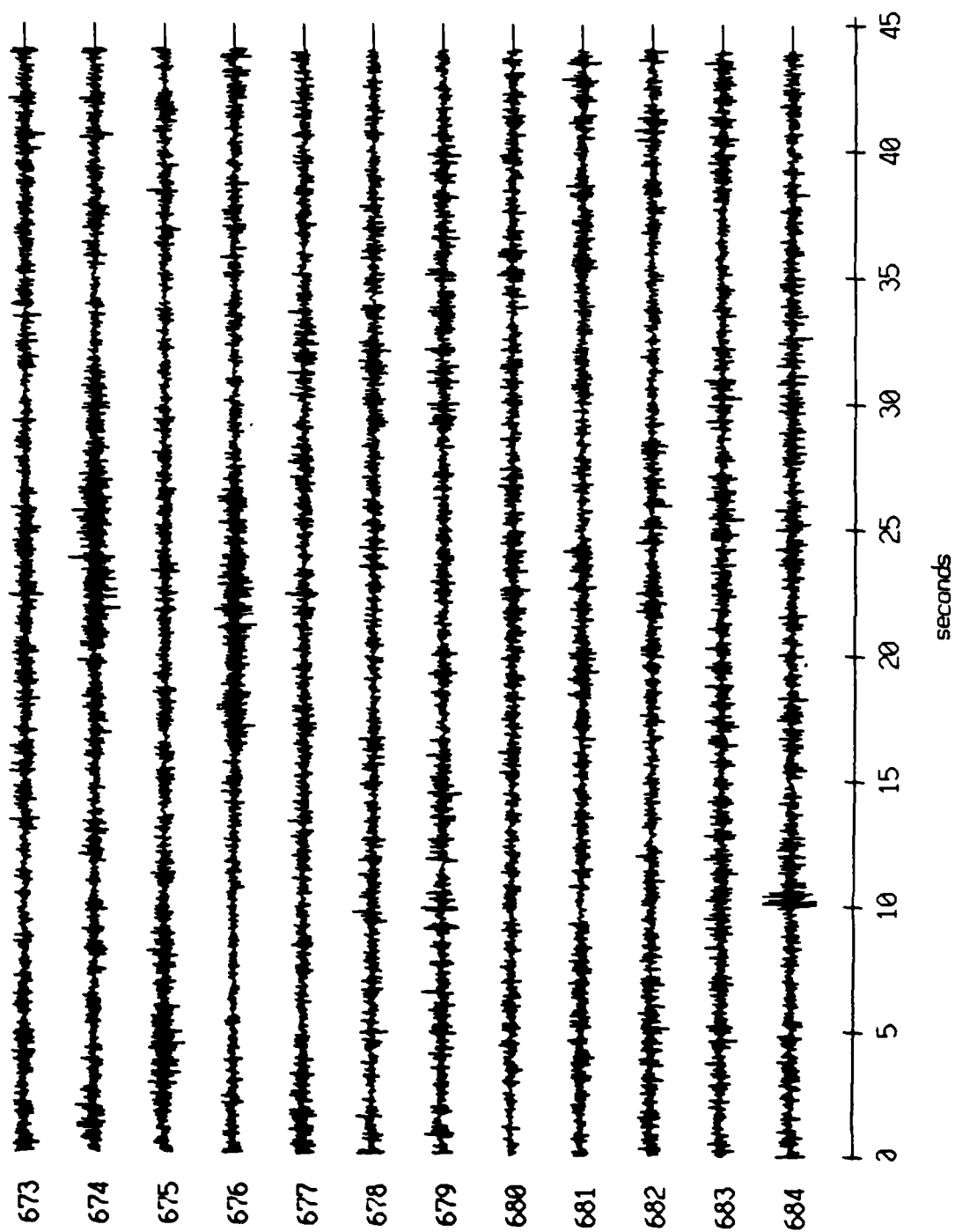


Figure X.12h

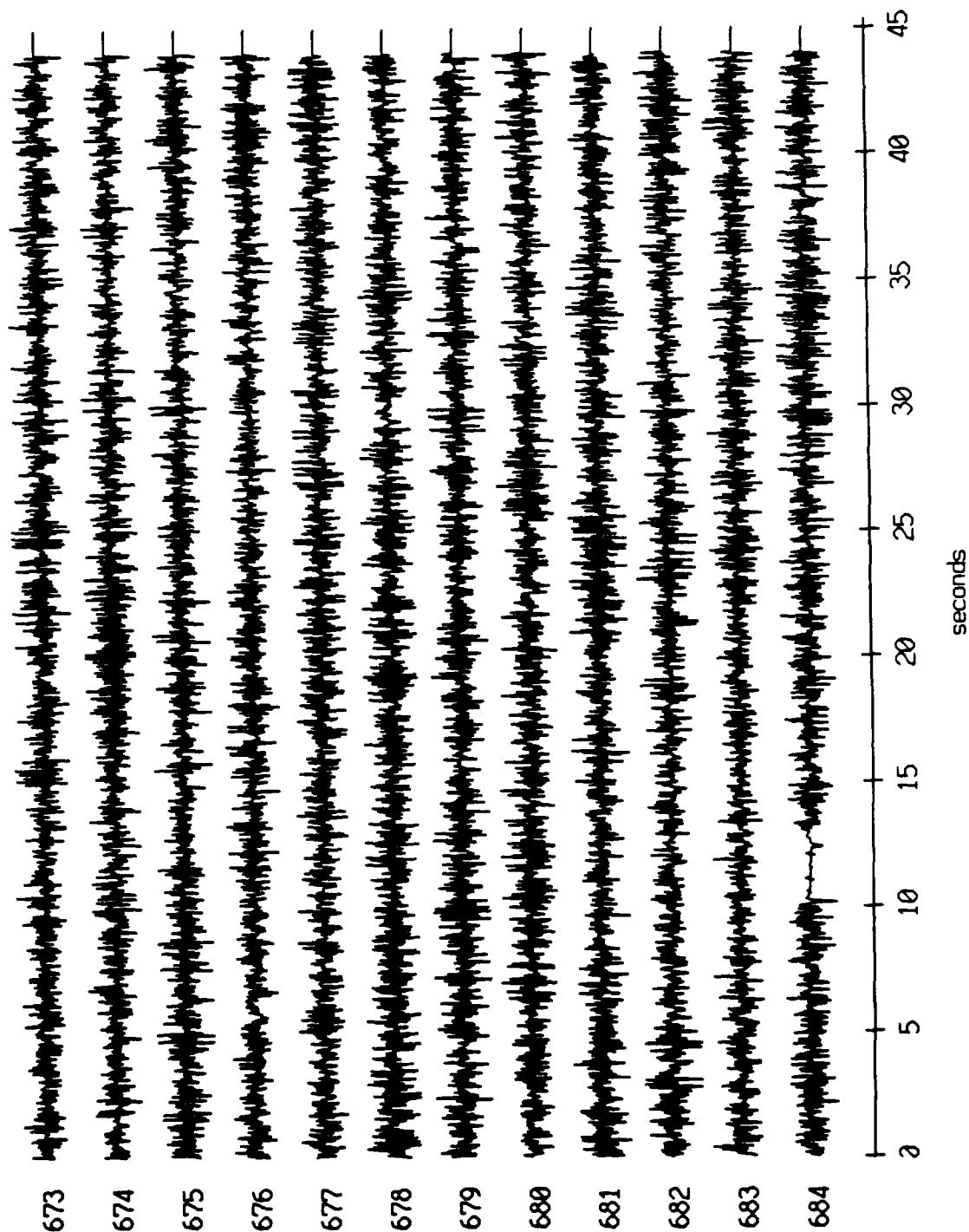
Float 0, July, 1989 Trip - records 673-684 (z-axis)  
vertical axis scale is approx. -2.0 to 2.0 volts



RGC corrected channel level (V)

Figure XI.1a

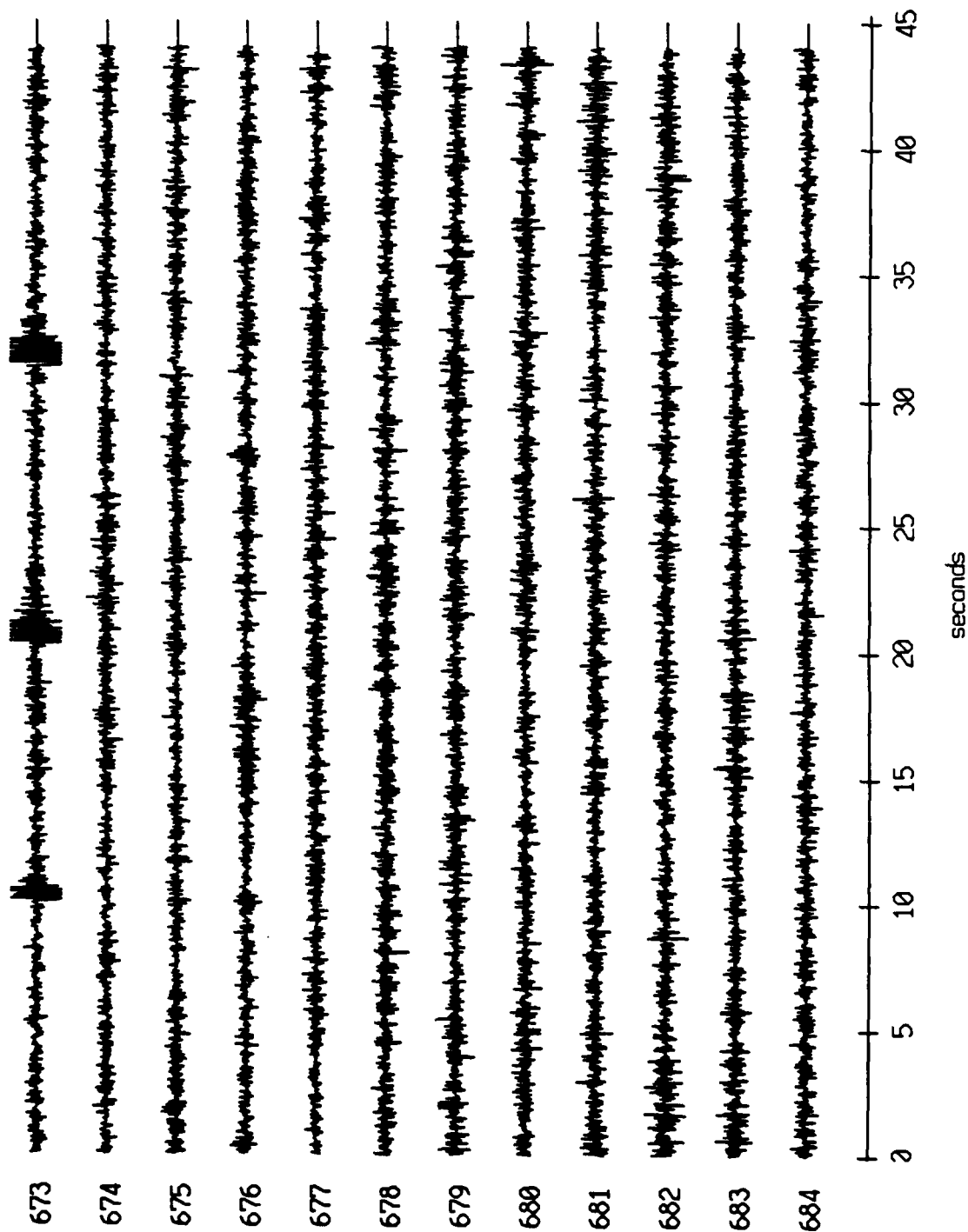
Float 0, July, 1989 Trip - records 673-684 (hydrophone)  
vertical axis scale is approx. -2.0 to 2.0 volts



PGC corrected channel level (V)

Figure XI.1b

Floq: 1, July, 1989 Trip - records 673-684 (z-axis)  
vertical axis scale is approx. -2.0 to 2.0 volts



AGC corrected channel level (V)

Figure XI.2a

Float 1, July, 1989 Trip - records 673-684 (hydrophone)  
vertical axis scale is approx. -2.0 to 2.0 volts

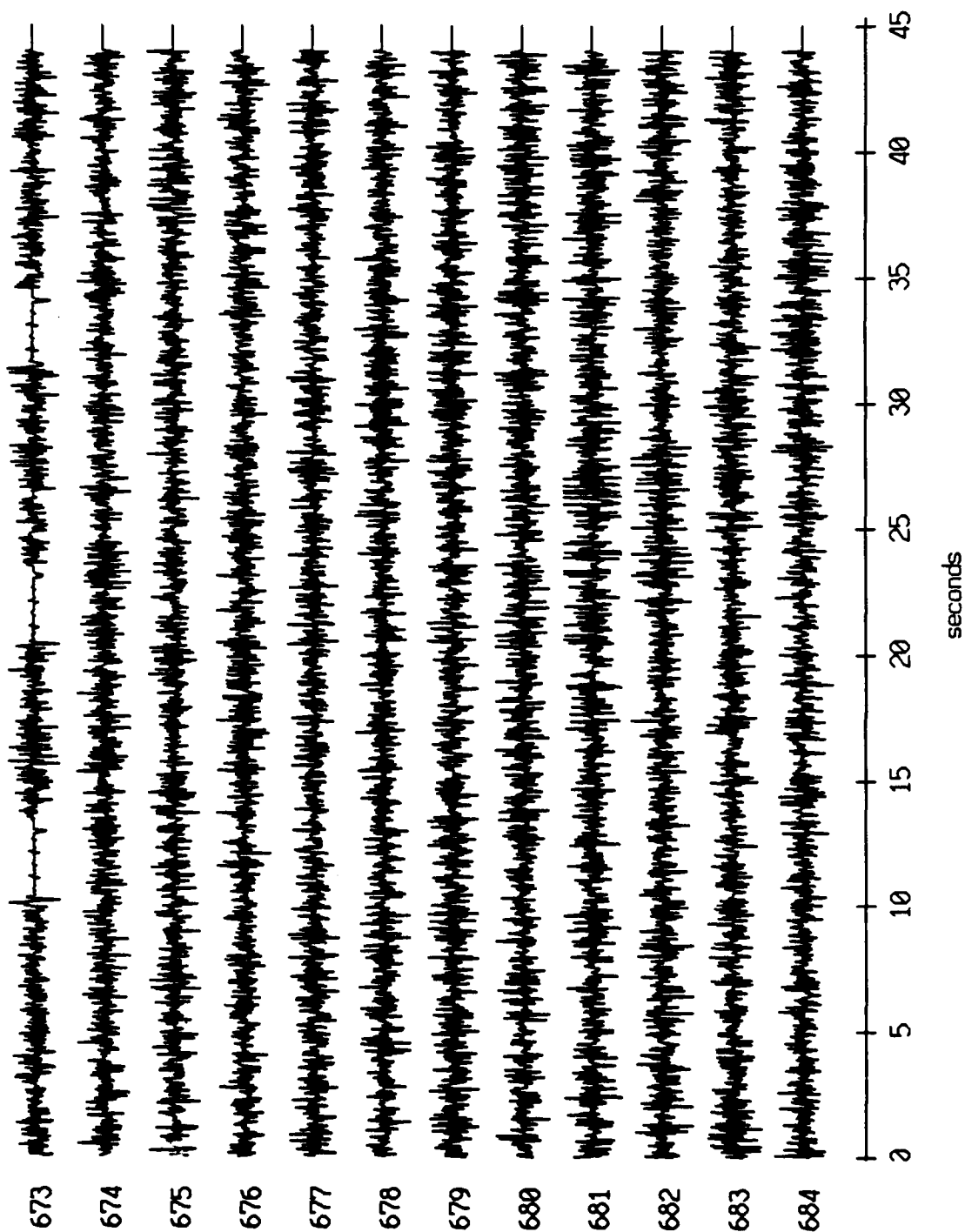


Figure XI.2b



Floot 2, July, 1989 Trip - records 673-684 (z-axis)  
vertical axis scale is approx. -2.0 to 2.0 volts

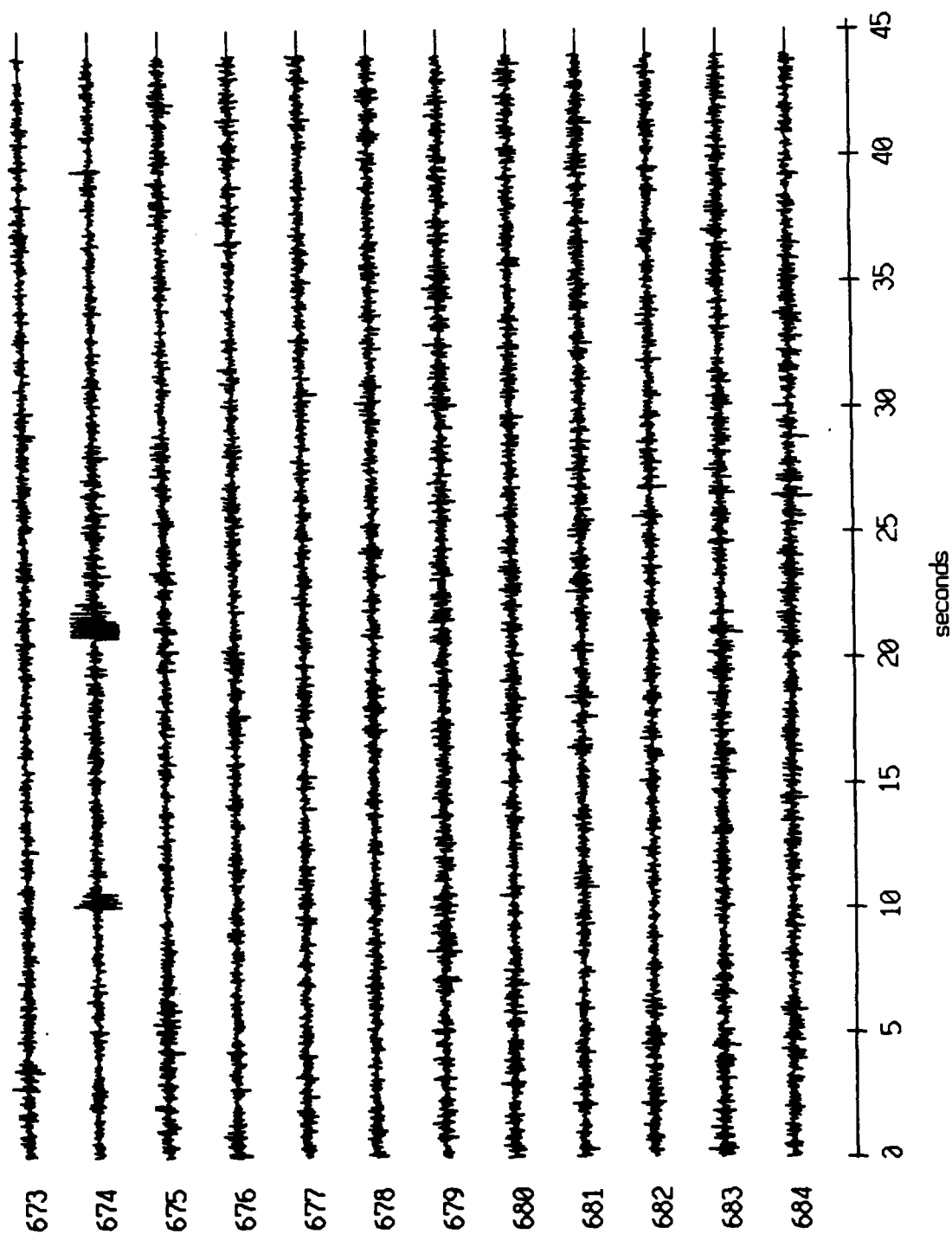


Figure XI.3a

Float 2, July, 1989 Trip - records 673-684 (hydrophone)  
 vertical axis scale is approx. -2.0 to 2.0 volts

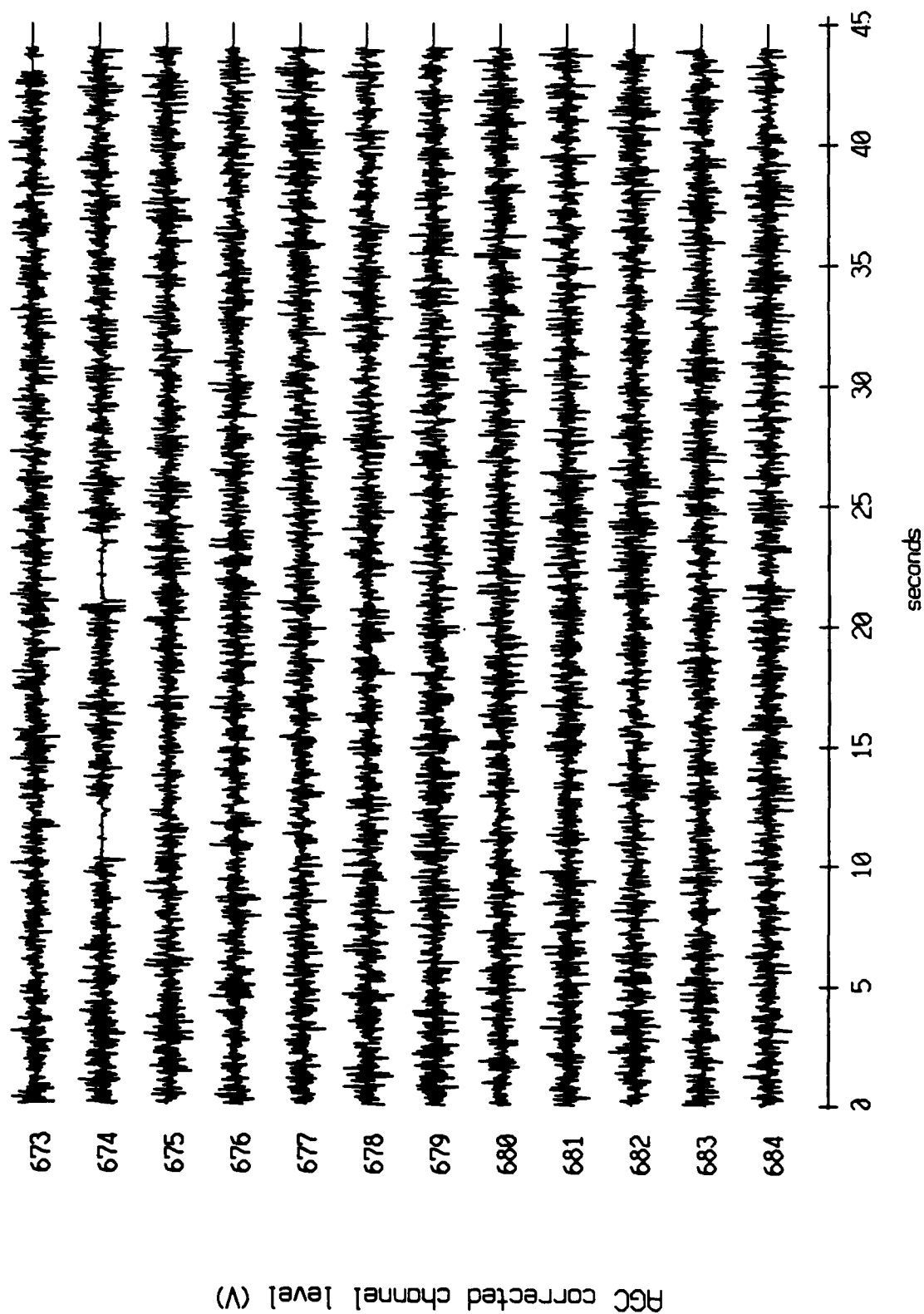
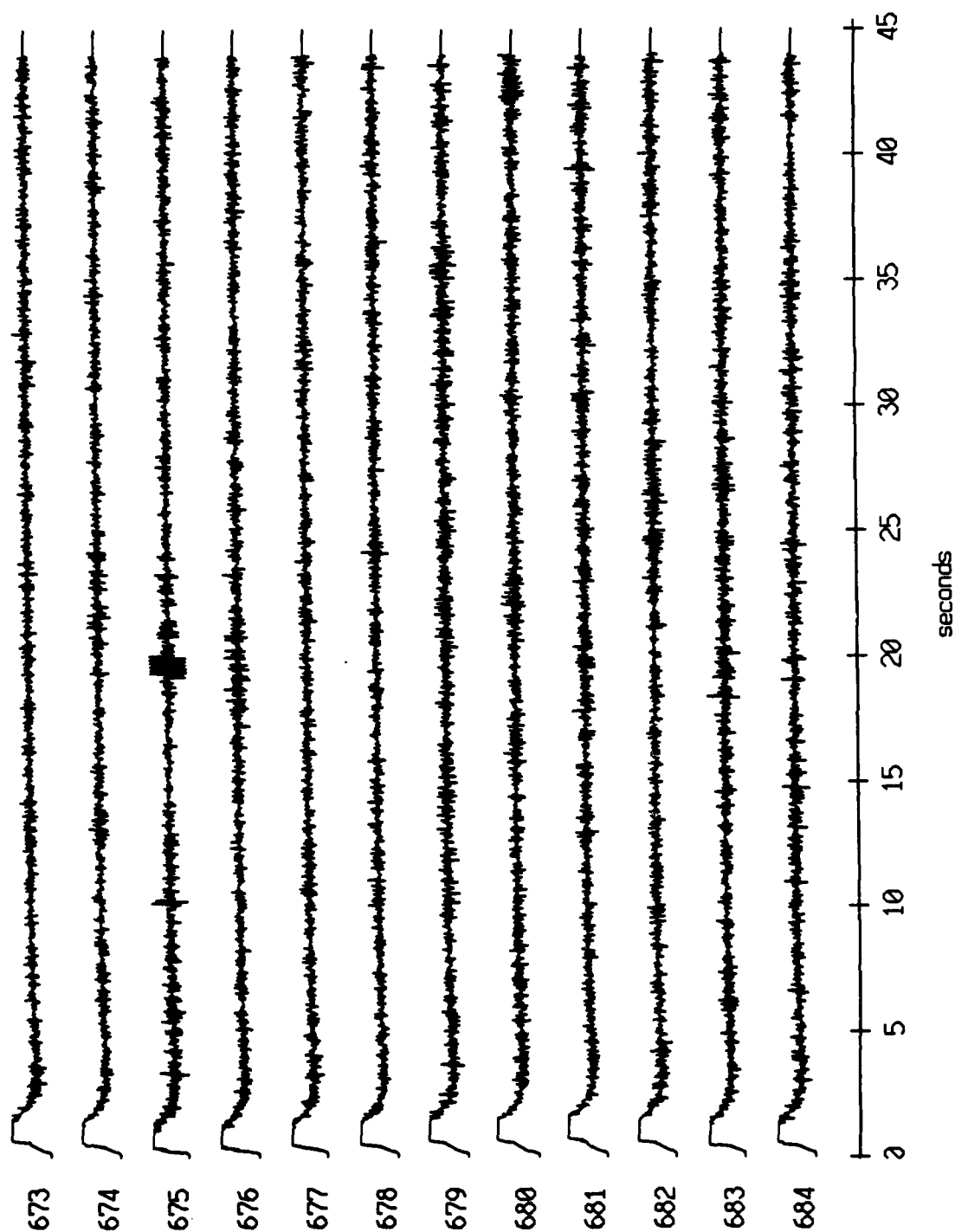


Figure XI.3b

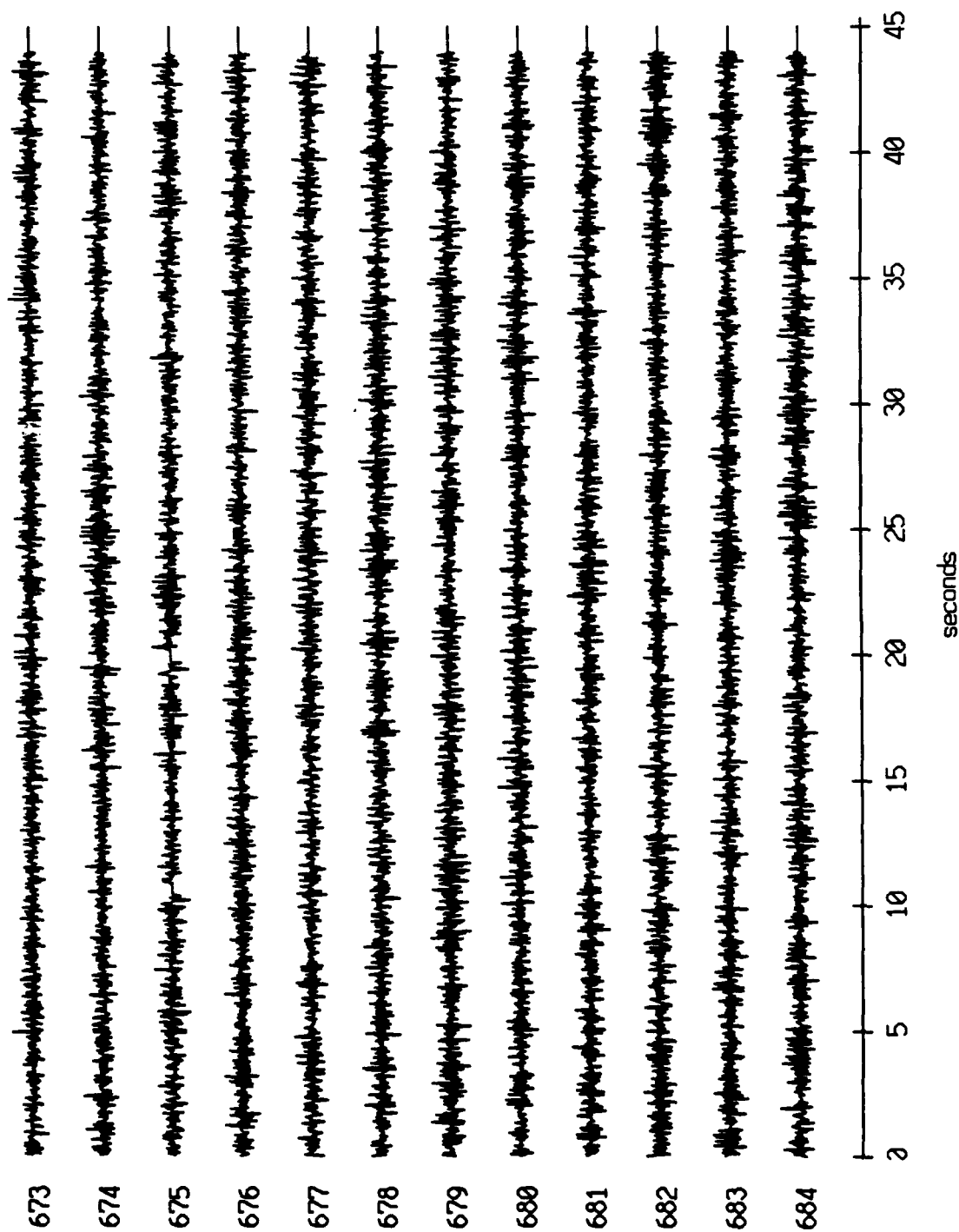
Float 3, July, 1989 Trip - records 673-684 (z-axis)  
vertical axis scale is approx. -2.0 to 2.0 volts



AGC corrected channel level (V)

Figure XI.4a

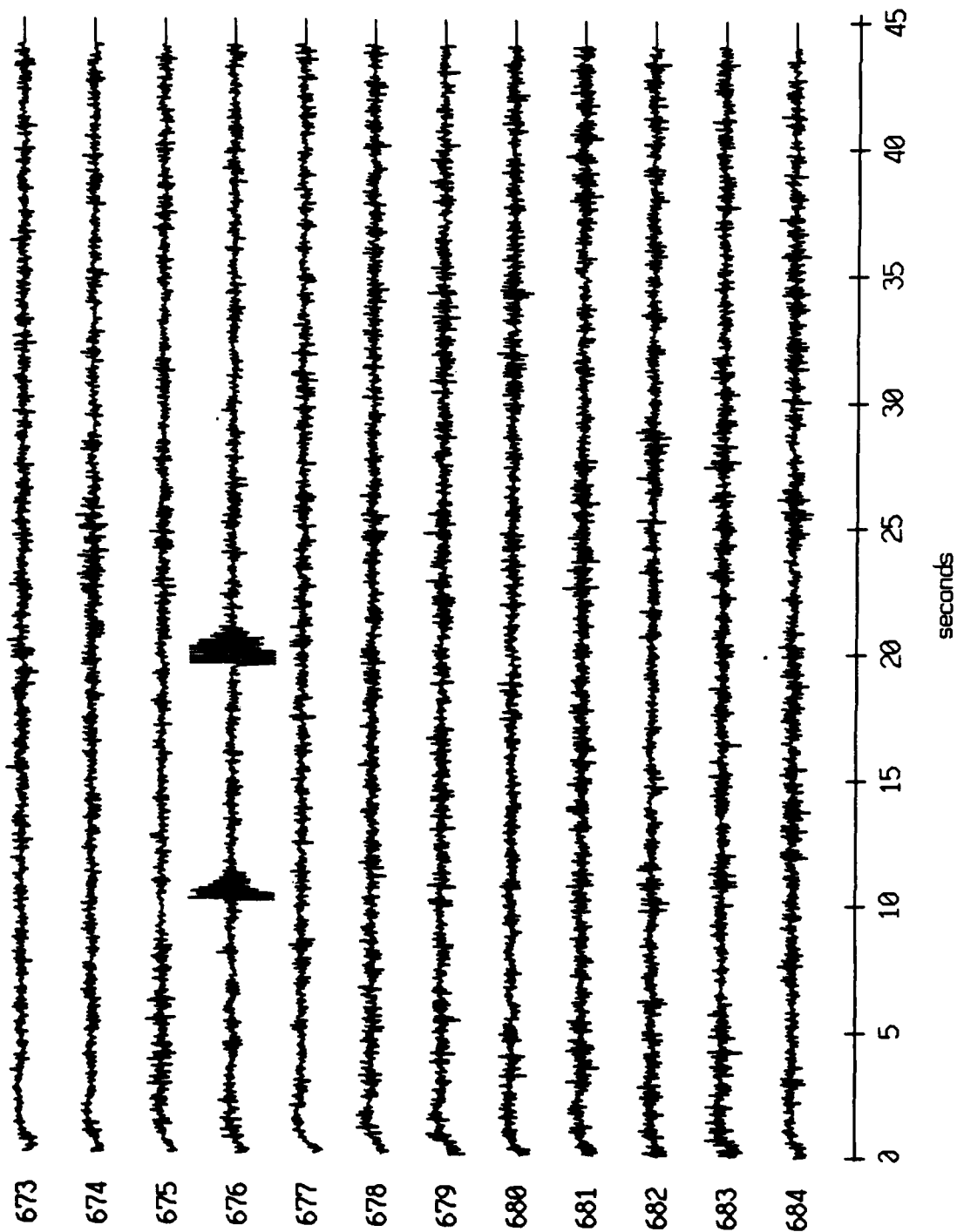
Floot 3, July, 1989 Trip - records 673-684 (hydrophone)  
vertical axis scale is approx. -2.0 to 2.0 volts



AGC corrected channel level (V)

Figure XI.4b

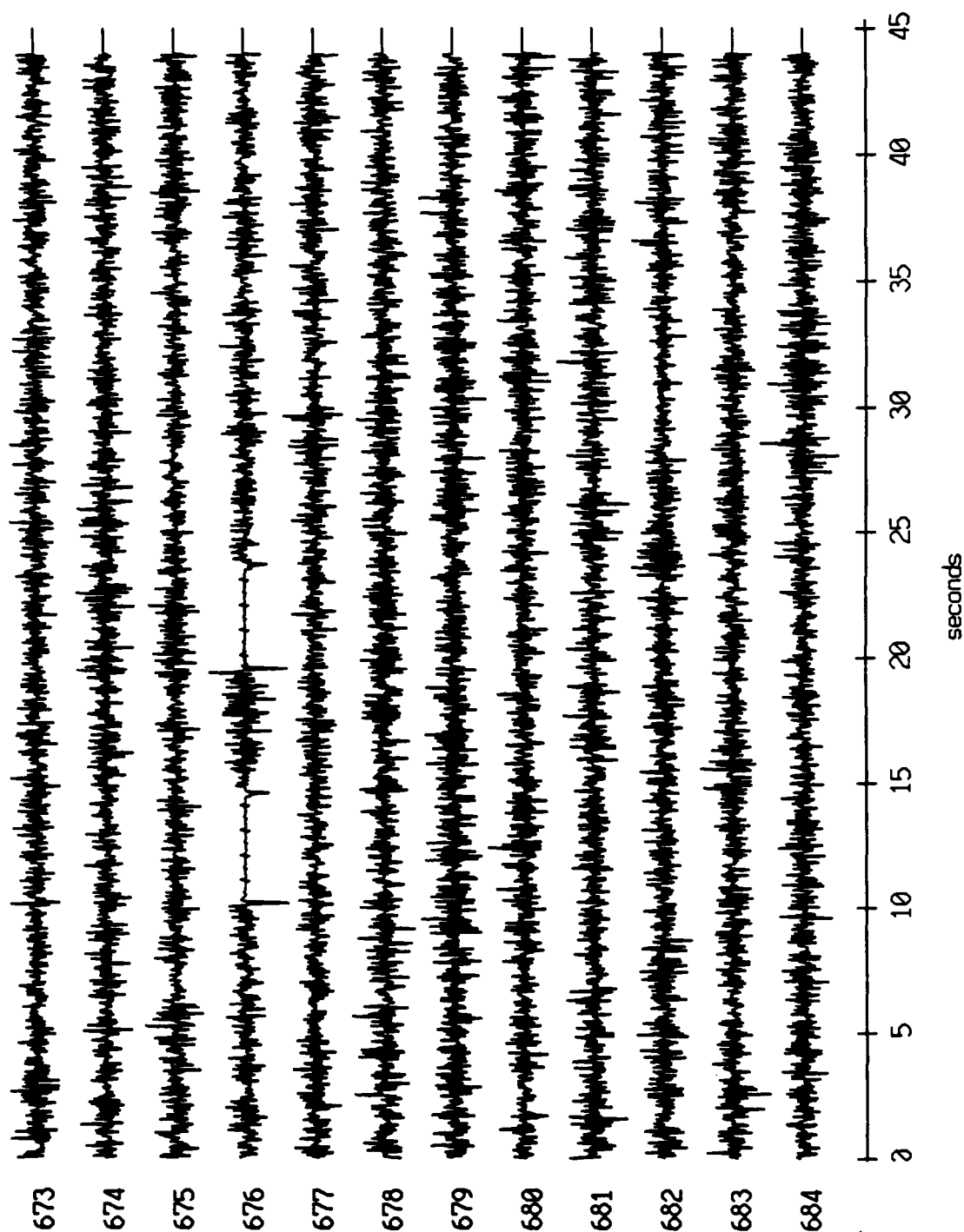
Float 4, July, 1989 Trip - records 673-684 (z-axis)  
vertical axis scale is approx. -2.0 to 2.0 volts



PGC corrected channel level (V)

Figure XI.5a

Float 4, July, 1989 Trip - records 673-684 (hydrophone)  
vertical axis scale is approx. -2.0 to 2.0 volts



AGC corrected channel level (V)

Figure XI.5b

Float 5, July, 1989 Trip - records 673-684 (z-axis)  
vertical axis scale is approx. -2.0 to 2.0 volts

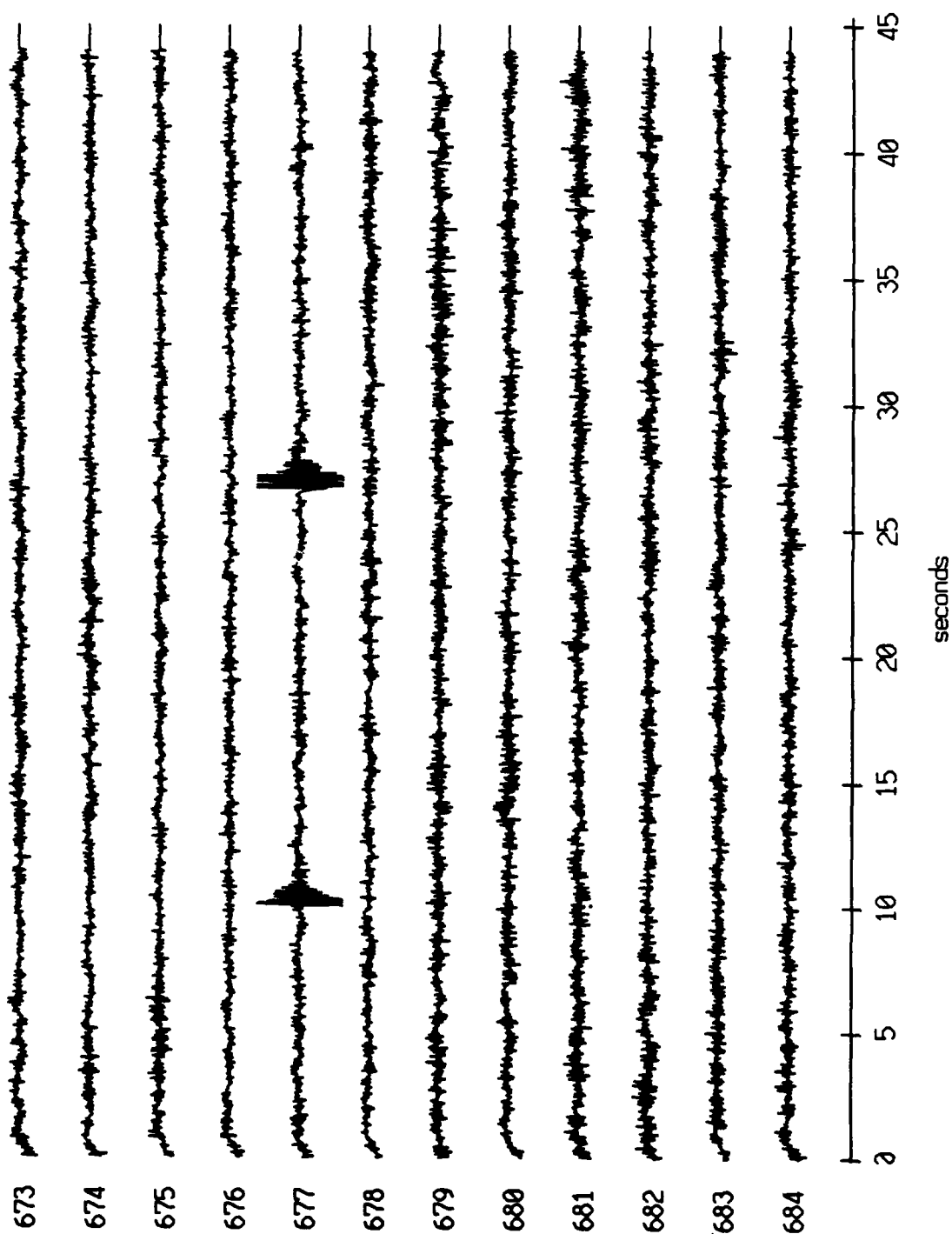
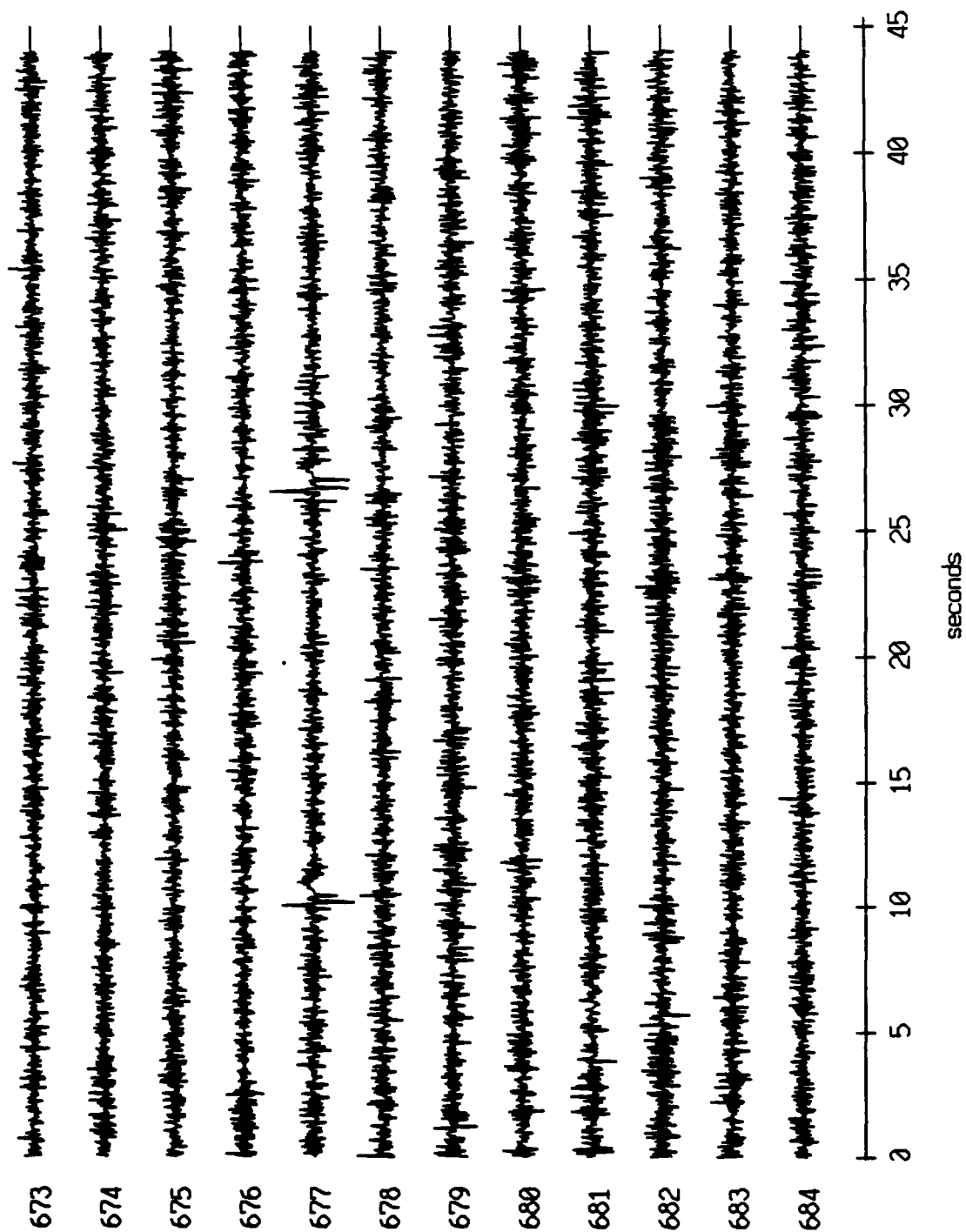


Figure XI.6a

Float 5, July, 1989 Trip - records 673-684 (hydrophone)  
vertical axis scale is approx. -2.0 to 2.0 volts

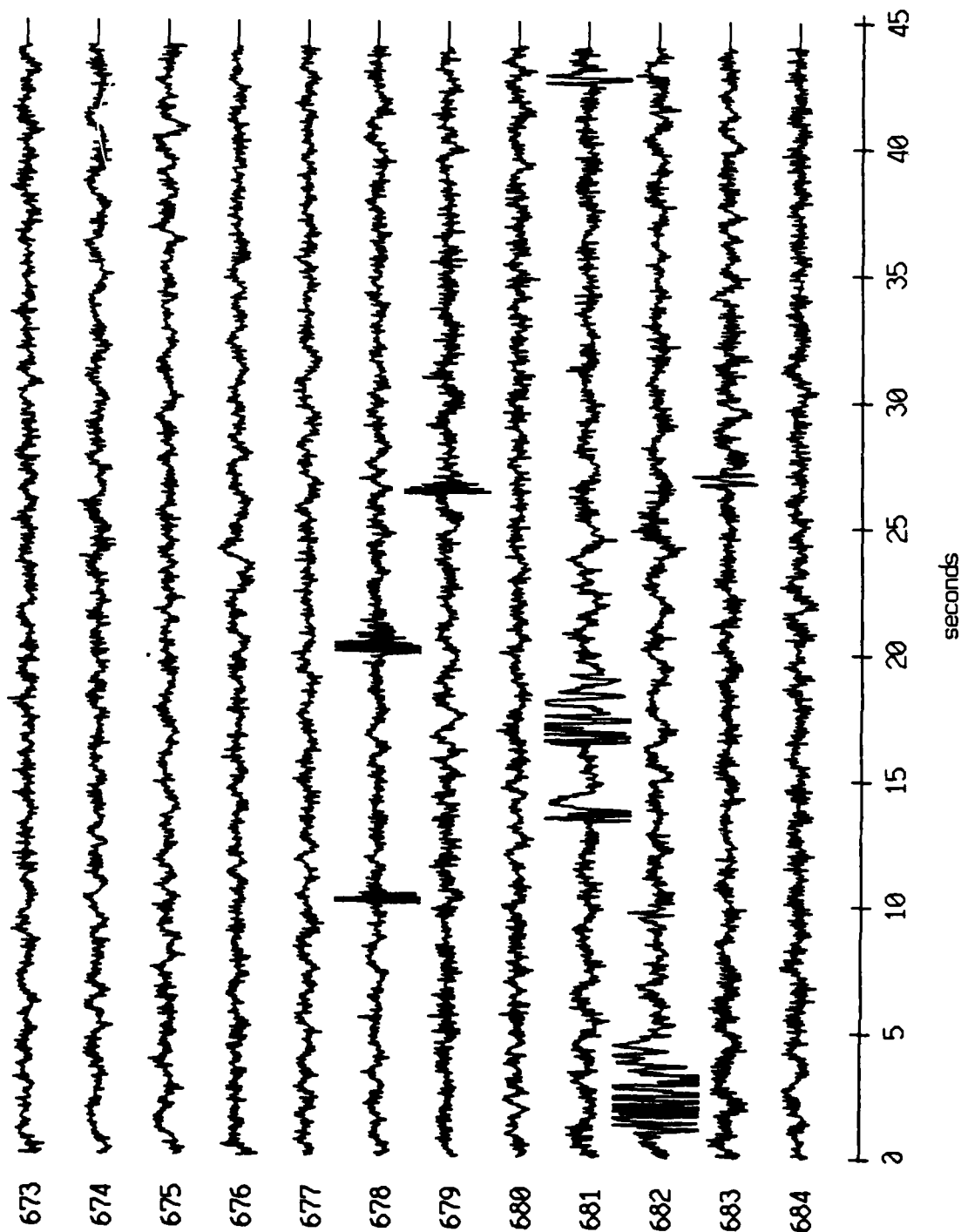


AGC corrected channel level (V)

Figure XI.6b



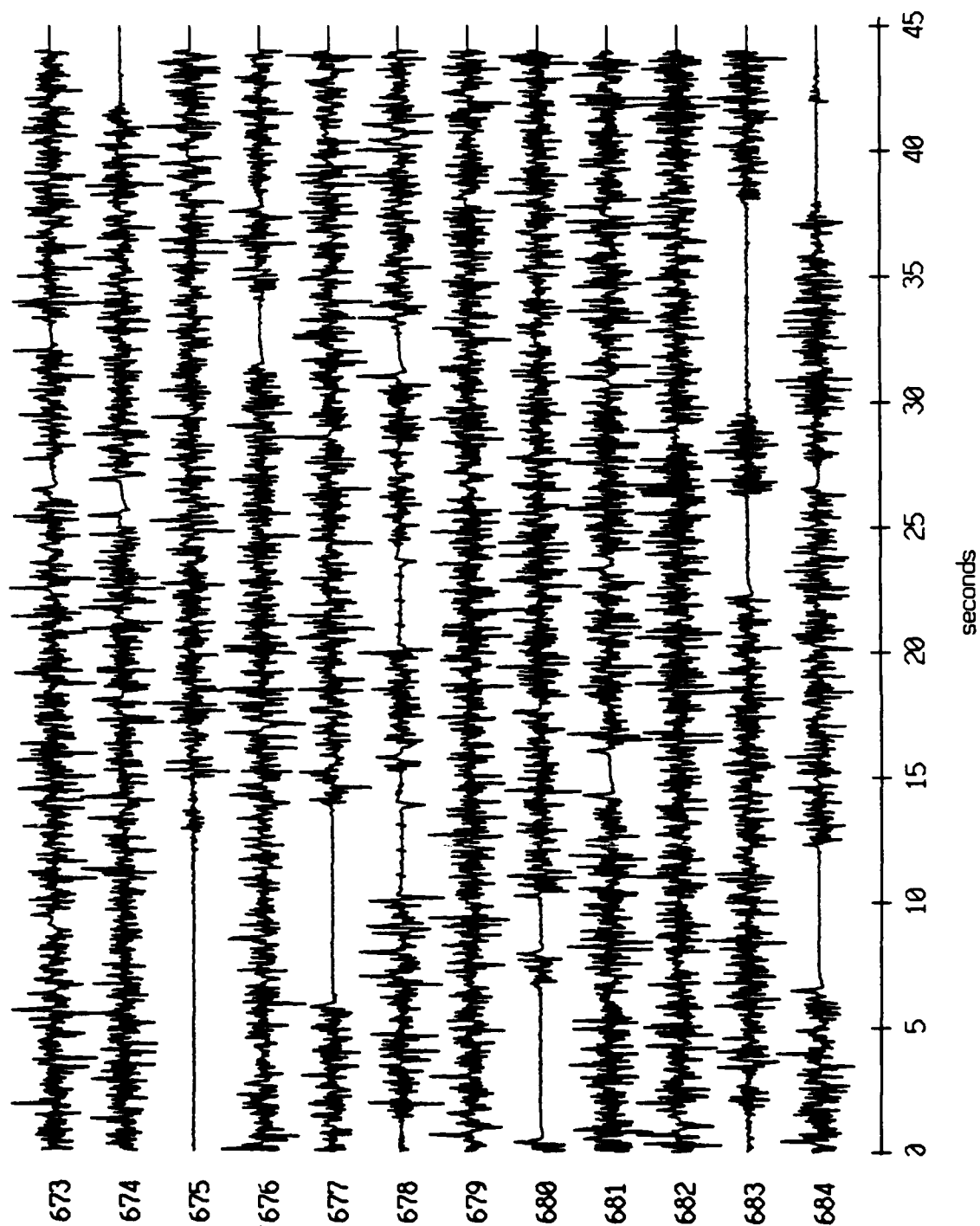
Floot 6, July, 1989 Trip - records 673-684 (z-axis)  
vertical axis scale is approx. -2.0 to 2.0 volts



RGC corrected channel level (V)

Figure XI.7a

Float 6, July, 1989 Trip - records 673-684 (hydrophone)  
vertical axis scale is approx. -2.0 to 2.0 volts



AGC corrected channel level (V)

Figure XI.7b

Float 7, July, 1989 Trip - records 673-684 (z-axis)  
vertical axis scale is approx. -2.0 to 2.0 volts

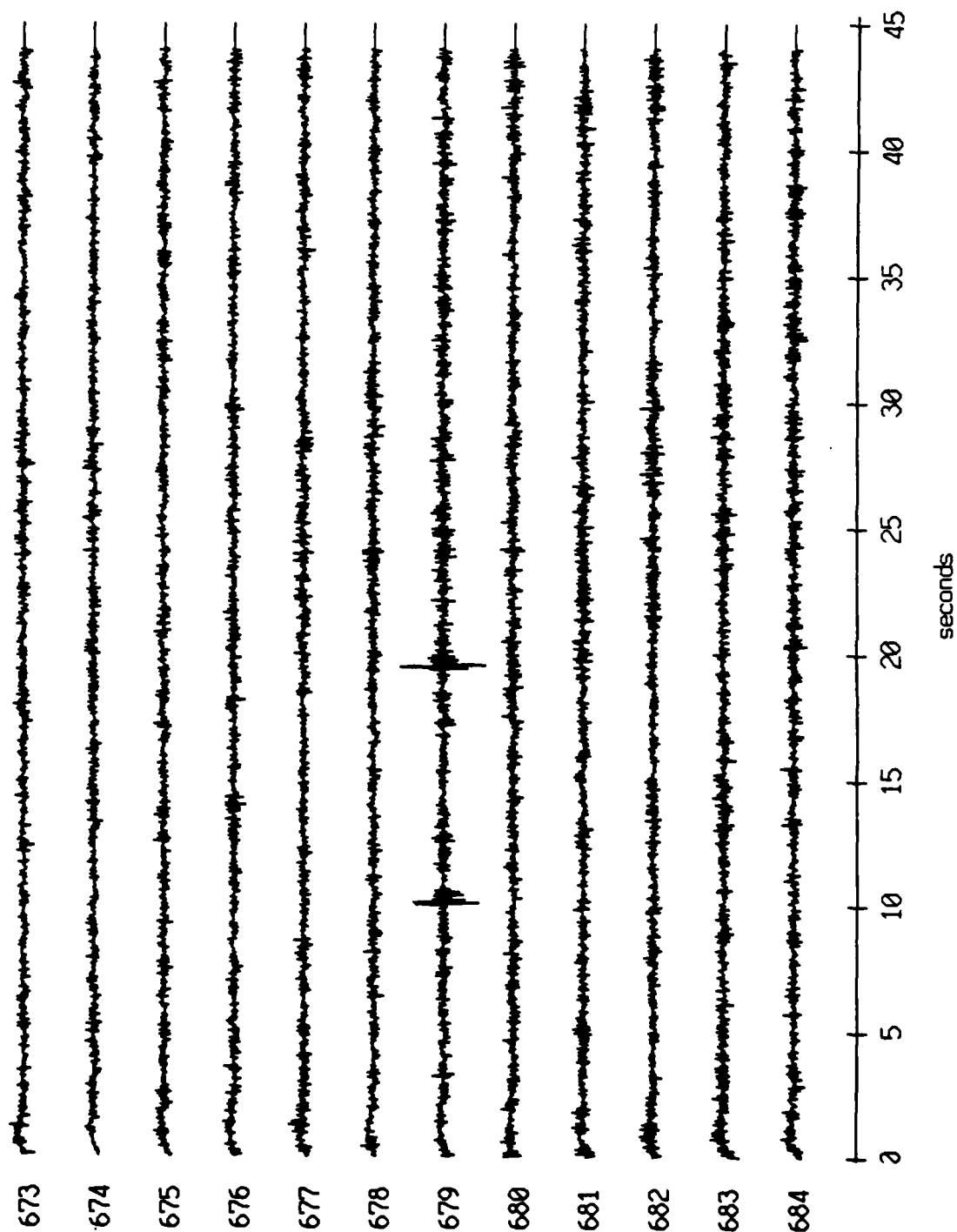
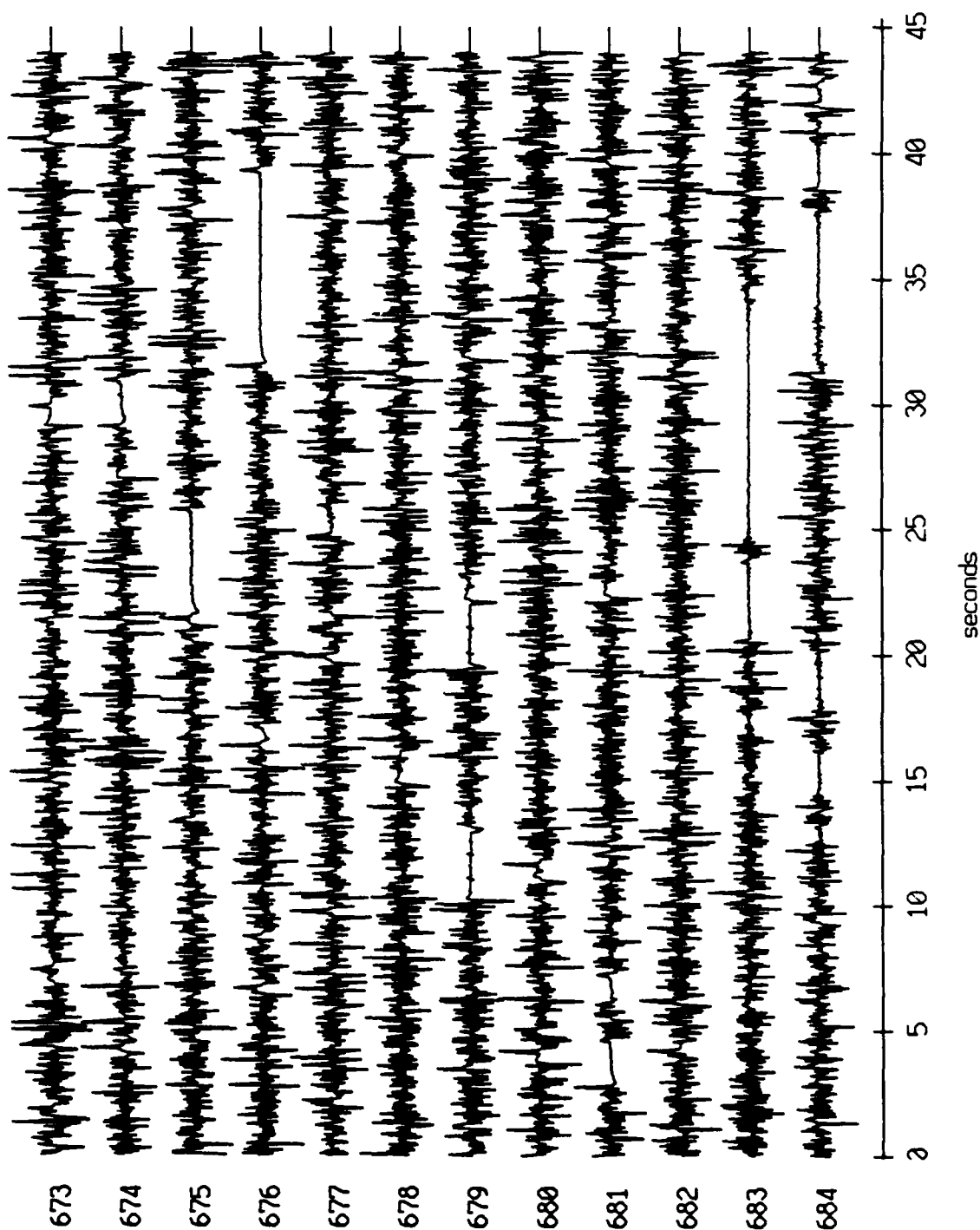


Figure XI.8a

Floot 7, July, 1989 Trip - records 673-684 (hydrophone)  
 vertical axis scale is approx. -2.0 to 2.0 volts



AGC corrected channel level (V)

Figure XI.8b

Floot 8, July, 1989 Trip - records 673-684 (z-axis)  
vertical axis scale is approx. -2.0 to 2.0 volts

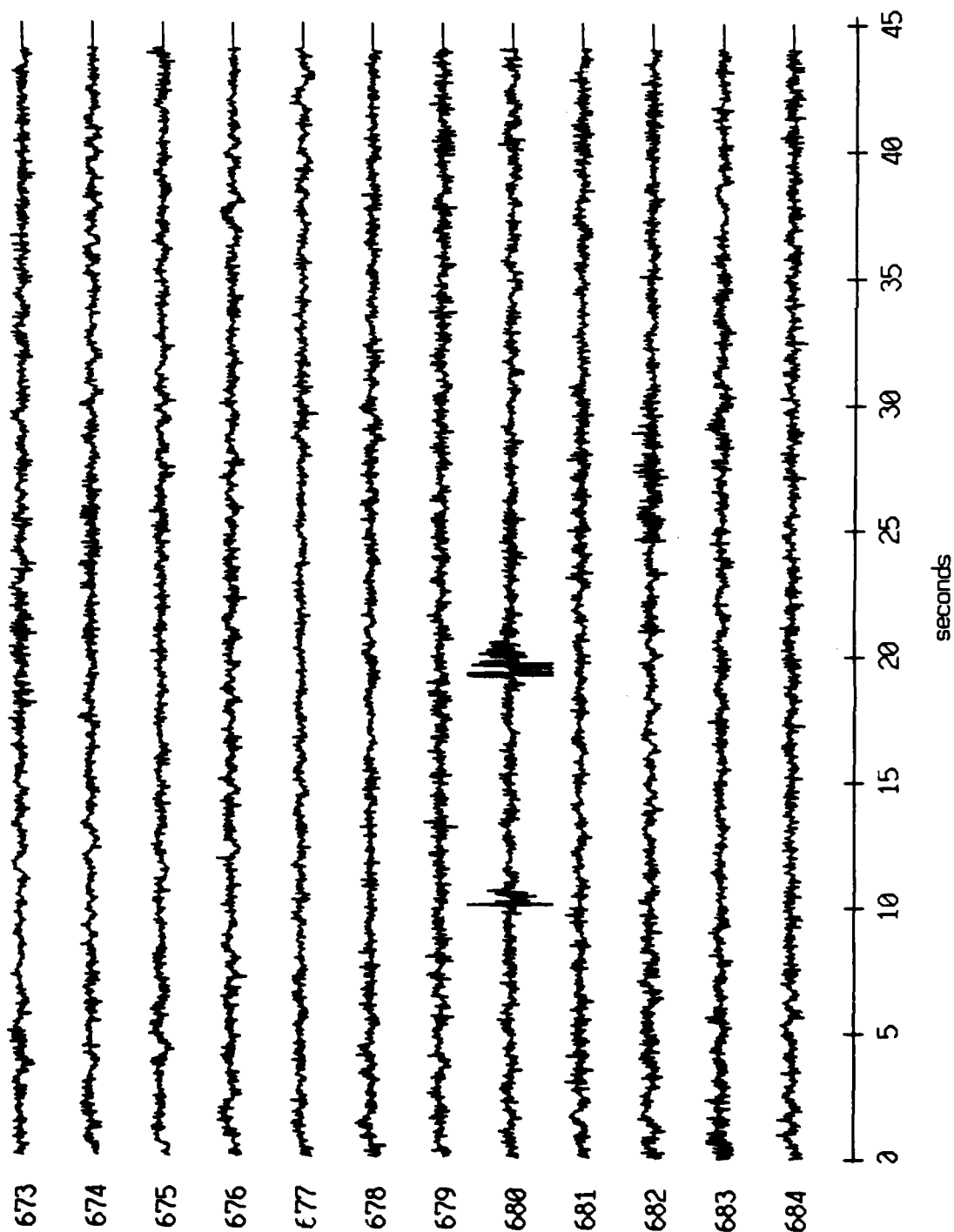


Figure XI.9a

Float 8, July, 1989 Trip - records 673-684 (hydrophone)  
vertical axis scale is approx. -2.0 to 2.0 volts

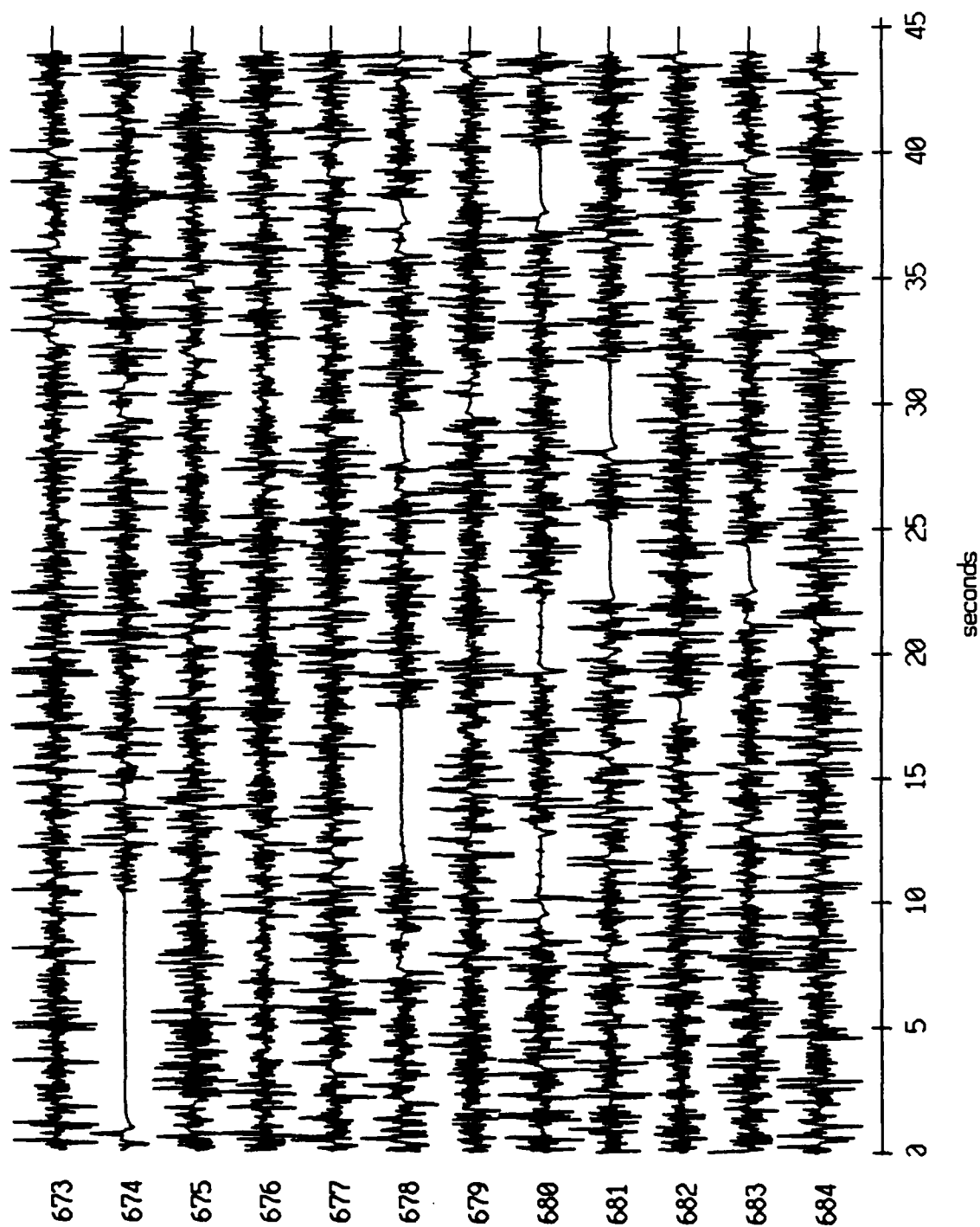


Figure XI.9b

Float 9, July, 1989 Trip - records 673-684 (z-axis)  
vertical axis scale is approx. -2.0 to 2.0 volts

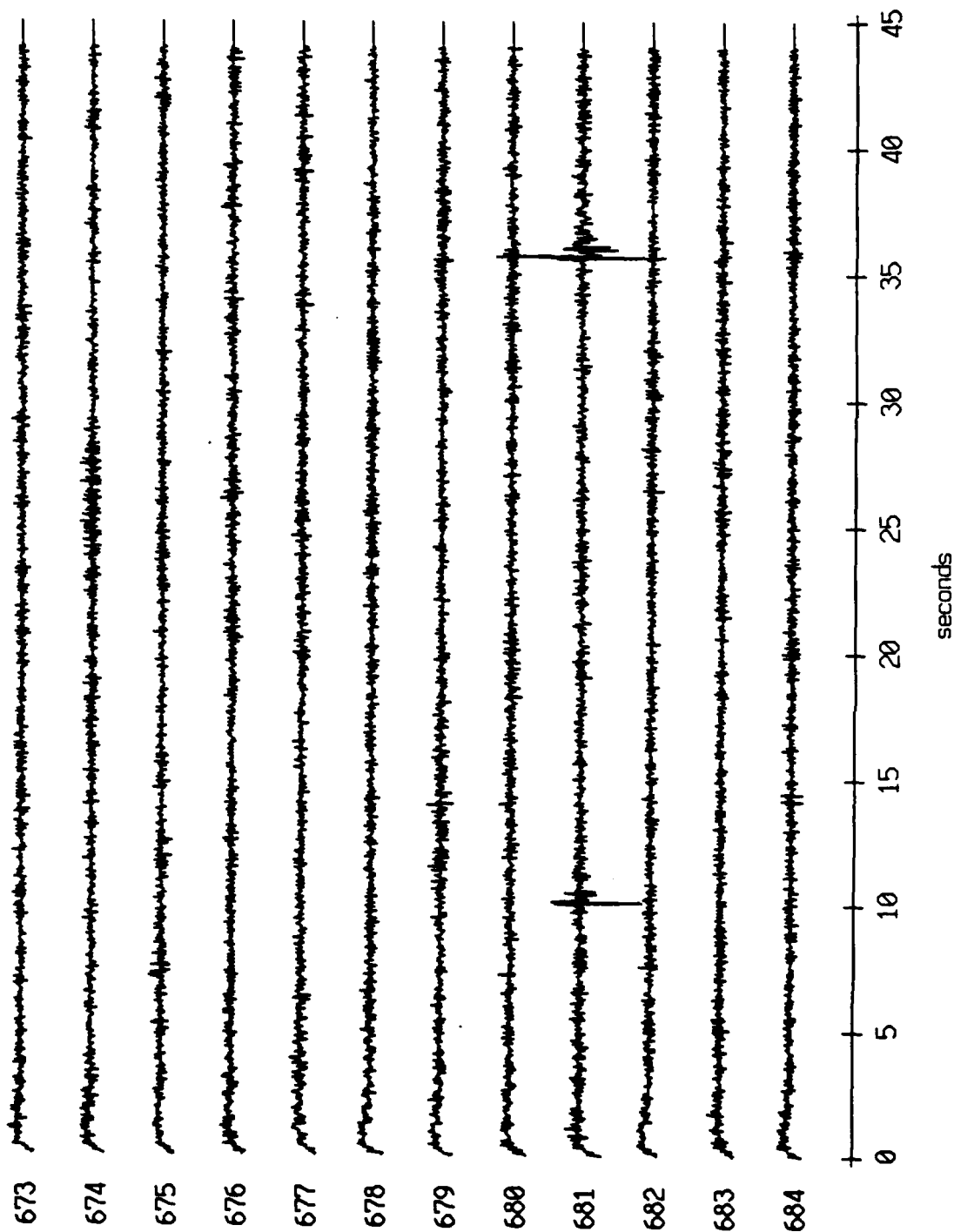
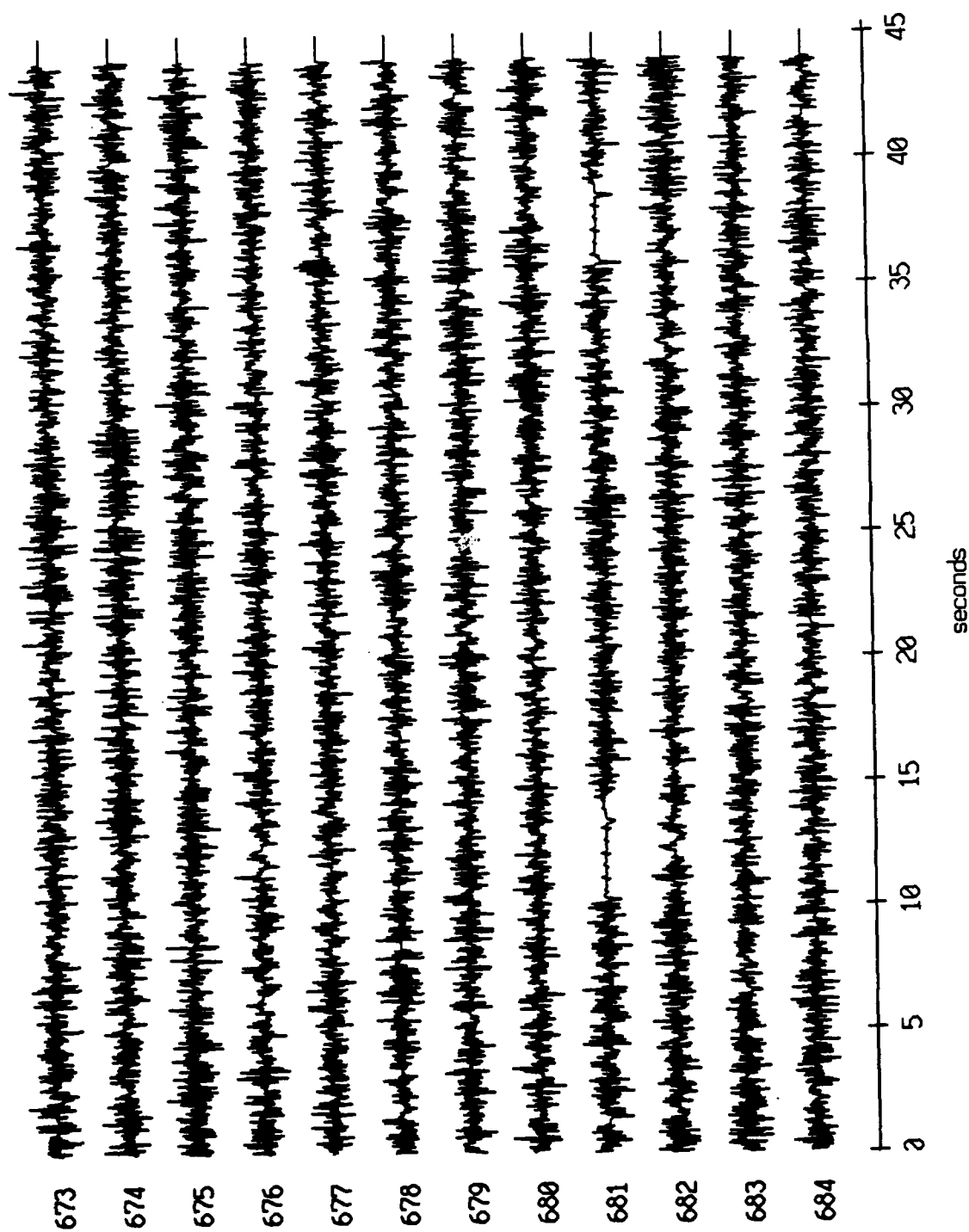


Figure XI.10a

Floot 9, July, 1989 Trip - records 673-684 (hydrophone)  
vertical axis scale is approx. -2.0 to 2.0 volts

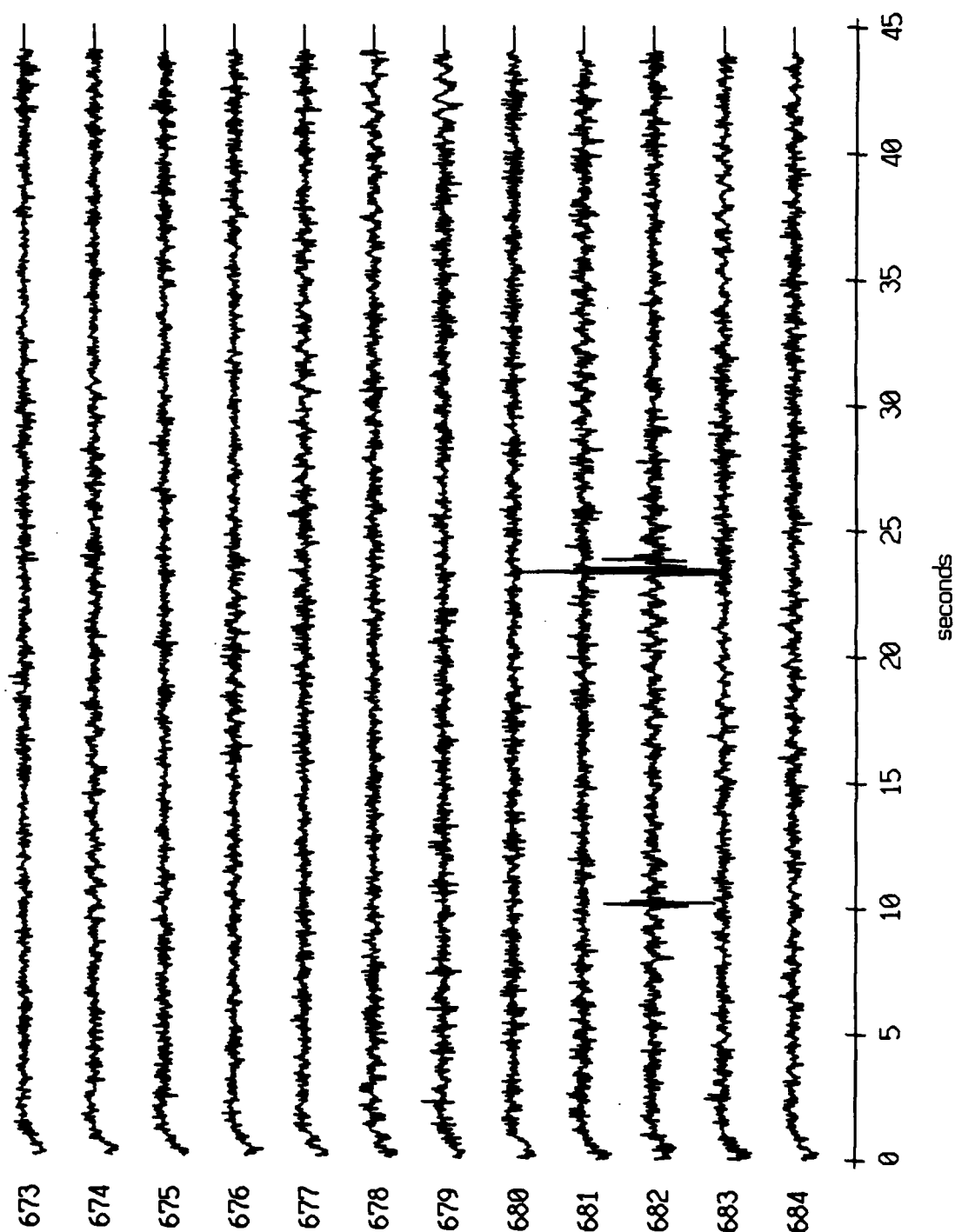


AGC corrected channel level (V)

Figure XI.10b



Floot 10, July, 1989 Trip - records 673-684 (z-axis)  
vertical axis scale is approx. -2.0 to 2.0 volts



RGC corrected channel level (V)

Figure XI.11a

Float 10, July, 1989 Trip - records 673-684 (hydrophone)  
vertical axis scale is approx. -2.0 to 2.0 volts

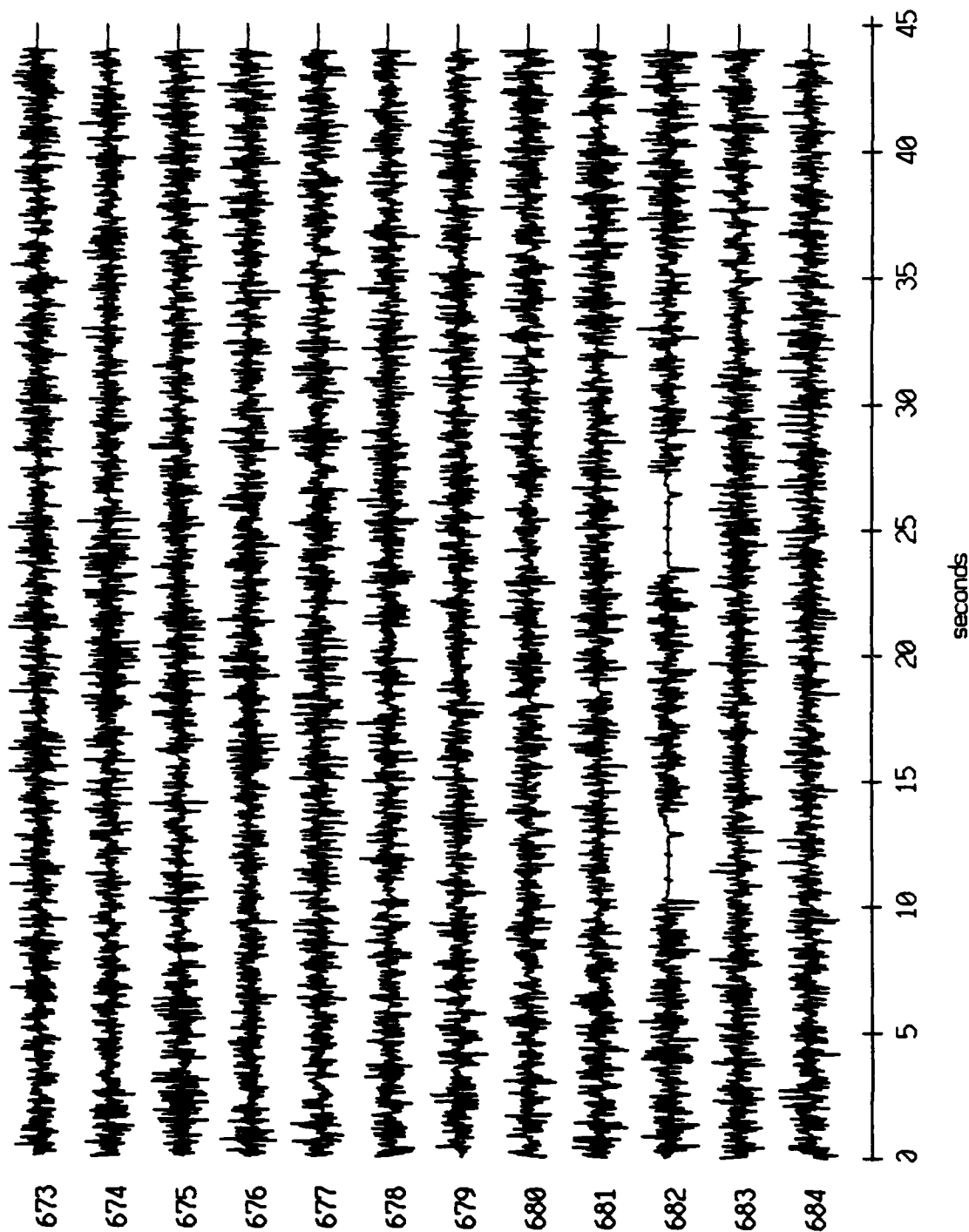


Figure XI.11b

Float 11, July, 1989 Trip - records 673-684 (z-axis)  
vertical axis scale is approx. -2.0 to 2.0 volts

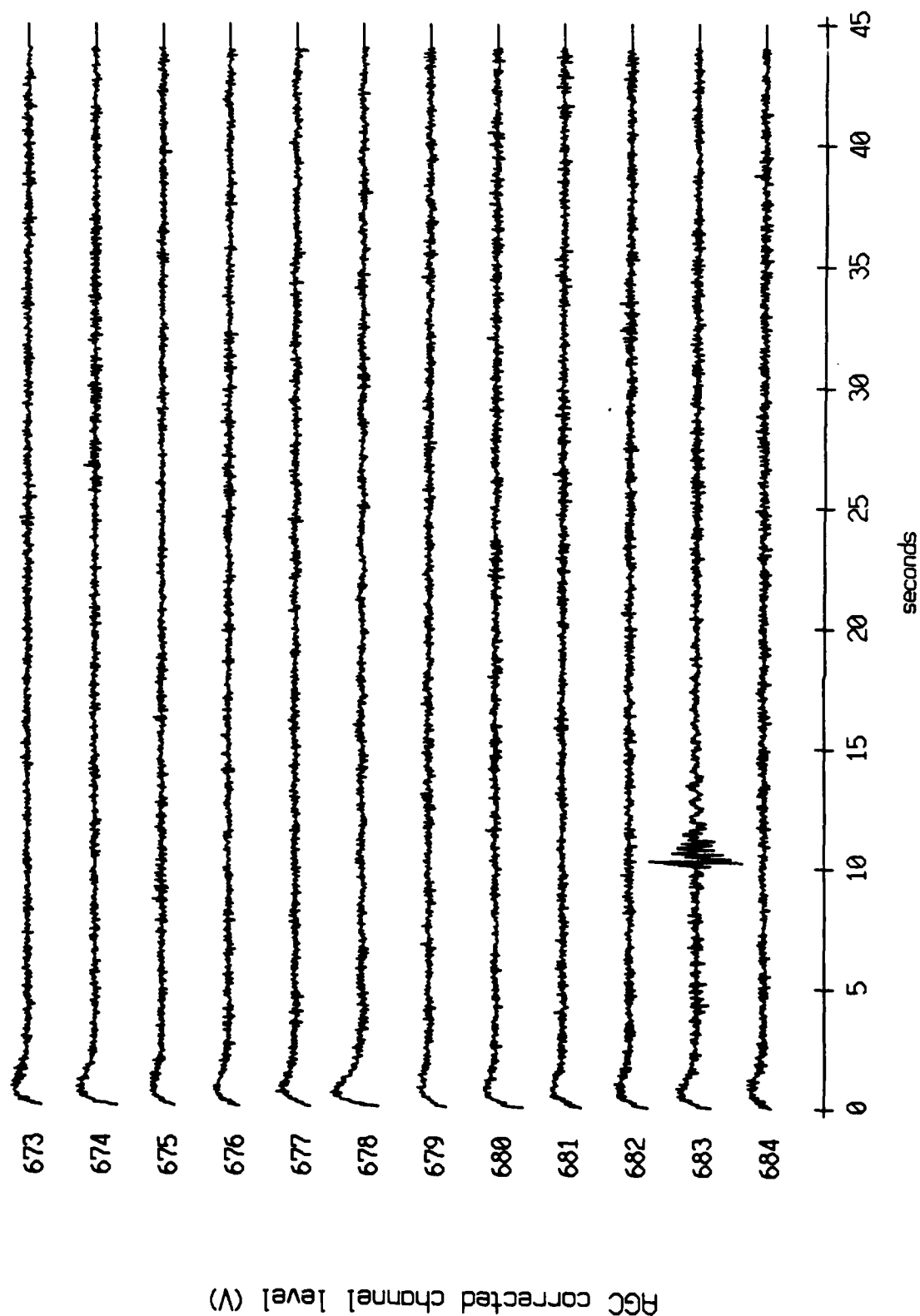


Figure XI.12a

Float 11, July, 1989 Trip - records 673-684 (hydrophone)  
vertical axis scale is approx. -2.0 to 2.0 volts

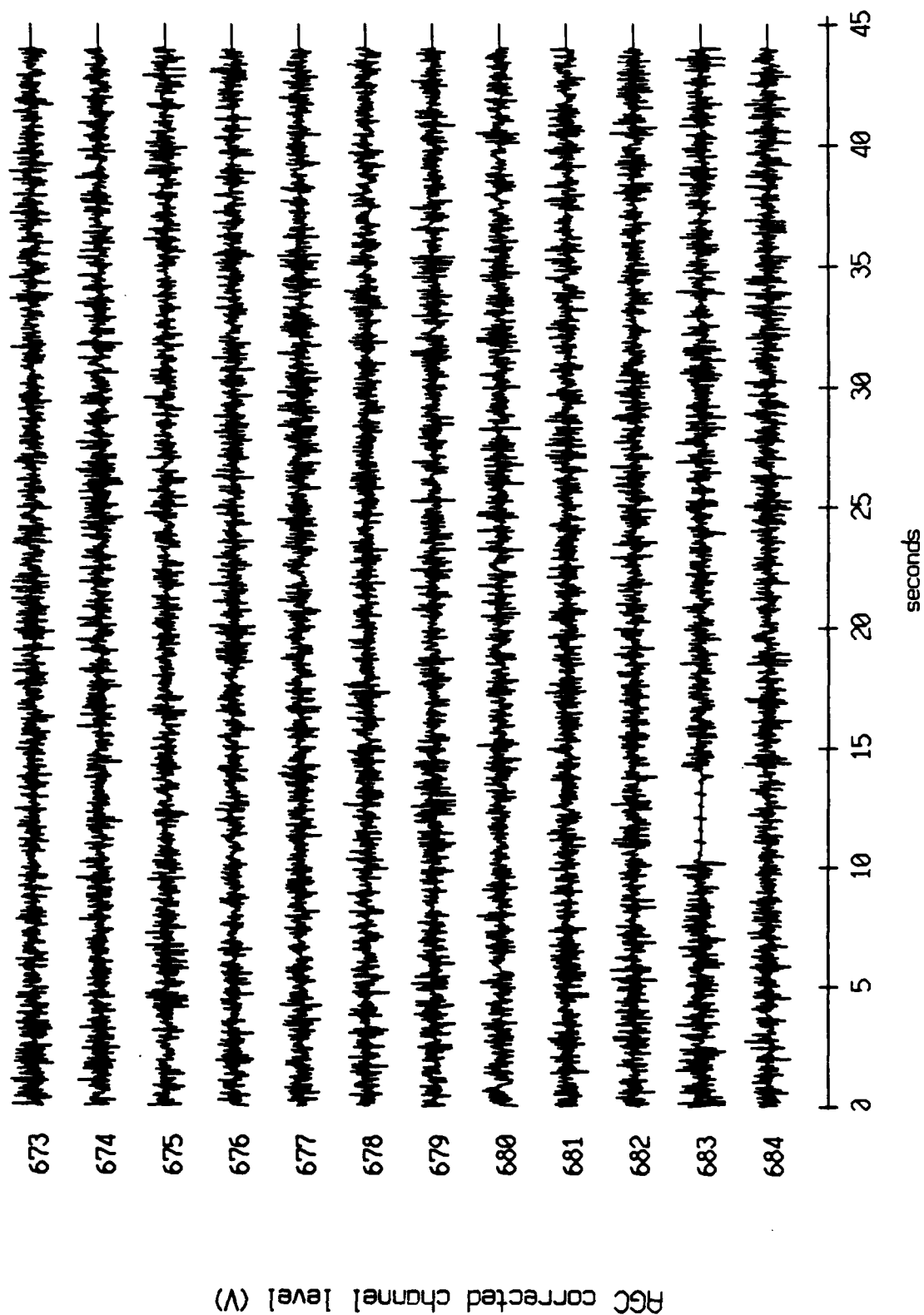


Figure XI.12b

Floot 1, July, 1989 Trip - records 738-749 (x-axis)  
vertical axis scale is approx. -1.5 to 1.5 volts

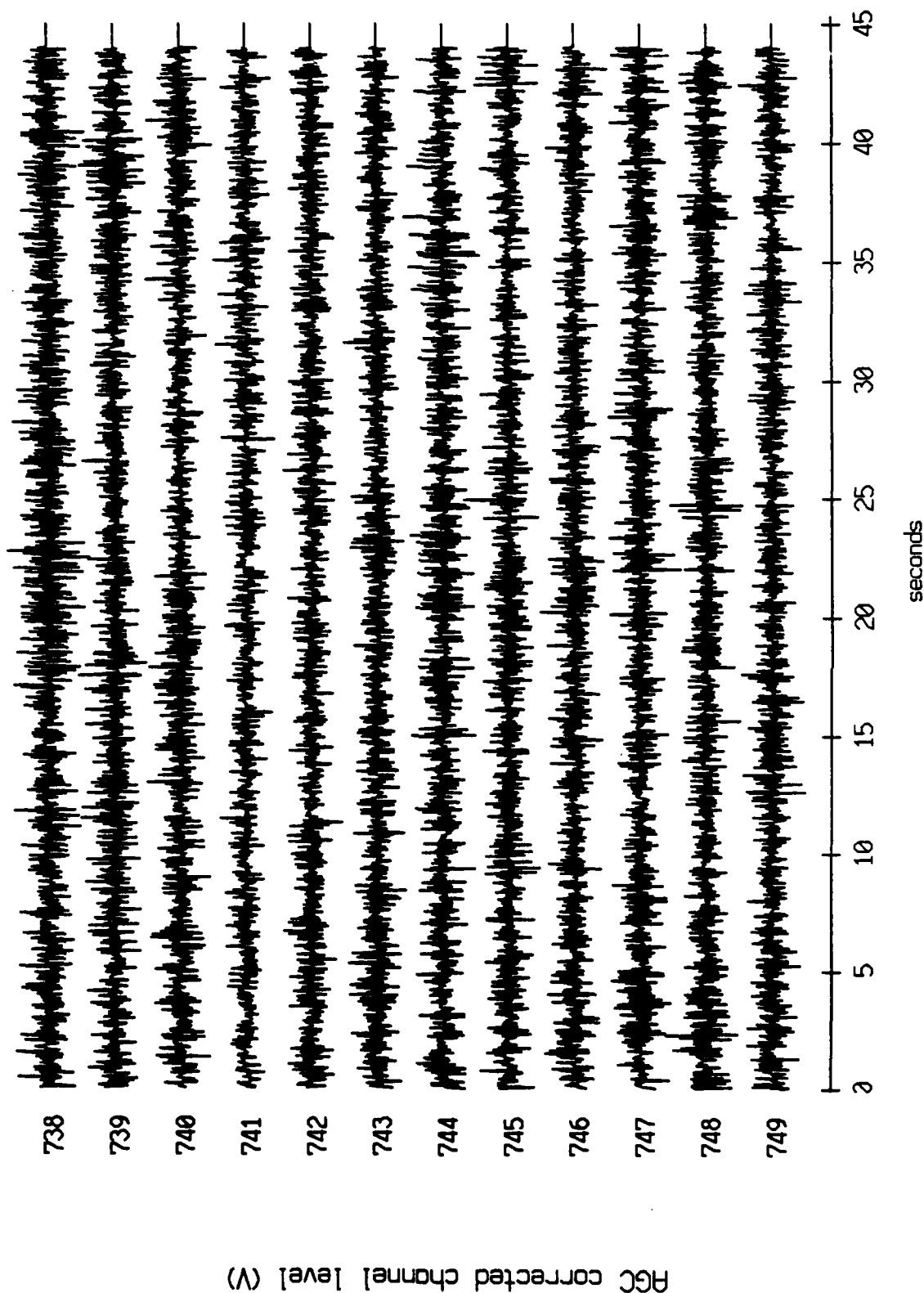
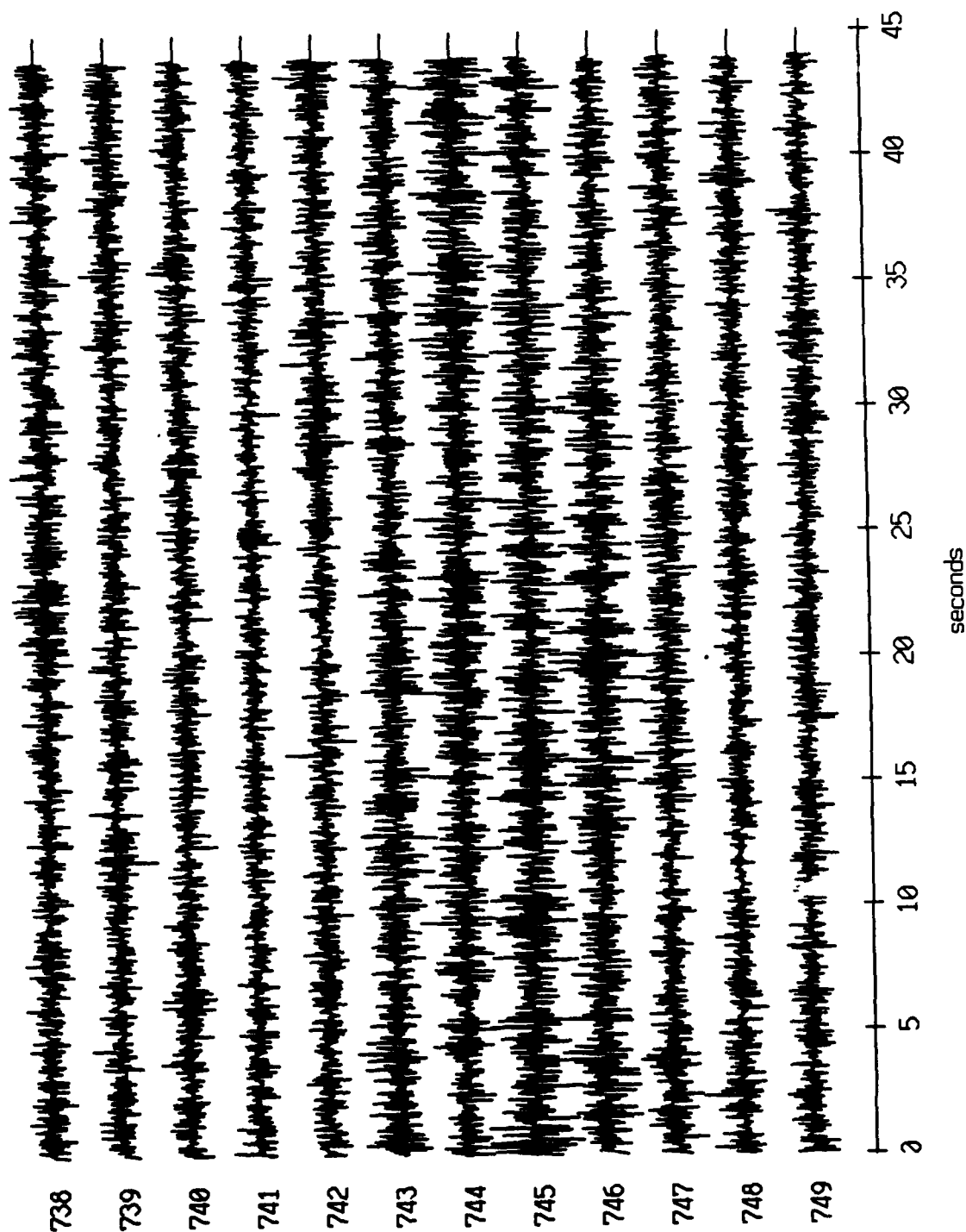


Figure XI.13a

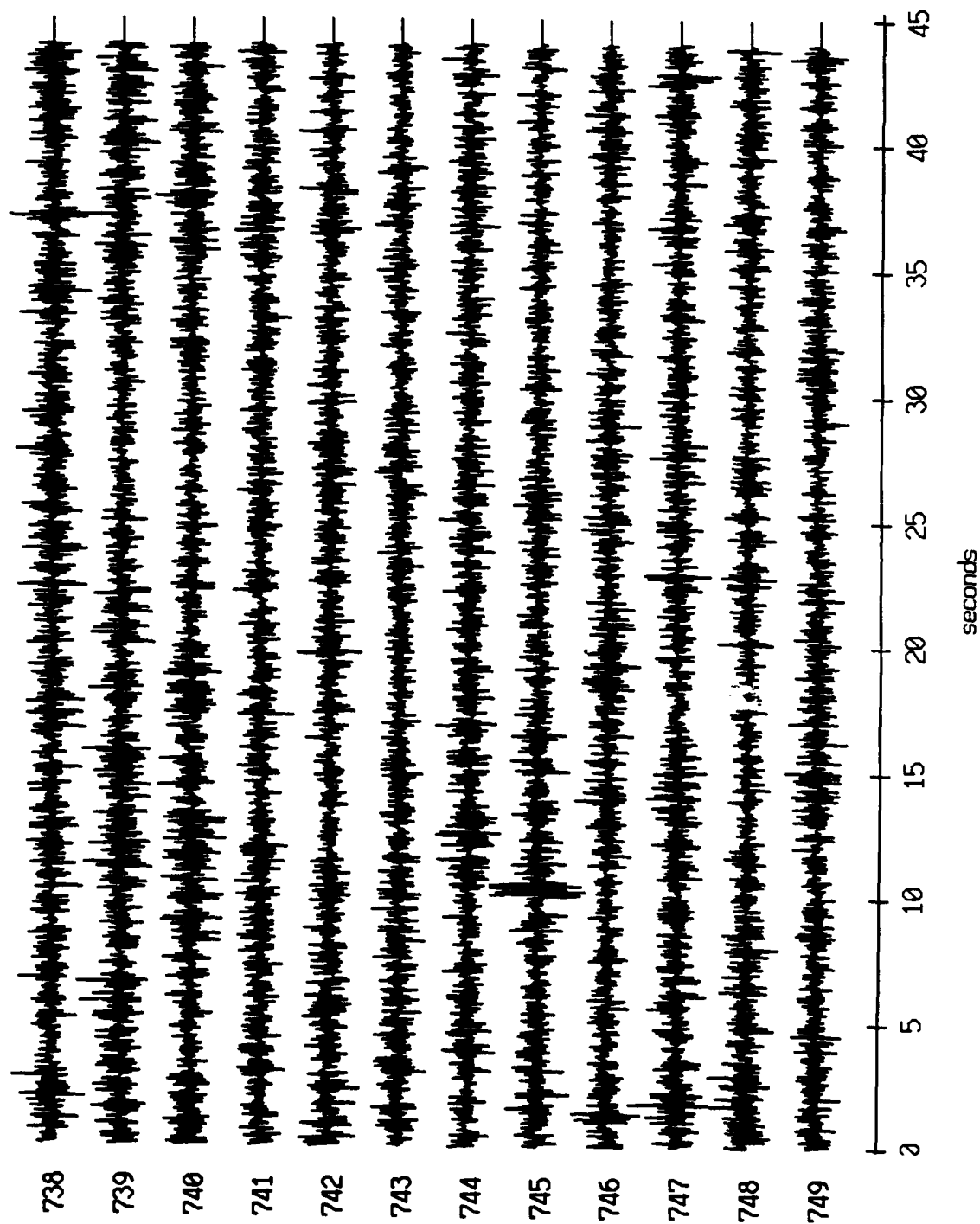
Floot 1, July, 1989 Trip - records 738-749 (y-axis)  
vertical axis scale is approx. -1.5 to 1.5 volts



RGC corrected channel level (V)

Figure XI.13b

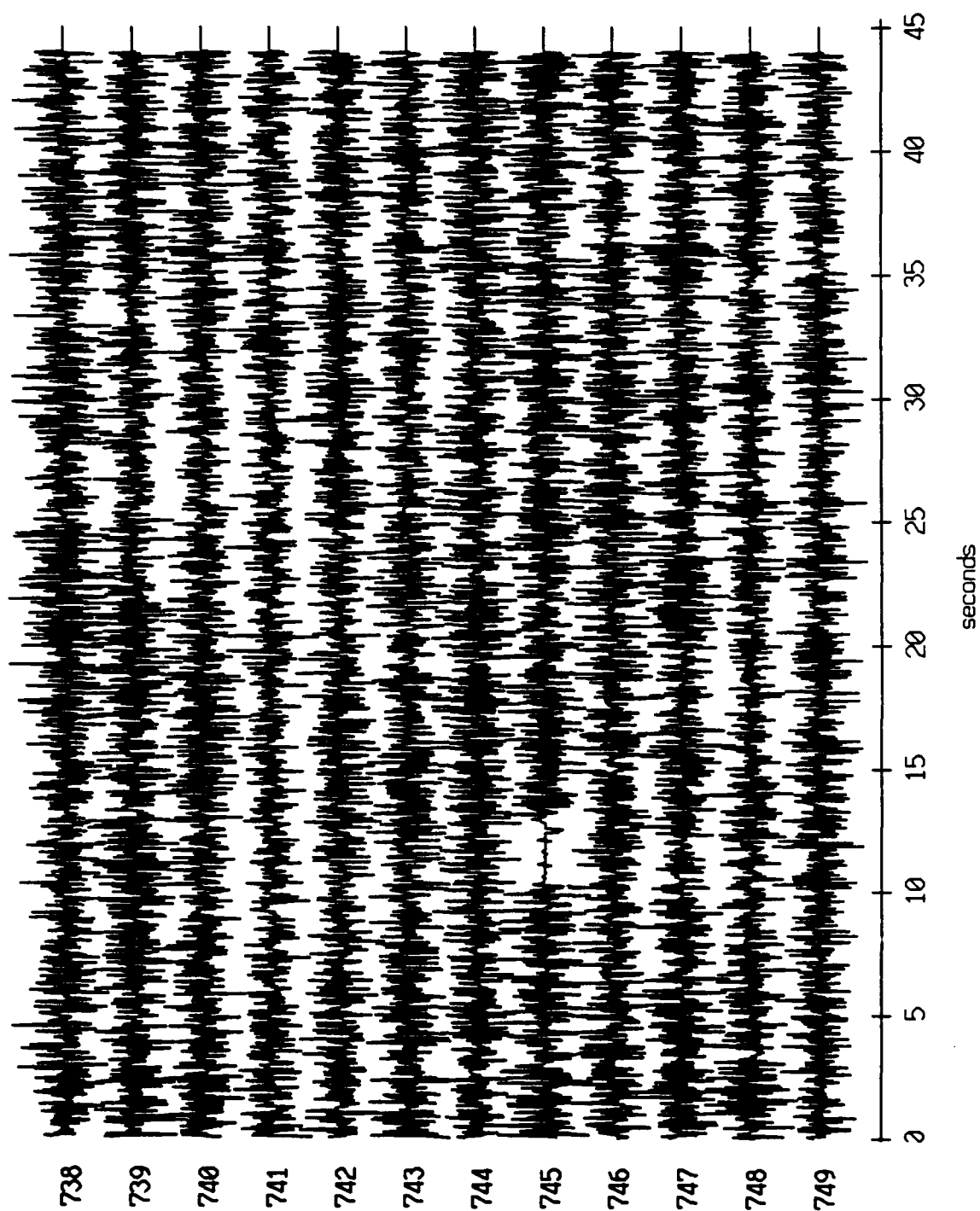
Float 1, July, 1989 Trip - records 738-749 (z-axis)  
vertical axis scale is approx. -1.5 to 1.5 volts



PGC corrected channel level (V)

Figure XI.13c

Float 1, July, 1989 Trip - records 738-749 (hydrophone)  
 vertical axis scale is approx. -1.5 to 1.5 volts

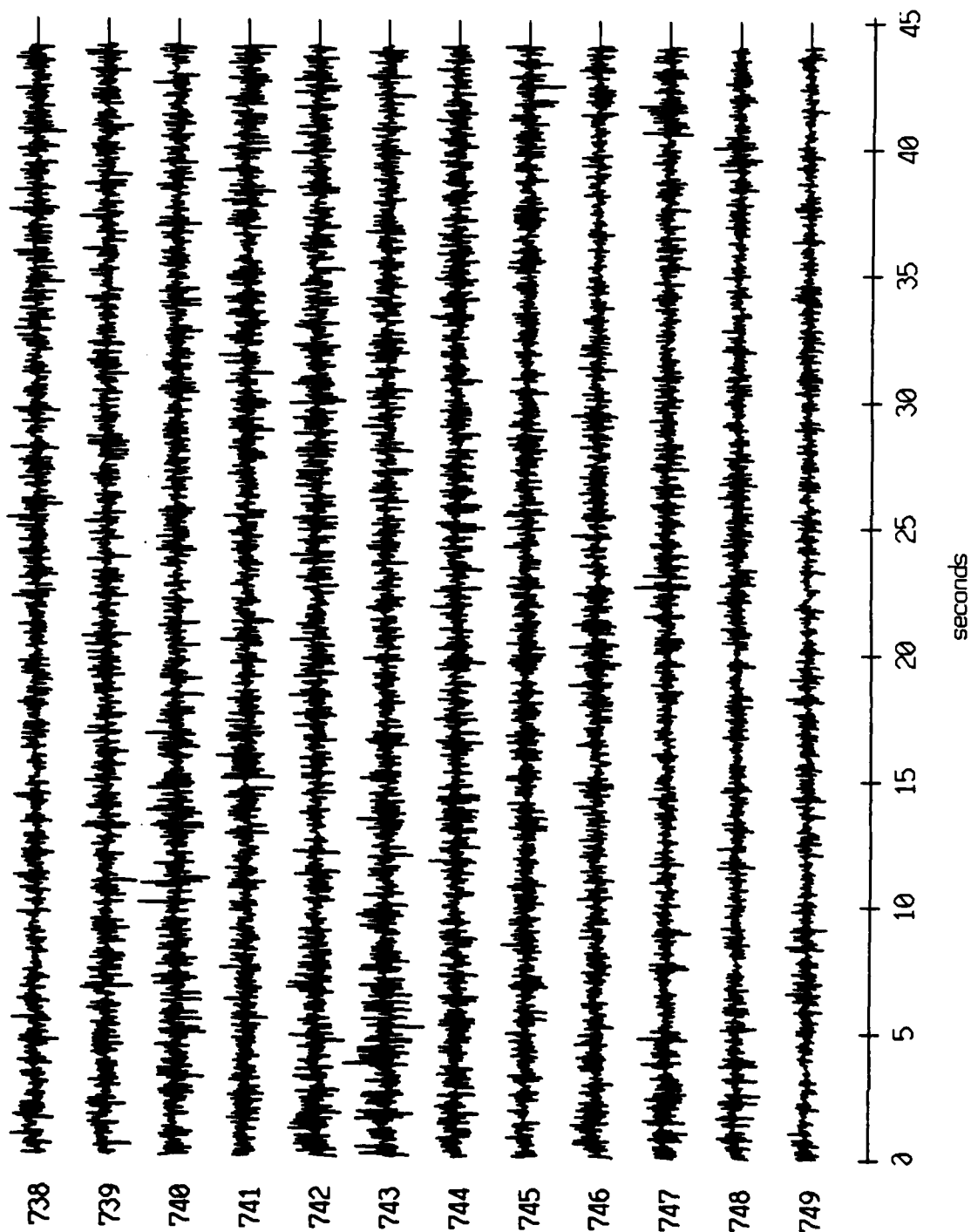


AGC corrected channel level (V)

Figure XI.13d



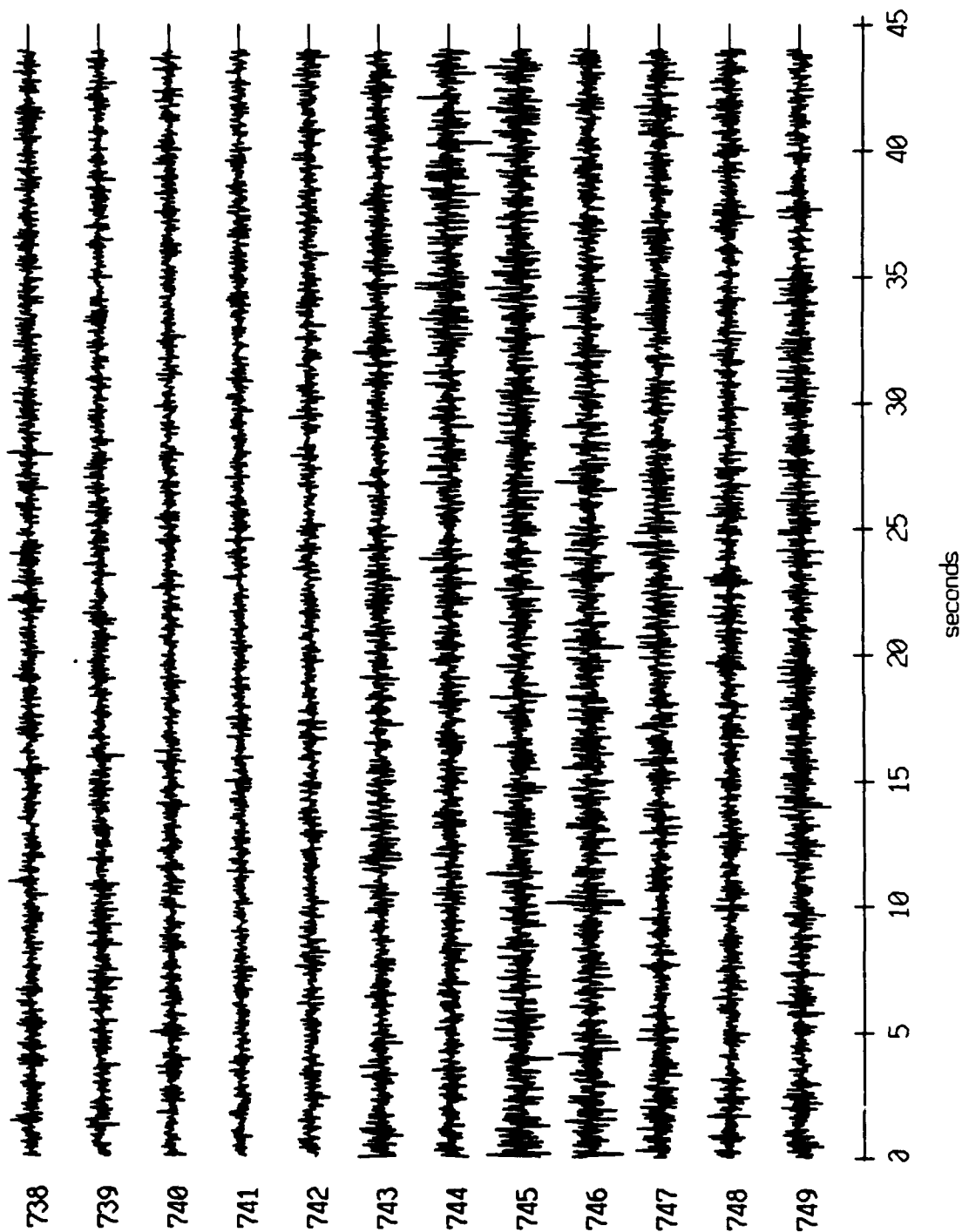
Float 2, July, 1989 Trip - records 738-749 (x-axis)  
vertical axis scale is approx. -1.5 to 1.5 volts



AGC corrected channel level (V)

Figure XI.14a

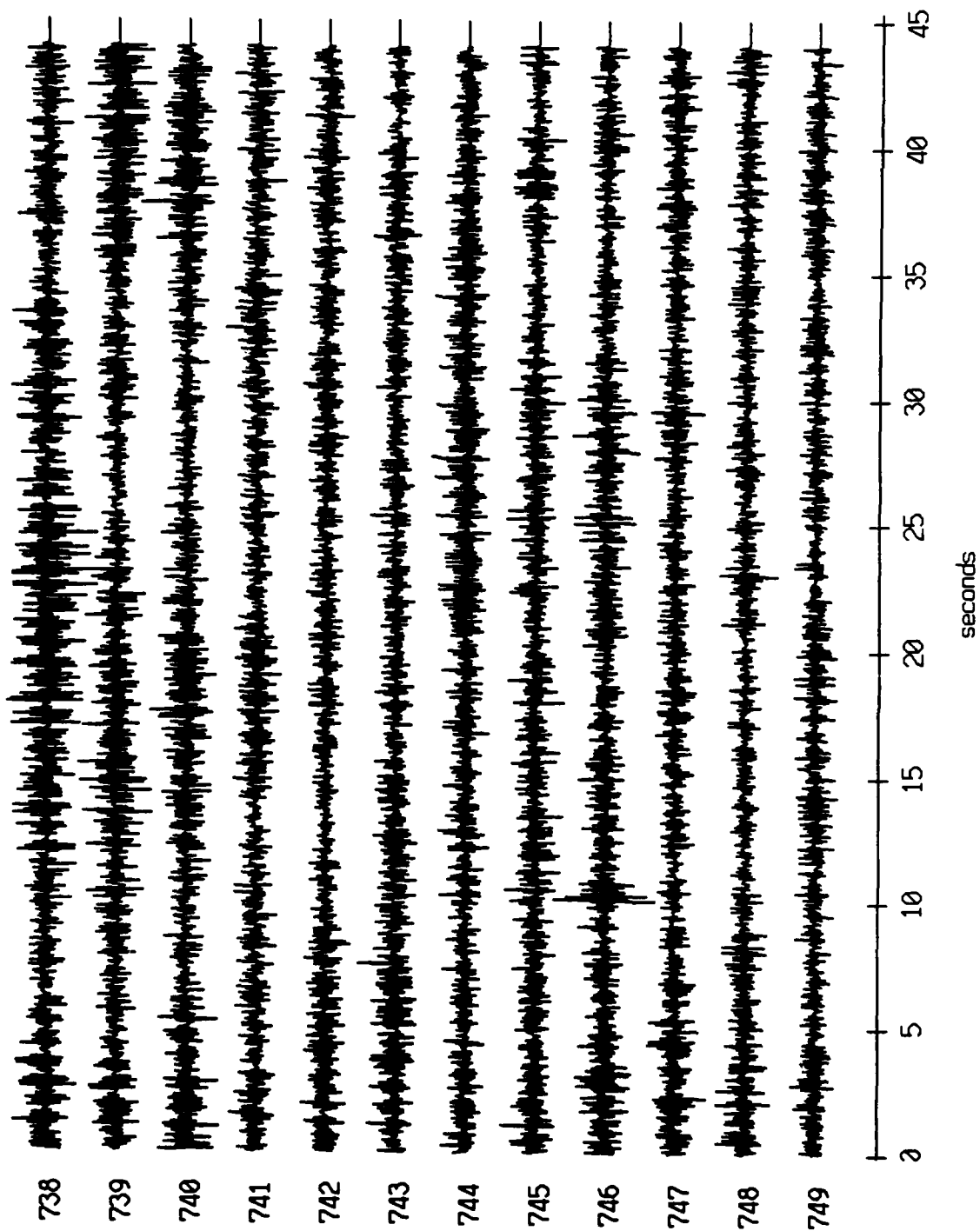
Float 2, July, 1989 Trip - records 738-749 (y-axis)  
vertical axis scale is approx. -1.5 to 1.5 volts



AGC corrected channel level (V)

Figure XI.14b

Float 2, July, 1989 Trip - records 738-749 (z-axis)  
vertical axis scale is approx. -1.5 to 1.5 volts



AGC corrected channel level (V)

Figure XI.14c

Float 2, July, 1989 Trip - records 738-749 (hydrophone)  
vertical axis scale is approx. -1.5 to 1.5 volts

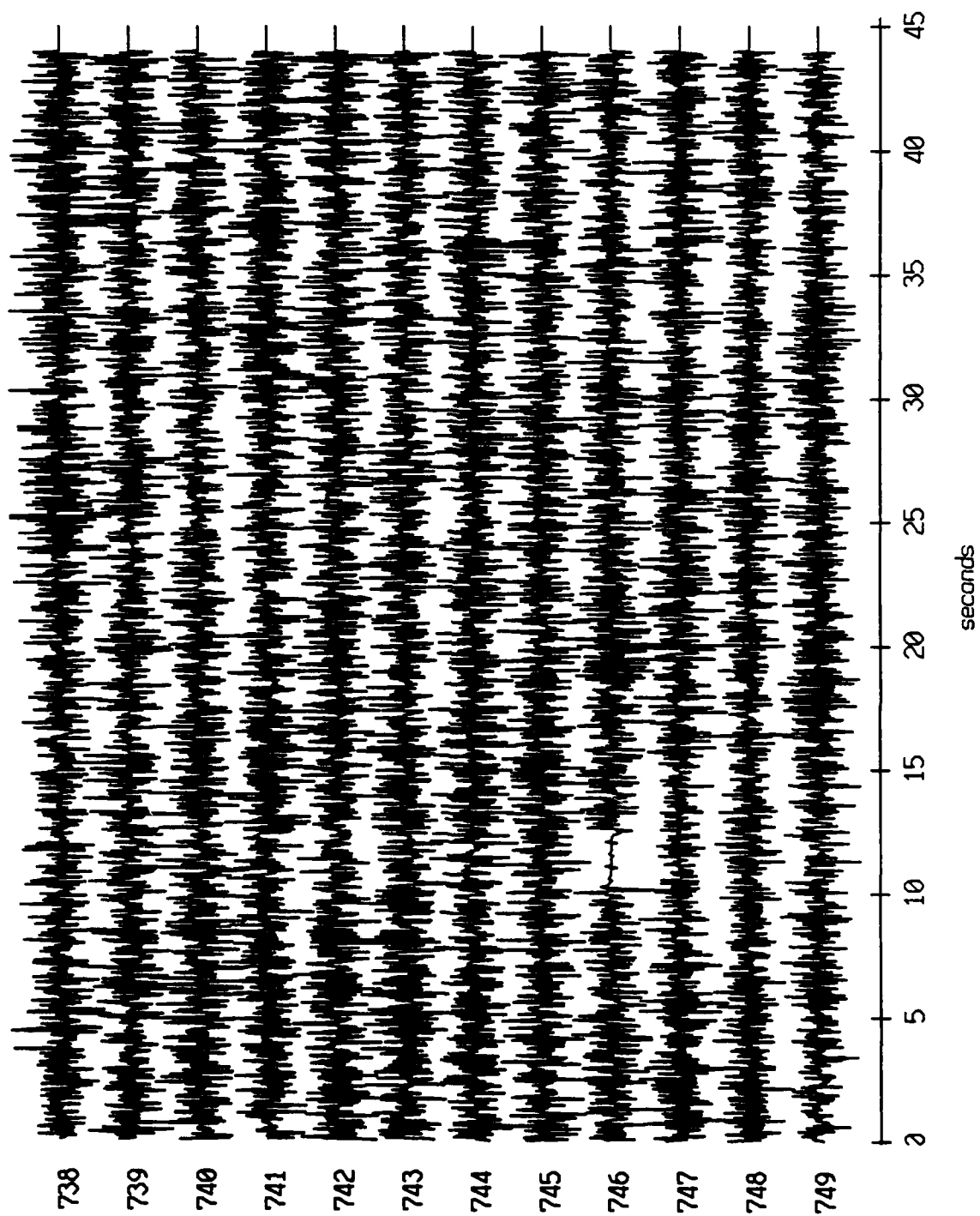


Figure XI.14d

Float 0, July, 1989 Trip - records 767-778 (x-axis)  
vertical axis scale is approx. -1.0 to 1.0 volts

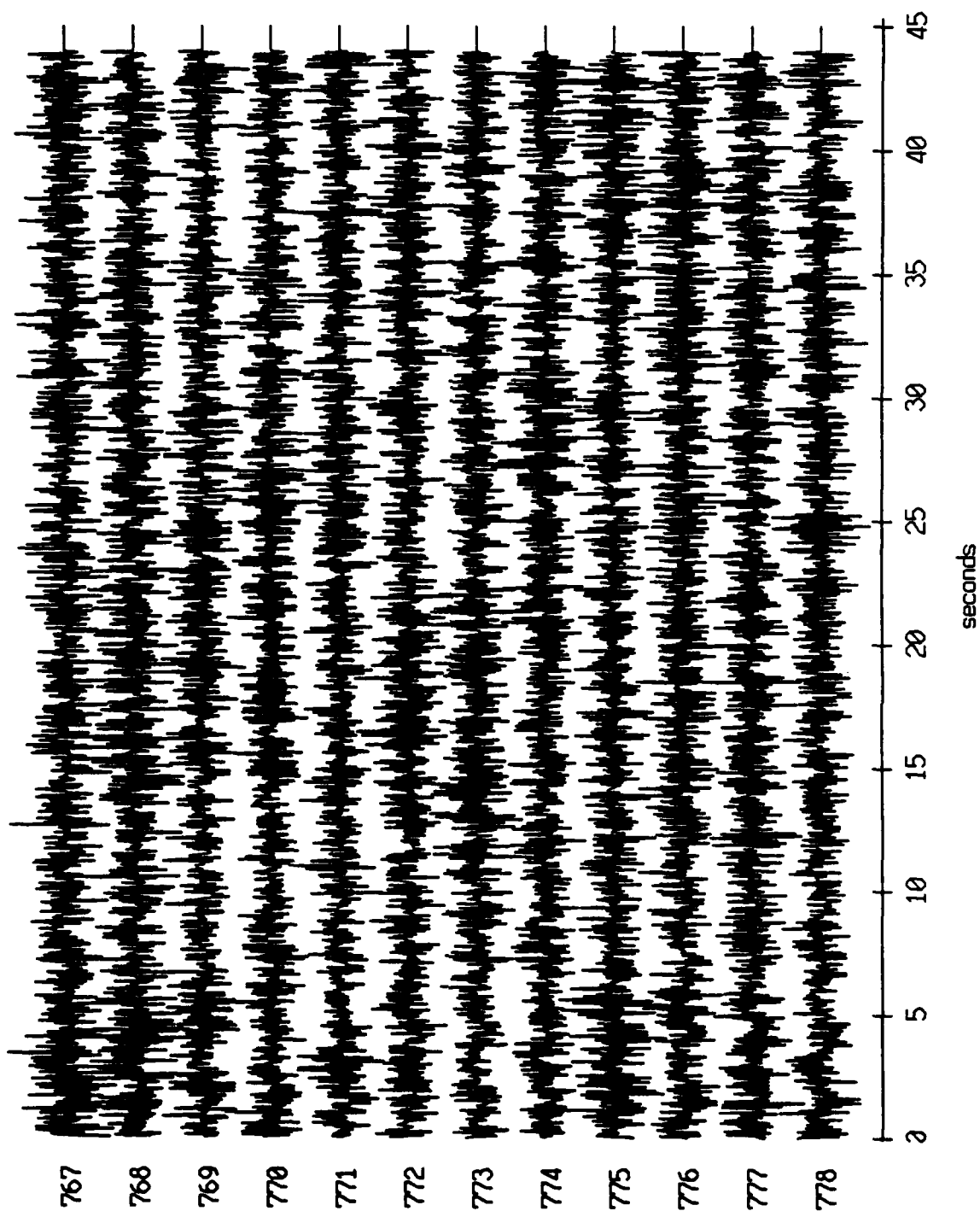


Figure XI.15a

Float 0, July, 1989 Trip - records 767-778 (y-axis)  
vertical axis scale is approx. -1.0 to 1.0 volts

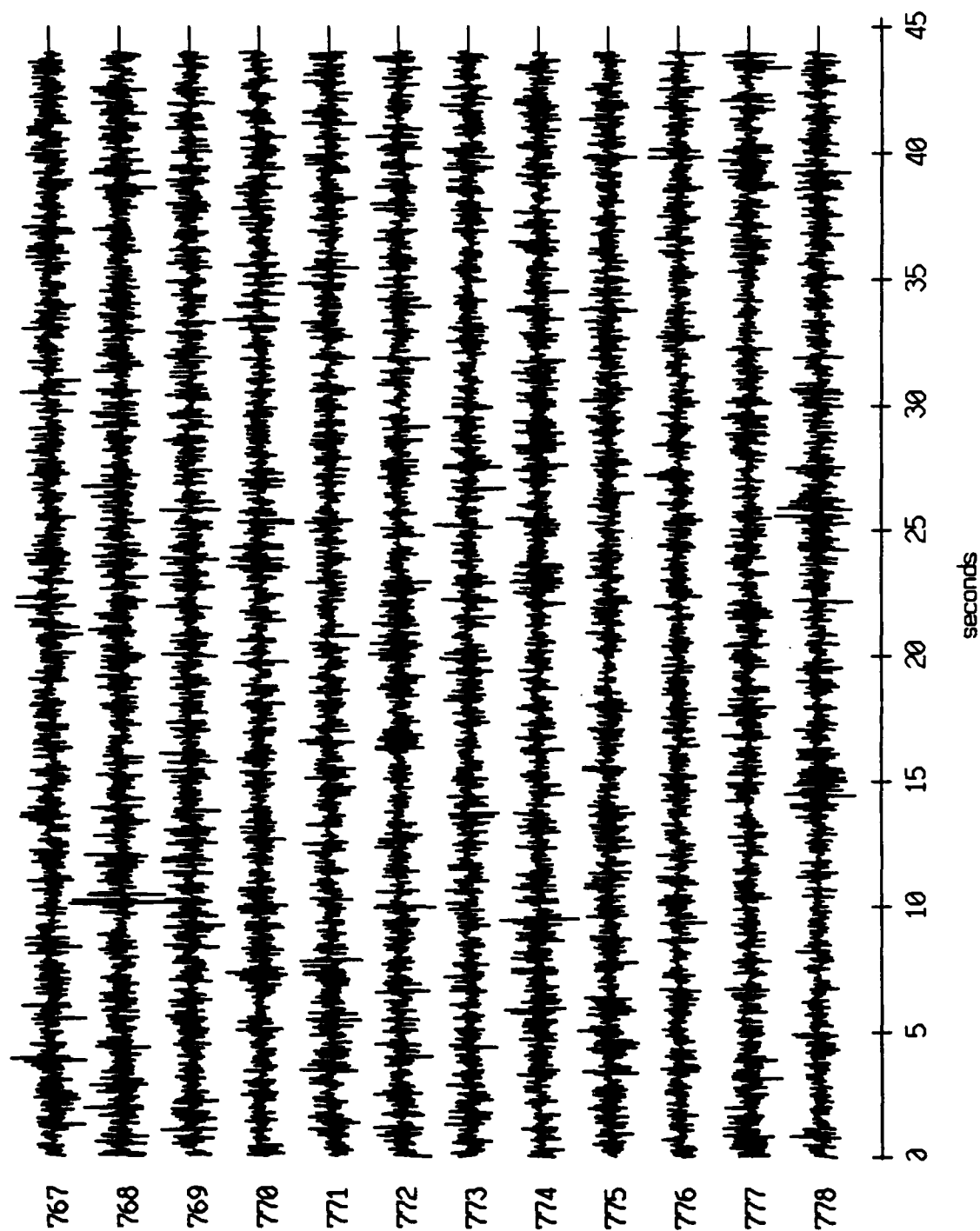


Figure XI.15b

Float 0, July, 1989 Trip - records 767-778 (z-axis)  
vertical axis scale is approx. -1.0 to 1.0 volts

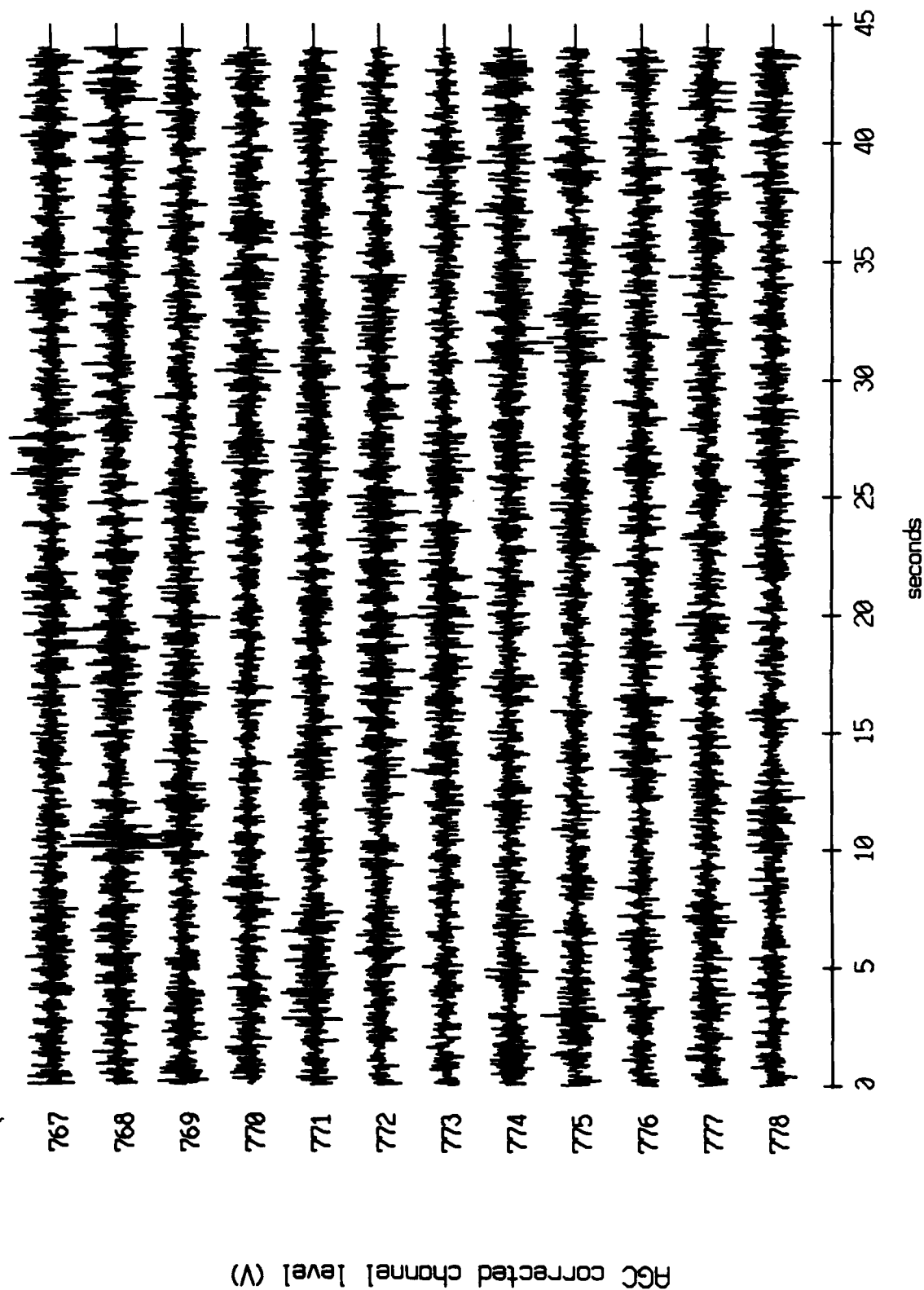


Figure XI.15c

Float 0, July, 1989 Trip - records 767-778 (hydrophone)  
 vertical axis scale is approx. -1.0 to 1.0 volts

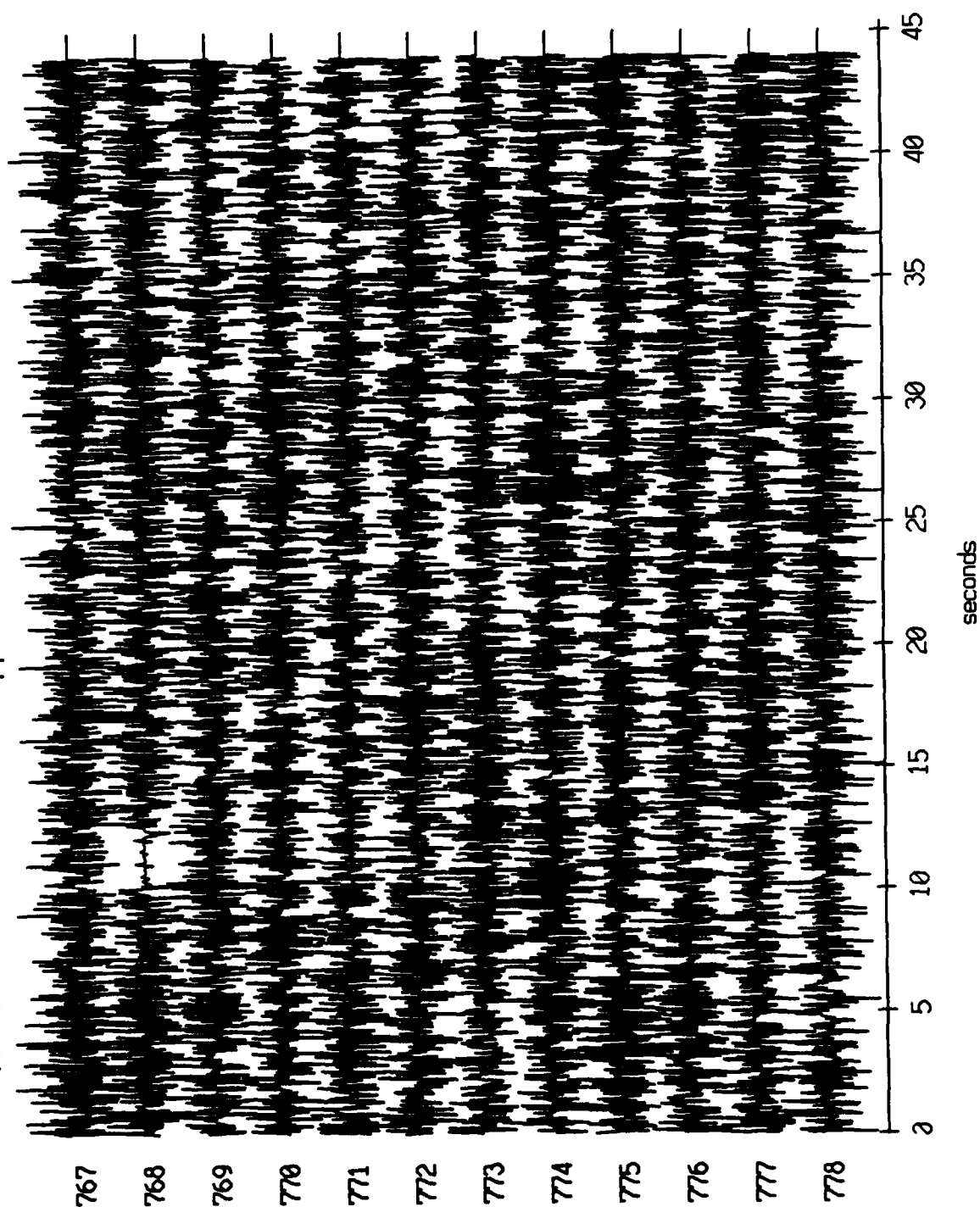
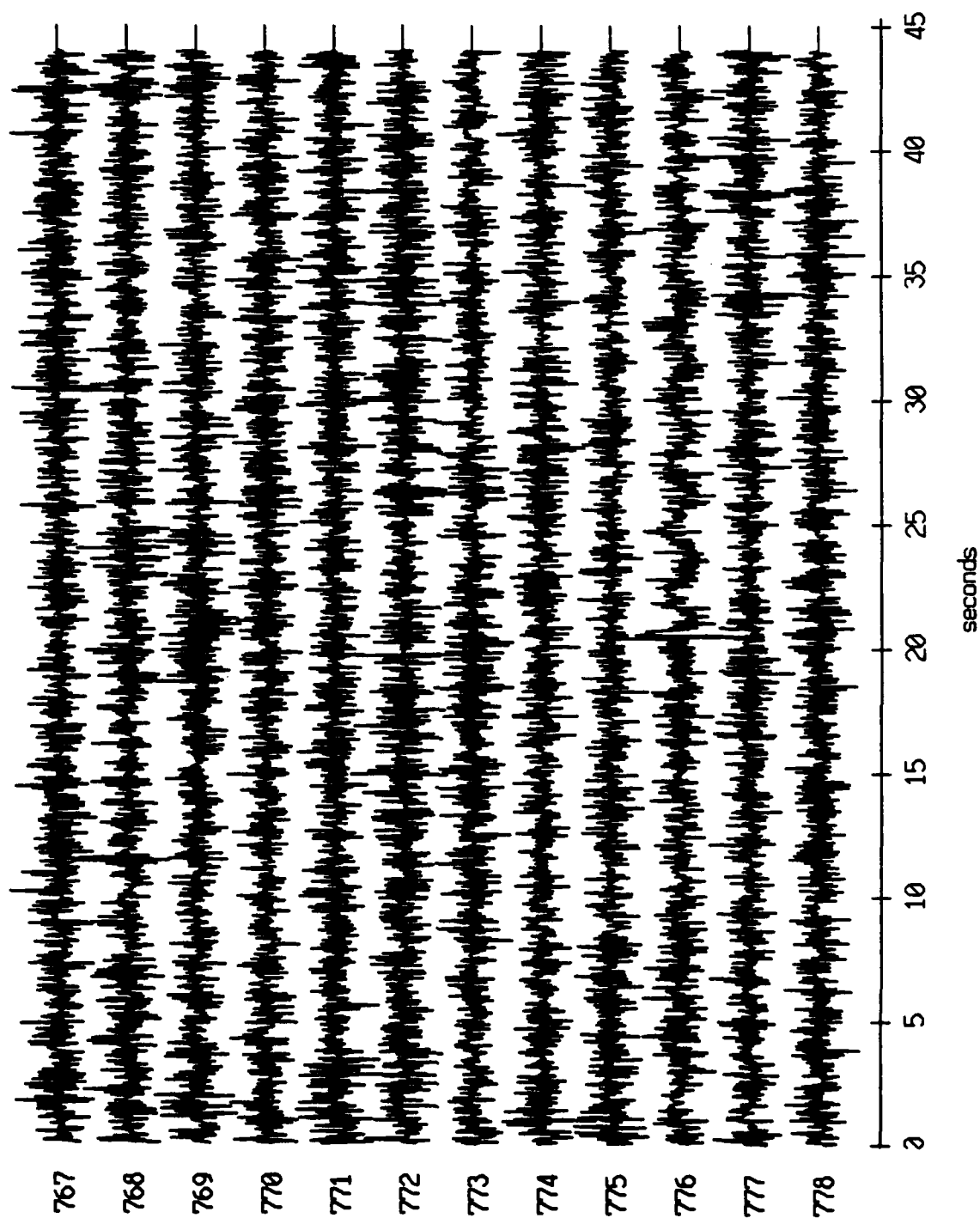


Figure XI.15d



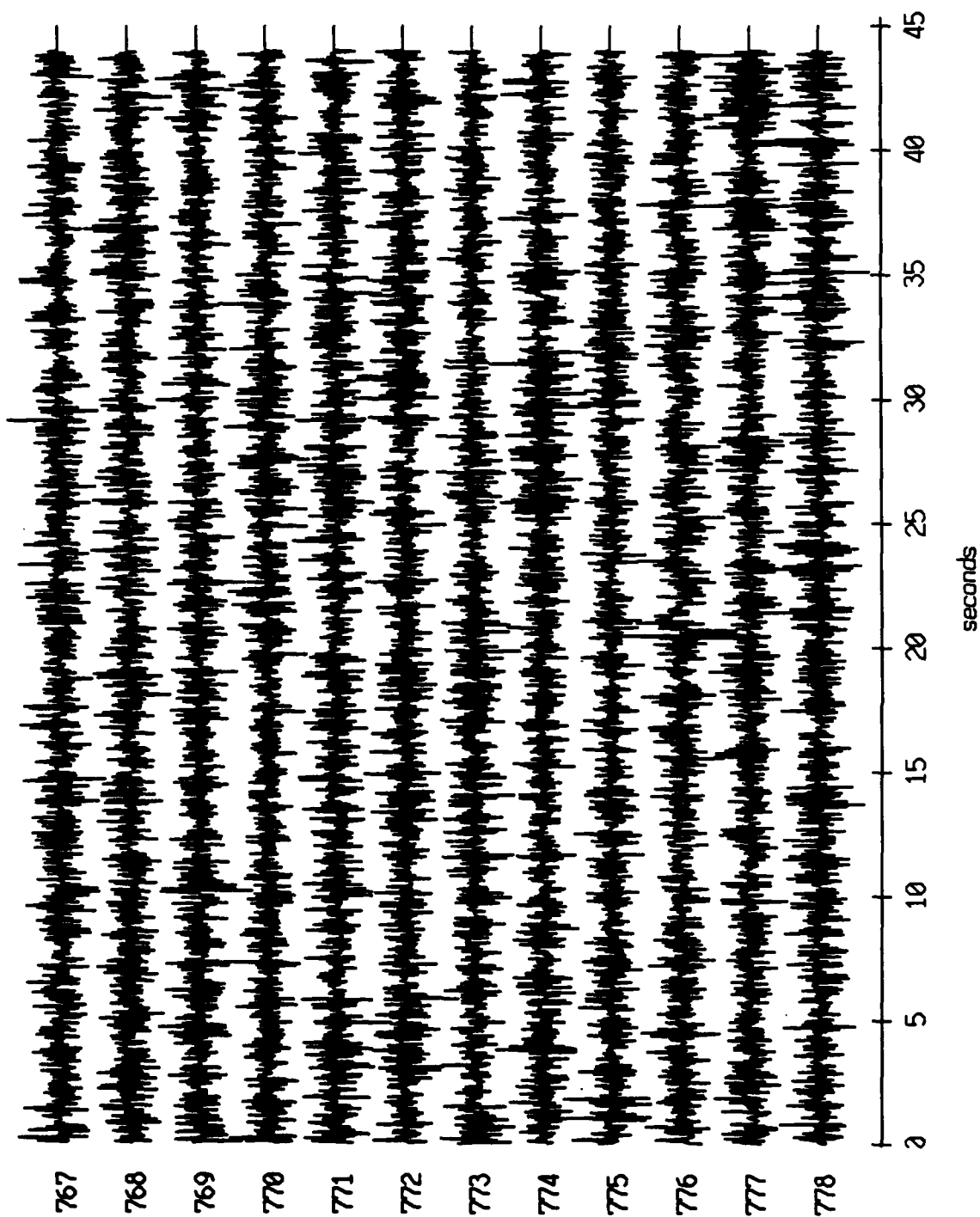
Float 1, July, 1989 Trip - records 767-778 (x-axis)  
vertical axis scale is approx. -1.0 to 1.0 volts



RGC corrected channel level (V)

Figure XI.16a

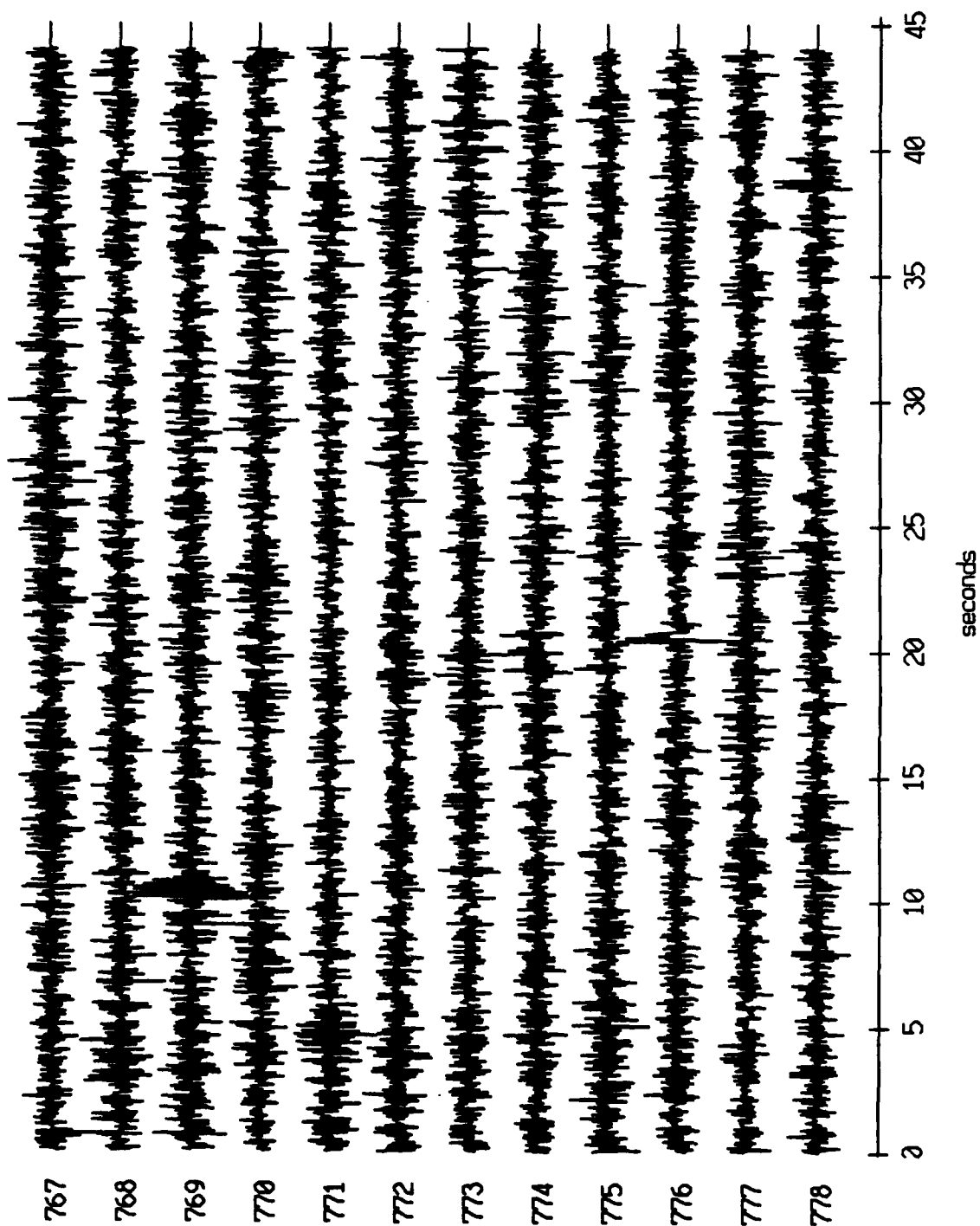
Float 1, July, 1989 Trip - records 767-778 (y-axis)  
vertical axis scale is approx. -1.0 to 1.0 volts



PGC corrected channel level (V)

Figure XI.16b

Float 1, July, 1989 Trip - records 767-778 (z-axis)  
vertical axis scale is approx. -1.0 to 1.0 volts



AGC corrected channel level (V)

Figure XI.16c

Float 1, July, 1989 Trip - records 767-778 (hydrophone)  
vertical axis scale is approx. -1.0 to 1.0 volts

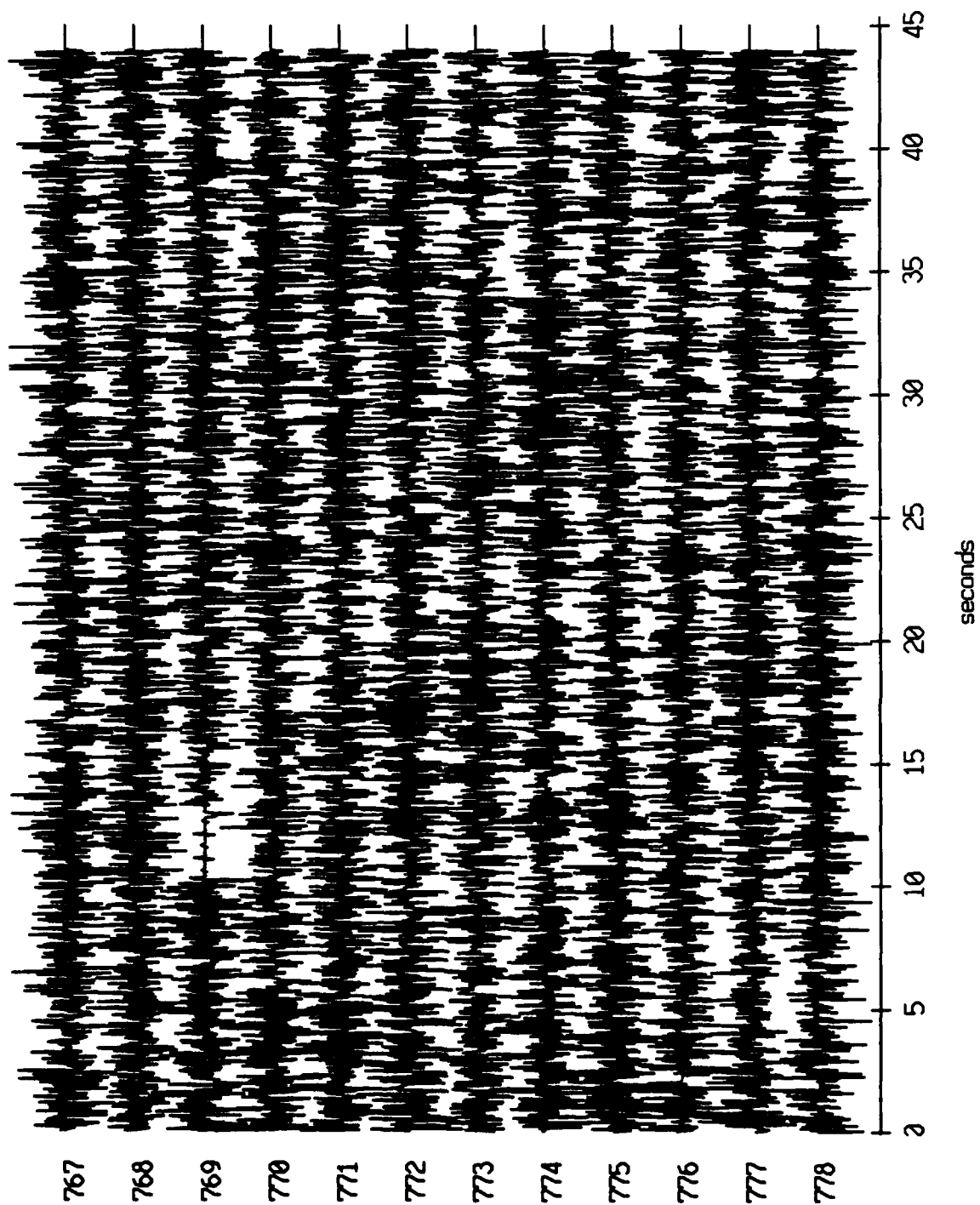


Figure XI.16d

Float 2, July, 1989 Trip - records 767-778 (x-axis)  
vertical axis scale is approx. -1.0 to 1.0 volts

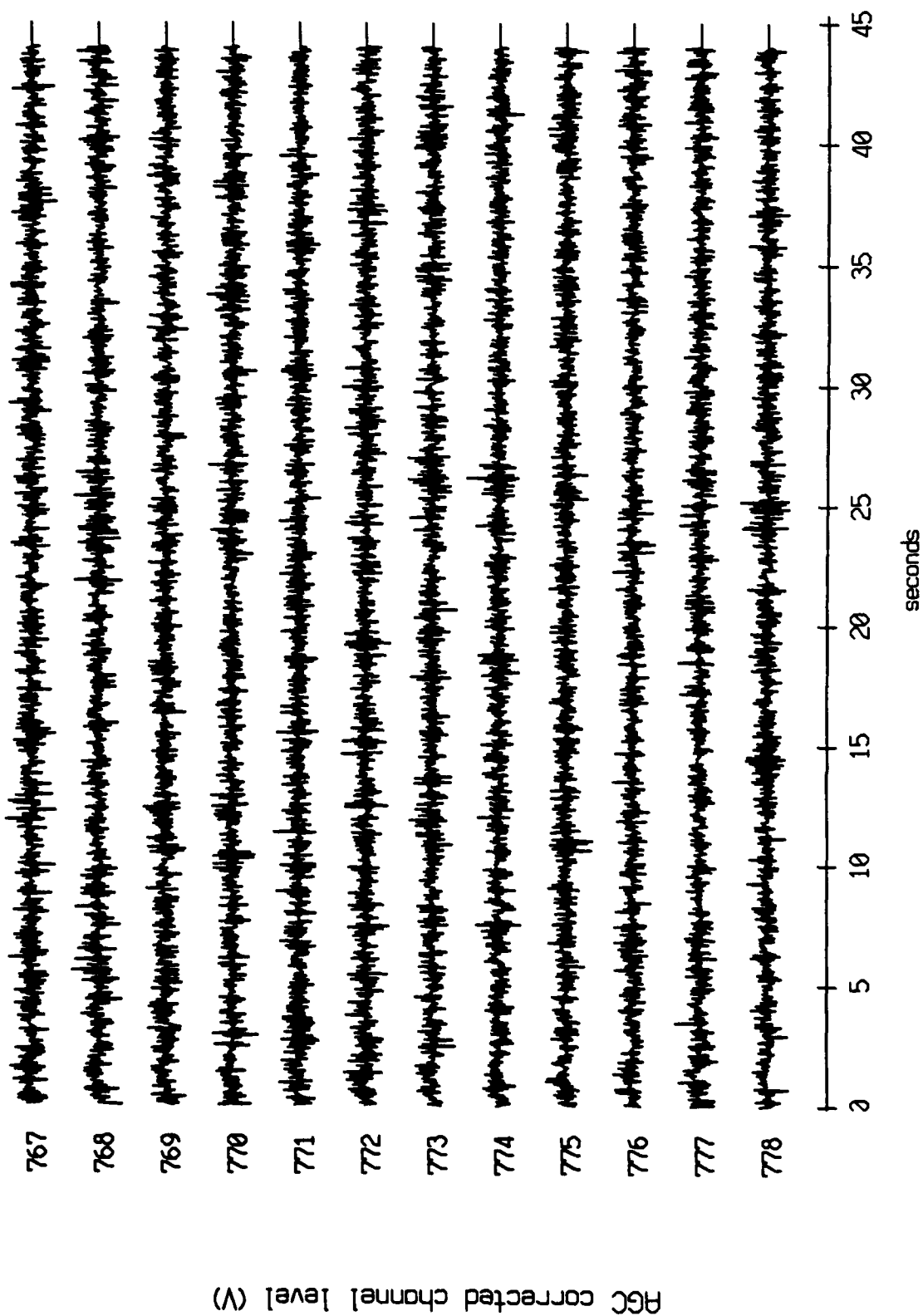


Figure XI.17a

Float 2, July, 1989 Trip - records 767-778 (y-axis)  
vertical axis scale is approx. -1.0 to 1.0 volts

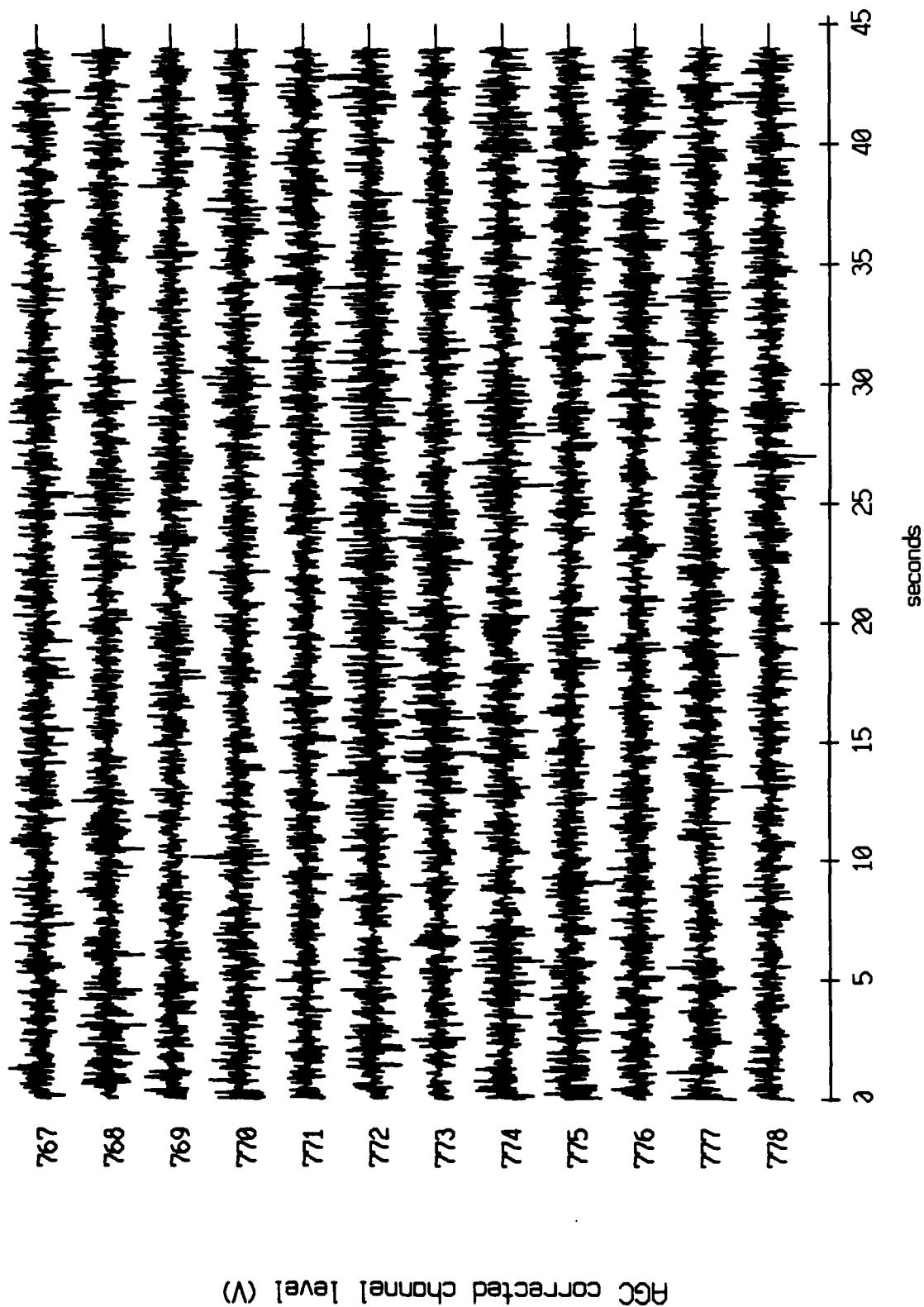


Figure XI.17b

Floot 2, July, 1989 Trip - records 767-778 (z-axis)  
vertical axis scale is approx. -1.0 to 1.0 volts

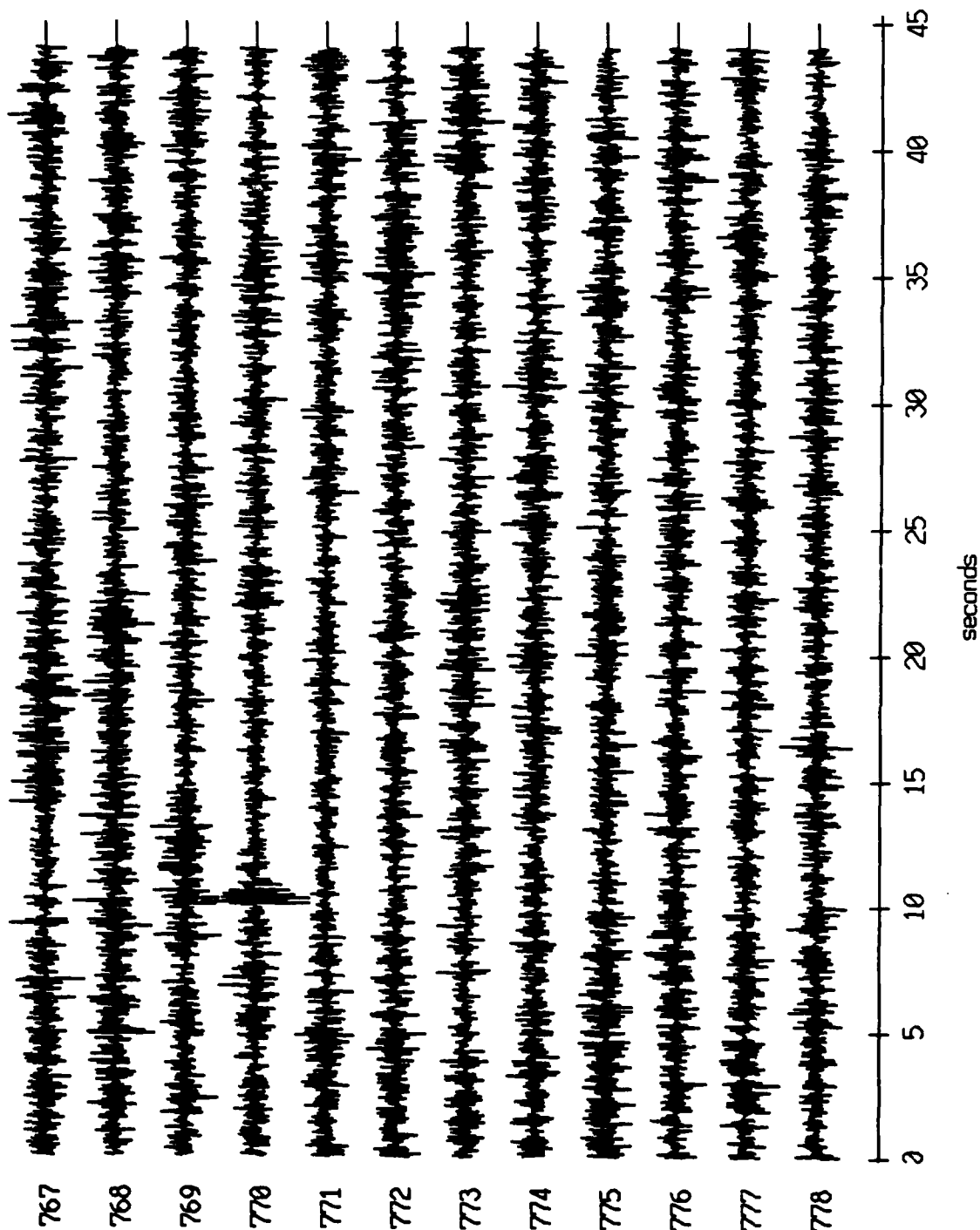


Figure XI.17c

Floot 2, July, 1989 Trip - records 767-778 (hydrophone)  
vertical axis scale is approx. -1.0 to 1.0 volts

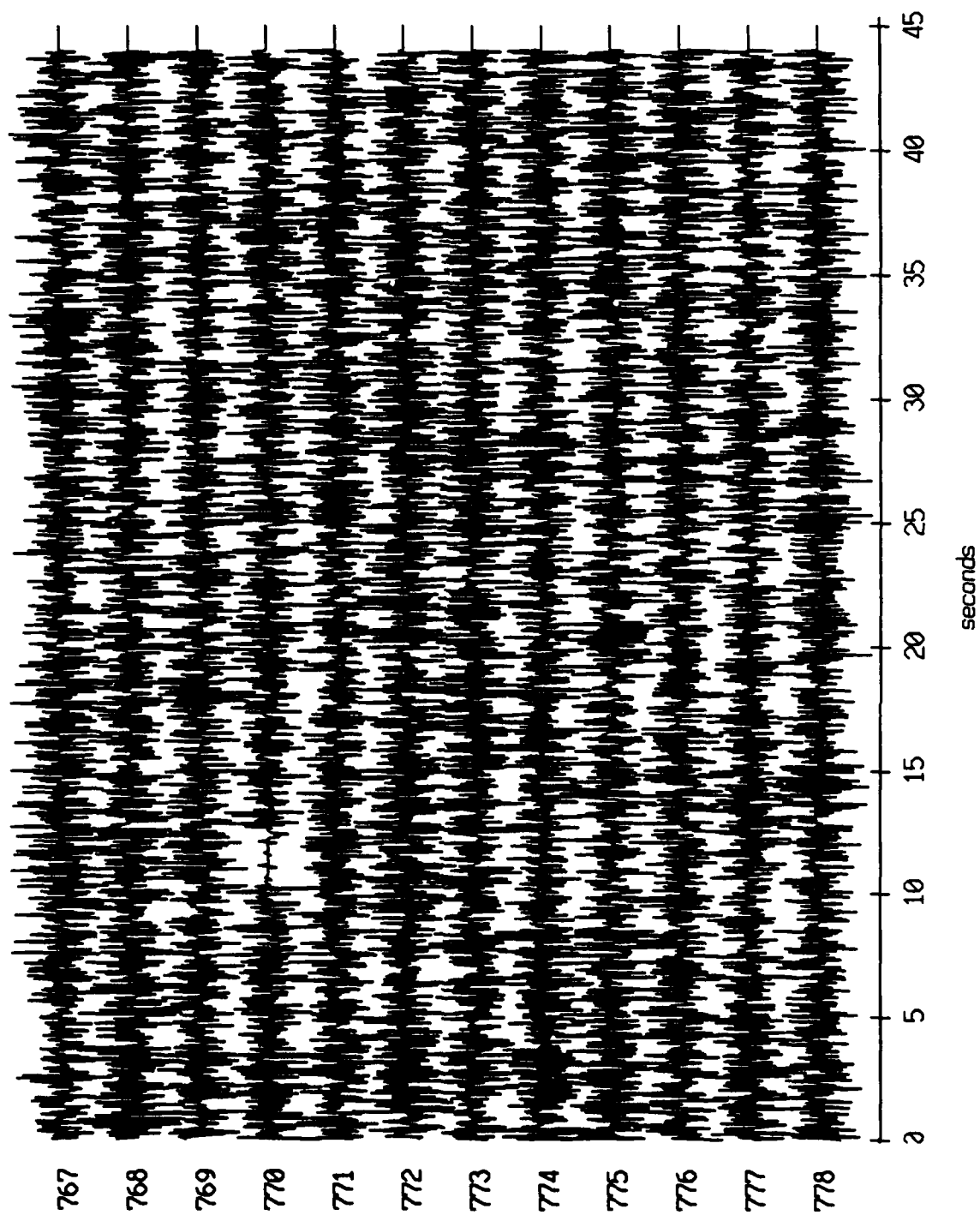


Figure XI.17d



Float 3, July, 1989 Trip - records 767-778 (x-axis)  
vertical axis scale is approx. -1.0 to 1.0 volts

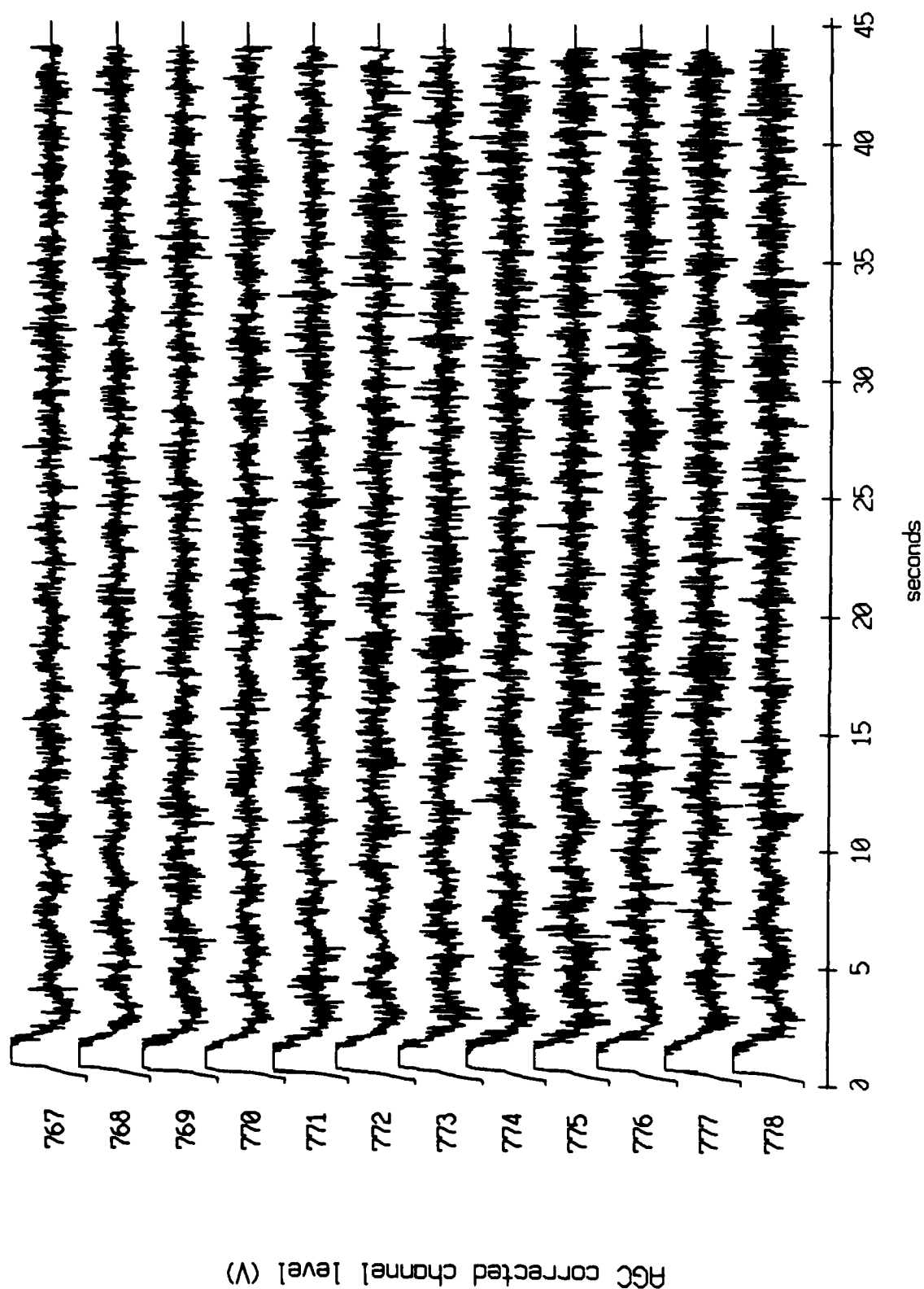


Figure XI.18a

Floot 3, July, 1989 Trip - records 767-778 (y-axis)  
vertical axis scale is approx. -1.0 to 1.0 volts

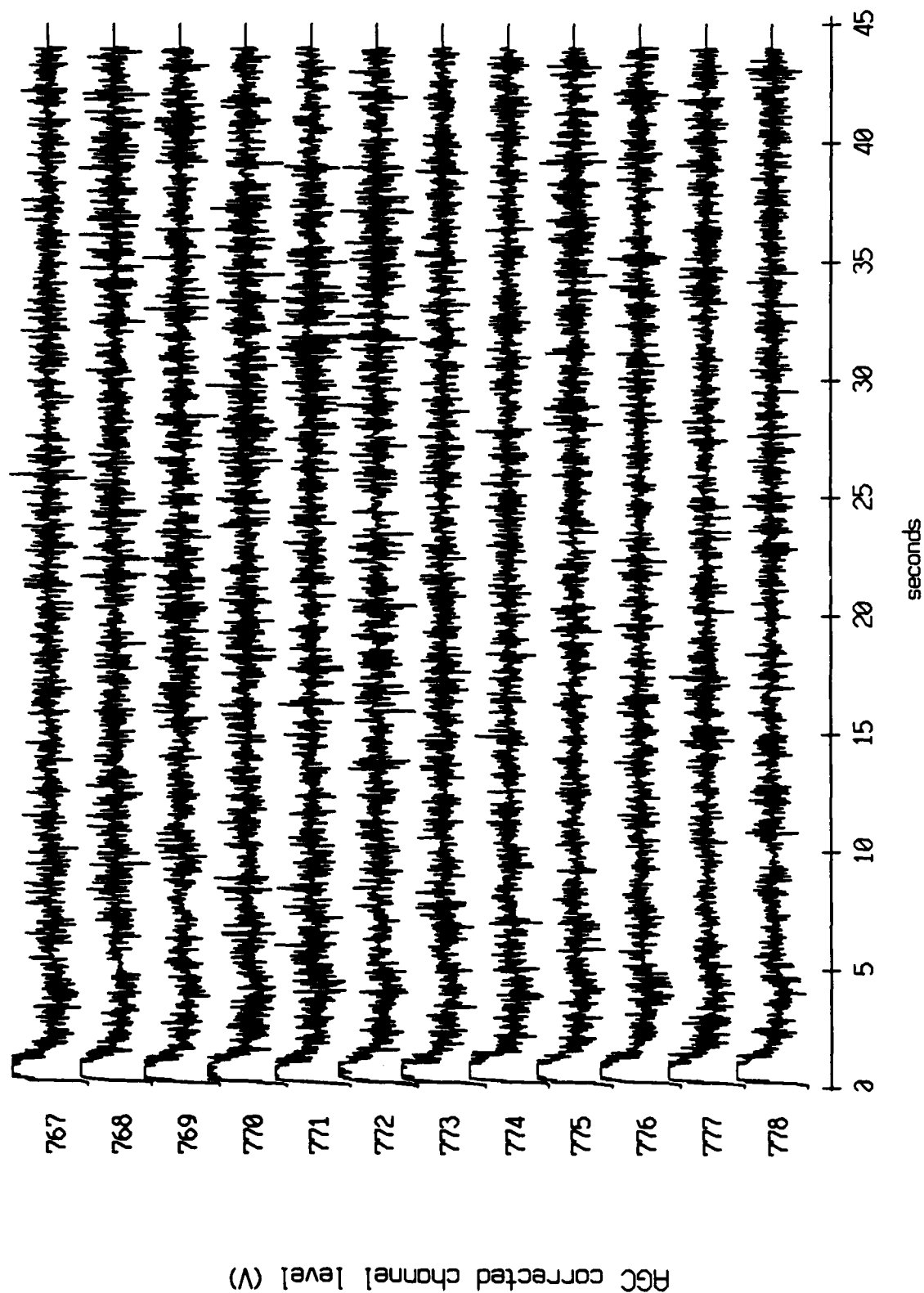


Figure XI.18b

Float 3, July, 1989 Trip - records 767-778 (z-axis)  
vertical axis scale is approx. -1.0 to 1.0 volts

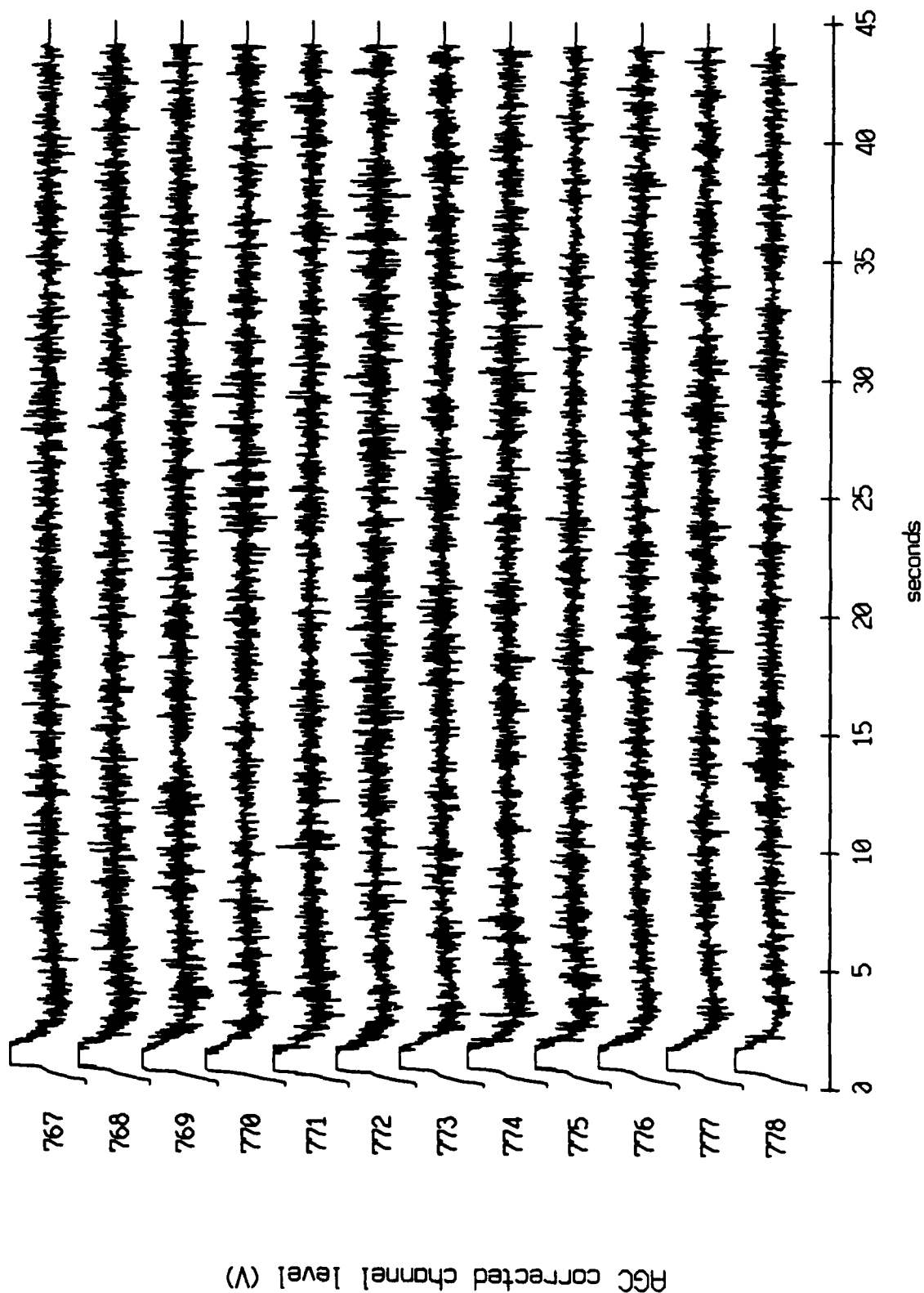


Figure XI.18c

Float 3, July, 1989 Trip - records 767-778 (hydrophone)  
vertical axis scale is approx. -1.0 to 1.0 volts

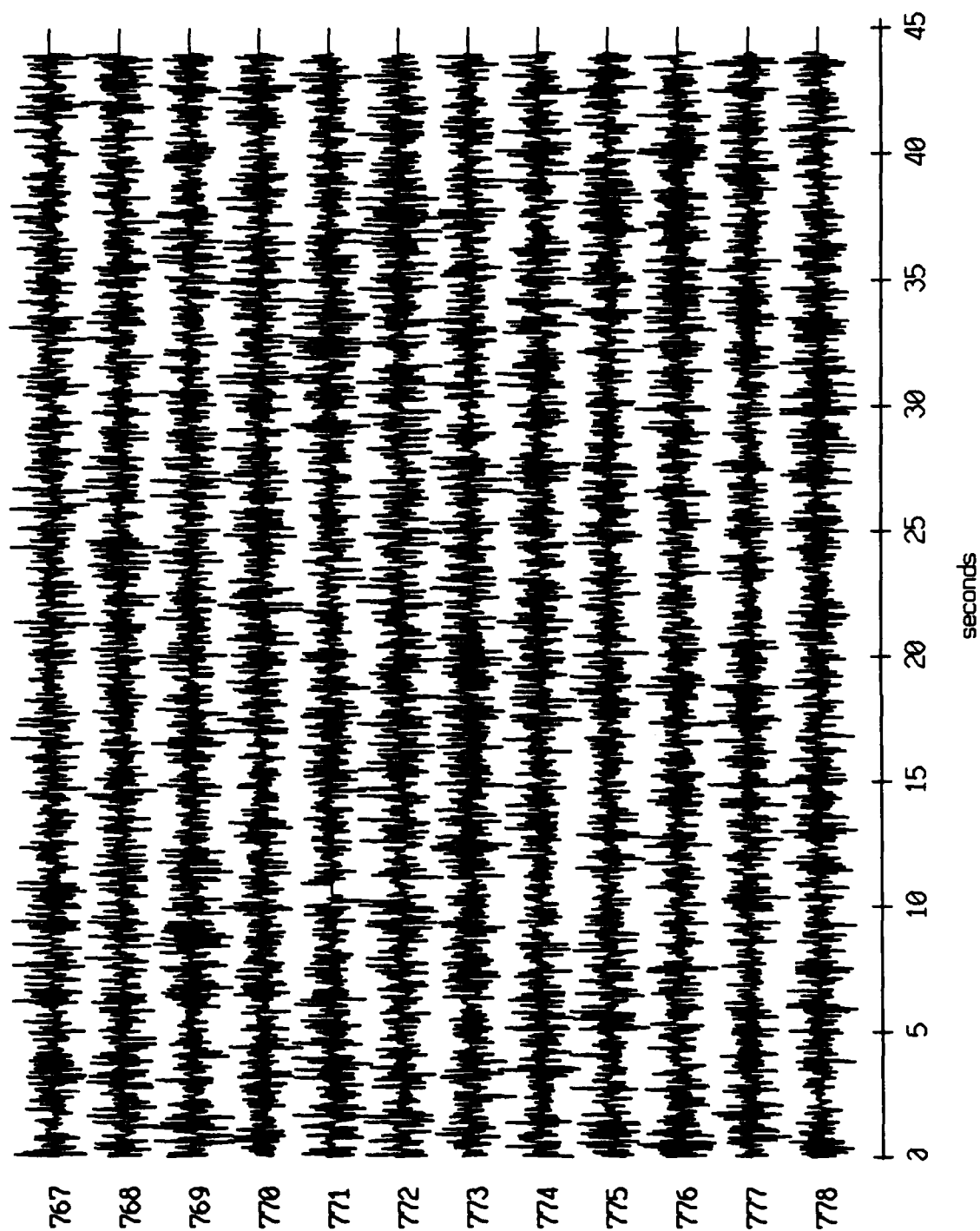
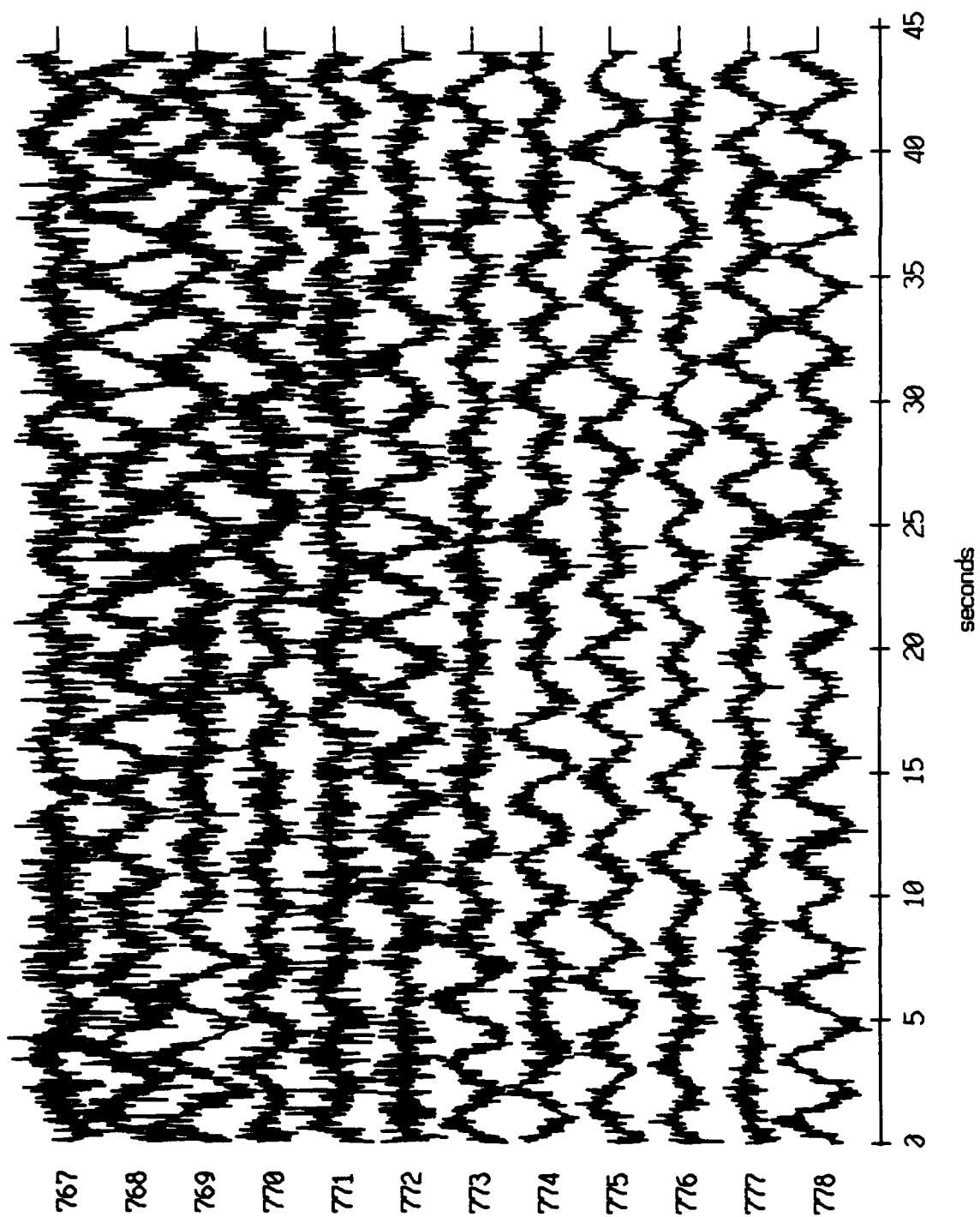


Figure XI.18d

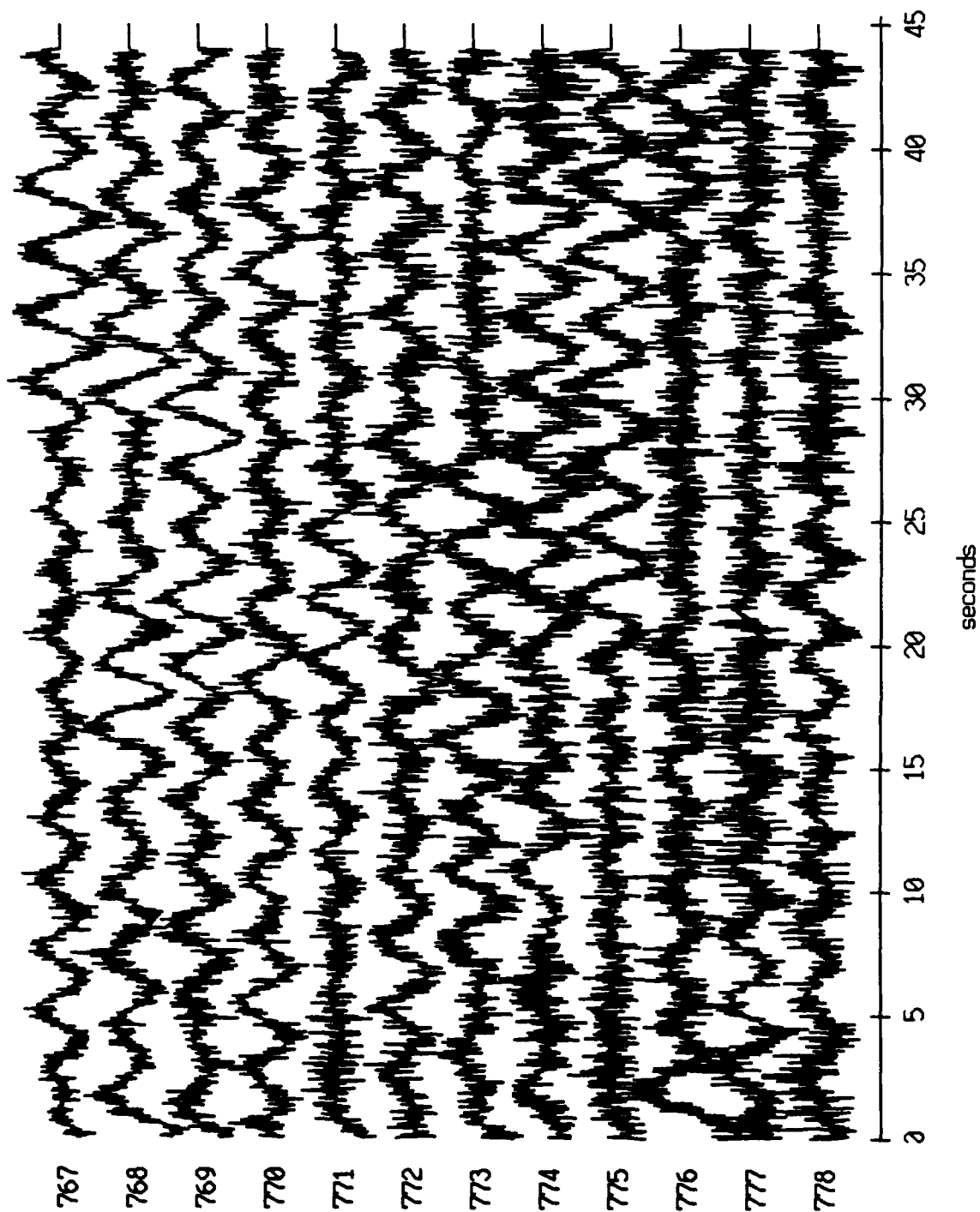
Float 4, July, 1989 Trip - records 767-778 (x-axis)  
vertical axis scale is approx. -1.0 to 1.0 volts



HGC corrected channel level (V)

Figure XI.19a

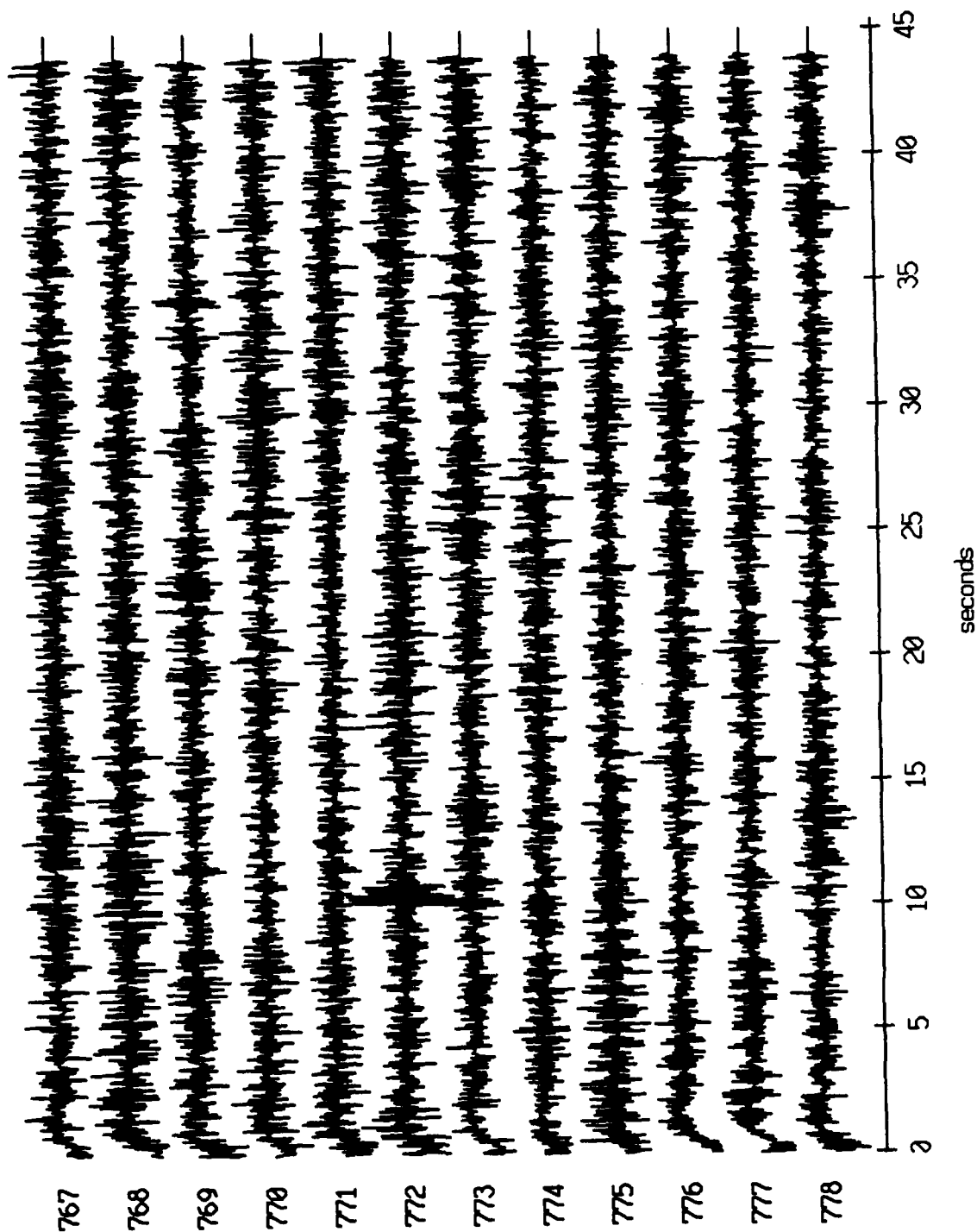
Floot 4, July, 1989 Trip - records 767-778 (y-axis)  
vertical axis scale is approx. -1.0 to 1.0 volts



RGC corrected channel level (V)

Figure XI.19b

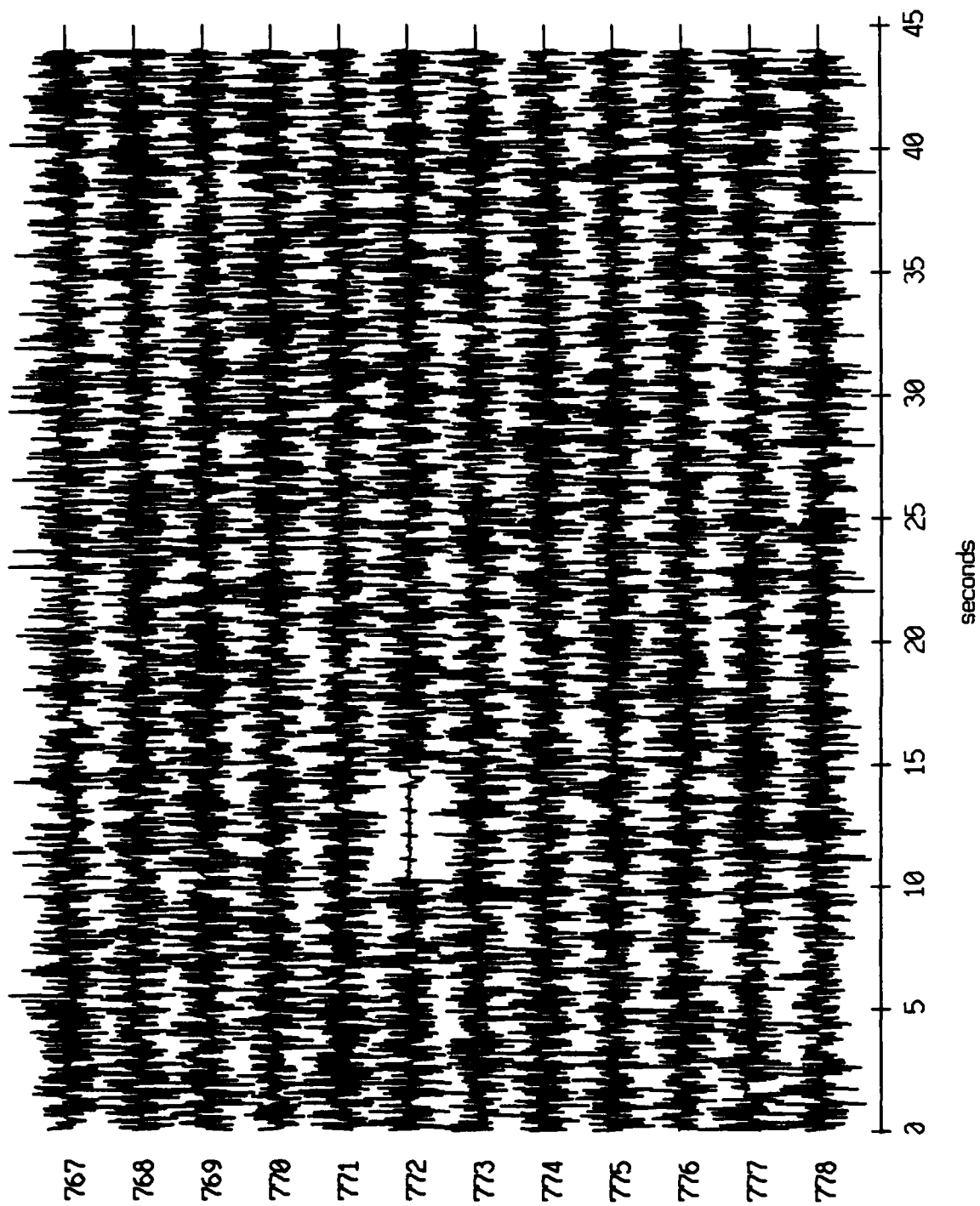
Floot 4, July, 1989 Trip - records 767-778 (z-axis)  
vertical axis scale is approx. -1.0 to 1.0 volts



AGC corrected channel level (V)

Figure XI.19c

Float 4, July, 1989 Trip - records 767-778 (hydrophone)  
vertical axis scale is approx. -1.0 to 1.0 volts

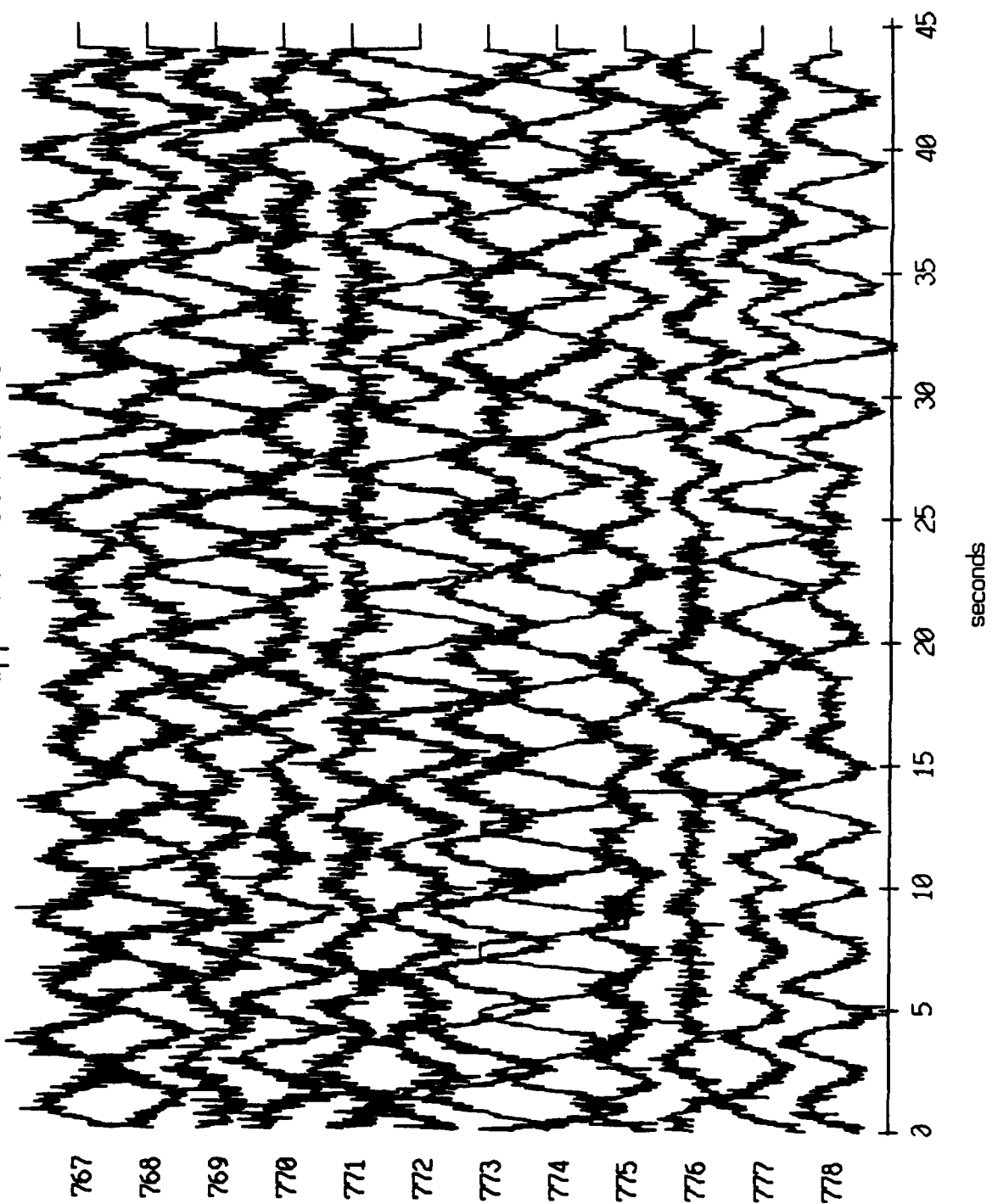


RGC corrected channel level (V)

Figure XI.19d



Float 5, July, 1989 Trip - records 767-778 (x-axis)  
vertical axis scale is approx. -1.0 to 1.0 volts



AGC corrected channel level (V)

Figure XI.20a

Float 5, July, 1989 Trip - records 767-778 (y-axis)  
vertical axis scale is approx. -1.0 to 1.0 volts

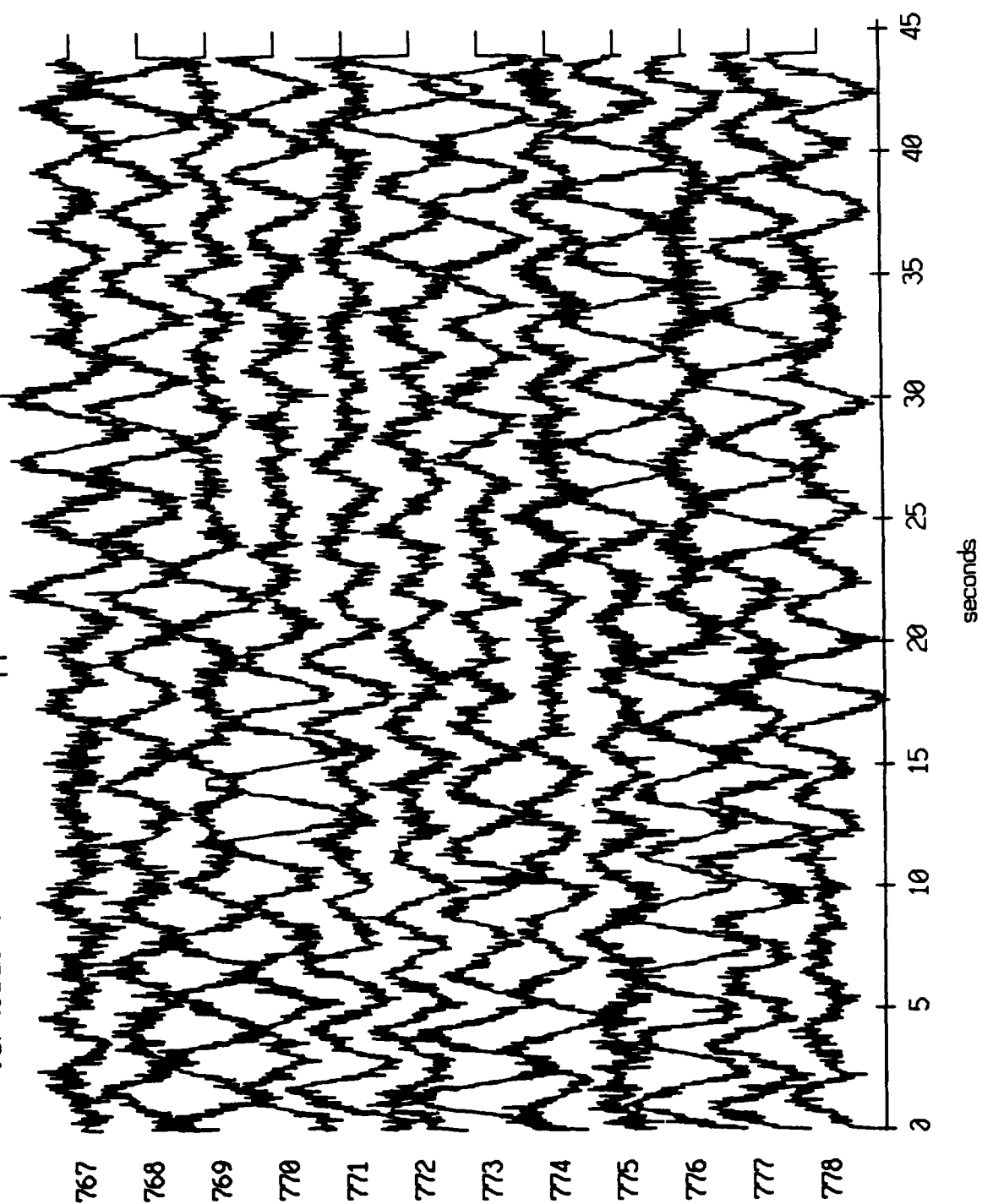
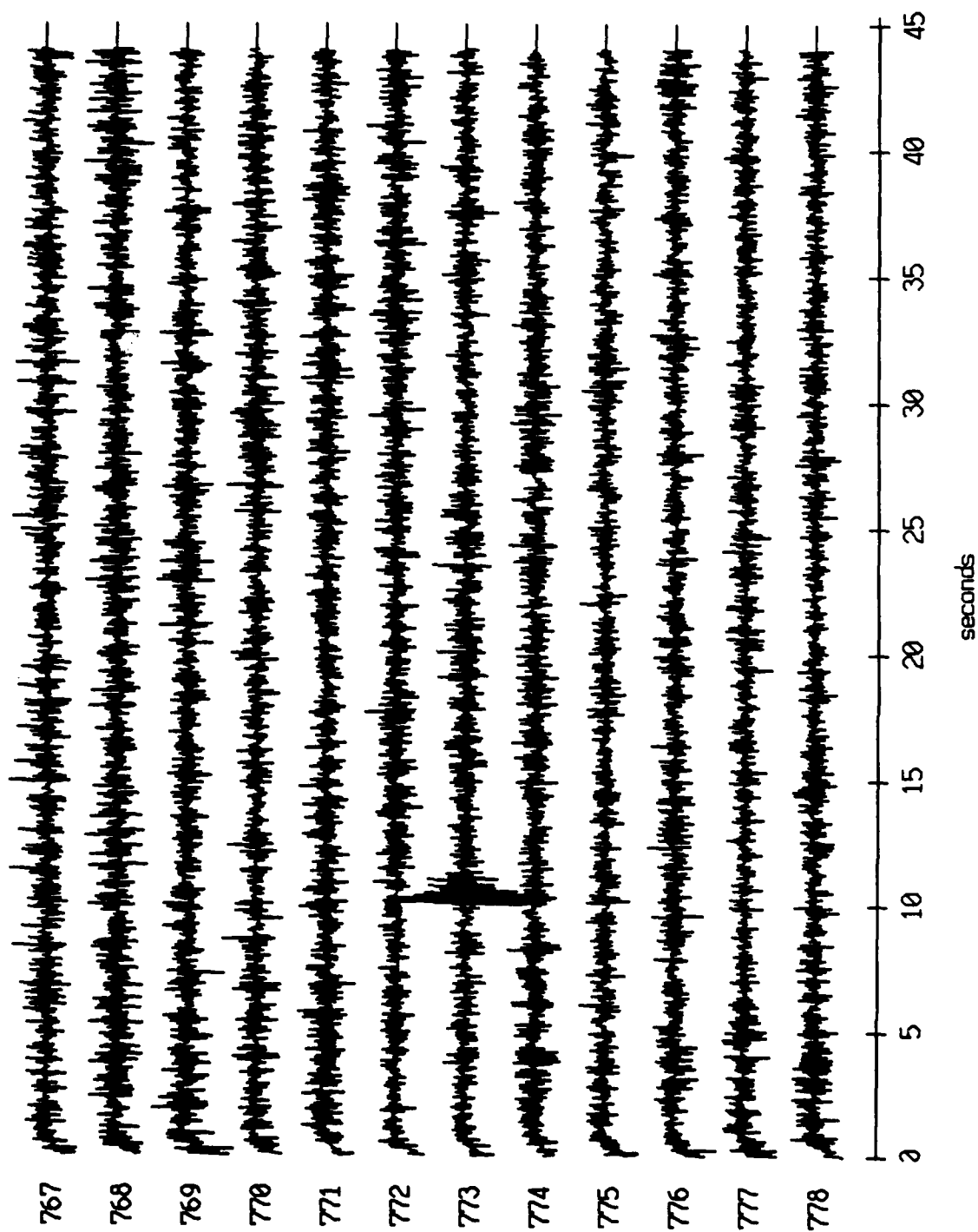


Figure XI.20b

Float 5, July, 1989 Trip - records 767-778 (z-axis)  
vertical axis scale is approx. -1.0 to 1.0 volts



PGC corrected channel level (V)

Figure XI.20c

Floot 5, July, 1989 Trip - records 767-778 (hydrophone)  
vertical axis scale is approx. -1.0 to 1.0 volts

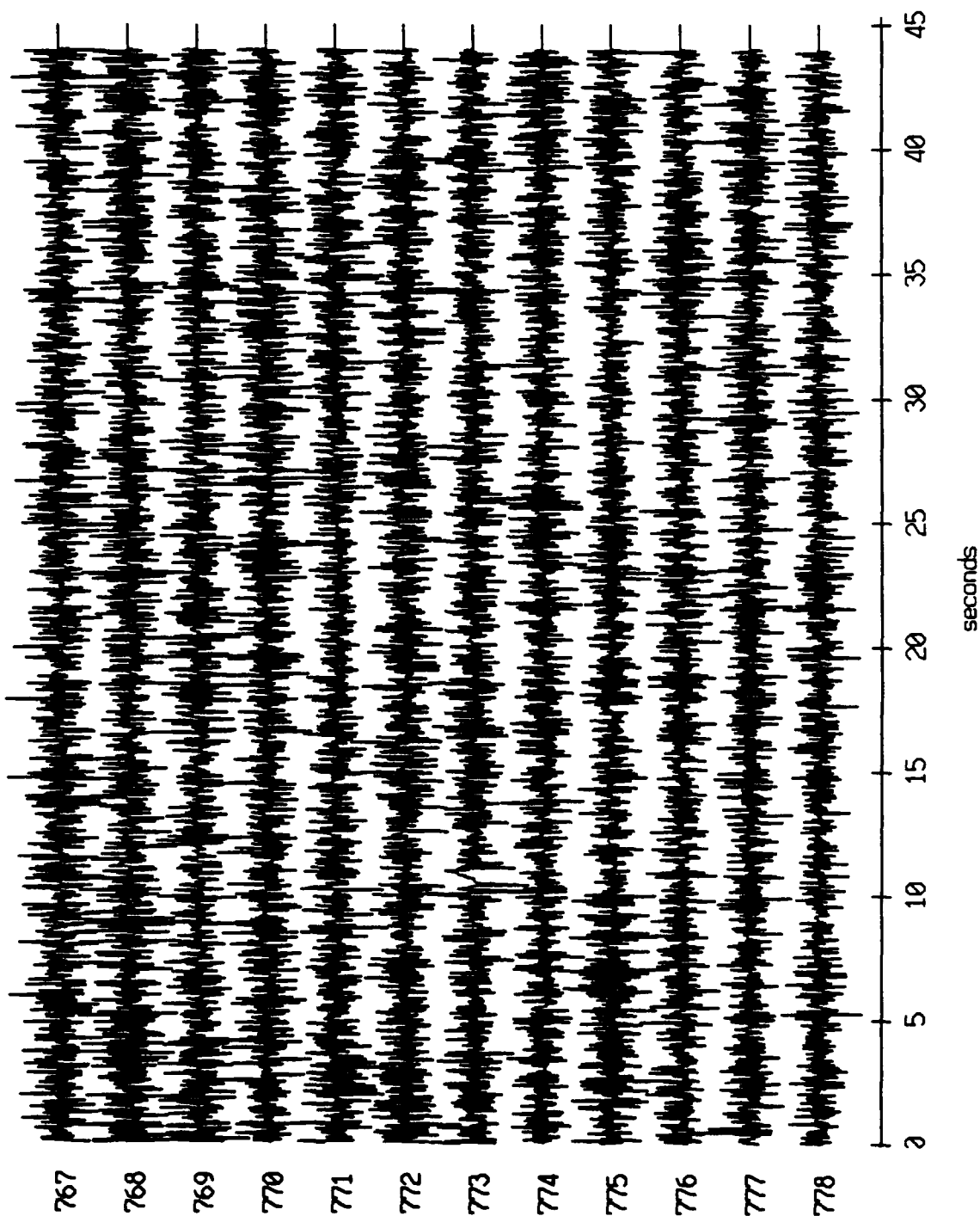
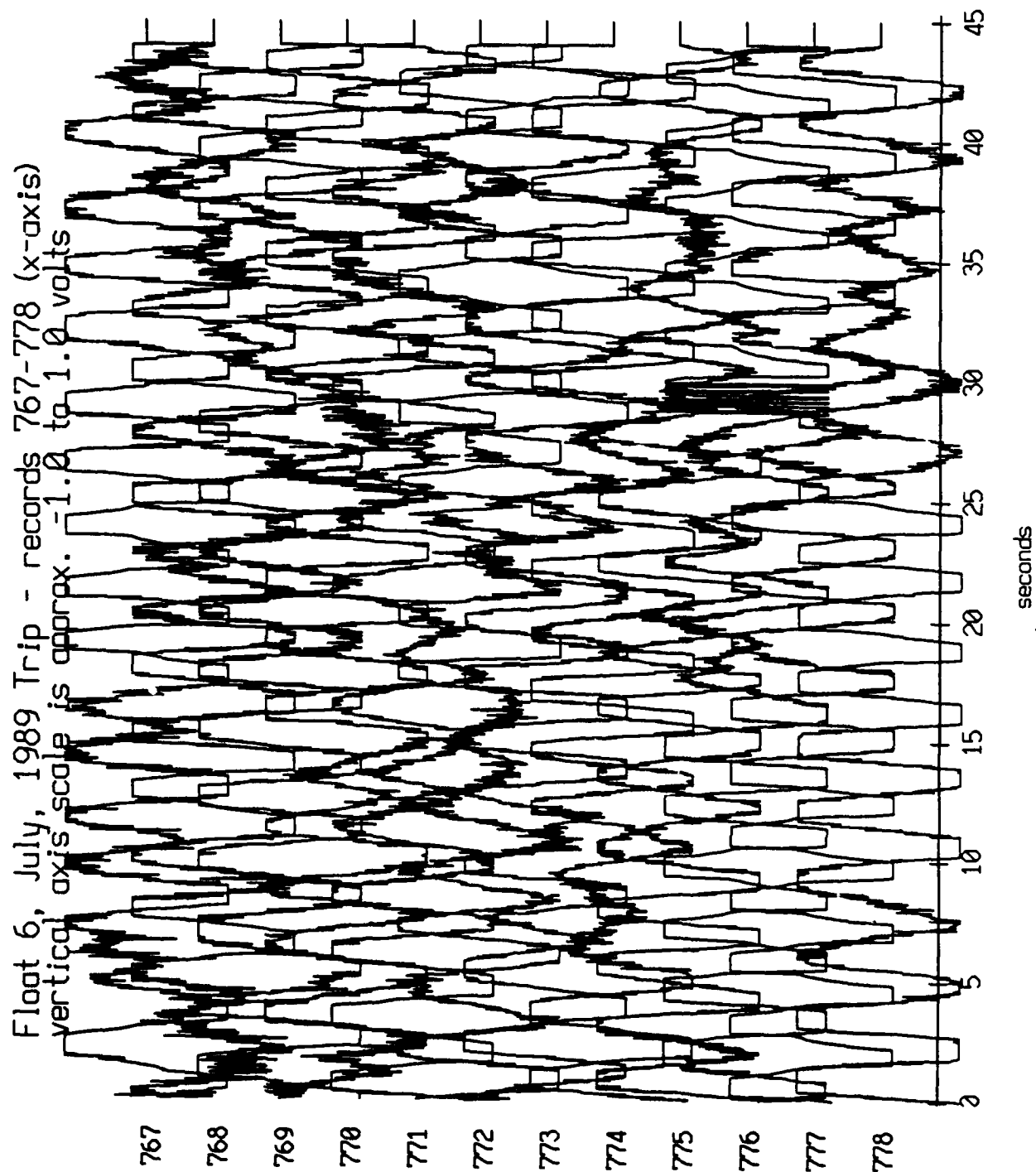


Figure X1.20d



AGC corrected channel level (V)

Figure XI.21a

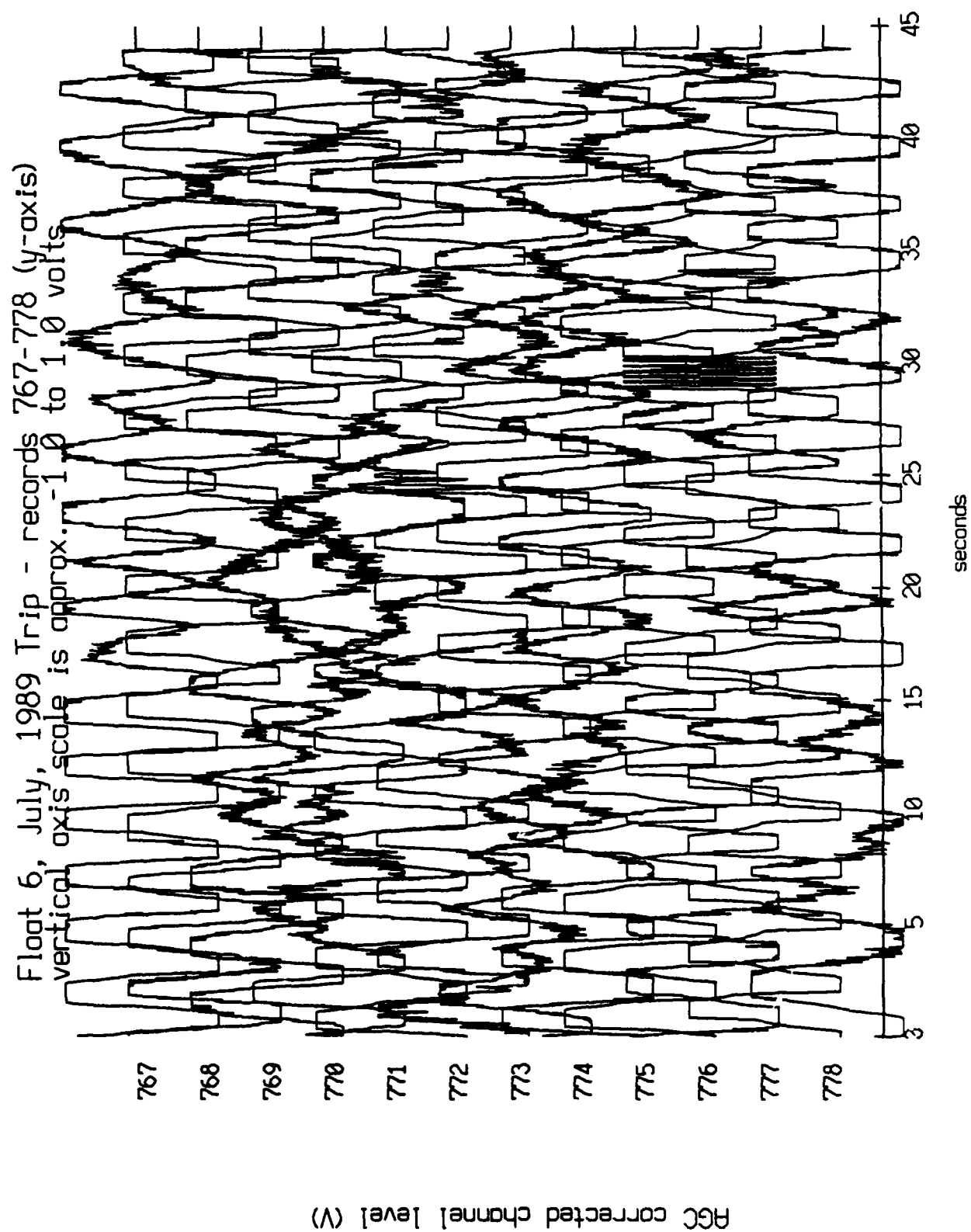


Figure XI.21b

Float 6, July, 1989 Trip - records 767-778 (z-axis)  
vertical axis scale is approx. -1.0 to 1.0 volts

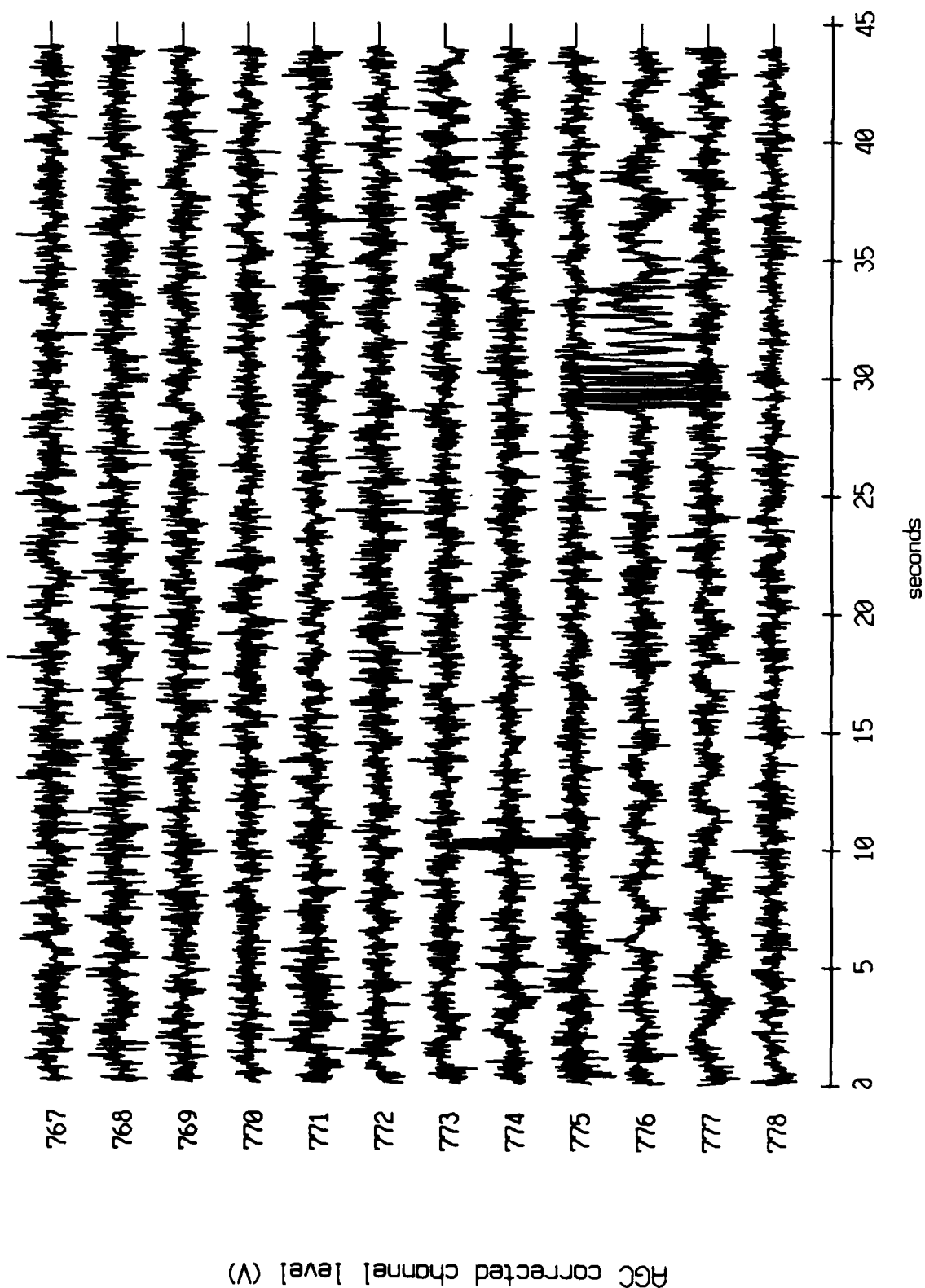
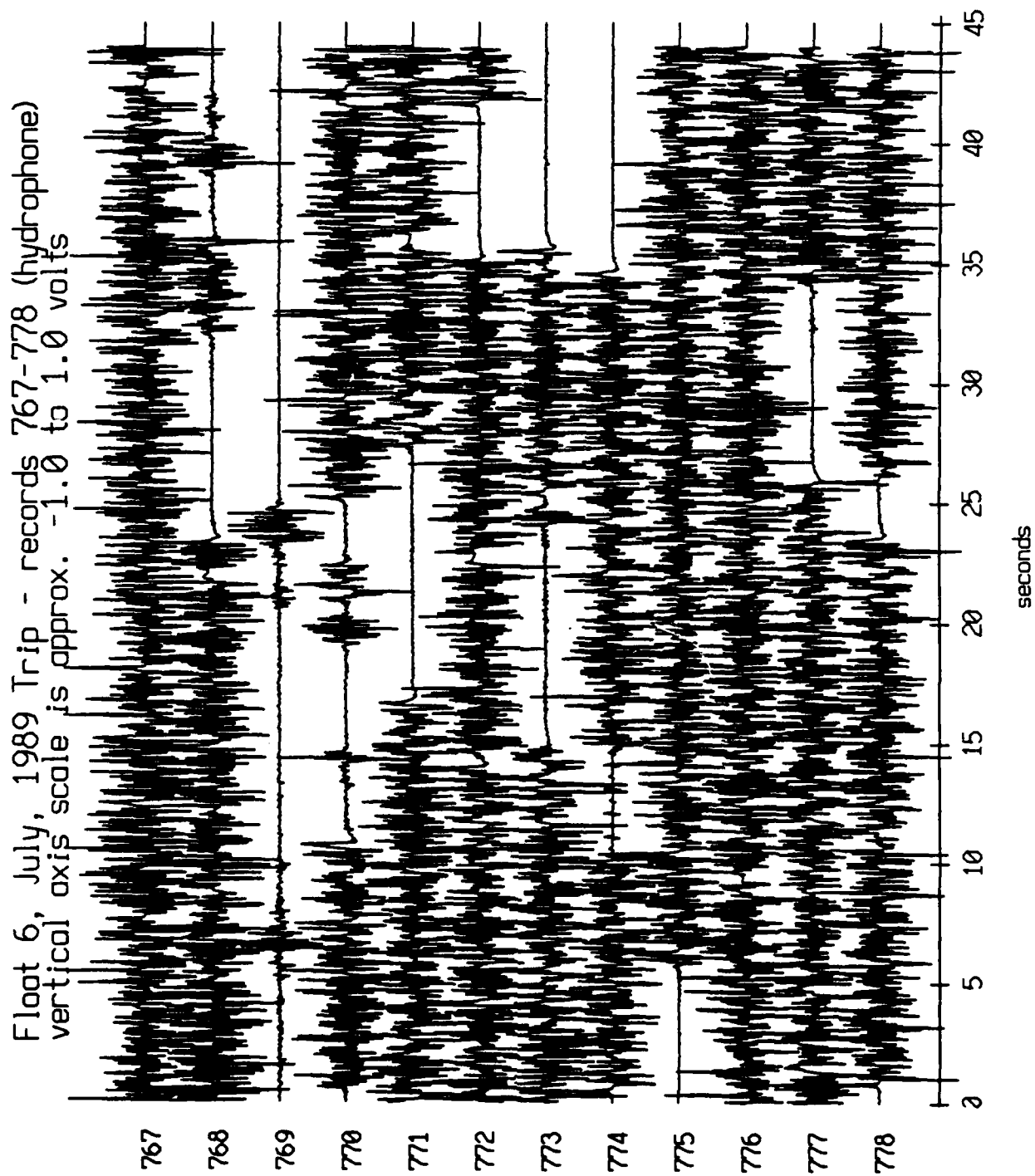


Figure XI.21c

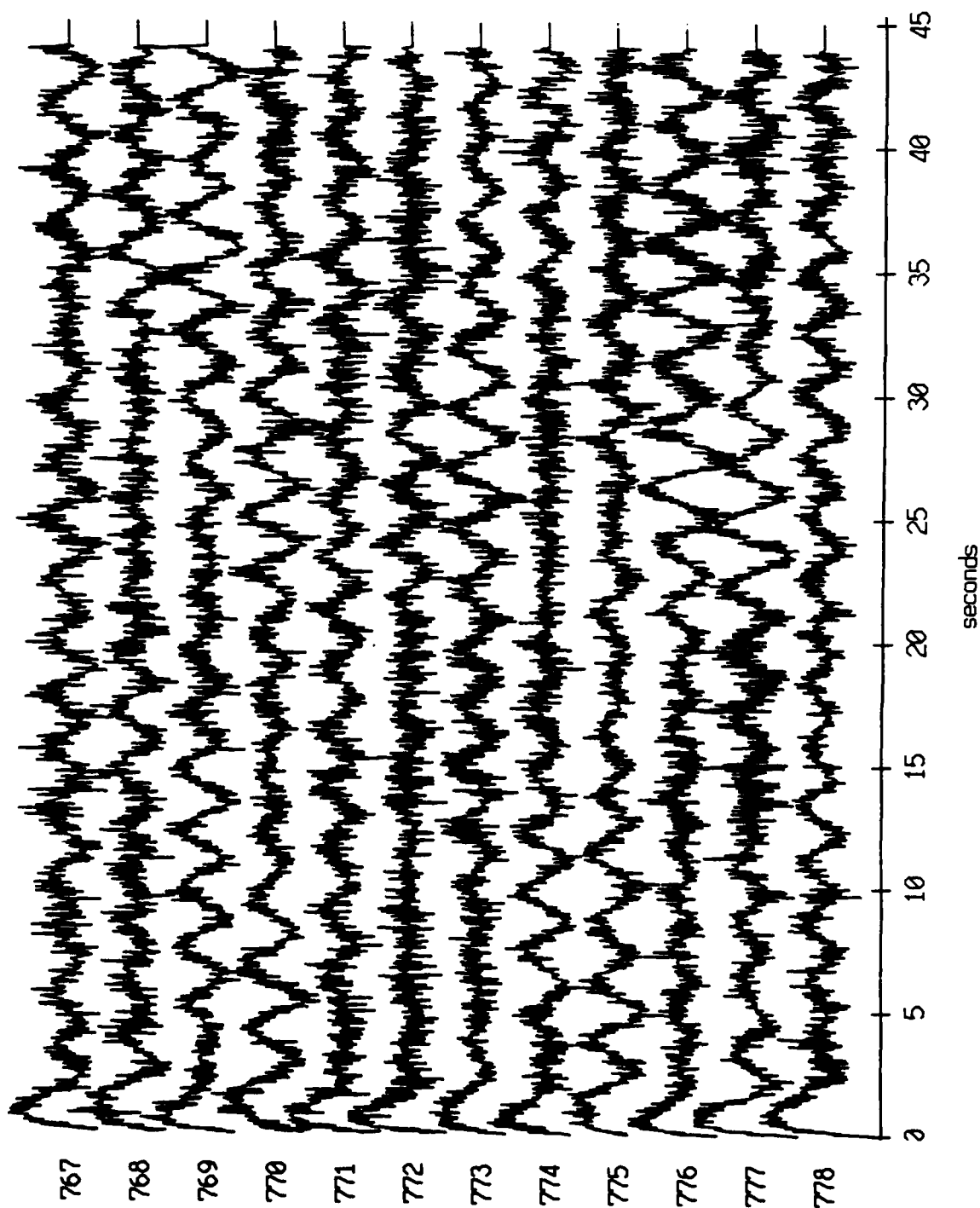


AGC corrected channel level (V)

Figure XI.21d



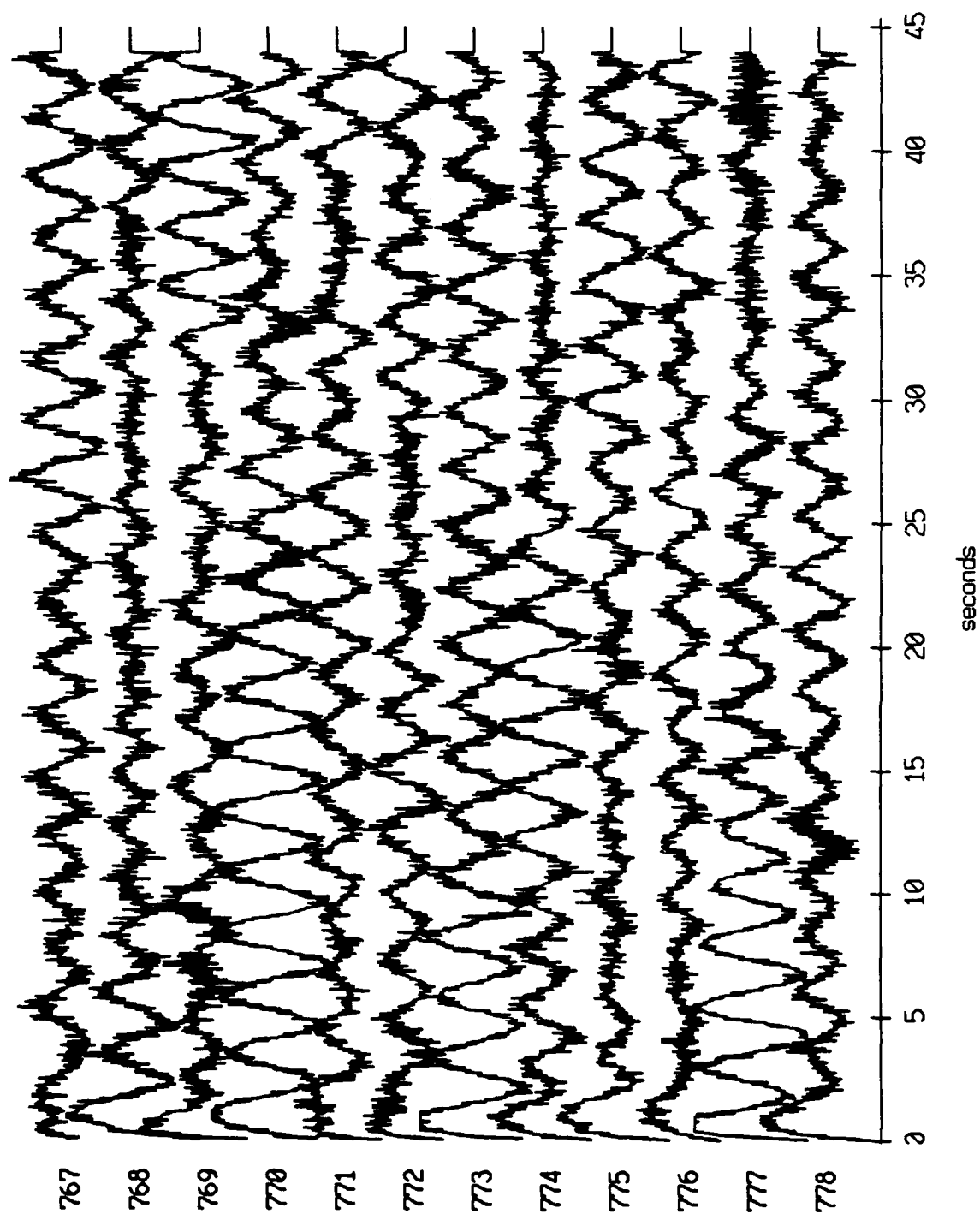
Floot 7, July, 1989 Trip - records 767-778 (x-axis)  
vertical axis scale is approx. -1.0 to 1.0 volts



RGC corrected channel level (V)

Figure XI.22a

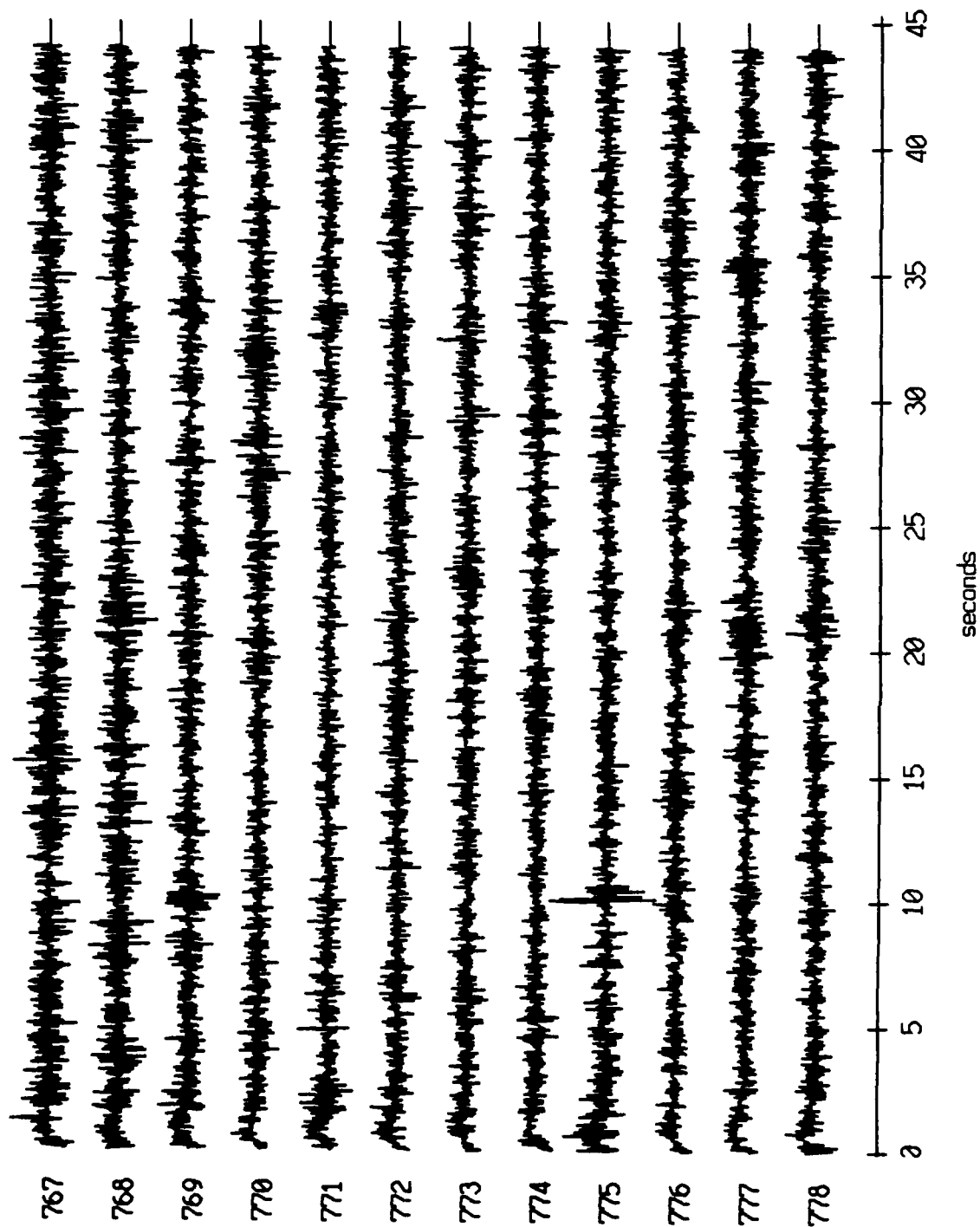
Floot 7, July, 1989 Trip - records 767-778 (y-axis)  
vertical axis scale is approx. -1.0 to 1.0 volts



AGC corrected channel level (V)

Figure XI.22b

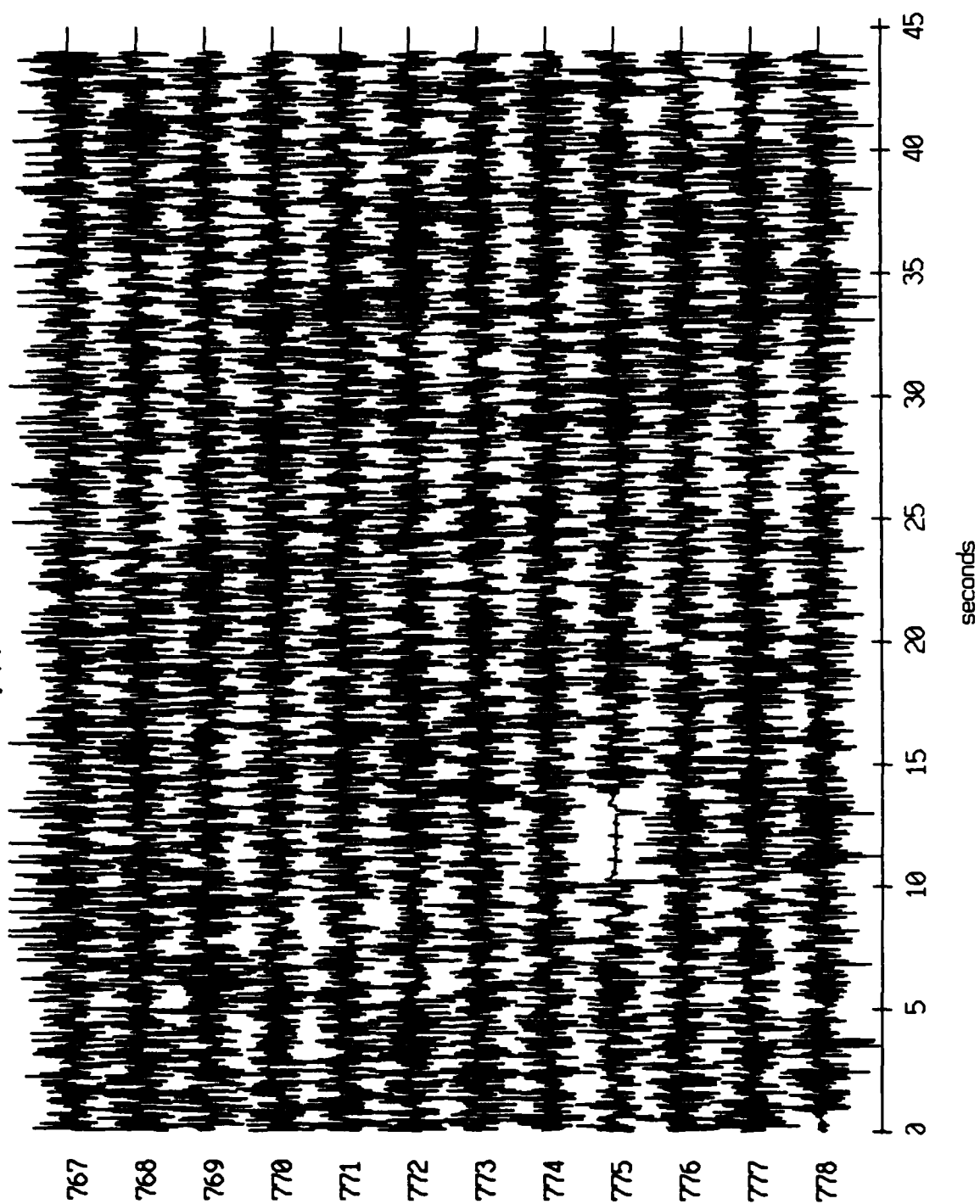
Floot 7, July, 1989 Trip - records 767-778 (z-axis)  
vertical axis scale is approx. -1.0 to 1.0 volts



HGC corrected channel level (V)

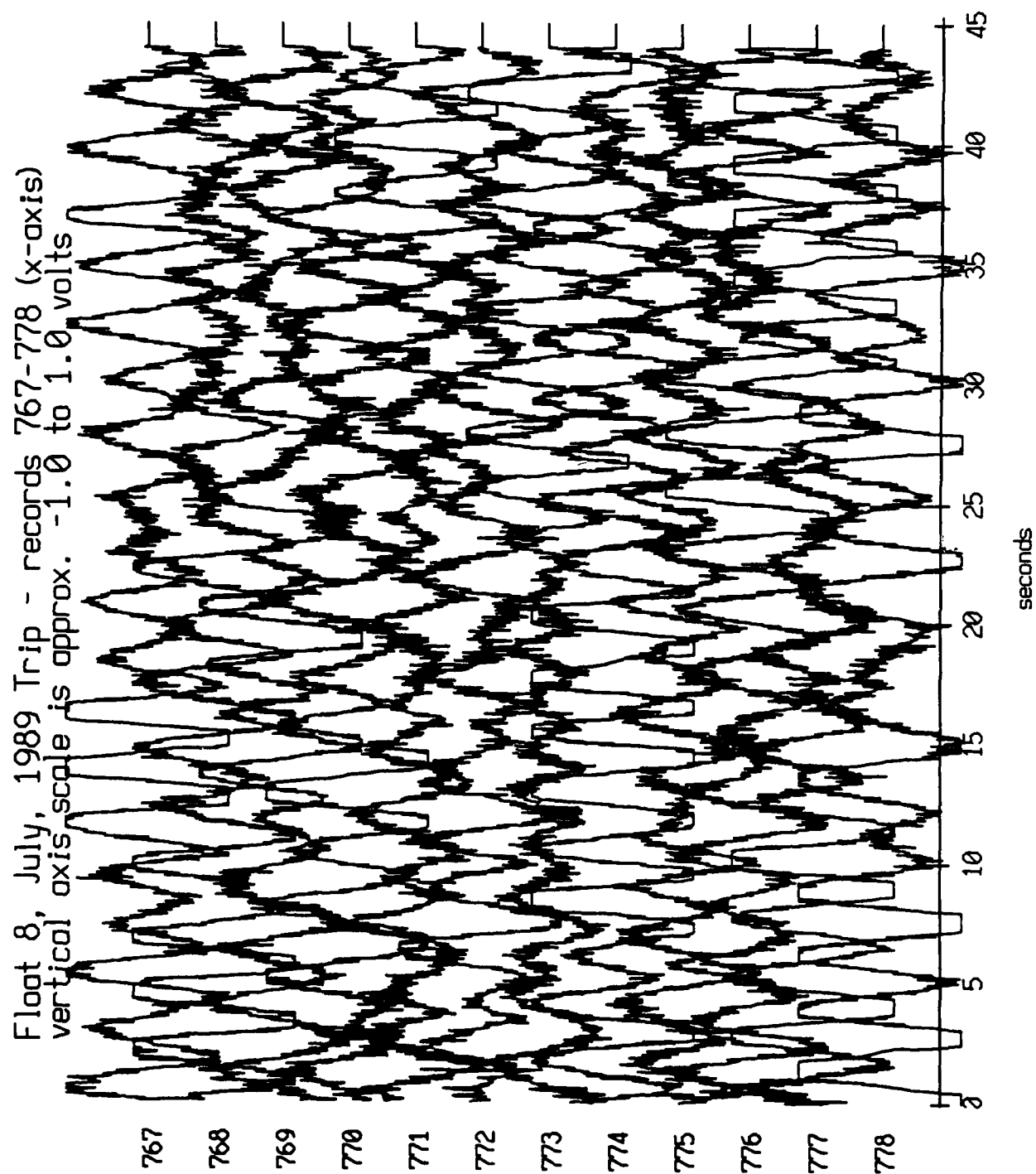
Figure XI.22c

Float 7, July, 1989 Trip - records 767-778 (hydrophone)  
vertical axis scale is approx. -1.0 to 1.0 volts



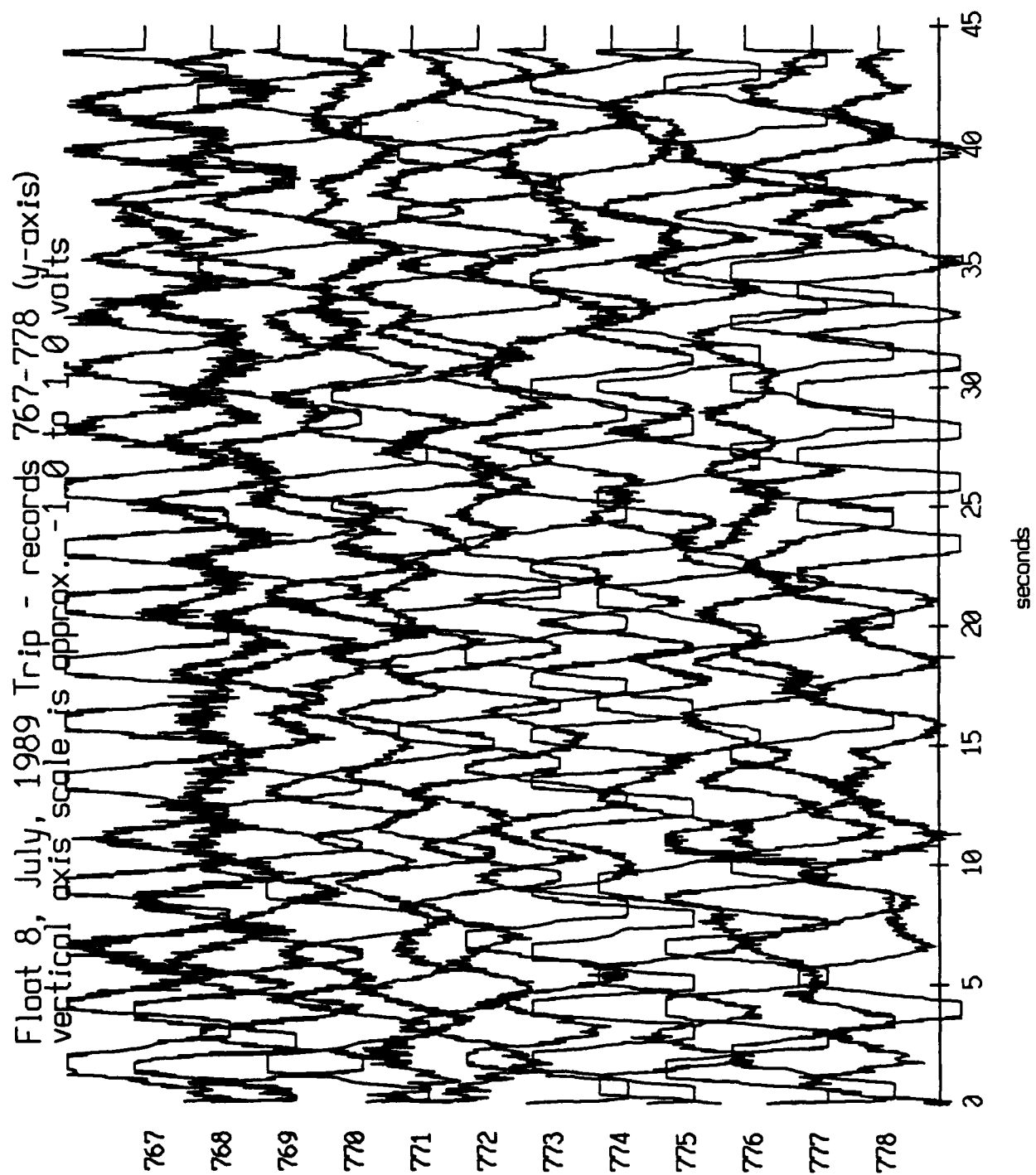
AGC corrected channel level (V)

Figure XI.22d



RGC corrected channel level (V)

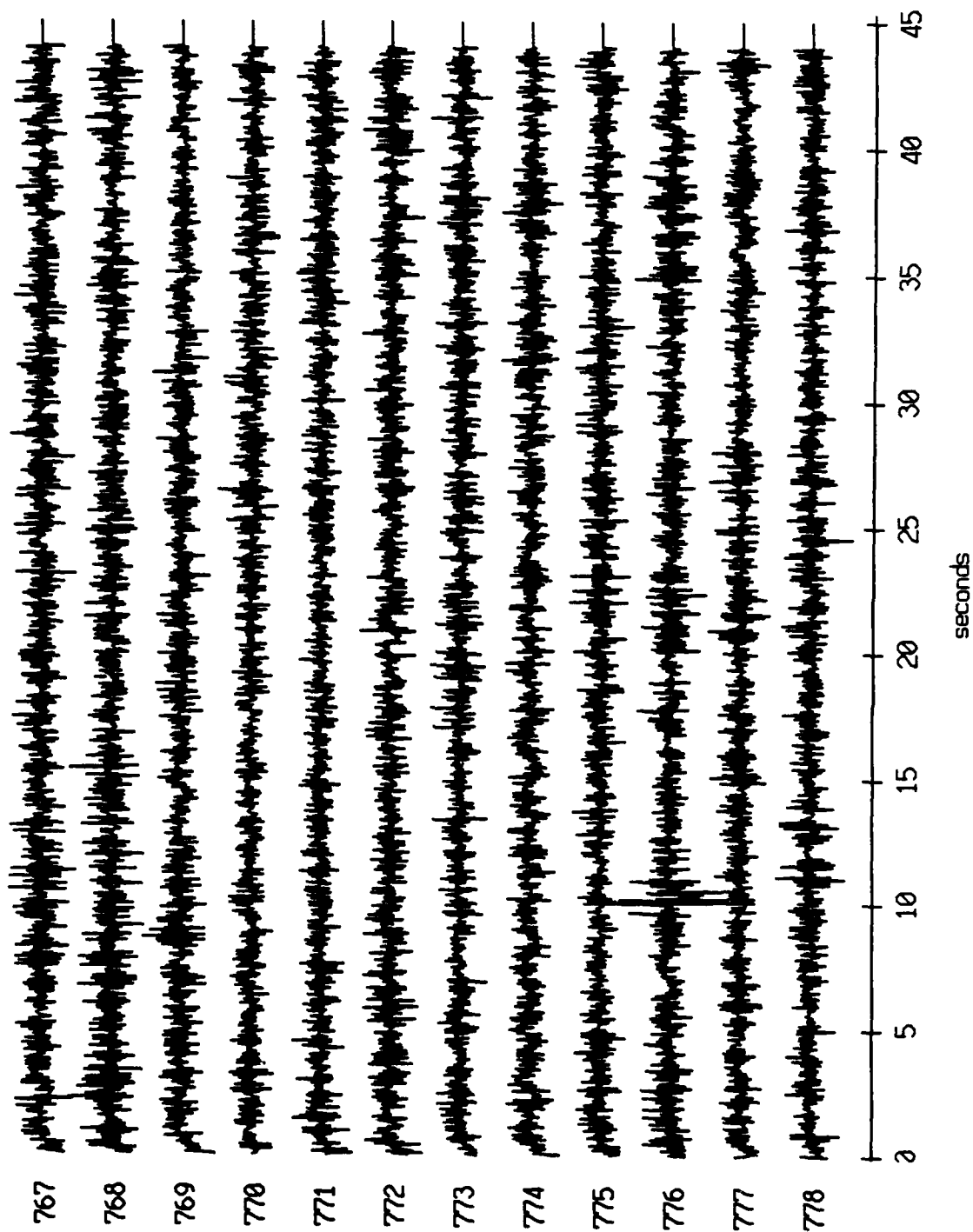
Figure XI.23a



AGC corrected channel level (V)

Figure XI.23b

Float 8, July, 1989 Trip - records 767-778 (z-axis)  
vertical axis scale is approx. -1.0 to 1.0 volts



RGC corrected channel level (V)

Figure XI.23c

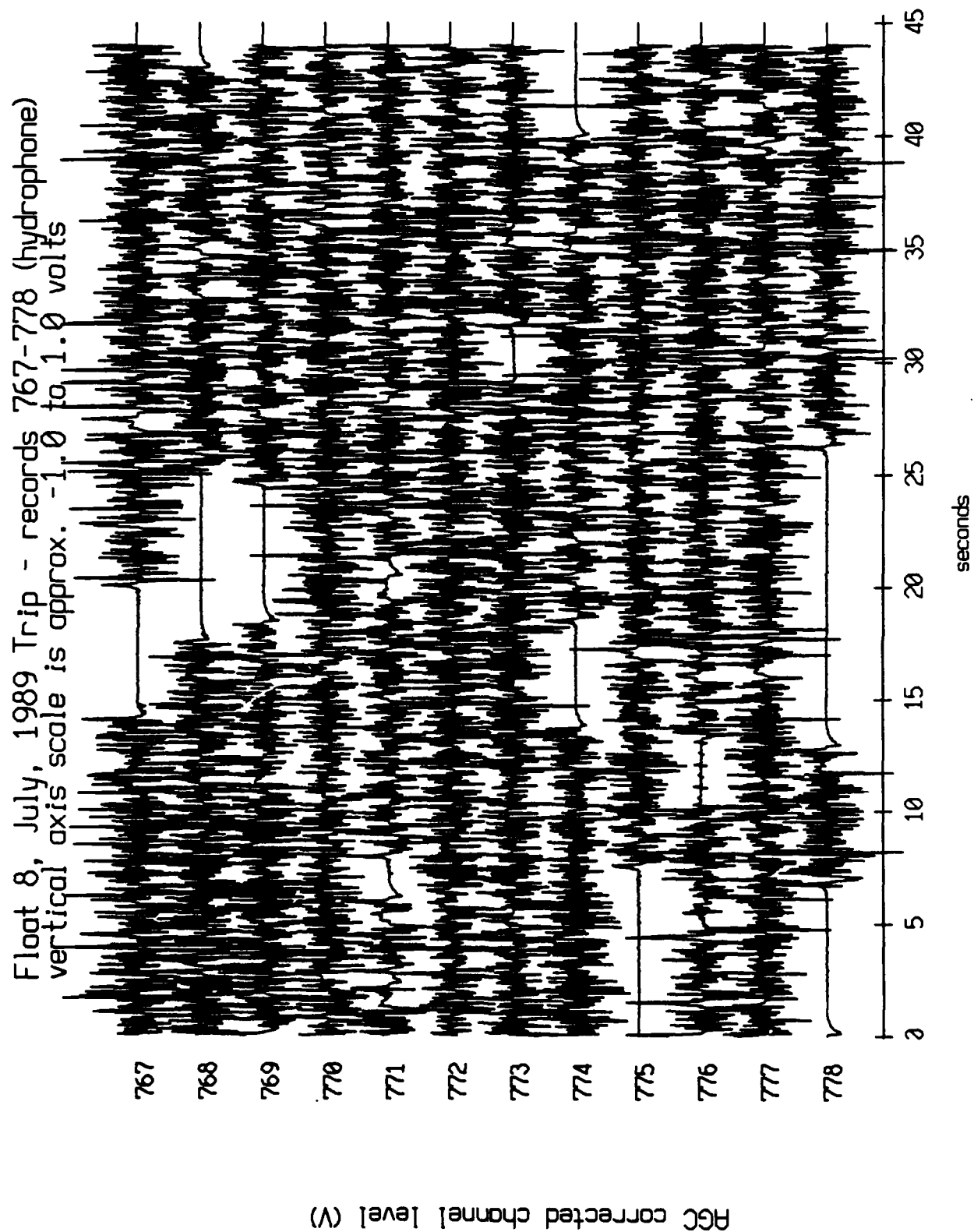
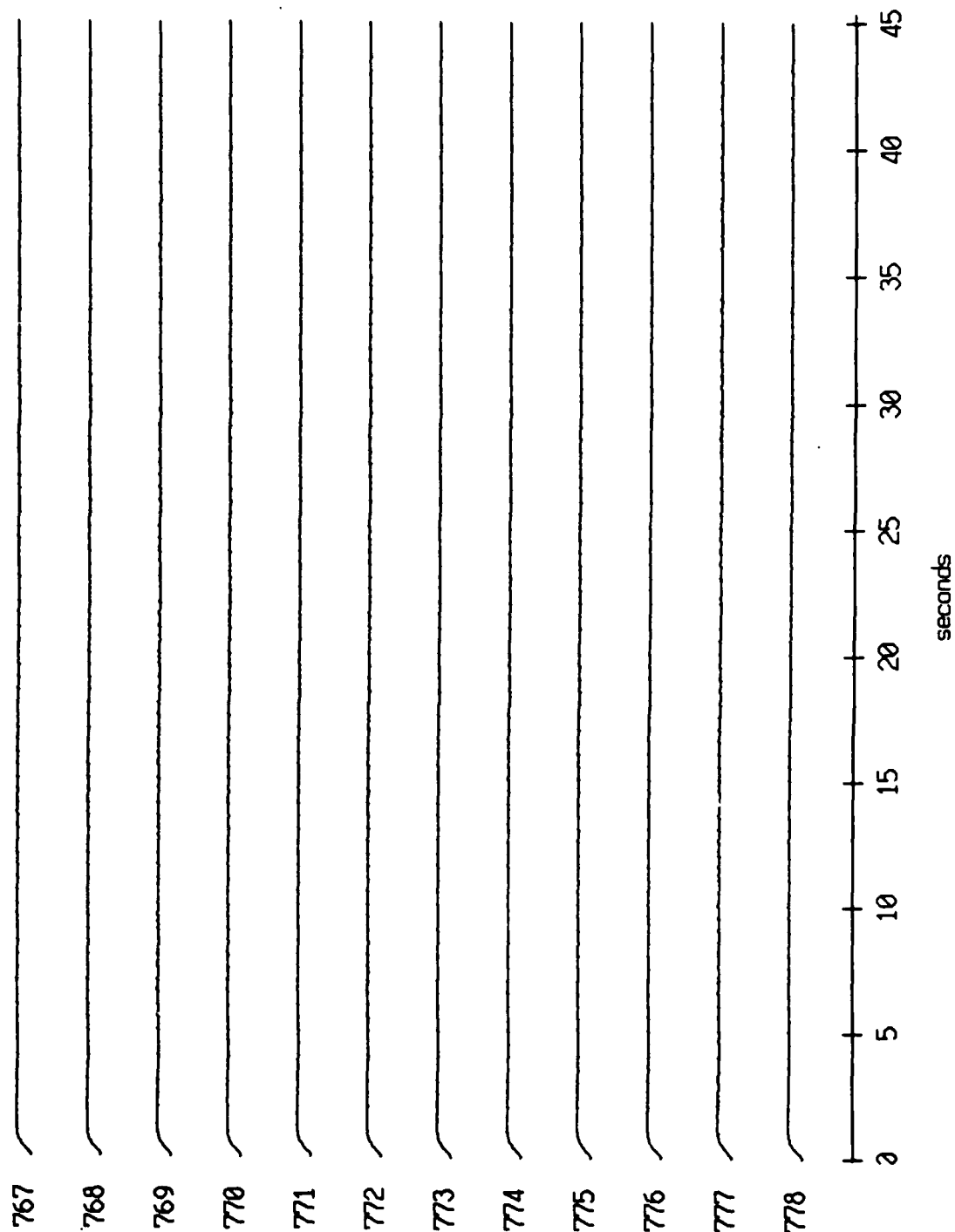


Figure XI.23d



Float 9, July, 1989 Trip - records 767-778 (x-axis)  
 vertical axis scale is approx. -1.0 to 1.0 volts



AGC corrected channel level (V)

Figure XI.24a

Float 9, July, 1989 Trip - records 767-778 (y-axis)  
vertical axis scale is approx. -1.0 to 1.0 volts

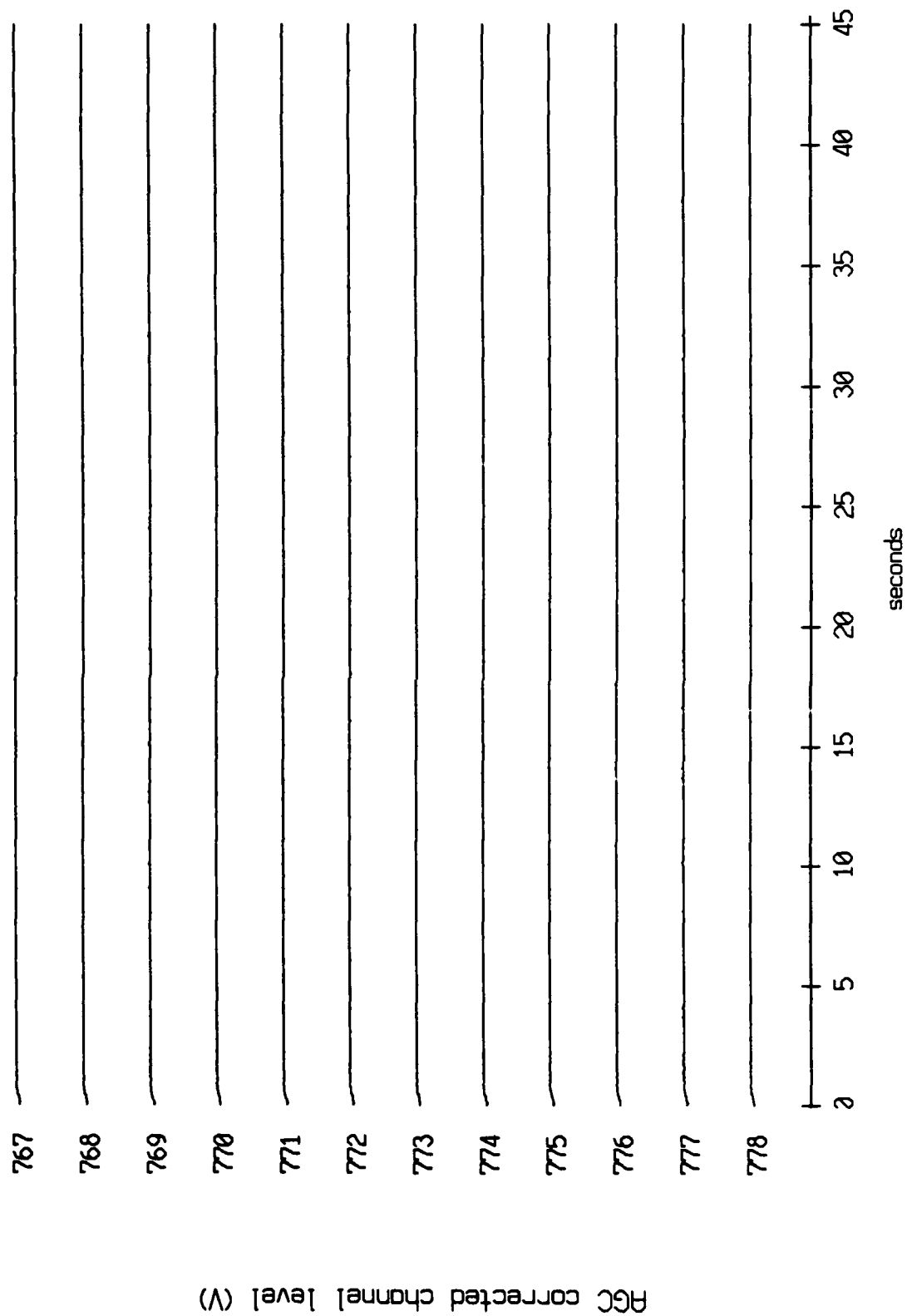


Figure XI.24b

Floot 9, July, 1989 Trip - records 767-778 (z-axis)  
vertical axis scale is approx. -1.0 to 1.0 volts

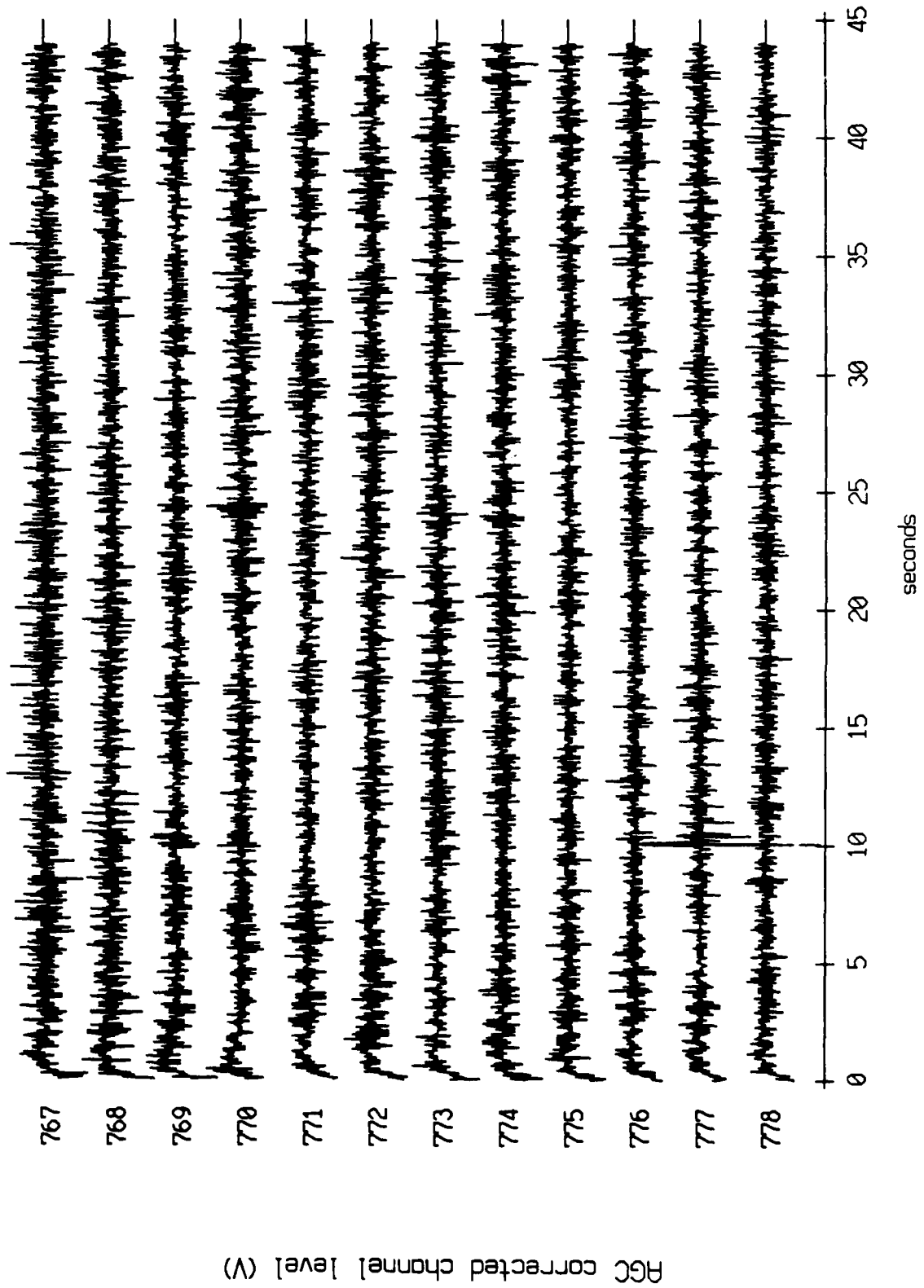
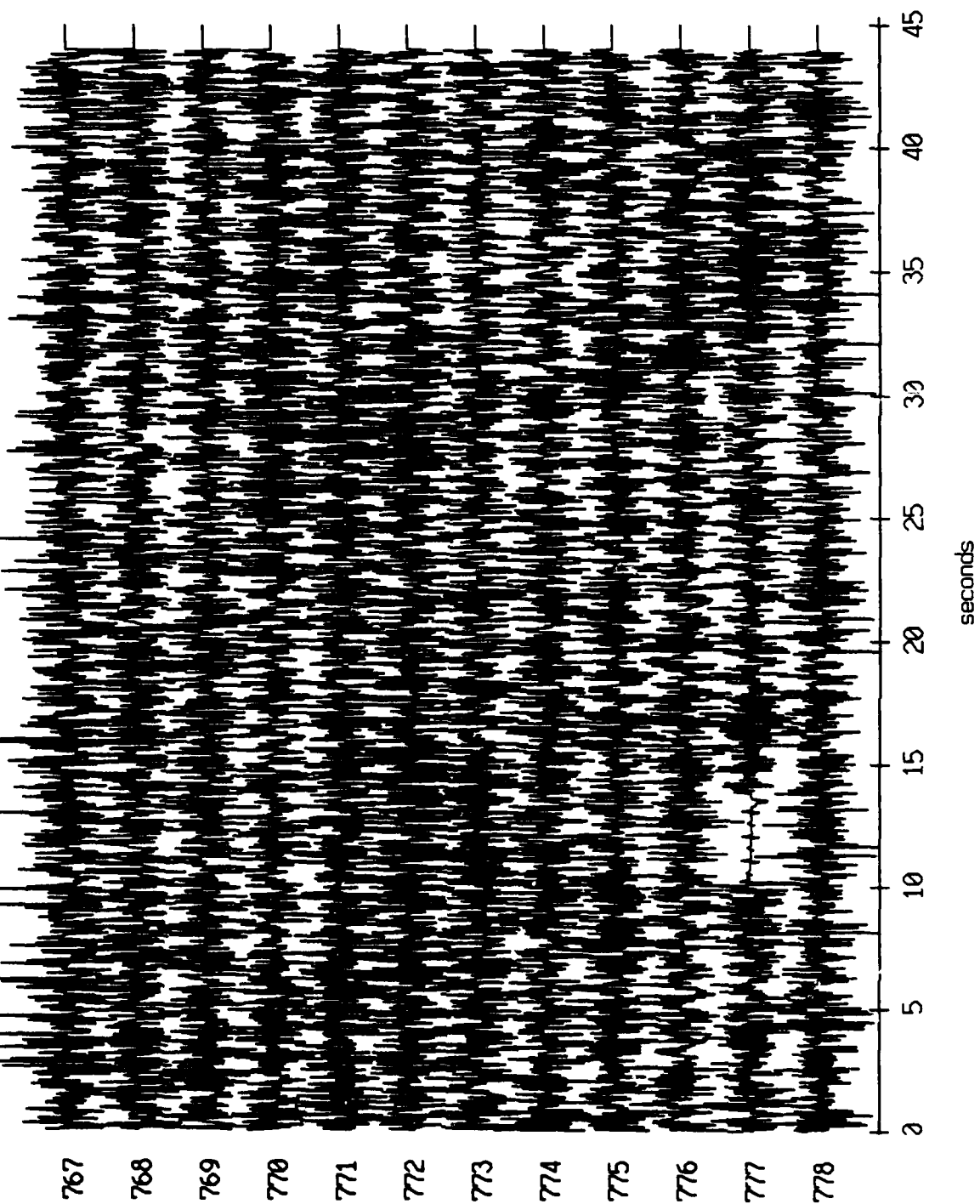


Figure XI.24c

Float 9, July, 1989 Trip - records 767-778 (hydrophone)  
vertical axis scale is approx. -1.0 to 1.0 volts



AGC corrected channel level (V)

Figure XI.24d

Float 10, July, 1989 Trip - records 767-778 (x-axis)  
vertical axis scale is approx. -1.0 to 1.0 volts

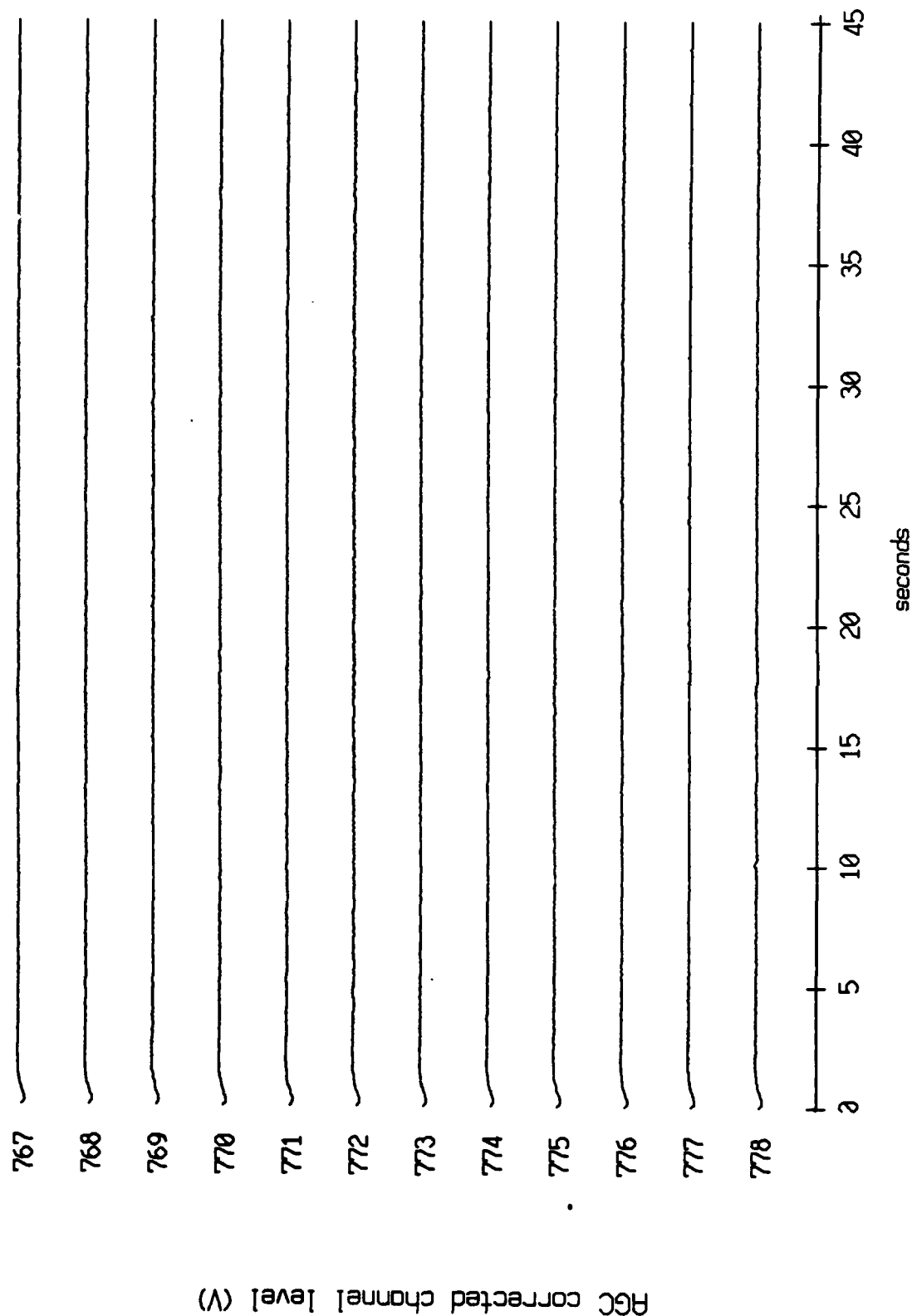
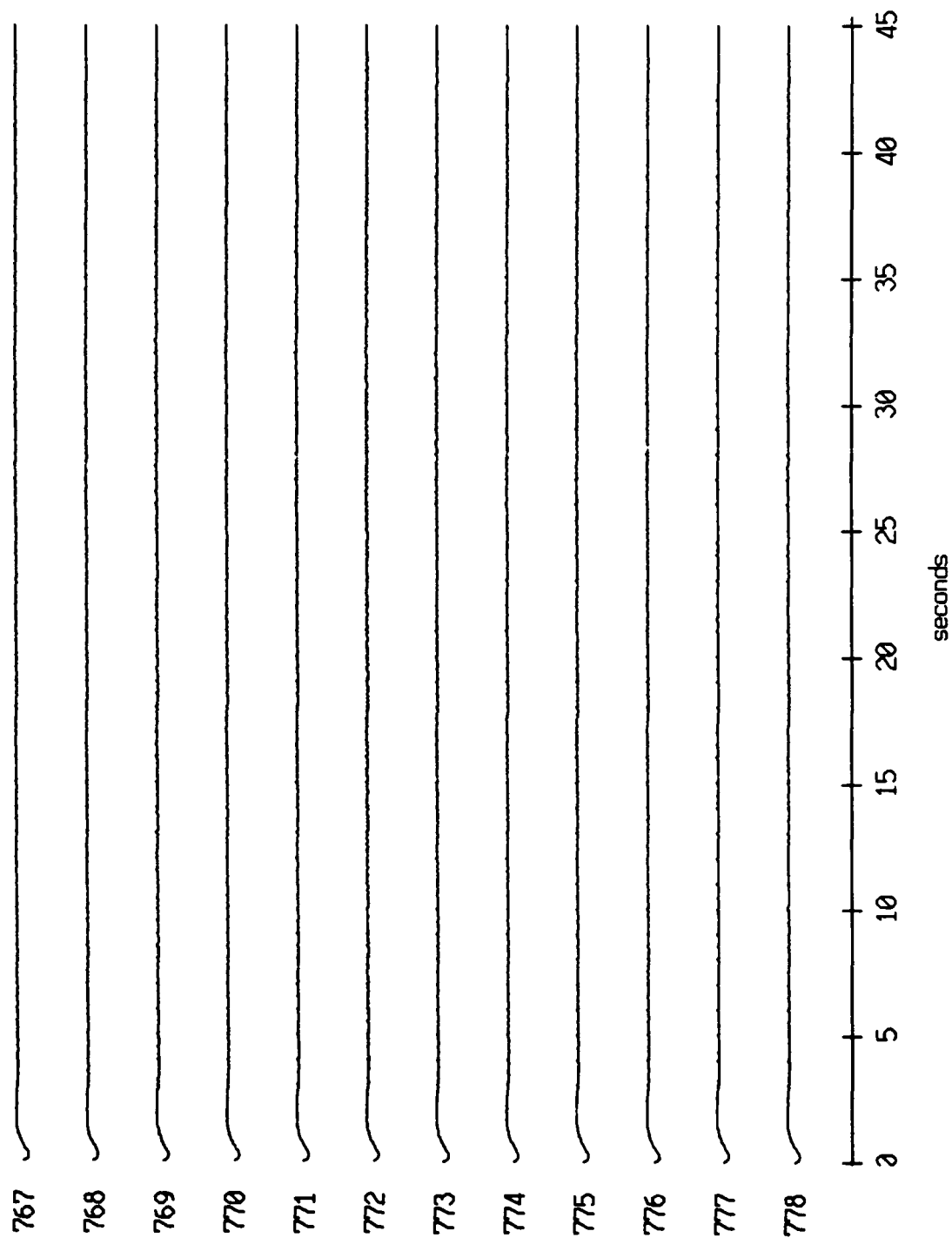


Figure XI.25a

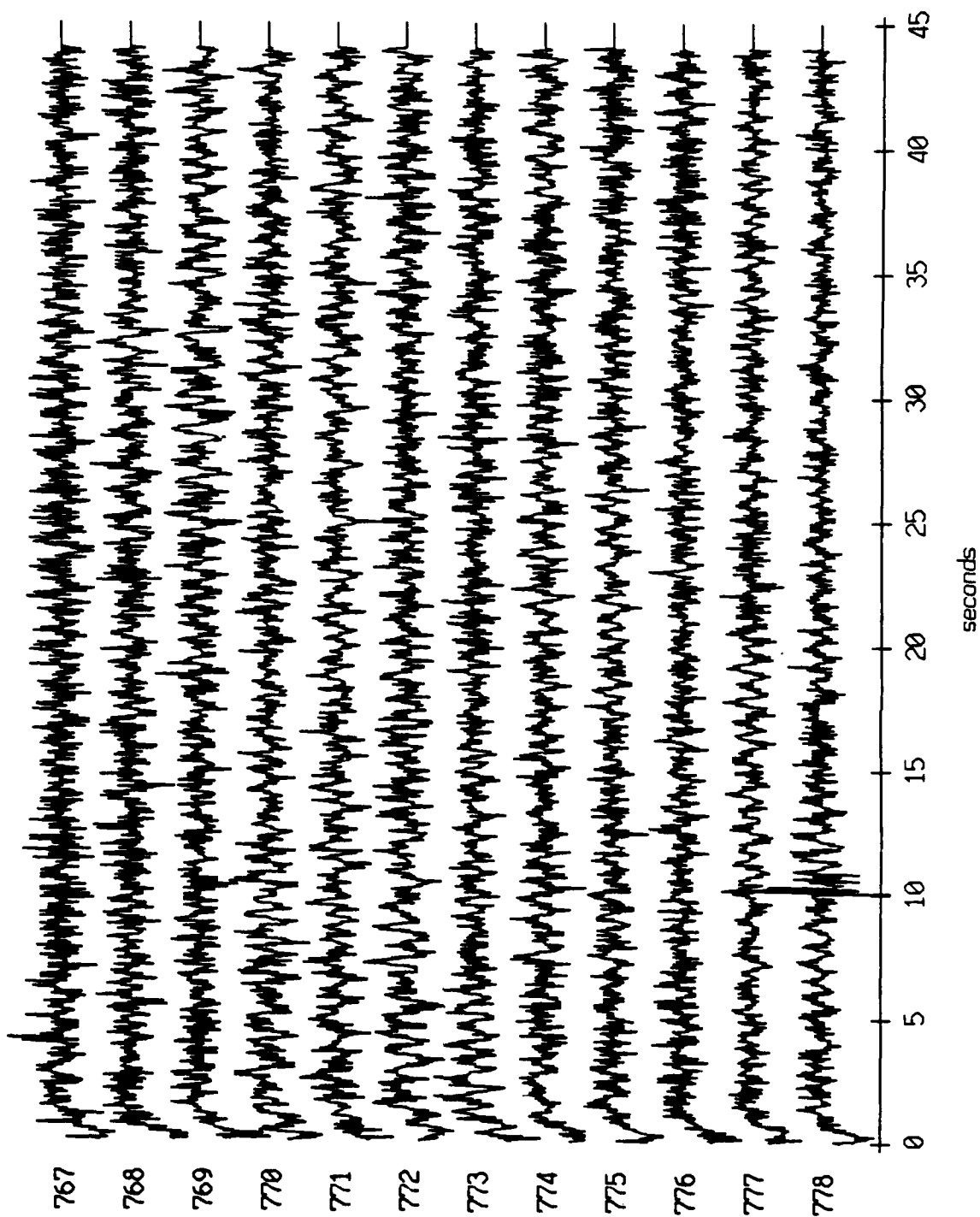
Float 10, July, 1989 Trip - records 767-778 (y-axis)  
vertical axis scale is approx. -1.0 to 1.0 volts



AGC corrected channel level (V)

Figure XI.25b

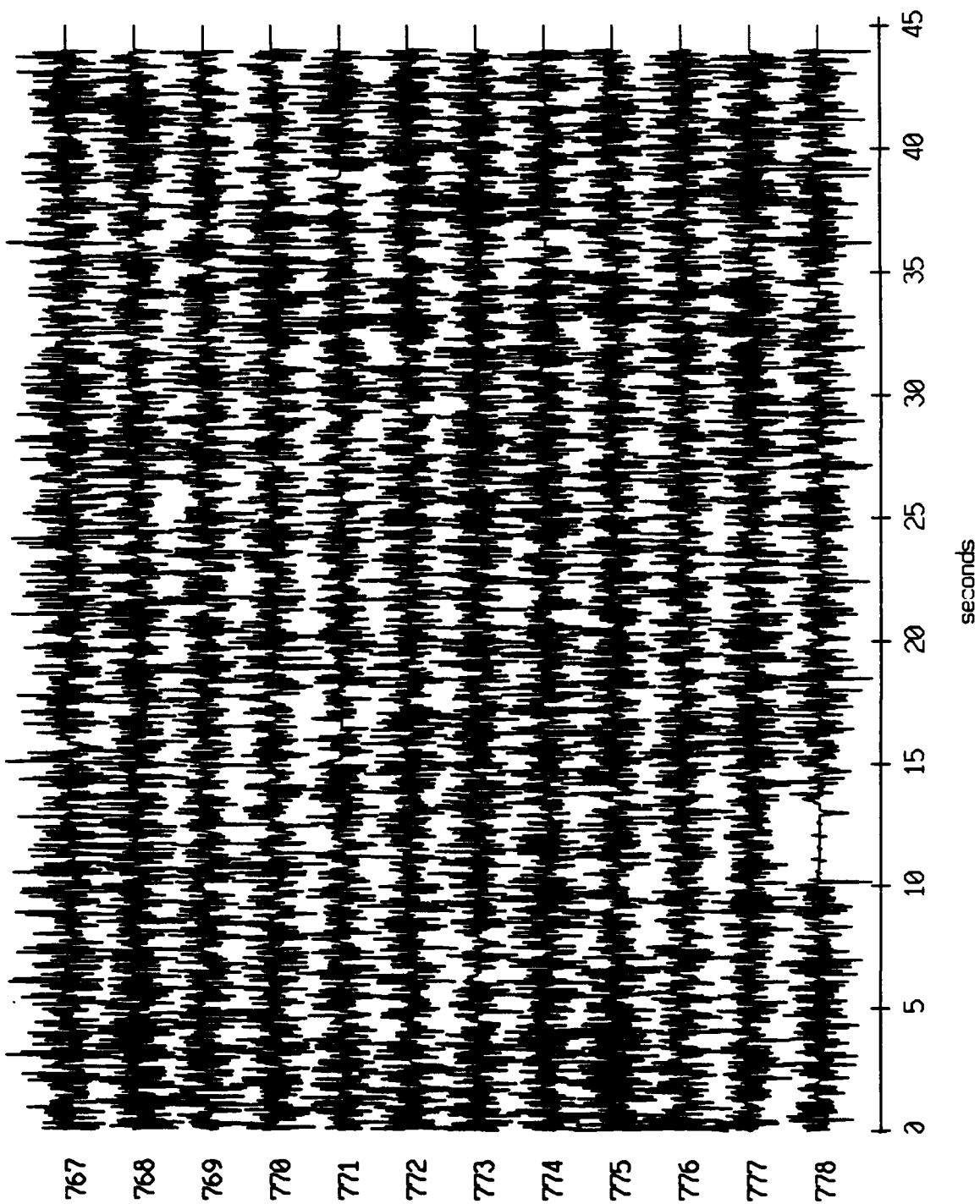
Float 10, July, 1989 Trip - records 767-778 (z-axis)  
vertical axis scale is approx. -1.0 to 1.0 volts



PGC corrected channel level (V)

Figure XI.25c

Float 10, July, 1989 Trip - records 767-778 (hydrophone)  
vertical axis scale is approx. -1.0 to 1.0 volts



AGC corrected channel level (V)

Figure XI.25d



Float 11, July, 1989 Trip - records 767-778 (x-axis)  
vertical axis scale is approx. -1.0 to 1.0 volts

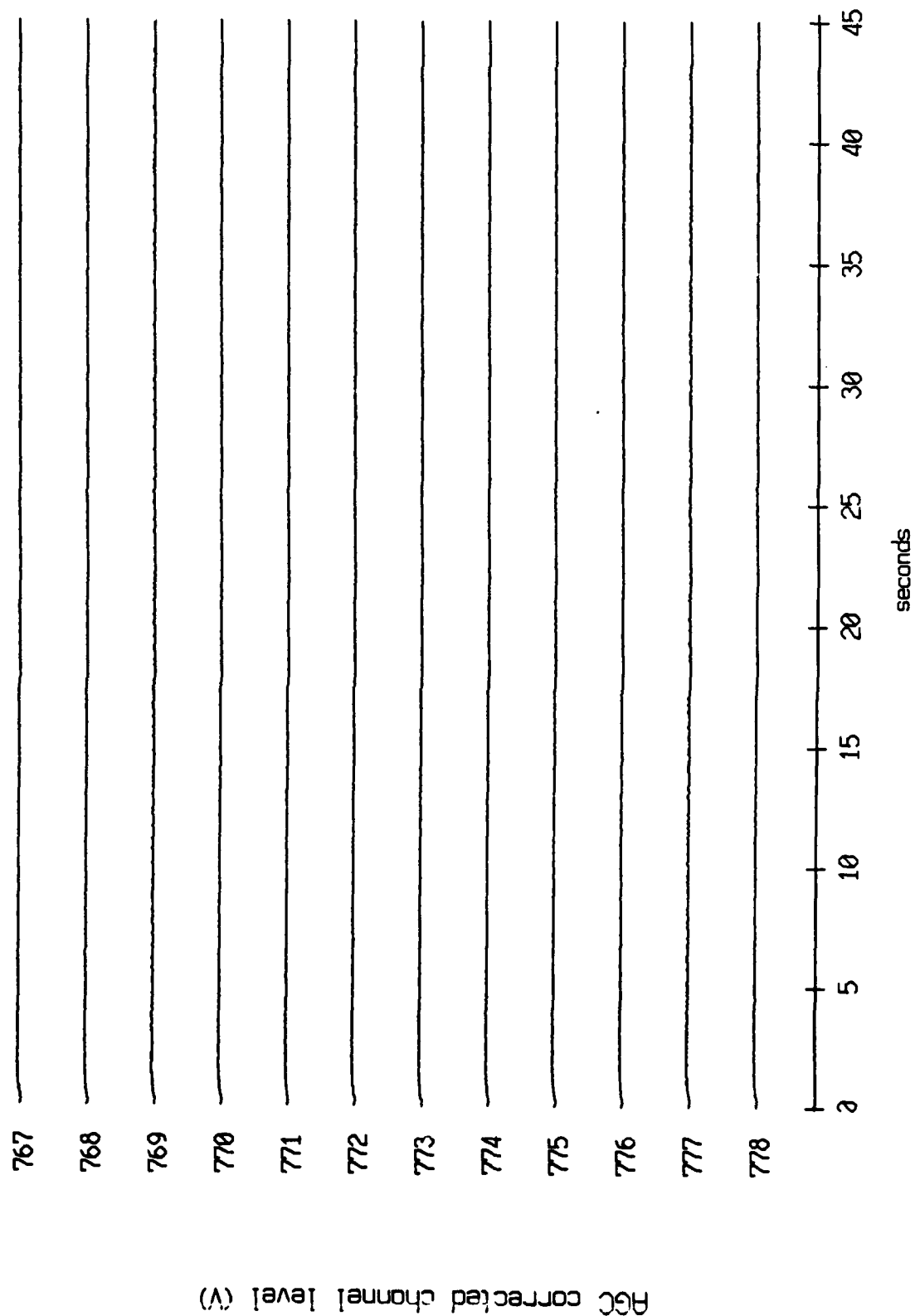


Figure XI.26a

Flot 11, July, 1989 Trip - records 767-778 (y-axis)  
vertical axis scale is approx. -1.0 to 1.0 volts

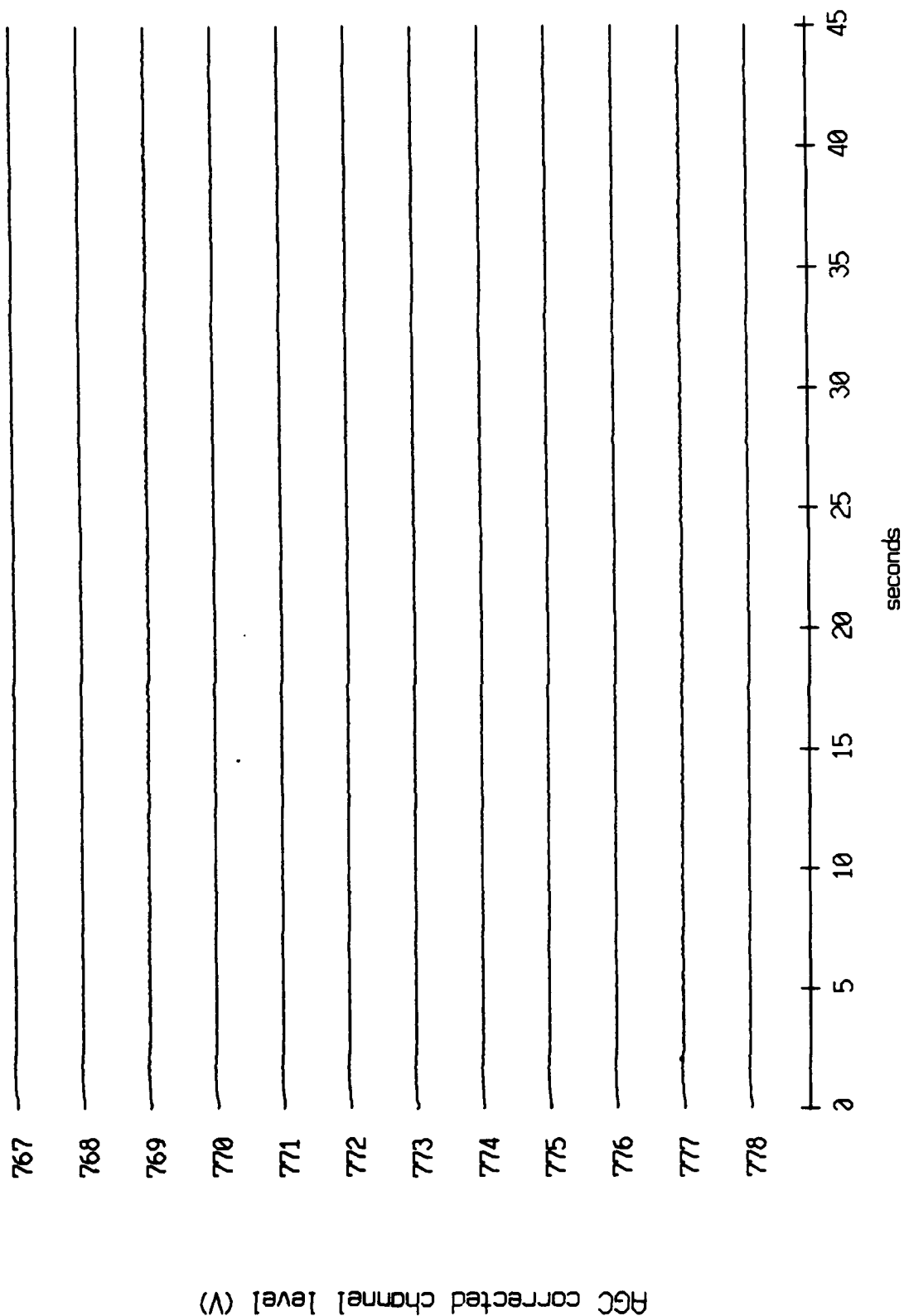
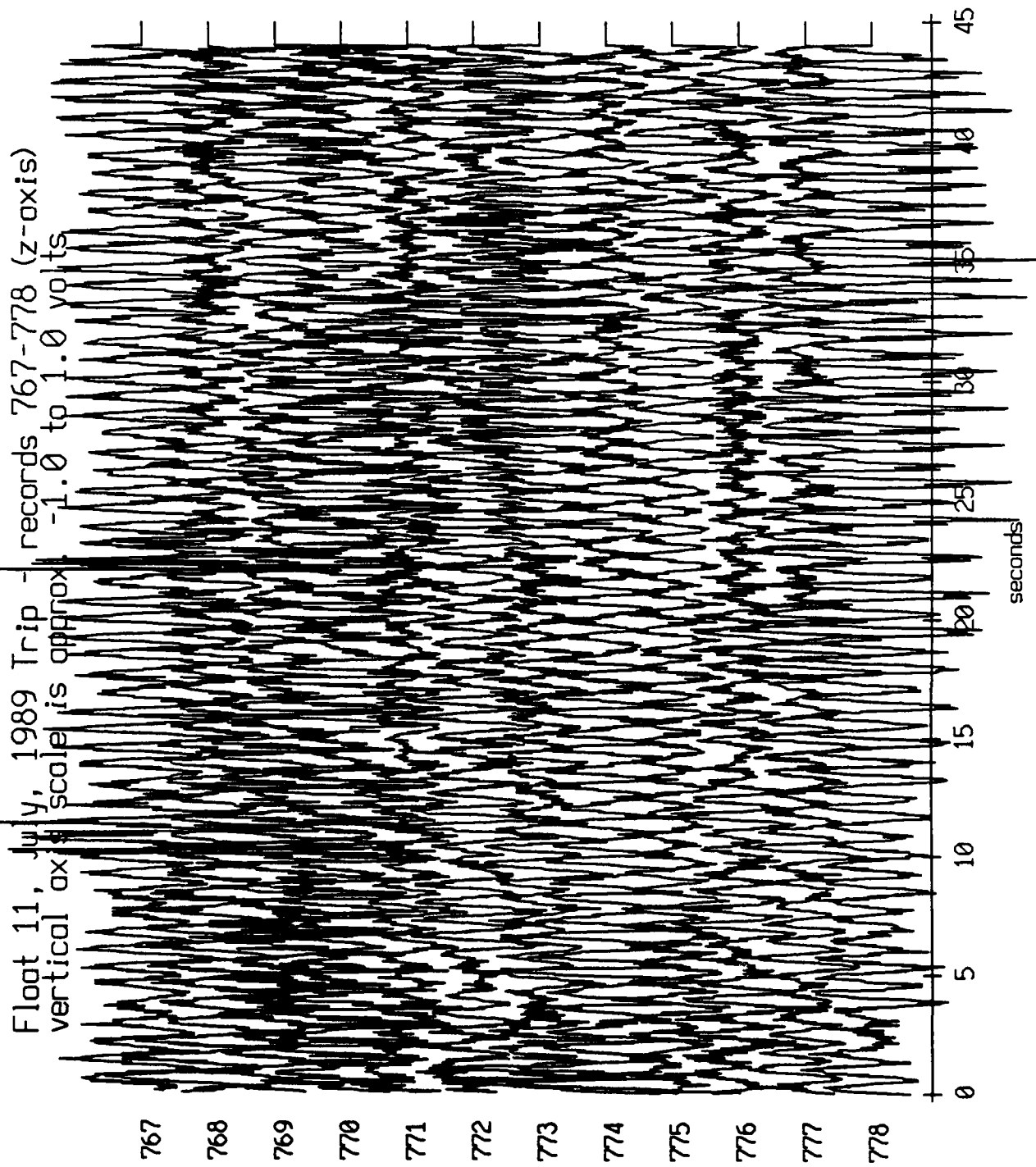


Figure XI.26b



AGC corrected channel level (V)

Figure XI.26c

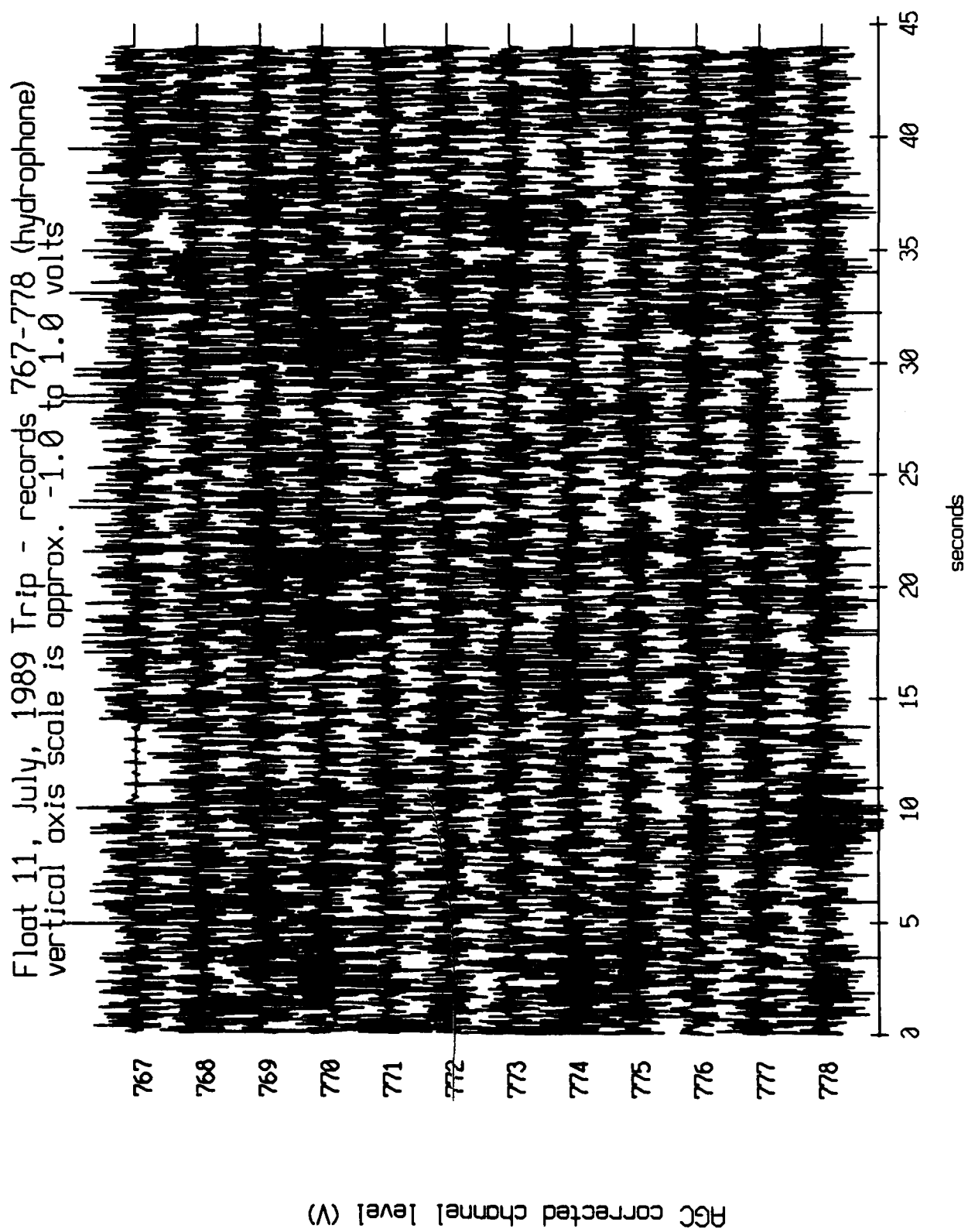


Figure XI.26d

Float 3, July, 1989 Trip - records 860-871 (x-axis)  
vertical axis scale is approx. -1.0 to 1.0 volts

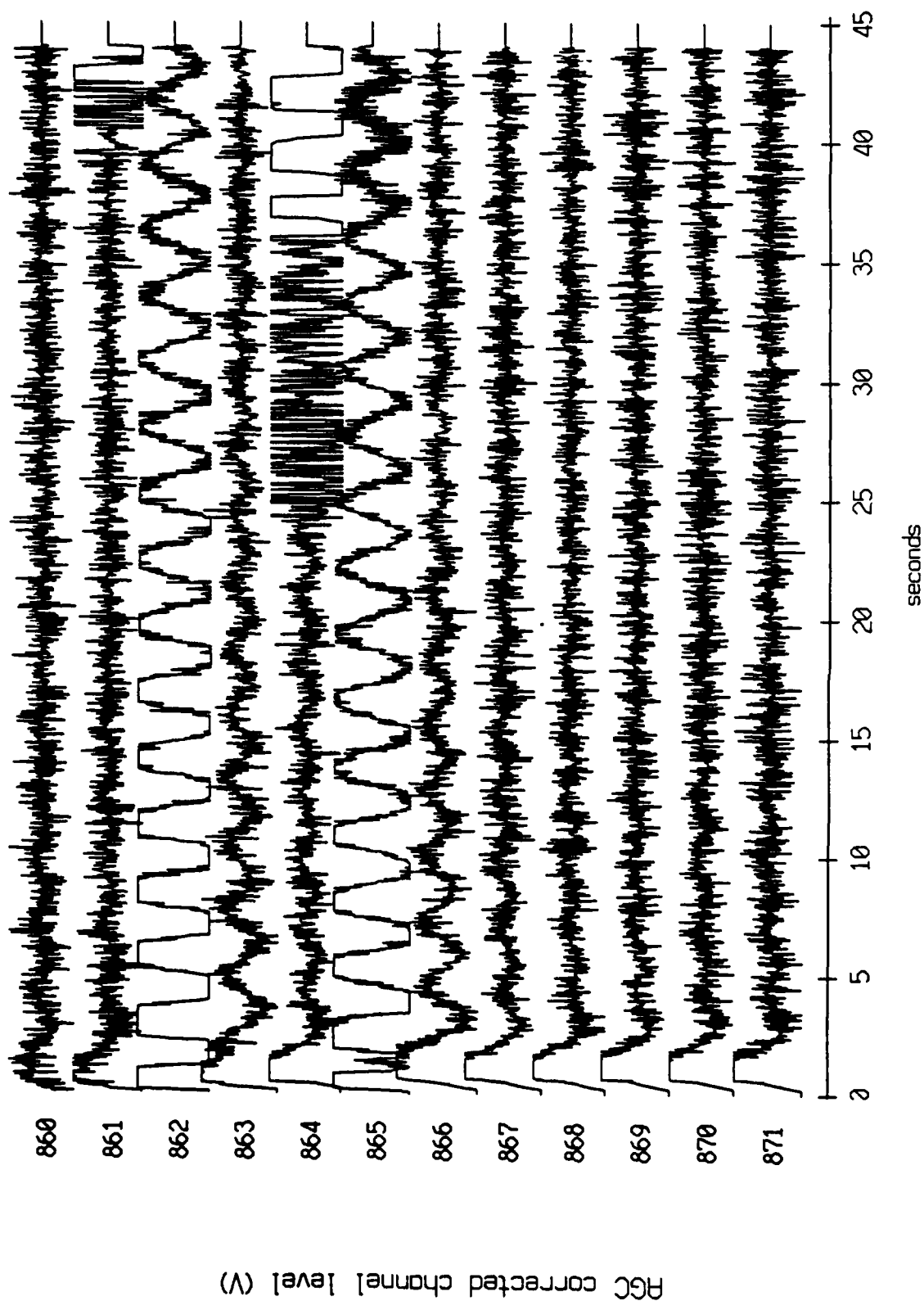


Figure XI.27a

Float 3, July, 1989 Trip - records 860-871 (y-axis)  
vertical axis scale is approx. -1.0 to 1.0 volts

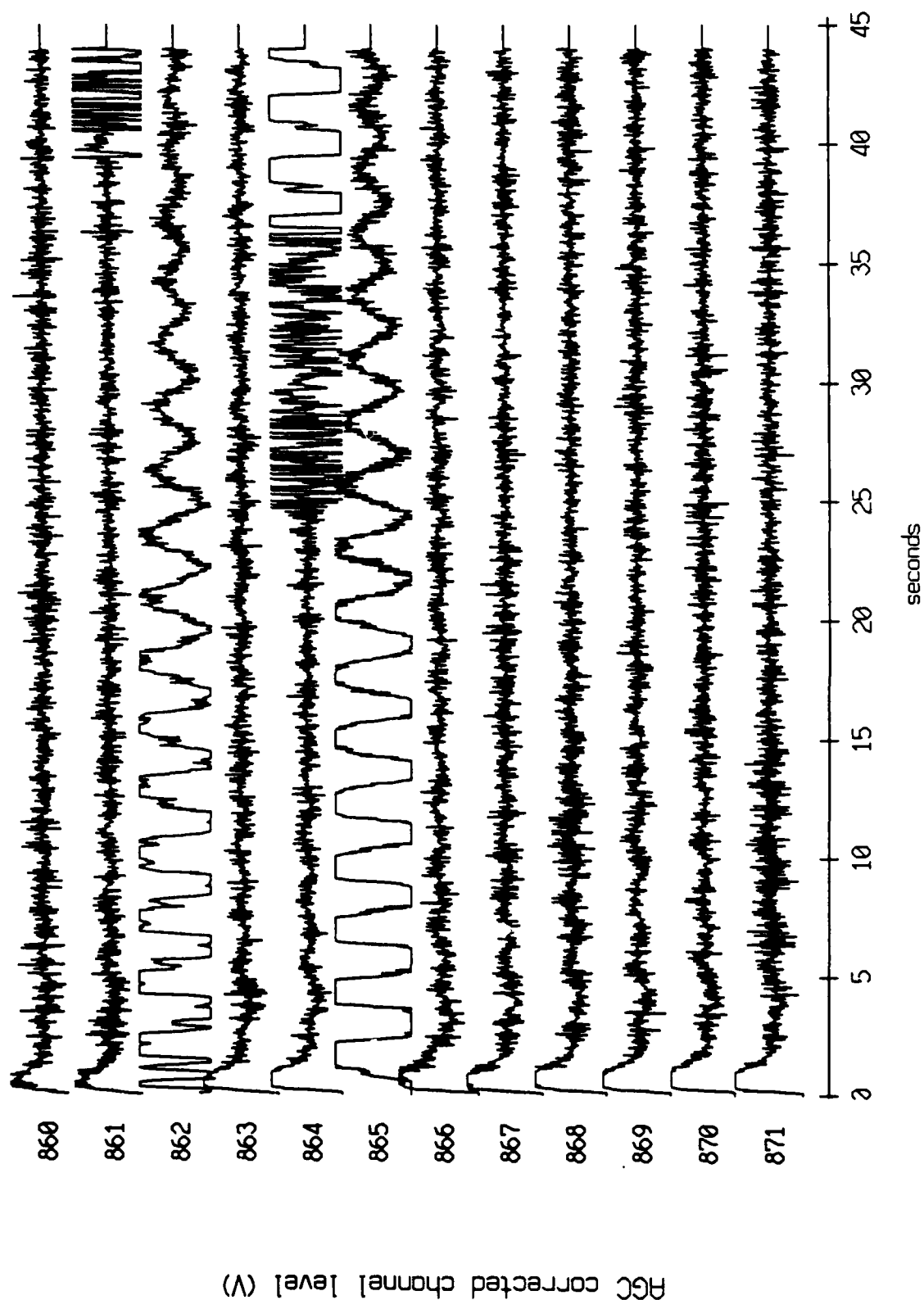


Figure XI.27b

Float 3, July, 1989 Trip - records 860-871 (z-axis)  
vertical axis scale is approx. -1.0 to 1.0 volts

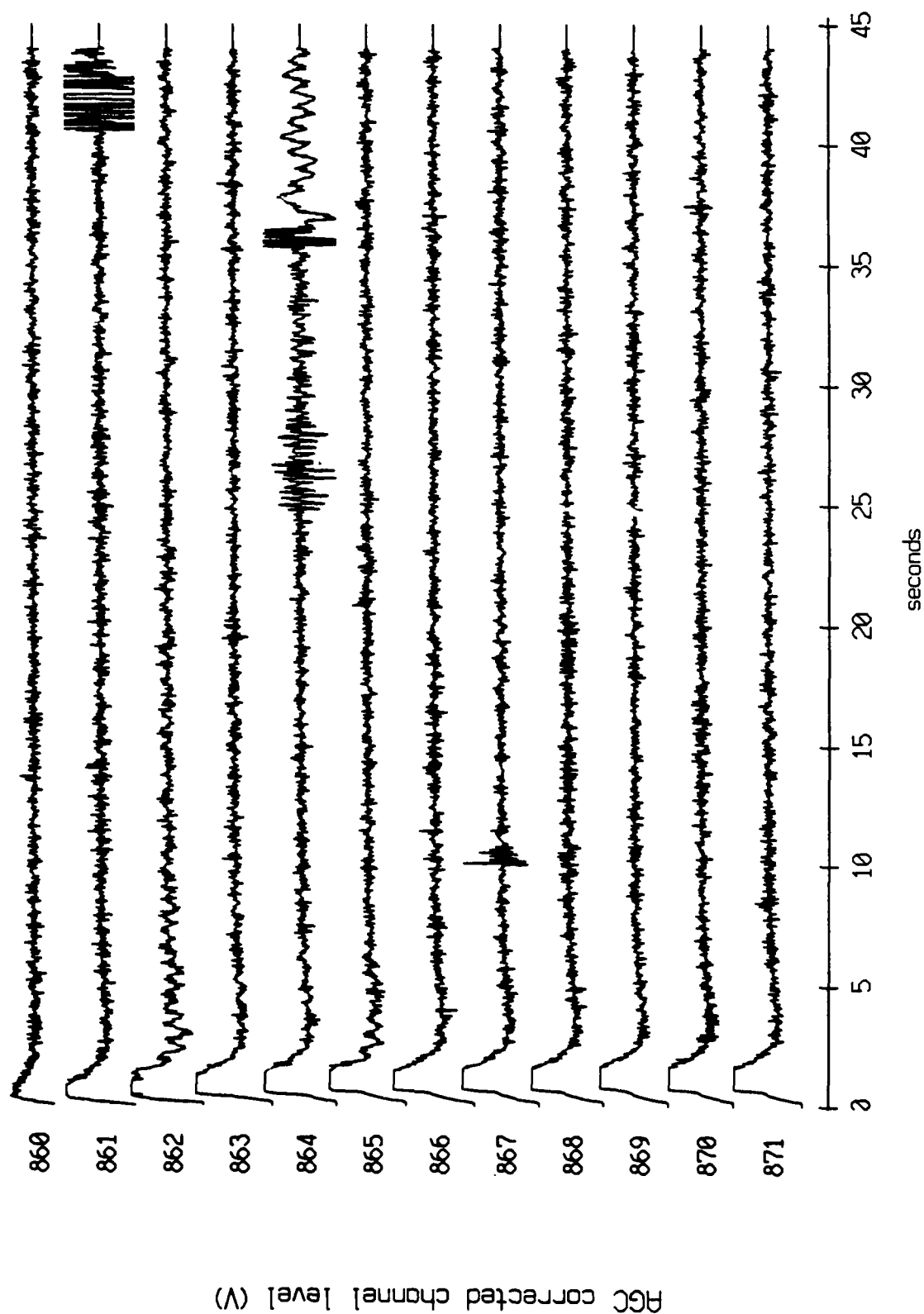
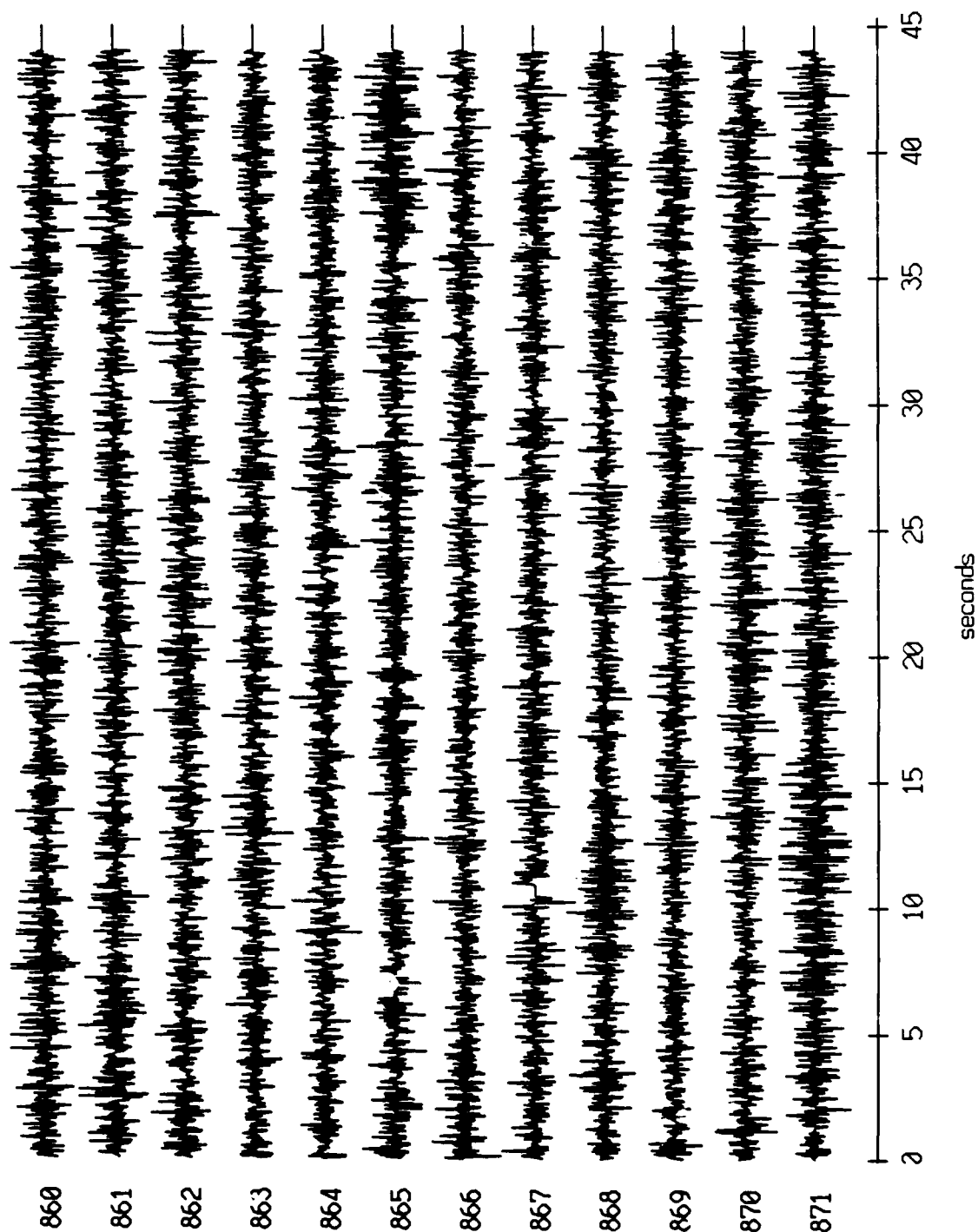


Figure XI.27c

Float 3, July, 1989 Trip - records 860-871 (hydrophone)  
vertical axis scale is approx. -1.0 to 1.0 volts



AGC corrected channel level (V)

Figure XI.27d



Float 2, July, 1989 Trip - records 1030-1041 (x-axis)  
vertical axis scale is approx. -1.0 to 1.0 volts

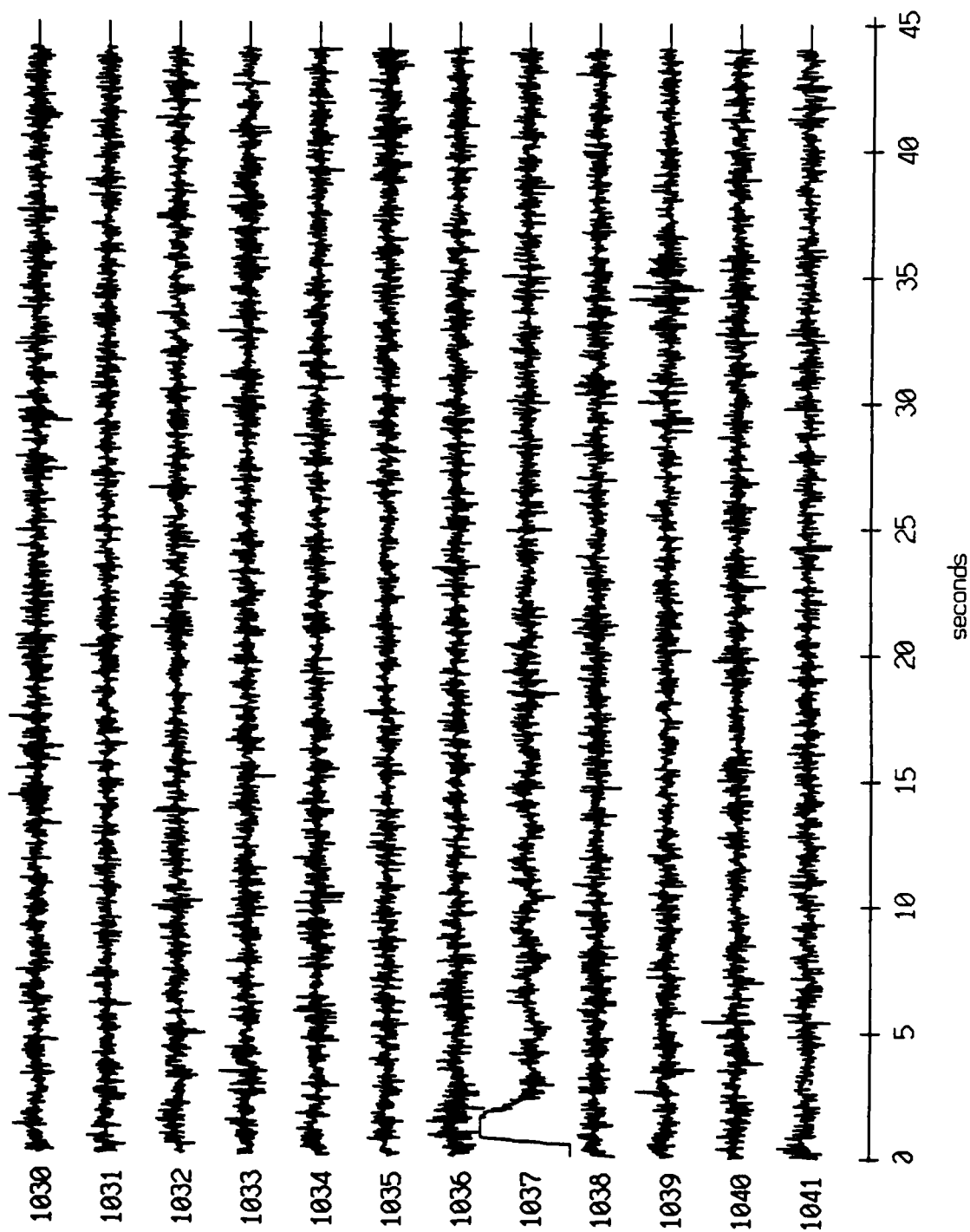
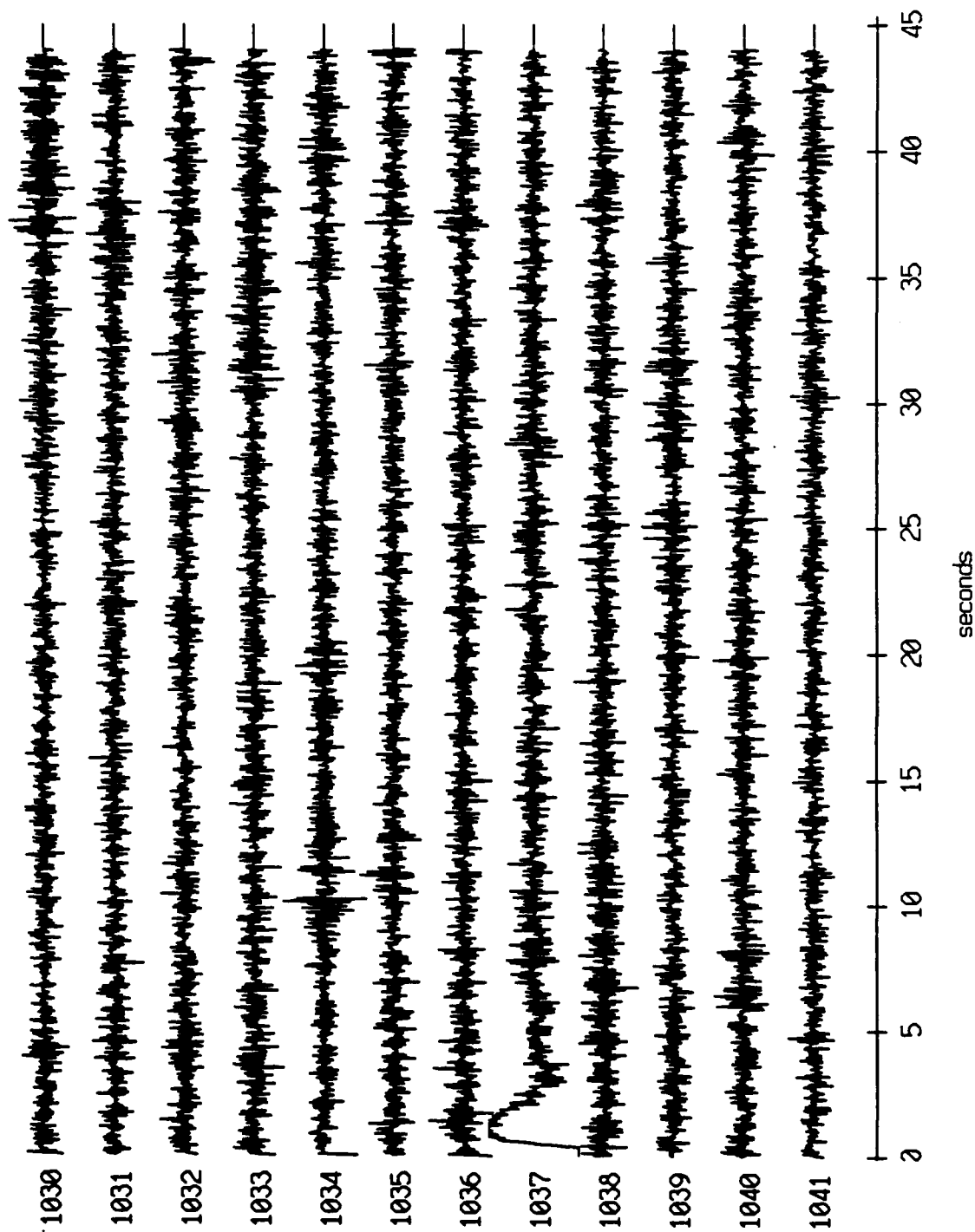


Figure XI.28a

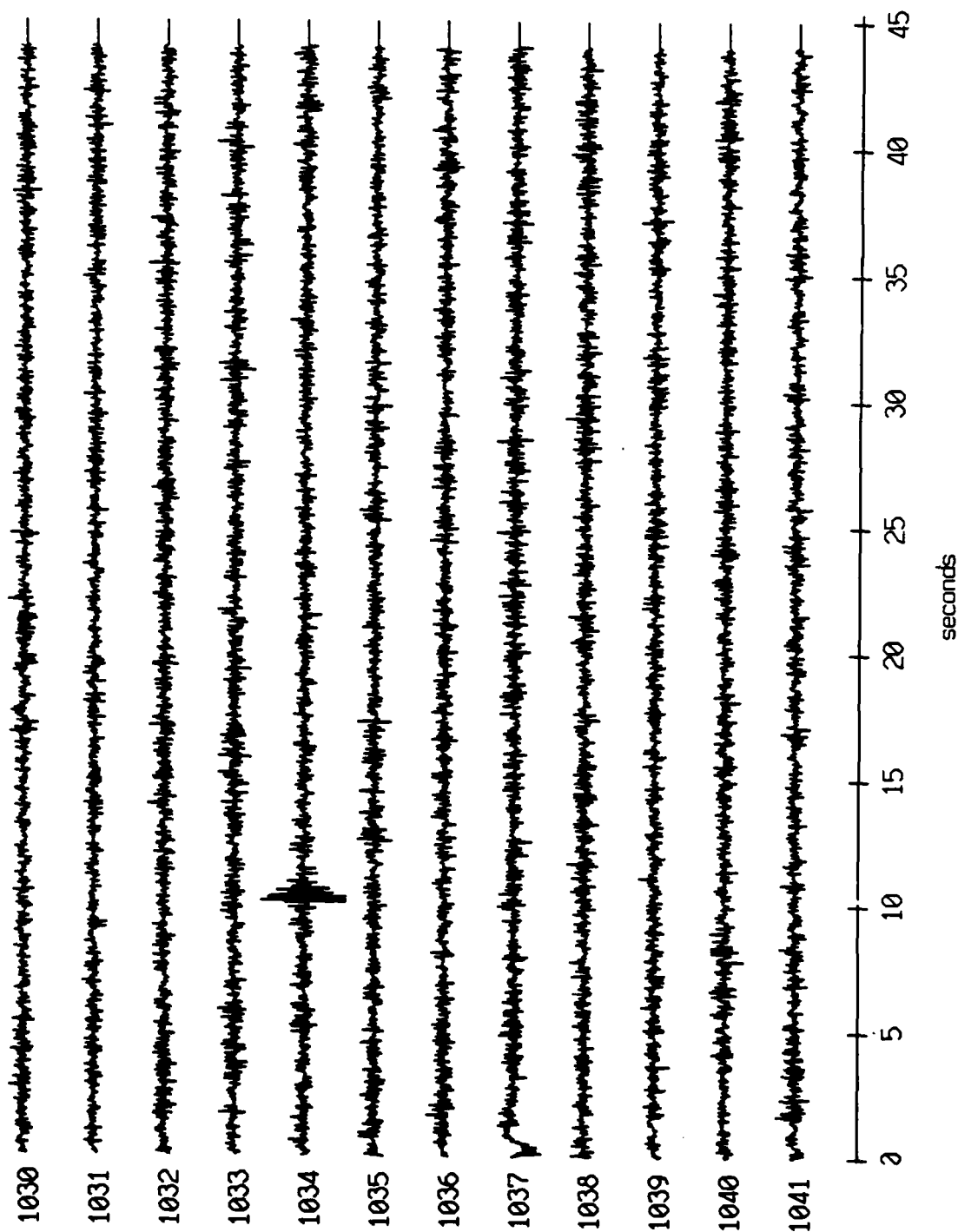
Float 2, July, 1989 Trip - records 1030-1041 (y-axis)  
vertical axis scale is approx. -1.0 to 1.0 volts



RGC corrected channel level (V)

Figure XI.28b

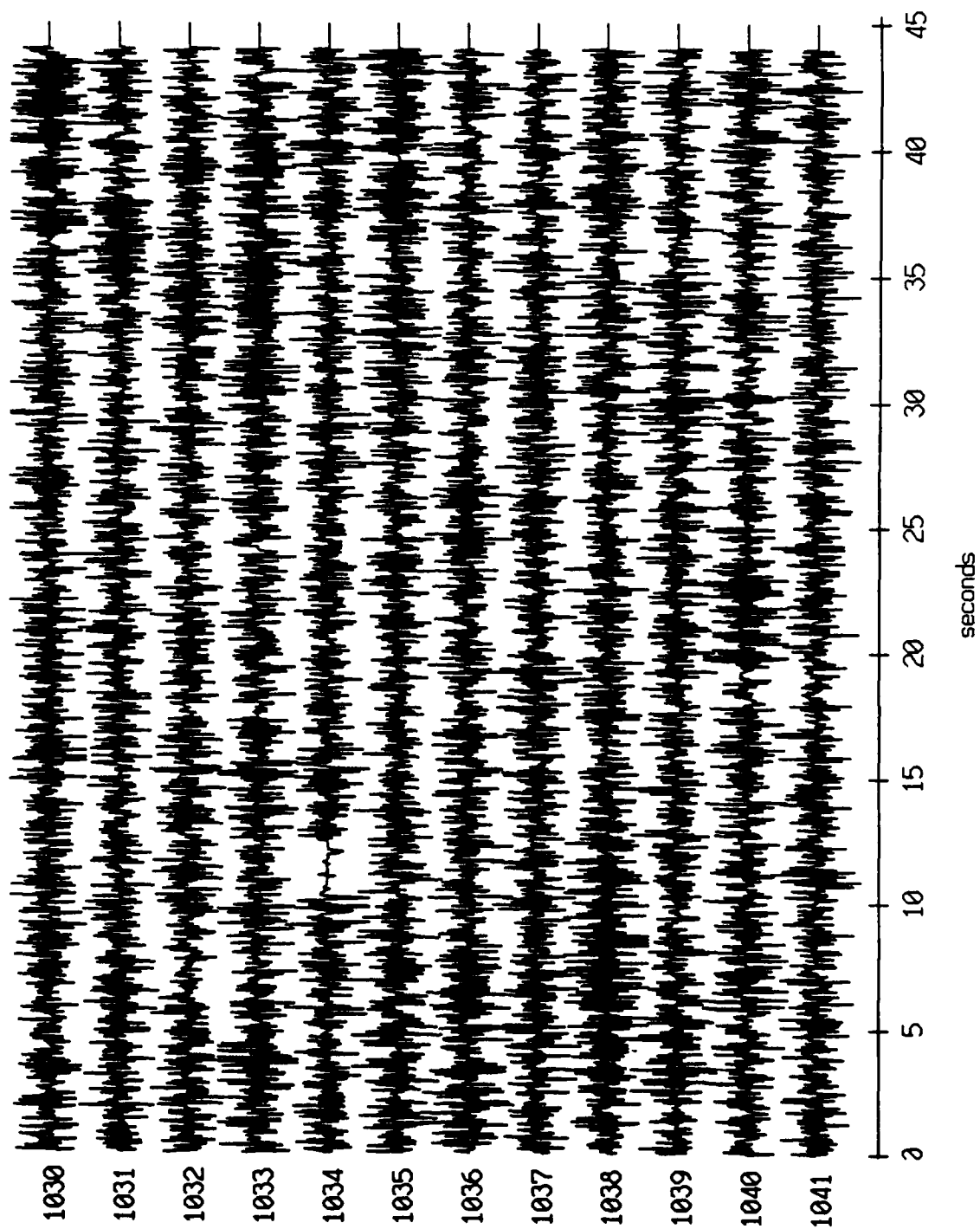
Float 2, July, 1989 Trip - records 1030-1041 (z-axis)  
vertical axis scale is approx. -1.0 to 1.0 volts



PGC corrected channel level (V)

Figure XI.28c

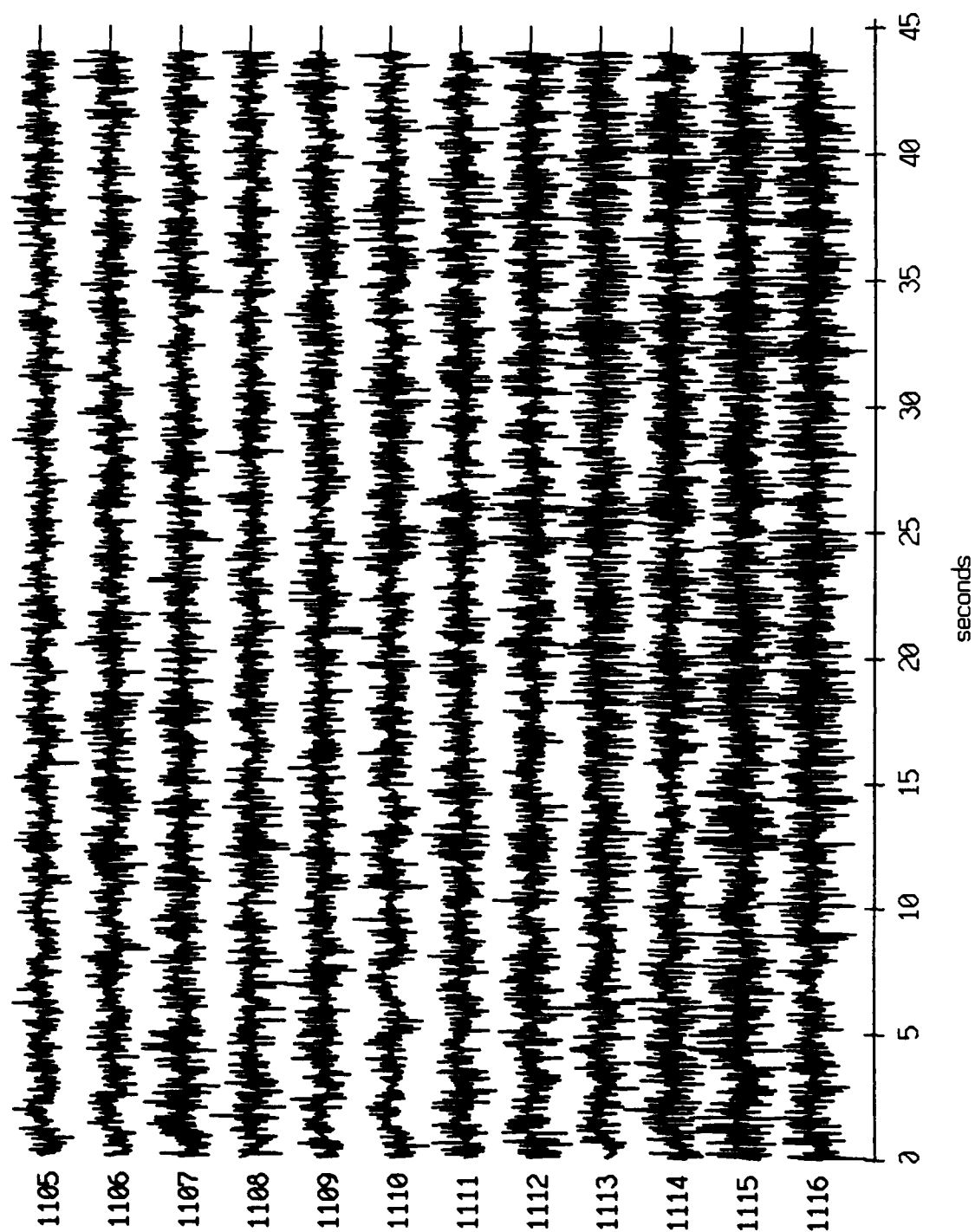
Float 2, July, 1989 Trip - records 1030-1041 (hydrophone)  
vertical axis scale is approx. -1.0 to 1.0 volts



AGC corrected channel level (V)

Figure XI.28d

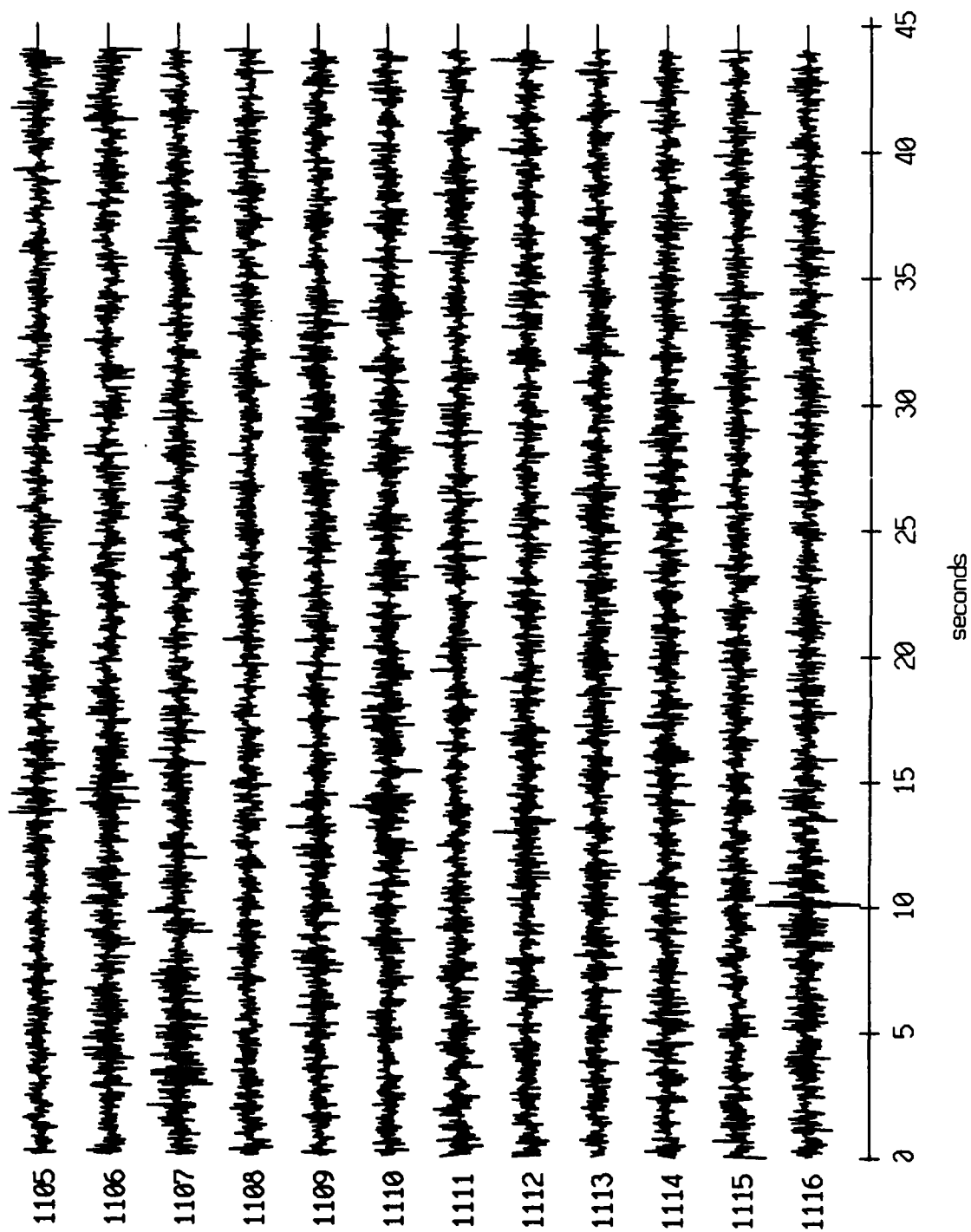
Float 0, July, 1989 Trip - records 1105-1116 (x-axis)  
vertical axis scale is approx. -1.0 to 1.0 volts



PGC corrected channel level (V)

Figure XI.29a

Floot 0, July, 1989 Trip - records 1105-1116 (y-axis)  
vertical axis scale is approx. -1.0 to 1.0 volts



RGC corrected channel level (V)

Figure X1.29b

Float 0, July, 1989 Trip - records 1105-1116 (z-axis)  
vertical axis scale is approx. -1.0 to 1.0 volts

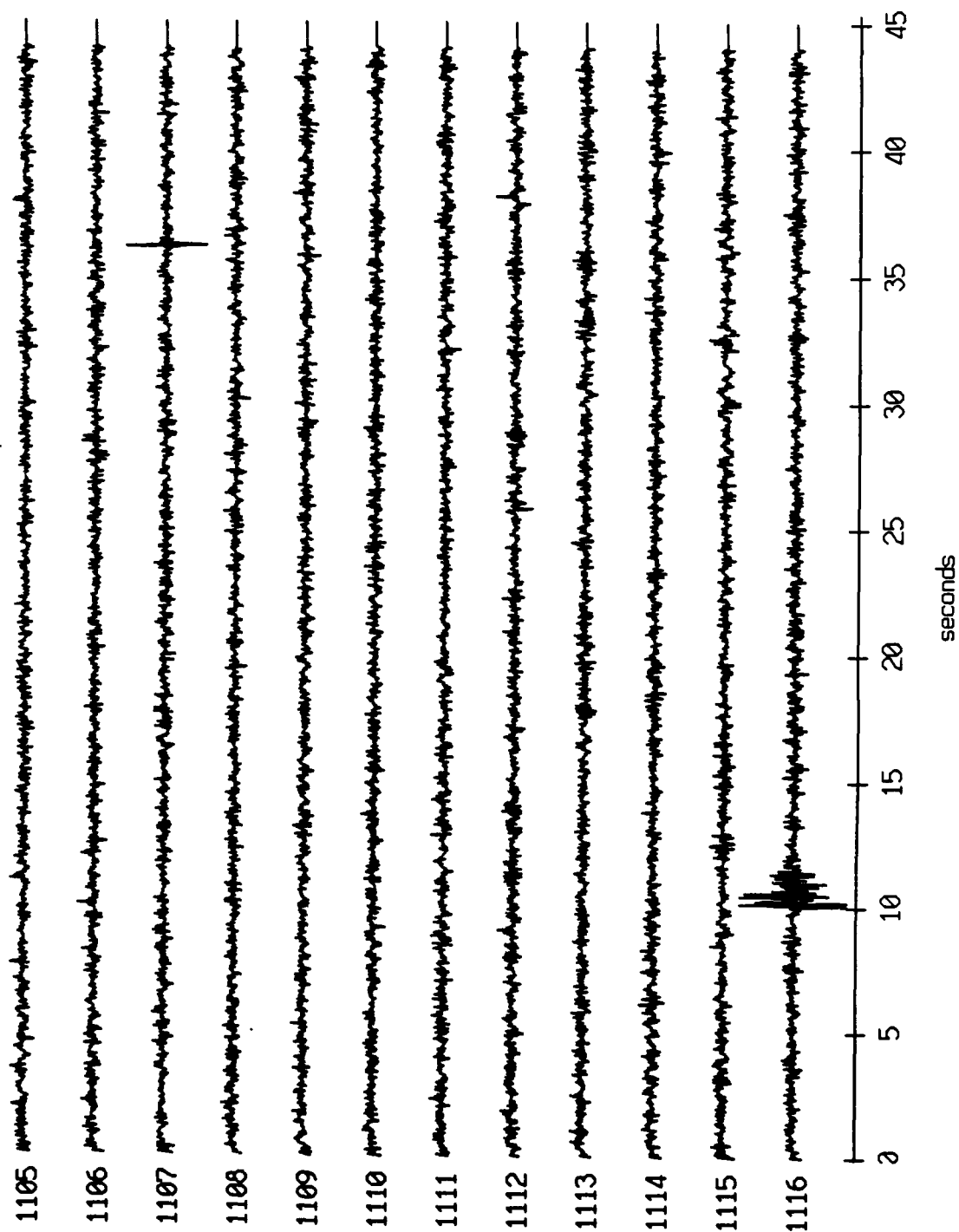
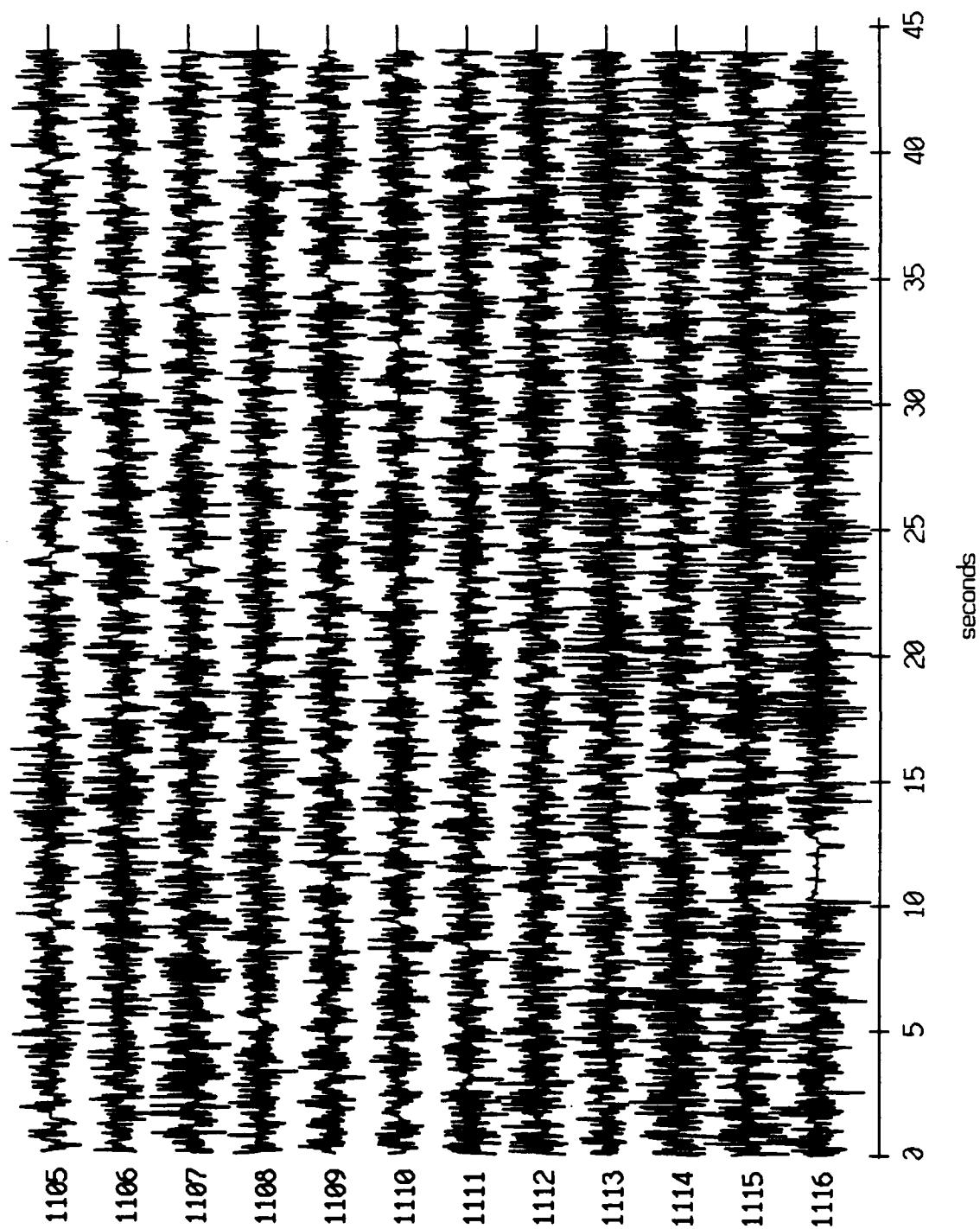


Figure XI.29c

Floot 0, July, 1989 Trip - records 1105-1116 (hydrophone)  
vertical axis scale is approx. -1.0 to 1.0 volts

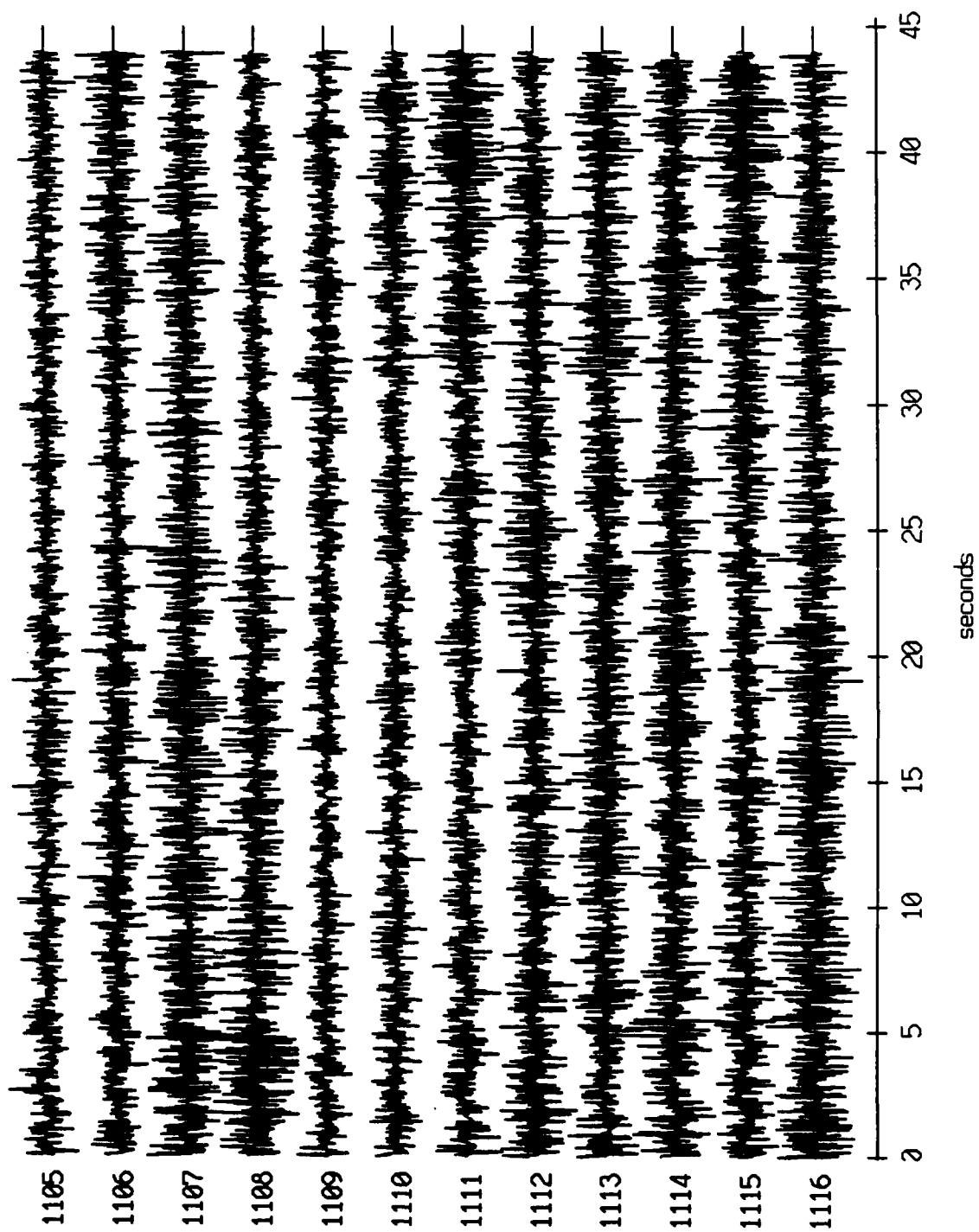


AGC corrected channel level (V)

Figure XI.29d



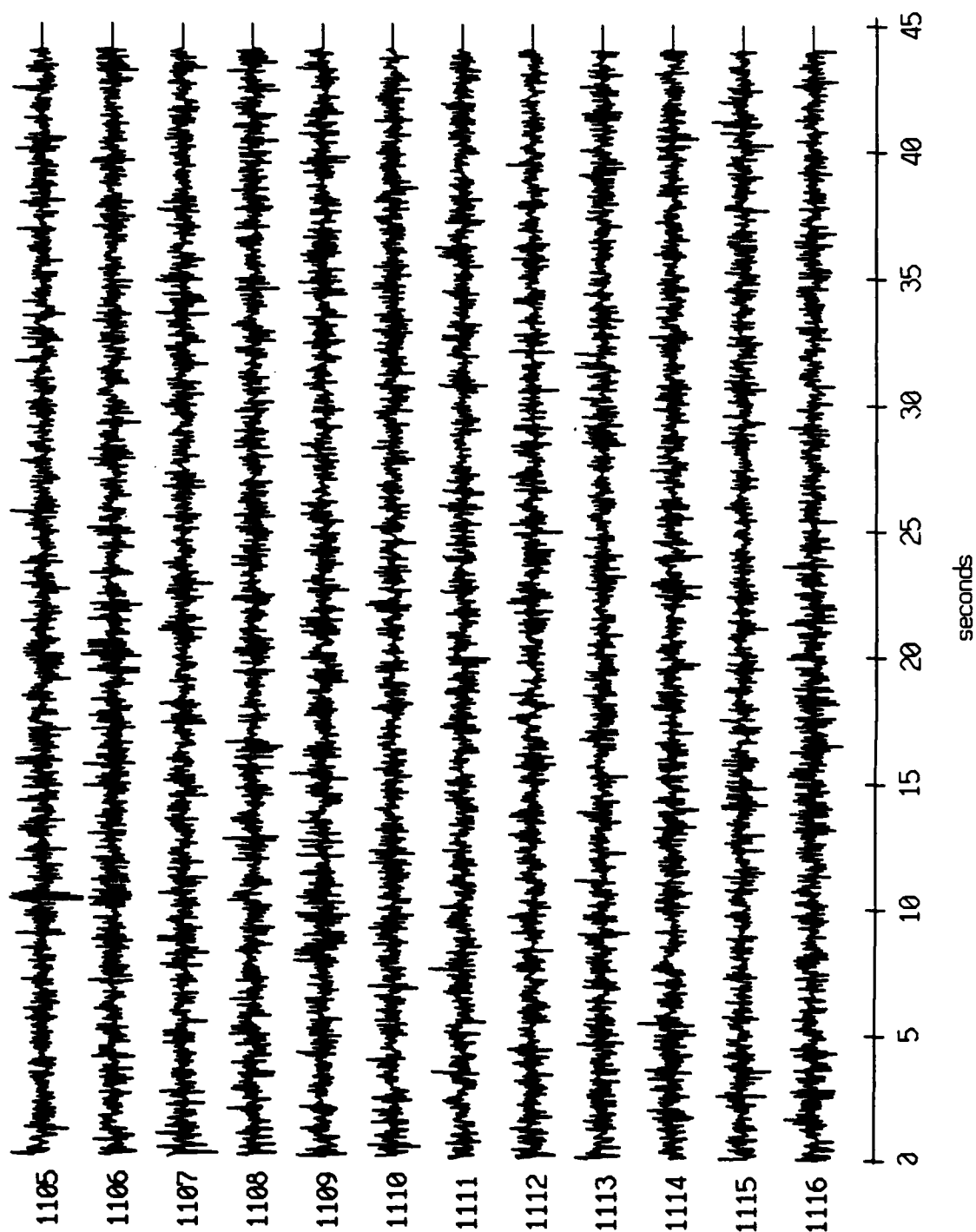
Float 1, July, 1989 Trip - records 1105-1116 (x-axis)  
vertical axis scale is approx. -1.0 to 1.0 volts



AGC corrected channel level (V)

Figure XI.30a

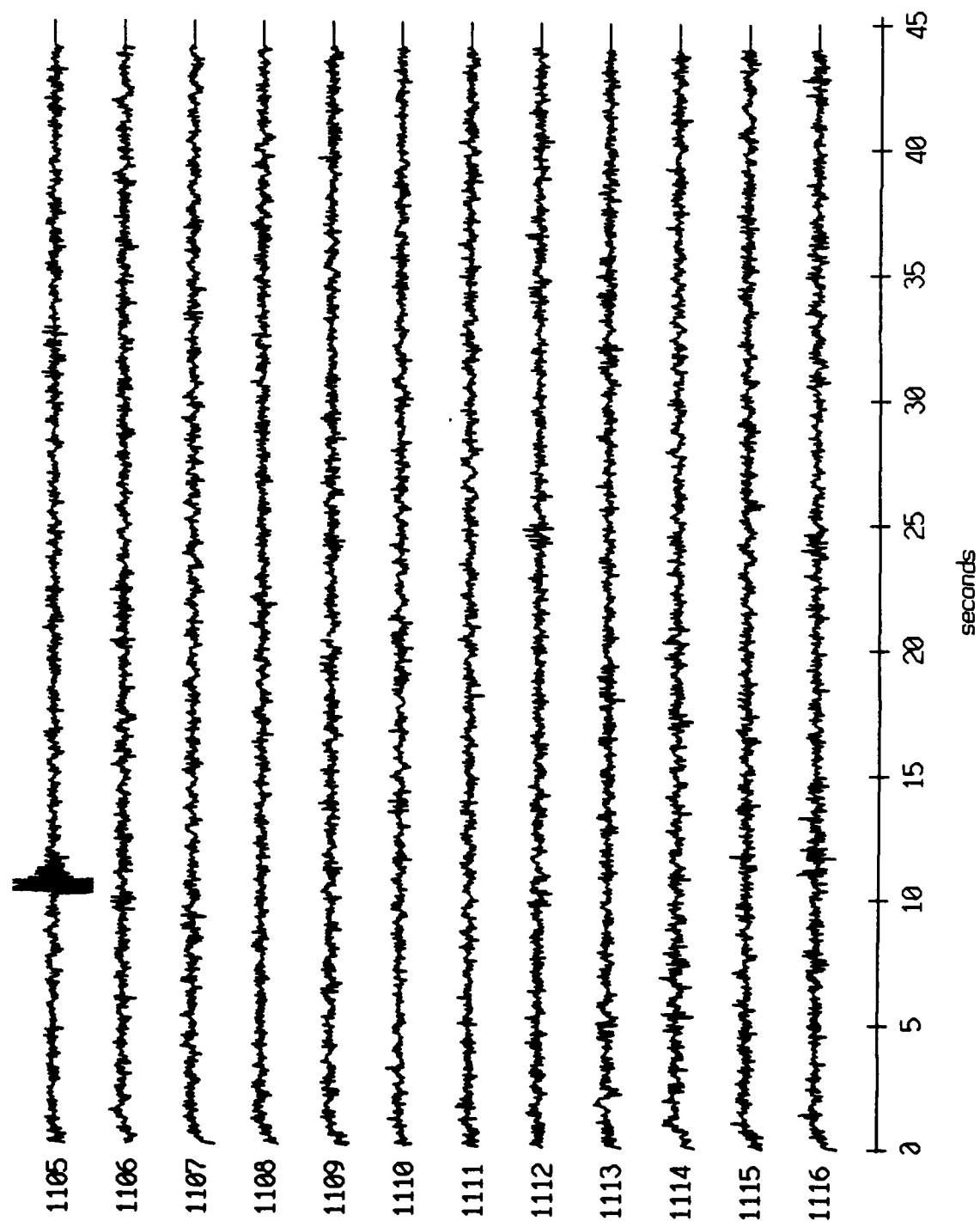
Float 1, July, 1989 Trip - records 1105-1116 (y-axis)  
vertical axis scale is approx. -1.0 to 1.0 volts



AGC corrected channel level (V)

Figure XI.30b

Floot 1, July, 1989 Trip - records 1105-1116 (z-axis)  
vertical axis scale is approx. -1.0 to 1.0 volts



PGC corrected channel level (V)

Figure XI.30c

Floot 1, July, 1989 Trip - records 1105-1116 (hydrophone)  
 vertical axis scale is approx. -1.0 to 1.0 volts

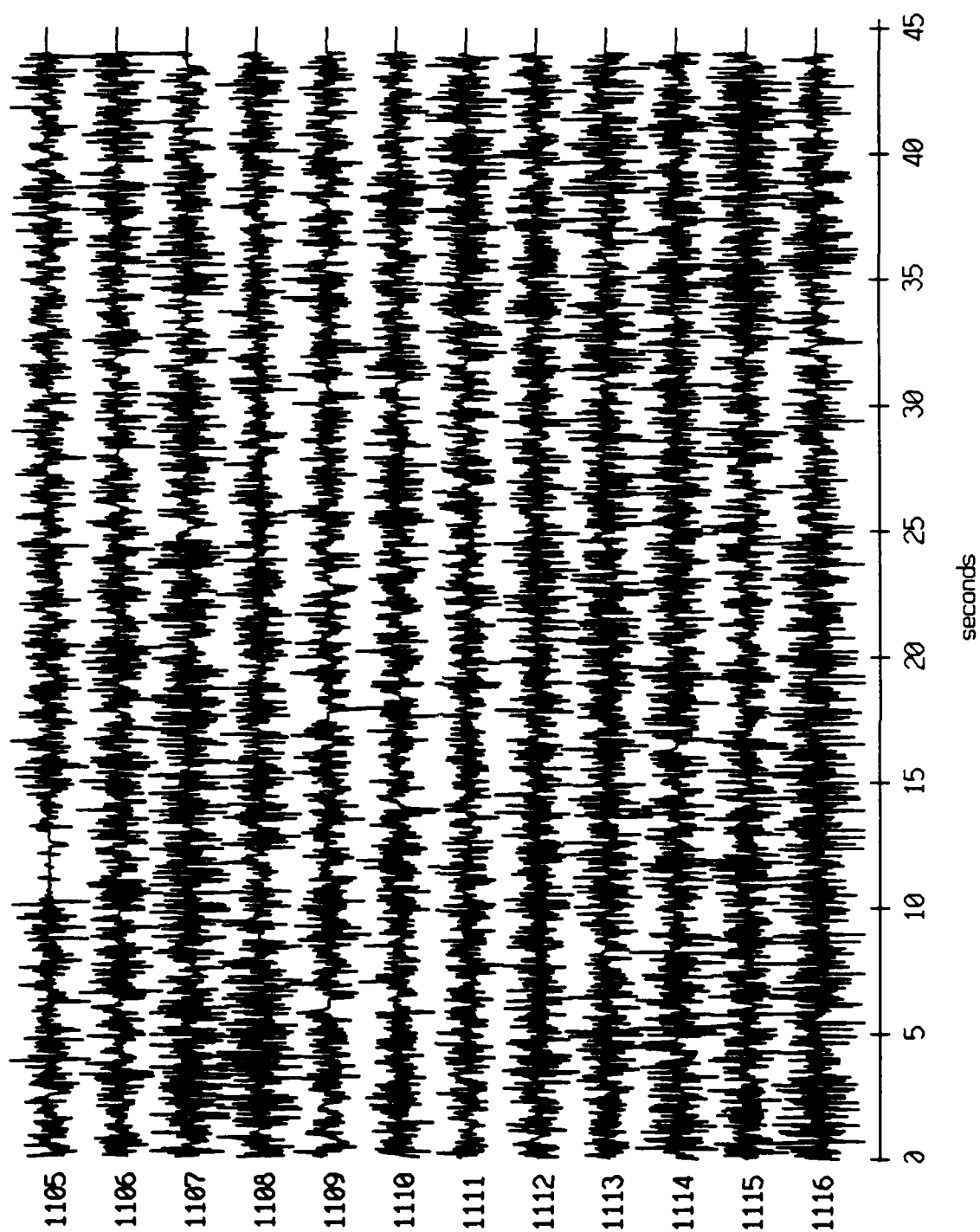
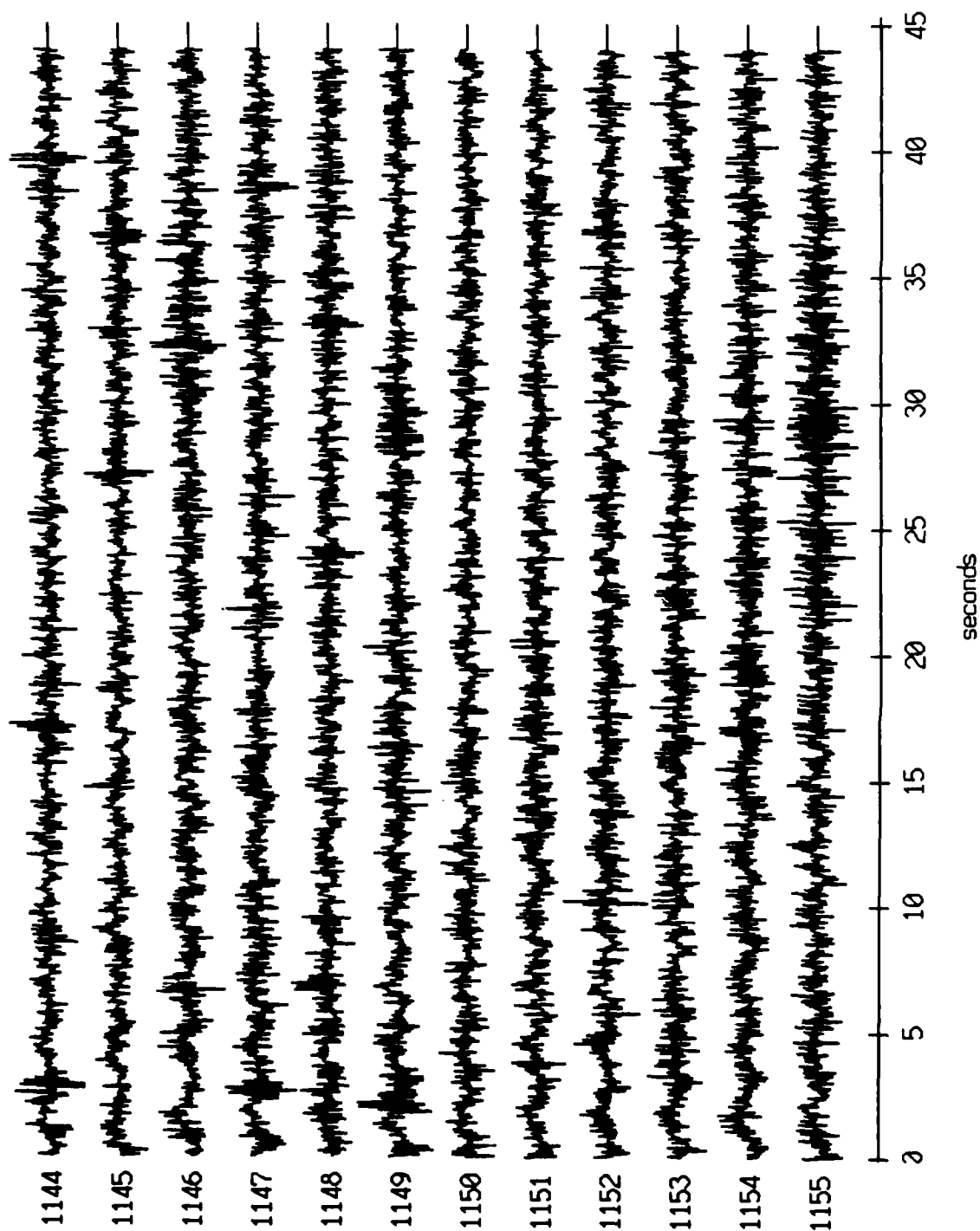


Figure XI.30d

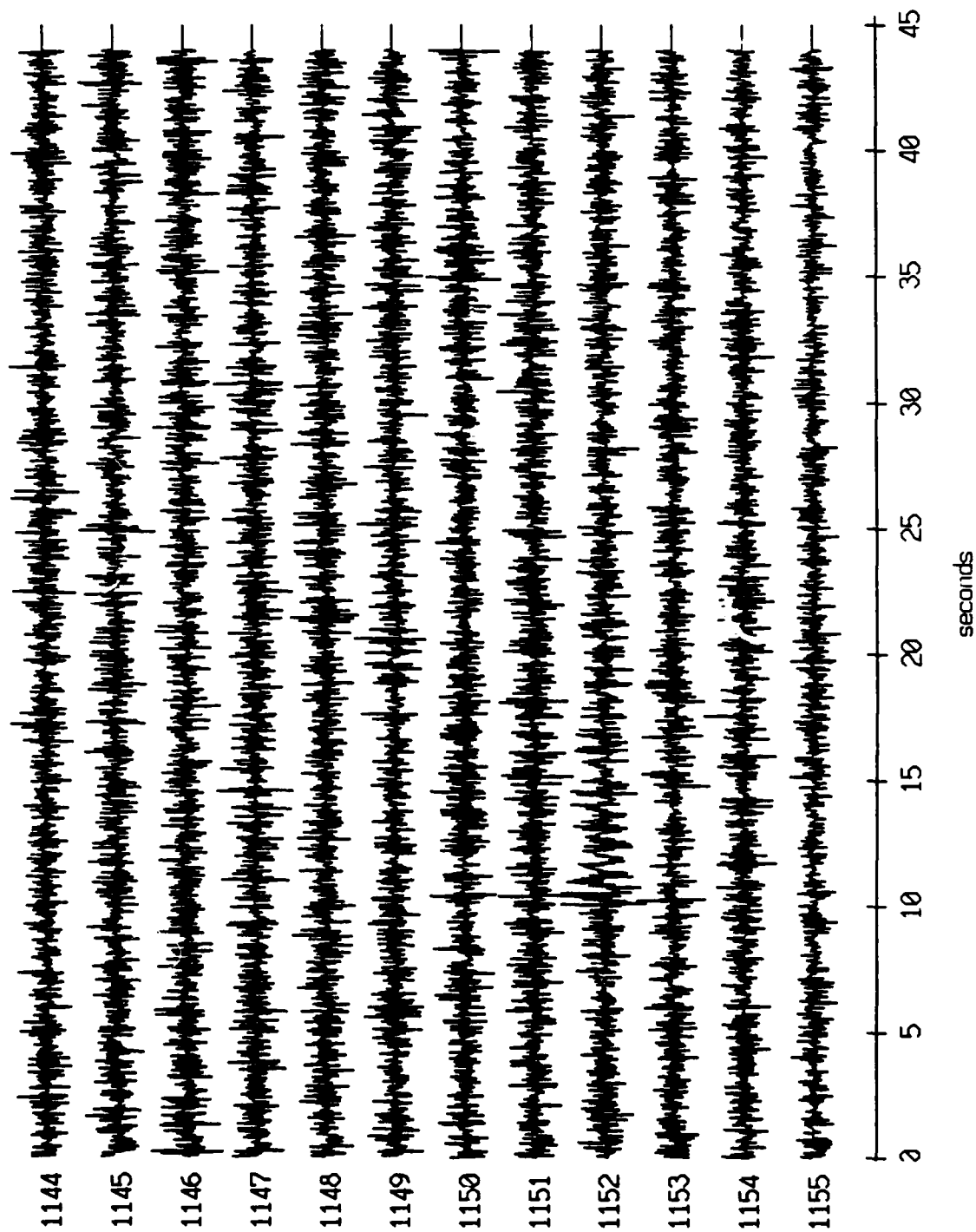
Floot 0, July, 1989 Trip - records 1144-1155 (x-axis)  
vertical axis scale is approx. -1.0 to 1.0 volts



RGC corrected channel level (V)

Figure XI.31a

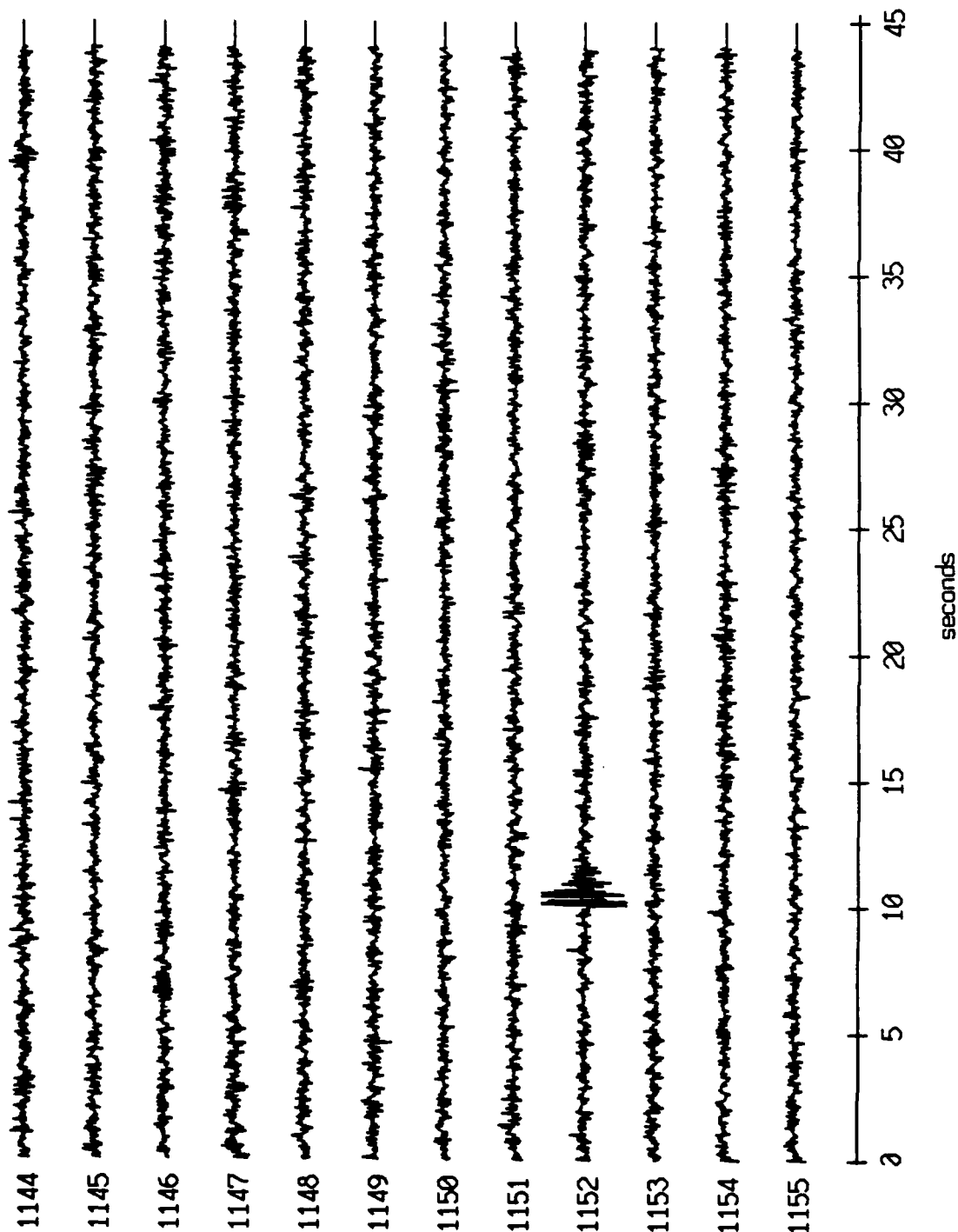
Float 0, July, 1989 Trip - records 1144-1155 (y-axis)  
vertical axis scale is approx. -1.0 to 1.0 volts



PGC corrected channel level (V)

Figure XI.31b

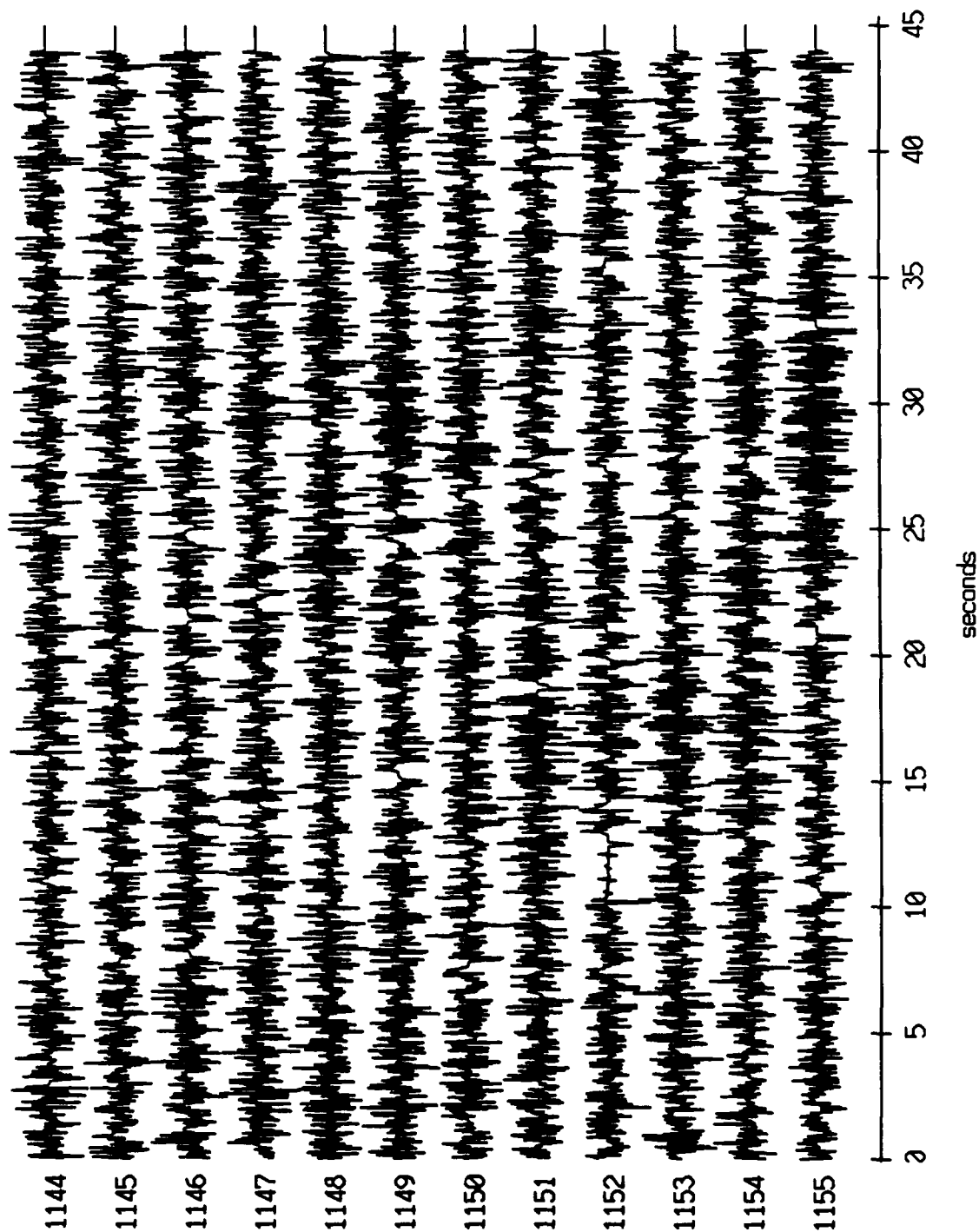
Float 0, July, 1989 Trip - records 1144-1155 (z-axis)  
vertical axis scale is approx. -1.0 to 1.0 volts



AGC corrected channel level (V)

Figure XI.31c

Float 0, July, 1989 Trip - records 1144-1155 (hydrophone)  
vertical axis scale is approx. -1.0 to 1.0 volts

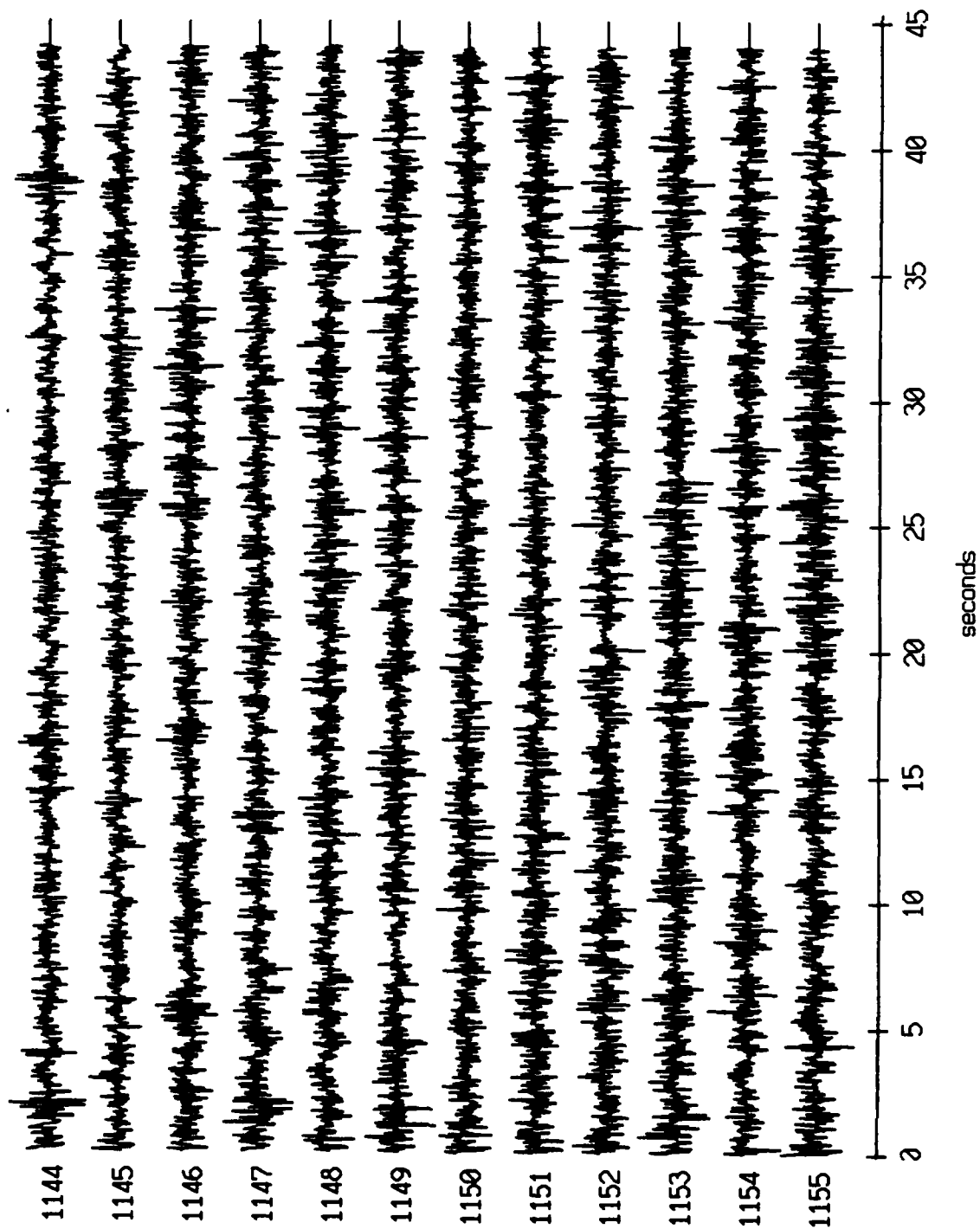


AGC corrected channel level (V)

Figure XI.31d



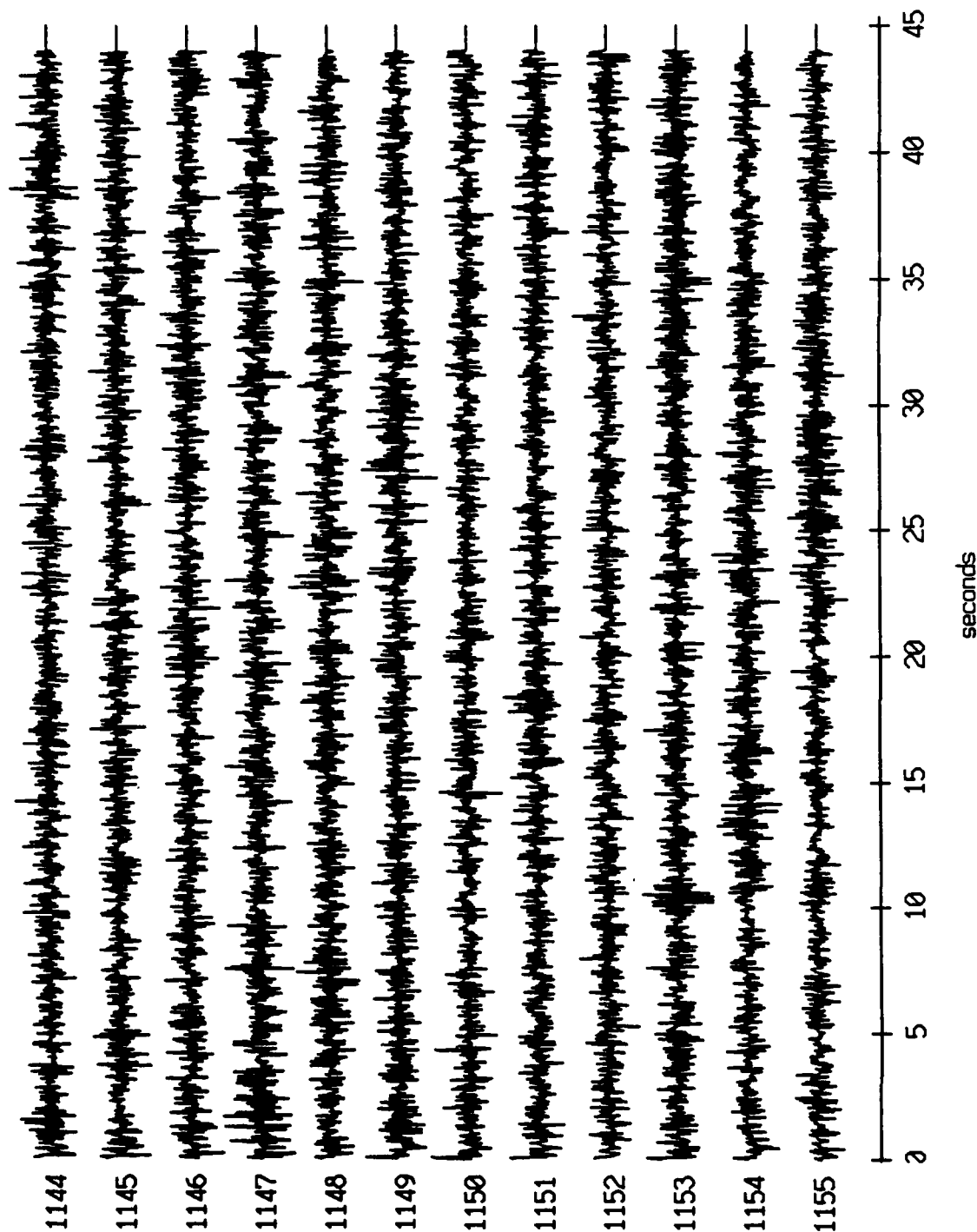
Float 1, July, 1989 Trip - records 1144-1155 (x-axis)  
vertical axis scale is approx. -1.0 to 1.0 volts



AGC corrected channel level (V)

Figure XI.32a

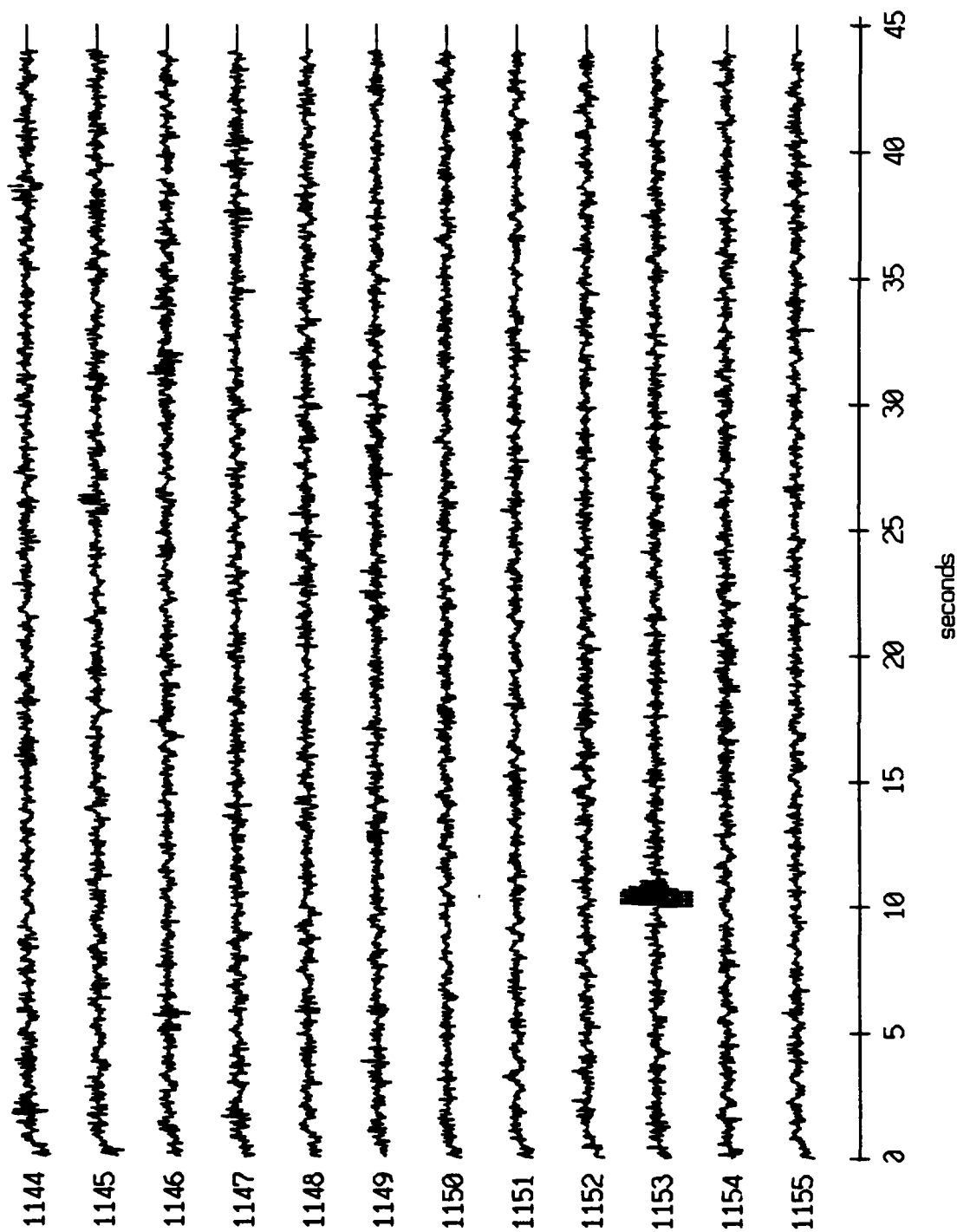
Floot 1, July, 1989 Trip - records 1144-1155 (y-axis)  
vertical axis scale is approx. -1.0 to 1.0 volts



RGC corrected channel level (V)

Figure XI.32b

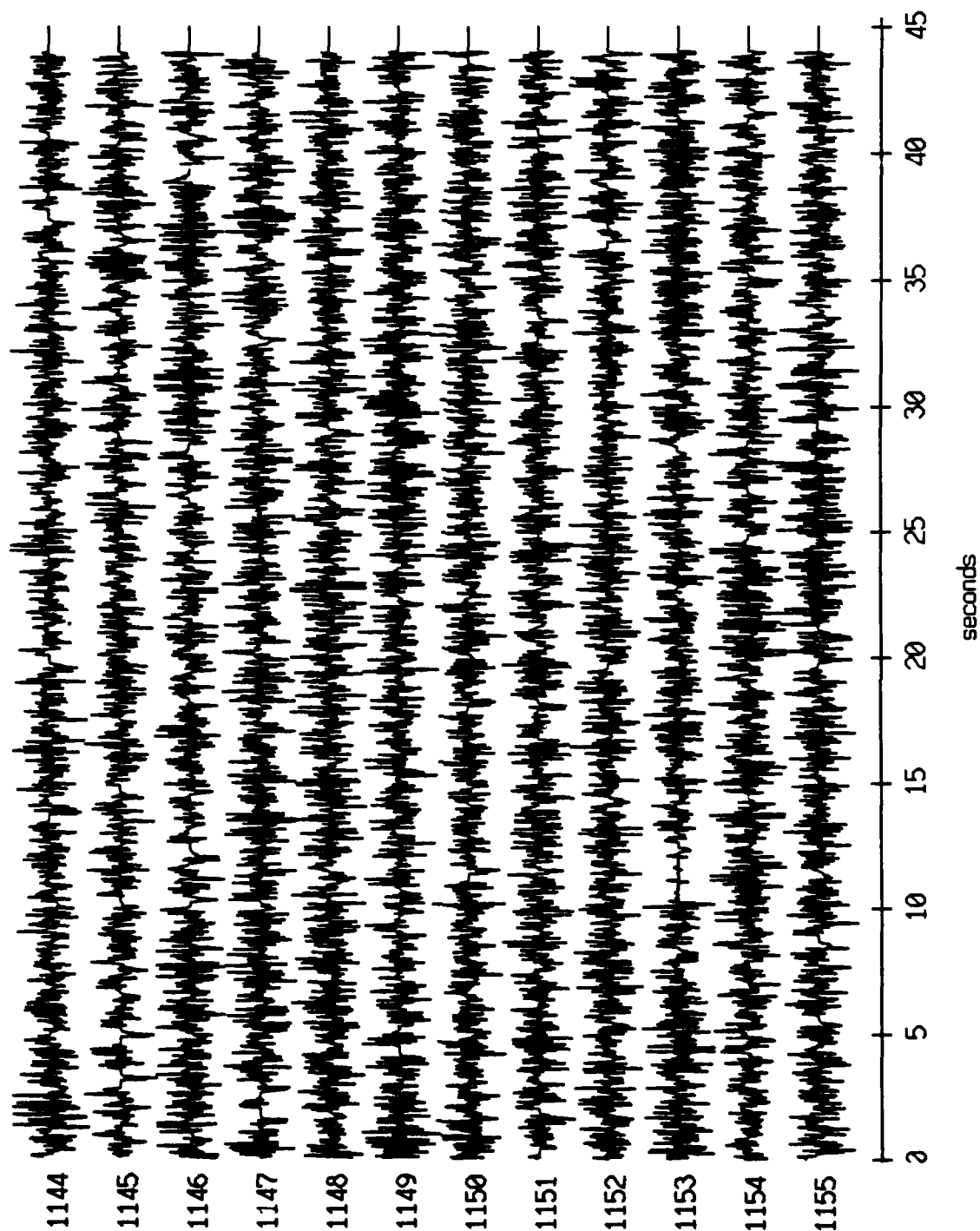
Floot 1, July, 1989 Trip - records 1144-1155 (z-axis)  
vertical axis scale is approx. -1.0 to 1.0 volts



AGC corrected channel level (V)

Figure XI.32c

Float 1, July, 1989 Trip - records 1144-1155 (hydrophone)  
vertical axis scale is approx. -1.0 to 1.0 volts



AGC corrected channel level (V)

Figure XI.32d

Float 2, July, 1989 Trip - records 1144-1155 (x-axis)  
vertical axis scale is approx. -1.0 to 1.0 volts

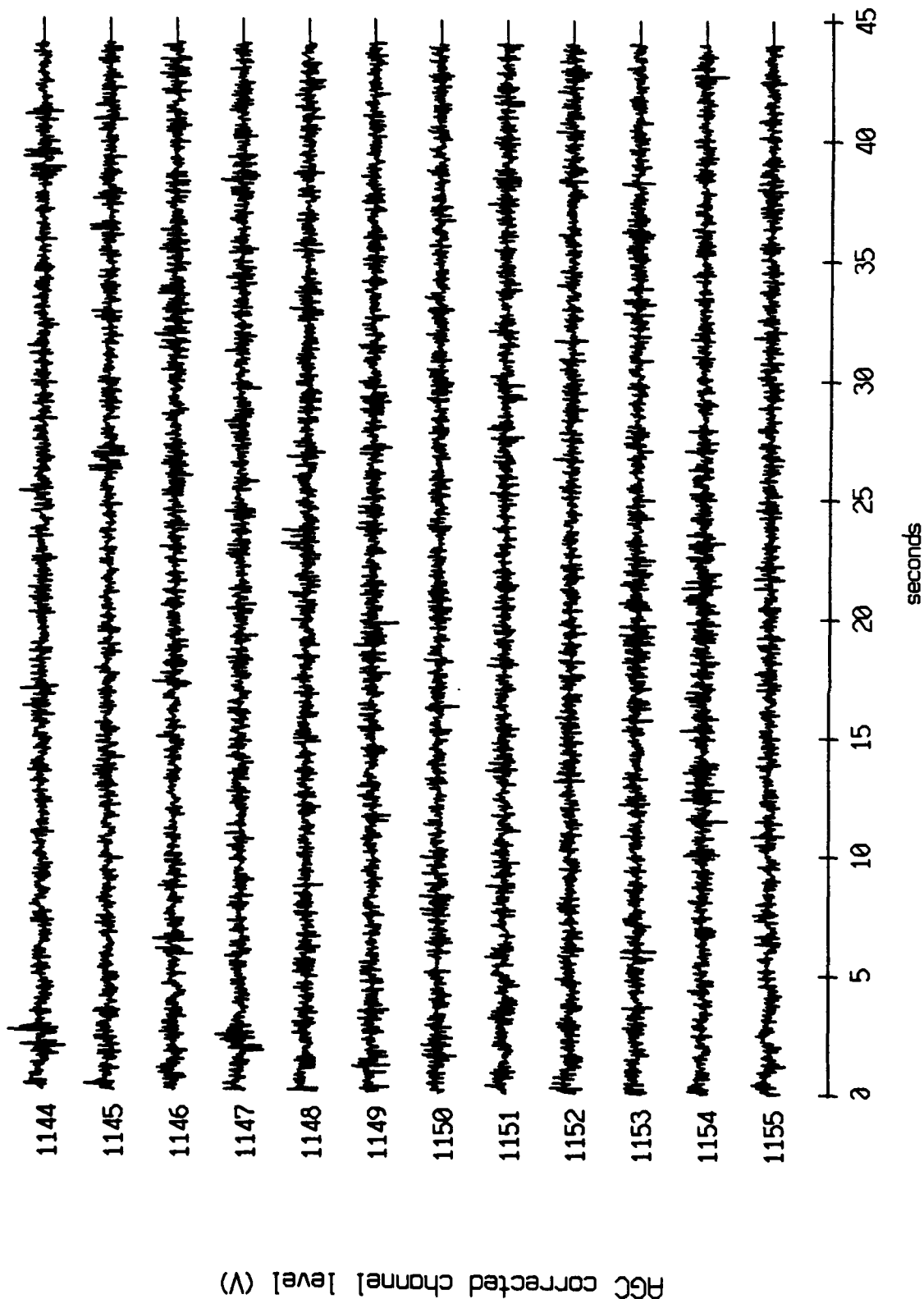
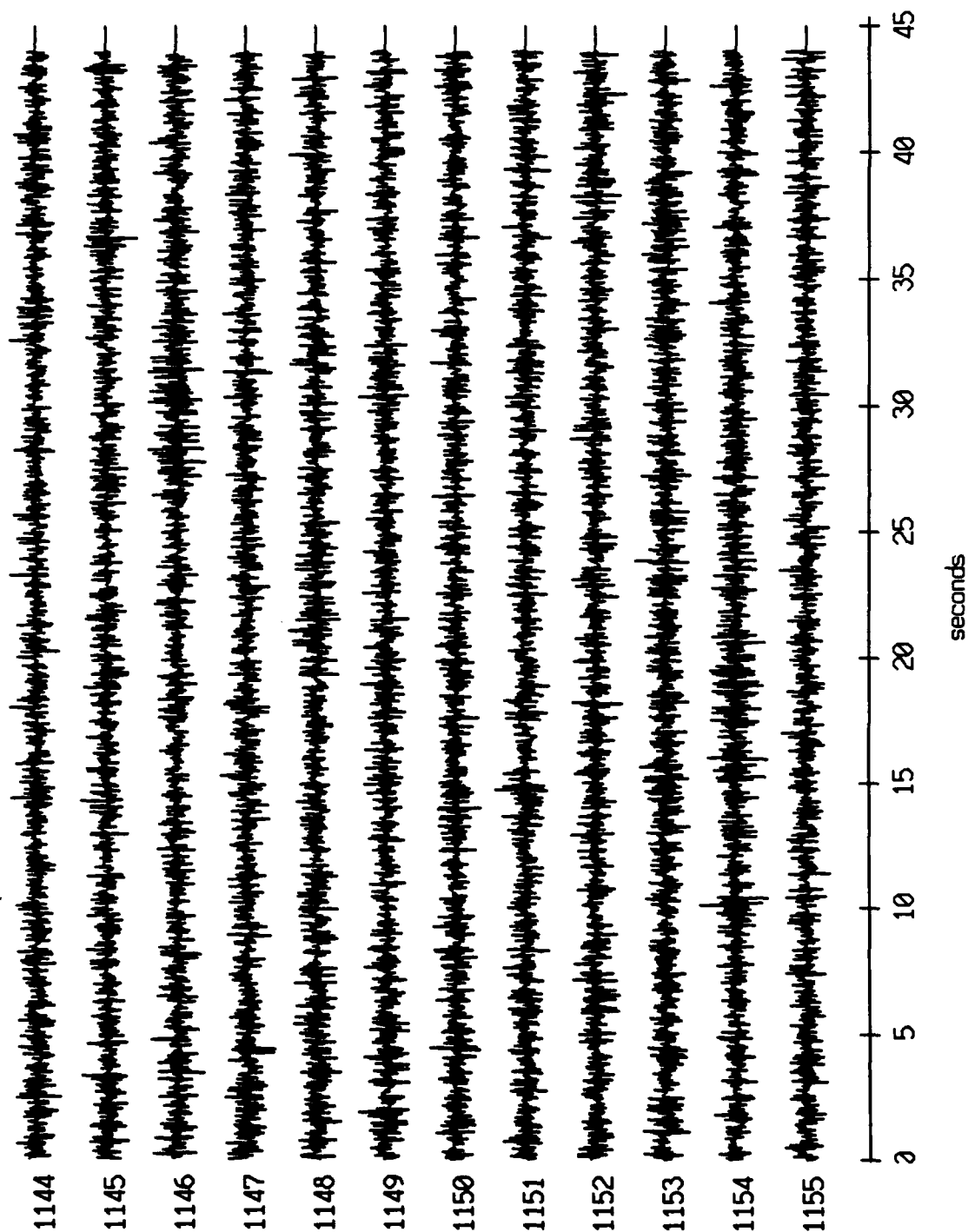


Figure XI.33a

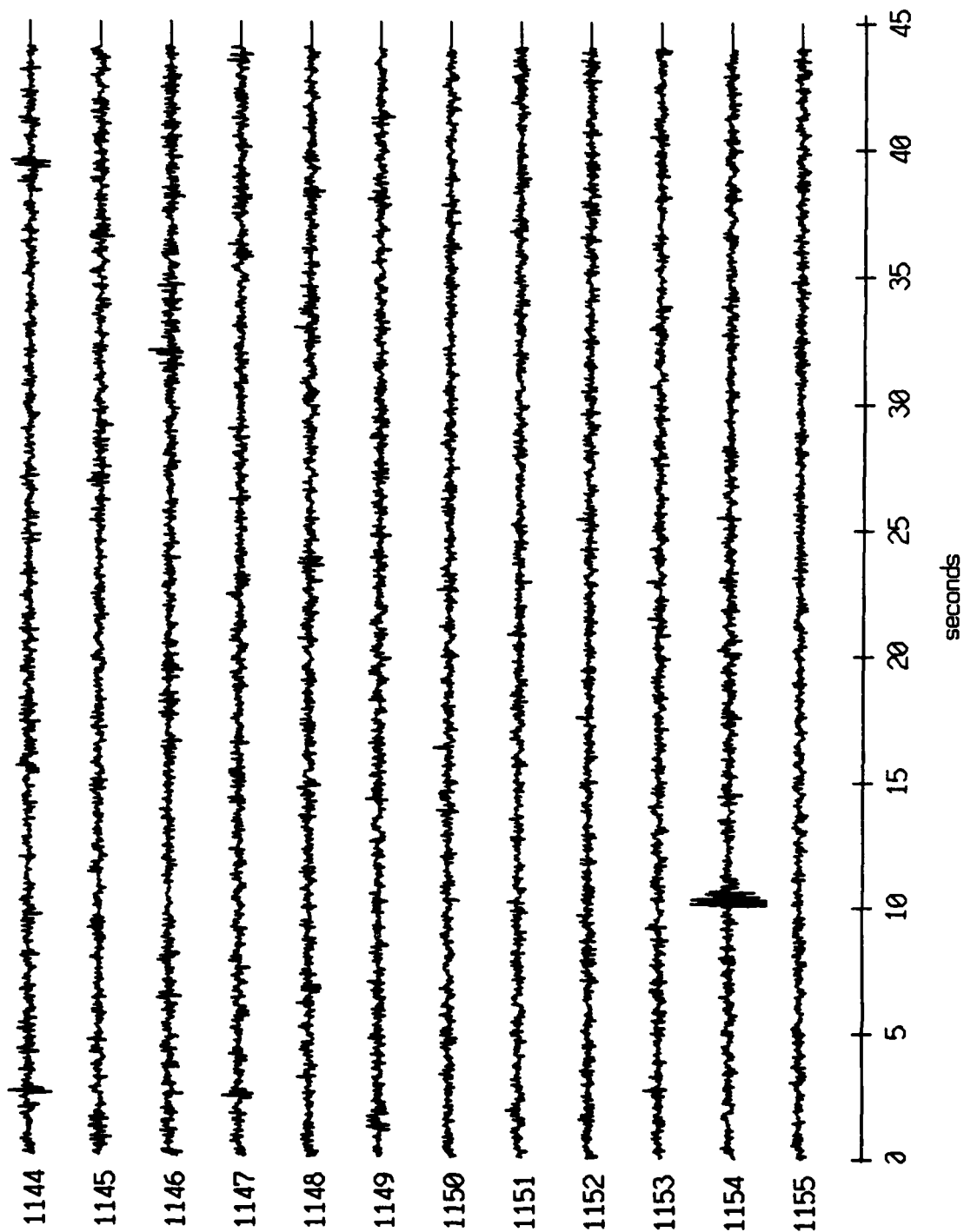
Float 2, July, 1989 Trip - records 1144-1155 (y-axis)  
vertical axis scale is approx. -1.0 to 1.0 volts



RGC corrected channel level (V)

Figure XI.33b

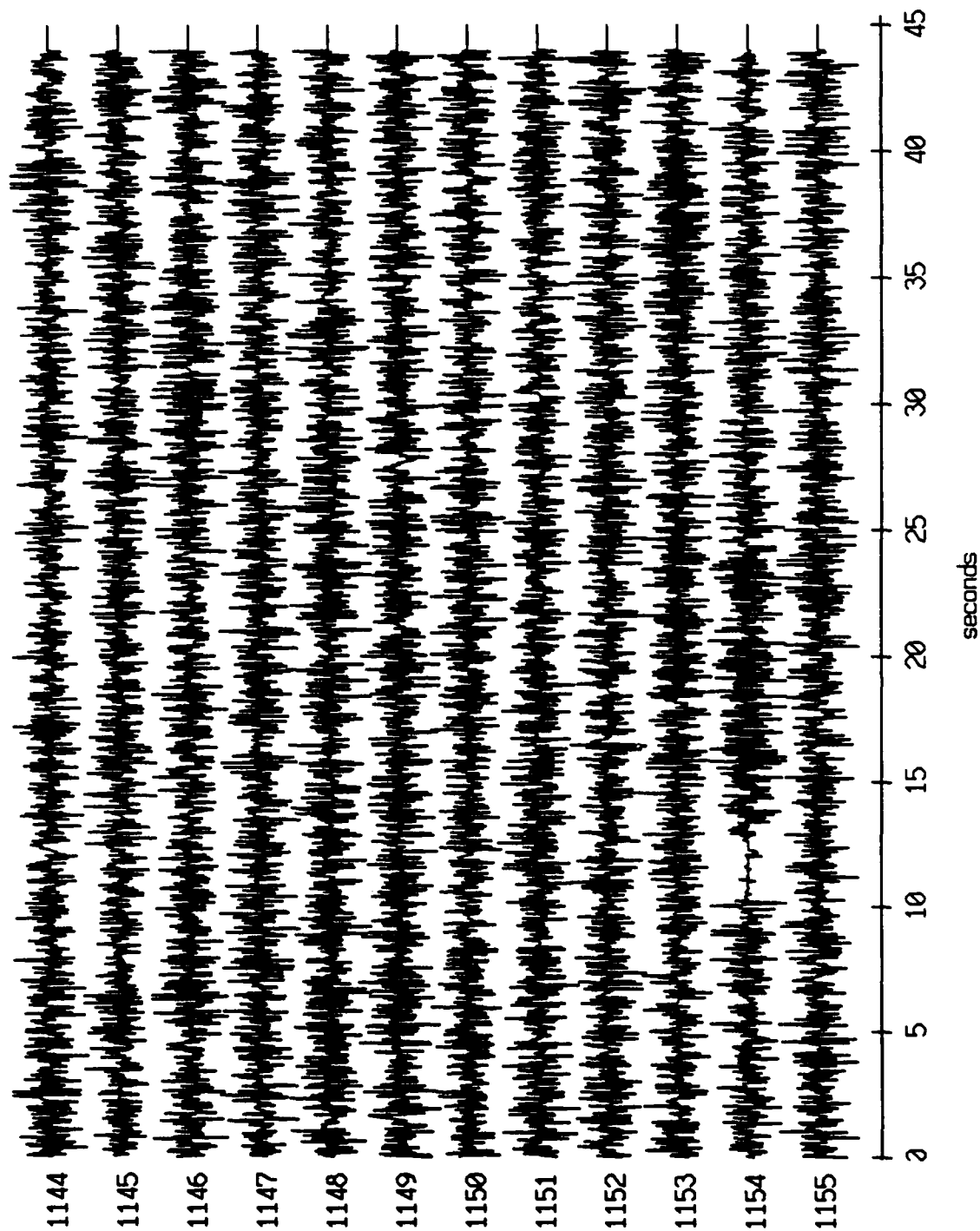
Floot 2, July, 1989 Trip - records 1144-1155 (z-axis)  
vertical axis scale is approx. -1.0 to 1.0 volts



AGC corrected channel level (V)

Figure XI.33c

Float 2, July, 1989 Trip - records 1144-1155 (hydrophone)  
vertical axis scale is approx. -1.0 to 1.0 volts



AGC corrected channel level (V)

Figure XI.33d



Float 3, July, 1989 Trip - records 1144-1155 (x-axis)  
vertical axis scale is approx. -1.0 to 1.0 volts

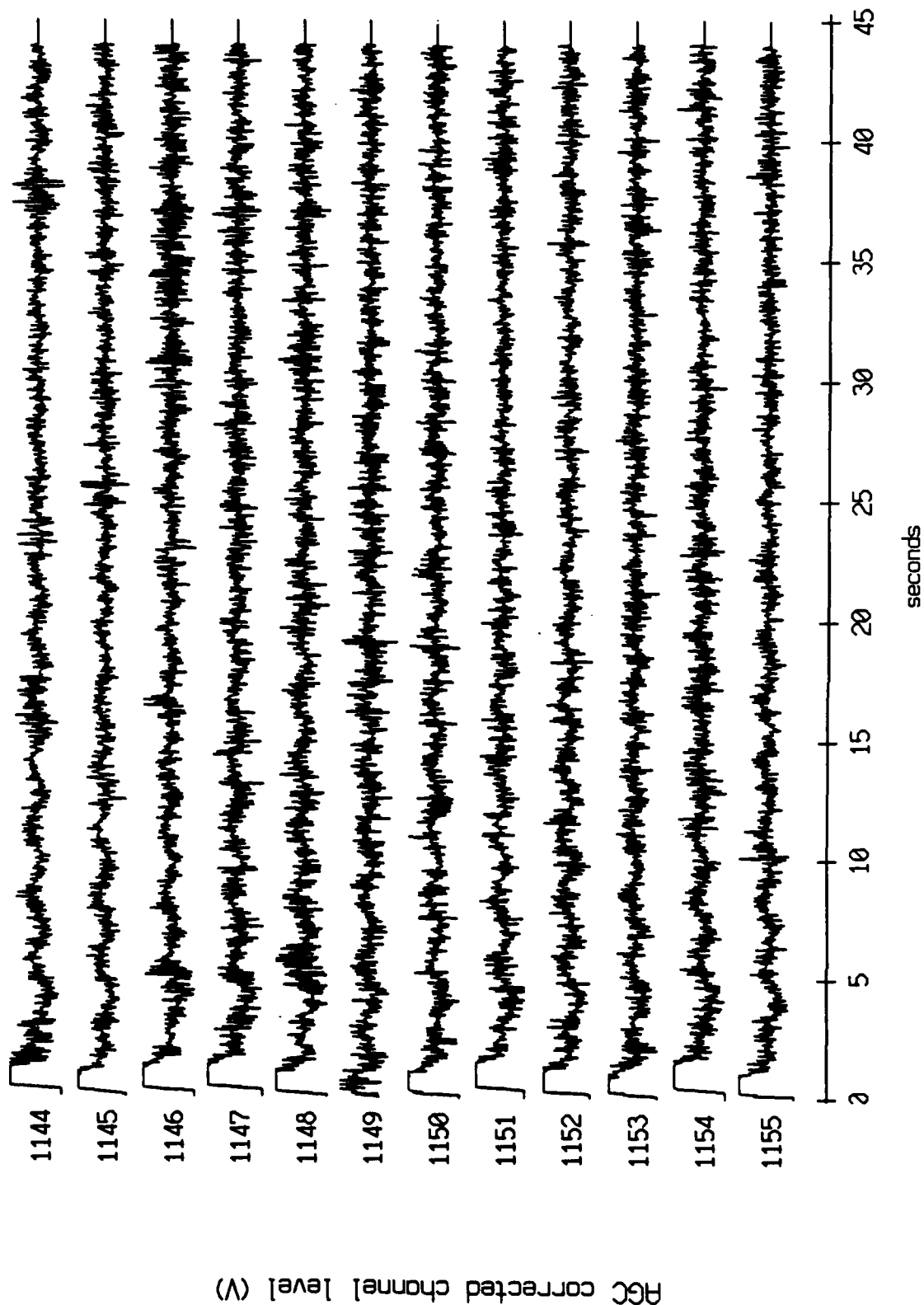


Figure XI.34a

Float 3, July, 1989 Trip - records 1144-1155 (y-axis)  
vertical axis scale is approx. -1.0 to 1.0 volts

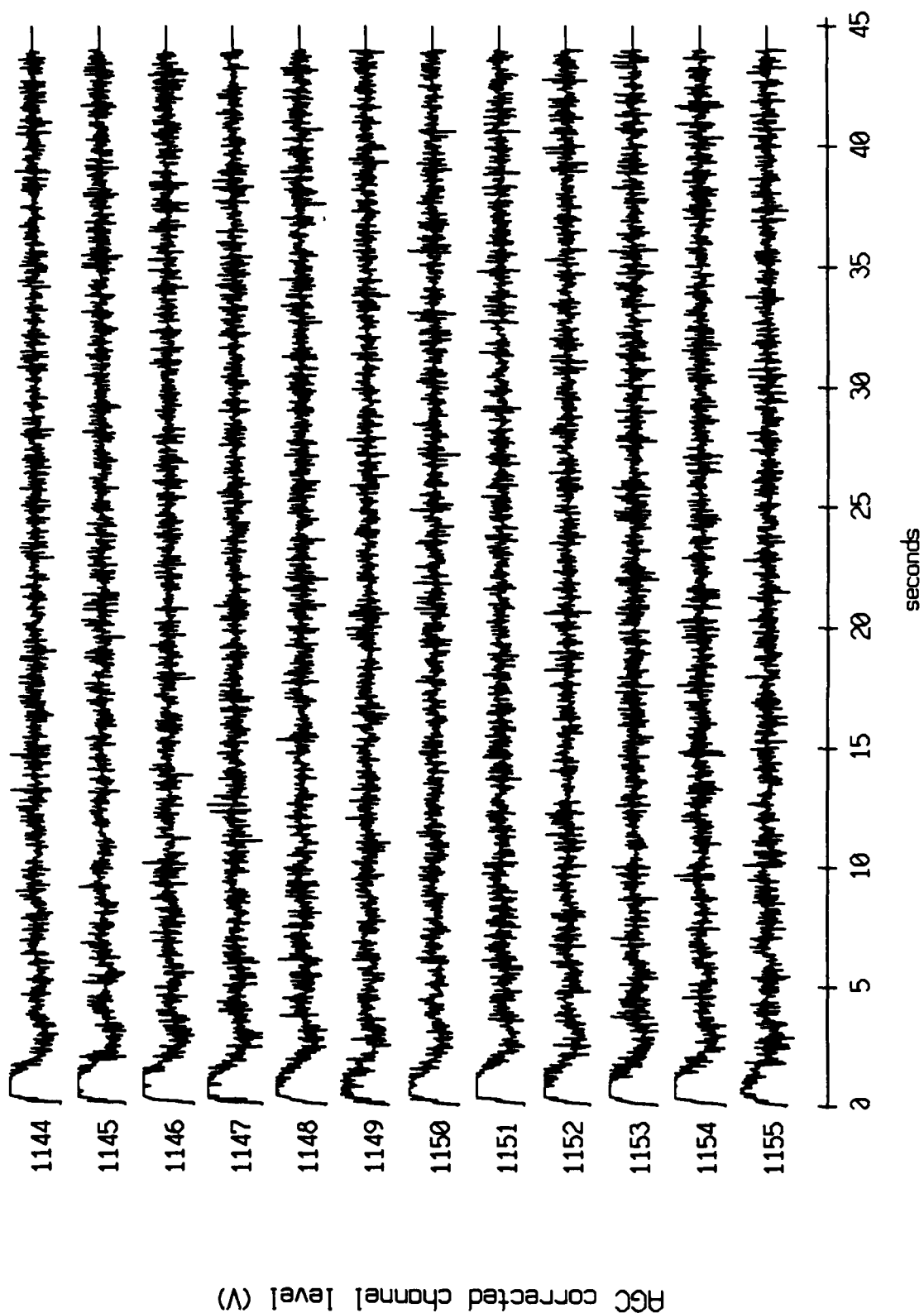


Figure XI.34b

Float 3, July, 1989 Trip - records 1144-1155 (z-axis)  
vertical axis scale is approx. -1.0 to 1.0 volts

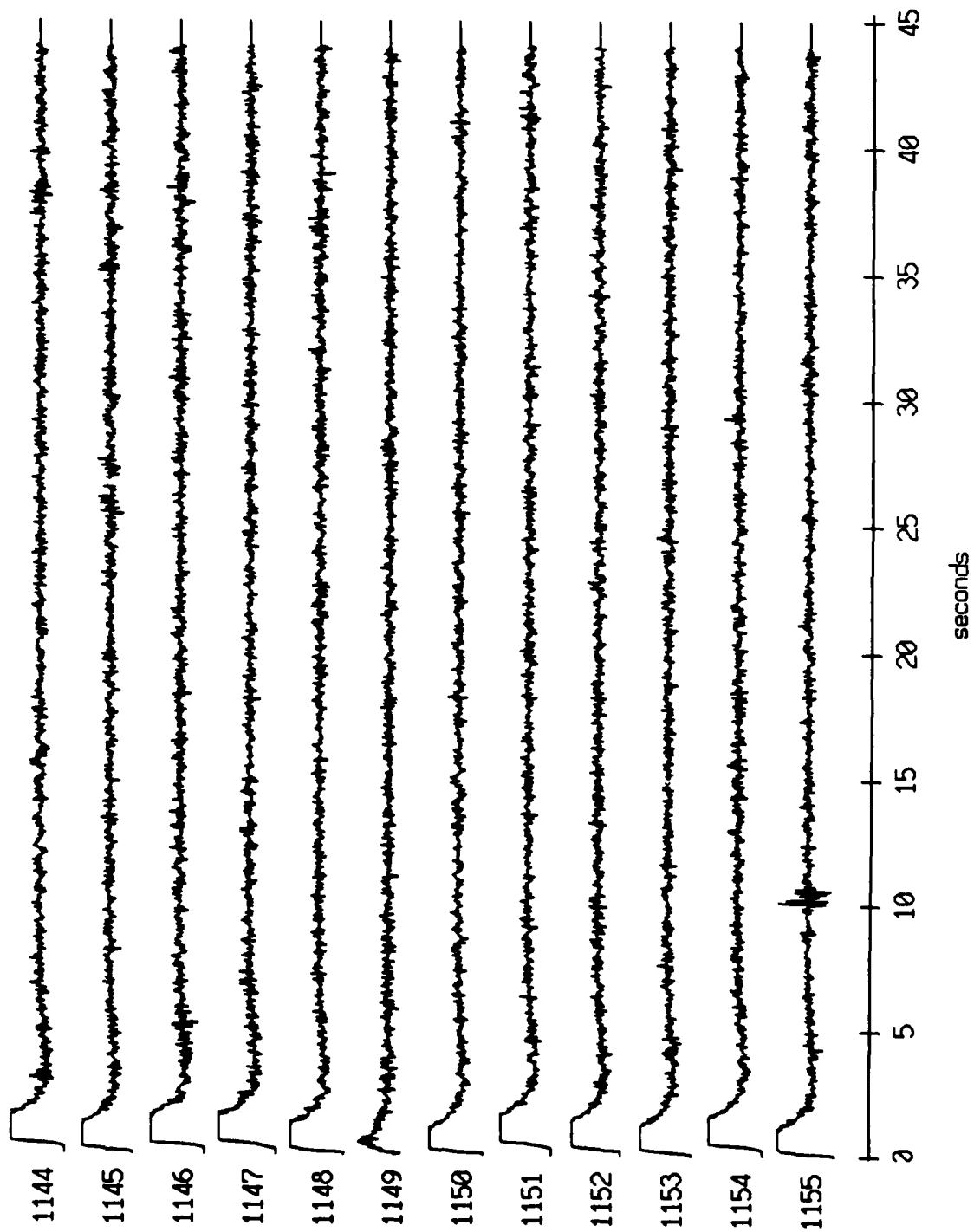
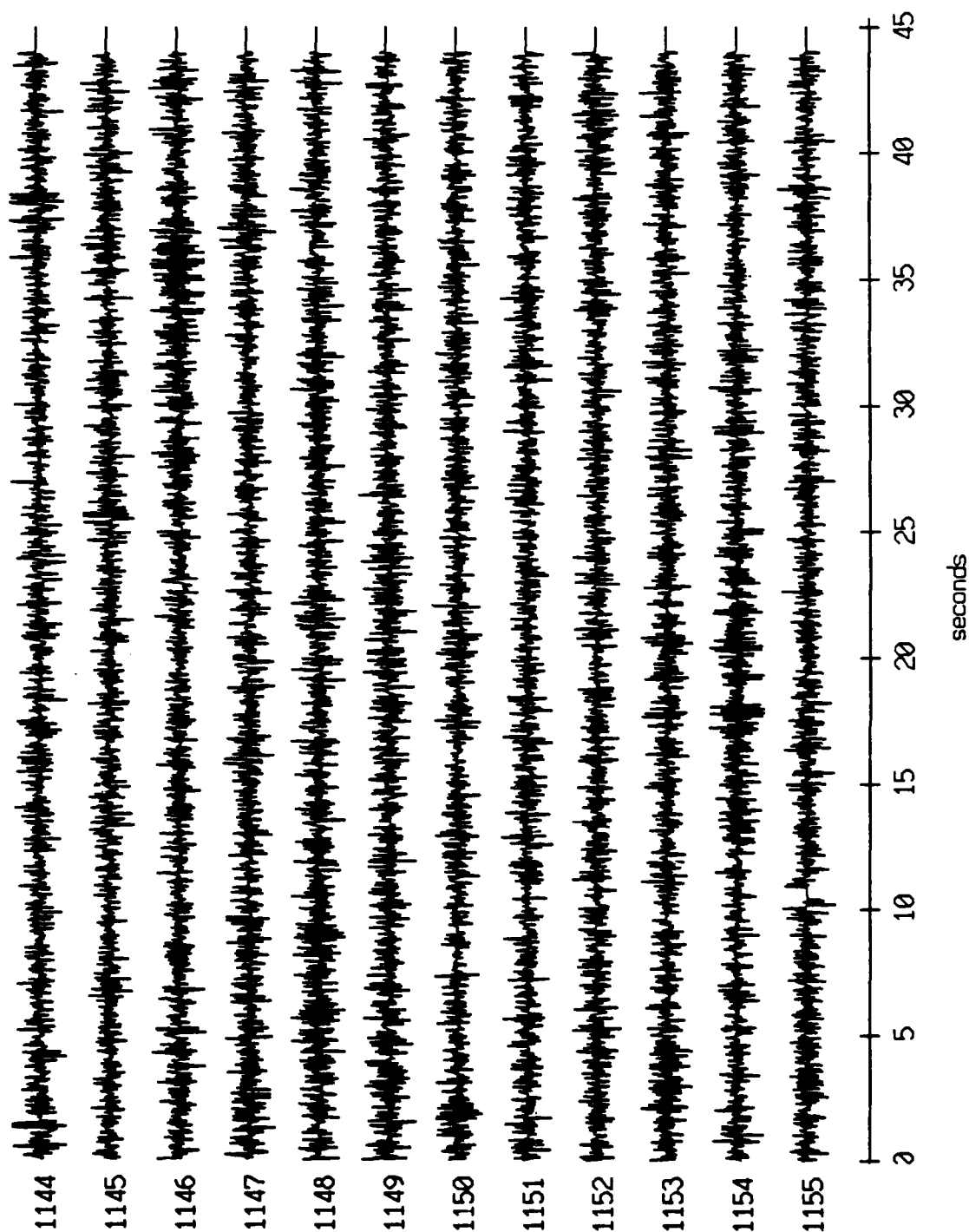


Figure XI.34c

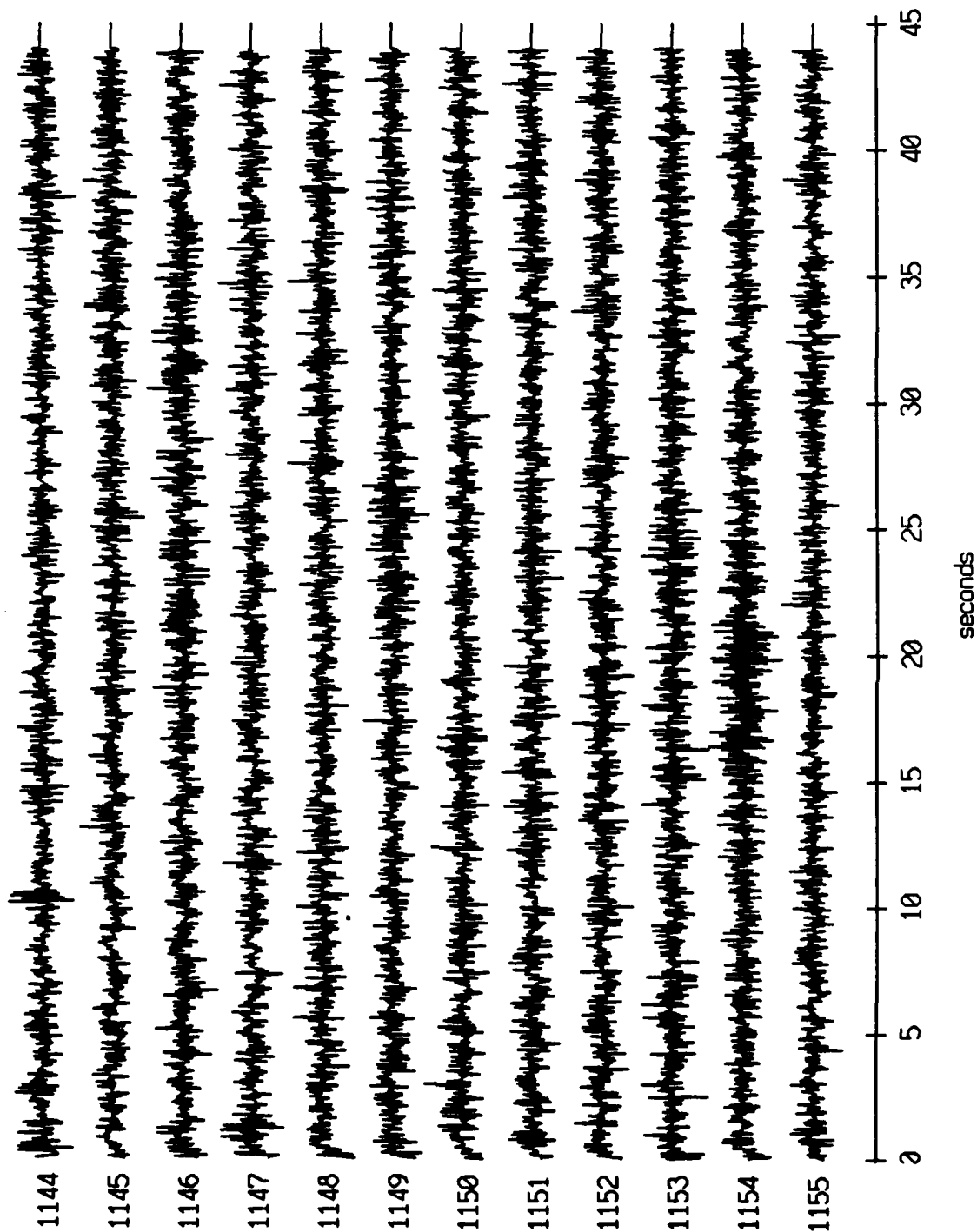
Float 3, July, 1989 Trip - records 1144-1155 (hydrophone)  
vertical axis scale is approx. -1.0 to 1.0 volts



AGC corrected channel level (V)

Figure XI.34d

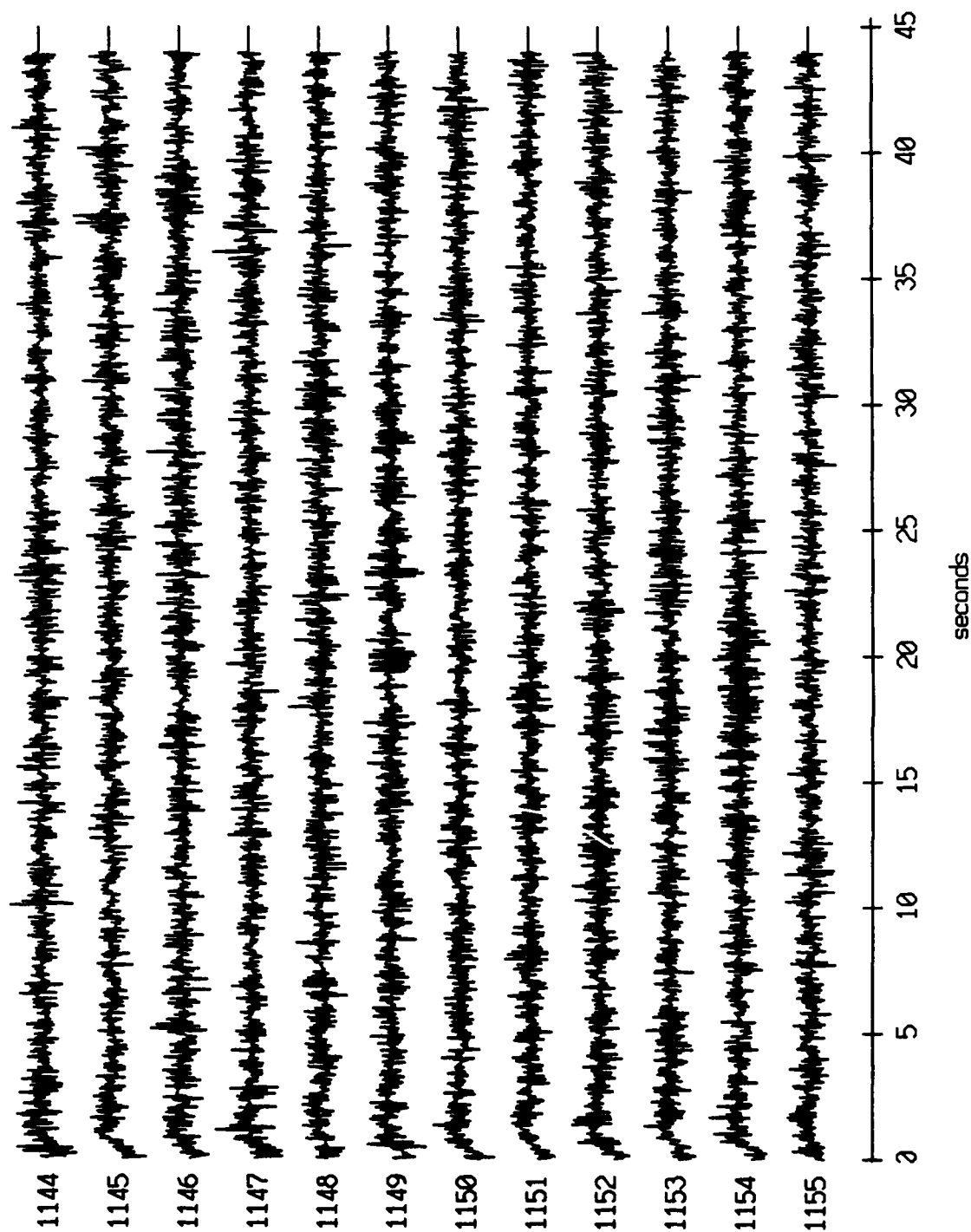
Floot 4, July, 1989 Trip - records 1144-1155 (x-axis)  
vertical axis scale is approx. -1.0 to 1.0 volts



PGC corrected channel level (V)

Figure XI.35a

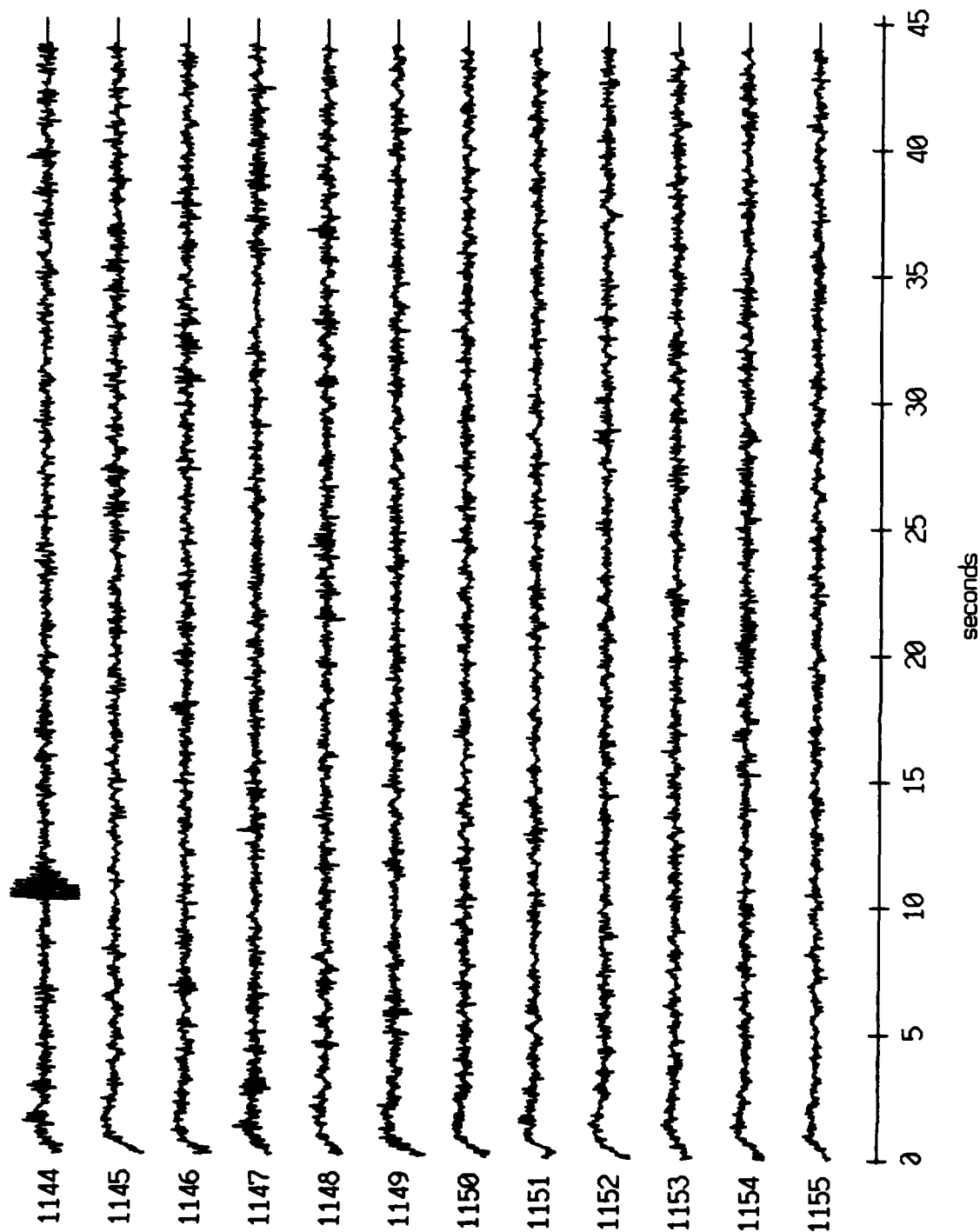
Floot 4, July, 1989 Trip - records 1144-1155 (y-axis)  
vertical axis scale is approx. -1.0 to 1.0 volts



AGC corrected channel level (V)

Figure XI.35b

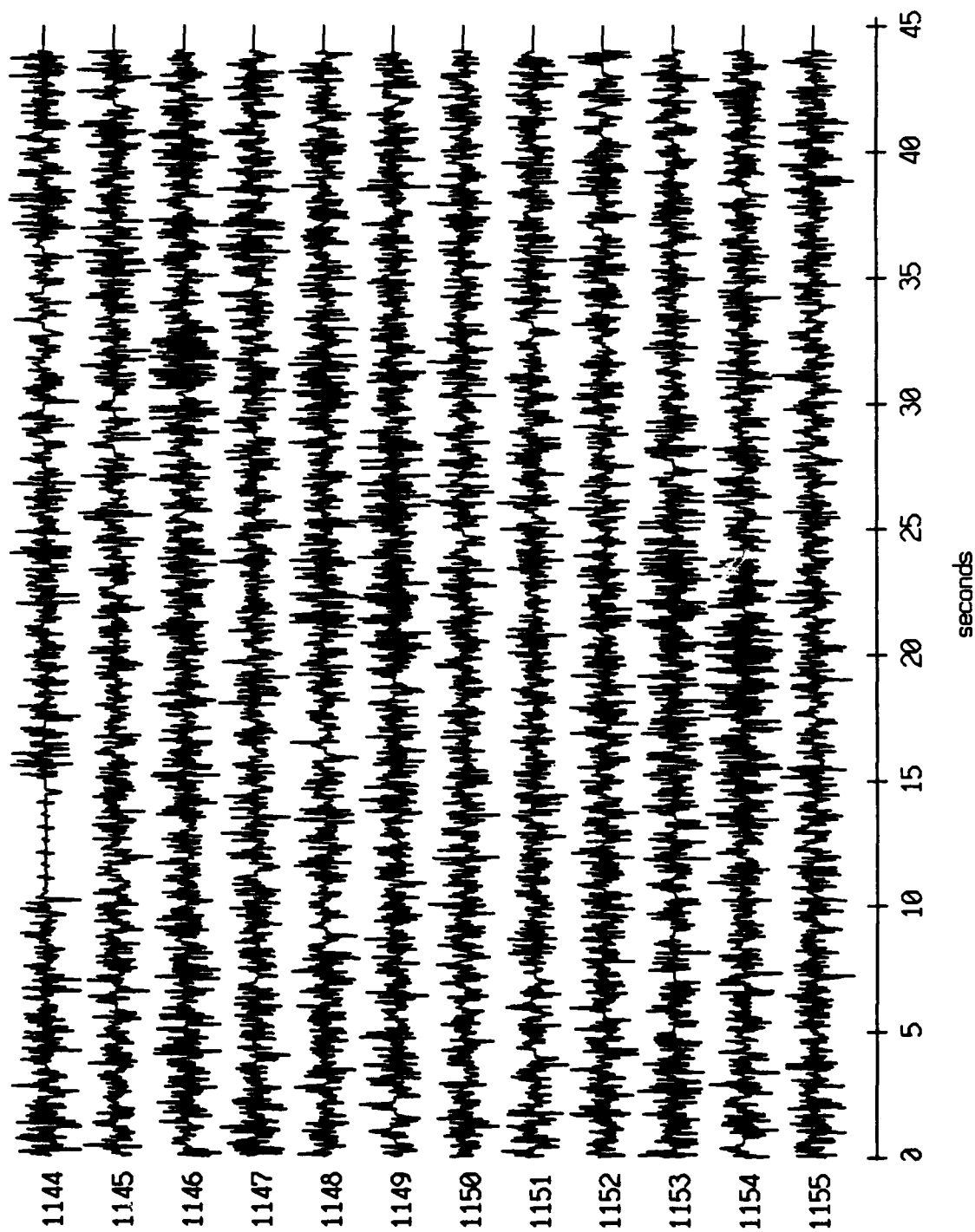
Floot 4, July, 1989 Trip - records 1144-1155 (z-axis)  
vertical axis scale is approx. -1.0 to 1.0 volts



PGC corrected channel level (V)

Figure XI.35c

Floot 4, July, 1989 Trip - records 1144-1155 (hydrophone)  
vertical axis scale is approx. -1.0 to 1.0 volts

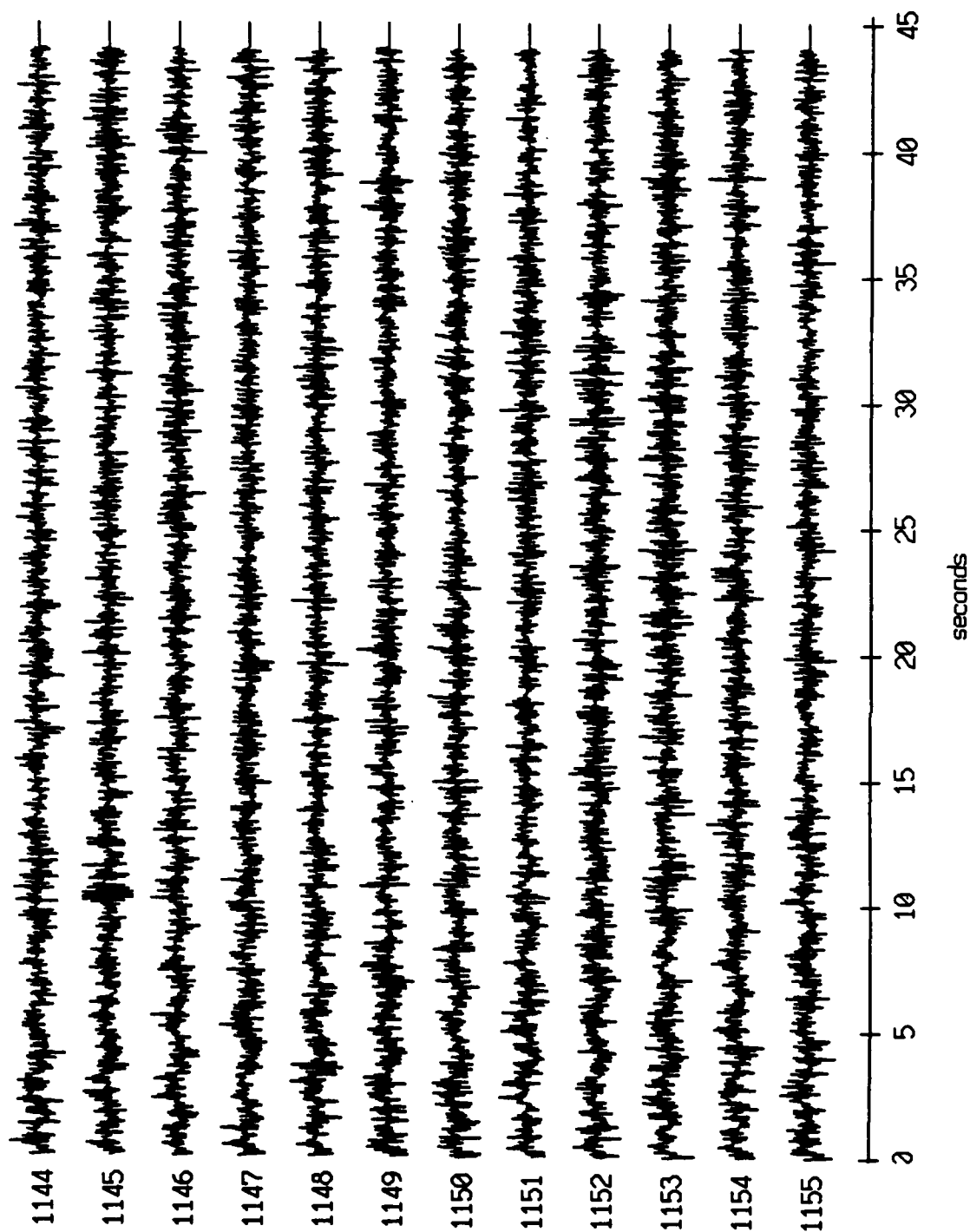


AGC corrected channel level (V)

Figure XI.35d



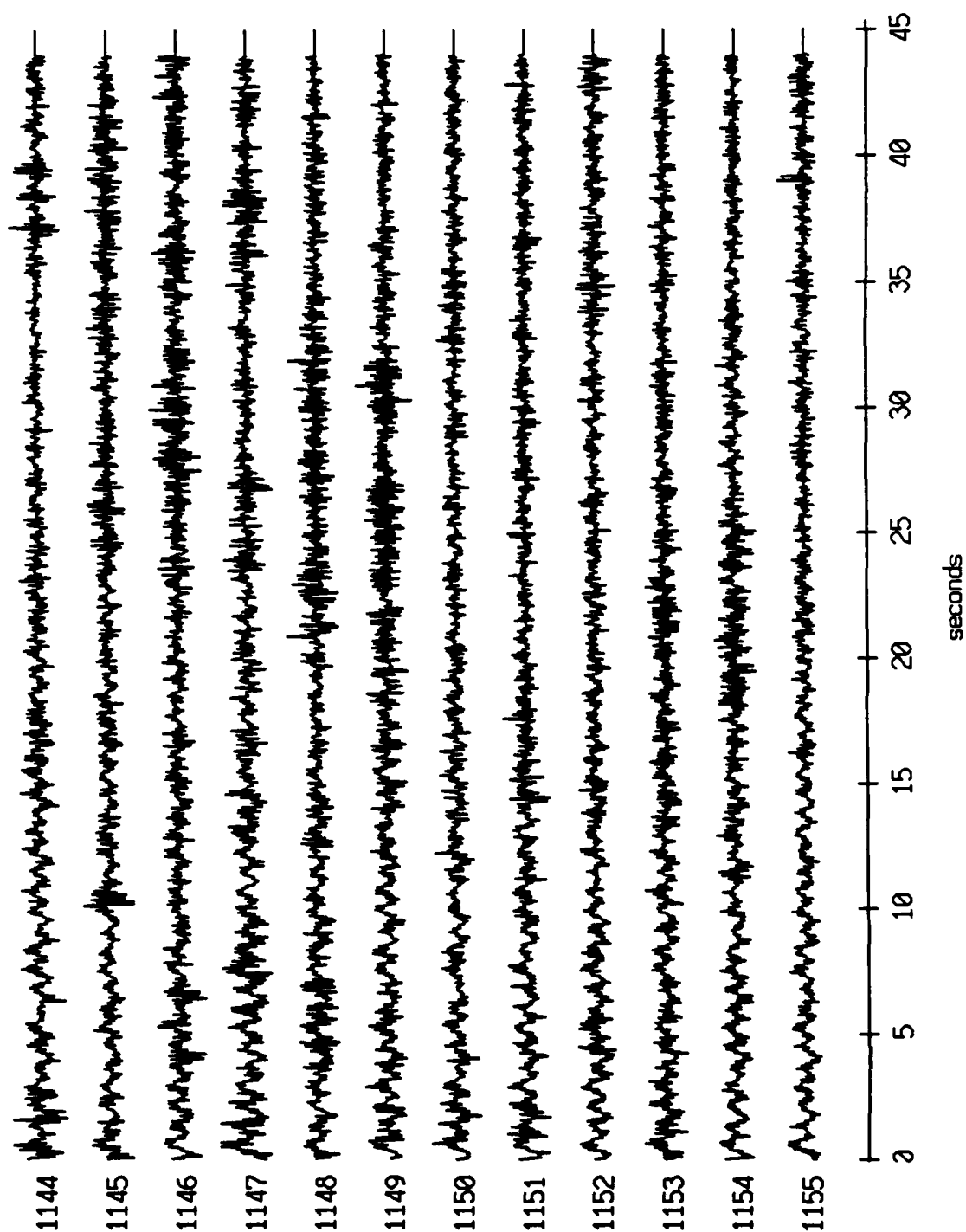
Floot 5, July, 1989 Trip - records 1144-1155 (x-axis)  
vertical axis scale is approx. -1.0 to 1.0 volts



RGC corrected channel level (V)

Figure XI.36a

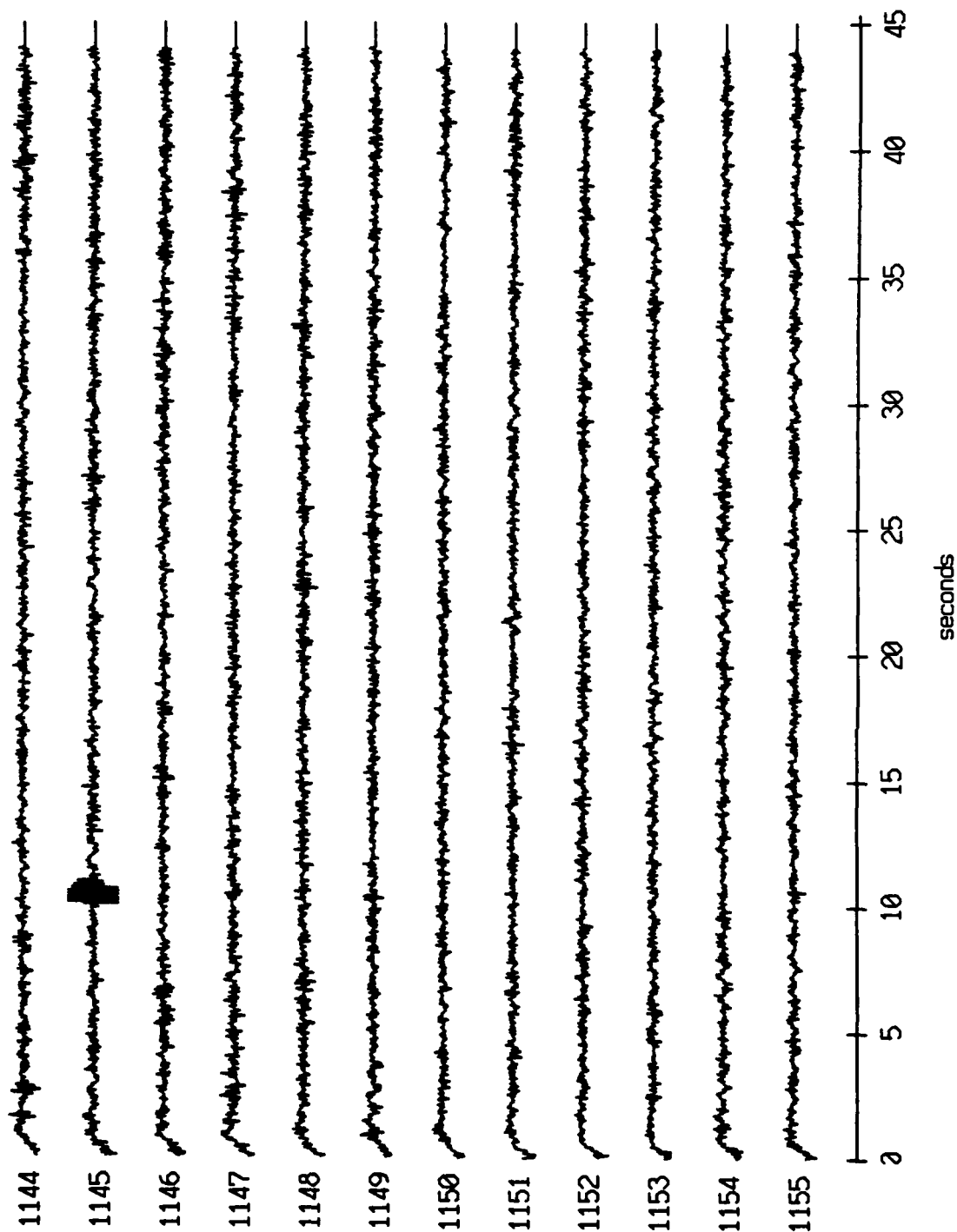
Float 5, July, 1989 Trip - records 1144-1155 (y-axis)  
vertical axis scale is approx. -1.0 to 1.0 volts



PGC corrected channel level (V)

Figure XI.36b

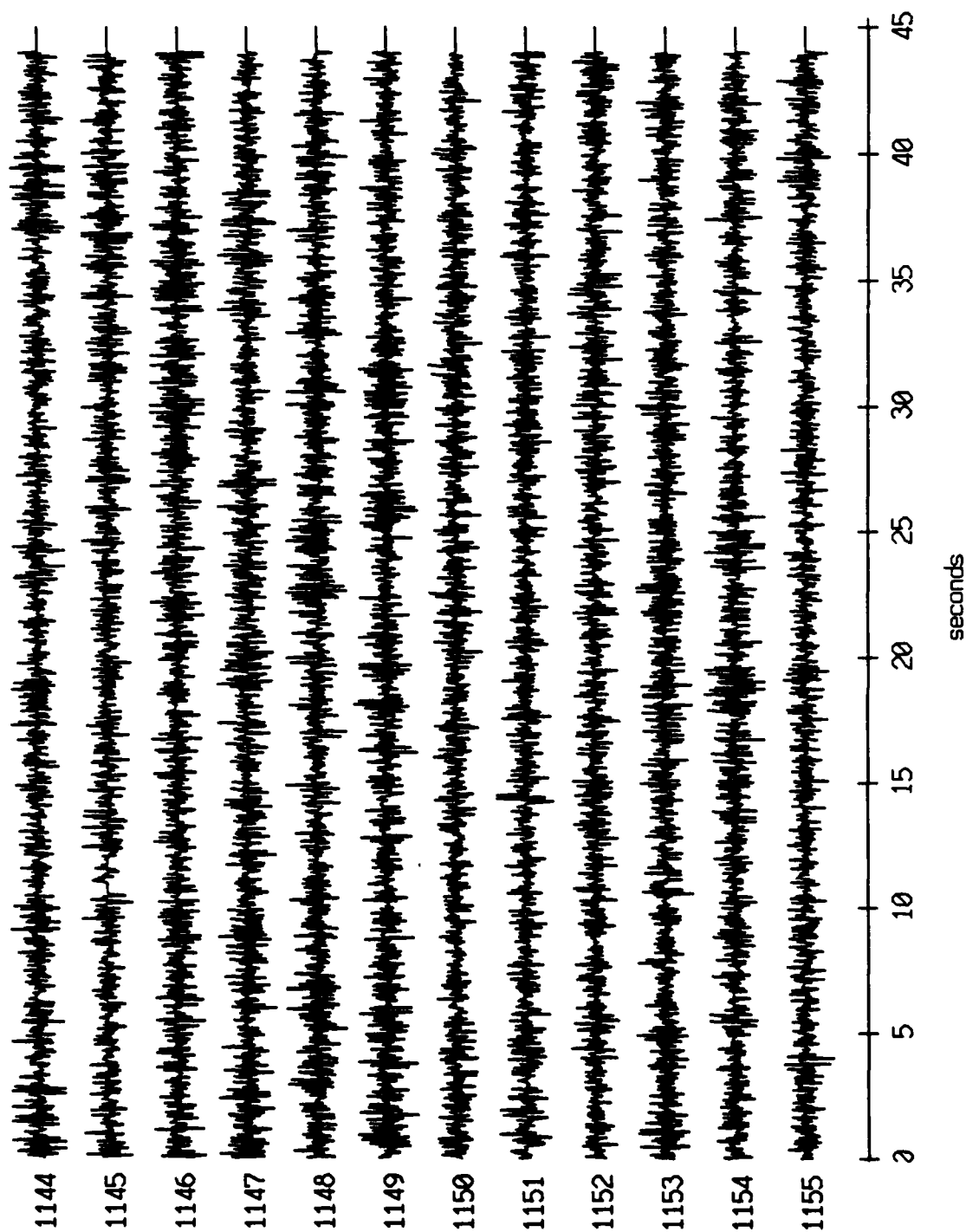
Floot 5, July, 1989 Trip - records 1144-1155 (z-axis)  
vertical axis scale is approx. -1.0 to 1.0 volts



PGC corrected channel level (V)

Figure XI.36c

Float 5, July, 1989 Trip - records 1144-1155 (hydrophone)  
vertical axis scale is approx. -1.0 to 1.0 volts



AGC corrected channel level (V)

Figure XI.36d

Float 6, July, 1989 Trip - records 1144-1155 (x-axis)  
vertical axis scale is approx. -1.0 to 1.0 volts

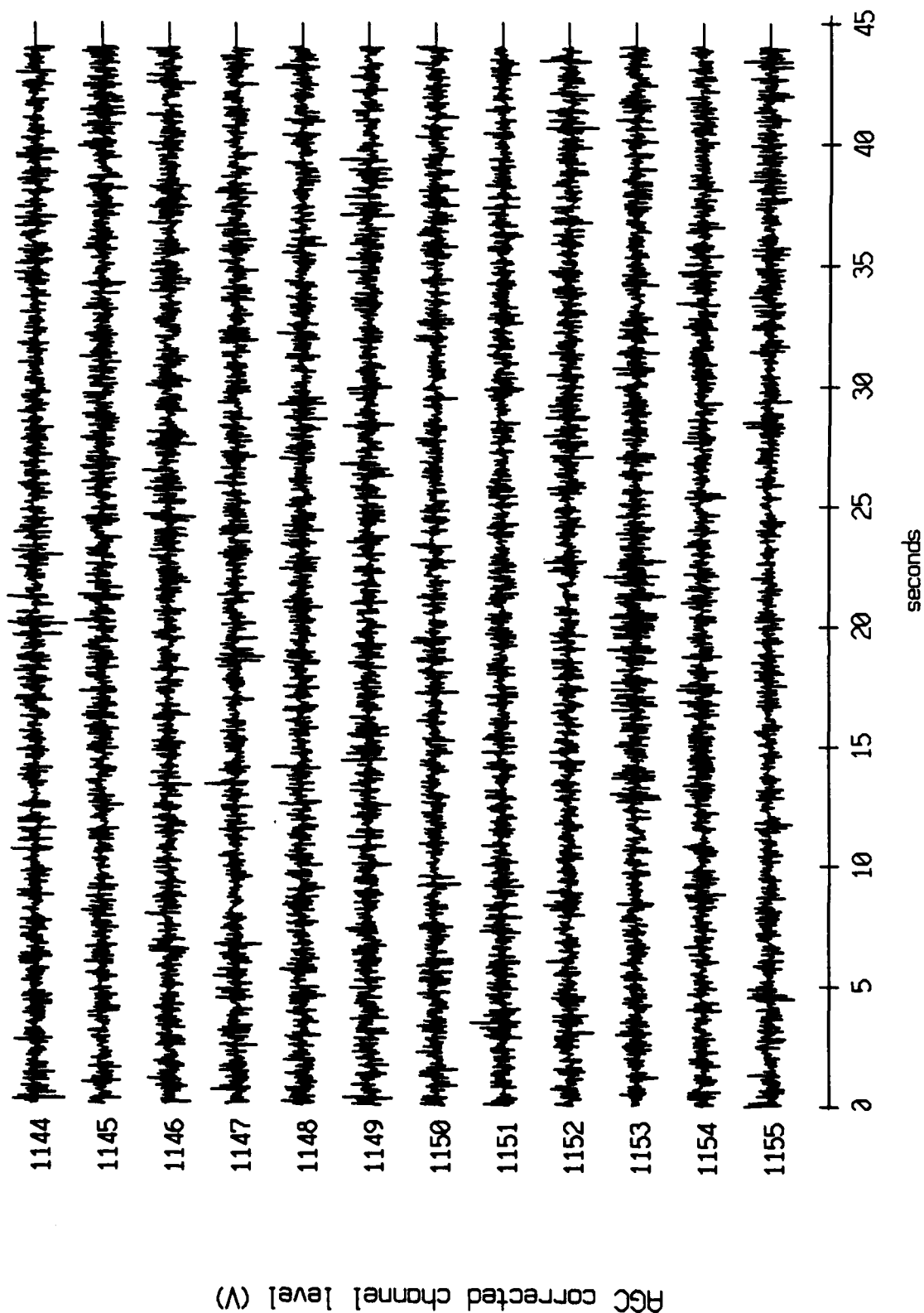
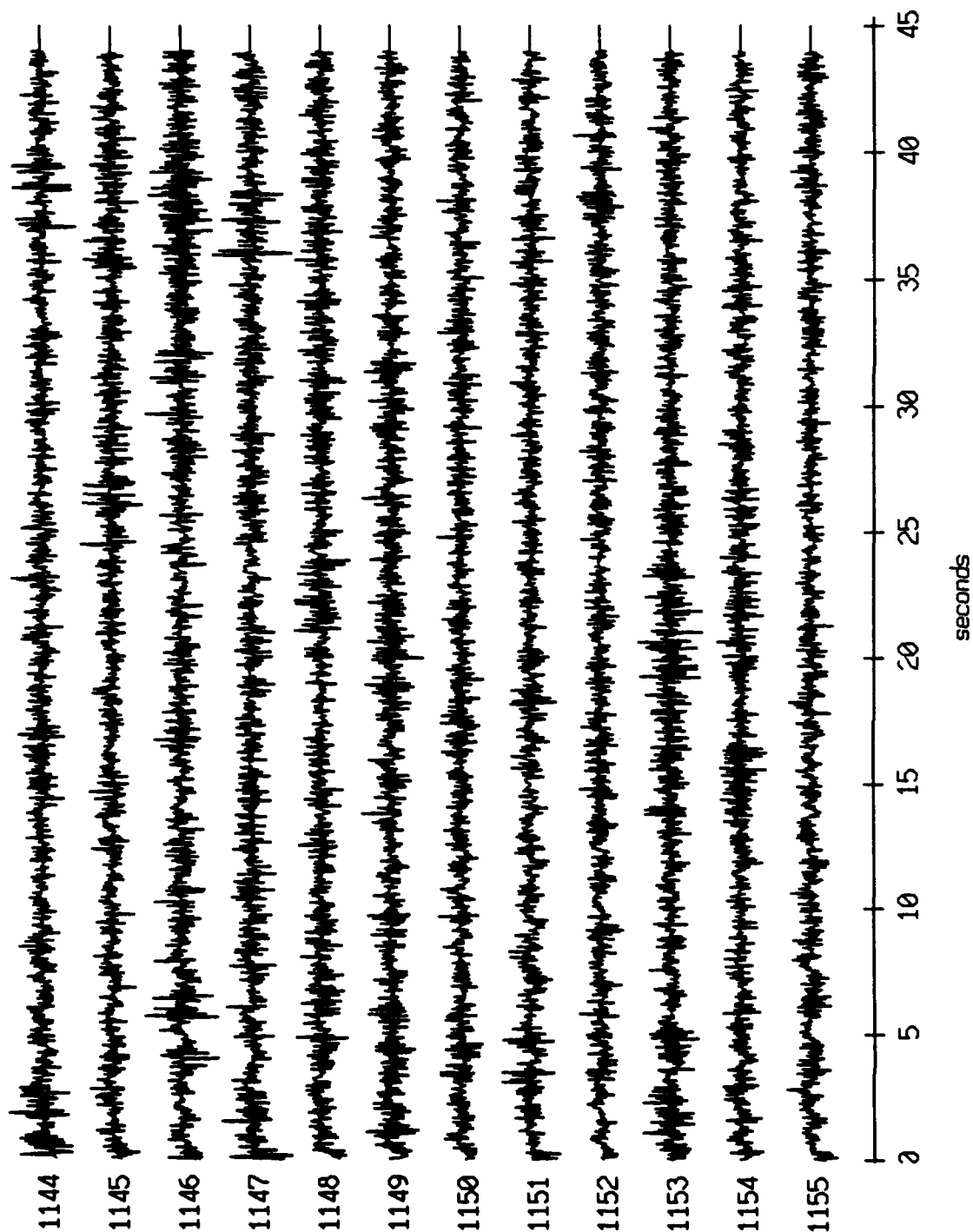


Figure XI.37a

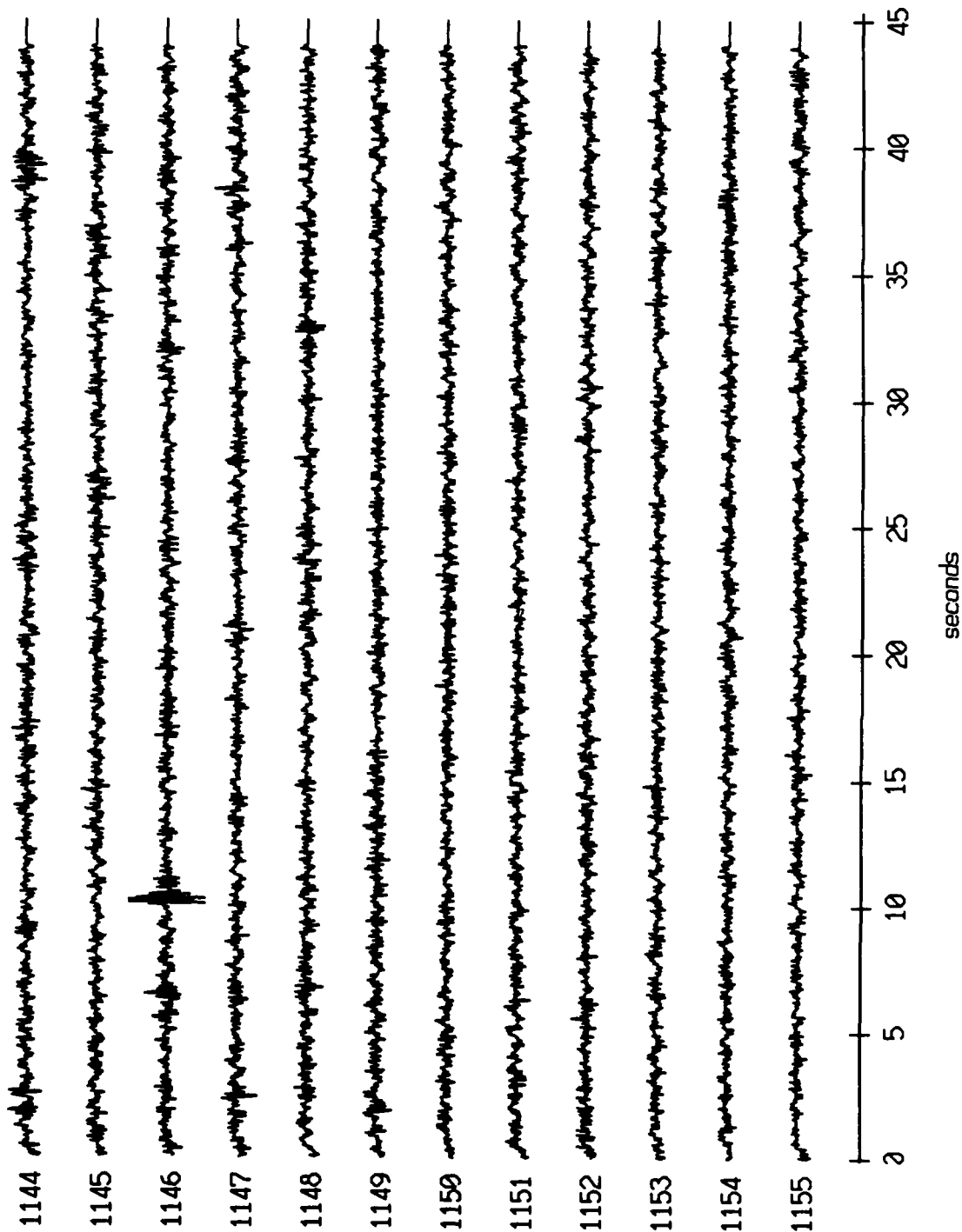
Float 6, July, 1989 Trip - records 1144-1155 (y-axis)  
vertical axis scale is approx. -1.0 to 1.0 volts



PGC corrected channel level (V)

Figure XI.37b

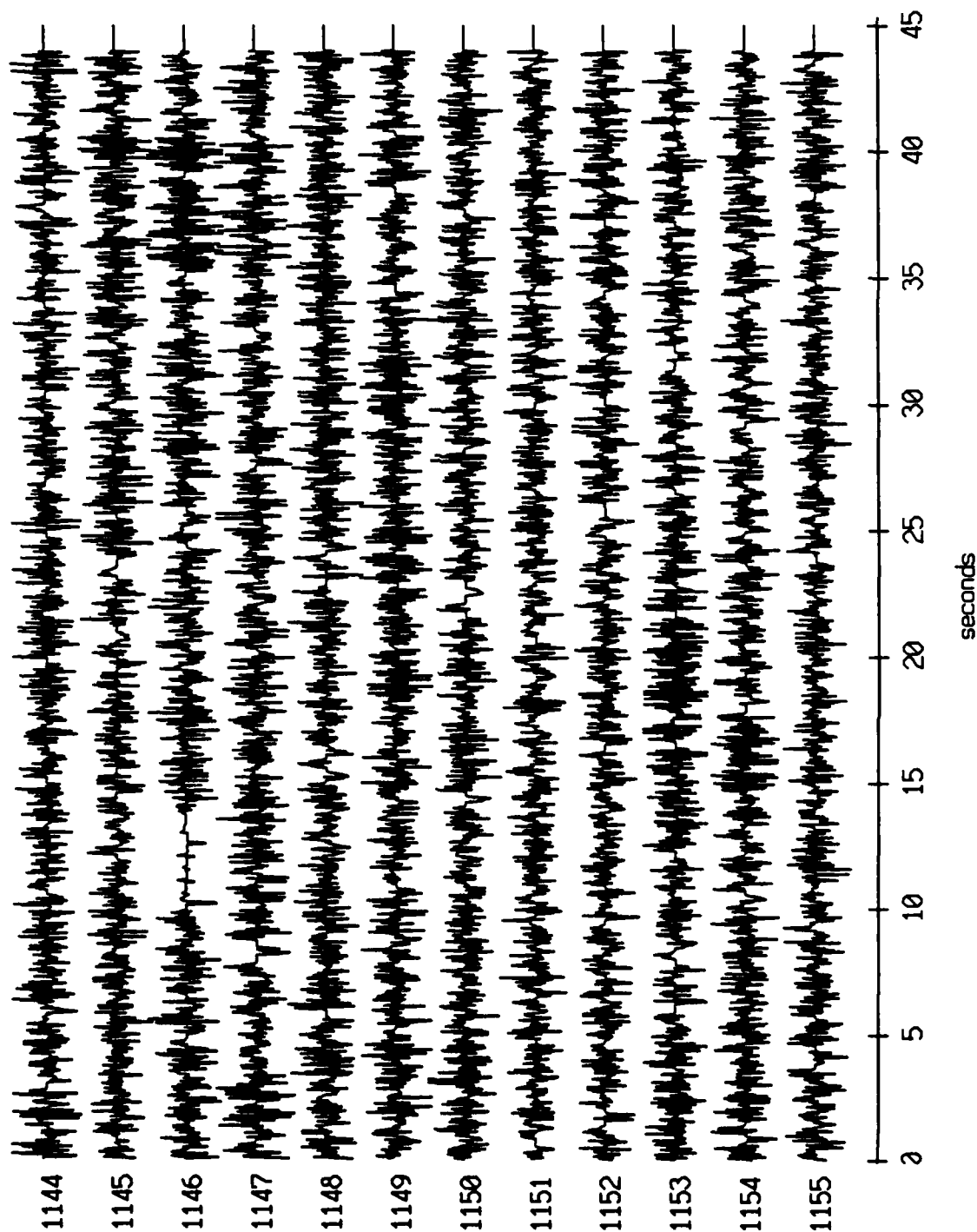
Float 6, July, 1989 Trip - records 1144-1155 (z-axis)  
vertical axis scale is approx. -1.0 to 1.0 volts



PGC corrected channel level (V)

Figure XI.37c

Float 6, July, 1989 Trip - records 1144-1155 (hydrophone)  
vertical axis scale is approx. -1.0 to 1.0 volts



AGC corrected channel level (V)

Figure XI.37d



Floot 7, July, 1989 Trip - records 1144-1155 (x-axis)  
vertical axis scale is approx. -1.0 to 1.0 volts

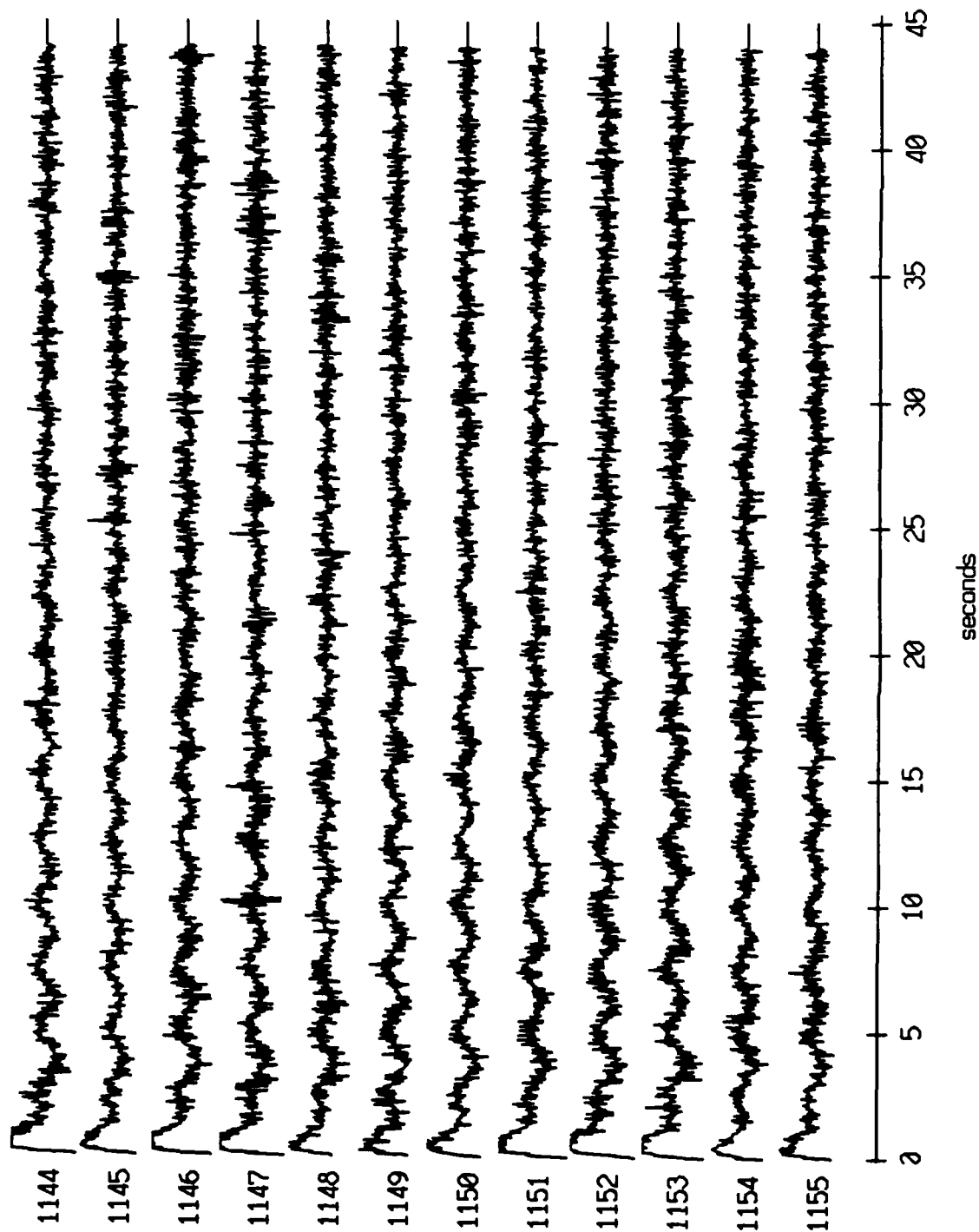
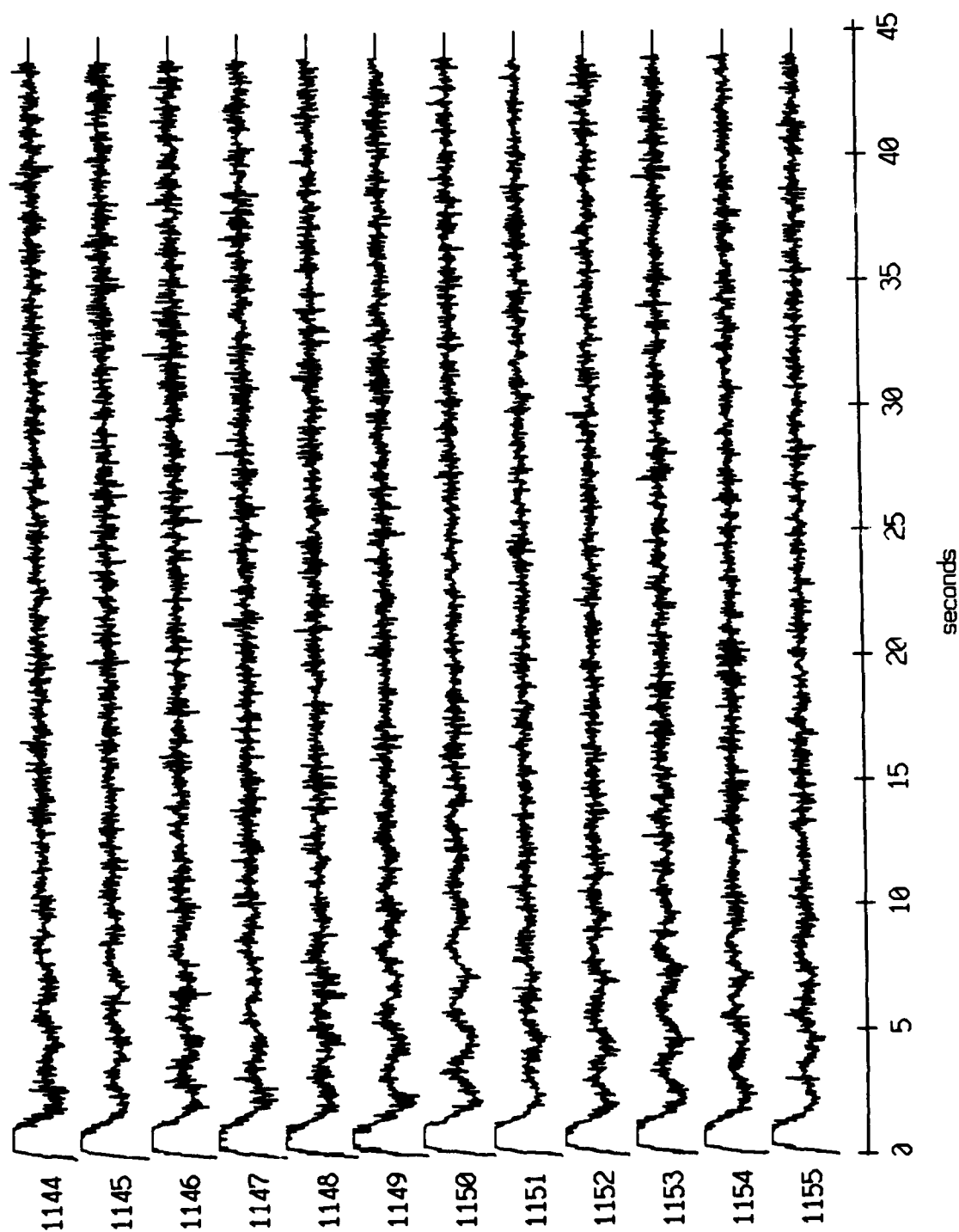


Figure XI.38a

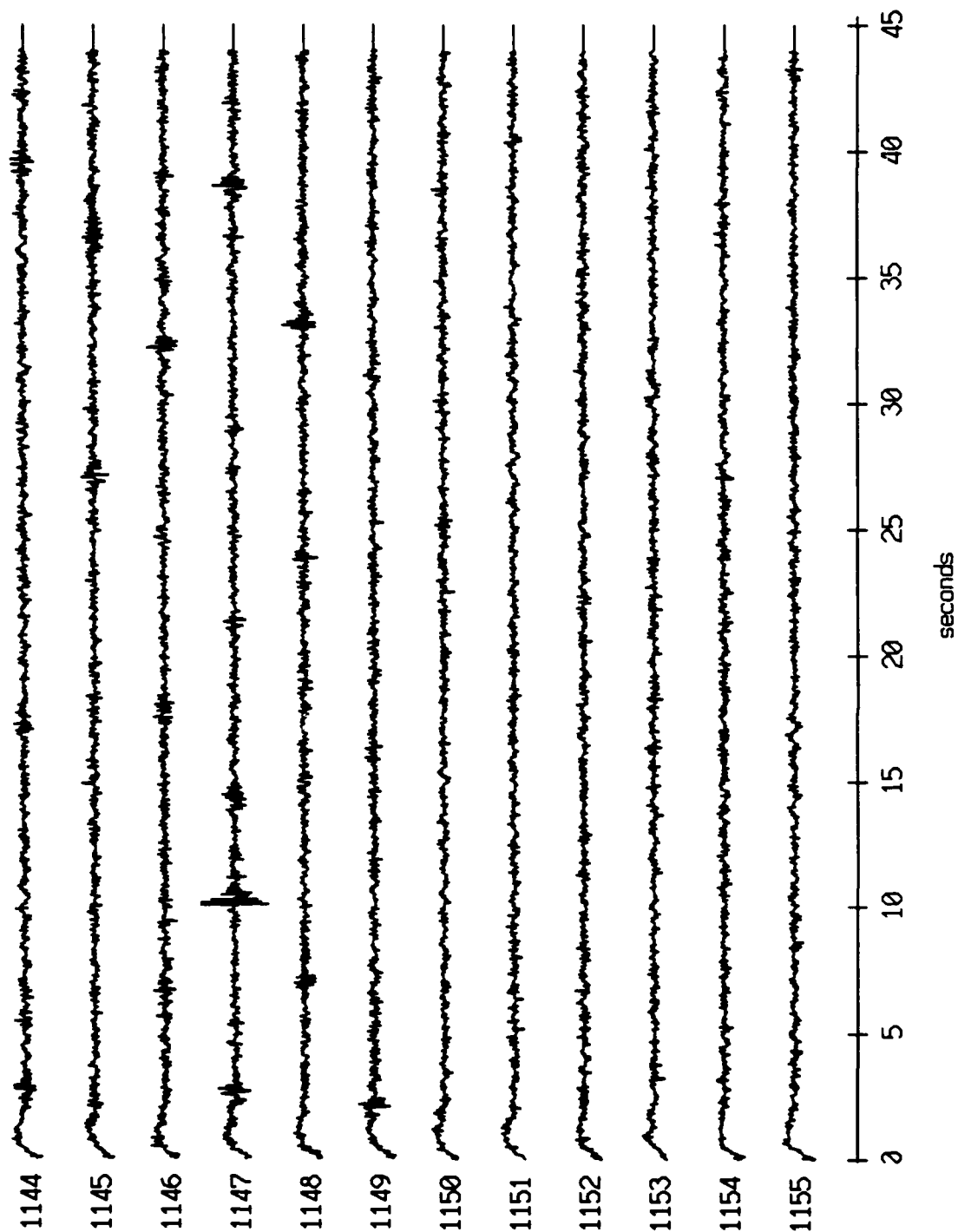
Floot 7, July, 1989 Trip - records 1144-1155 (y-axis)  
vertical axis scale is approx. -1.0 to 1.0 volts



RGC corrected channel level (V)

Figure XI.38b

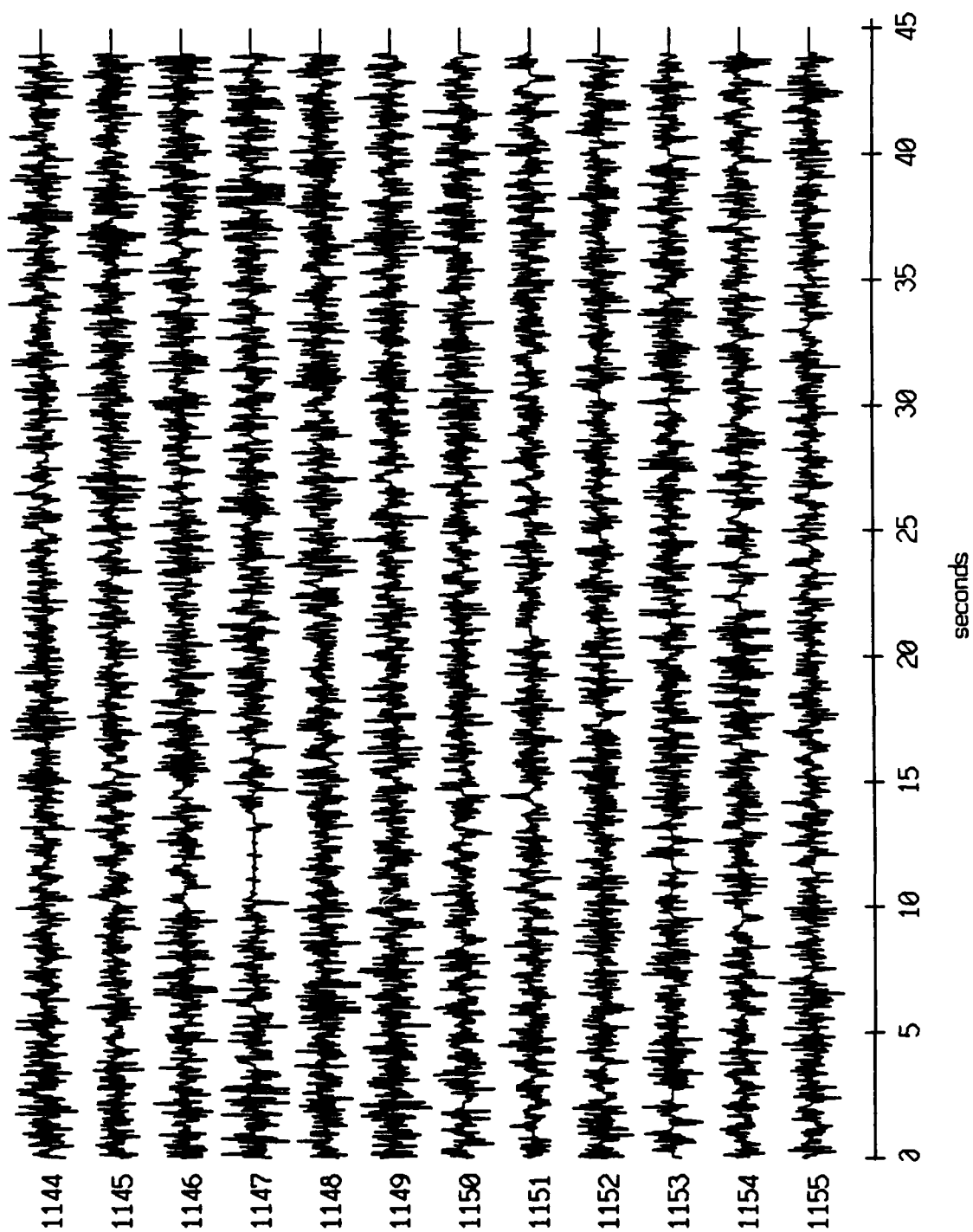
Floot 7, July, 1989 Trip - records 1144-1155 (z-axis)  
vertical axis scale is approx. -1.0 to 1.0 volts



PGC corrected channel level (V)

Figure XI.38c

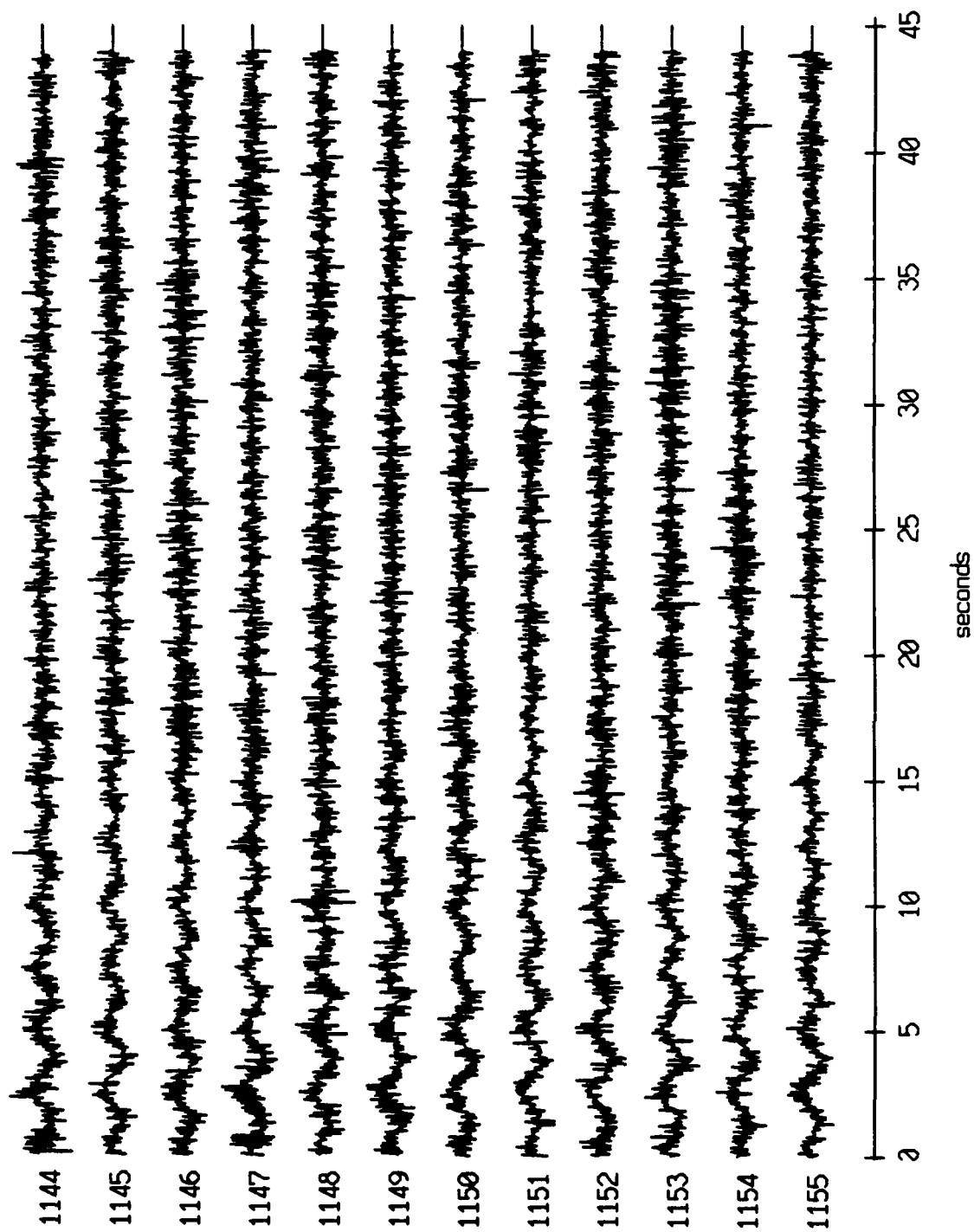
Floot 7, July, 1989 Trip - records 1144-1155 (hydrophone)  
vertical axis scale is approx. -1.0 to 1.0 volts



PGC corrected channel level (V)

Figure XI.38d

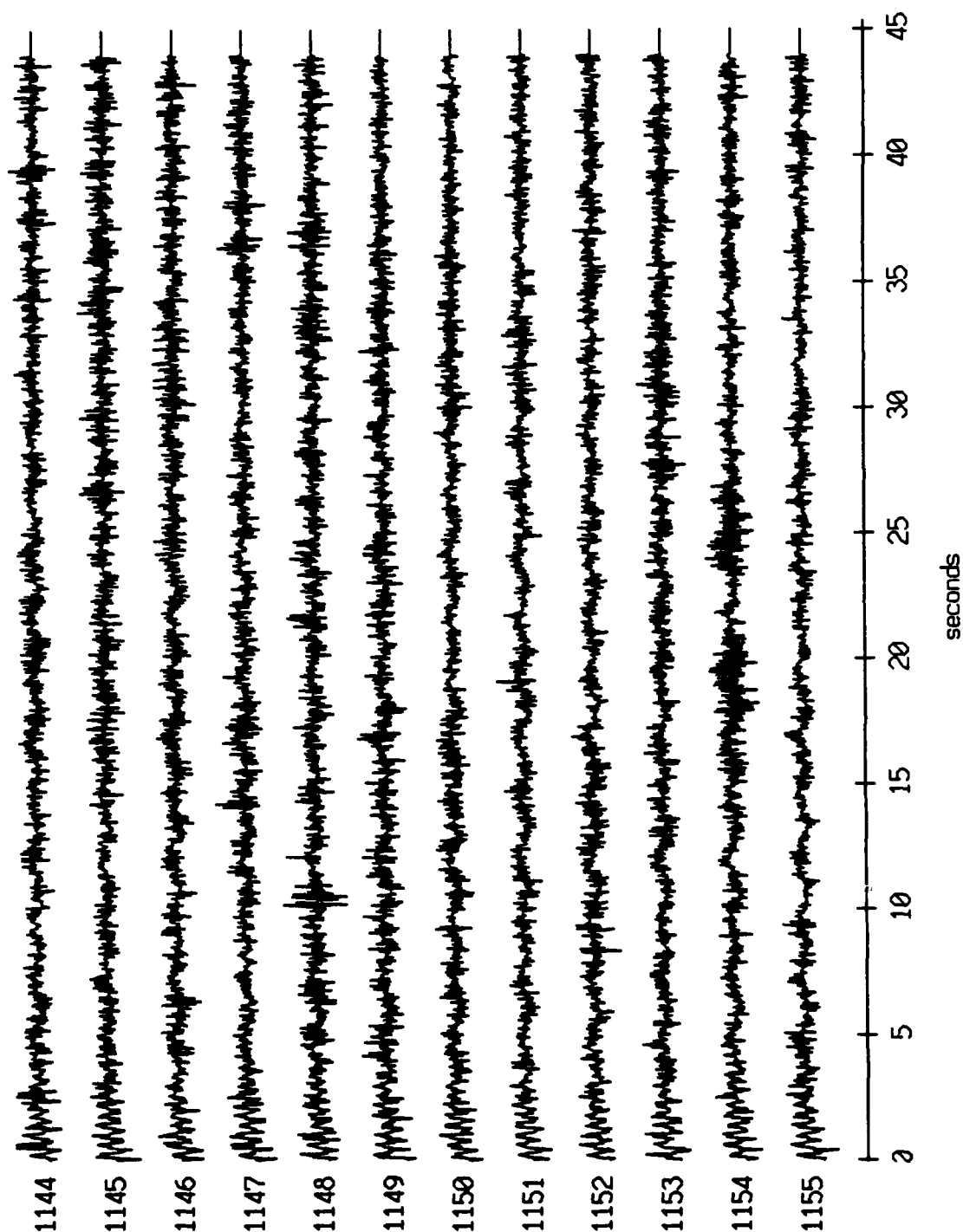
Float 8, July, 1989 Trip - records 1144-1155 (x-axis)  
vertical axis scale is approx. -1.0 to 1.0 volts



RG corrected channel level (V)

Figure XI.39a

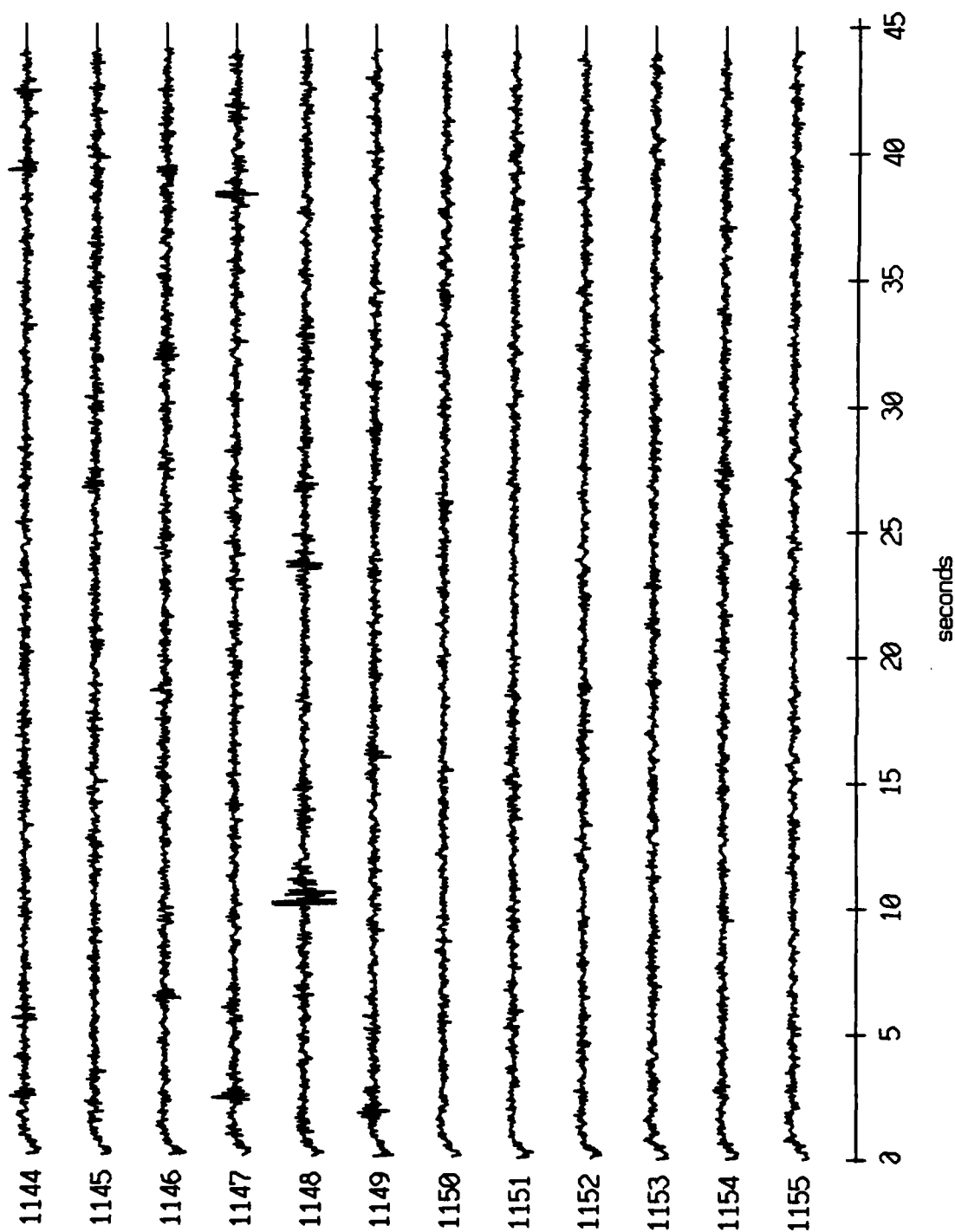
Float 8, July, 1989 Trip - records 1144-1155 (y-axis)  
vertical axis scale is approx. -1.0 to 1.0 volts



PGC corrected channel level (V)

Figure XI.39b

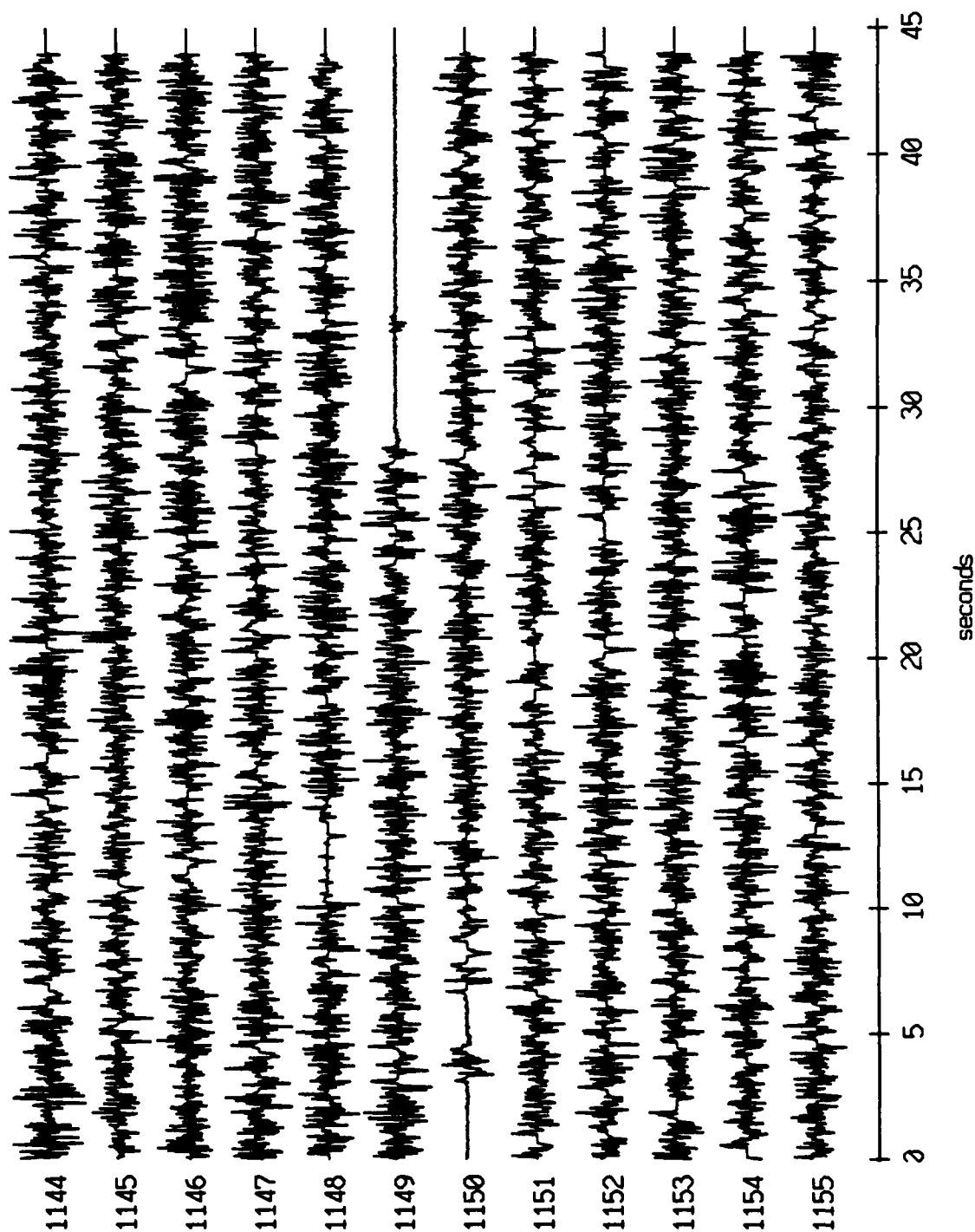
Float 8, July, 1989 Trip - records 1144-1155 (z-axis)  
vertical axis scale is approx. -1.0 to 1.0 volts



PGC corrected channel level (V)

Figure XI.39c

Floot 8, July, 1989 Trip - records 1144-1155 (hydrophone)  
vertical axis scale is approx. -1.0 to 1.0 volts

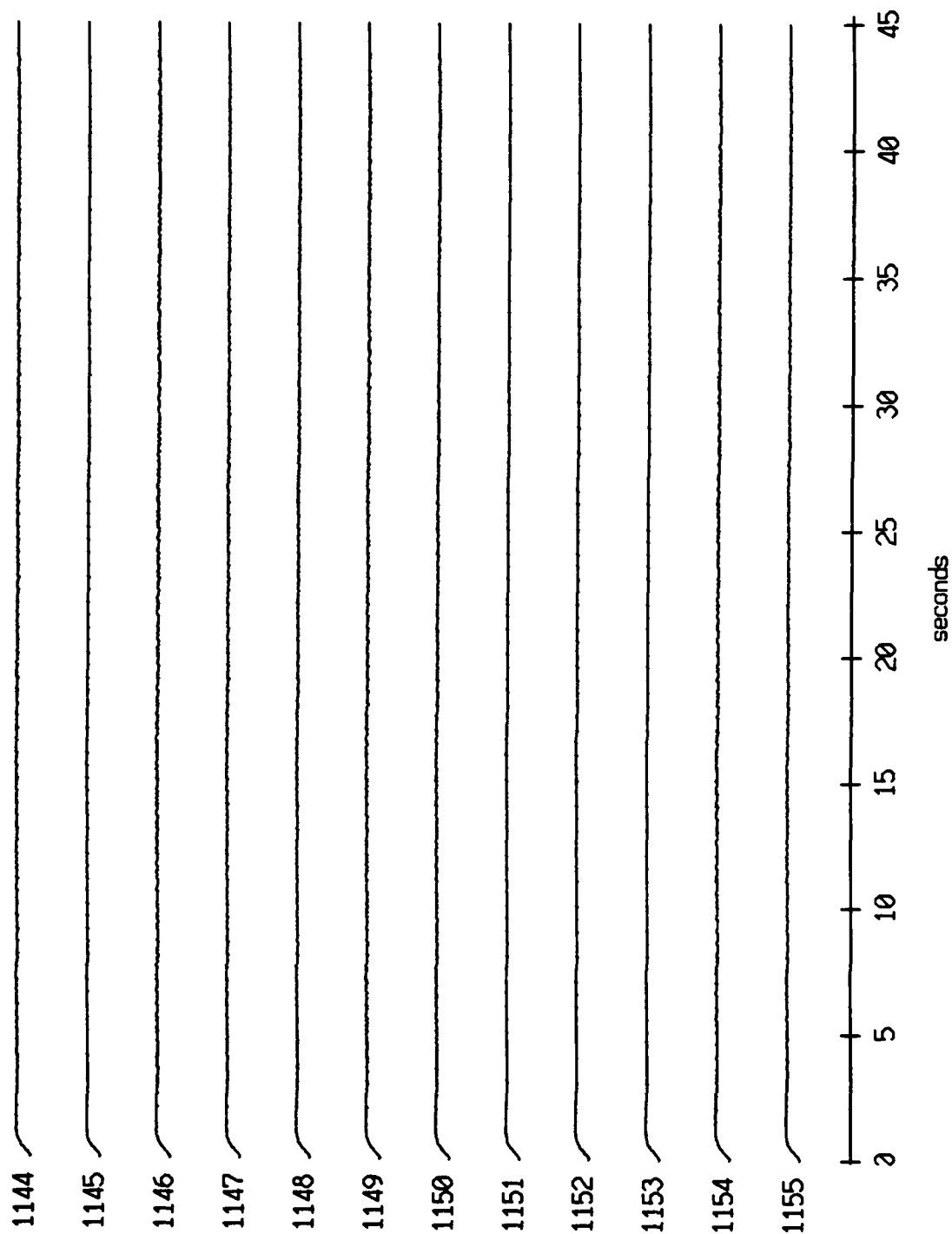


AGC corrected channel level (V)

Figure XI.39d



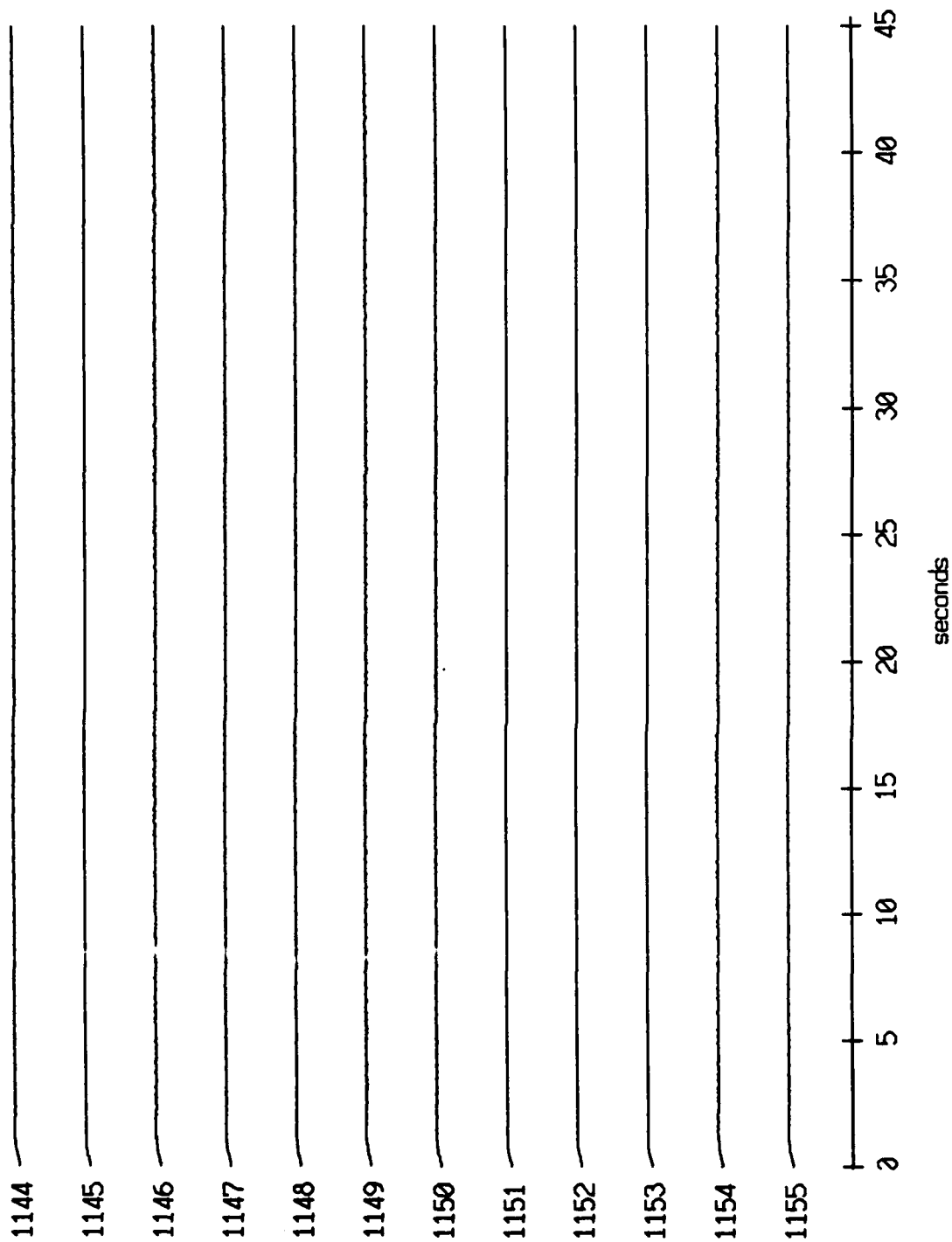
Float 9, July, 1989 Trip - records 1144-1155 (x-axis)  
vertical axis scale is approx. -1.0 to 1.0 volts



AGC corrected channel level (V)

Figure XI.40a

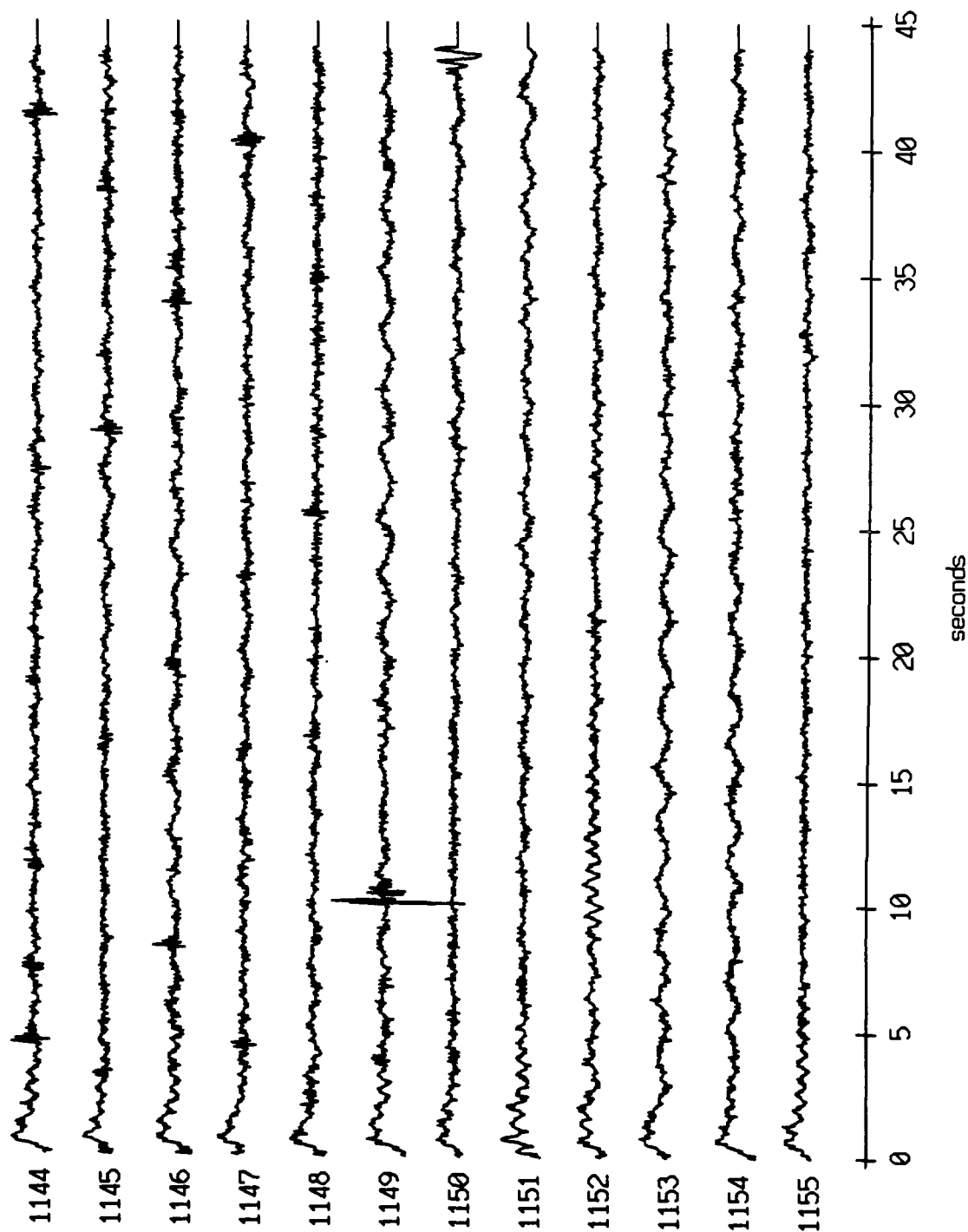
Float 9, July, 1989 Trip - records 1144-1155 (y-axis)  
 vertical axis scale is approx. -1.0 to 1.0 volts



AGC corrected channel level (V)

Figure XI.40b

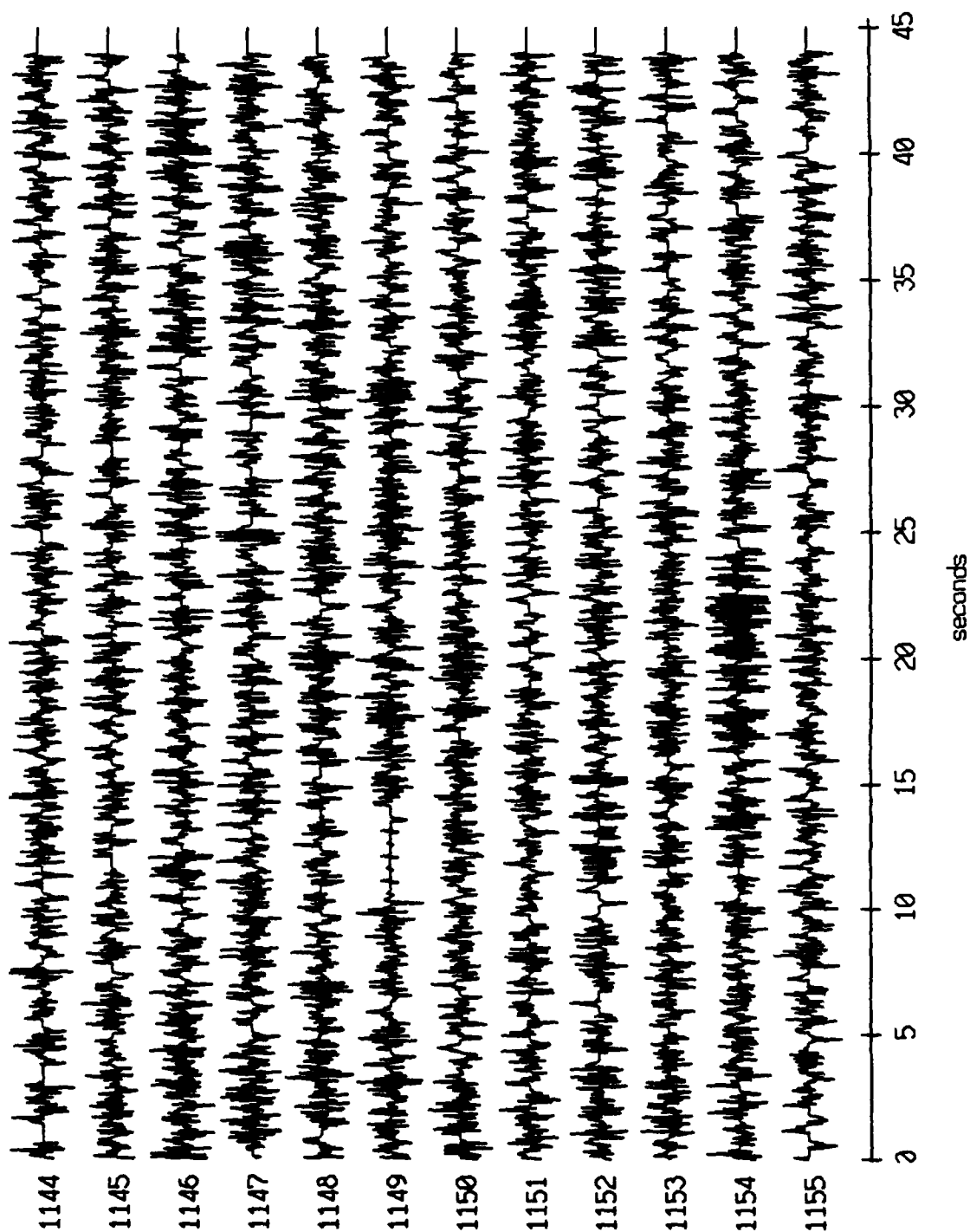
Float 9, July, 1989 Trip - records 1144-1155 (z-axis)  
vertical axis scale is approx. -1.0 to 1.0 volts



PGC corrected channel level (V)

Figure XI.40c

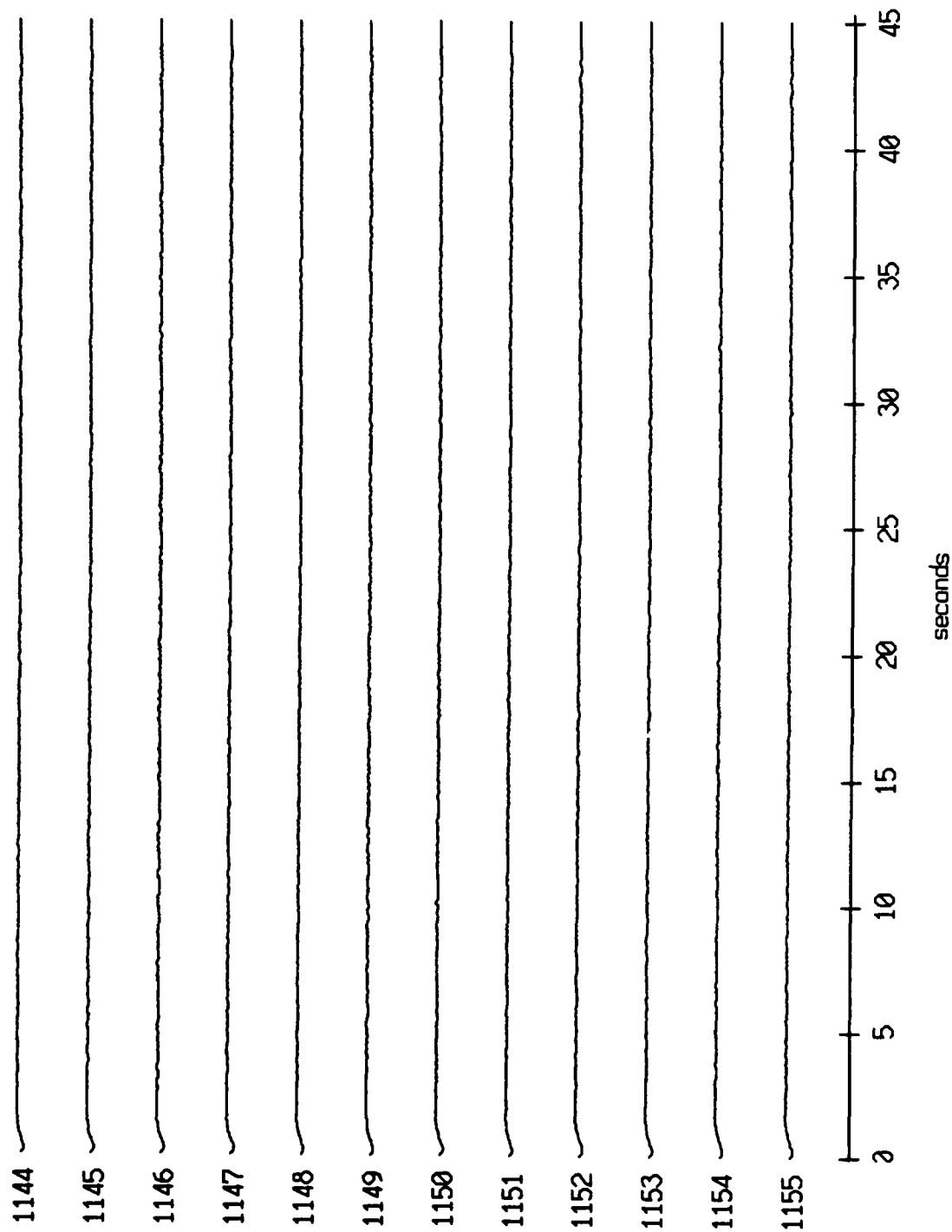
Float 9, July, 1989 Trip - records 1144-1155 (hydrophone)  
vertical axis scale is approx. -1.0 to 1.0 volts



RGC corrected channel level (V)

Figure XI.40d

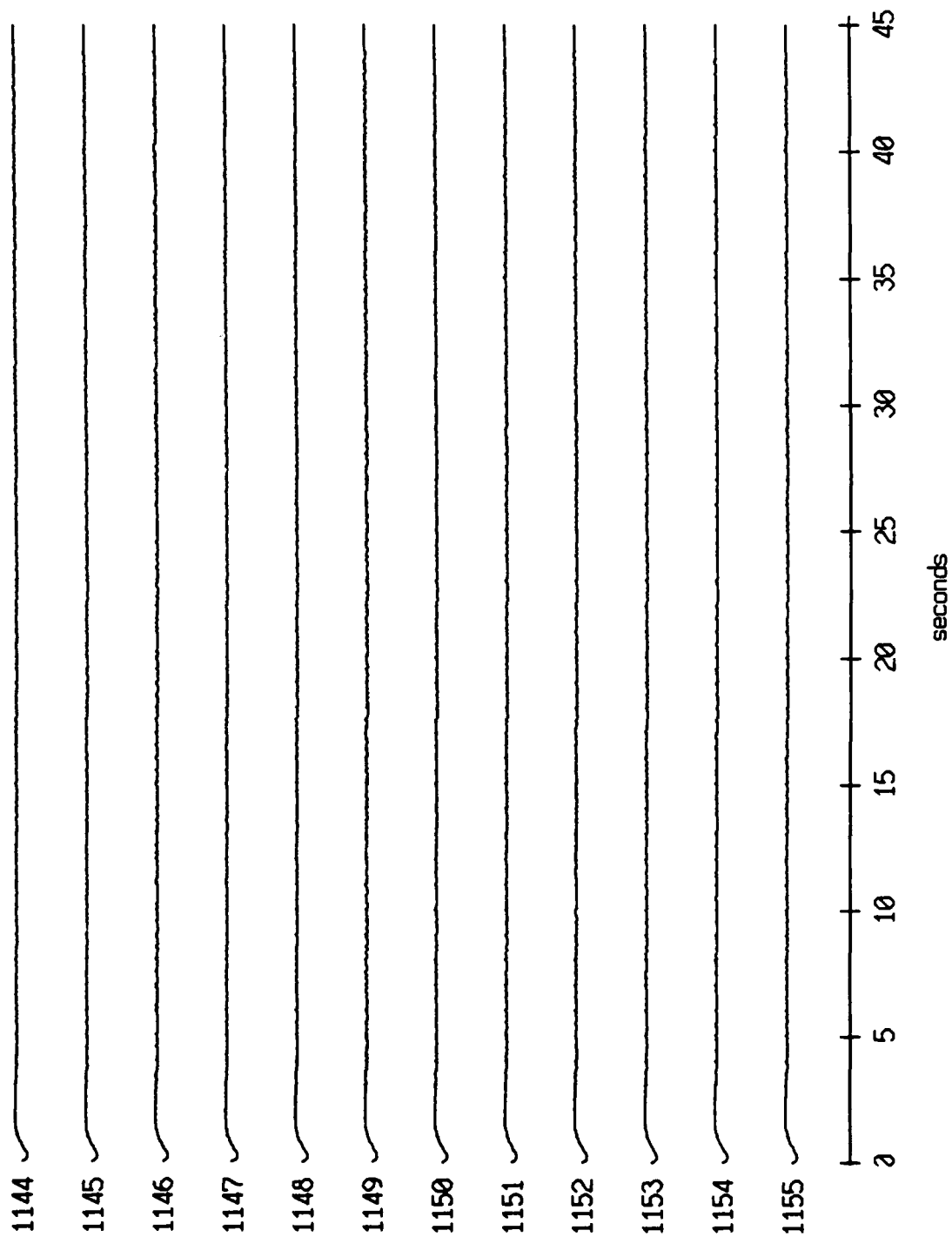
Float 10, July, 1989 Trip - records 1144-1155 (x-axis)  
vertical axis scale is approx. -1.0 to 1.0 volts



AGC corrected channel level (V)

Figure XI.41a

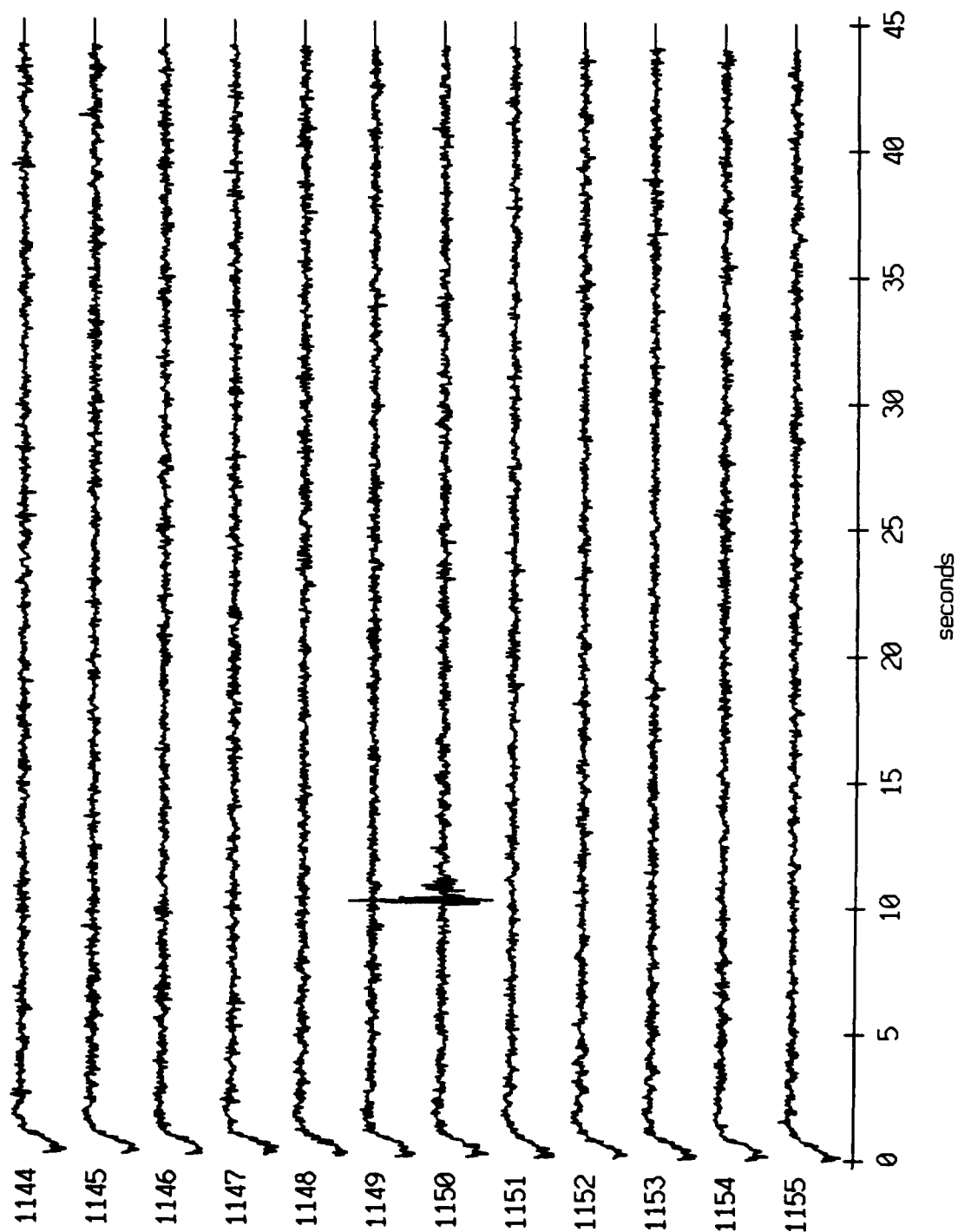
Float 10, July, 1989 Trip - records 1144-1155 (y-axis)  
 vertical axis scale is approx. -1.0 to 1.0 volts



AGC corrected channel level (V)

Figure XI.41b

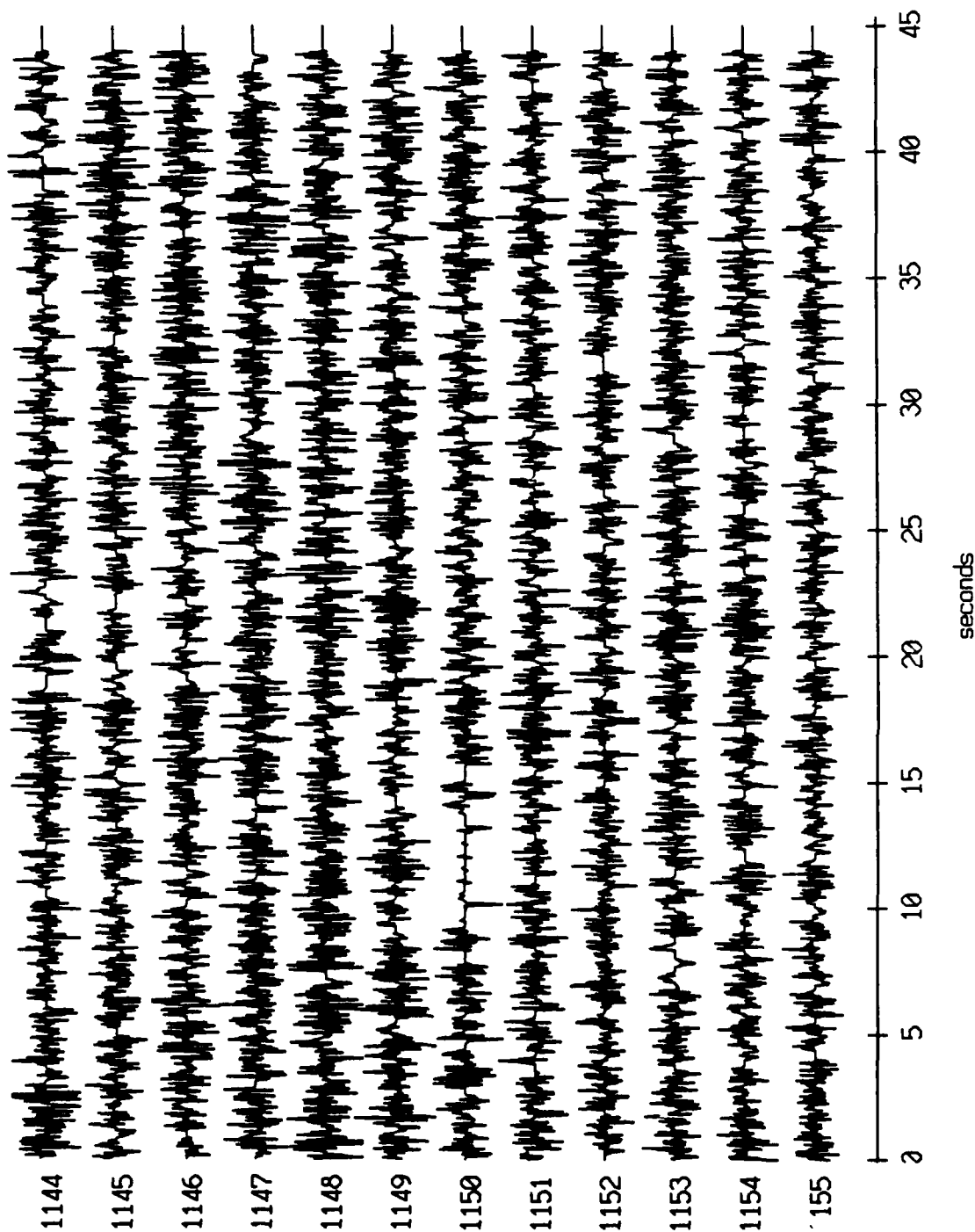
Float 10, July, 1989 Trip - records 1144-1155 (z-axis)  
vertical axis scale is approx. -1.0 to 1.0 volts



RGC corrected channel level (V)

Figure XI.41c

Floot 10, July, 1989 Trip - records 1144-1155 (hydrophone)  
vertical axis scale is approx. -1.0 to 1.0 volts



RCC corrected channel level (V)

Figure XI.41d



Float 11, July, 1989 Trip - records 1144-1155 (x-axis)  
 vertical axis scale is approx. -1.0 to 1.0 volts

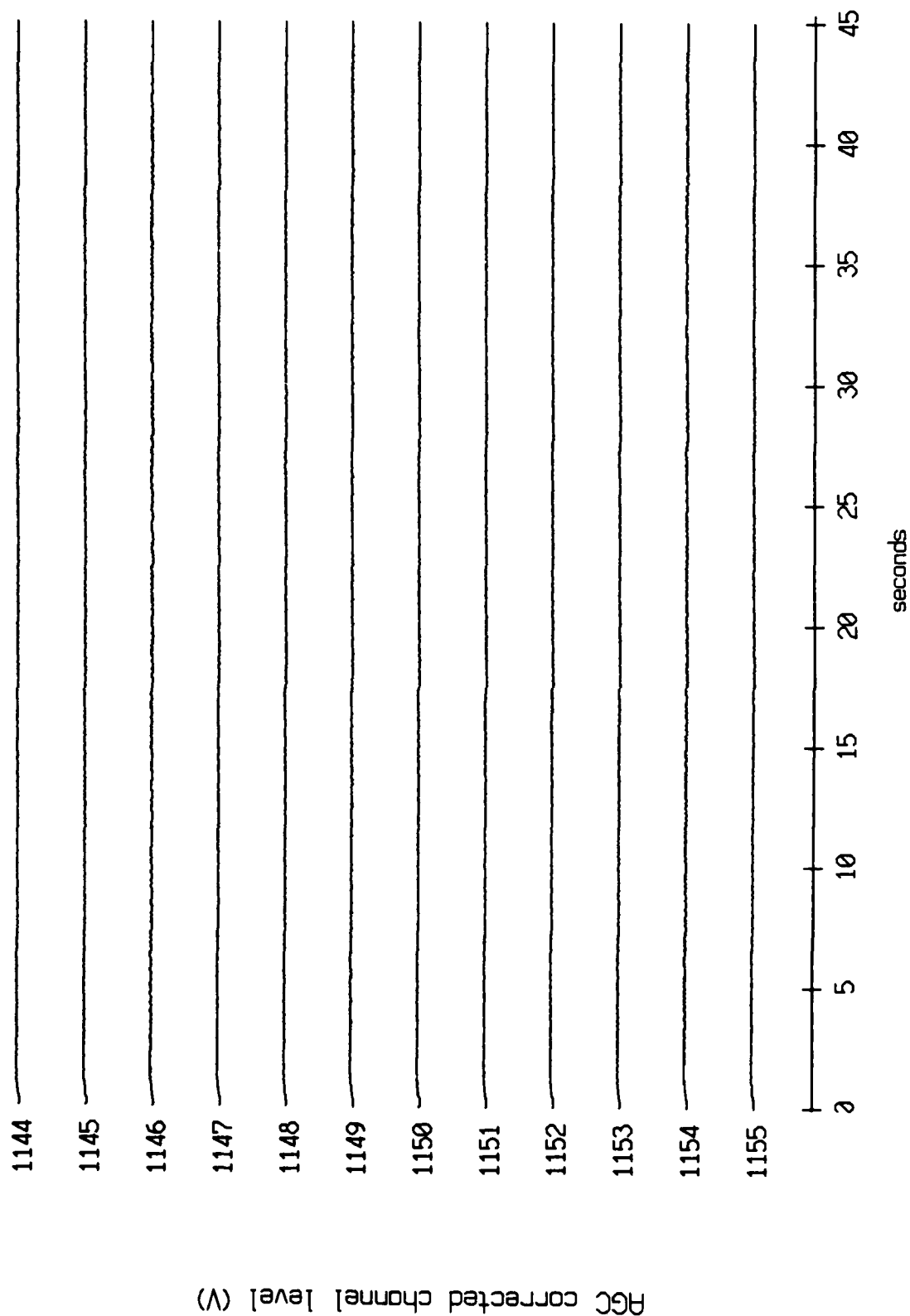


Figure X1.42a

Float 11, July, 1989 Trip - records 1144-1155 (y-axis)  
vertical axis scale is approx. -1.0 to 1.0 volts

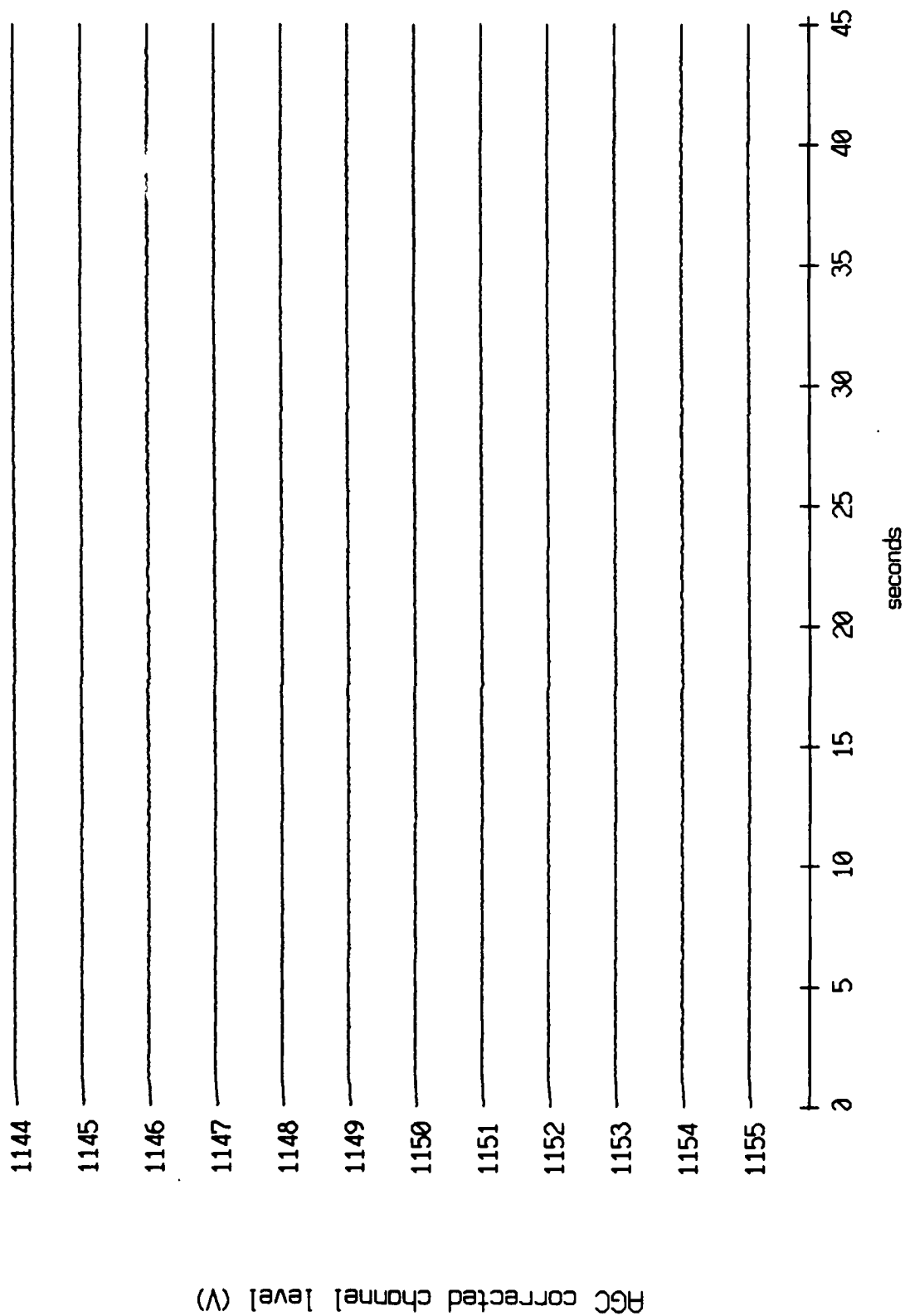


Figure XI.42b

Float 11, July, 1989 Trip - records 1144-1155 (z-axis)  
vertical axis scale is approx. -1.0 to 1.0 volts

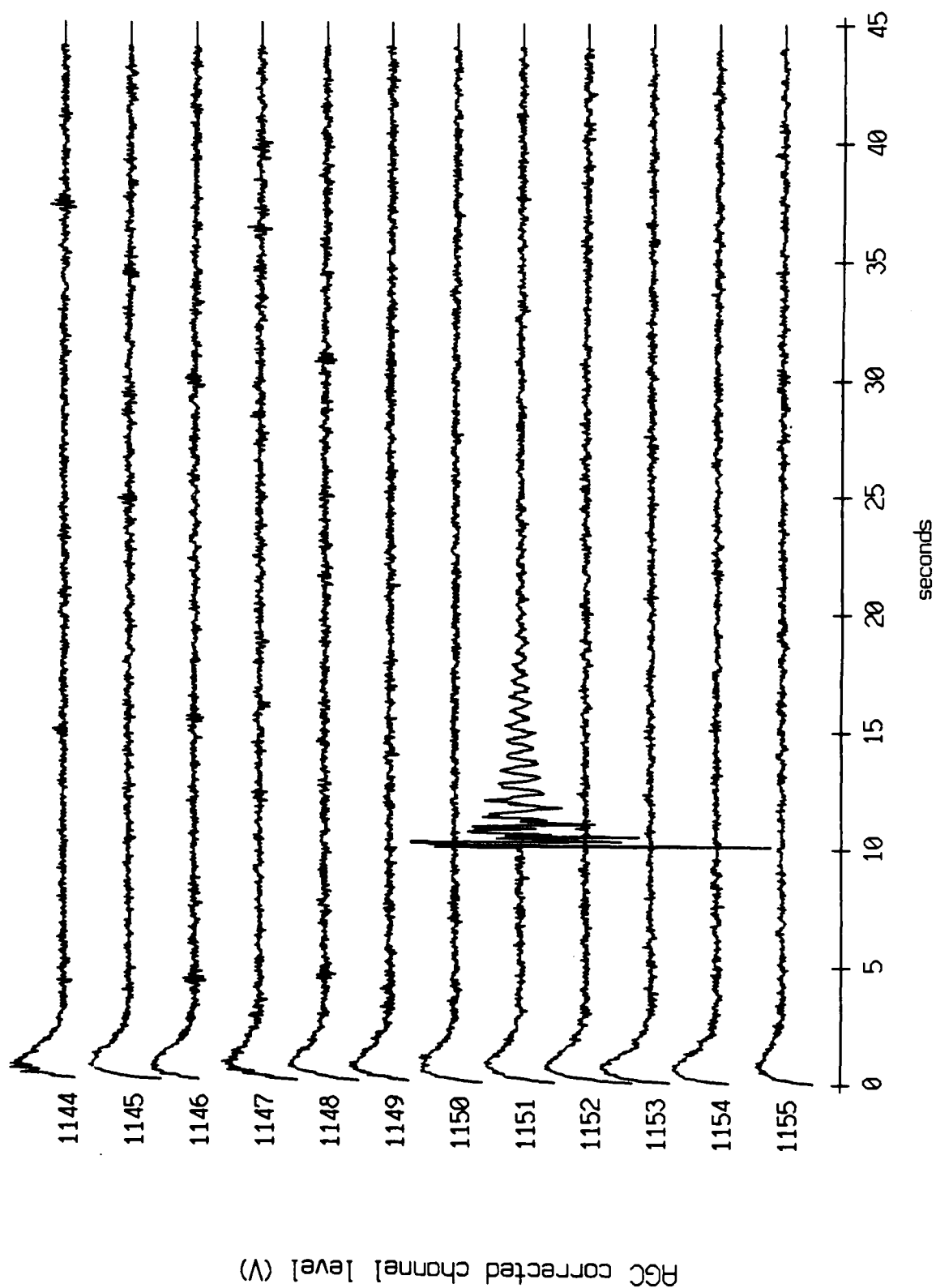
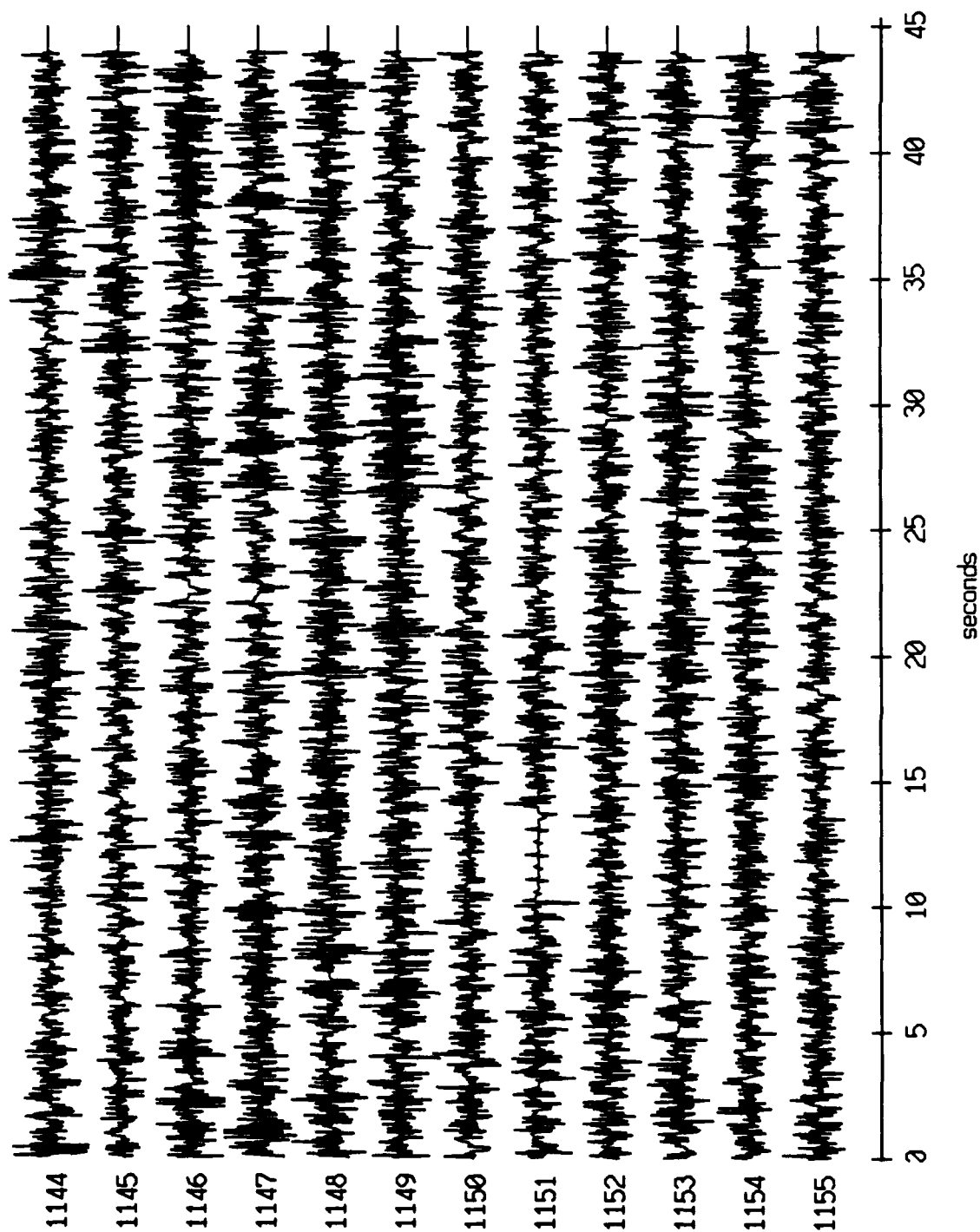


Figure XI.42c

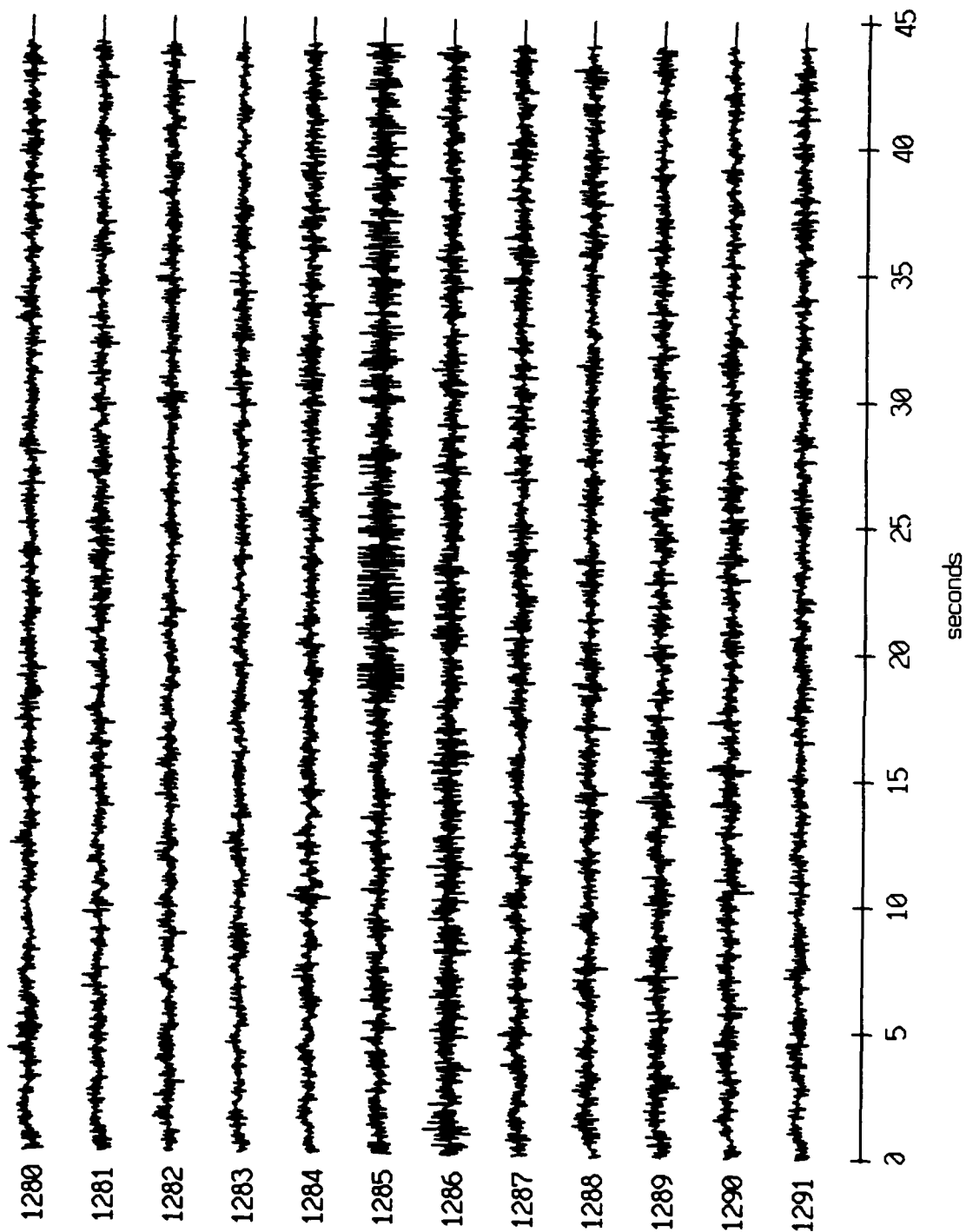
Float 11, July, 1989 Trip - records 1144-1155 (hydrophone)  
vertical axis scale is approx. -1.0 to 1.0 volts



AGC corrected channel level (V)

Figure XI.42d

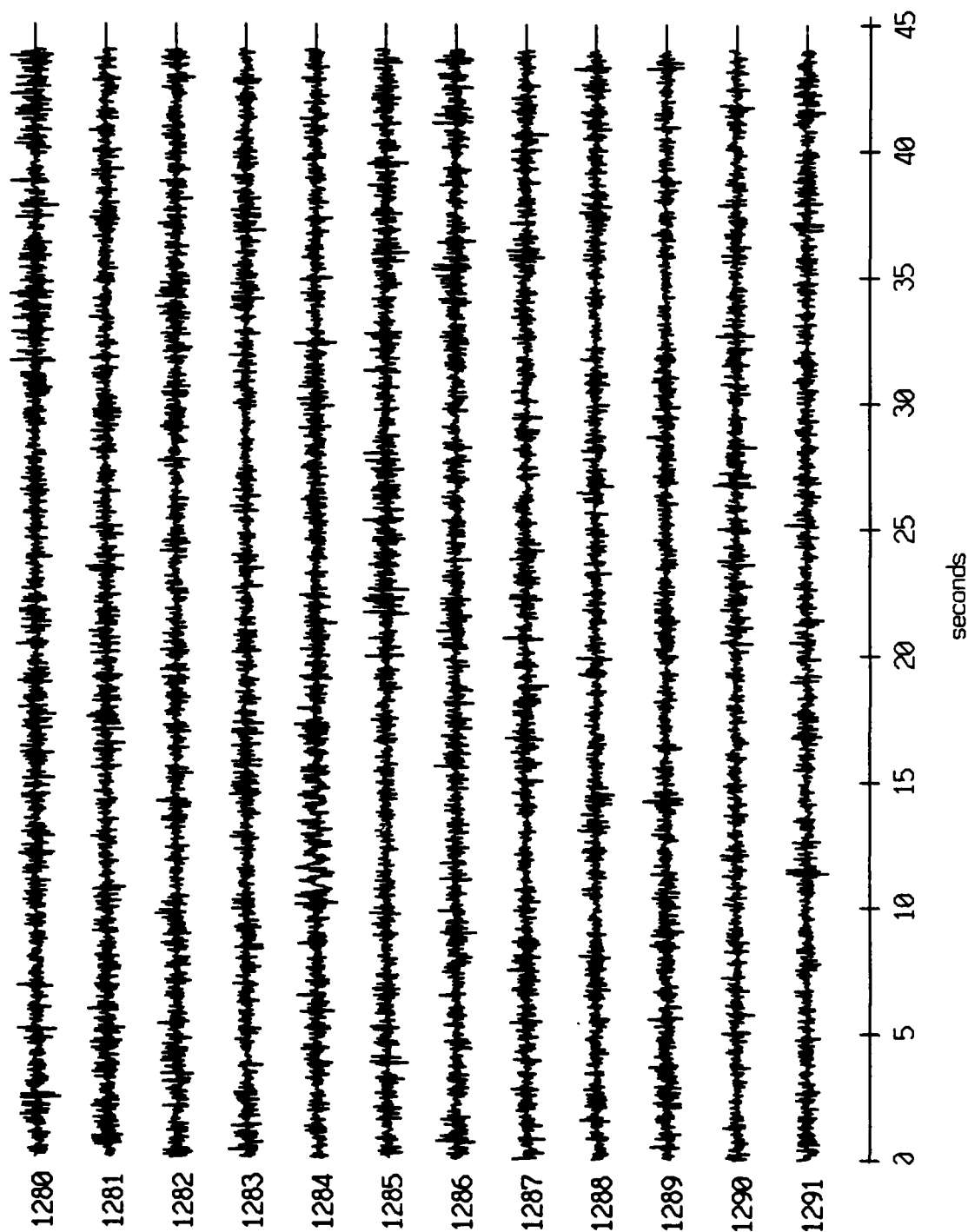
Floot 0, July, 1989 Trip - records 1280-1291 (x-axis)  
vertical axis scale is approx. -2.0 to 2.0 volts



PGC corrected channel level (V)

Figure XI.43a

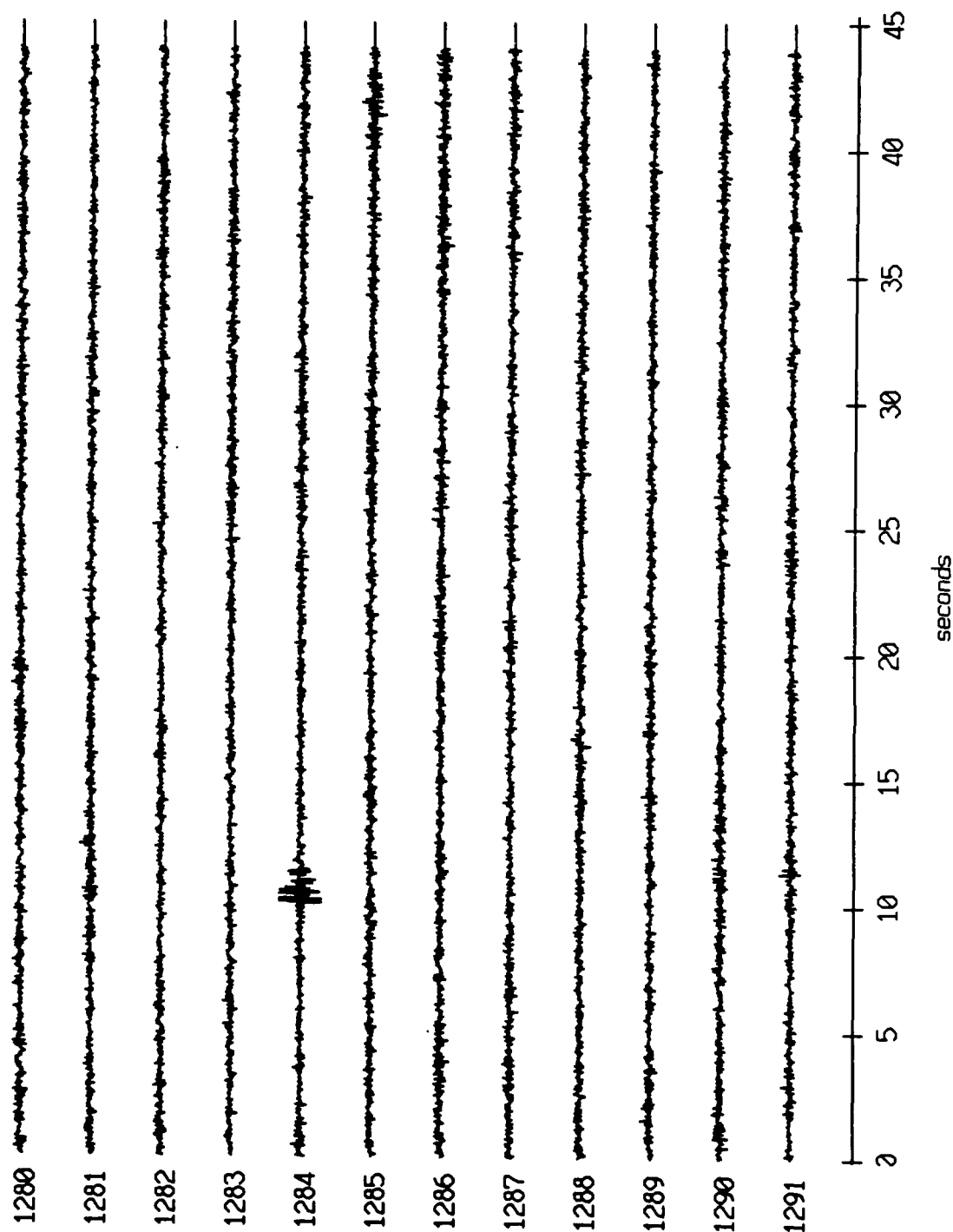
Float 0, July, 1989 Trip - records 1280-1291 (y-axis)  
vertical axis scale is approx. -2.0 to 2.0 volts



AGC corrected channel level (V)

Figure XI.43b

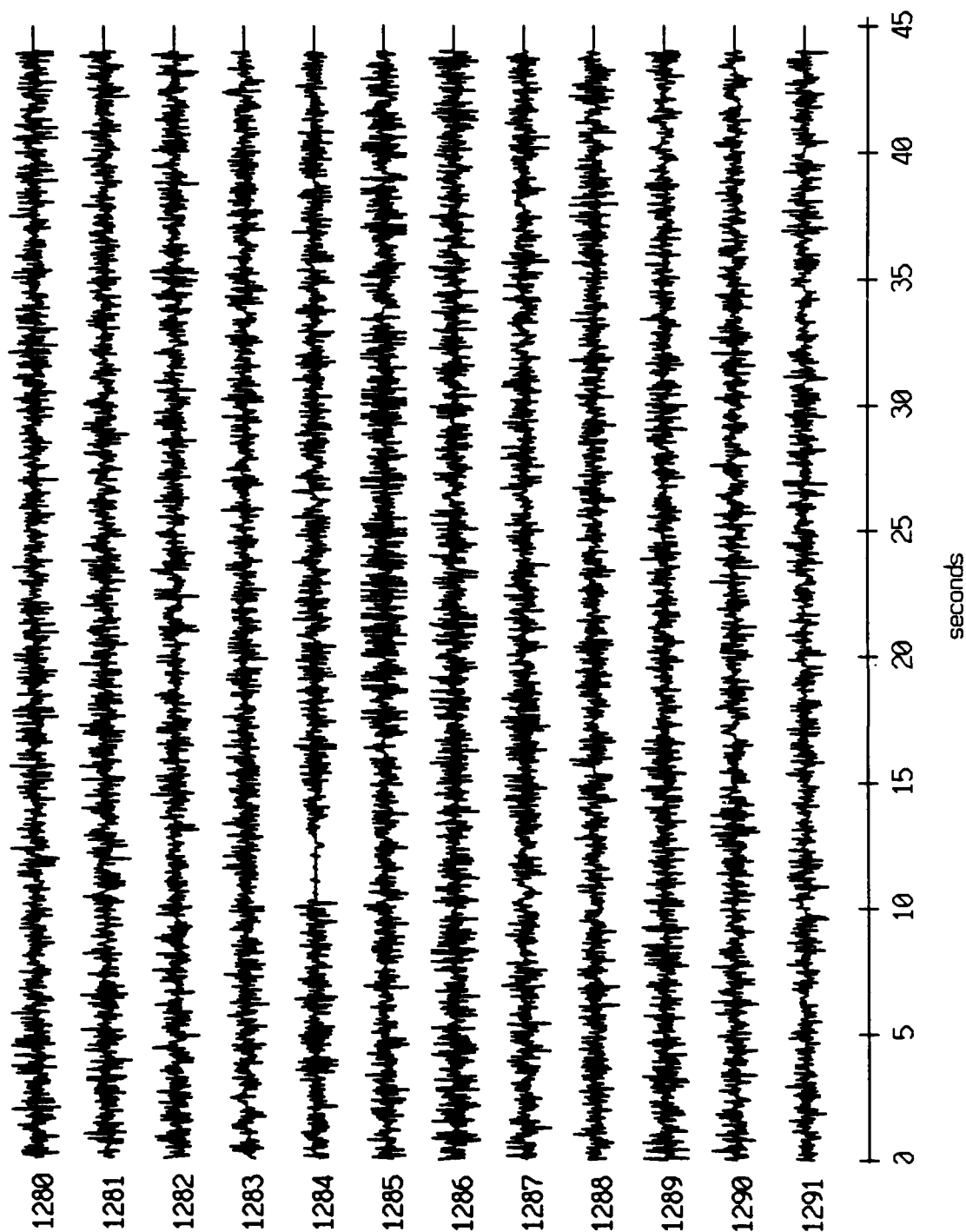
Float 0, July, 1989 Trip - records 1280-1291 (z-axis)  
vertical axis scale is approx. -2.0 to 2.0 volts



HGC corrected channel level (V)

Figure XI.43c

Float 0, July, 1989 Trip - records 1280-1291 (hydrophone)  
vertical axis scale is approx. -2.0 to 2.0 volts

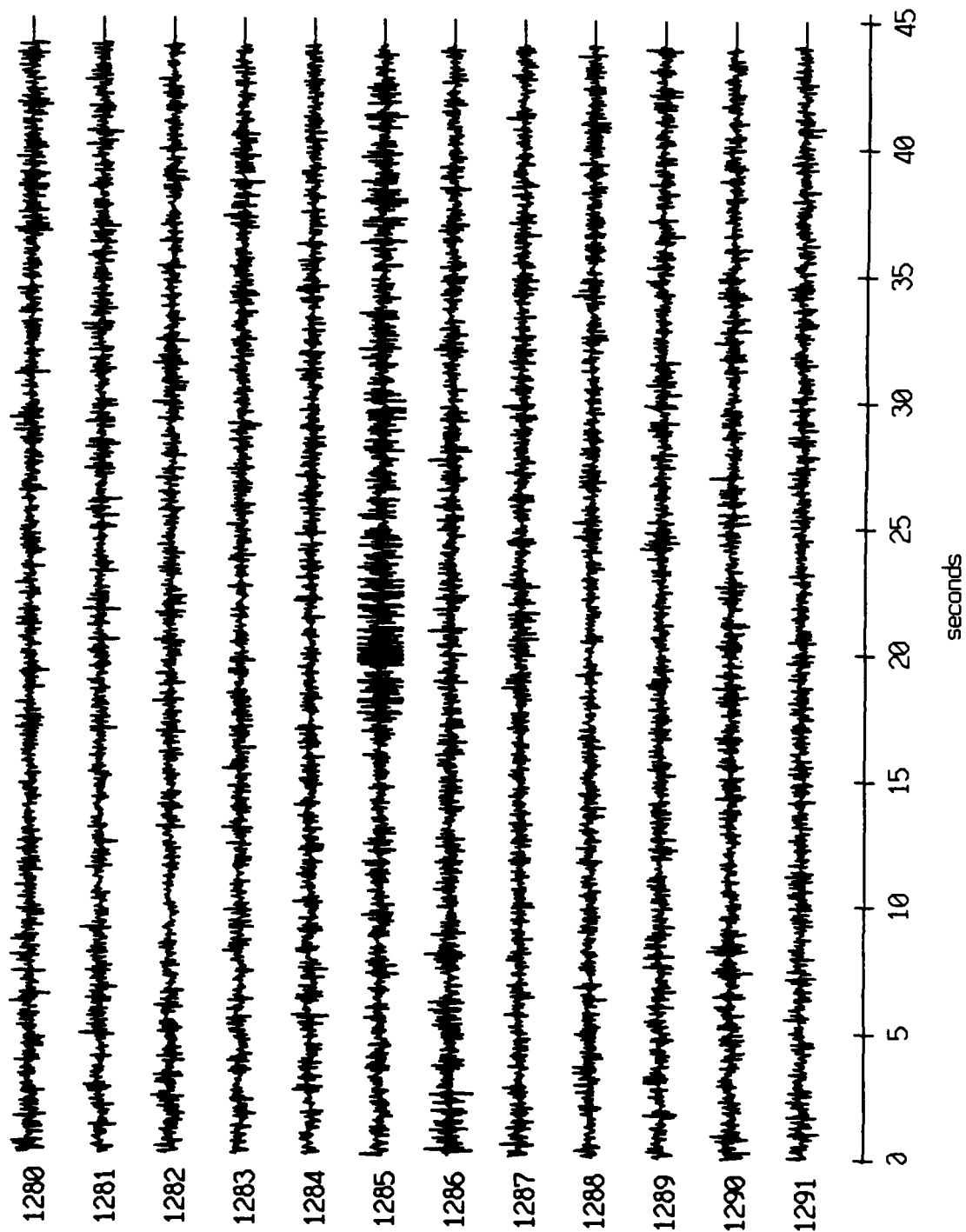


AGC corrected channel level (V)

Figure XI.43d



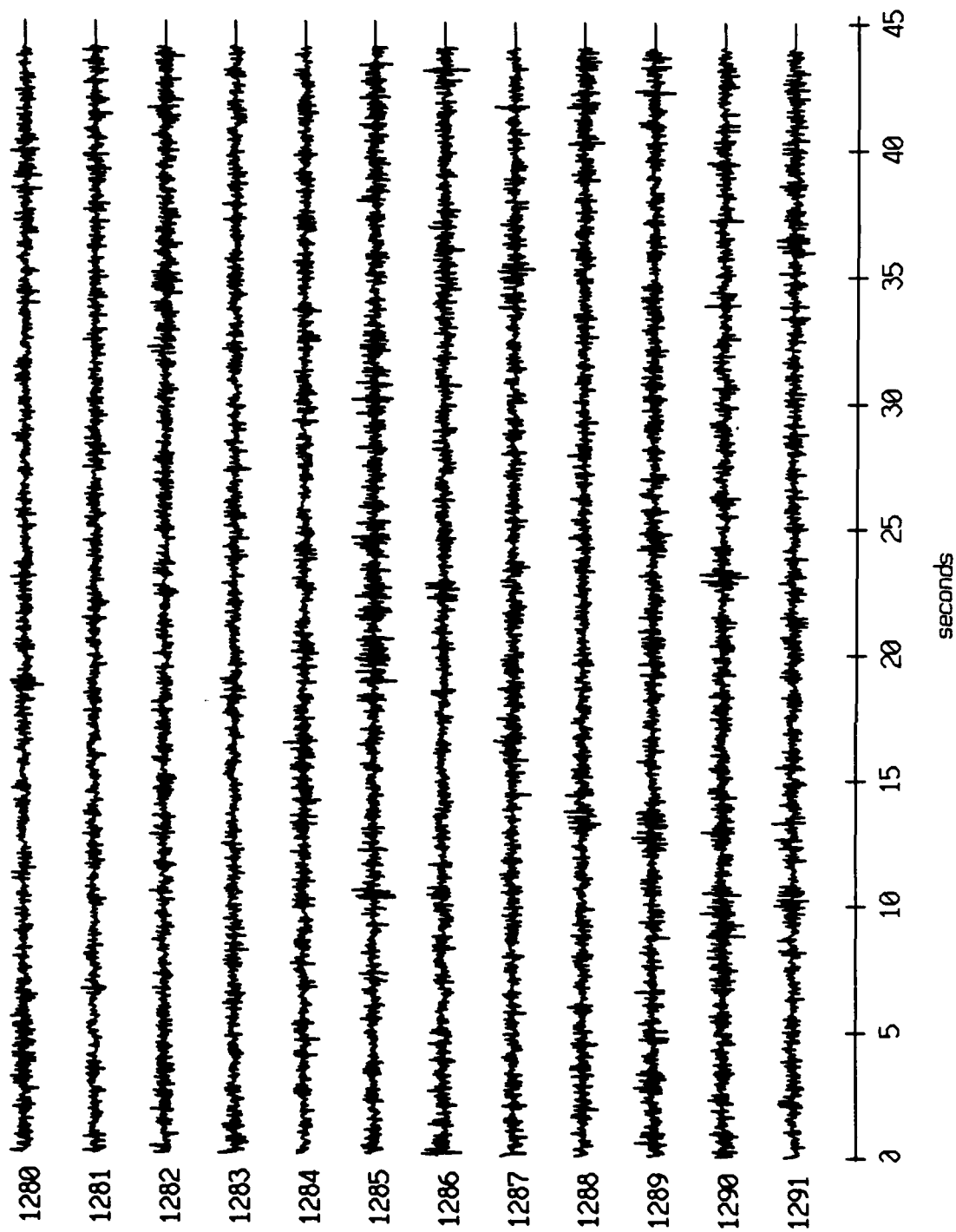
Float 1, July, 1989 Trip - records 1280-1291 (x-axis)  
vertical axis scale is approx. -2.0 to 2.0 volts



PGC corrected channel level (V)

Figure XI.44a

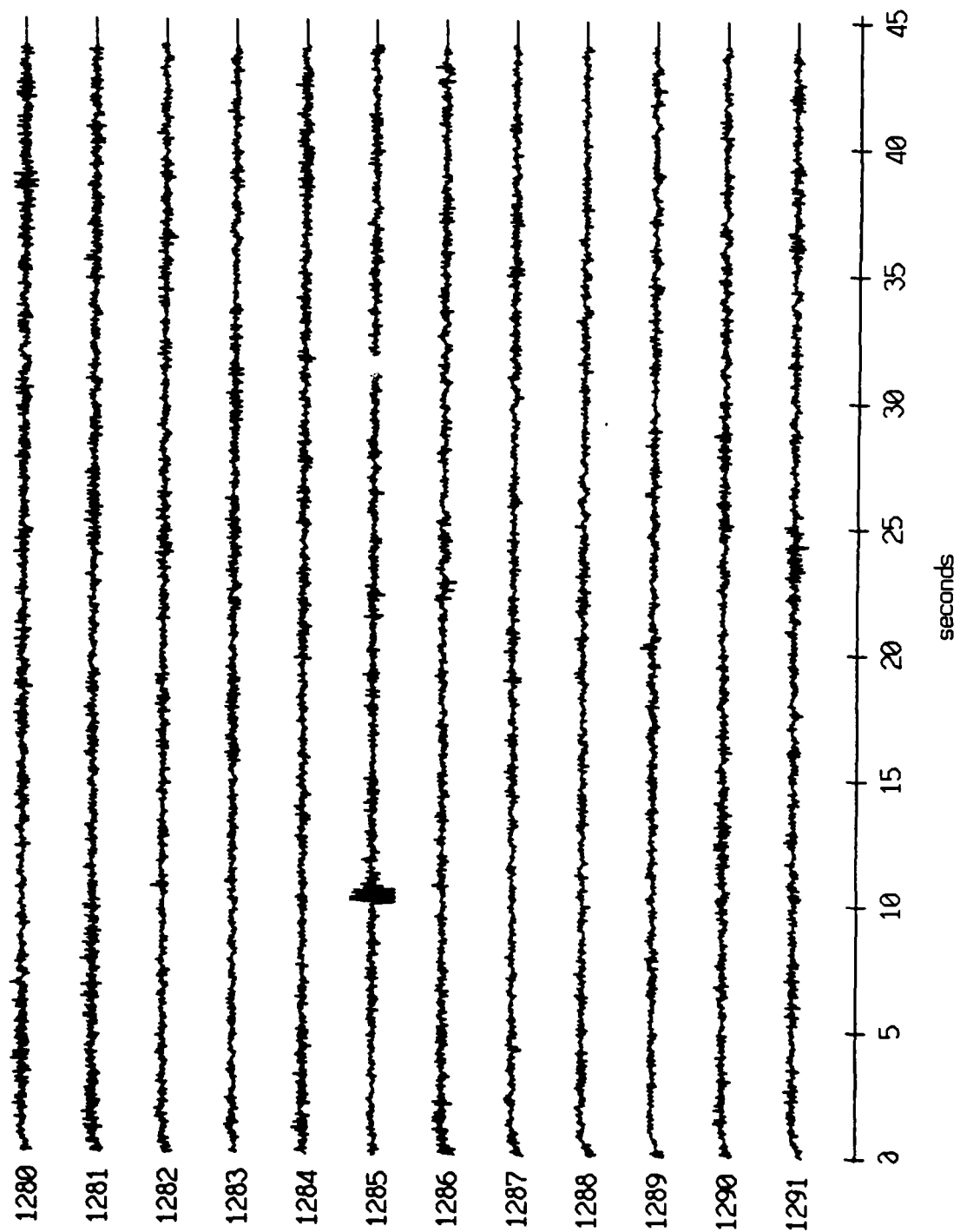
Floot 1, July, 1989 Trip - records 1280-1291 (y-axis)  
vertical axis scale is approx. -2.0 to 2.0 volts



RGC corrected channel level (V)

Figure XI.44b

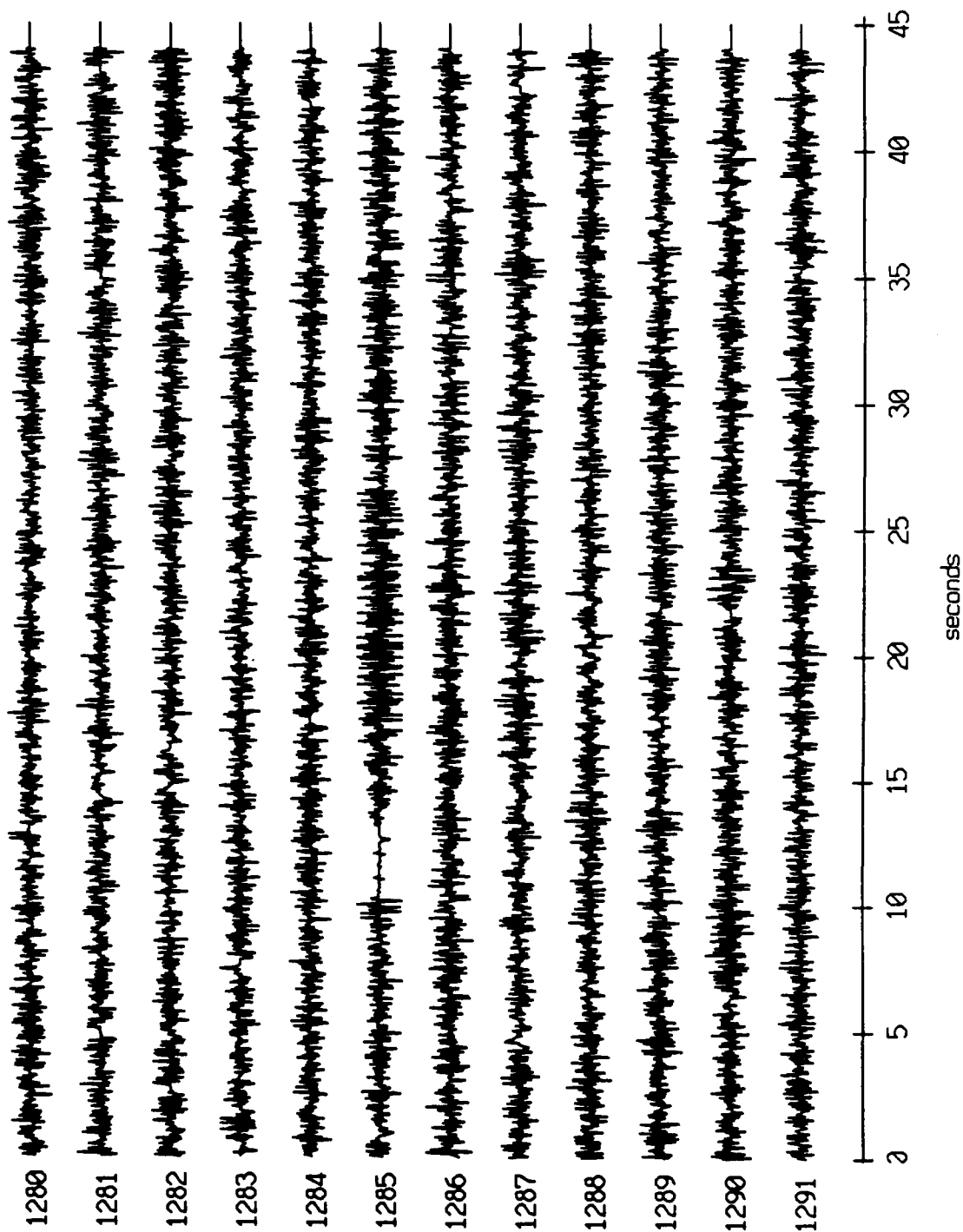
Float 1, July, 1989 Trip - records 1280-1291 (z-axis)  
vertical axis scale is approx. -2.0 to 2.0 volts



HGC corrected channel level (V)

Figure XI.44c

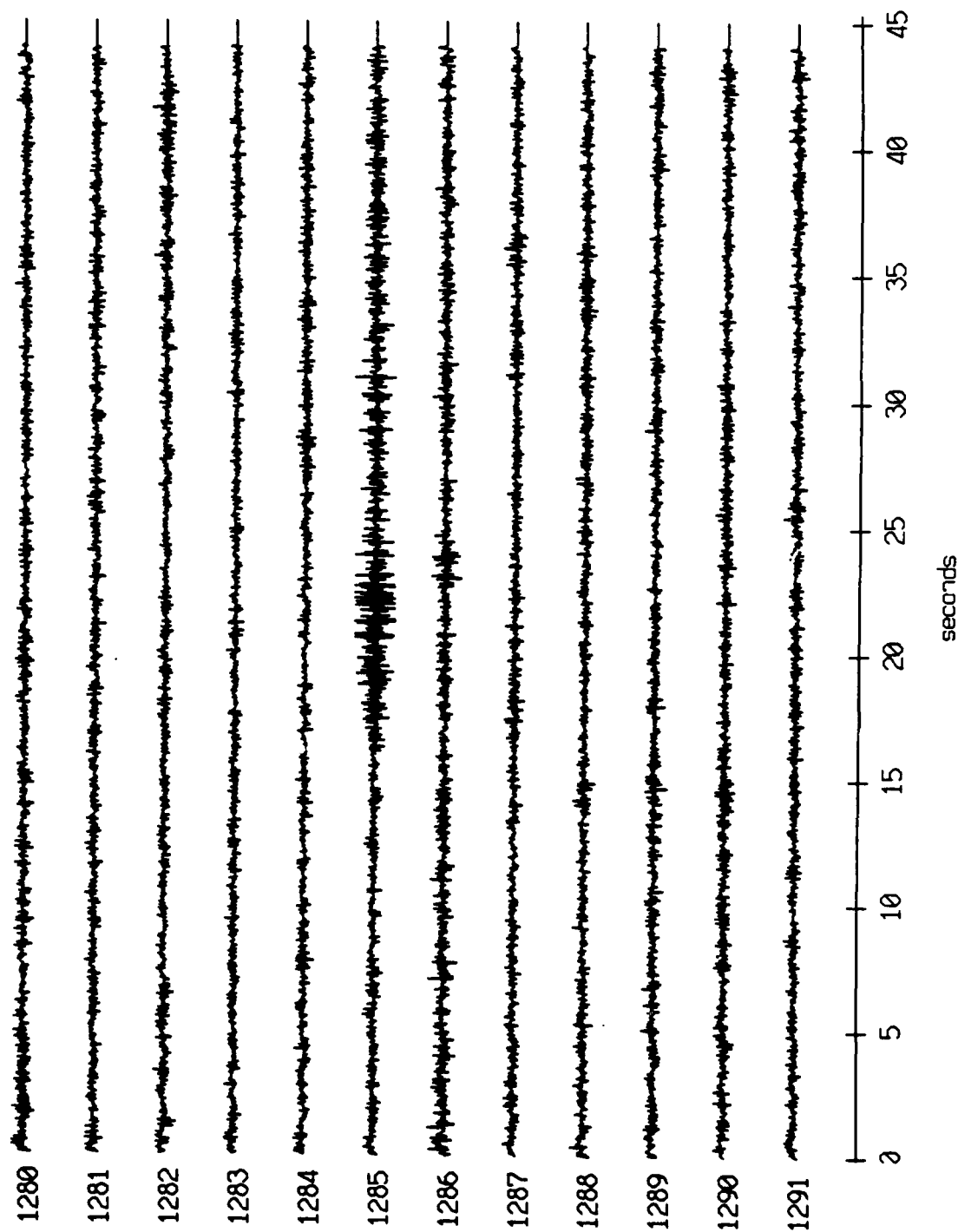
Floot 1, July, 1989 Trip - records 1280-1291 (hydrophone)  
vertical axis scale is approx. -2.0 to 2.0 volts



HGC corrected channel level (V)

Figure XI.44d

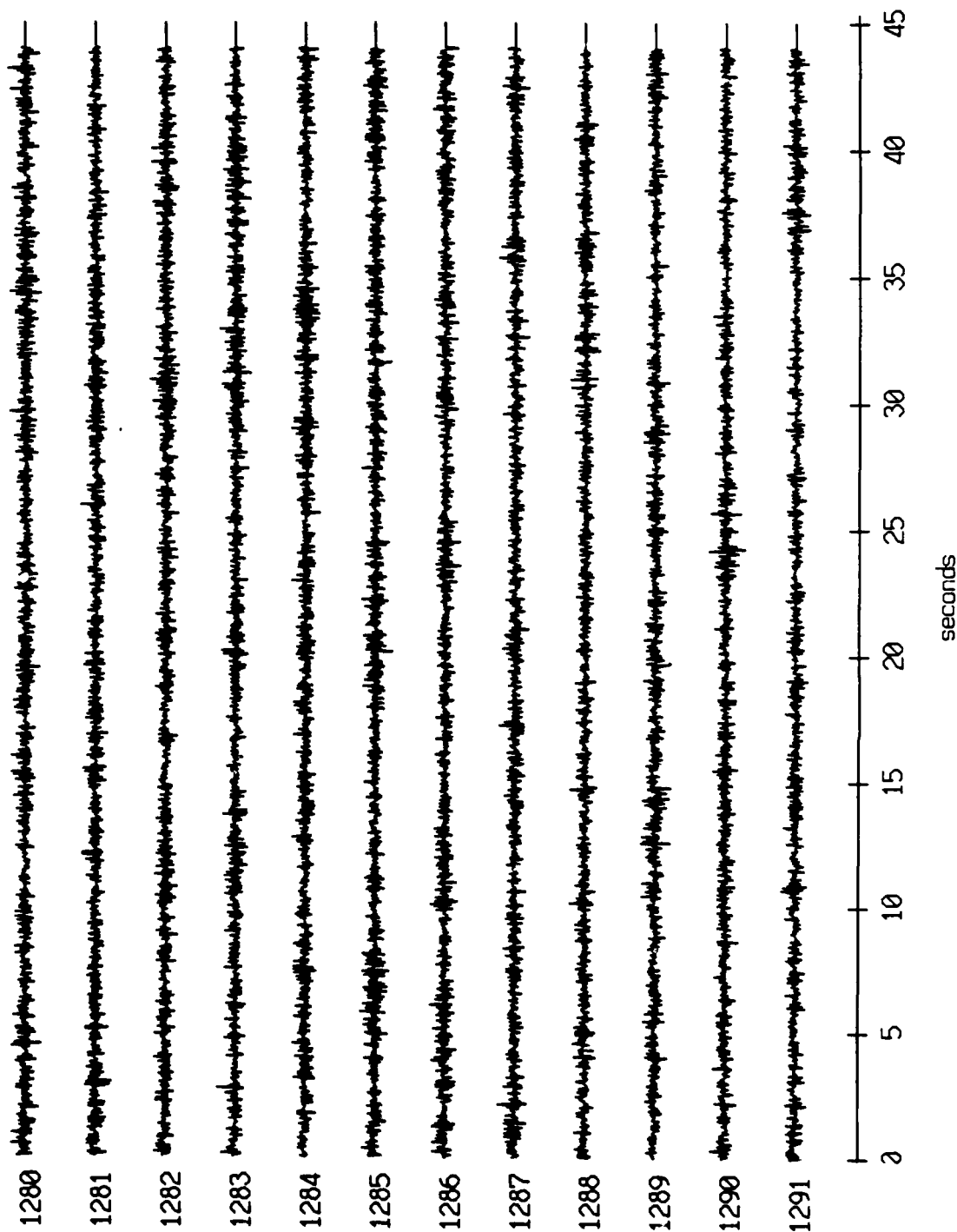
Float 2, July, 1989 Trip - records 1280-1291 (x-axis)  
vertical axis scale is approx. -2.0 to 2.0 volts



HGC corrected channel level (V)

Figure XI.45a

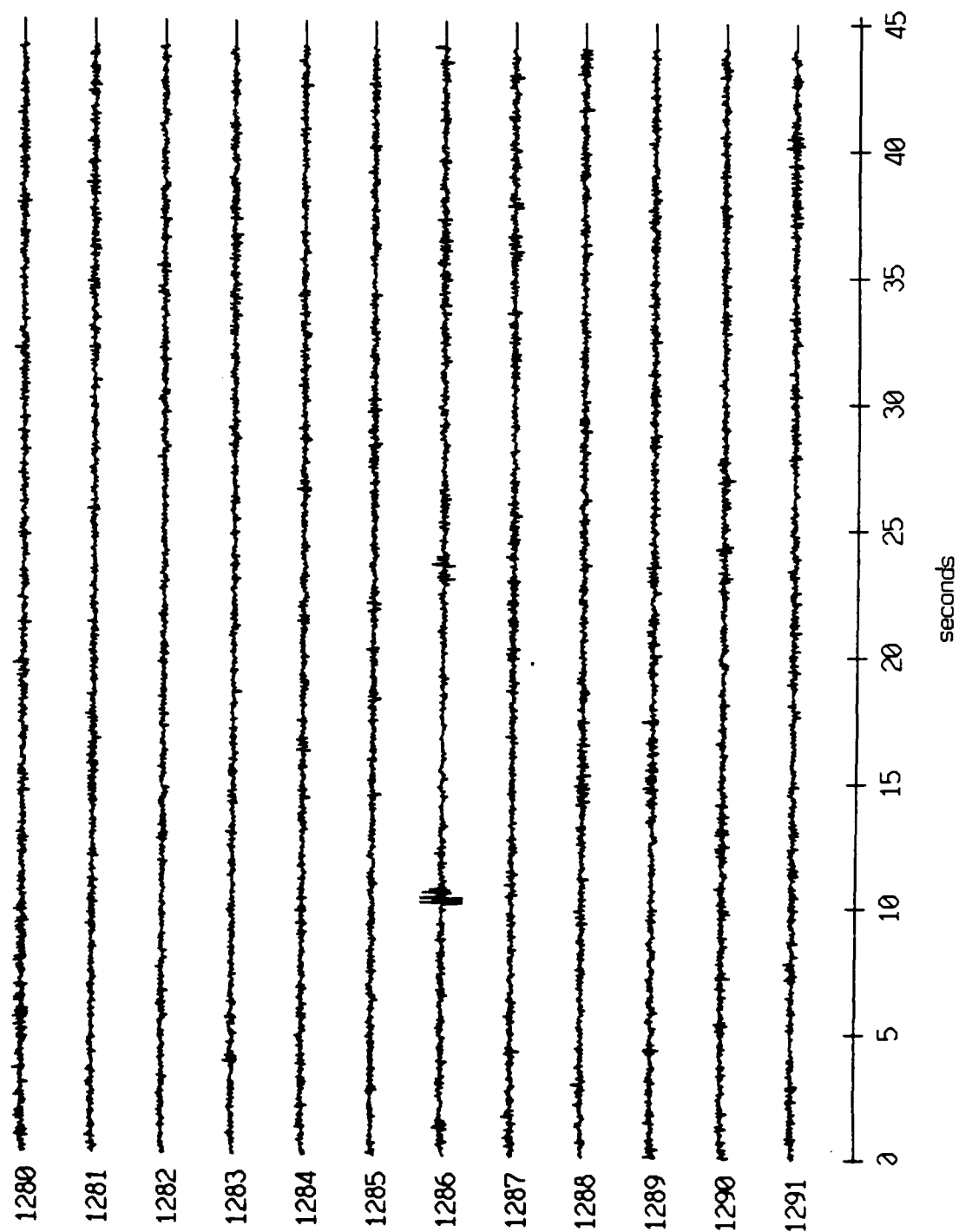
Float 2, July, 1989 Trip - records 1280-1291 (y-axis)  
vertical axis scale is approx. -2.0 to 2.0 volts



HGC corrected channel level (V)

Figure XI.45b

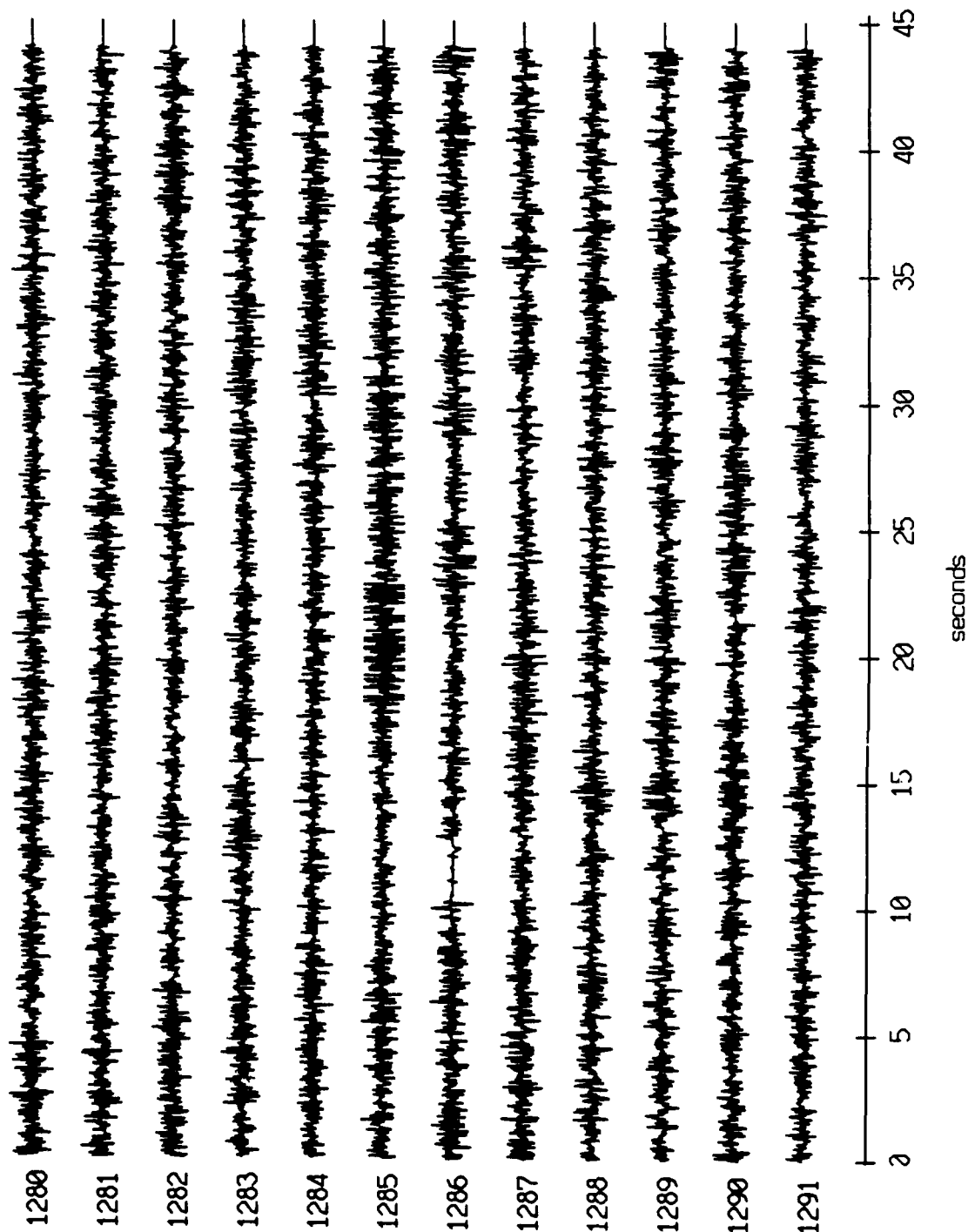
Float 2, July, 1989 Trip - records 1280-1291 (z-axis)  
vertical axis scale is approx. -2.0 to 2.0 volts



HGC corrected channel level (V)

Figure XI.45c

Float 2, July, 1989 Trip - records 1280-1291 (hydrophone)  
vertical axis scale is approx. -2.0 to 2.0 volts

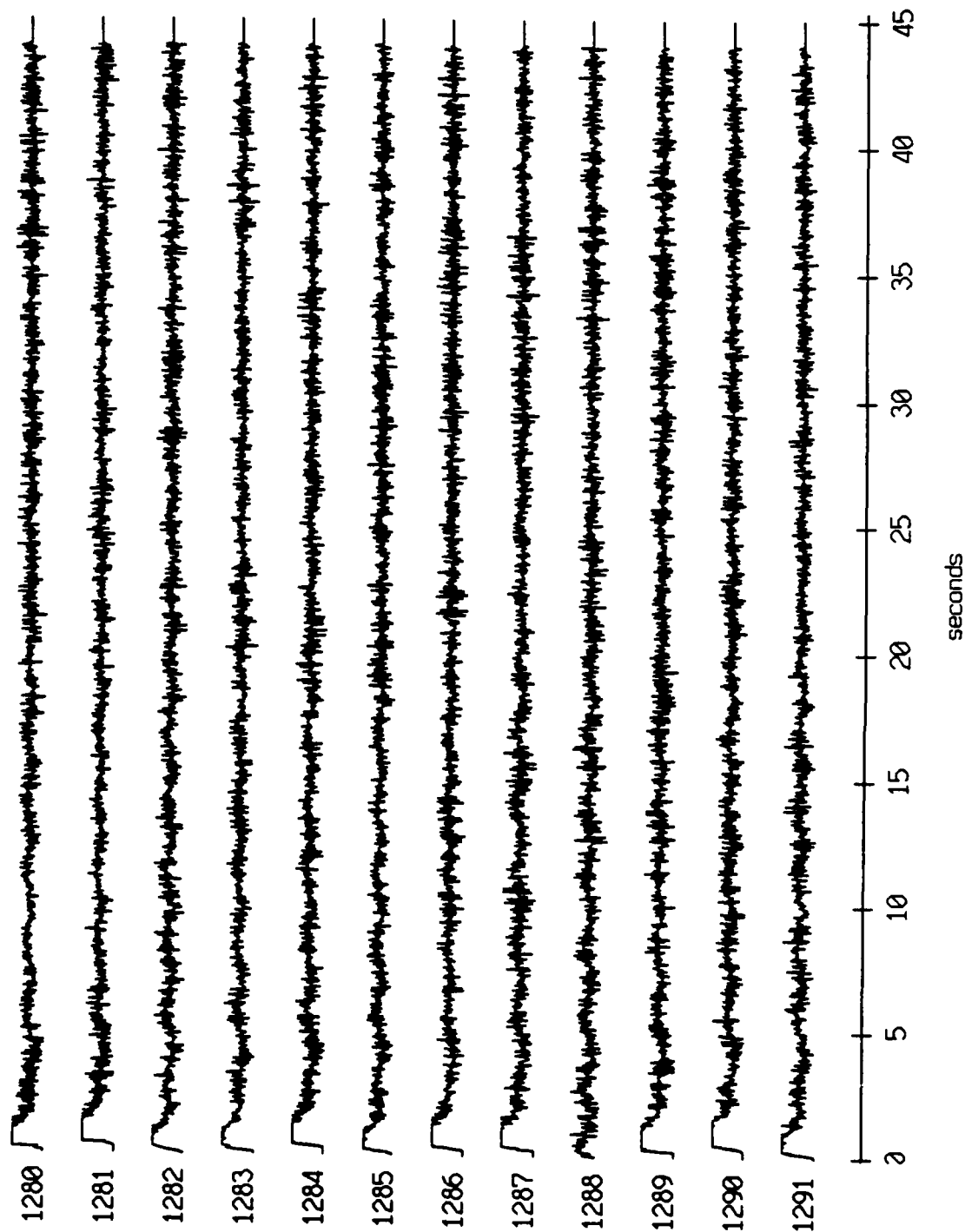


AGC corrected channel level (V)

Figure XI.45d



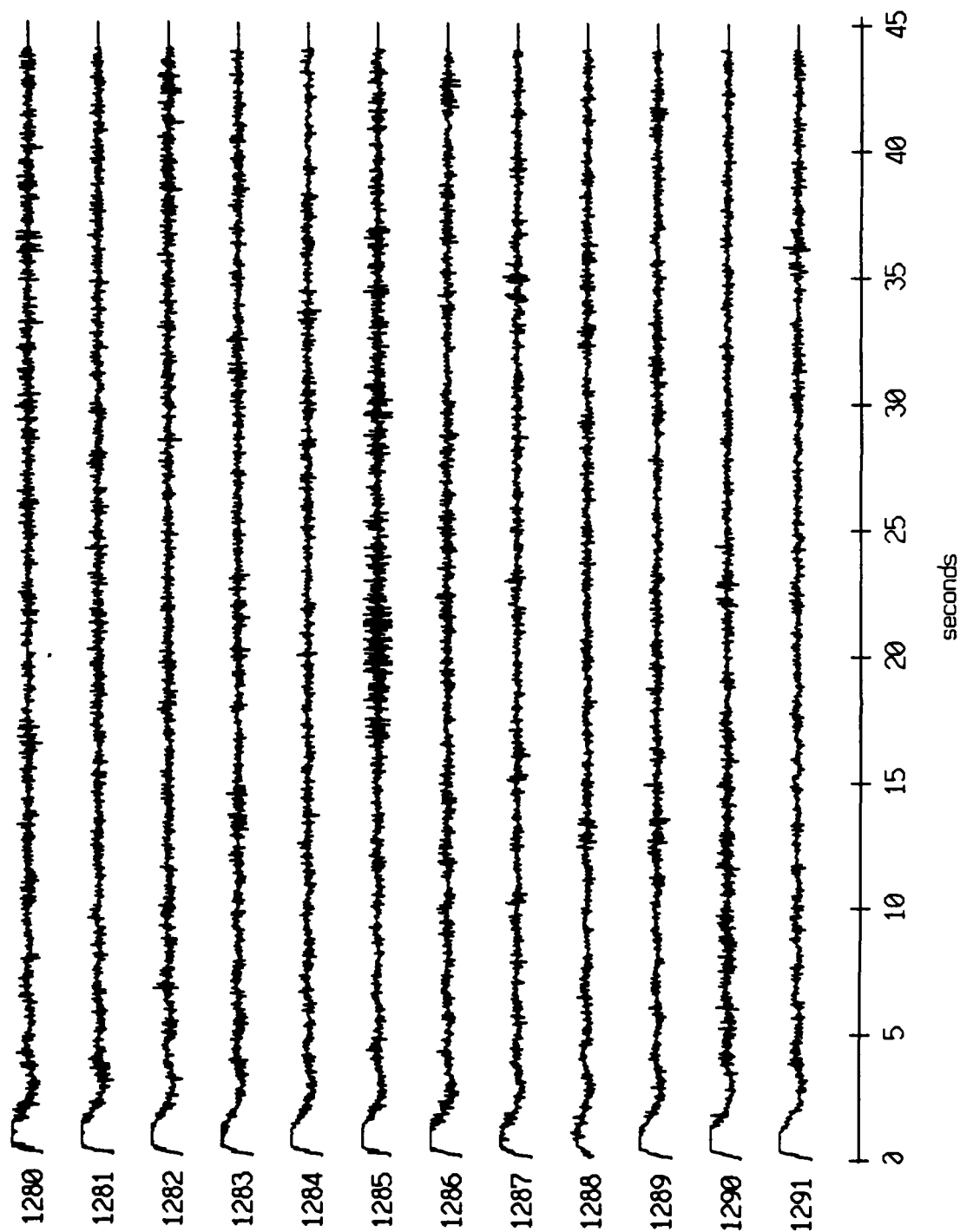
Float 3, July, 1989 Trip - records 1280-1291 (x-axis)  
vertical axis scale is approx. -2.0 to 2.0 volts



PGC corrected channel level (V)

Figure XI.46a

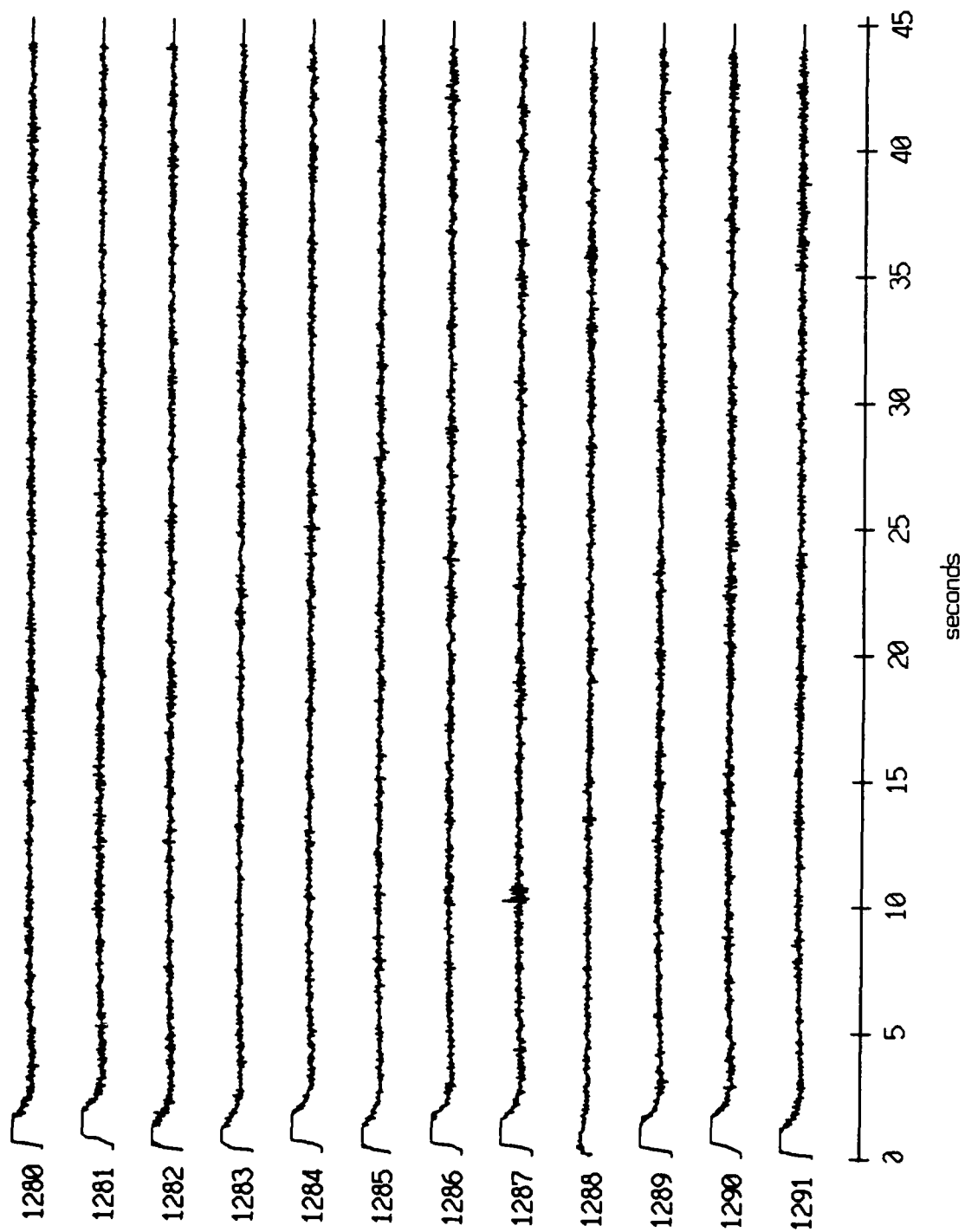
Float 3, July, 1989 Trip - records 1280-1291 (y-axis)  
vertical axis scale is approx. -2.0 to 2.0 volts



AGC corrected channel level (V)

Figure XI.46b

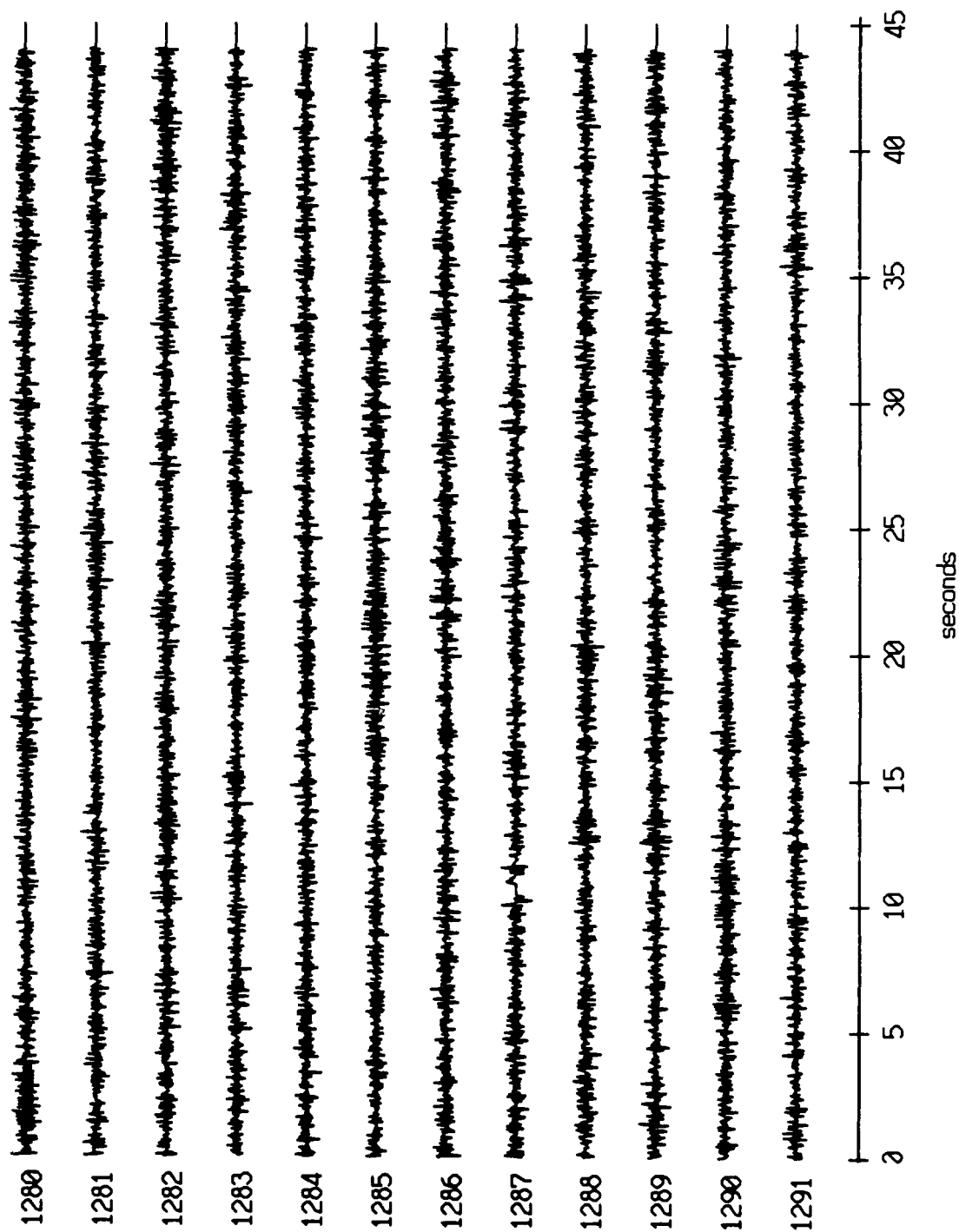
Float 3, July, 1989 Trip - records 1280-1291 (z-axis)  
vertical axis scale is approx. -2.0 to 2.0 volts



PGC corrected channel level (V)

Figure XI.46c

Float 3, July, 1989 Trip - records 1280-1291 (hydrophone)  
vertical axis scale is approx. -2.0 to 2.0 volts



AGC corrected channel level (V)

Figure XI.46d

Floot 0, July, 1989 Trip - records 1530-1541 (x-axis)  
 vertical axis scale is approx. -2.0 to 2.0 volts

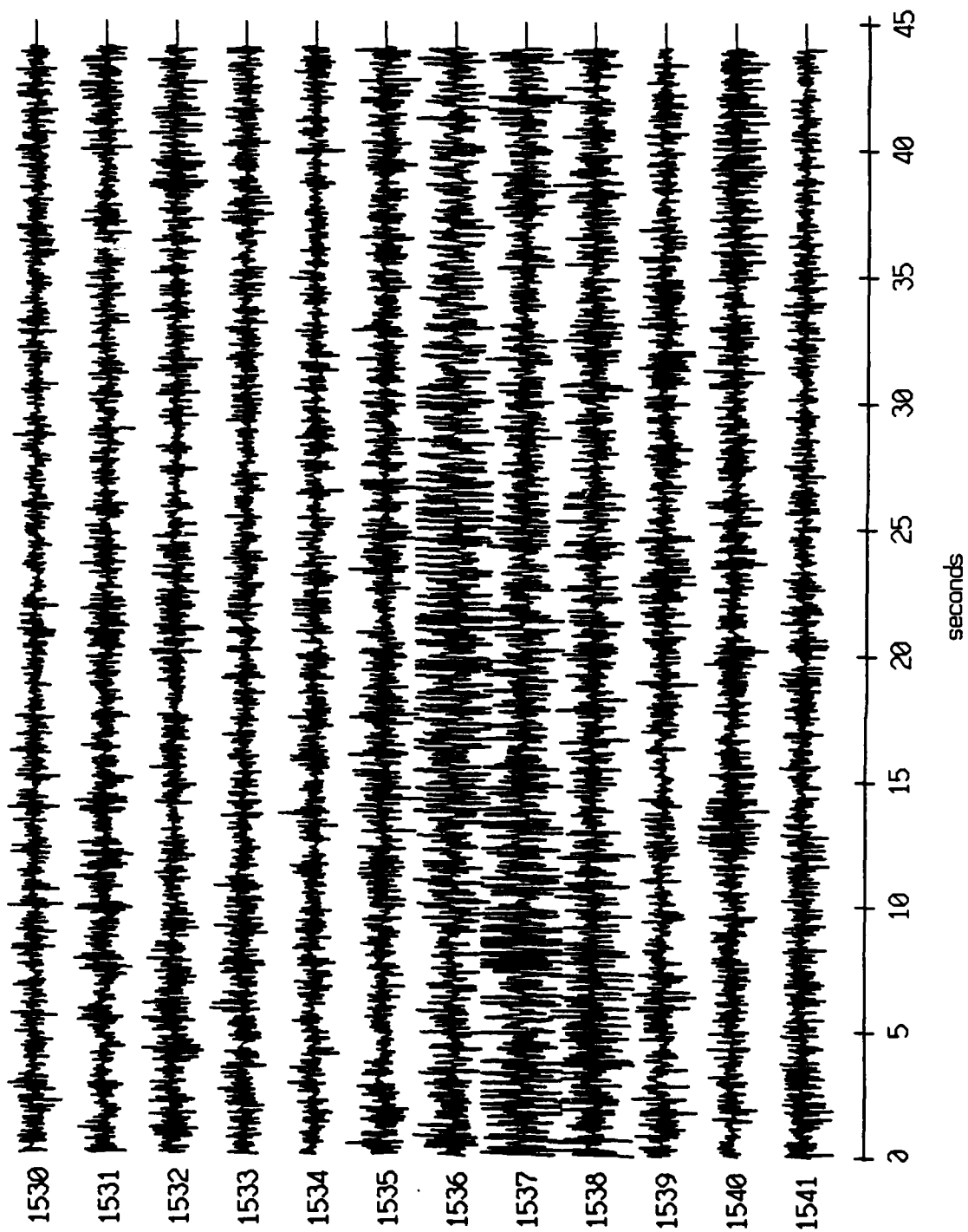
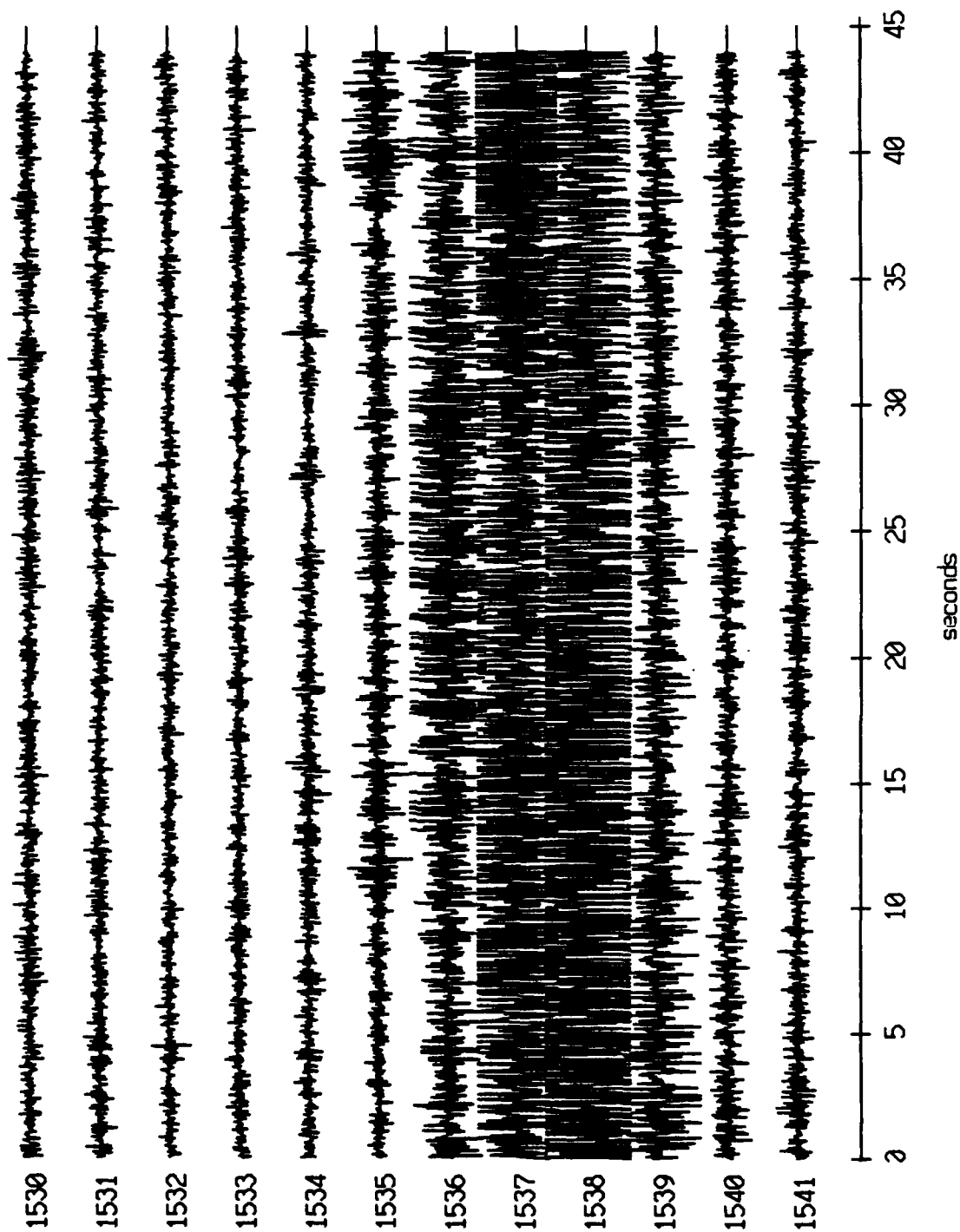


Figure XI.47a

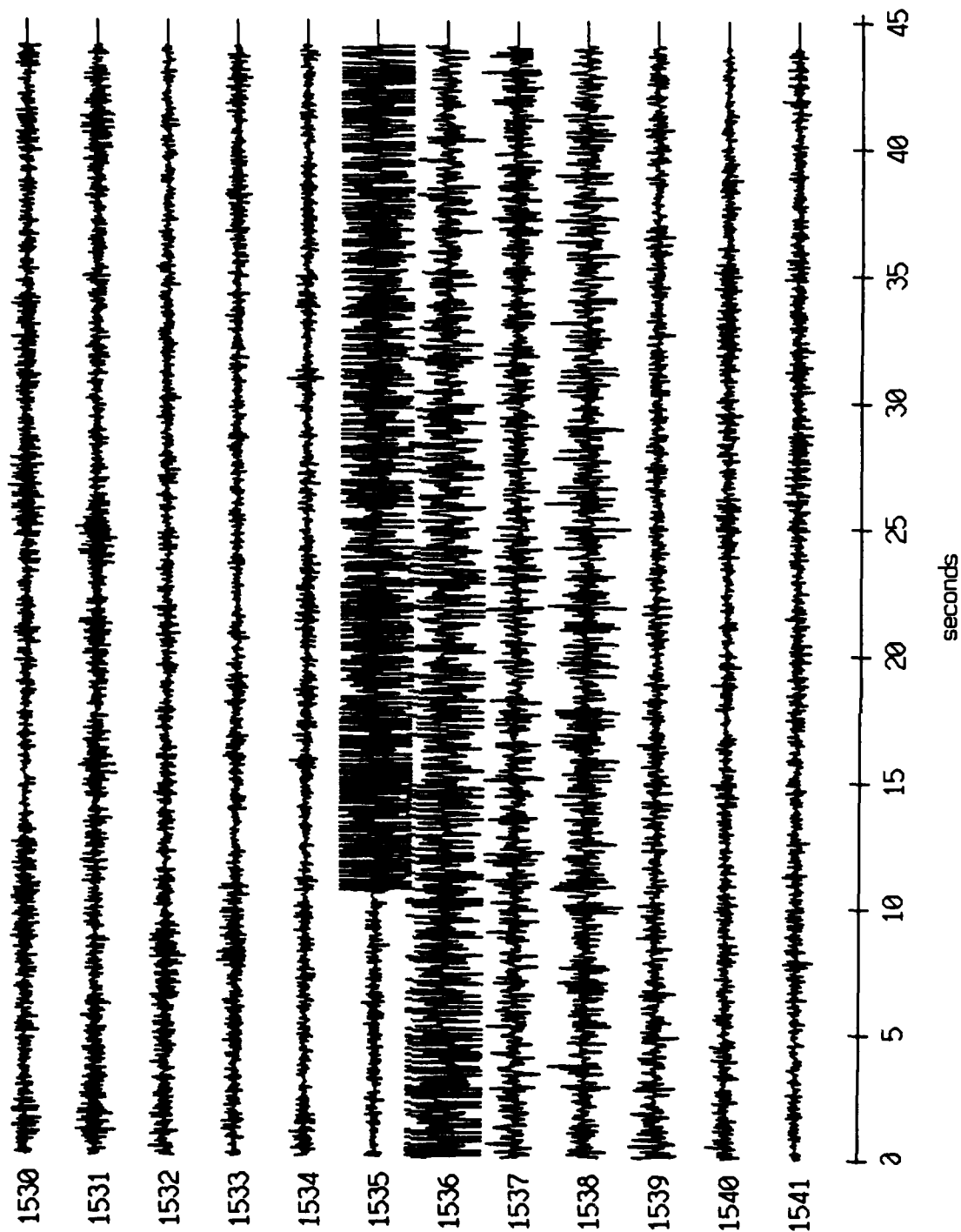
Floot 0, July, 1989 Trip - records 1530-1541 (y-axis)  
vertical axis scale is approx. -2.0 to 2.0 volts



HGC corrected channel level (V)

Figure XI.47b

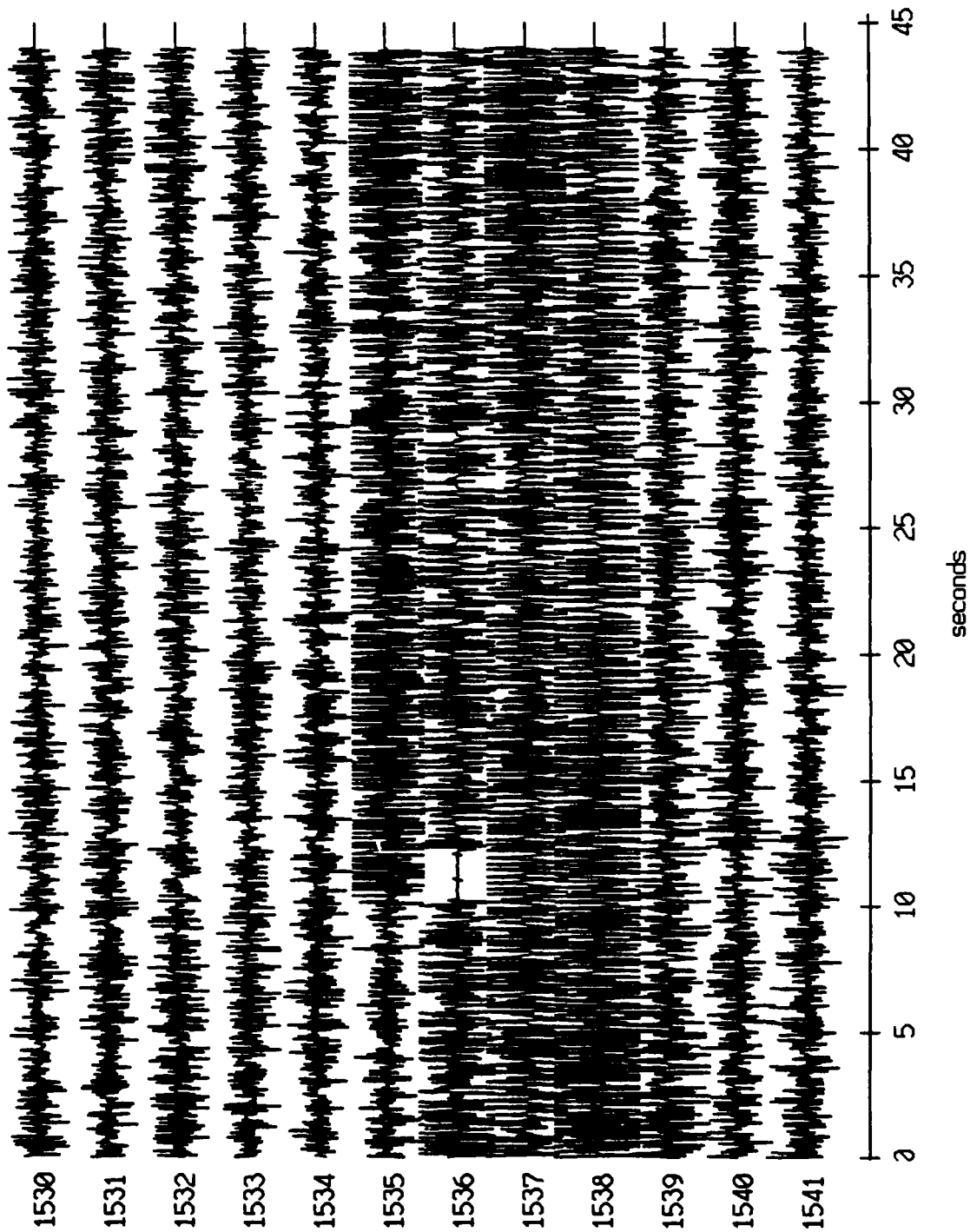
Floot 0, July, 1989 Trip - records 1530-1541 (z-axis)  
vertical axis scale is approx. -2.0 to 2.0 volts



RGC corrected channel level (V)

Figure XI.47c

Float 0, July, 1989 Trip - records 1530-1541 (hydrophone)  
 vertical axis scale is approx. -2.0 to 2.0 volts

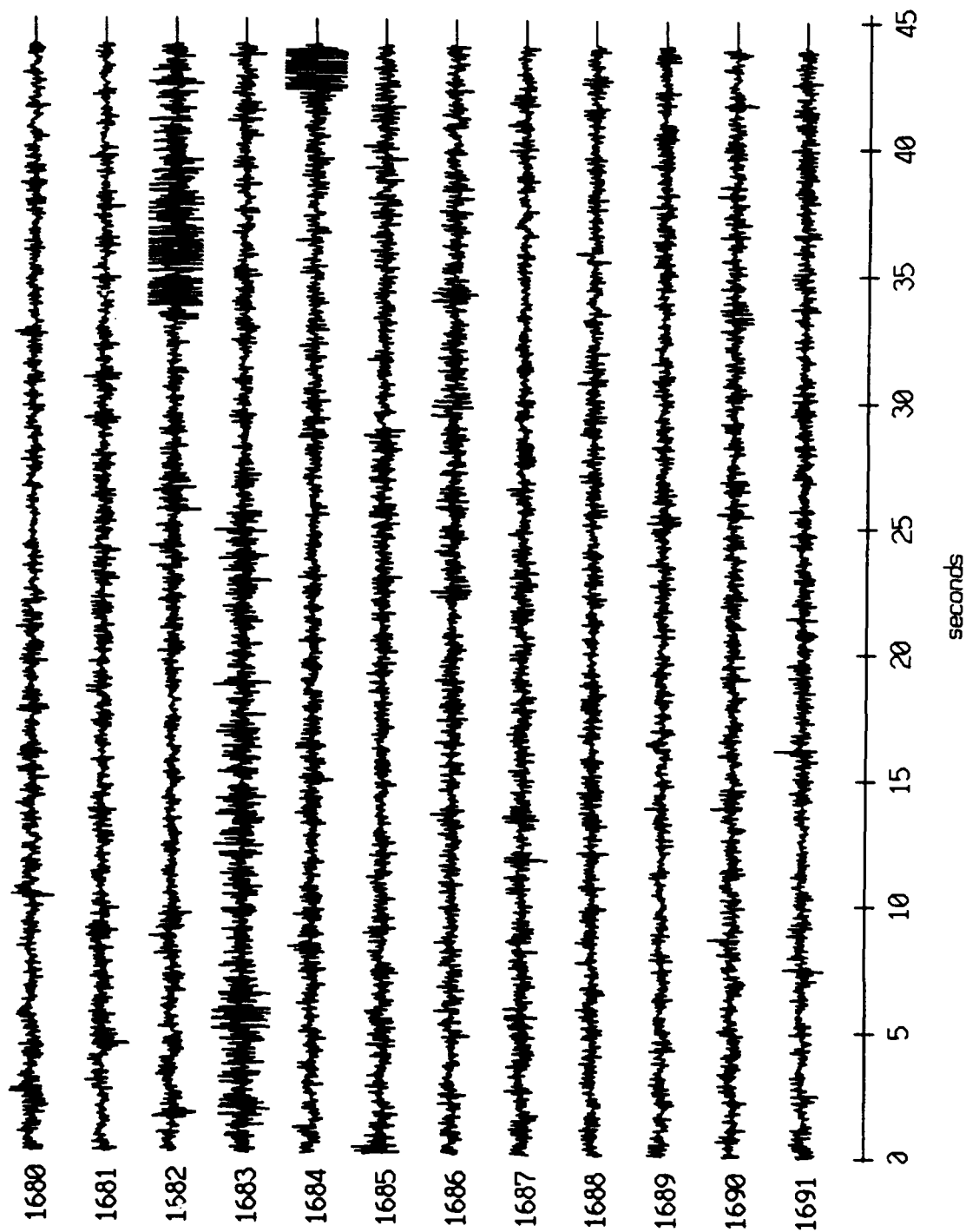


RGC corrected channel level (V)

Figure XI.47d



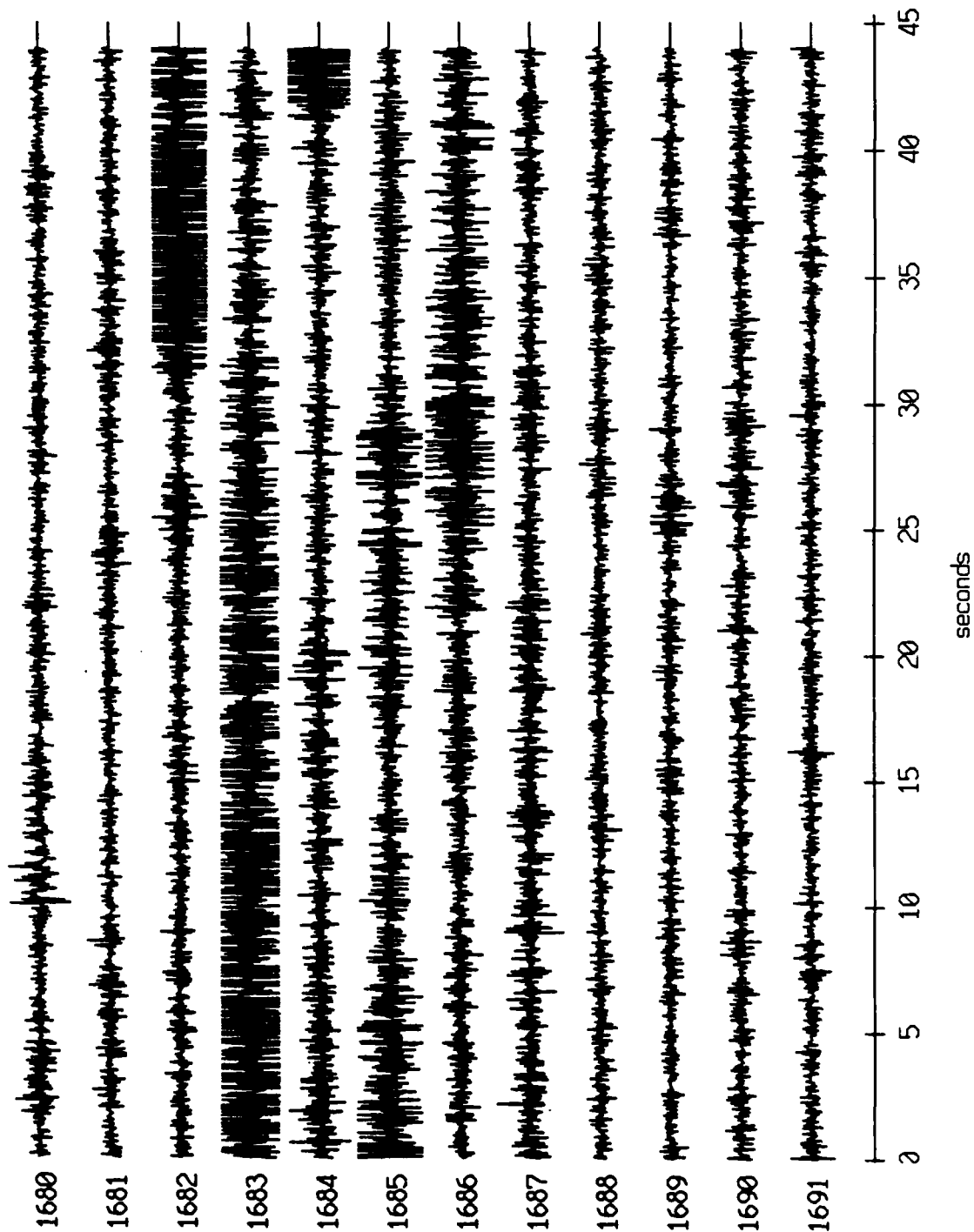
Float 0, July, 1989 Trip - records 1680-1691 (x-axis)  
vertical axis scale is approx. -2.0 to 2.0 volts



RGC corrected channel level (V)

Figure XI.48a

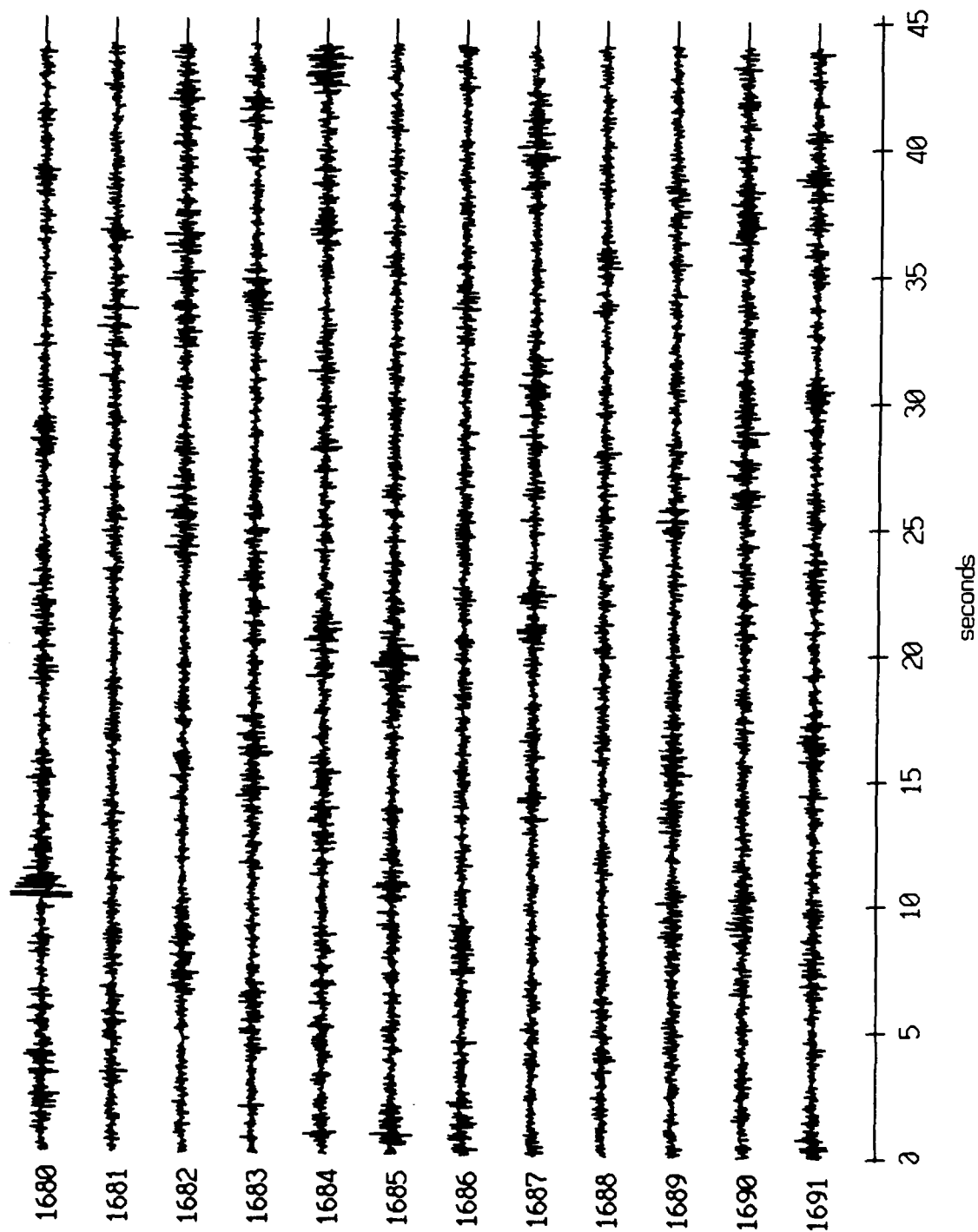
Float 0, July, 1989 Trip - records 1680-1691 (y-axis)  
vertical axis scale is approx. -2.0 to 2.0 volts



PGC corrected channel level (V)

Figure XI.48b

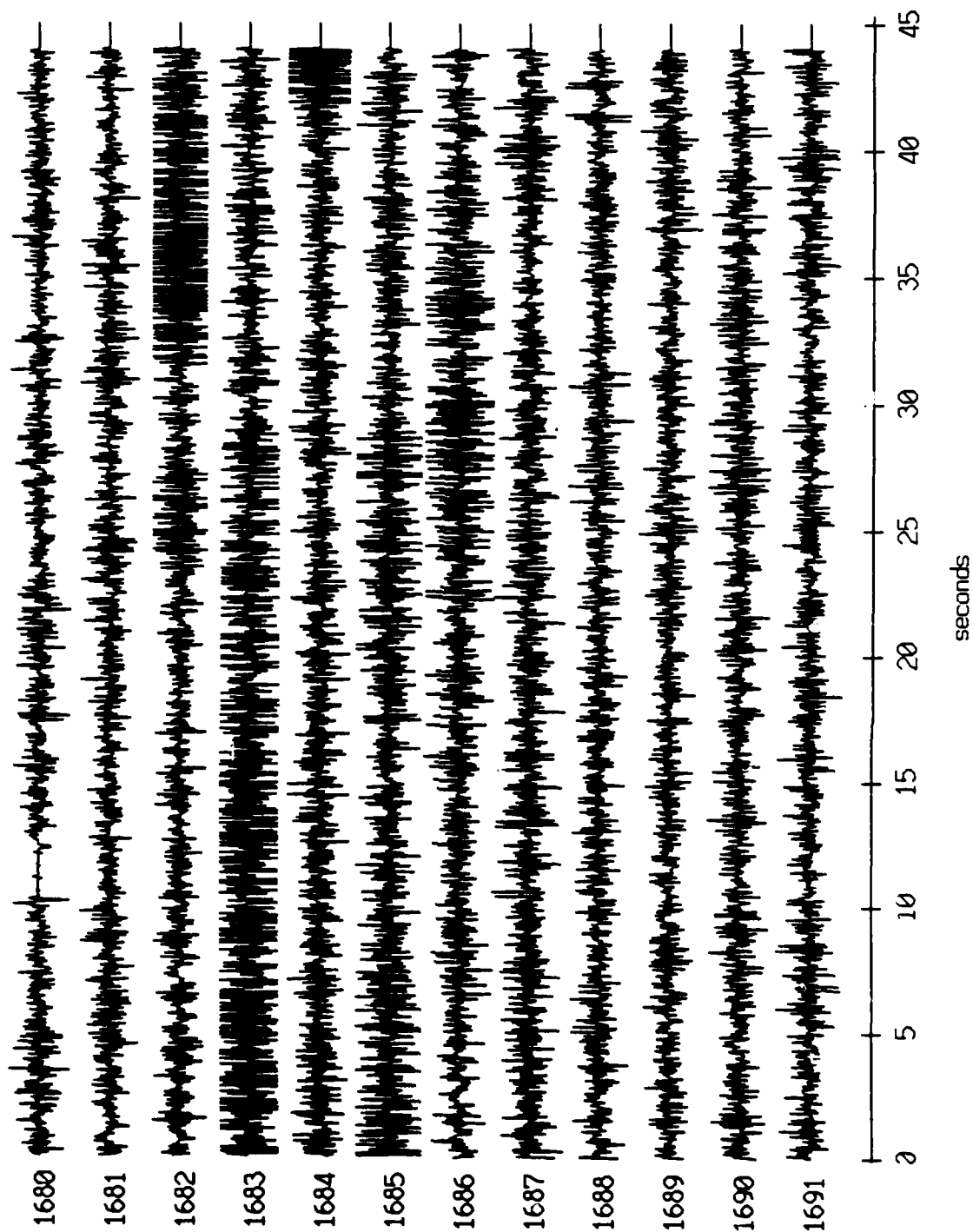
Floot 0, July, 1989 Trip - records 1680-1691 (z-axis)  
vertical axis scale is approx. -2.0 to 2.0 volts



PGC corrected channel level (V)

Figure XI.48c

Float 0, July, 1989 Trip - records 1680-1691 (hydrophone)  
vertical axis scale is approx. -2.0 to 2.0 volts



AGC corrected channel level (V)

Figure XI.48d

Float 1, July, 1989 Trip - records 1680-1691 (x-axis)  
vertical axis scale is approx. -2.0 to 2.0 volts

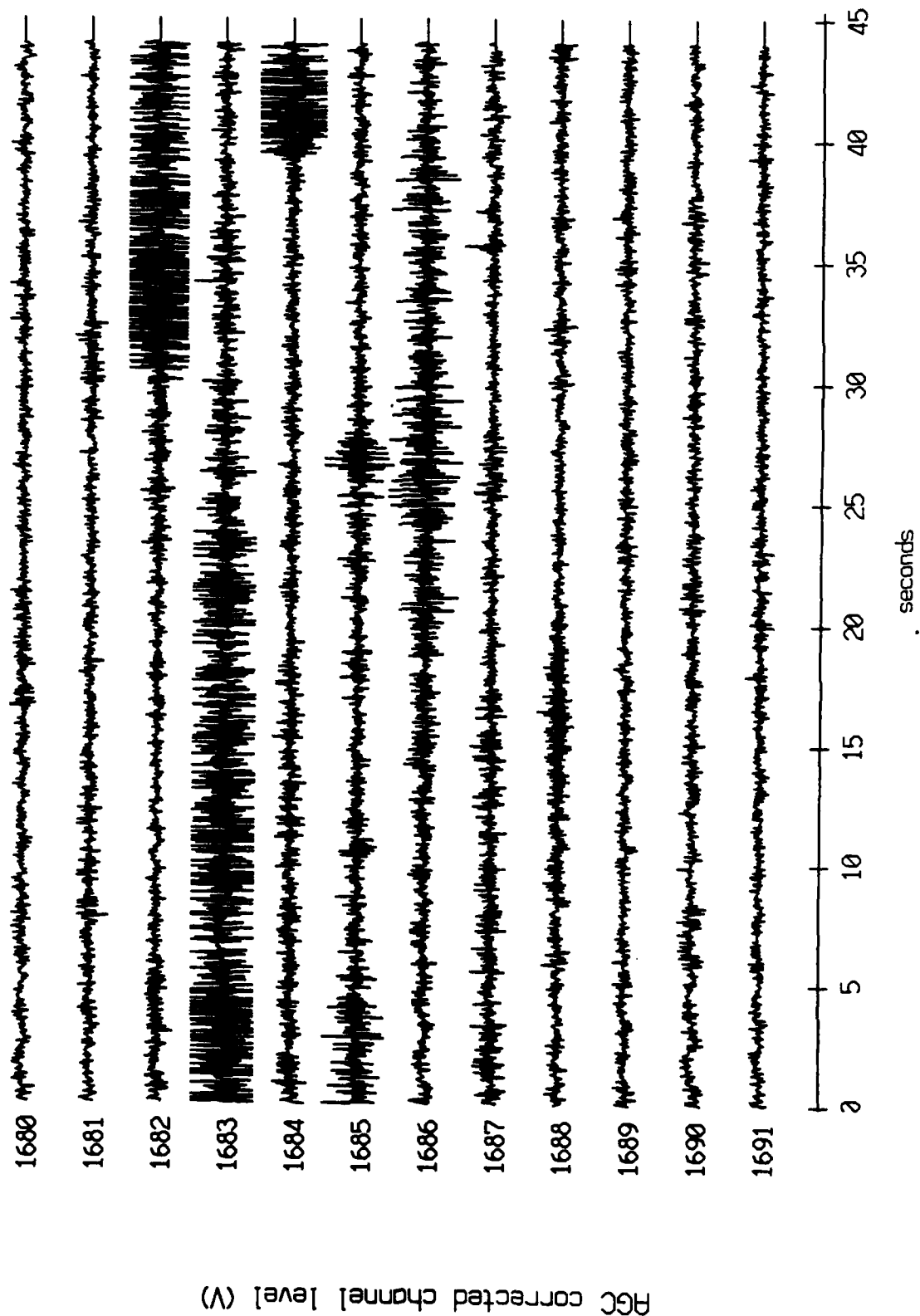
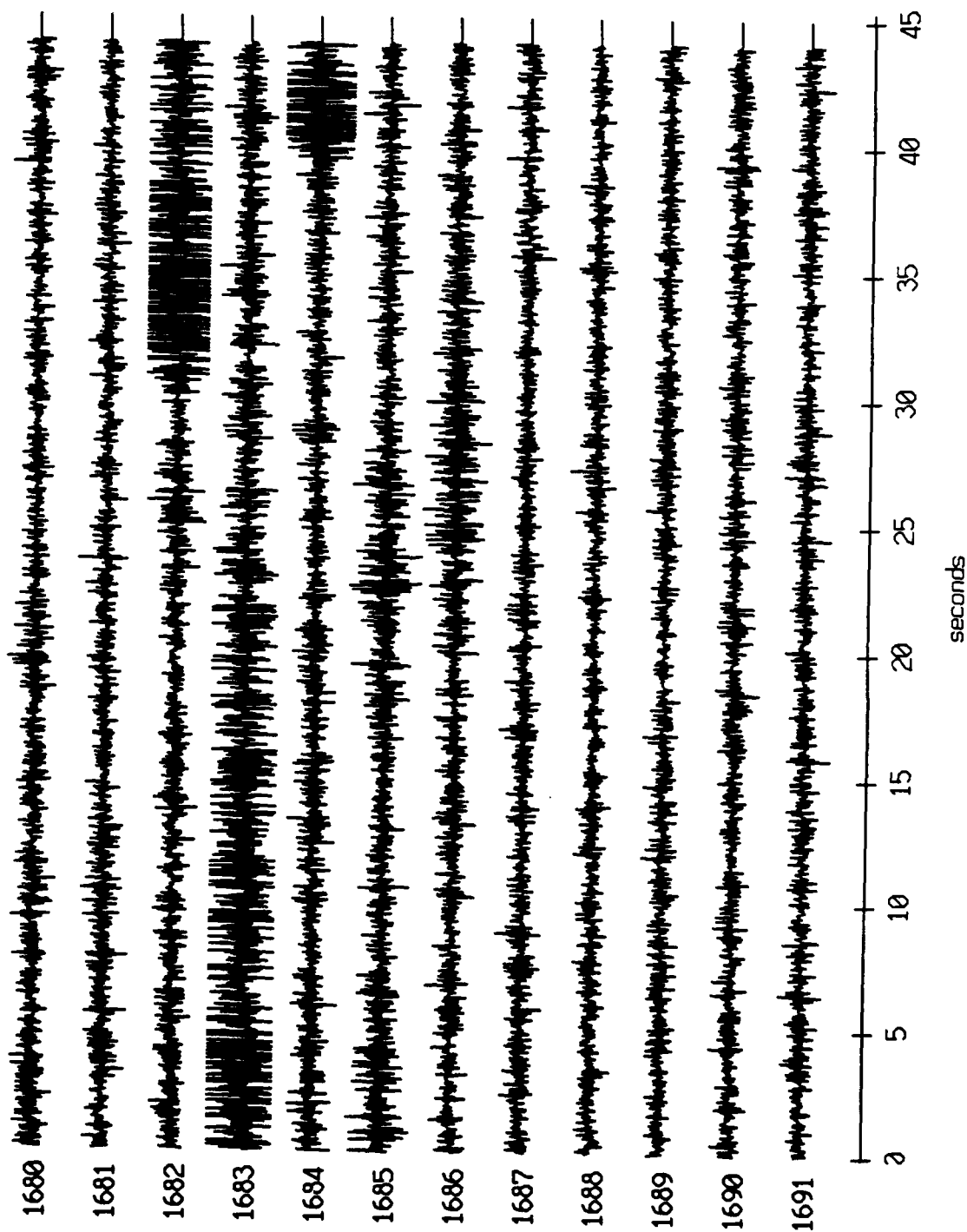


Figure XI.49a

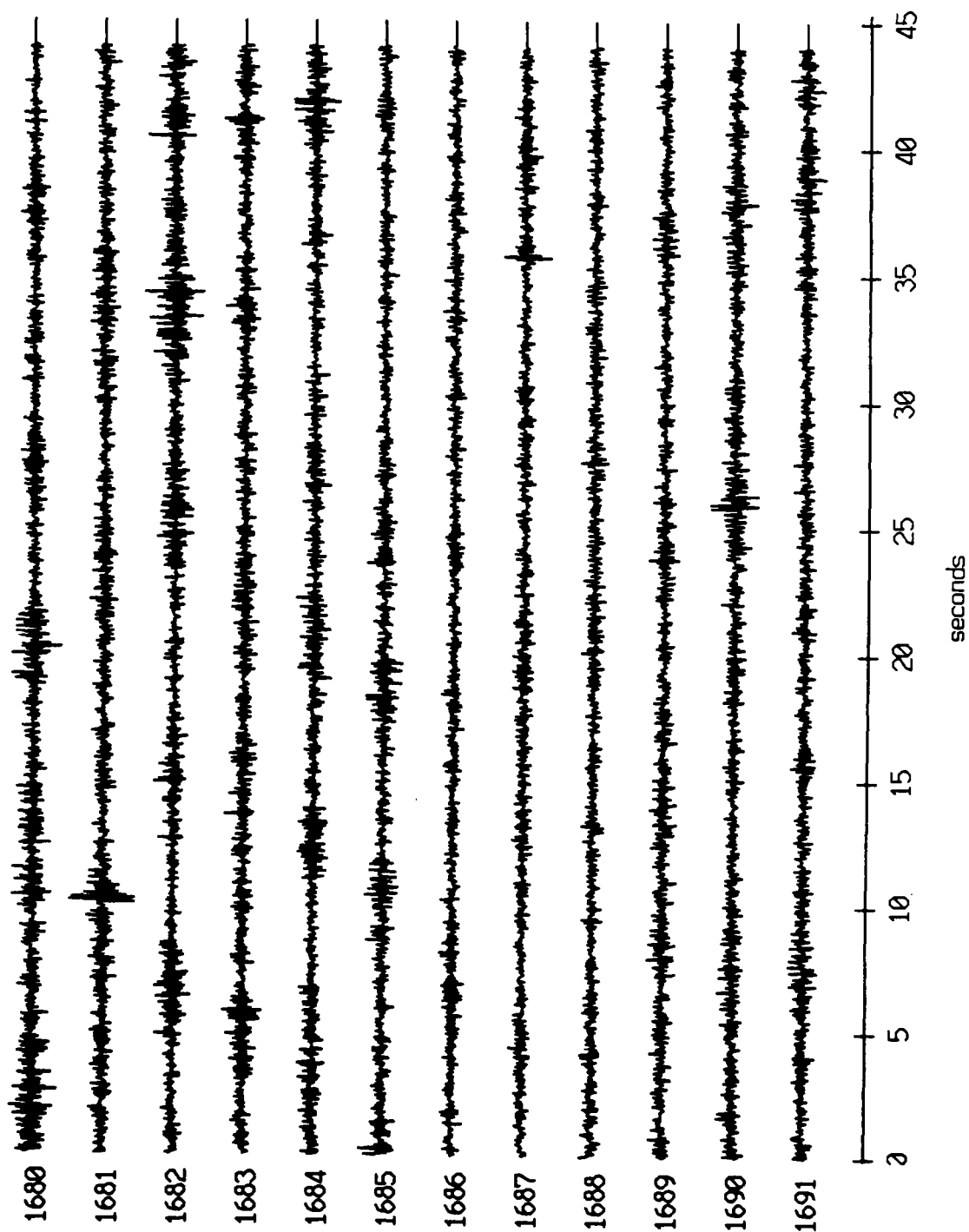
Float 1, July, 1989 Trip - records 1680-1691 (y-axis)  
vertical axis scale is approx. -2.0 to 2.0 volts



AGC corrected channel level (V)

Figure XI.49b

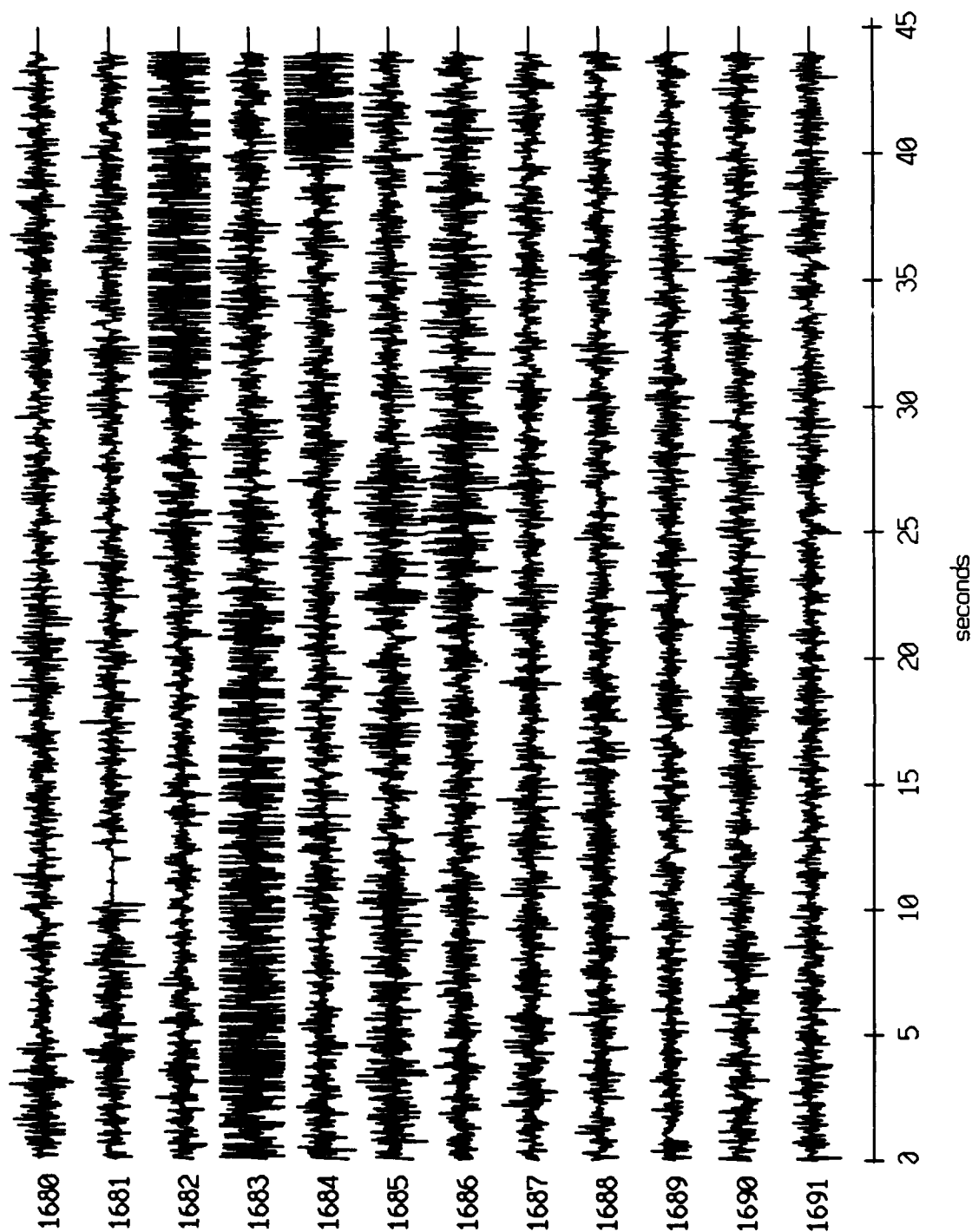
Float 1, July, 1989 Trip - records 1680-1691 (z-axis)  
vertical axis scale is approx. -2.0 to 2.0 volts



PGC corrected channel level (V)

Figure XI.49c

Float 1, July, 1989 Trip - records 1680-1691 (hydrophone)  
vertical axis scale is approx. -2.0 to 2.0 volts

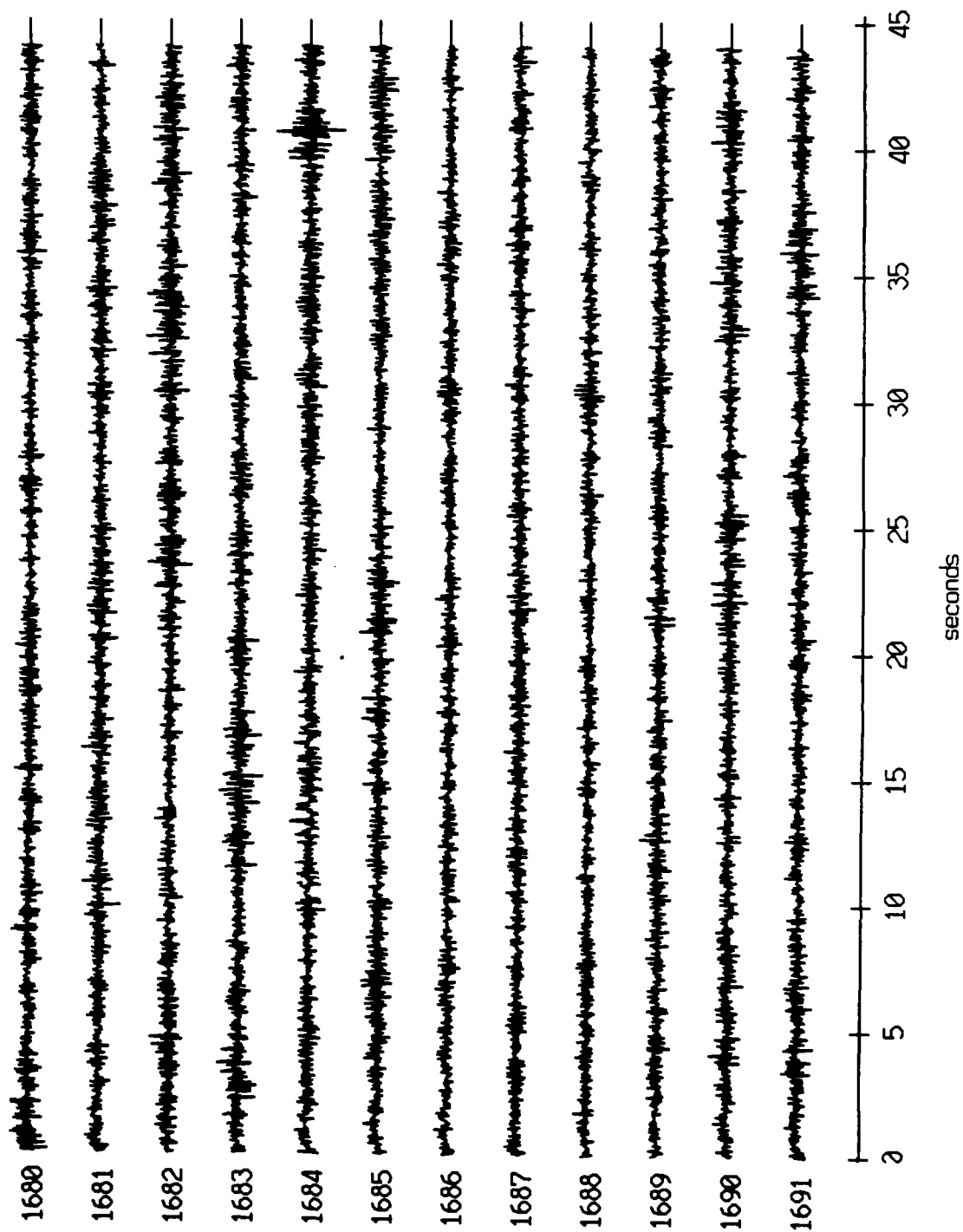


AGC corrected channel level (V)

Figure XI.49d



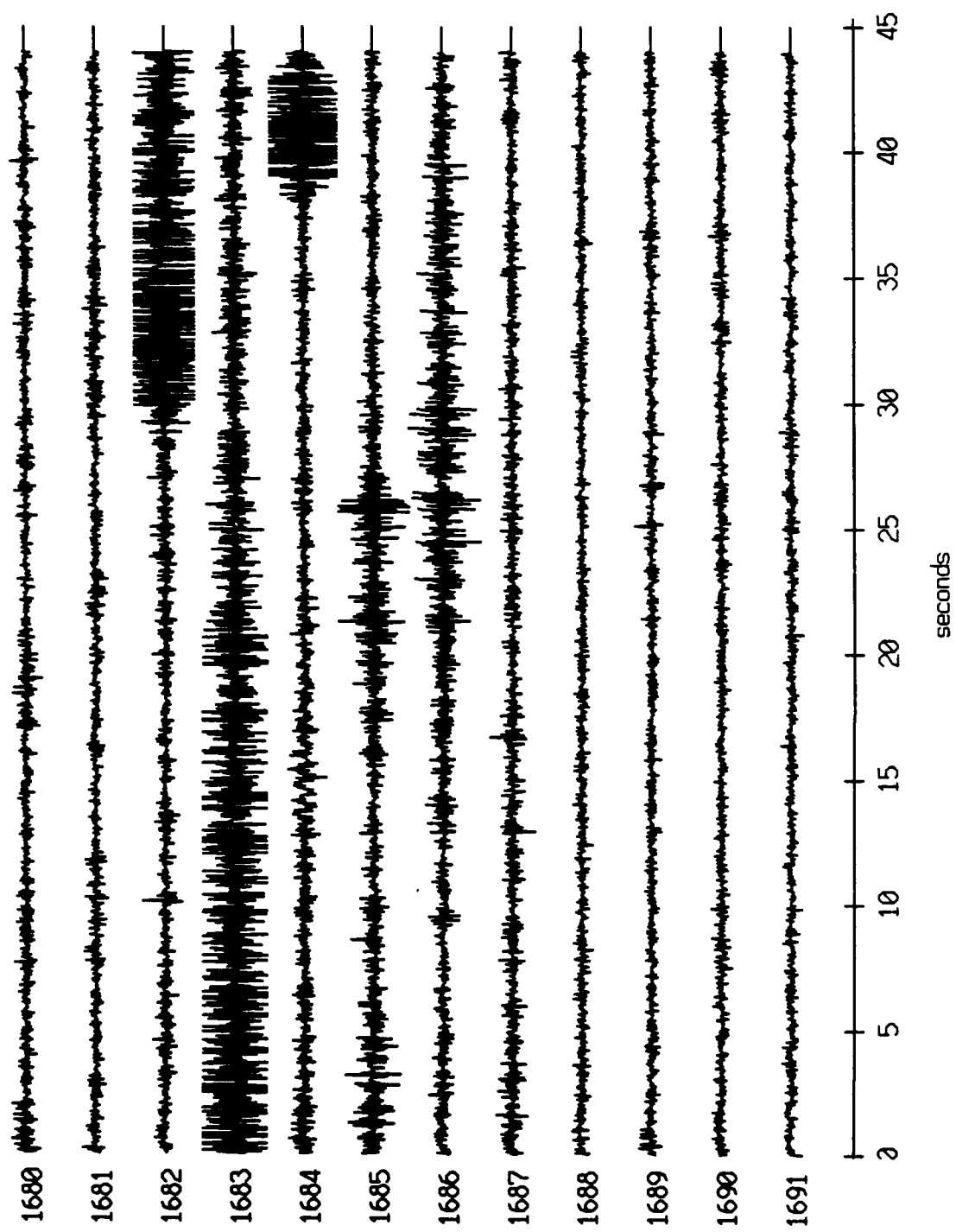
Float 2, July, 1989 Trip - records 1680-1691 (x-axis)  
vertical axis scale is approx. -2.0 to 2.0 volts



AGC corrected channel level (V)

Figure XI.50a

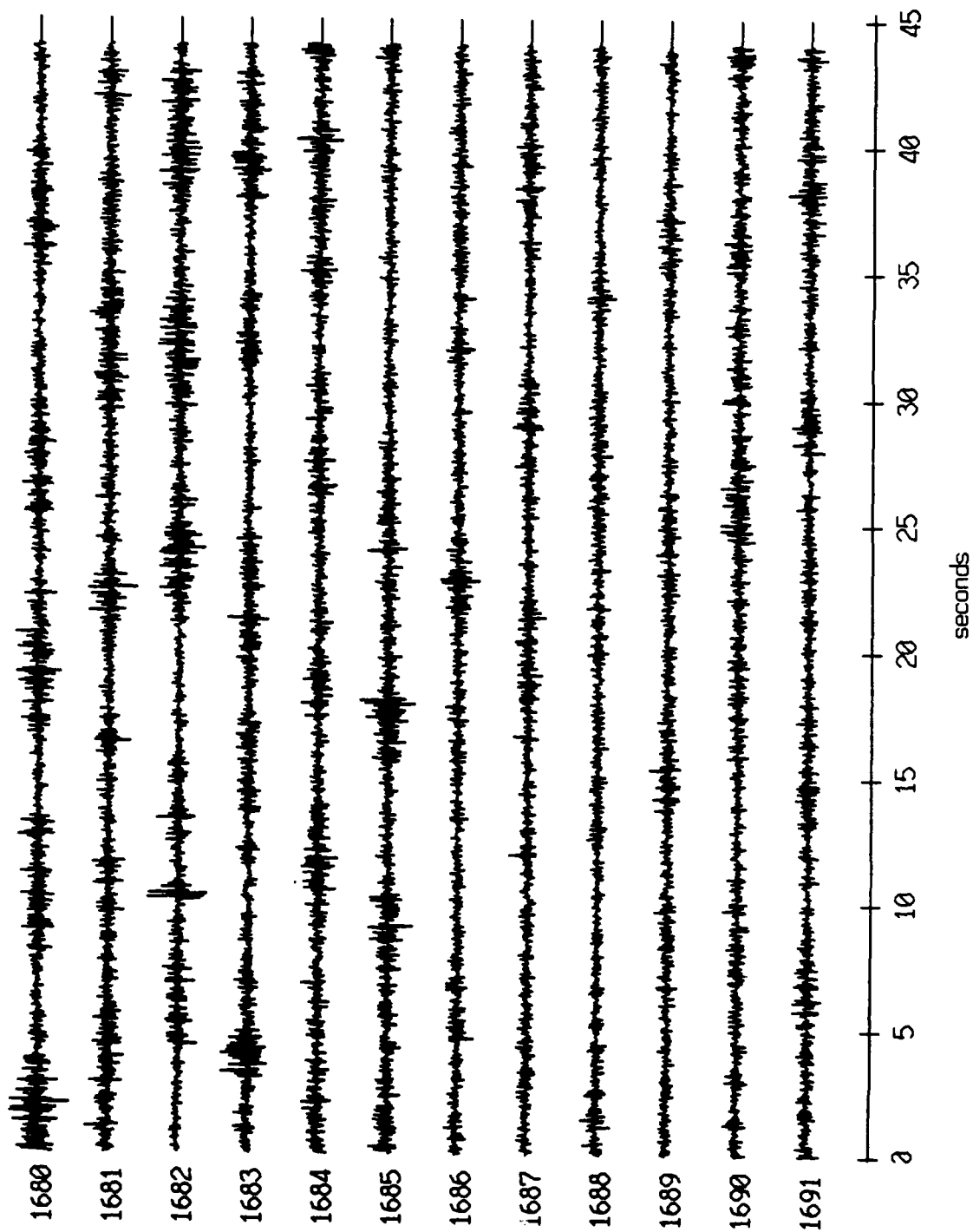
Float 2, July, 1989 Trip - records 1680-1691 (y-axis)  
 vertical axis scale is approx. -2.0 to 2.0 volts



AGC corrected channel level (V)

Figure XI.50b

Float 2, July, 1989 Trip - records 1680-1691 (z-axis)  
vertical axis scale is approx. -2.0 to 2.0 volts



PGC corrected channel level (V)

Figure XI.50c

Float 2, July, 1989 Trip - records 1680-1691 (hydrophone)  
vertical axis scale is approx. -2.0 to 2.0 volts

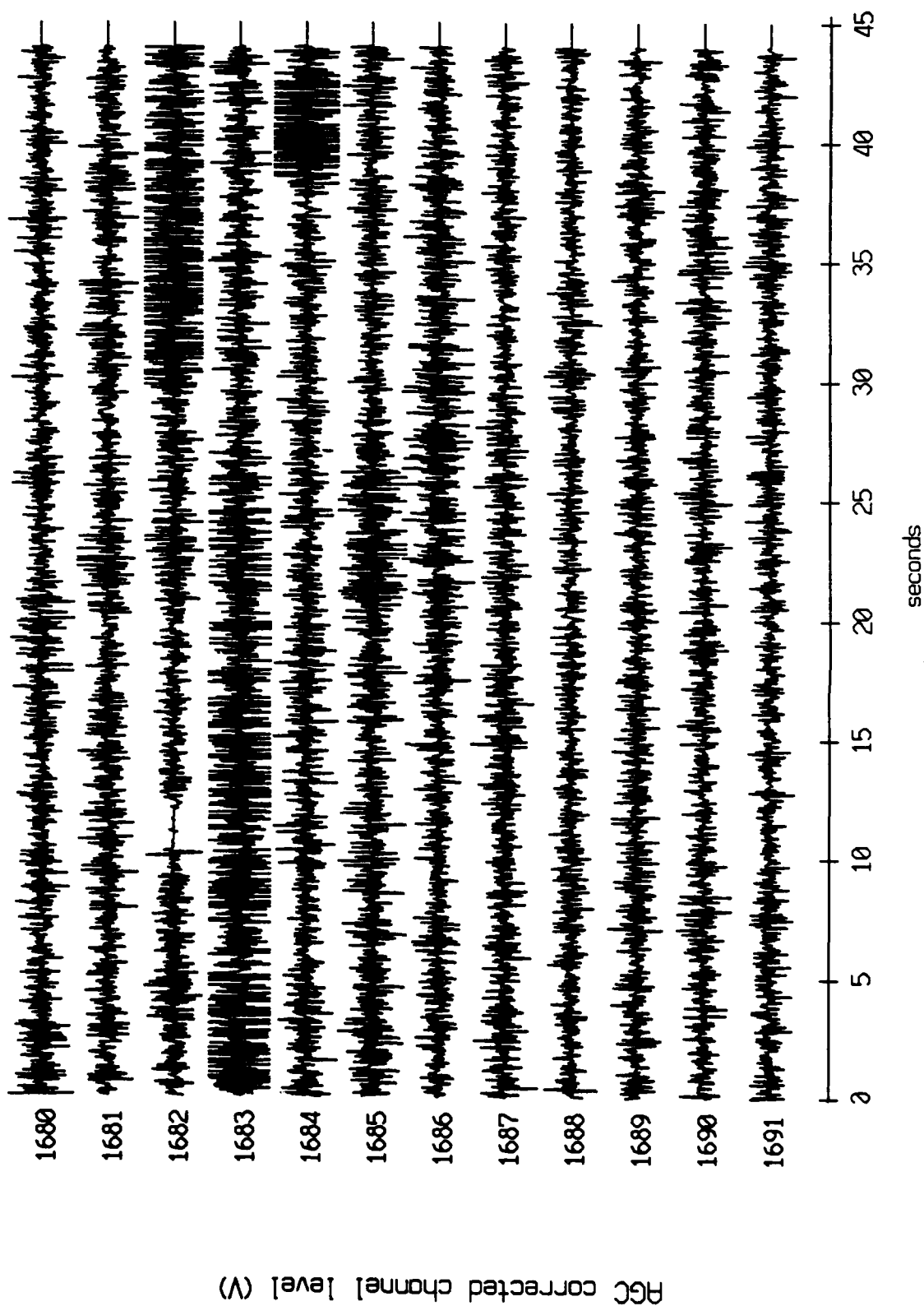
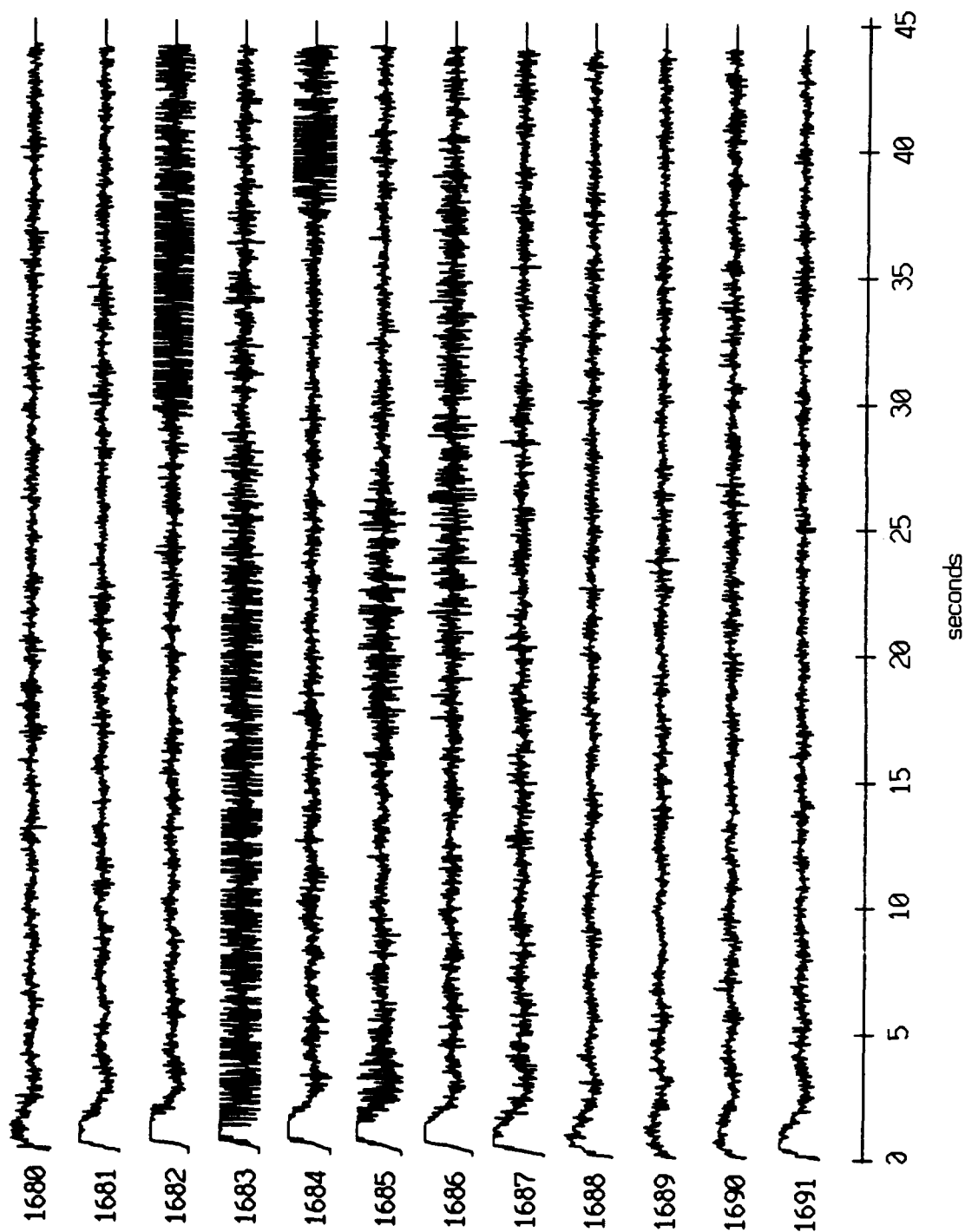


Figure XI.50d

Floot 3, July, 1989 Trip - records 1680-1691 (x-axis)  
vertical axis scale is approx. -2.0 to 2.0 volts



HGC corrected channel level (V)

Figure XI.51a

Float 3, July, 1989 Trip - records 1680-1691 (y-axis)  
vertical axis scale is approx. -2.0 to 2.0 volts

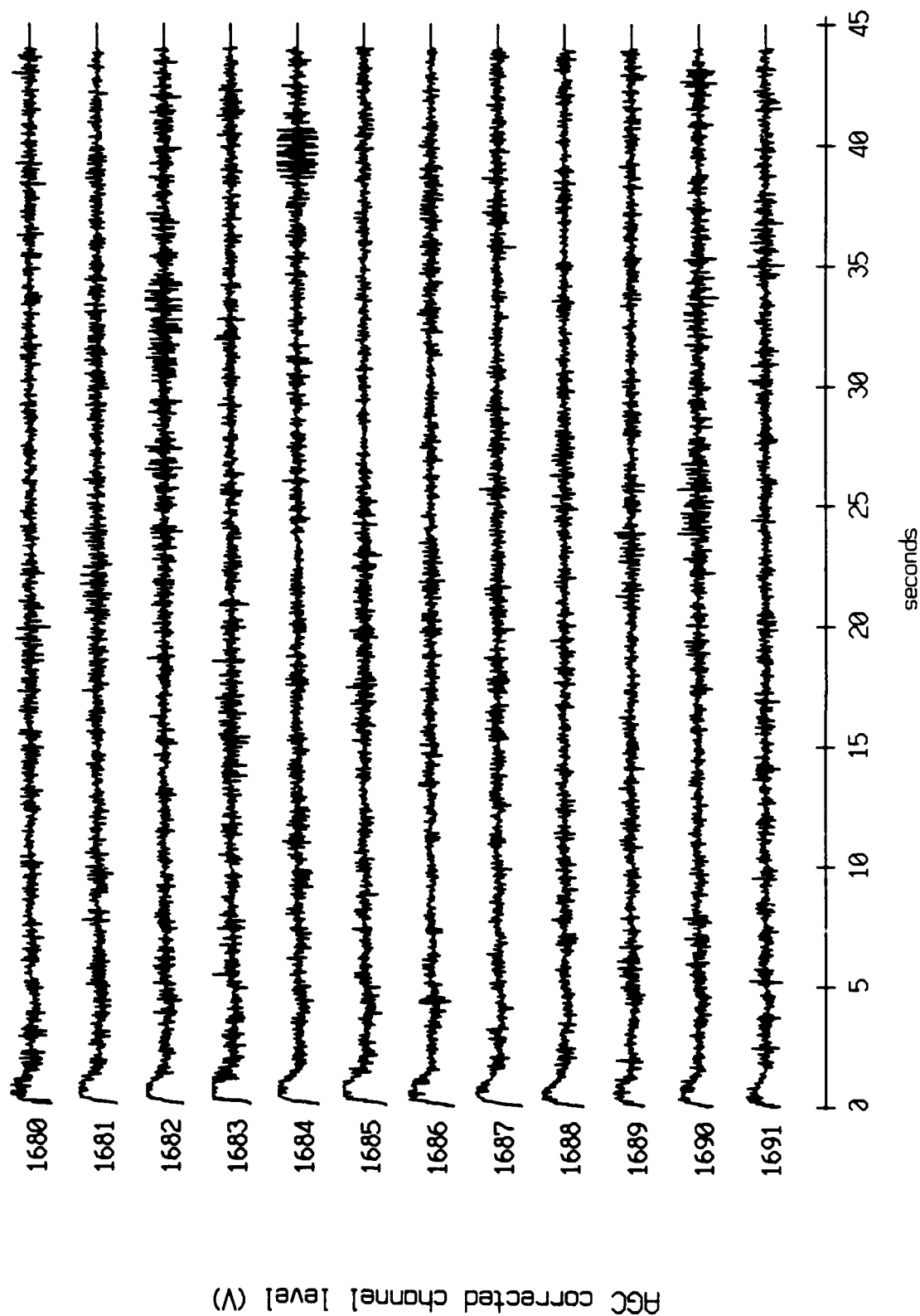


Figure XI.51b

Floot 3, July, 1989 Trip - records 1680-1691 (z-axis)  
vertical axis scale is approx. -2.0 to 2.0 volts

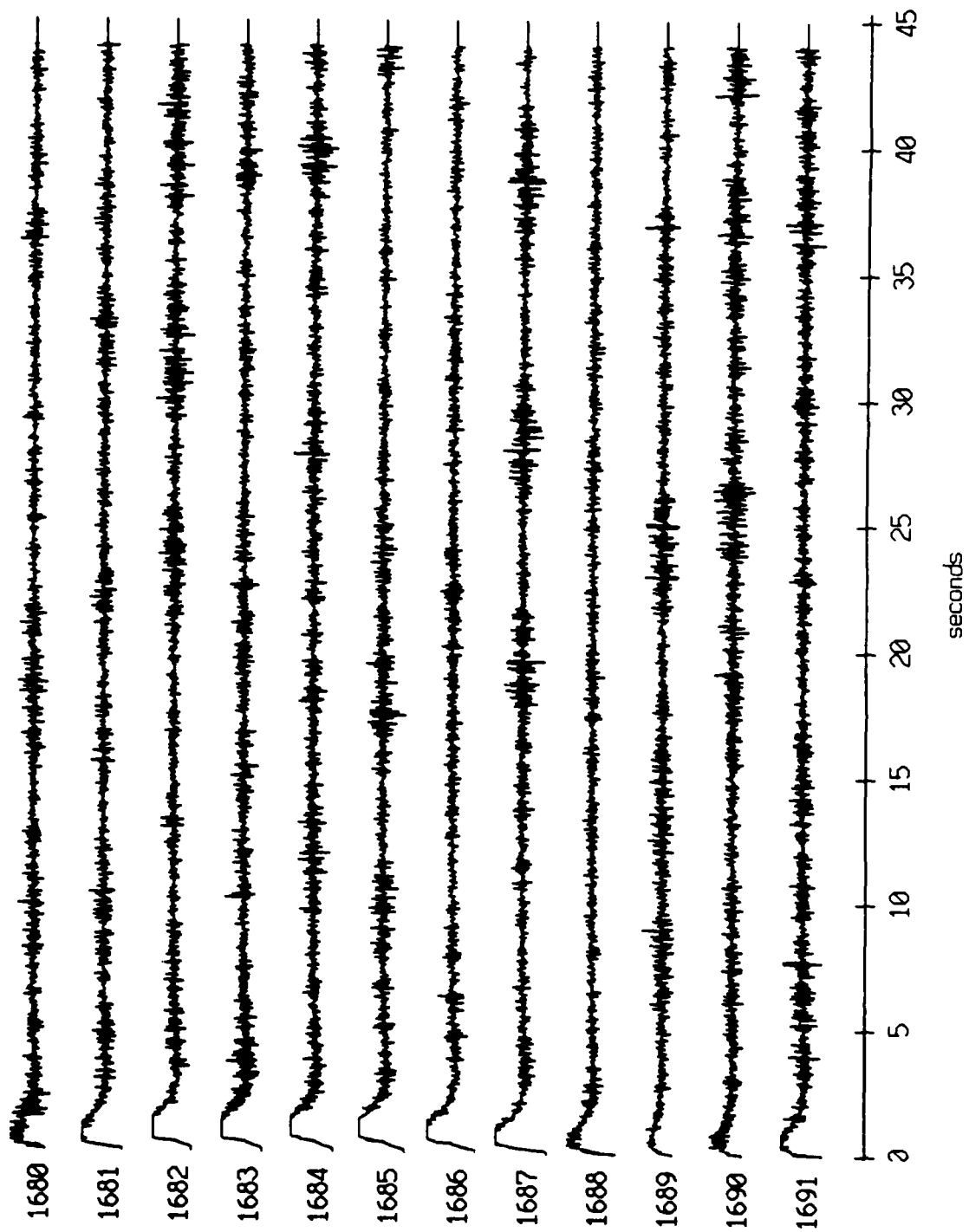
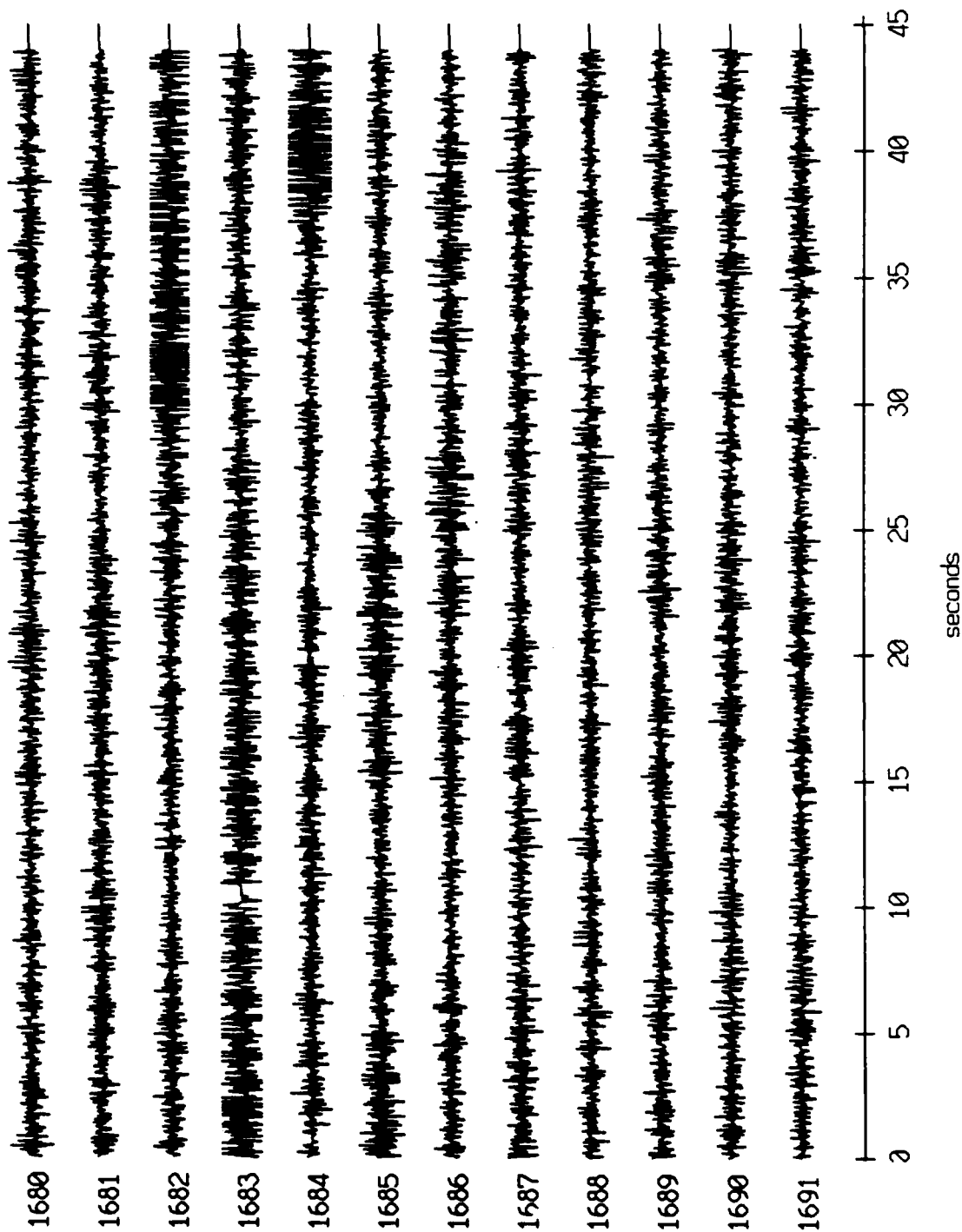


Figure XI.51c

Float 3, July, 1989 Trip - records 1680-1691 (hydrophone)  
vertical axis scale is approx. -2.0 to 2.0 volts



AGC corrected channel level (V)

Figure XI.51d



Float 4, July, 1989 Trip - records 1680-1691 (x-axis)  
vertical axis scale is approx. -2.0 to 2.0 volts

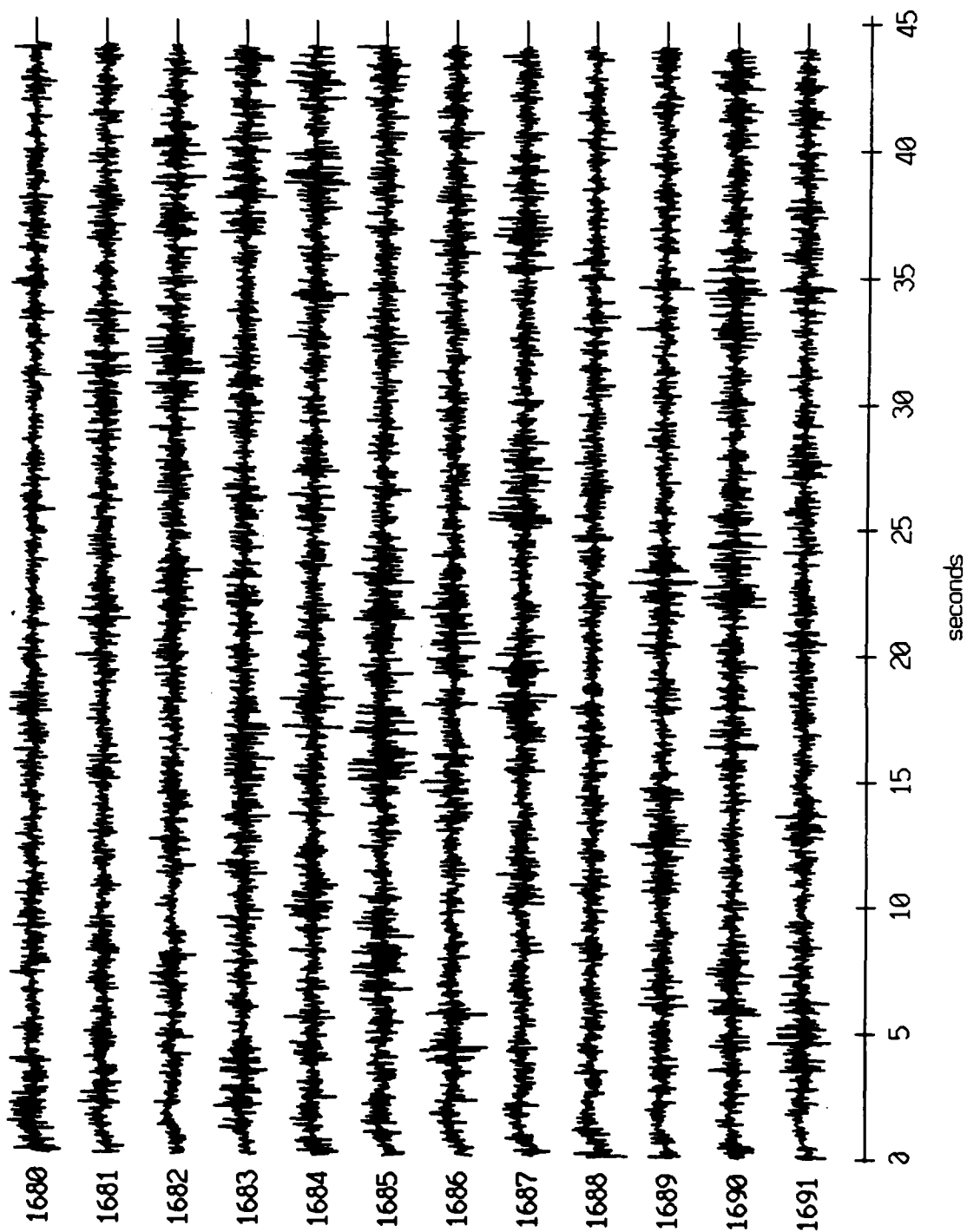
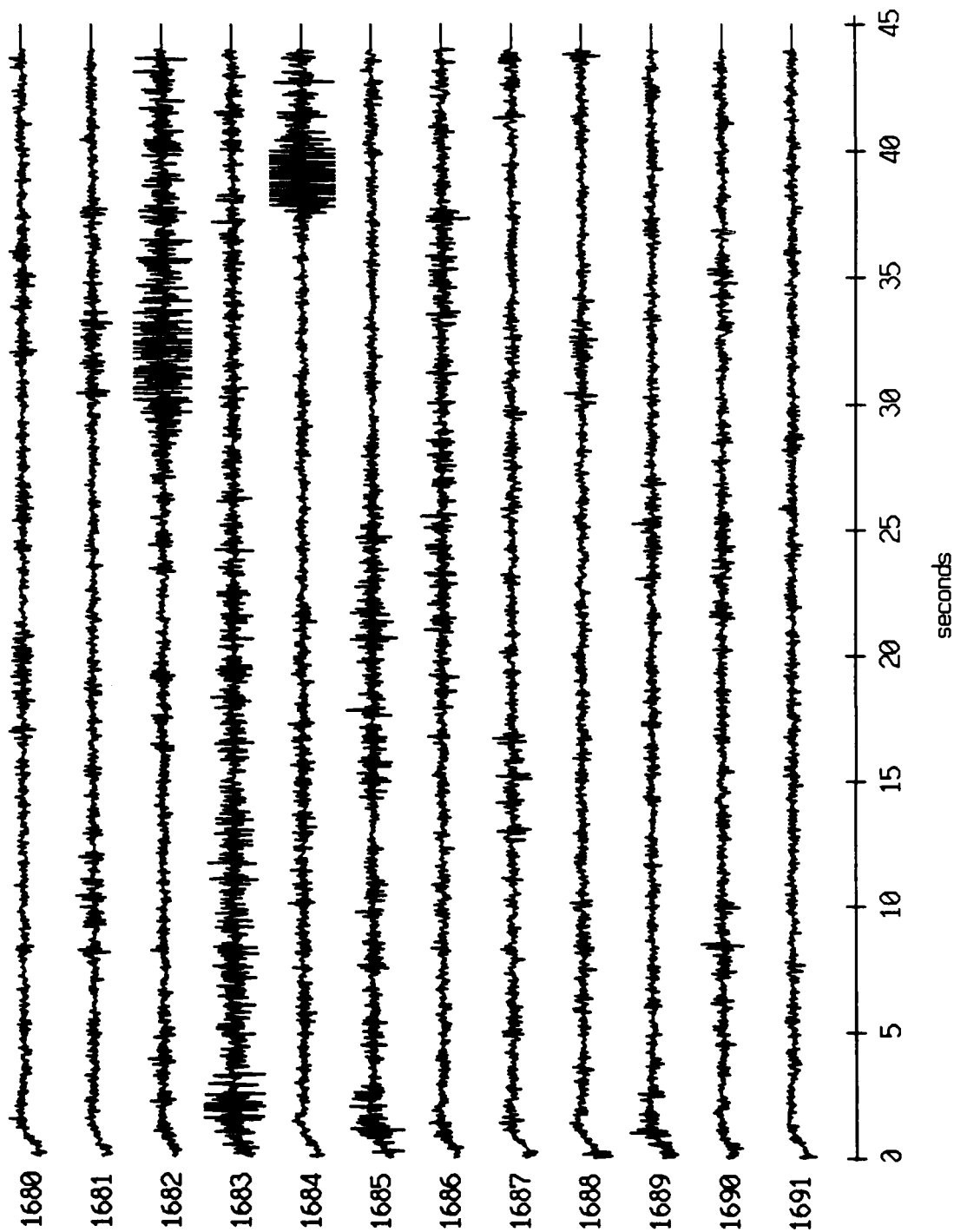


Figure XI.52a

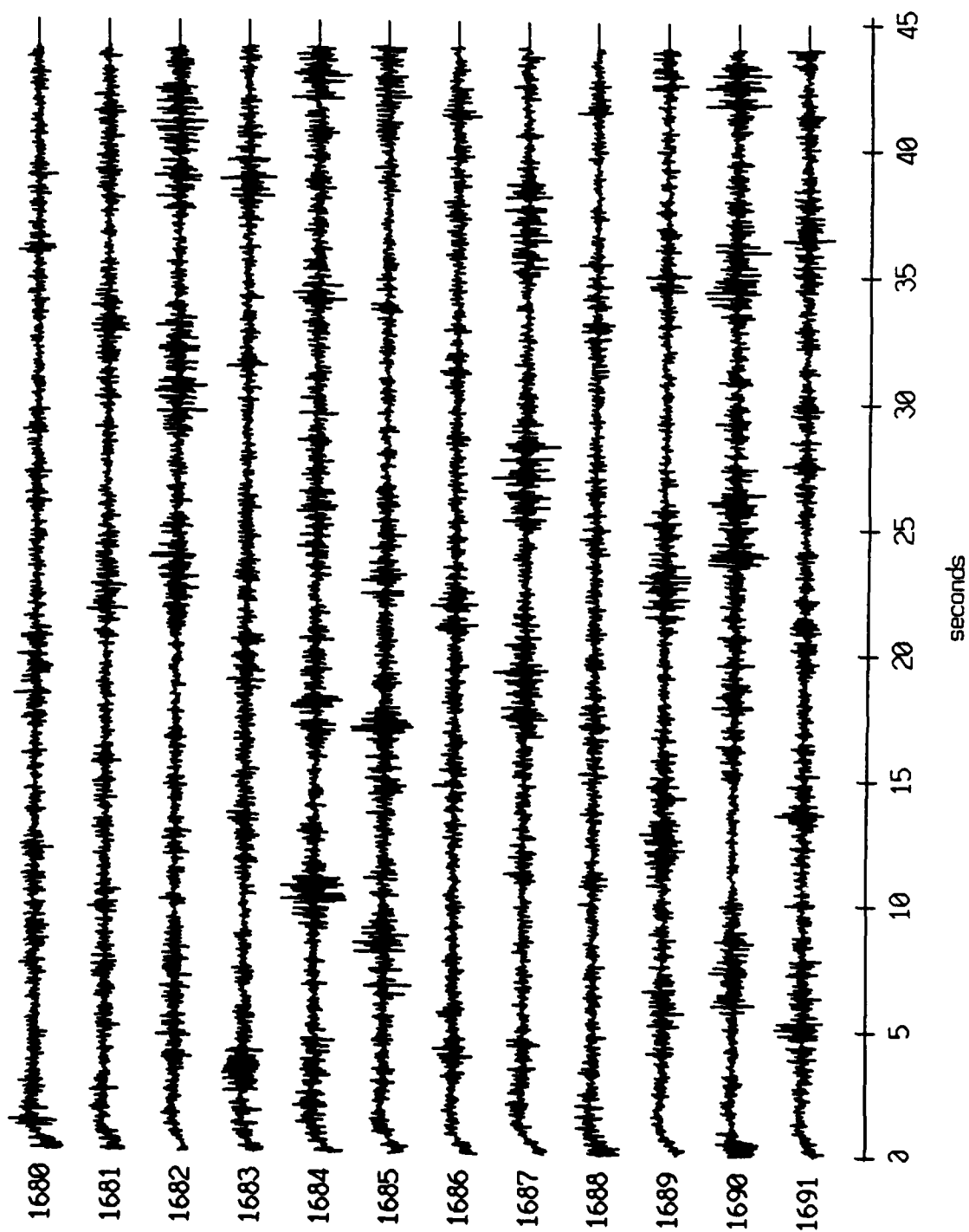
Float 4, July, 1989 Trip - records 1680-1691 (y-axis)  
vertical axis scale is approx. -2.0 to 2.0 volts



RGC corrected channel level (V)

Figure XI.52b

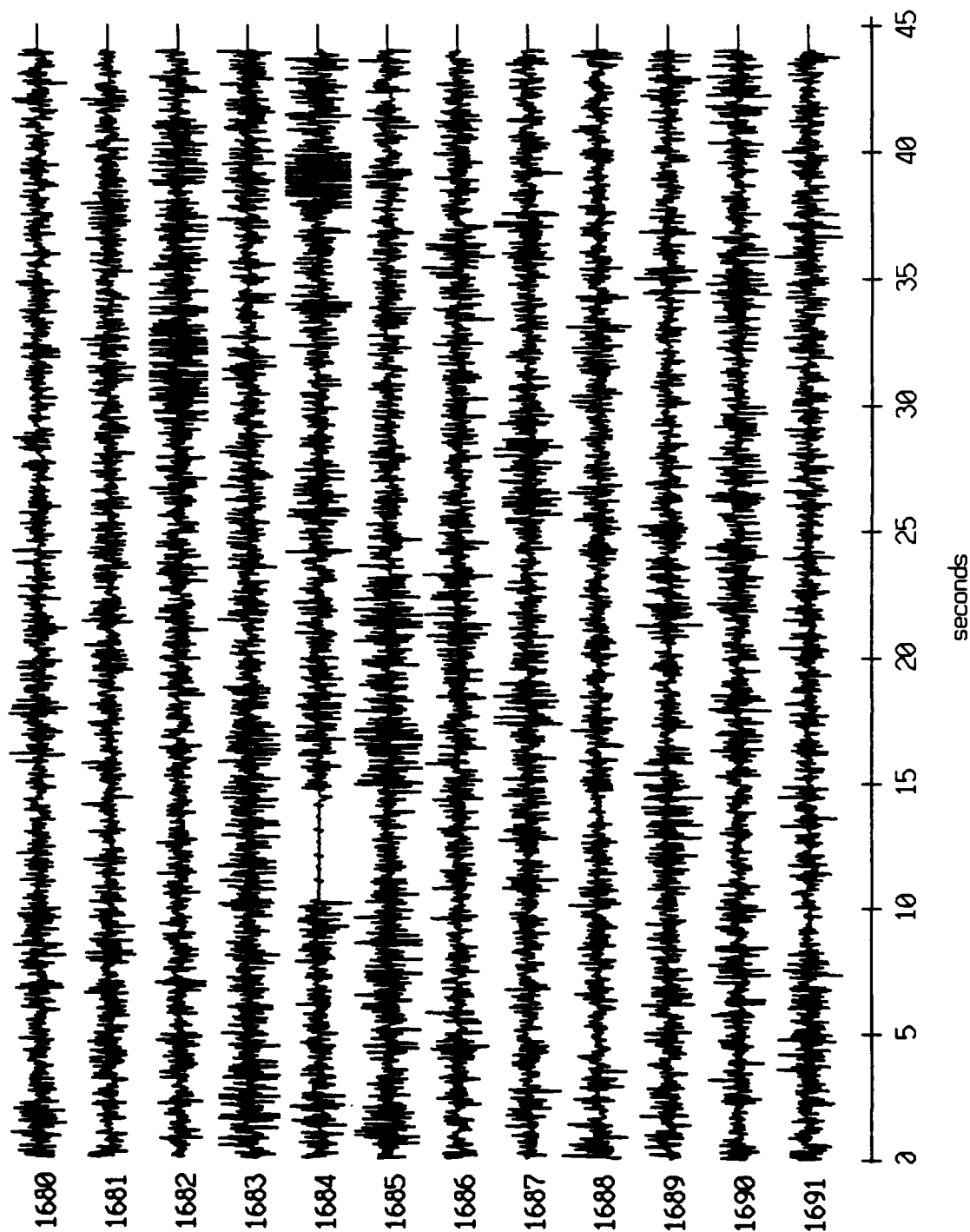
Floot 4, July, 1989 Trip - records 1680-1691 (z-axis)  
vertical axis scale is approx. -2.0 to 2.0 volts



AGC corrected channel level (V)

Figure XI.52c

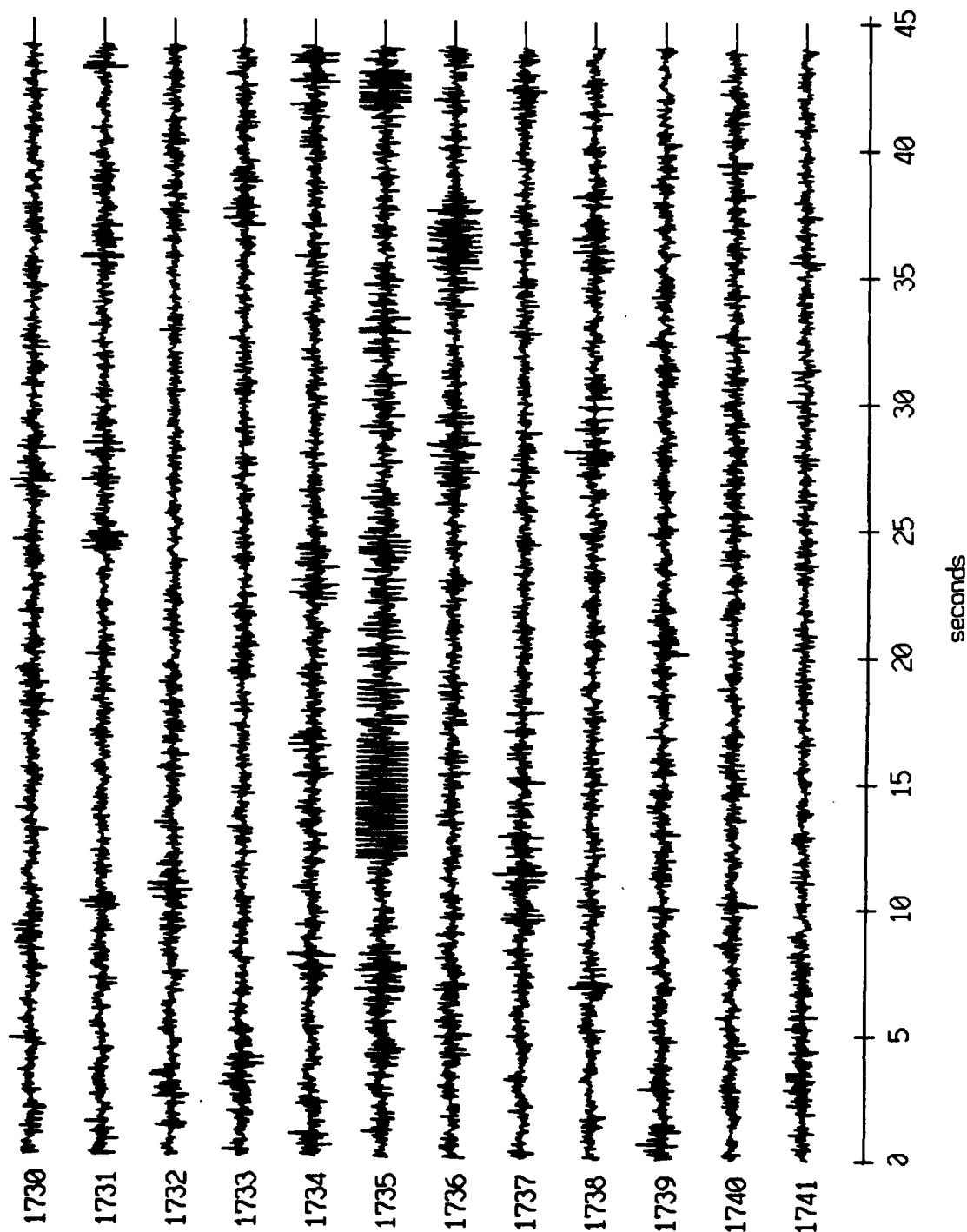
Float 4, July, 1989 Trip - records 1680-1691 (hydrophone)  
vertical axis scale is approx. -2.0 to 2.0 volts



PGC corrected channel level (V)

Figure XI.52d

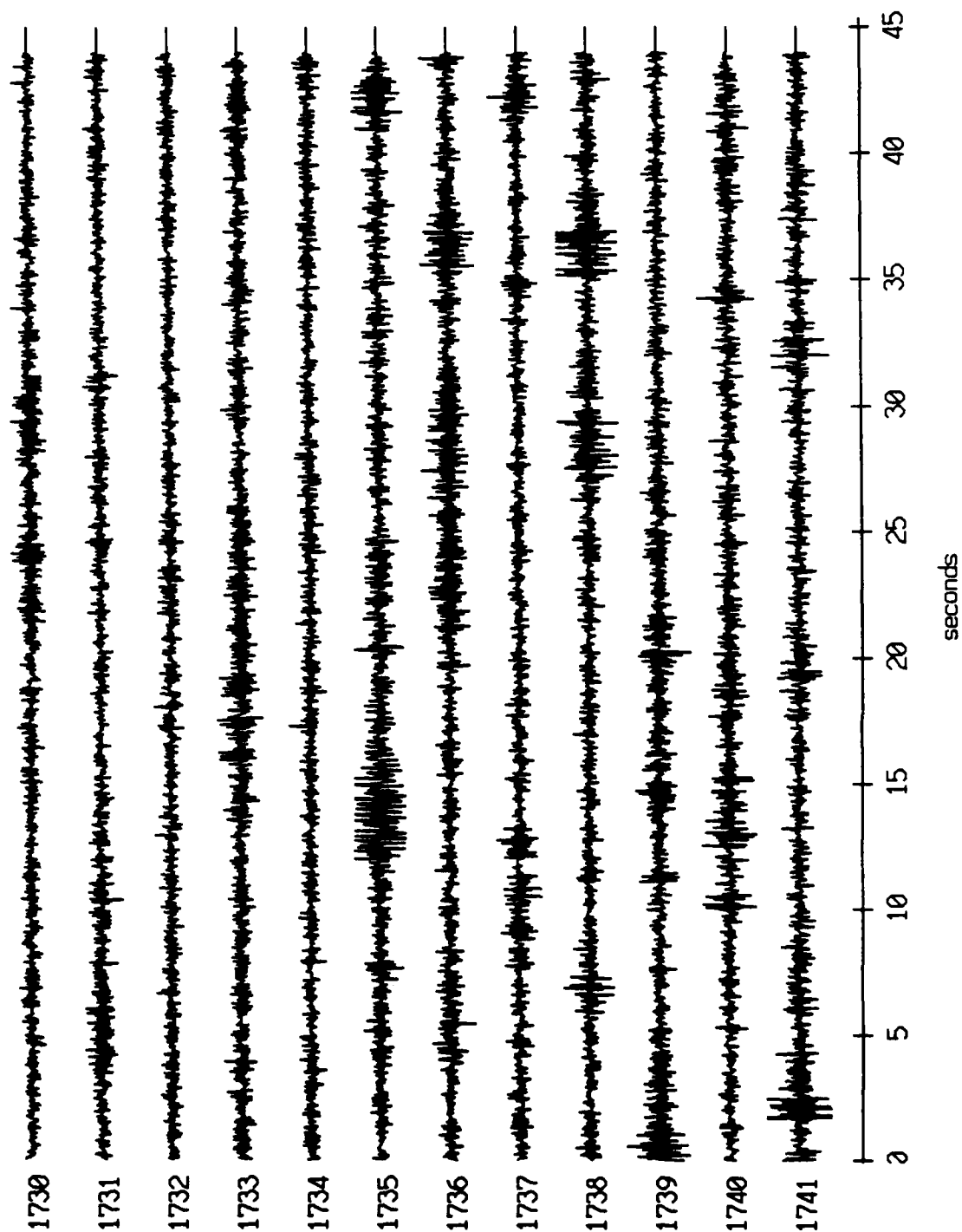
Float 0, July, 1989 Trip - records 1730-1741 (x-axis)  
vertical axis scale is approx. -2.0 to 2.0 volts



AGC corrected channel level (V)

Figure XI.53a

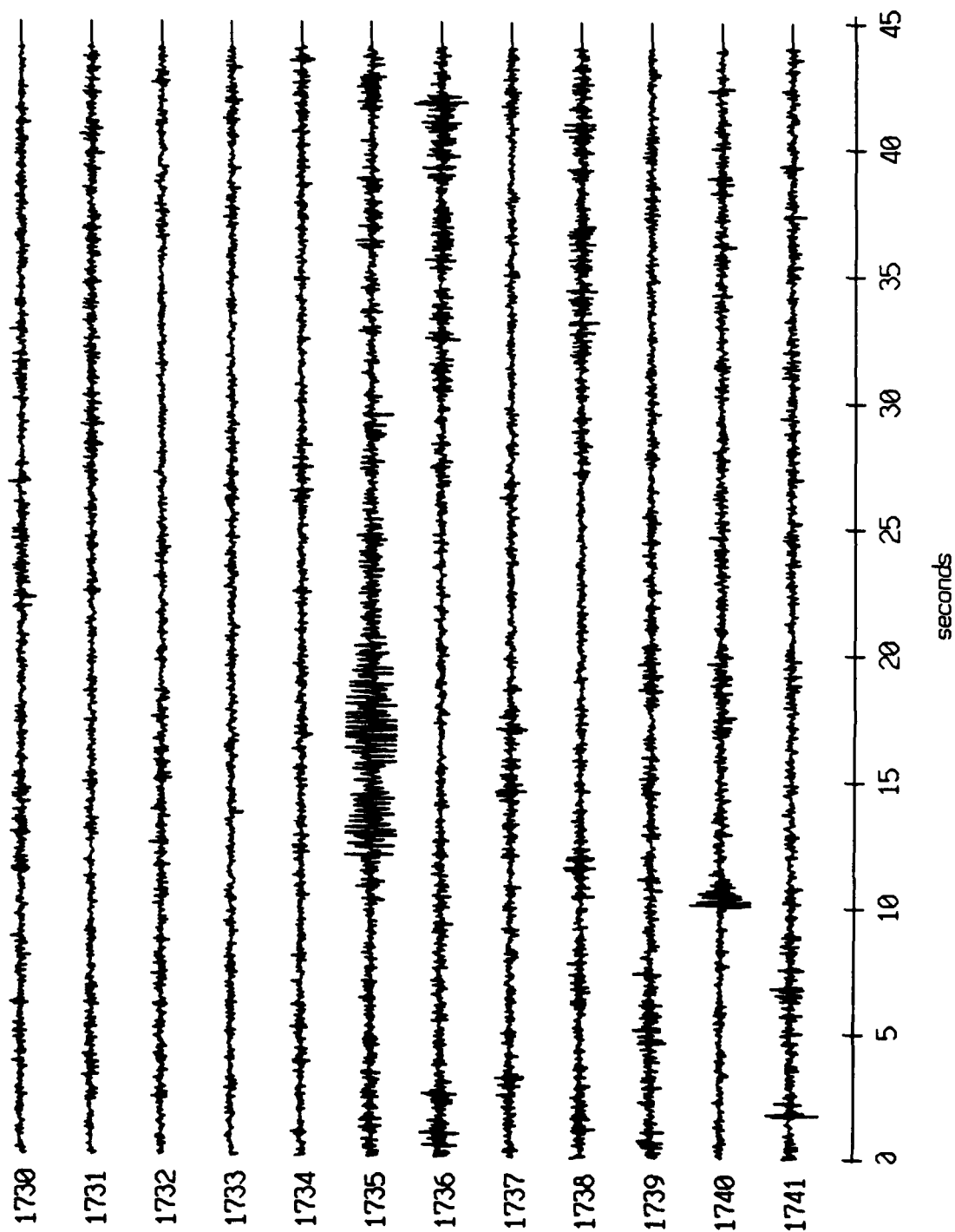
Float 0, July, 1989 Trip - records 1730-1741 (y-axis)  
vertical axis scale is approx. -2.0 to 2.0 volts



AGC corrected channel level (V)

Figure XI.53b

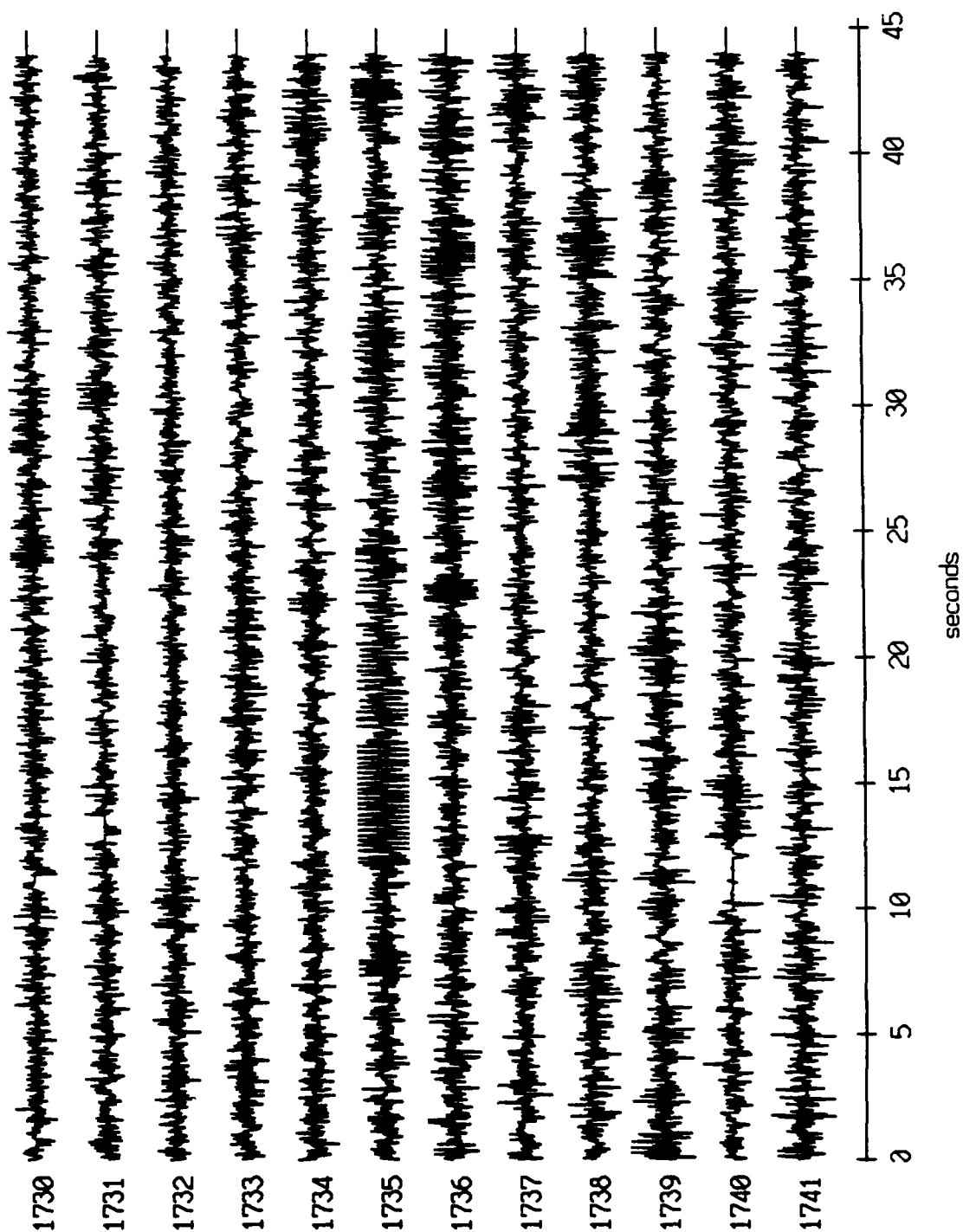
Float 0, July, 1989 Trip - records 1730-1741 (z-axis)  
vertical axis scale is approx. -2.0 to 2.0 volts



AGC corrected channel level (V)

Figure XI.53c

Float 0, July, 1989 Trip - records 1730-1741 (hydrophone)  
vertical axis scale is approx. -2.0 to 2.0 volts

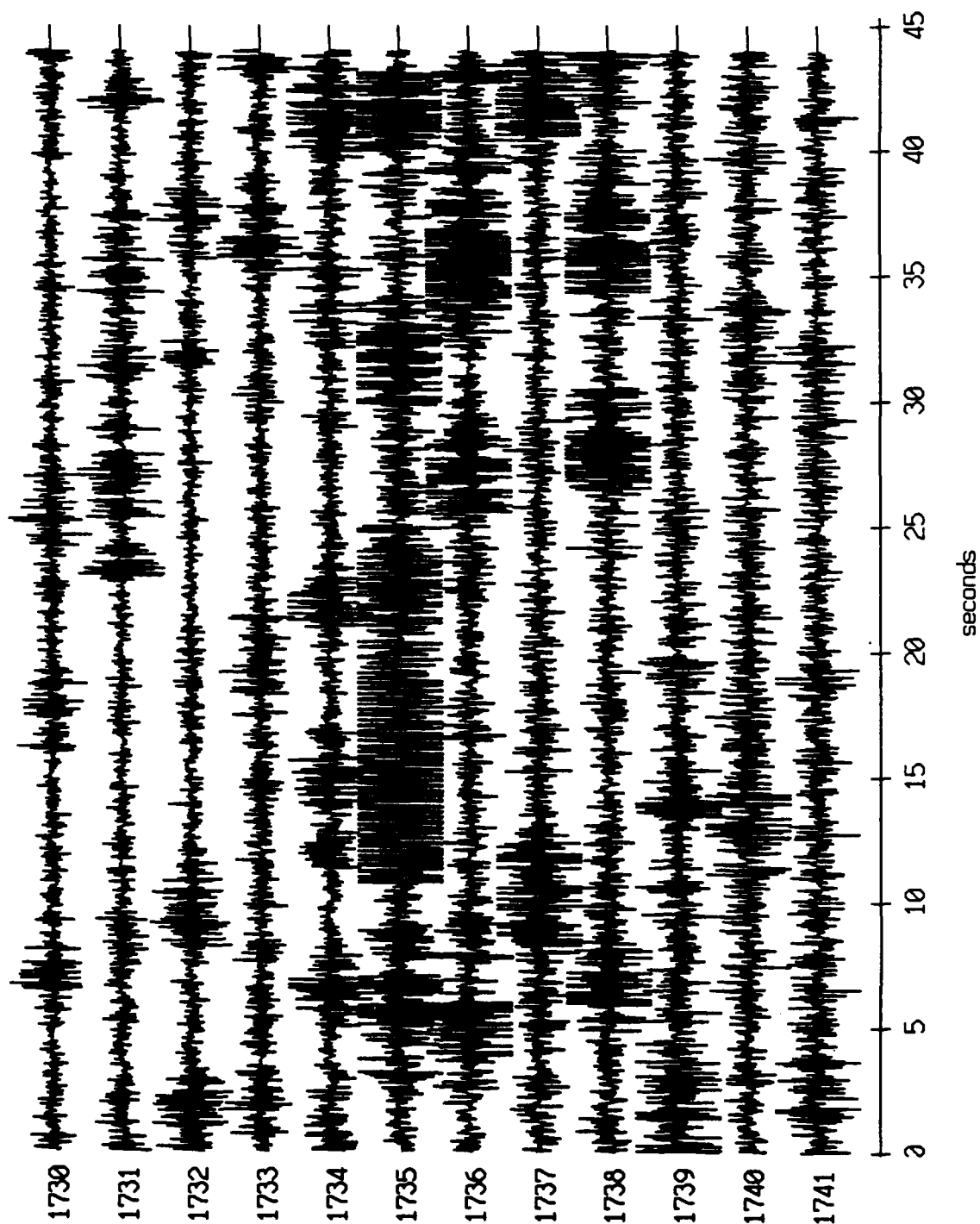


AGC corrected channel level (V)

Figure XI.53d



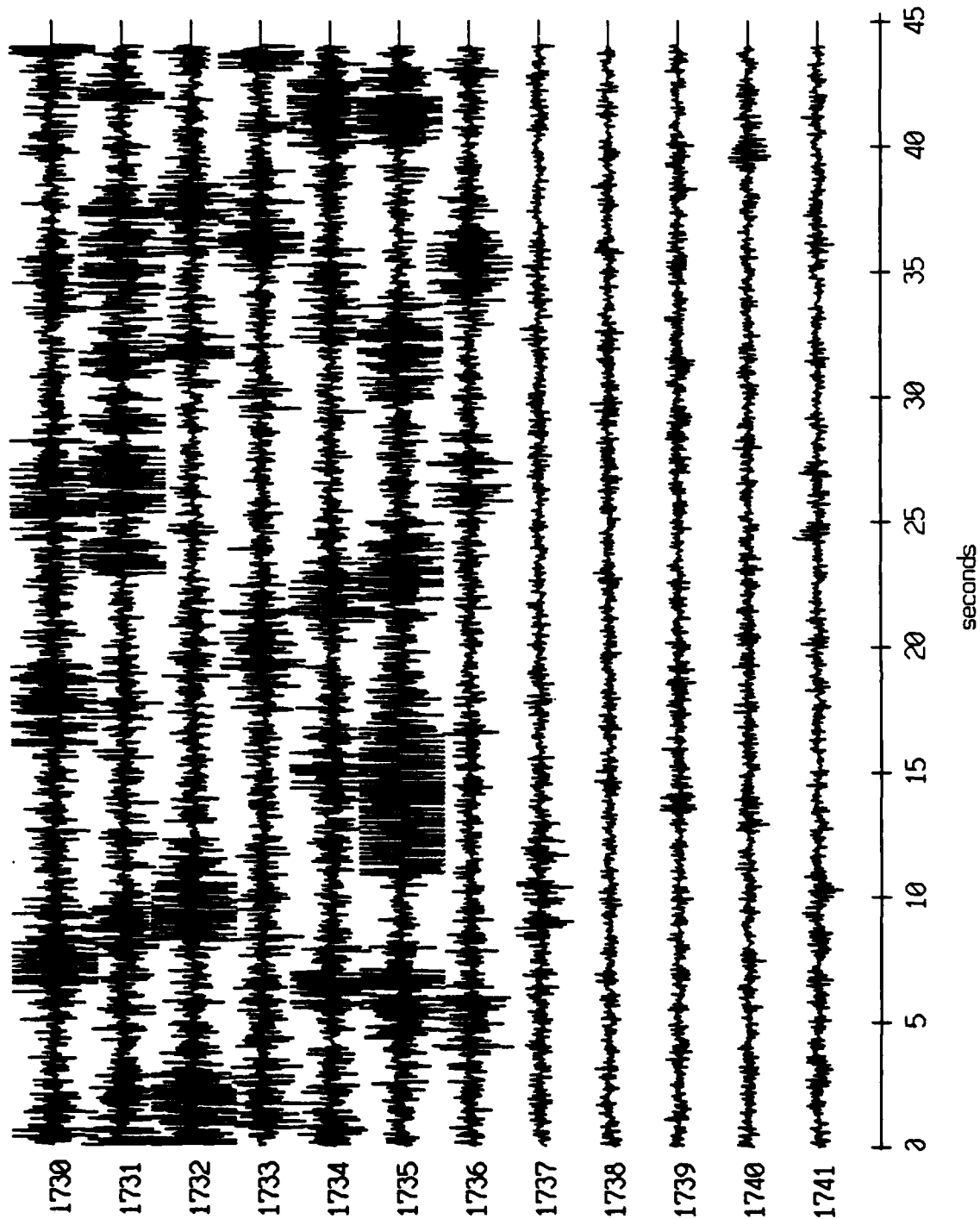
Float 1, July, 1989 Trip - records 1730-1741 (x-axis)  
vertical axis scale is approx. -2.0 to 2.0 volts



AGC corrected channel level (V)

Figure XI.54a

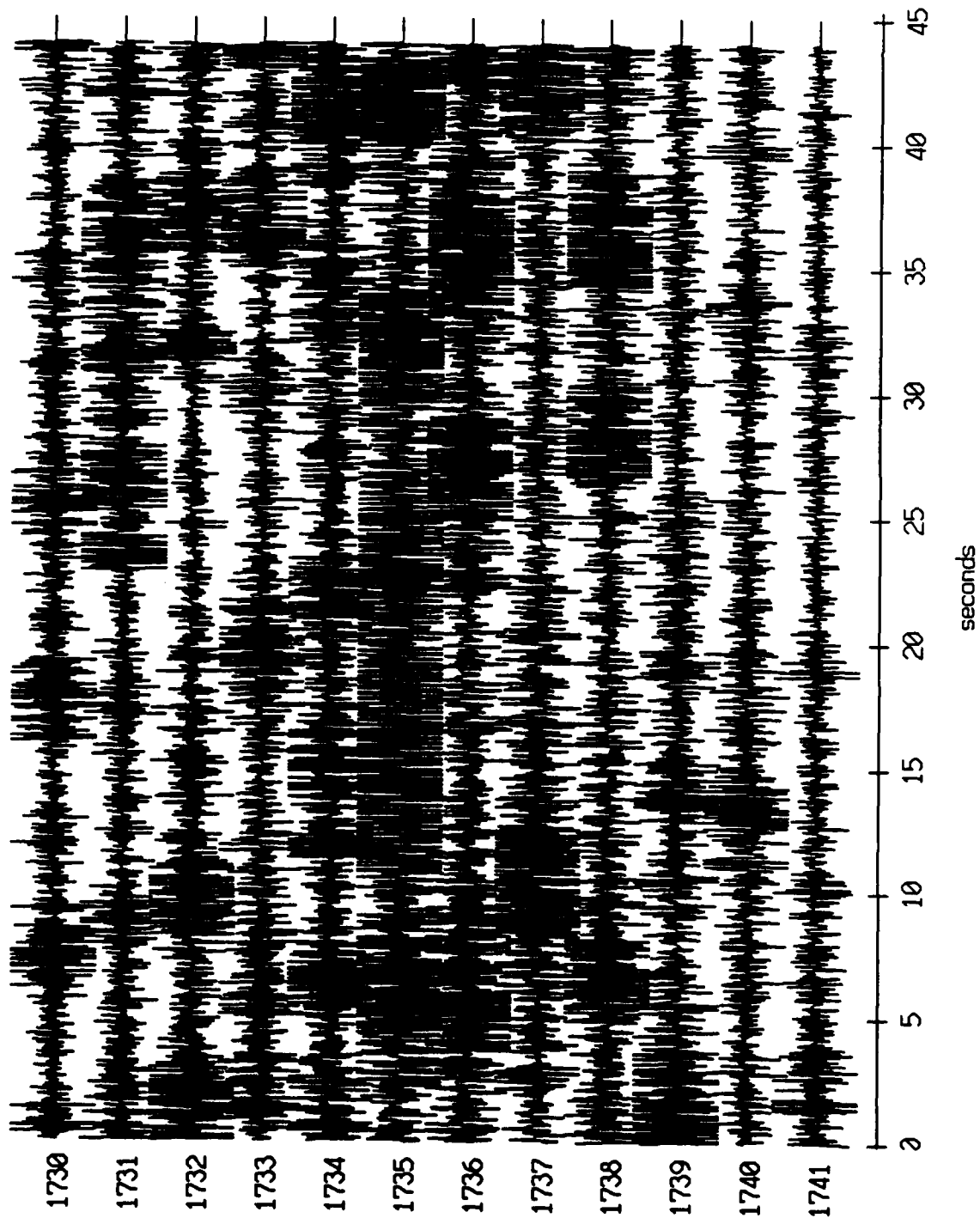
Float 1, July, 1989 Trip - records 1730-1741 (y-axis)  
vertical axis scale is approx. -2.0 to 2.0 volts



RGC corrected channel level (V)

Figure XI.54b

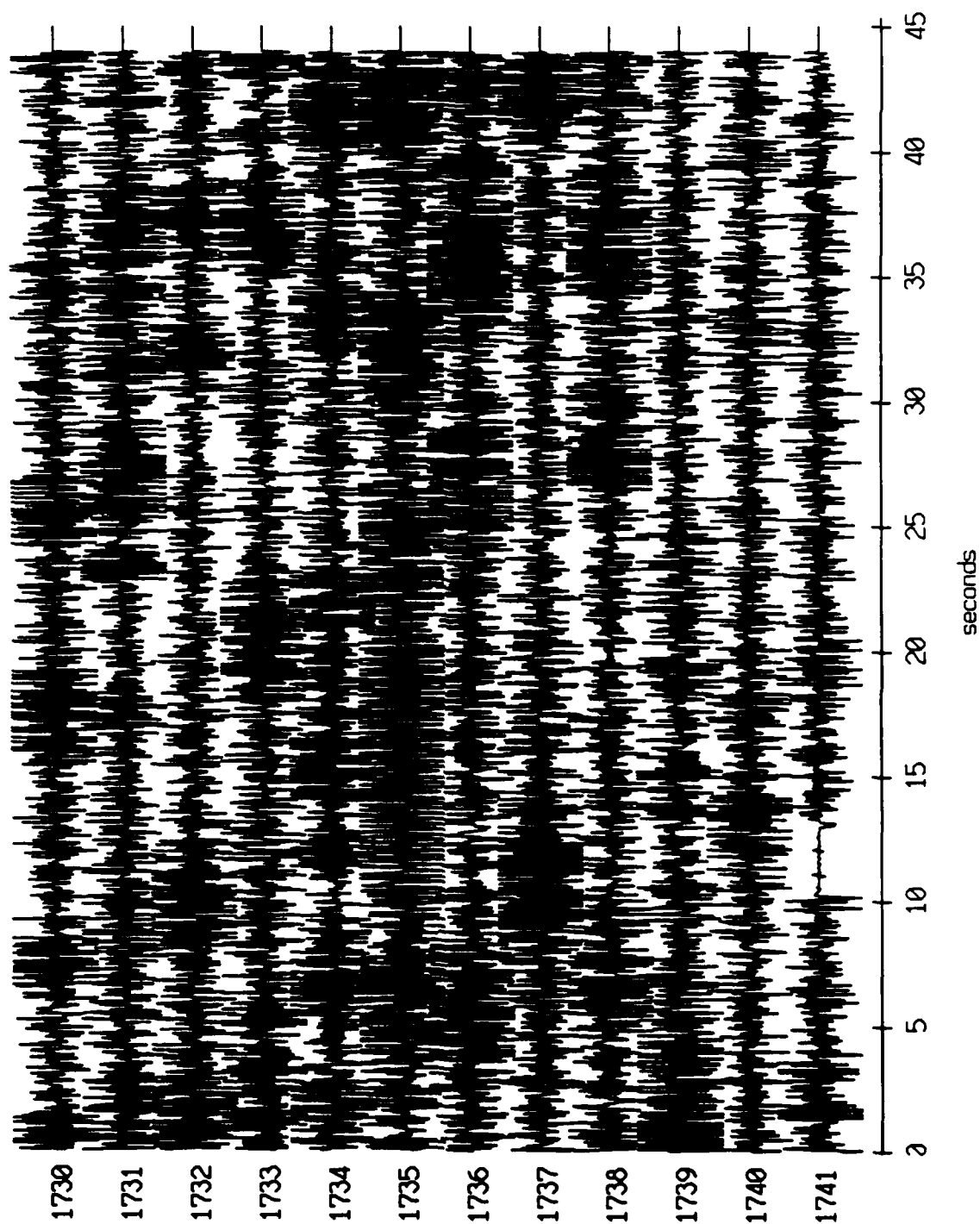
Float 1, July, 1989 Trip - records 1730-1741 (z-axis)  
vertical axis scale is approx. -2.0 to 2.0 volts



AGC corrected channel level (V)

Figure XI.54c

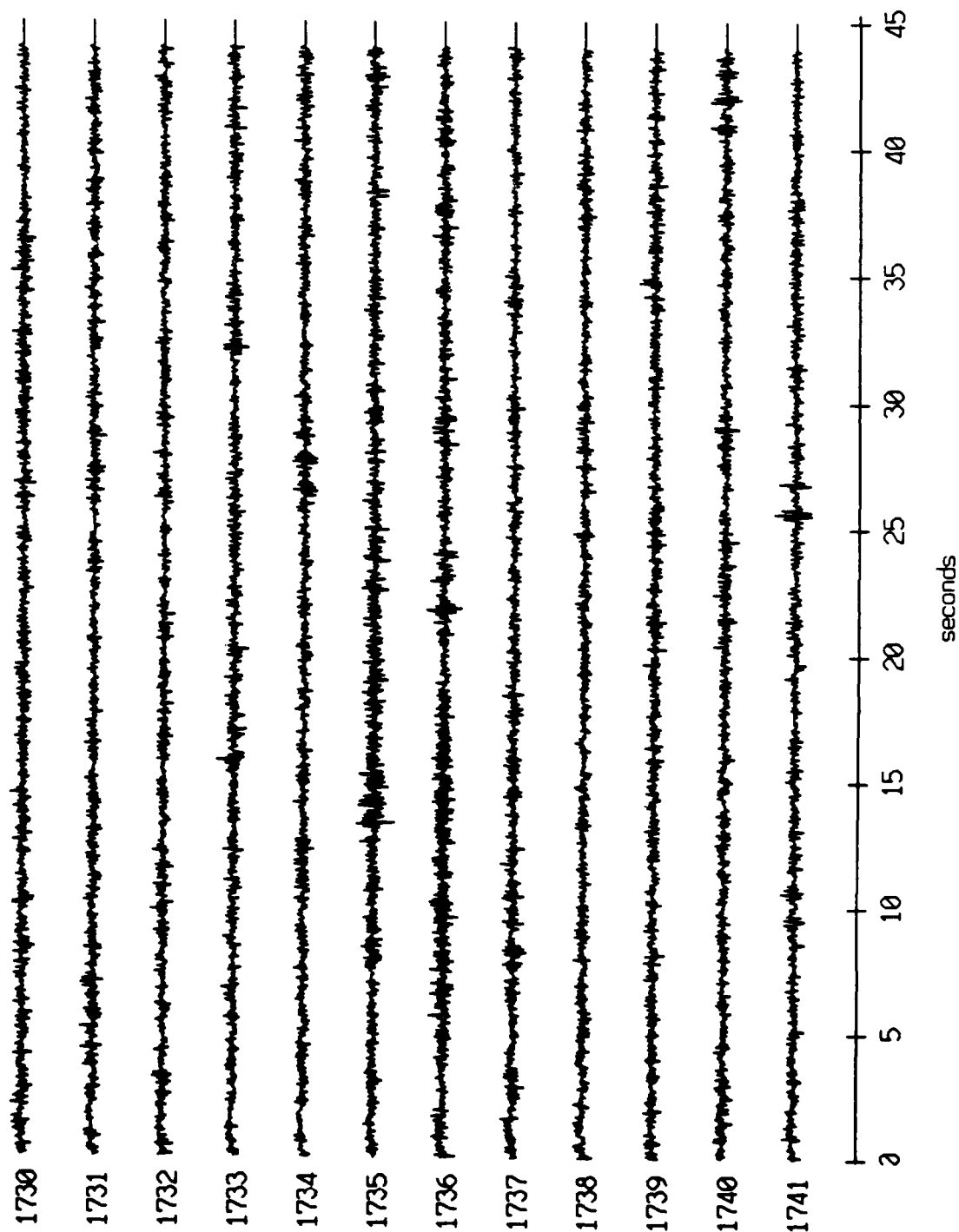
Float 1, July, 1989 Trip - records 1730-1741 (hydrophone)  
vertical axis scale is approx. -2.0 to 2.0 volts



AGC corrected channel level (V)

Figure XI.54d

Float 2, July, 1989 Trip - records 1730-1741 (x-axis)  
vertical axis scale is approx. -2.0 to 2.0 volts



AGC corrected channel level (V)

Figure XI.55a

Float 2, July, 1989 Trip - records 1730-1741 (y-axis)  
vertical axis scale is approx. -2.0 to 2.0 volts

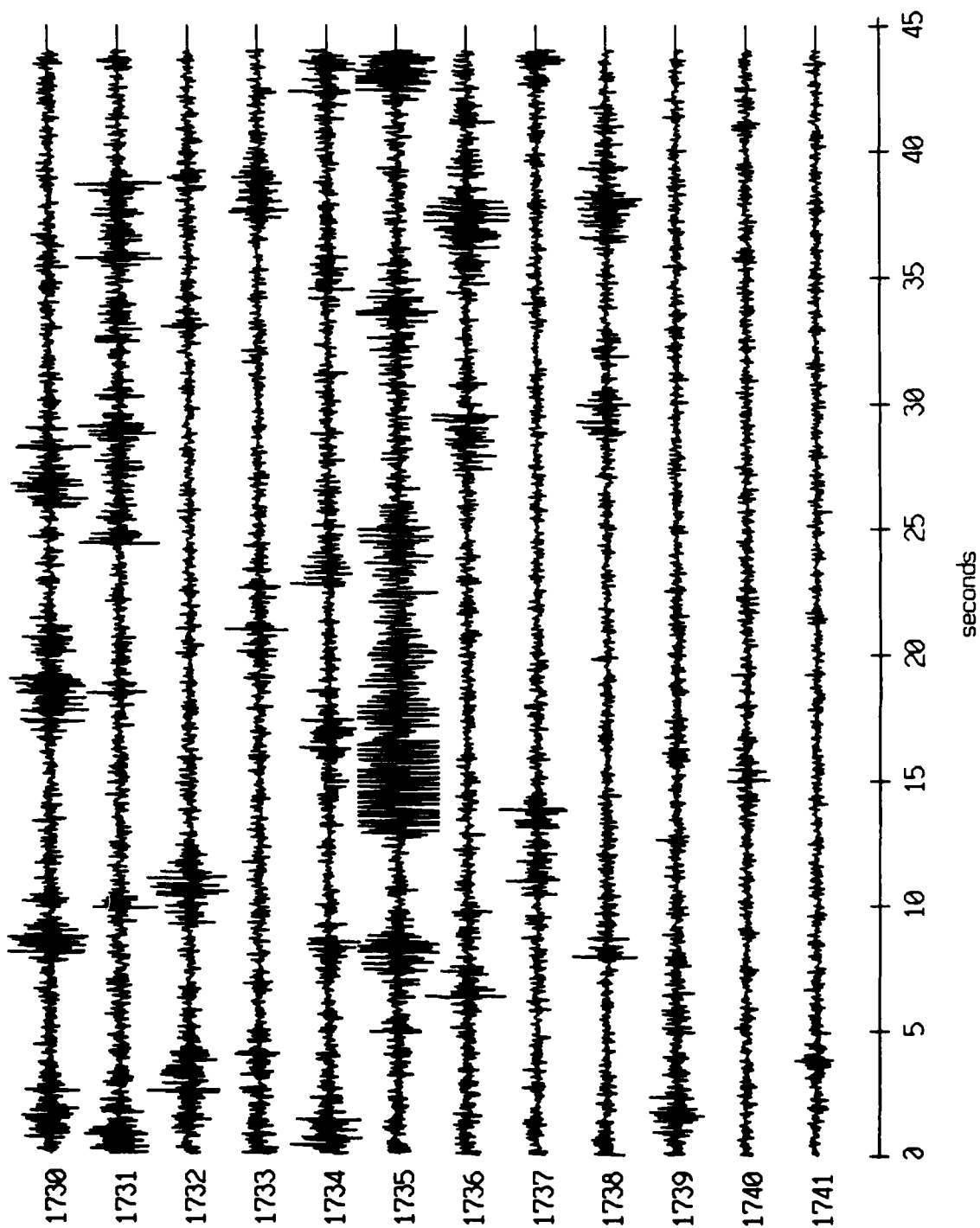
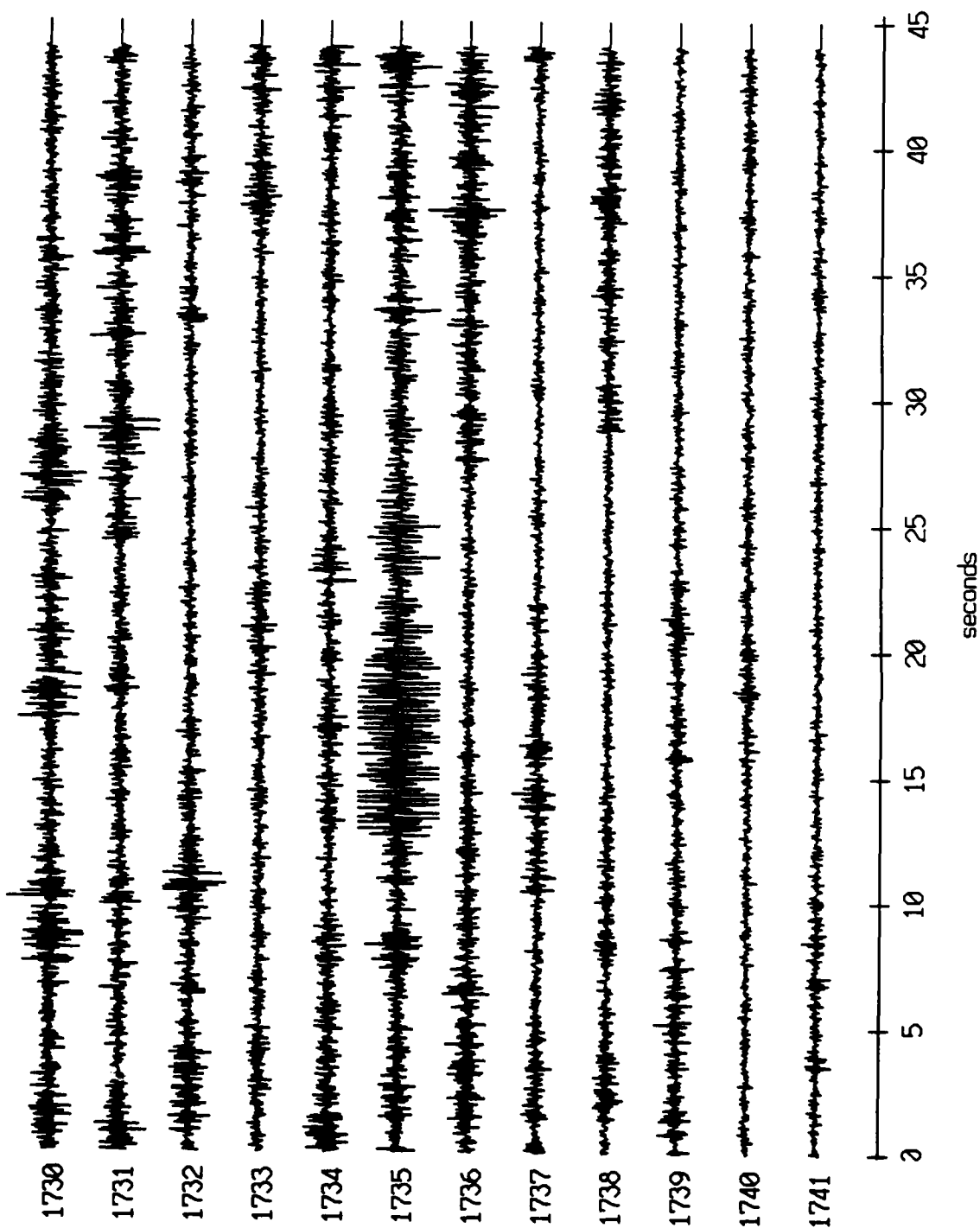


Figure XI.55b

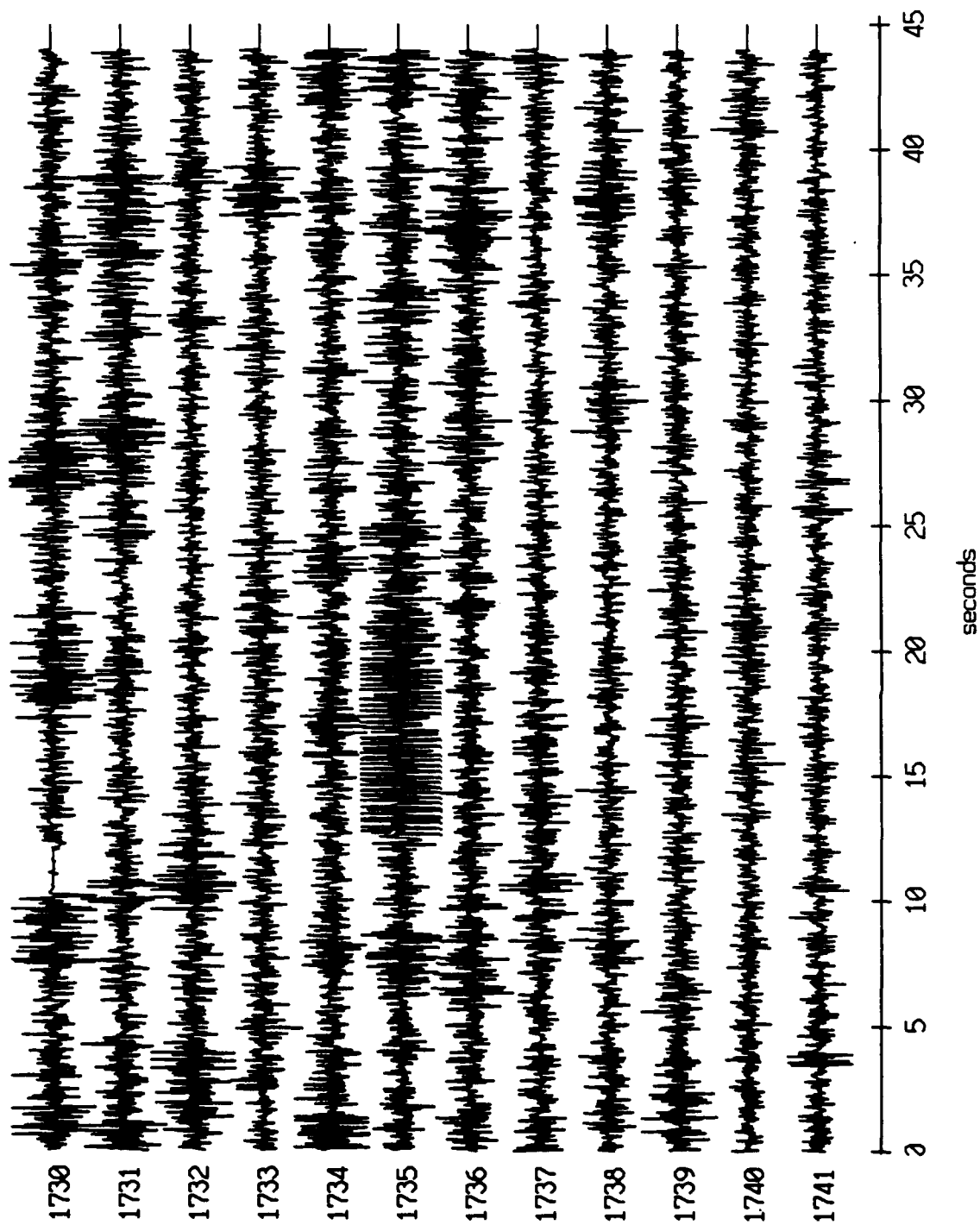
Floot 2, July, 1989 Trip - records 1730-1741 (z-axis)  
vertical axis scale is approx. -2.0 to 2.0 volts



PGC corrected channel level (V)

Figure XI.55c

Float 2, July, 1989 Trip - records 1730-1741 (hydrophone)  
vertical axis scale is approx. -2.0 to 2.0 volts



AGC corrected channel level (V)

Figure XI.55d



Float 3, July, 1989 Trip - records 1730-1741 (x-axis)  
vertical axis scale is approx. -2.0 to 2.0 volts

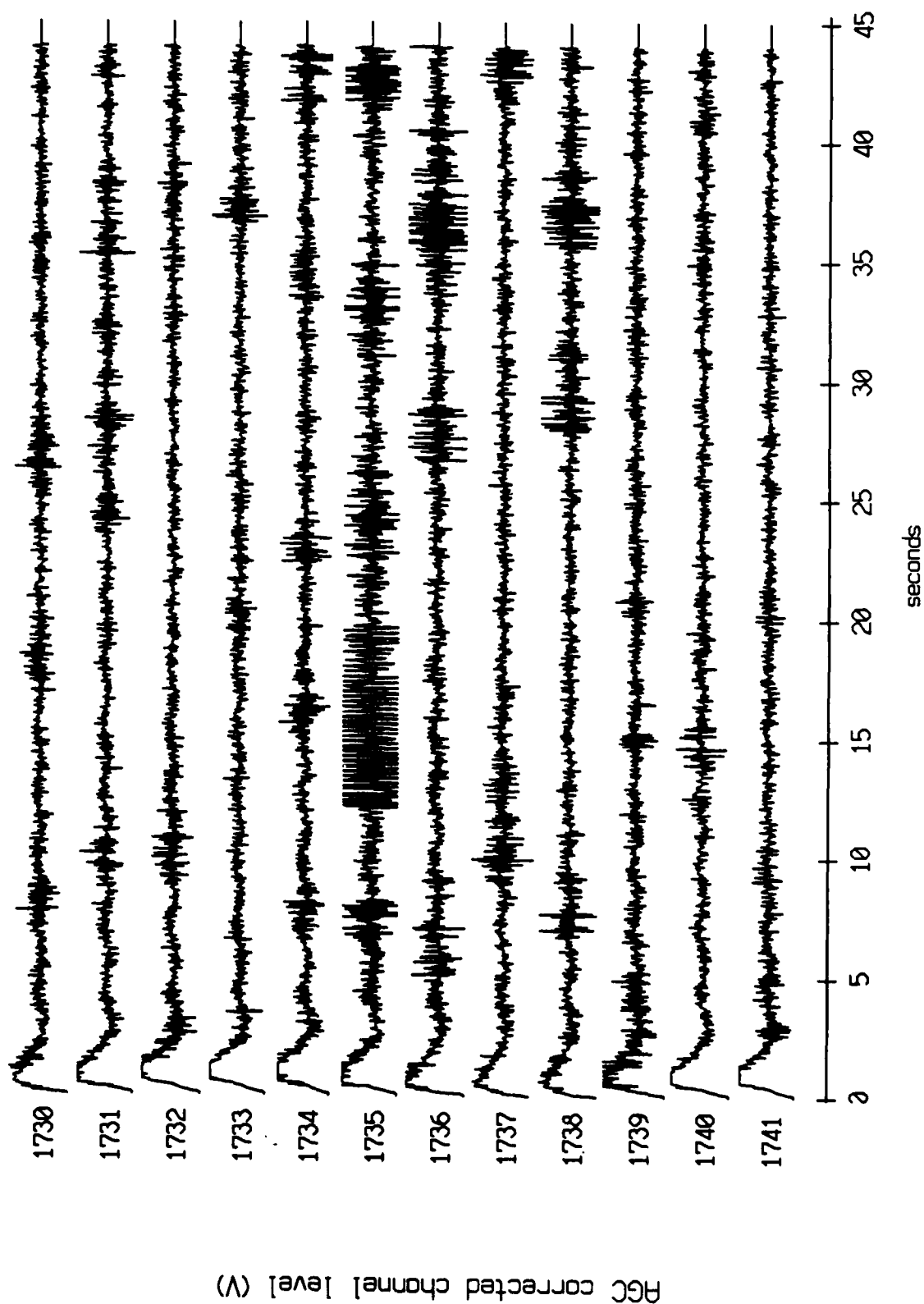
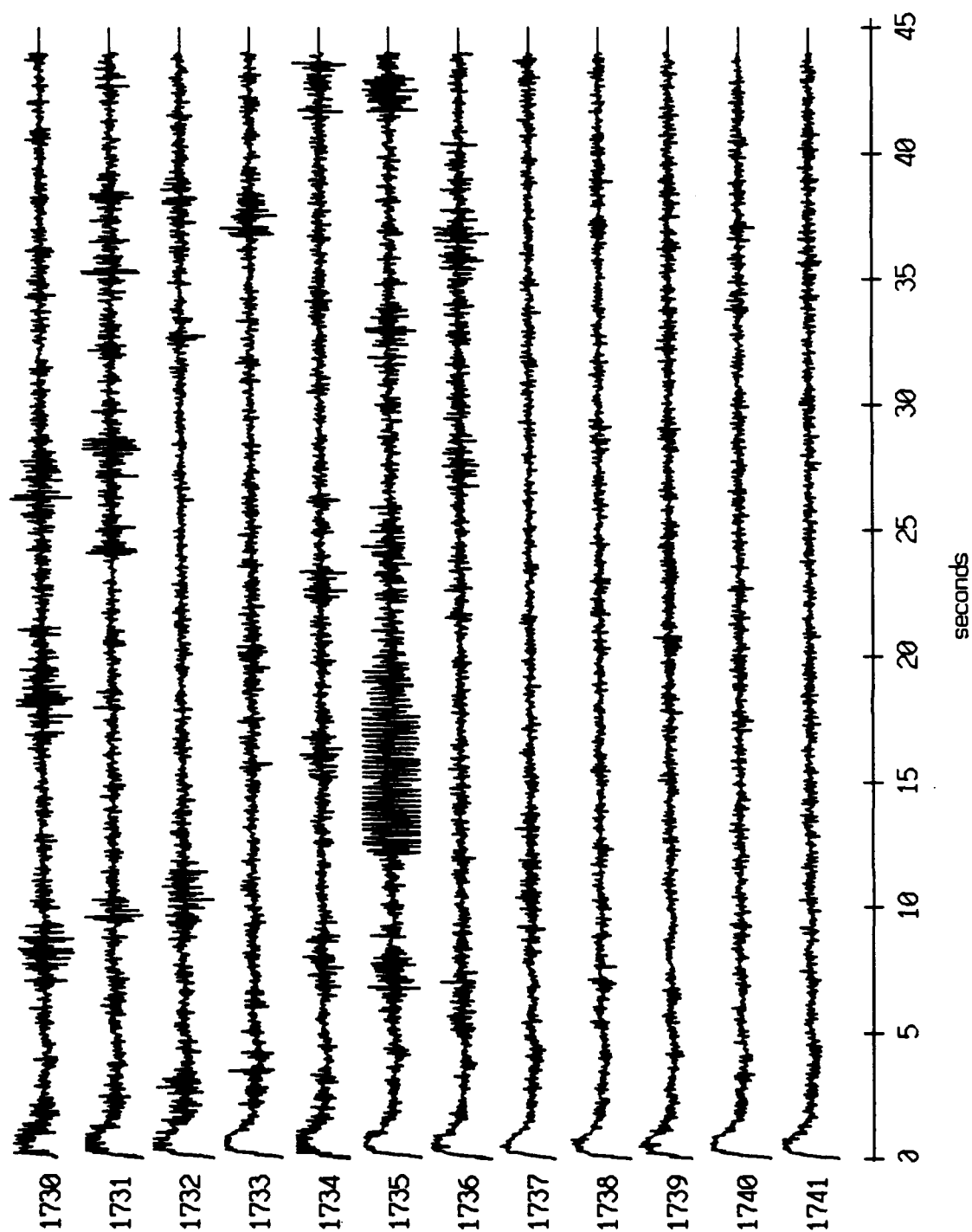


Figure XI.56a

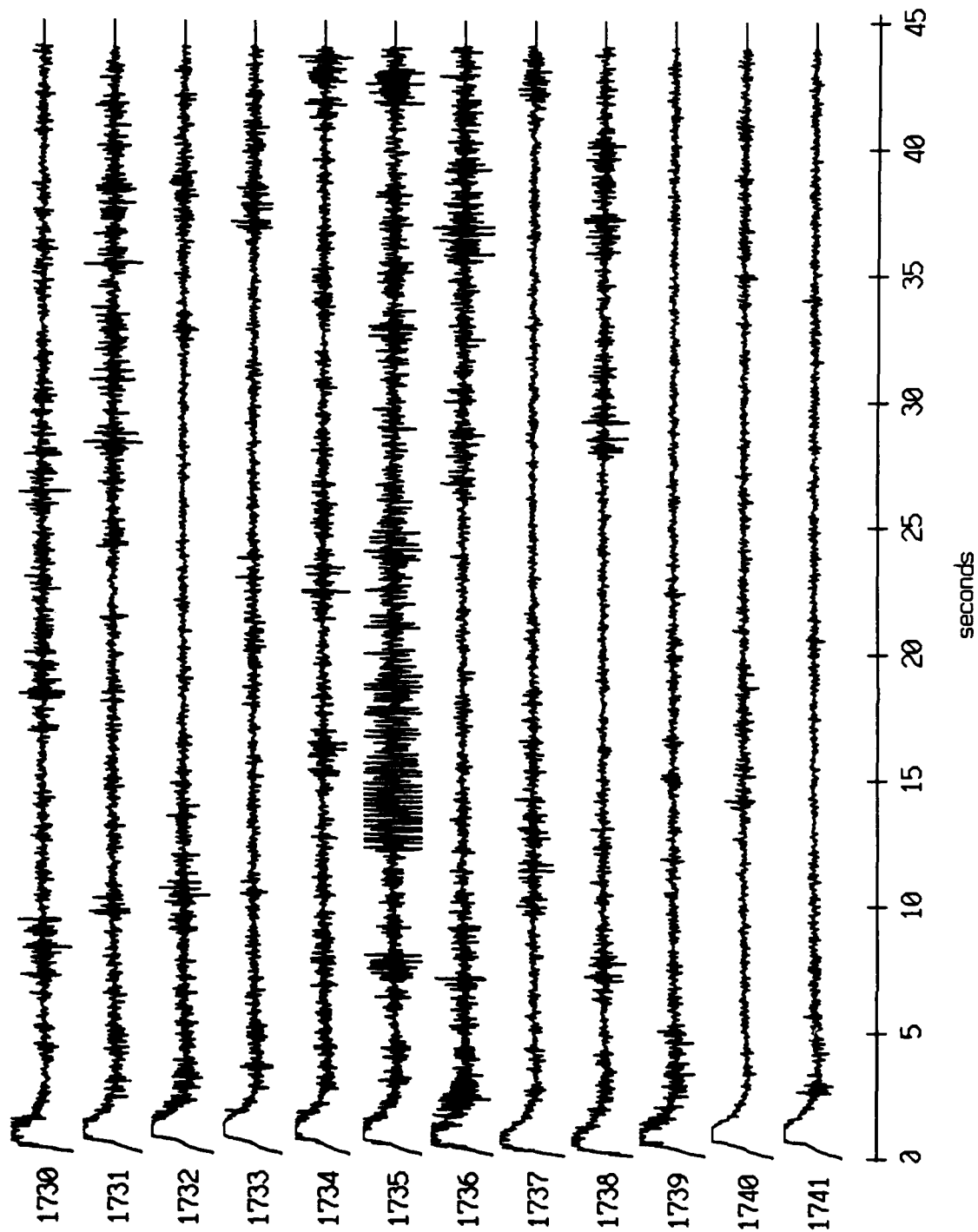
Float 3, July, 1989 Trip - records 1730-1741 (y-axis)  
vertical axis scale is approx. -2.0 to 2.0 volts



PGC corrected channel level (V)

Figure XI.56b

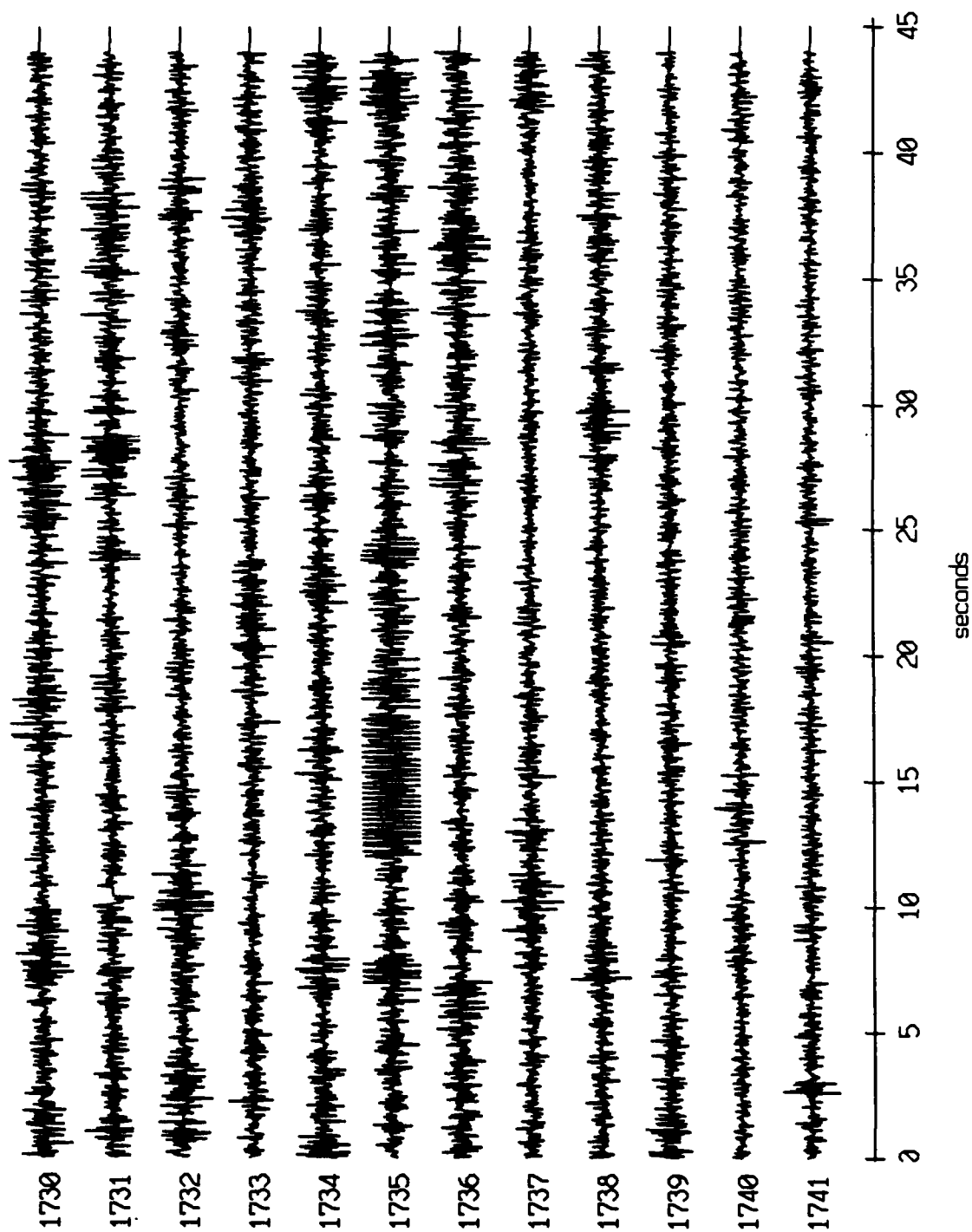
Float 3, July, 1989 Trip - records 1730-1741 (z-axis)  
vertical axis scale is approx. -2.0 to 2.0 volts



AGC corrected channel level (V)

Figure XI.56c

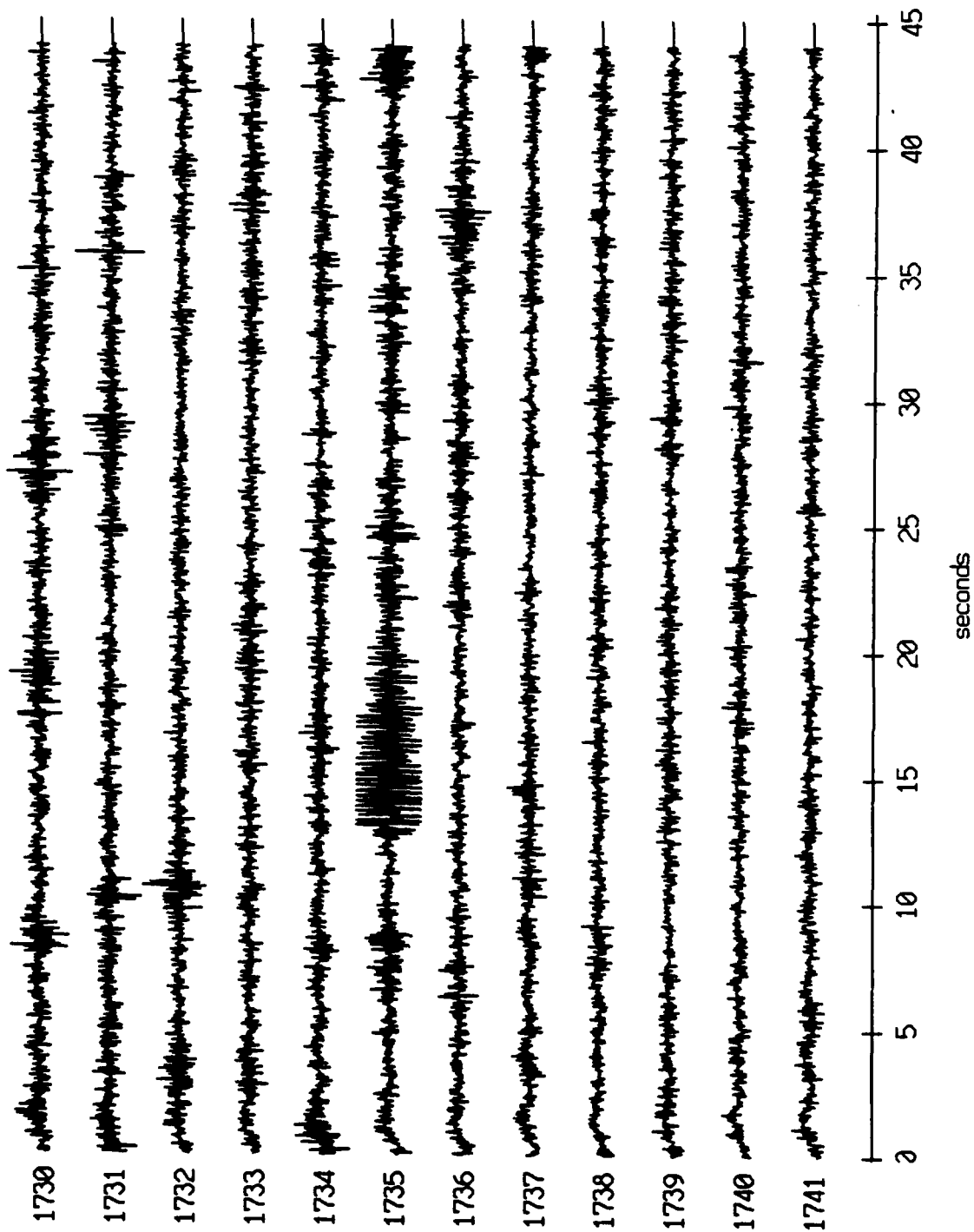
Float 3, July, 1989 Trip - records 1730-1741 (hydrophone)  
vertical axis scale is approx. -2.0 to 2.0 volts



AGC corrected channel level (V)

Figure XI.56d

Floot 4, July, 1989 Trip - records 1730-1741 (x-axis)  
vertical axis scale is approx. -2.0 to 2.0 volts



PGC corrected channel level (V)

Figure XI.57a

Float 4, July, 1989 Trip - records 1730-1741 (y-axis)  
vertical axis scale is approx. -2.0 to 2.0 volts

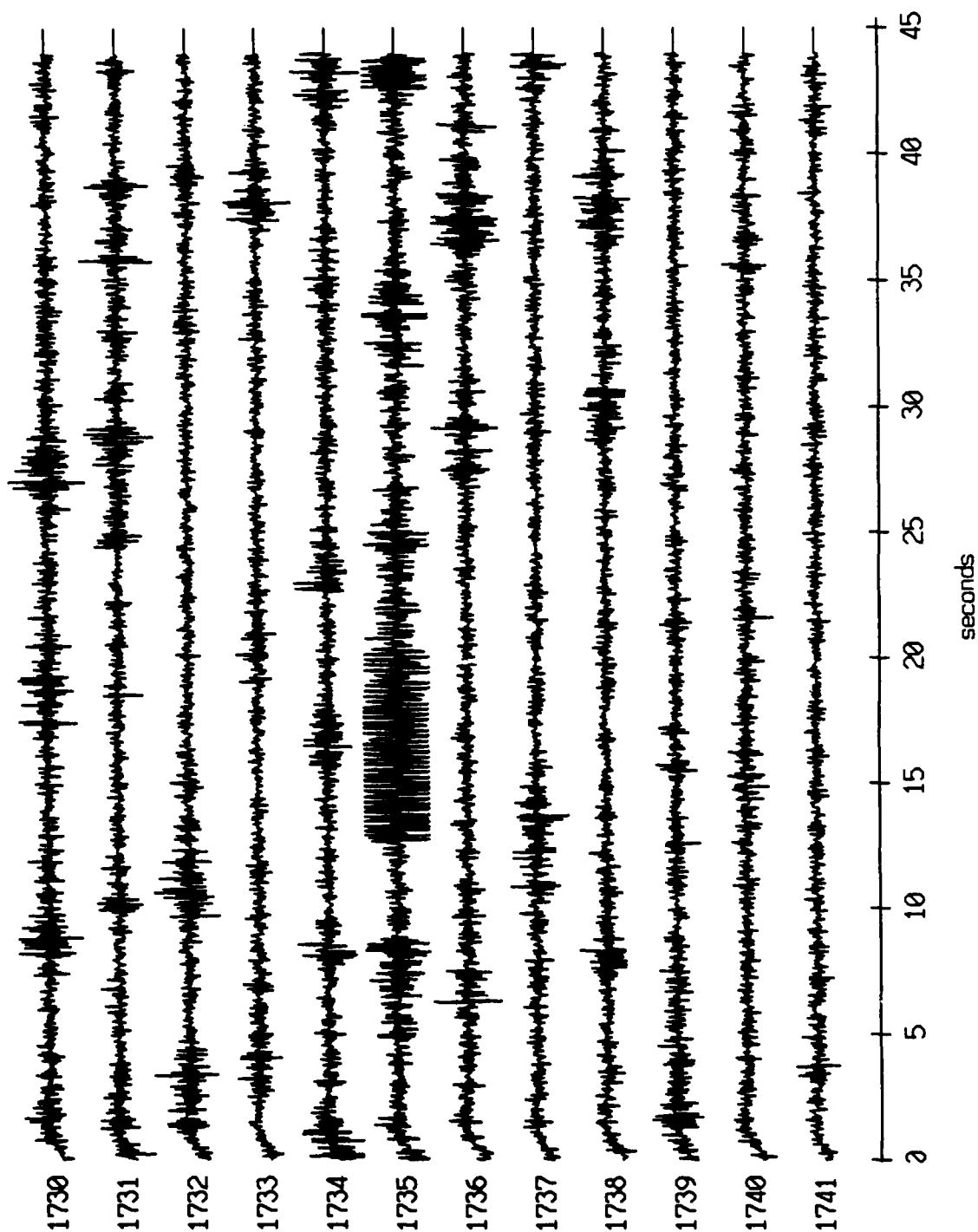
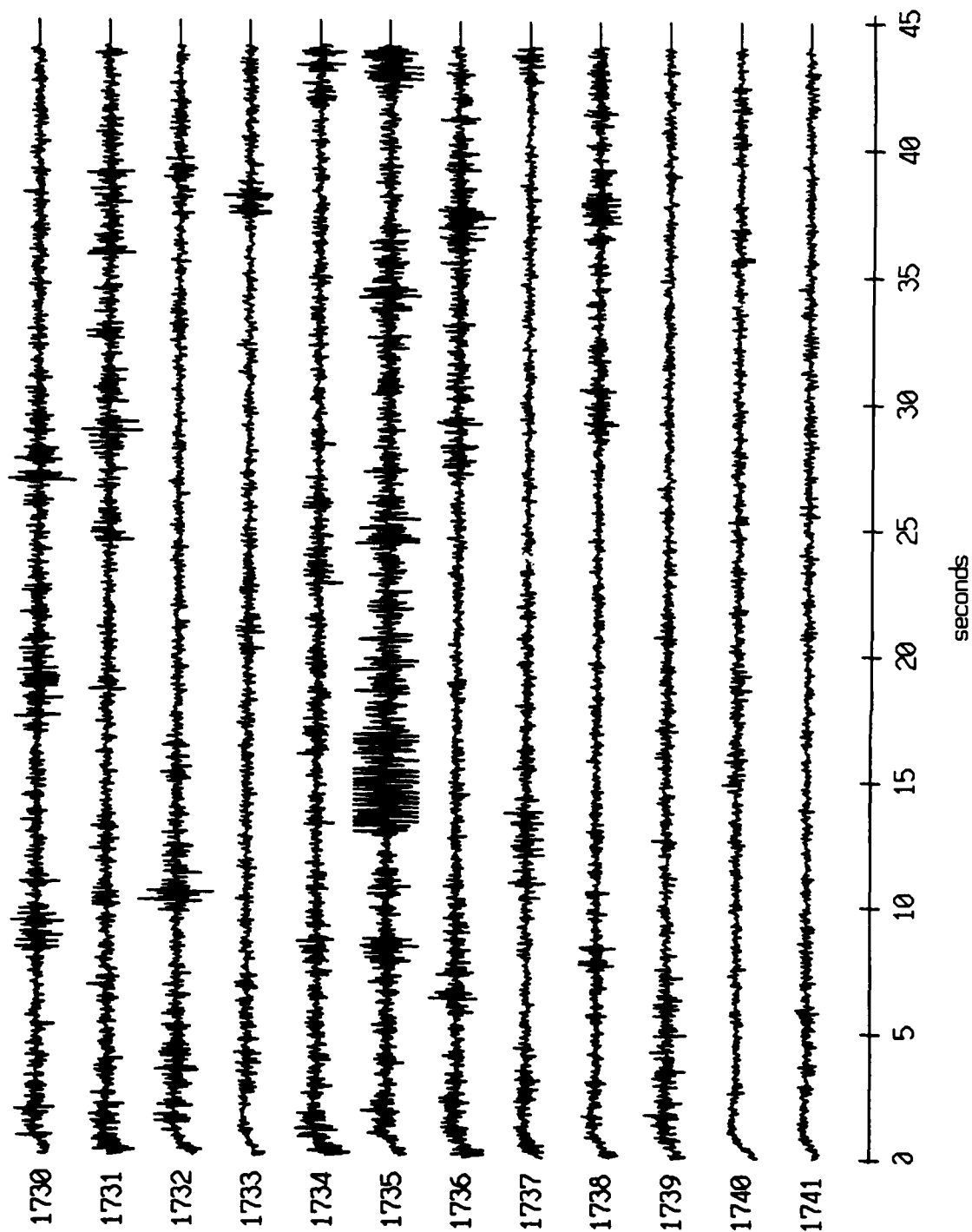


Figure XI.57b

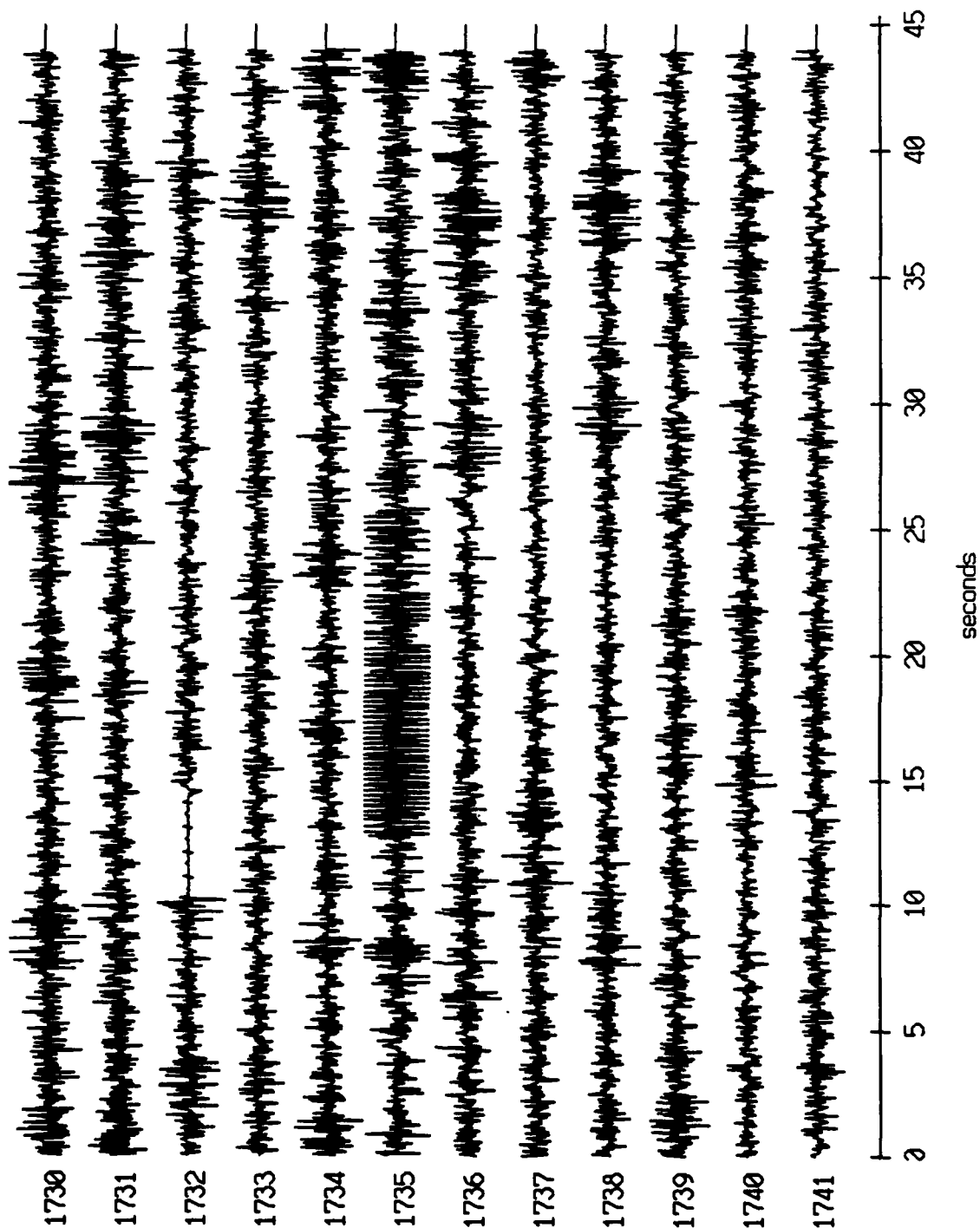
Float 4, July, 1989 Trip - records 1730-1741 (z-axis)  
vertical axis scale is approx. -2.0 to 2.0 volts



AGC corrected channel level (V)

Figure XI.57c

Float 4, July, 1989 Trip - records 1730-1741 (hydrophone)  
vertical axis scale is approx. -2.0 to 2.0 volts

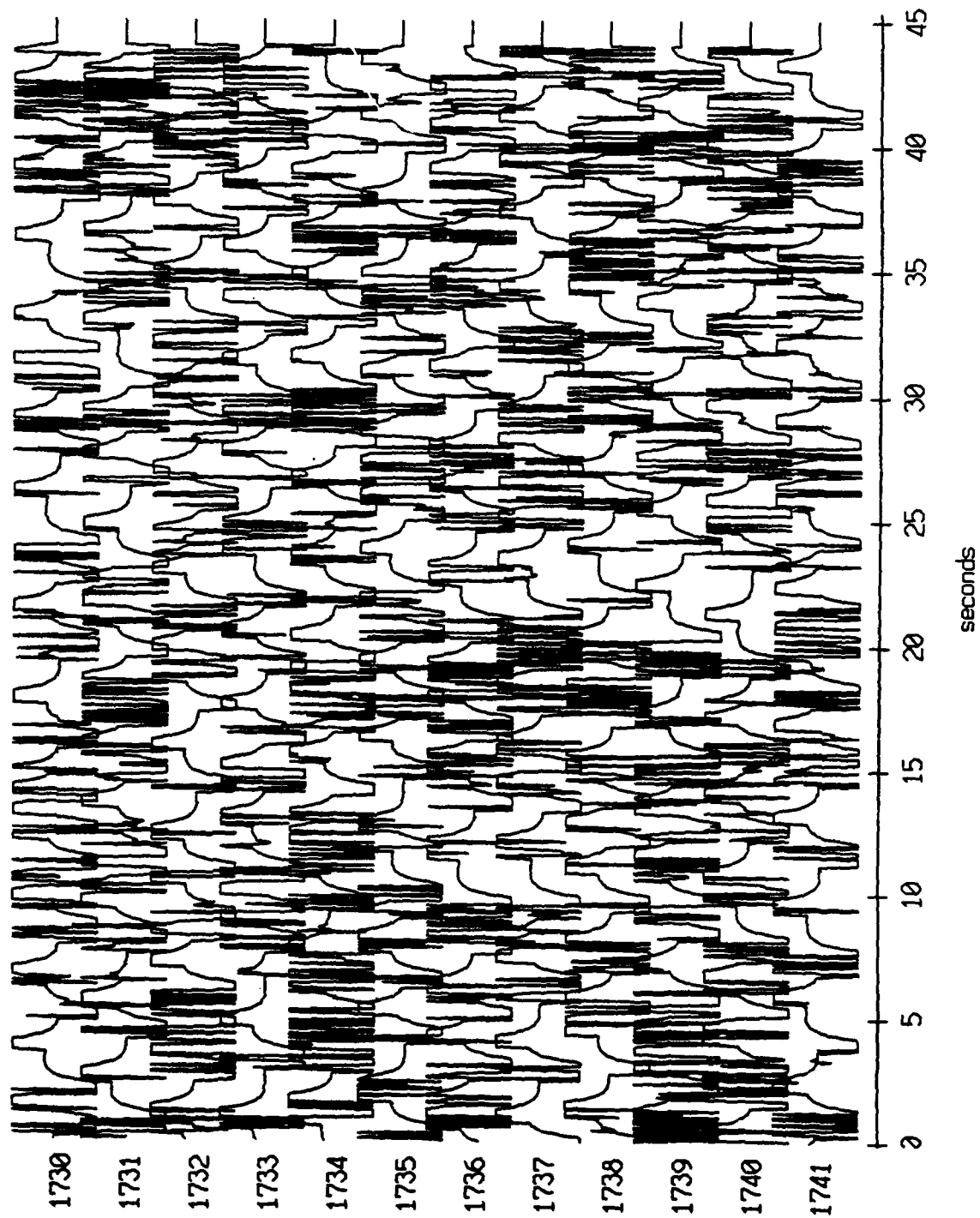


AGC corrected channel level (V)

Figure XI.57d



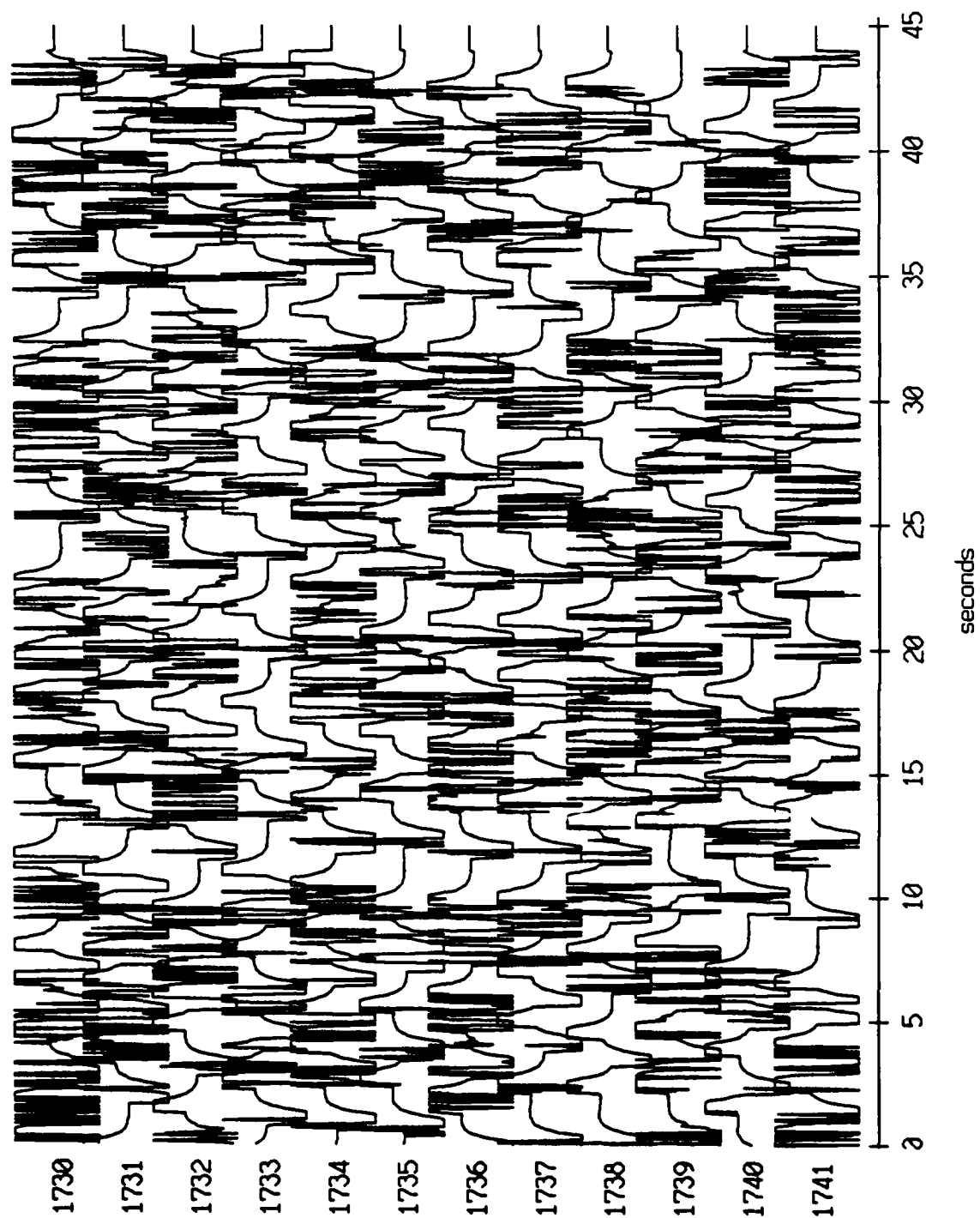
Float 5, July, 1989 Trip - records 1730-1741 (x-axis)  
vertical axis scale is approx. -2.0 to 2.0 volts



AGC corrected channel level (V)

Figure XI.58a

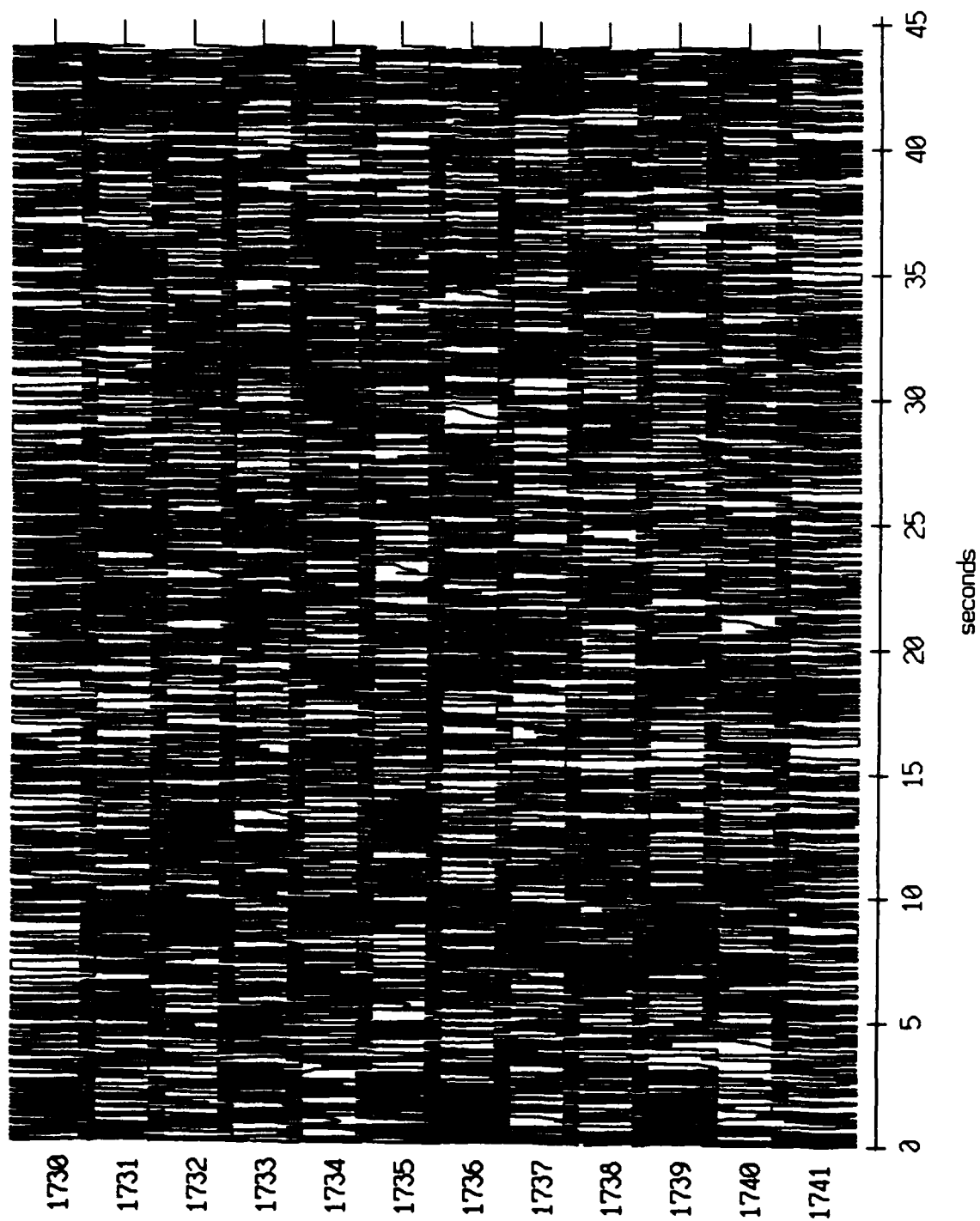
Float 5, July, 1989 Trip - records 1730-1741 (y-axis)  
vertical axis scale is approx. -2.0 to 2.0 volts



RGC corrected channel level (V)

Figure XI.58b

Float 5, July, 1989 Trip - records 1730-1741 (z-axis)  
vertical axis scale is approx. -2.0 to 2.0 volts



AGC corrected channel level (V)

Figure XI.58c

Float 5, July, 1989 Trip - records 1730-1741 (hydrophone)  
vertical axis scale is approx. -2.0 to 2.0 volts

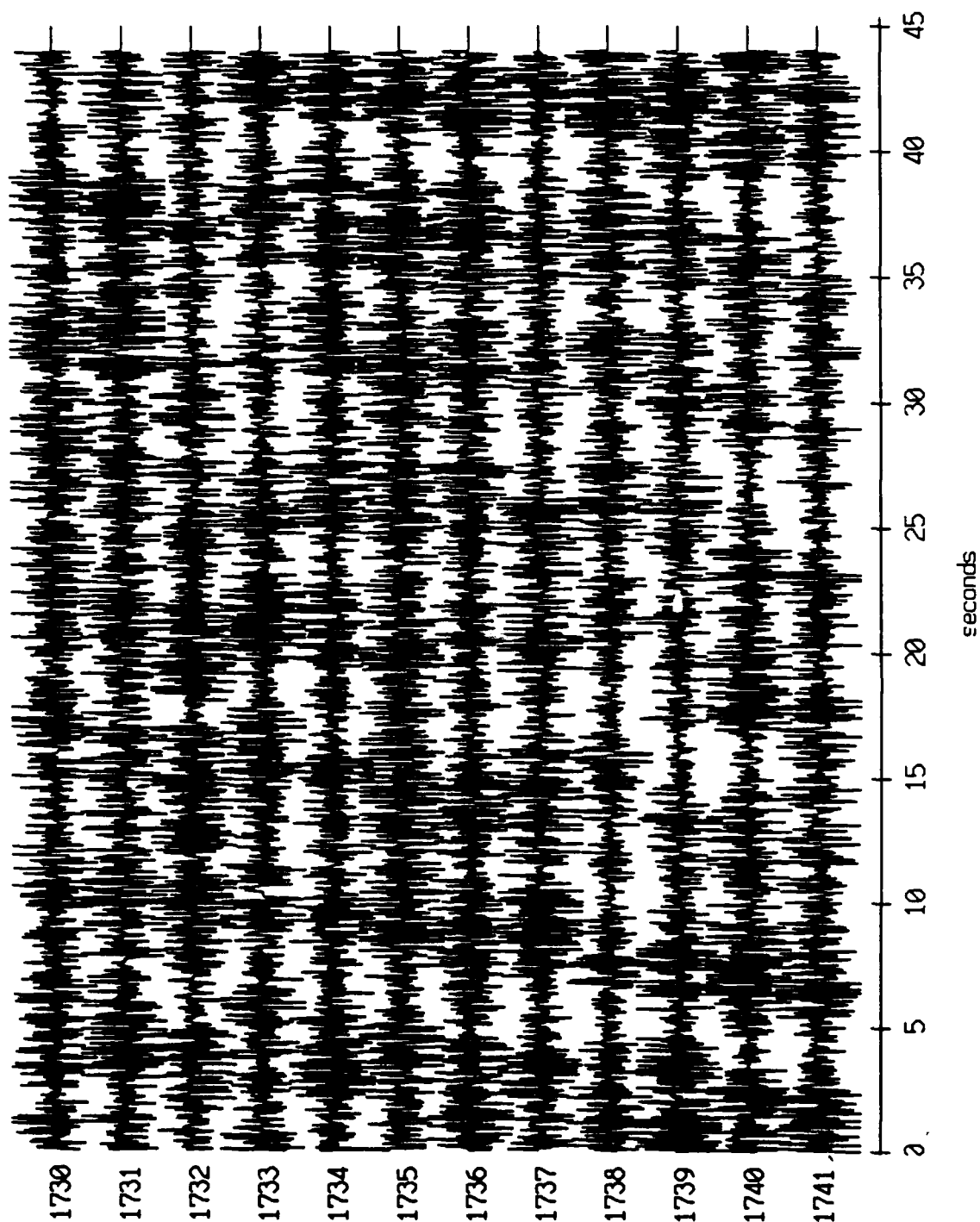
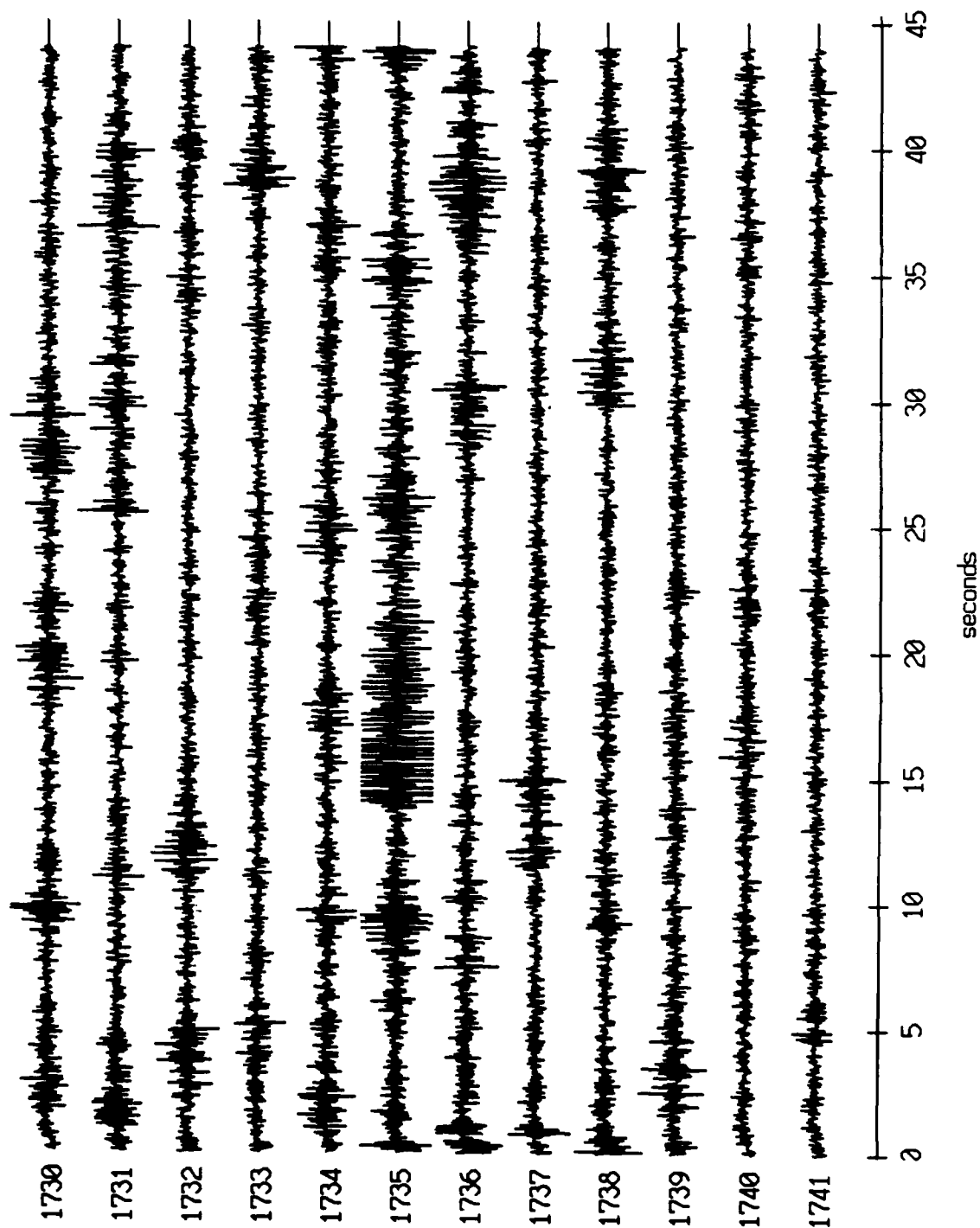


Figure XI.58d

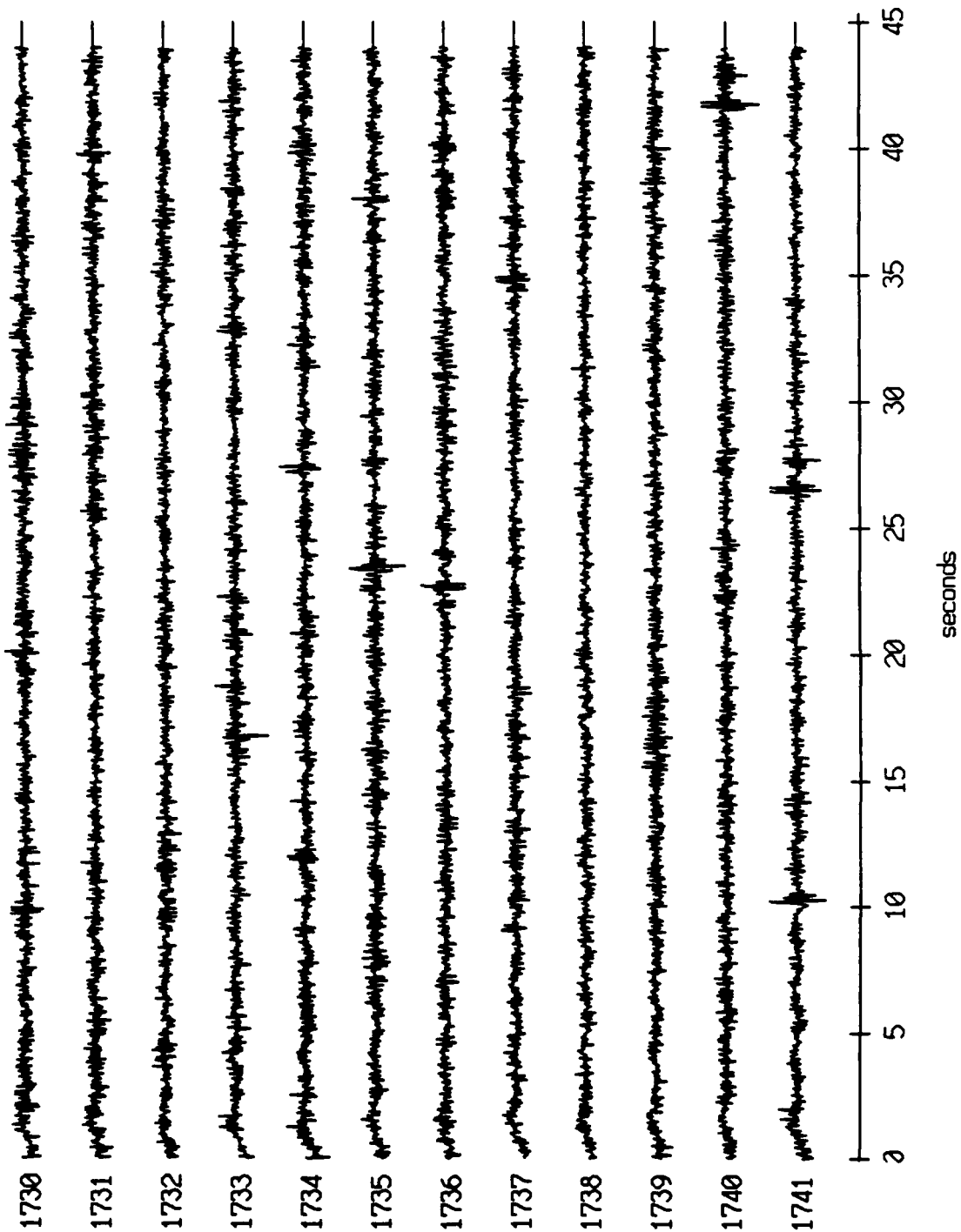
Float 6, July, 1989 Trip - records 1730-1741 (x-axis)  
vertical axis scale is approx. -2.0 to 2.0 volts



AGC corrected channel level (V)

Figure XI.59a

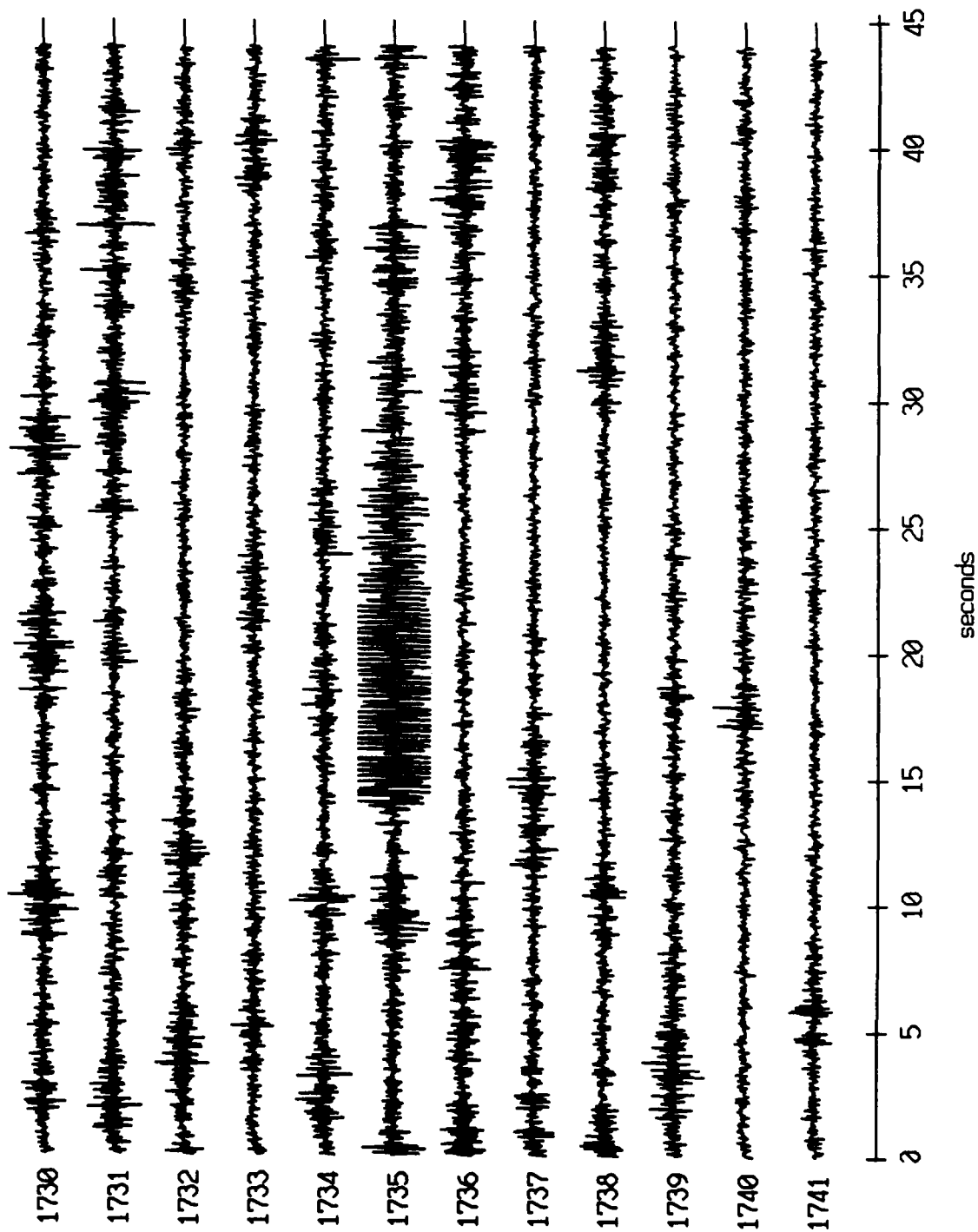
Float 6, July, 1989 Trip - records 1730-1741 (y-axis)  
vertical axis scale is approx. -2.0 to 2.0 volts



AGC corrected channel level (V)

Figure XI.59b

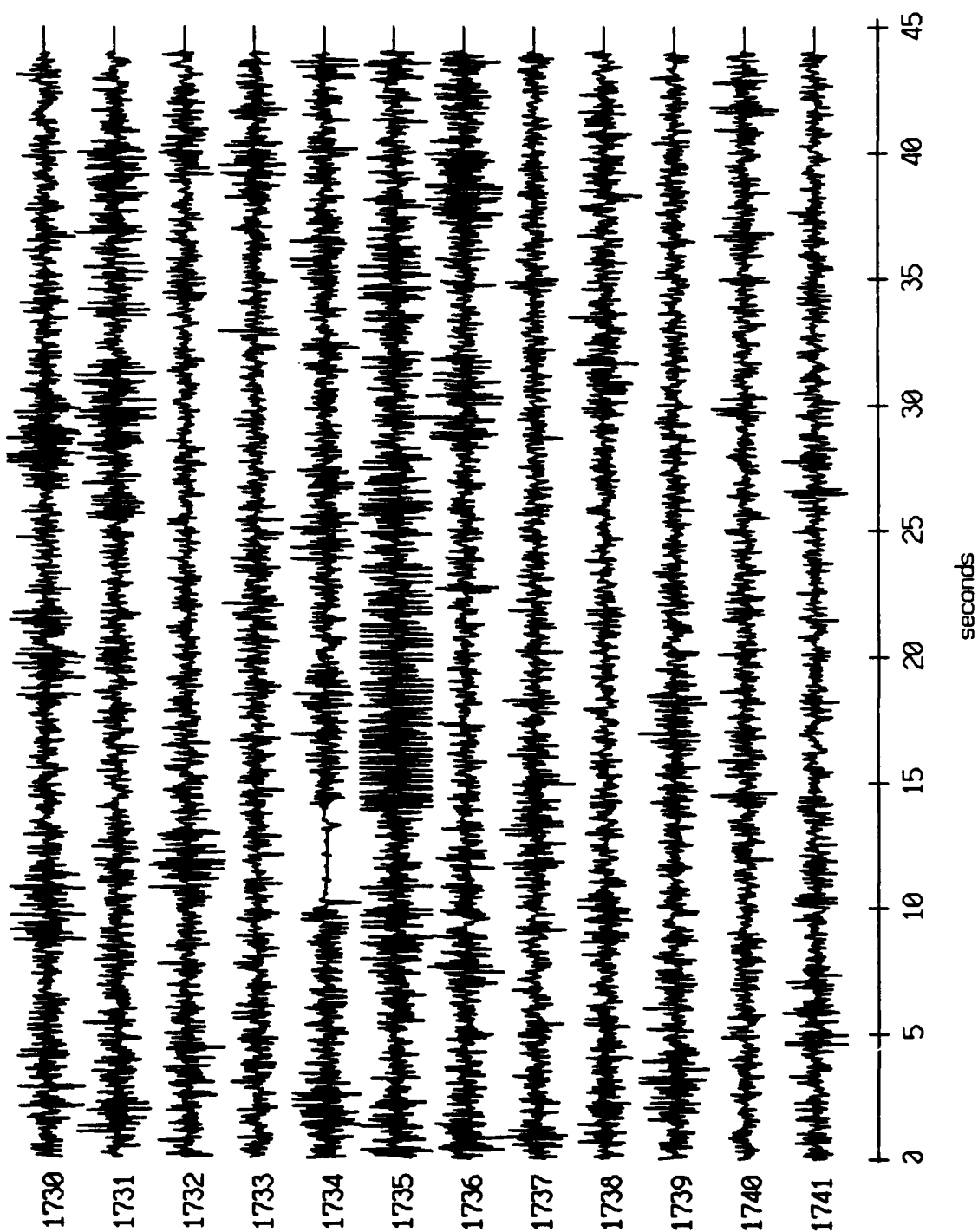
Float 6, July, 1989 Trip - records 1730-1741 (z-axis)  
vertical axis scale is approx. -2.0 to 2.0 volts



AGC corrected channel level (V)

Figure XI.59c

Float 6, July, 1989 Trip - records 1730-1741 (hydrophone)  
vertical axis scale is approx. -2.0 to 2.0 volts

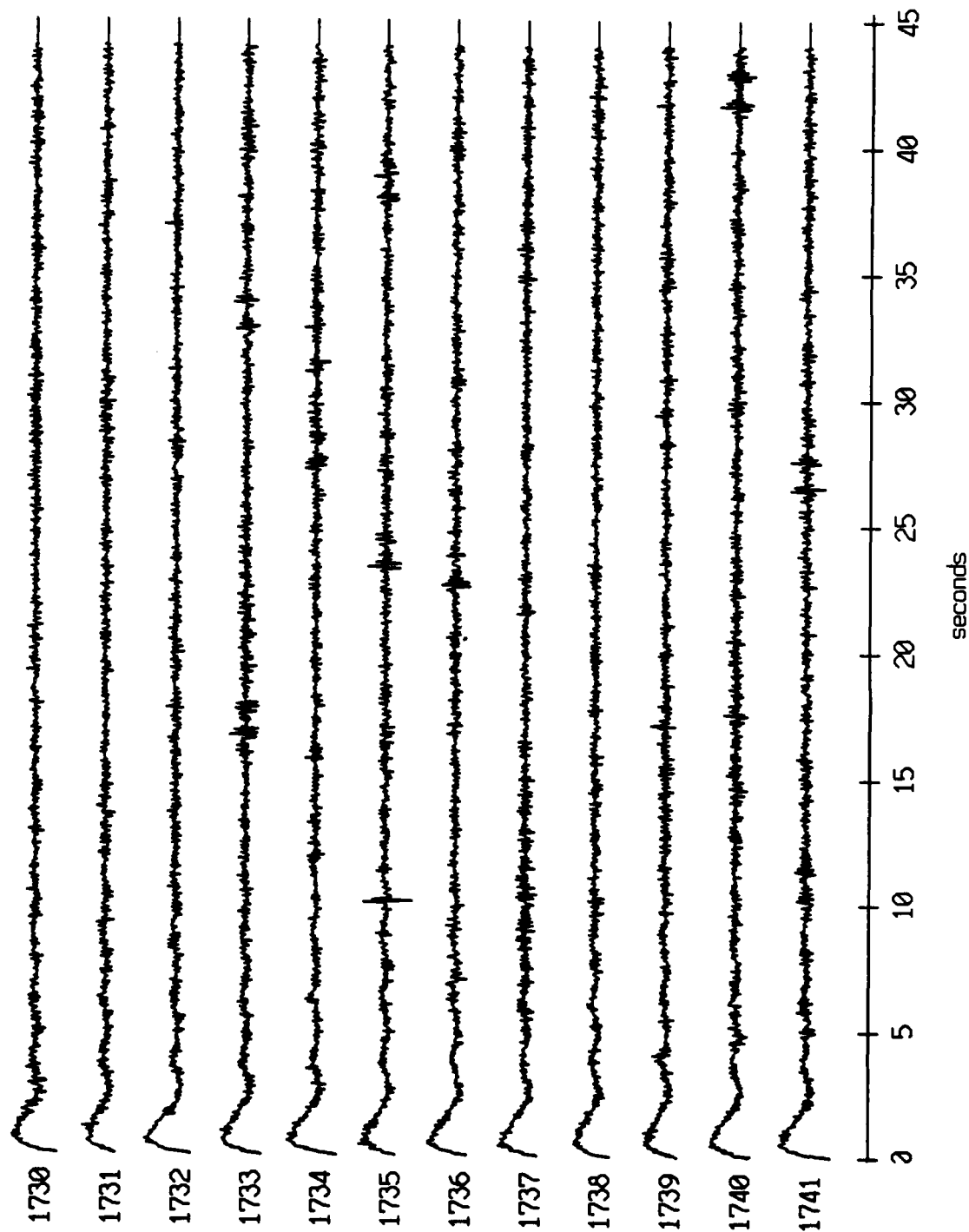


AGC corrected channel level (V)

Figure XI.59d



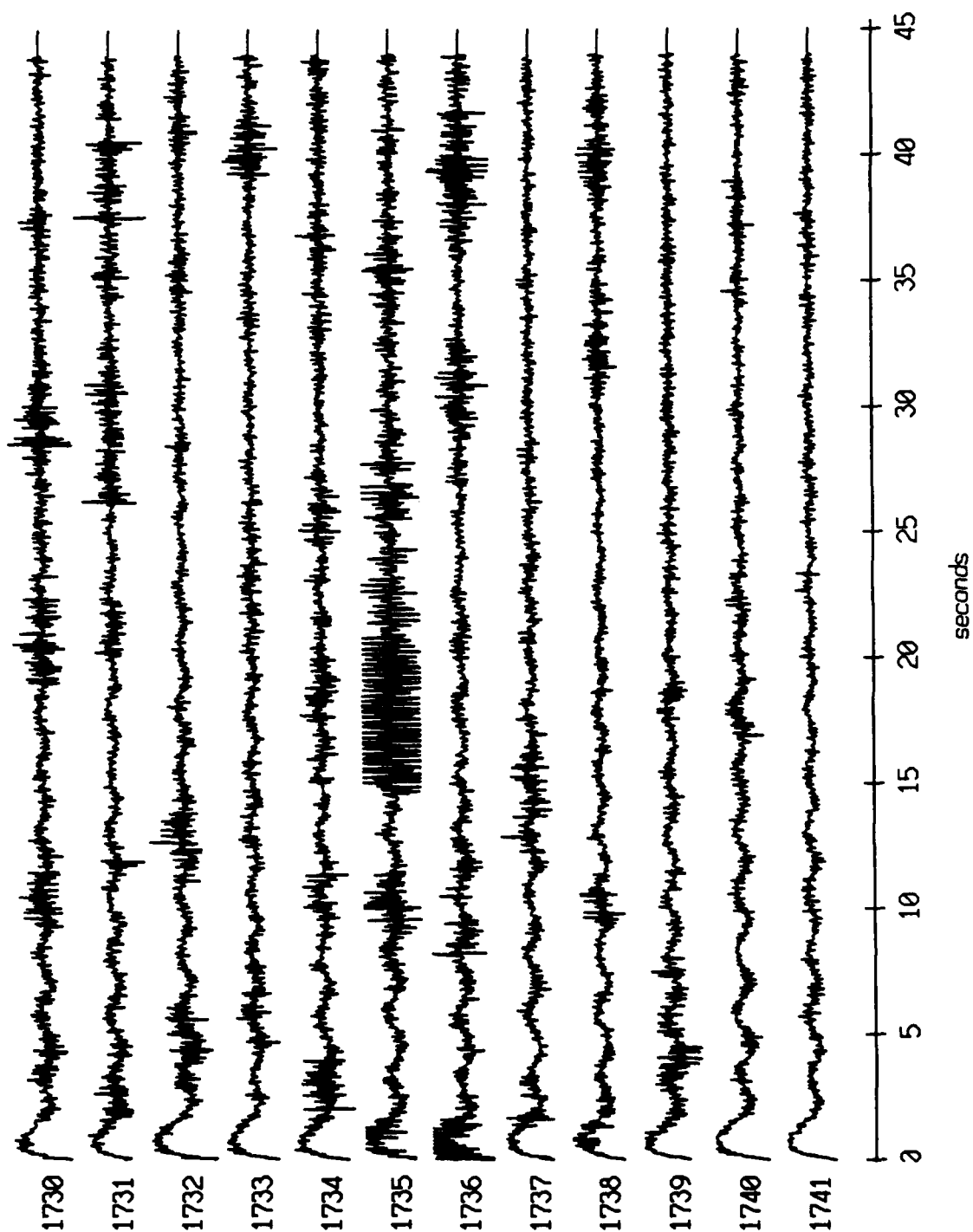
Float 7, July, 1989 Trip - records 1730-1741 (x-axis)  
vertical axis scale is approx. -2.0 to 2.0 volts



PGC corrected channel level (V)

Figure XI.60a

Float 7, July, 1989 Trip - records 1730-1741 (y-axis)  
vertical axis scale is approx. -2.0 to 2.0 volts



RGC corrected channel level (V)

Figure XI.60b

Float 7, July, 1989 Trip - records 1730-1741 (z-axis)  
vertical axis scale is approx. -2.0 to 2.0 volts

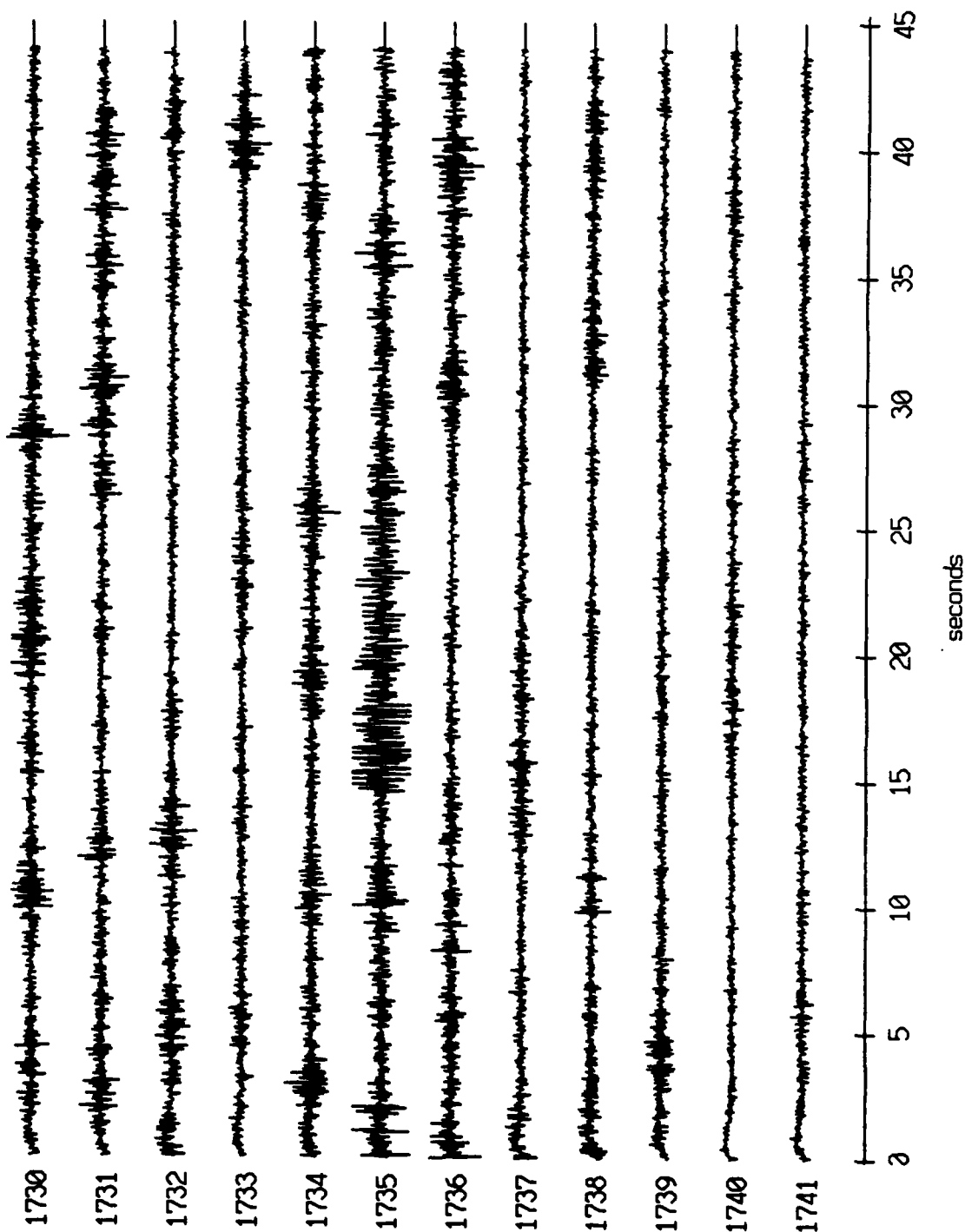
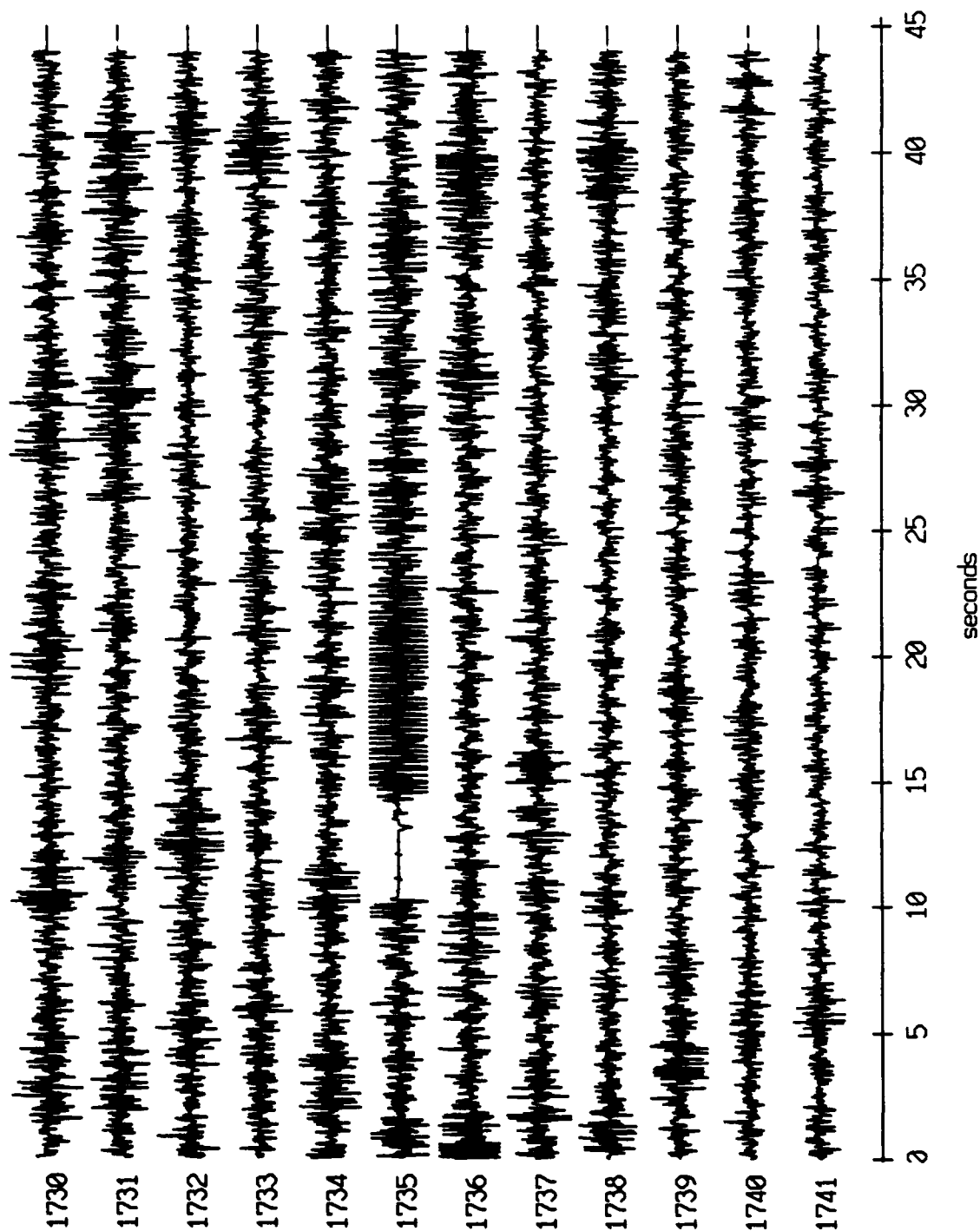


Figure XI.60c

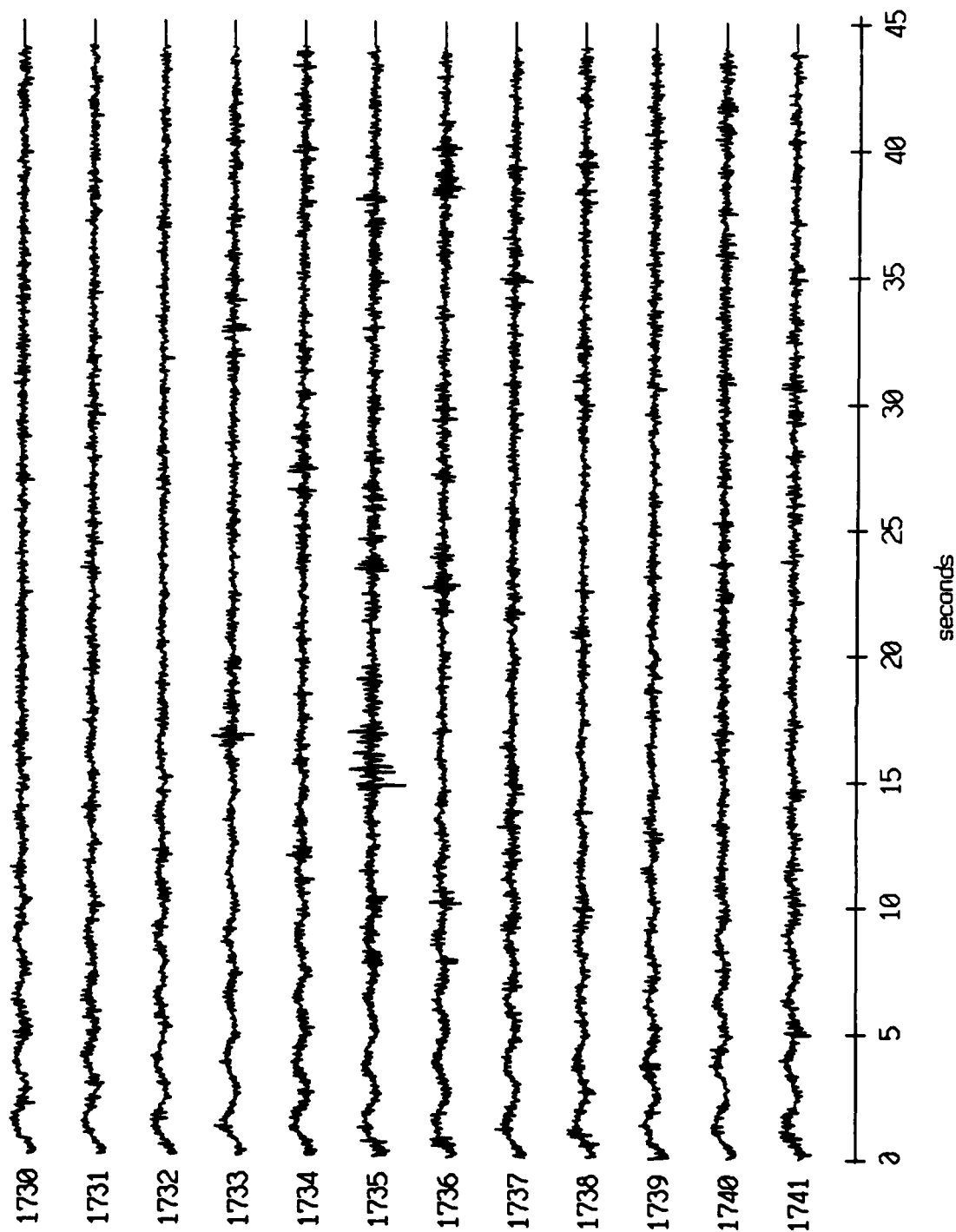
Float 7, July, 1989 Trip - records 1730-1741 (hydrophone)  
vertical axis scale is approx. -2.0 to 2.0 volts



AGC corrected channel level (V)

Figure XI.60d

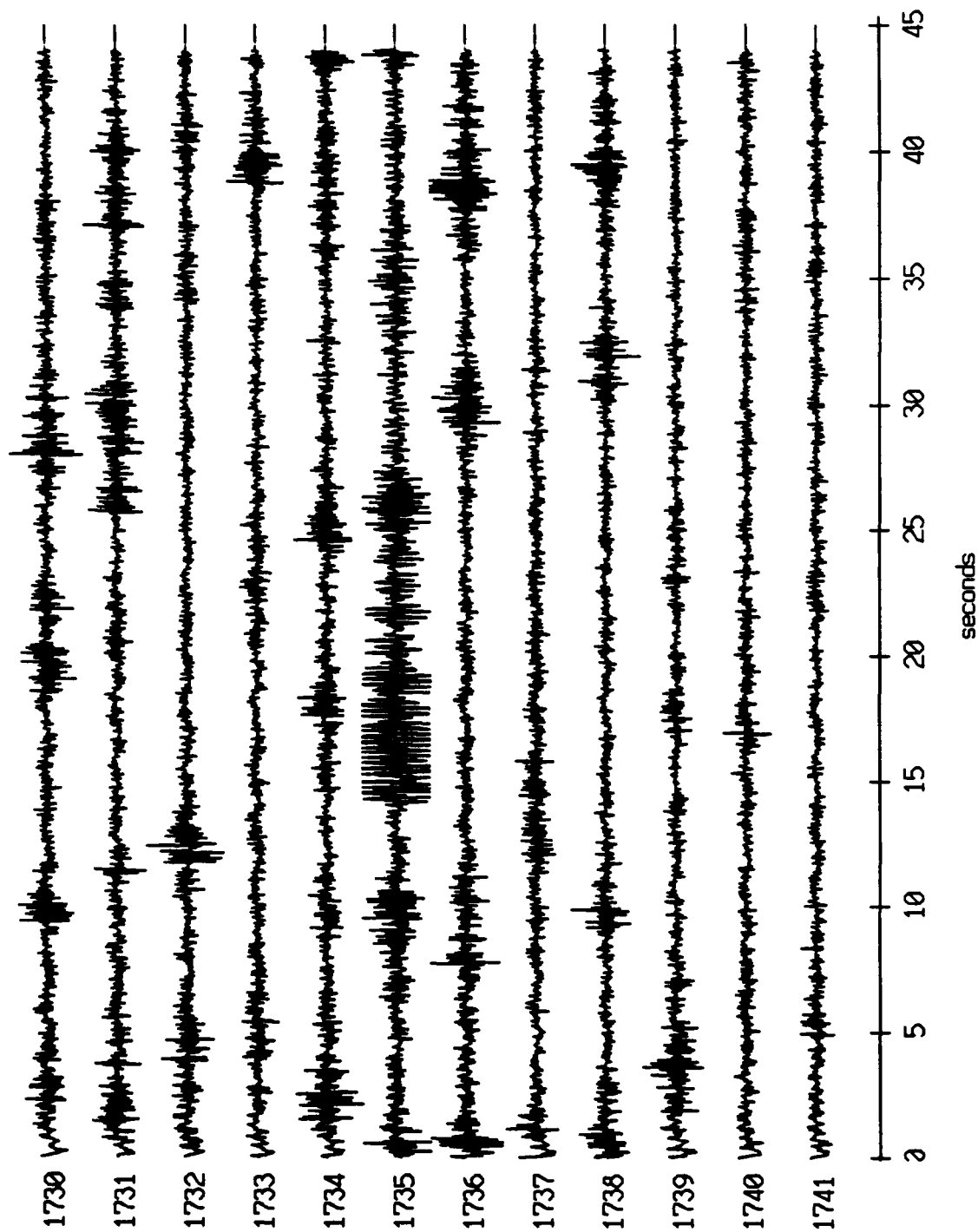
Float 8, July, 1989 Trip - records 1730-1741 (x-axis)  
vertical axis scale is approx. -2.0 to 2.0 volts



AGC corrected channel level (V)

Figure XI.61a

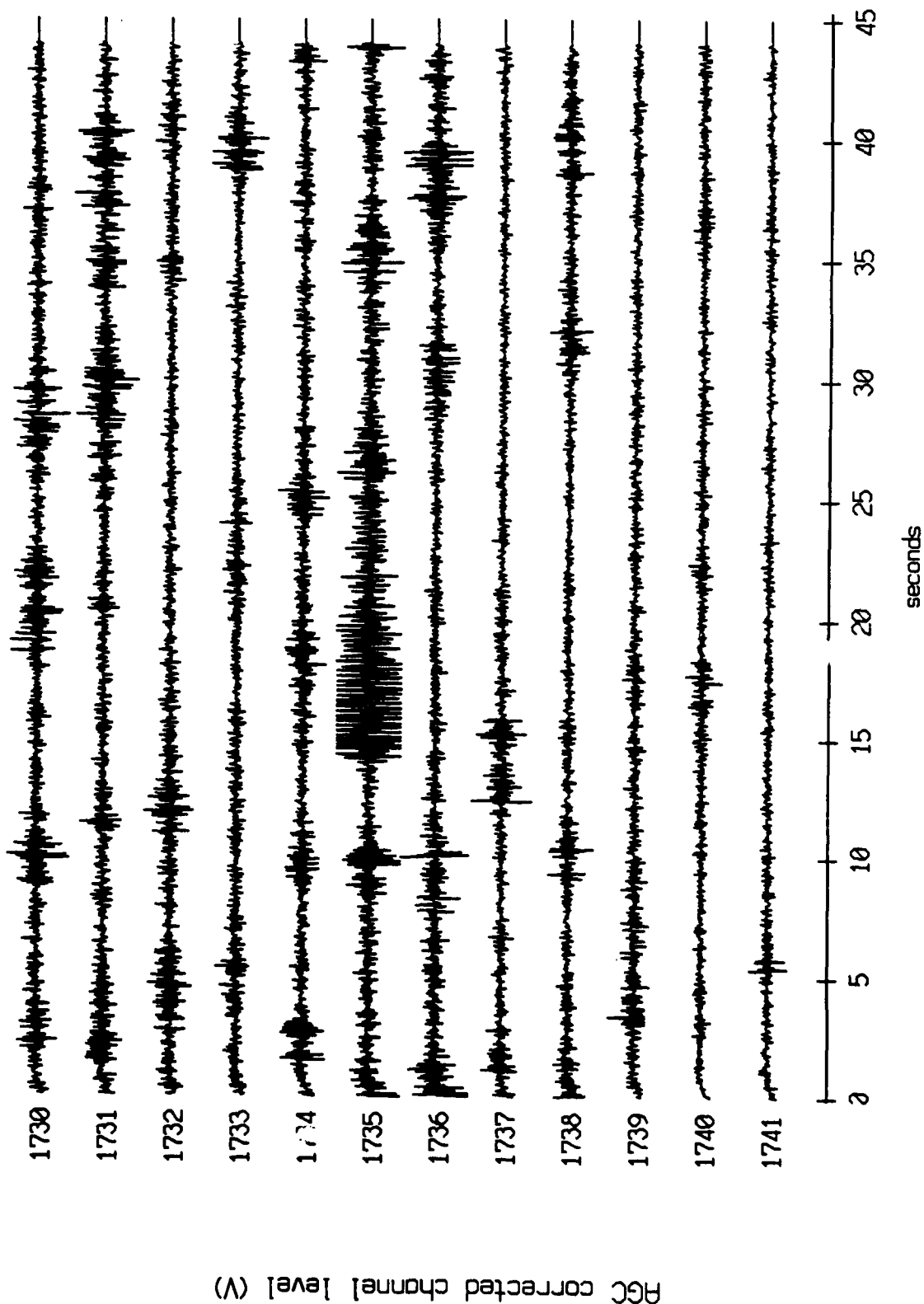
Float 8, July, 1989 Trip - records 1730-1741 (y-axis)  
vertical axis scale is approx. -2.0 to 2.0 volts



RGC corrected channel level (V)

Figure XI.61b

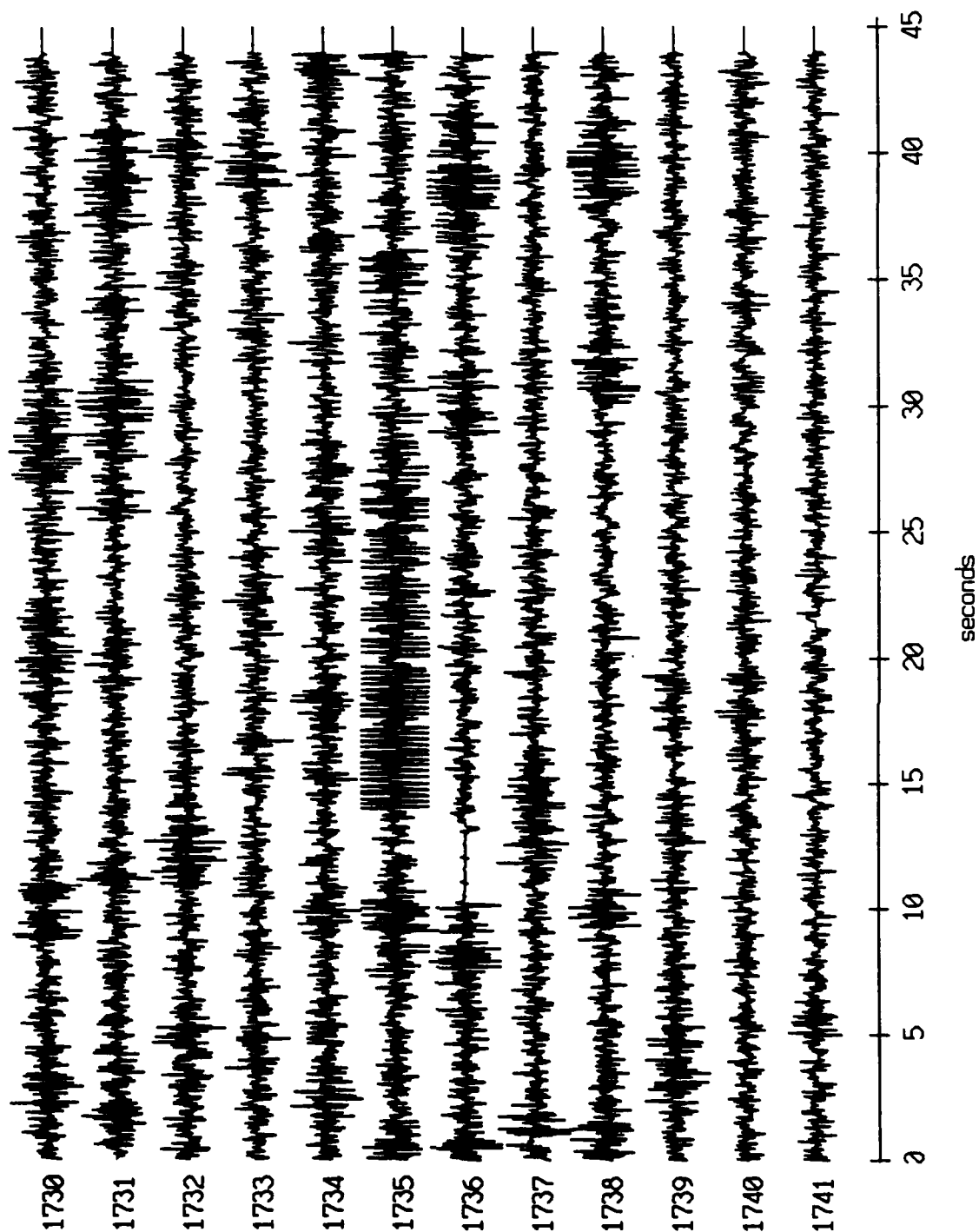
Float 8, July, 1989 Trip - records 1730-1741 (z-axis)  
vertical axis scale is approx. -2.0 to 2.0 volts



RGC corrected channel level (V)

Figure XI.61c

Float 8, July, 1989 Trip - records 1730-1741 (hydrophone)  
vertical axis scale is approx. -2.0 to 2.0 volts

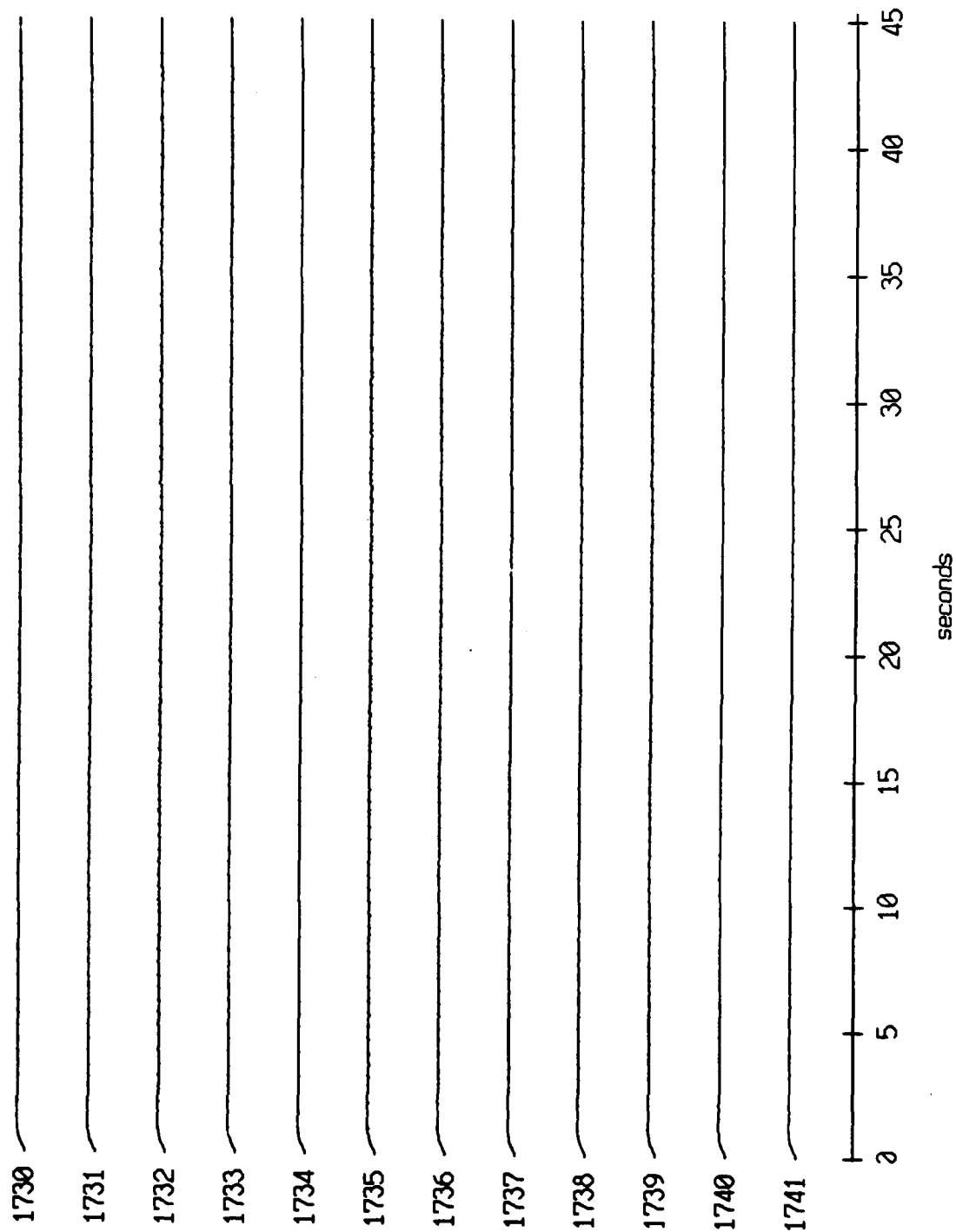


AGC corrected channel level (V)

Figure XI.61d



Float 9, July, 1989 Trip - records 1730-1741 (x-axis)  
vertical axis scale is approx. -2.0 to 2.0 volts



AGC corrected channel level (V)

Figure XI.62a

Float 9, July, 1989 Trip - records 1730-1741 (y-axis)  
vertical axis scale is approx. -2.0 to 2.0 volts

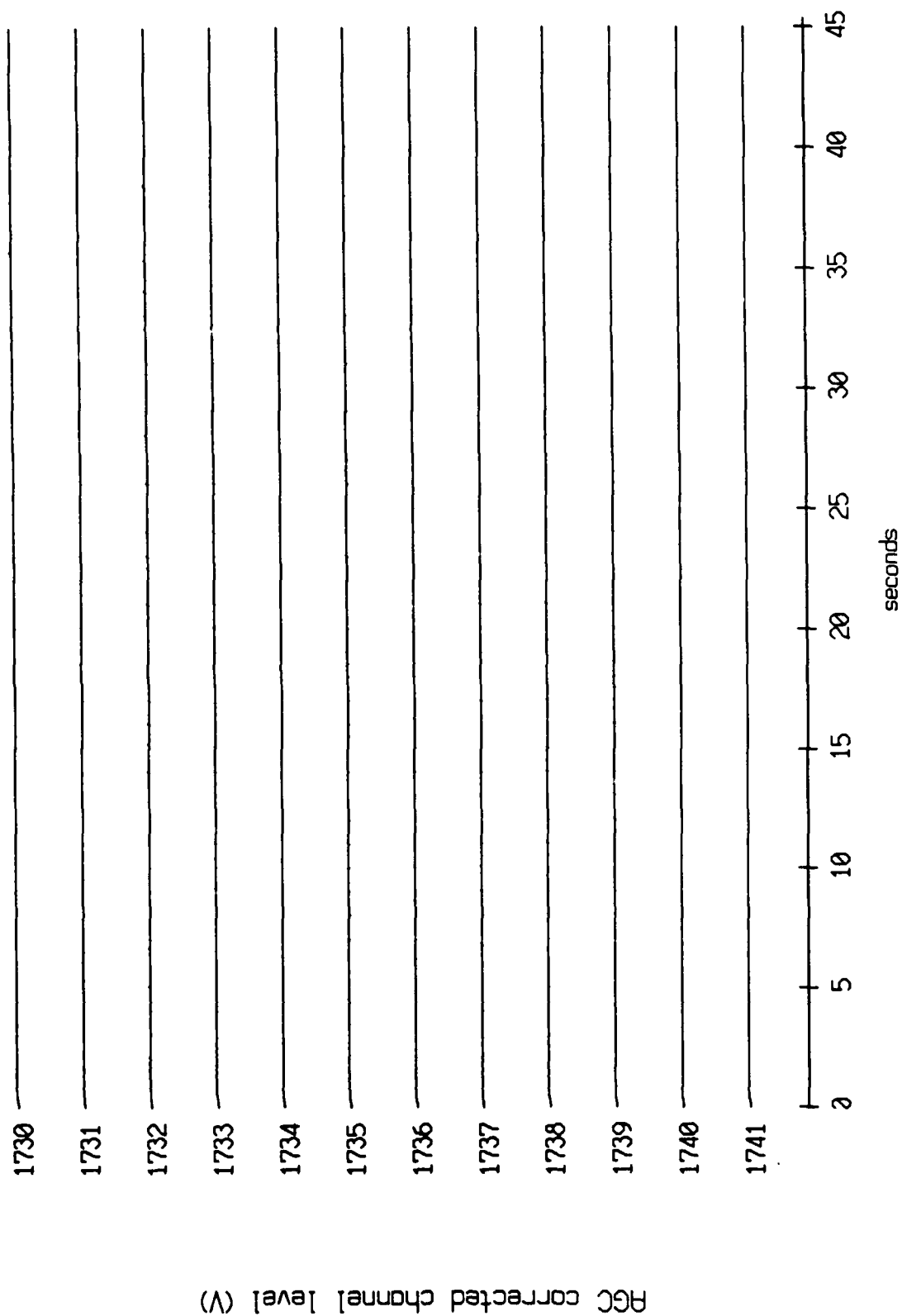
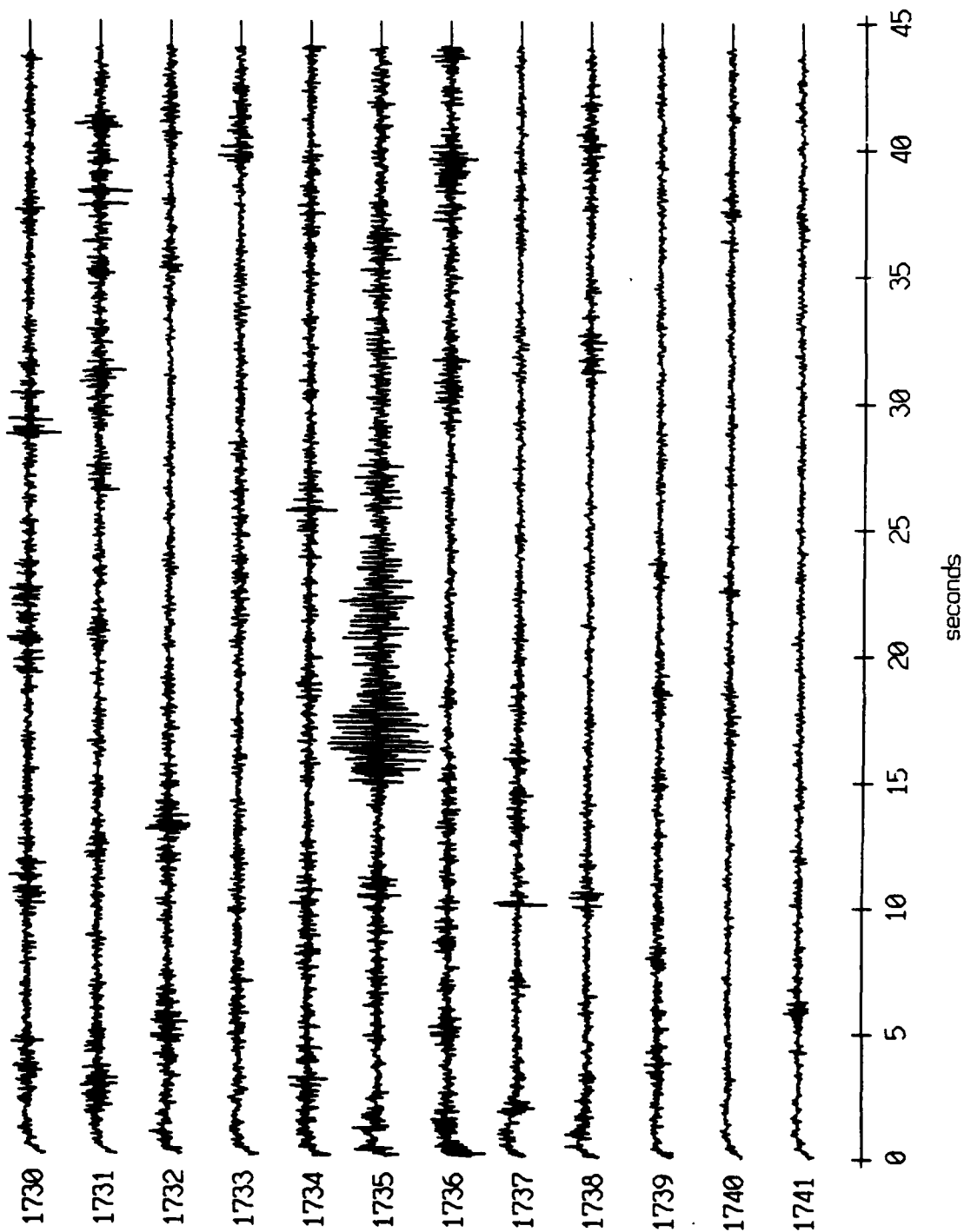


Figure XI.62b

Float 9, July, 1989 Trip - records 1730-1741 (z-axis)  
vertical axis scale is approx. -2.0 to 2.0 volts



AGC corrected channel level (V)

Figure XI.62c

Floot 9, July, 1989 Trip - records 1730-1741 (hydrophone)  
vertical axis scale is approx. -2.0 to 2.0 volts

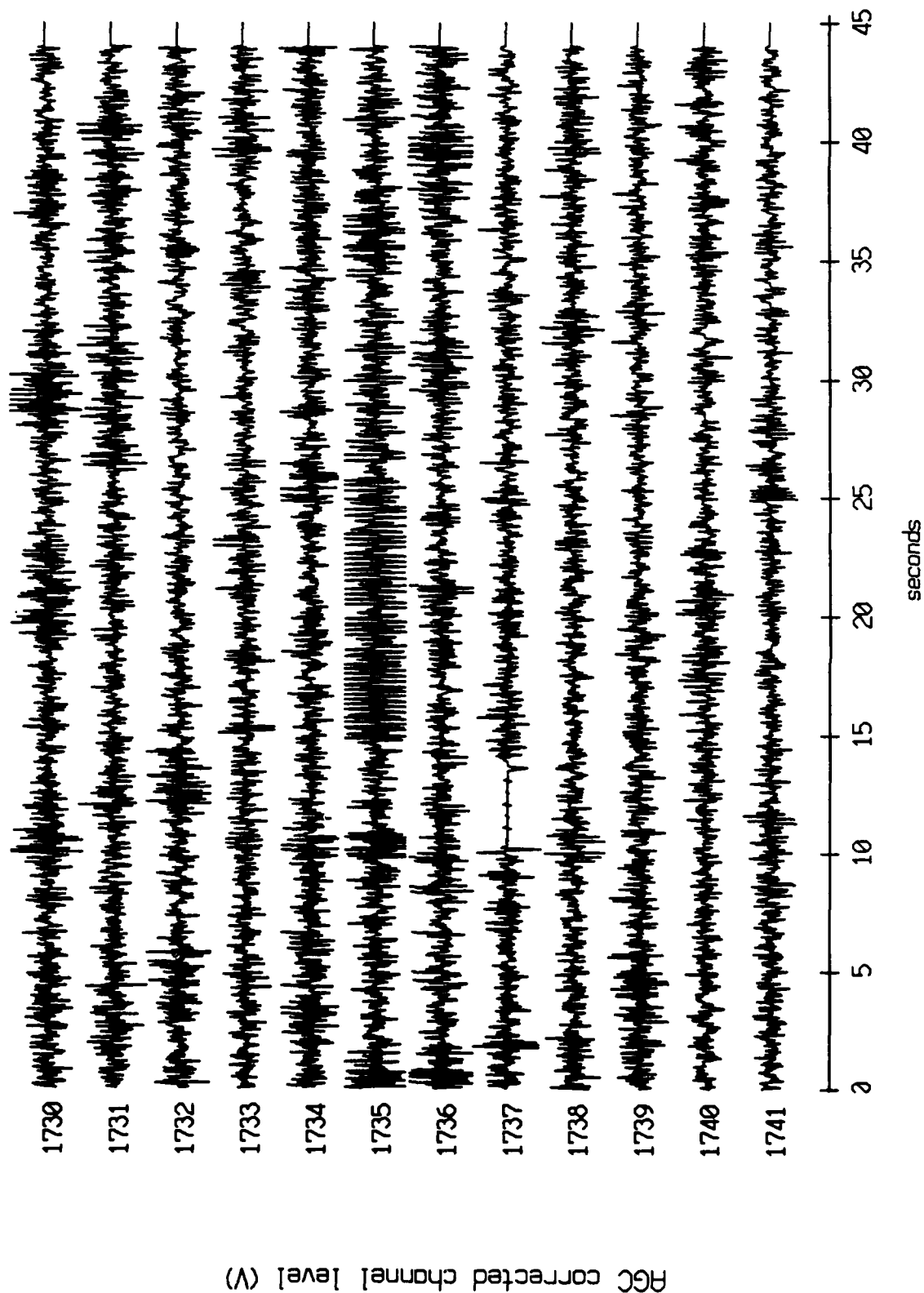


Figure XI.62d

Float 10, July, 1989 Trip - records 1730-1741 (x-axis)  
vertical axis scale is approx. -2.0 to 2.0 volts

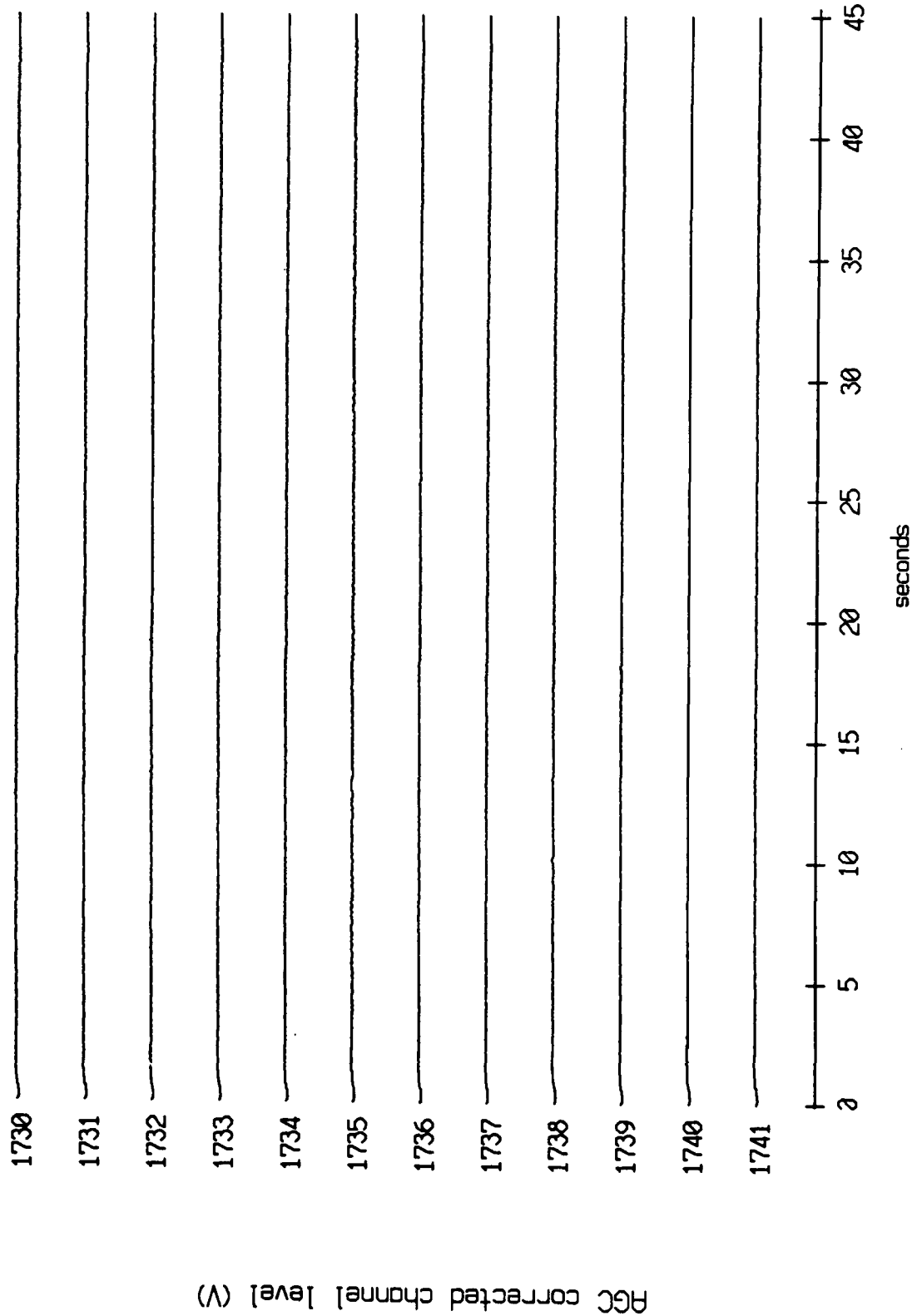
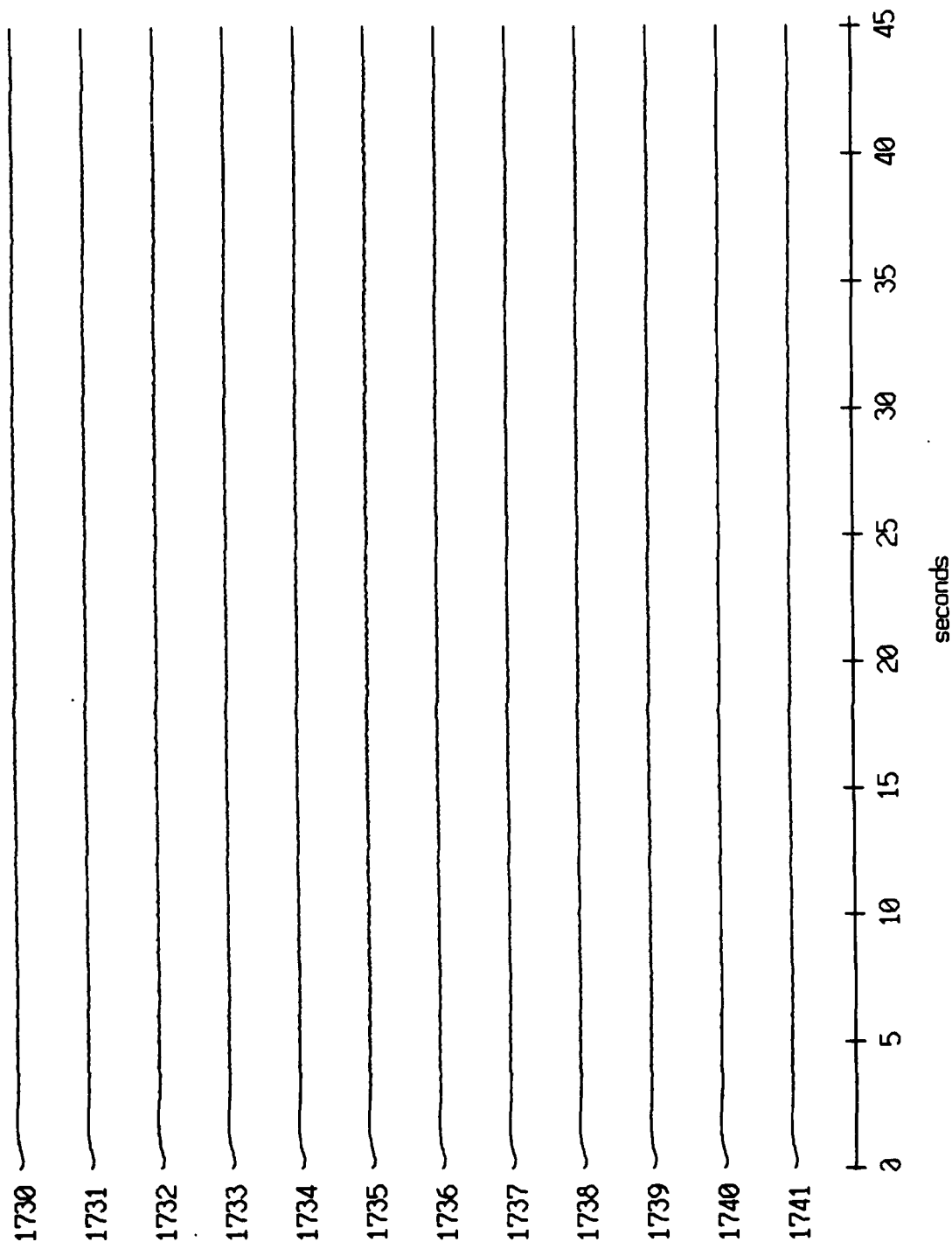


Figure XI.63a

Floot 10, July, 1989 Trip - records 1730-1741 (y-axis)  
 vertical axis scale is approx. -2.0 to 2.0 volts



AGC corrected channel level (V)

Figure XI.63b

Float 10, July, 1989 Trip - records 1730-1741 (z-axis)  
vertical axis scale is approx. -2.0 to 2.0 volts

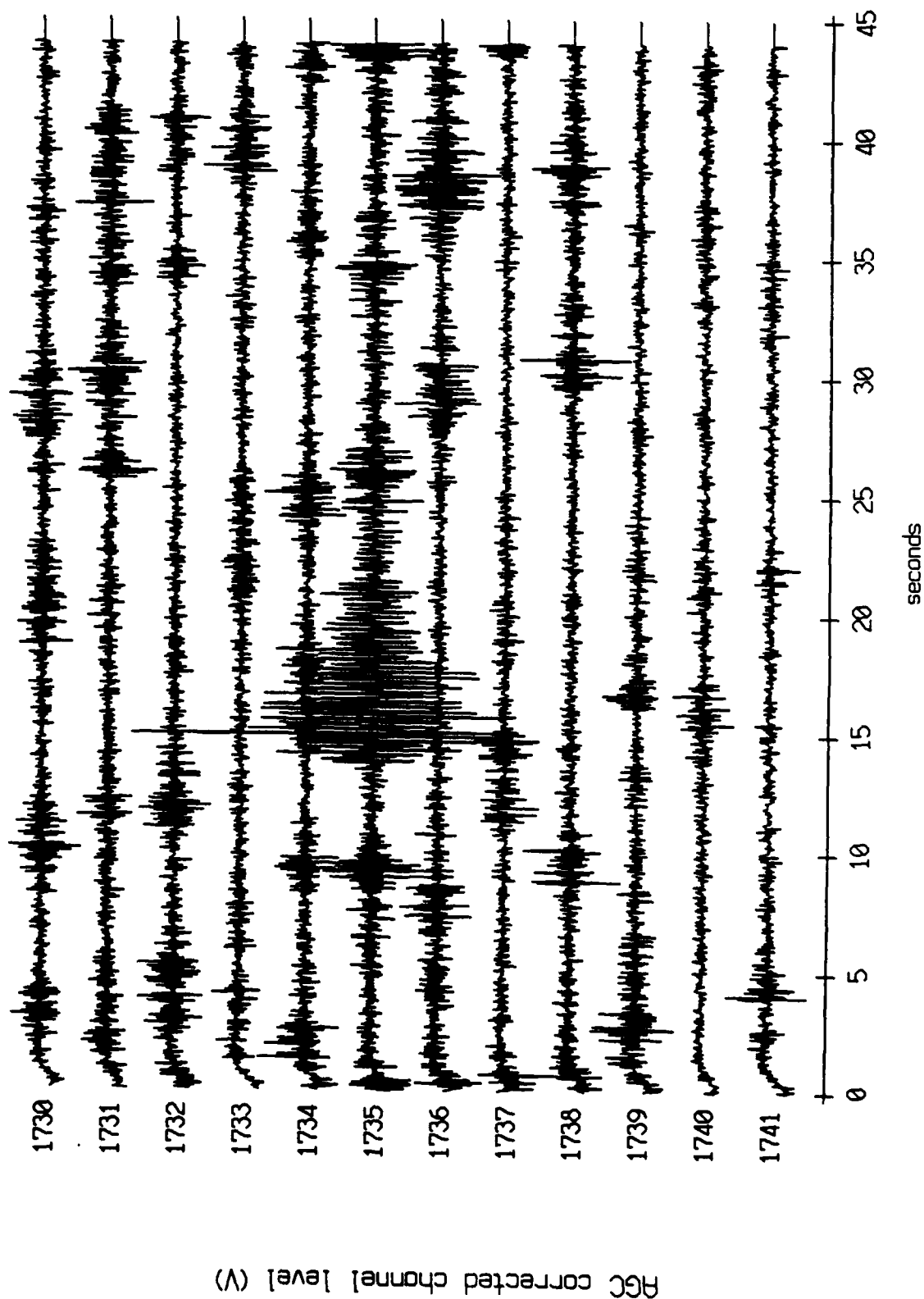
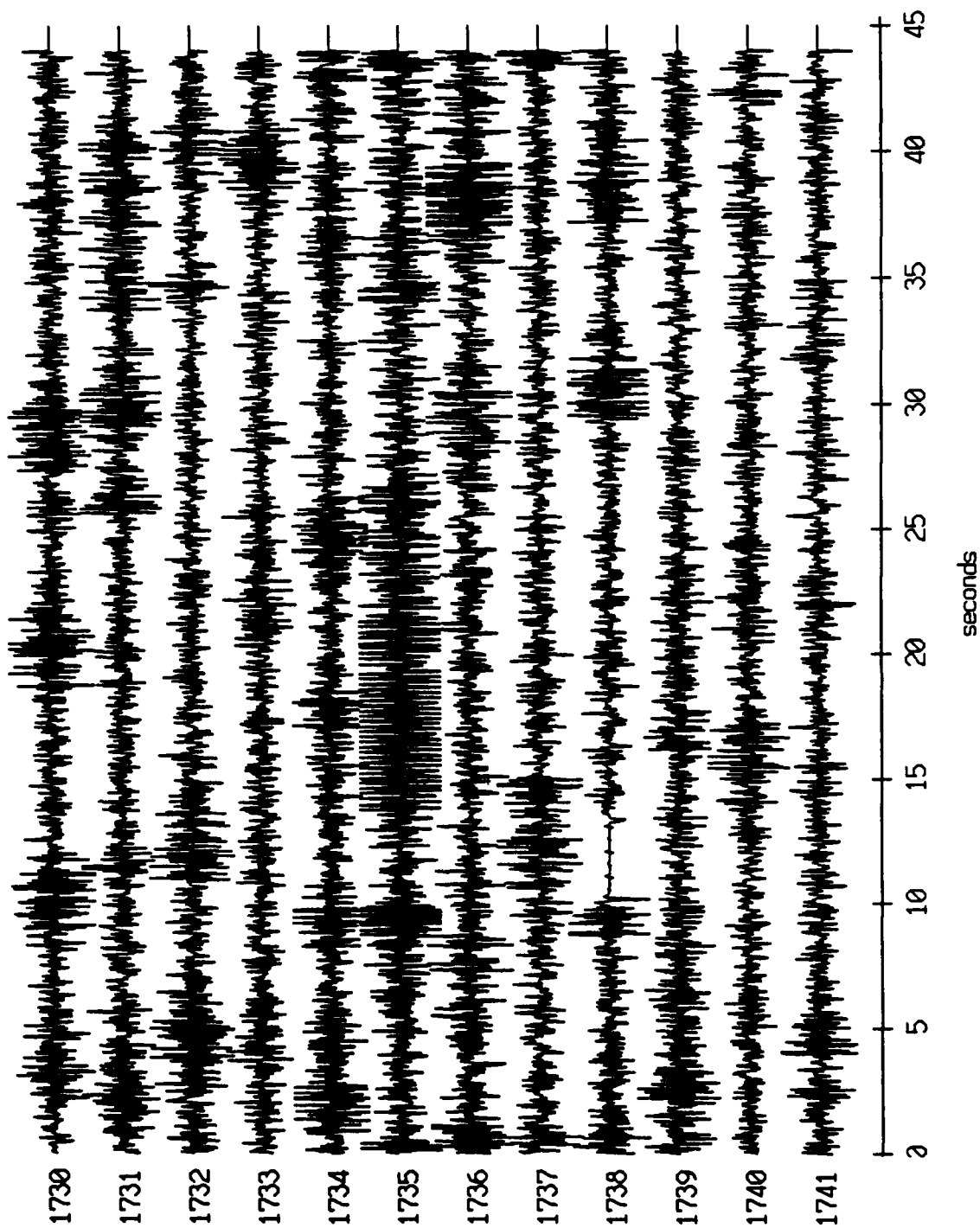


Figure XI.63c

Float 10, July, 1989 Trip - records 1730-1741 (hydrophone)  
vertical axis scale is approx. -2.0 to 2.0 volts

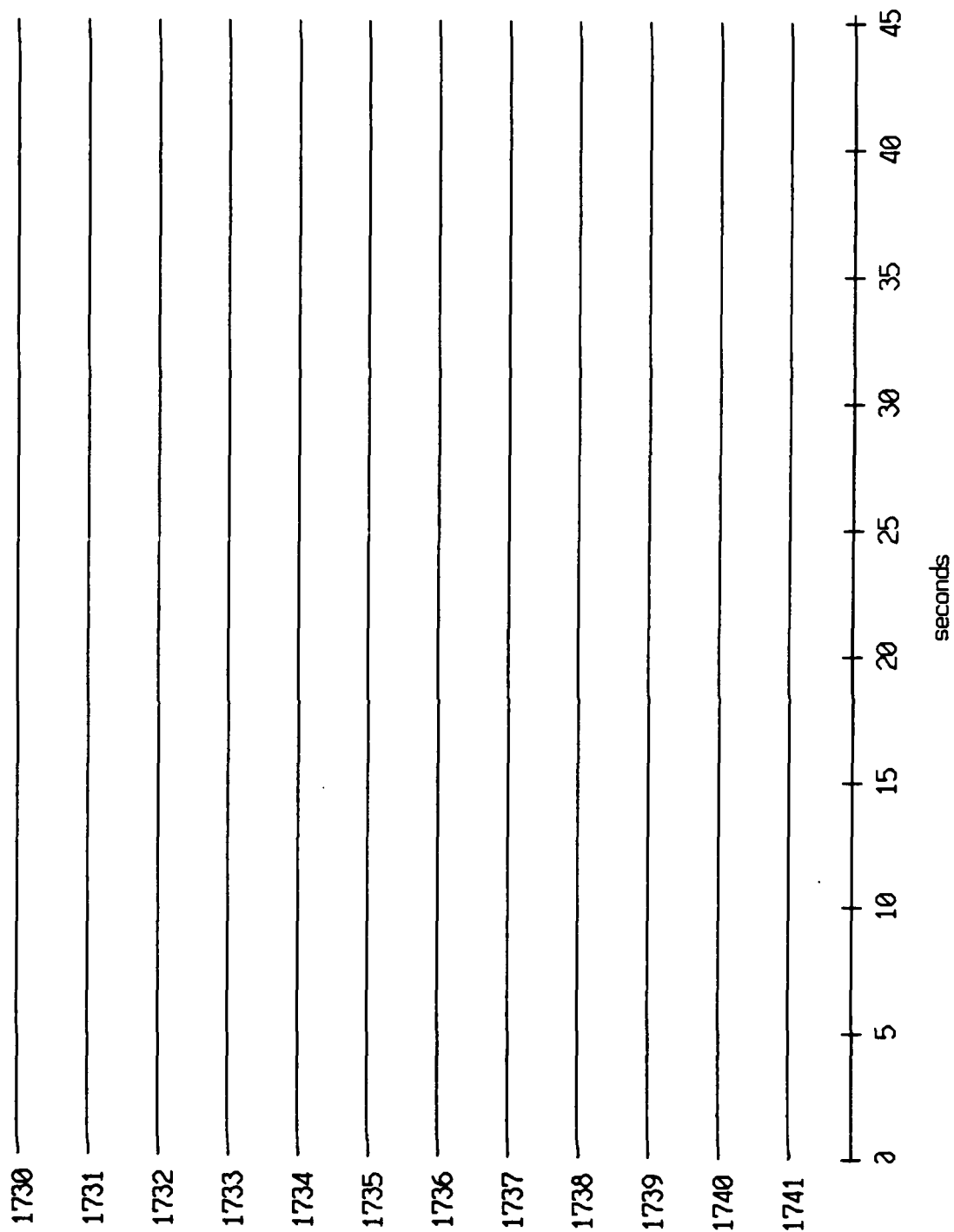


PGC corrected channel level (V)

Figure XI.63d



Floot 11, July, 1989 Trip - records 1730-1741 (x-axis)  
 vertical axis scale is approx. -2.0 to 2.0 volts



AGC corrected channel level (V)

Figure XI.64a

Float 11, July, 1989 Trip - records 1730-1741 (y-axis)  
 vertical axis scale is approx. -2.0 to 2.0 volts

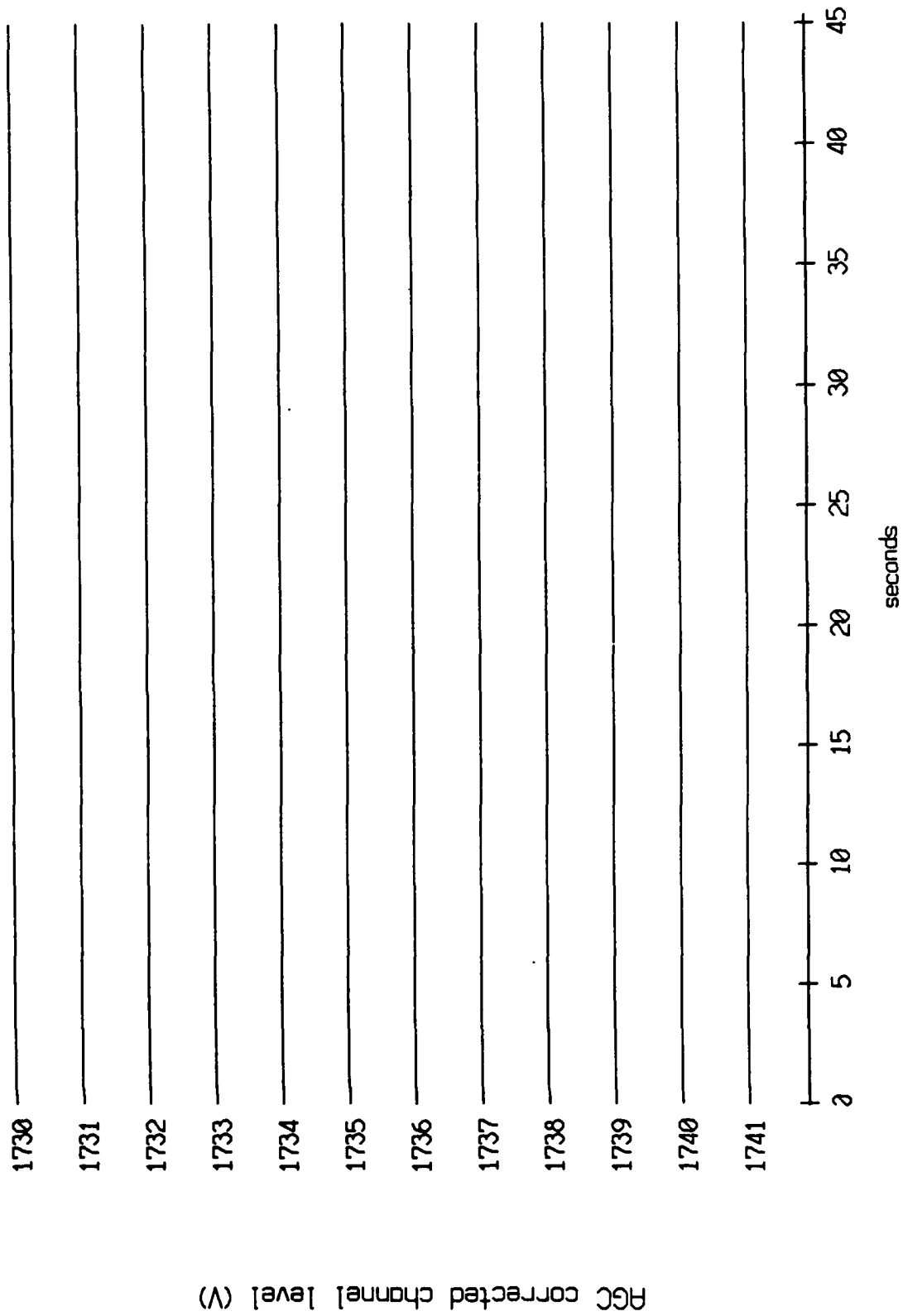
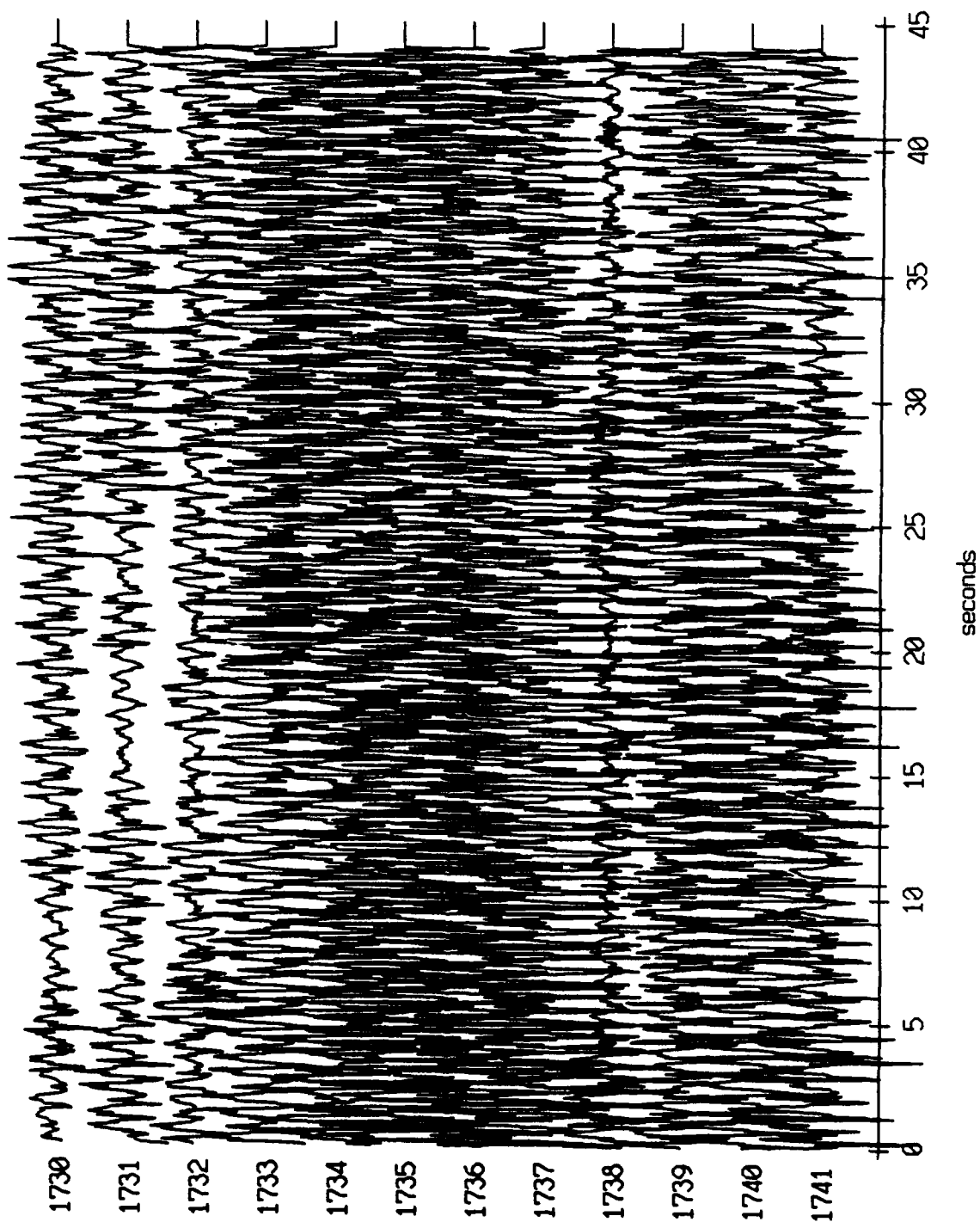


Figure XI.64b

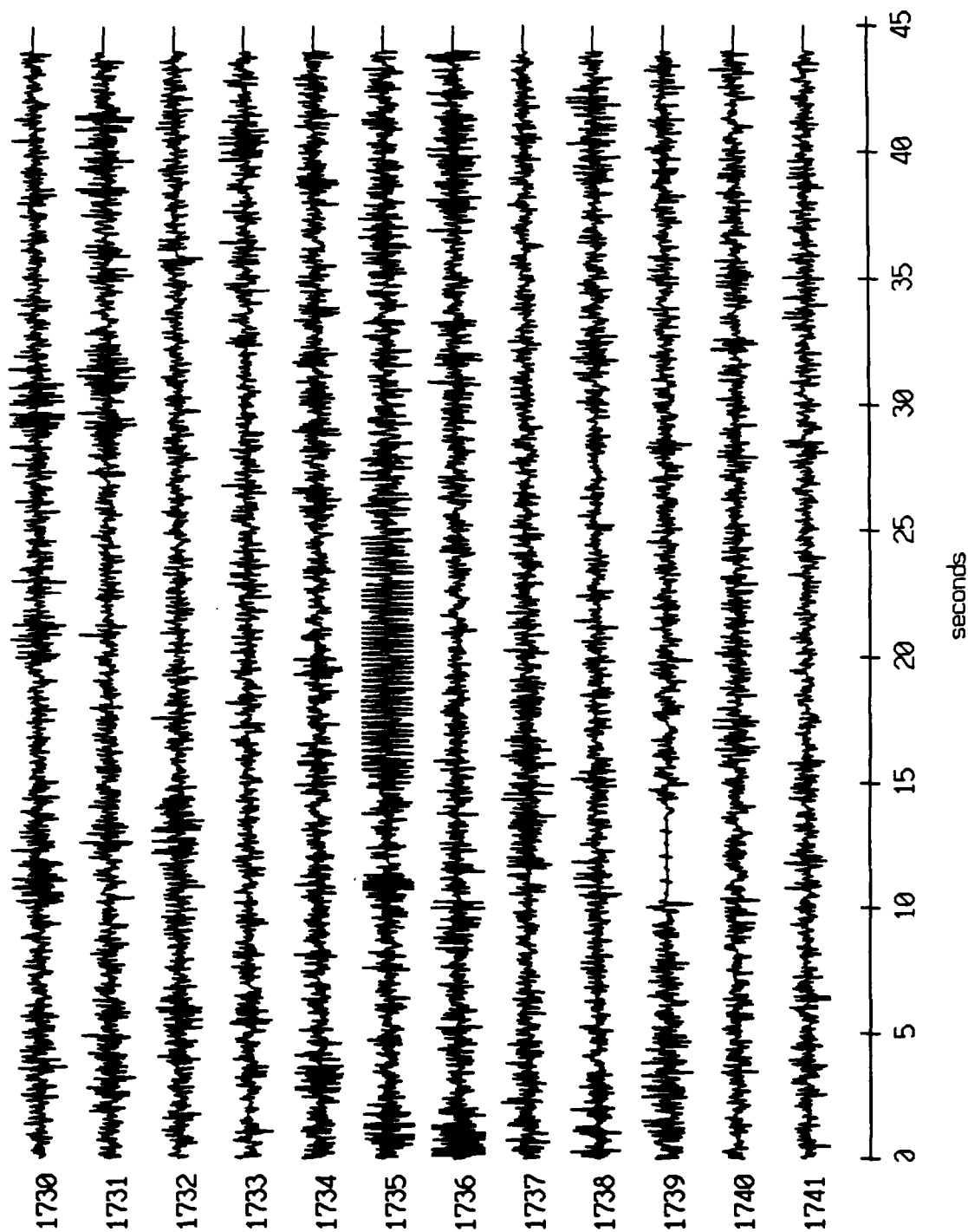
Floot 11, July, 1989 Trip - records 1730-1741 (z-axis)  
vertical axis scale is approx. -2.0 to 2.0 volts



AGC corrected channel level (V)

Figure XI.64c

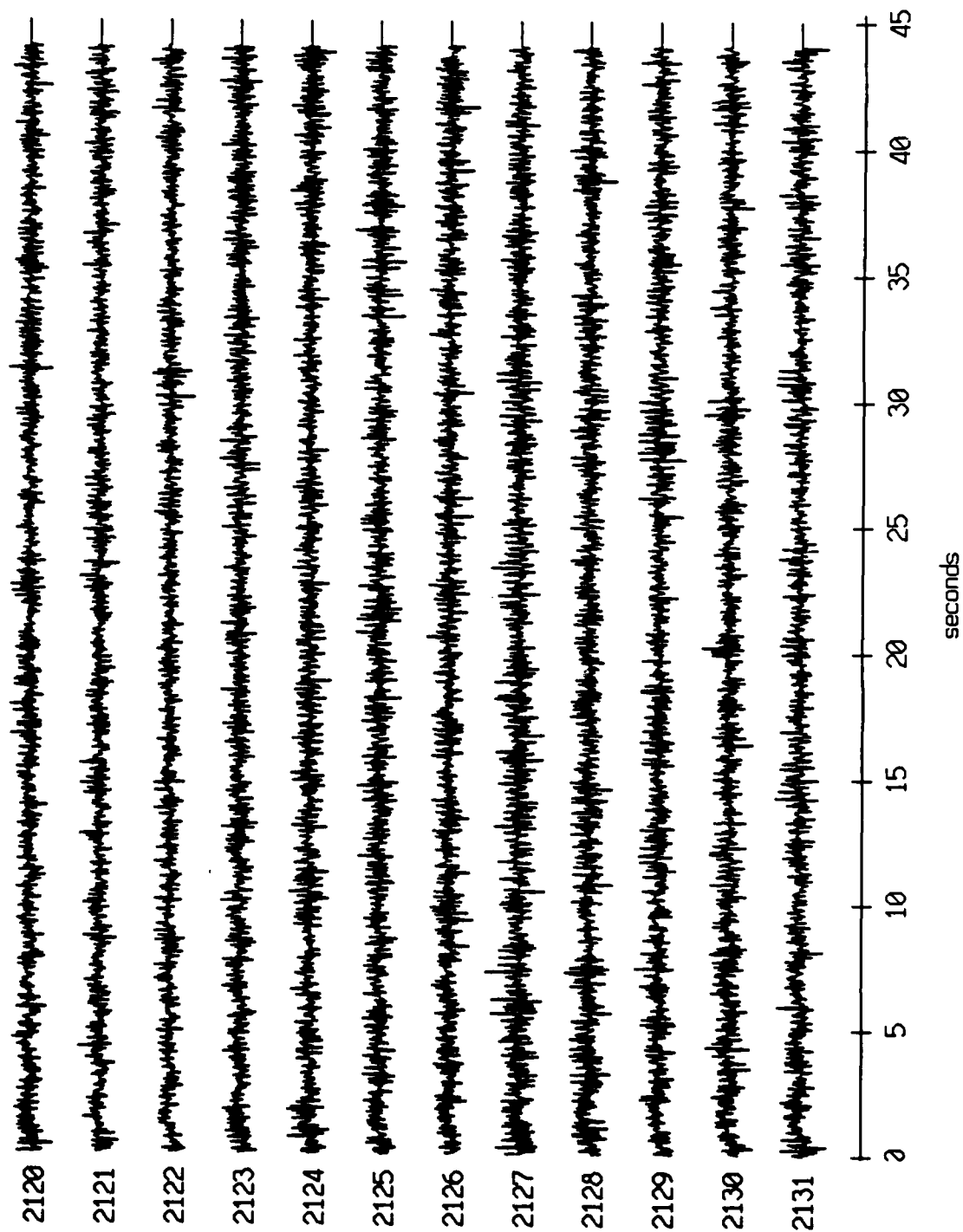
Floot 11, July, 1989 Trip - records 1730-1741 (hydrophone)  
vertical axis scale is approx. -2.0 to 2.0 volts



AGC corrected channel level (V)

Figure XI.64d

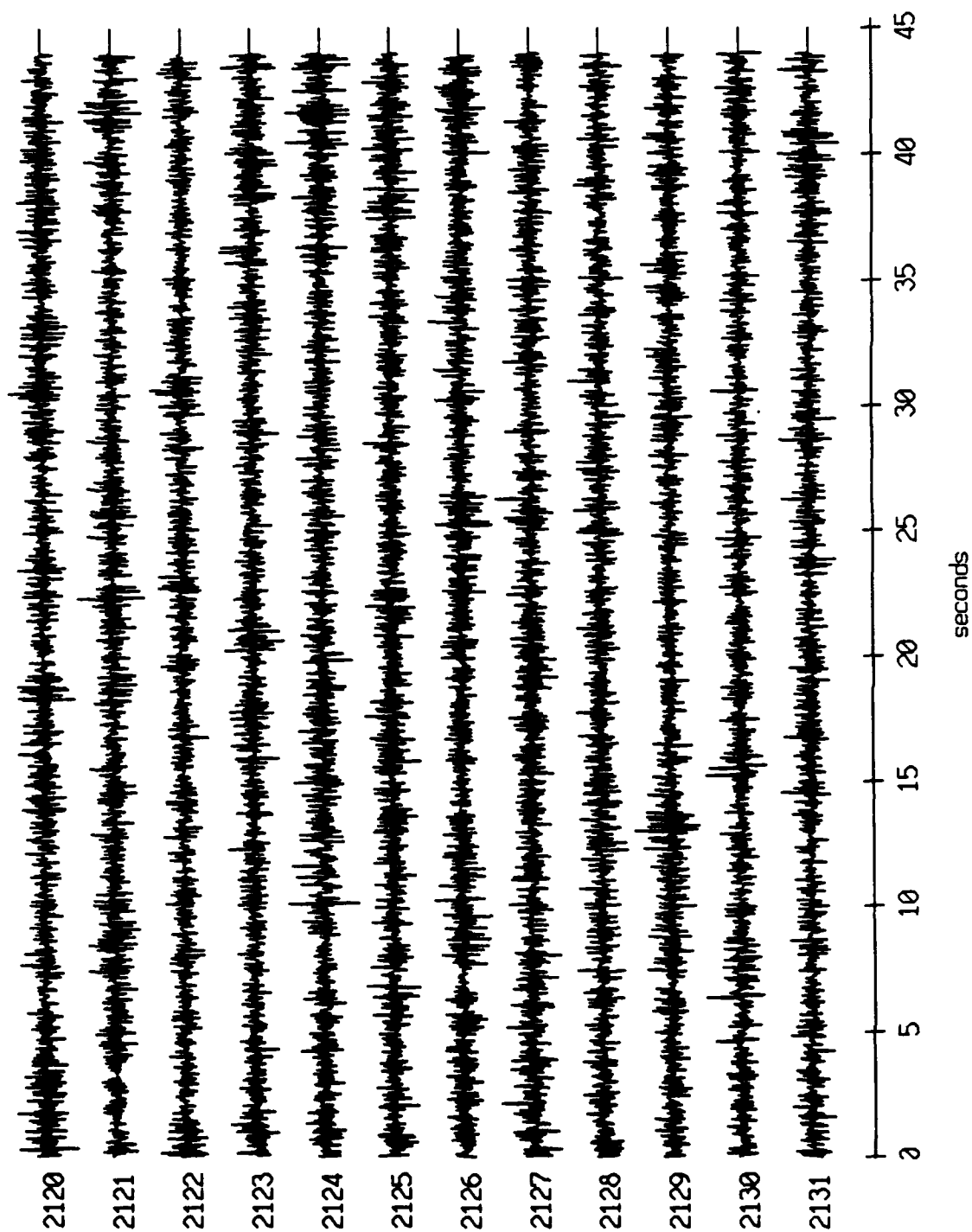
Float 0, July, 1989 Trip - records 2120-2131 (x-axis)  
vertical axis scale is approx. -2.0 to 2.0 volts



AGC corrected channel level (V)

Figure XI.65a

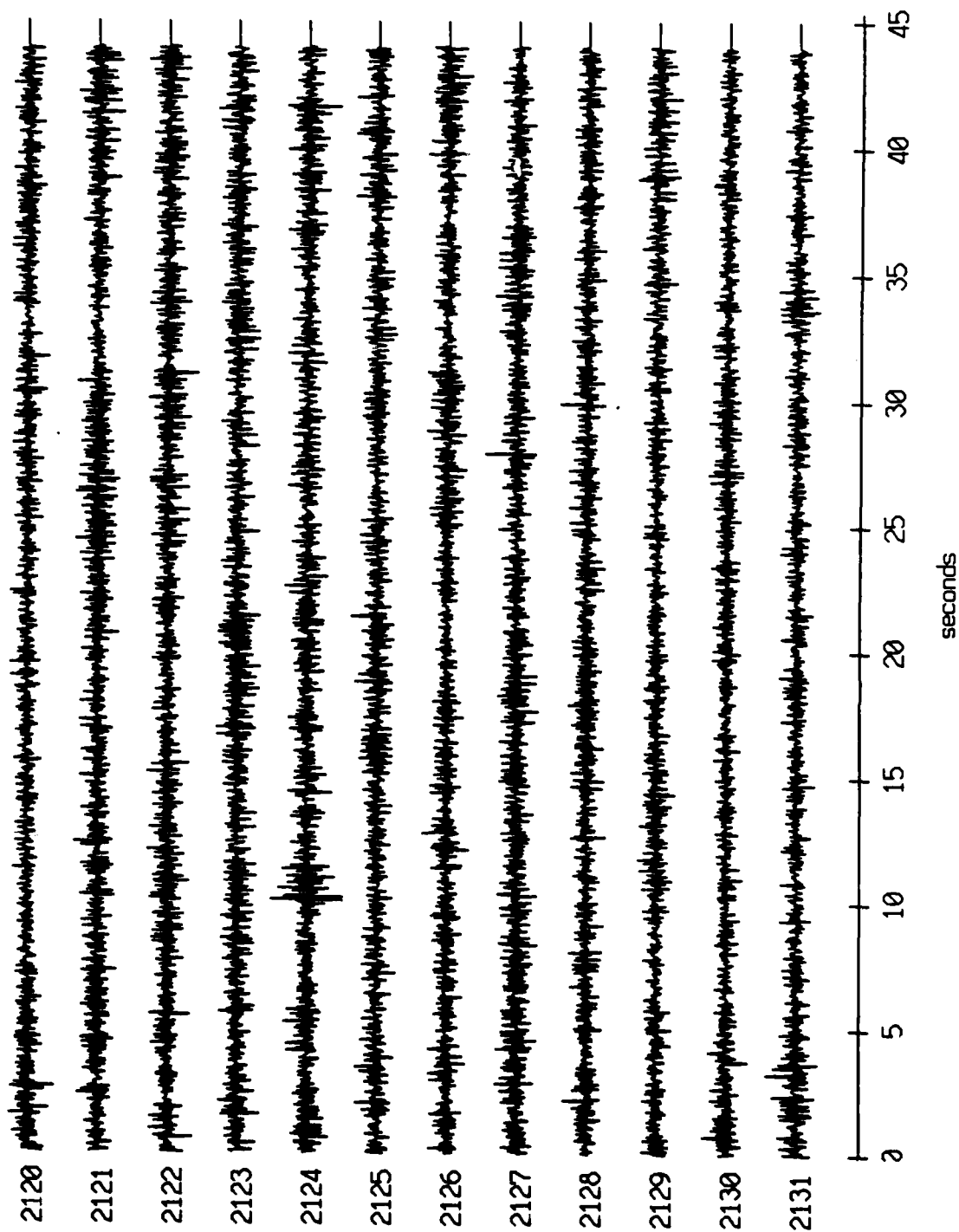
Floot 0, July, 1989 Trip - records 2120-2131 (y-axis)  
vertical axis scale is approx. -2.0 to 2.0 volts



AGC corrected channel level (V)

Figure XI.65b

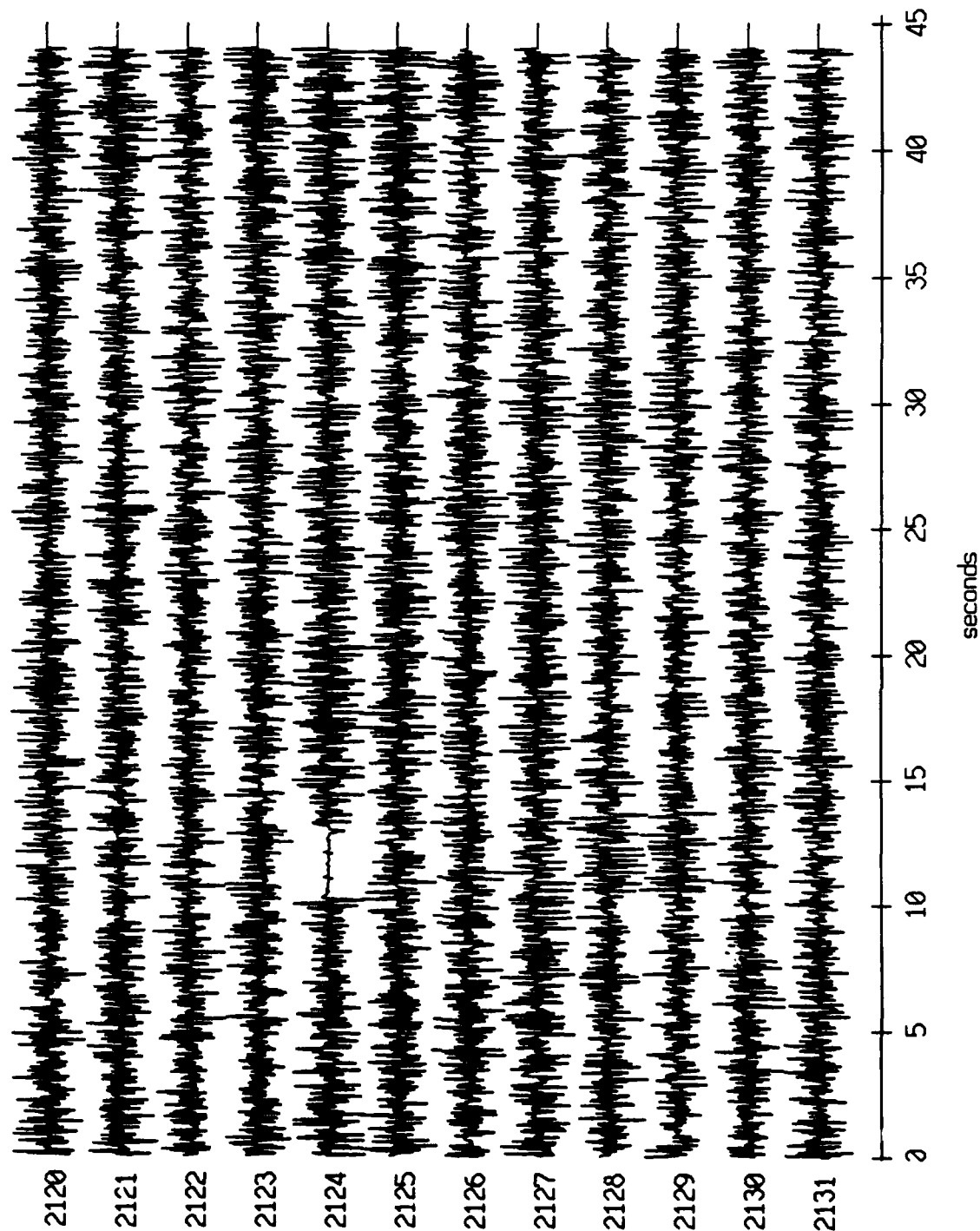
Float 0, July, 1989 Trip - records 2120-2131 (z-axis)  
vertical axis scale is approx. -2.0 to 2.0 volts



PGC corrected channel level (V)

Figure XI.65c

Float 0, July, 1989 Trip - records 2120-2131 (hydrophone)  
vertical axis scale is approx. -2.0 to 2.0 volts

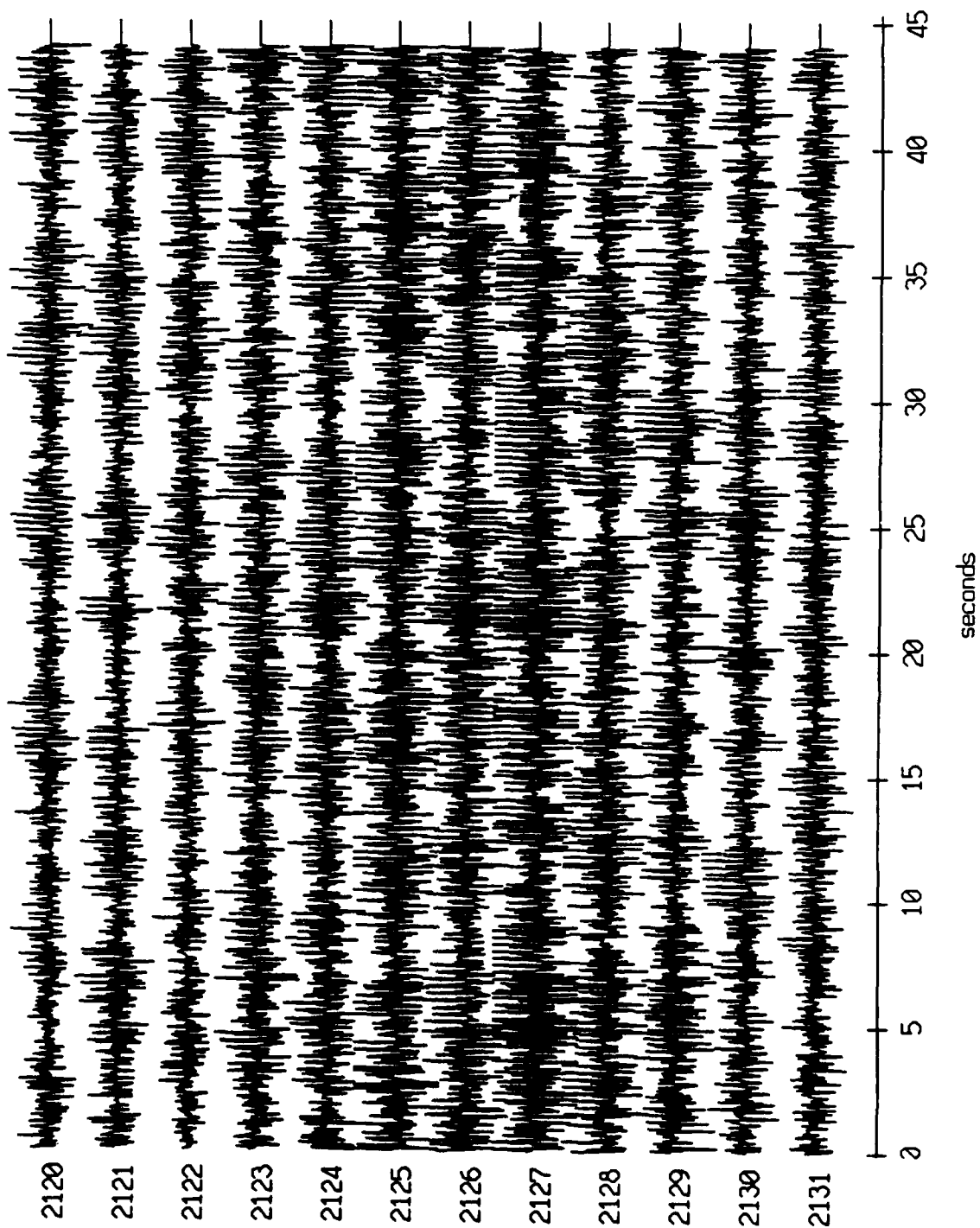


AGC corrected channel level (V)

Figure XI.65d



Floot 1, July, 1989 Trip - records 2120-2131 (x-axis)  
vertical axis scale is approx. -2.0 to 2.0 volts



PGC corrected channel level (V)

Figure XI.66a

Float 1, July, 1989 Trip - records 2120-2131 (y-axis)  
vertical axis scale is approx. -2.0 to 2.0 volts

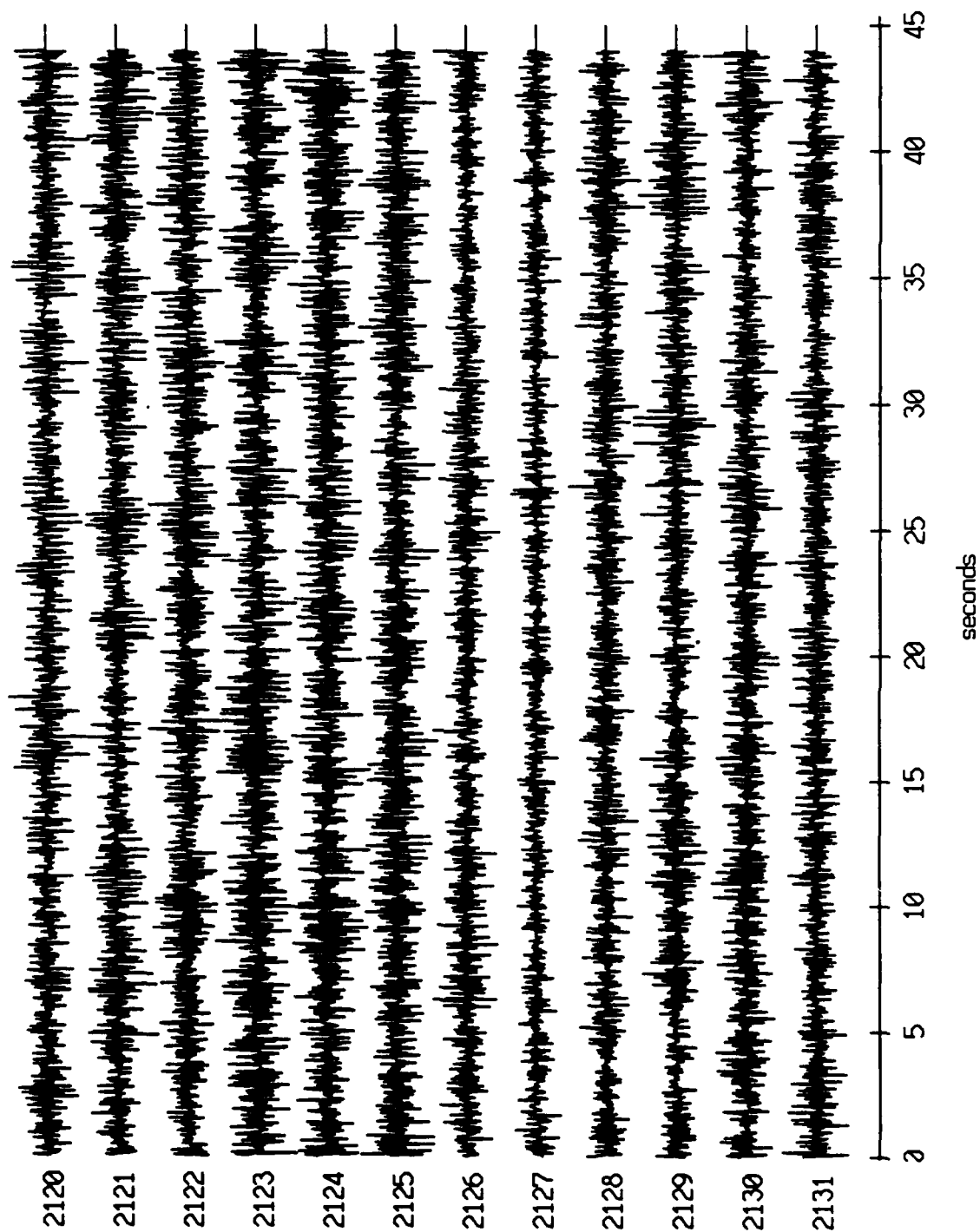


Figure XI.66b

Floot 1, July, 1989 Trip - records 2120-2131 (z-axis)  
vertical axis scale is approx. -2.0 to 2.0 volts

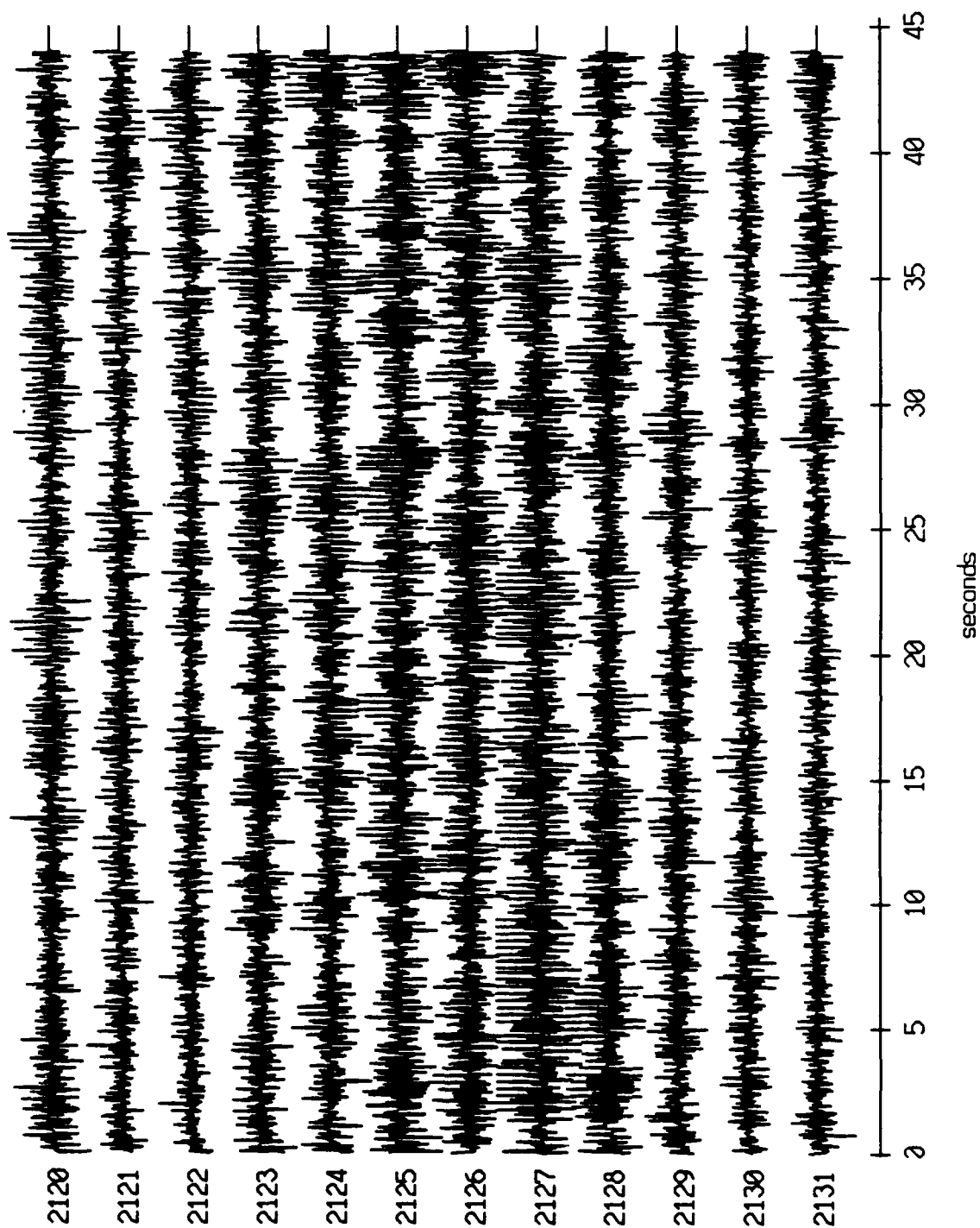
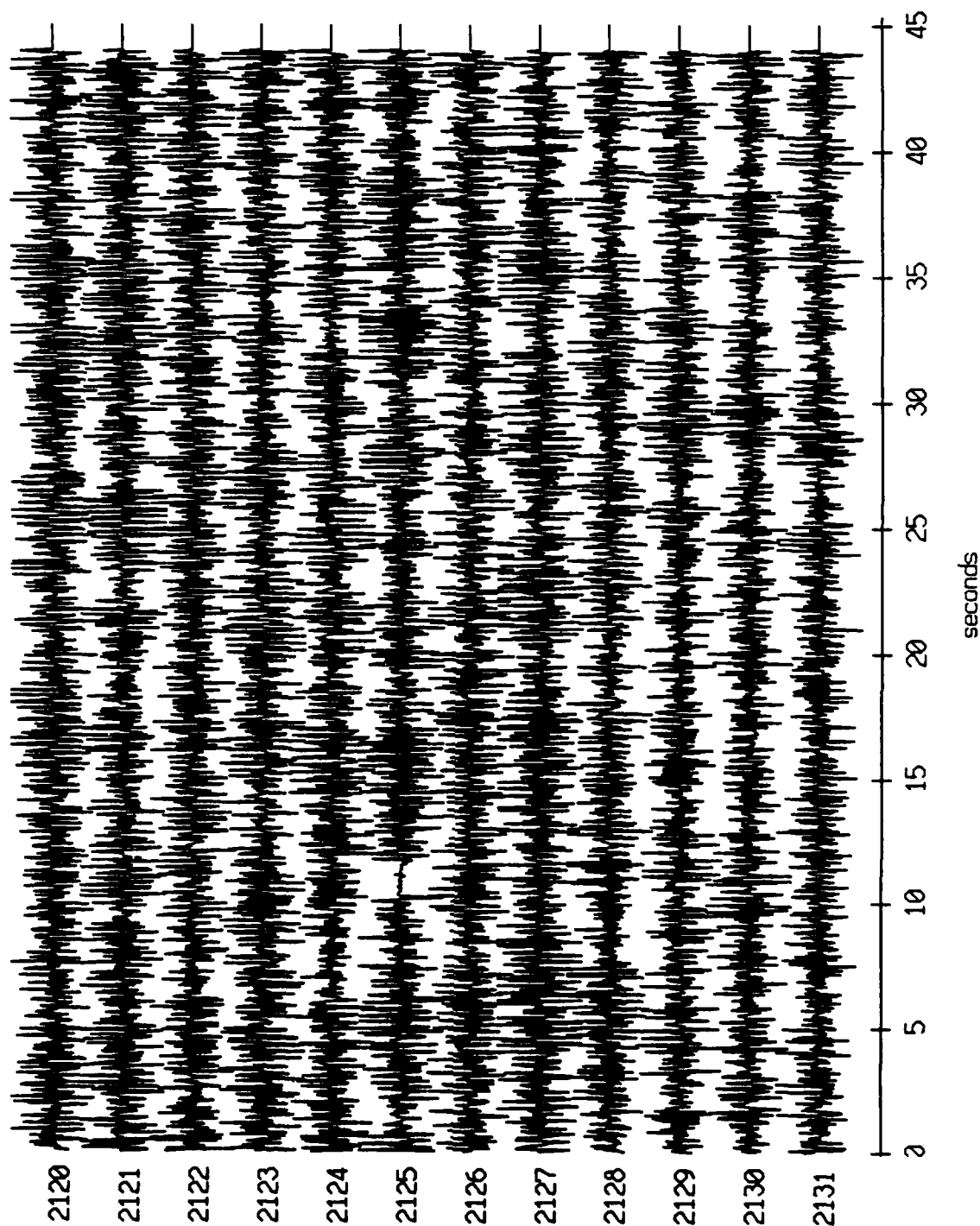


Figure XI.66c

Float 1, July, 1989 Trip - records 2120-2131 (hydrophone)  
vertical axis scale is approx. -2.0 to 2.0 volts



AGC corrected channel level (V)

Figure XI.66d

Floot 2, July, 1989 Trip - records 2120-2131 (x-axis)  
vertical axis scale is approx. -2.0 to 2.0 volts

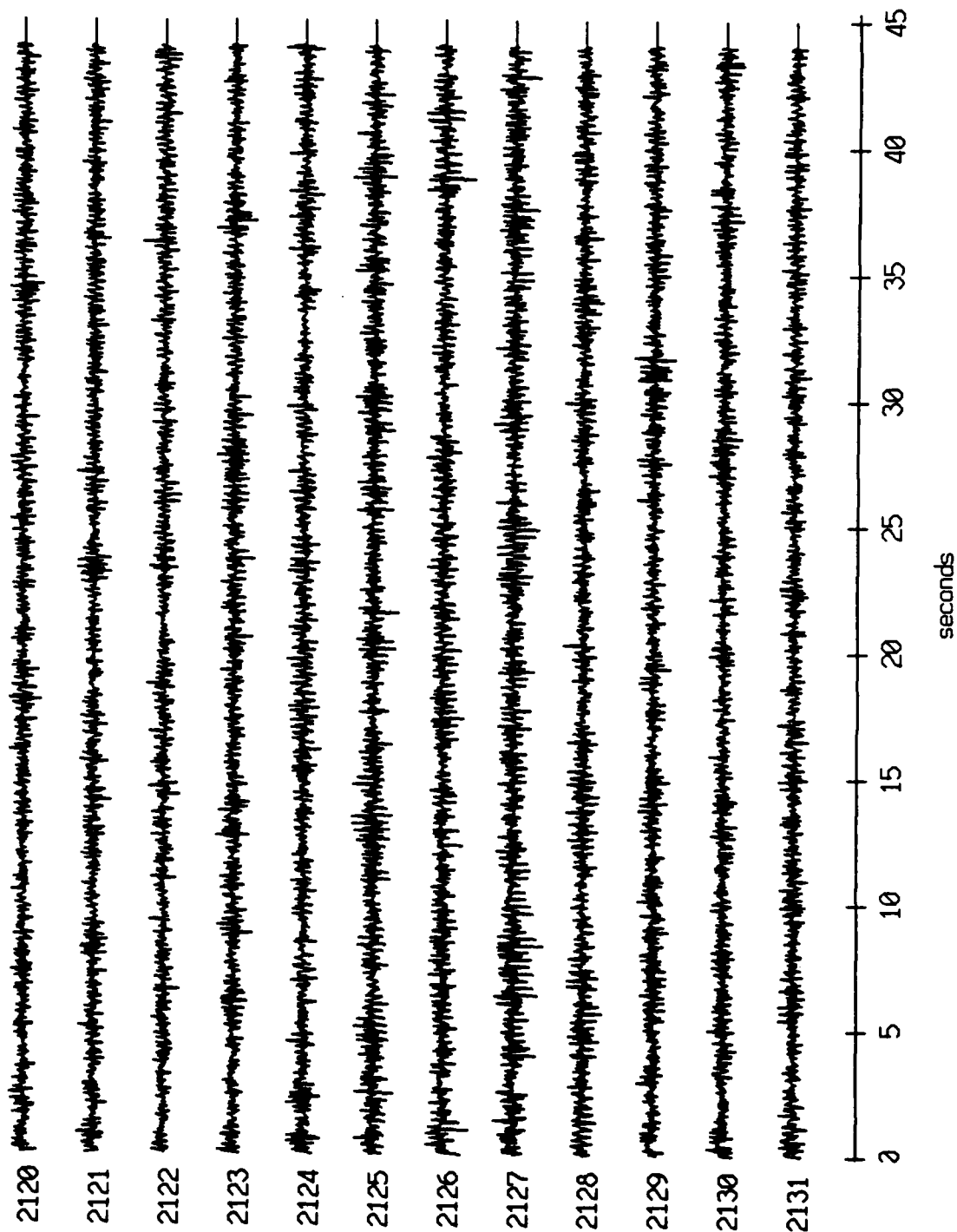


Figure XI.67a

Floot 2, July, 1989 Trip - records 2120-2131 (y-axis)  
vertical axis scale is approx. -2.0 to 2.0 volts

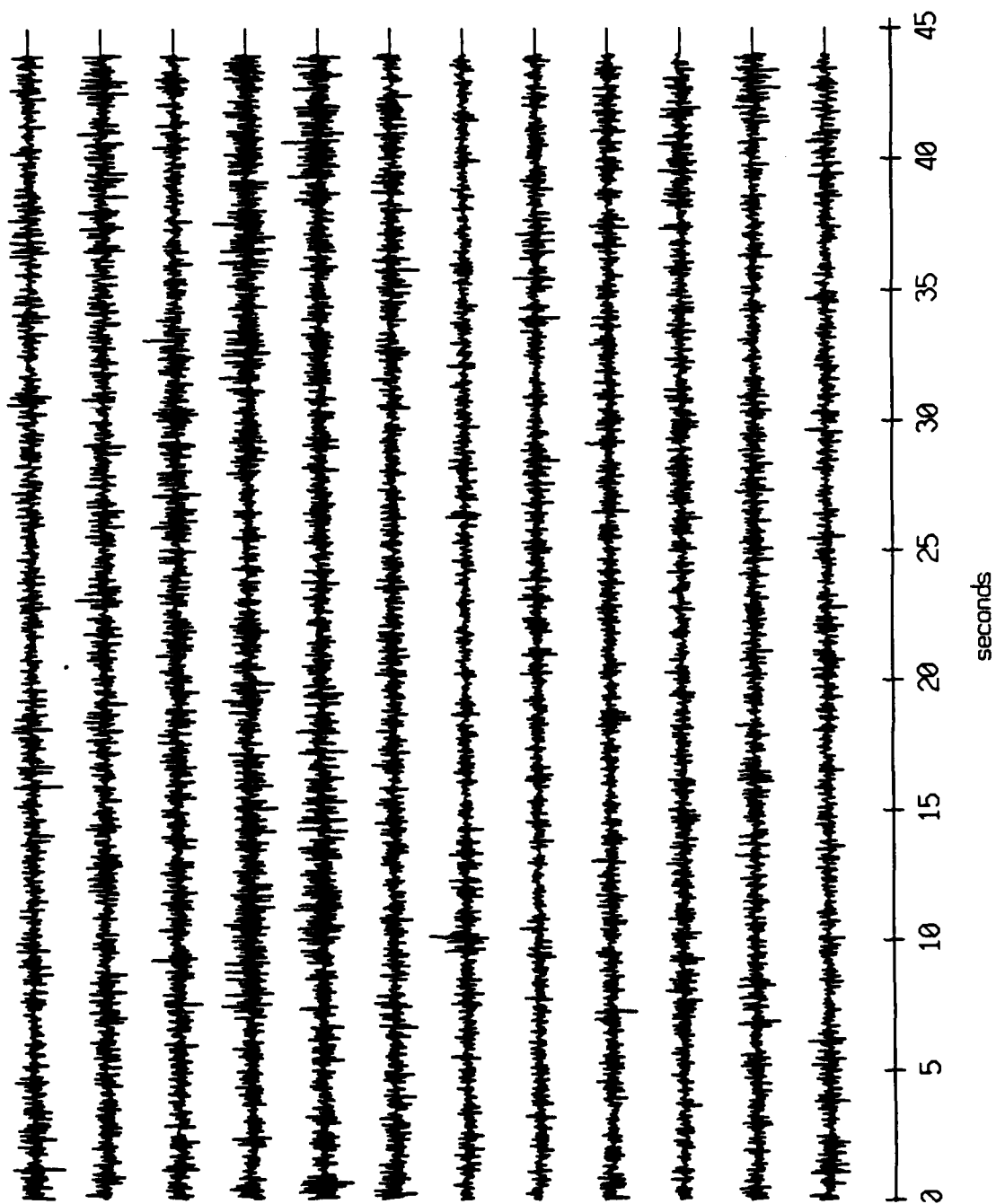
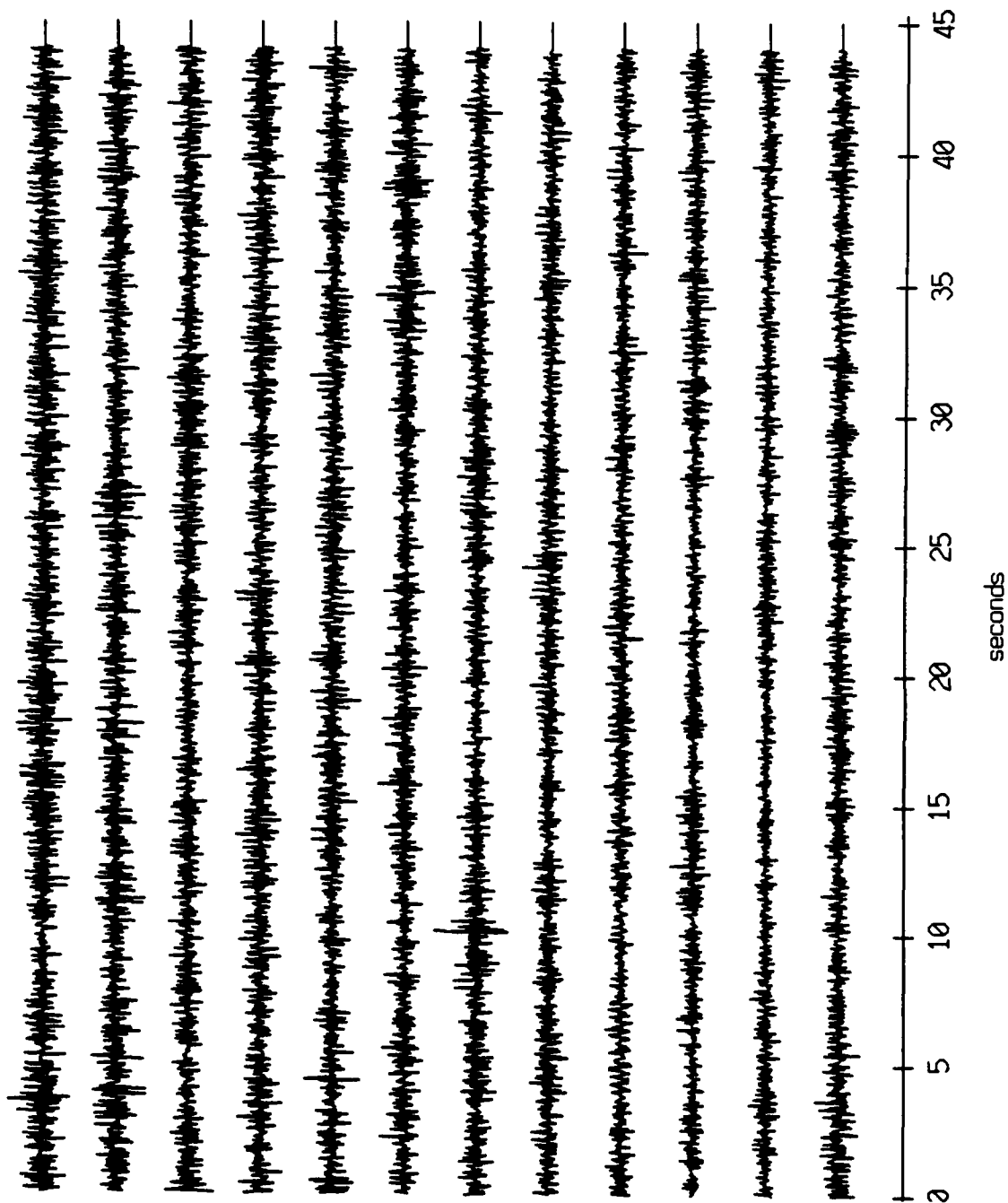


Figure XI.67b

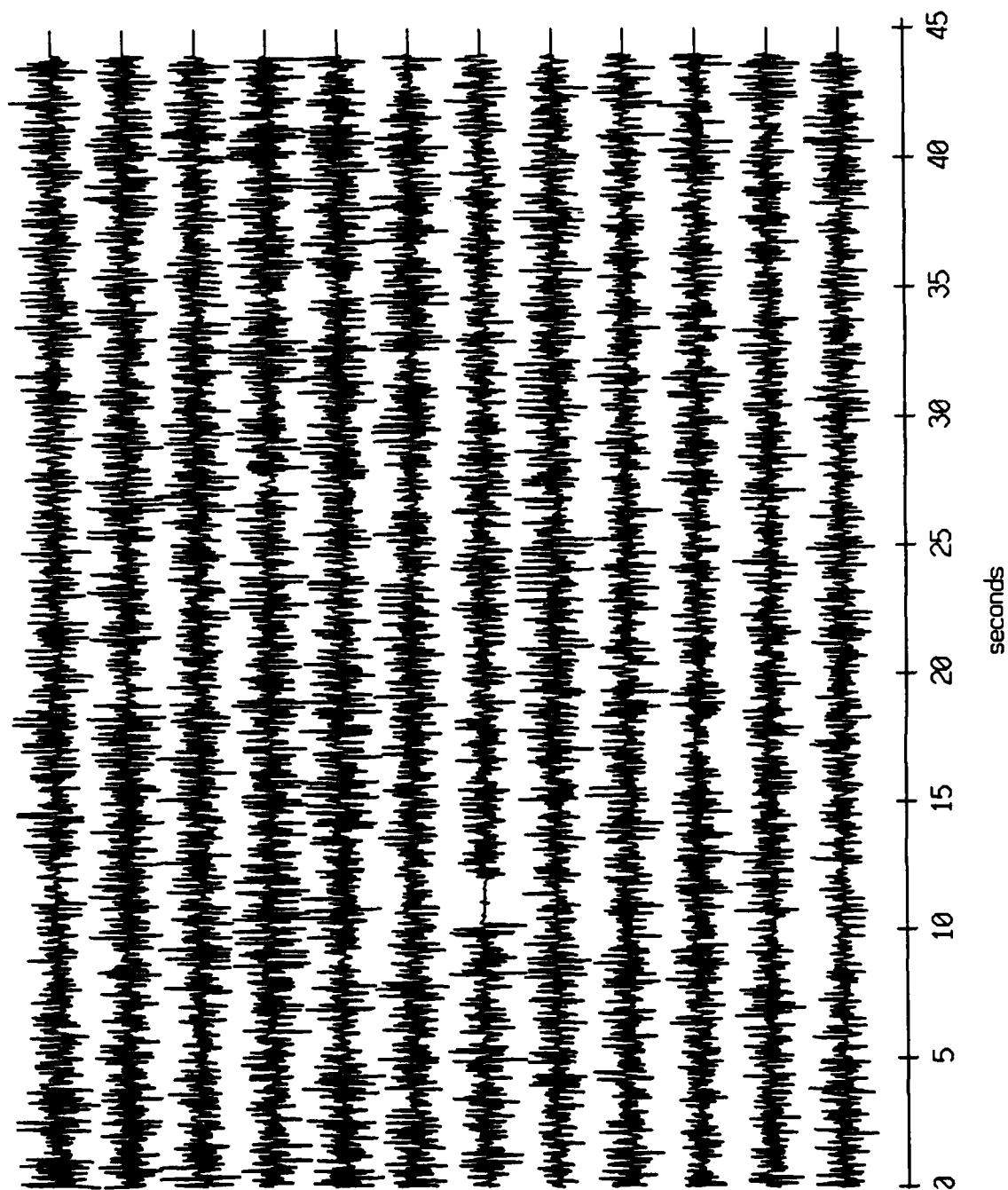
Float 2, July, 1989 Trip - records 2120-2131 (z-axis)  
vertical axis scale is approx. -2.0 to 2.0 volts



AGC corrected channel level (V)

Figure XI.67c

Float 2, July, 1989 Trip - records 2120-2131 (hydrophone)  
vertical axis scale is approx. -2.0 to 2.0 volts

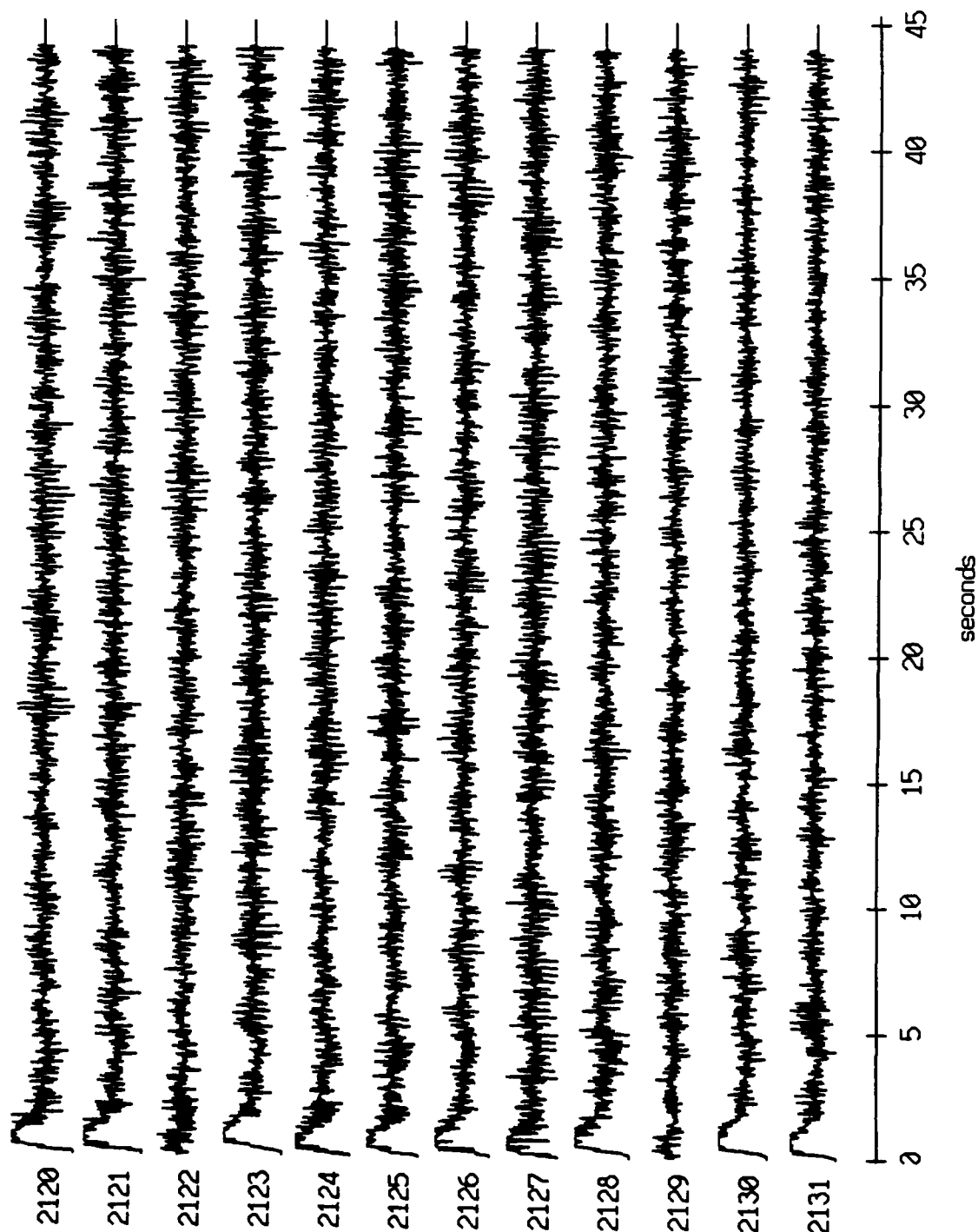


AGC corrected channel level (V)

Figure XI.67d



Float 3, July, 1989 Trip - records 2120-2131 (x-axis)  
vertical axis scale is approx. -2.0 to 2.0 volts



HGC corrected channel level (V)

Figure XI.68a

Floot 3, July, 1989 Trip - records 2120-2131 (y-axis)  
vertical axis scale is approx. -2.0 to 2.0 volts

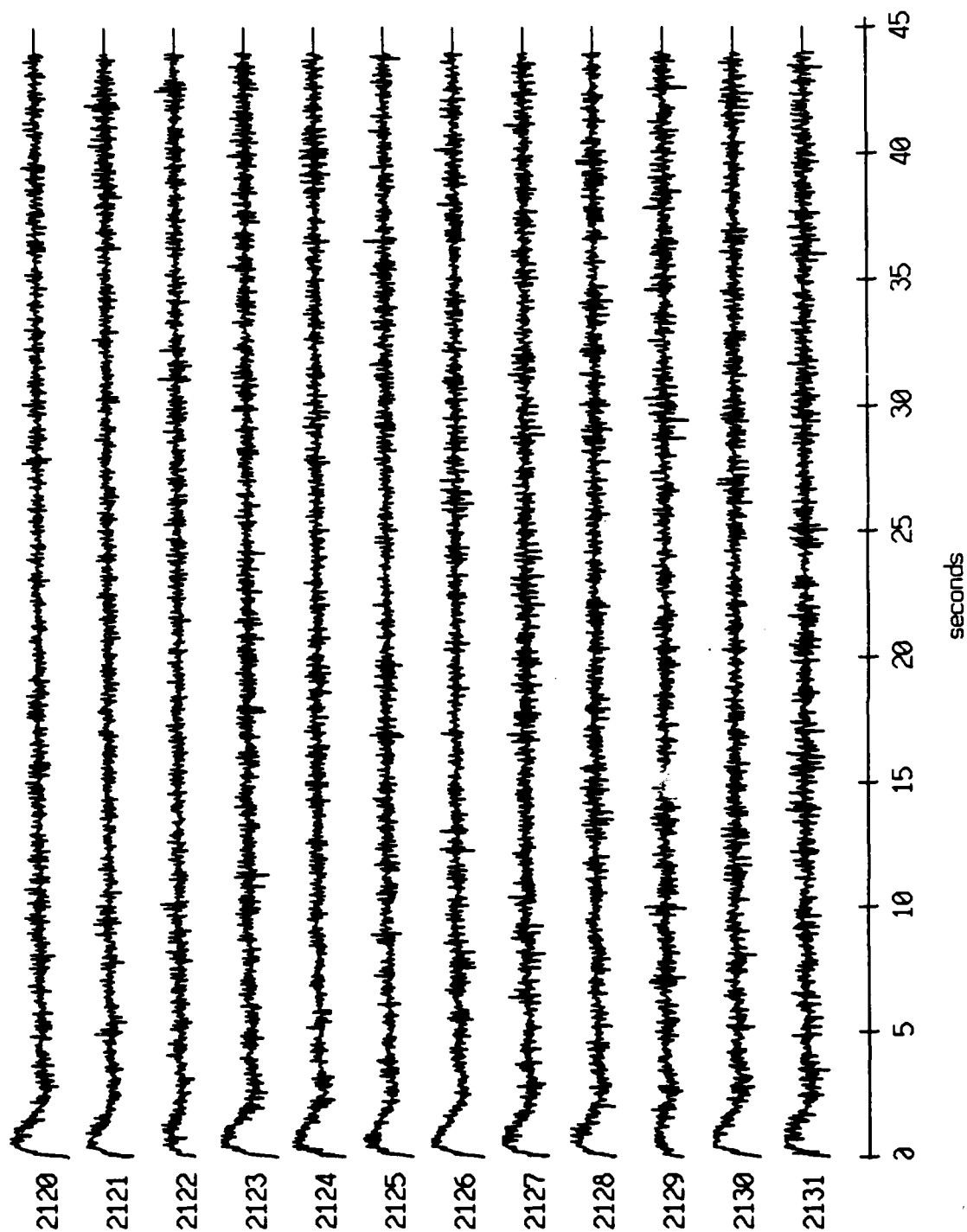


Figure XI.68b

Floot 3, July, 1989 Trip - records 2120-2131 (z-axis)  
vertical axis scale is approx. -2.0 to 2.0 volts

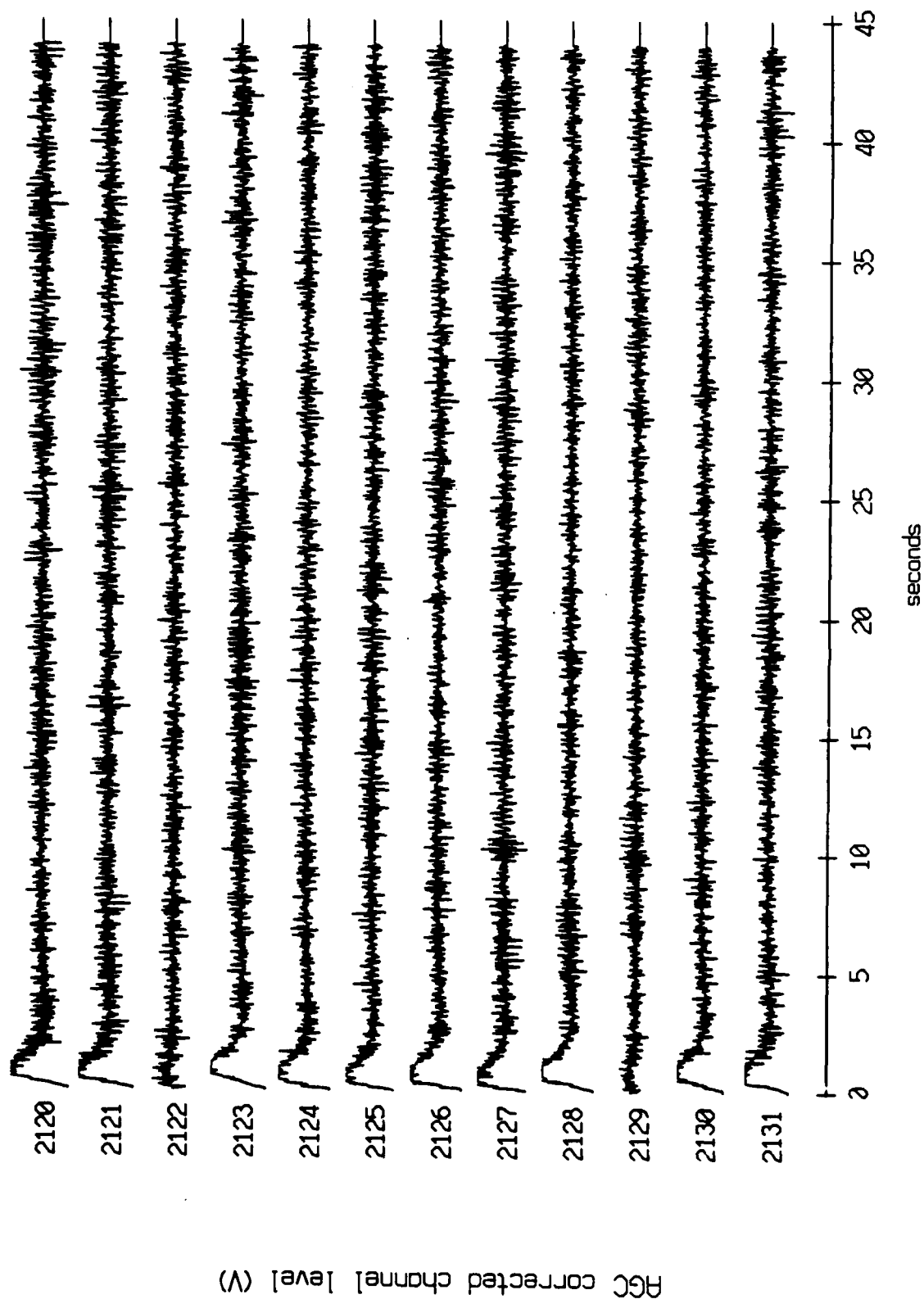
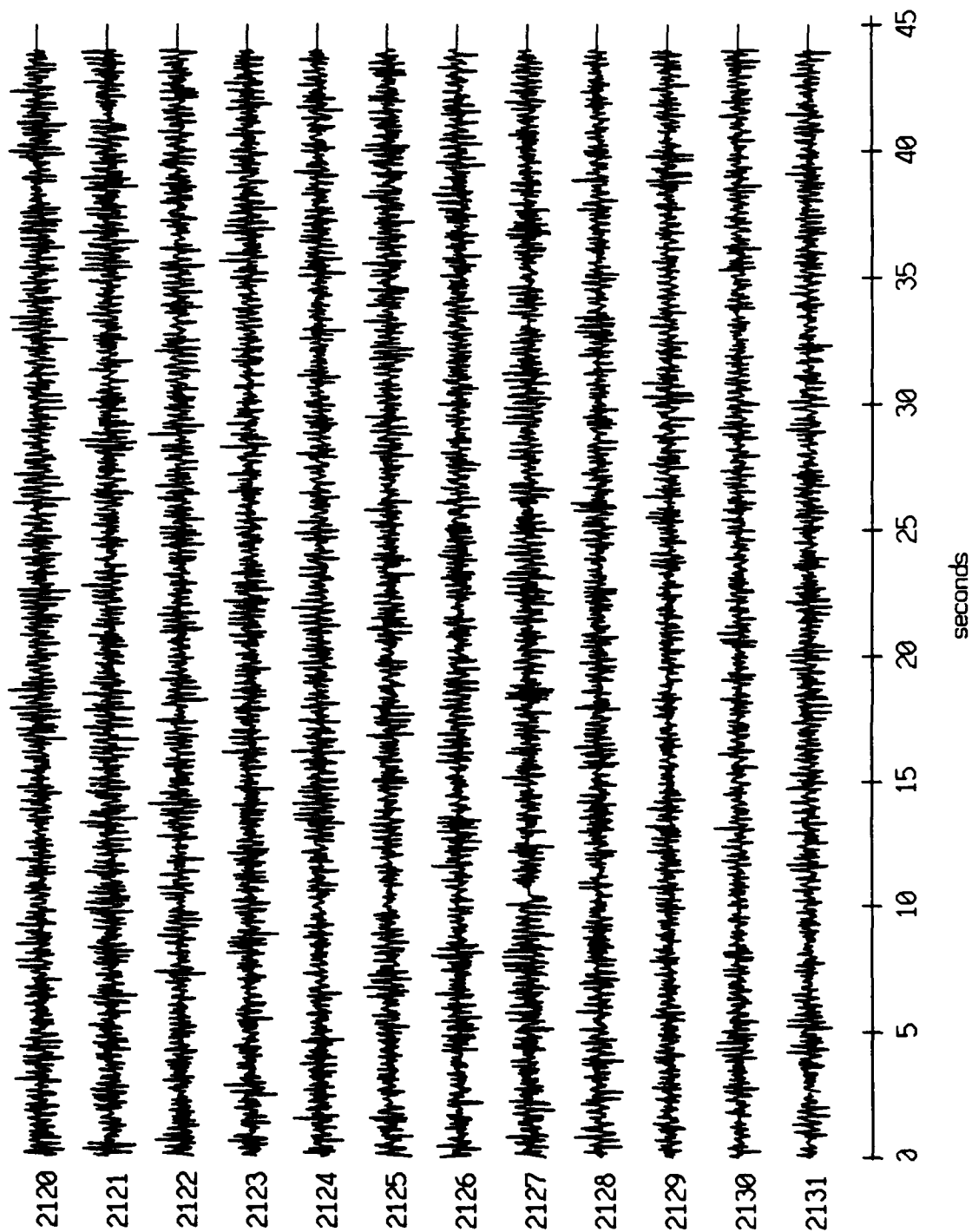


Figure XI.68c

Float 3, July, 1989 Trip - records 2120-2131 (hydrophone)  
vertical axis scale is approx. -2.0 to 2.0 volts



PGC corrected channel level (V)

Figure XI.68d

Float 5, July, 1989 Trip - records 2120-2131 (x-axis)  
vertical axis scale is approx. -2.0 to 2.0 volts

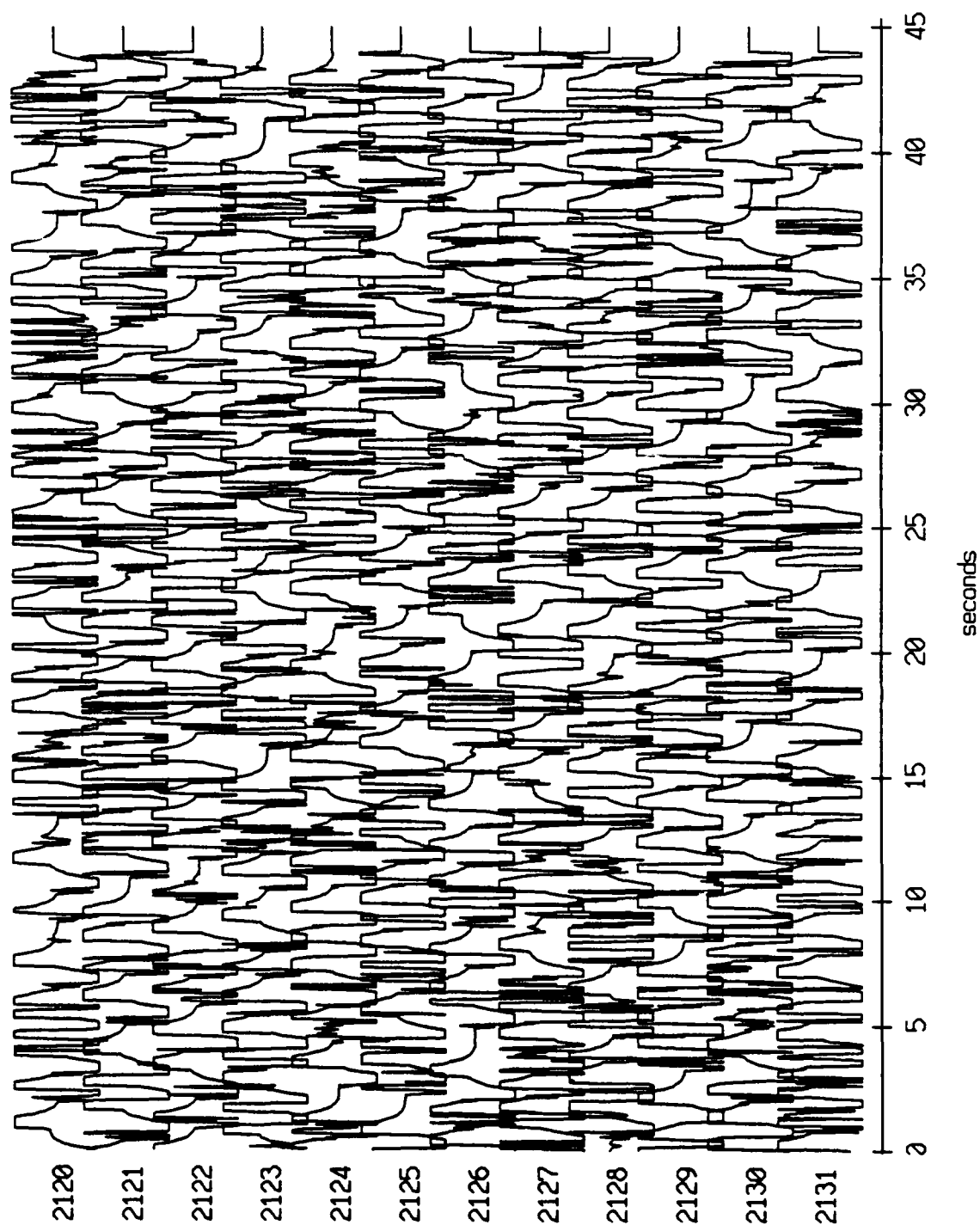
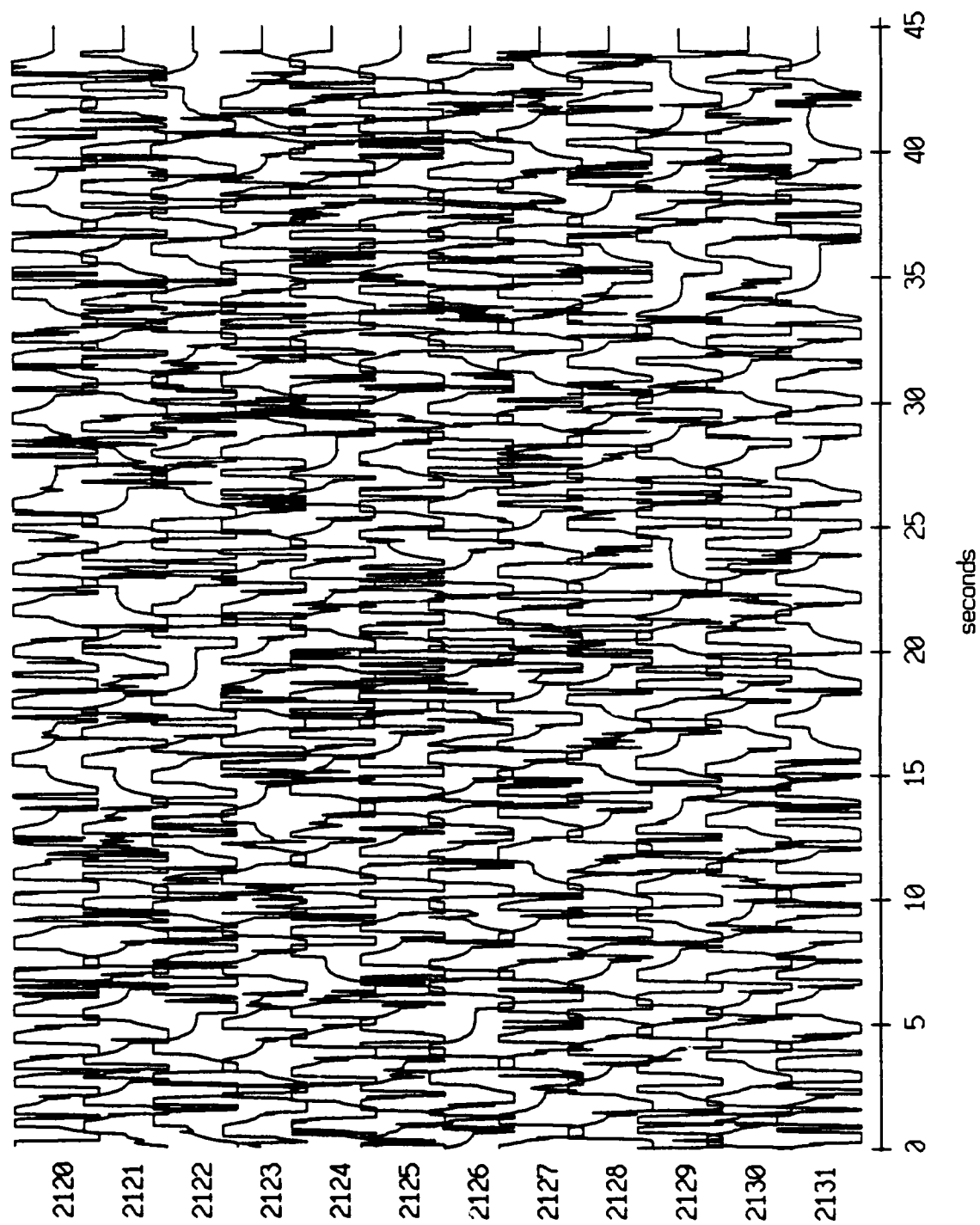


Figure XI.69a

Floot 5, July, 1989 Trip - records 2120-2131 (y-axis)  
vertical axis scale is approx. -2.0 to 2.0 volts



AGC corrected channel level (V)

Figure XI.69b

Float 5, July, 1989 Trip - records 2120-2131 (z-axis)  
vertical axis scale is approx. -2.0 to 2.0 volts

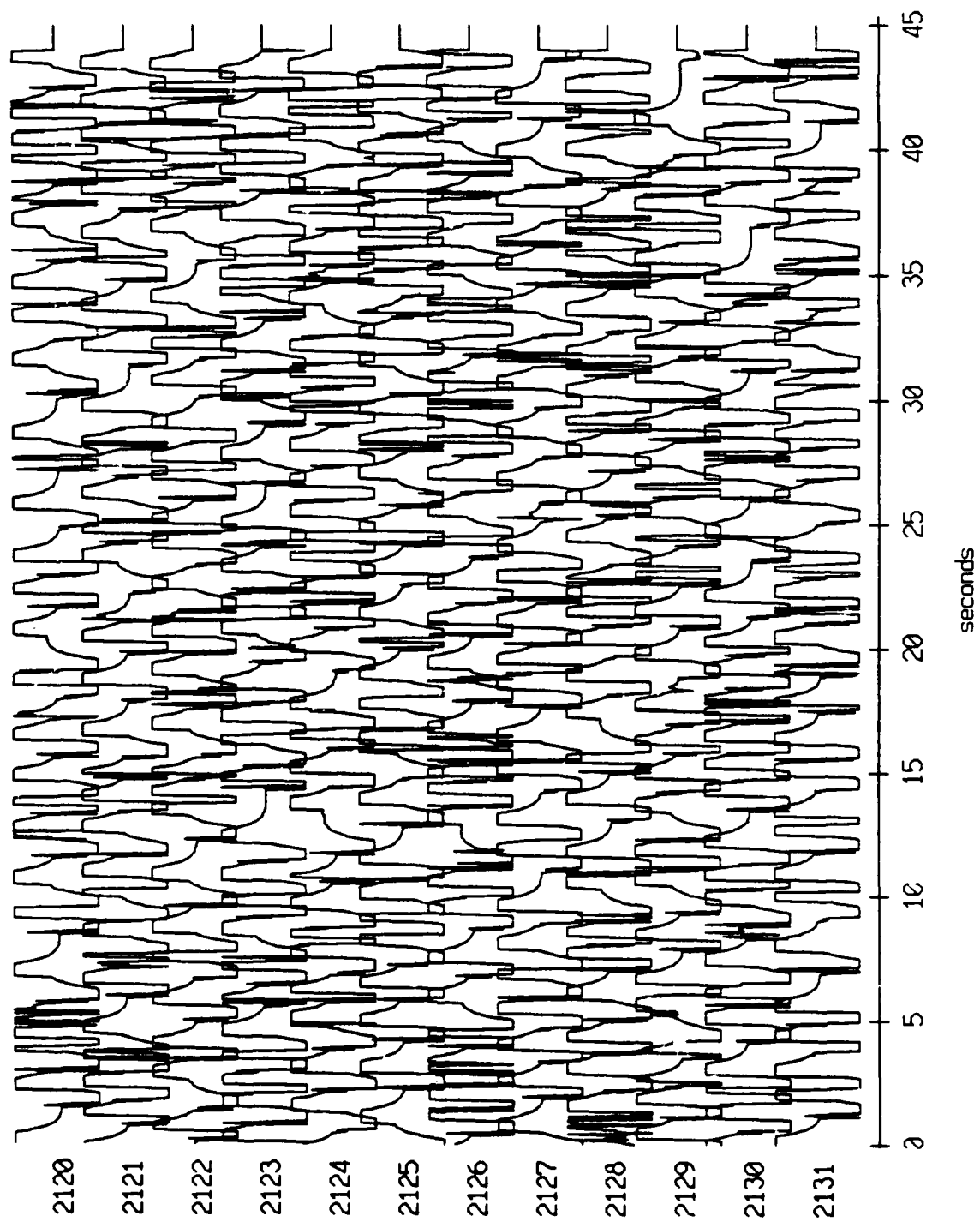
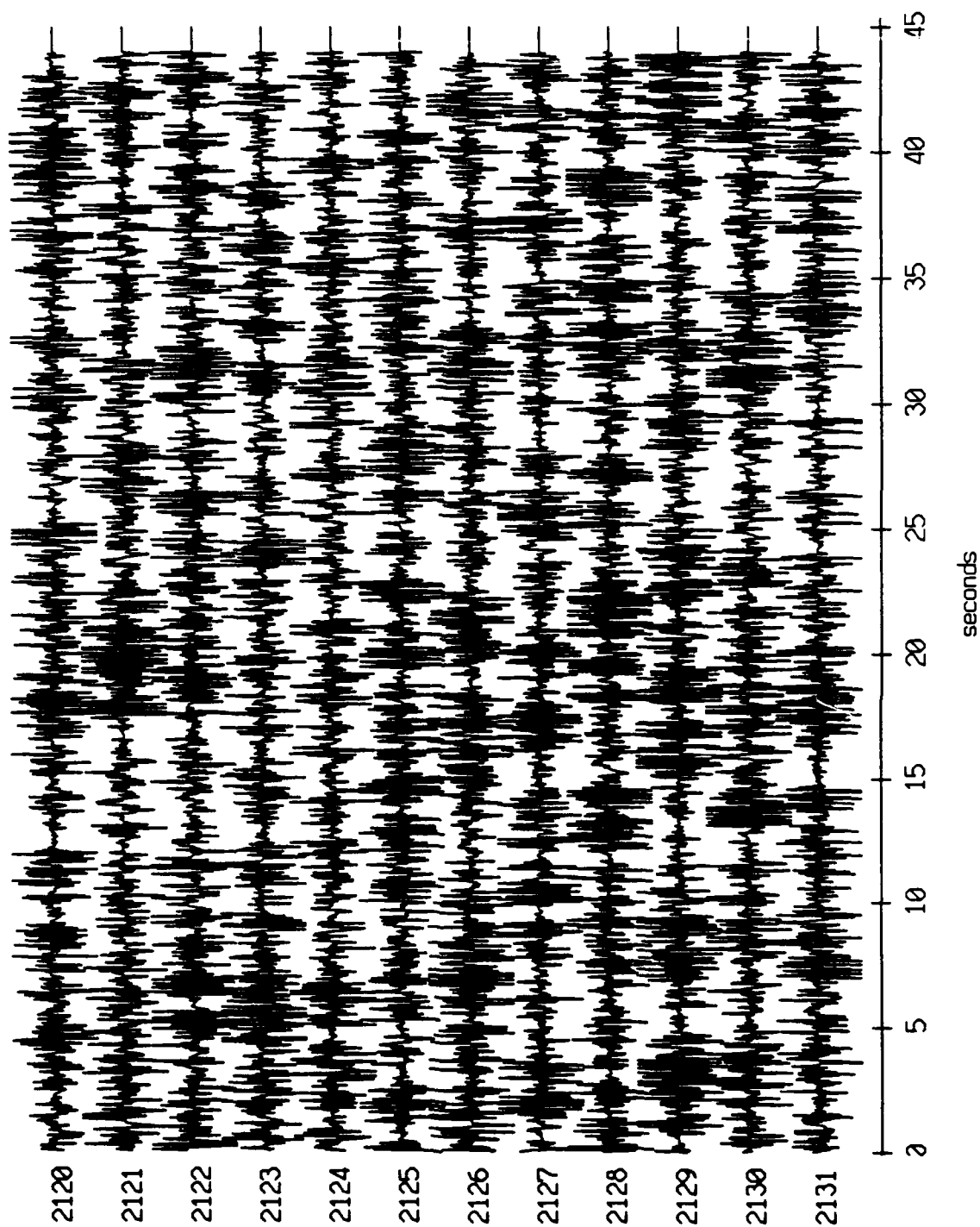


Figure XI.69c

Floot 5, July, 1989 Trip - records 2120-2131 (hydrophone)  
 vertical axis scale is approx. -2.0 to 2.0 volts

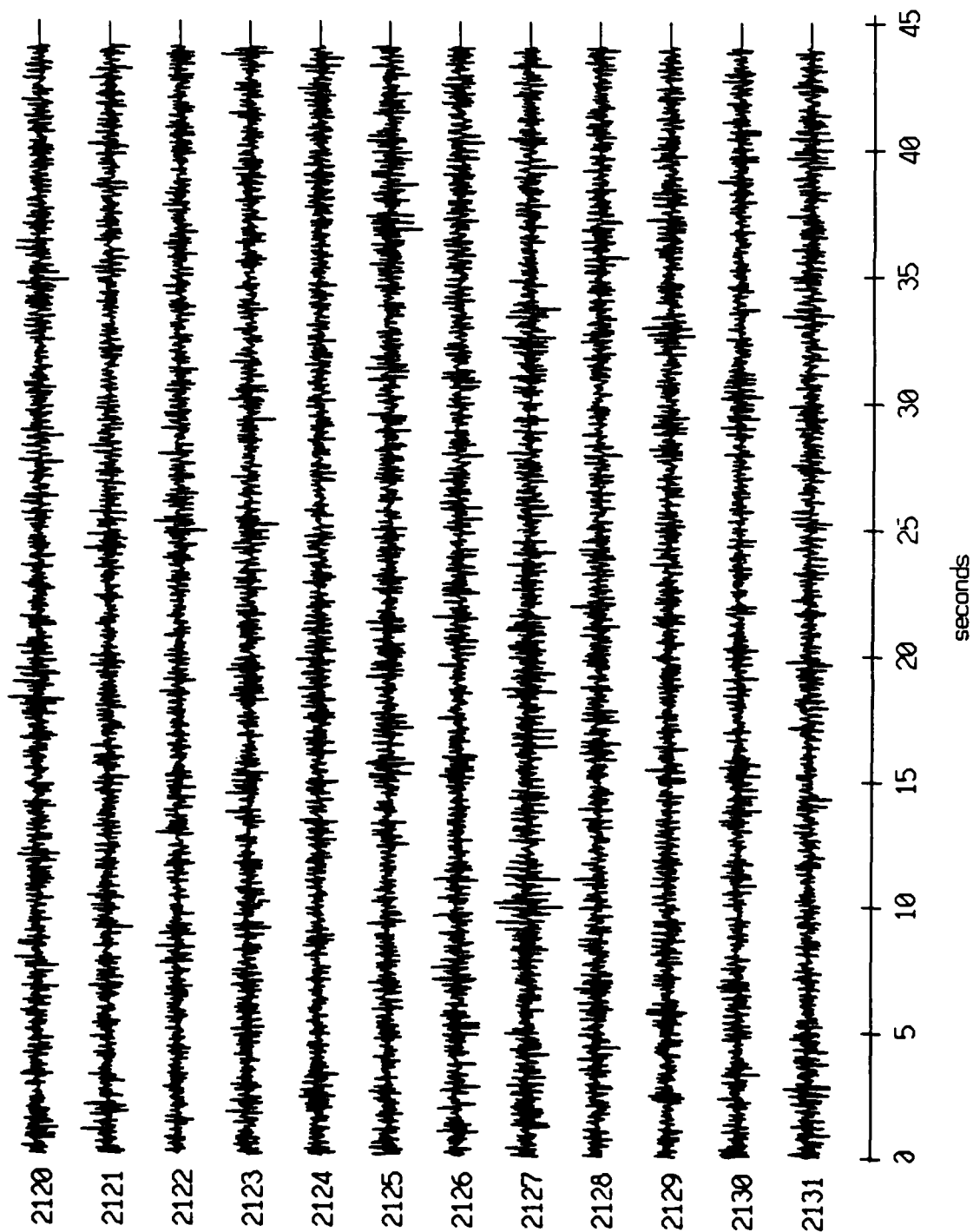


RGC corrected channel level (V)

Figure XI.69d



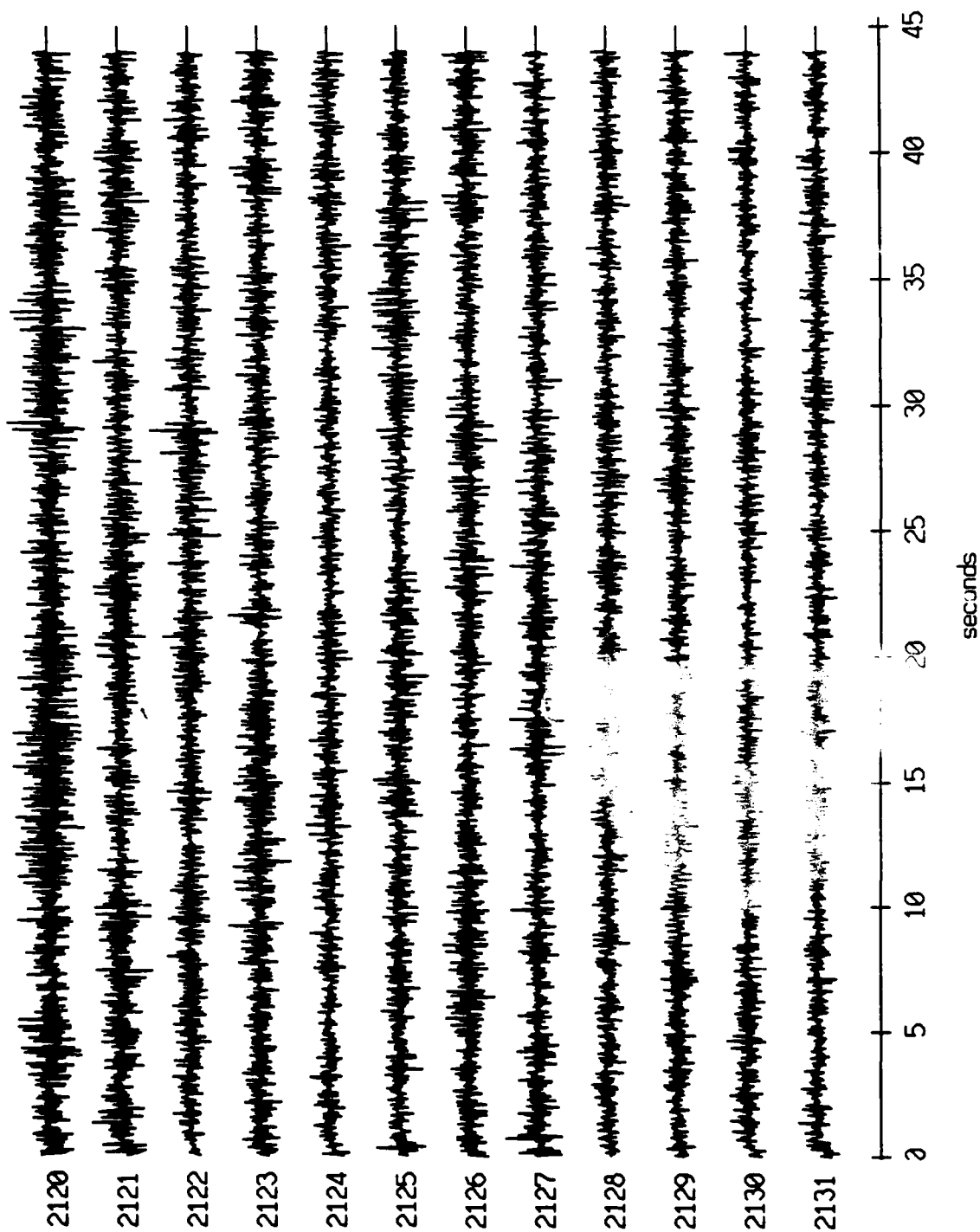
Floot 6, July, 1989 Trip - records 2120-2131 (x-axis)  
vertical axis scale is approx. -2.0 to 2.0 volts



PGC corrected channel level (V)

Figure XI.70a

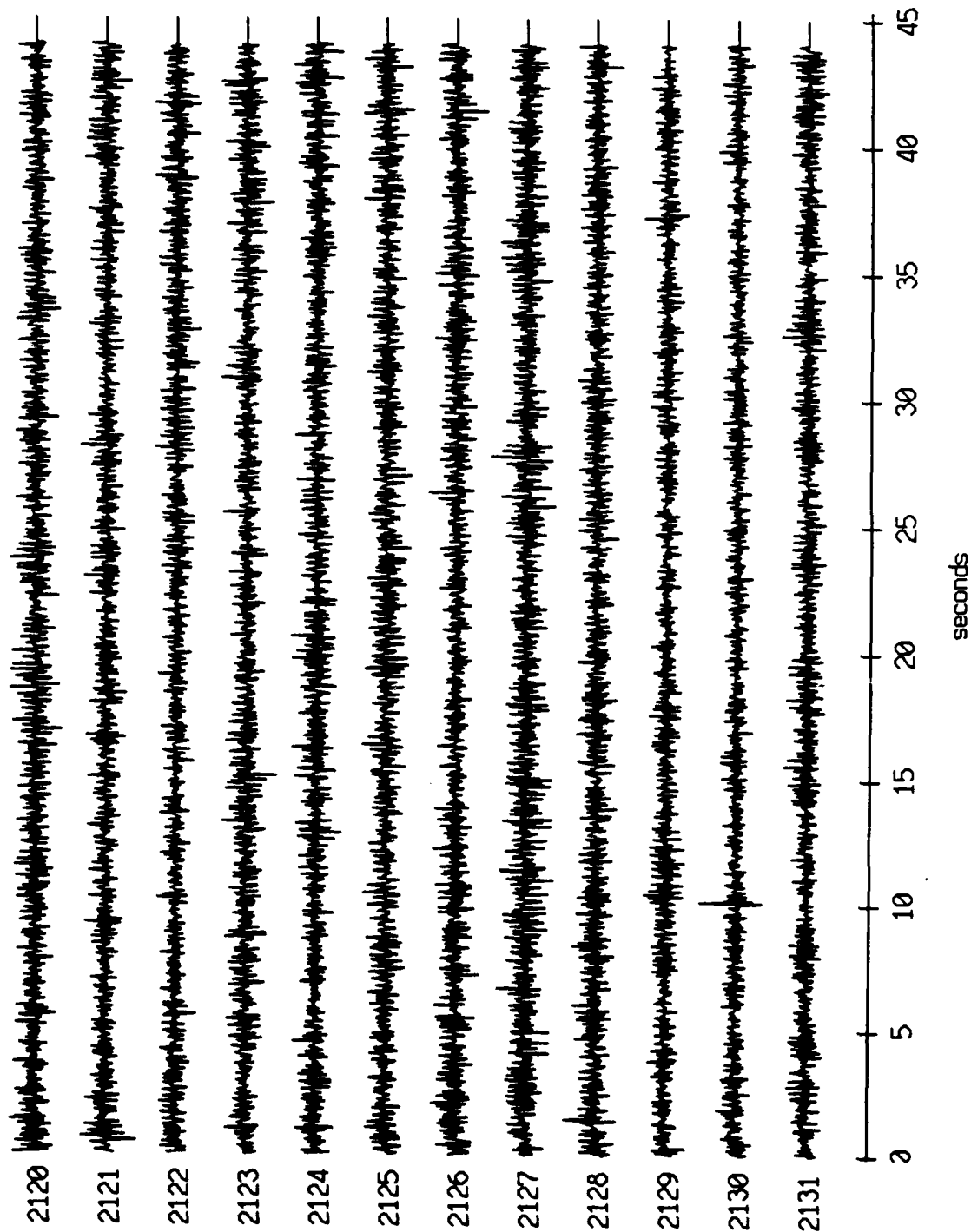
Floot 6, July, 1989 Trip - records 2120-2131 (y-axis)  
vertical axis scale is approx. -2.0 to 2.0 volts



HGC corrected channel level (V)

Figure XI.70b

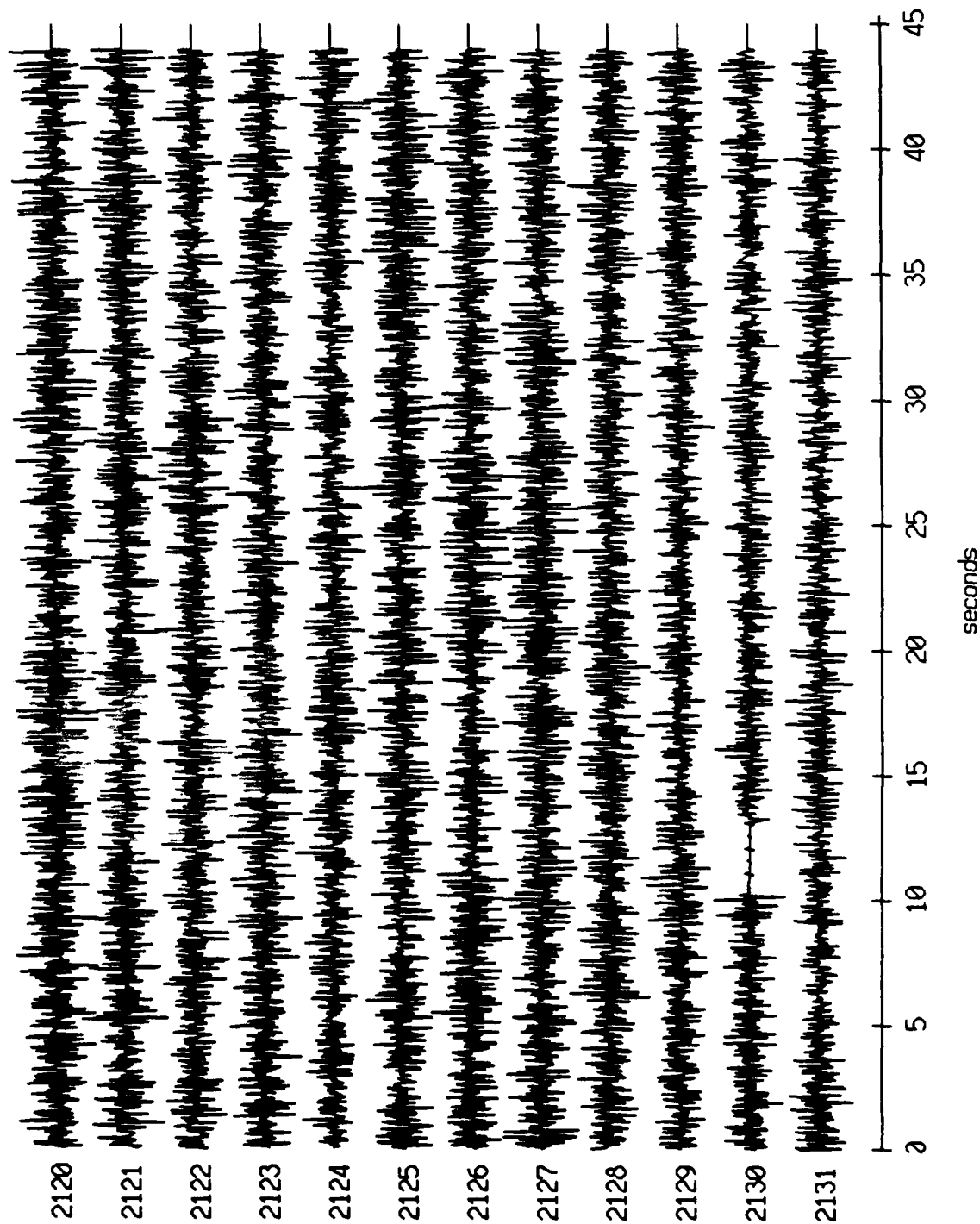
Float 6, July, 1989 Trip - records 2120-2131 (z-axis)  
vertical axis scale is approx. -2.0 to 2.0 volts



RGC corrected channel level (V)

Figure XI.70c

Float 6, July, 1989 Trip - records 2120-2131 (hydrophone)  
vertical axis scale is approx. -2.0 to 2.0 volts



PGC corrected channel level (V)

Figure XI.70d

Float 7, July, 1989 Trip - records 2120-2131 (x-axis)  
vertical axis scale is approx. -2.0 to 2.0 volts

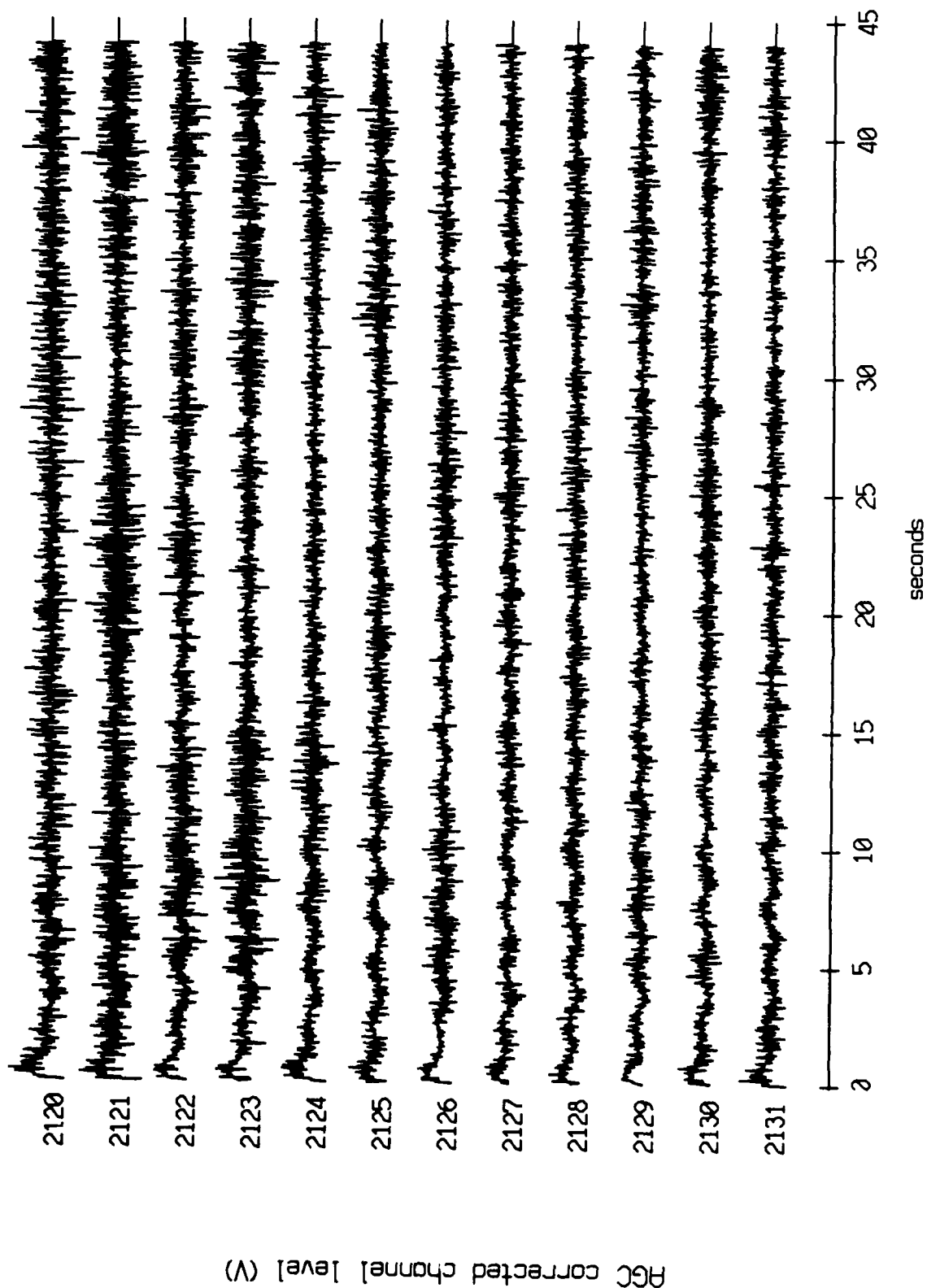


Figure XI.71a

Float 7, July, 1989 Trip - records 2120-2131 (y-axis)  
vertical axis scale is approx. -2.0 to 2.0 volts

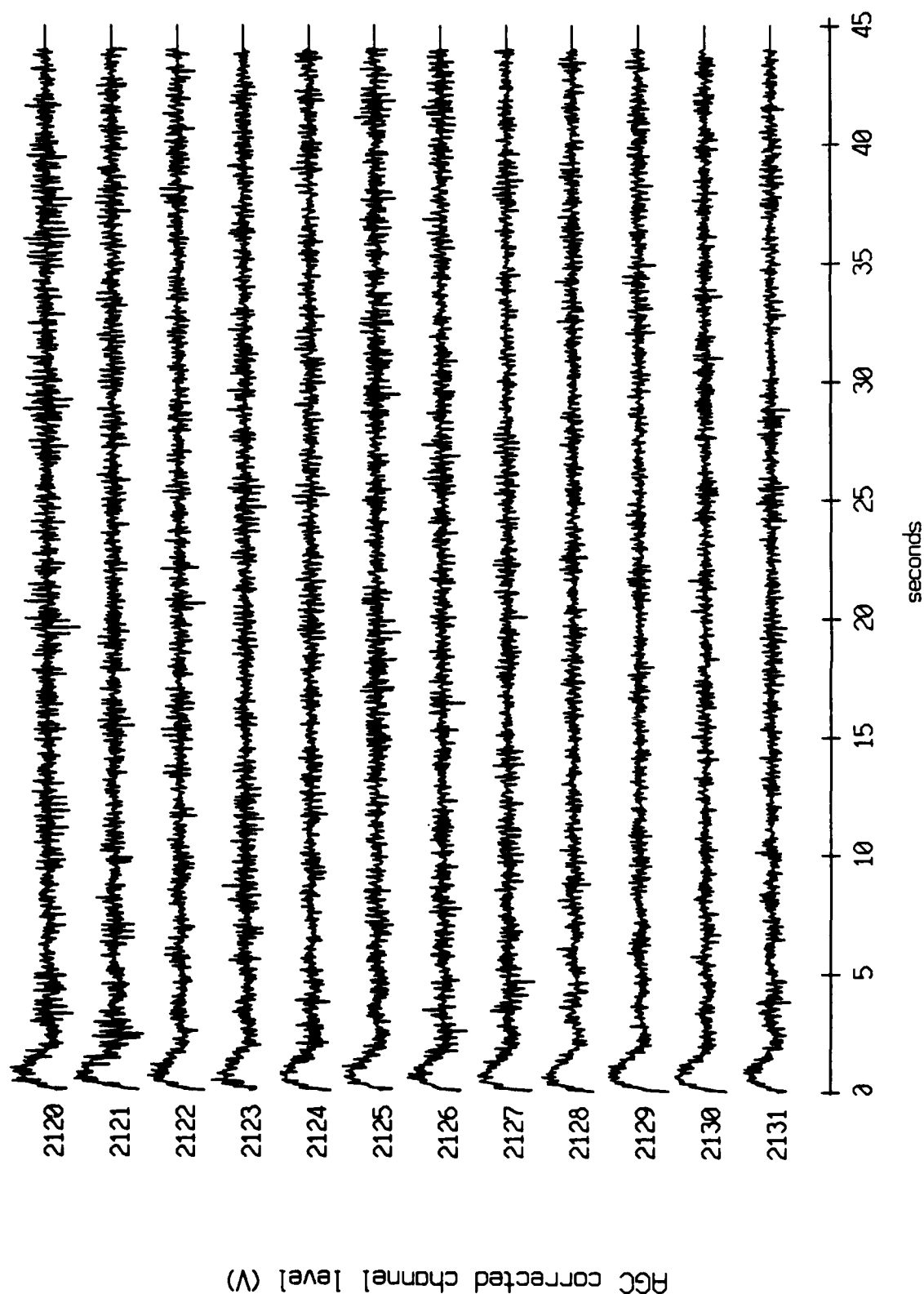


Figure XI.71b

Float 7, July, 1989 Trip - records 2120-2131 (z-axis)  
vertical axis scale is approx. -2.0 to 2.0 volts

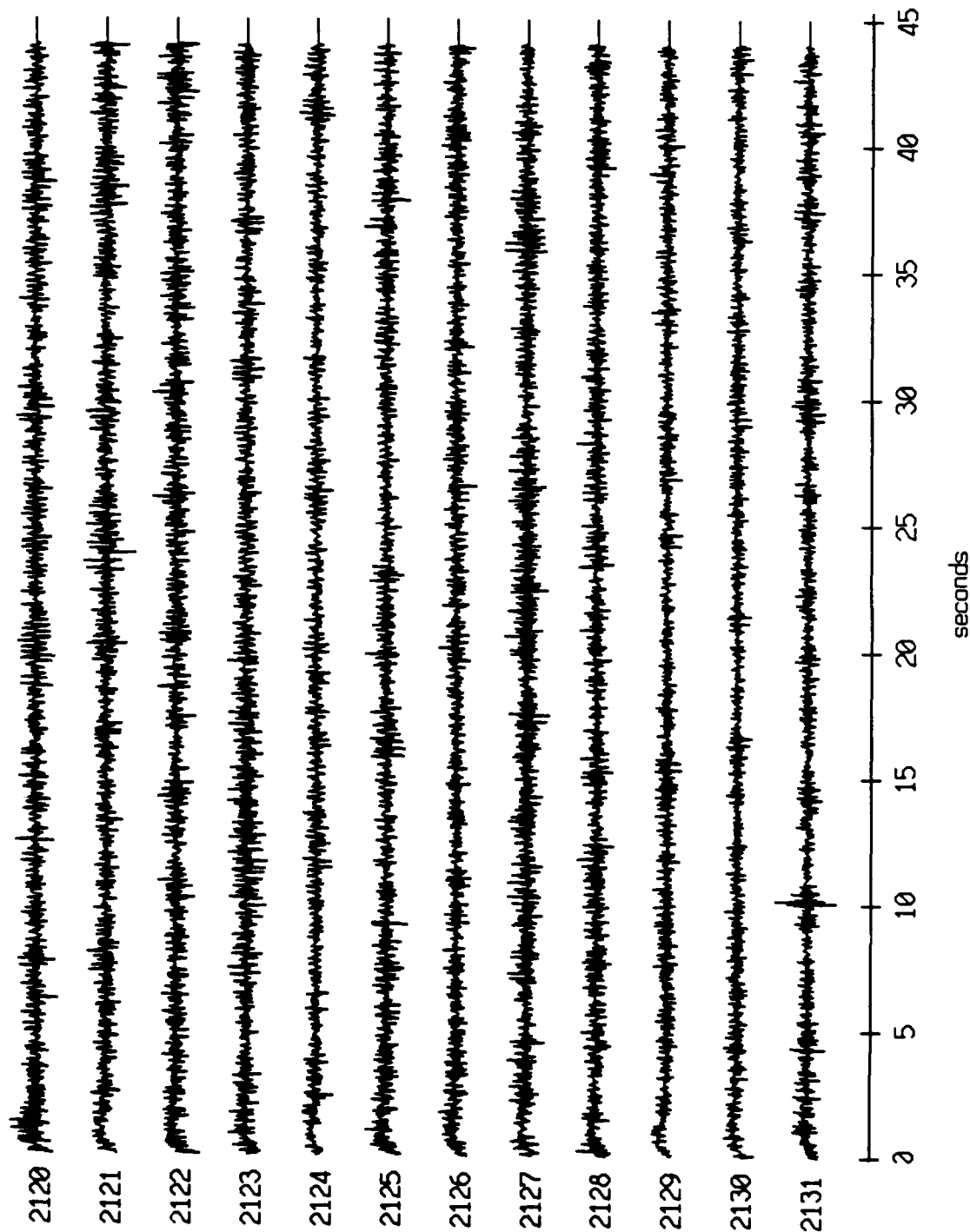
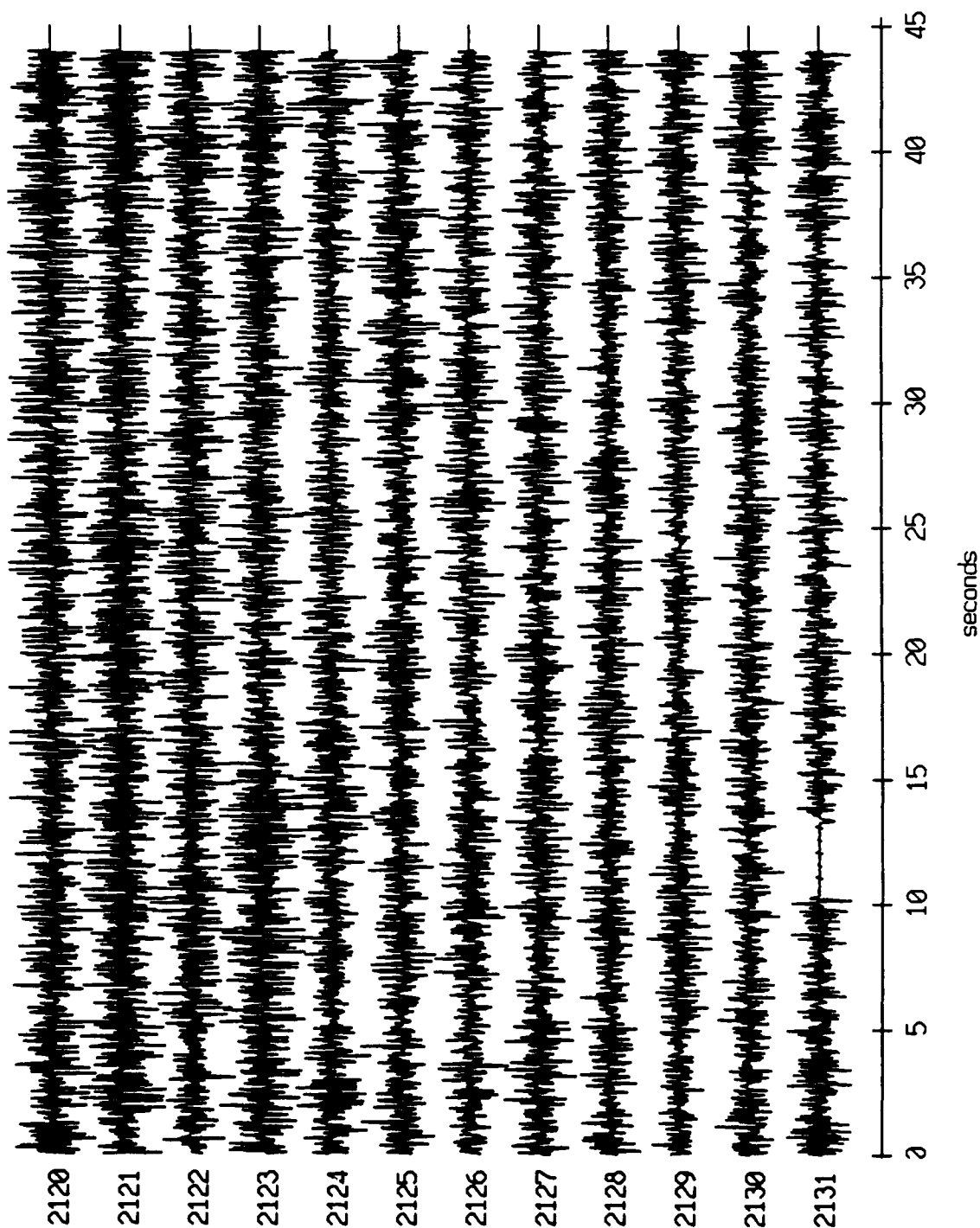


Figure XI.71c

Float 7, July, 1989 Trip - records 2120-2131 (hydrophone)  
 vertical axis scale is approx. -2.0 to 2.0 volts

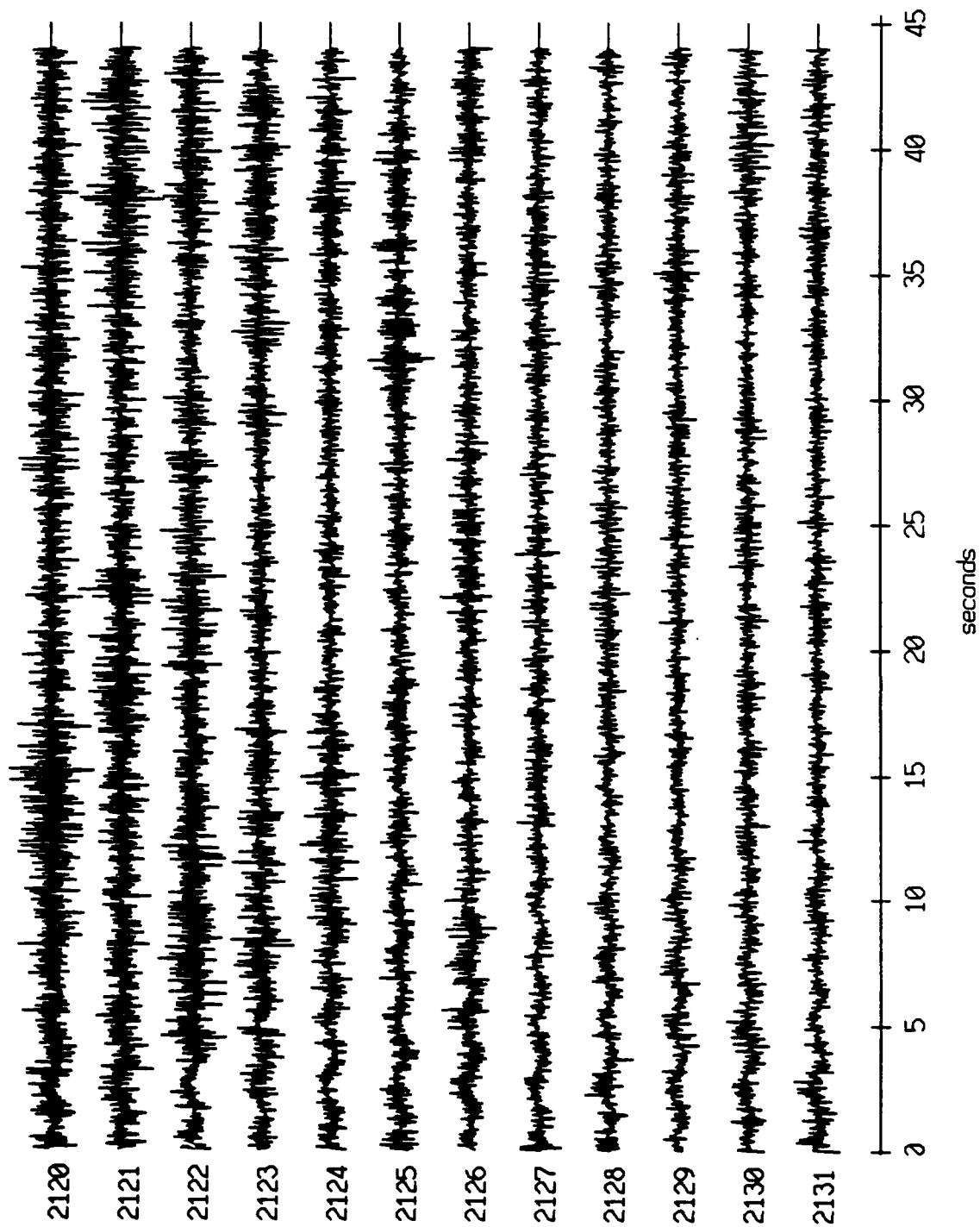


AGC corrected channel level (V)

Figure XI.71d



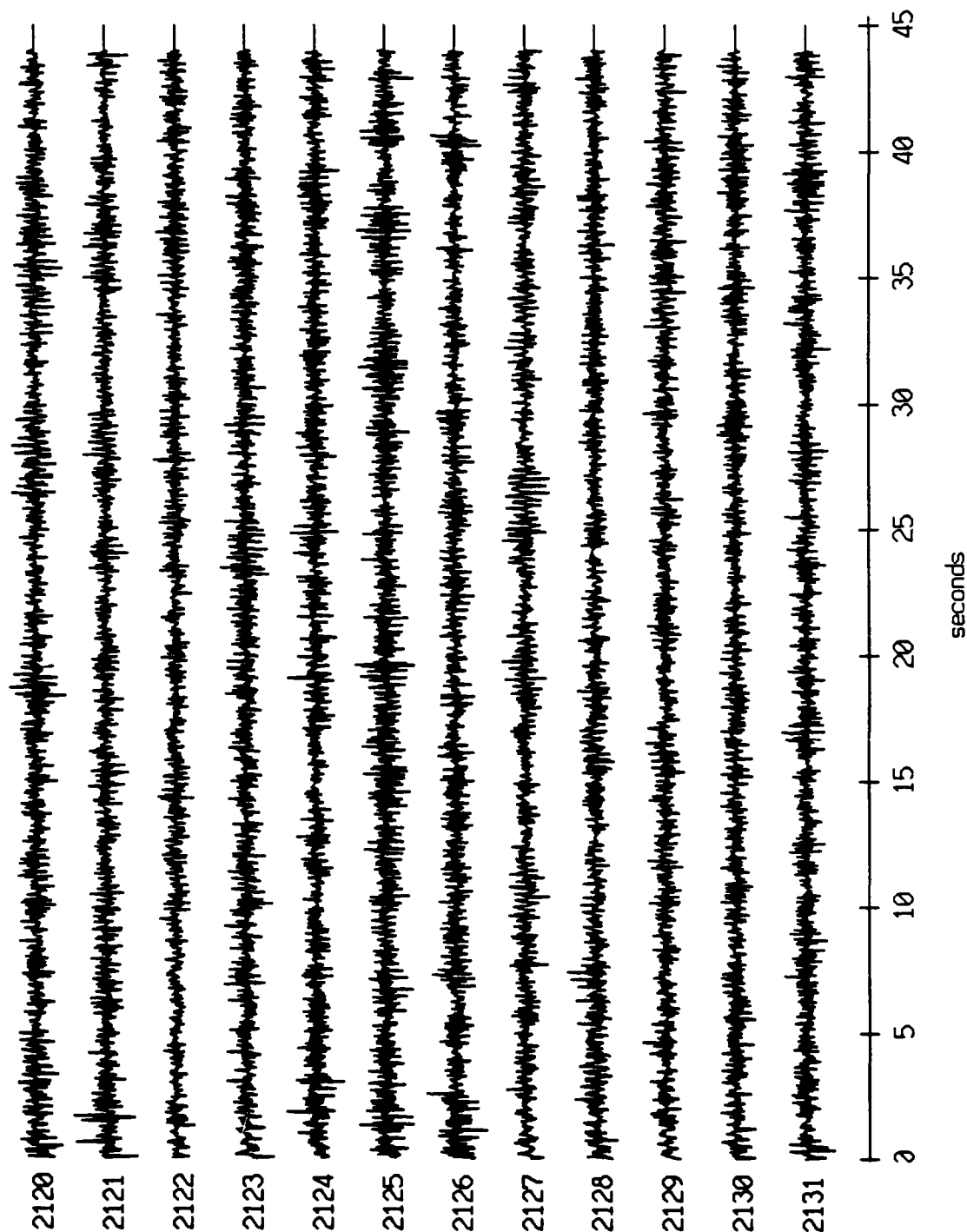
Float 8, July, 1989 Trip - records 2120-2131 (x-axis)  
vertical axis scale is approx. -2.0 to 2.0 volts



AGC corrected channel level (V)

Figure XI.72a

Flot 8, July, 1989 Trip - records 2120-2131 (y-axis)  
vertical axis scale is approx. -2.0 to 2.0 volts



AGC corrected channel level (V)

Figure XI.72b

Float 8, July, 1989 Trip - records 2120-2131 (z-axis)  
vertical axis scale is approx. -2.0 to 2.0 volts

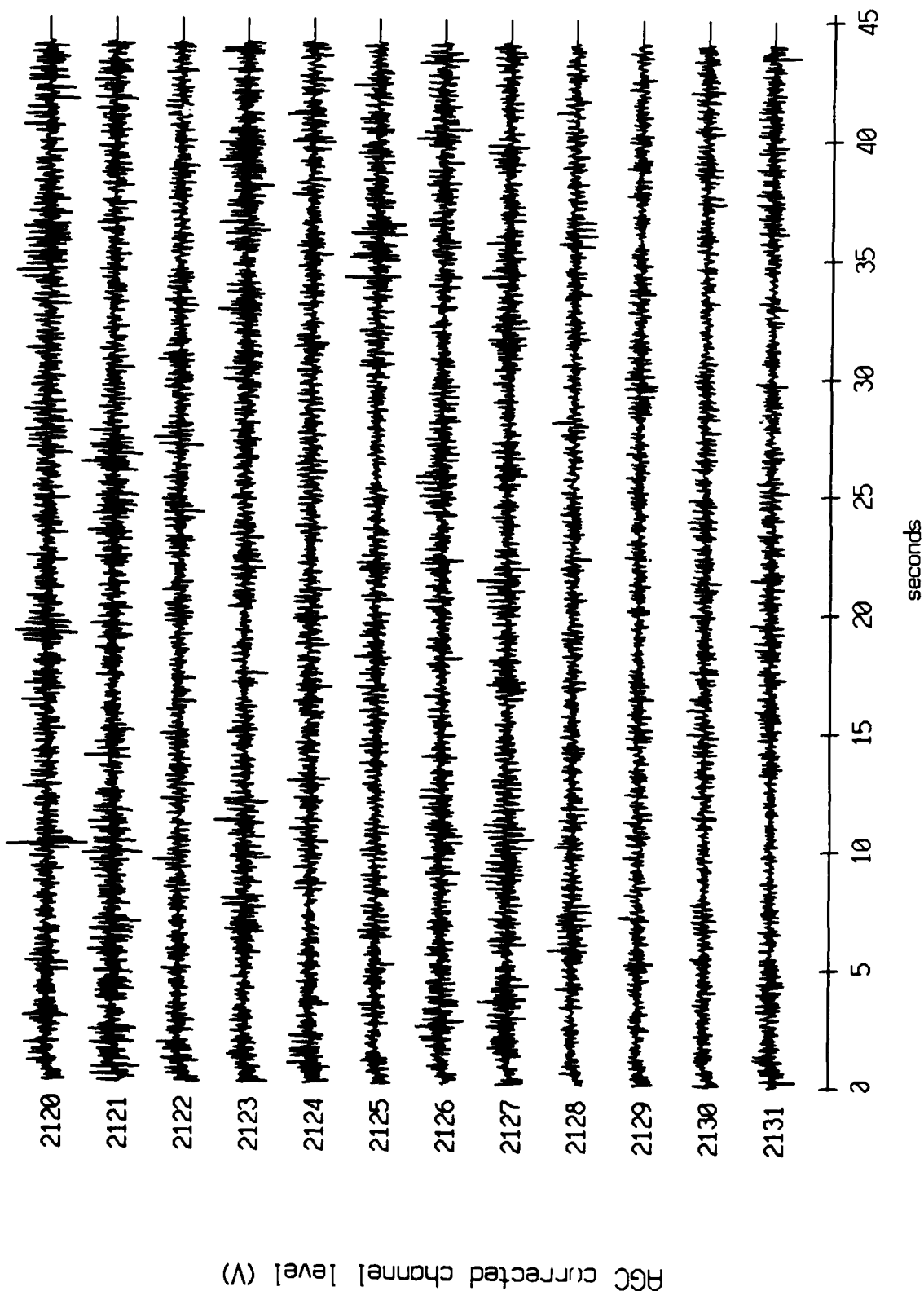


Figure XI.72c

Float 8, July, 1989 Trip - records 2120-2131 (hydrophone)  
vertical axis scale is approx. -2.0 to 2.0 volts

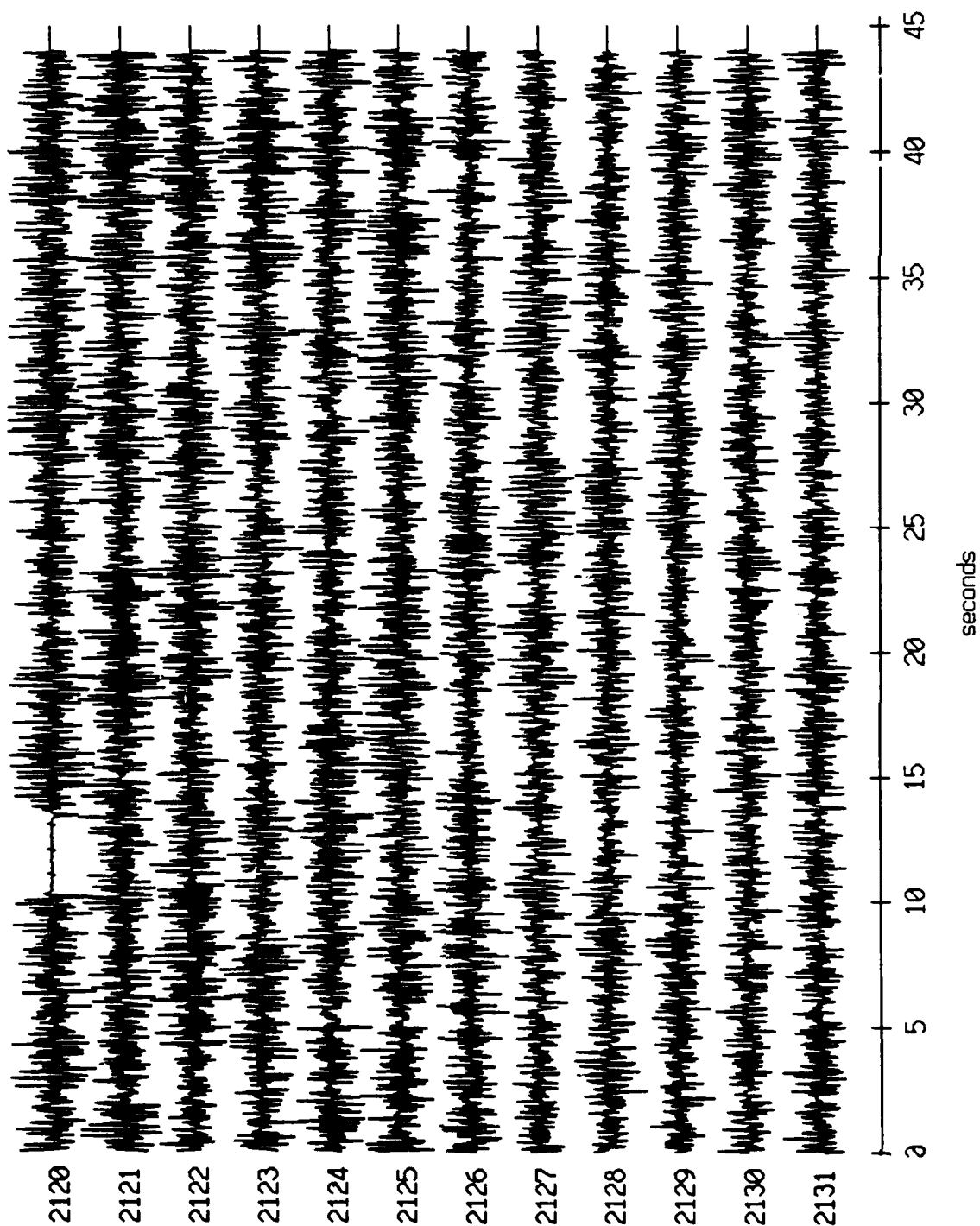
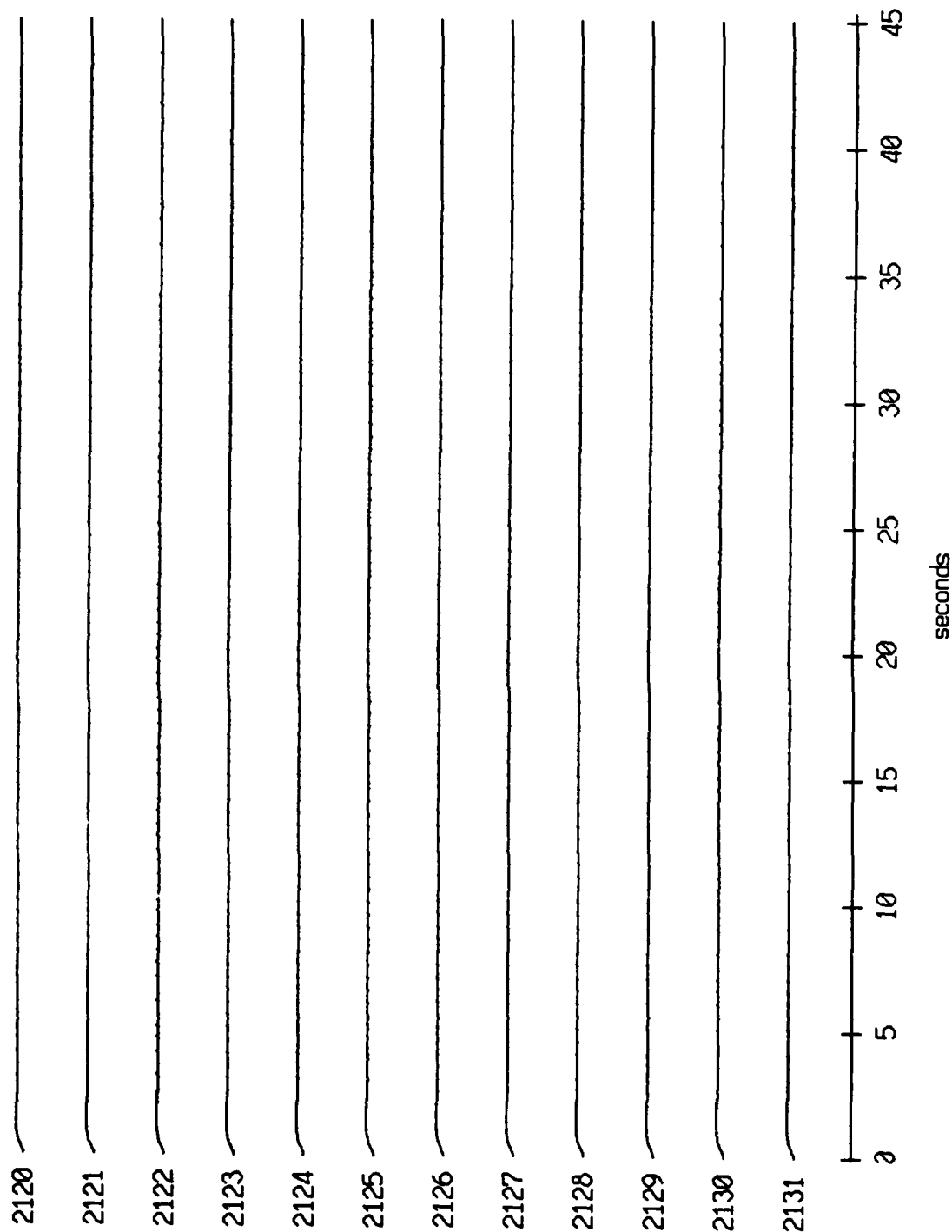


Figure XI.72d

Floot 9, July, 1989 Trip - records 2120-2131 (x-axis)  
vertical axis scale is approx. -2.0 to 2.0 volts



RGC corrected channel level (V)

Figure XI.73a

Float 9, July, 1989 Trip - records 2120-2131 (y-axis)  
vertical axis scale is approx. -2.0 to 2.0 volts

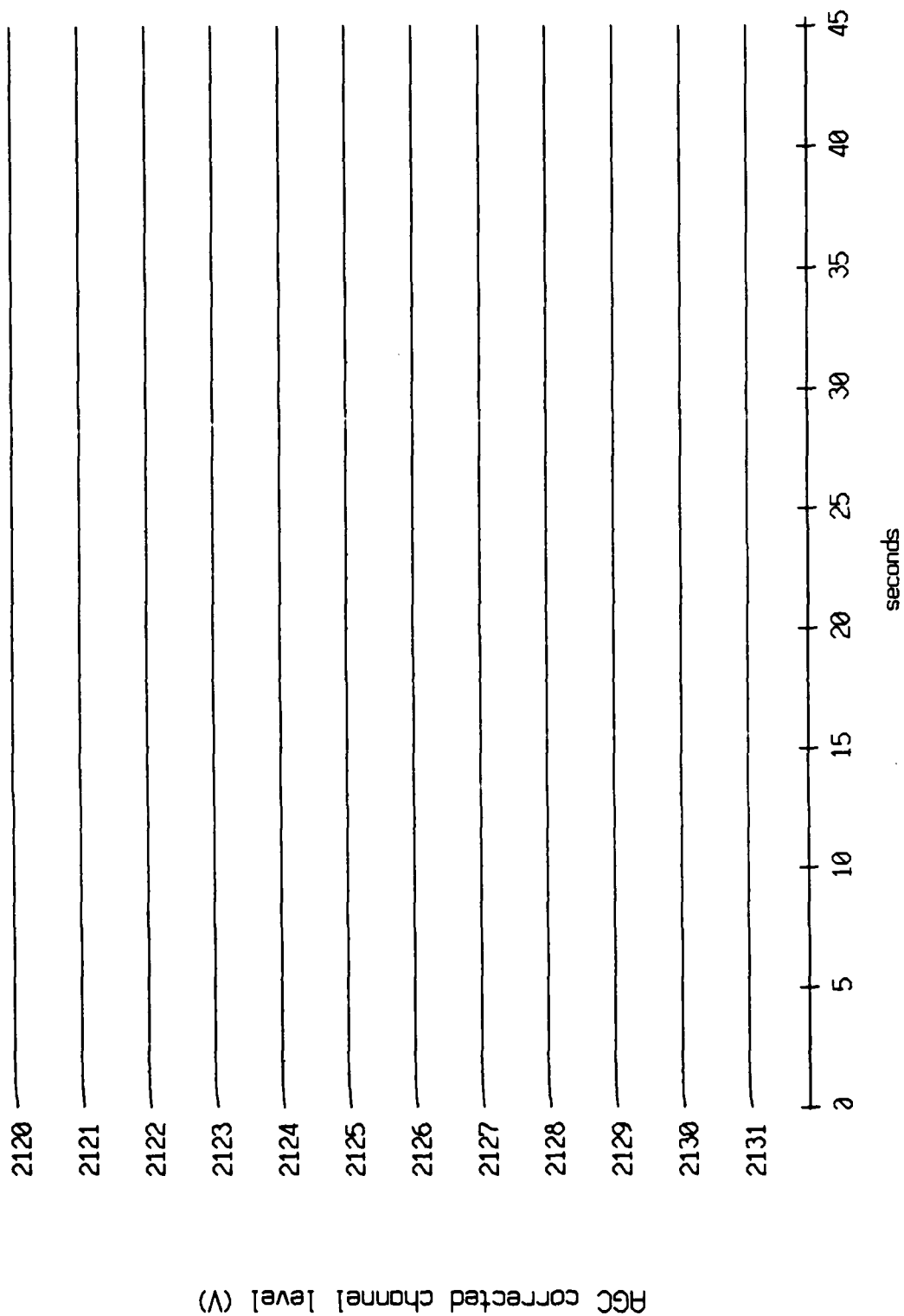
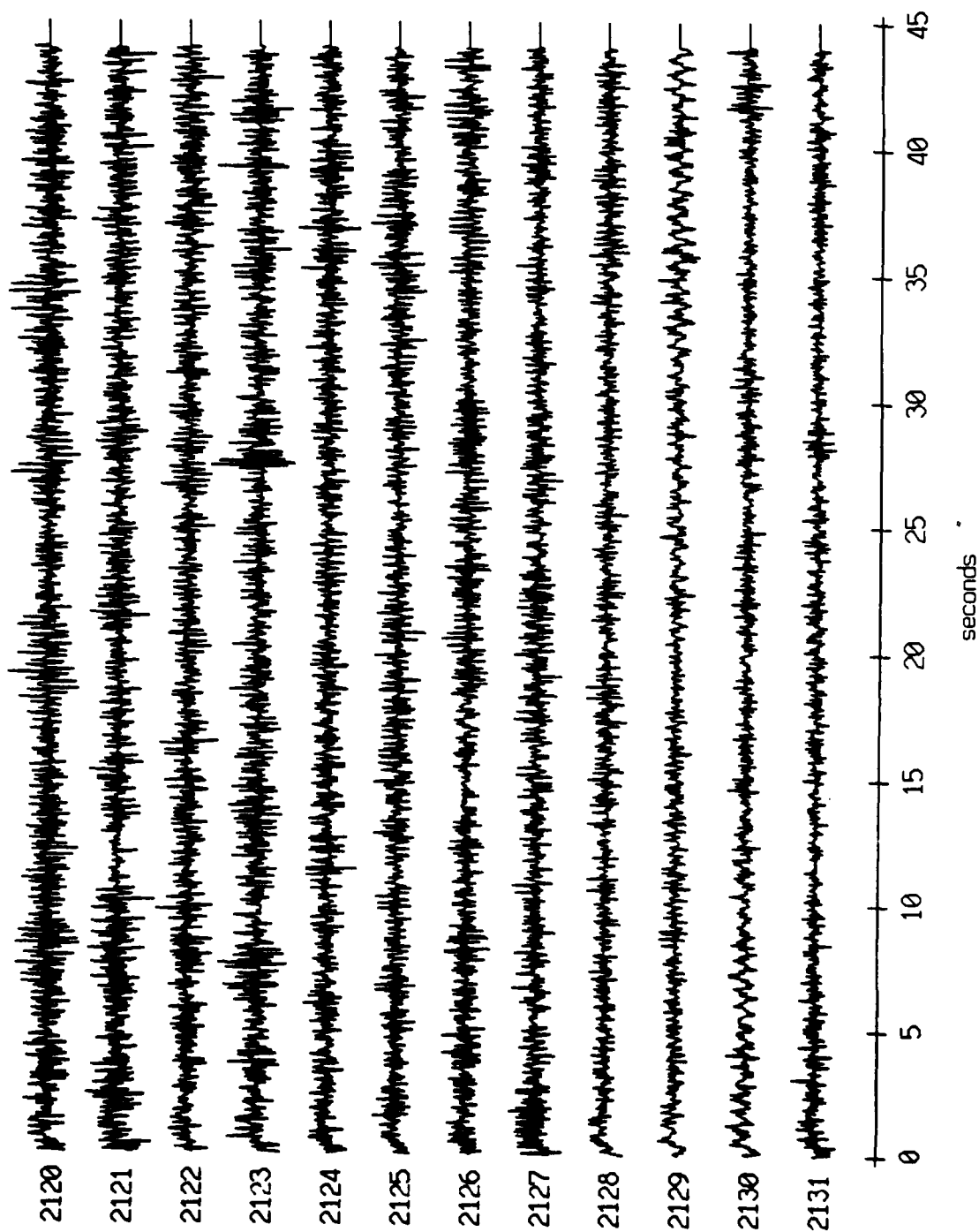


Figure XI.73b

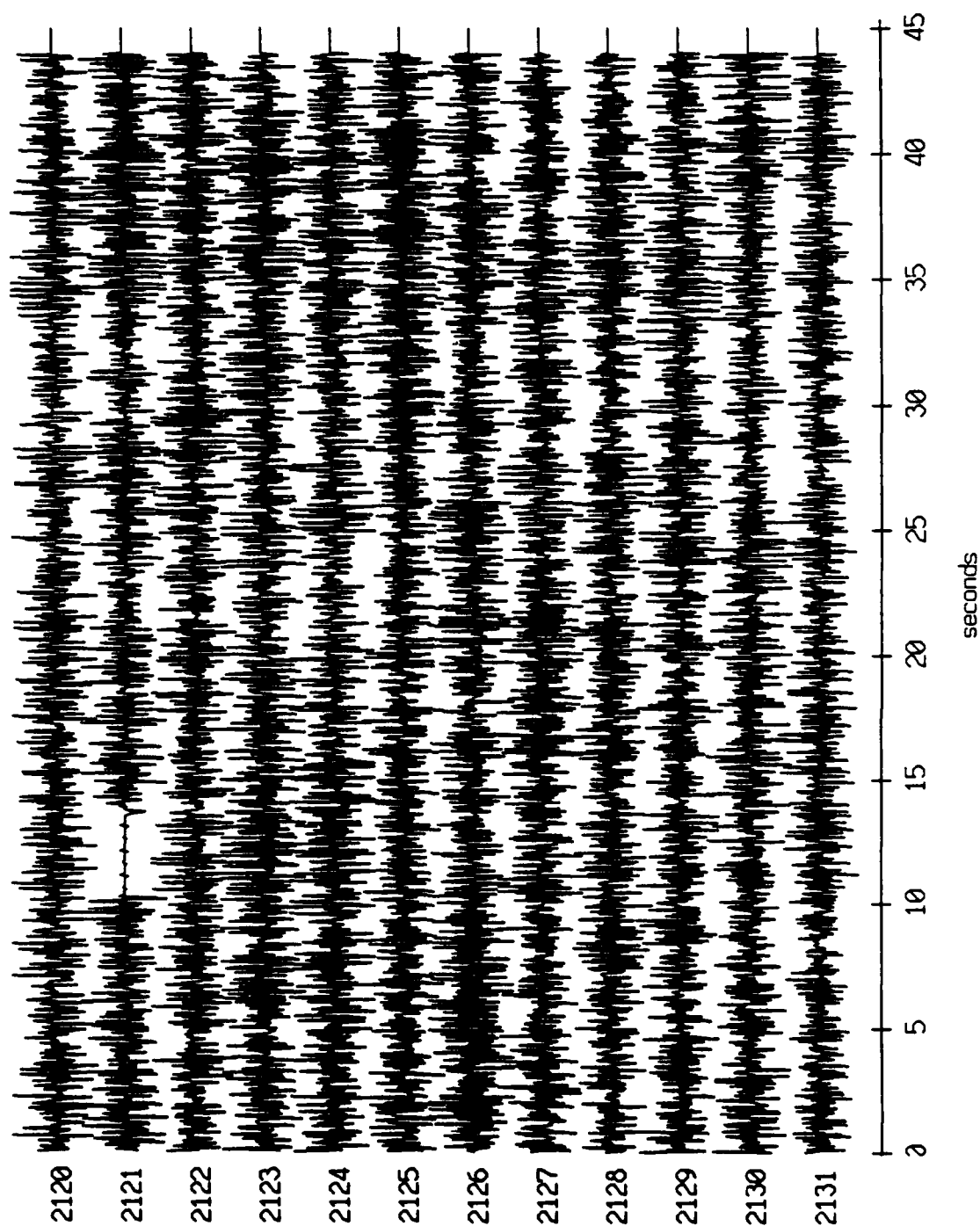
Floot 9, July, 1989 Trip - records 2120-2131 (z-axis)  
vertical axis scale is approx. -2.0 to 2.0 volts



HGC corrected channel level (V)

Figure XI.73c

Float 9, July, 1989 Trip - records 2120-2131 (hydrophone)  
vertical axis scale is approx. -2.0 to 2.0 volts



AGC corrected channel level (V)

Figure XI.73d



Float 10, July, 1989 Trip - records 2120-2131 (x-axis)  
vertical axis scale is approx. -2.0 to 2.0 volts

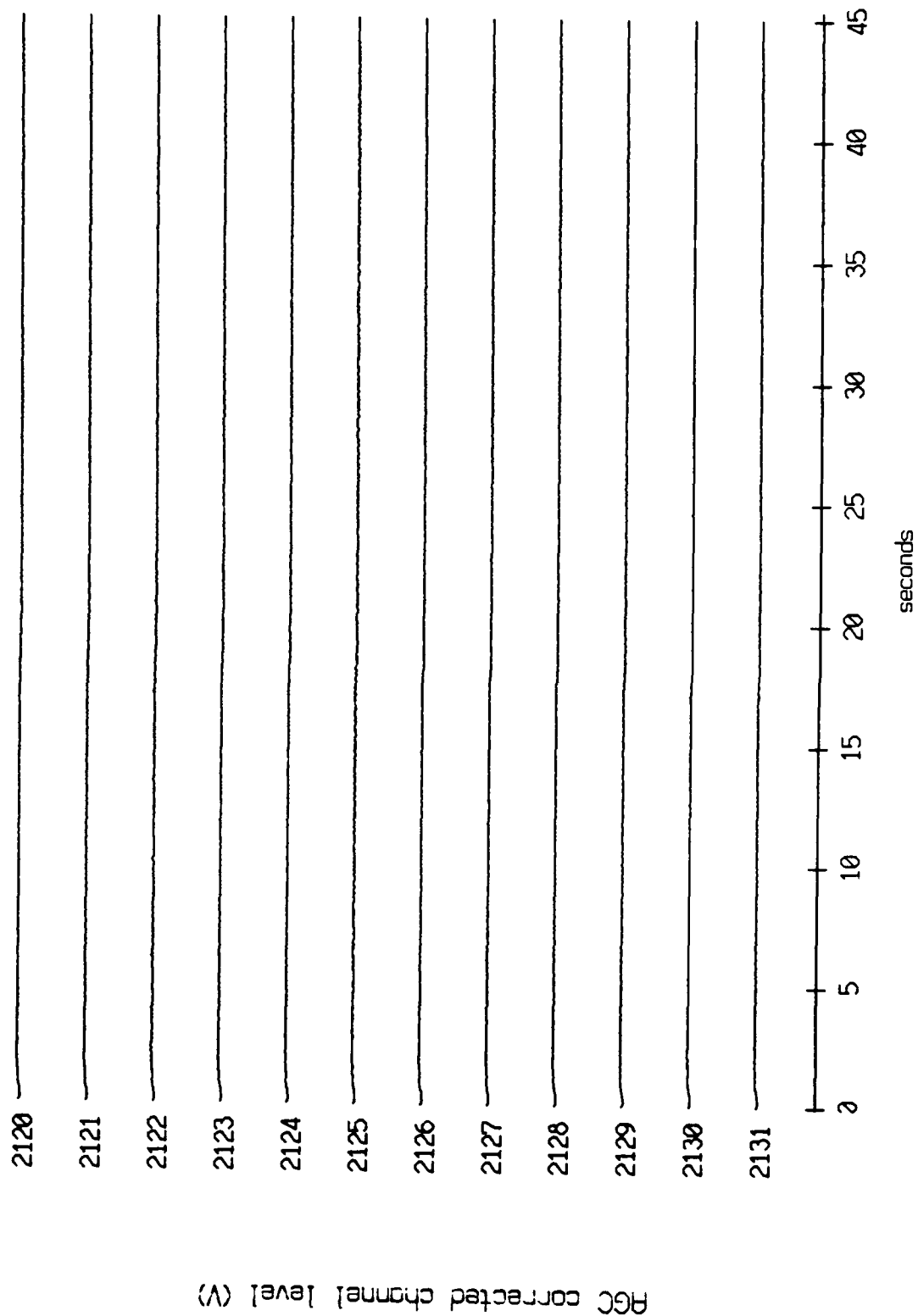


Figure XI.74a

Floot 10, July, 1989 Trip - records 2120-2131 (y-axis)  
 vertical axis scale is approx. -2.0 to 2.0 volts

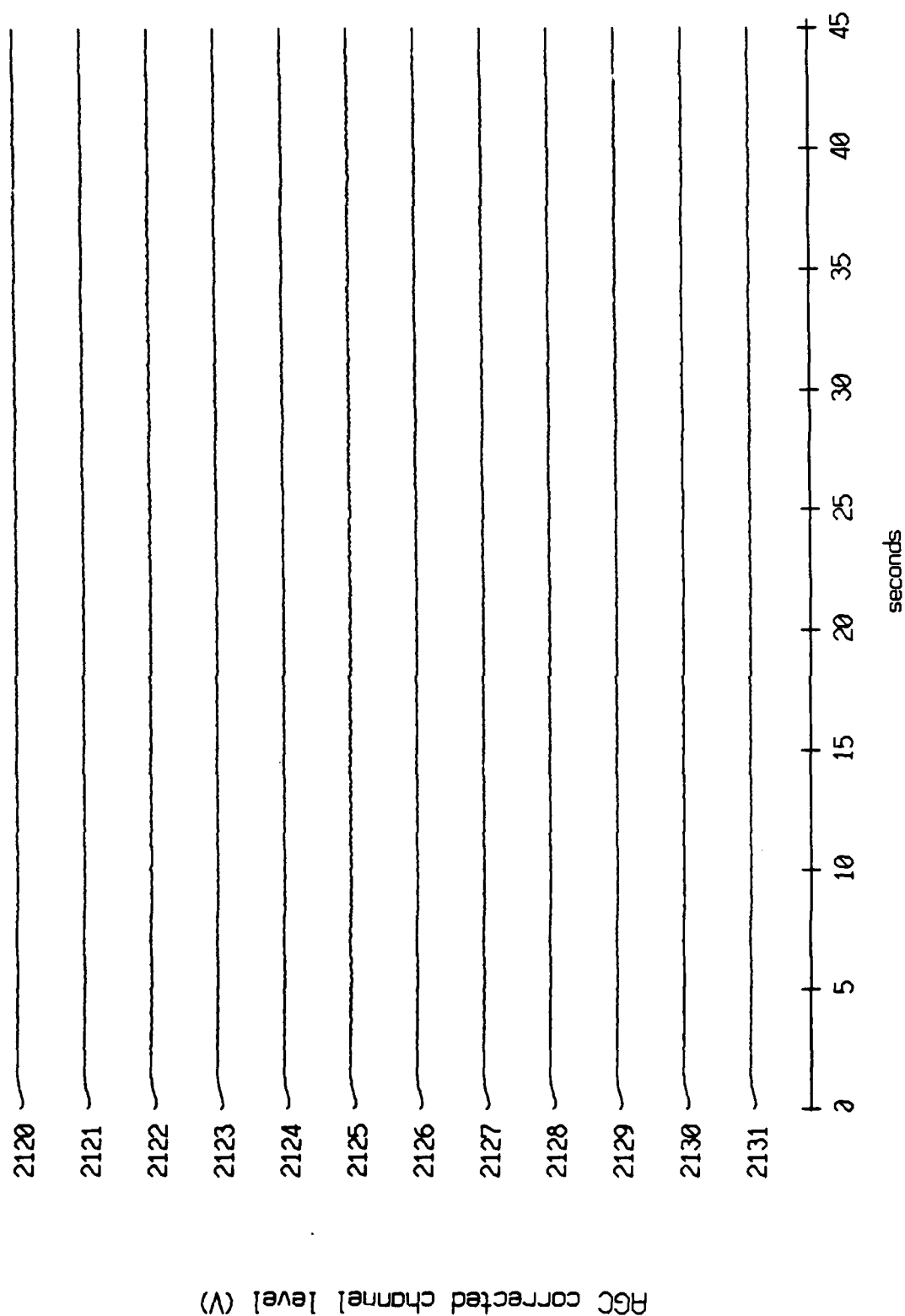


Figure XI.74b

Float 10, July, 1989 Trip - records 2120-2131 (z-axis)  
vertical axis scale is approx. -2.0 to 2.0 volts

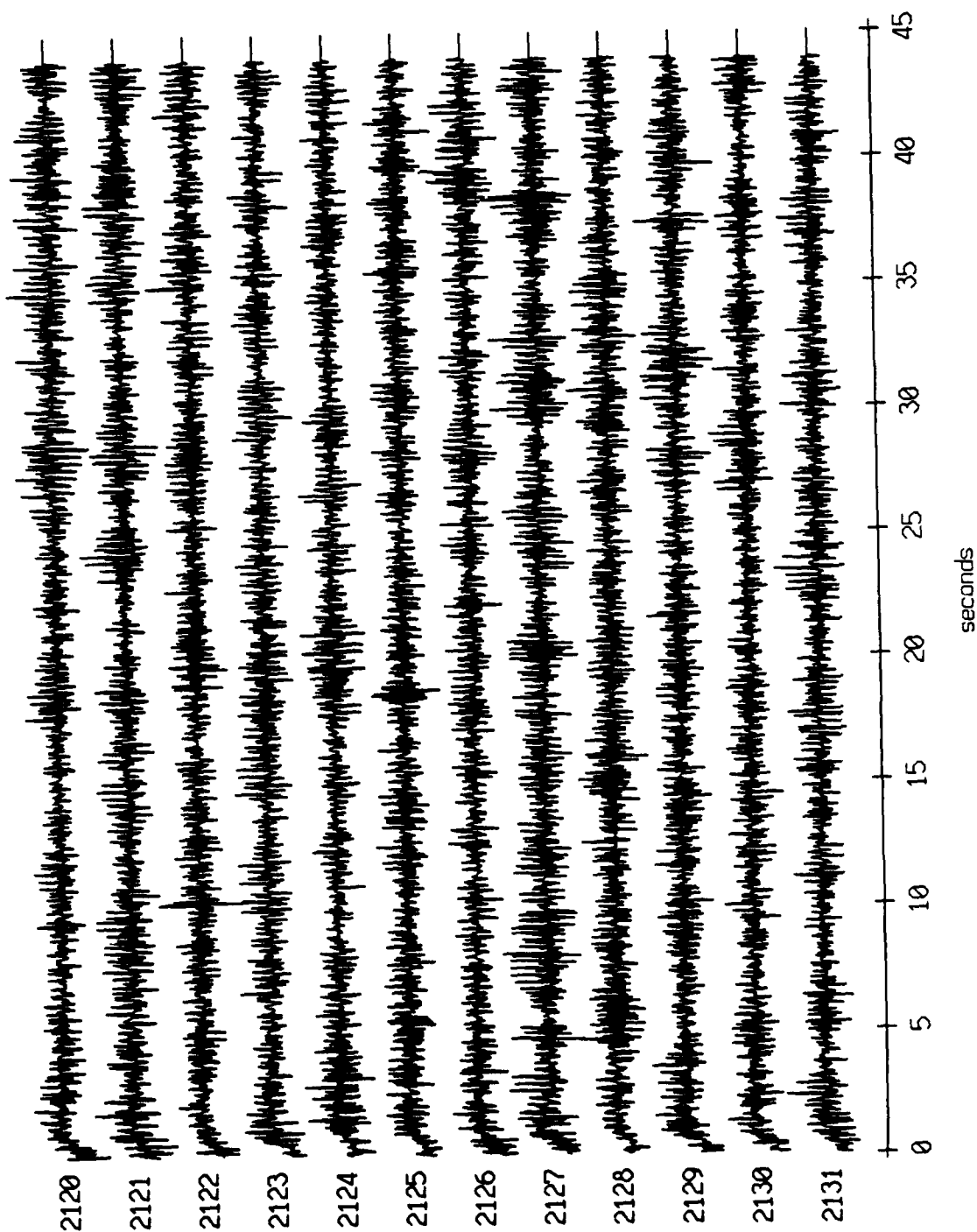


Figure XI.74c

Float 10, July, 1989 Trip - records 2120-2131 (hydrophone)  
vertical axis scale is approx. -2.0 to 2.0 volts

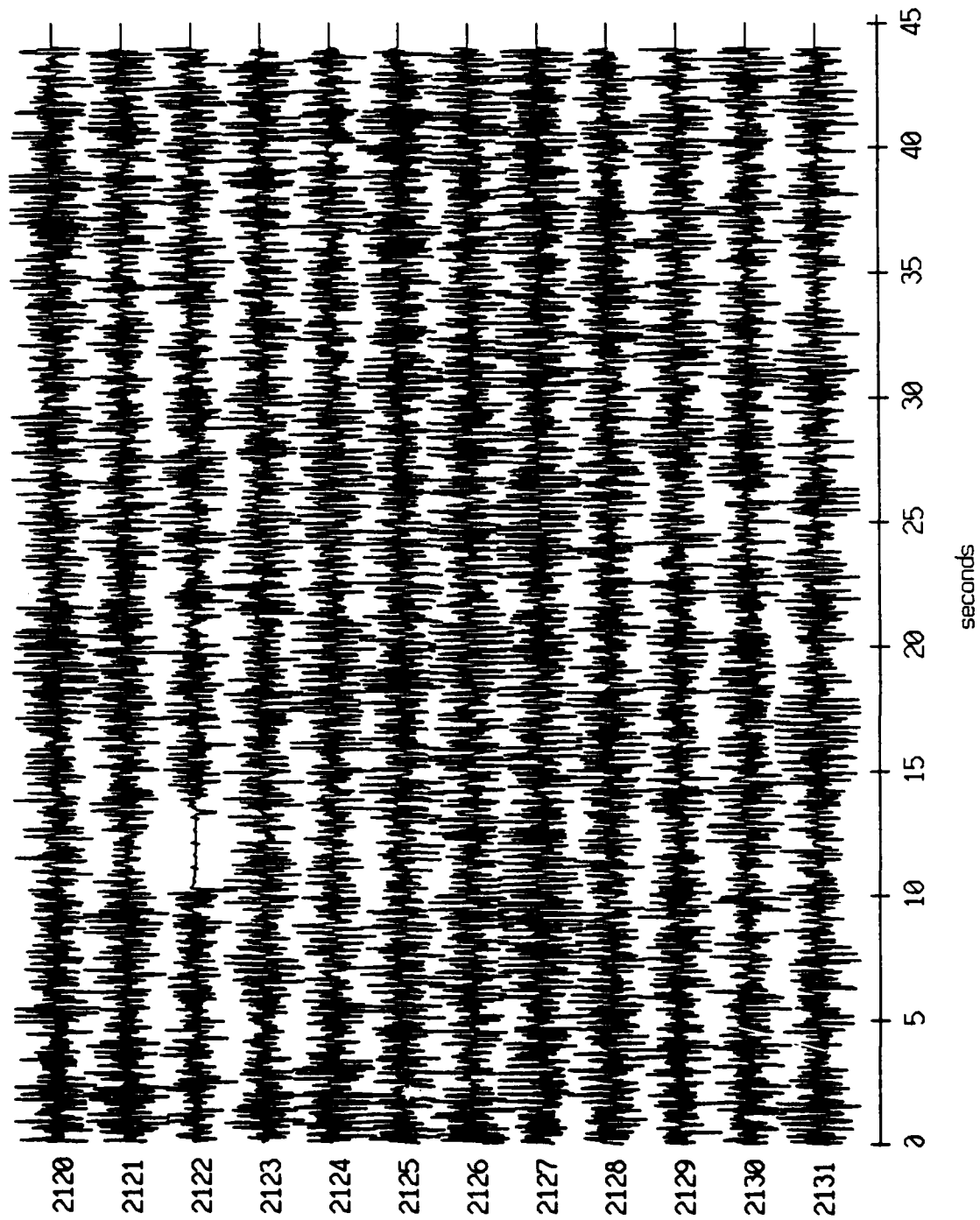


Figure XI.74d

Float 11, July, 1989 Trip - records 2120-2131 (x-axis)  
vertical axis scale is approx. -2.0 to 2.0 volts

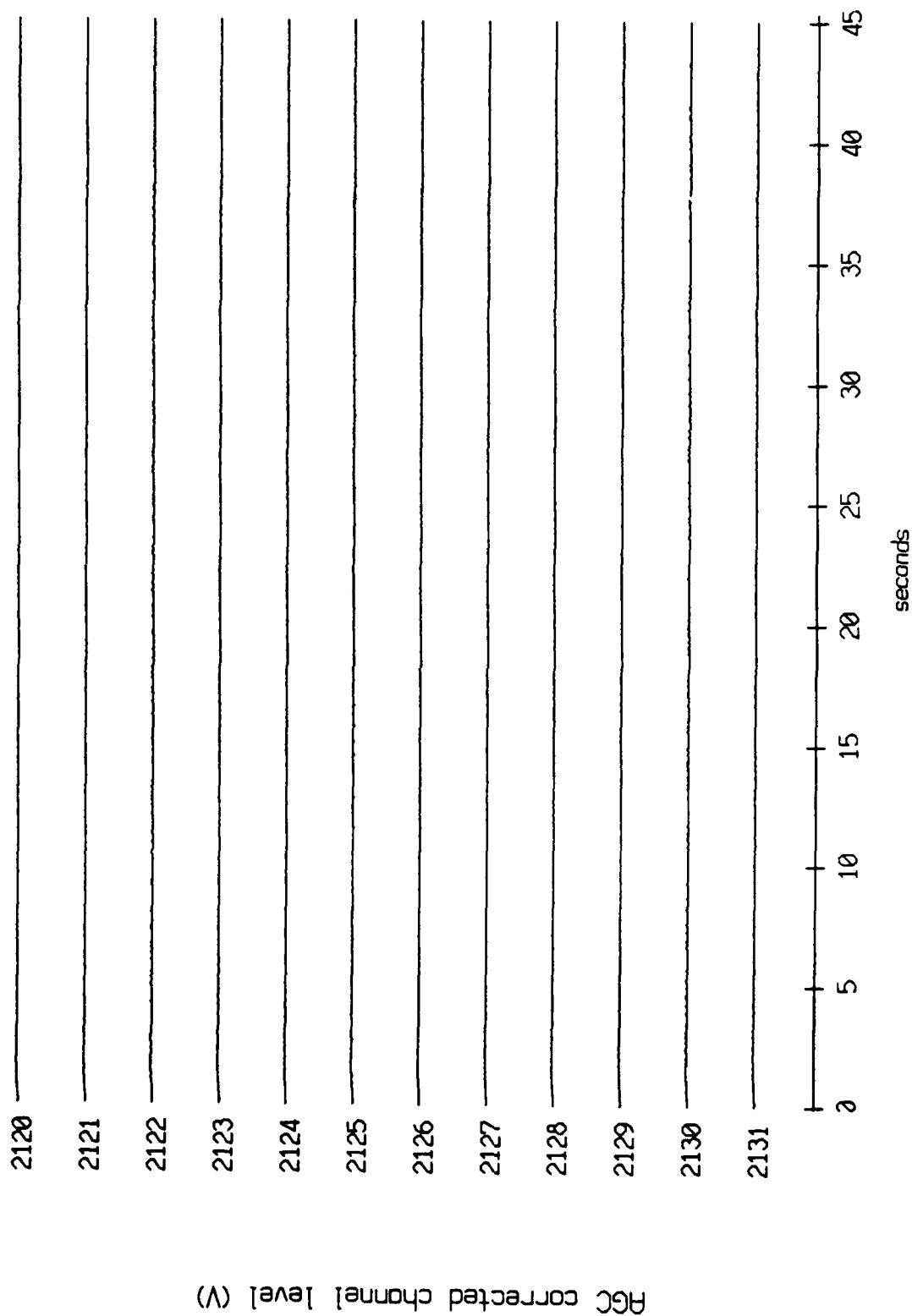


Figure XI.75a

Float 11, July, 1989 Trip - records 2120-2131 (y-axis)  
vertical axis scale is approx. -2.0 to 2.0 volts

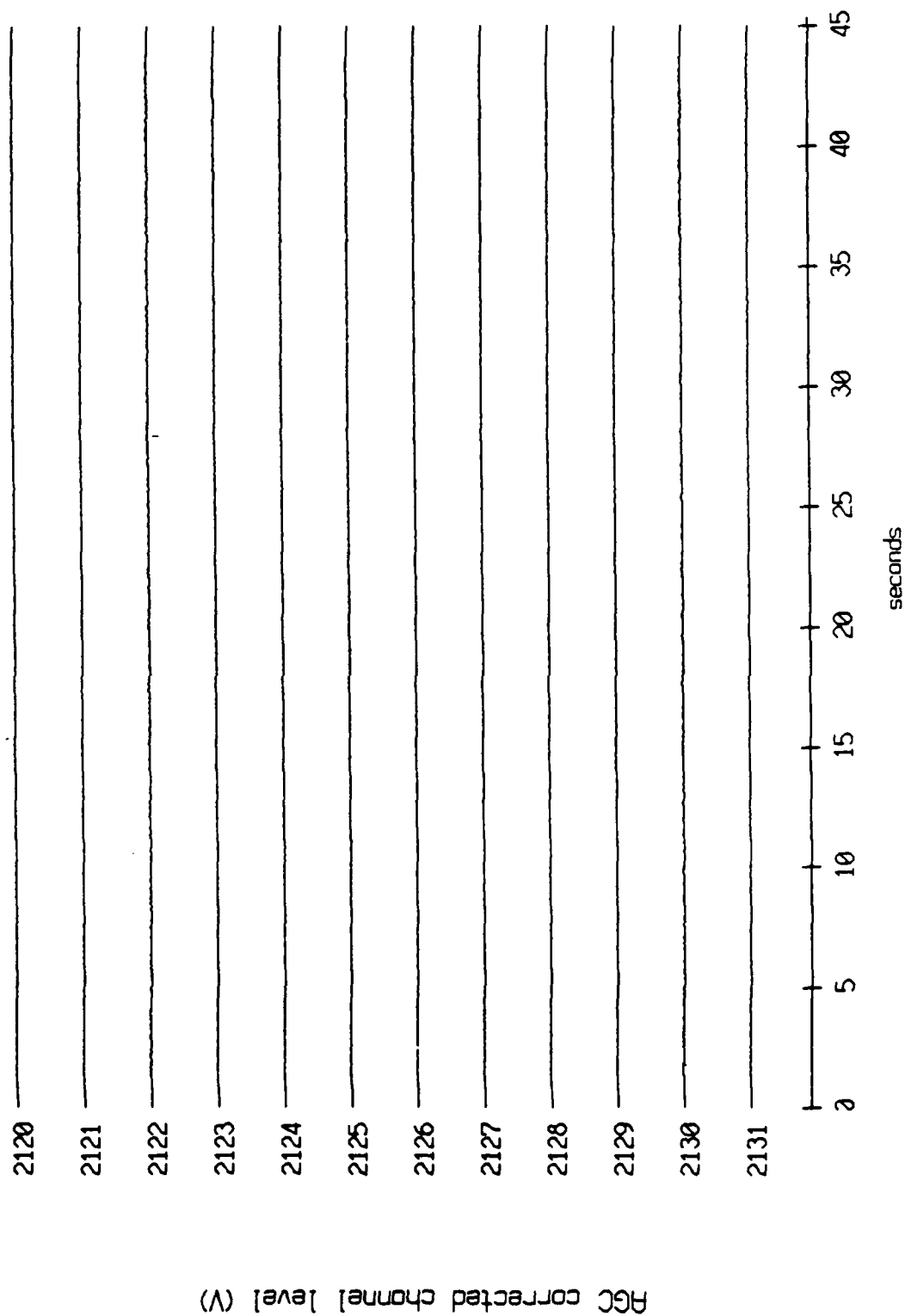


Figure XI.75b

Floot 11, July, 1989 Trip - records 2120-2131 (z-axis)  
vertical axis scale is approx. -2.0 to 2.0 volts

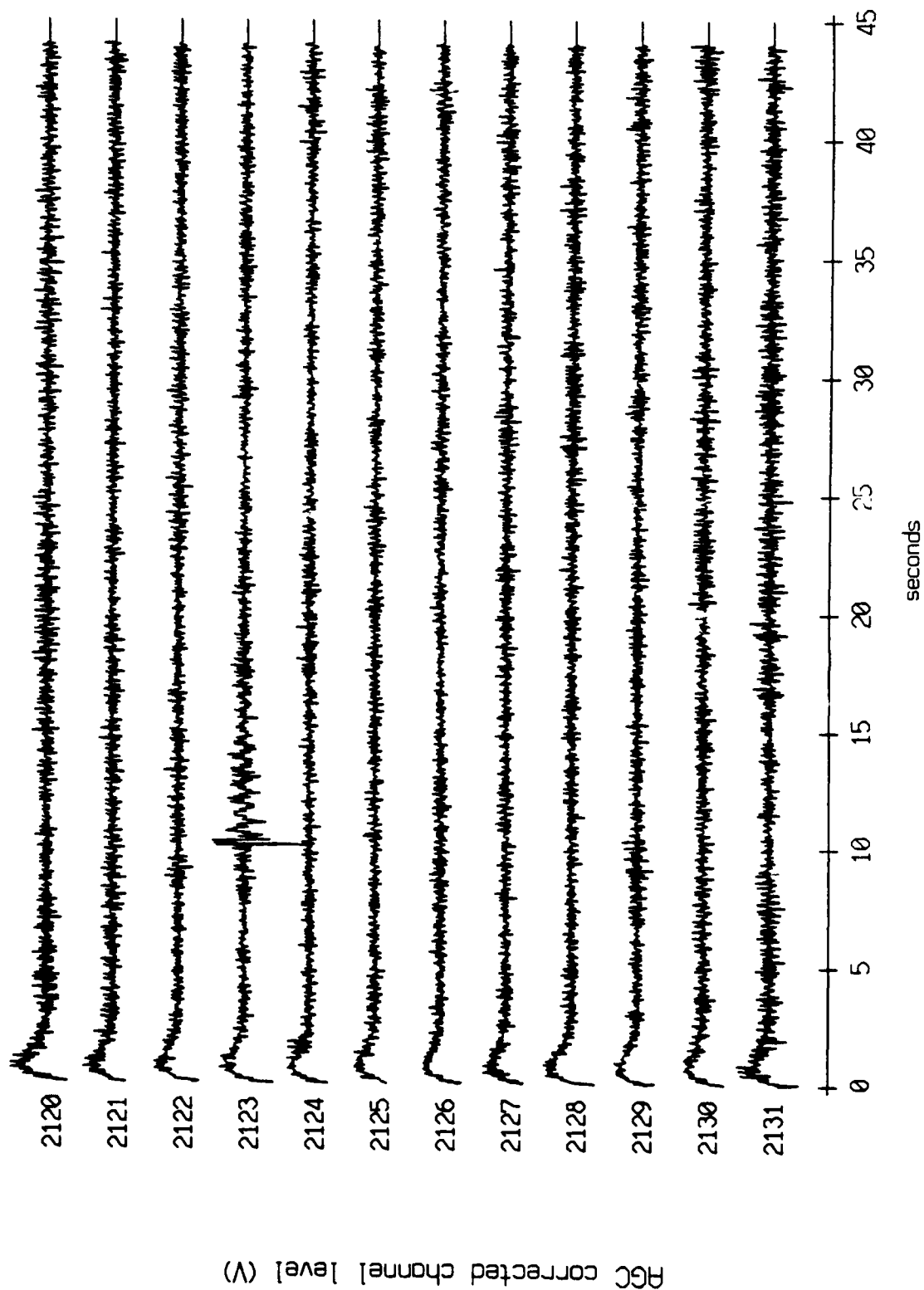
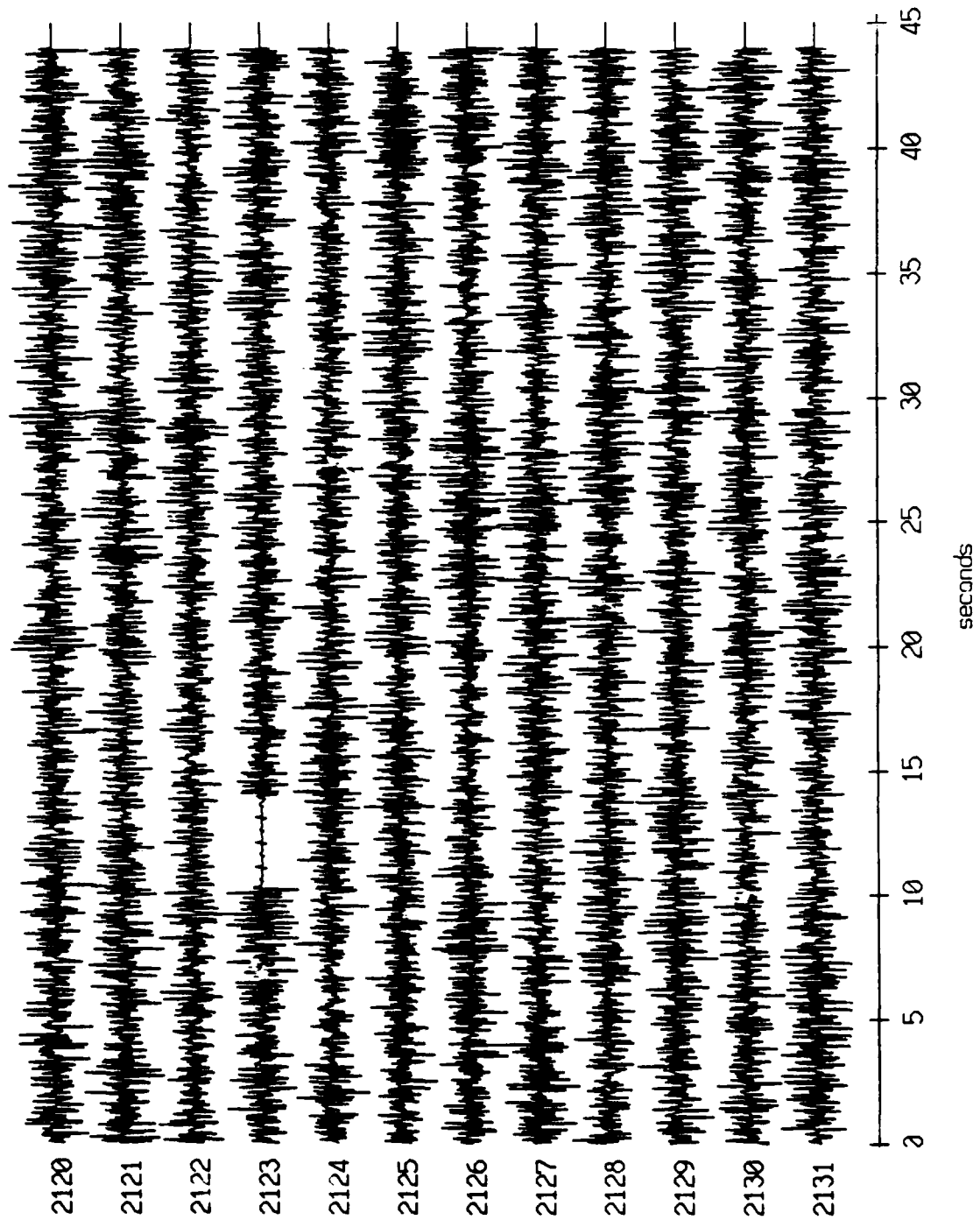


Figure XI.75c

Float 11, July, 1989 Trip - records 2120-2131 (hydrophone)  
vertical axis scale is approx. -2.0 to 2.0 volts

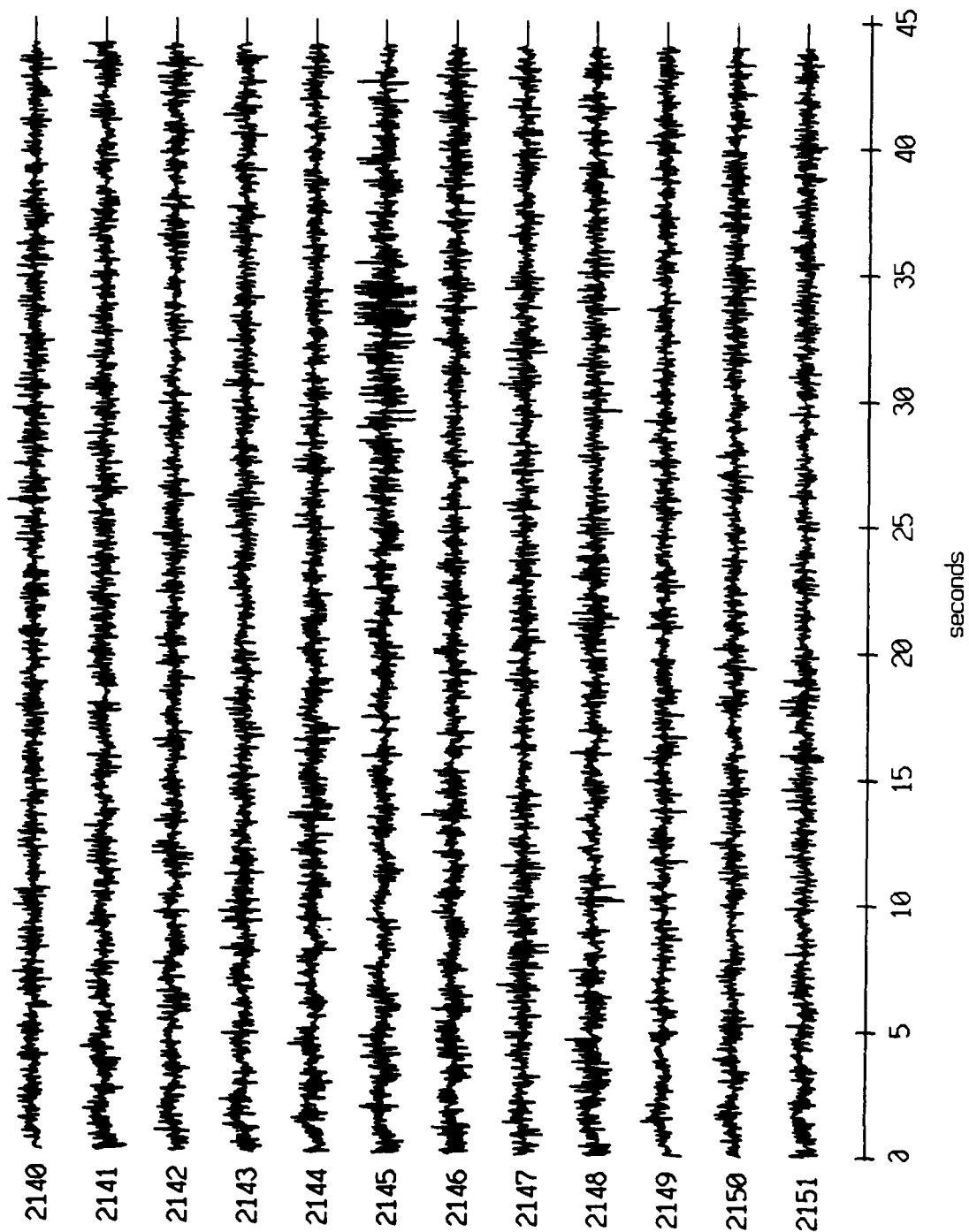


AGC corrected channel level (V)

Figure XI.75d



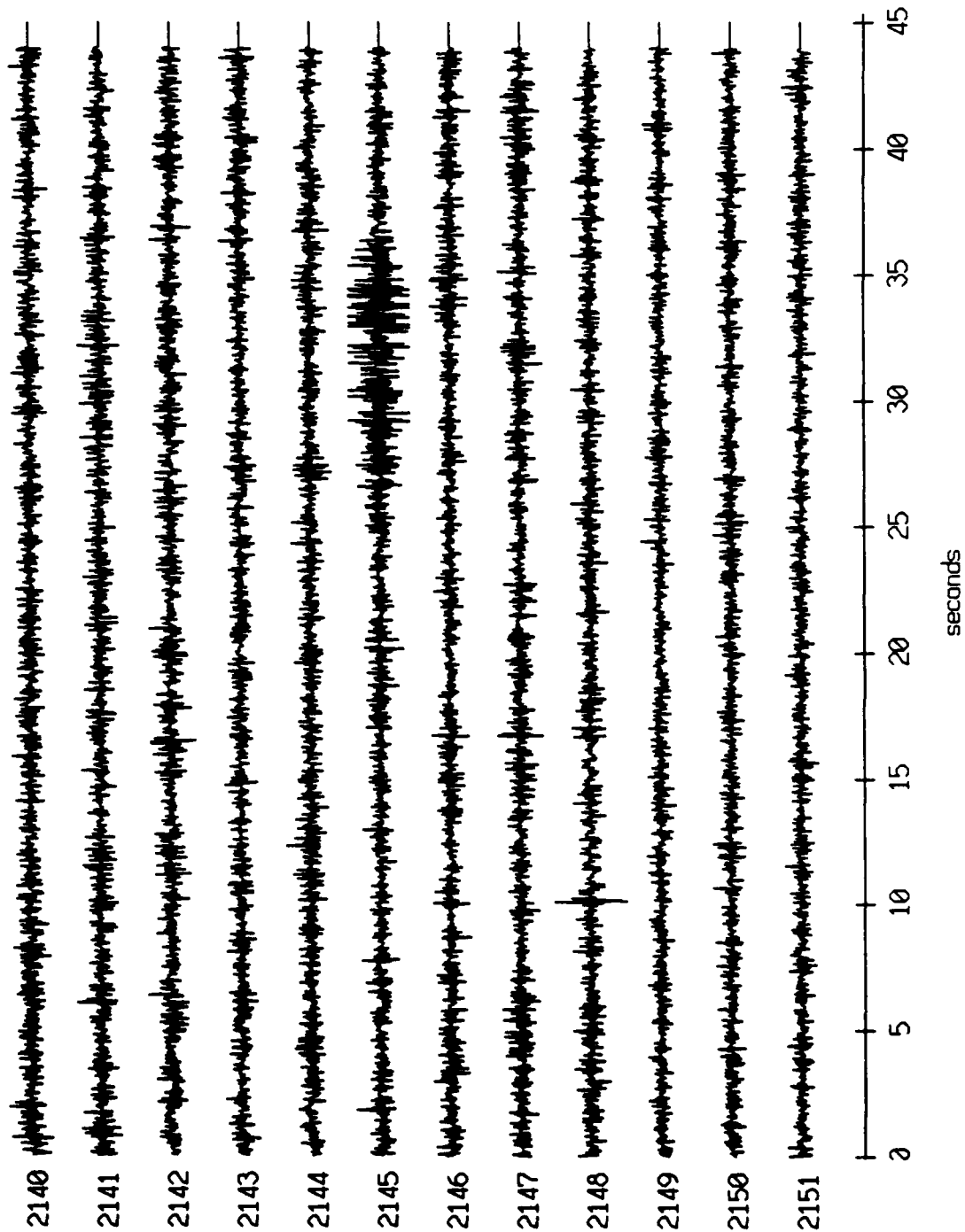
Float 0, July, 1989 Trip - records 2140-2151 (x-axis)  
vertical axis scale is approx. -2.0 to 2.0 volts



AGC corrected channel level (V)

Figure XI.76a

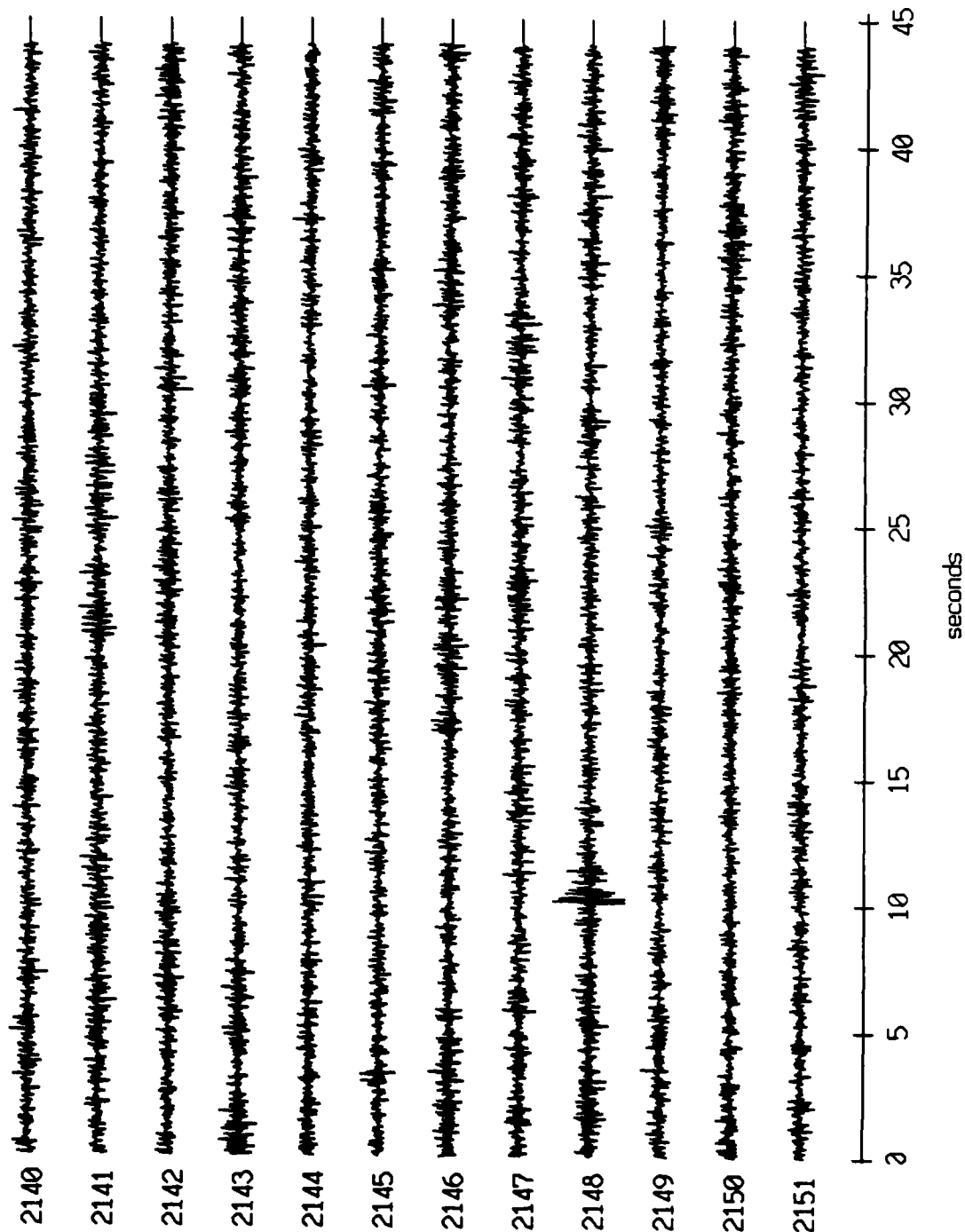
Floot 0, July, 1989 Trip - records 2140-2151 (y-axis)  
vertical axis scale is approx. -2.0 to 2.0 volts



AGC corrected channel level (V)

Figure XI.76b

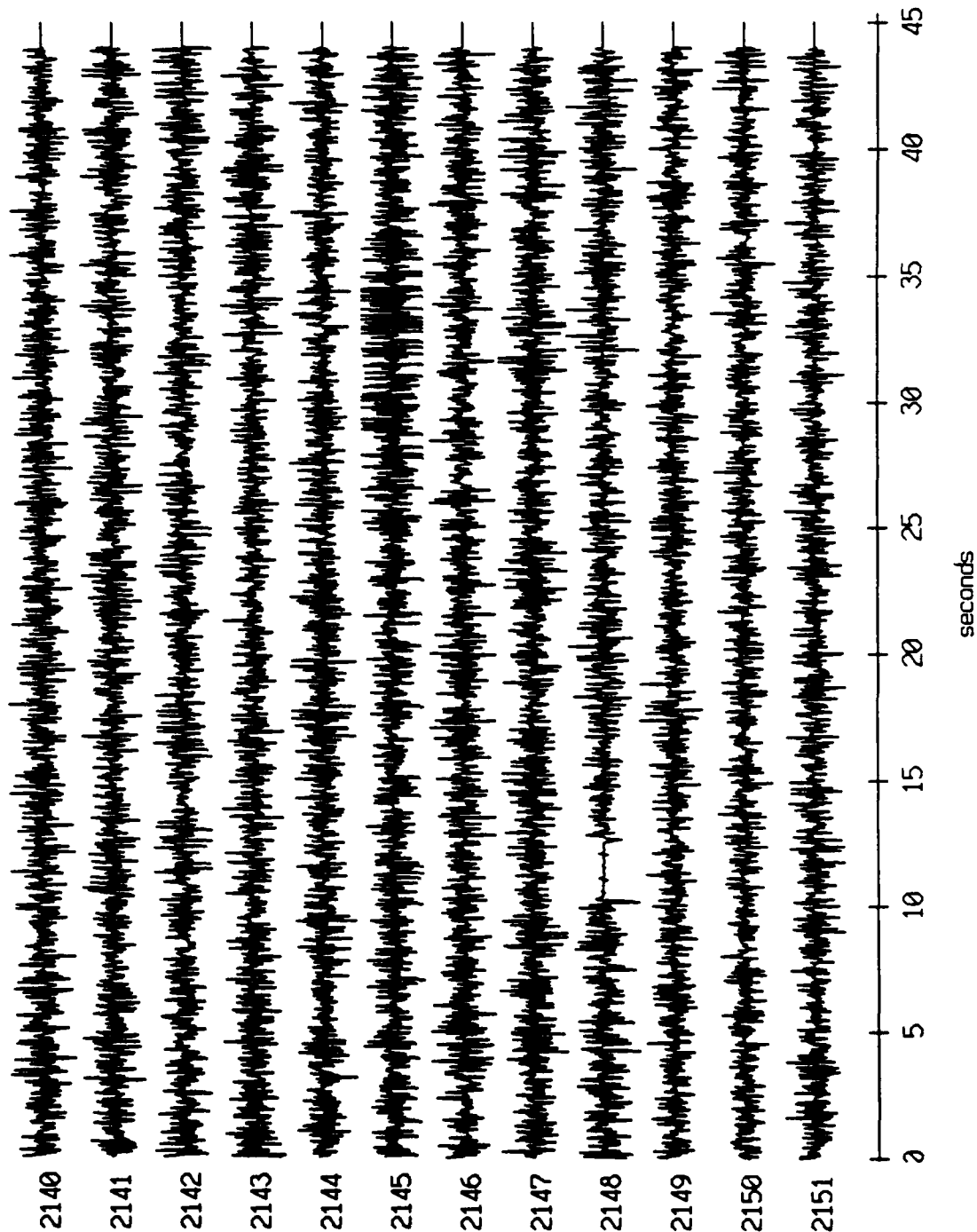
Float 0, July, 1989 Trip - records 2140-2151 (z-axis)  
vertical axis scale is approx. -2.0 to 2.0 volts



AGC corrected channel level (V)

Figure XI.76c

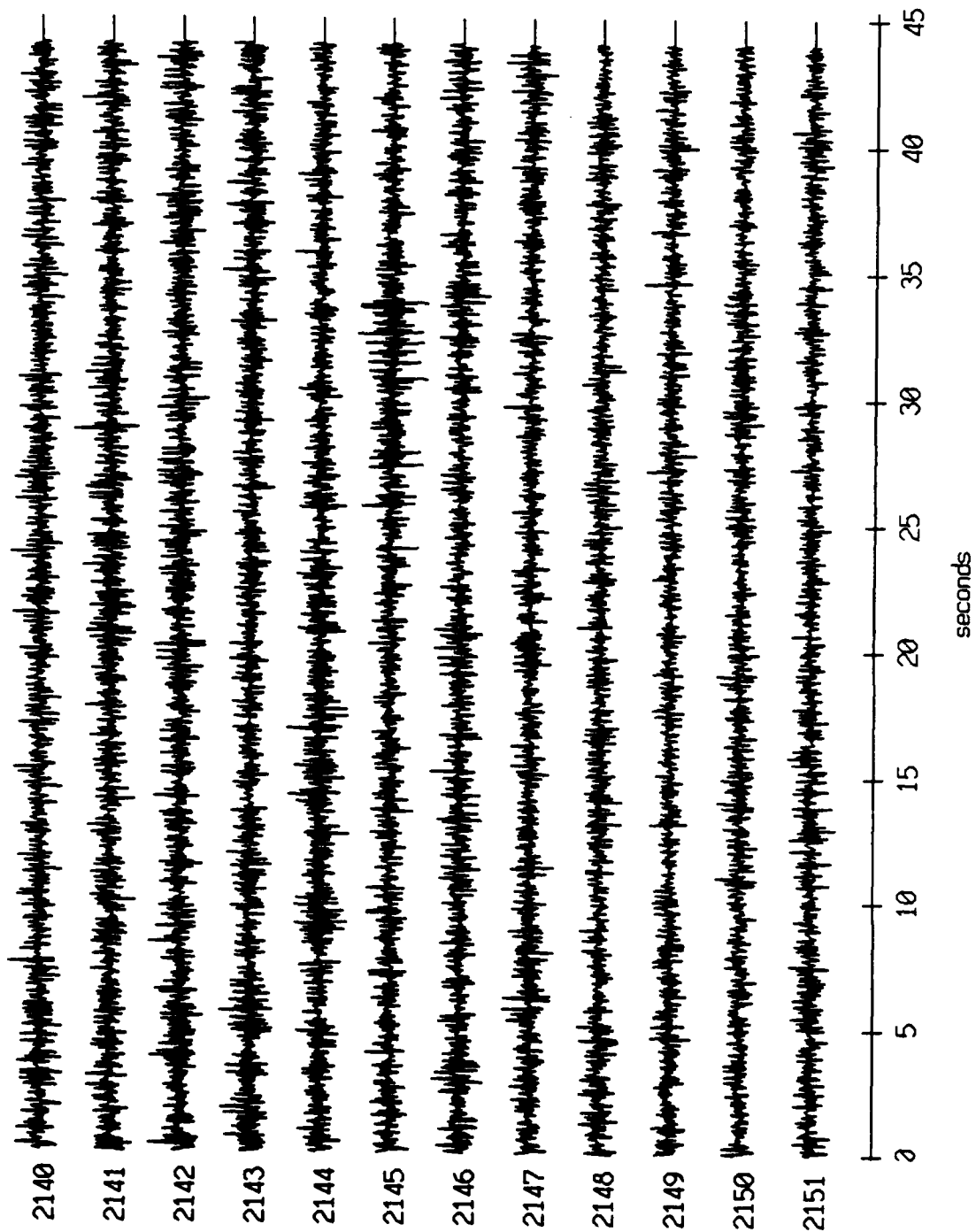
Float 0, July, 1989 Trip - records 2140-2151 (hydrophone)  
vertical axis scale is approx. -2.0 to 2.0 volts



RGC corrected channel level (V)

Figure XI.76d

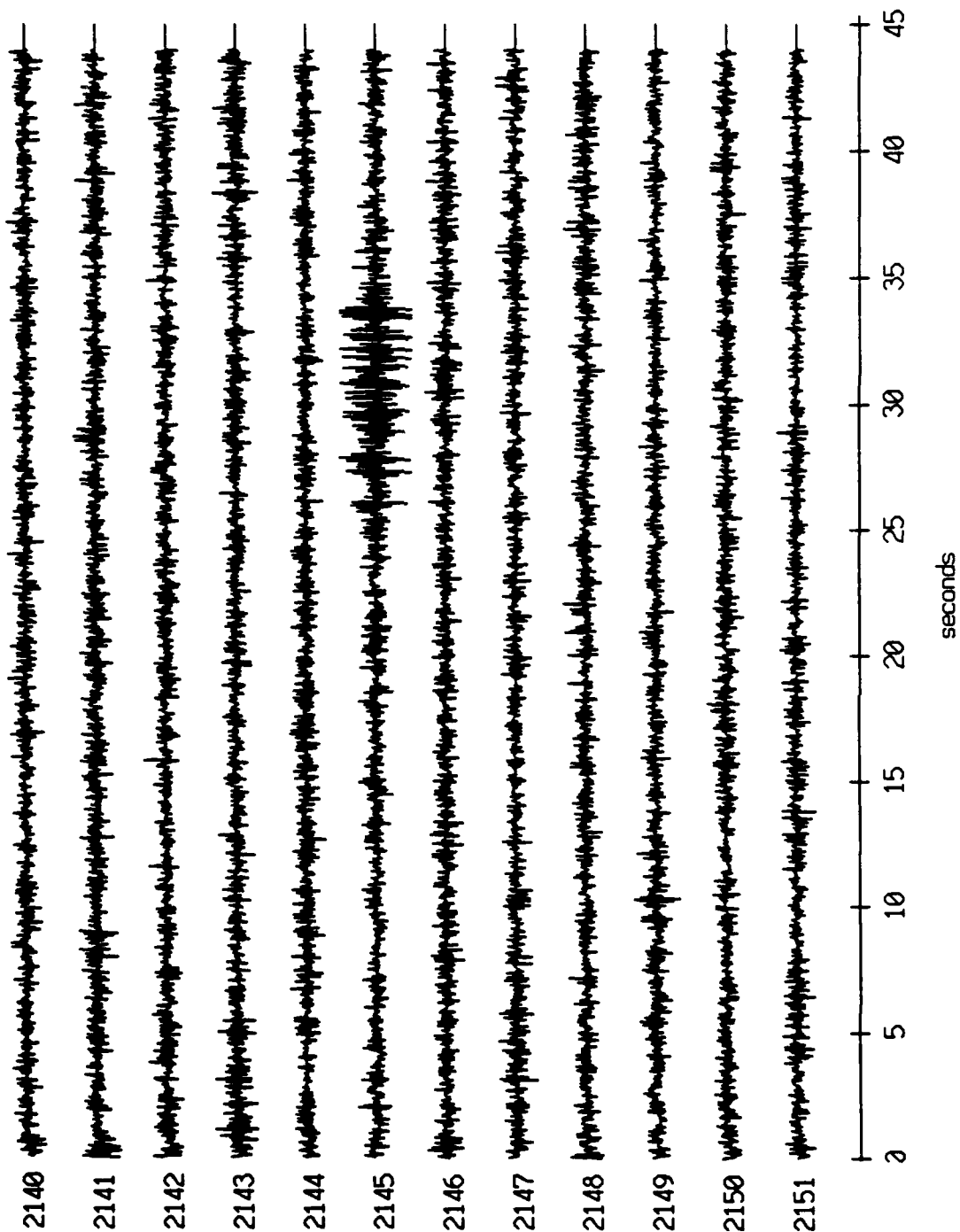
Float 1, July, 1989 Trip - records 2140-2151 (x-axis)  
vertical axis scale is approx. -2.0 to 2.0 volts



PGC corrected channel level (V)

Figure XI.77a

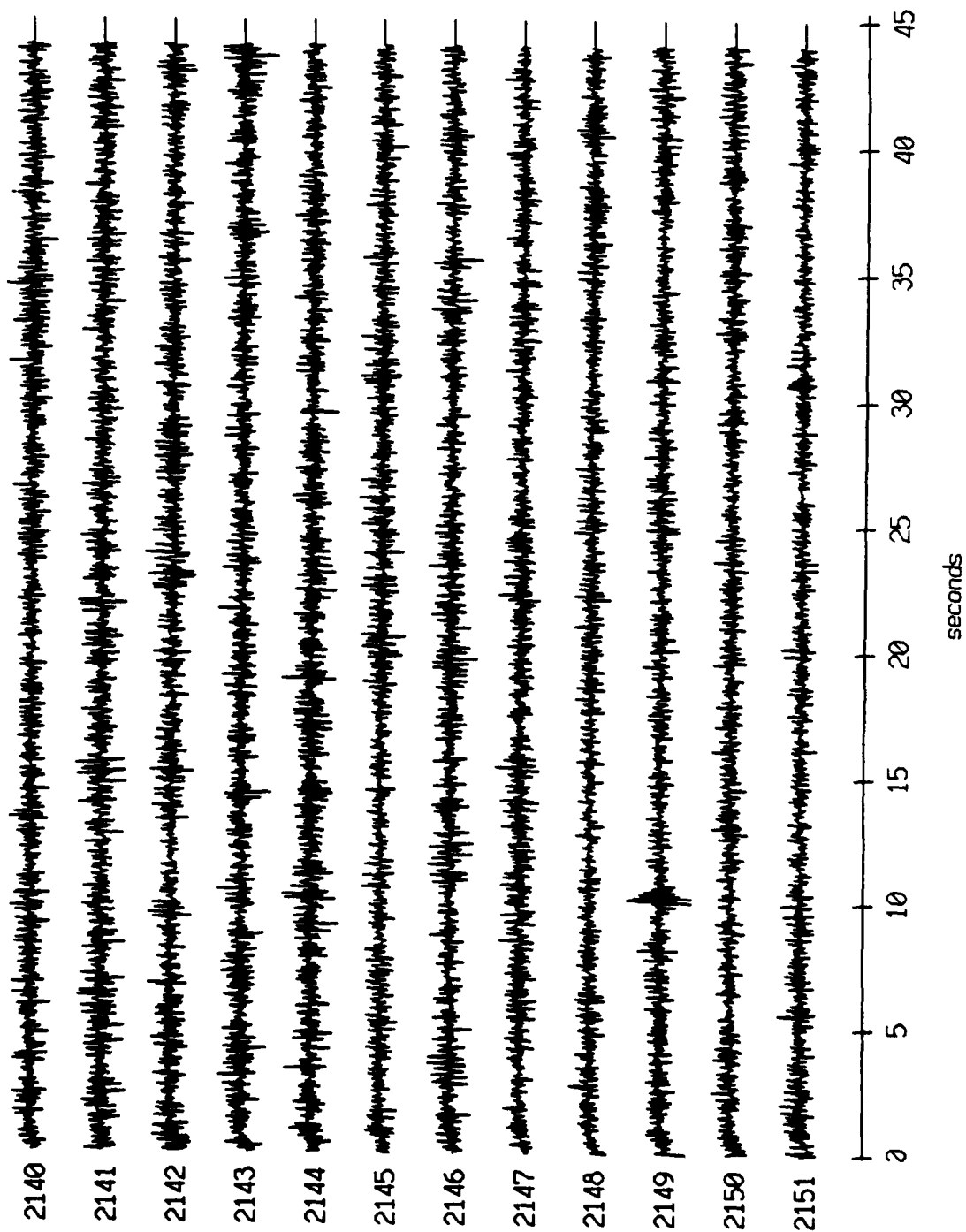
Float 1, July, 1989 Trip - records 2140-2151 (y-axis)  
vertical axis scale is approx. -2.0 to 2.0 volts



RGC corrected channel level (V)

Figure XI.77b

Float 1, July, 1989 Trip - records 2140-2151 (z-axis)  
vertical axis scale is approx. -2.0 to 2.0 volts



PGC corrected channel level (V)

Figure XI.77c

Float 1, July, 1989 Trip - records 2140-2151 (hydrophone)  
vertical axis scale is approx. -2.0 to 2.0 volts

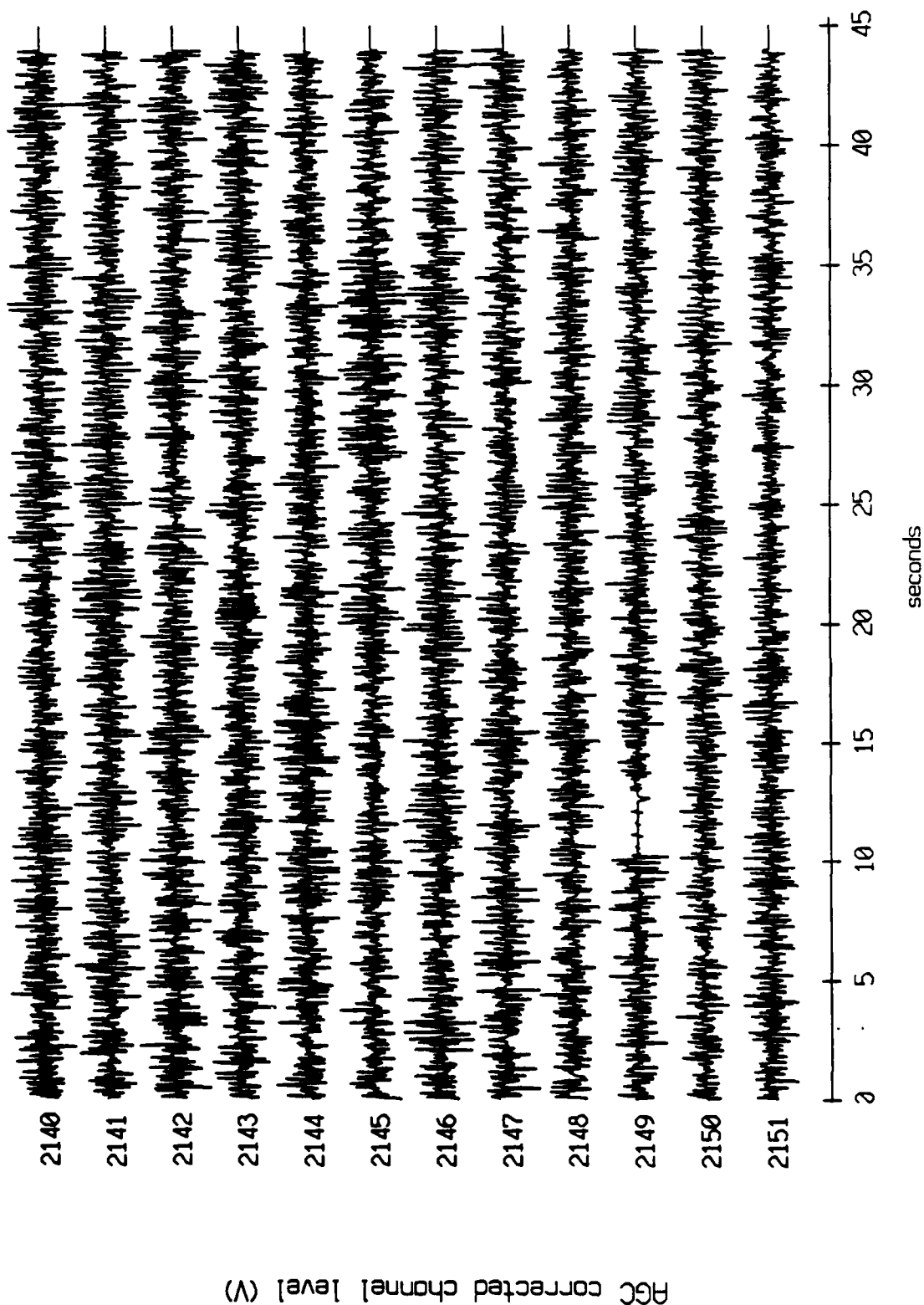
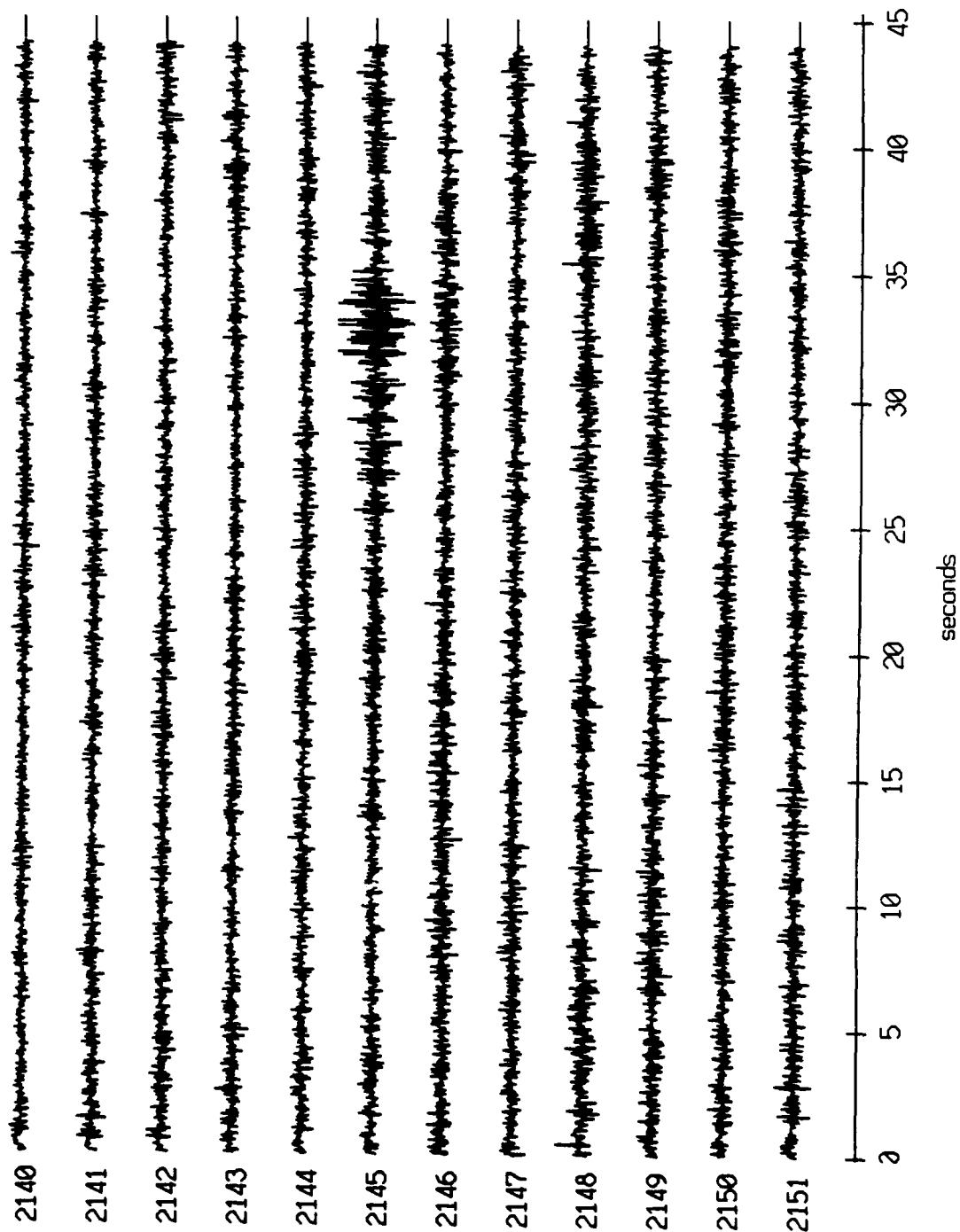


Figure XL77d



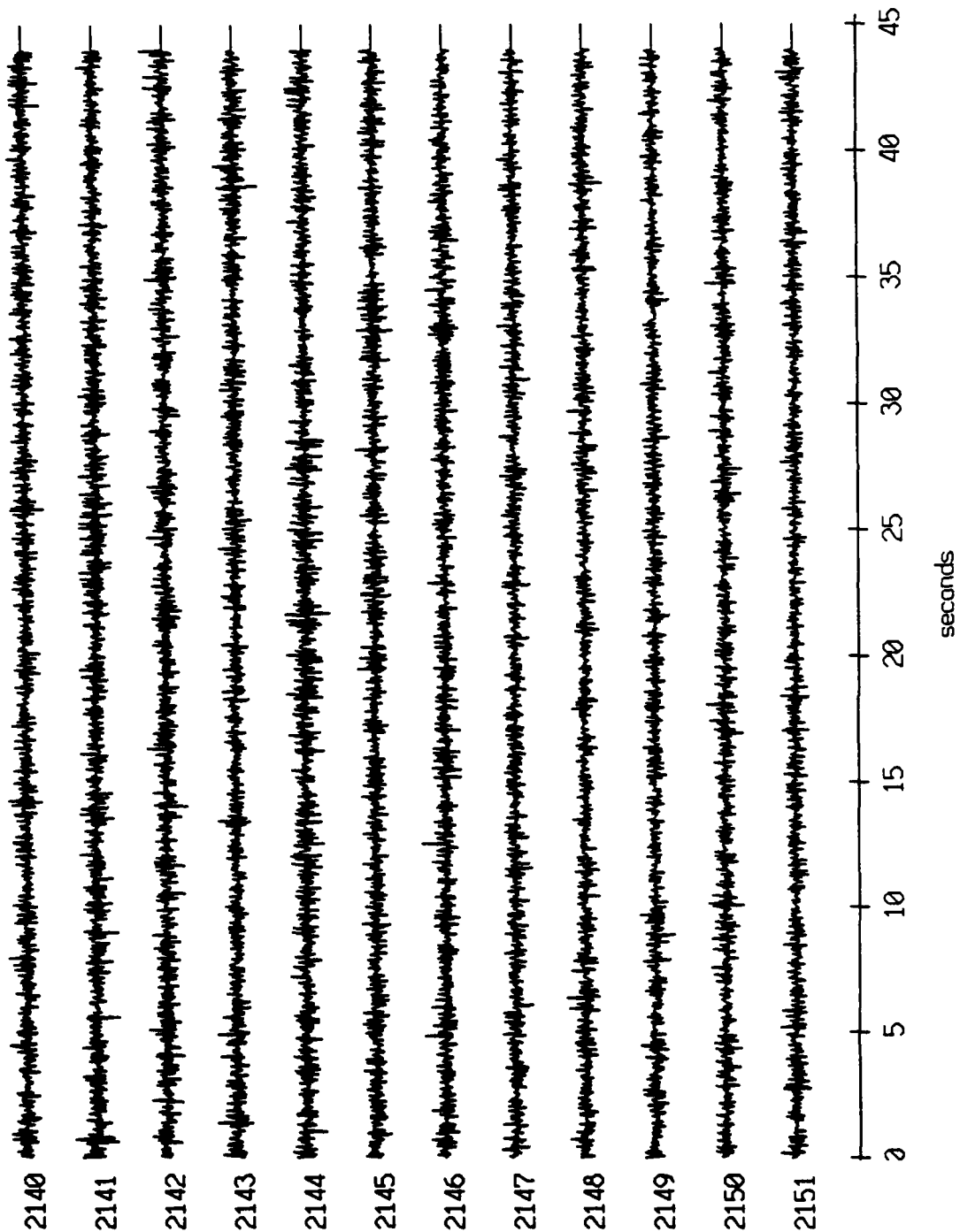
Float 2, July, 1989 Trip - records 2140-2151 (x-axis)  
vertical axis scale is approx. -2.0 to 2.0 volts



AGC corrected channel level (V)

Figure XI.78a

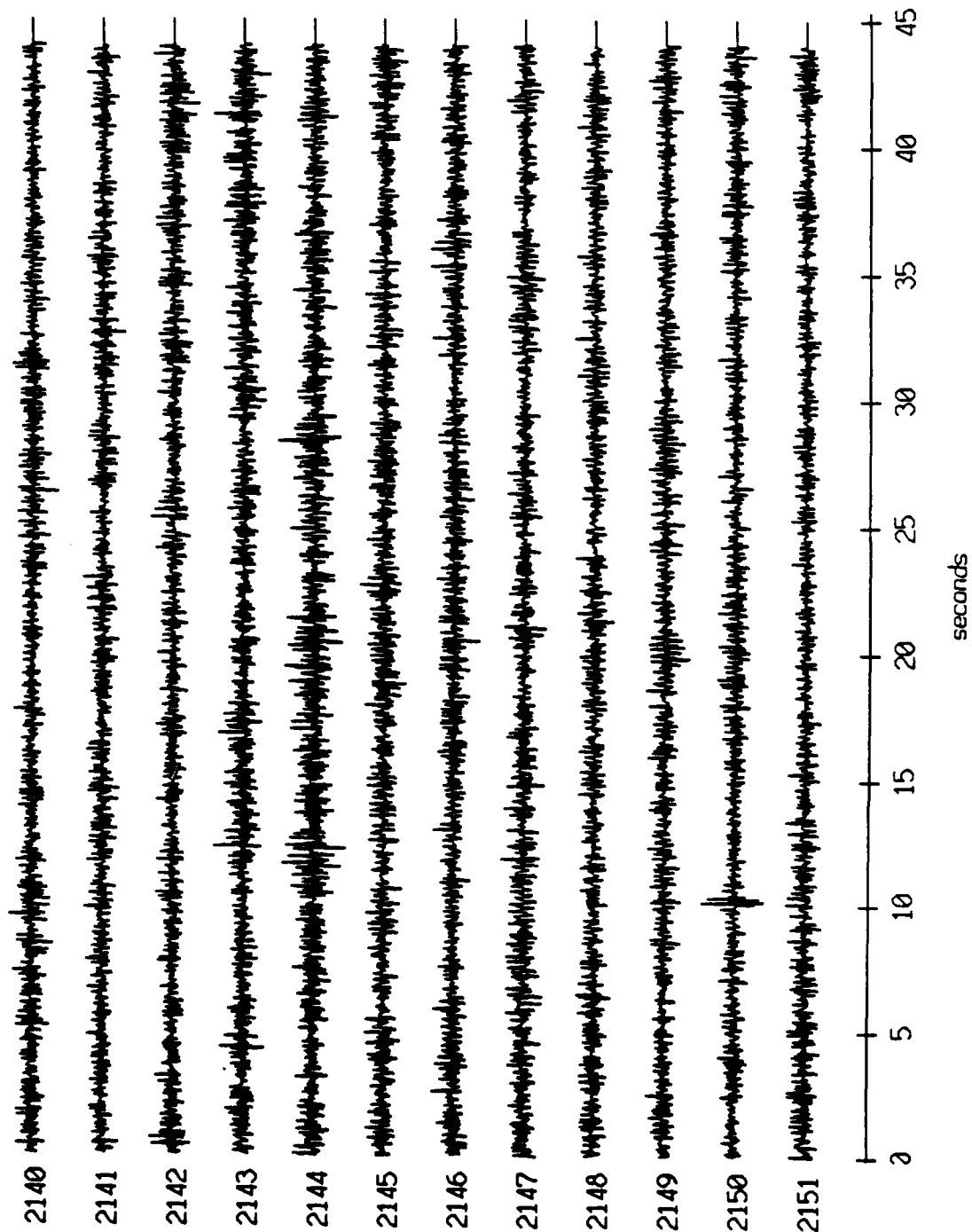
Float 2, July, 1989 Trip - records 2140-2151 (y-axis)  
vertical axis scale is approx. -2.0 to 2.0 volts



AGC corrected channel level (V)

Figure XI.78b

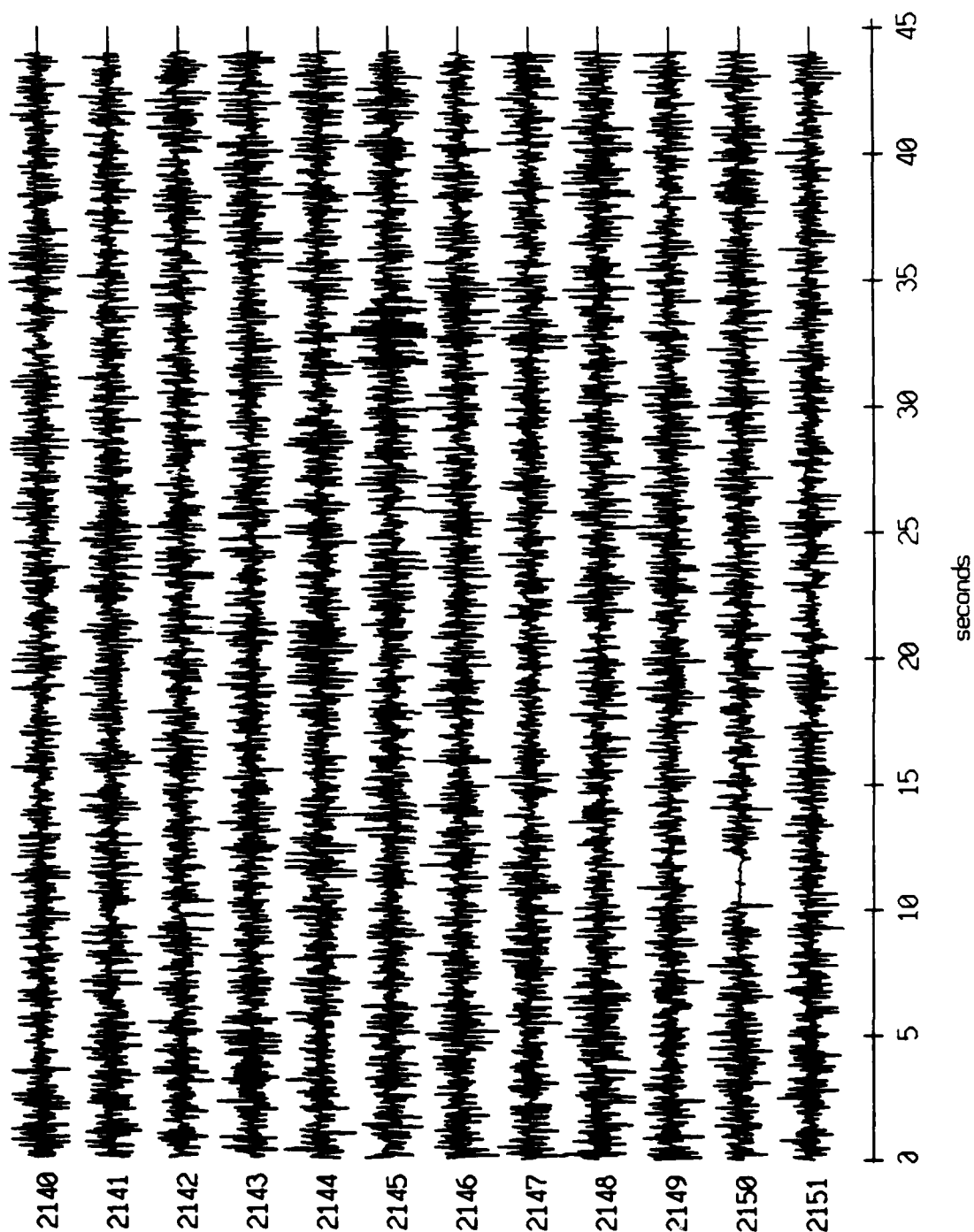
Float 2, July, 1989 Trip - records 2140-2151 (z-axis)  
vertical axis scale is approx. -2.0 to 2.0 volts



PGC corrected channel level (V)

Figure XI.78c

Float 2, July, 1989 Trip - records 2140-2151 (hydrophone)  
vertical axis scale is approx. -2.0 to 2.0 volts



AGC corrected channel level (V)

Figure XI.78d

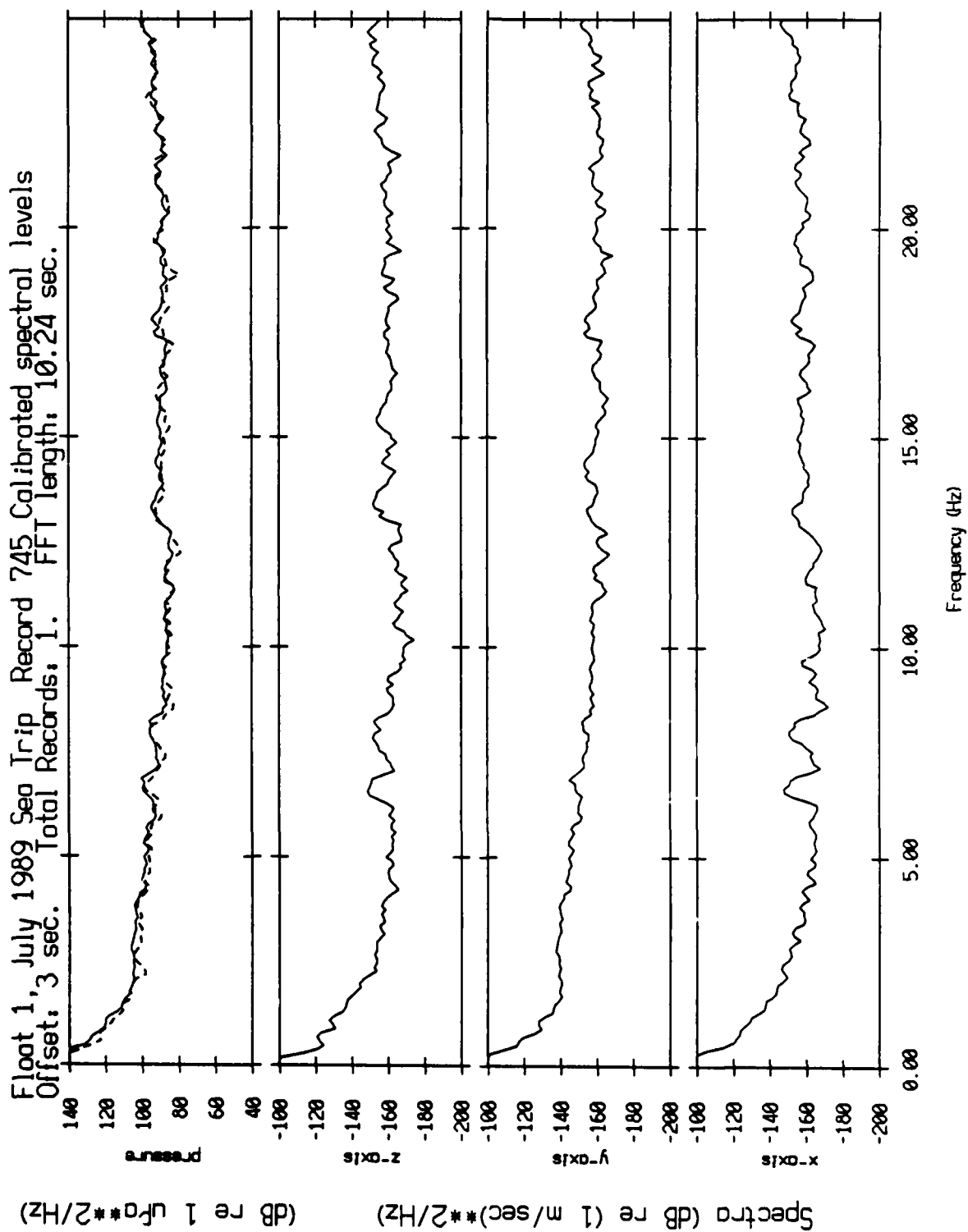


Figure XII.1a

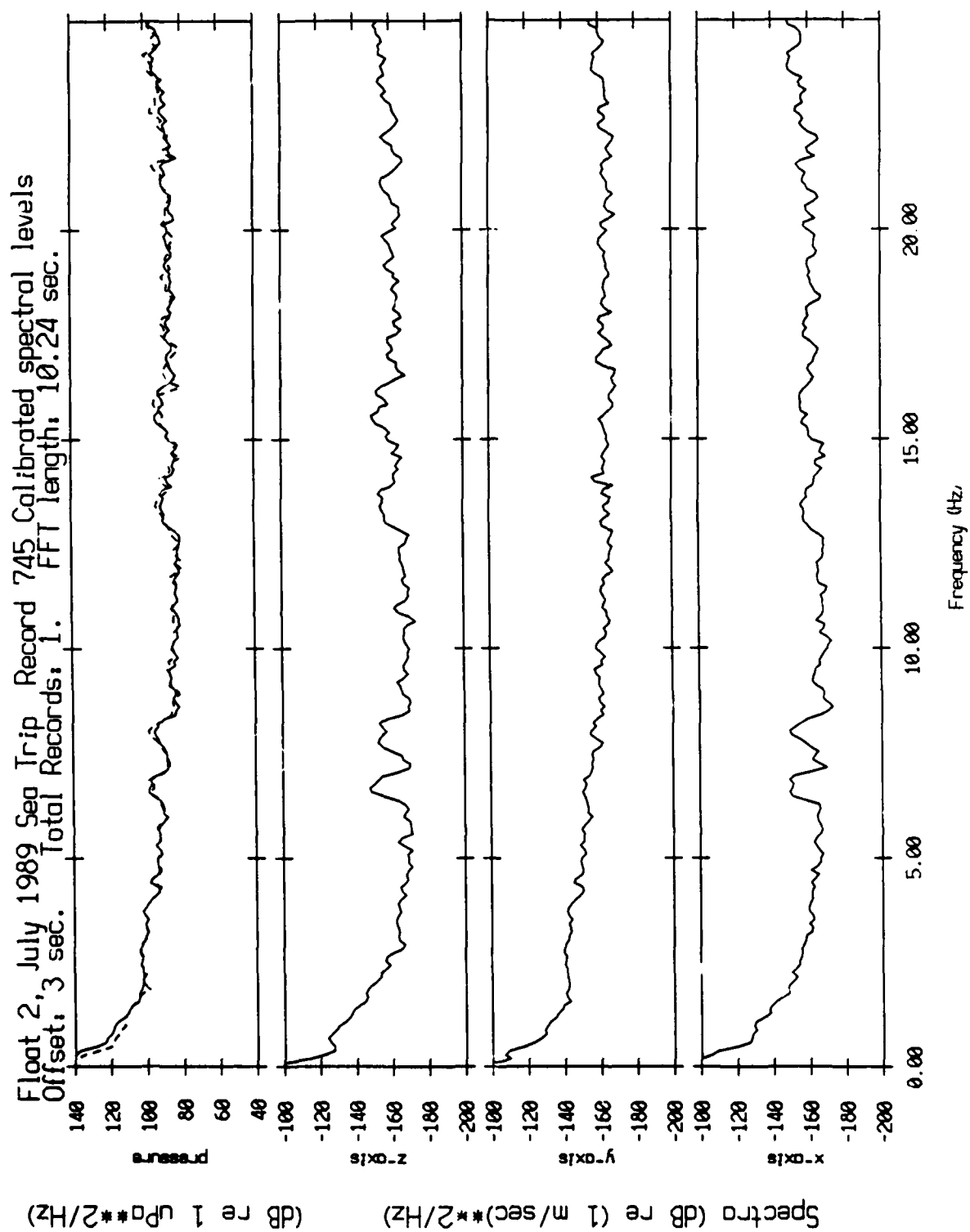


Figure XII.1b

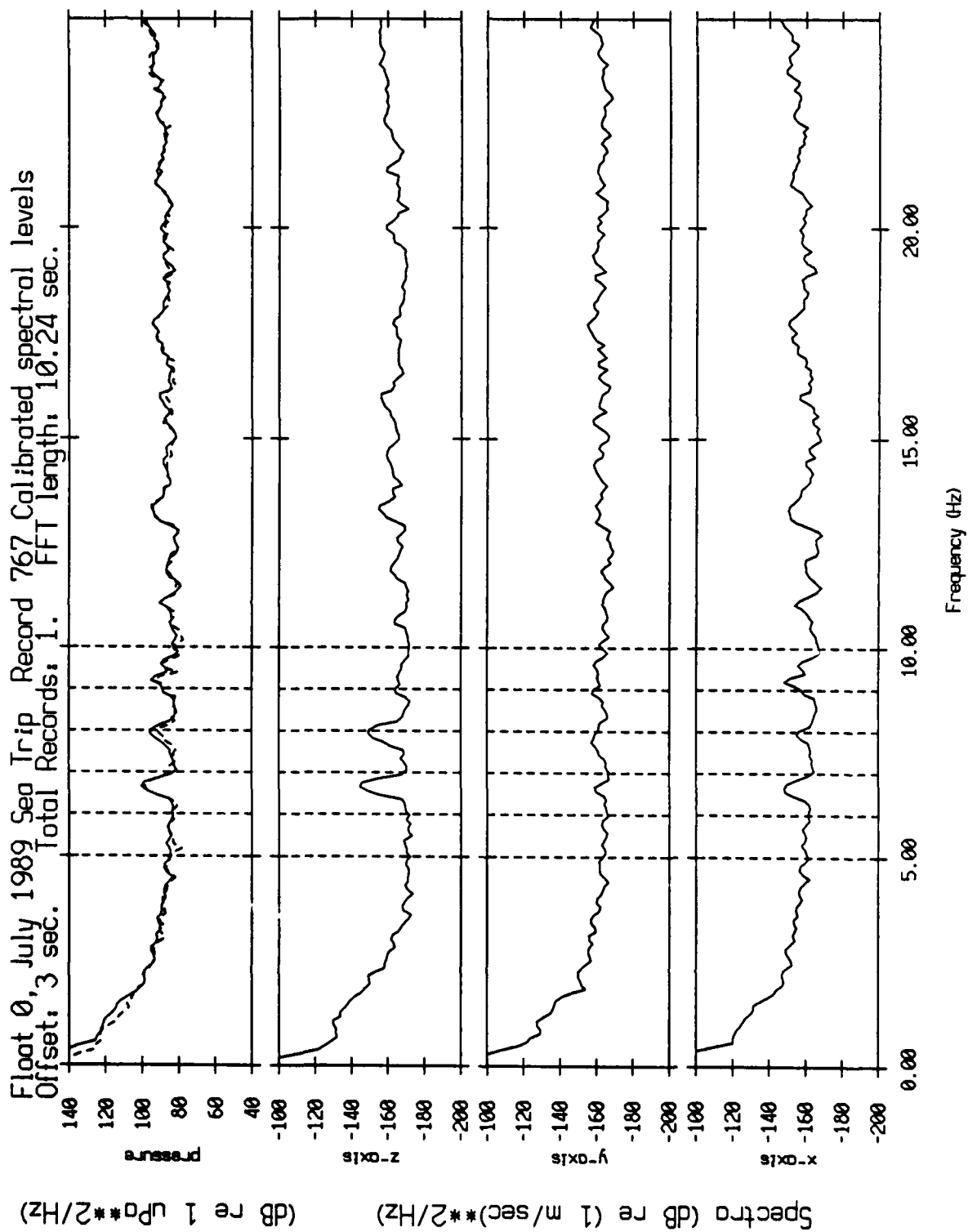


Figure XII.2a

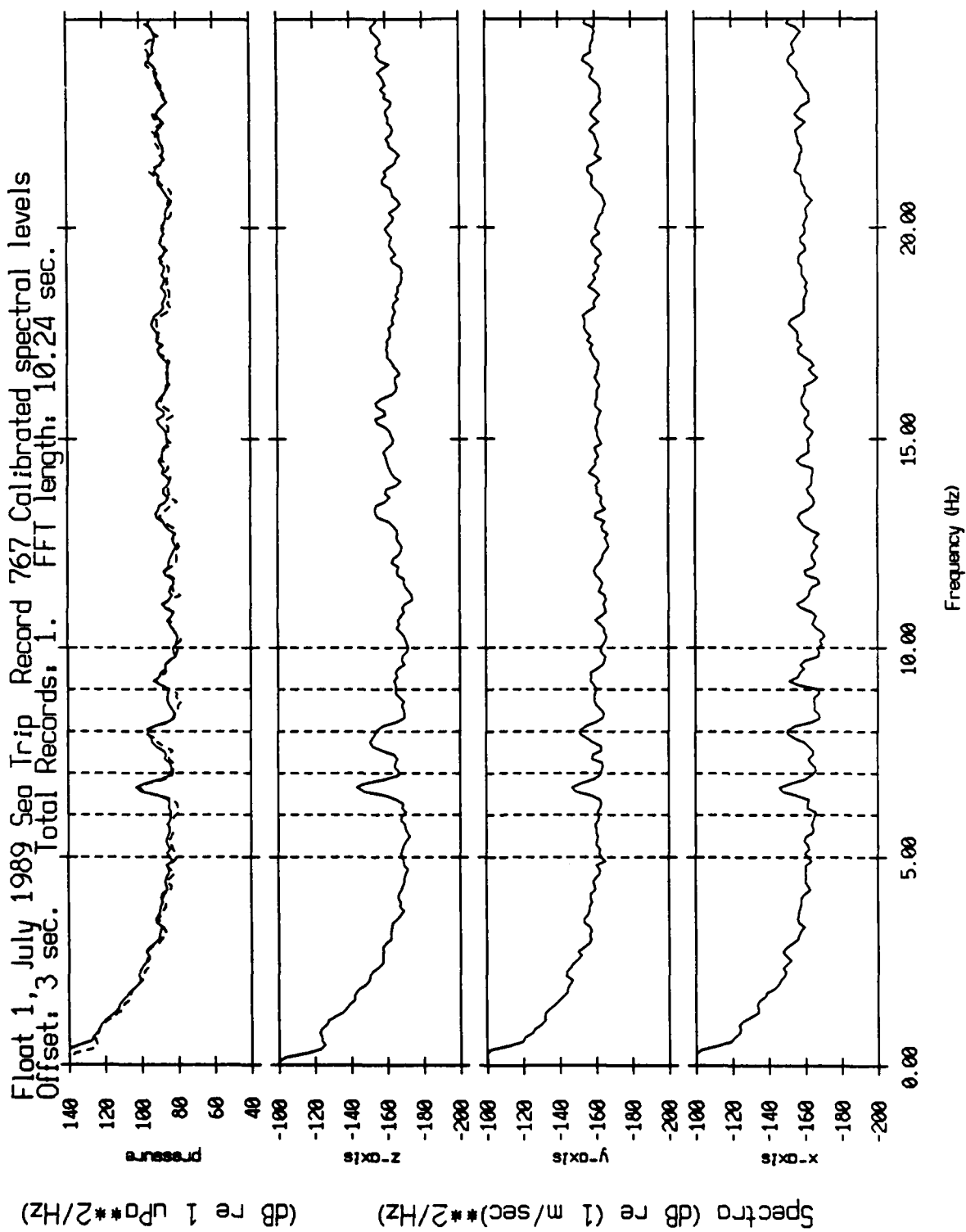


Figure XII.2b



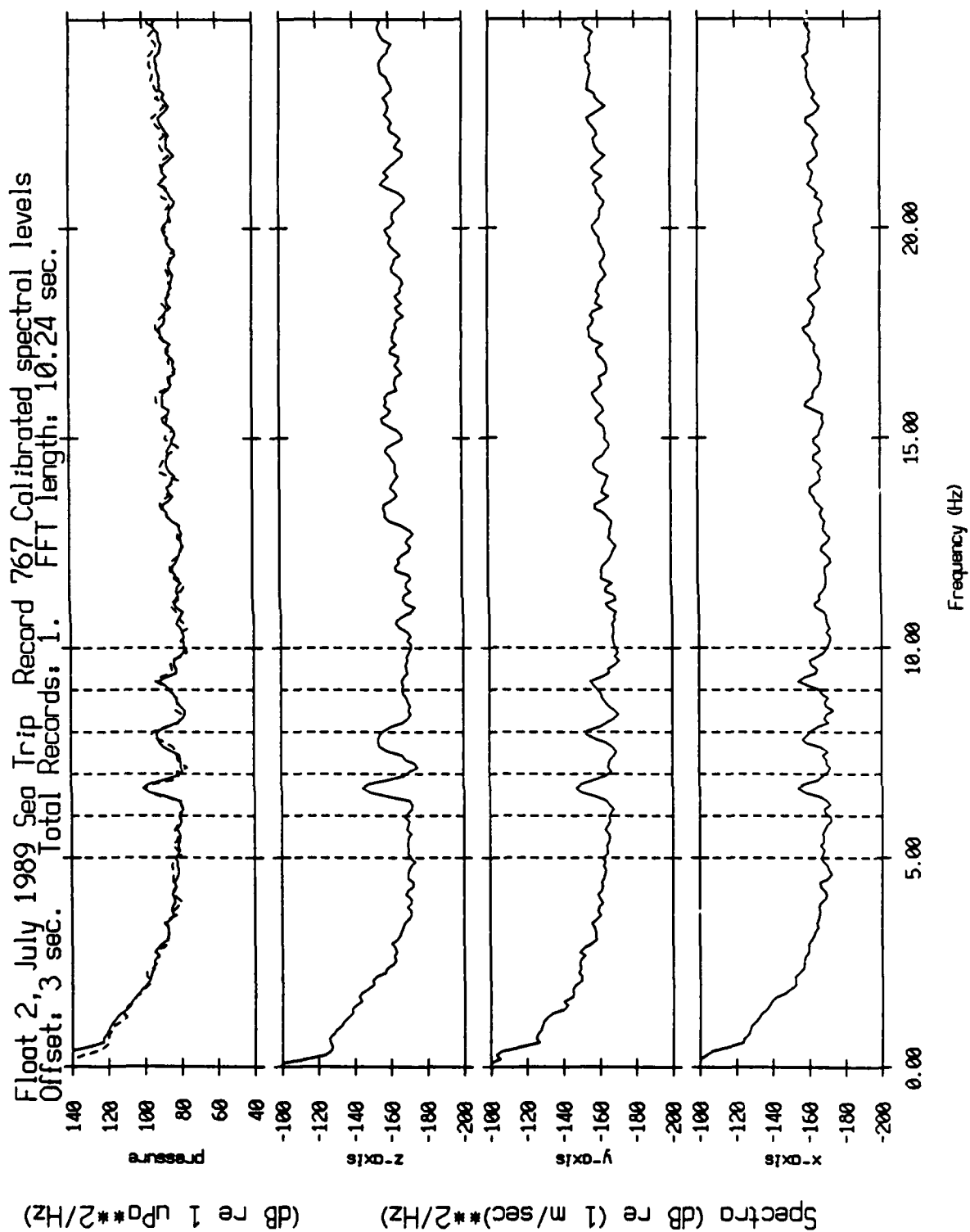


Figure XII.2c

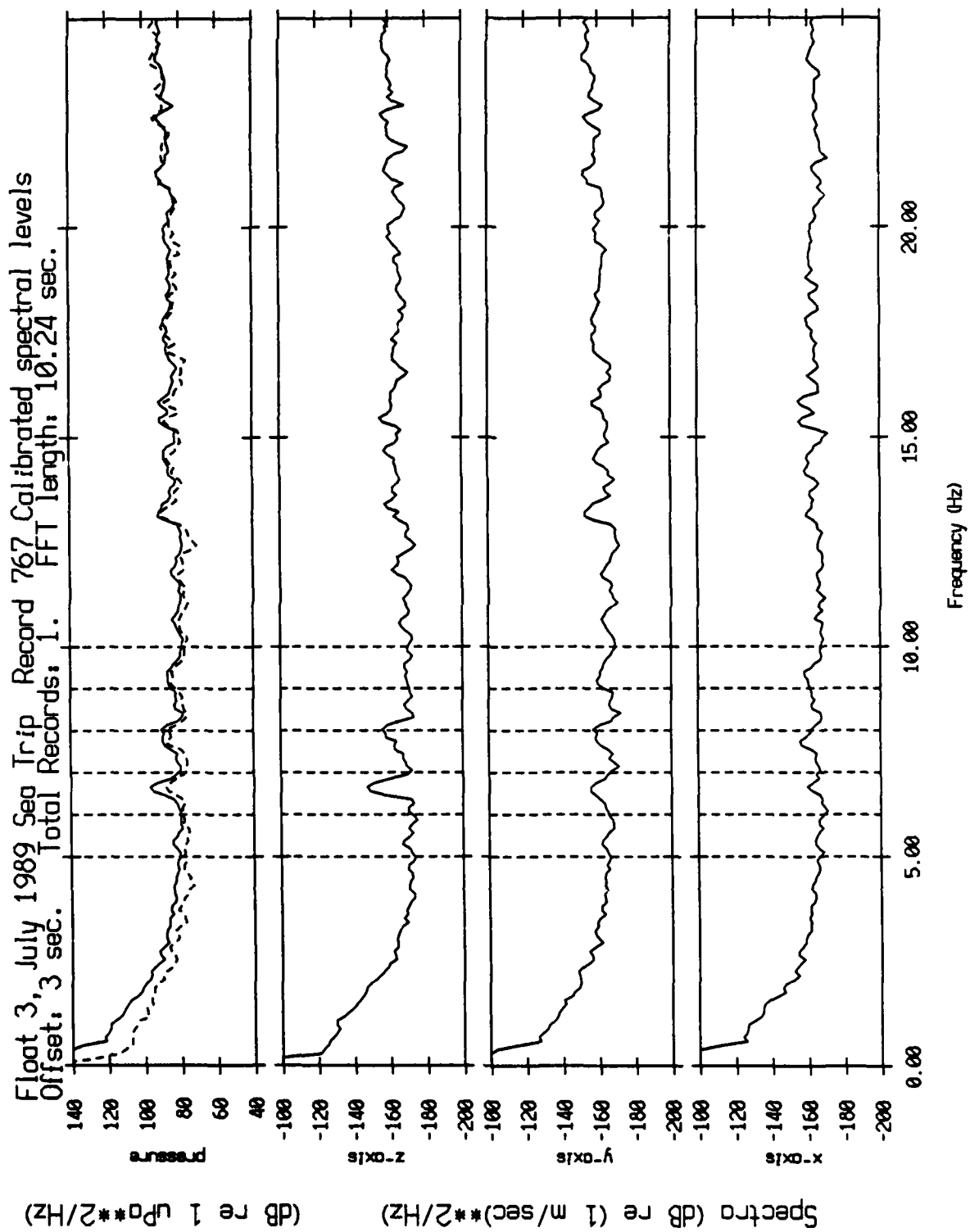


Figure XII.2d

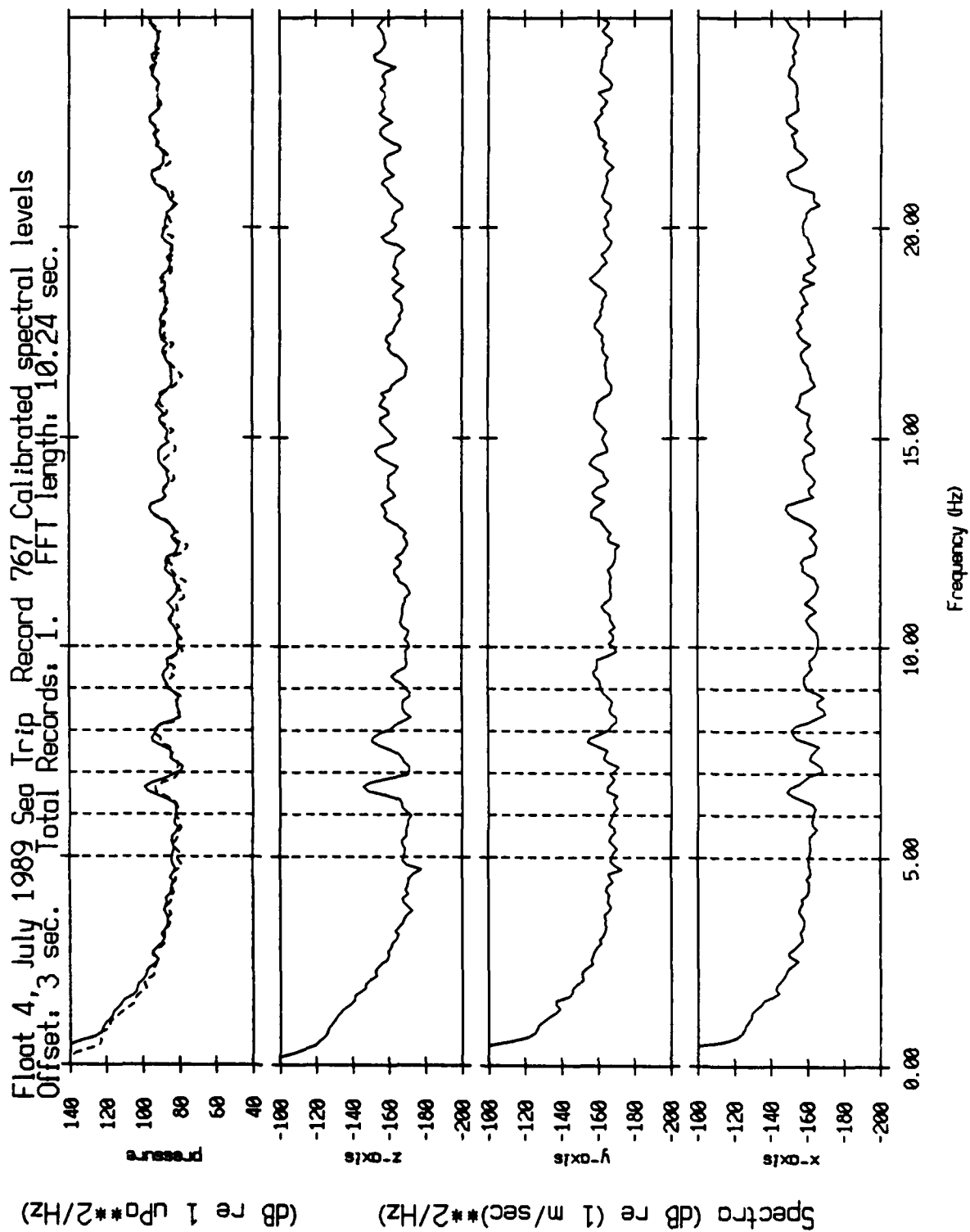


Figure XII.2e

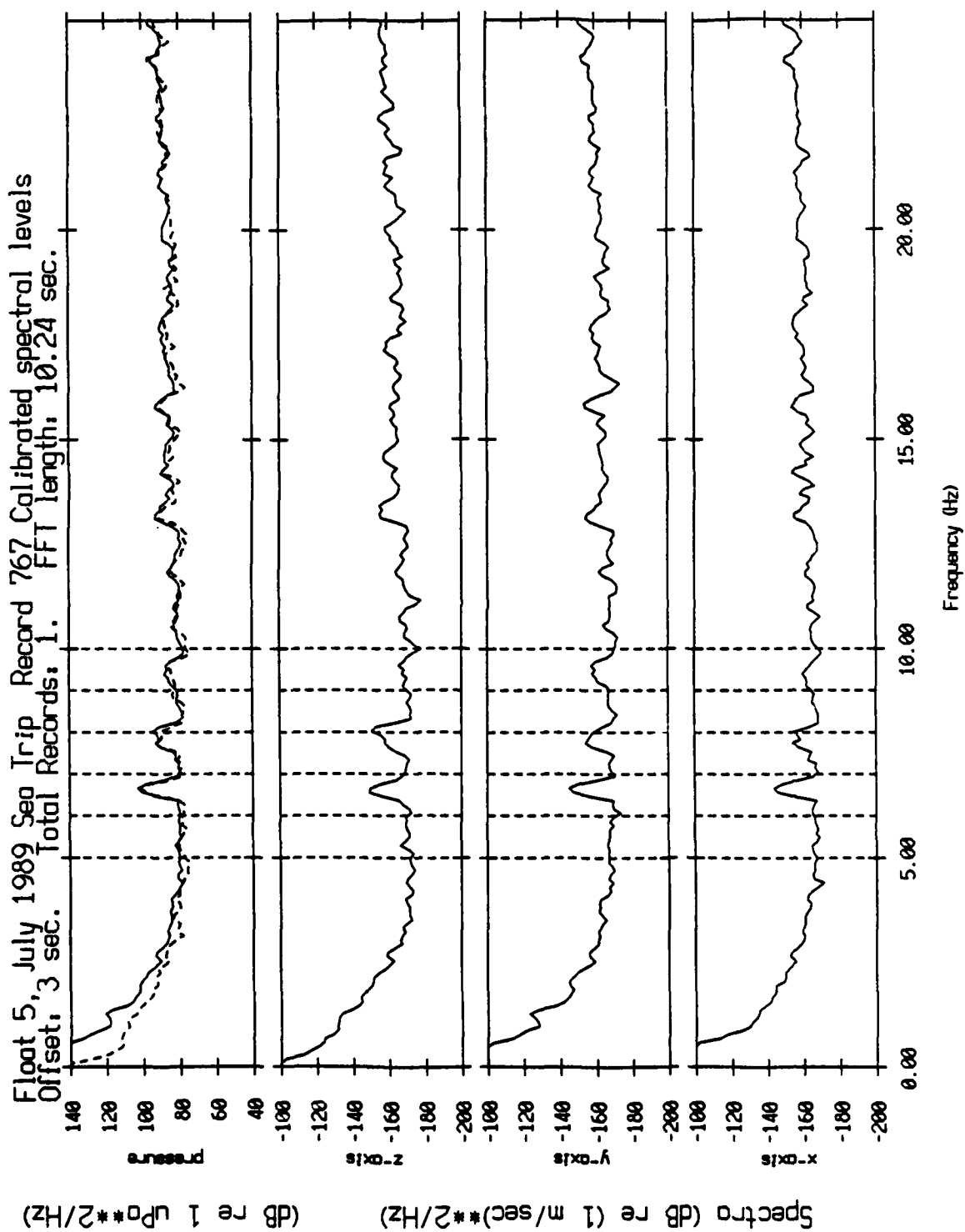


Figure XII.2f

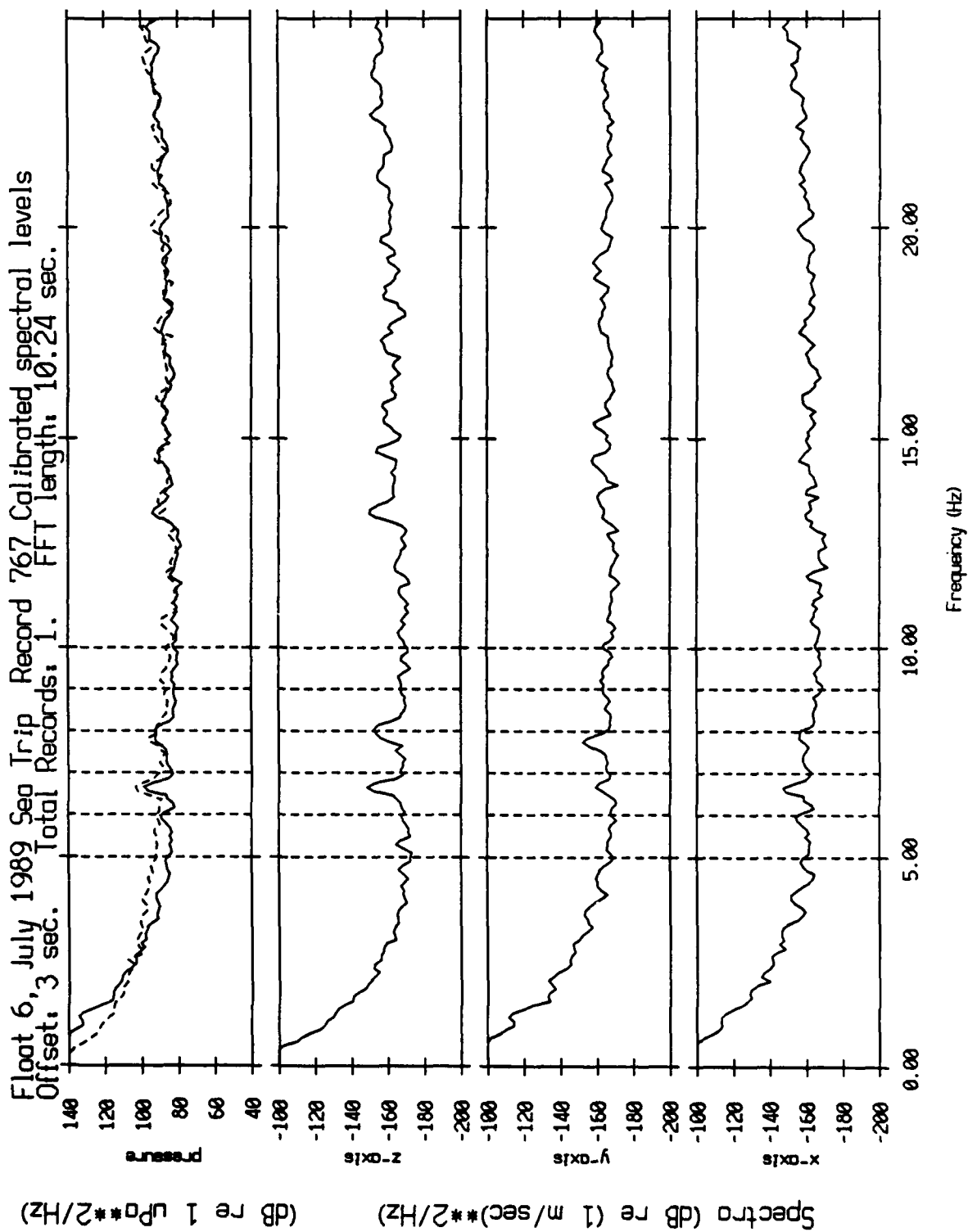


Figure XII.2g

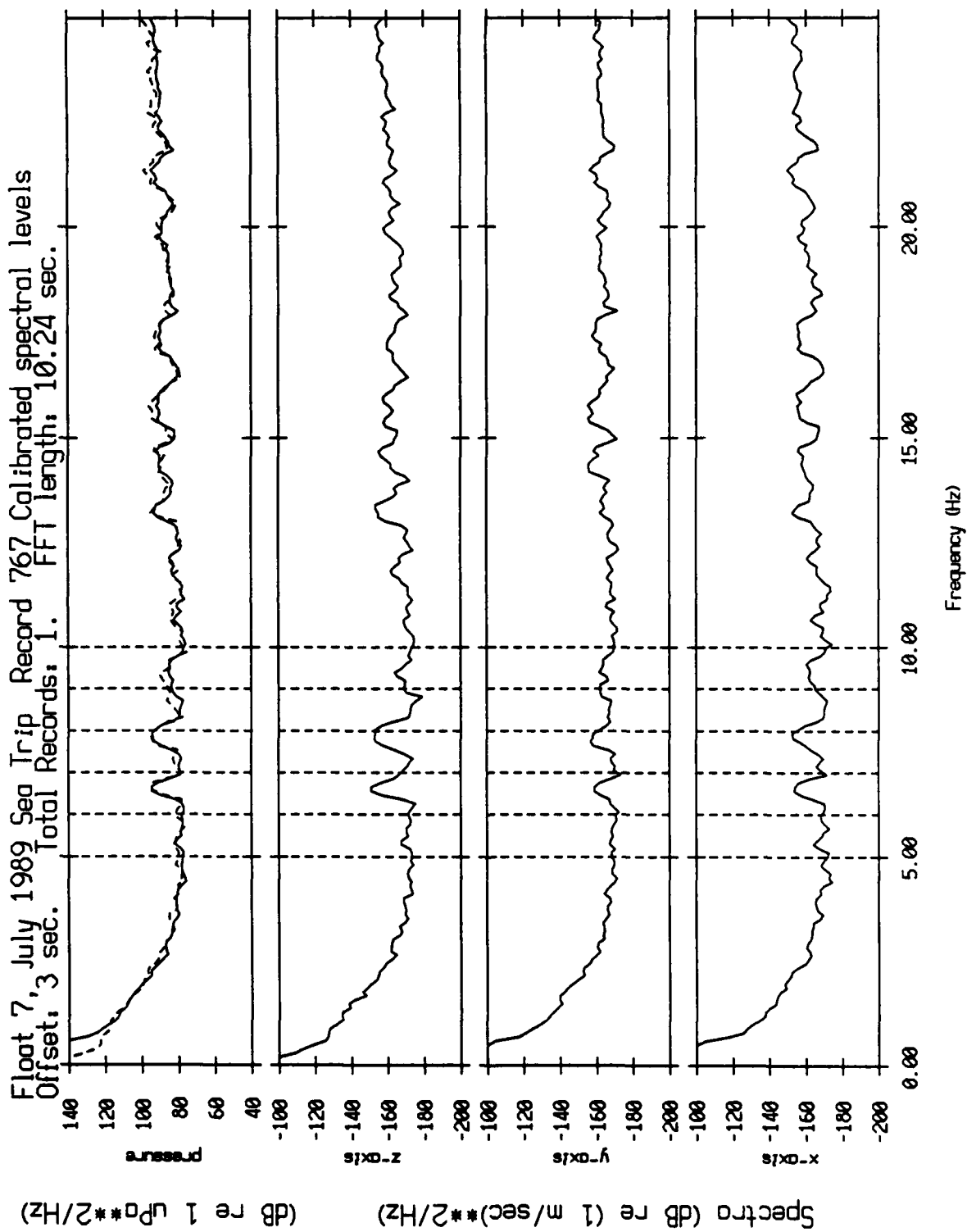


Figure XII.2h

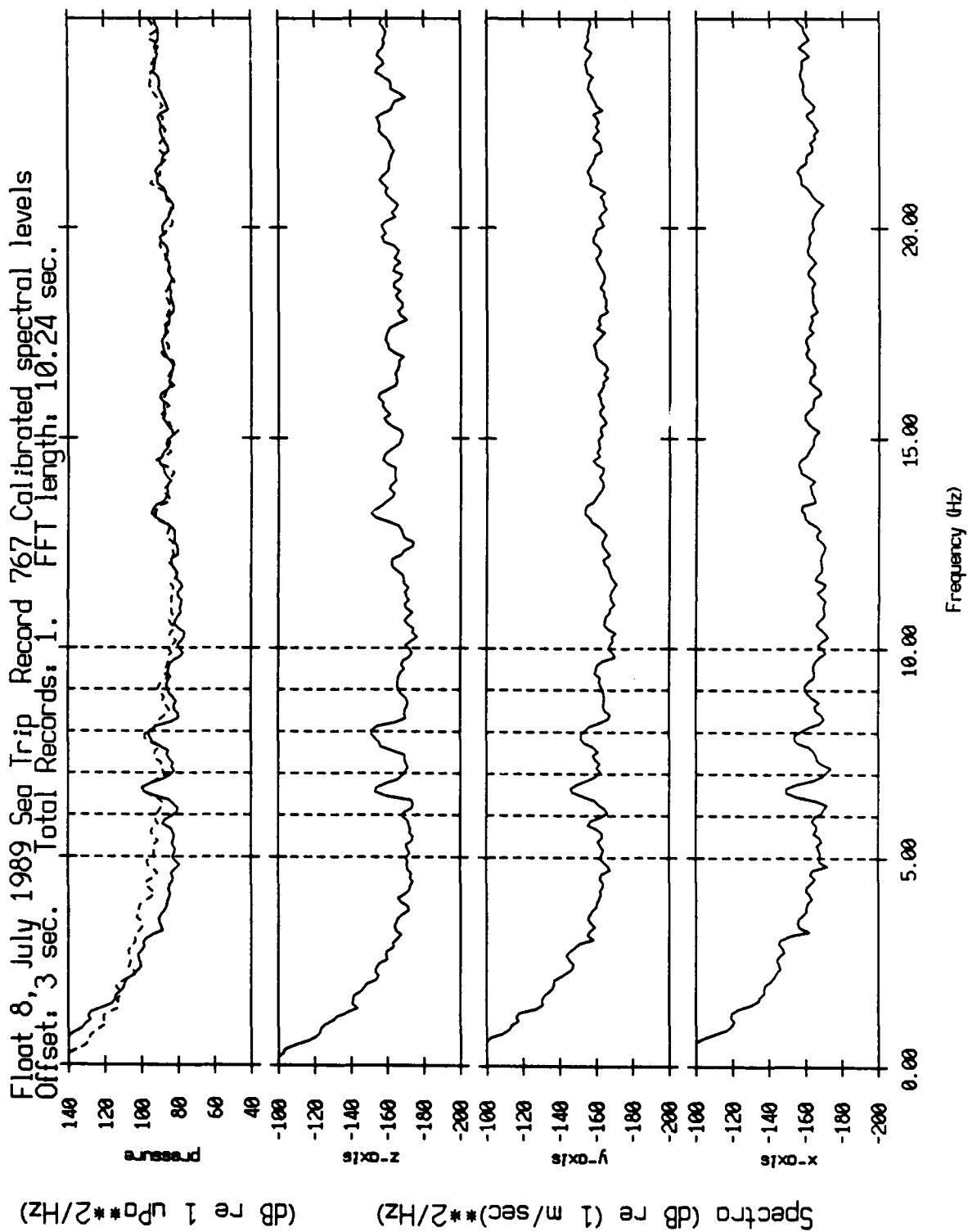


Figure XII.21

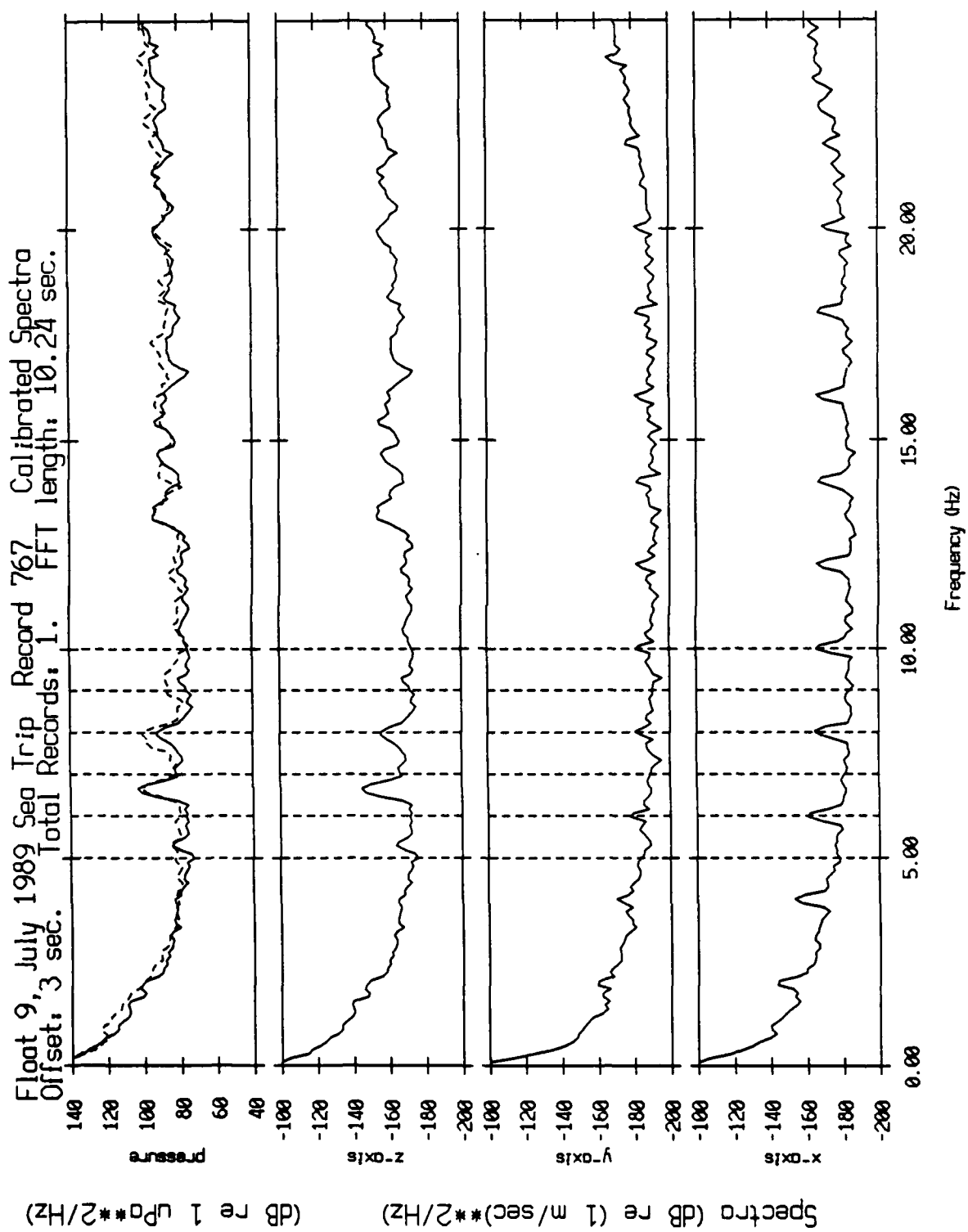


Figure XII.2]



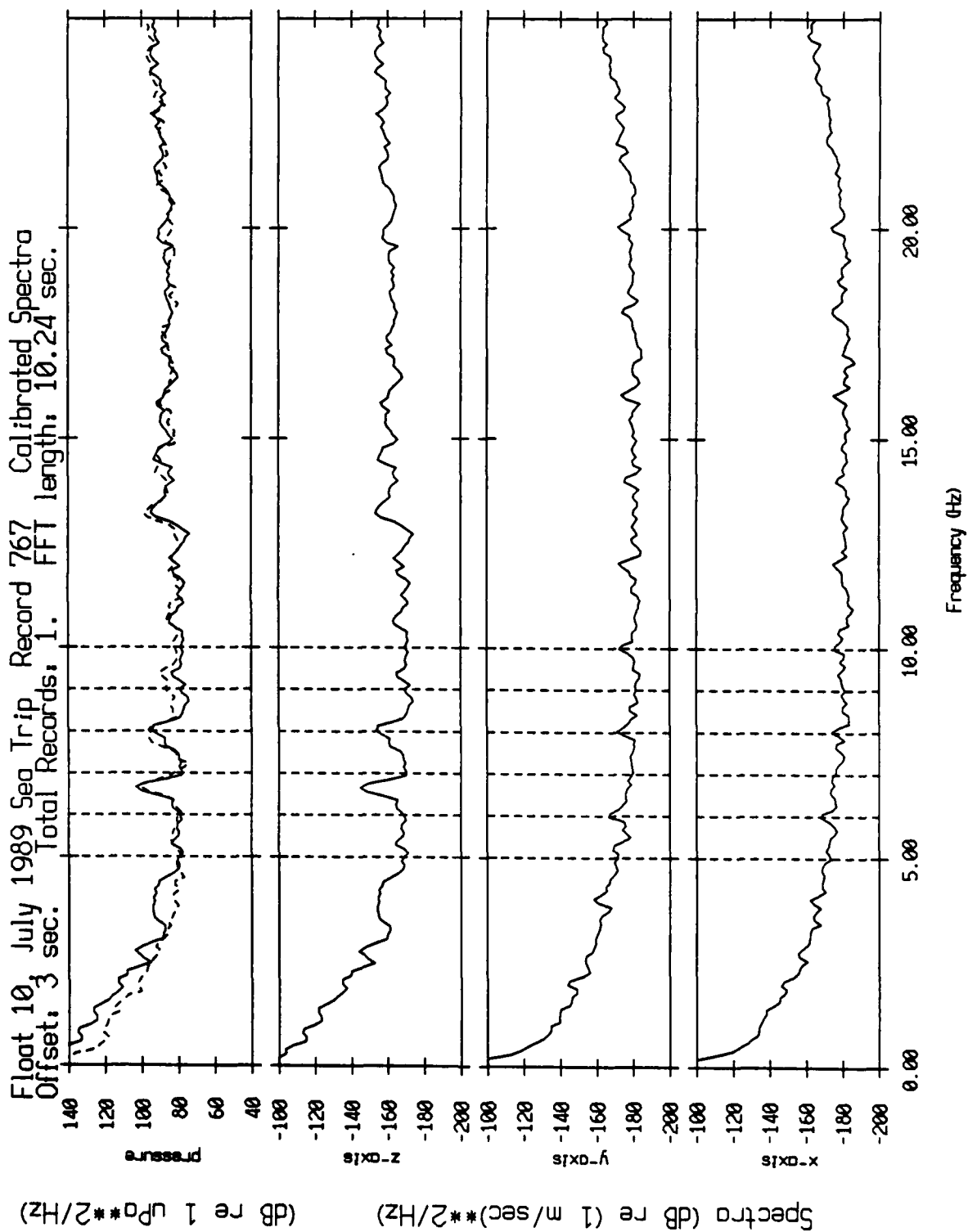


Figure XII.2k

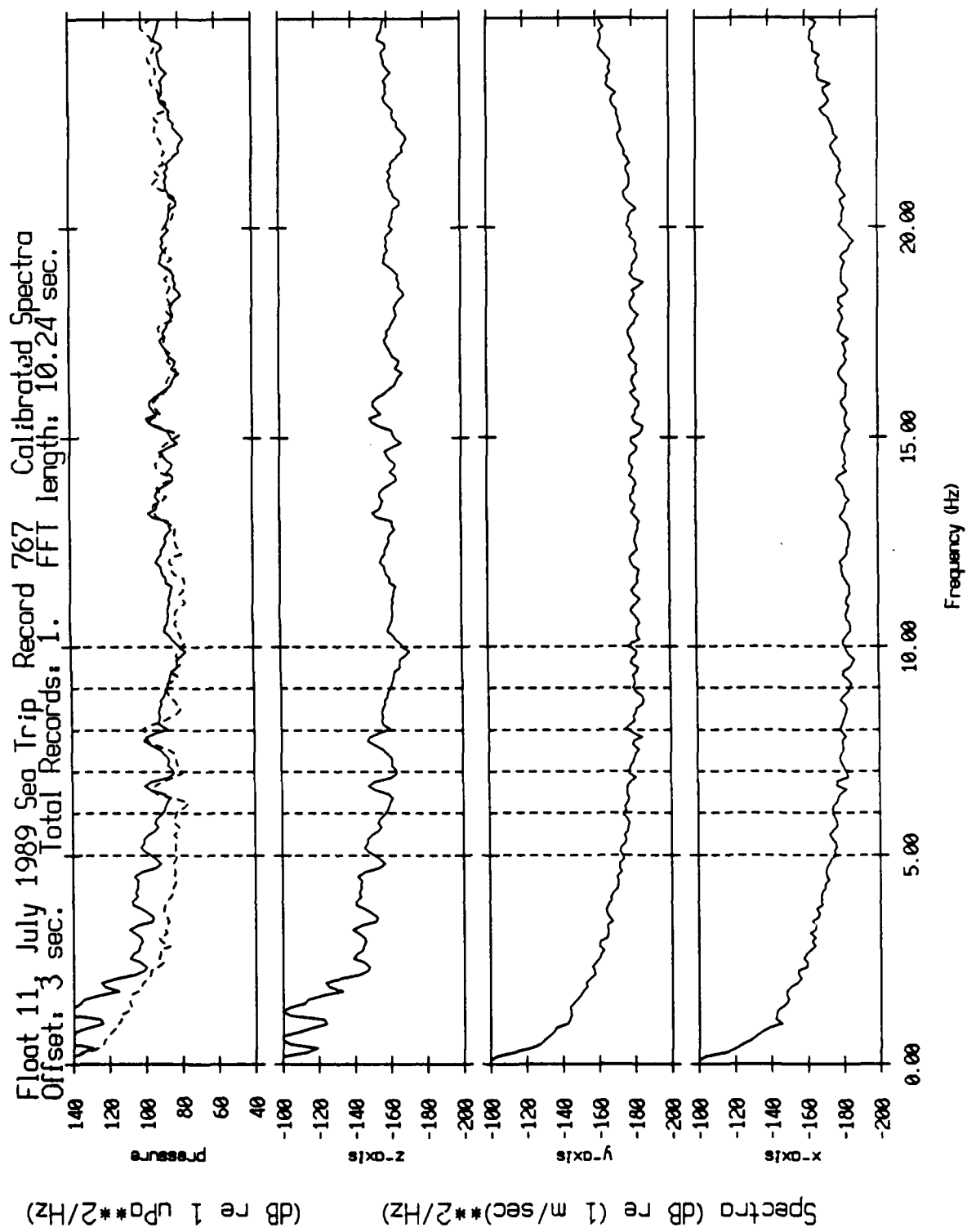


Figure XII.21

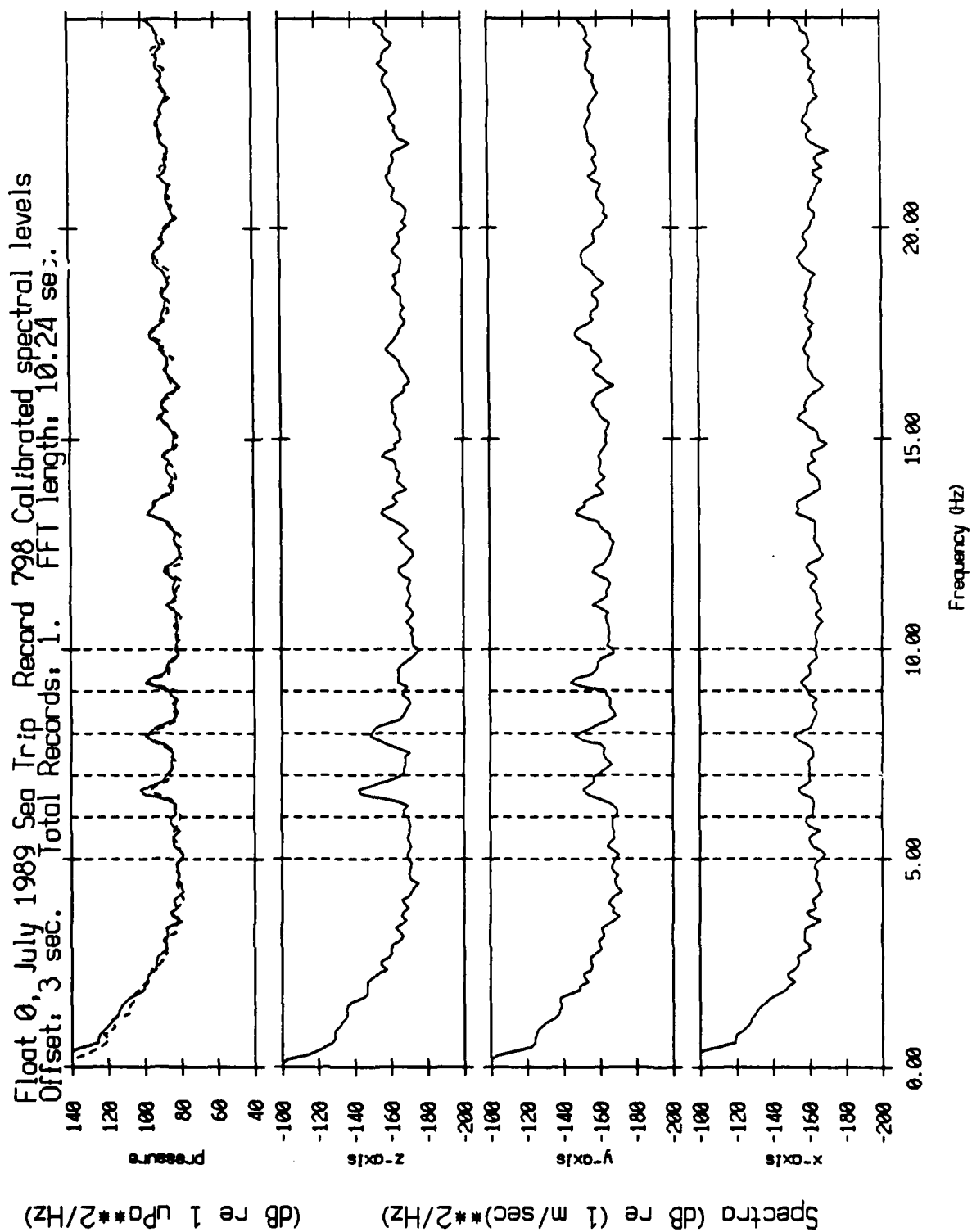


Figure XII.3a

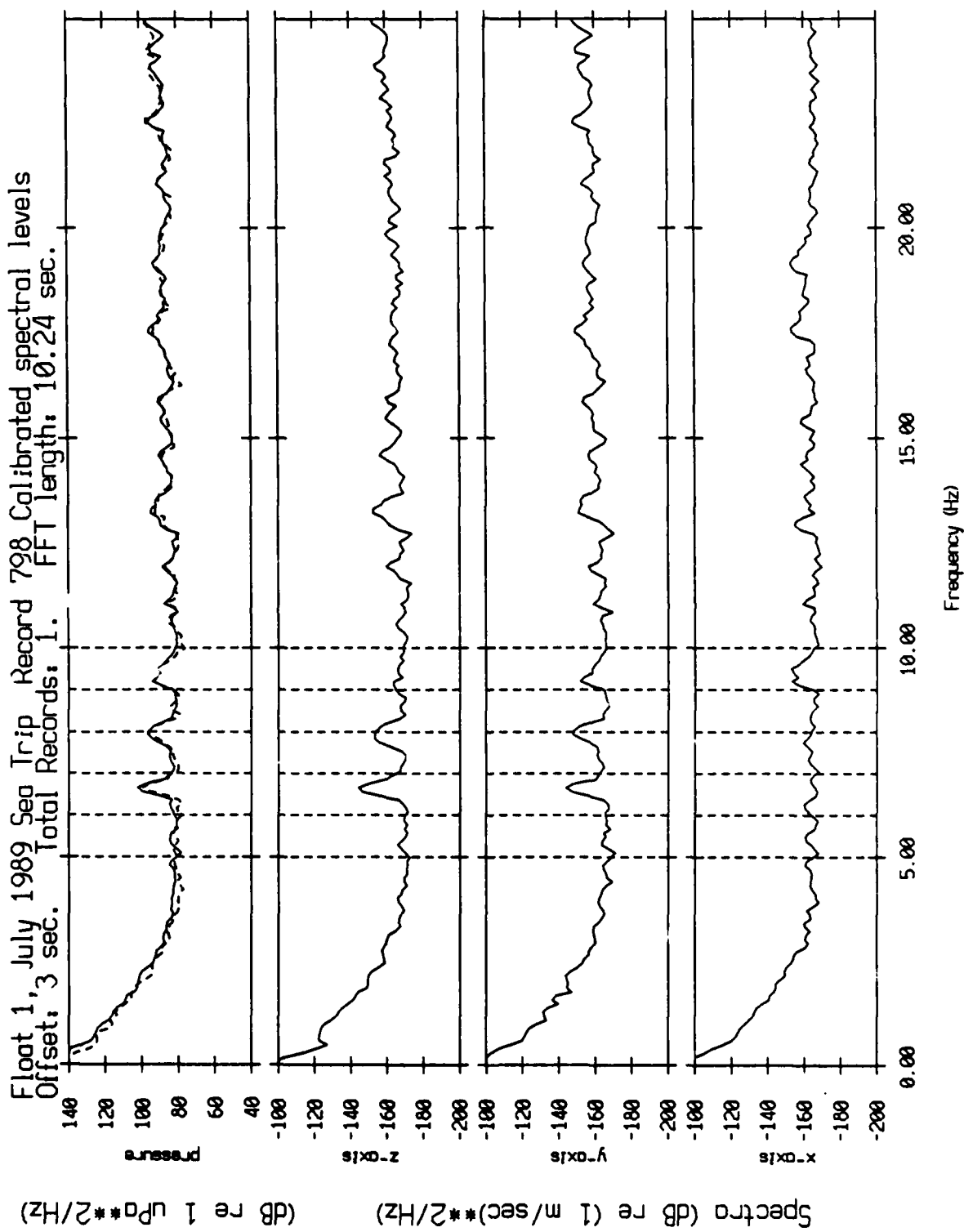


Figure XII.3b

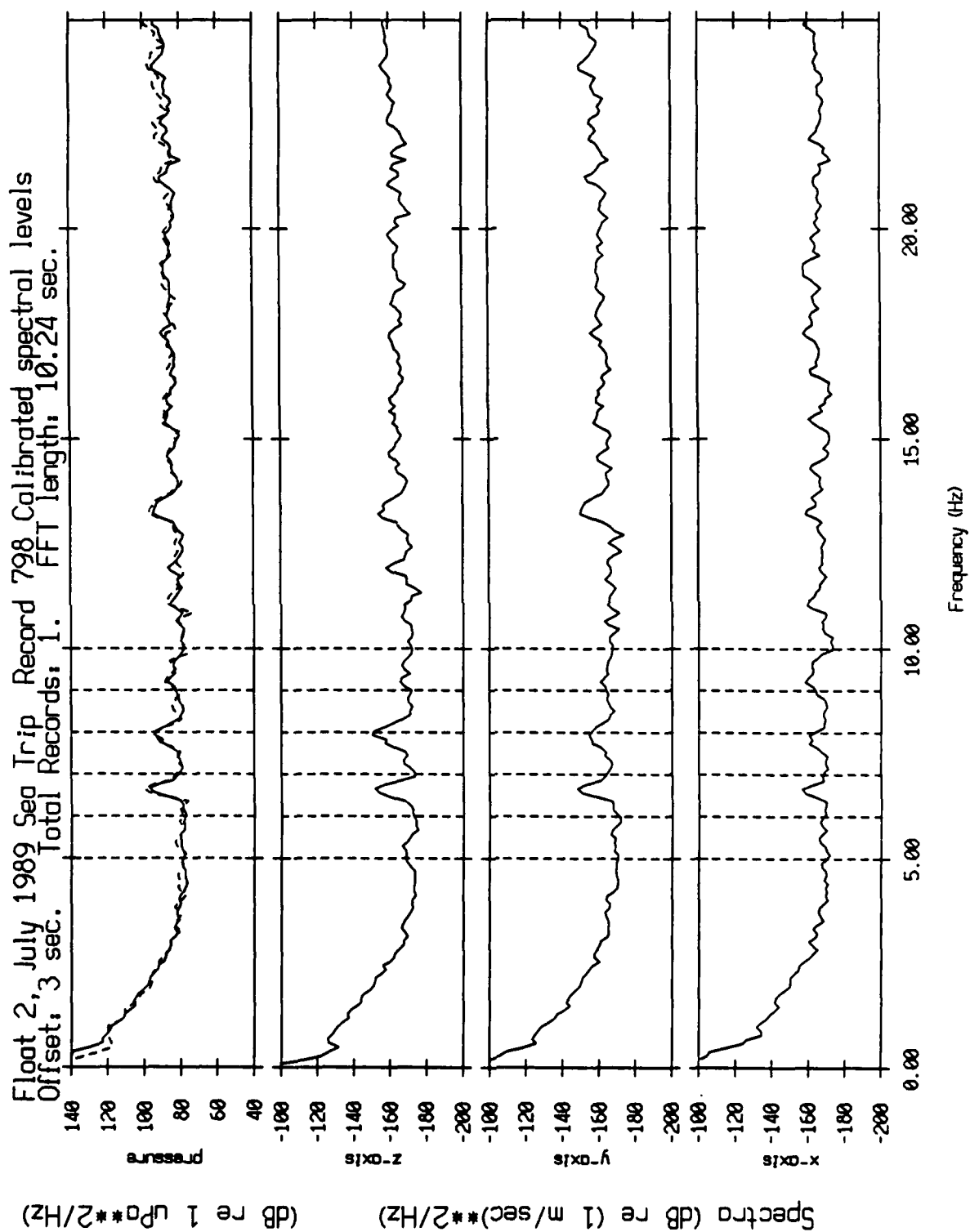


Figure XII.3c

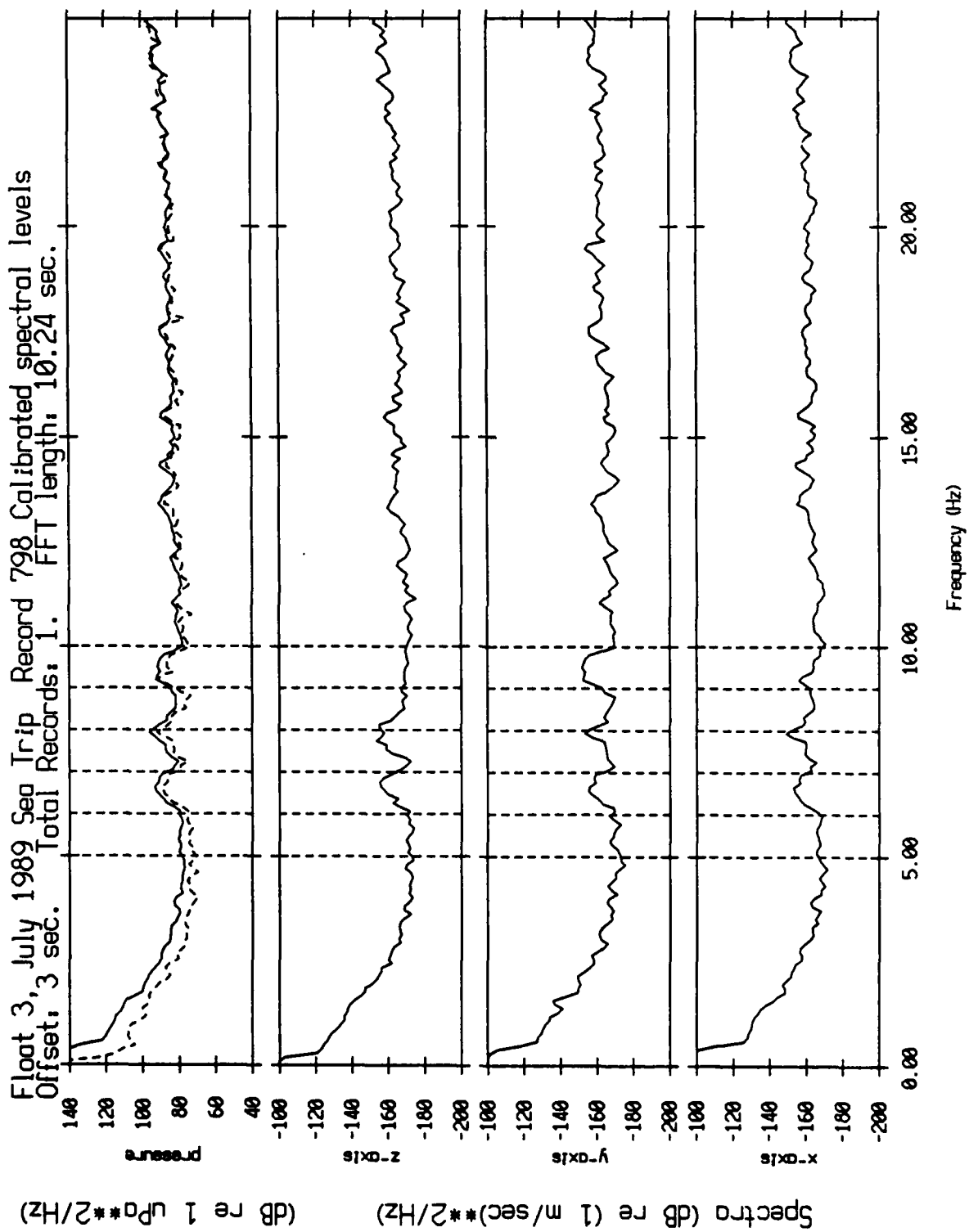


Figure XII.3d

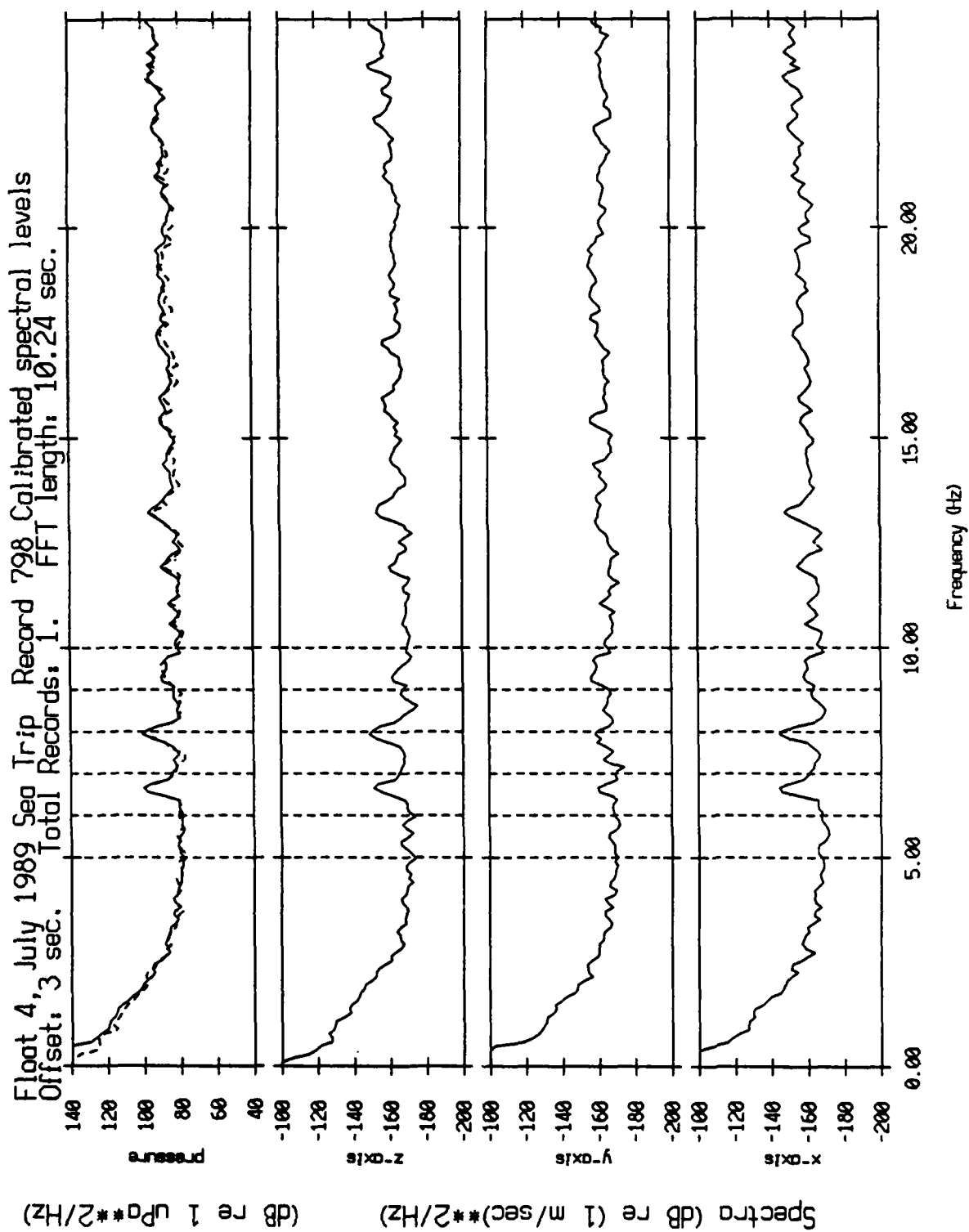


Figure XII.3e

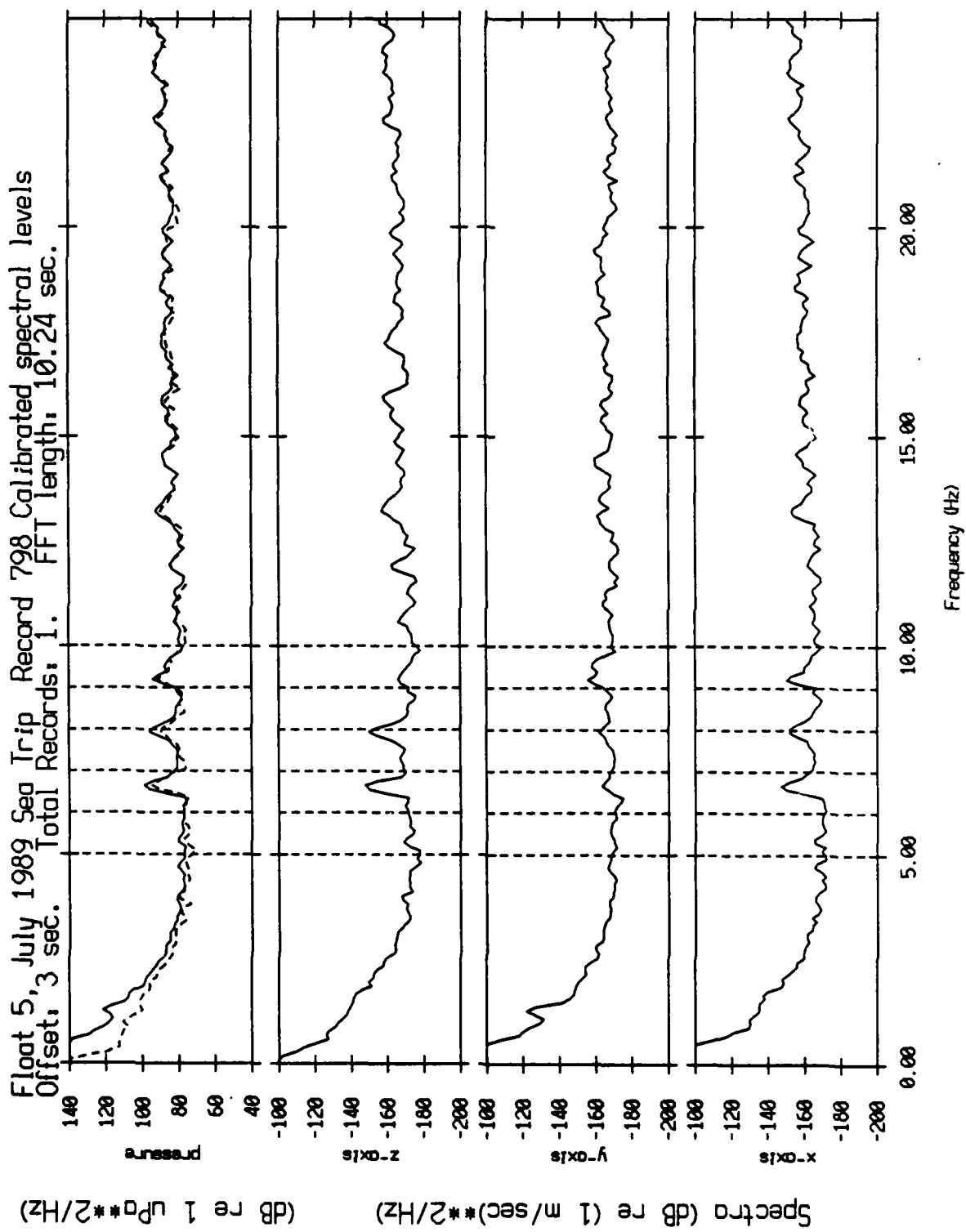


Figure XII.3f



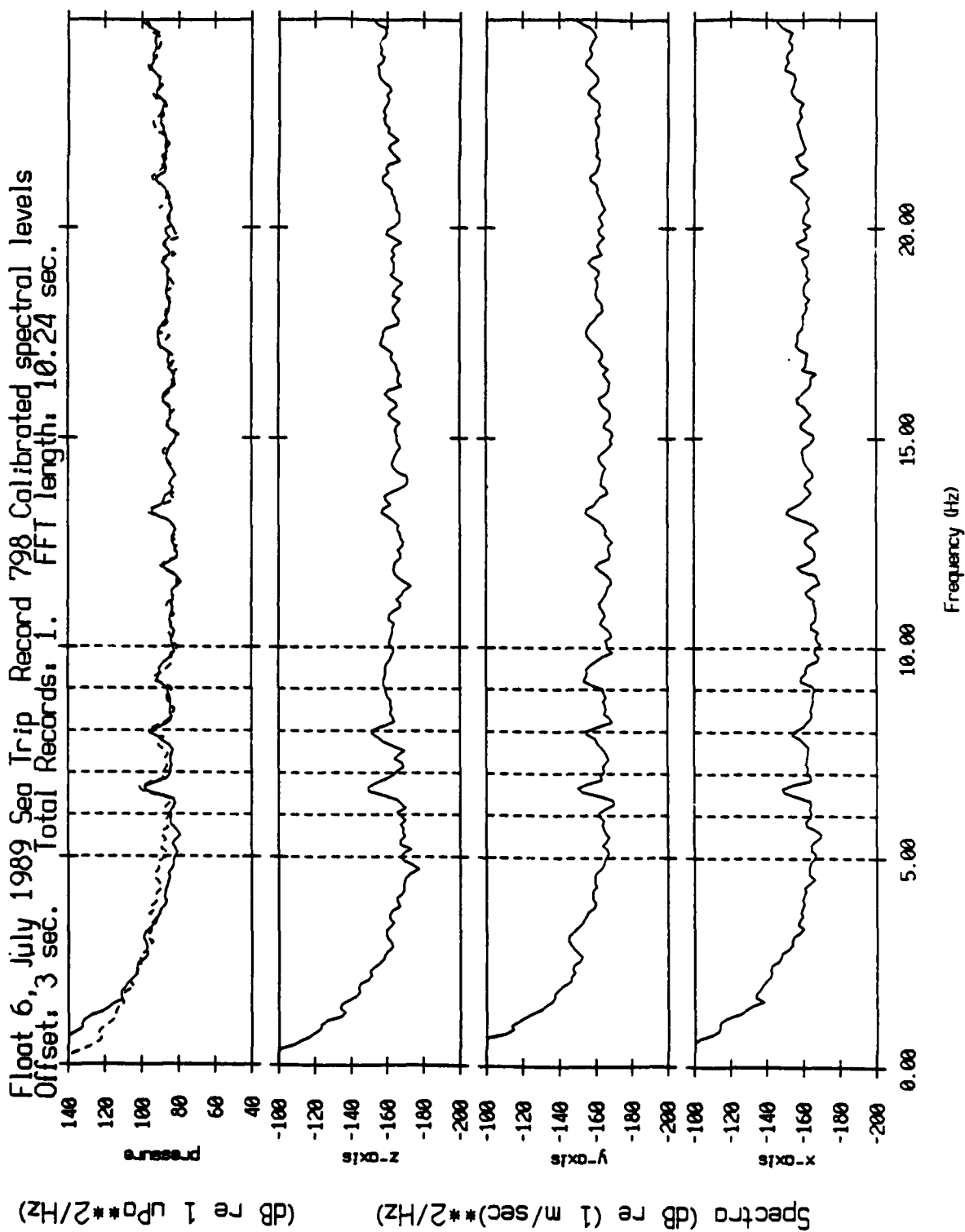


Figure XII.3g

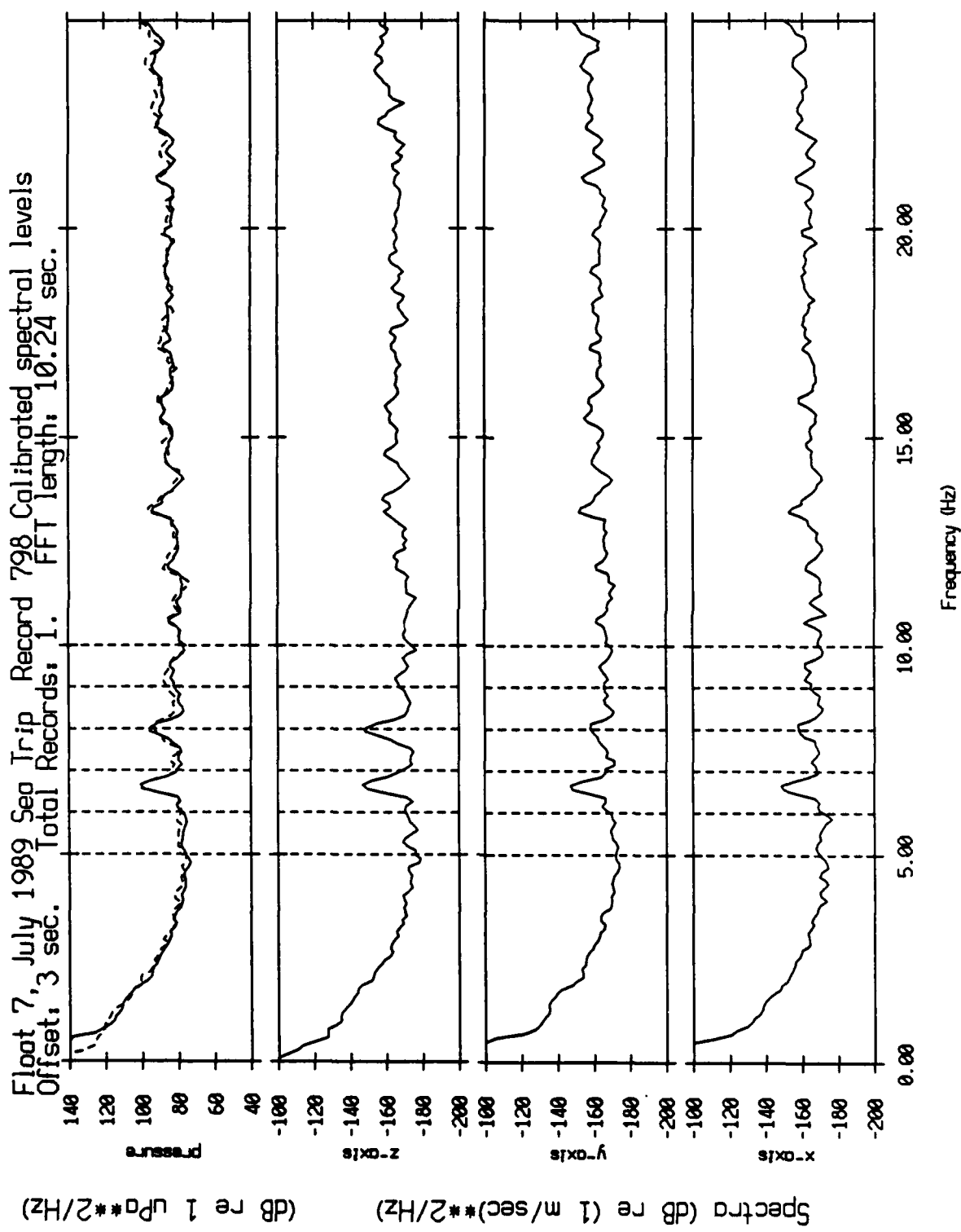


Figure XII.3h

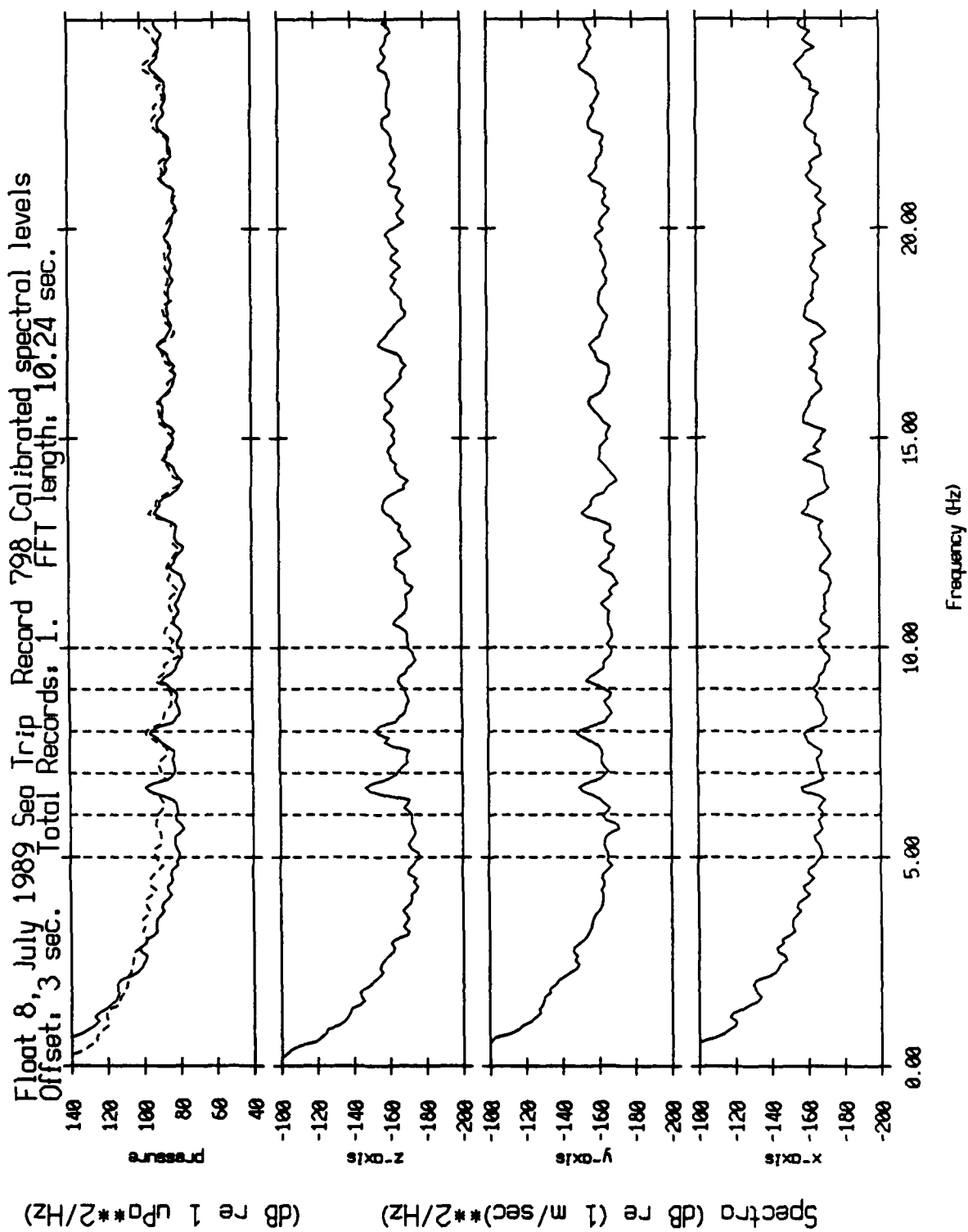


Figure XII.31

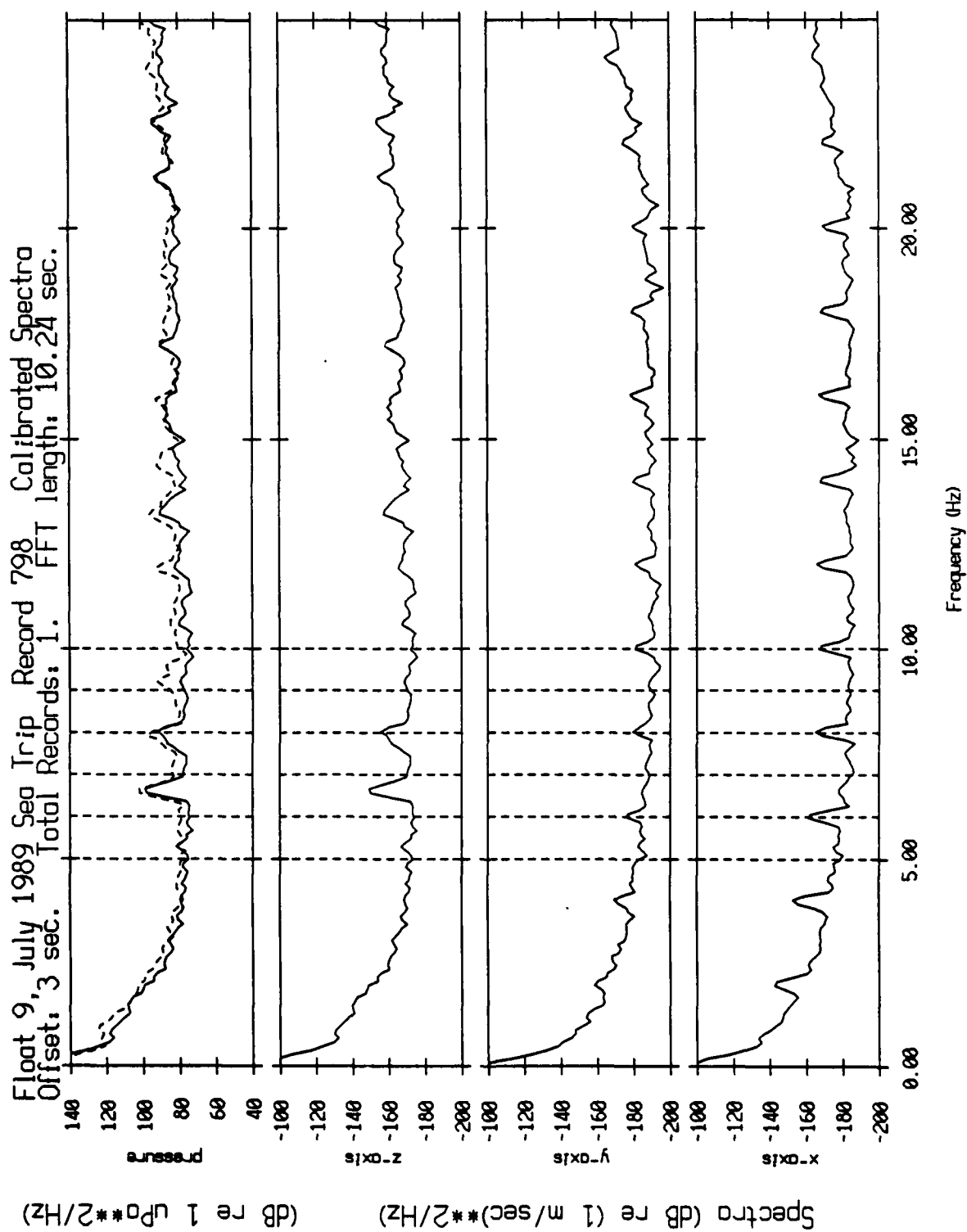


Figure XII.3j

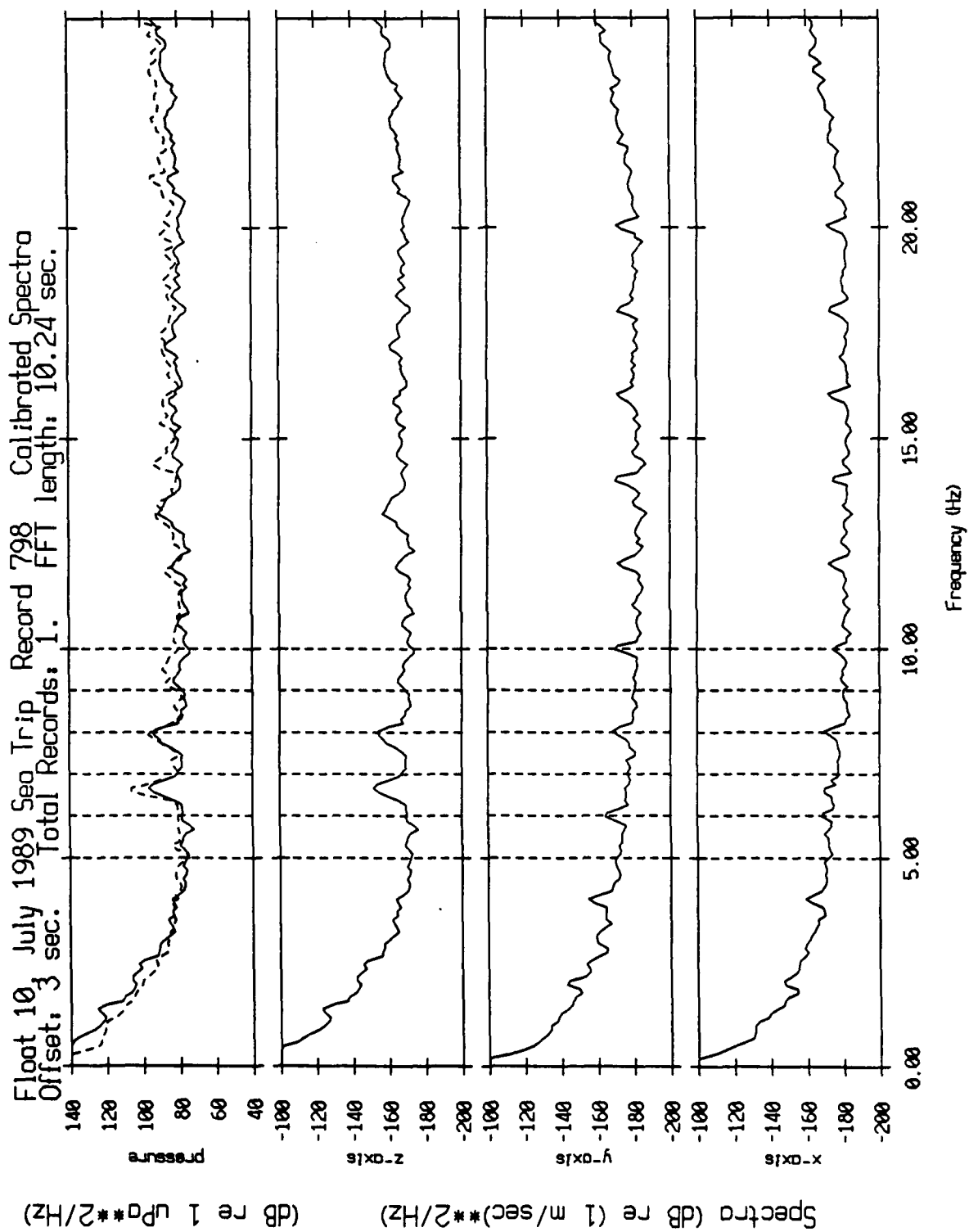


Figure XII.3k

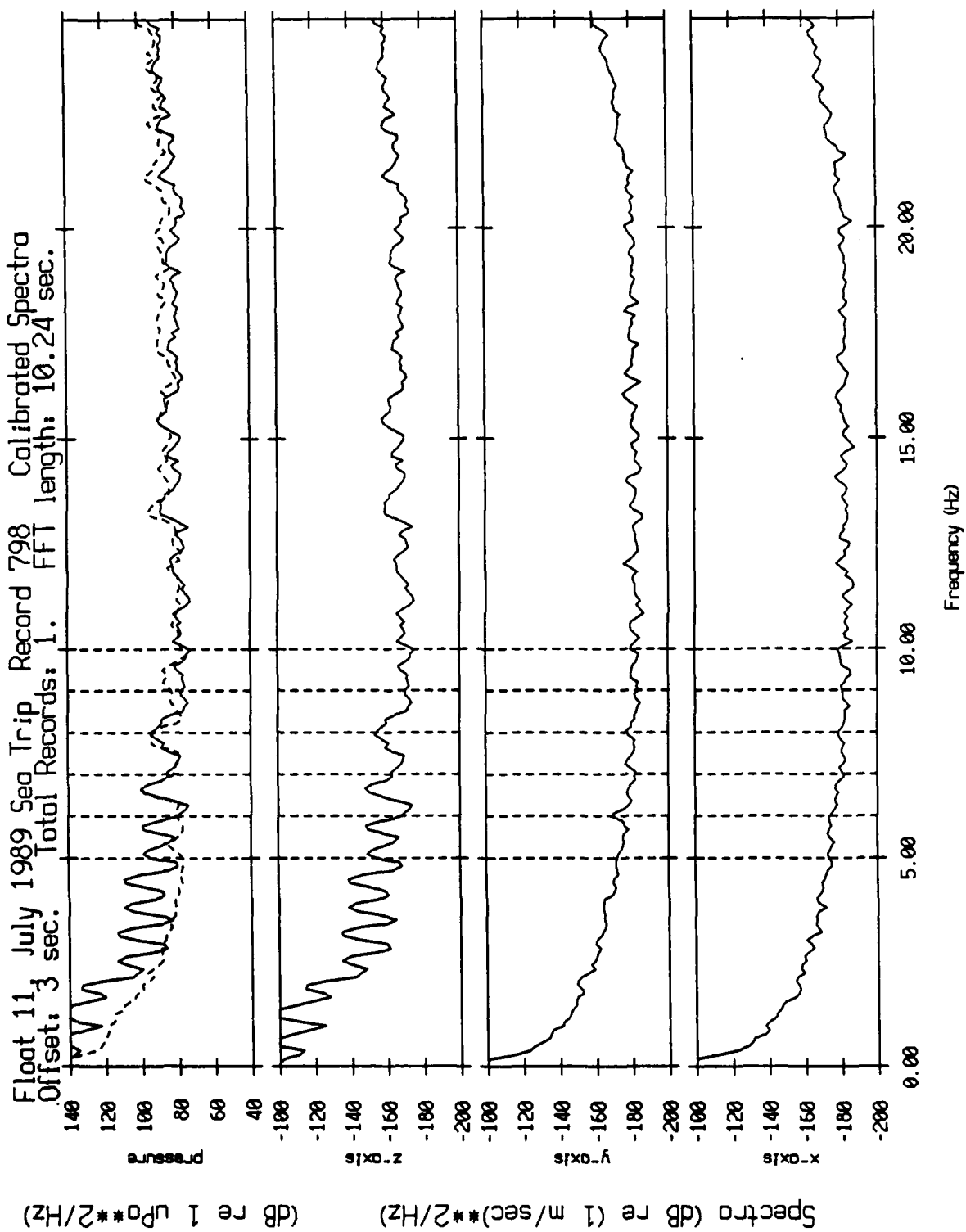


Figure XII.31

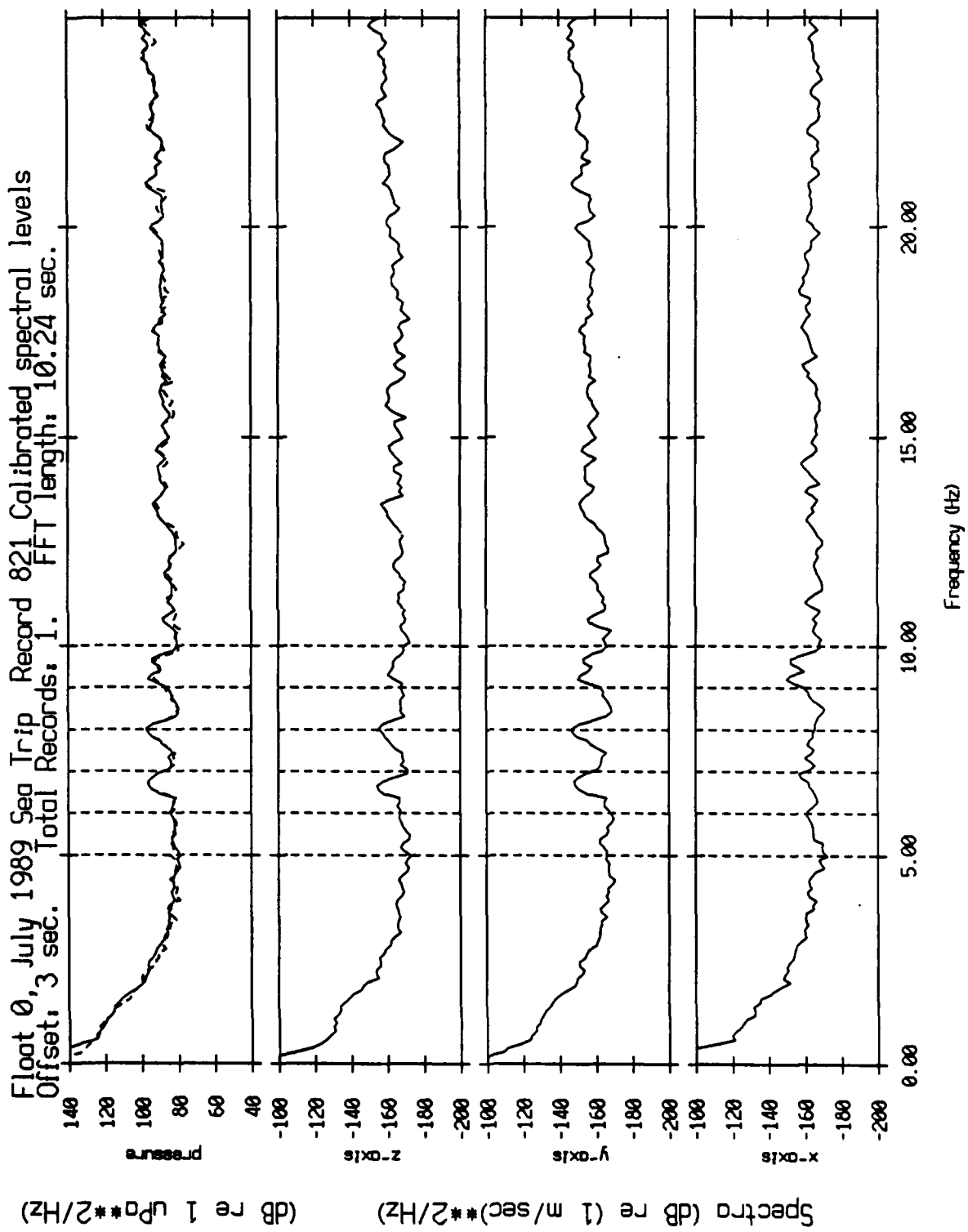


Figure XII.4a

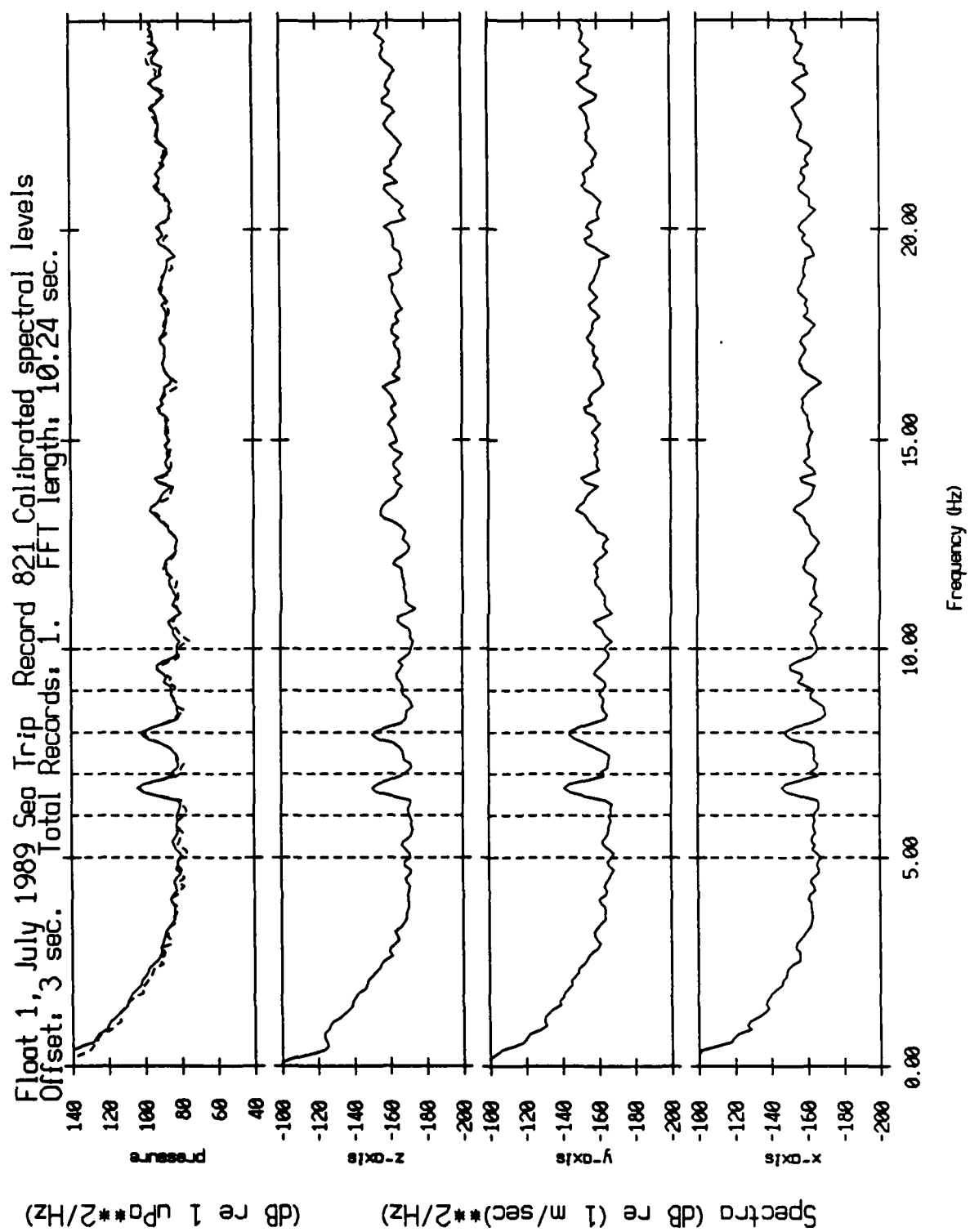


Figure XII.4b



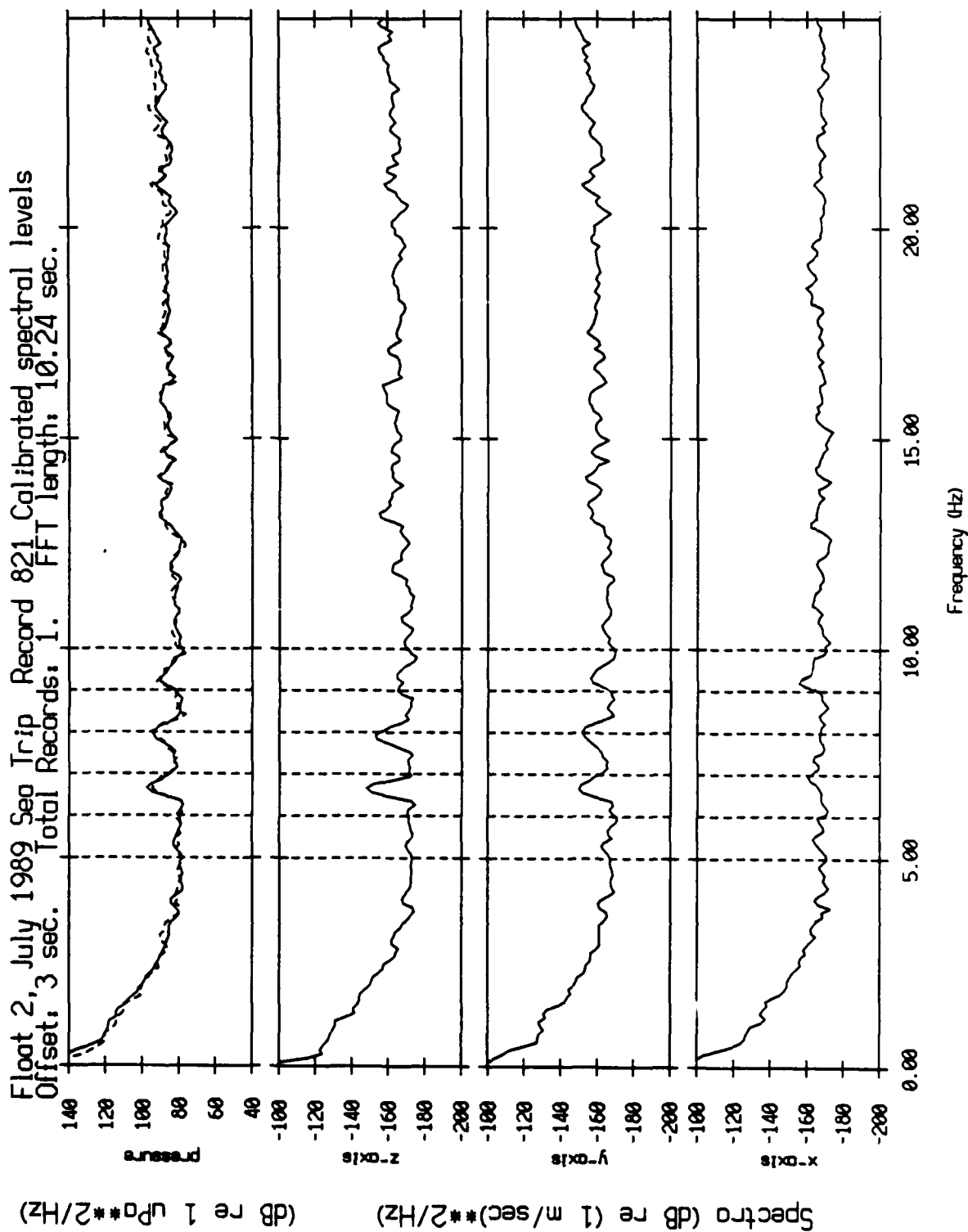


Figure XII.4c

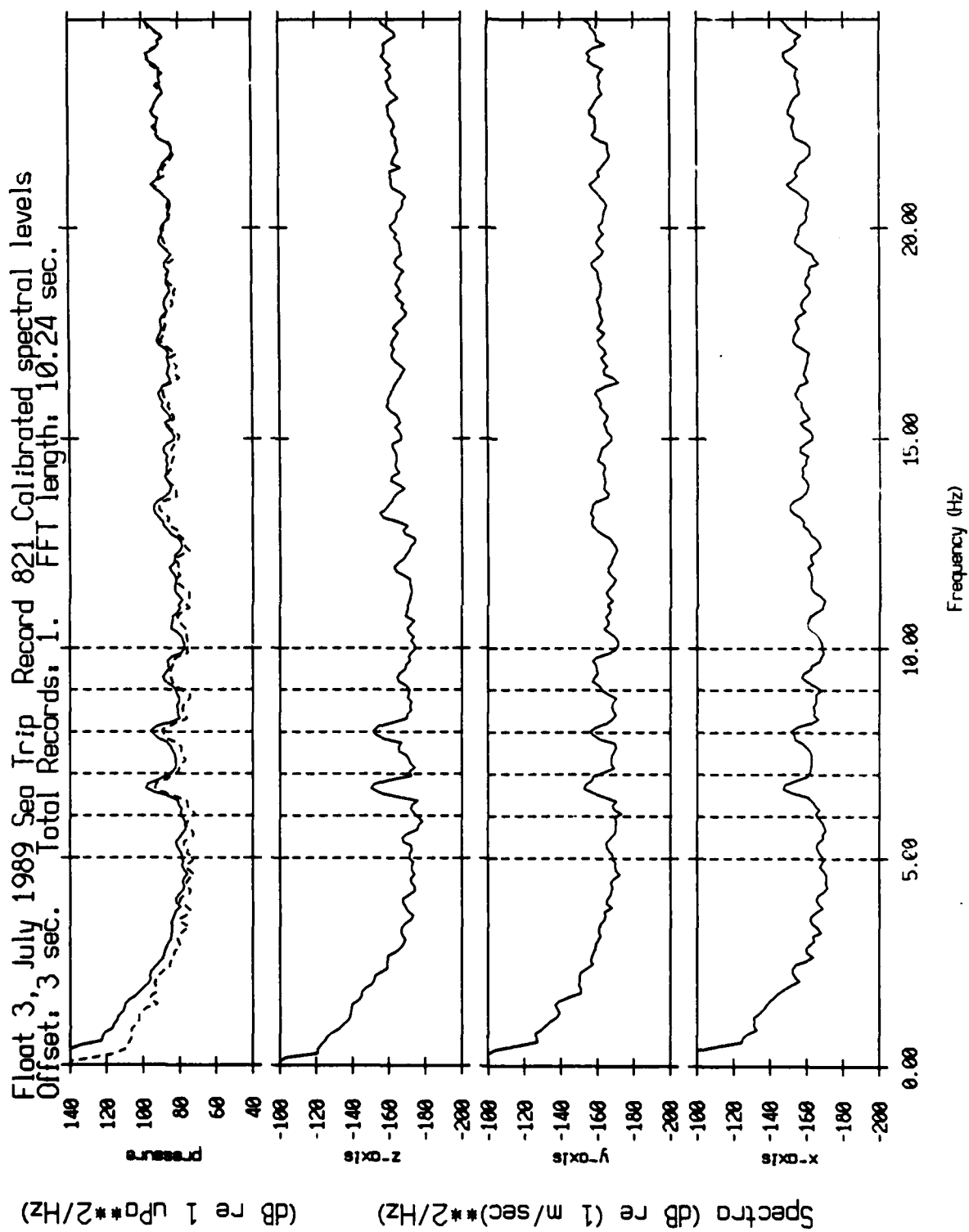


Figure XII.4d

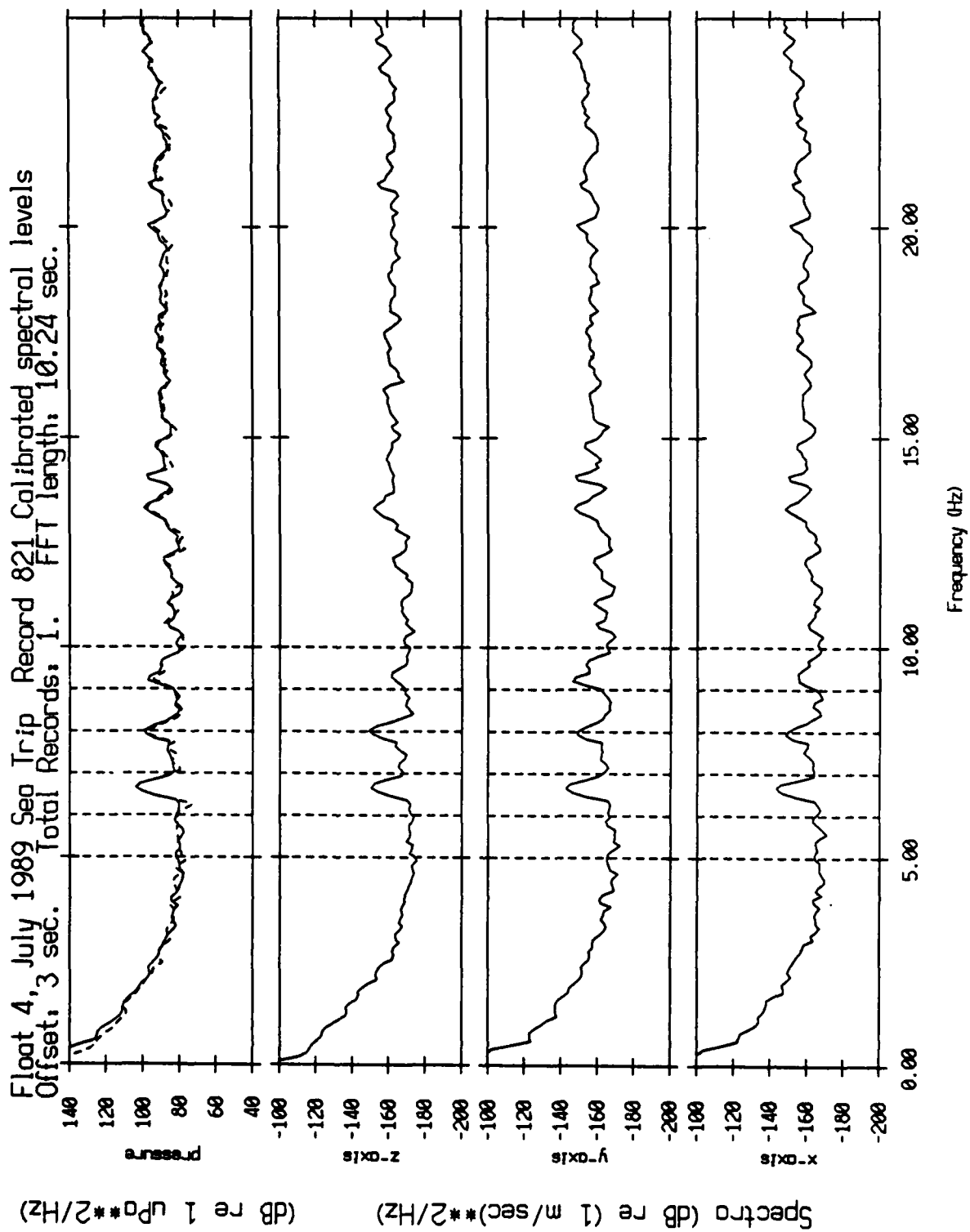


Figure XII.4e

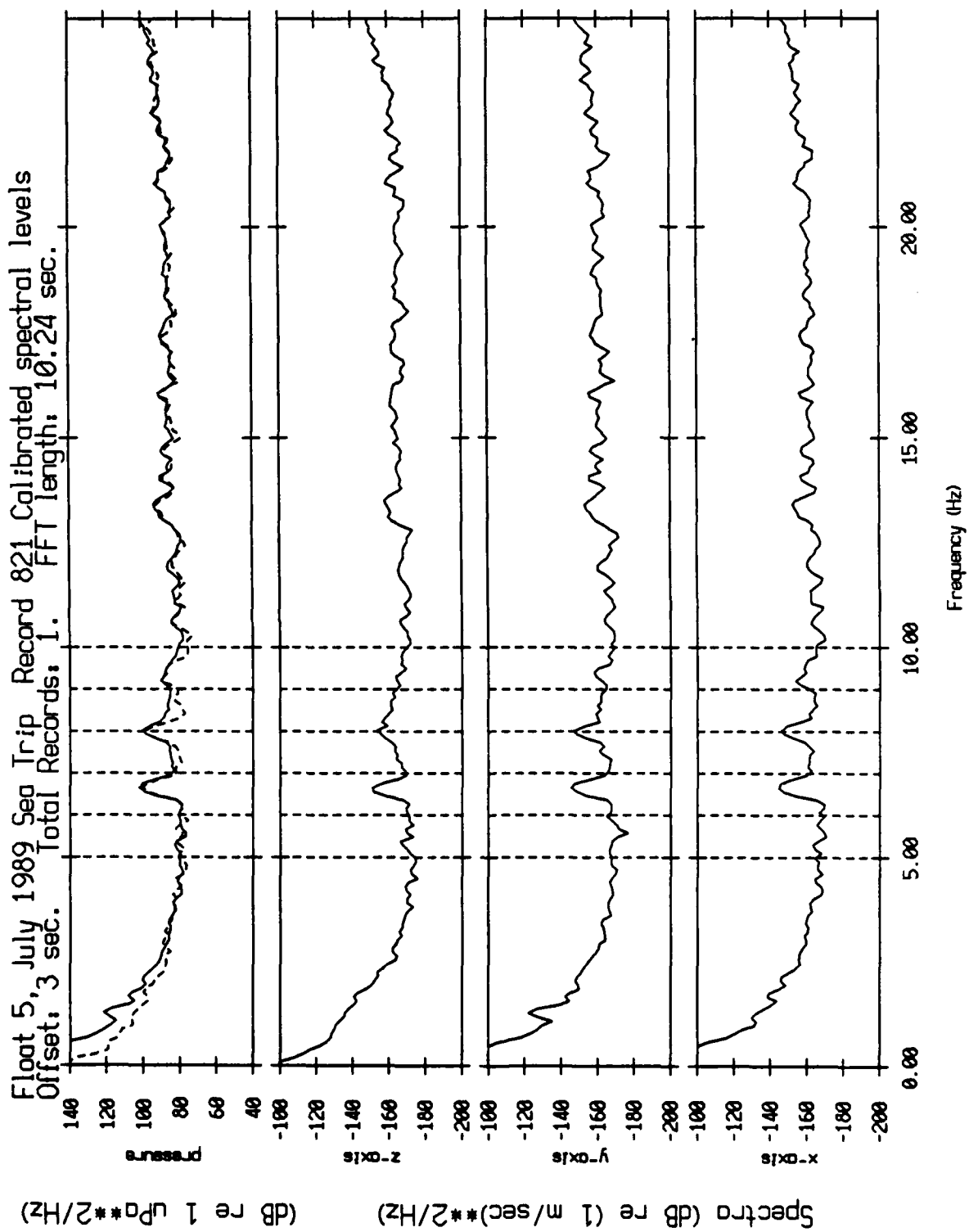


Figure XII.4f

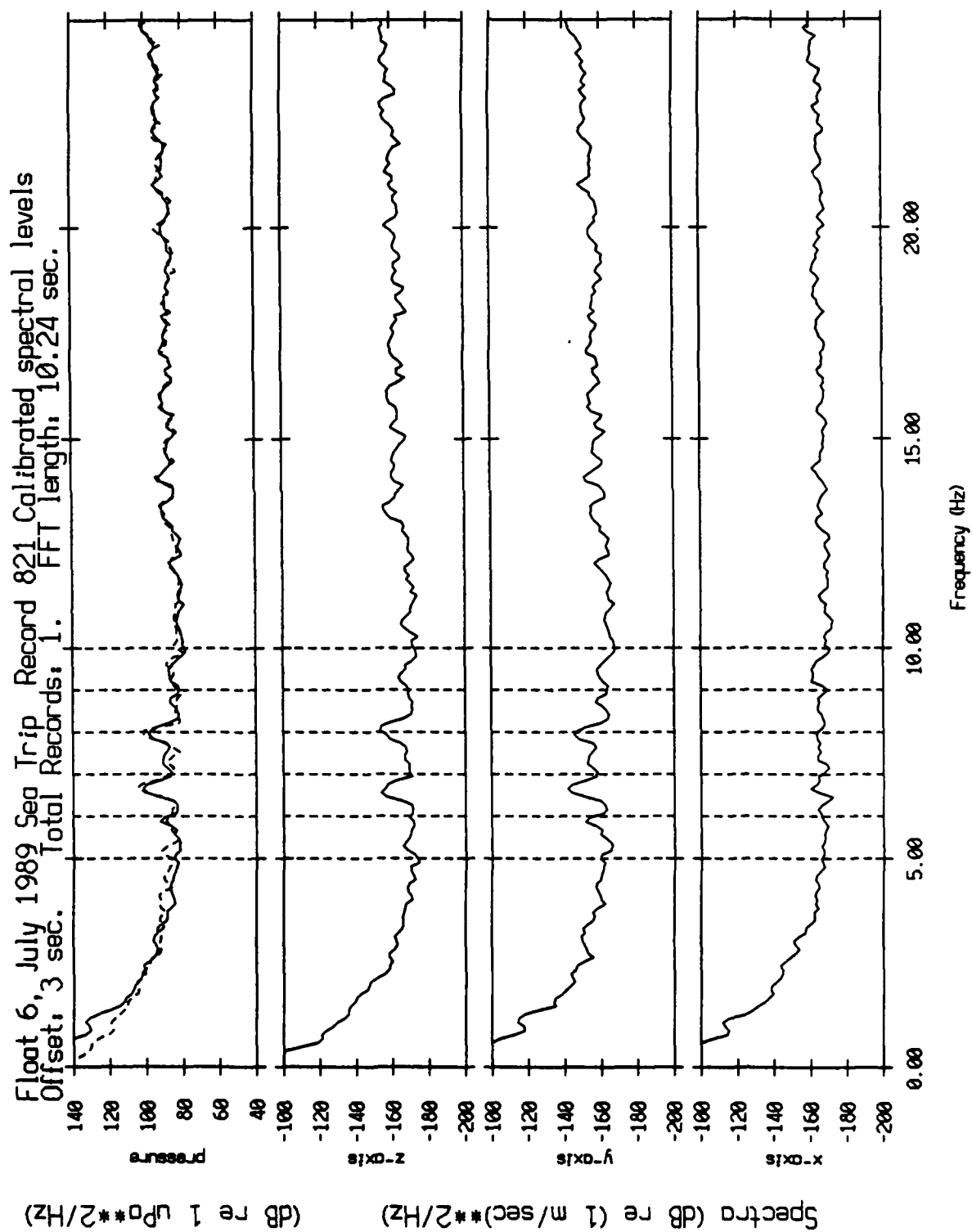


Figure XII.4g

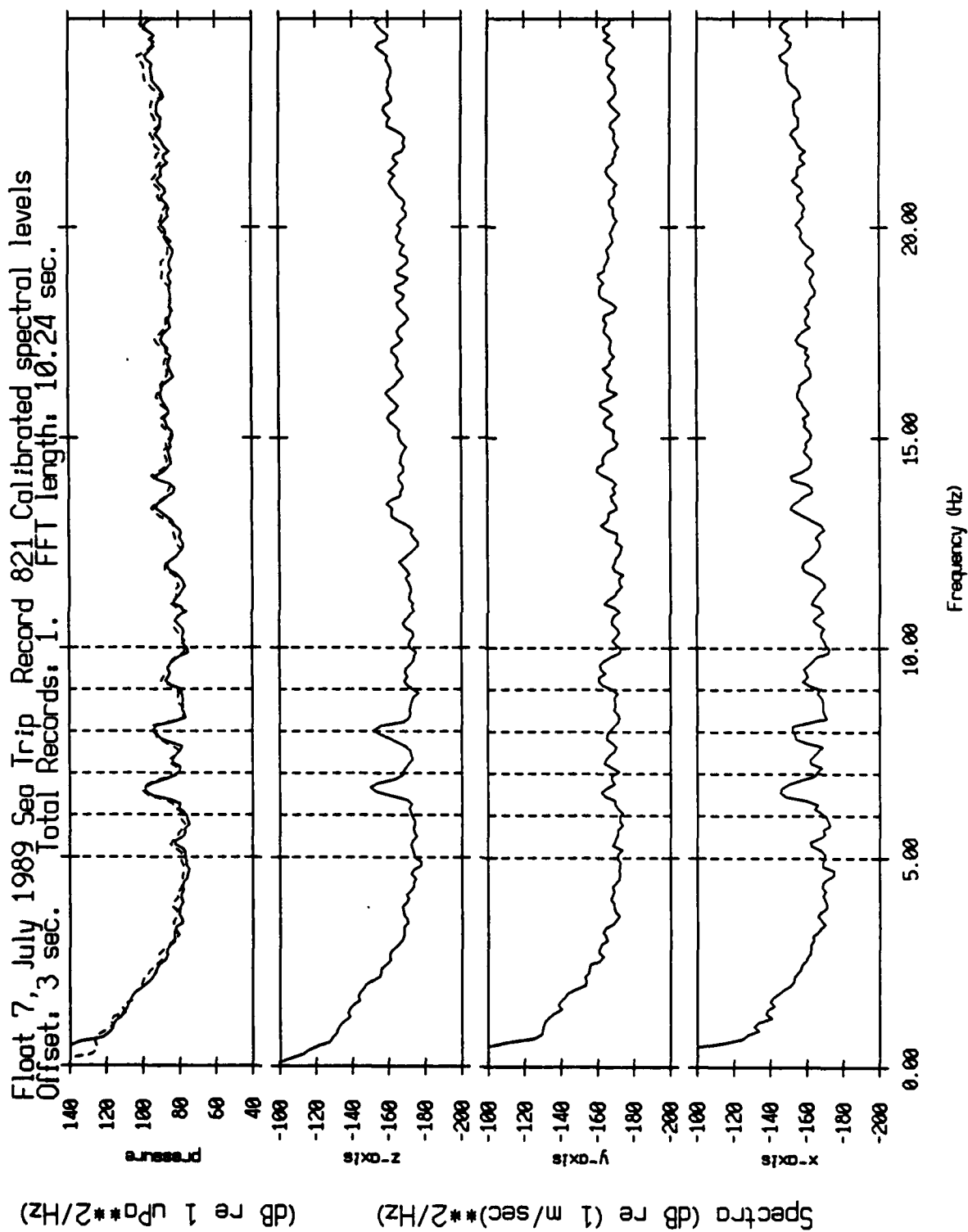


Figure XII.4h

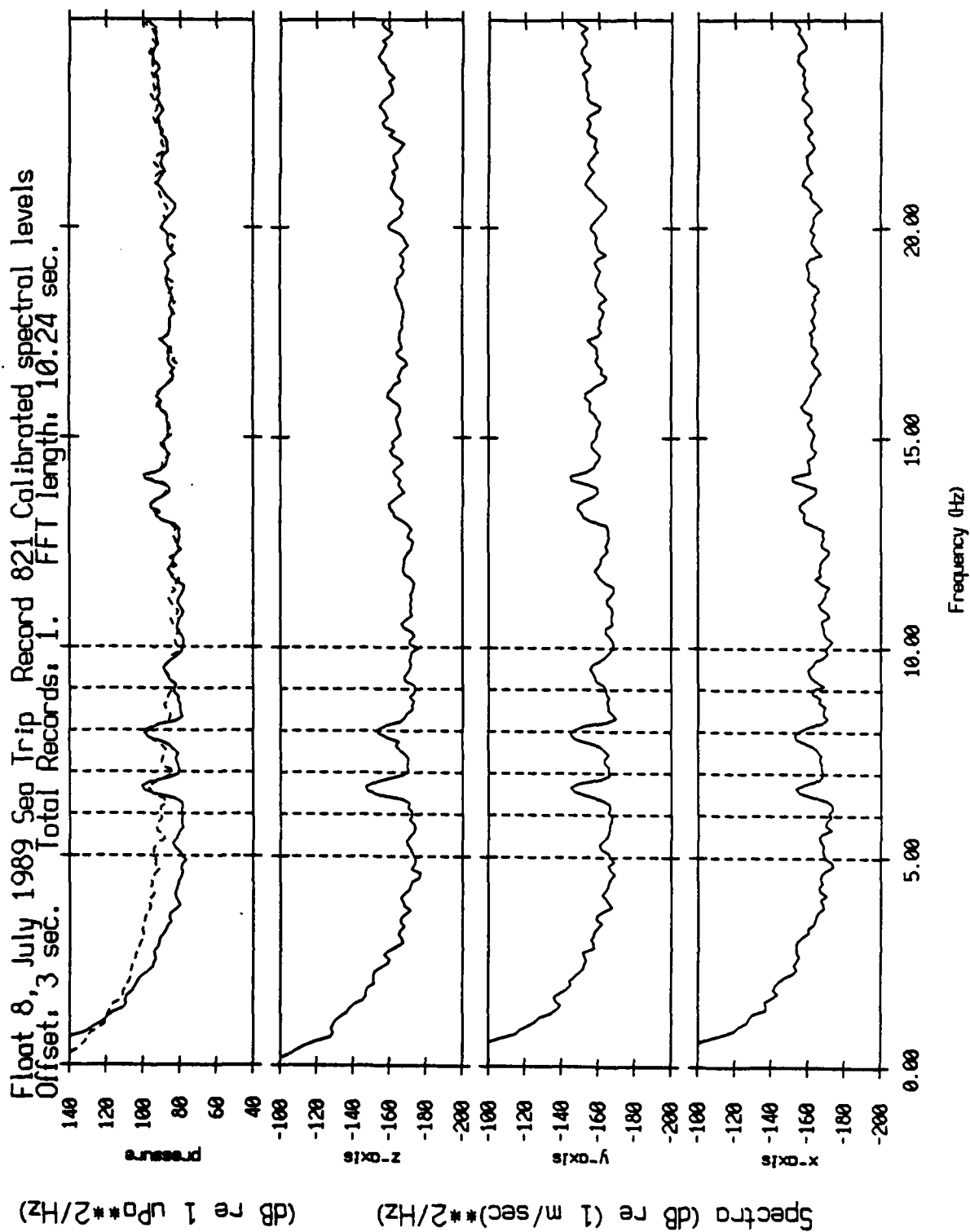


Figure XII.41

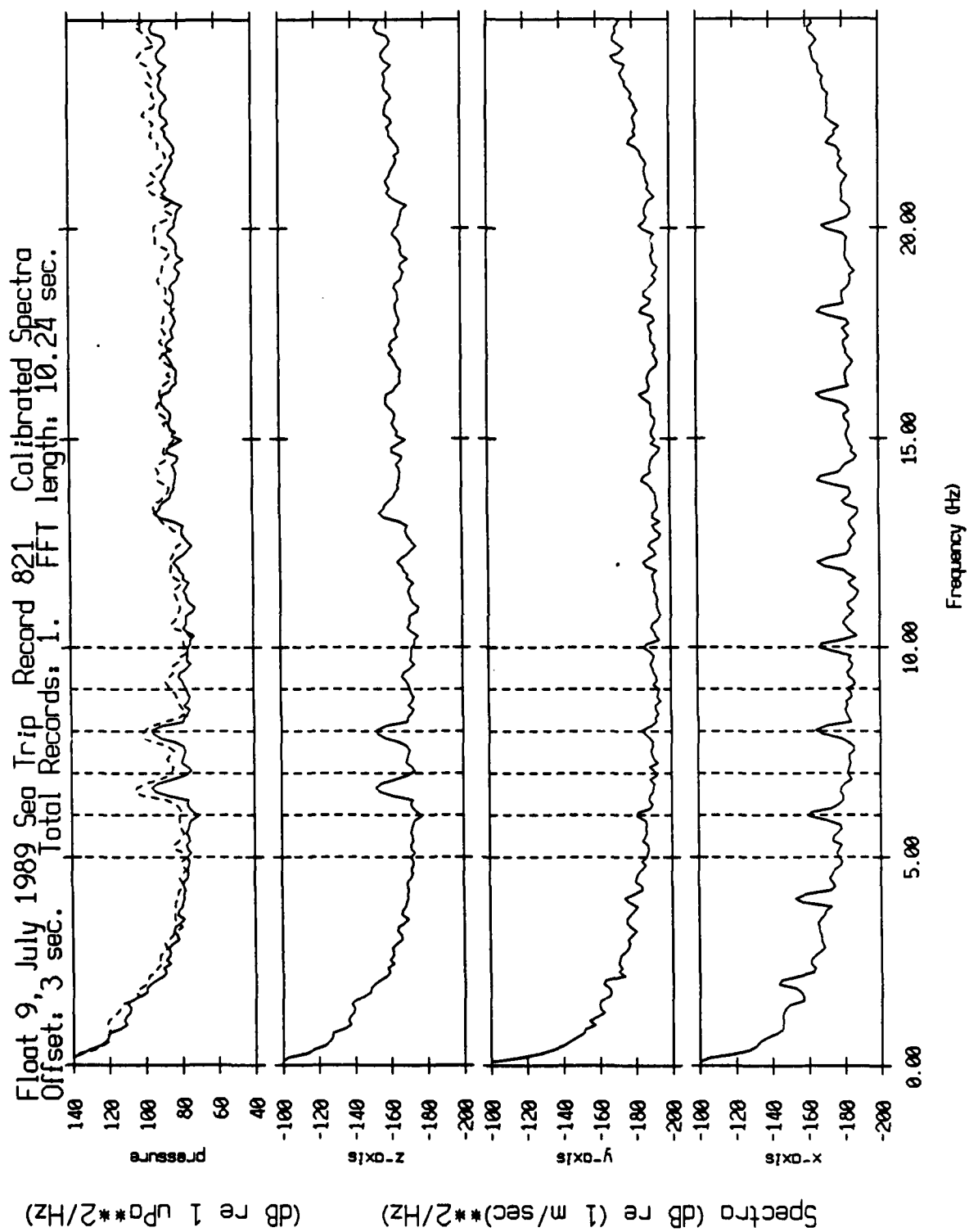


Figure XII.4j



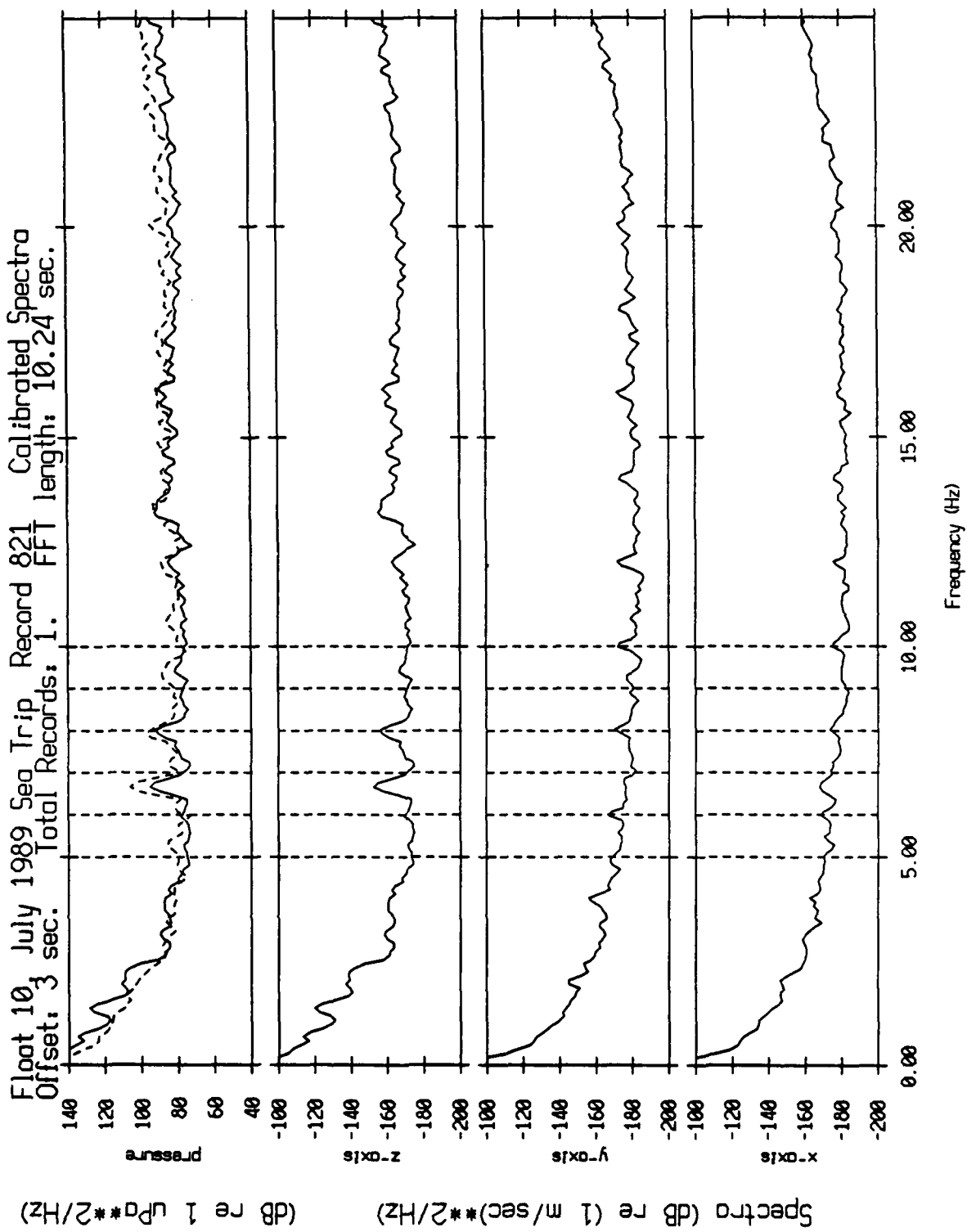


Figure XII.4k

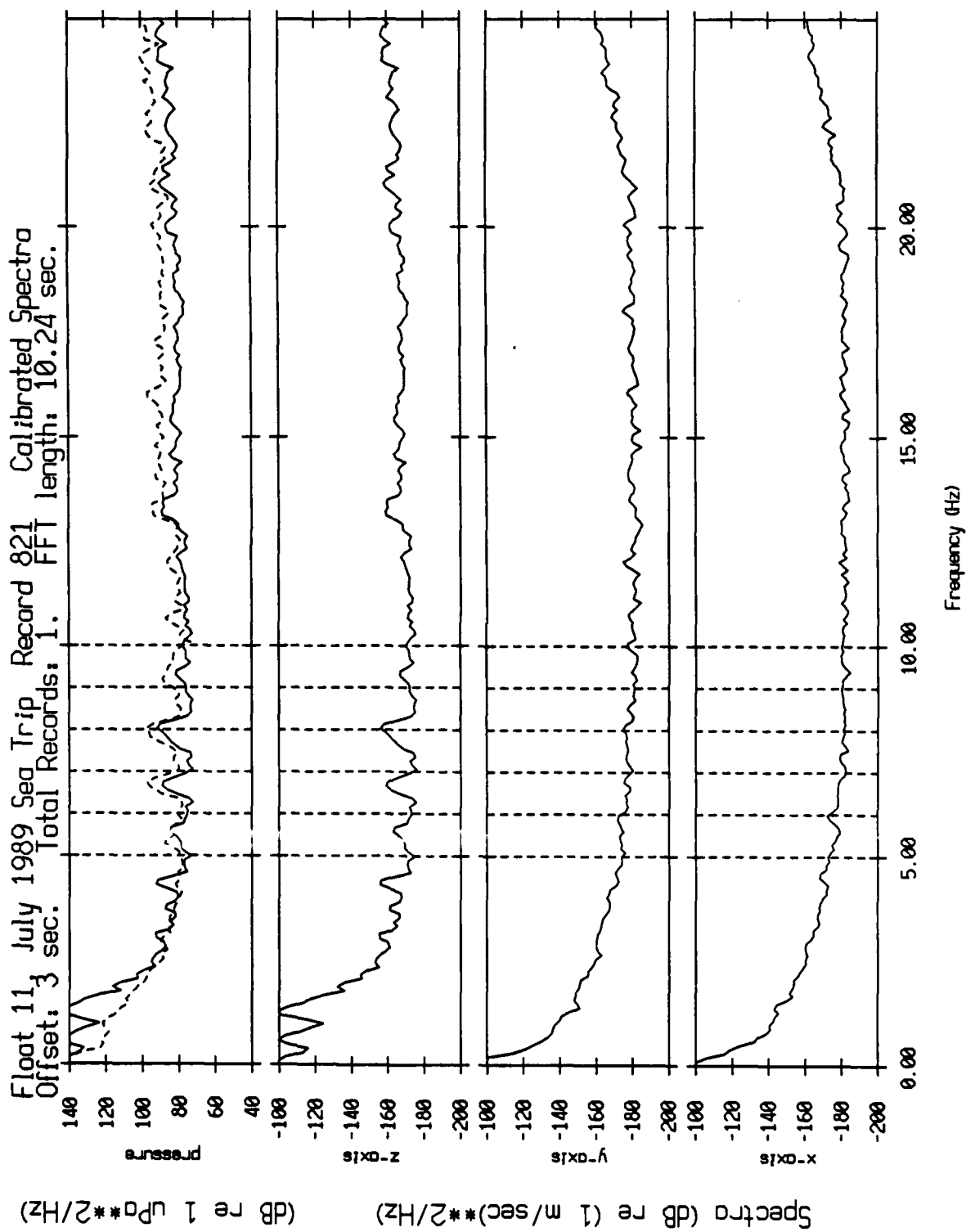


Figure XII.41

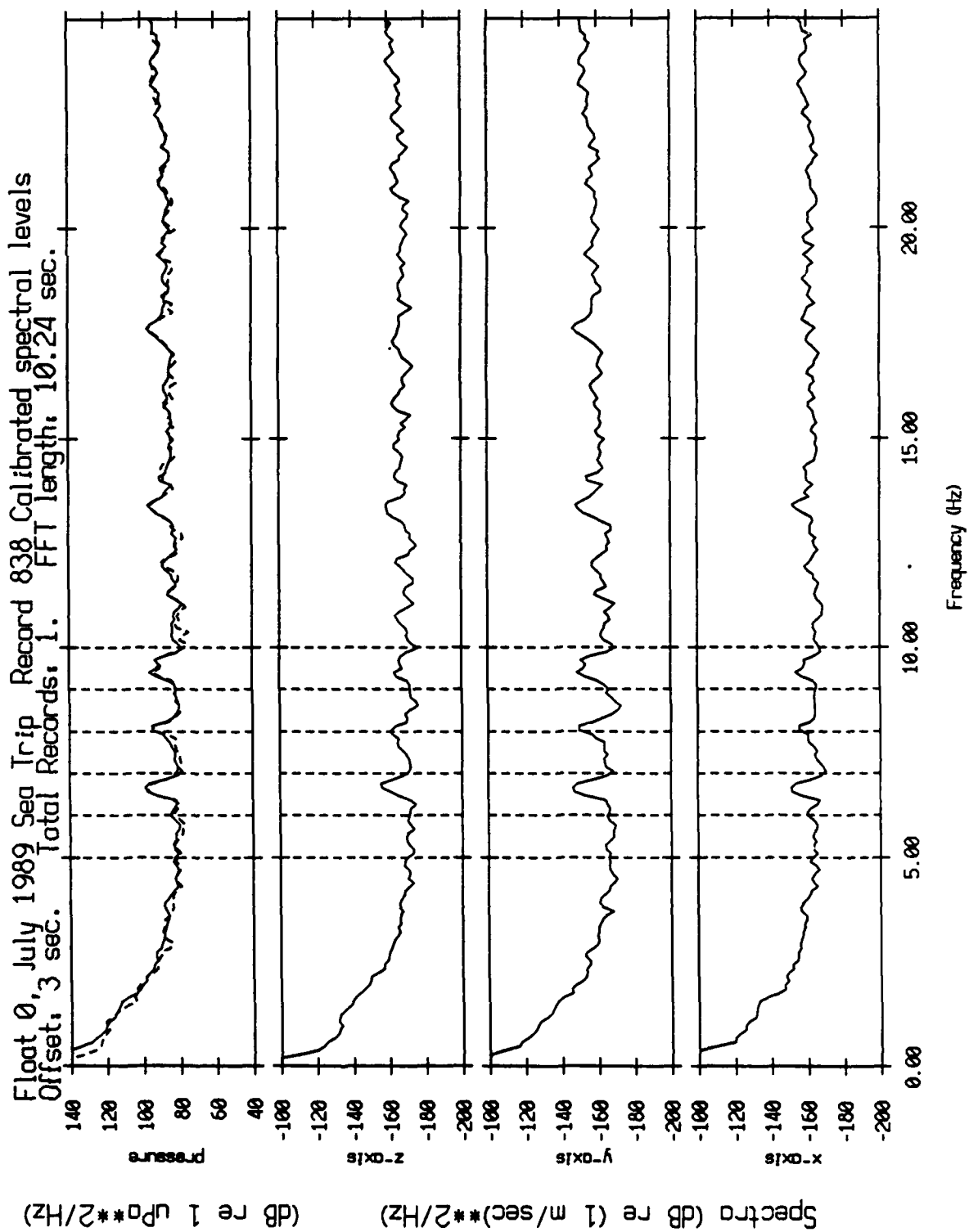


Figure XII.5a

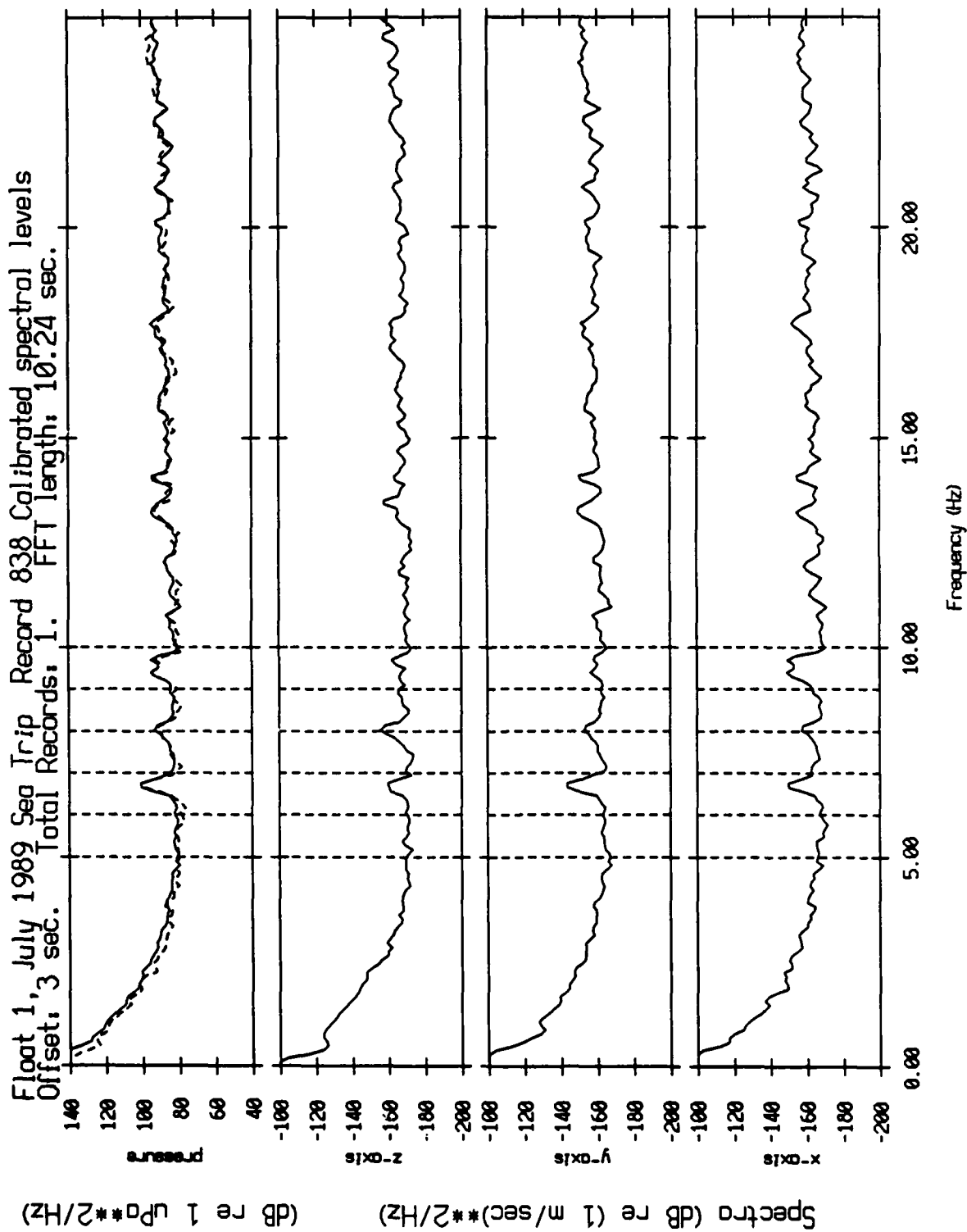


Figure XII.5b

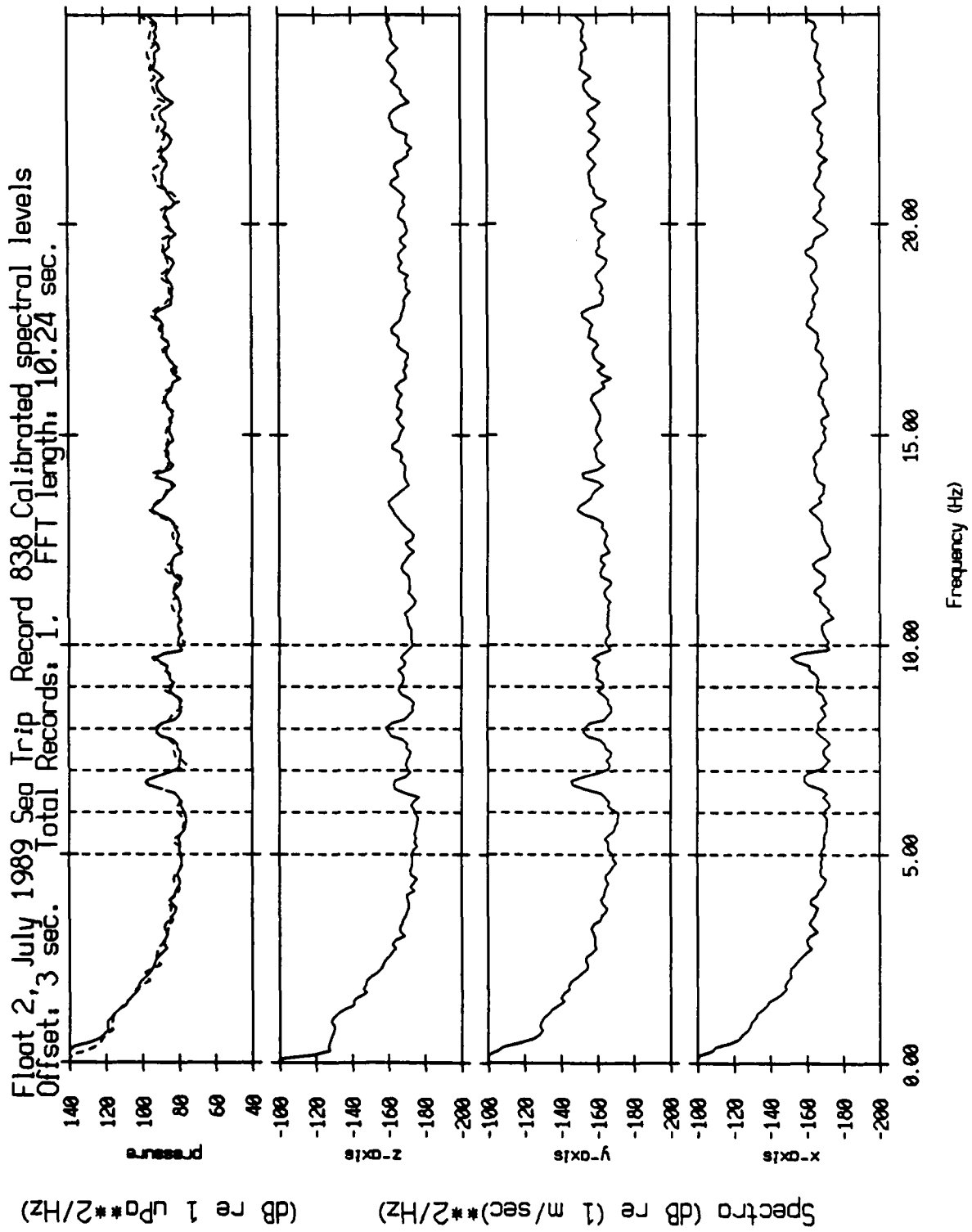


Figure XII.5c

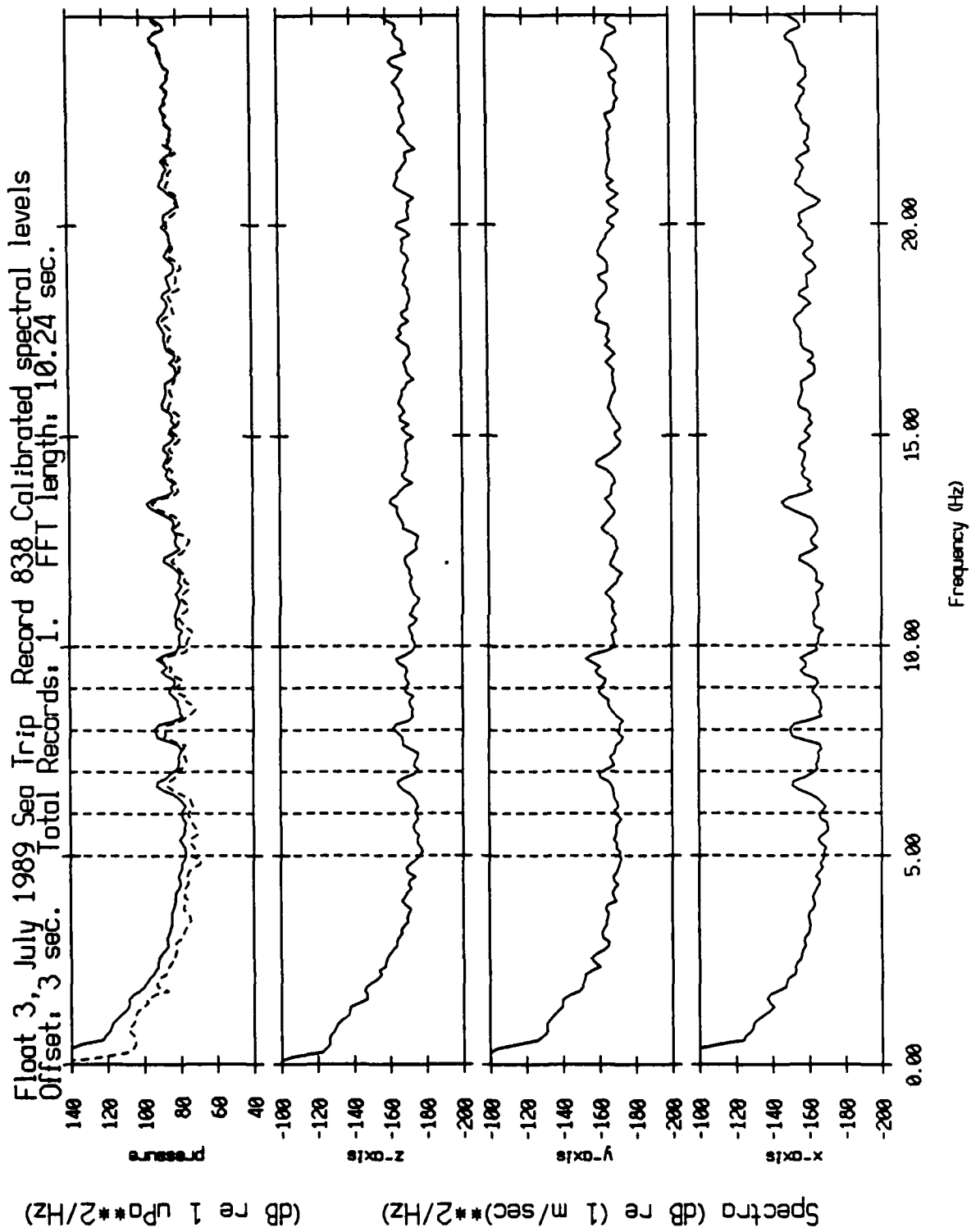


Figure XII.5d

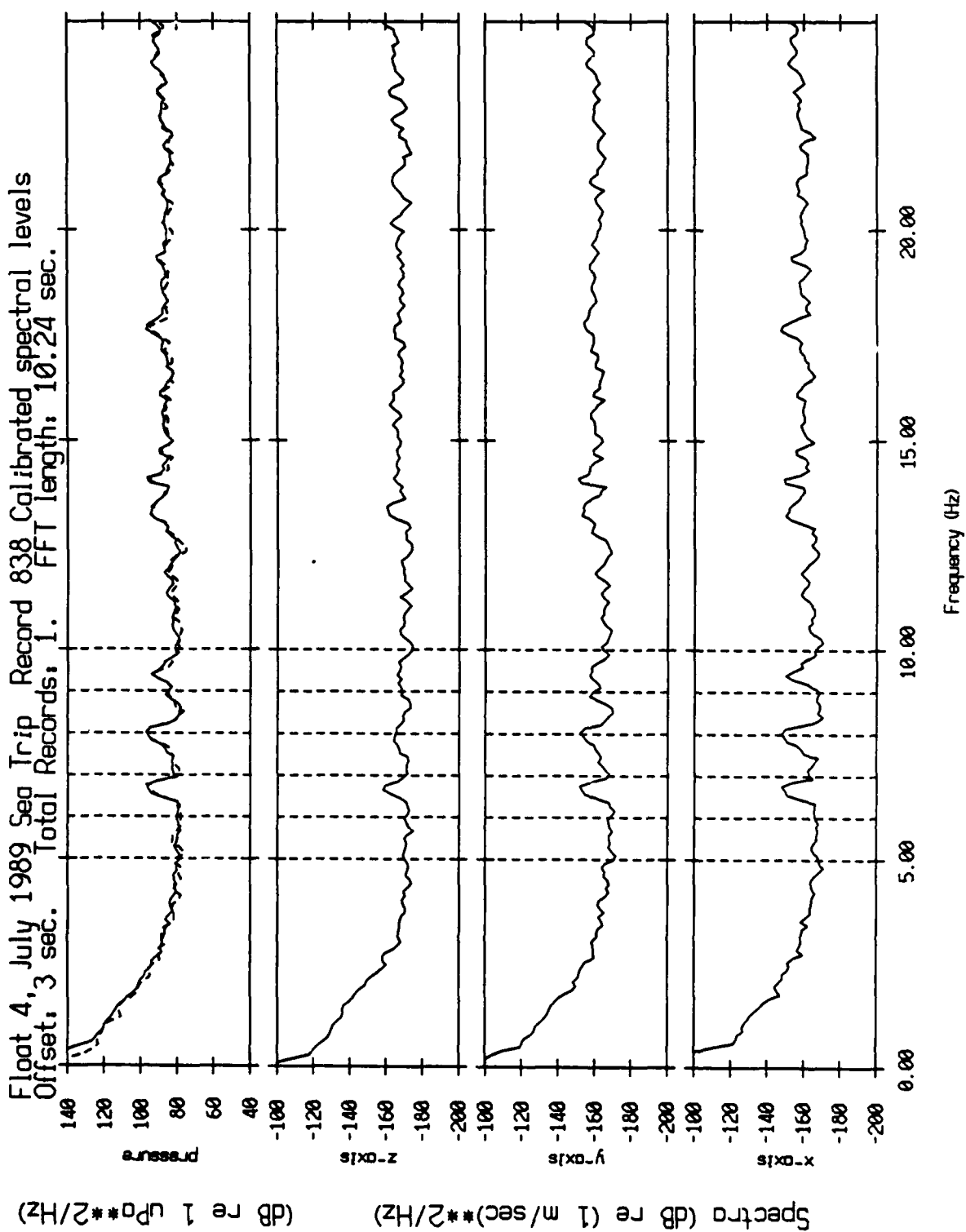


Figure XII.5e

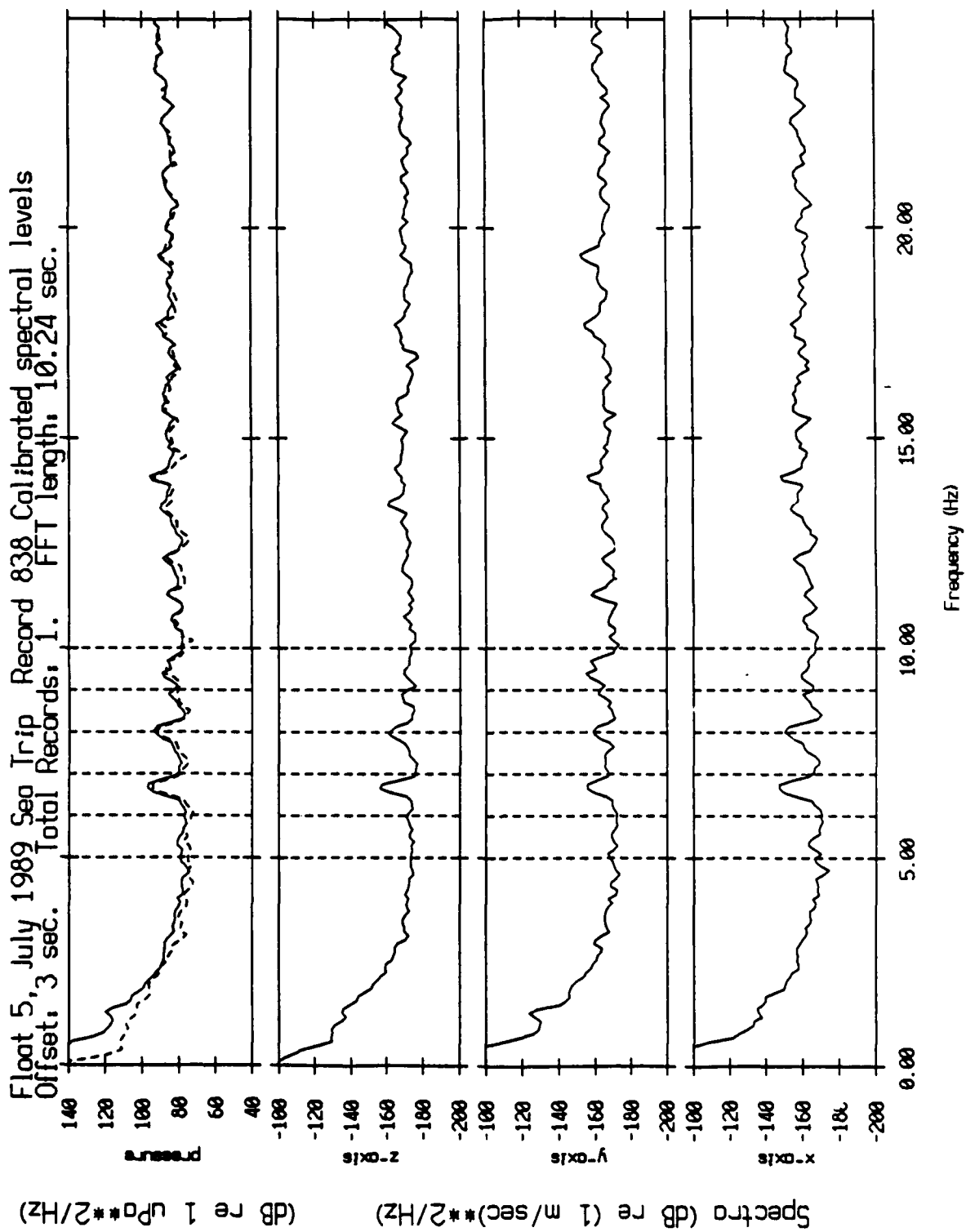


Figure XII.5f



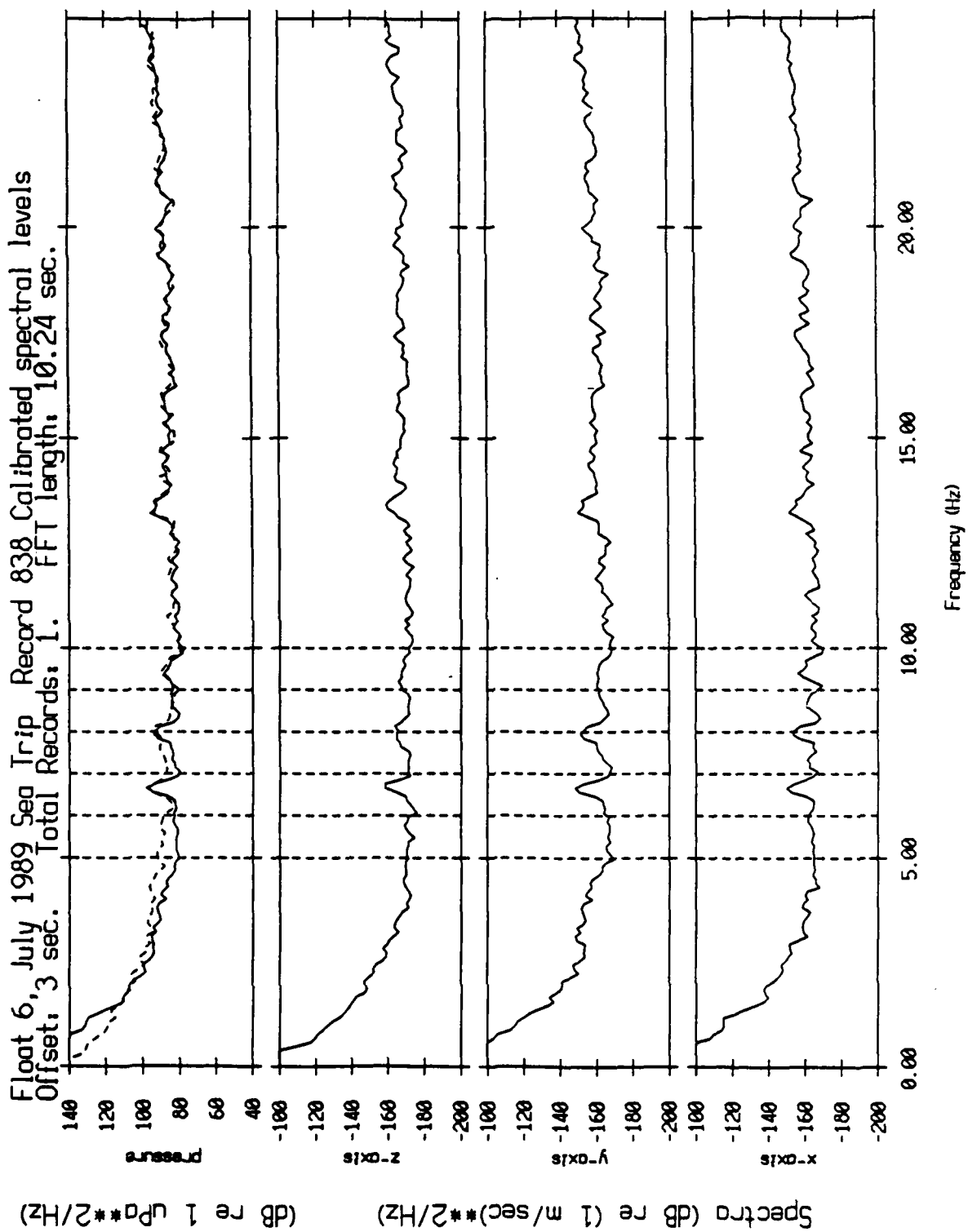


Figure XII.5g

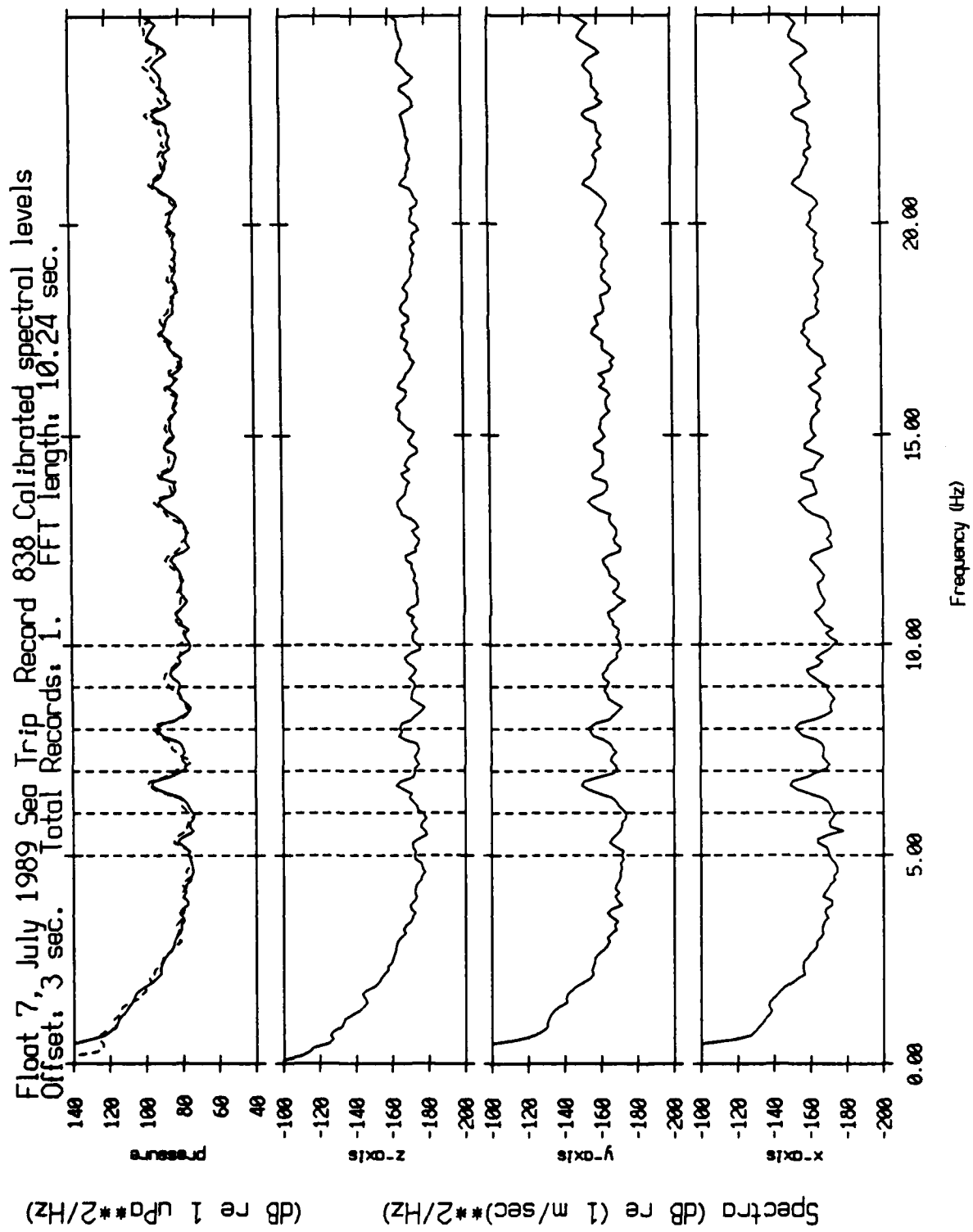


Figure XII.5h

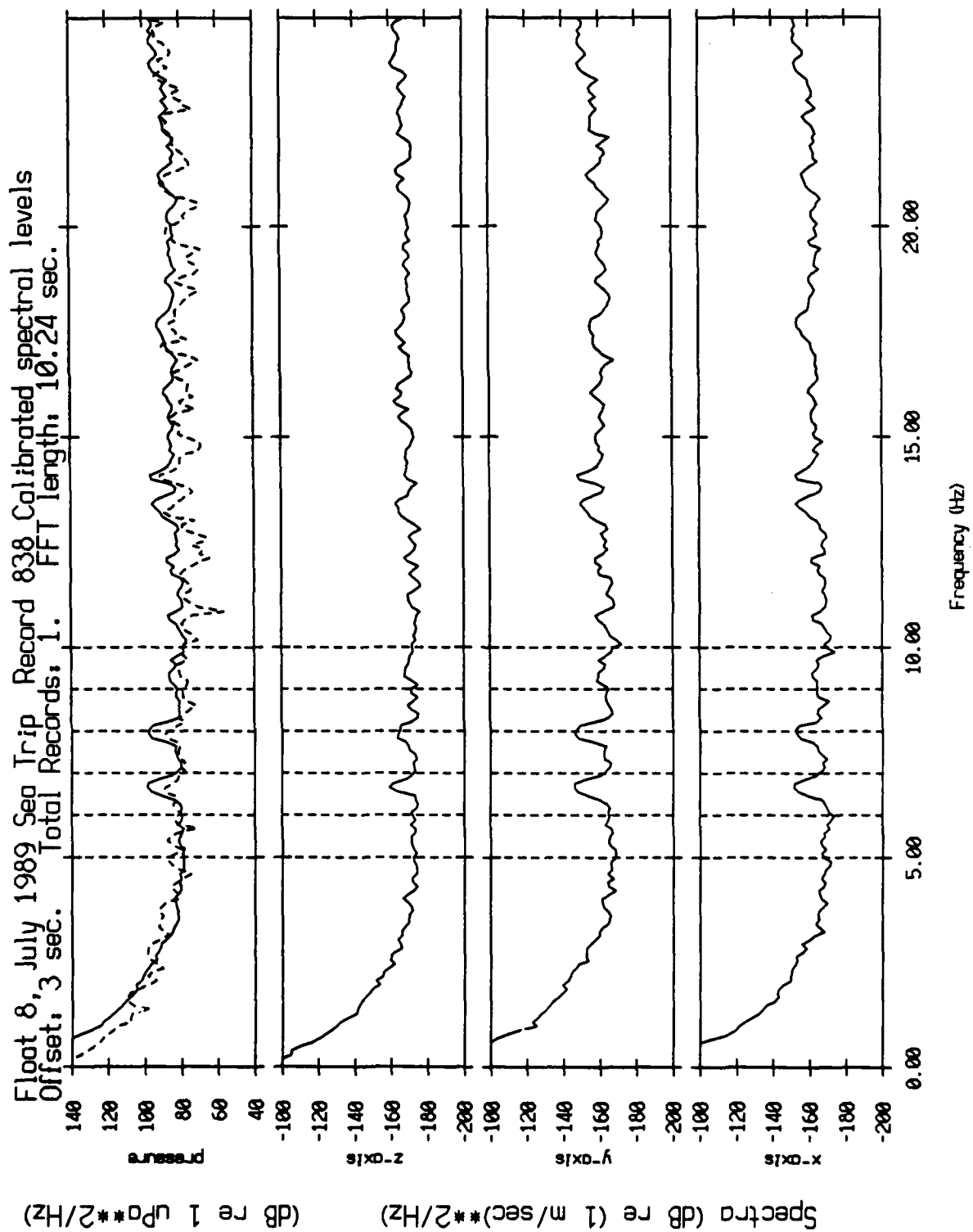


Figure XII.5i

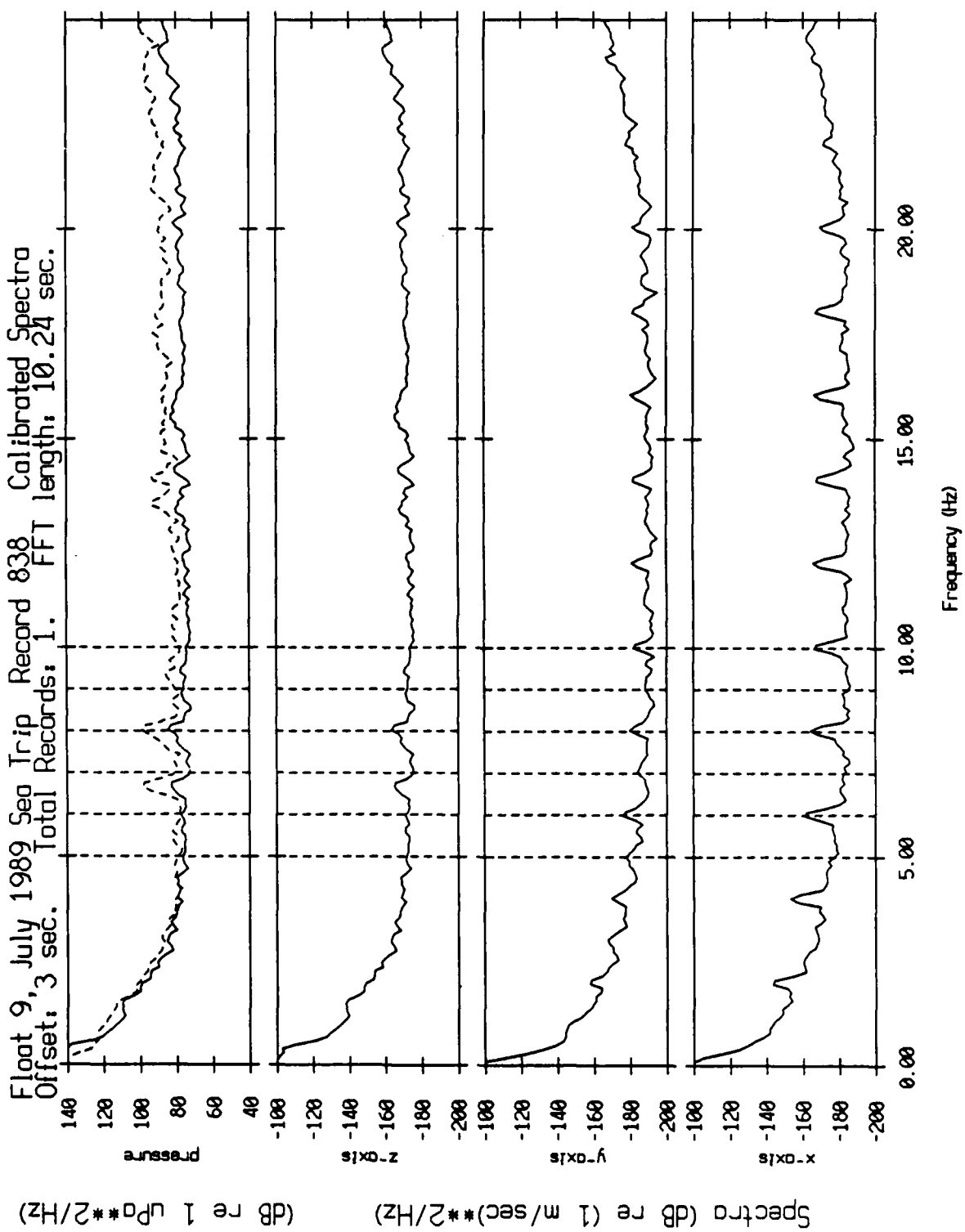


Figure XII.5j

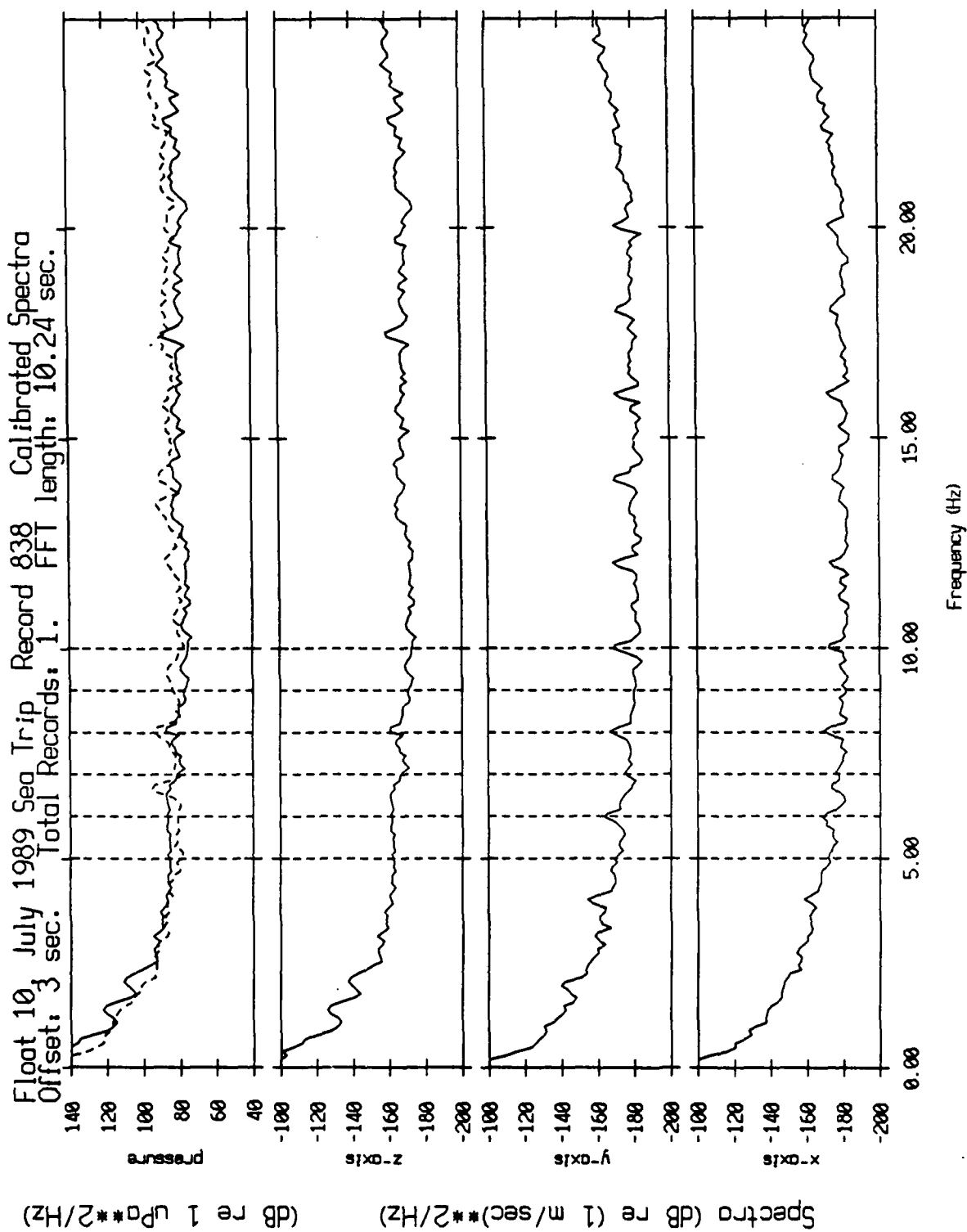


Figure XII.5k

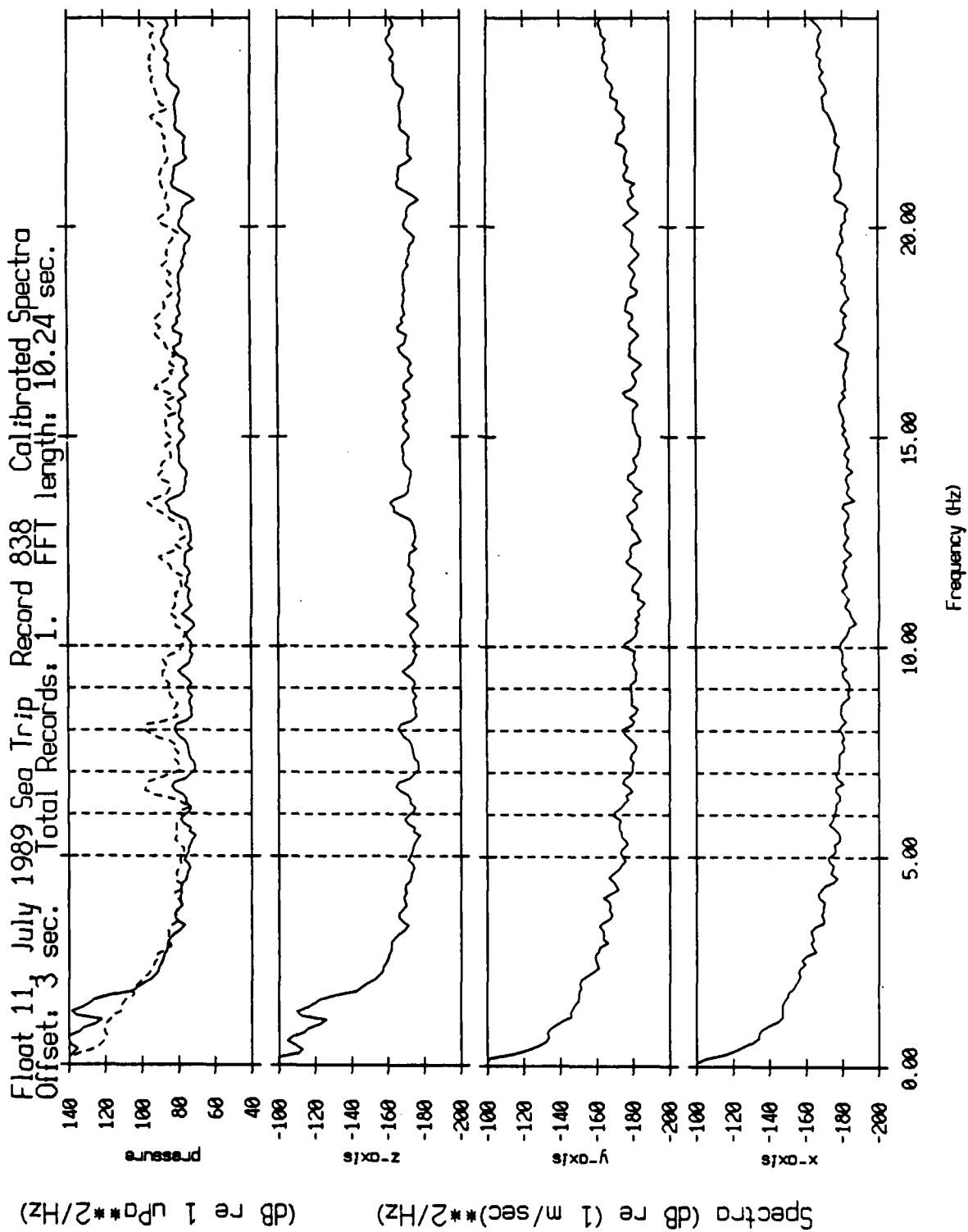


Figure XII.51

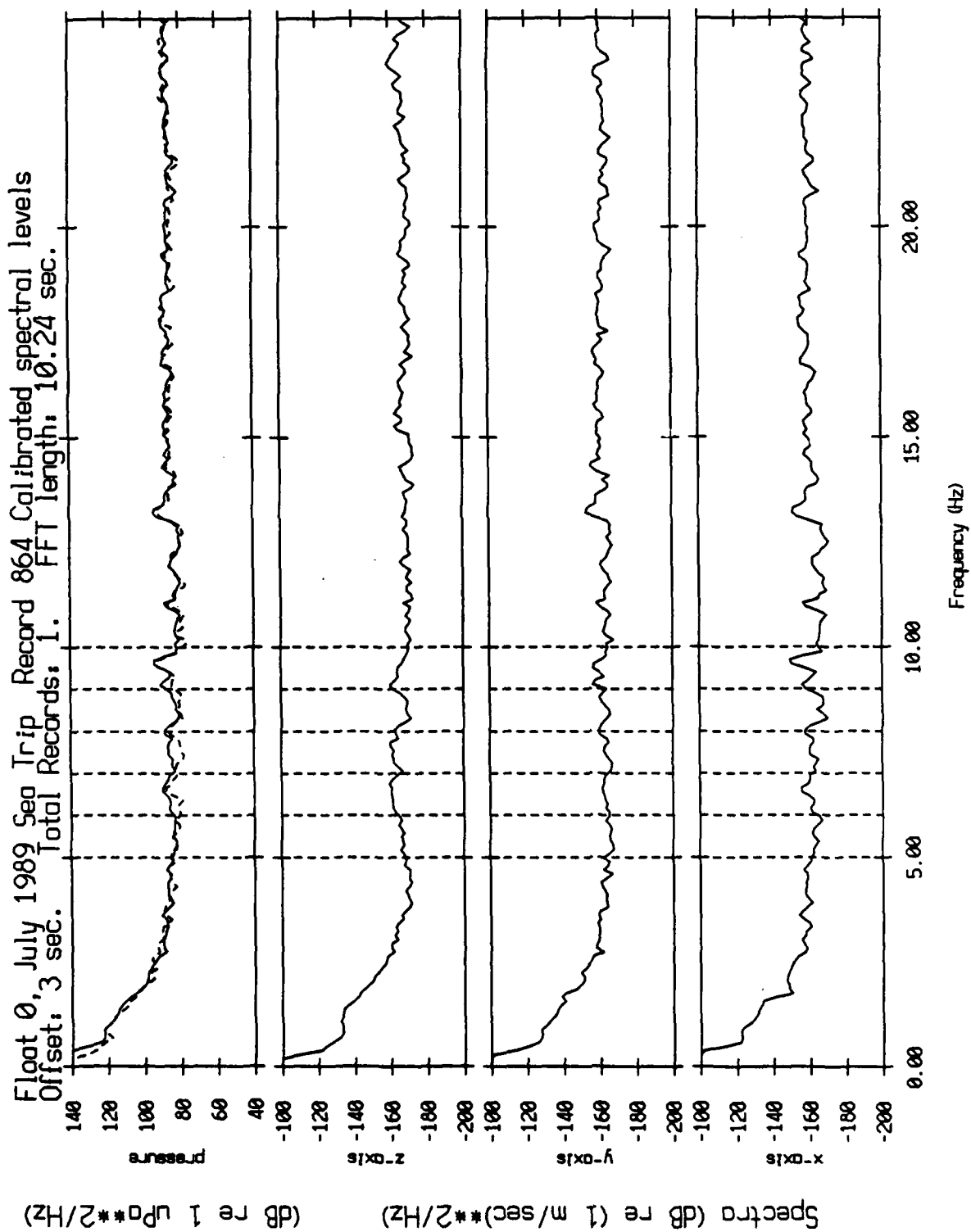


Figure XII.6a

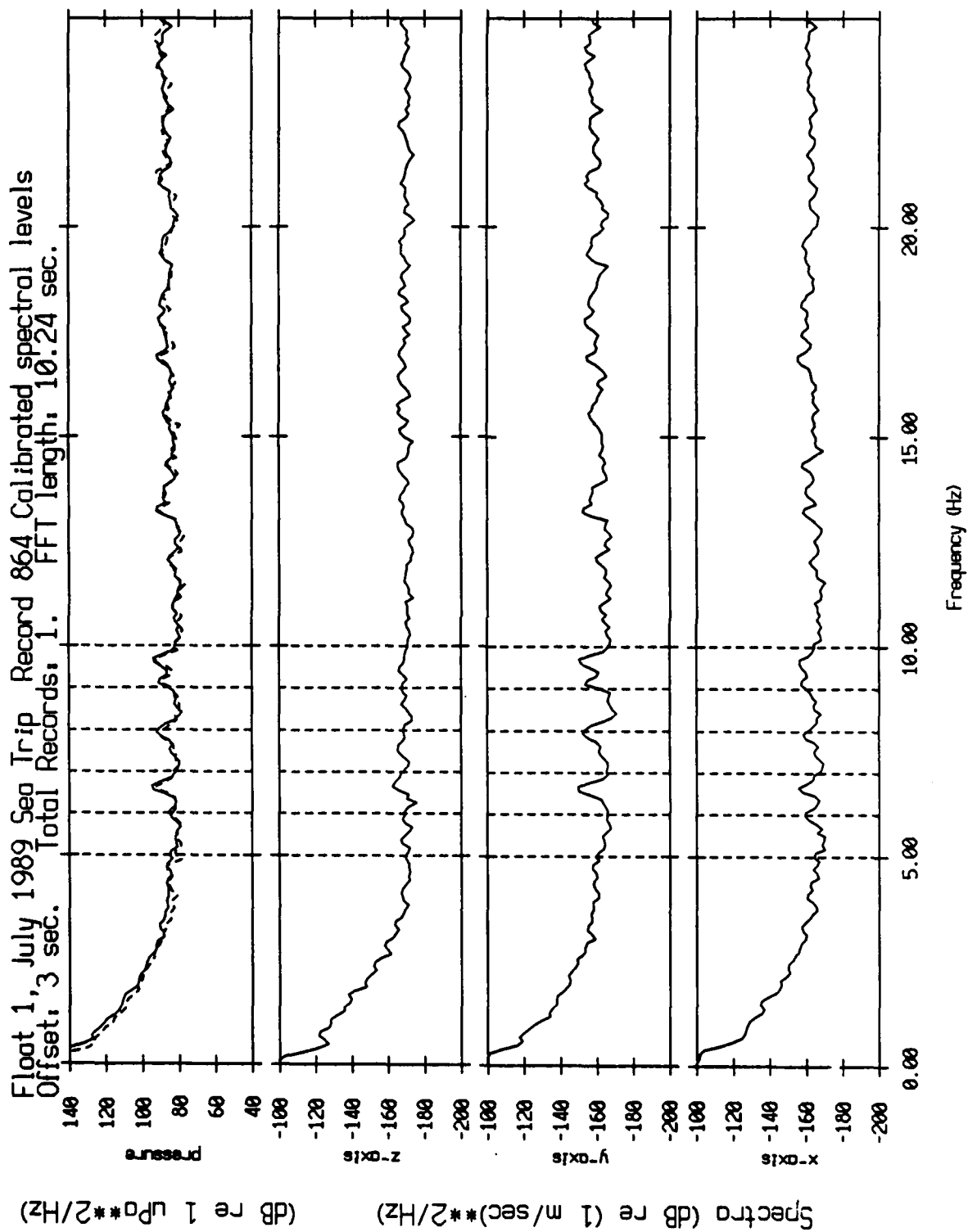


Figure XII.6b



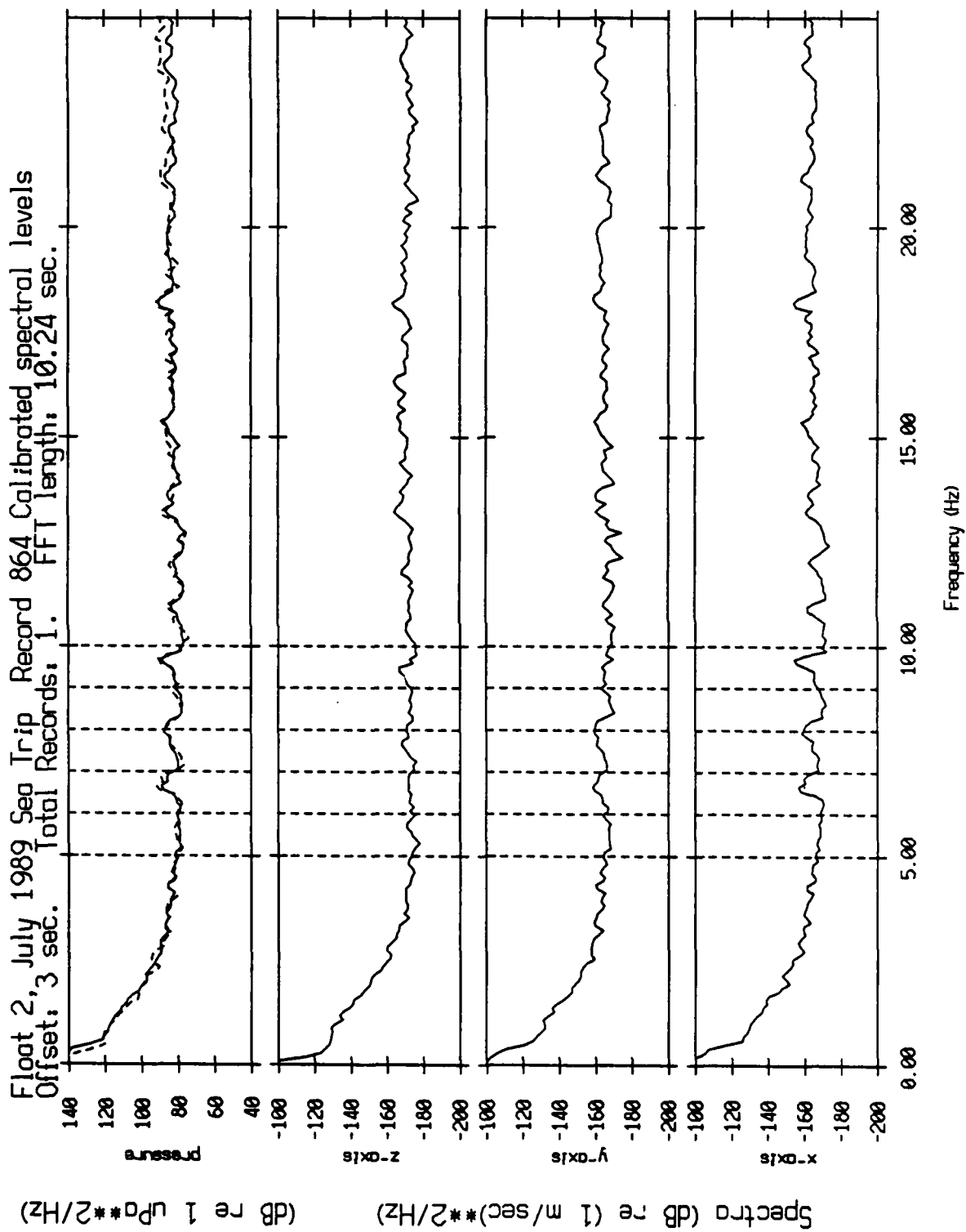


Figure XII.6c

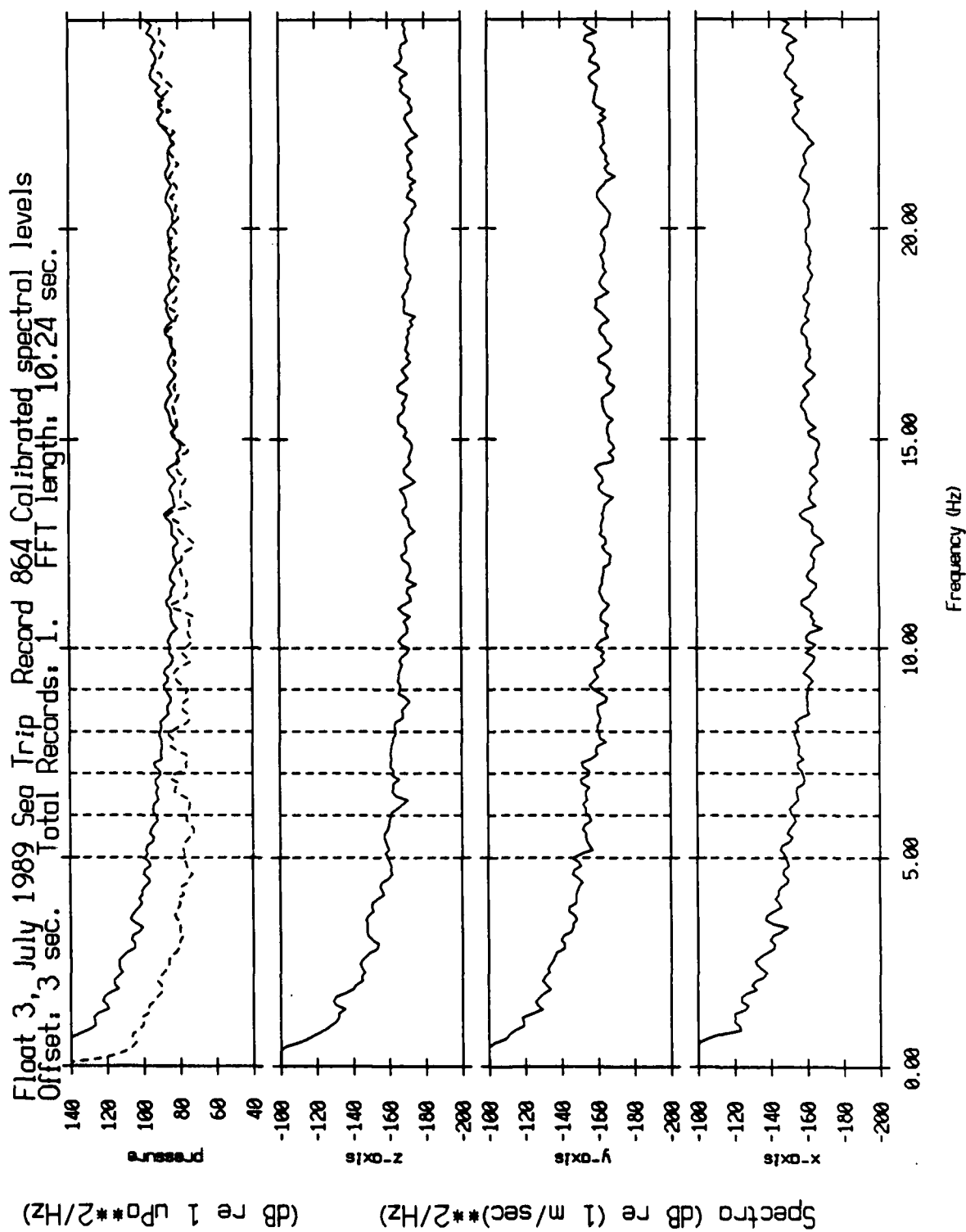


Figure XII.6d

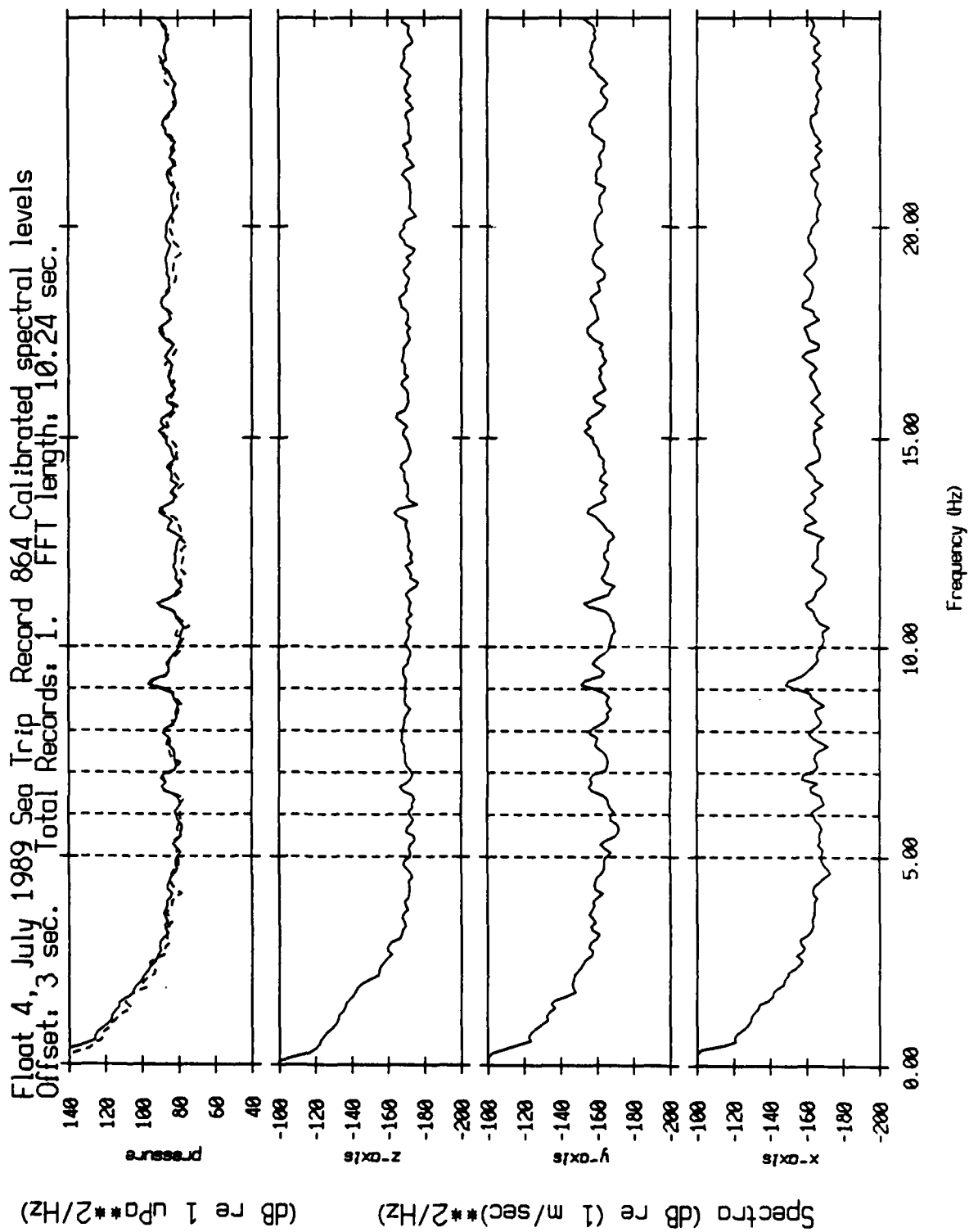


Figure XII.6e

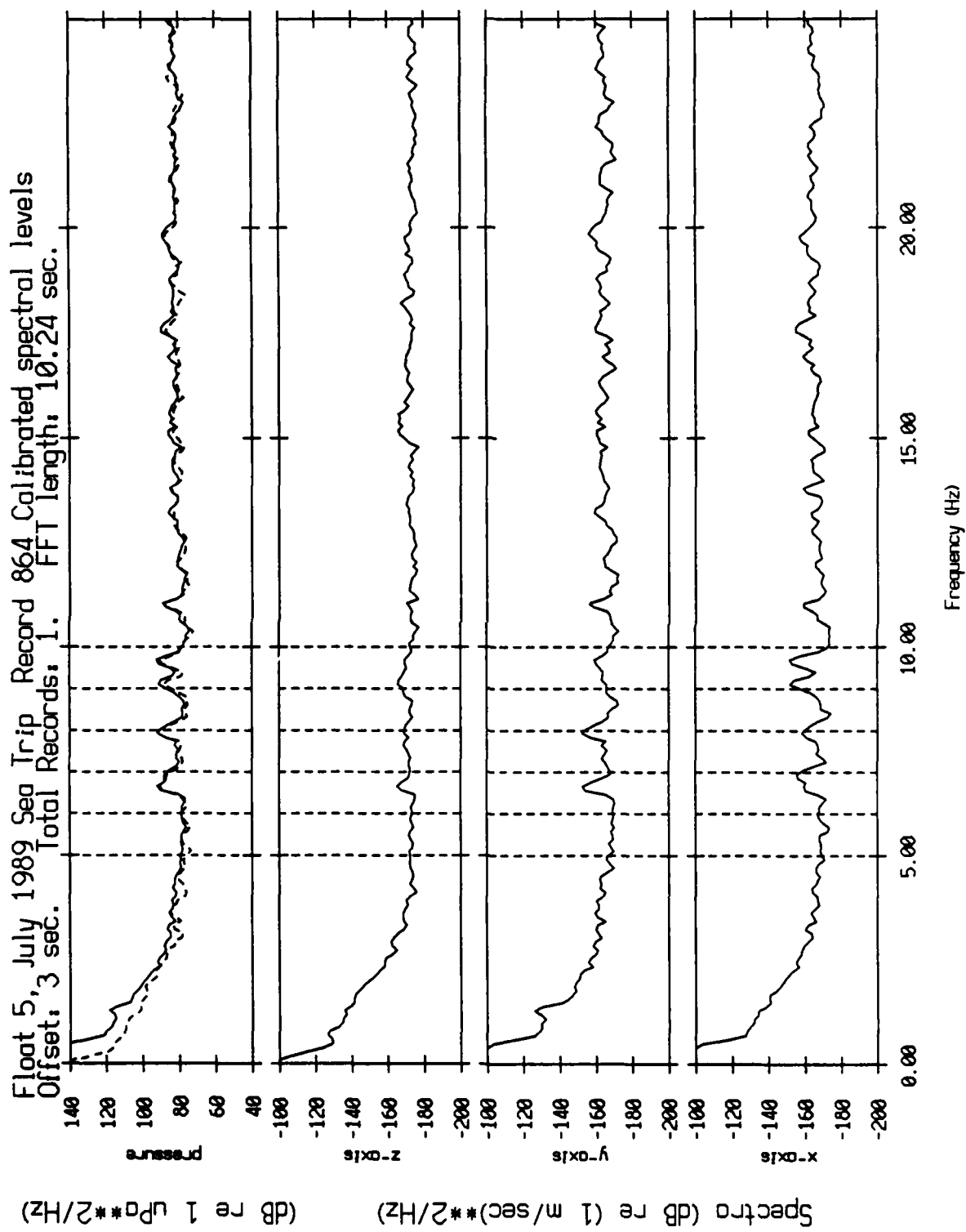


Figure XII.6f

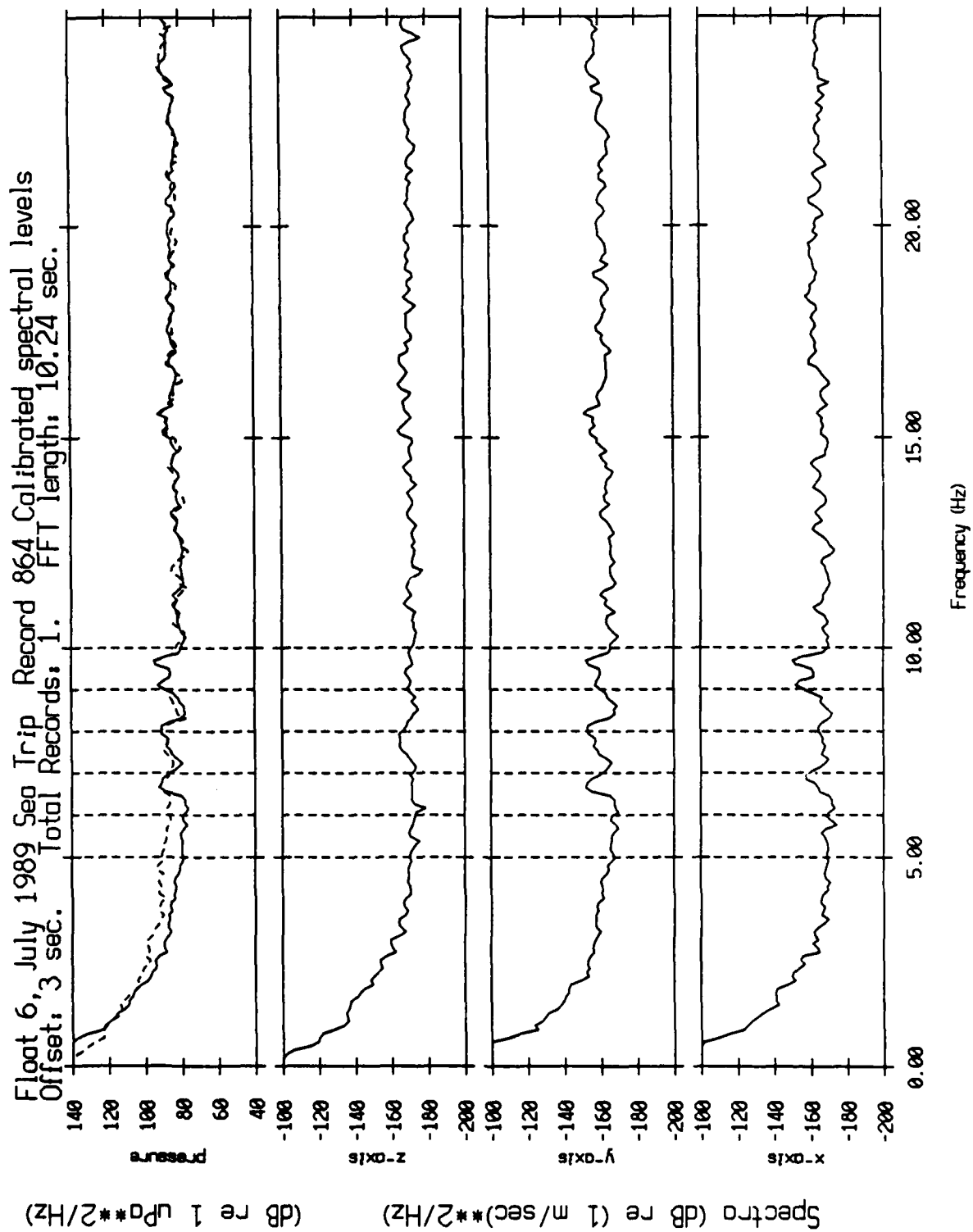


Figure XII.6g

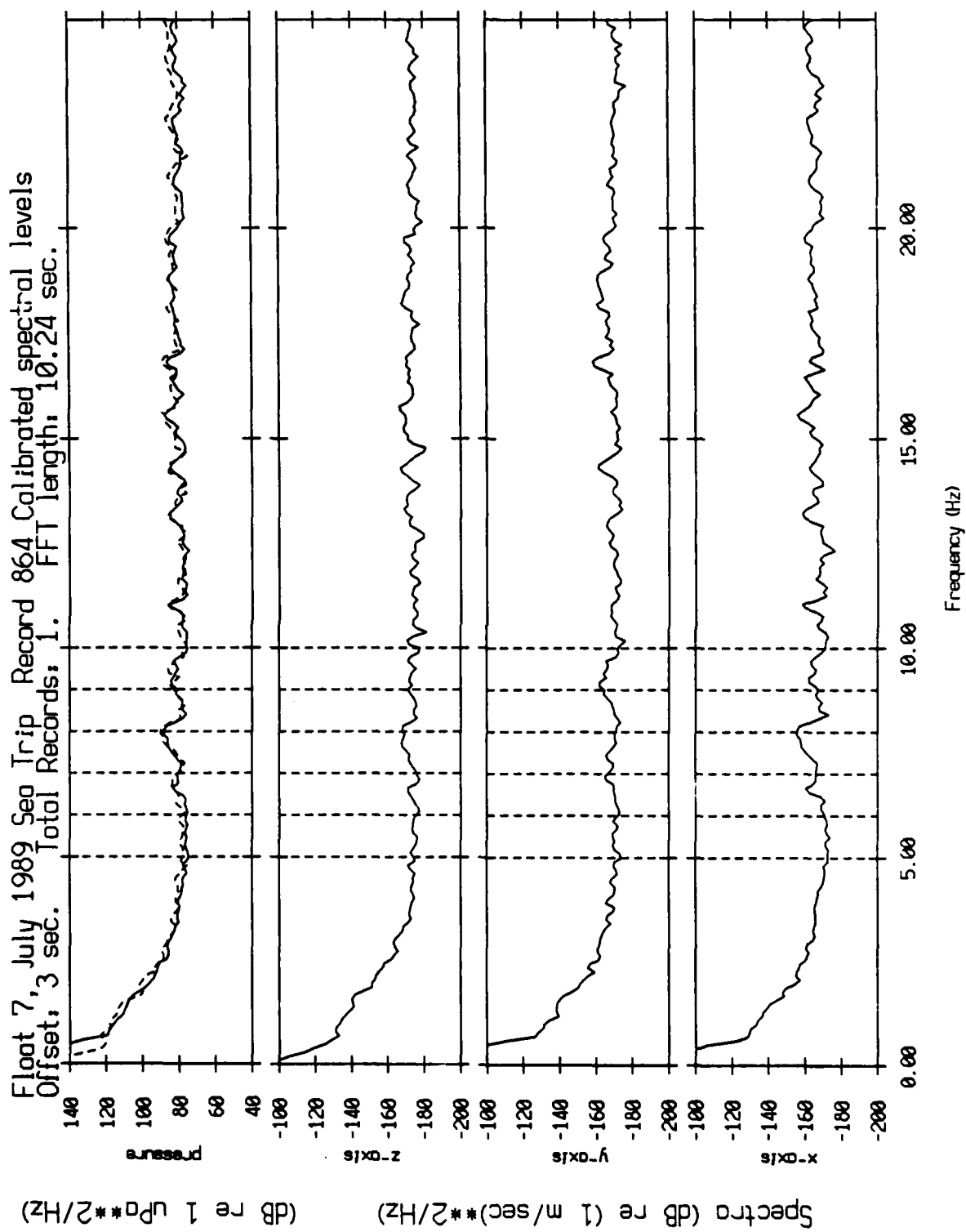


Figure XII.6h

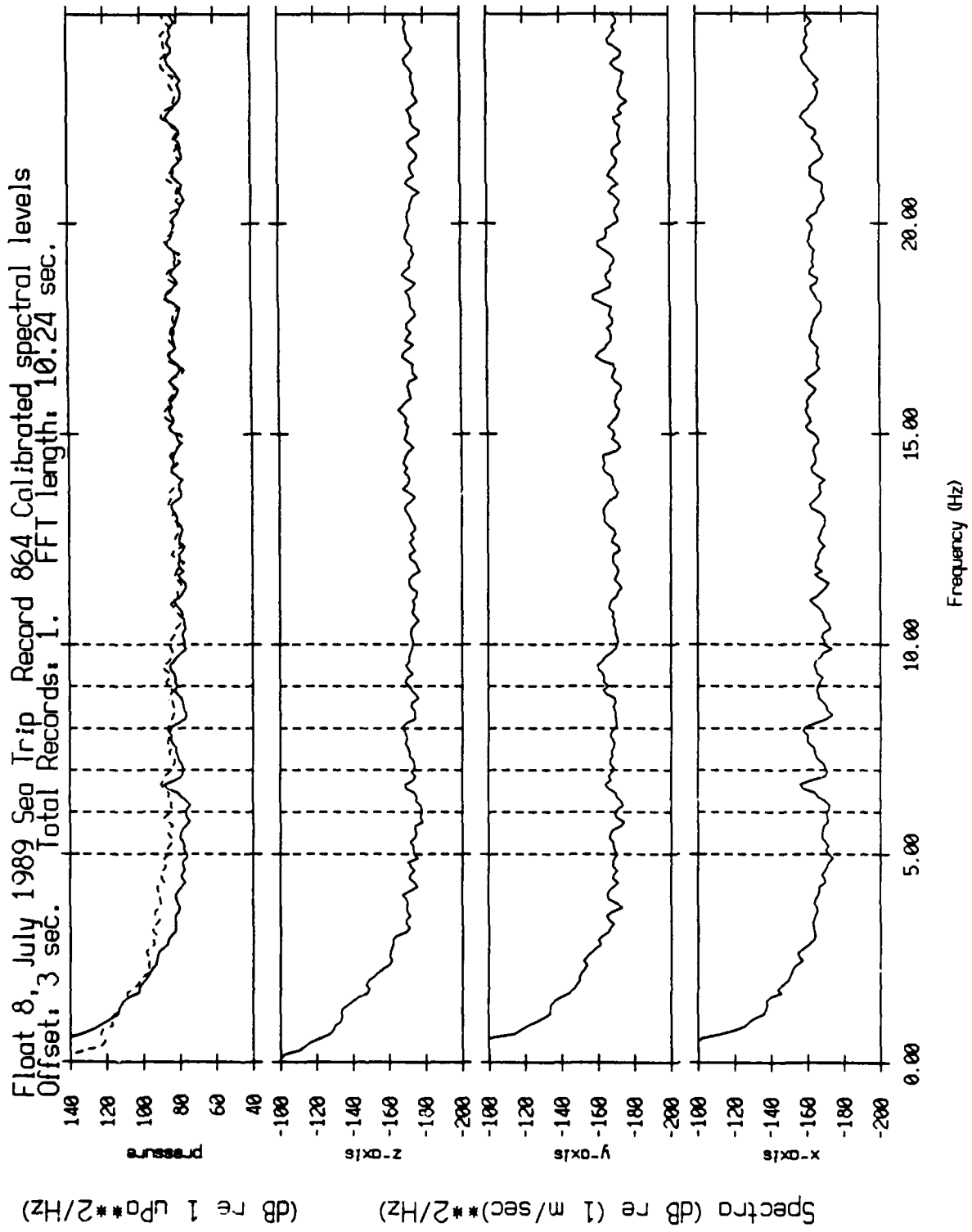


Figure XII.6i

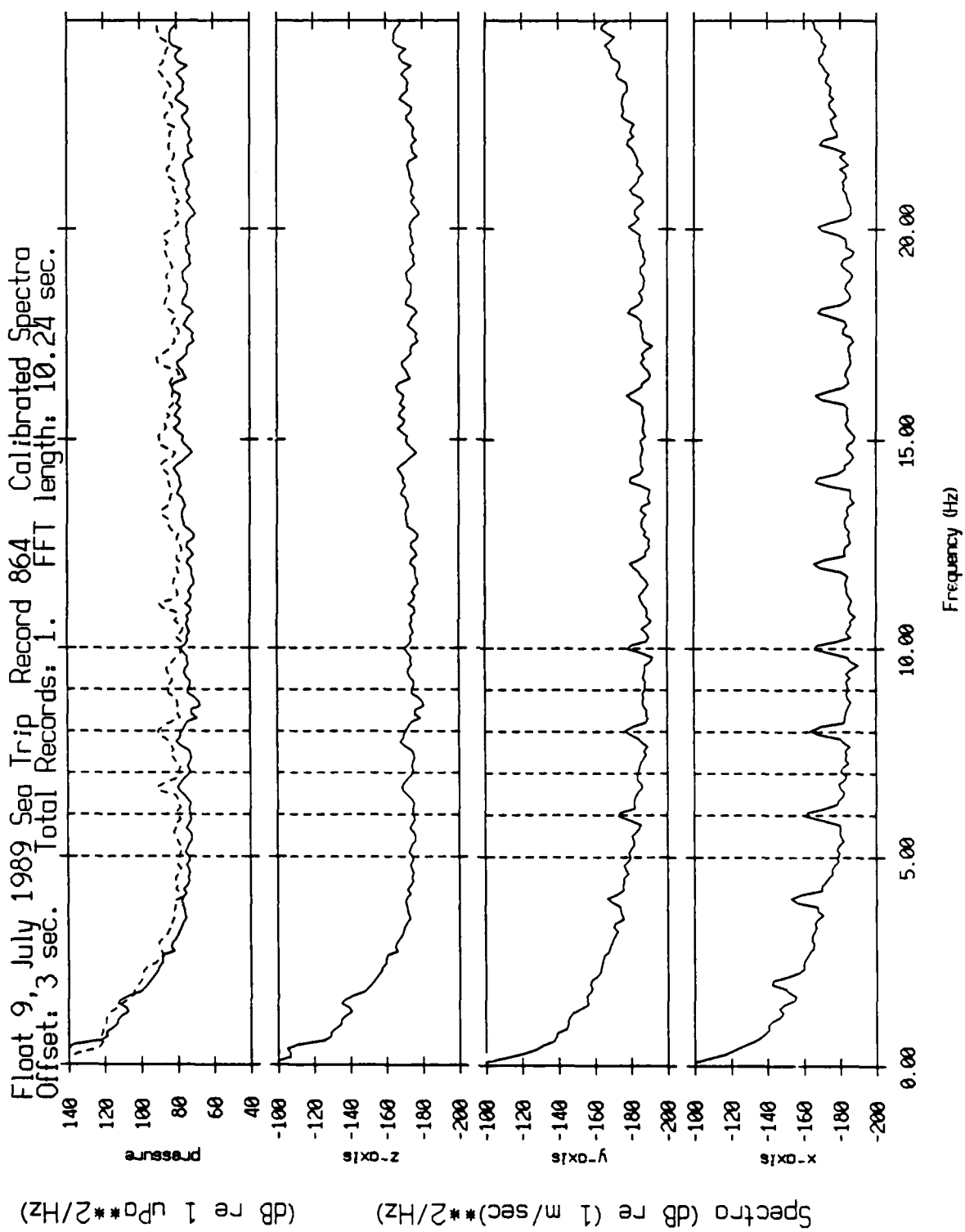


Figure XII.6j



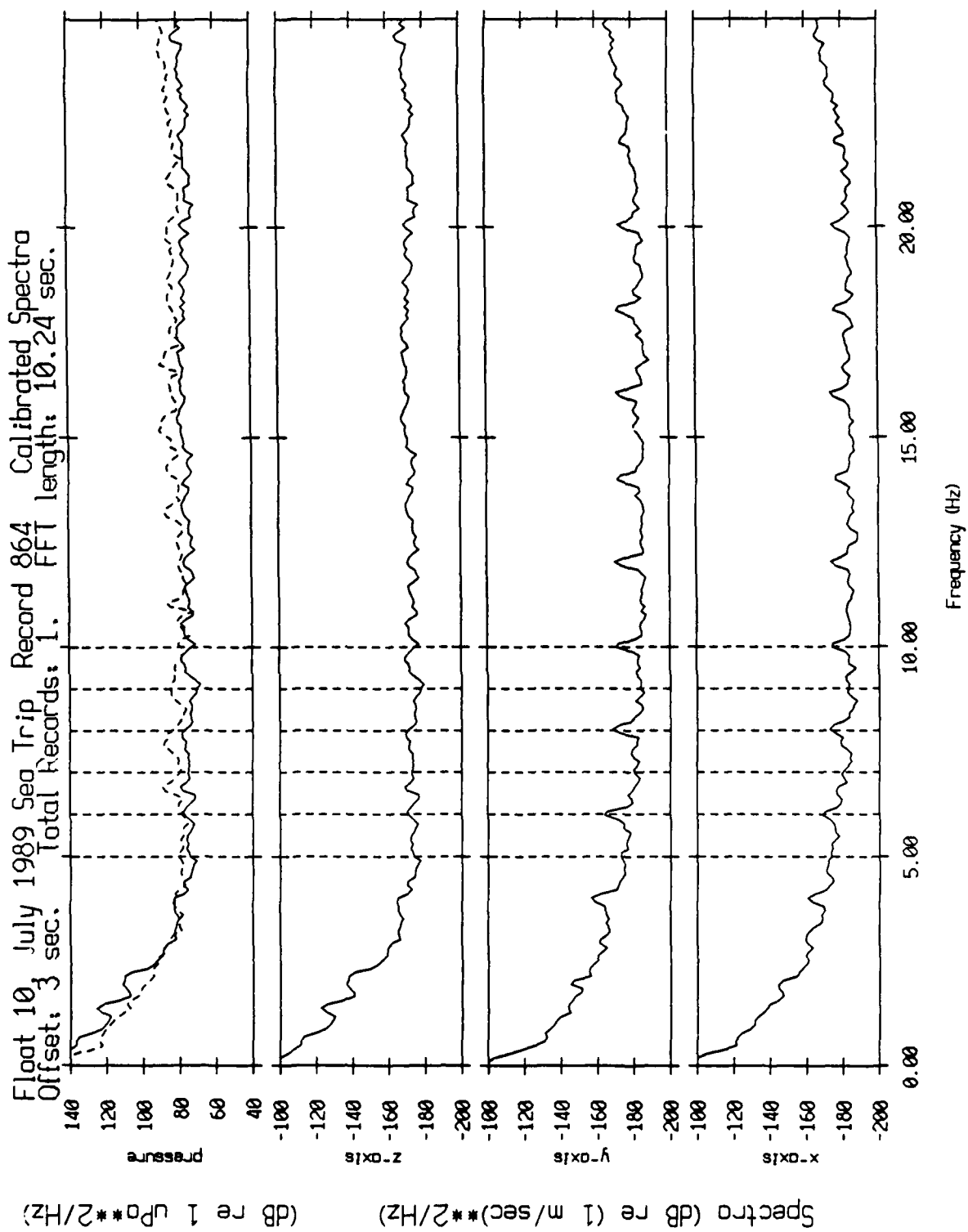


Figure XII.6k

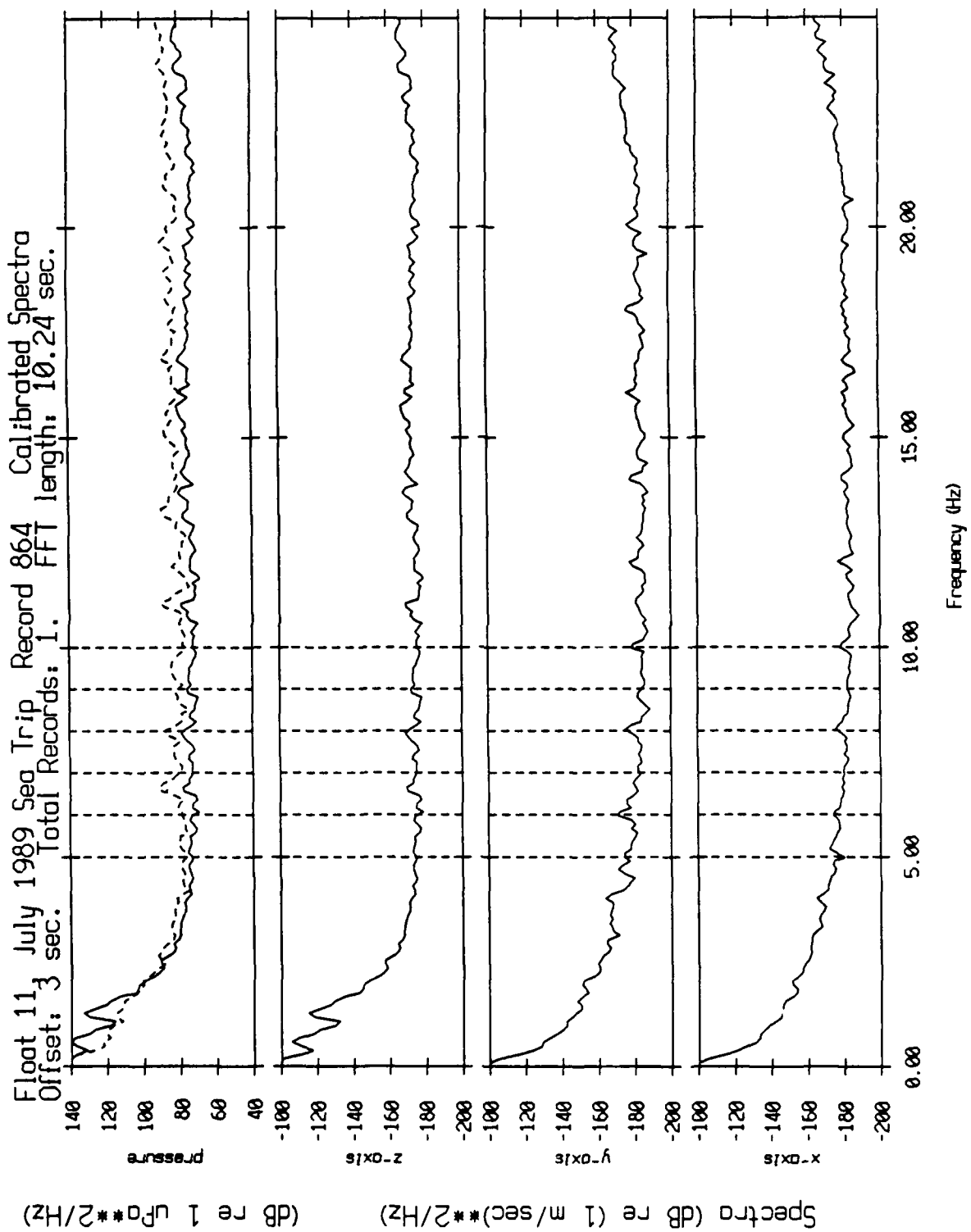


Figure XII.61

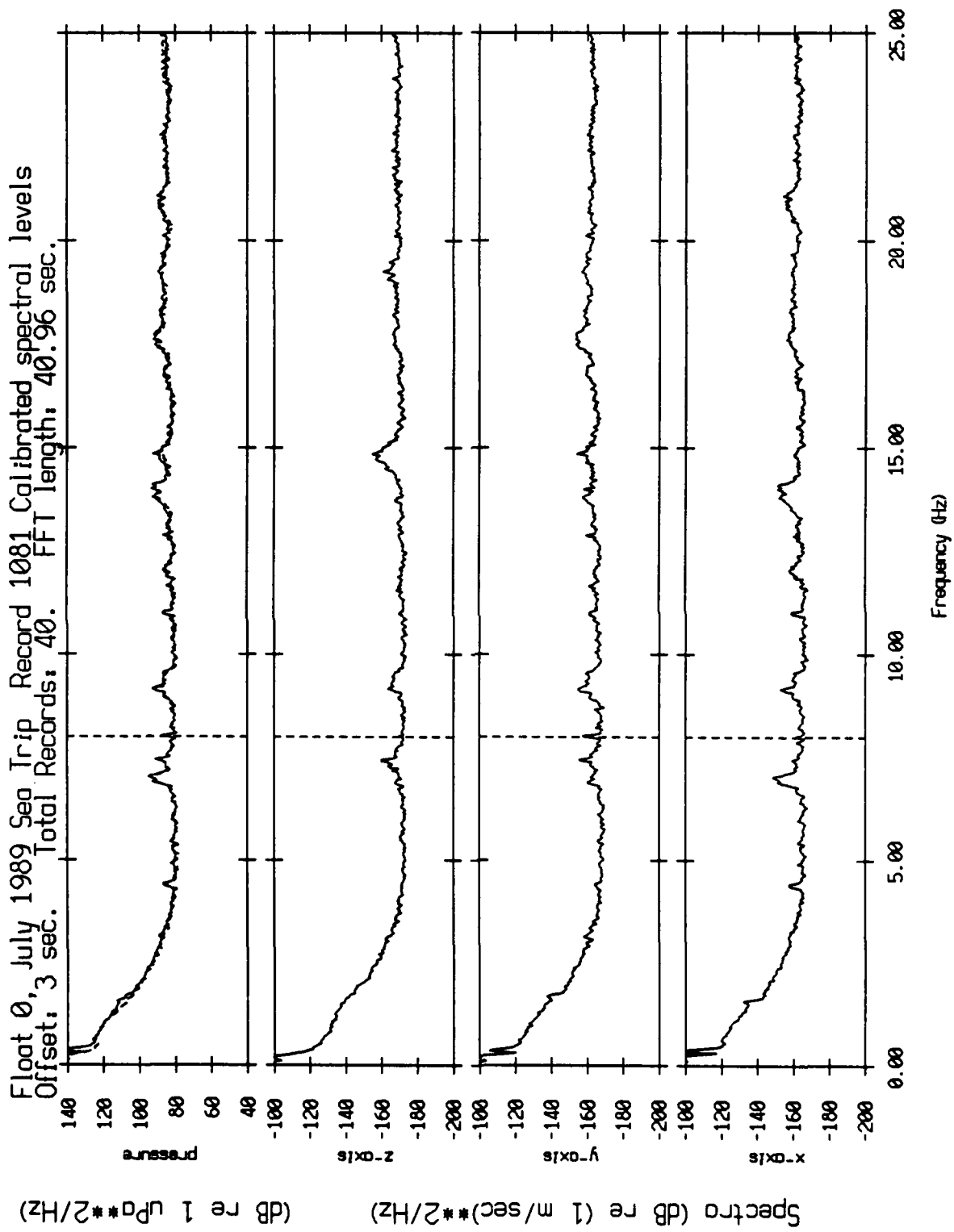


Figure XII.7a

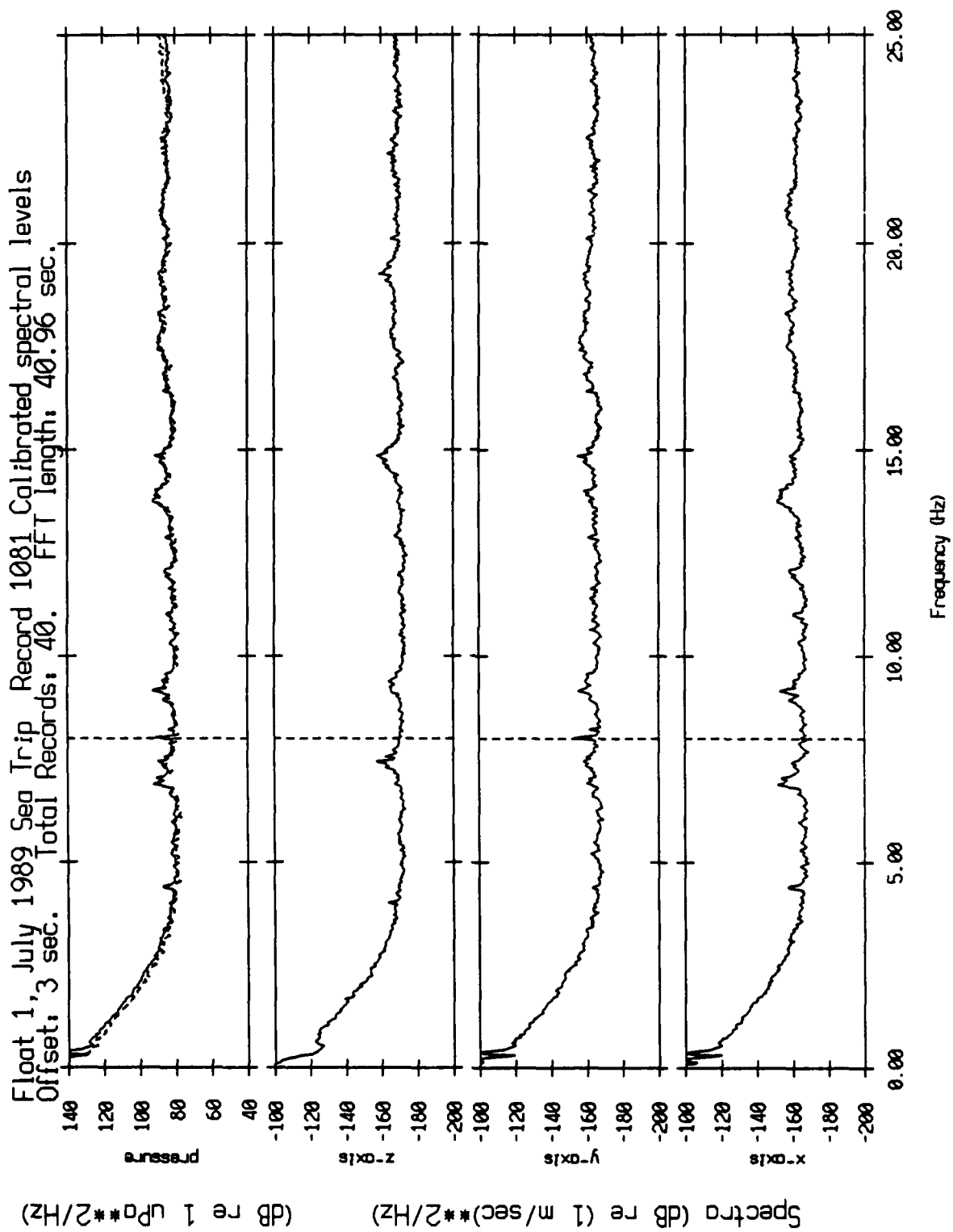


Figure XII.7b

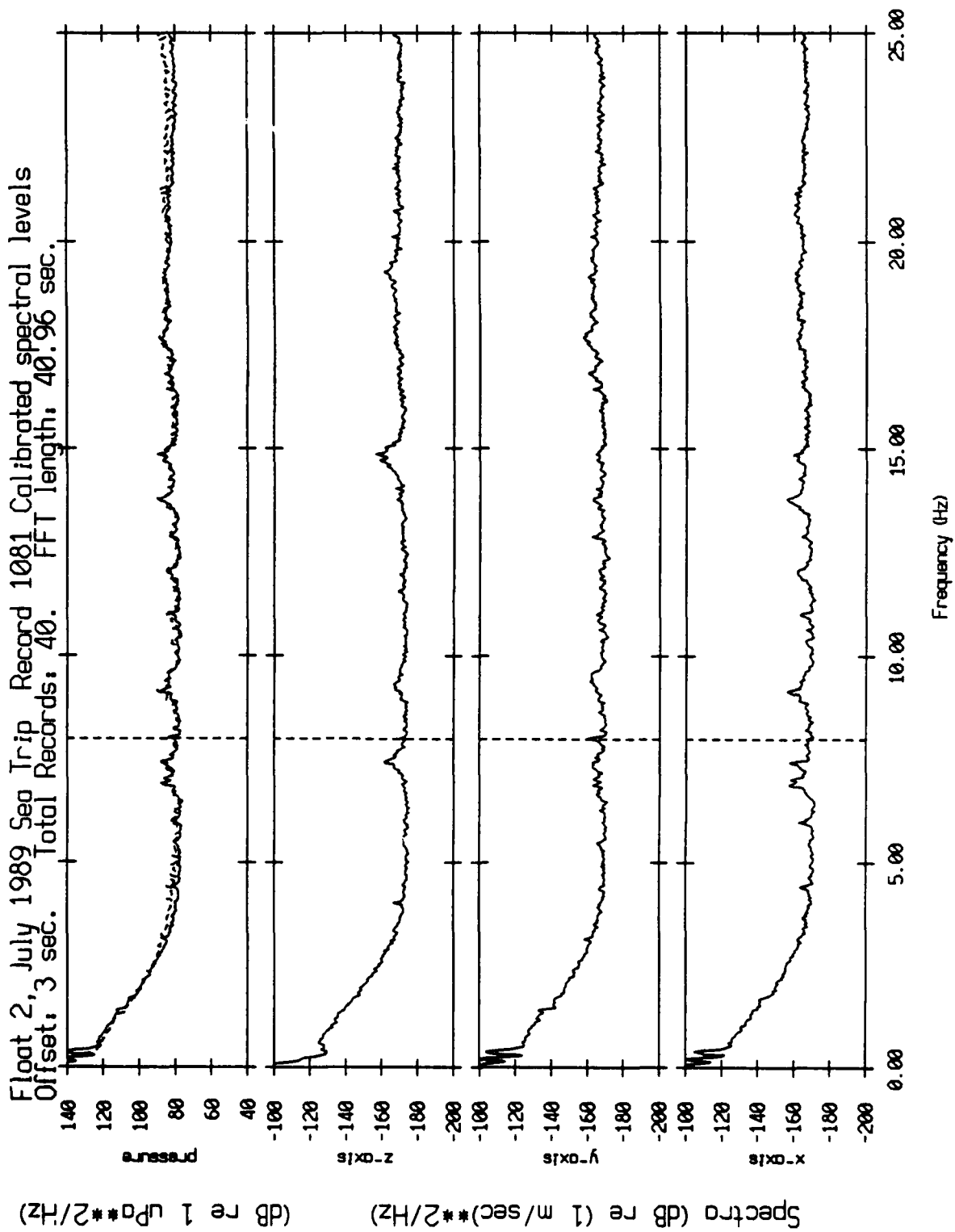


Figure XII.7c

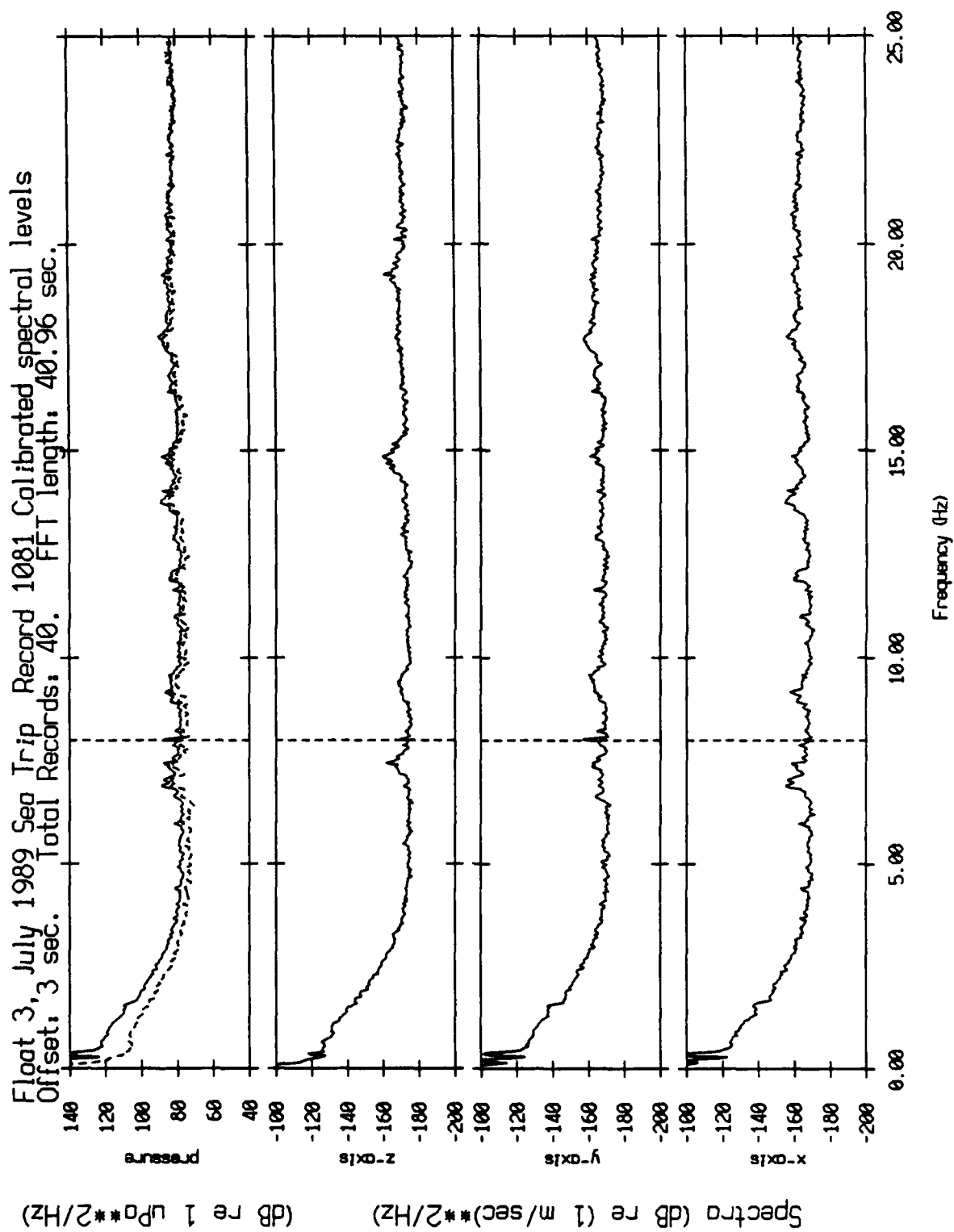


Figure XII.7d

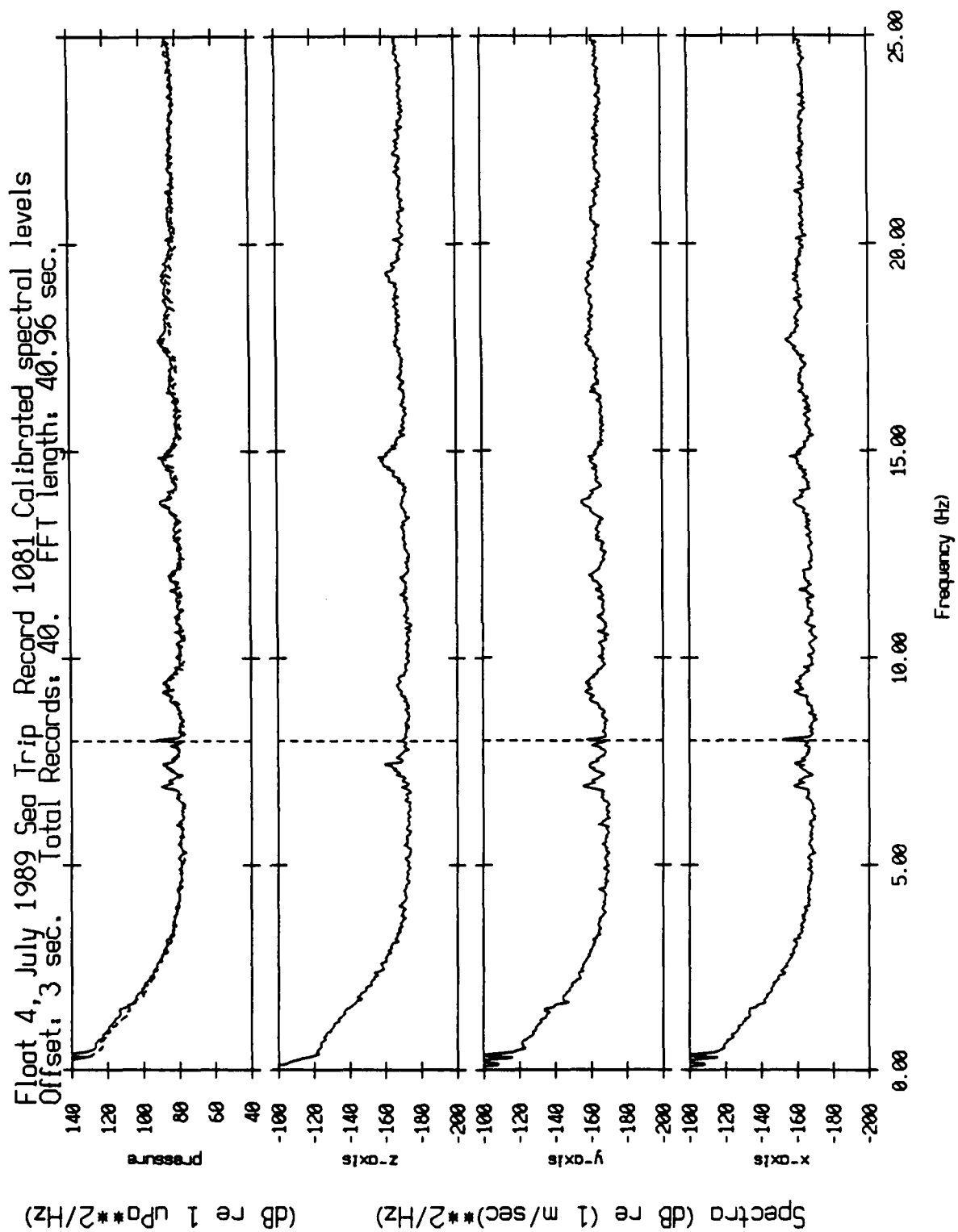


Figure XII.7e

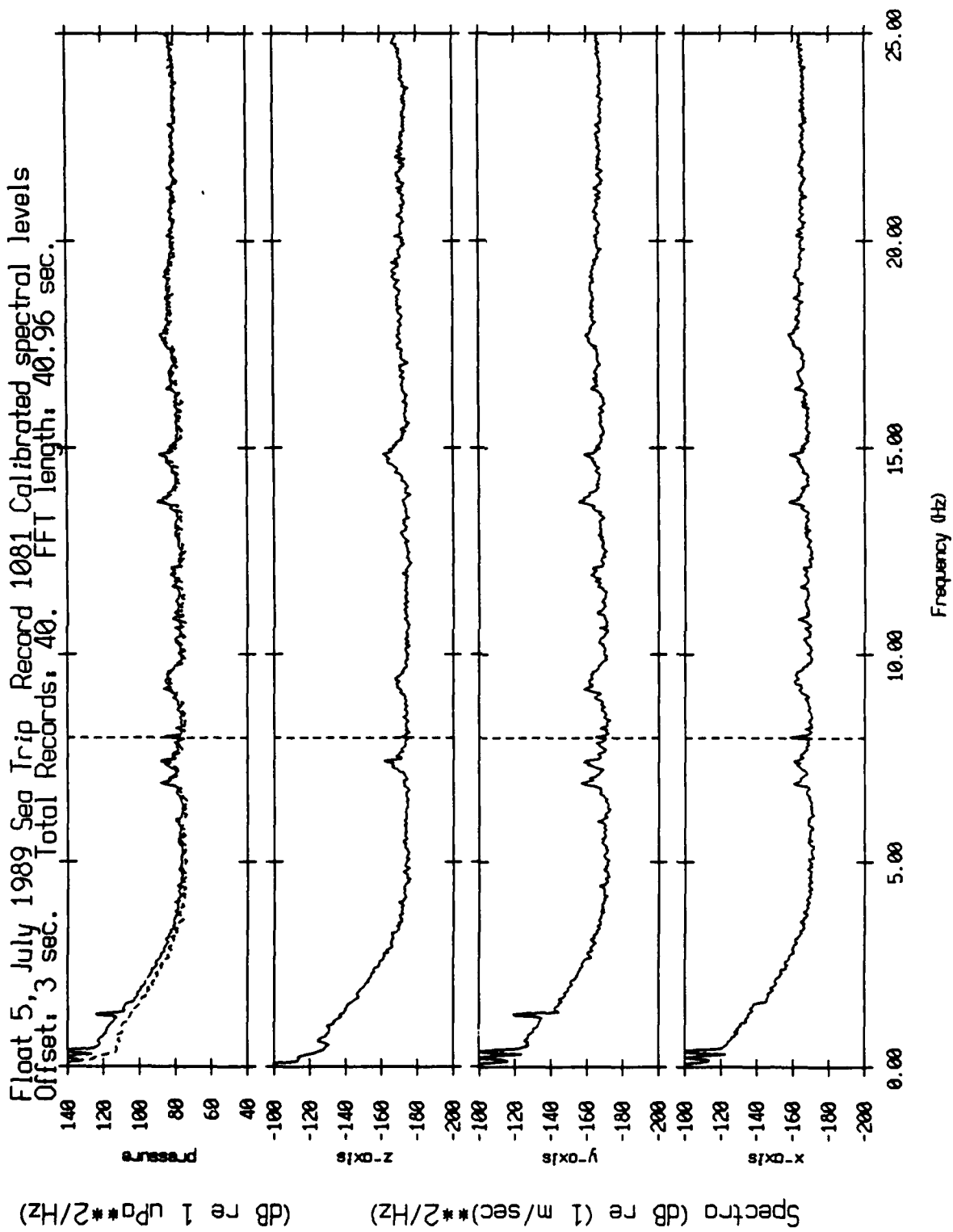


Figure XII.7f



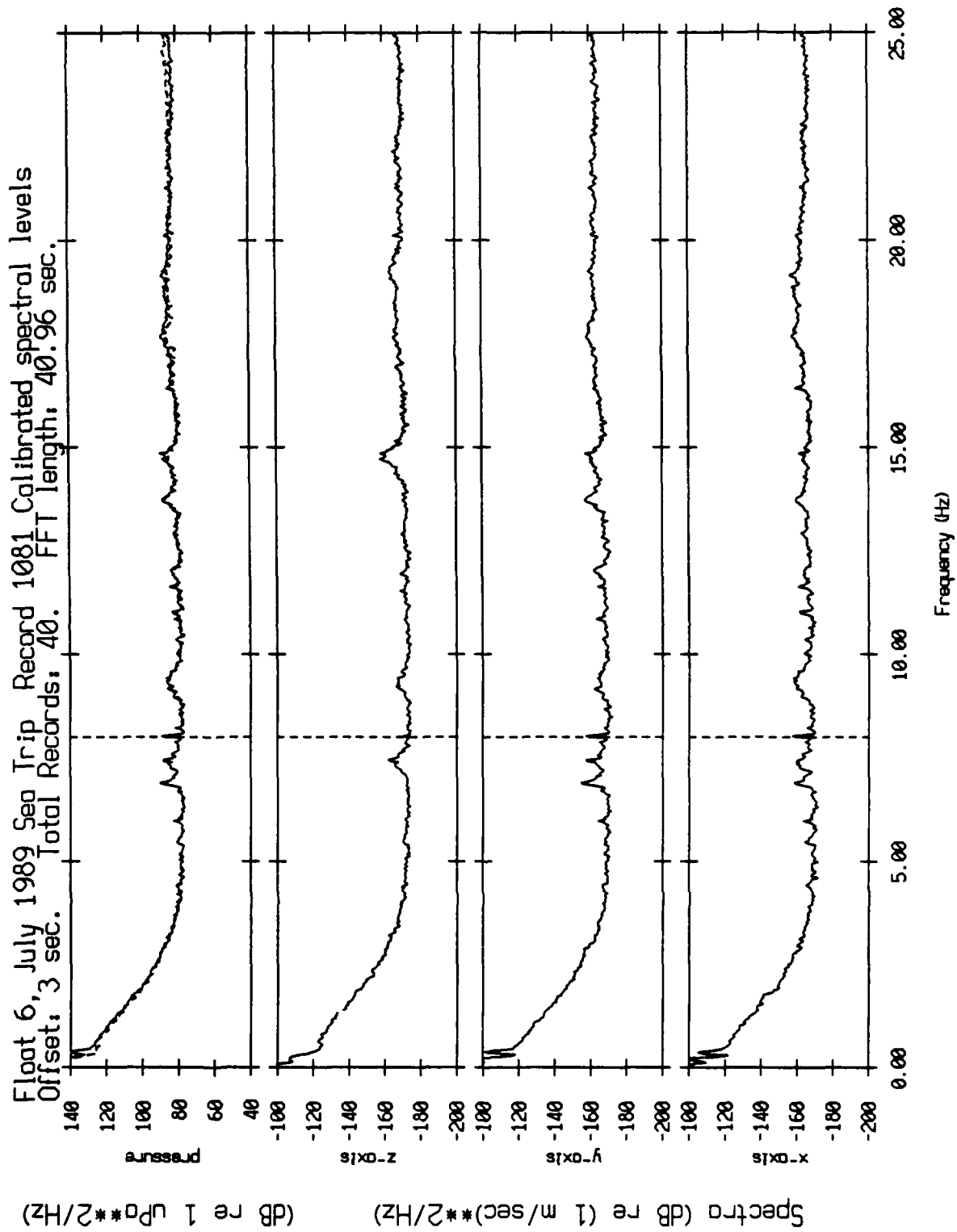


Figure XII.7g

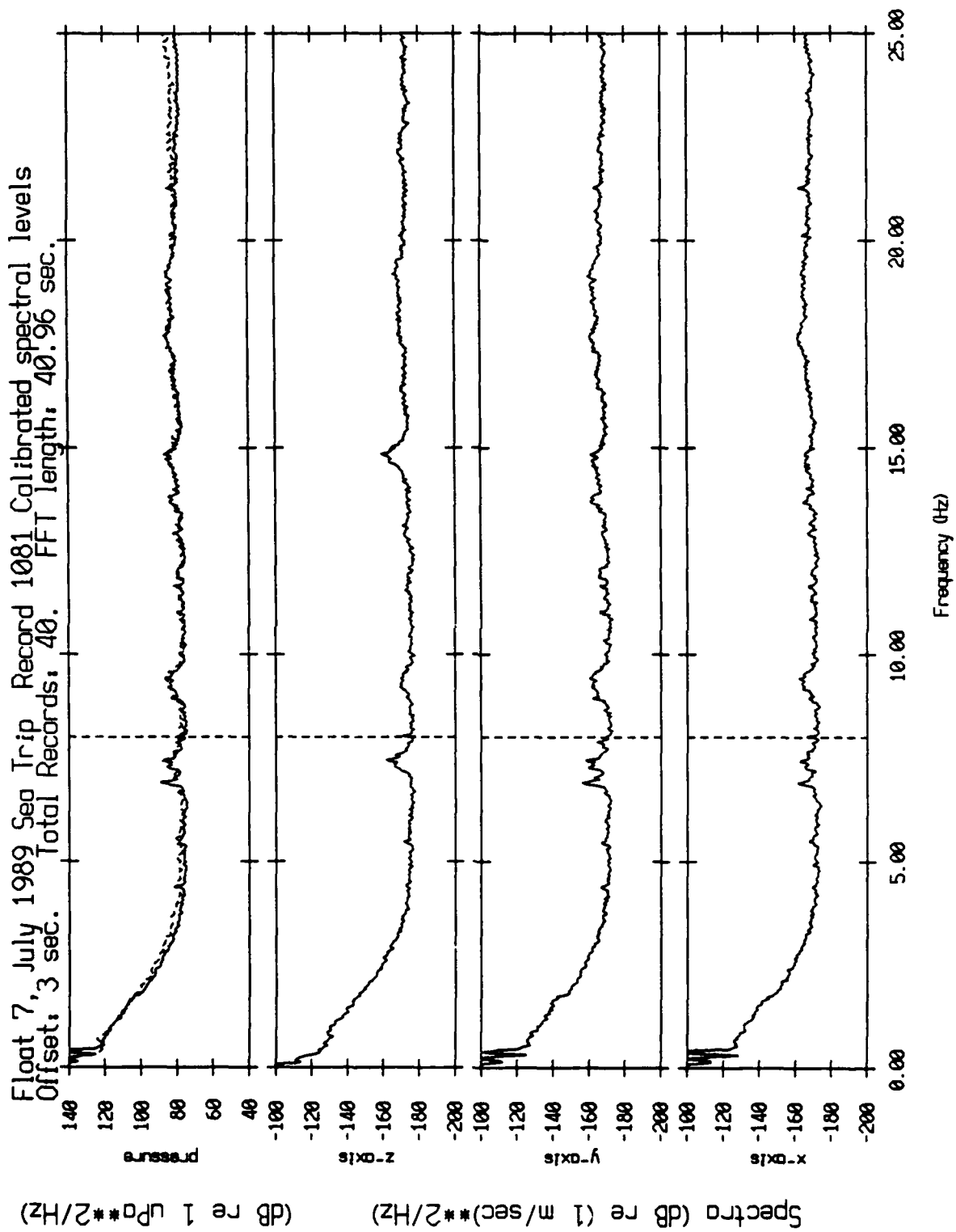


Figure XII.7h

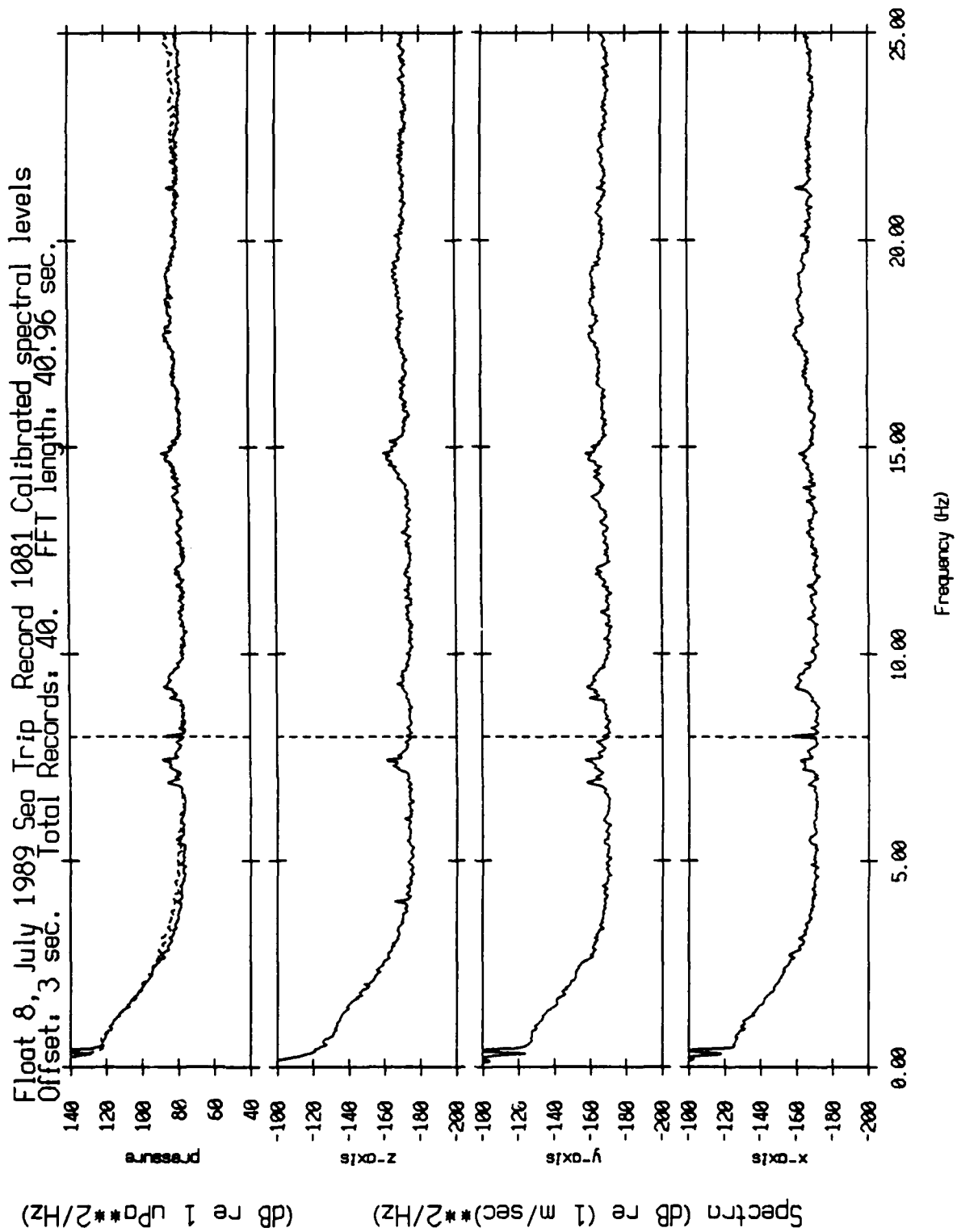


Figure XII.7i

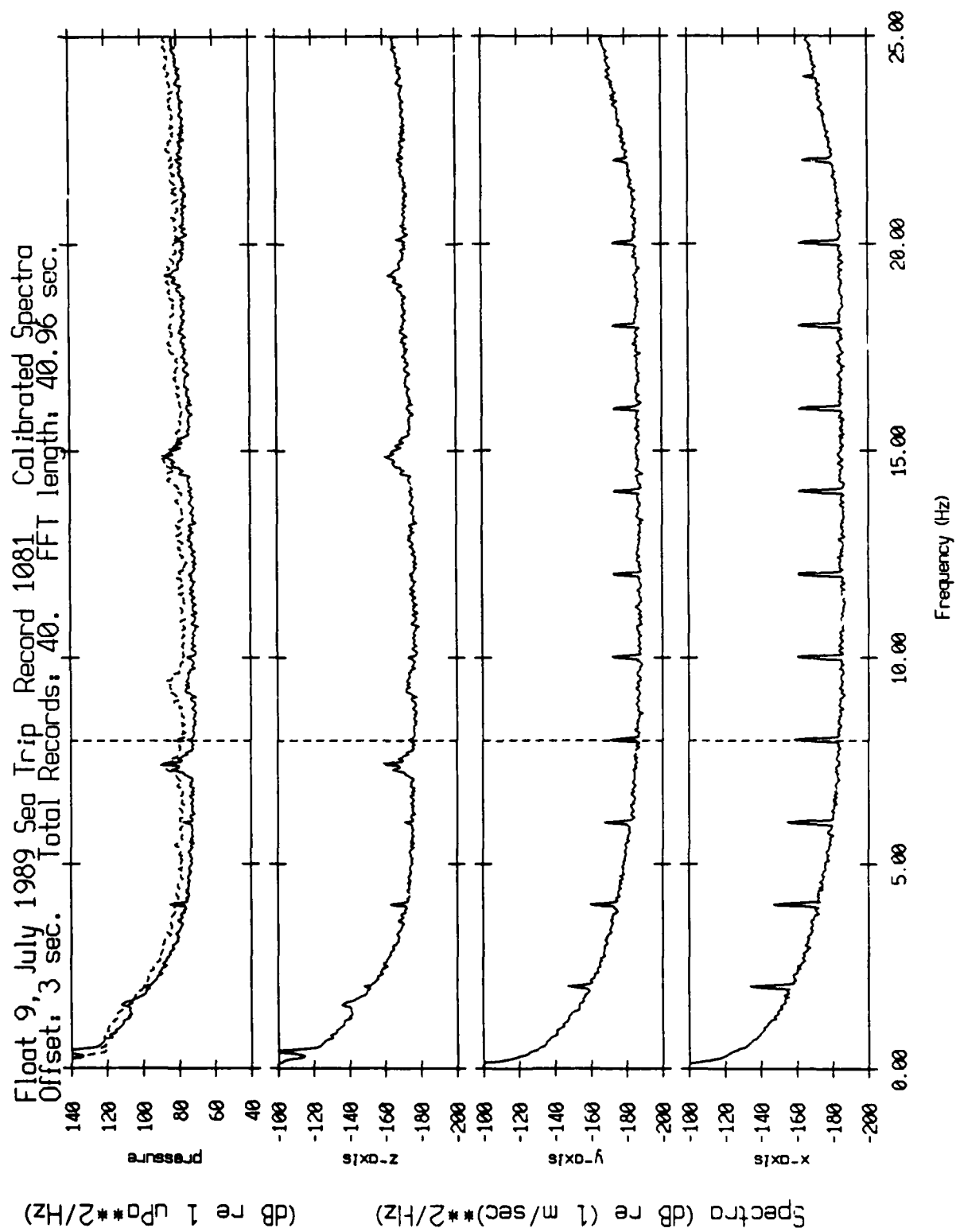


Figure XII.7j

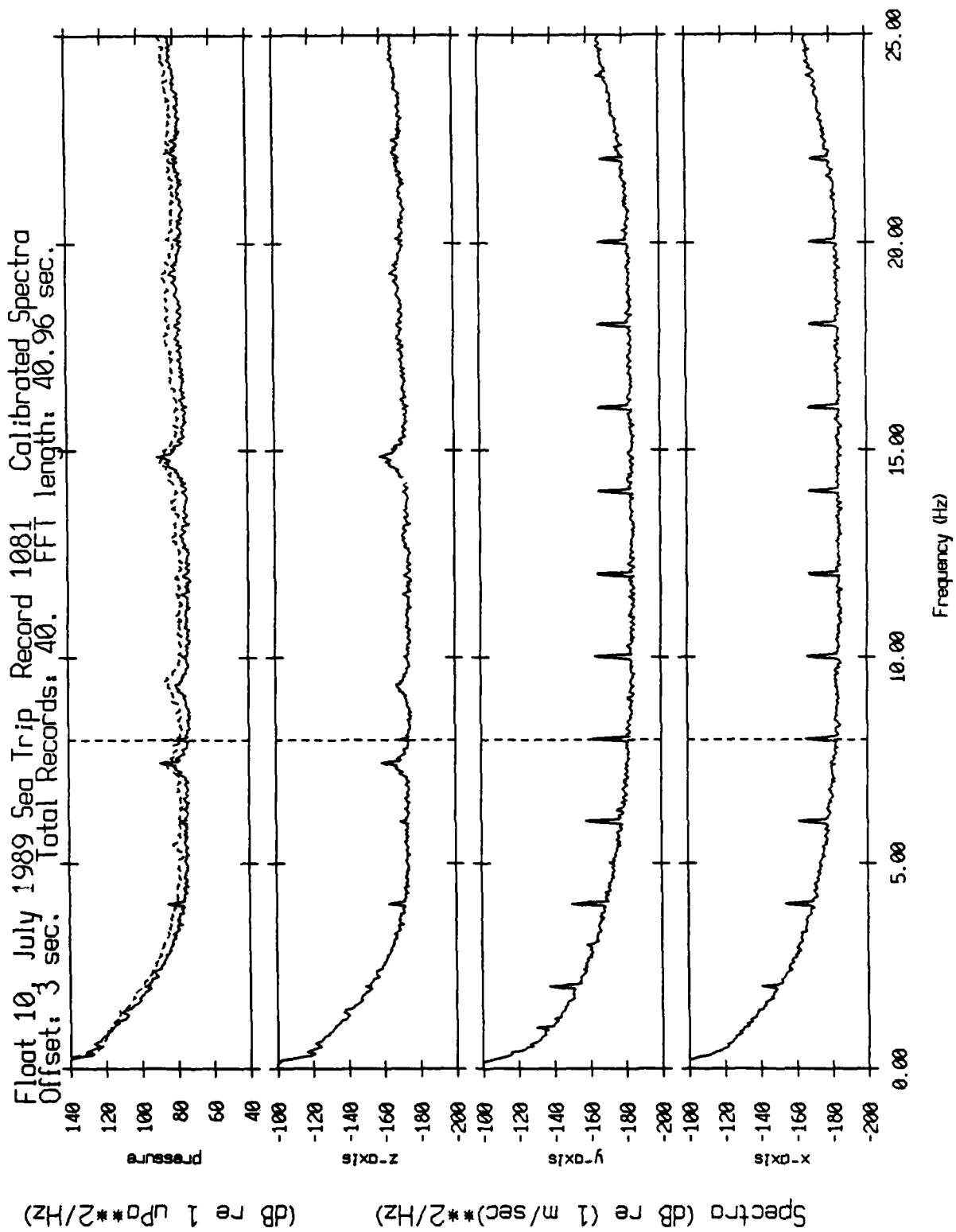


Figure X11.7k

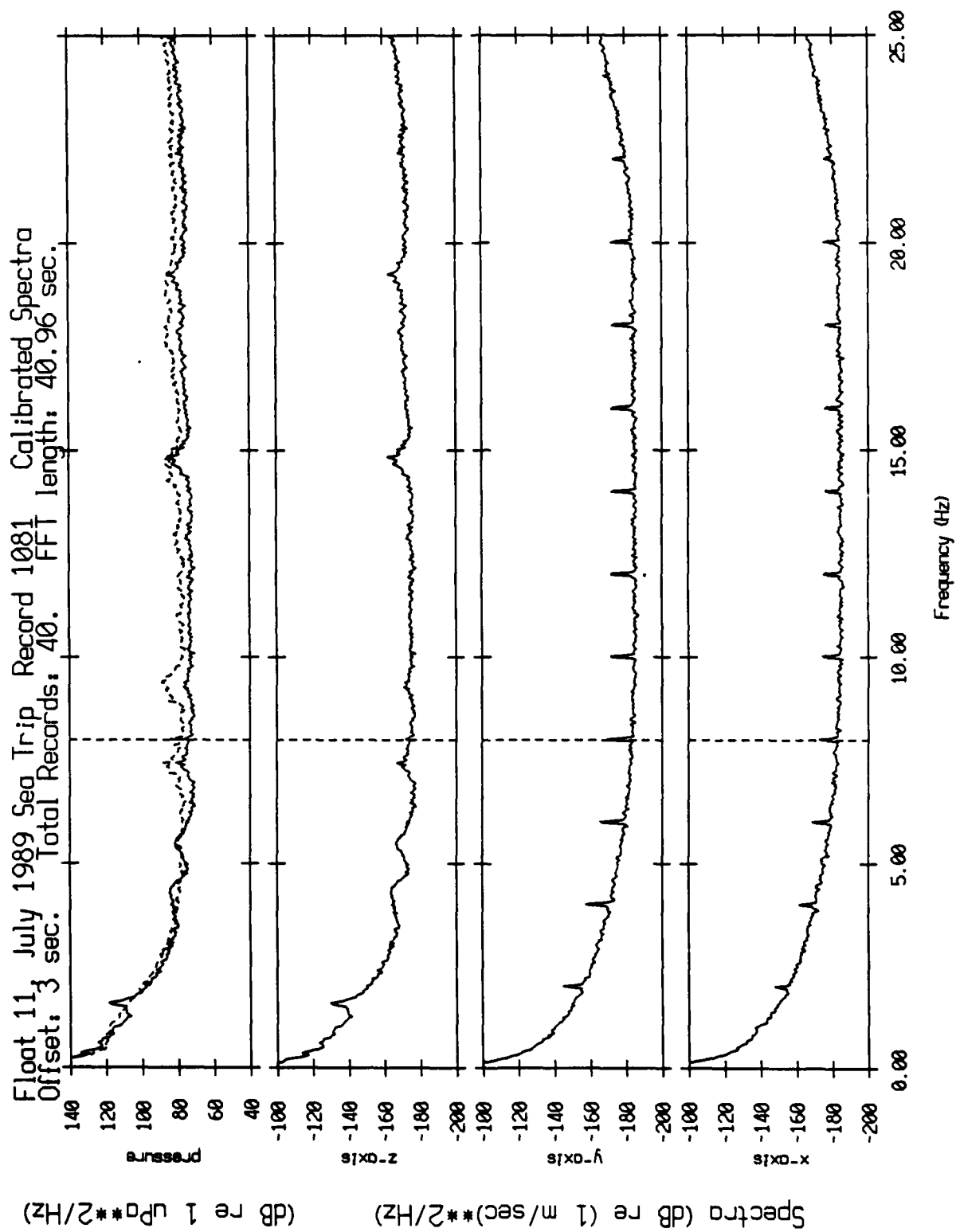


Figure XII.71

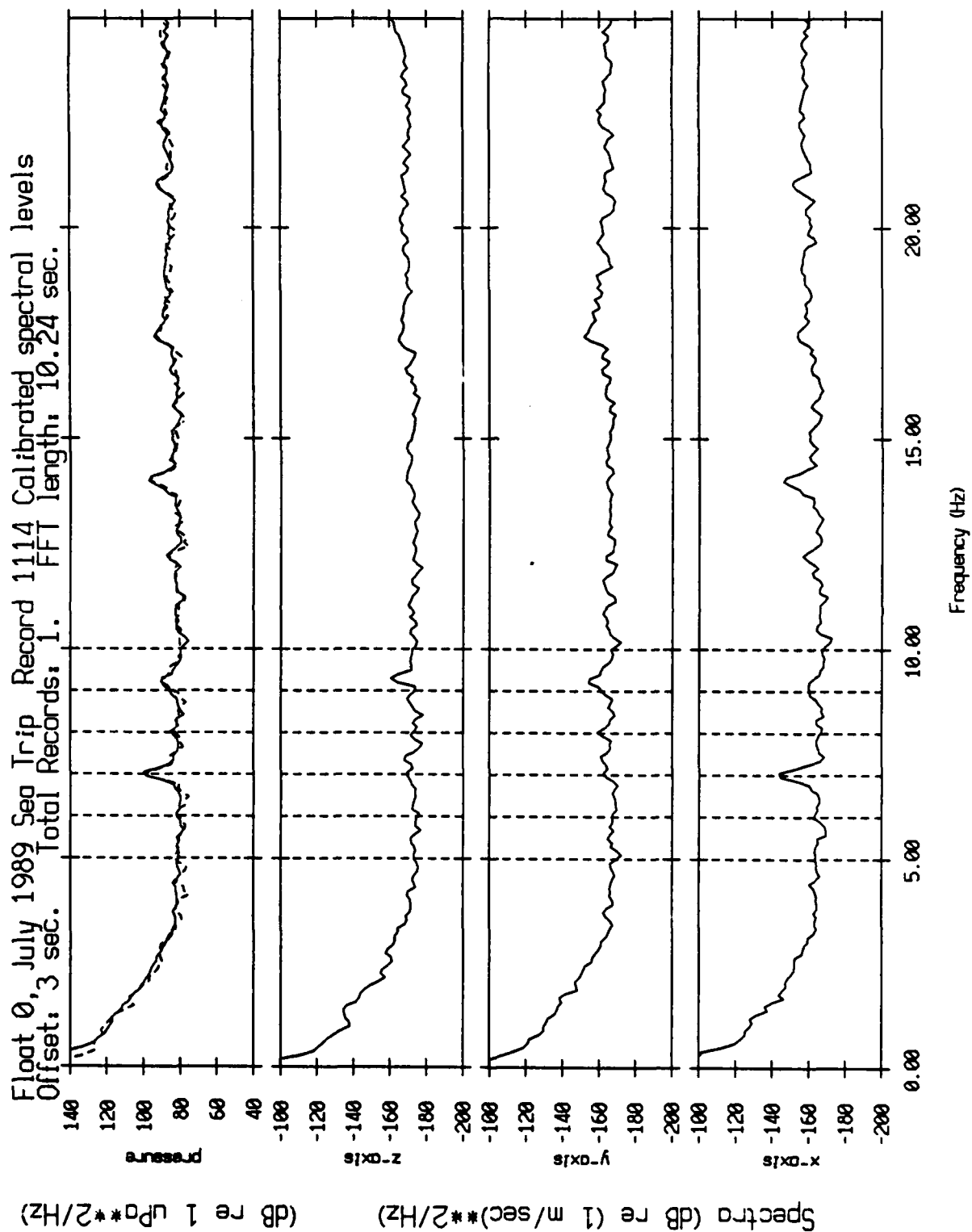


Figure XII.8a

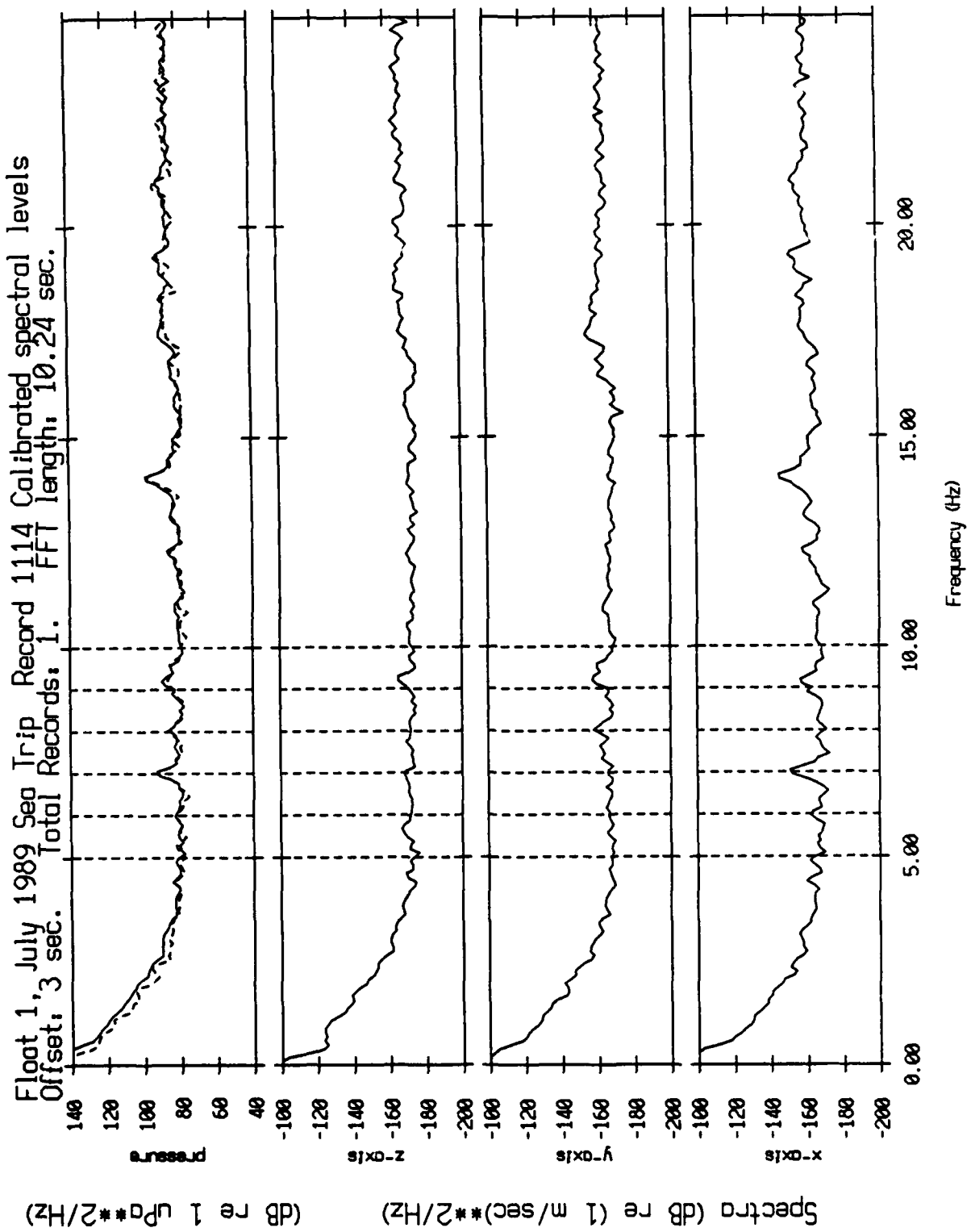


Figure XII.8b



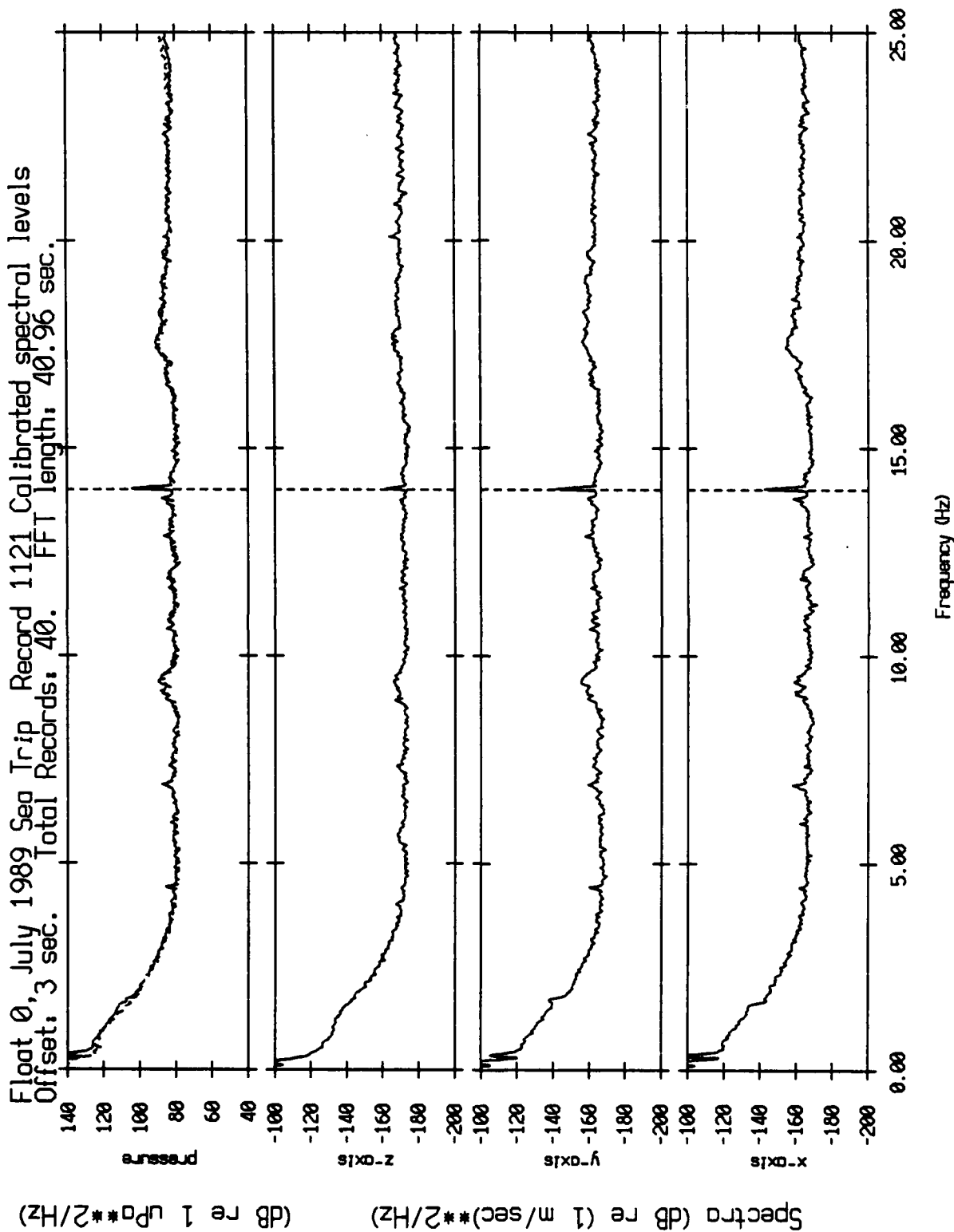


Figure XII.9a

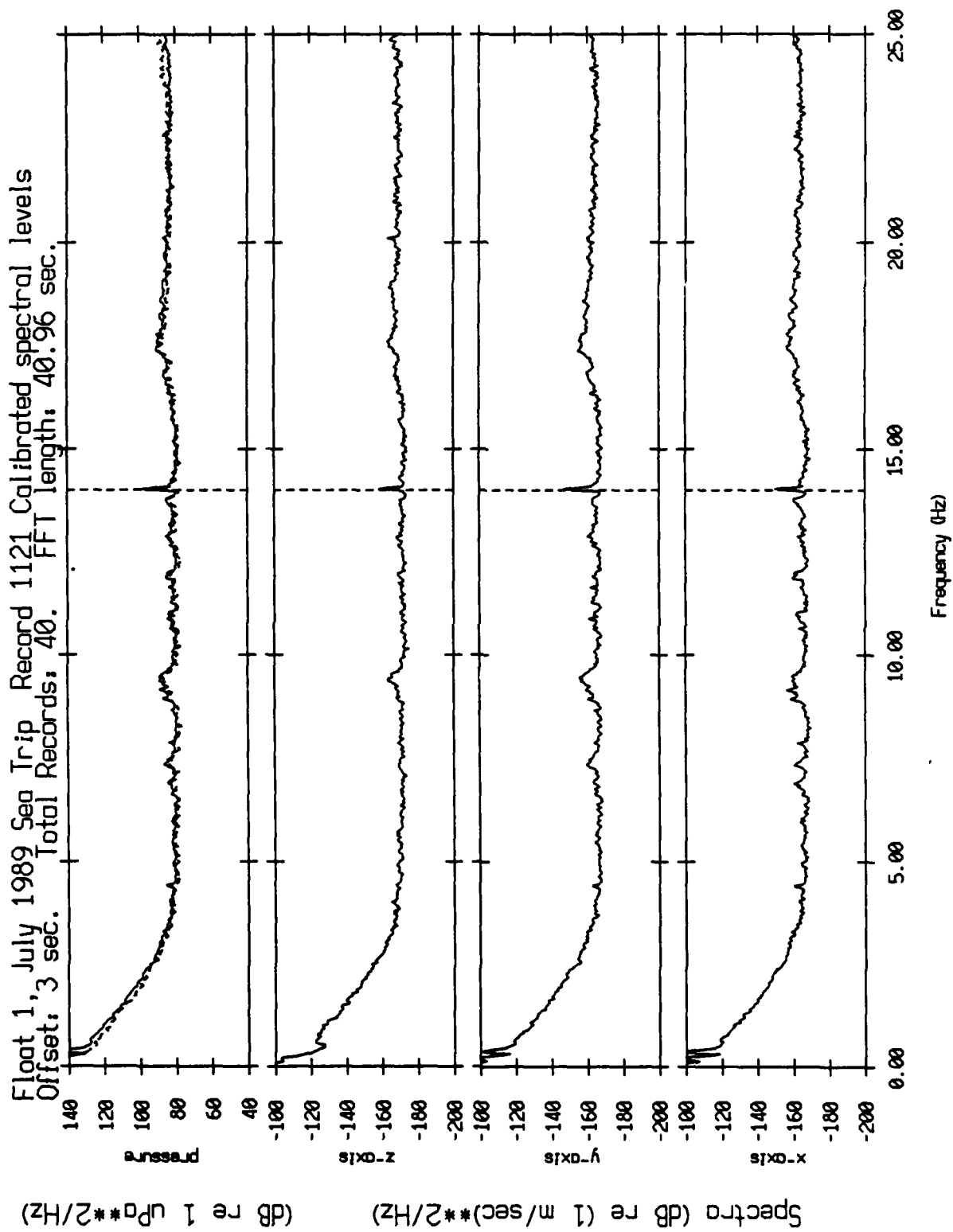


Figure XII.9b

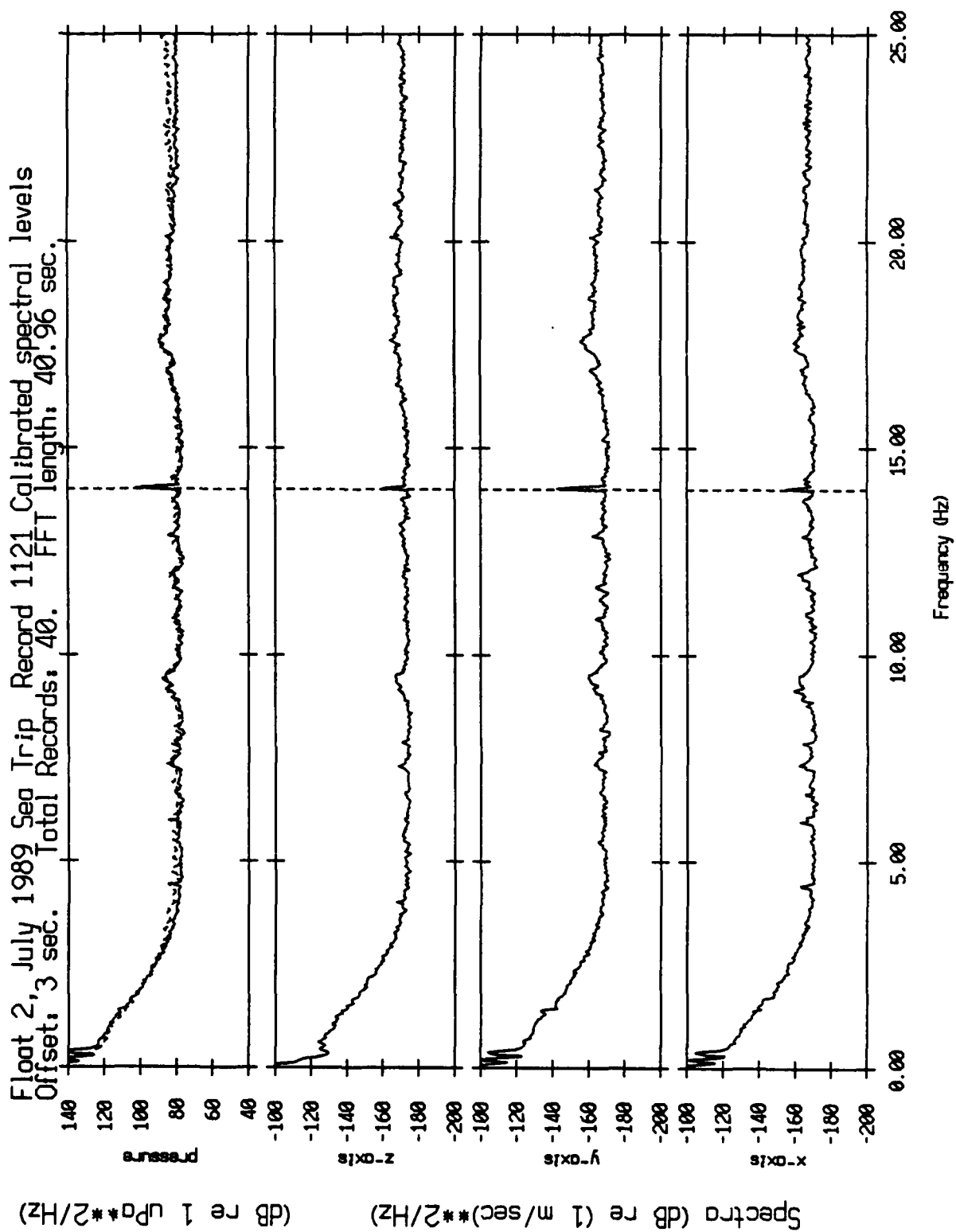


Figure XII.9c

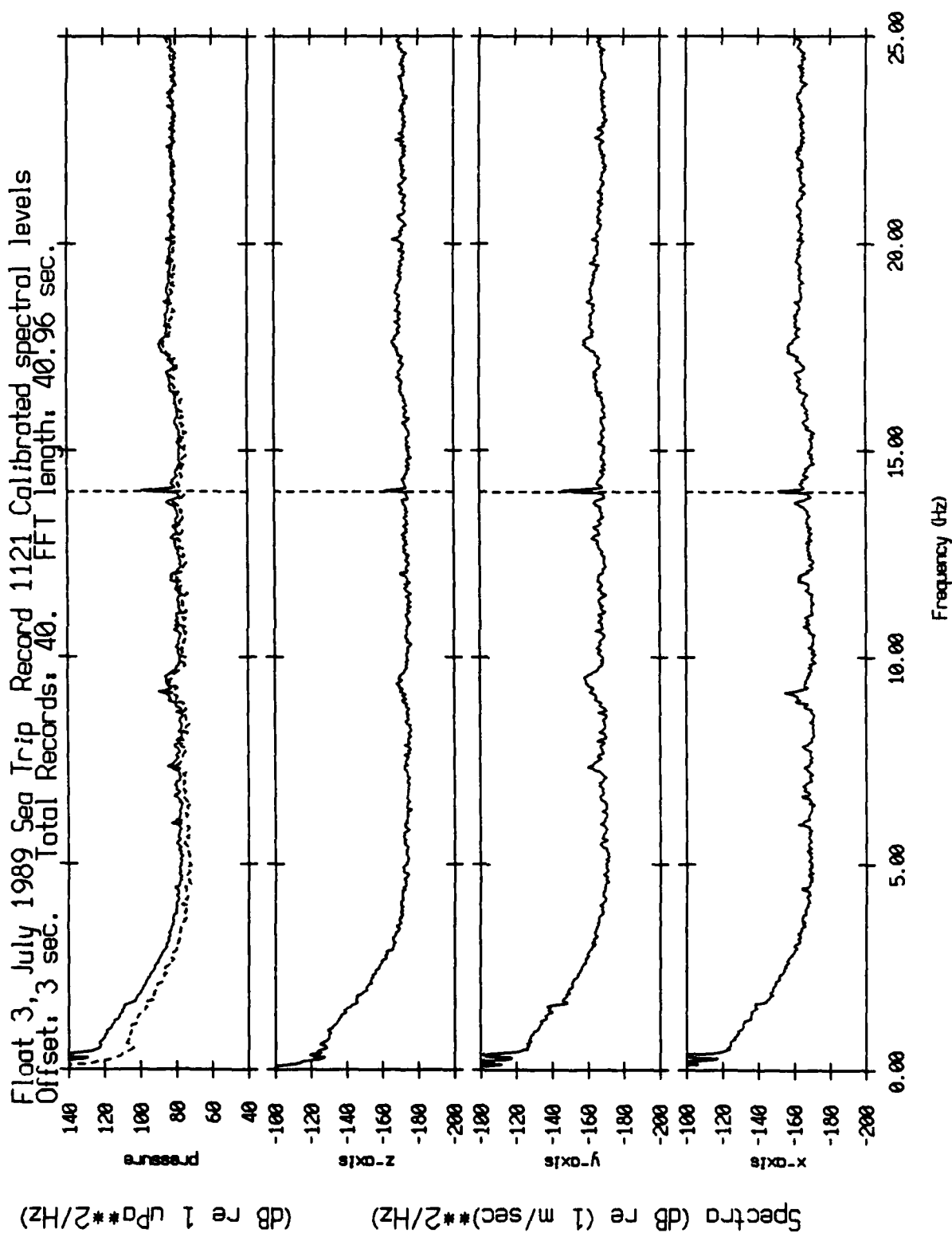


Figure XII.9d

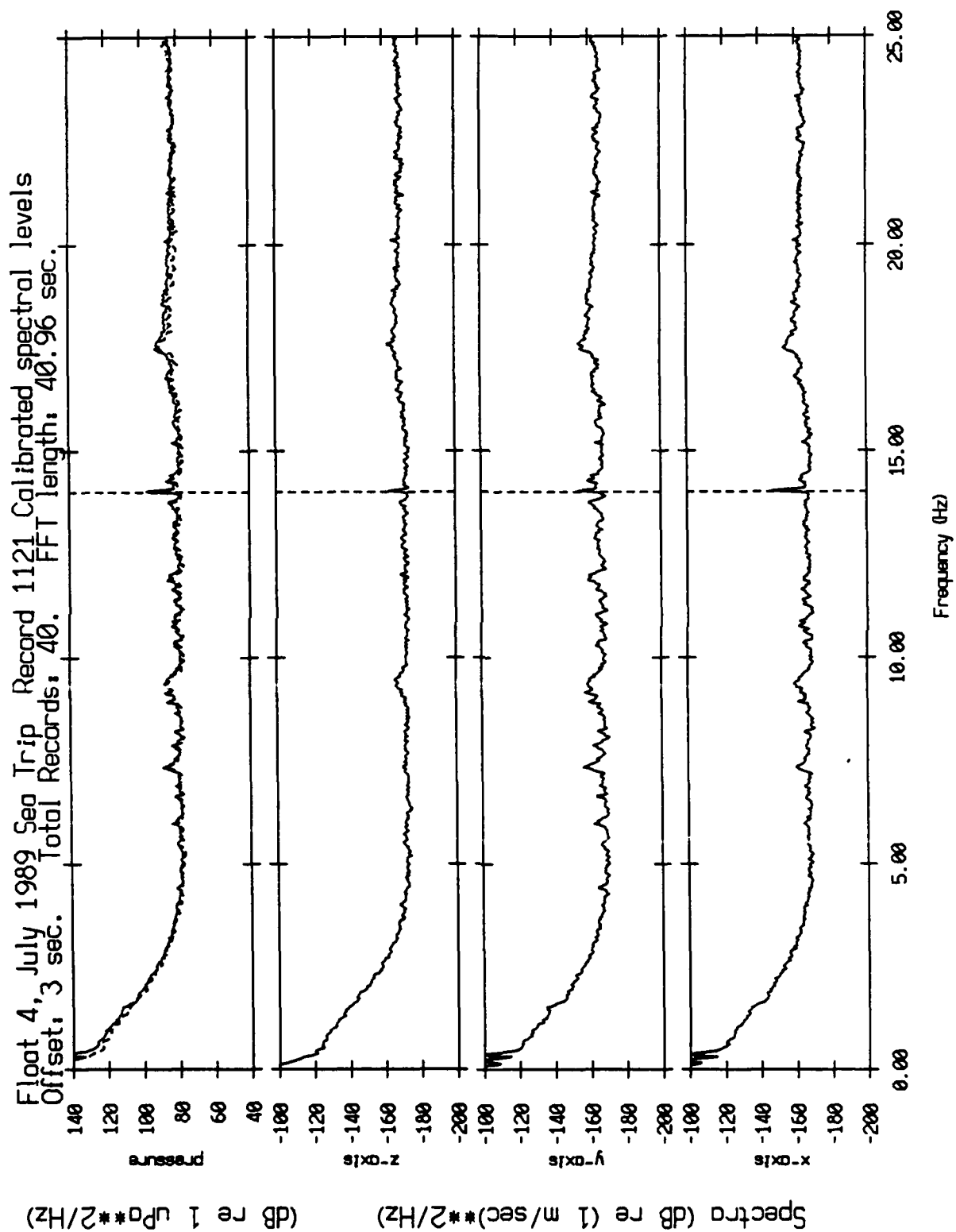


Figure XII.9e

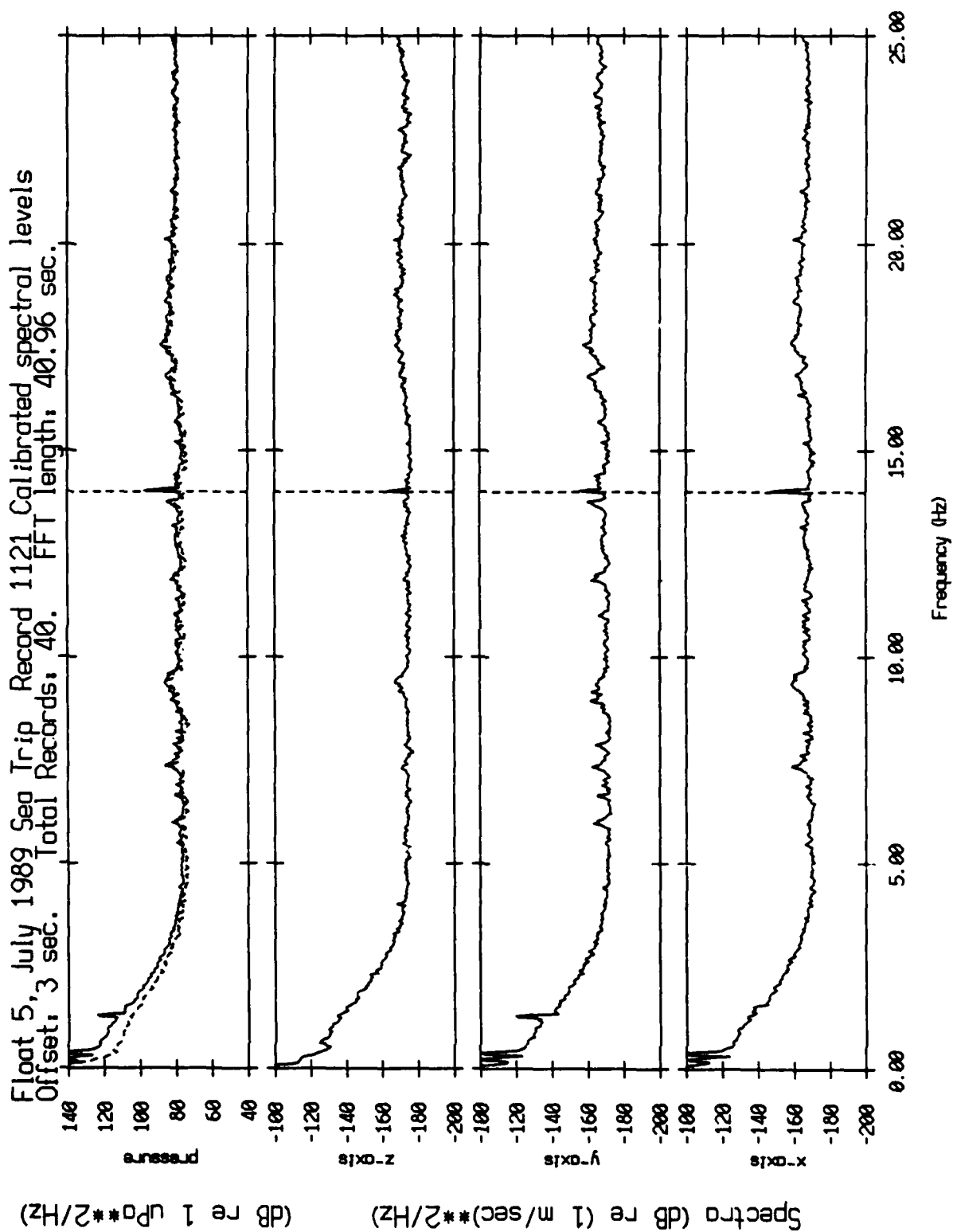


Figure XII.9f

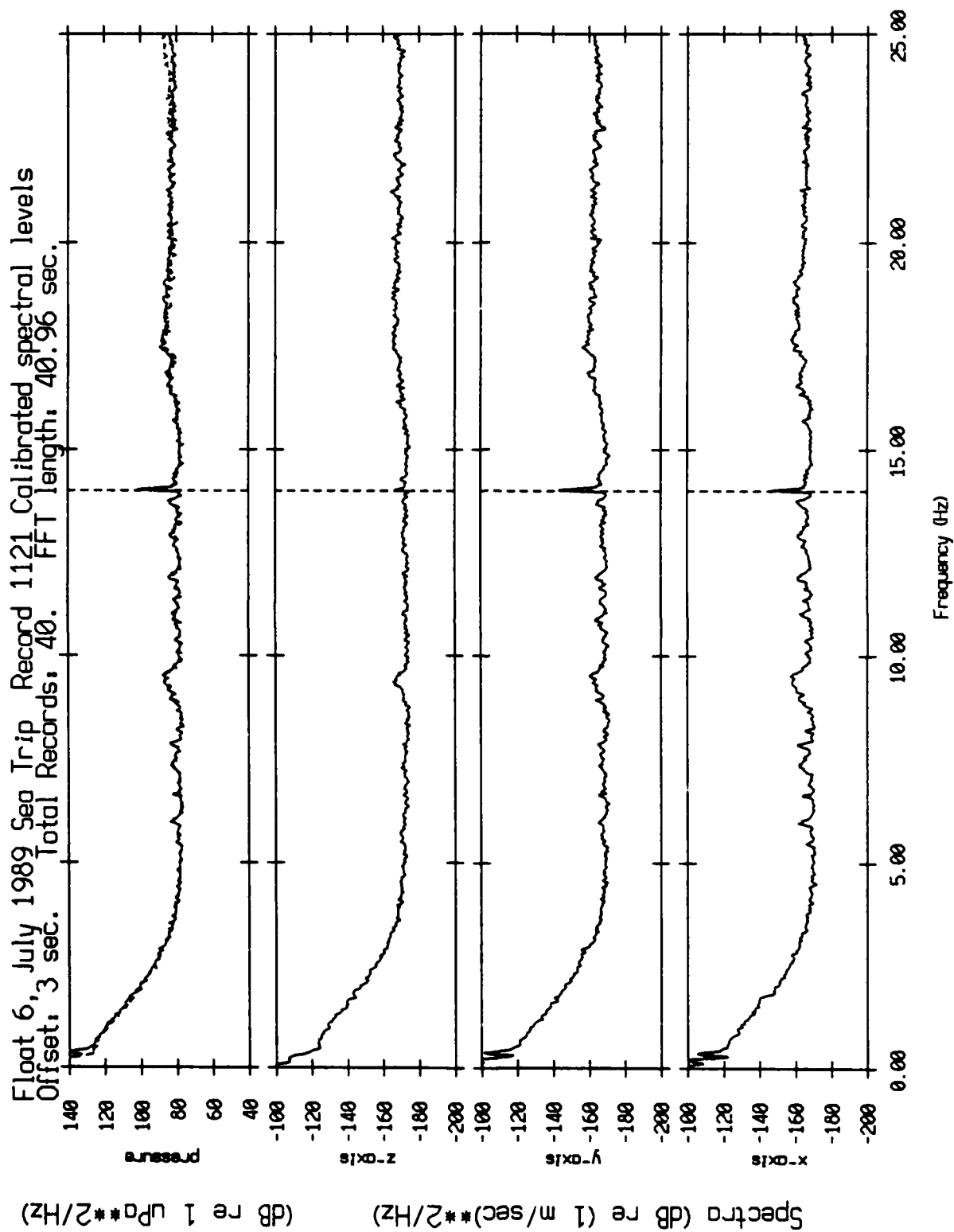


Figure XII.9g

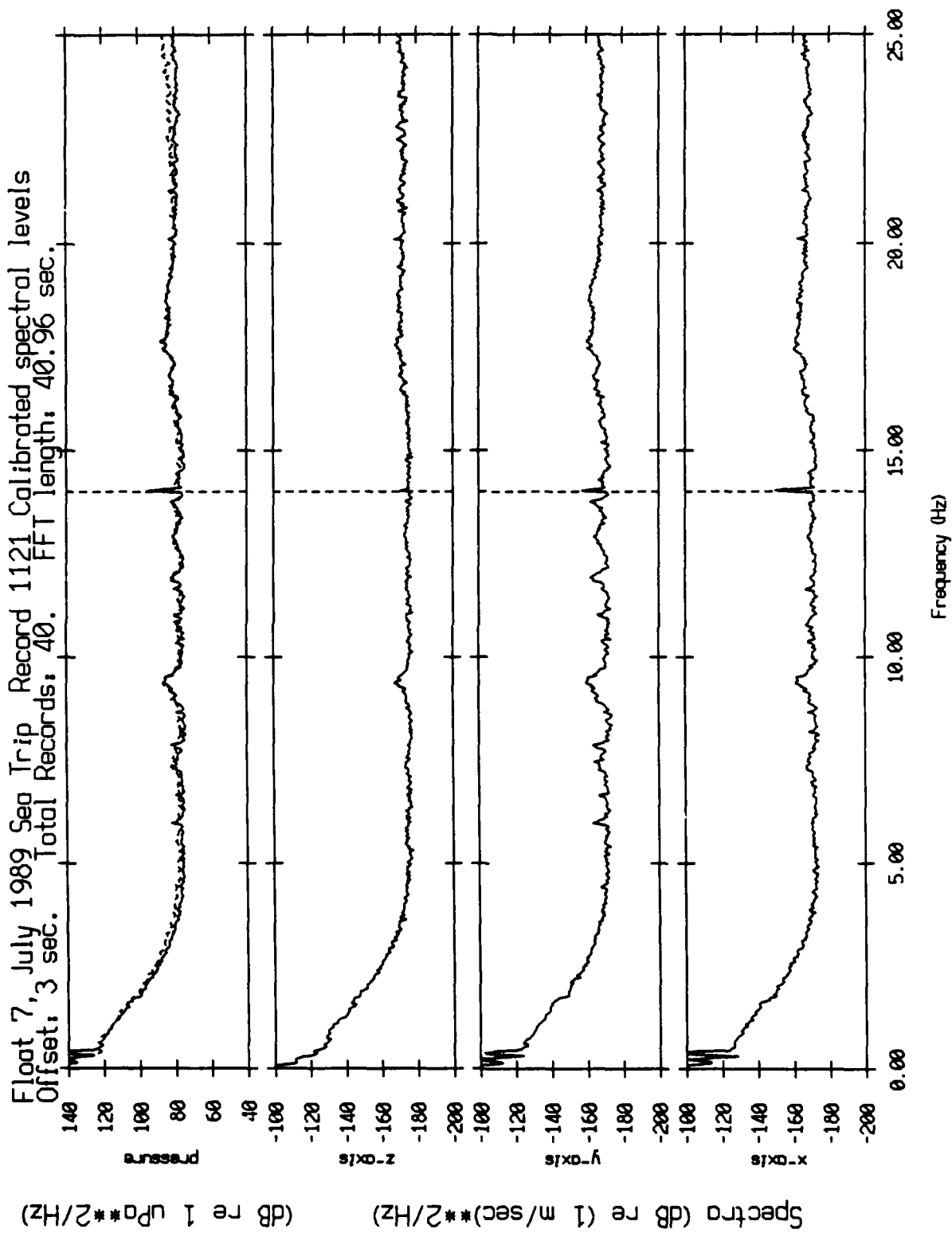


Figure XII.9h



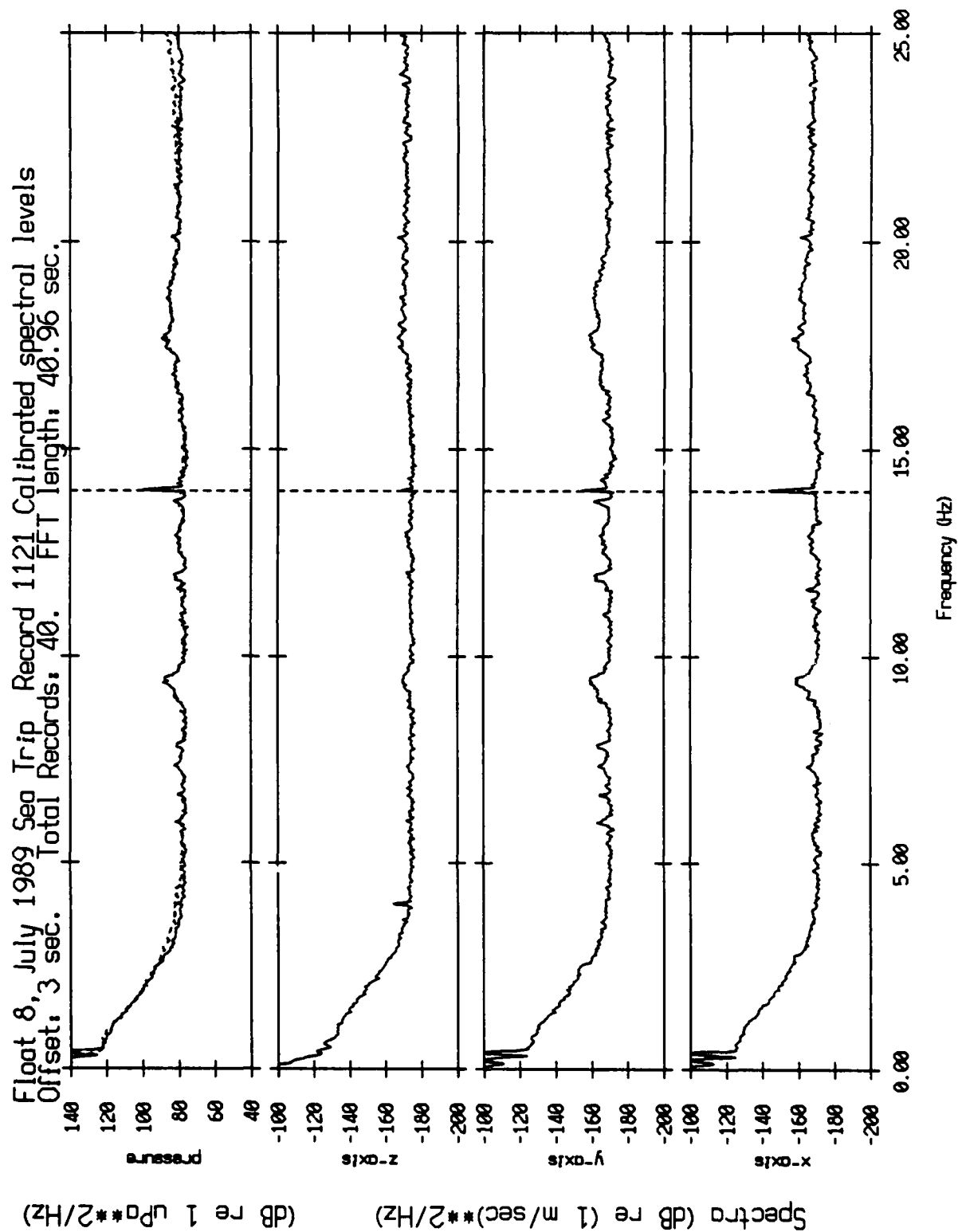


Figure XII.91

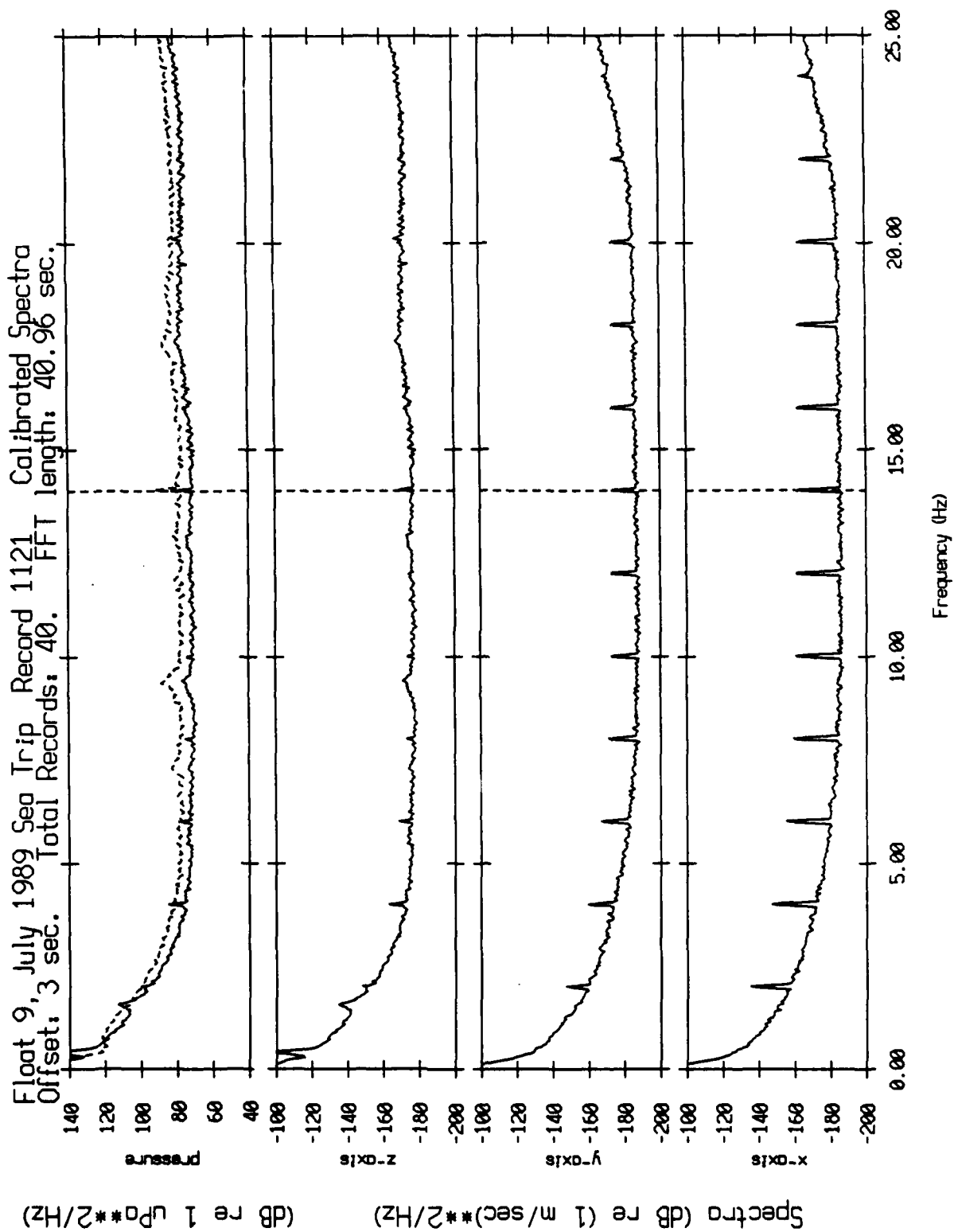


Figure XII.9j

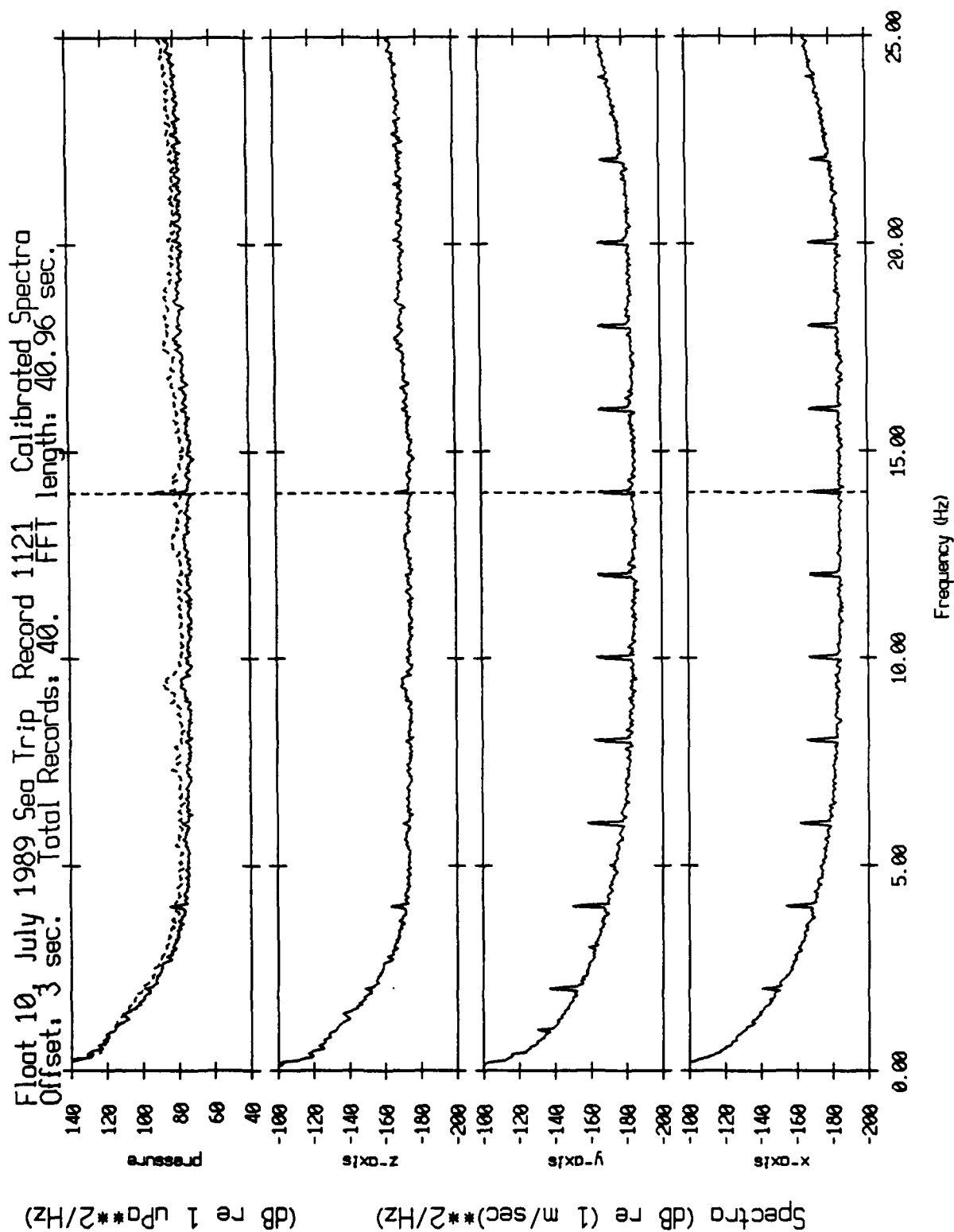


Figure XII.9k

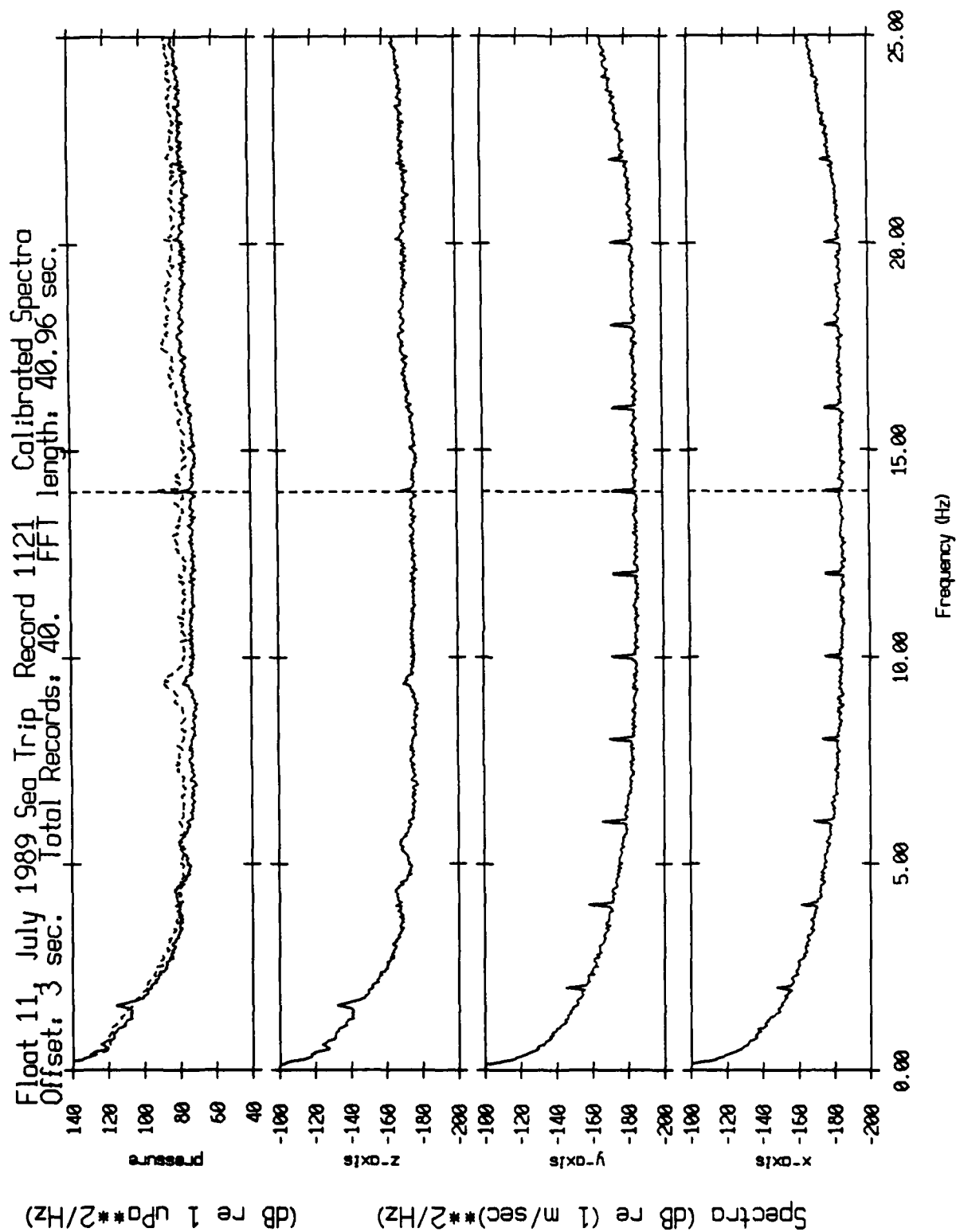


Figure XII.91

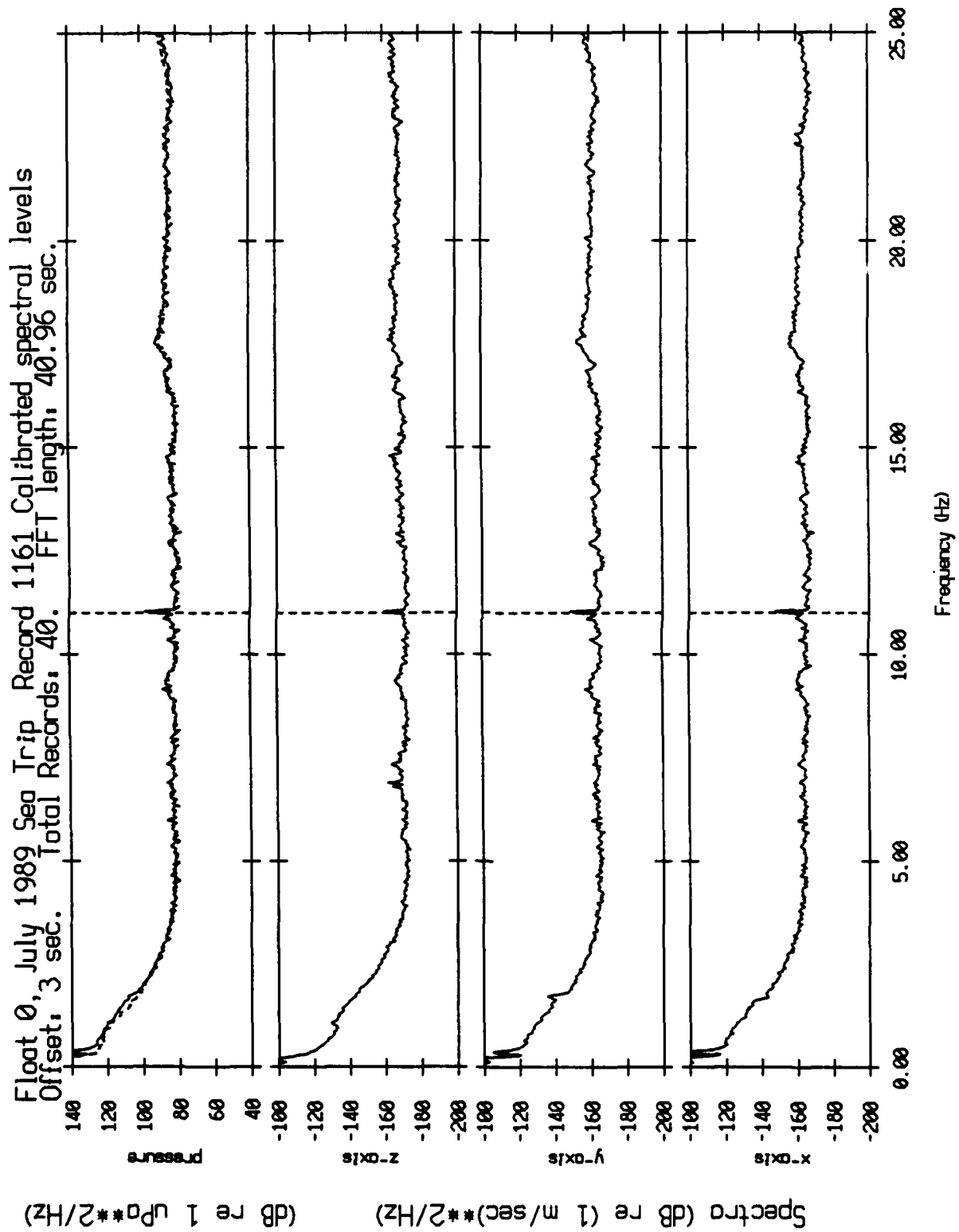


Figure XII.10a

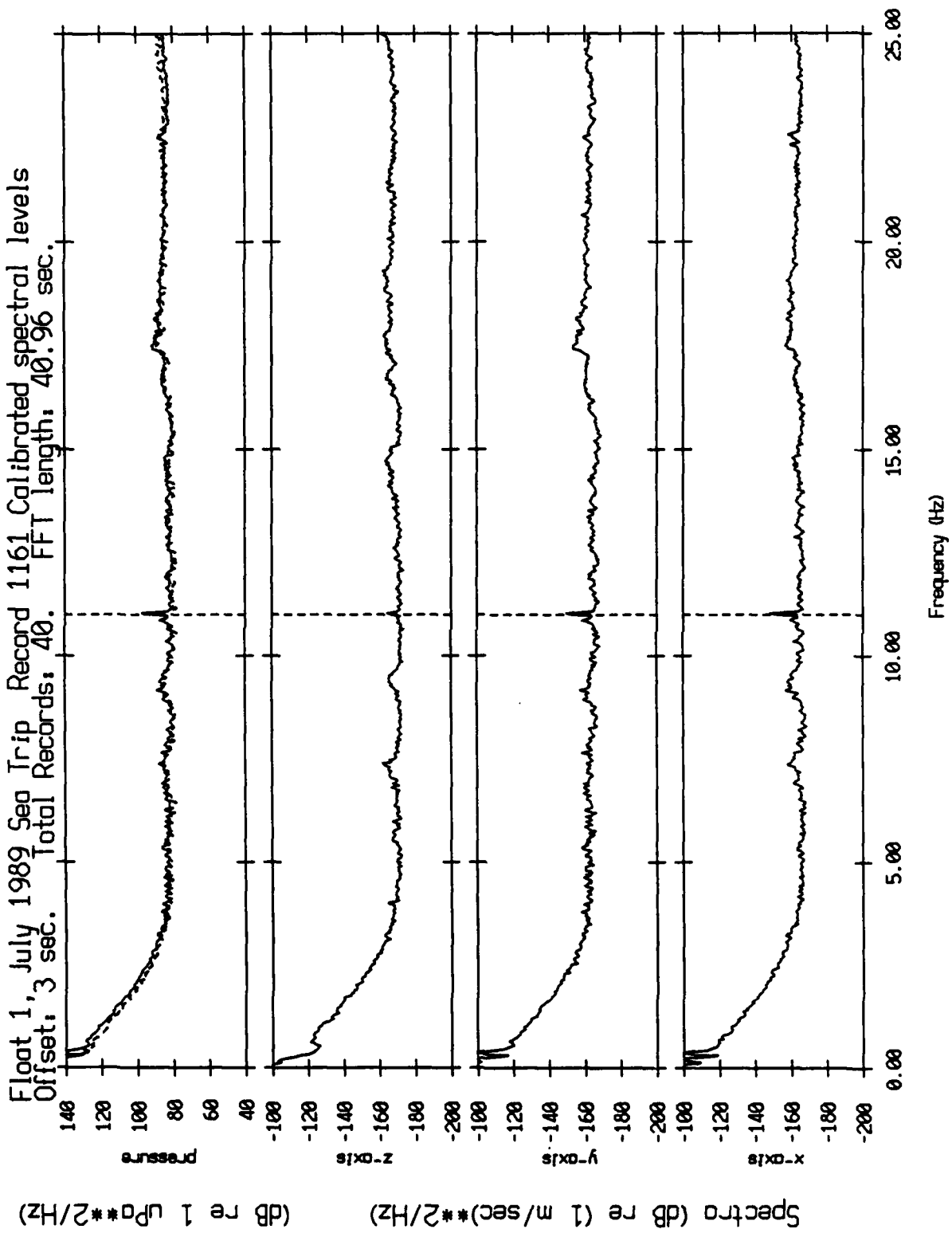


Figure XII.10b

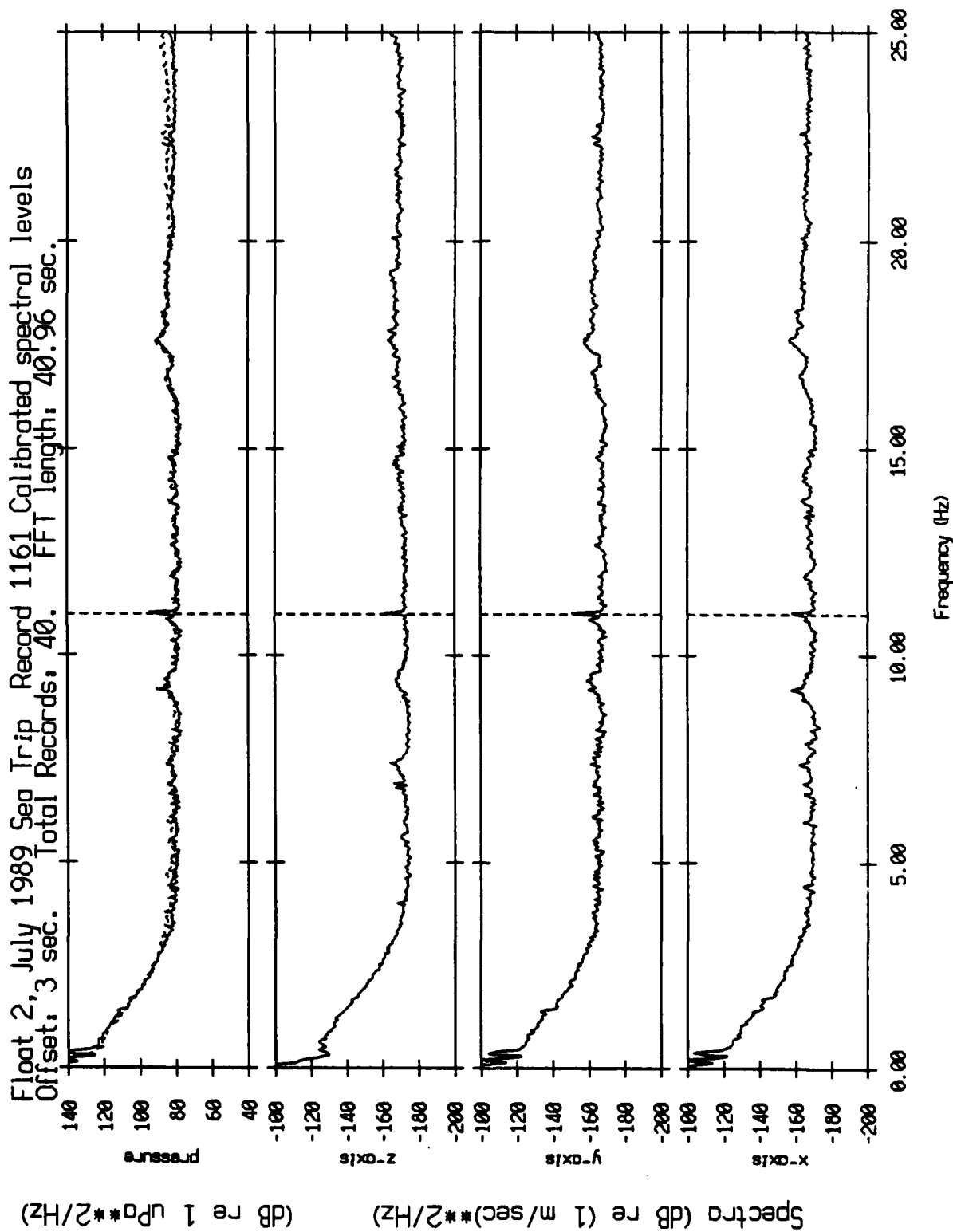


Figure XII.10c

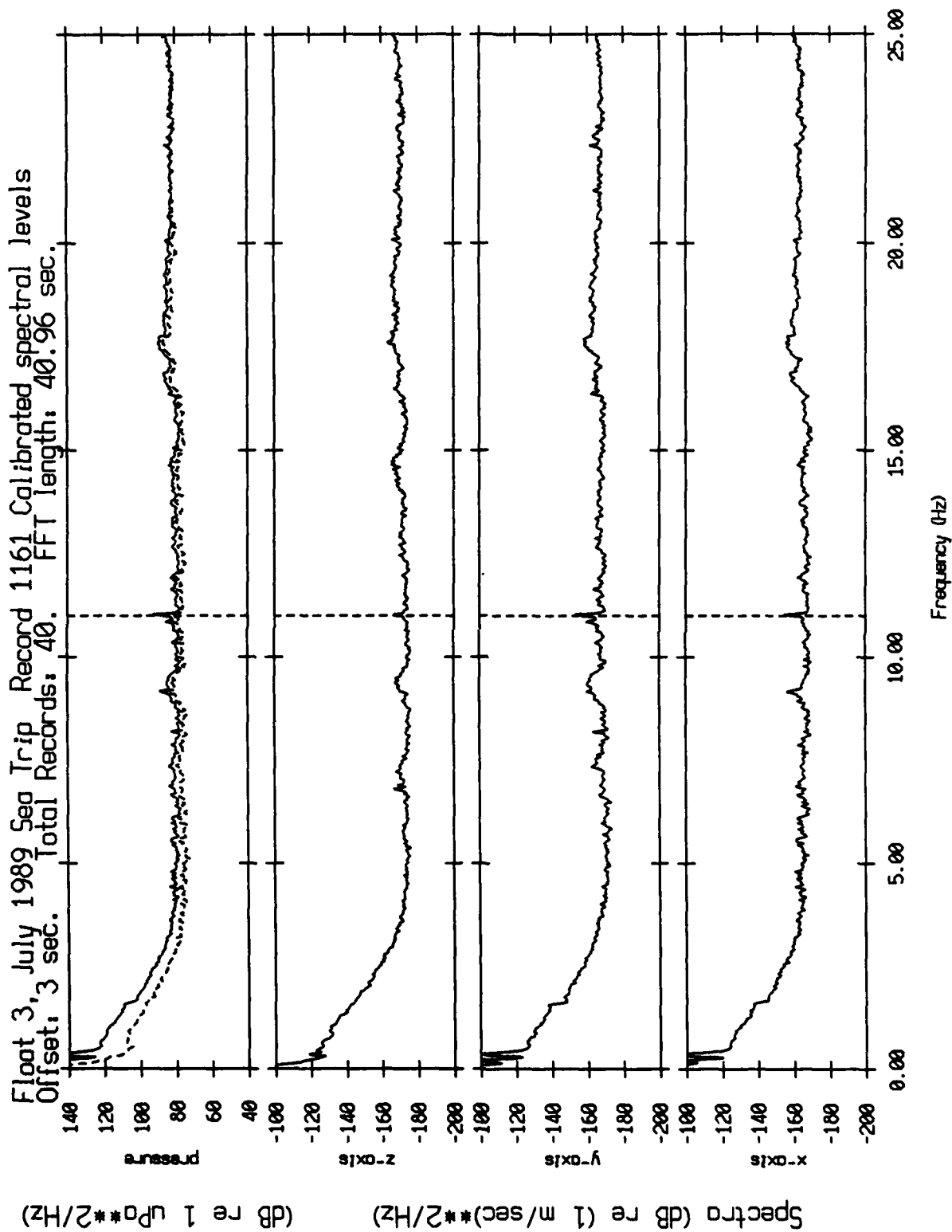


Figure XII.10d



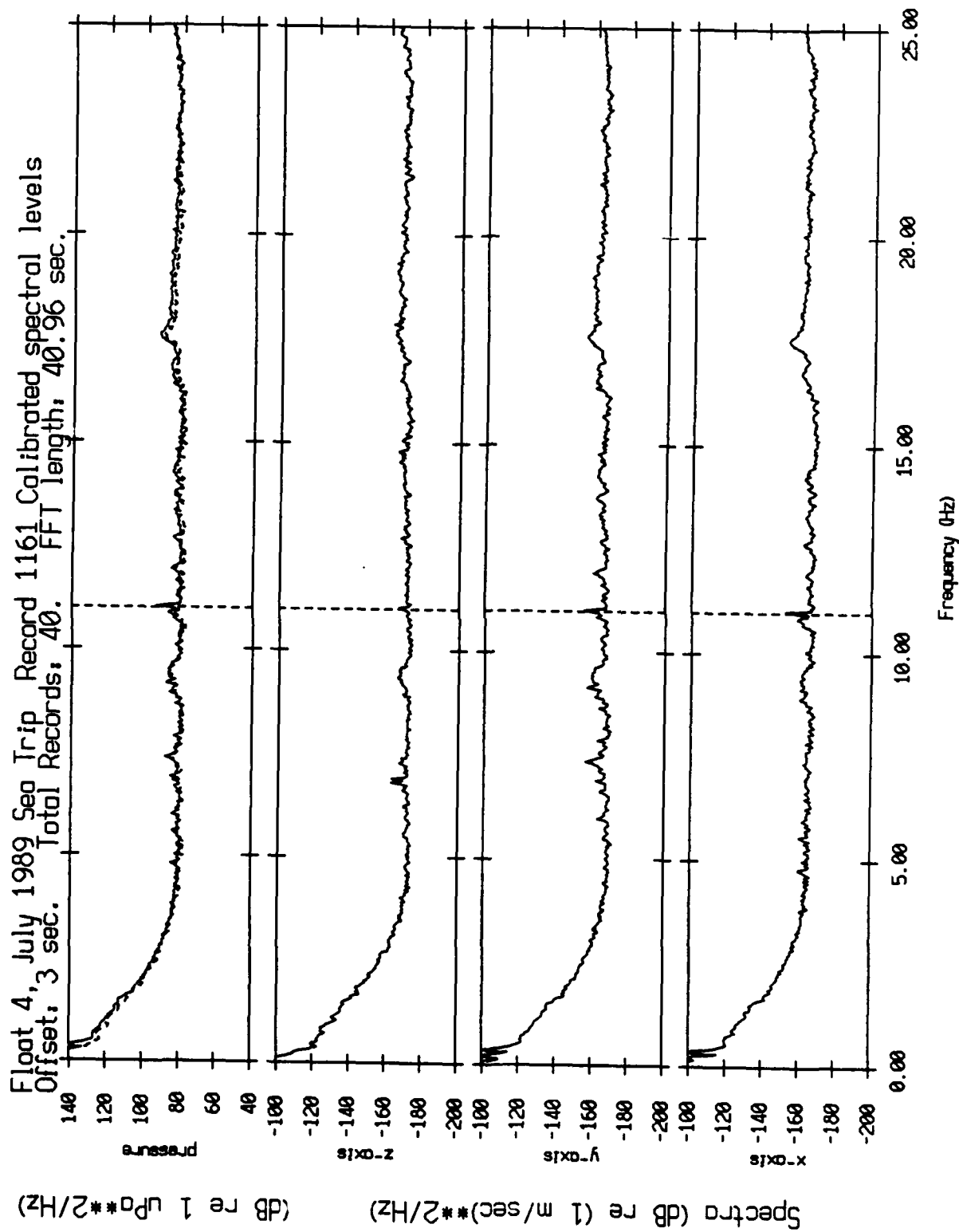


Figure XII.10e

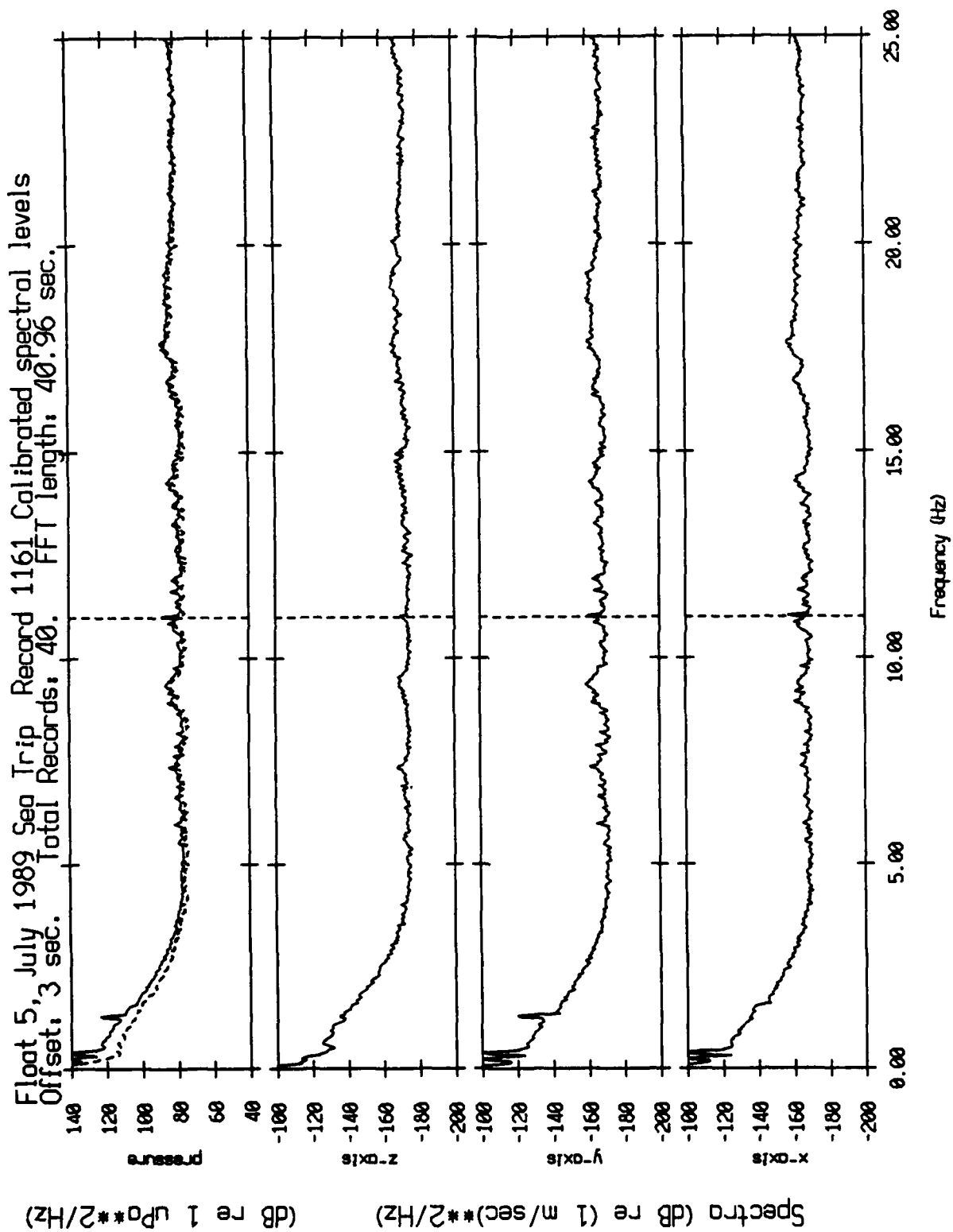


Figure XII.10f

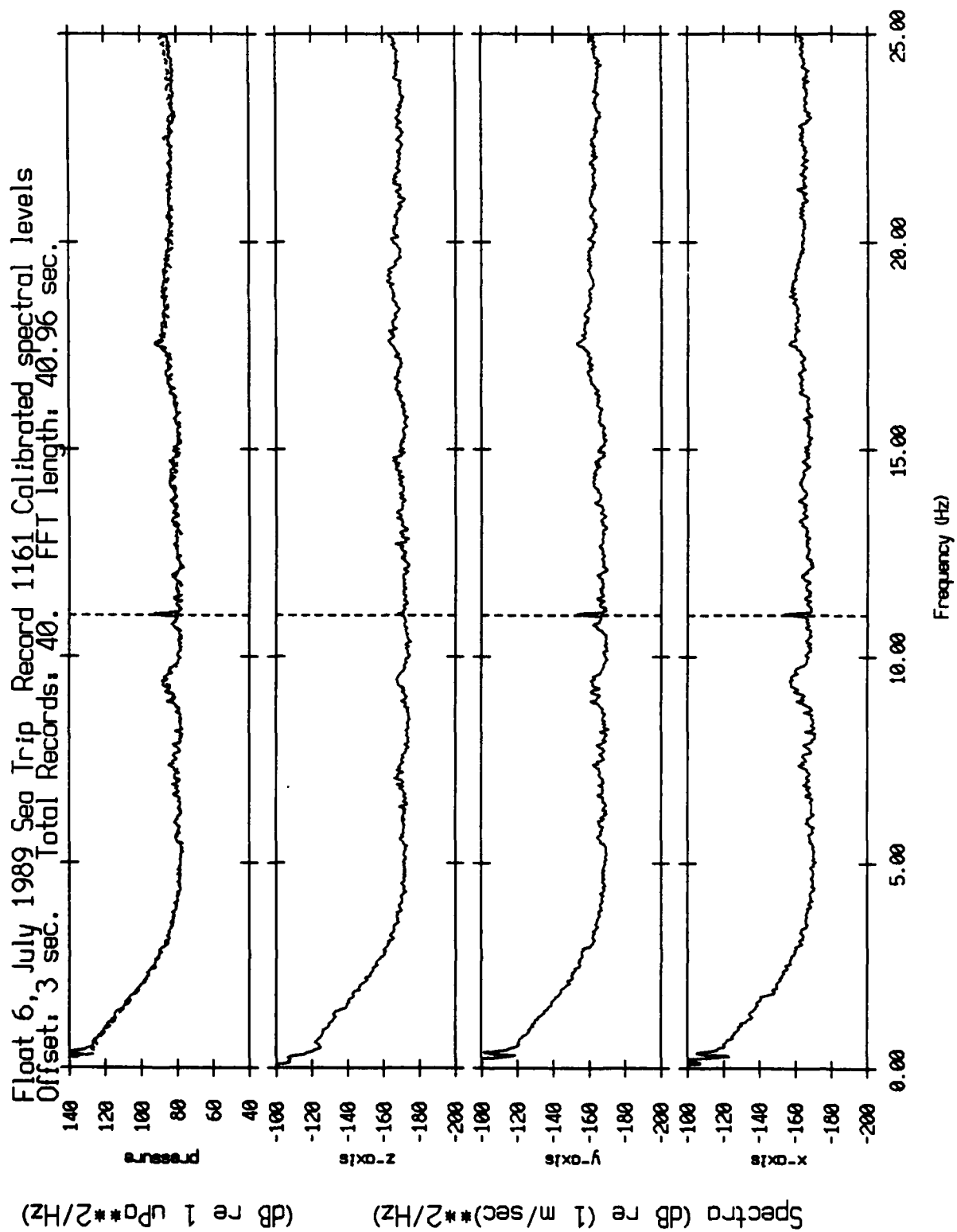


Figure XII.10g

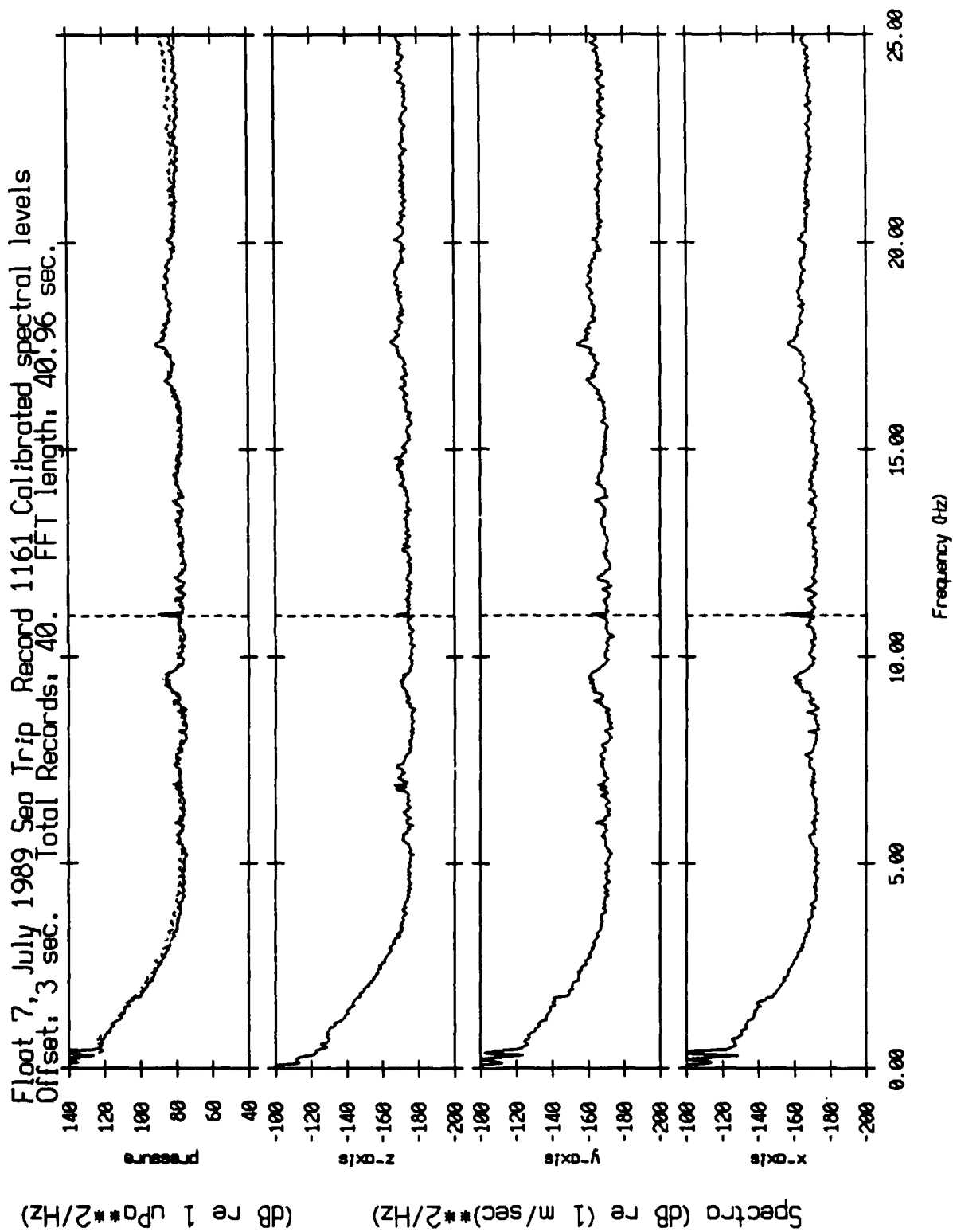


Figure XII.10h

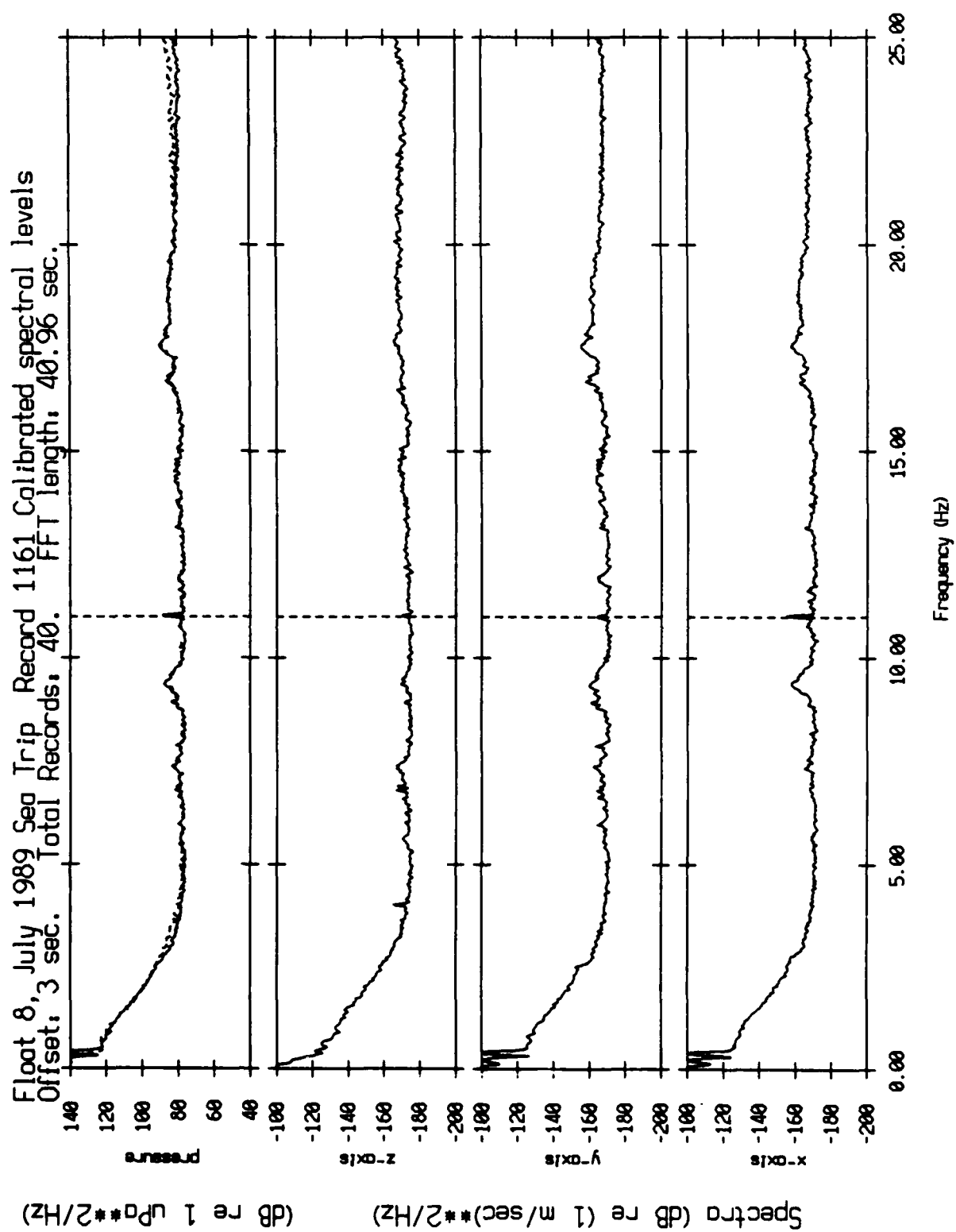


Figure XII.10i

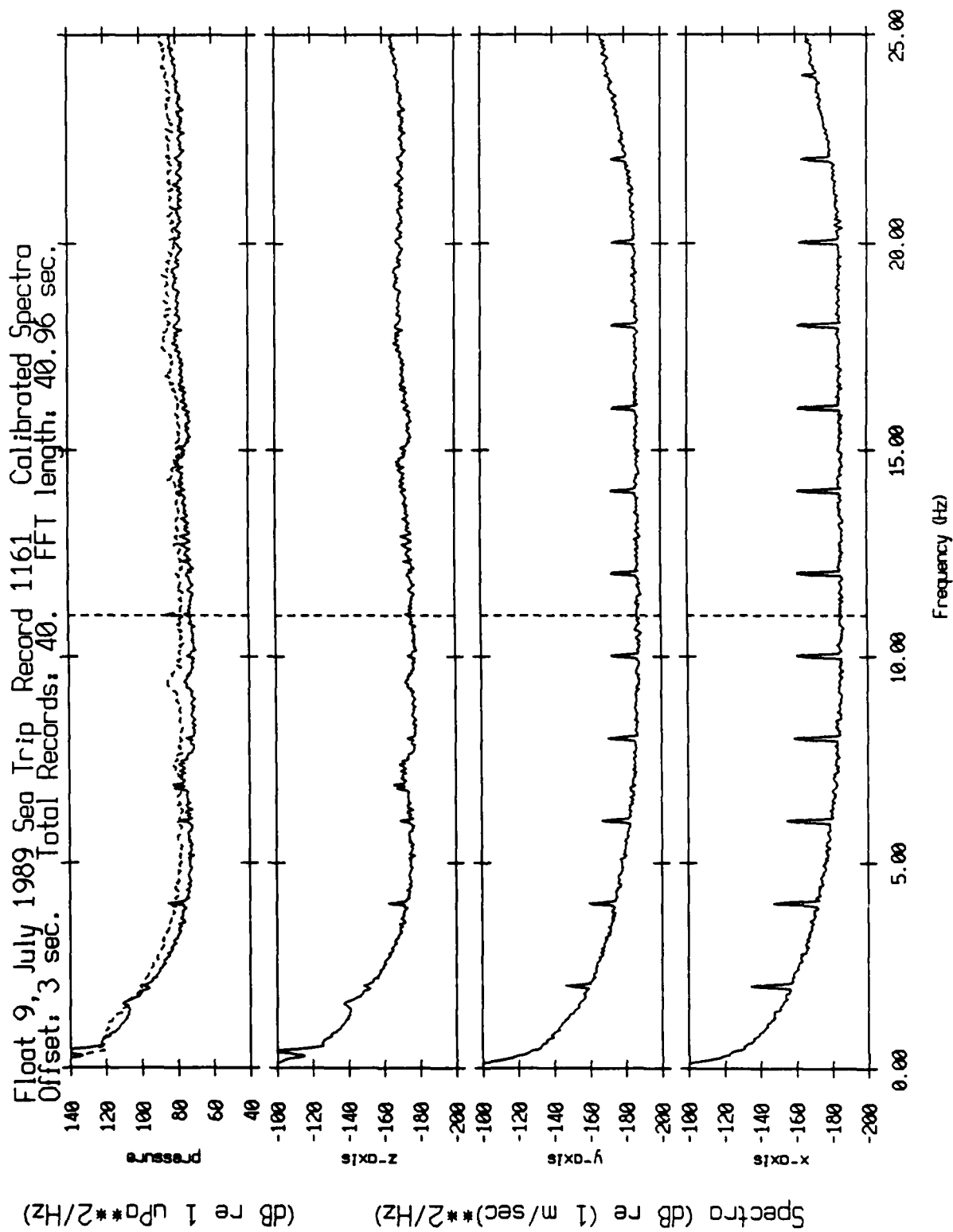


Figure XII.10j

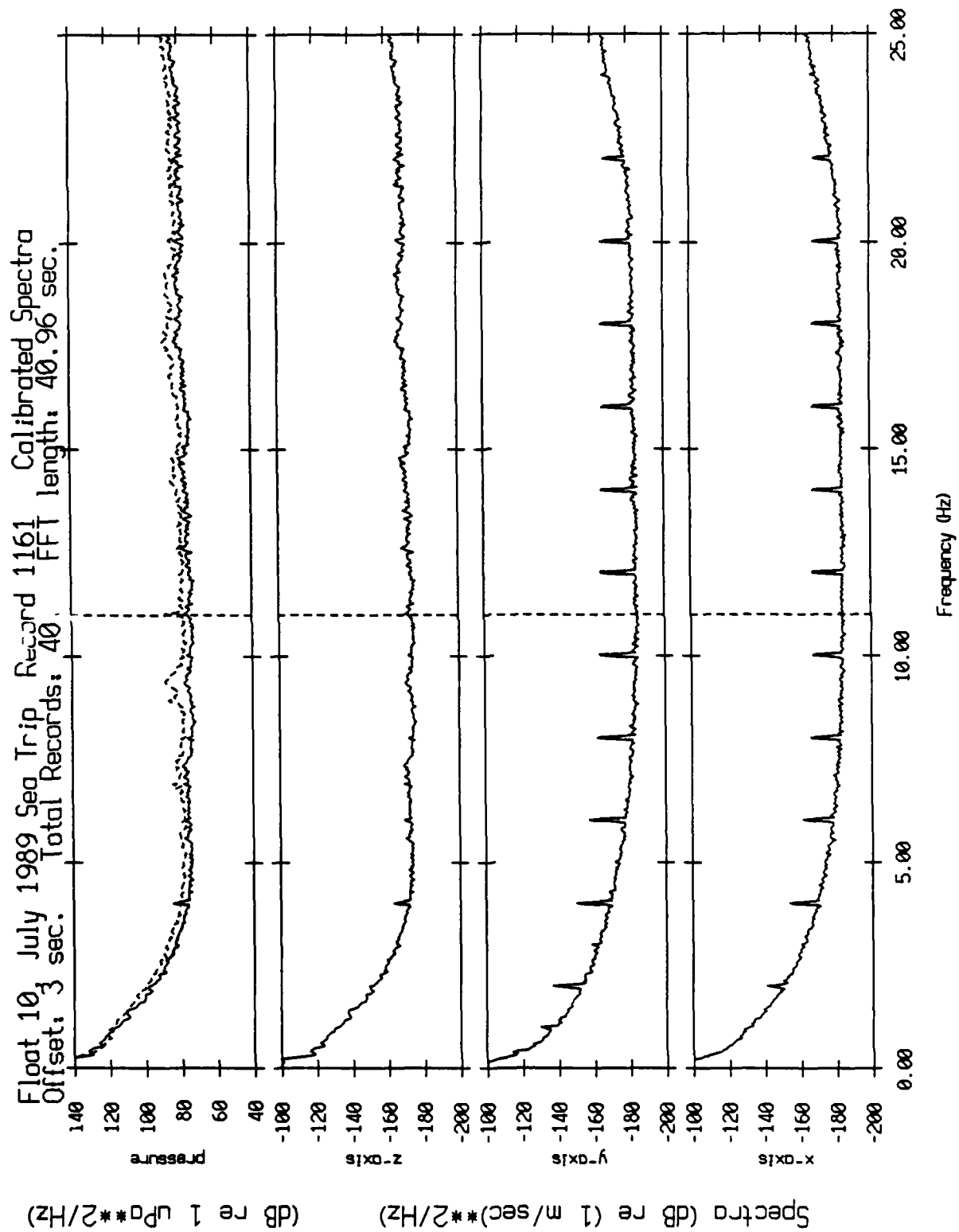


Figure XII.10k

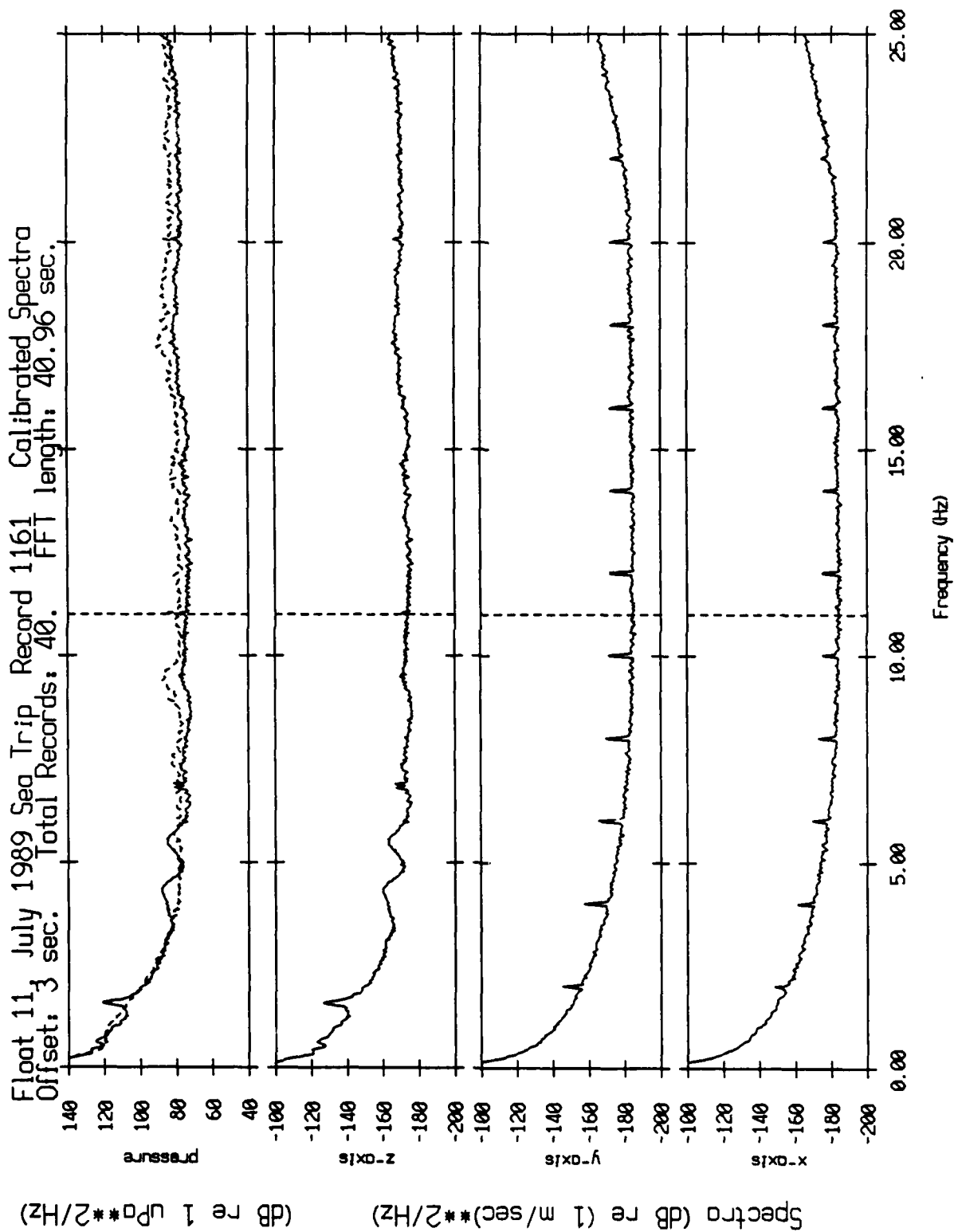


Figure XII.101



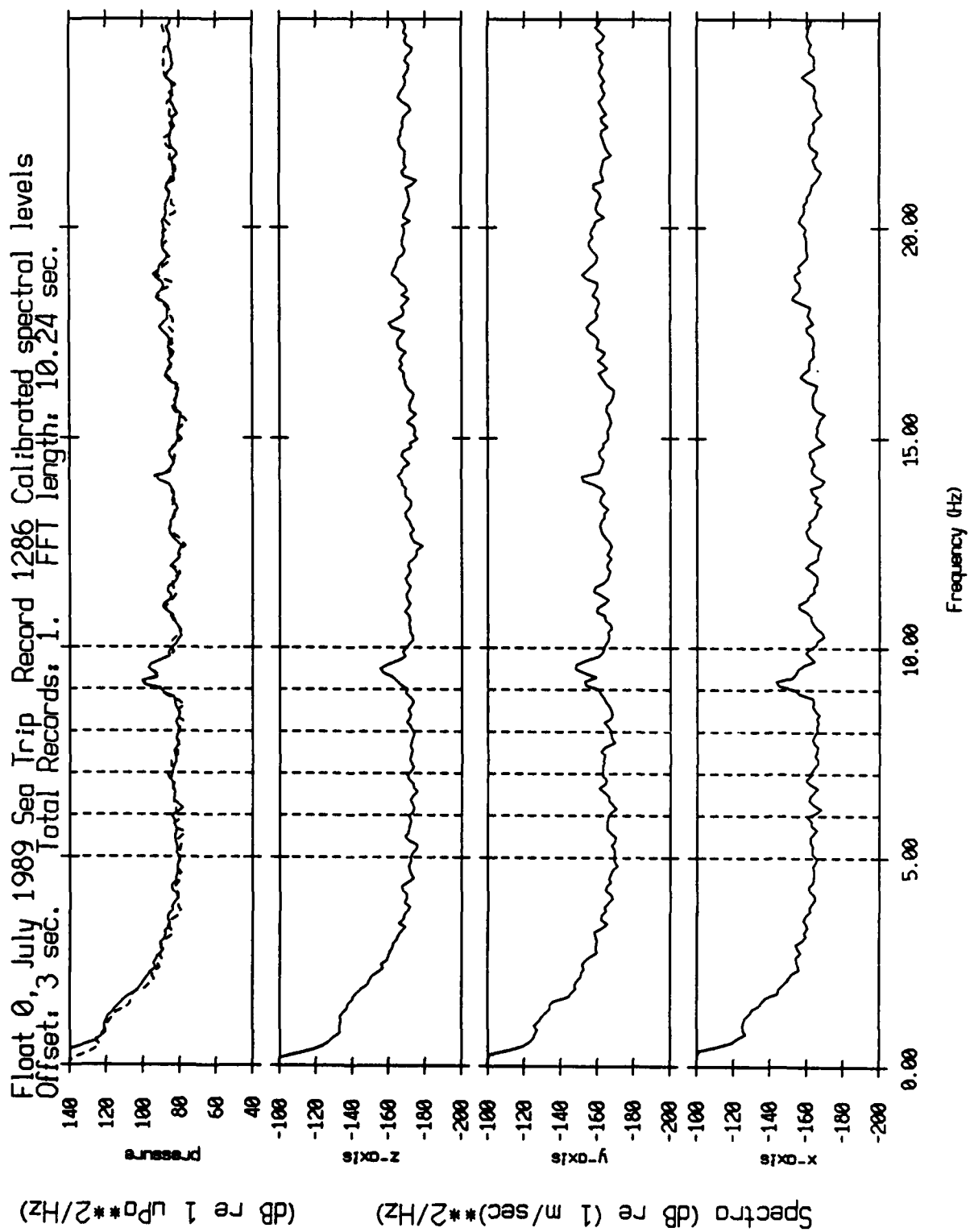


Figure XII.11a

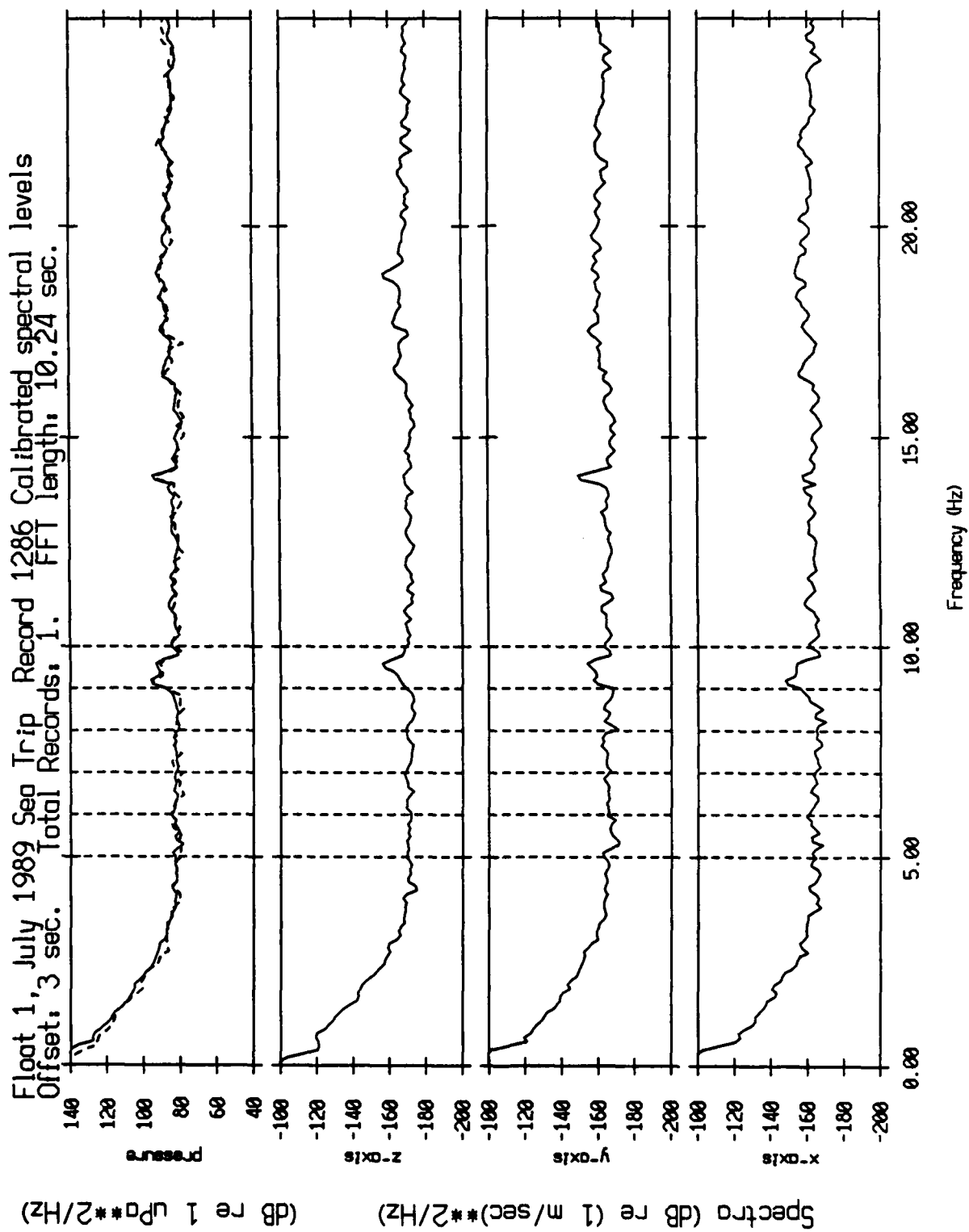


Figure XII.11b

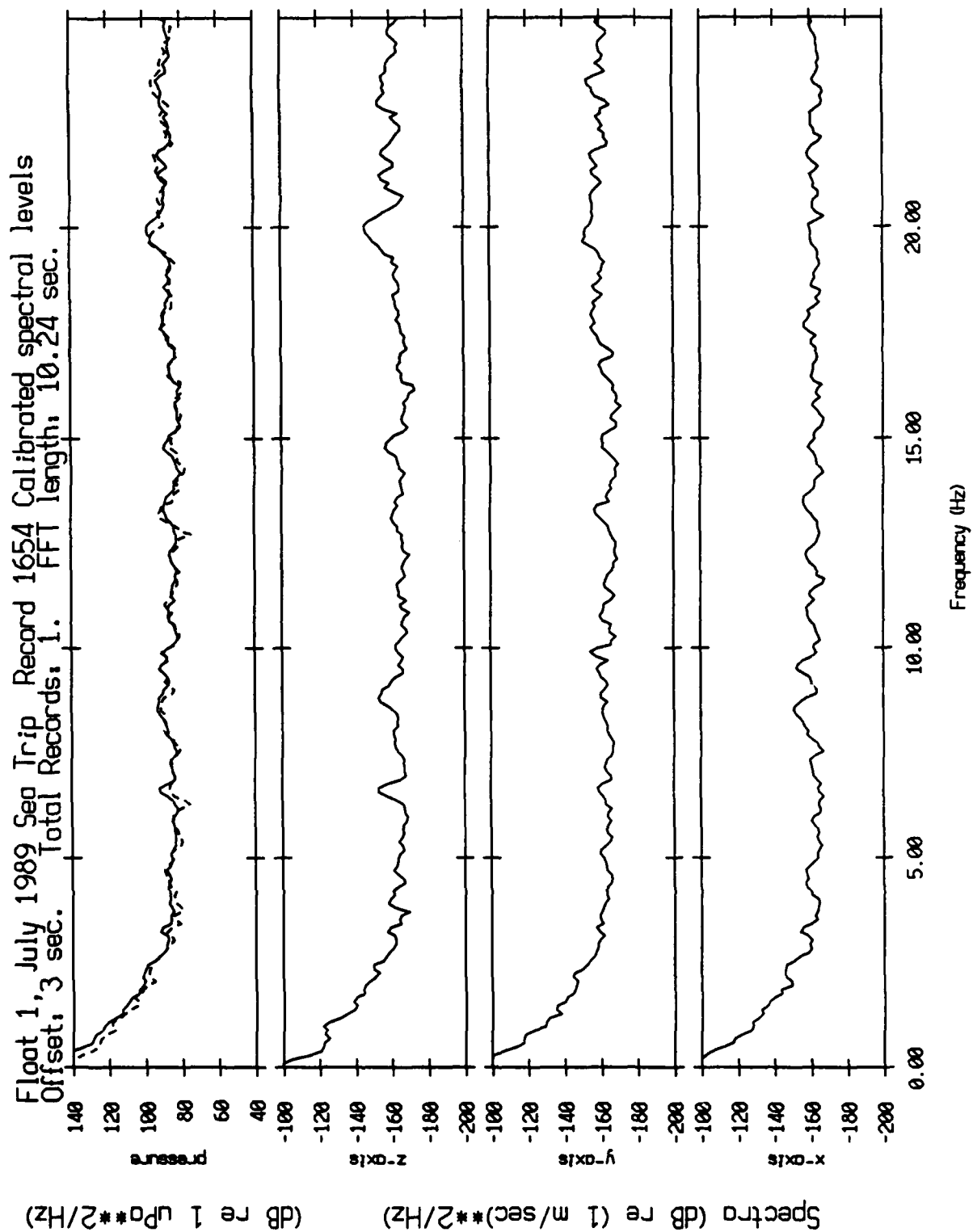


Figure XII.12

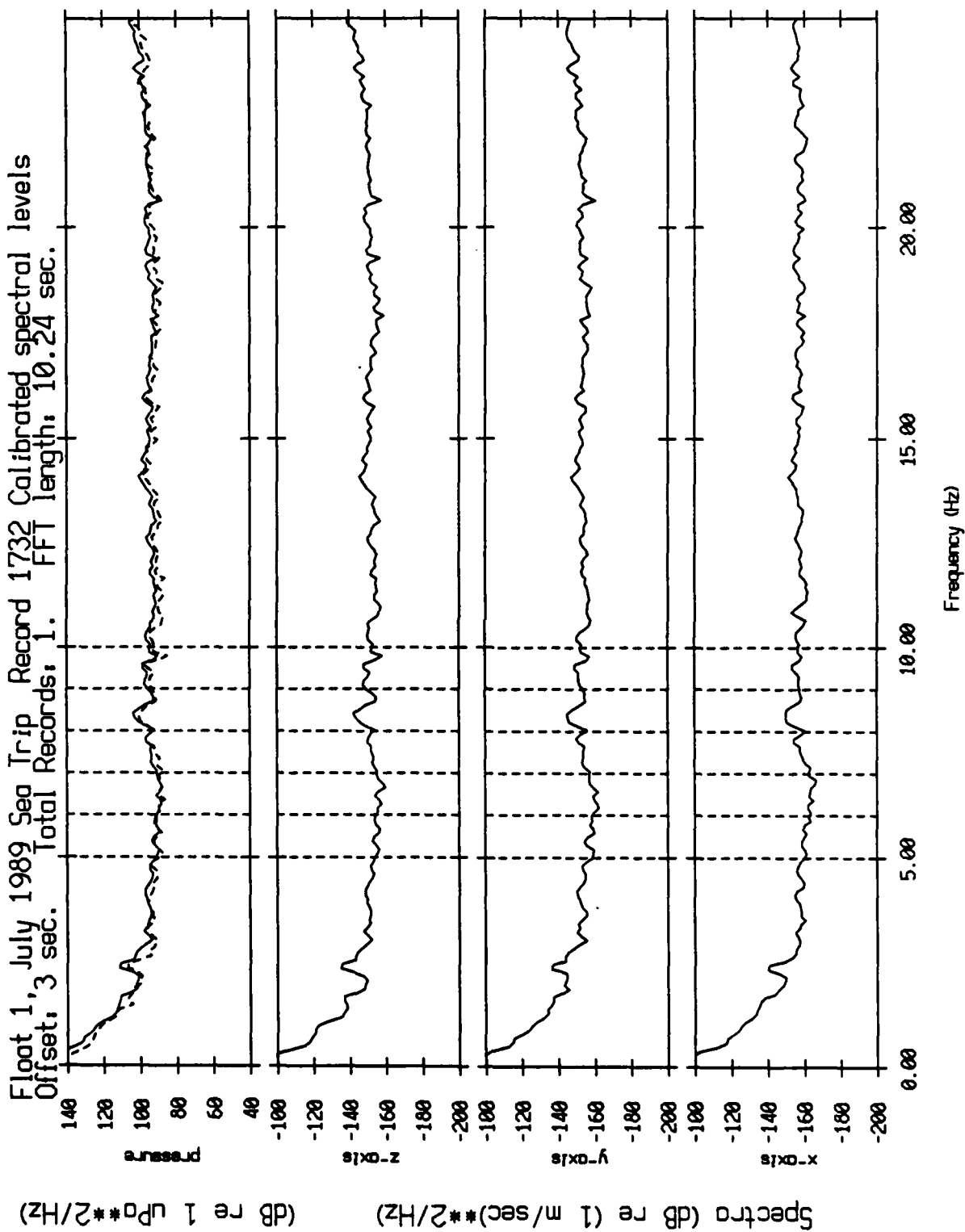


Figure XII.13

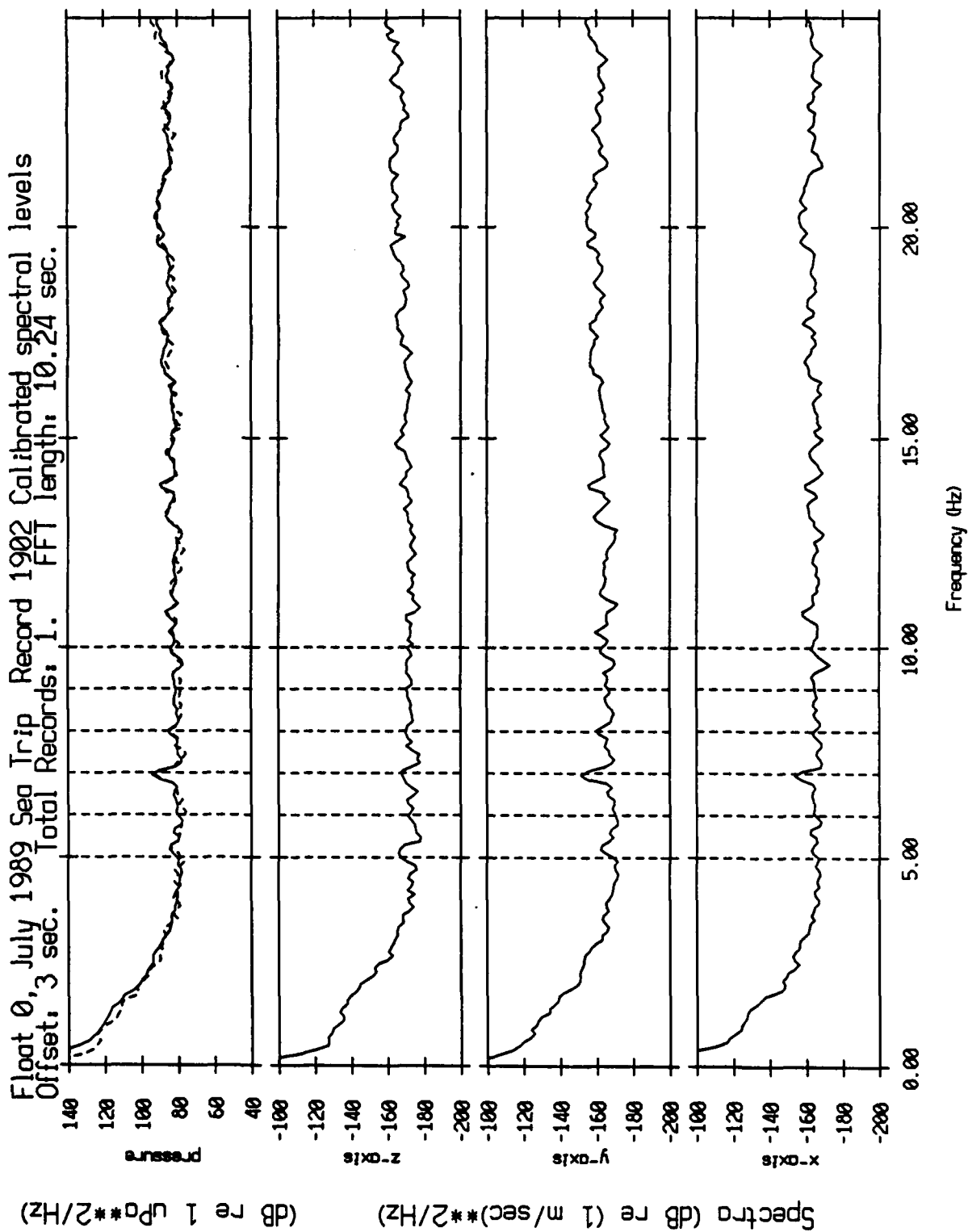


Figure XII.14a

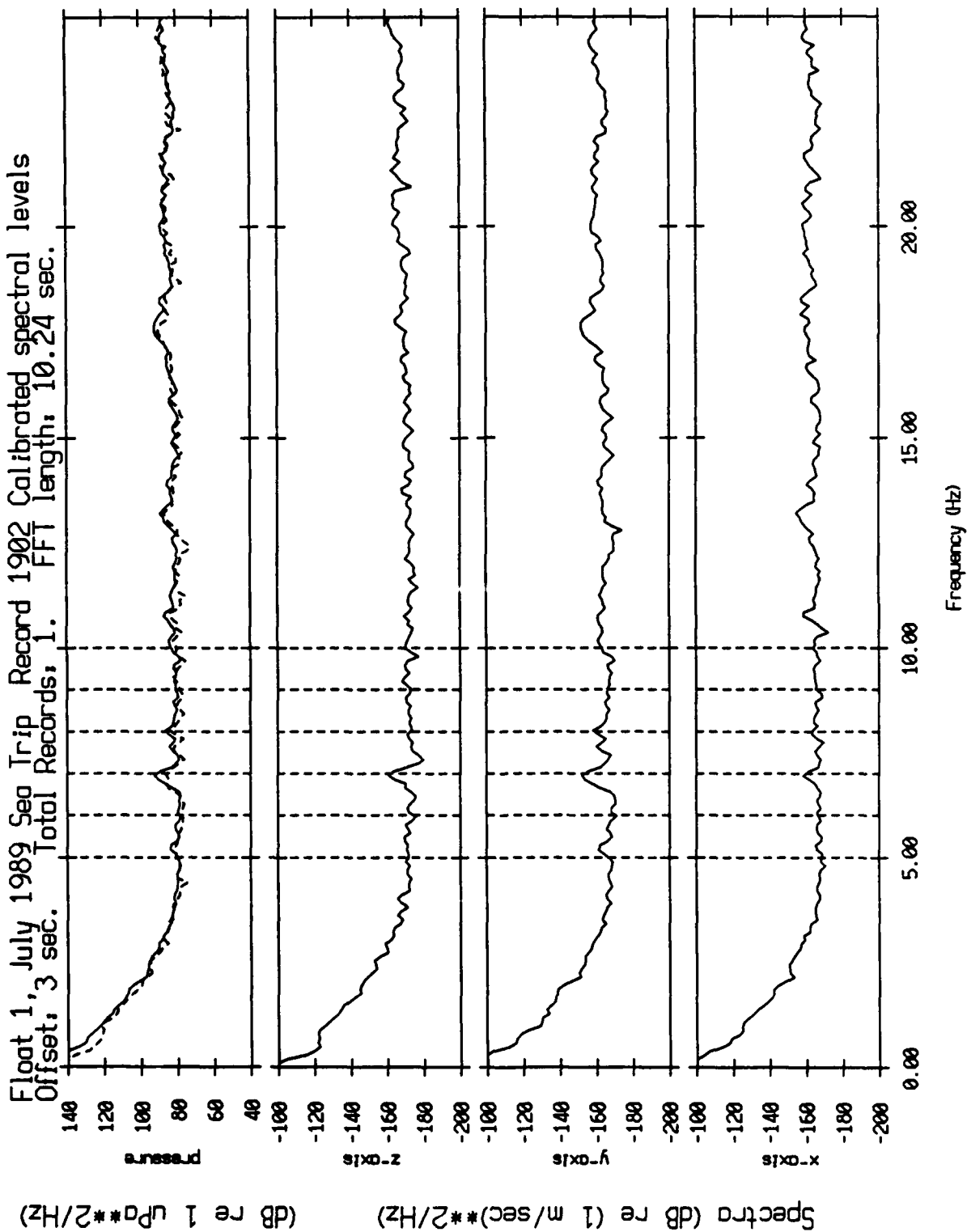


Figure XII.14b

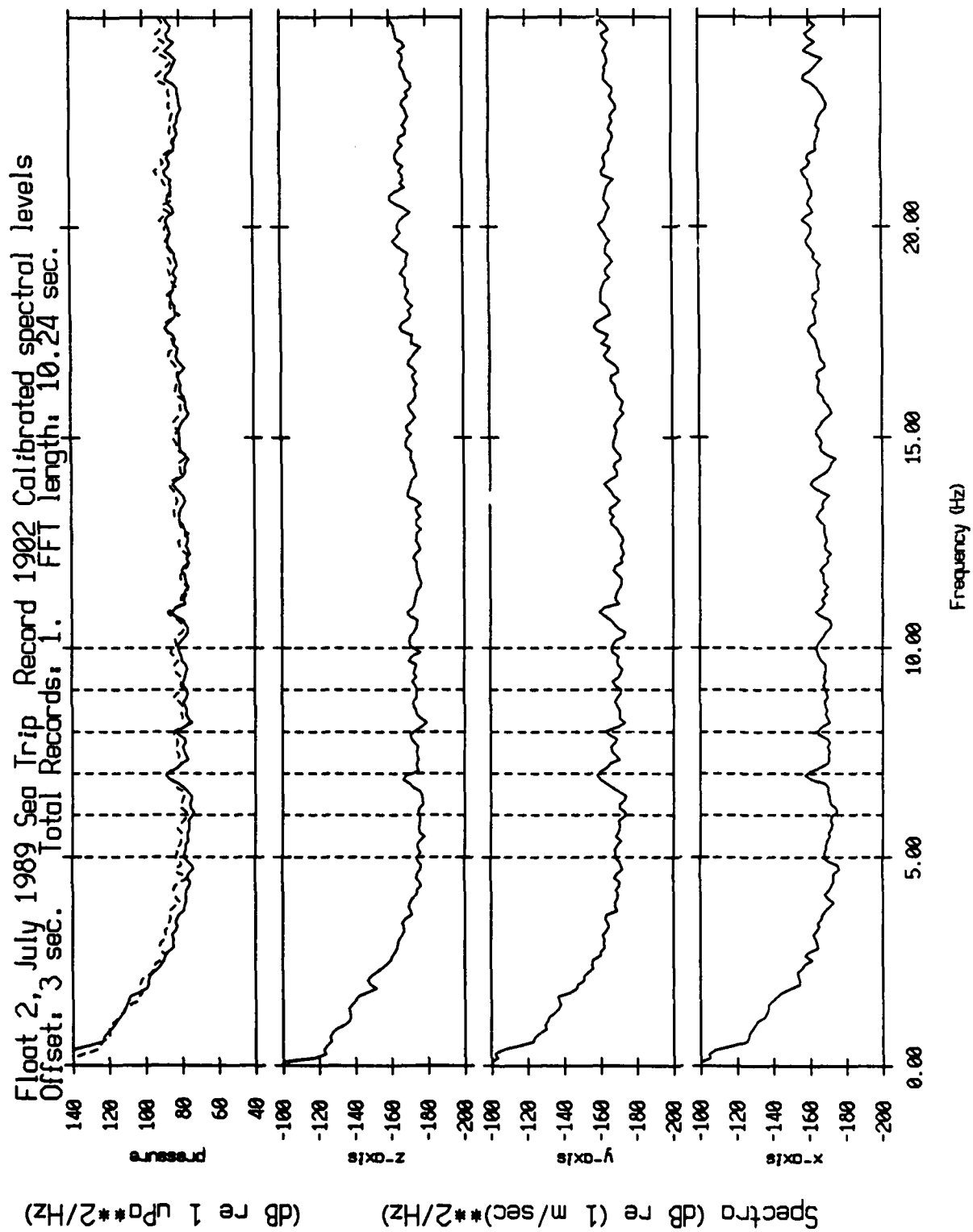


Figure XII.14c

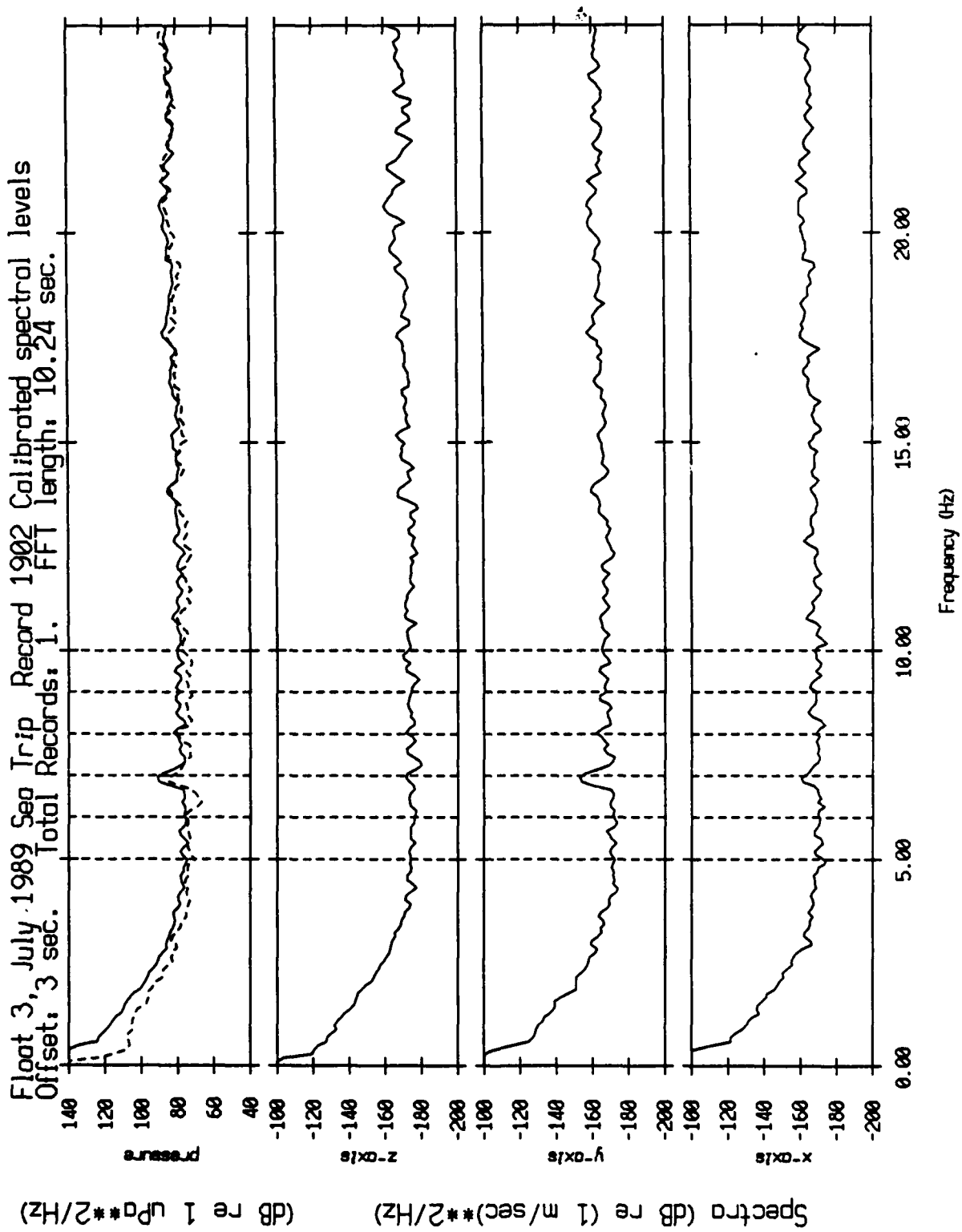


Figure XII.14d



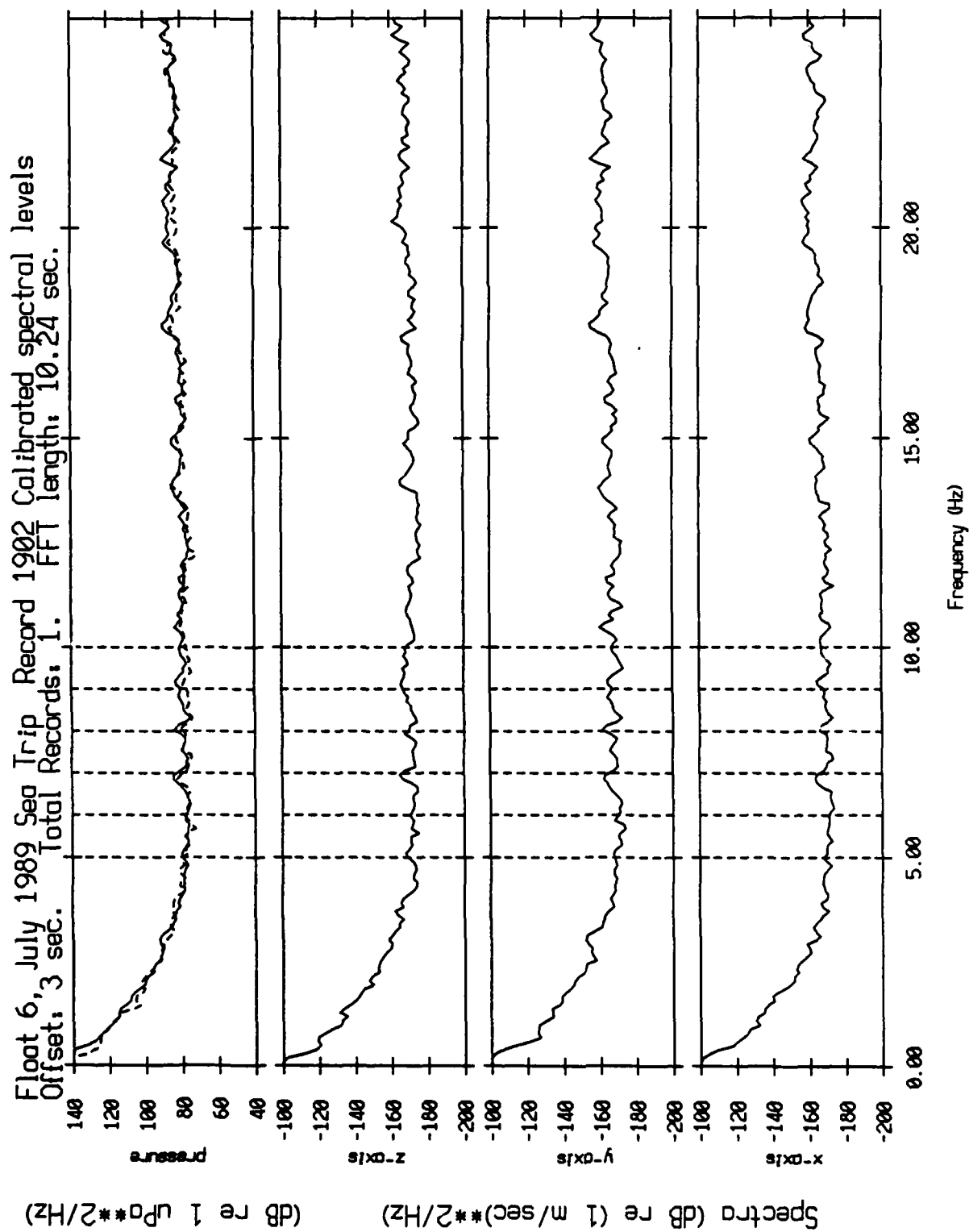


Figure XII.14e

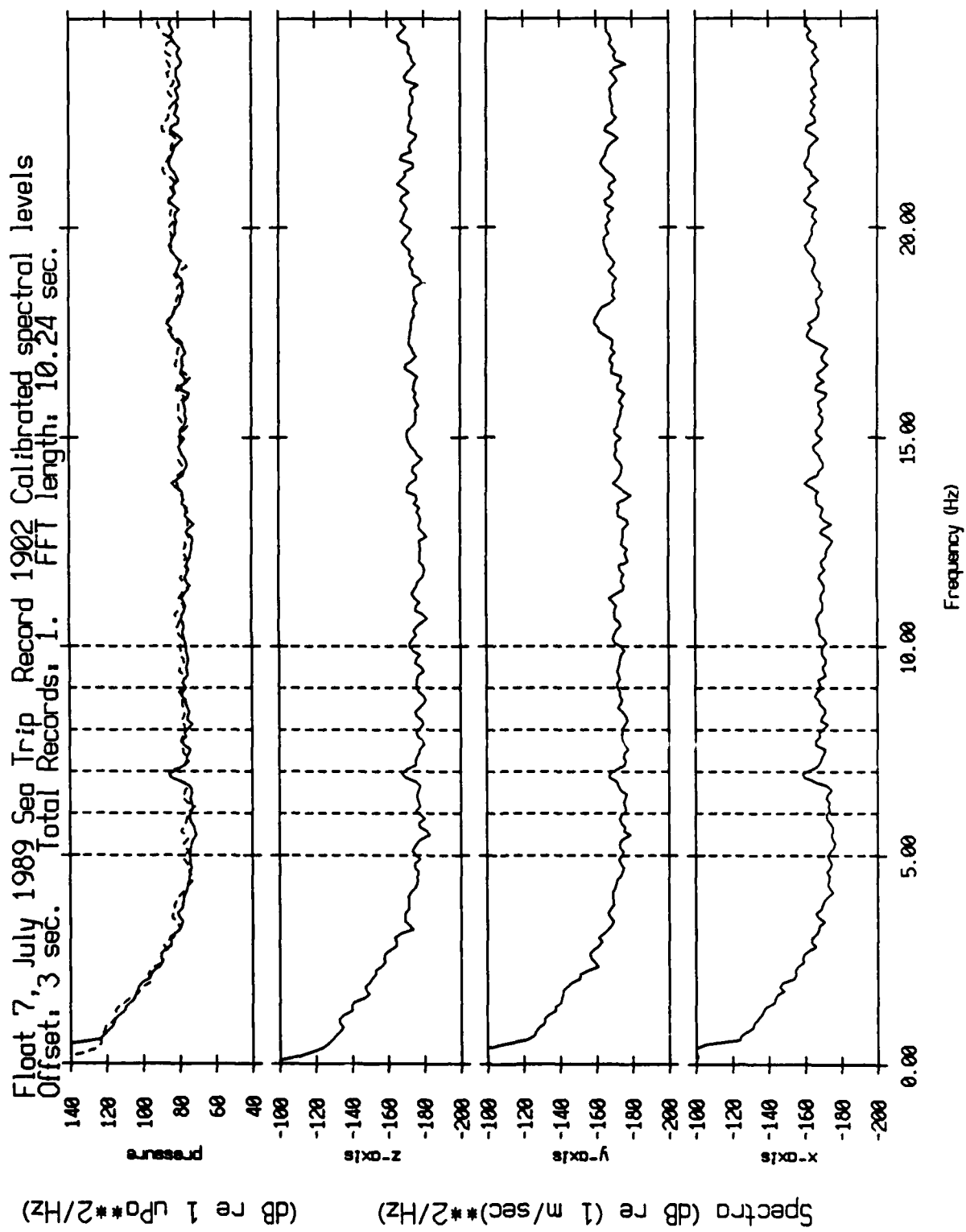


Figure XII.14f

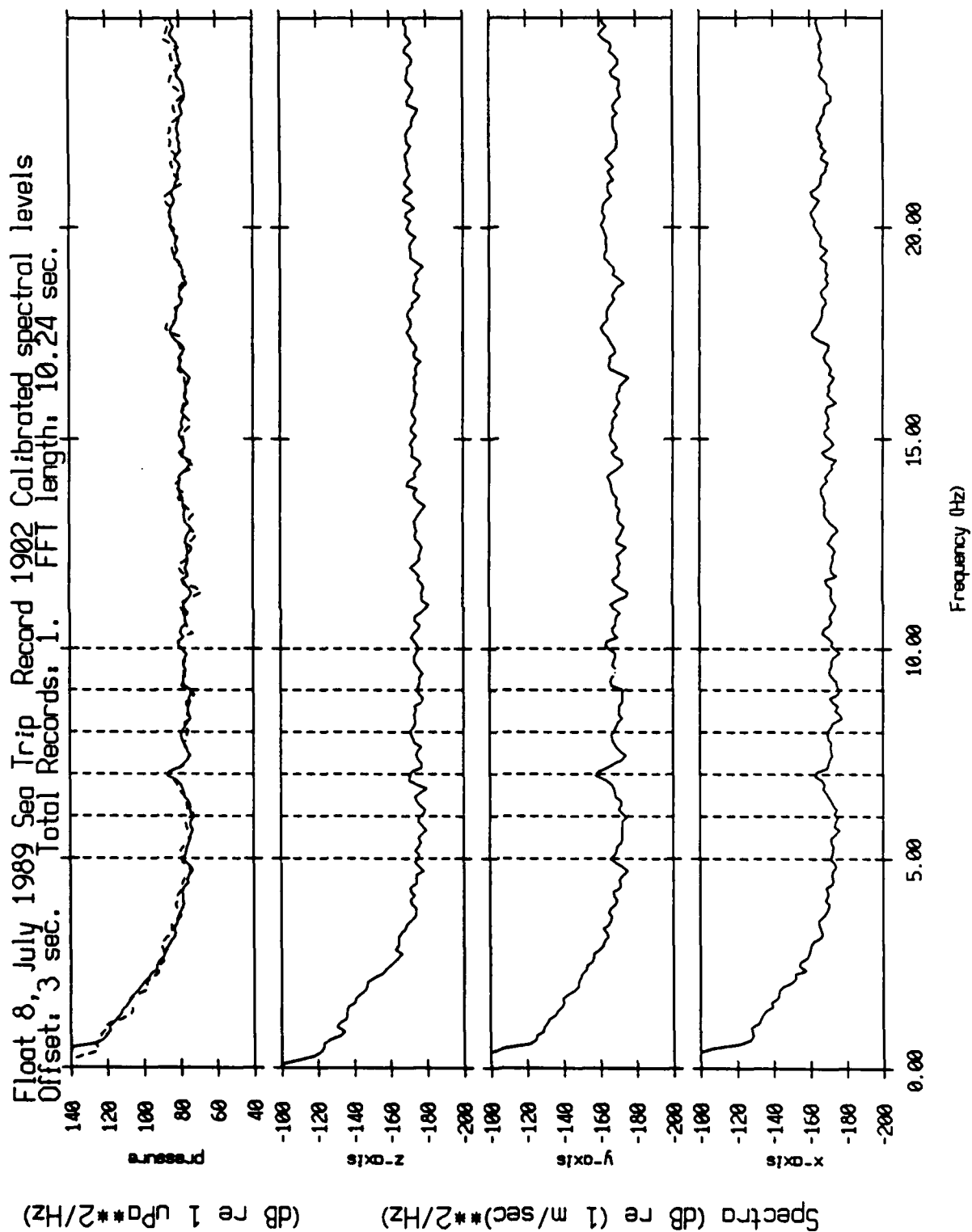


Figure XII.14g

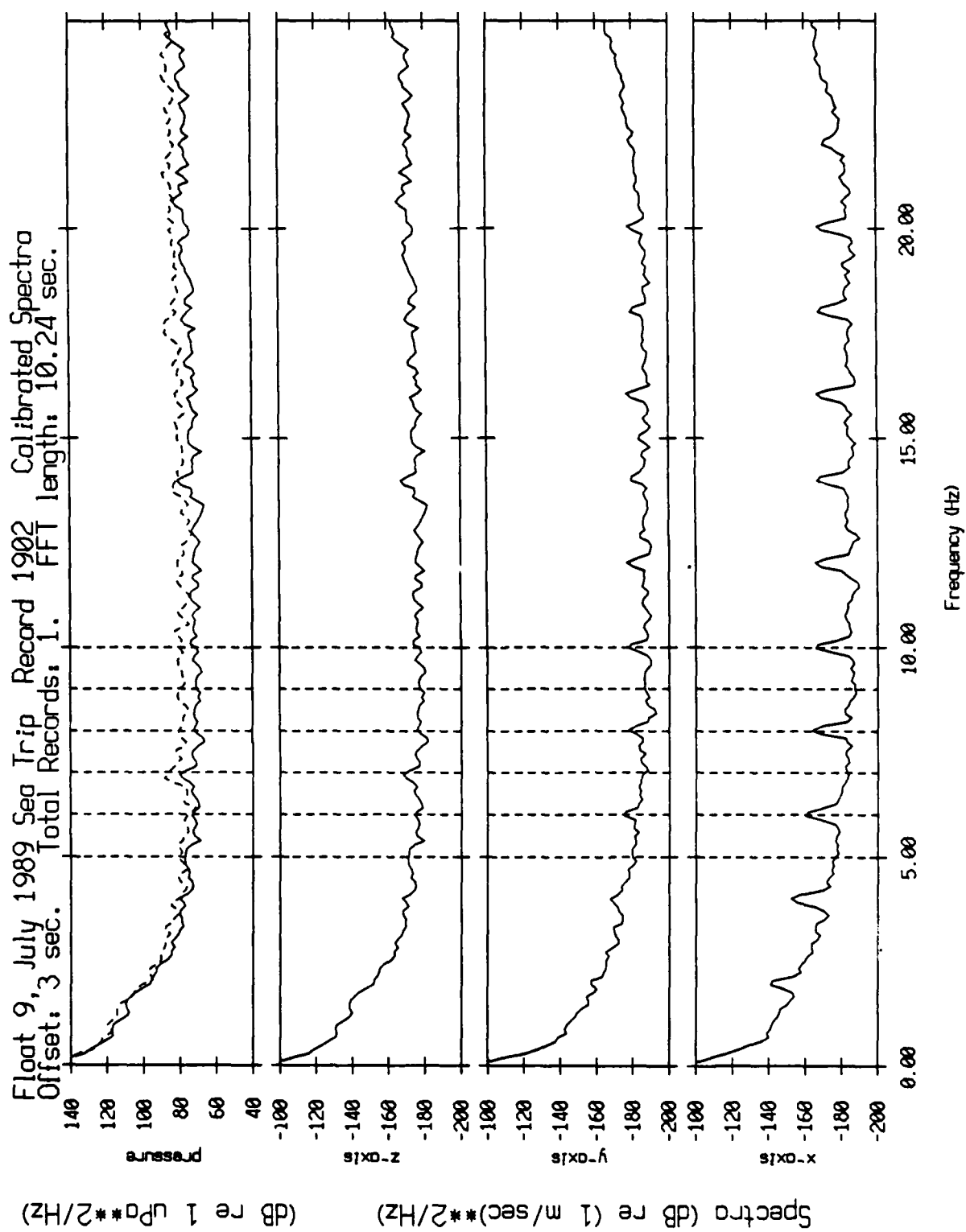


Figure XII.14h

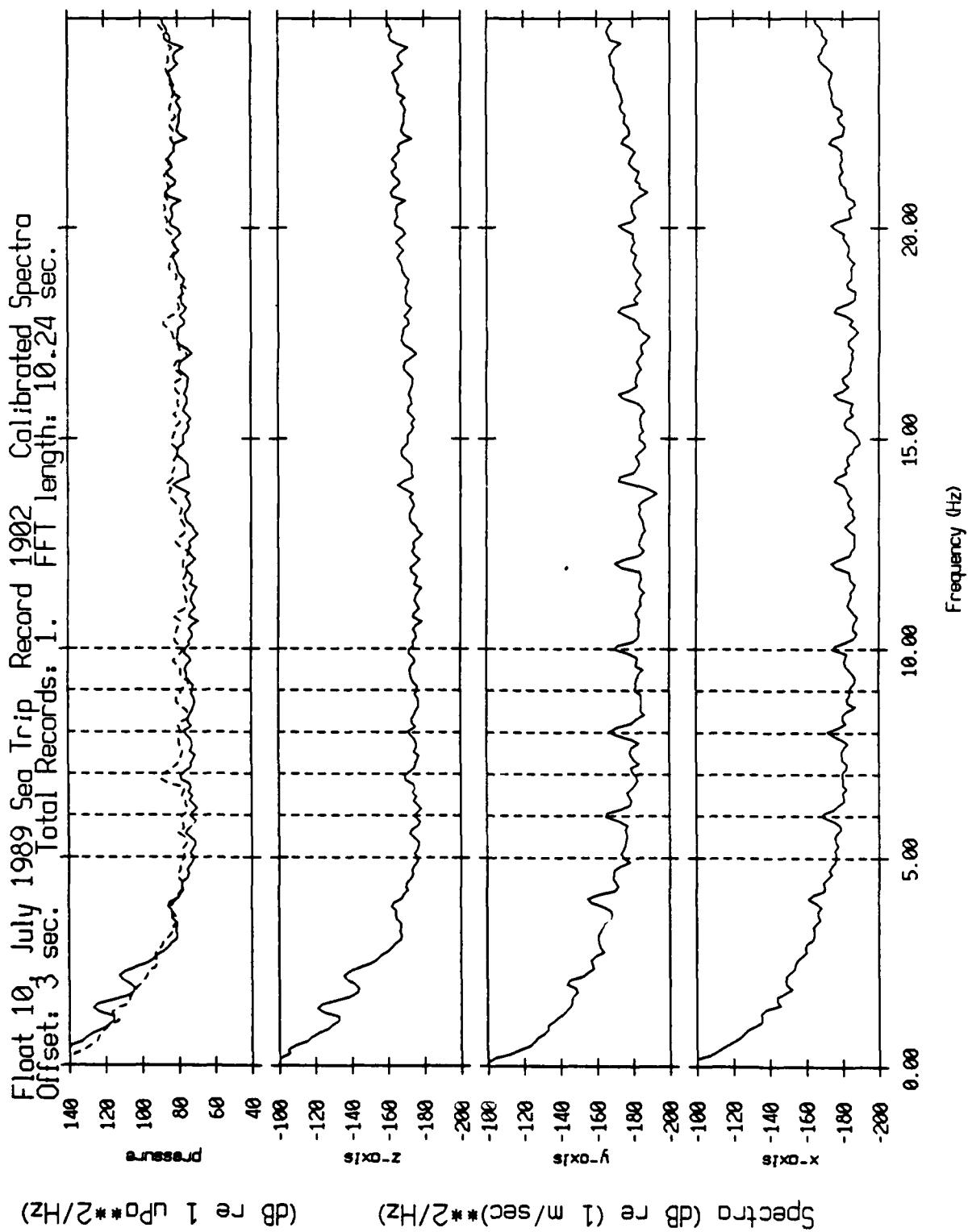


Figure XII.14i

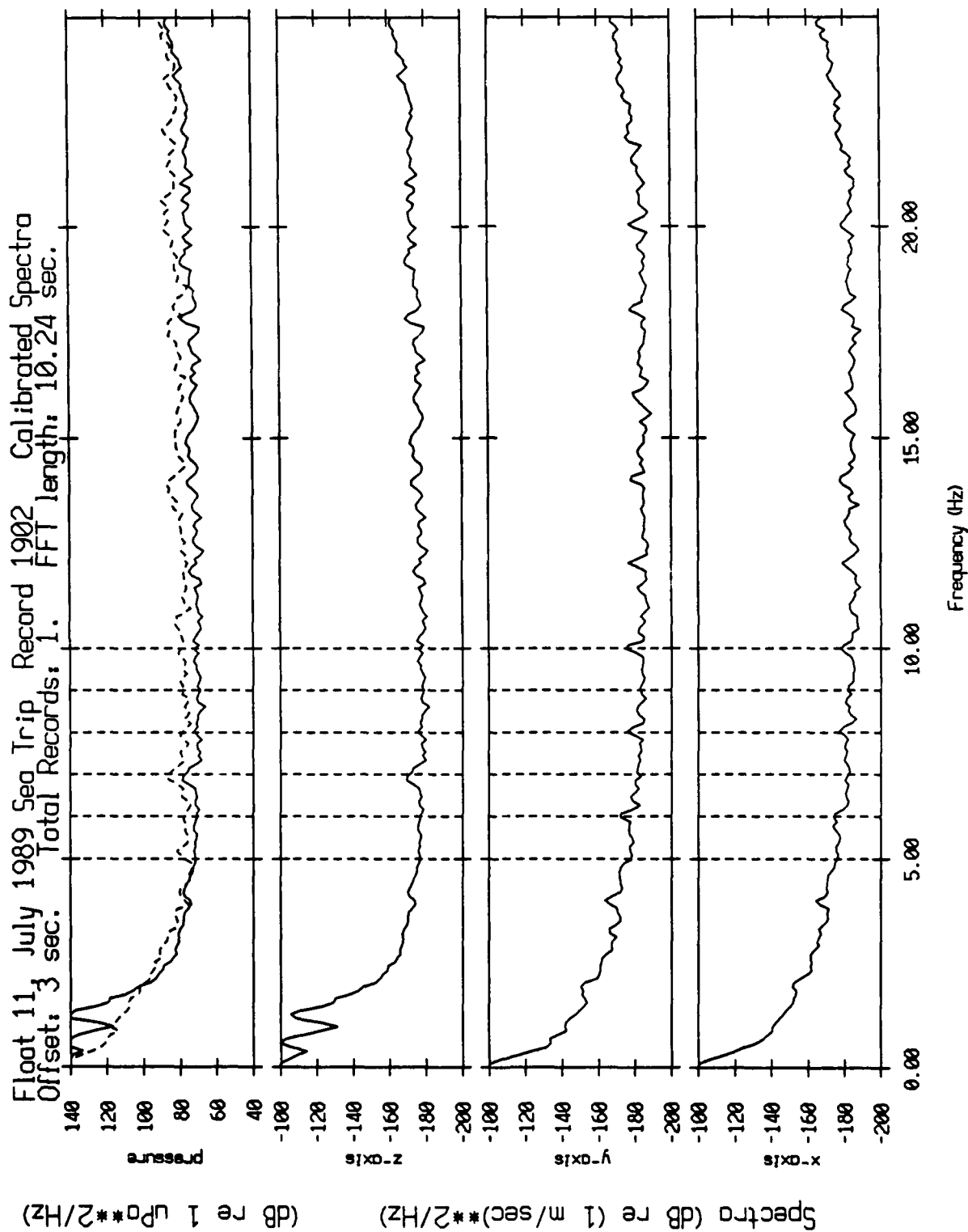


Figure XII.14j

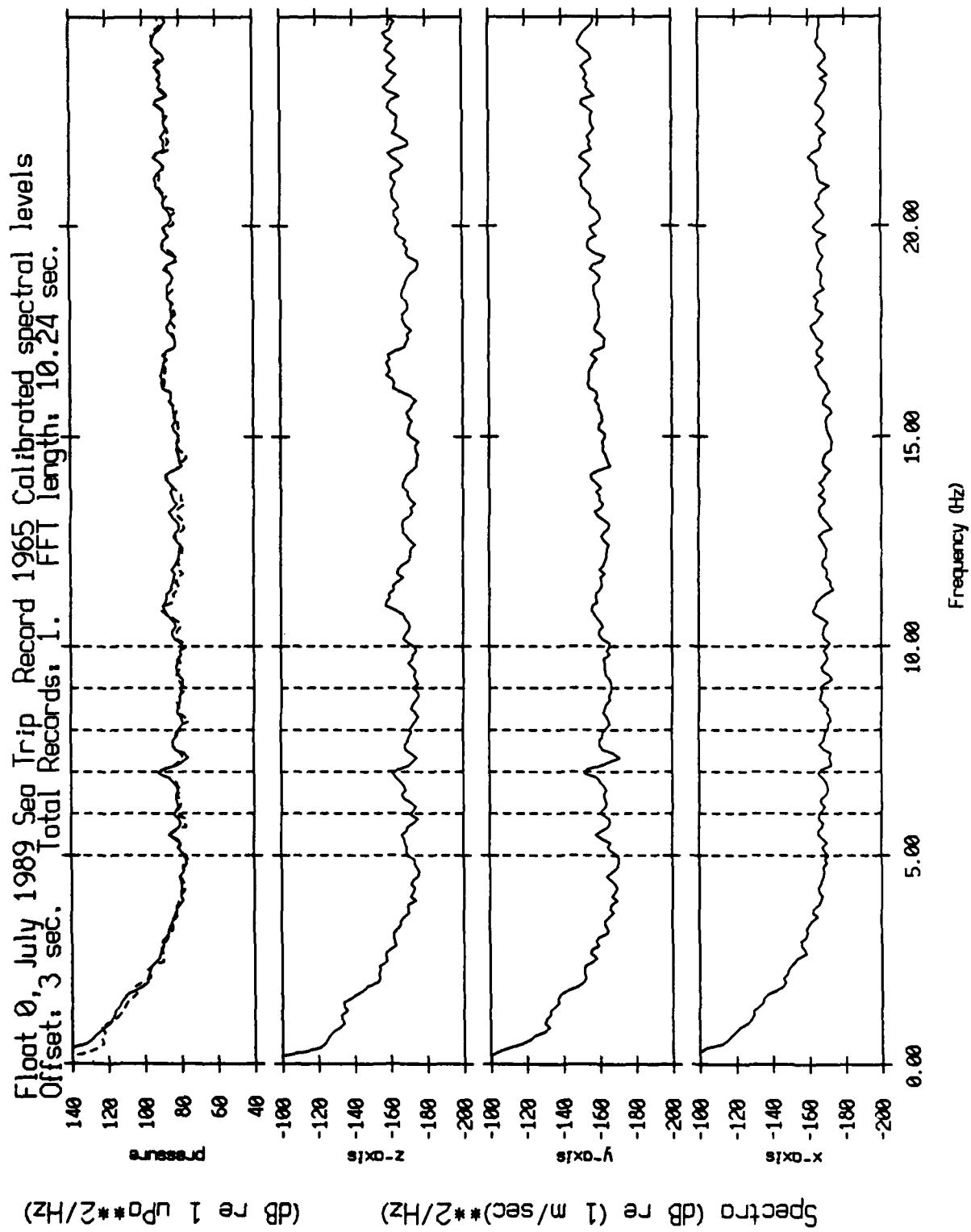


Figure XII.15a

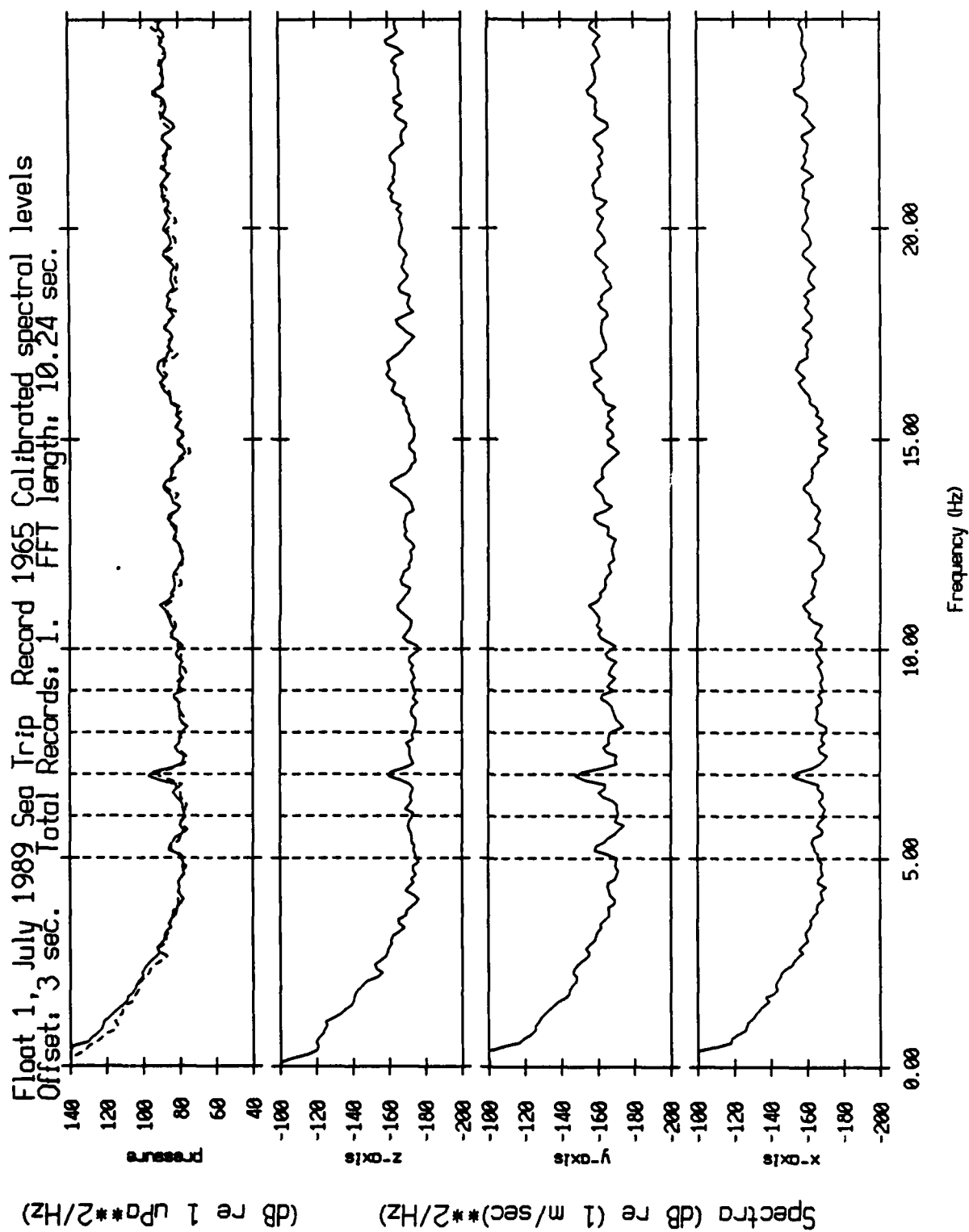


Figure XII.15b



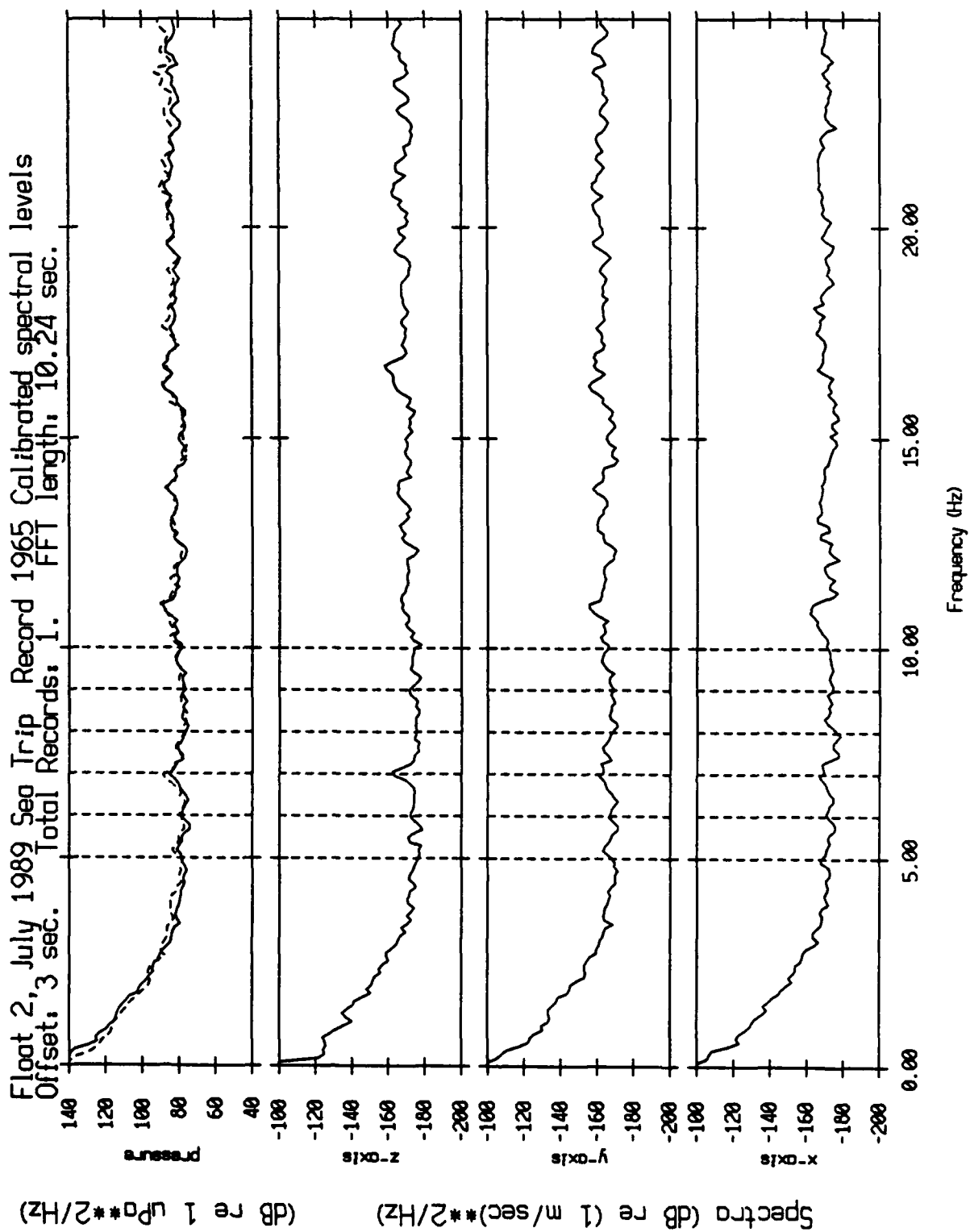


Figure XII.15c

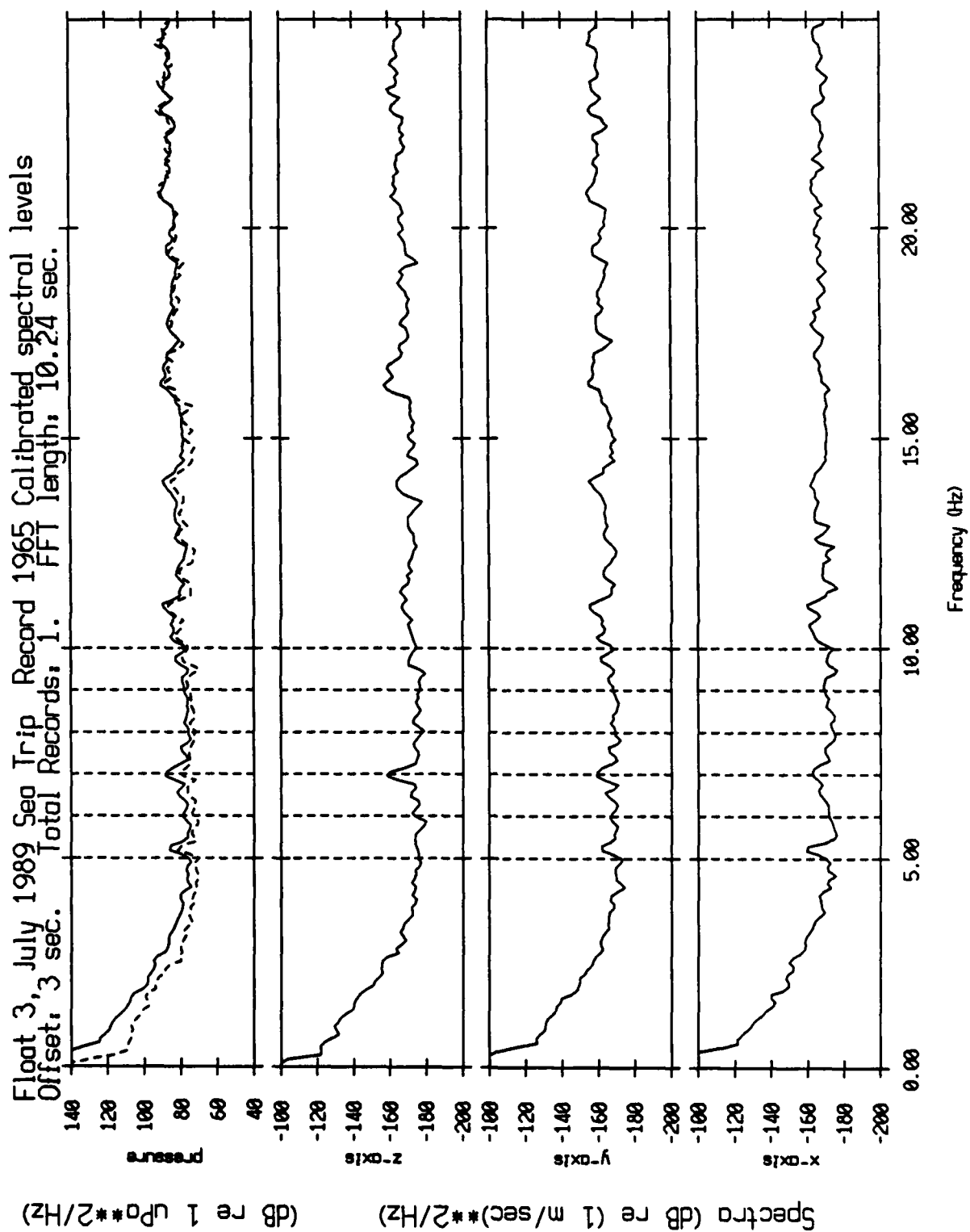


Figure XII.15d

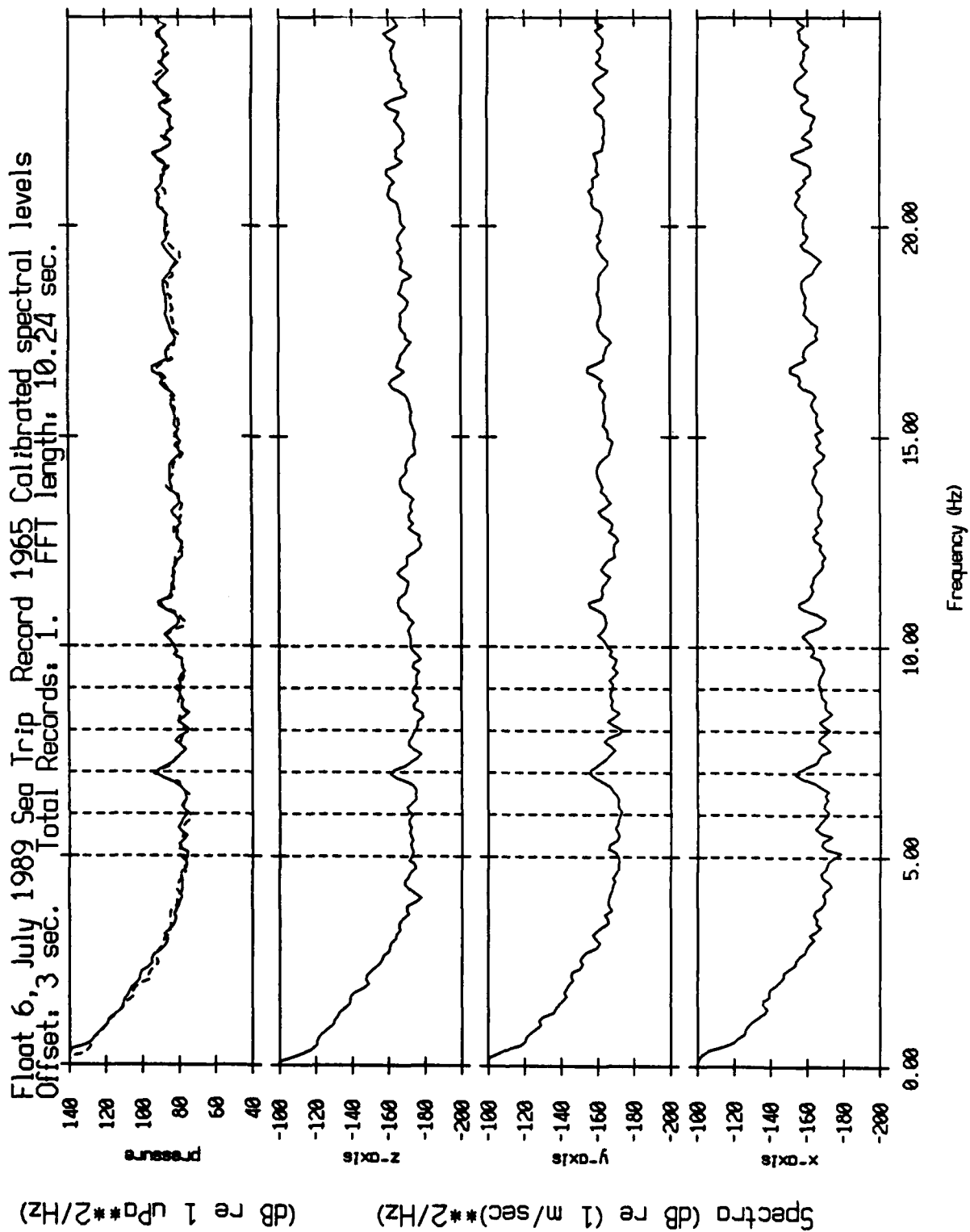


Figure XII.15e

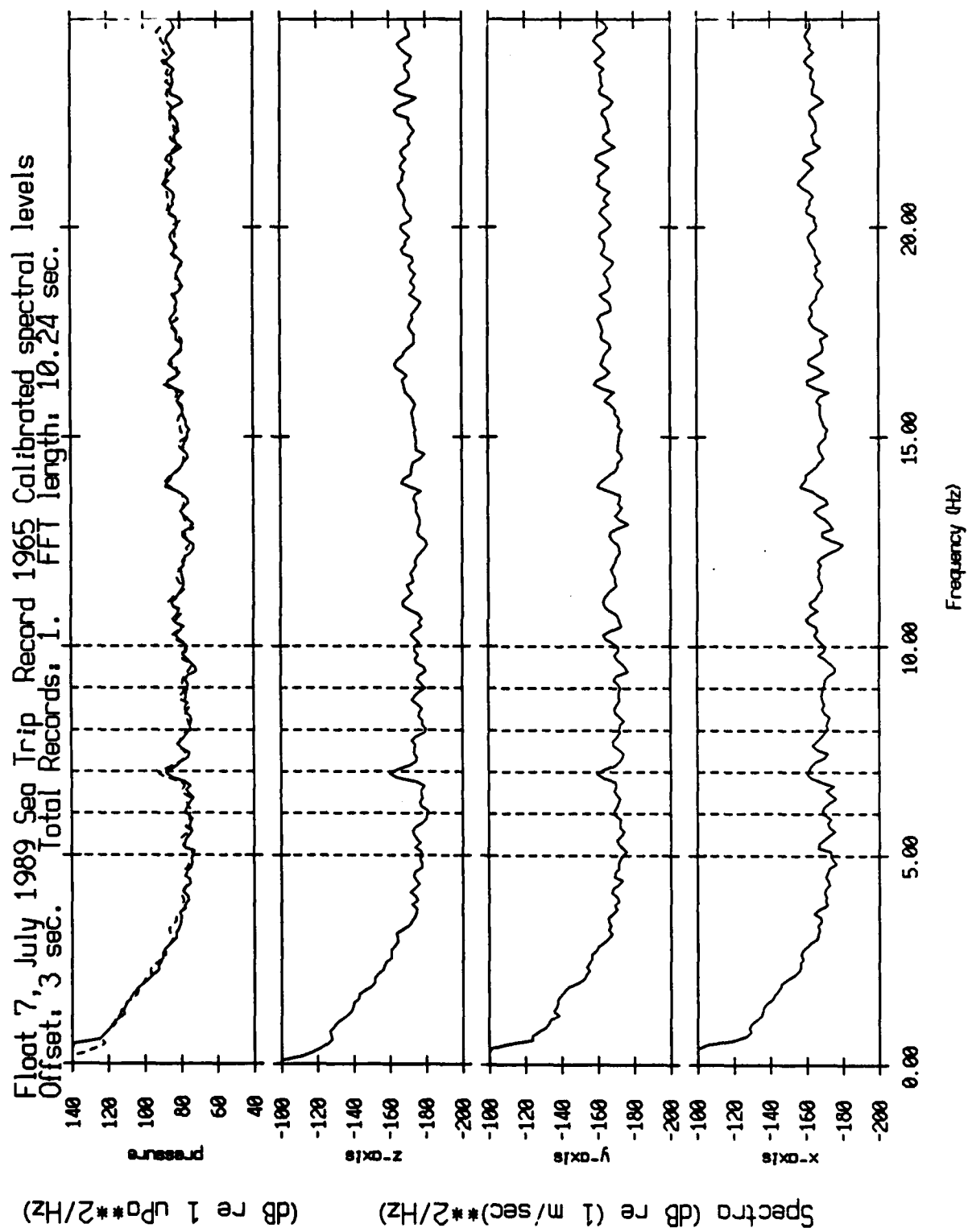


Figure XII.15f

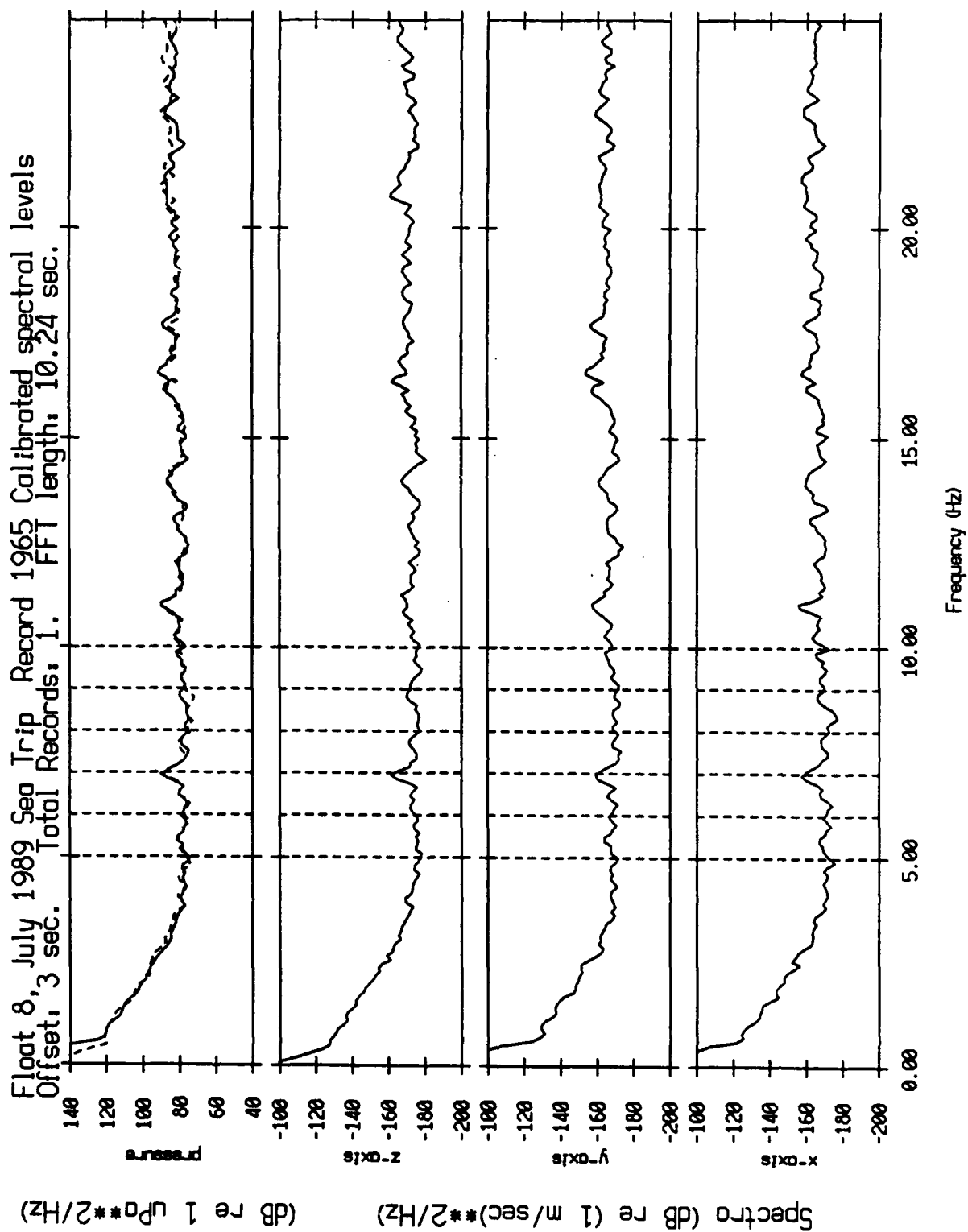


Figure XII.15g

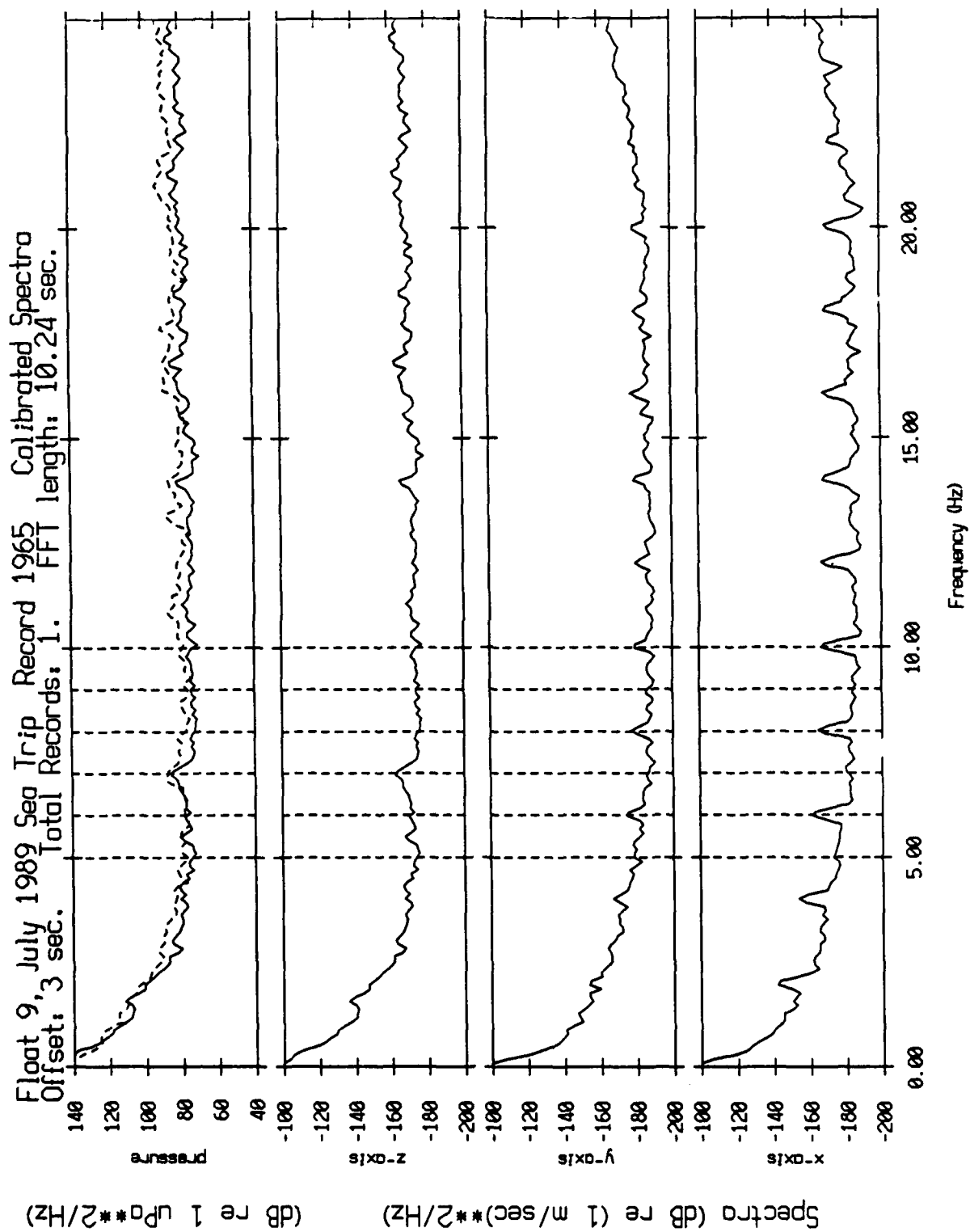


Figure XII.15h

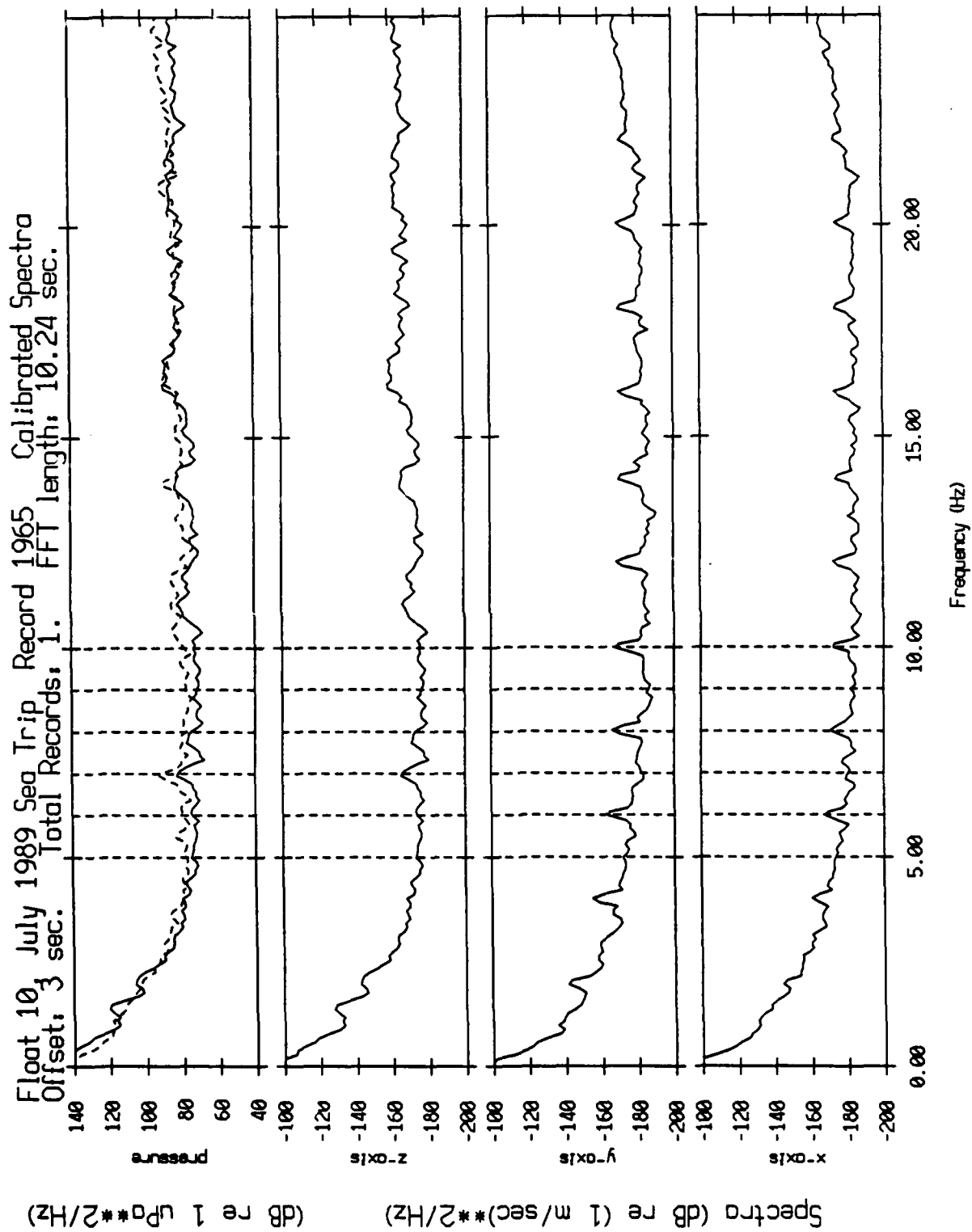


Figure XII.15i

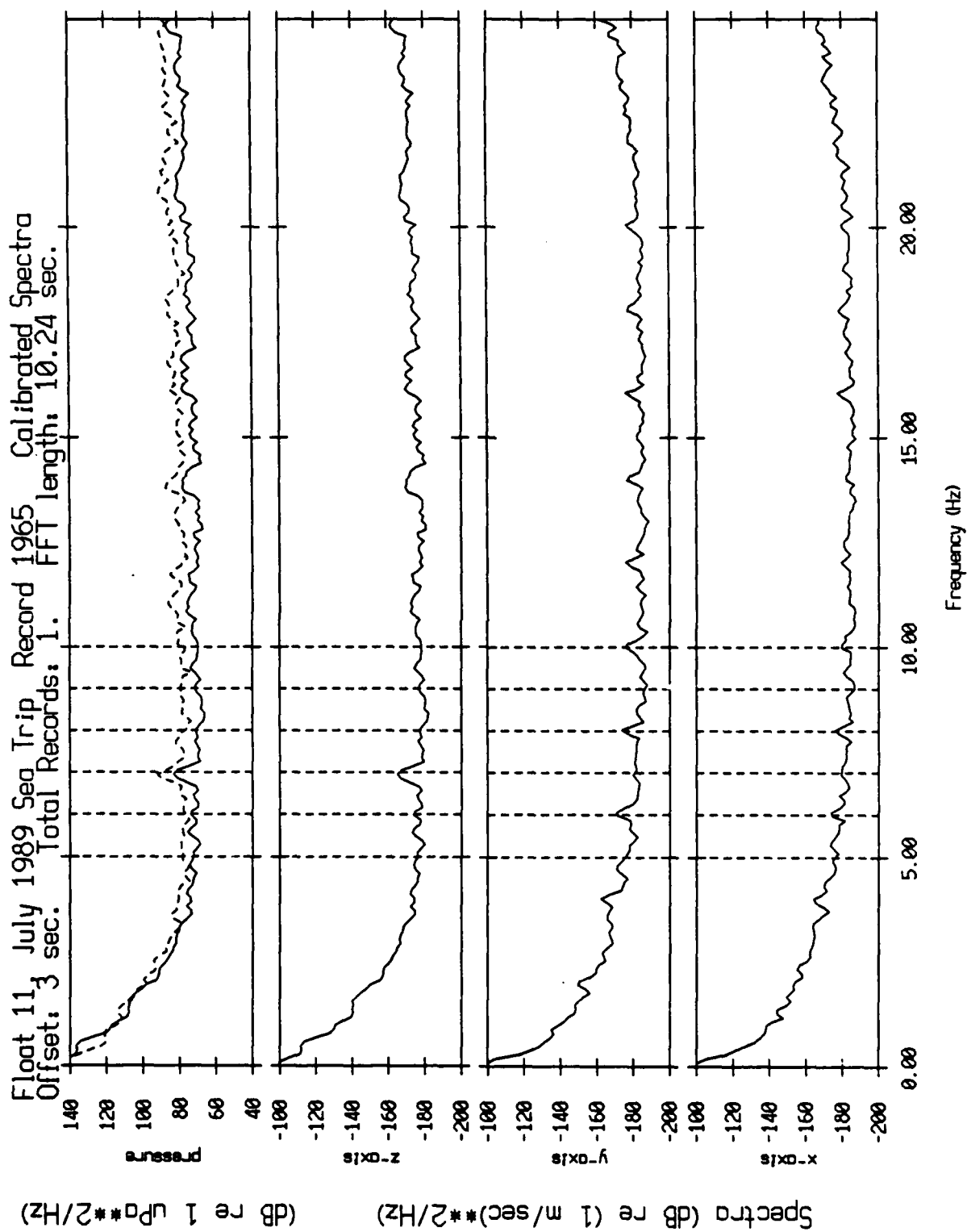


Figure XII.15j



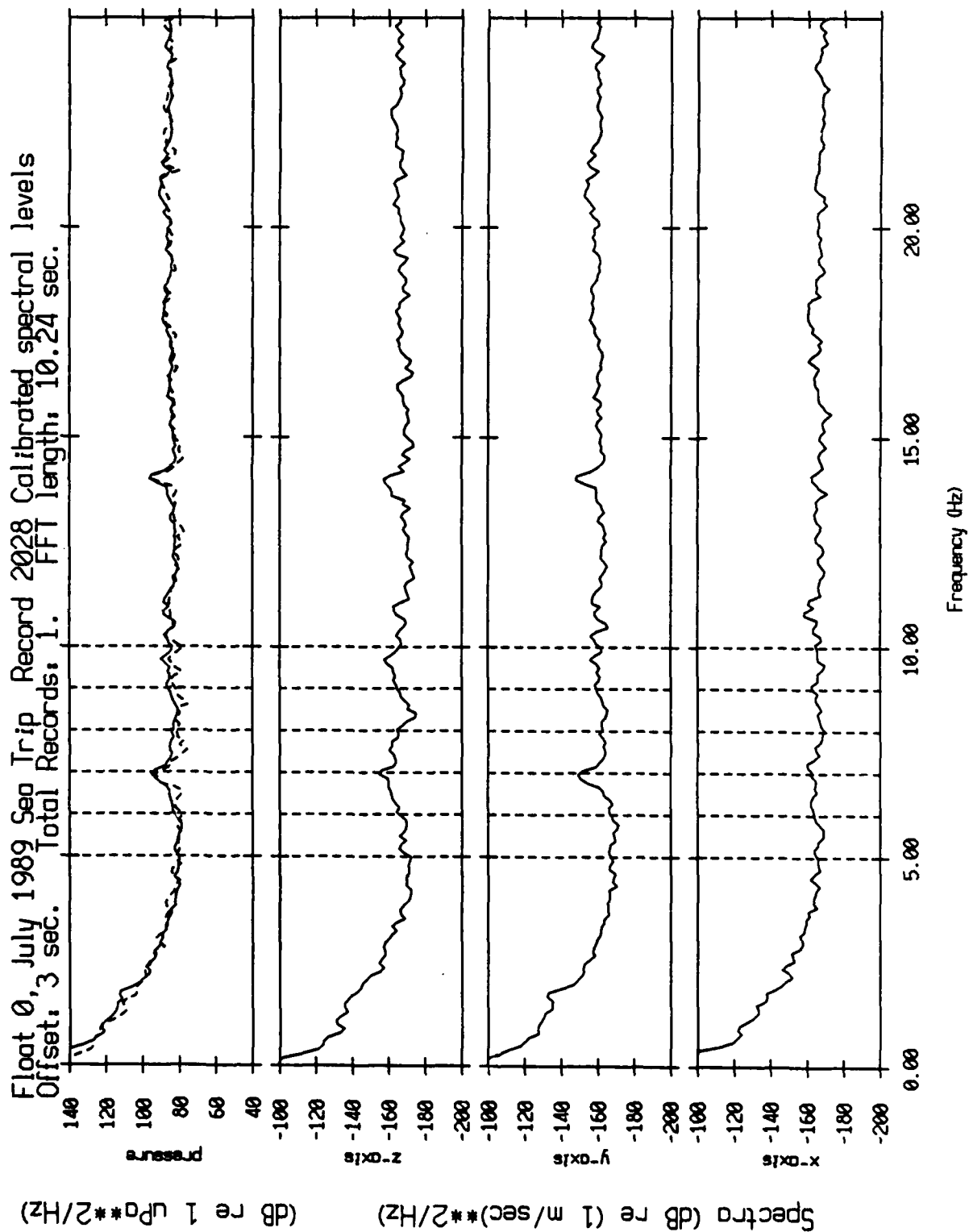


Figure XII.16a

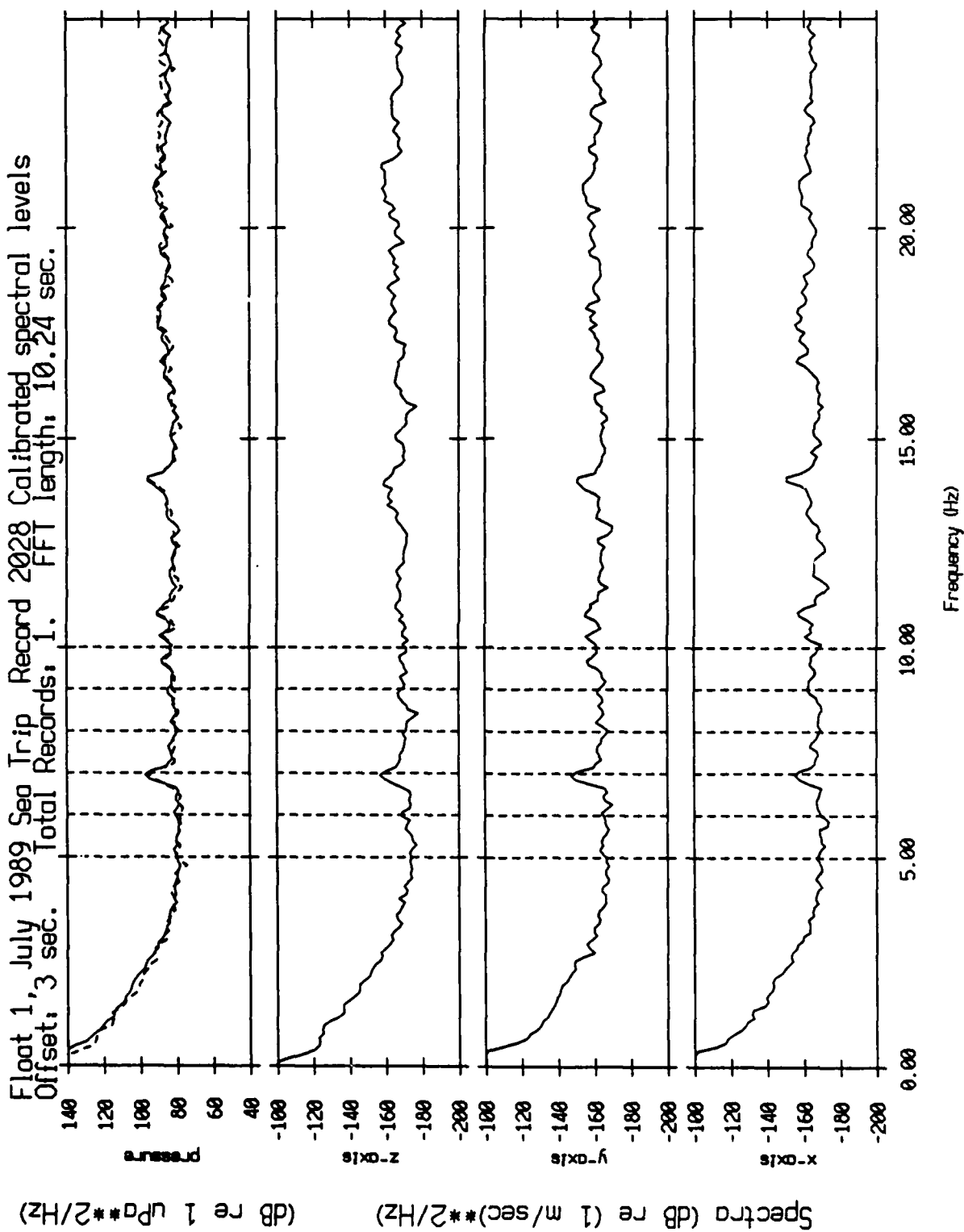


Figure XII.16b

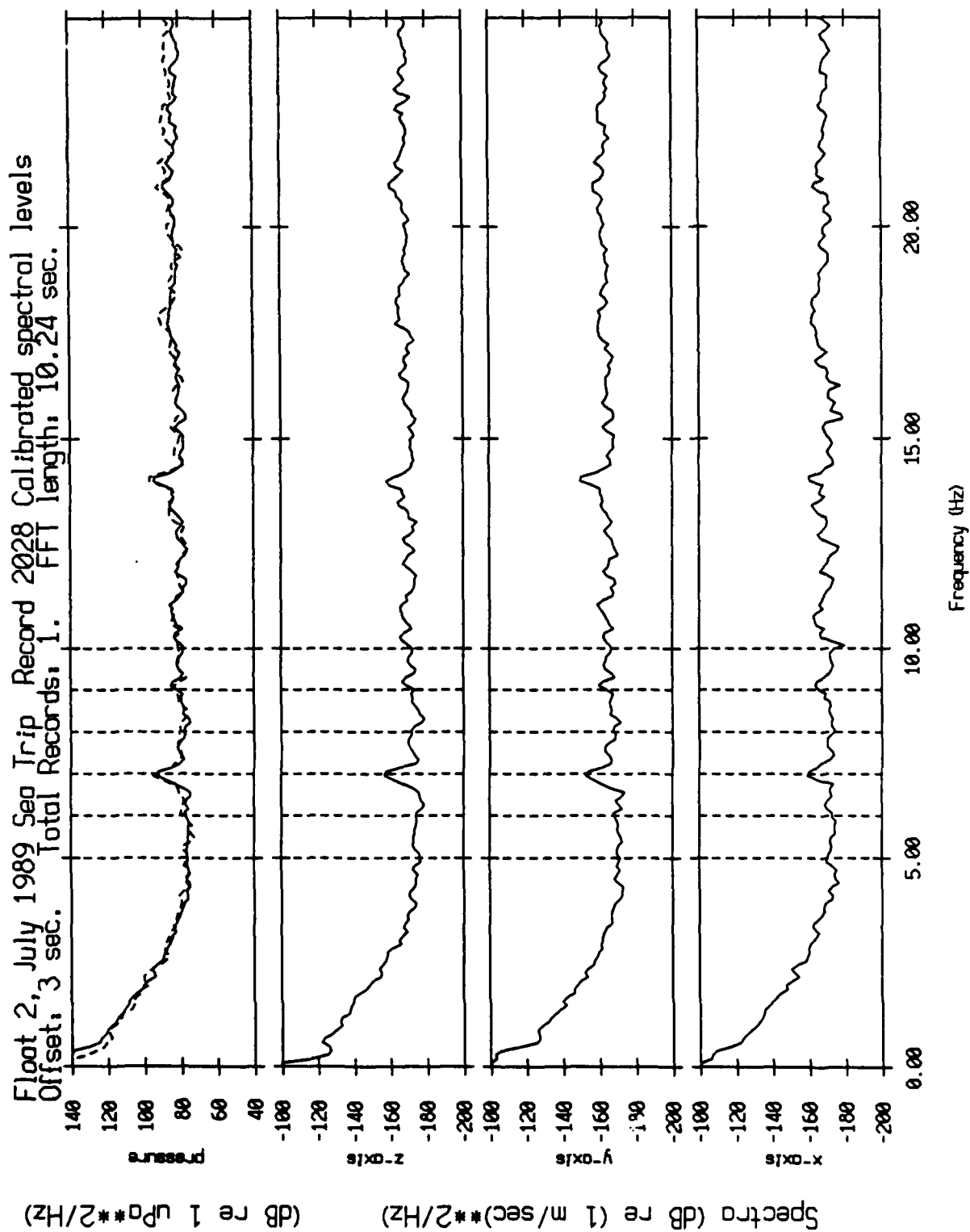


Figure XII.16c

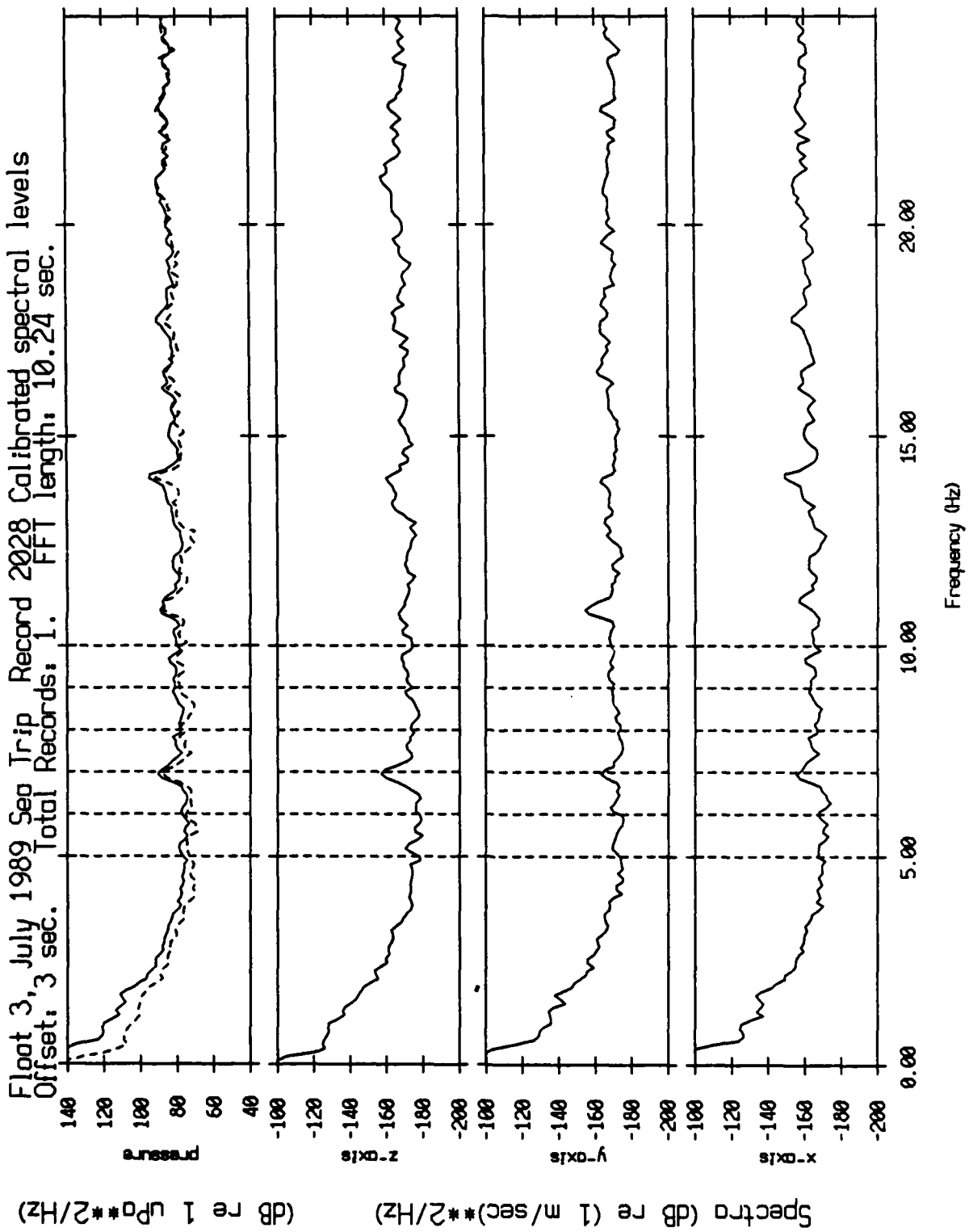


Figure XII.16d

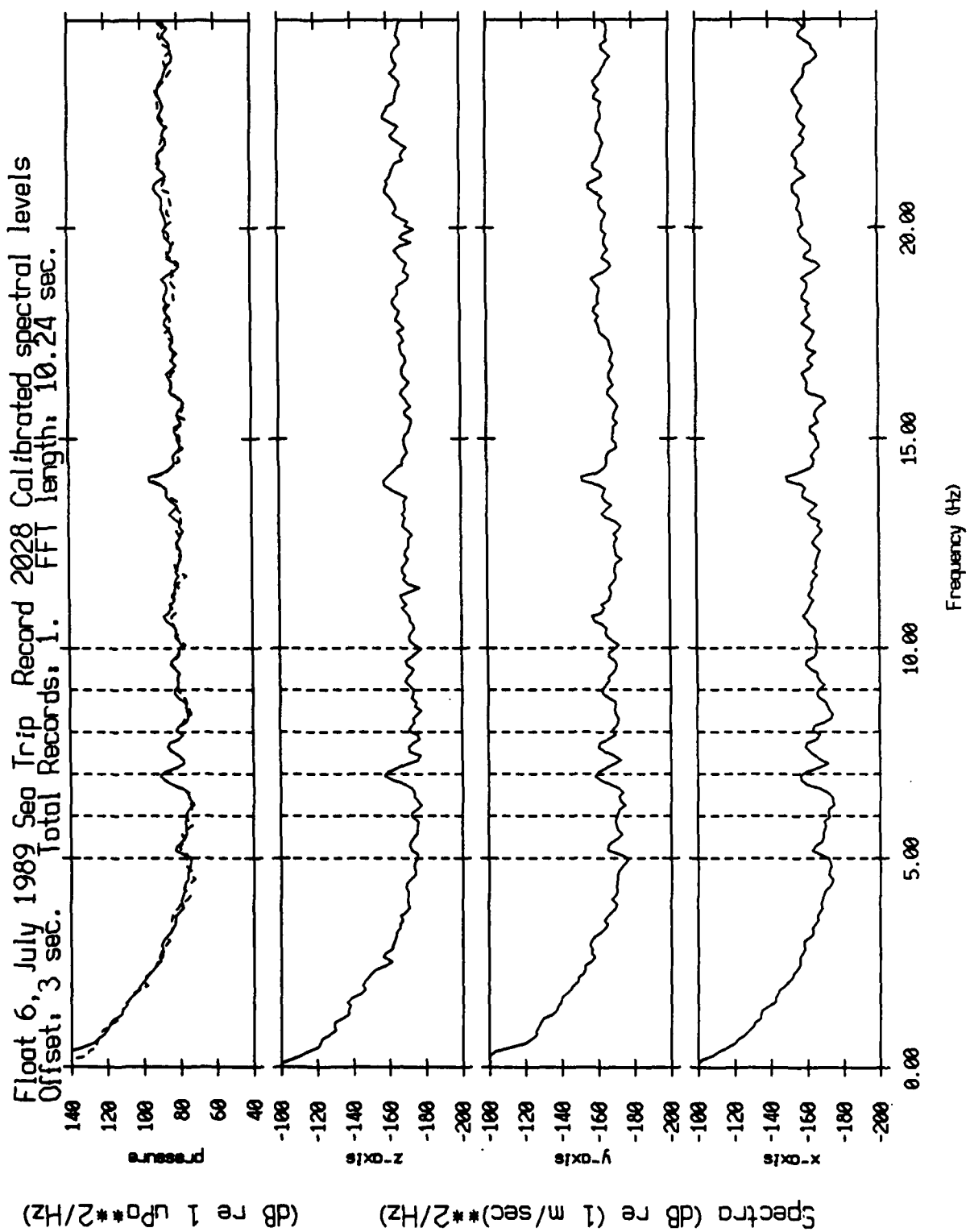


Figure XII.16e

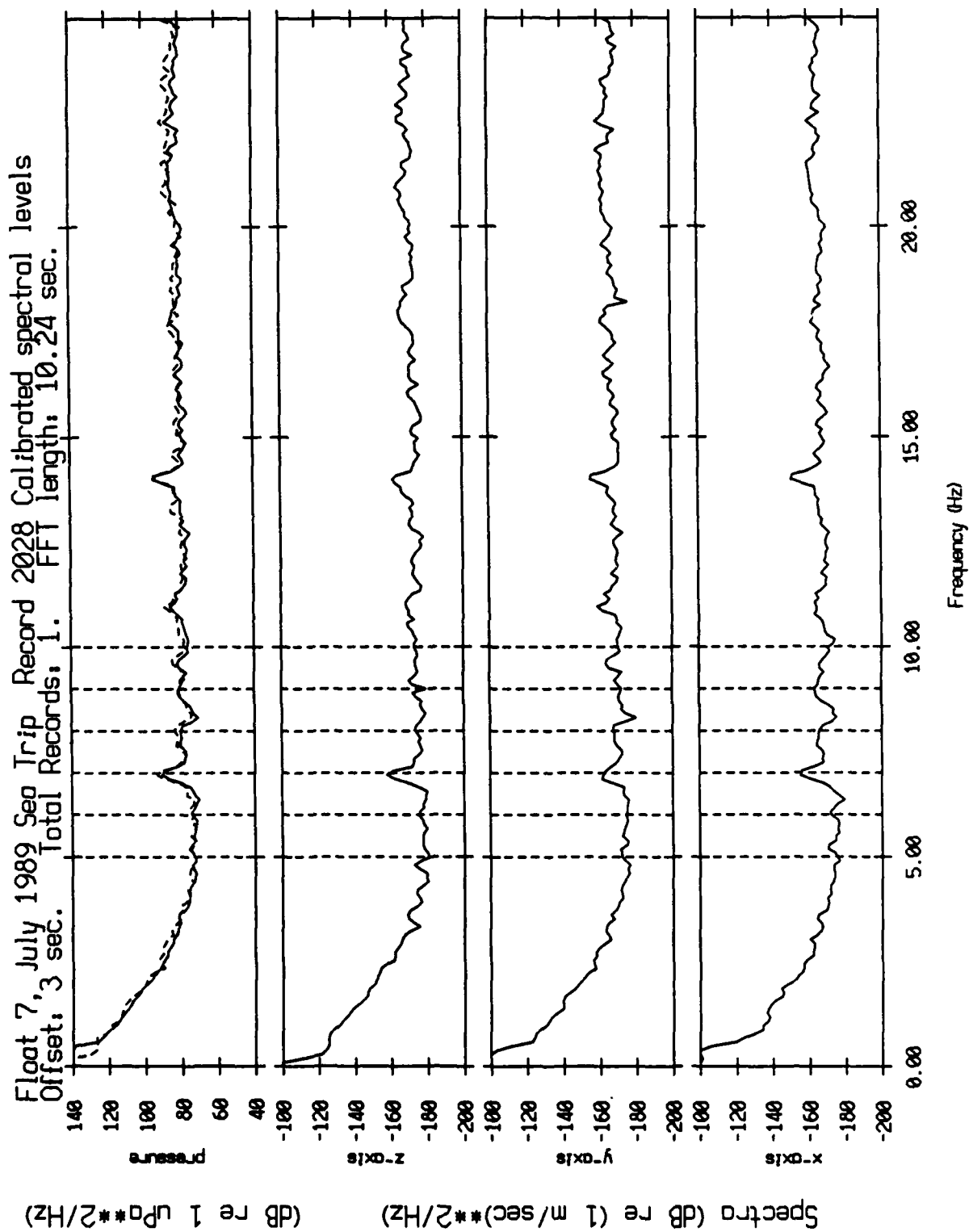


Figure XII.16f

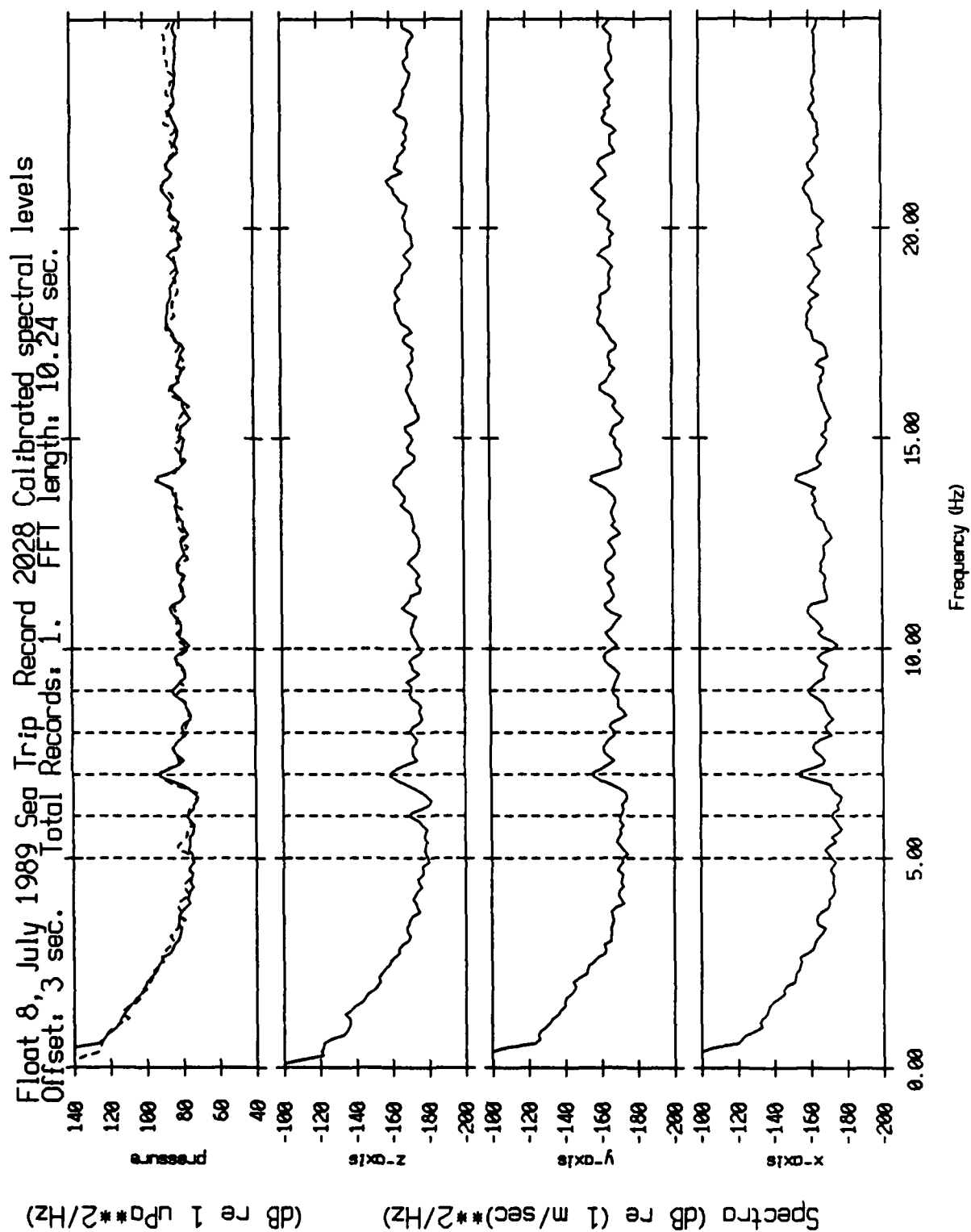


Figure XII.16g

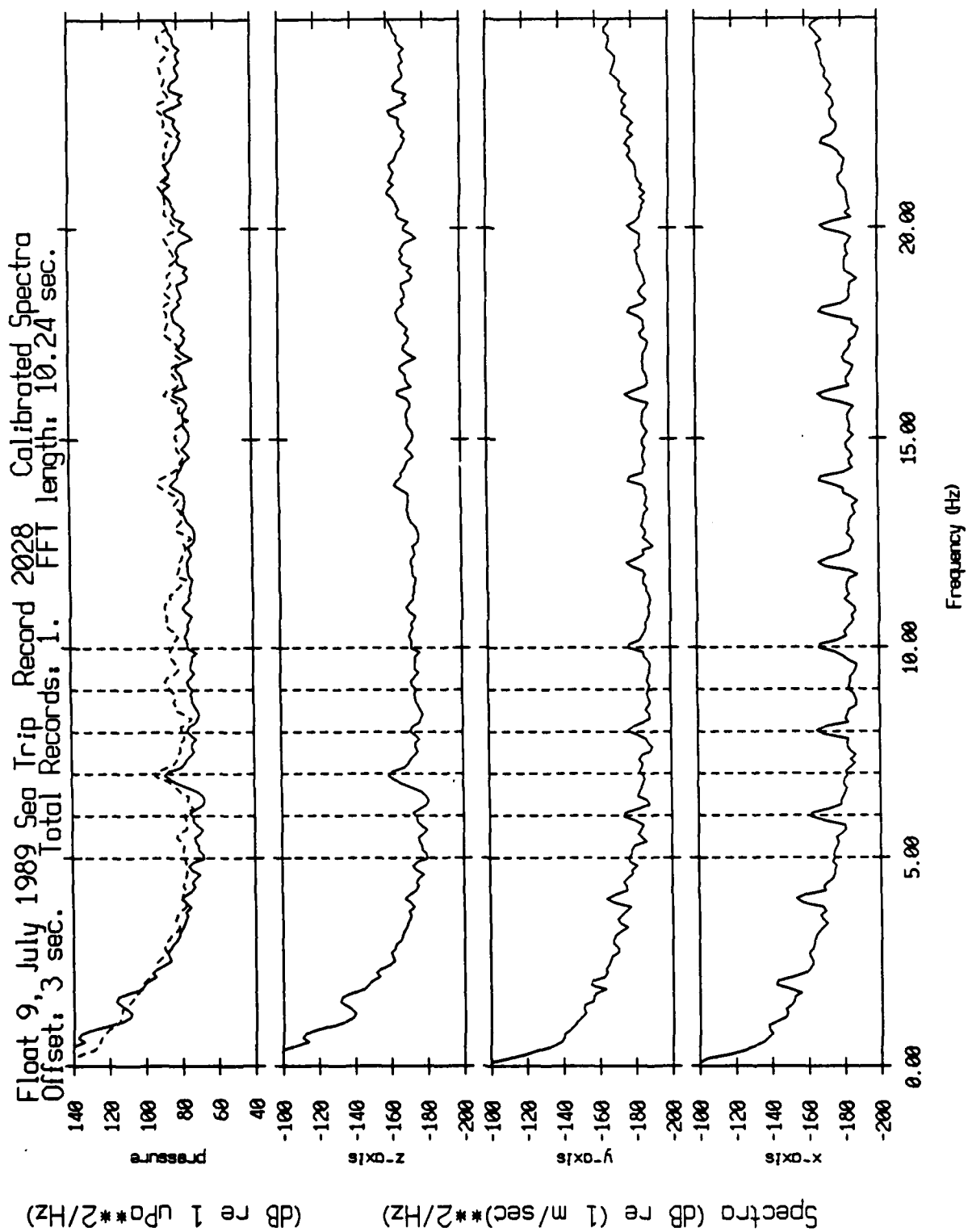


Figure XII.16h



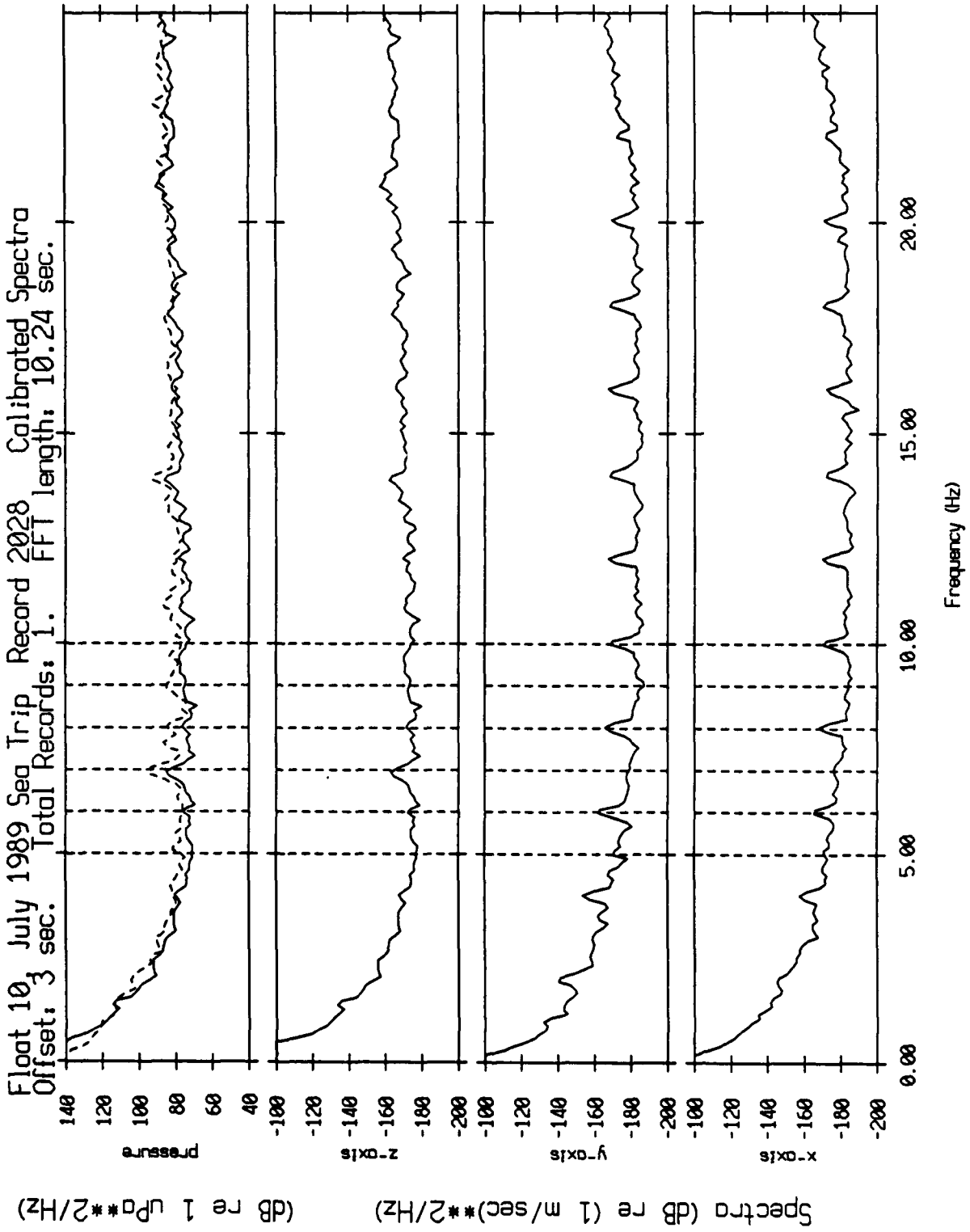


Figure XII.16i

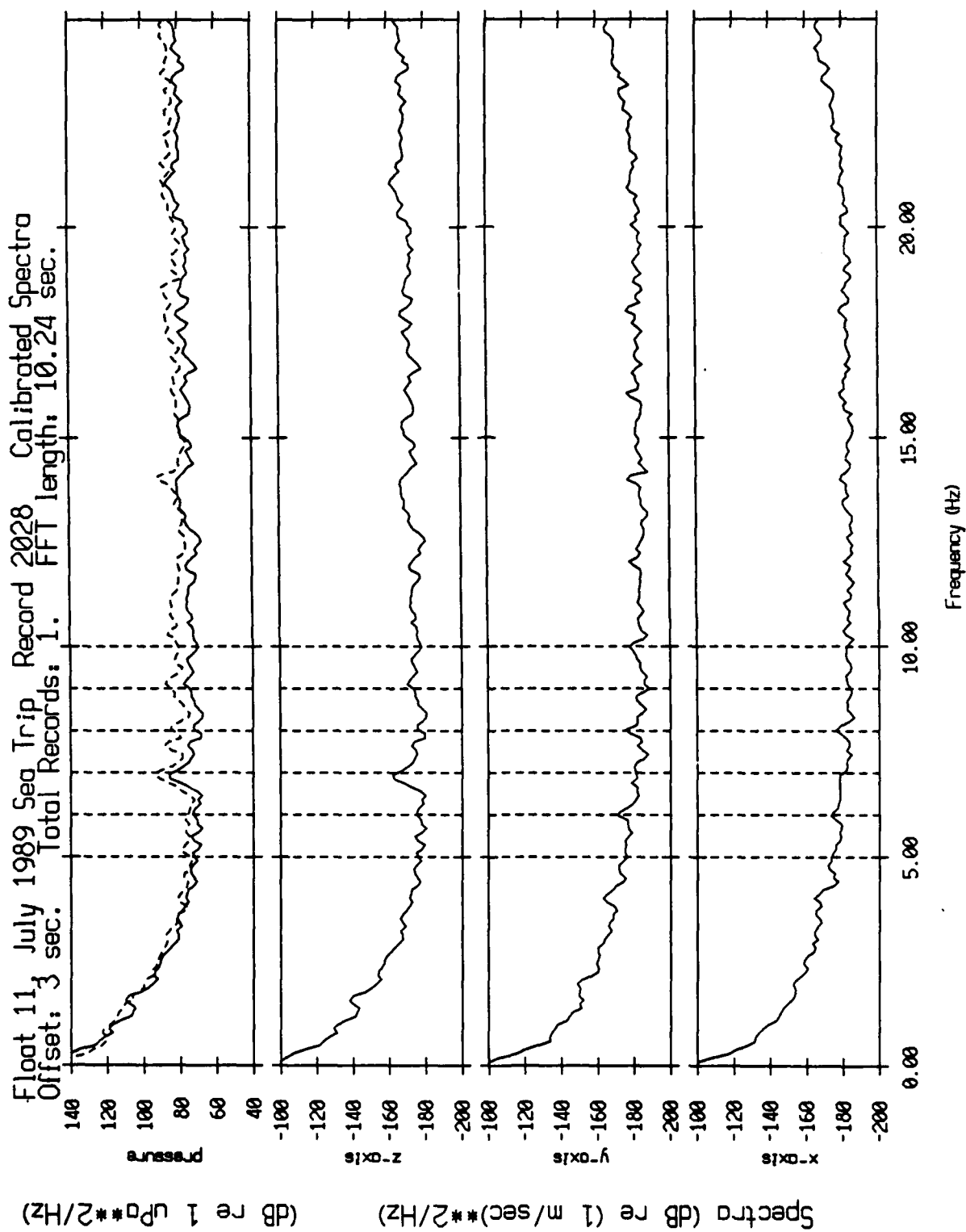


Figure XII.16j

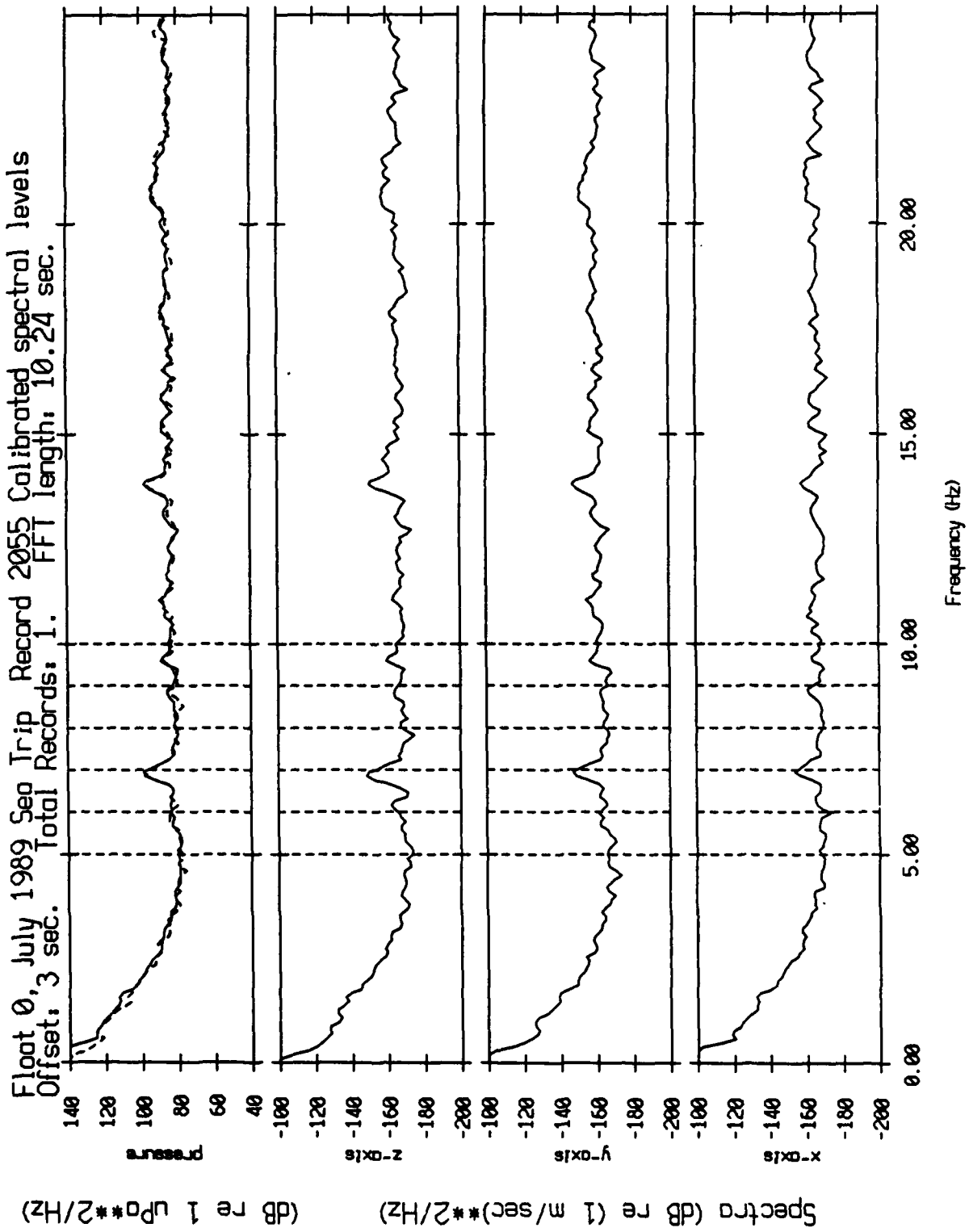


Figure XII.17a

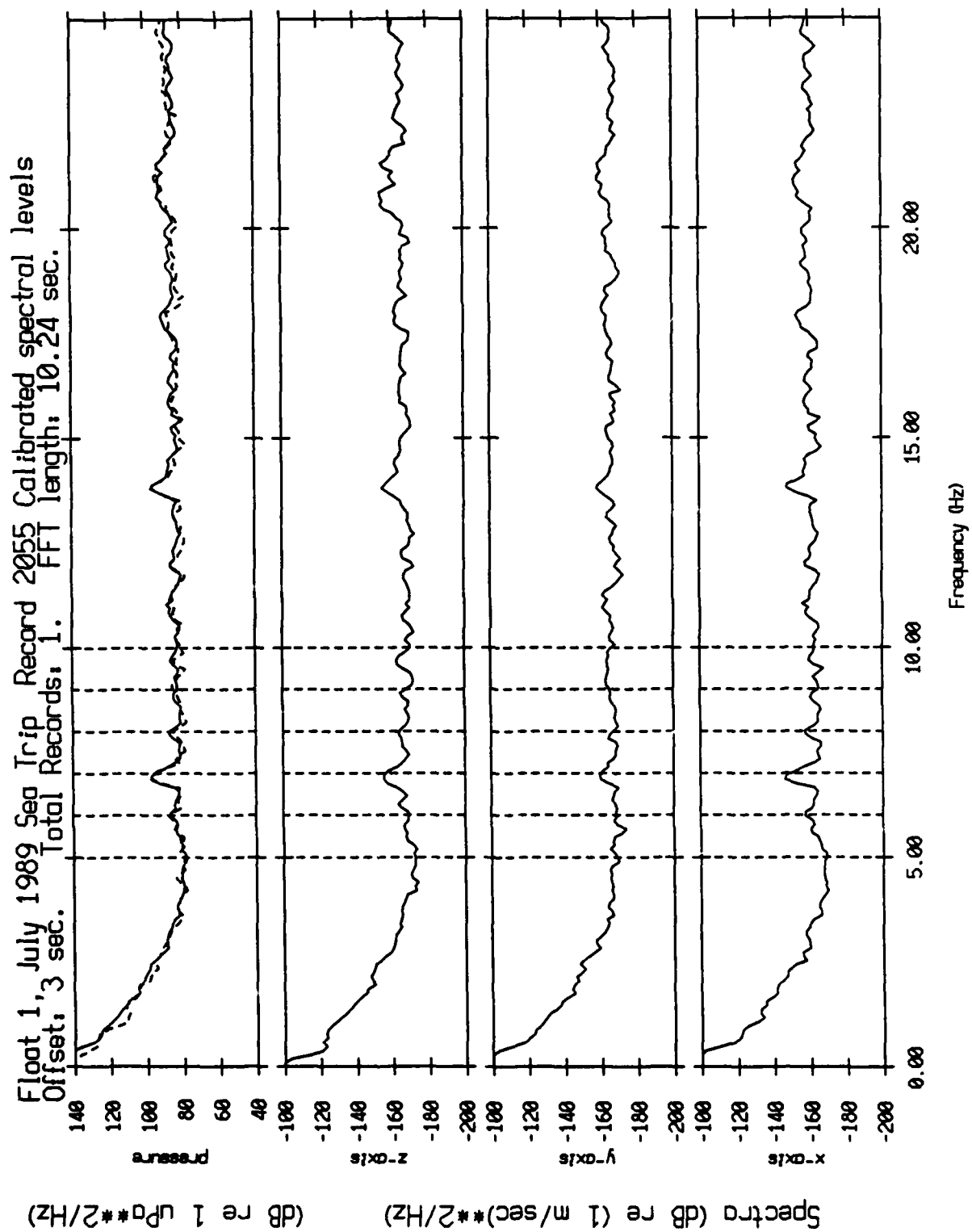


Figure XII.17b

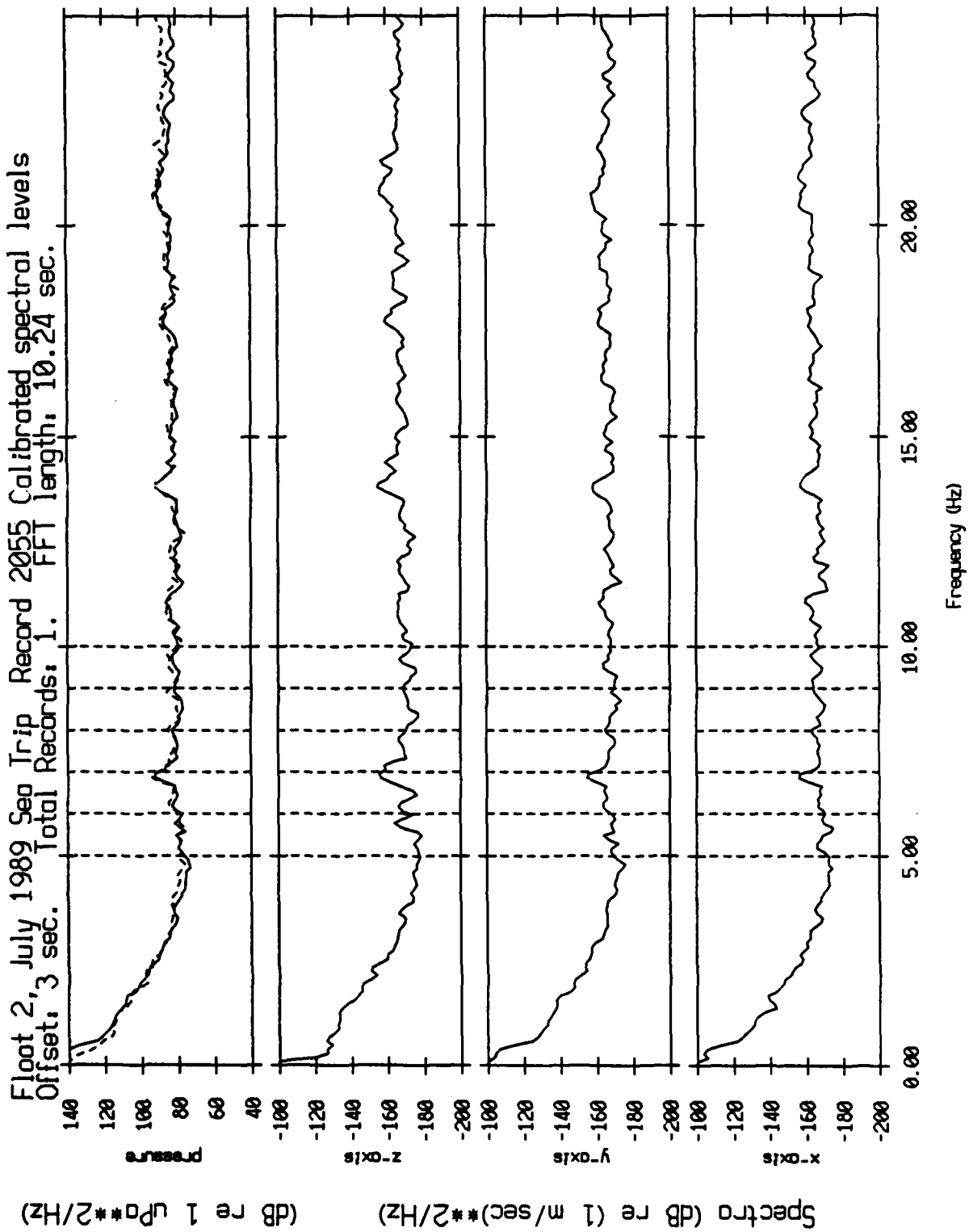


Figure XII.17c

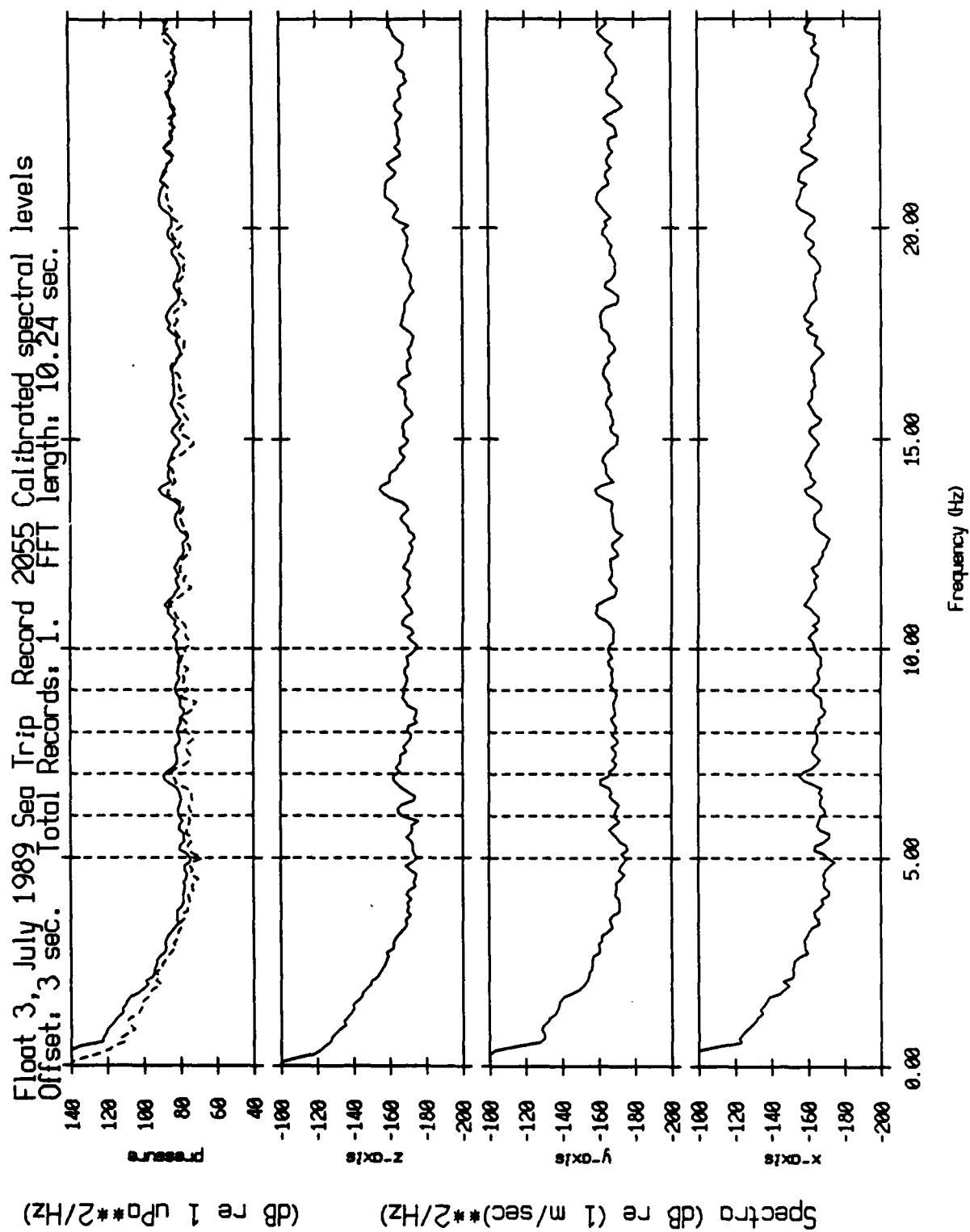


Figure XII.17d

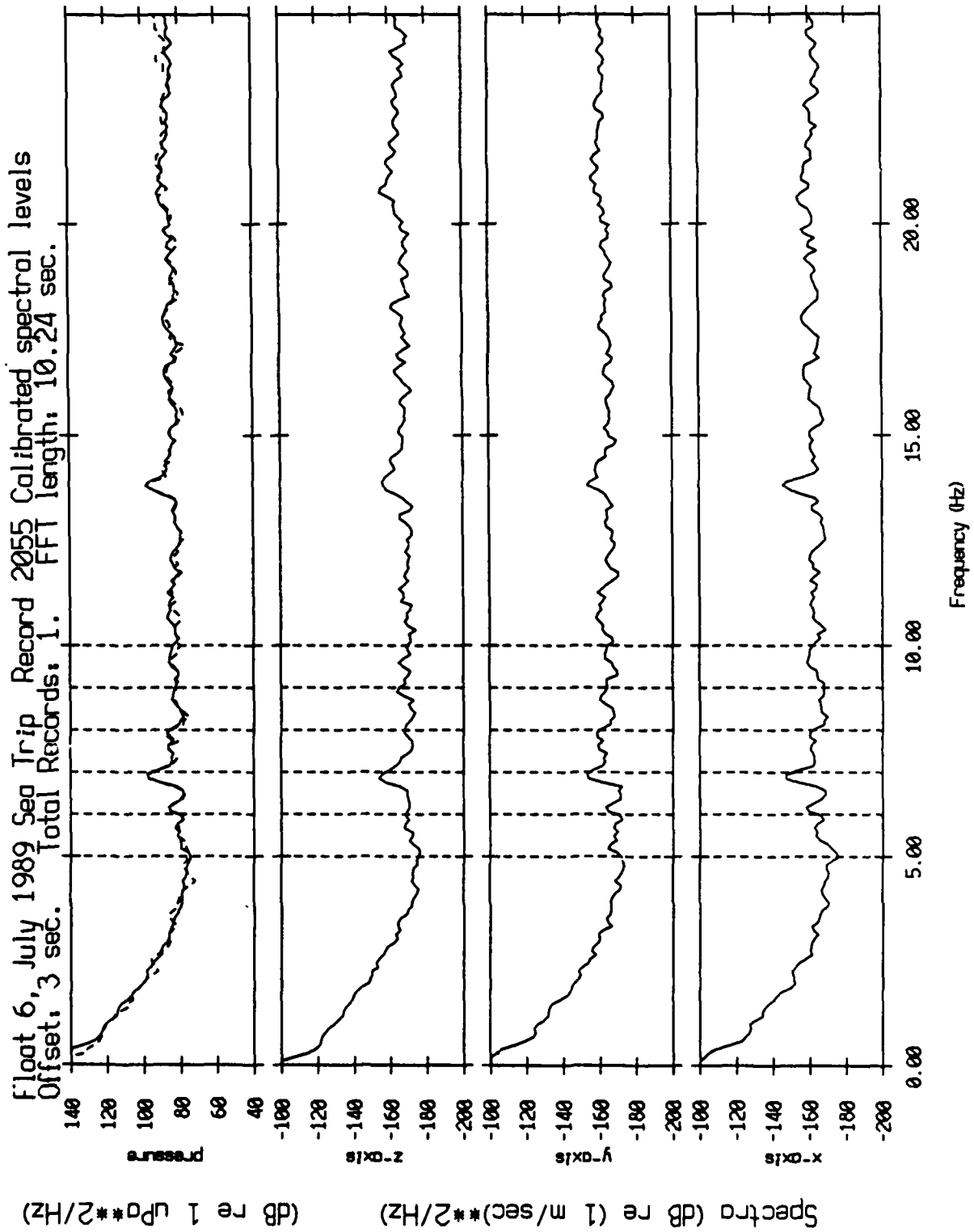


Figure XII.17e

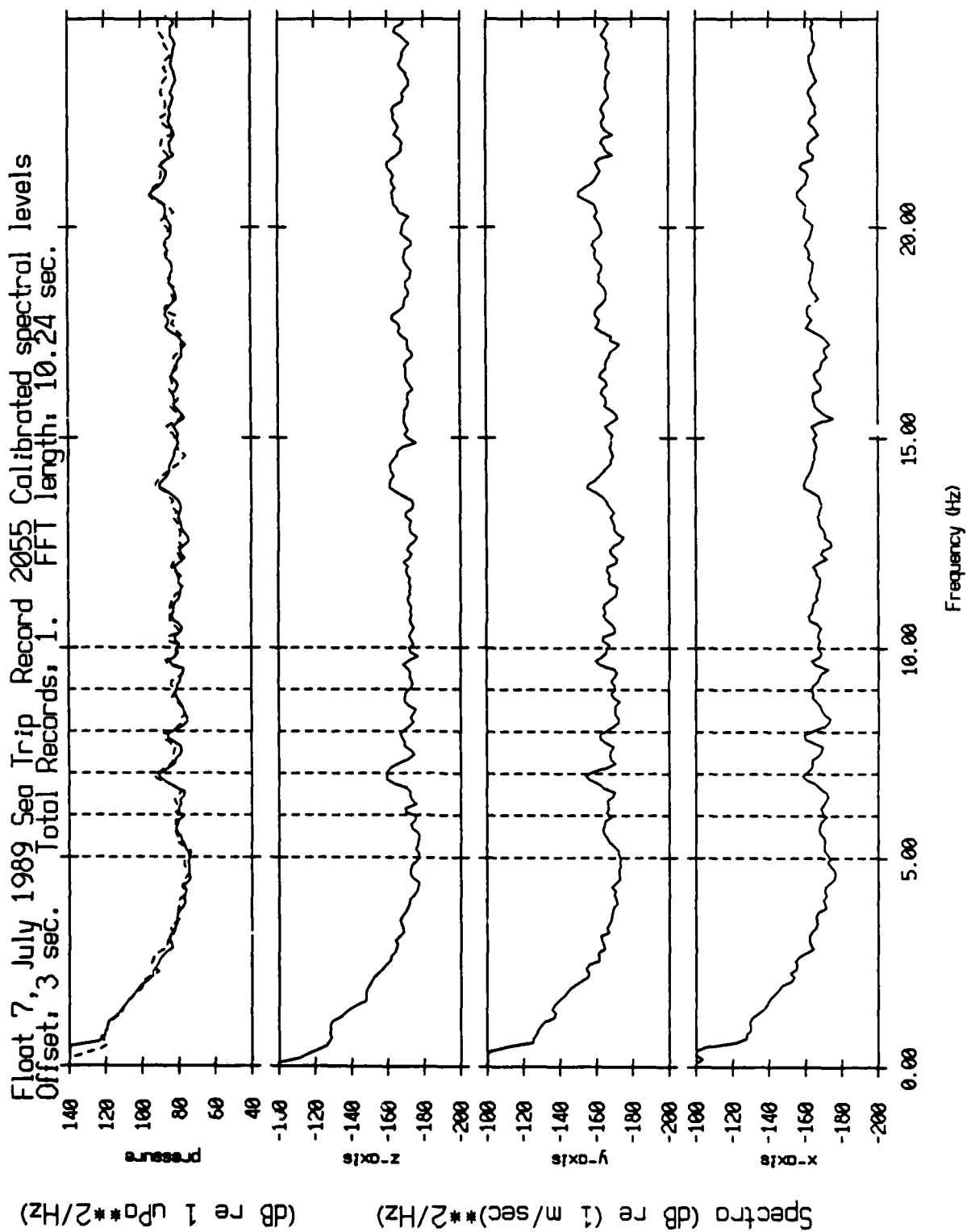


Figure XII.17f



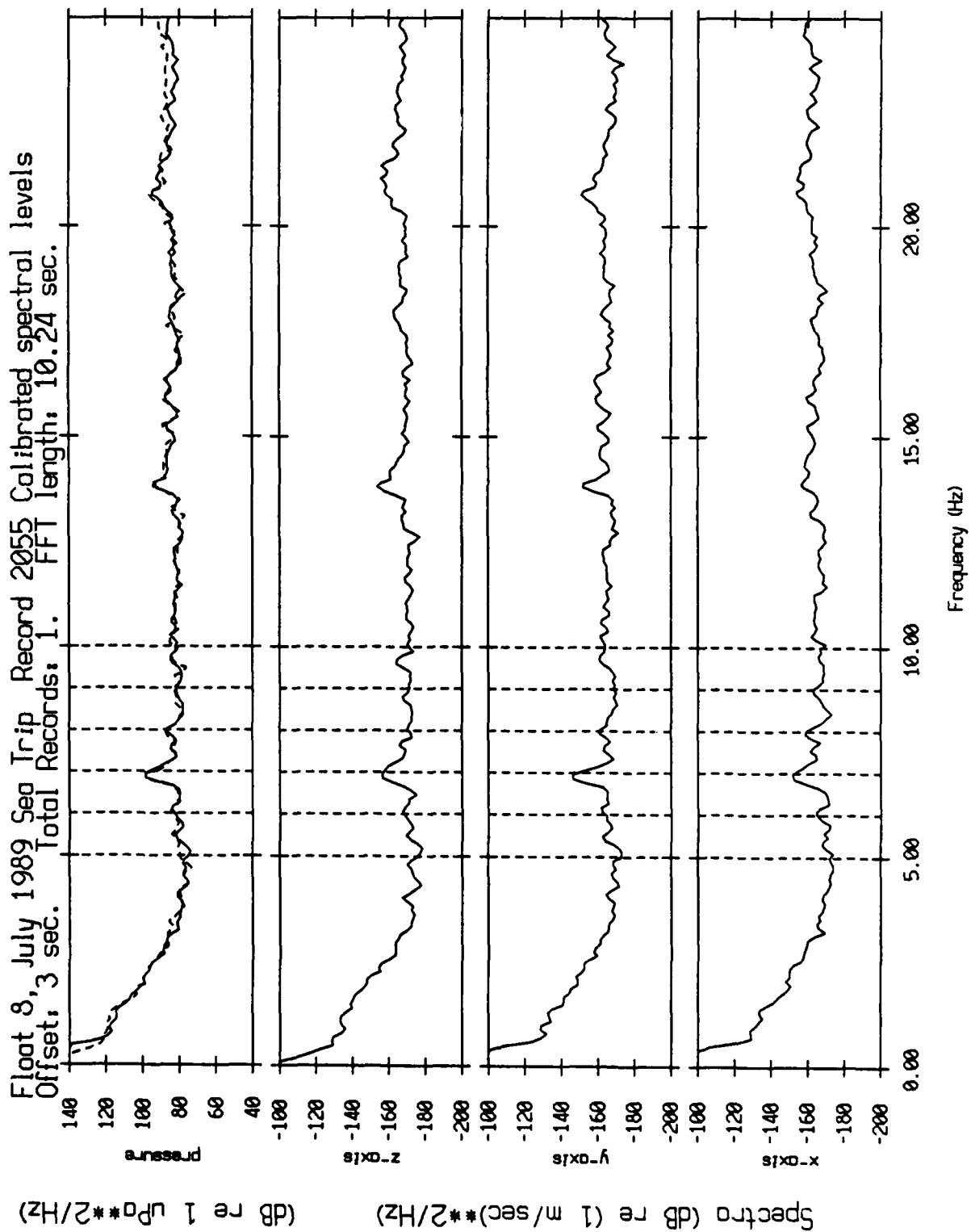


Figure XII.17g

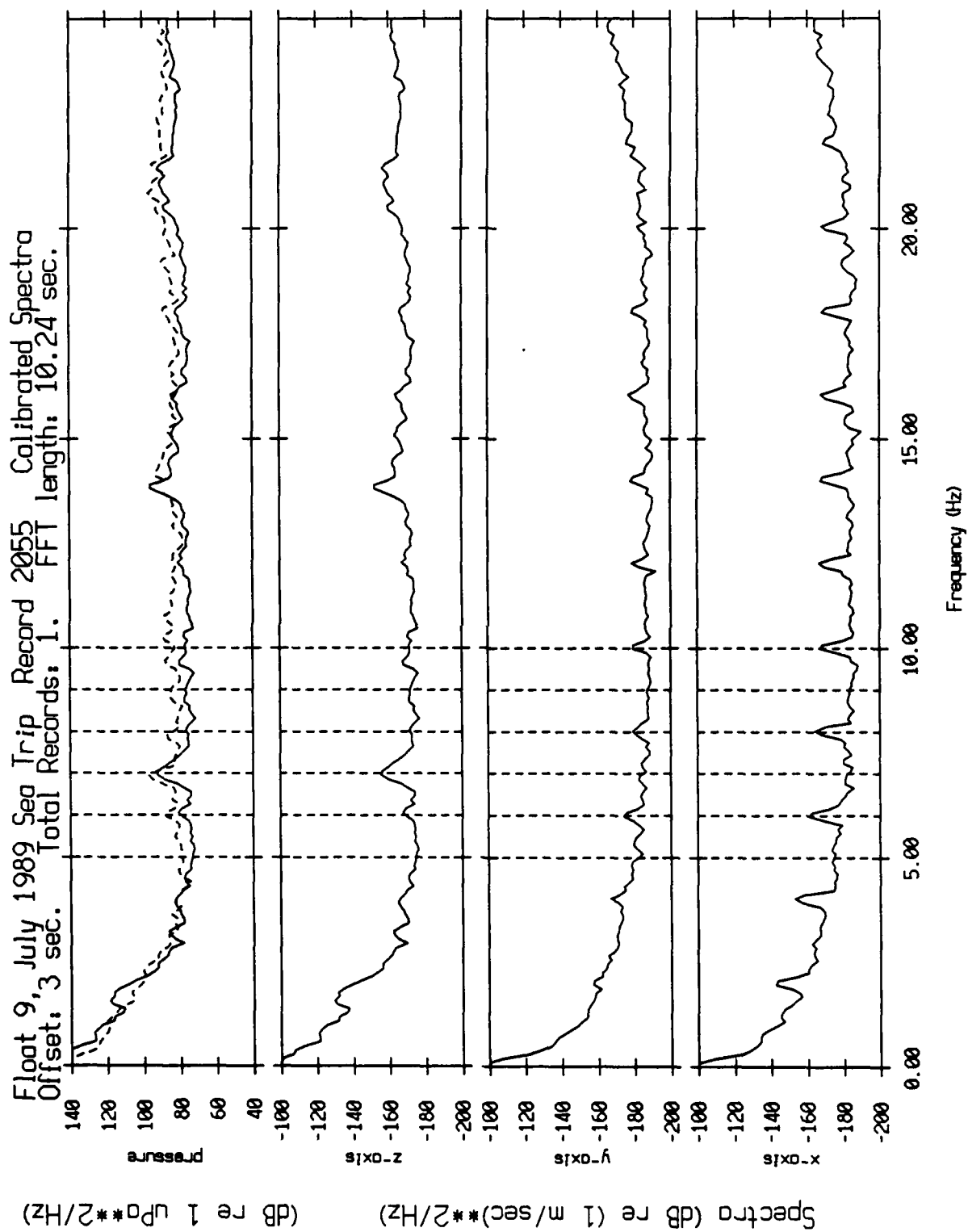


Figure XII.17h

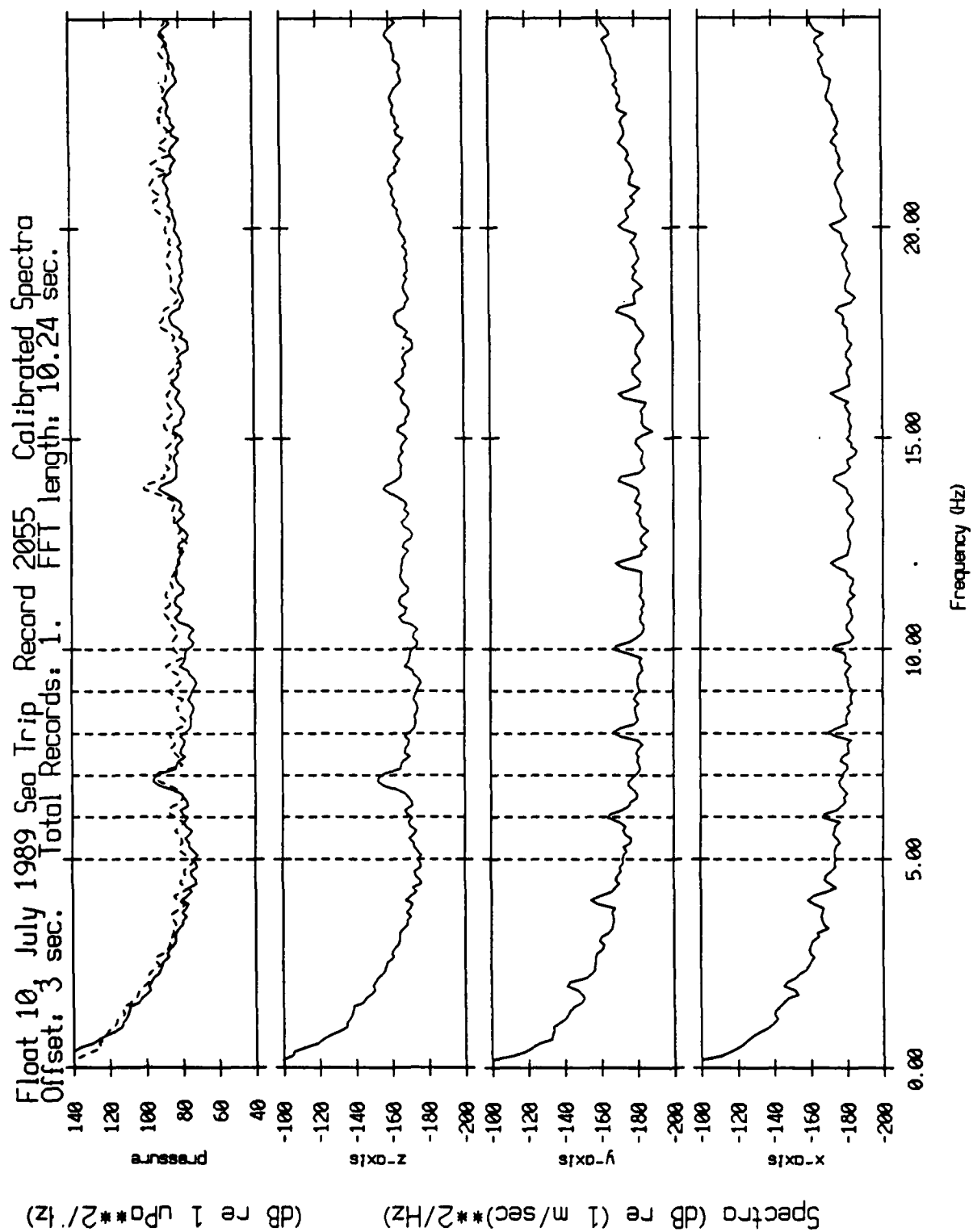


Figure XII.171

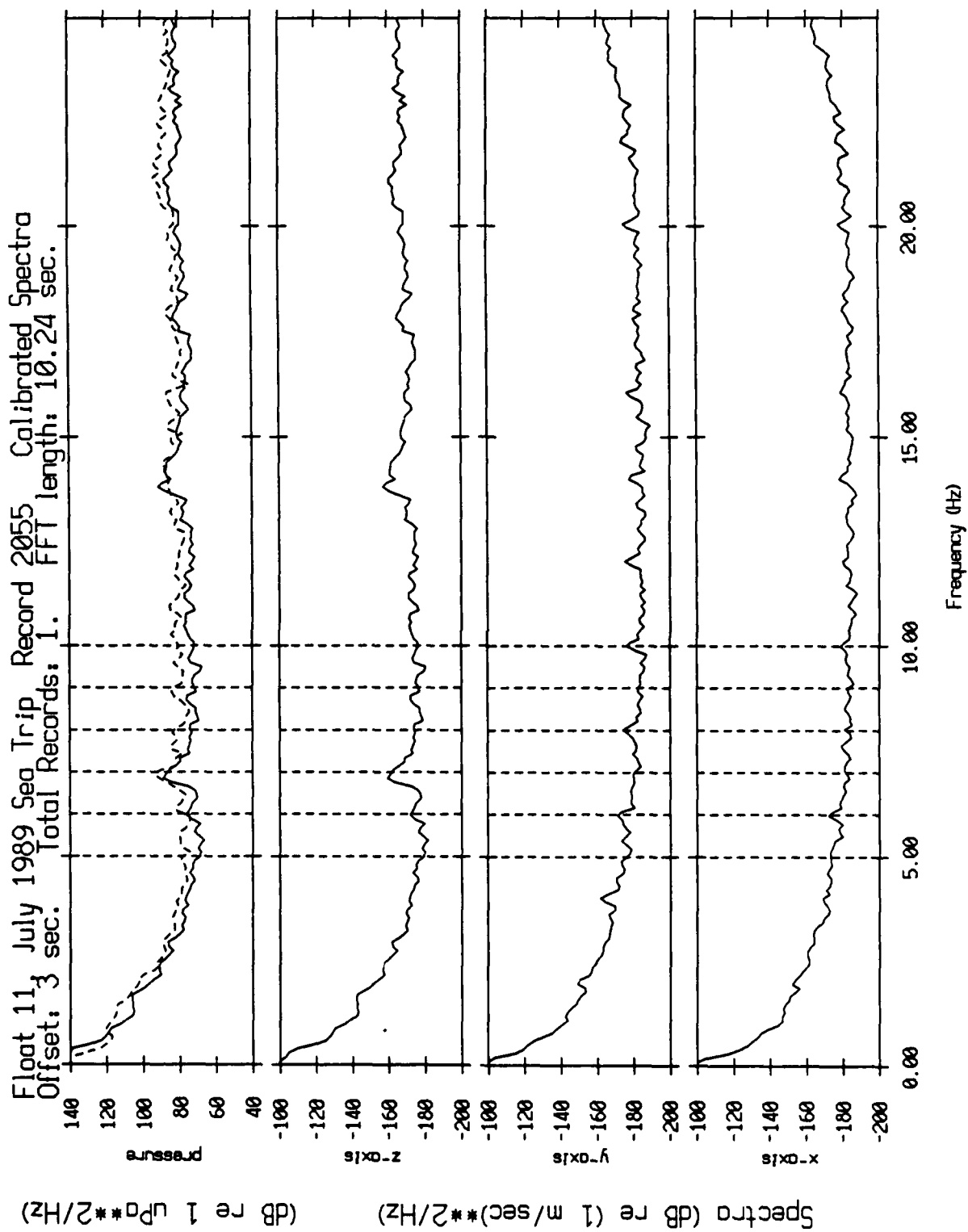


Figure XII.17J

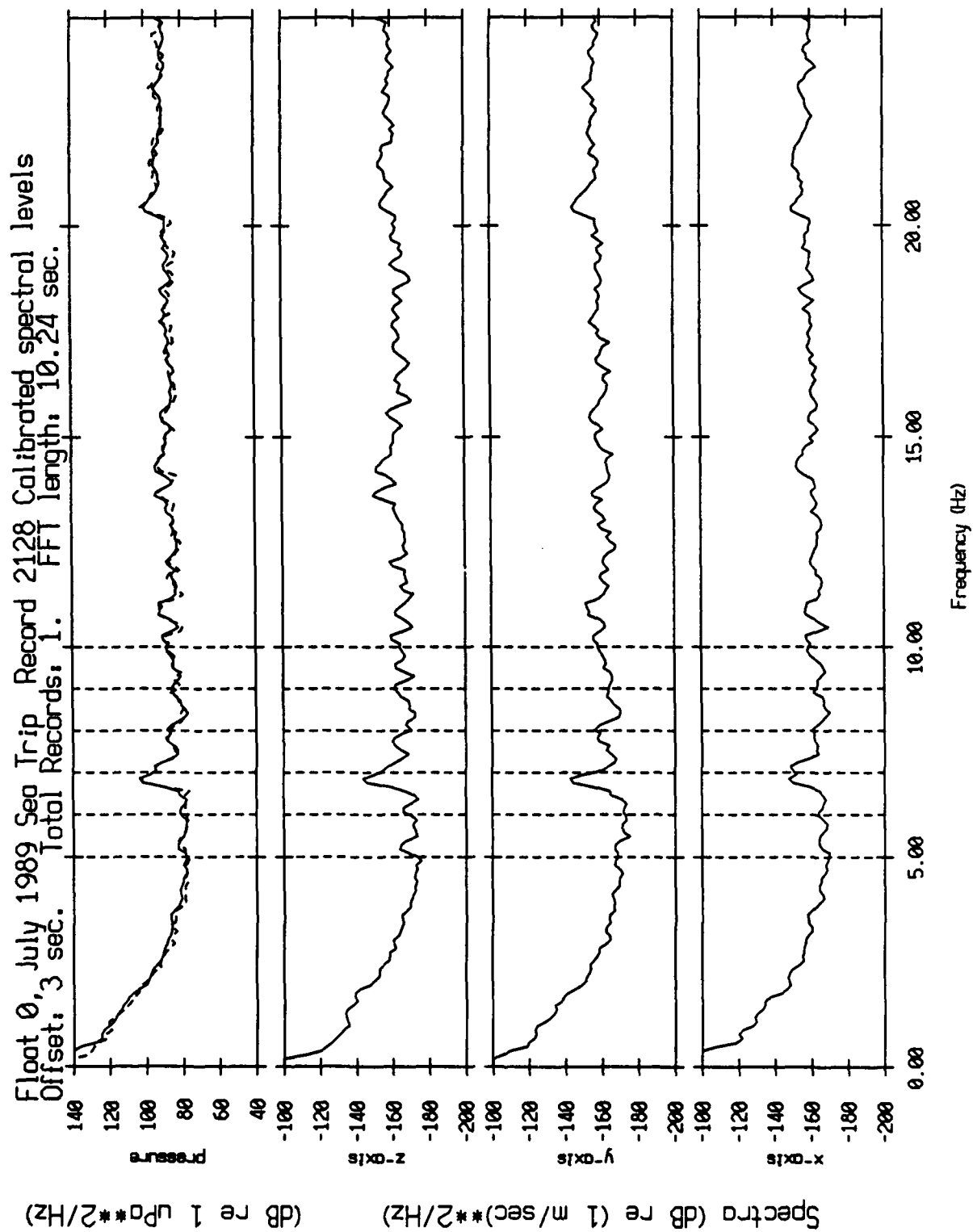


Figure XII.18a

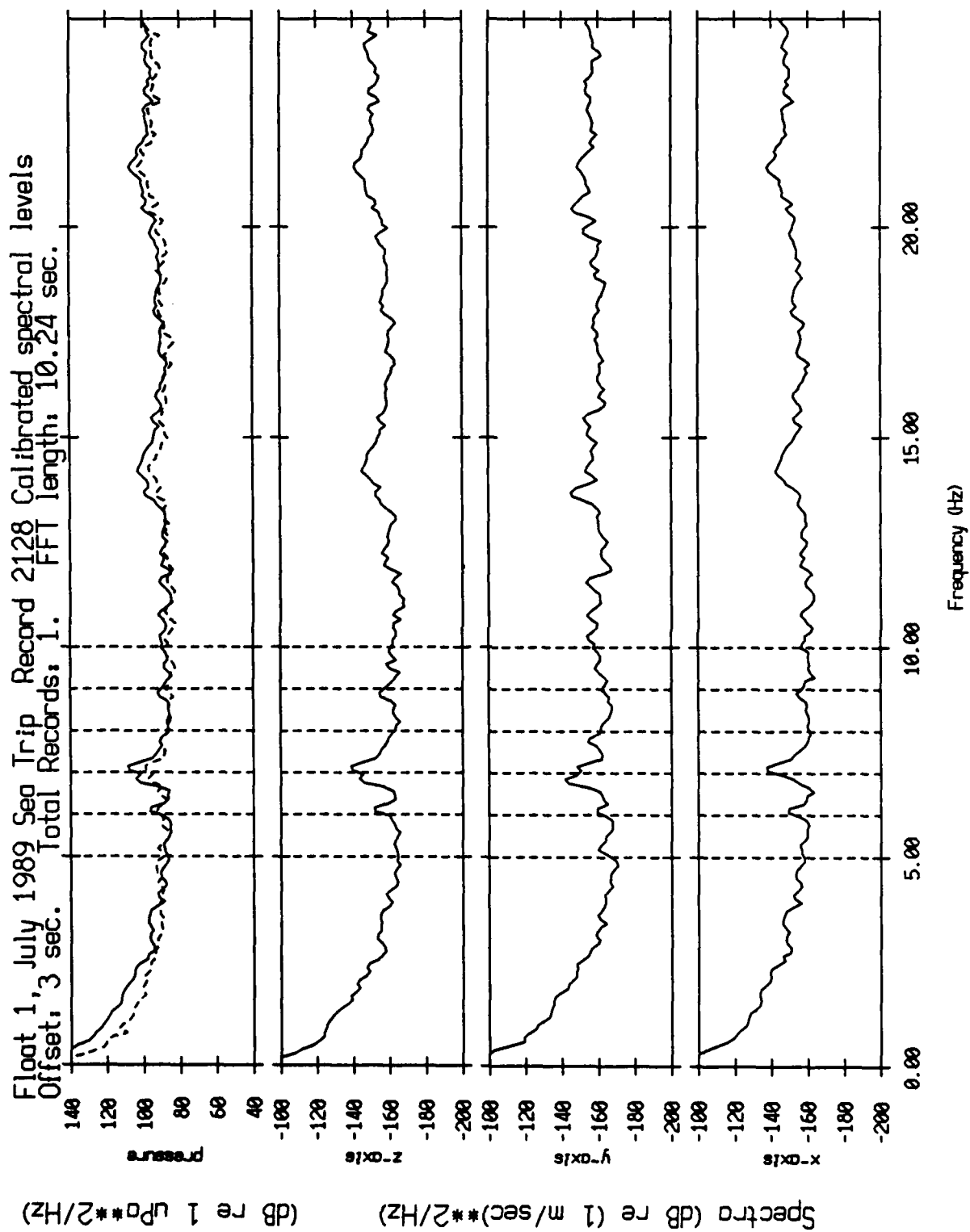


Figure XII.18b

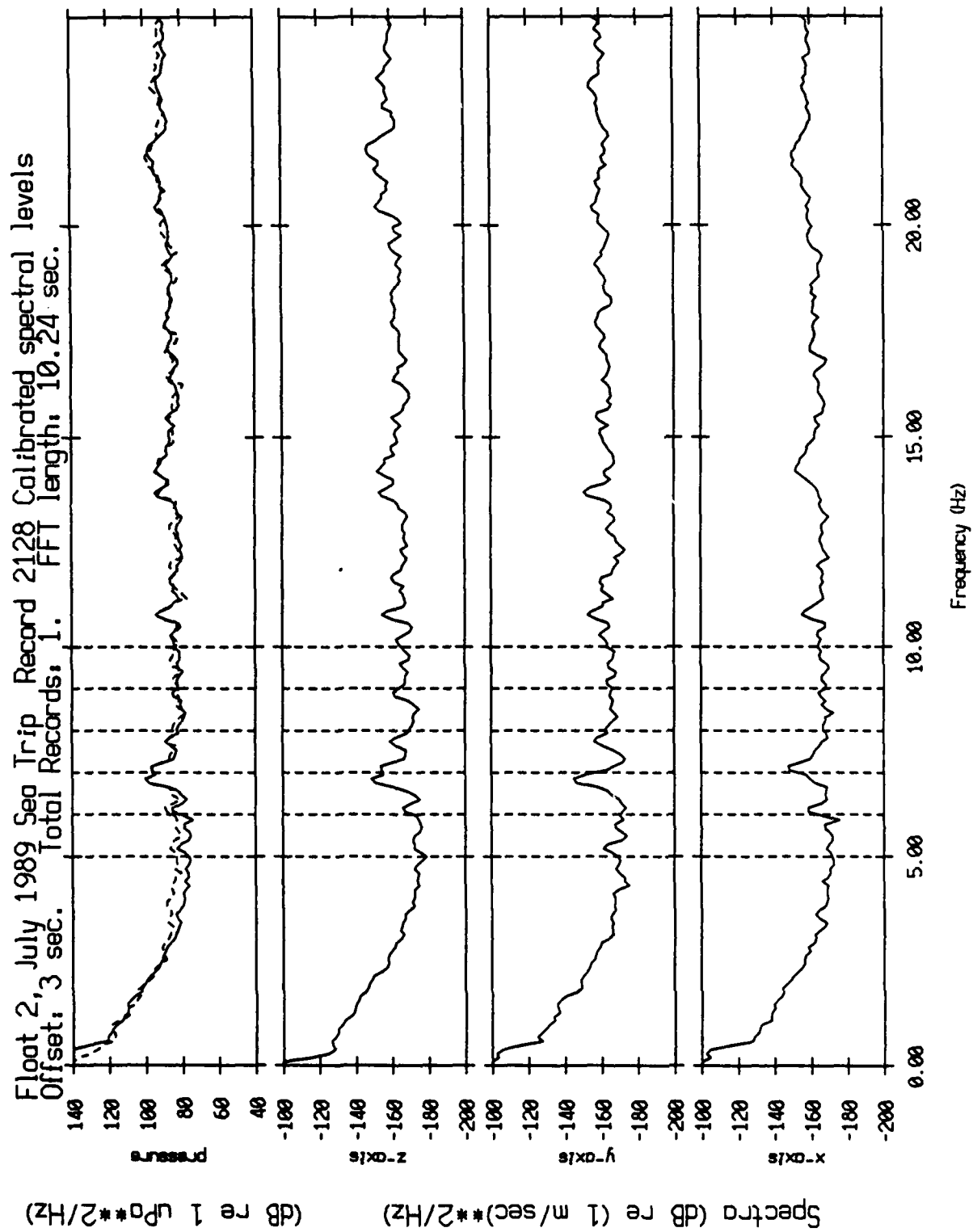


Figure XII.18c

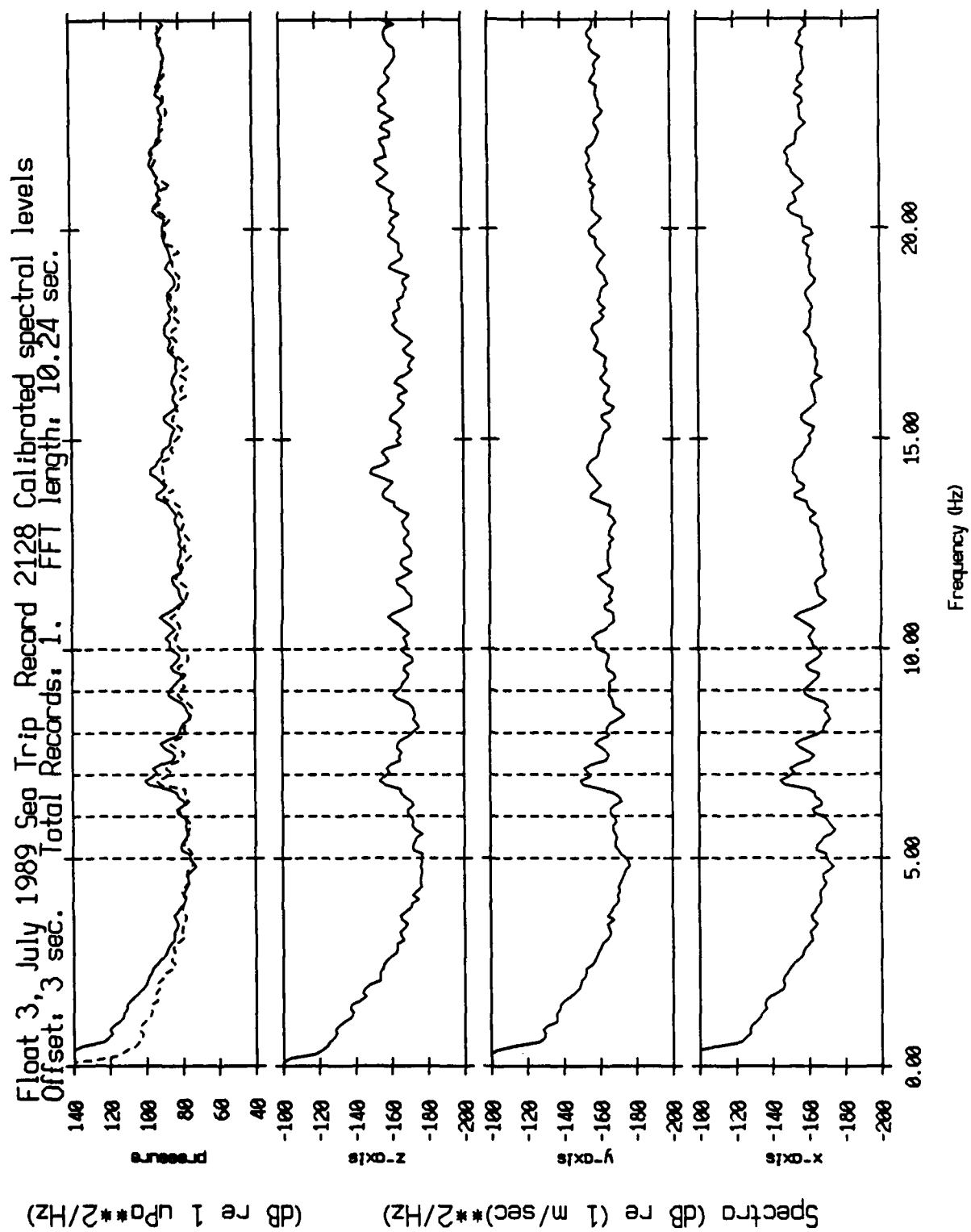


Figure XII.18d



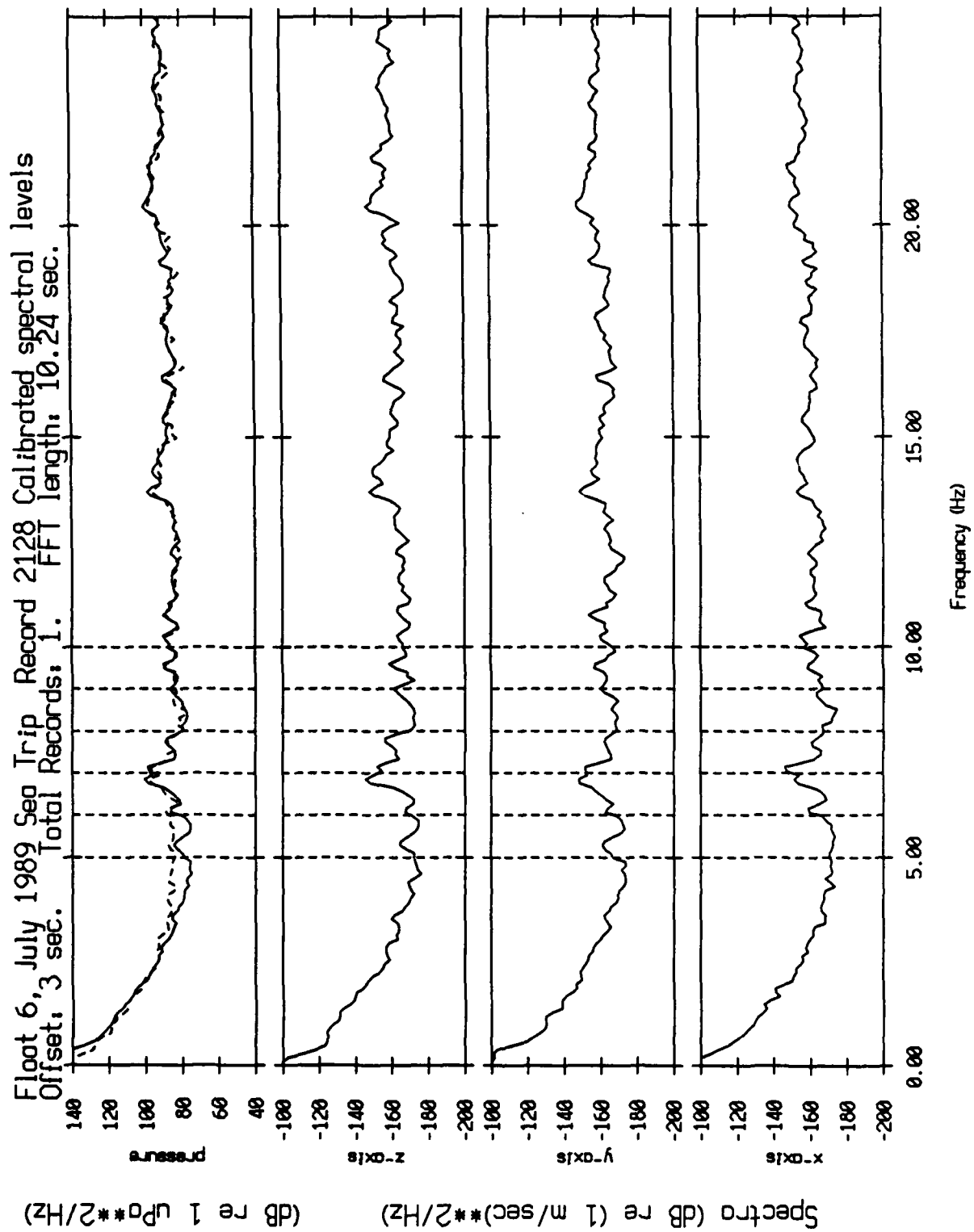


Figure XII.18e

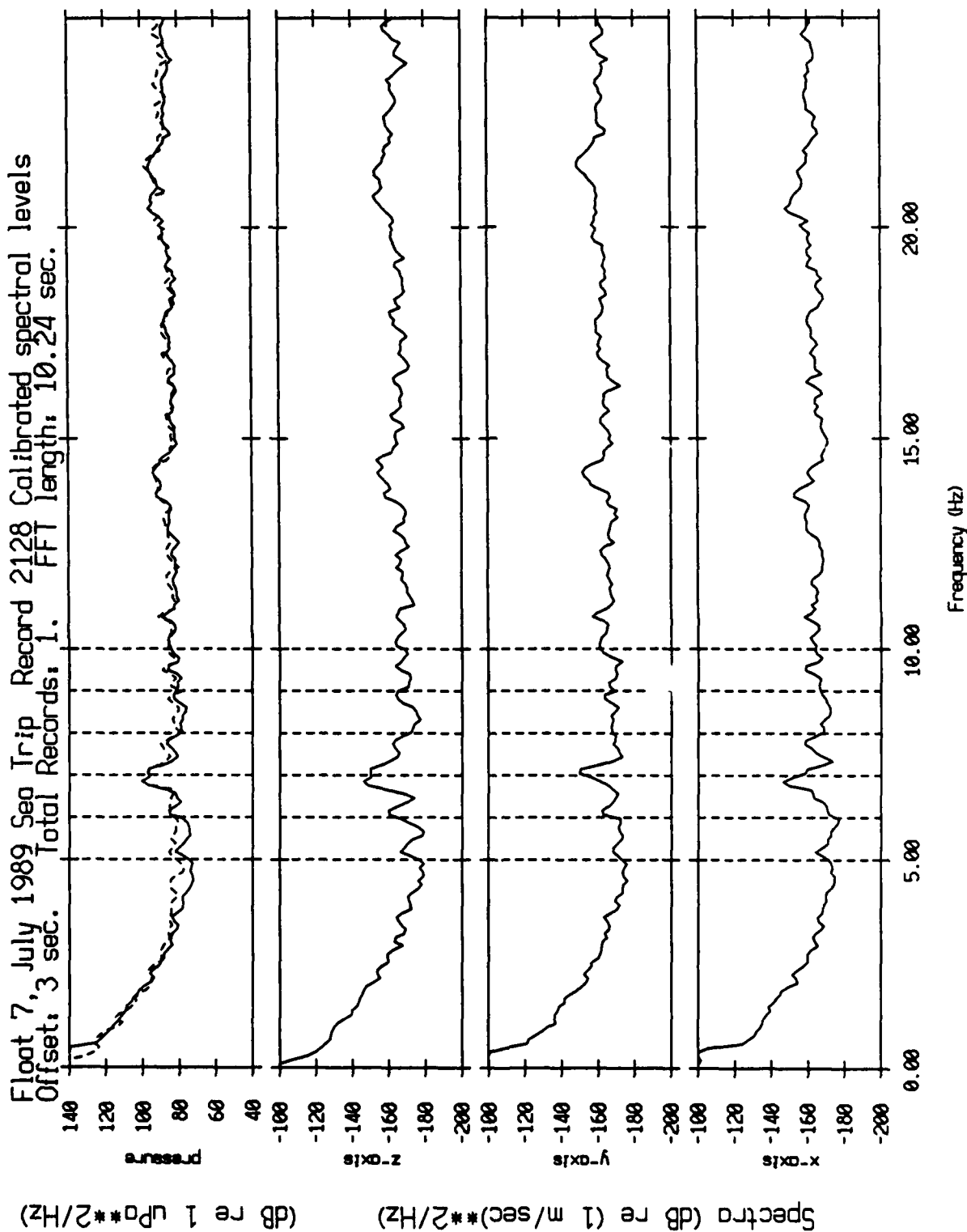


Figure XII.18f

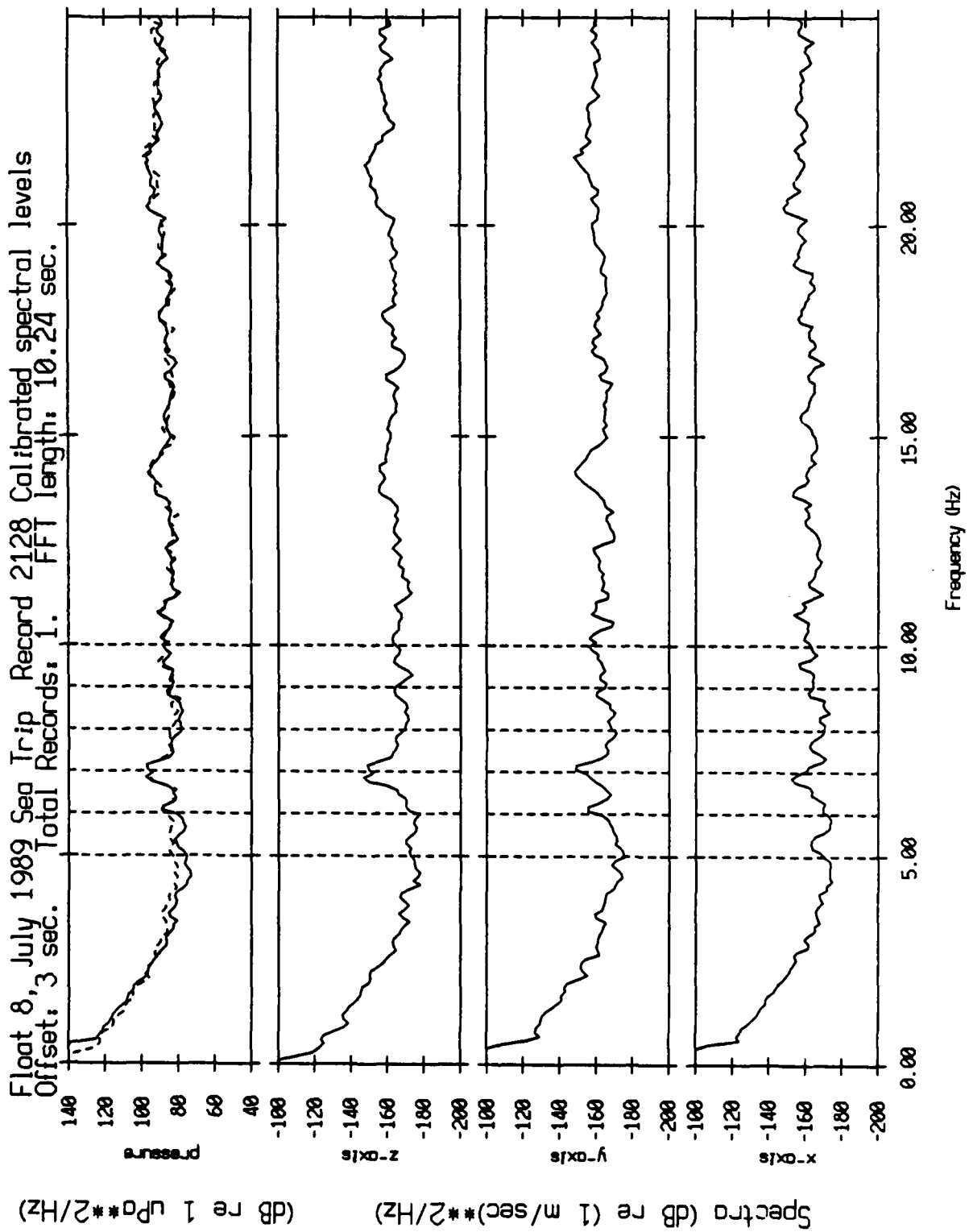


Figure XII.18g

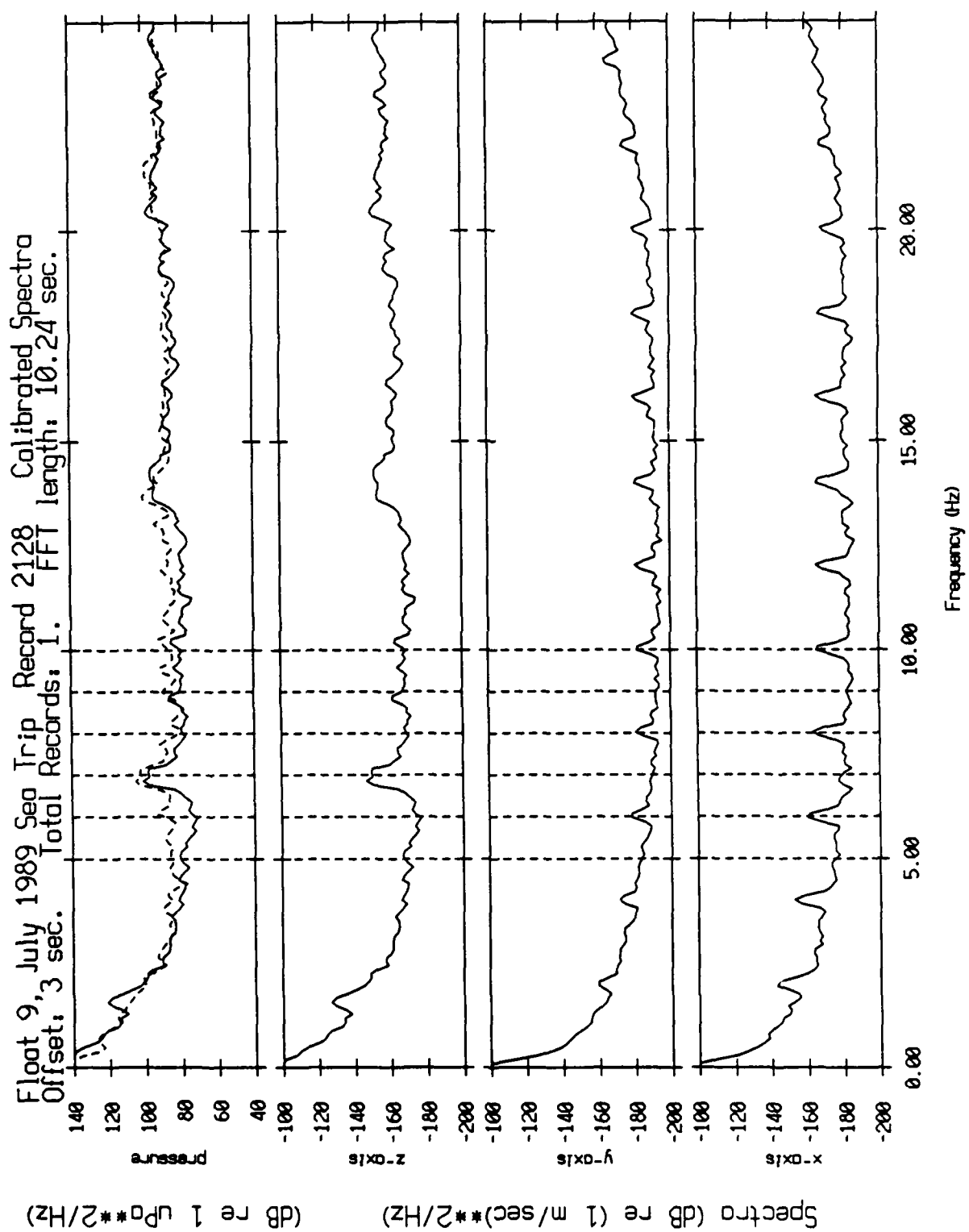


Figure XII.18h

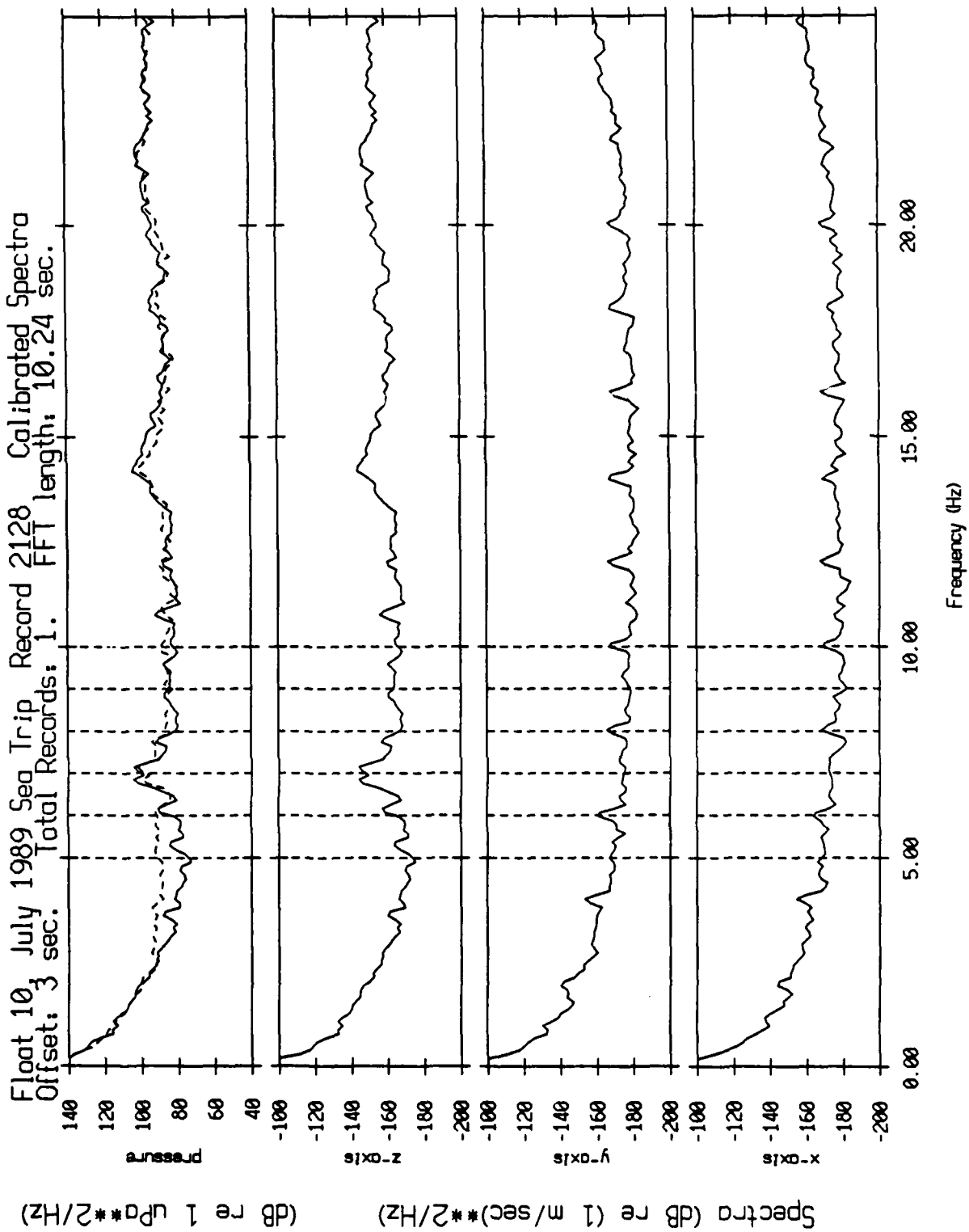


Figure XII.18i

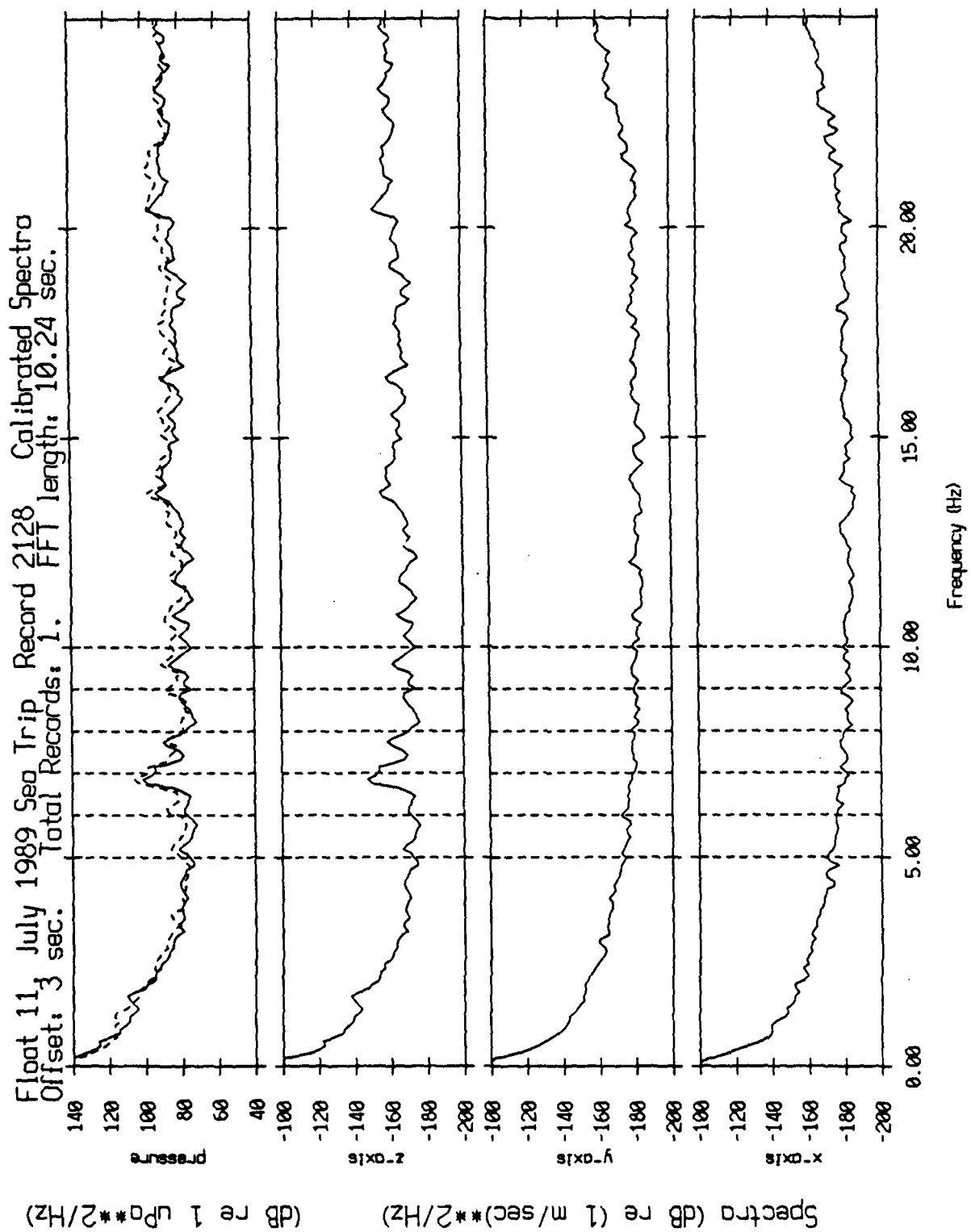


Figure XII.18j

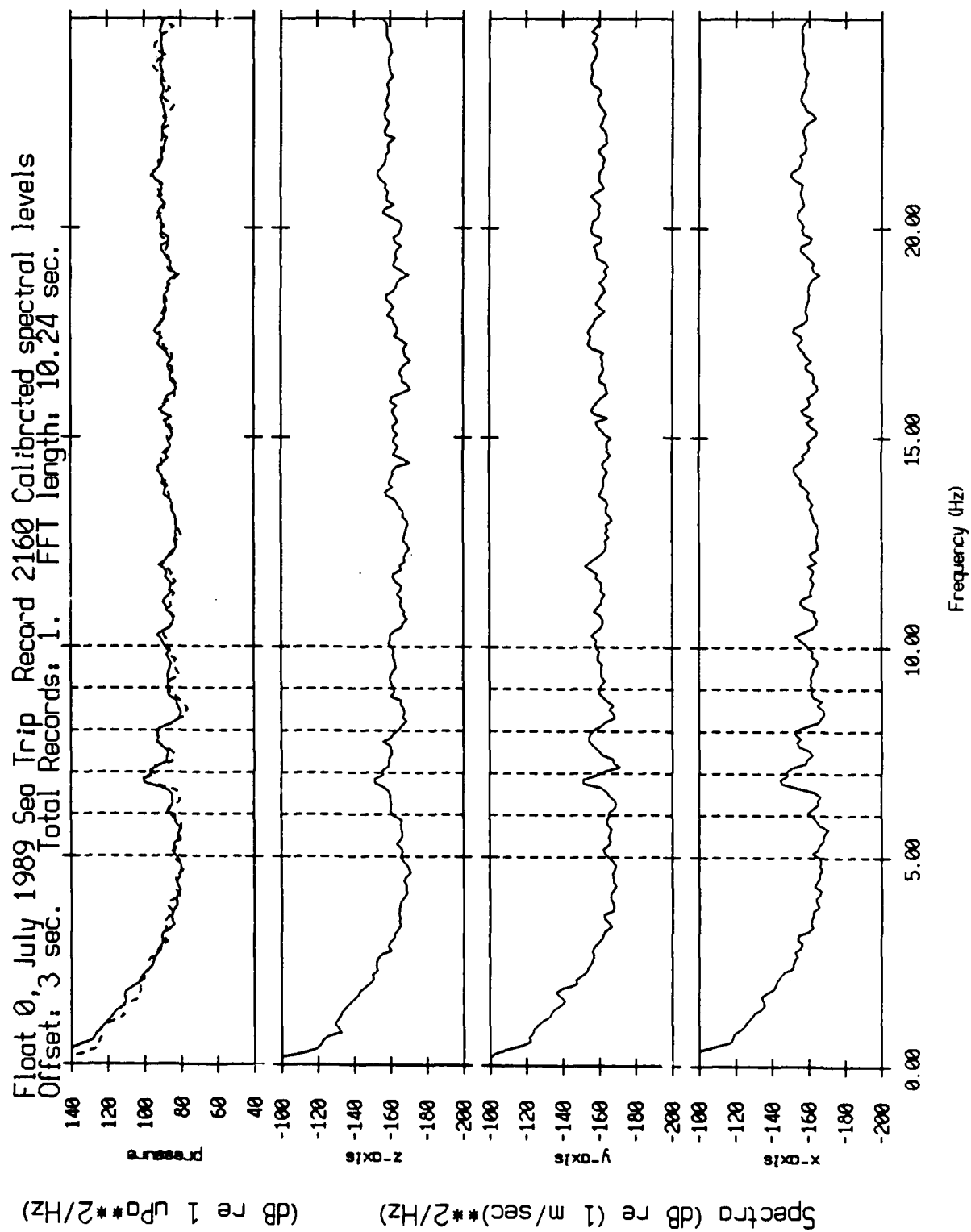


Figure XII.19a

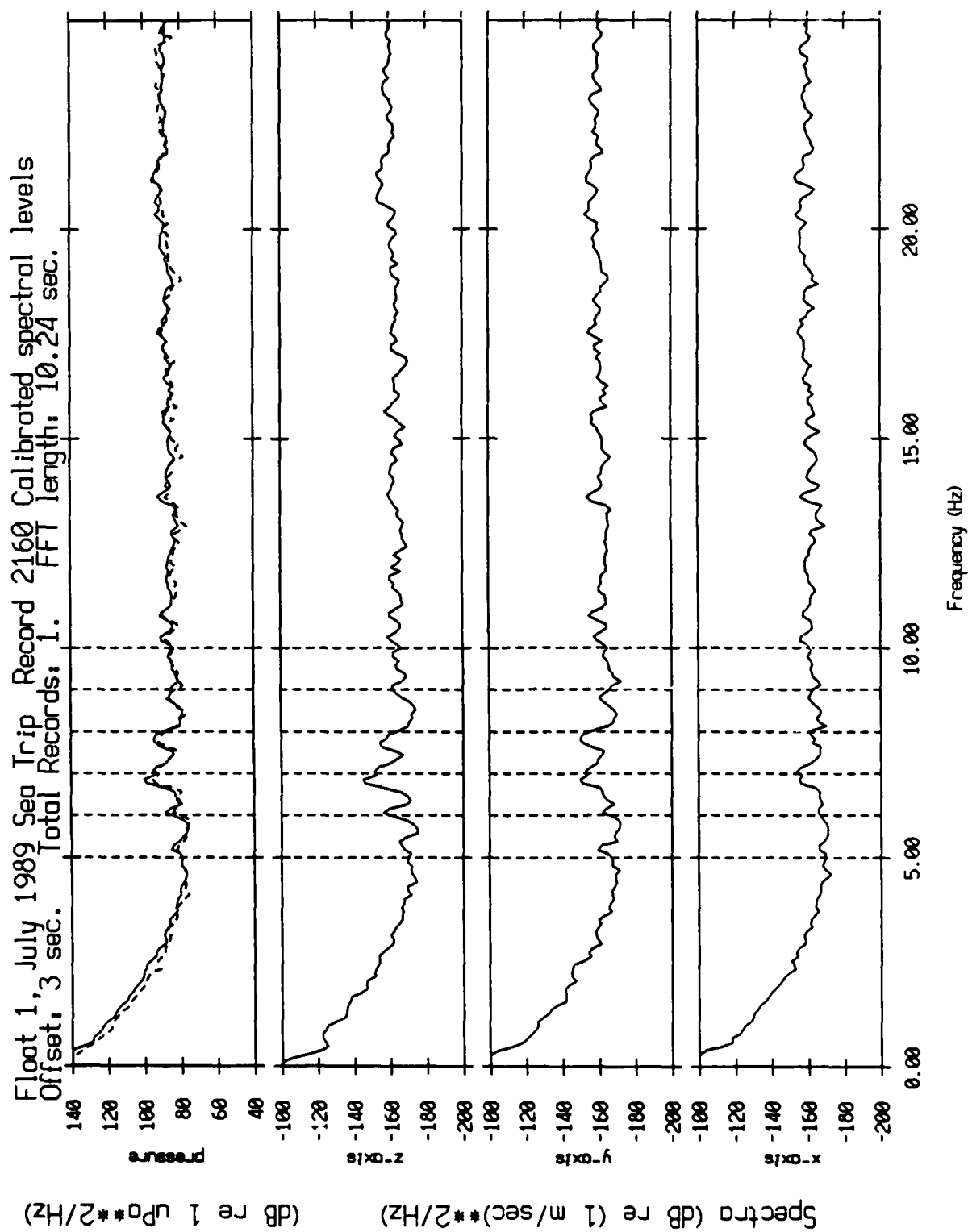


Figure XII.19b



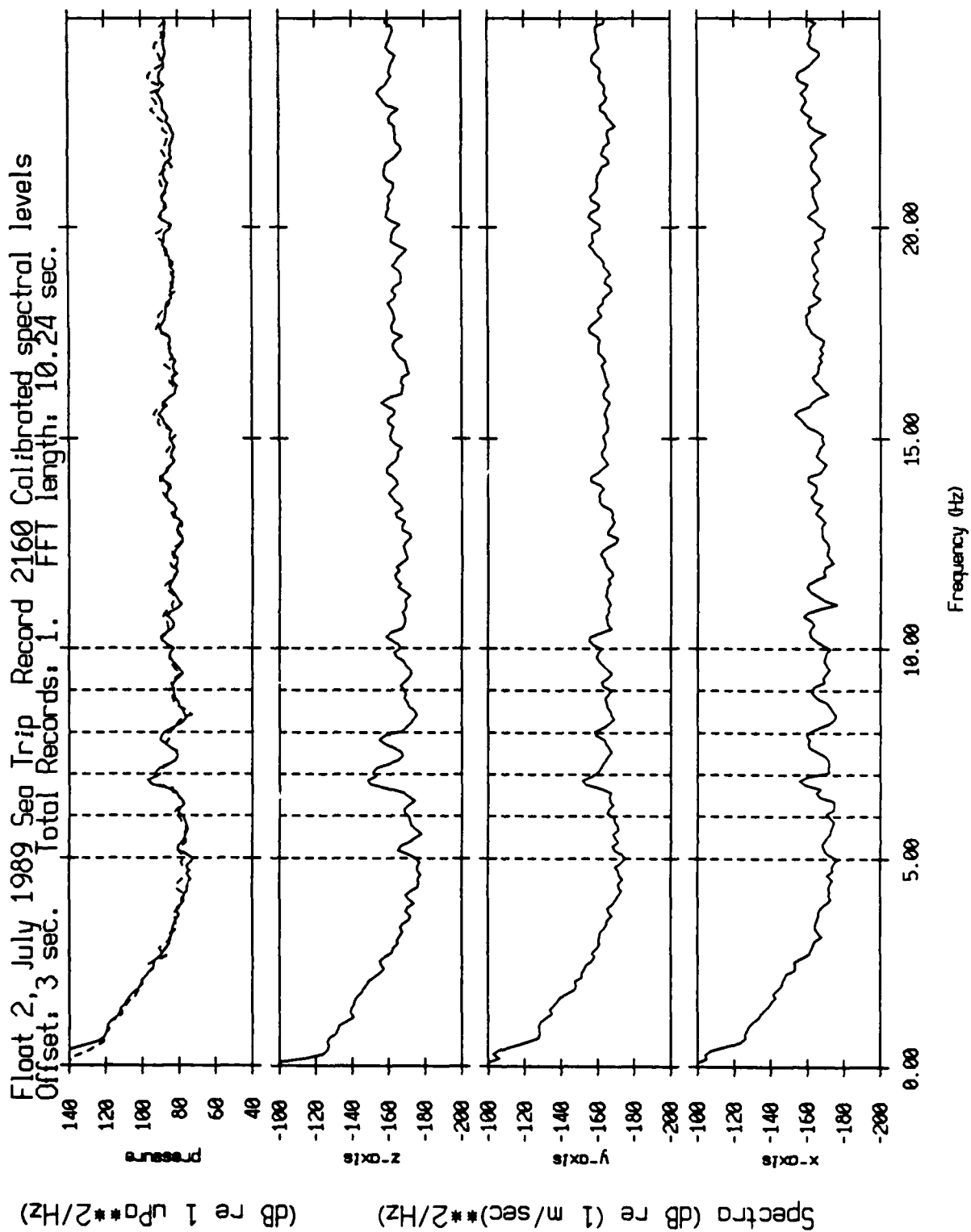


Figure XII.19c

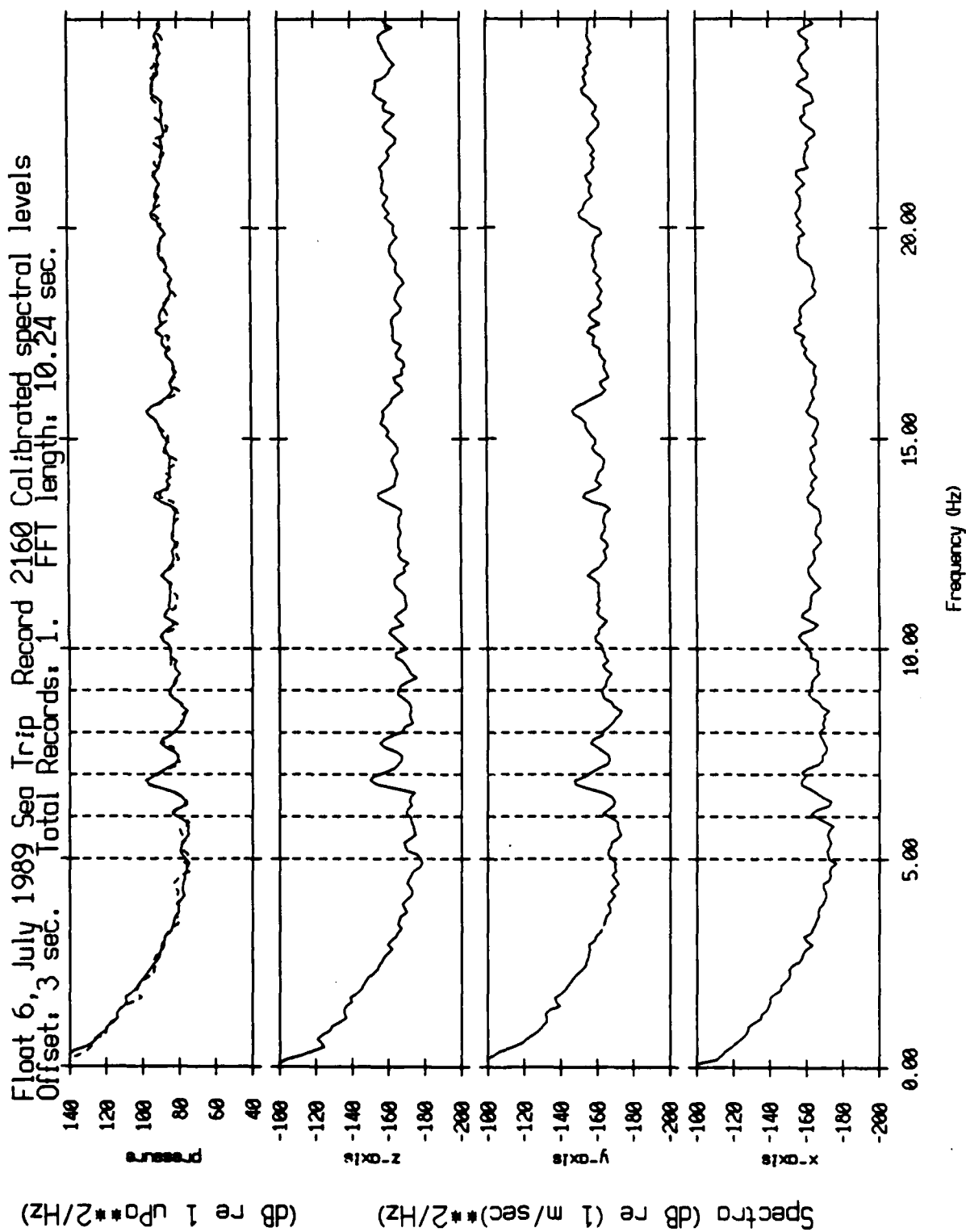


Figure XII.19d

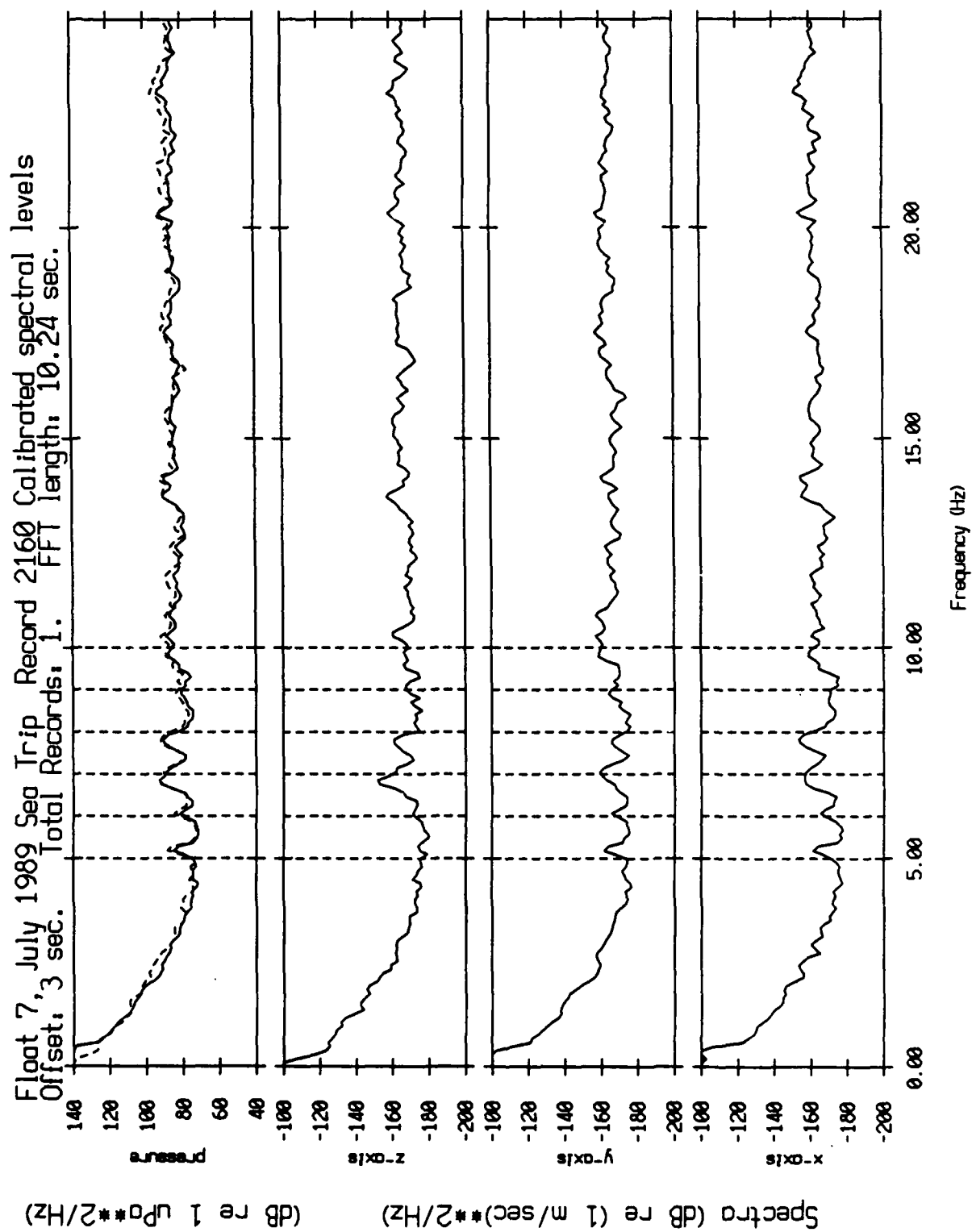


Figure XII.19e

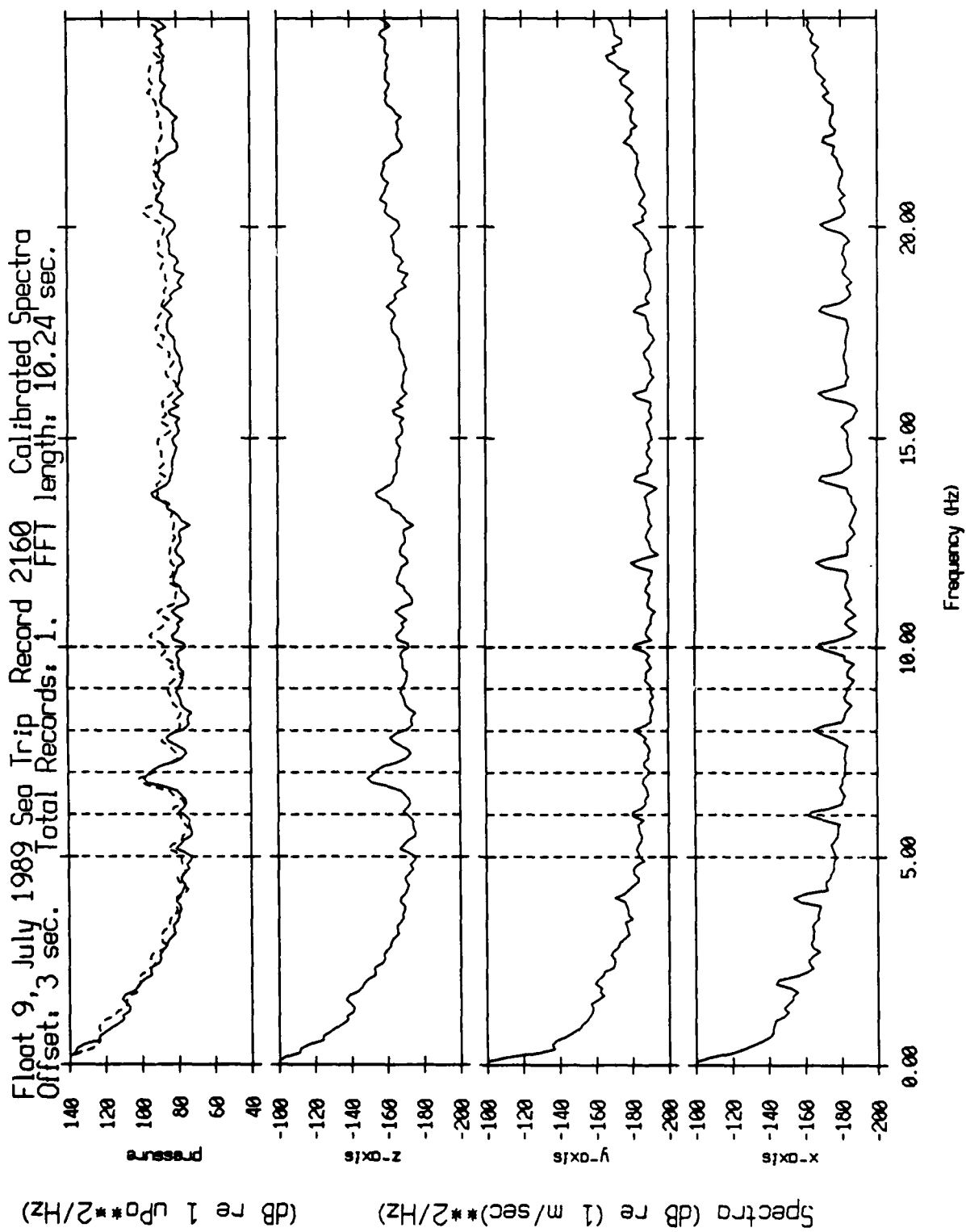


Figure XII.19f

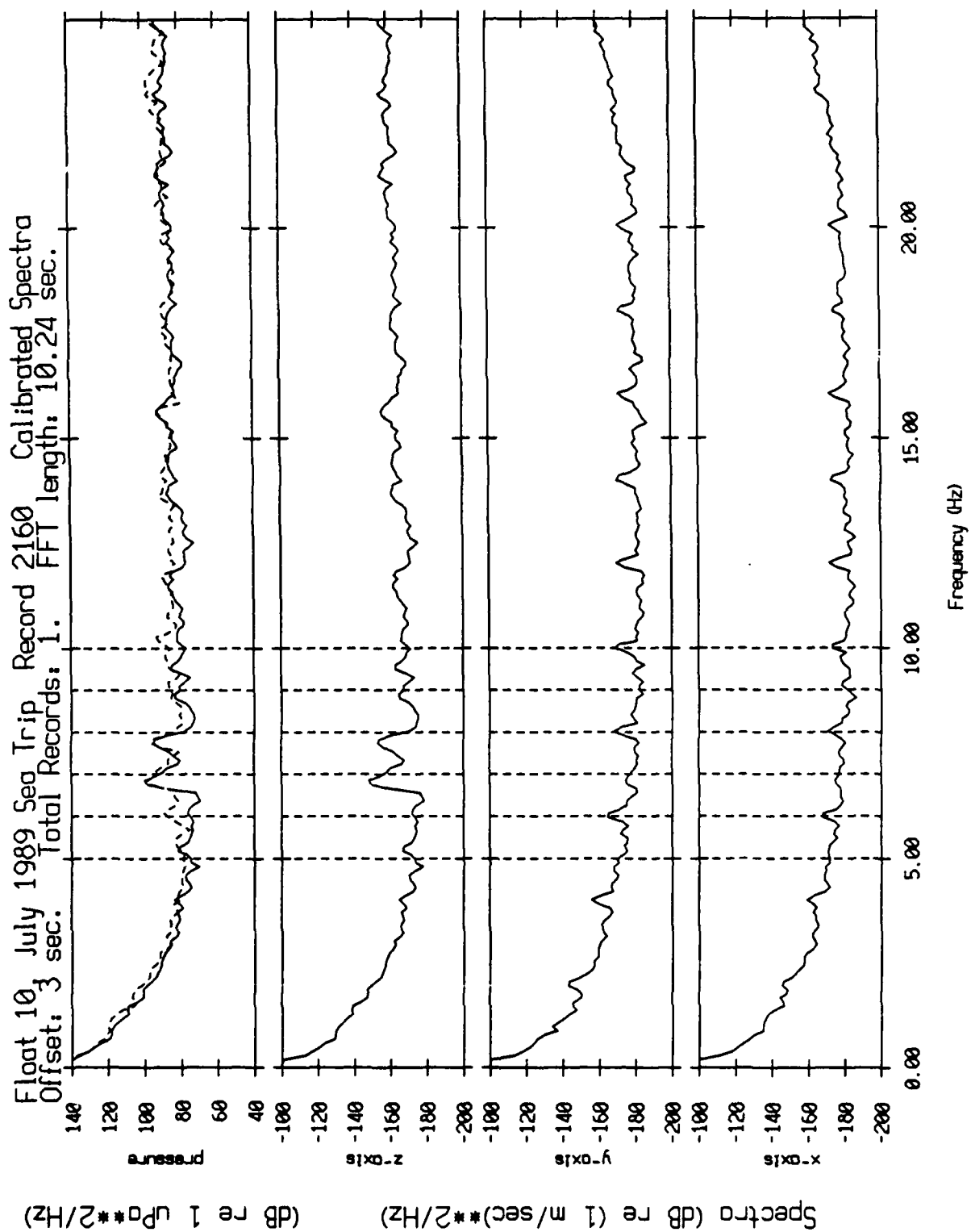


Figure XII.19g

# SWALLOW FLOAT VLF DATA ACQUISITION SYSTEM

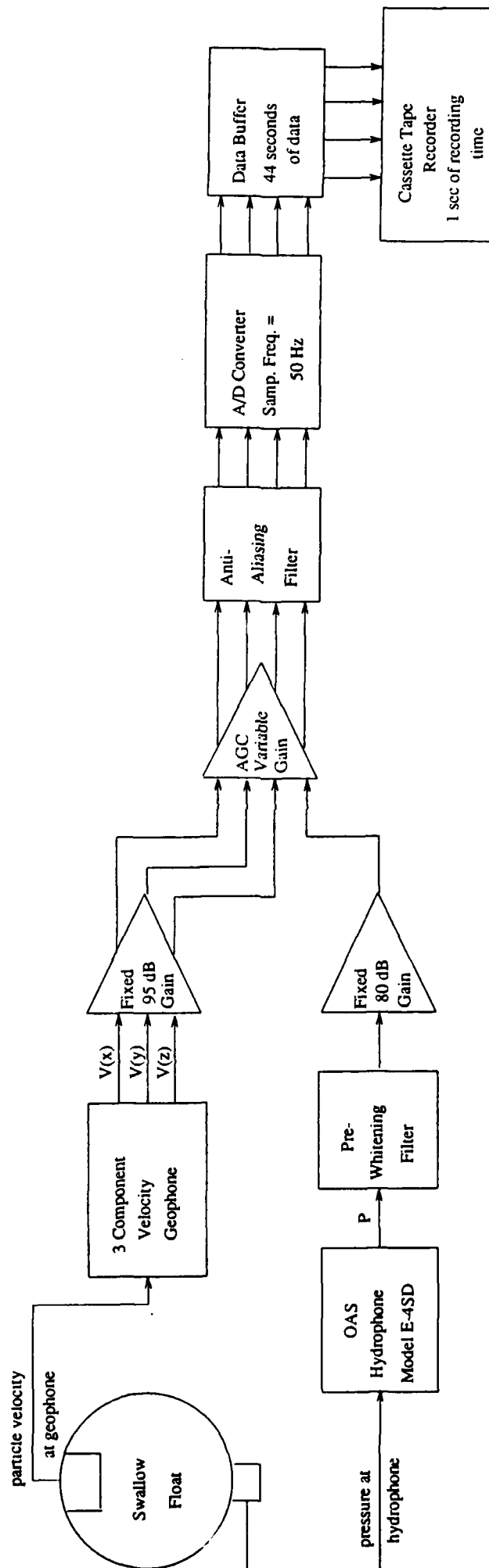


Figure A1.1

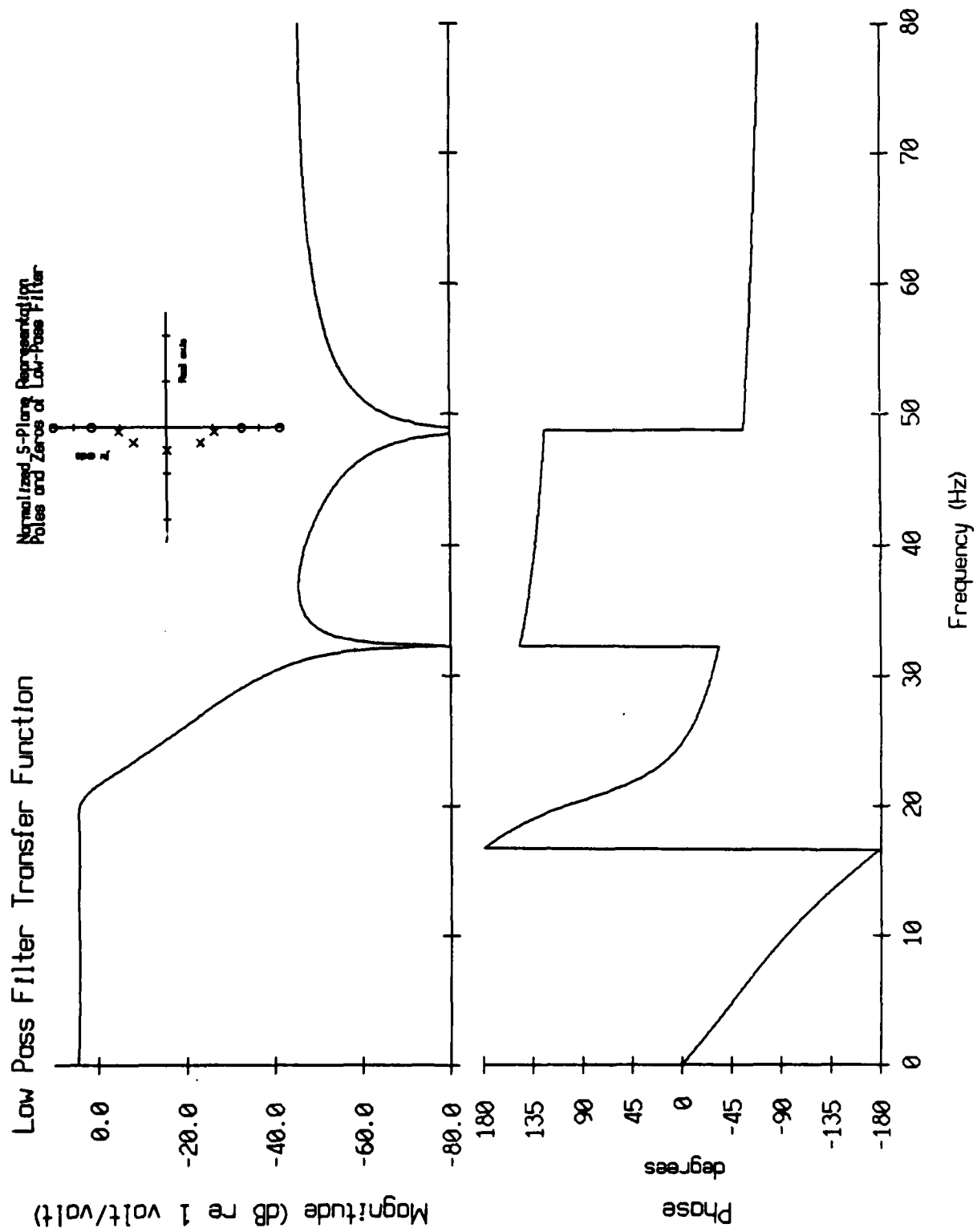


Figure A1.2

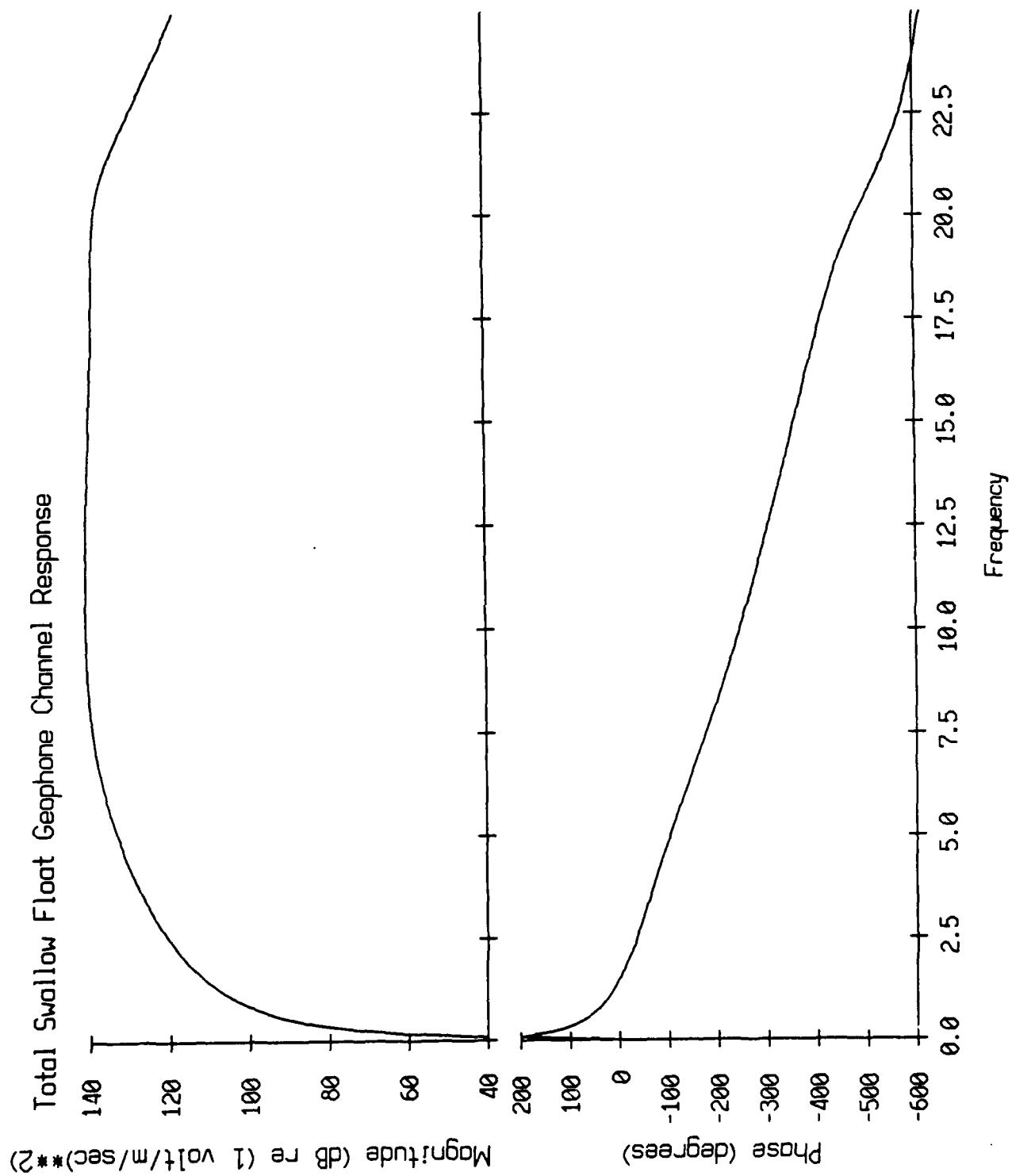


Figure A1.3



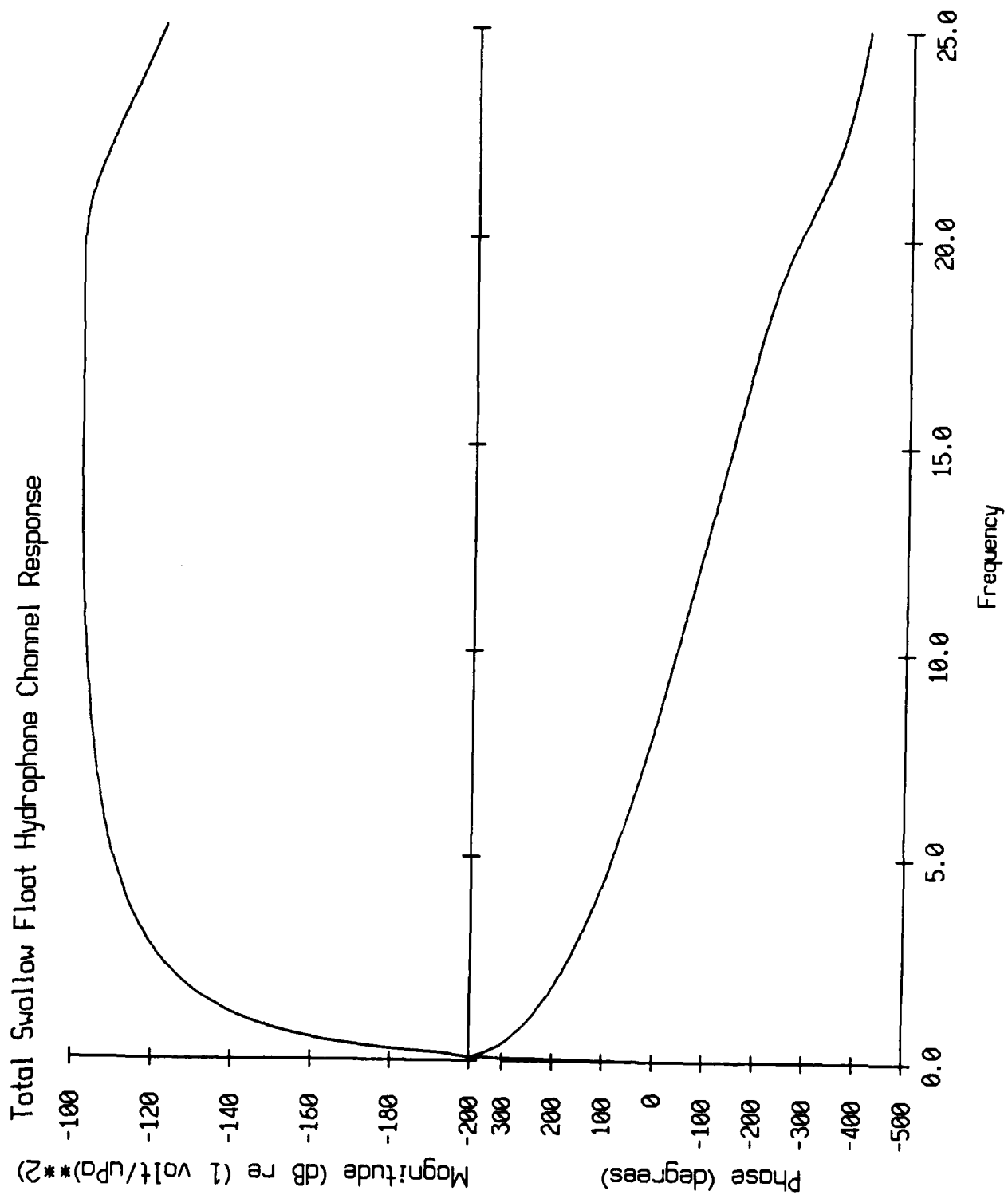


Figure A1.4

Geophone Channel Transfer Function Error  
amount to be added to old spectra to get true spectra

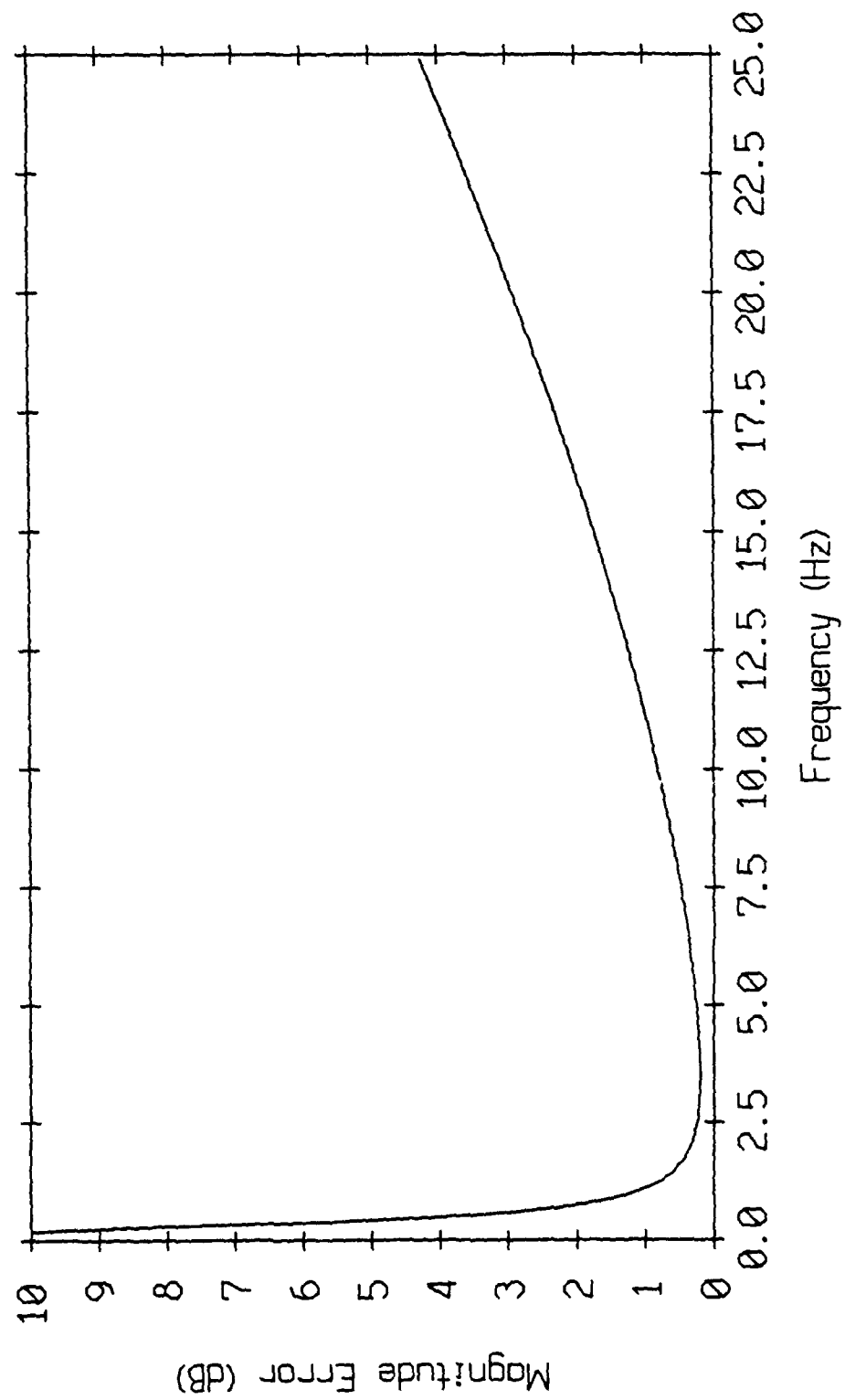


Figure A1.5

Hydrophone Channel Transfer Function Error  
amount to be added to reported spectra to get true spectra

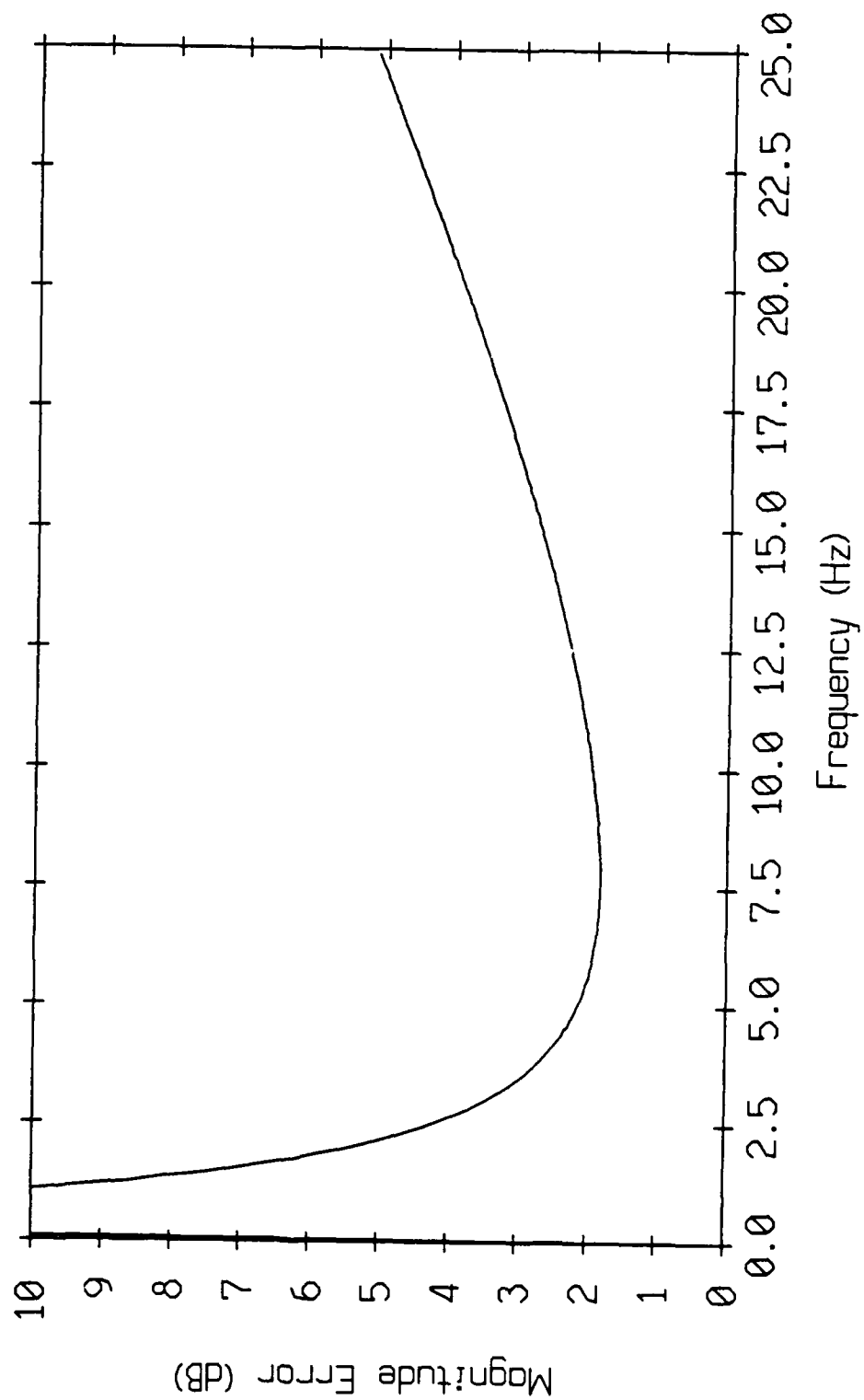


Figure A1.6

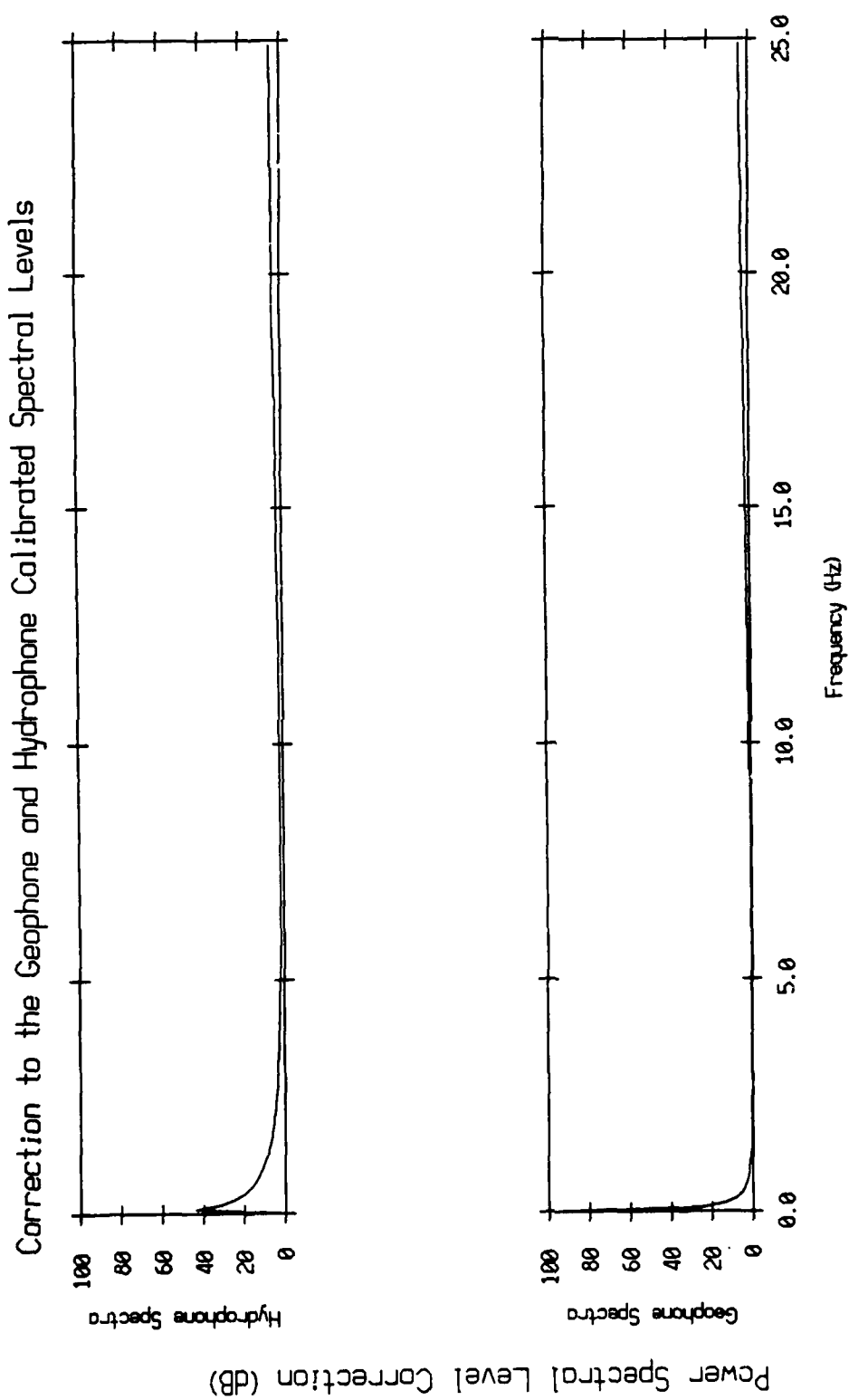


Figure A1.7

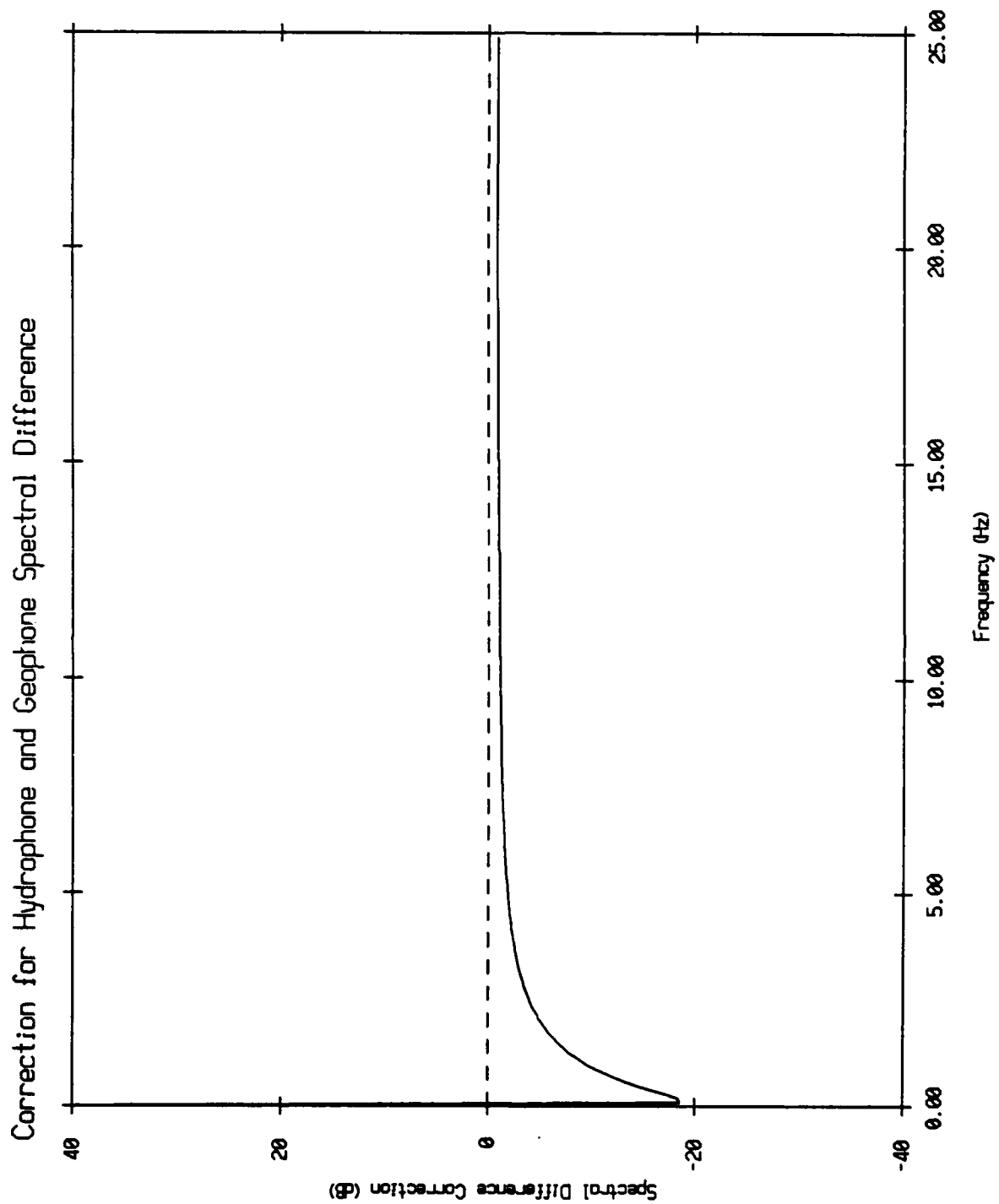


Figure A1.8

1	RECORD # (LB)	H	527	RESYNC (AA)	V
	RECORD # (HB)	E		RESYNC (AA)	L
	AGC CODE	A		RESYNC (01)	F
	COMPASS	D		CHAN X	
	BUOY ID	E		CHAN Y	A
	BATTERY	R		CHAN Z	C
	TAPE TRACK			CHAN X	O
	CHECKSUM (LB)			CHAN Y	U
	CHECKSUM (HB)			CHAN Z	S
10	RESYNC (AA)				T
	RESYNC (AA)				I
	RESYNC (01)			CHECKSUM (LB)	C
13	RANGE INDEX 1	R		CHECKSUM (HB)	
	DETECTION	A	607	RESYNC (AA)	D
	TIME (LB)	N		RESYNC (AA)	A
	TIME (HB)	G		RESYNC (01)	T
	DETECTION	E		CHAN X	A
	TIME (LB)			CHAN Y	
	TIME (HB)	P		CHAN Z	
		U			
		L			
	DETECTION	S		CHECKSUM (LB)	
	TIME (LB)	E	7646	CHECKSUM (HB)	
	TIME (HB)				G
269	RANGE INDEX 2	D			A
	DETECTION	A			P
	TIME (LB)	T	1	RECORD # (LB)	
	TIME (HB)	A			N
	DETECTION				E
	TIME (LB)				X
	TIME (HB)				T
					R
	DETECTION				E
	TIME (LB)				C
	TIME (HB)				O
	CHKSUM (LB)				R
526	CHKSUM (HB)				D

FIG. SWALLOW DATA RECORD FORMAT

1	RECORD # (LB)	H	527	RESYNC (AA)	V
	RECORD # (HB)	E		RESYNC (AA)	L
	AGC CODE	A		RESYNC (01)	F
	COMPASS	D		CHAN X	
	BUOY ID	E		CHAN Y	A
	BATTERY	R		CHAN Z	C
	TAPE TRACK			CHAN HYD	O
	CHECKSUM (LB)				U
	CHECKSUM (HB)				S
10	RESYNC (AA)				T
	RESYNC (AA)				I
	RESYNC (01)			CHECKSUM (LB)	C
13	RANGE INDEX 1	R		CHECKSUM (HB)	
	DETECTION	A	632	RESYNC (AA)	D
	TIME (LB)	N		RESYNC (AA)	A
	TIME (HB)	G		RESYNC (01)	T
	DETECTION	E		CHAN X	A
	TIME (LB)			CHAN Y	
	TIME (HB)	P		CHAN Z	
		U		CHAN HYD	
		L			
	DETECTION	S		CHECKSUM (LB)	
	TIME (LB)	E	9766	CHECKSUM (HB)	
	TIME (HB)				G
269	RANGE INDEX 2	D			A
	DETECTION	A			P
	TIME (LB)	T	1	RECORD # (LB)	
	TIME (HB)	A			N
	DETECTION				E
	TIME (LB)				X
	TIME (HB)				T
					R
	DETECTION				E
	TIME (LB)				C
	TIME (HB)				O
	CHKSUM (LB)				R
526	CHKSUM (HB)				D

FIG. SWALLOW DATA RECORD FORMAT WITH HYDROPHONE